DESIGN of CONCRETE STRUCTURES

Winter-Urquhrat 'O'Rourke-Nilson



SEVENTH EDITION

INTERNATIONAL STUDENT EDITION

Scanned with CamScanner

Scanned with CamScanner

CONTENTS

Preface v

Chapter 1 Concrete and Reinforcing Steel 1

Concrete, Reinforced and Prestressed—*1*; Cement—*5*; Aggregate—*7*; Proportioning—*9*; Mixing—*11*; Placing and Curing—*11*; Quality Control—*12*; Stress-Strain Curves—*14*; Creep—*17*; Tension Strength—*18*; Combined Stress—*19*; Volume Changes—*21*. Reinforcing Steels—*23*; Steel Grades—*26*; Stress-Strain Curves—*27*.

Chapter 2 Mechanics and Behavior of Reinforced Concrete 29

Fundamental Propositions—*29*. Axial Compression—*31*; Elastic Stresses—*32*; Ultimate Strength—*35*. Axial Tension—*37*. Bending—*39*; Elastic Stresses—*44*; Ultimate Strength—*48*; Equivalent Rectangular Stress Block—*53*. Shear and Diagonal Tension—*56*; Beams without Web Reinforcement—*59*; Beams with Web Reinforcement—*67*. Bond and Anchorage—*72*. Deflections—*79*. Compression plus Bending—*83*; Elastic Stresses—*84*; Ultimate Strength—*87*. Prestressed Concrete—*93*; Elastic Stresses—*95*; Ultimate Strength—*98*.

Scanned with CamScanner

Chapter 3 Beams 106

Design Methods—*106*. Historical Summary—*108*. Safety Provisions—*109*; Applied Loads—*110*; Structural Strength—*112*; ACI Code Safety Provisions—*113*. Flexural Design by Ultimate-strength Methods—*116*; Flexural Design by Working-stress Methods—*134*. Shear and Diagonal Tension—*150*; Ultimate-strength Design for Diagonal Tension—*152*; Working-stress Design for Diagonal Tension—*159*. Bond and Anchorage—*161*. Design Details—*168*; Crack Control—*178*. Deflection—*180*.

Chapter 4 Slabs 186

Types of Slabs—*186*; One-way Slabs—*188*; Two-way Slabs—*194*; Flat Slabs—*207*; Flat Plates—*221*; Slabs on Ground—*225*; Yield-line Theory—*231*.

Chapter 5 Columns: Axial Compression plus Bending 243

Types of Columns—*243*. Ties and Spirals—*244*. Ultimate-strength Design: Safety Provisions—*248*; Rectangular Columns—*250*; Biaxial Bending—*261*; Circular Spiral-reinforced Columns—*263*. Working-stress Design: General—*265*; Axially Loaded Columns—*267*; Compression plus Bending—*268*; Biaxial Bending—*274*. Slender Columns: General—*276*; Effects of Slenderness—*277*; Design by ACI Code—*287*.

Chapter 6 Footings 298

Types and Function—*298*; Wall Footings—*300*; Single-column Footings—303. Multiple-column Footings—*309*; Footings on Piles—*317*.

Chapter 7 Retaining Walls 320

Types and Function—*320*; Earth Pressure—*321*; External Stability—*326*; Drainage and Other Details—*330*; Gravity Retaining Walls—*331*; Cantilever Retaining Walls—*332*; Counterfort Retaining Walls—*338*.

Chapter 8 Continuous Beams and Frames 341

Continuity of Reinforced-concrete Structures—*341*; Continuous Beams—*343*; Slope-deflection Method—*346*; Moment-distribution Method—*361*; Building Frames: Vertical Loads—*372*; Building Frame: Horizontal Loads—*383*; Effective Span Length—*387*; Moments of Inertia—*389*; Support Conditions—*390*; Preliminary Design—*392*; Inelastic Redistribution of Moments—*393*.

Chapter 9 Reinforced-concrete Buildings 402

Floor and Roof Loads—*403*; Floor and Roof Systems—*406*; Walls and Partitions—*419*; Stairways—*422*; Design of Beam-and-girder Floor—*423*; Design of Ribbed Floor—*434*; Design of a Flat-slab Building—*440*.

Chapter 10 Arch and Shell Roofs 468

Arches—*469*; Theory of Two-hinged Arches—*472*; Theory of Fixed Arches—*477*; Preliminary Arch Design—*484*; Hinges in Reinforced-concrete Structures—*489*; Design of Two-hinged Arch—*492*; Cylindrical Shells—*501*; Folded Plates—*507*; Hyperbolic Paraboloids—*512*; Spherical Domes—*517*.

Chapter 11 Prestressed Concrete 523

Historical Development—*523*; Sources of Prestress Force—*525*; Prestressing Steels—*527*; Concrete—*531*; General Equations for Flexural Design—*532*; Cable Profiles—*546*; Losses in Prestress—*549*; Ultimate Flexural Strength—*553*; Shear and Diagonal Tension—*557*; Bond—*562*; End-block Design—*563*.

Chapter 12 Reinforced-concrete Bridges 568

Types of Bridges—*568*; Loads and Design Specifications—*572*; Abutments—*579*; Construction Details—*582*; Design of a Slab Bridge—*585*; Design of a Deck-girder Bridge—*587*; Composite-bridge Construction—*595*; Design of a Composite Bridge—*598*.

Appendix A Flat Slabs with Square or Rectangular Panels (ACI 1963) 607

Appendix B Tables and Diagrams 624

Appendix C Analysis and Design of Beams for Torsion 647

Index 653

Scanned with CamScanner

chapter **1**

CONCRETE AND REINFORCING STEEL

1.1 Introduction: Concrete, Reinforced Concrete, Prestressed Concrete / *Concrete* is a stonelike material obtained by permitting a carefully proportioned mixture of cement, sand and gravel or other aggregate, and water to harden in forms of the shape and dimensions of the desired structure. The bulk of the material consists of fine and coarse aggregate. Cement and water interact chemically to bind the aggregate particles into a solid mass. Additional water, over and above that needed for this chemical reaction, is necessary to give the mixture the workability that enables it to fill the forms and surround the embedded reinforcing steel prior to hardening. Concretes in a wide range of strength properties can be obtained by appropriate adjustment of the proportions of the constituent materials. Special cements (such as high-early-strength cements), special aggregates (such as various lightweight or heavyweight aggre-

Scanned with CamScanner

gates), and special curing methods (such as steam-curing) permit an even wider variety of properties to be obtained.

These properties depend to a very substantial degree on the proportions of the mix, on the thoroughness with which the various constituents are intermixed, and on the conditions of humidity and temperature in which the mix is maintained from the moment it is placed in the forms until it is fully hardened. The process of controlling these conditions is known as *curing*. To protect against the unintentional production of substandard concrete, a high degree of skillful control and supervision is necessary throughout the process, from the proportioning by weight of the individual components, through mixing and placing, until the completion of curing.

The factors which make concrete a universal building material are so pronounced that it has been used, in more primitive kinds and ways than at present, for thousands of years, probably beginning in Egyptian antiquity. The facility with which, while plastic, it can be deposited and made to fill forms or moulds of almost any practical shape is one of these factors. Its high fire and weather resistance are evident advantages. Most of the constituent materials, with the possible exception of cement, are usually available at low cost locally or at small distances from the construction site. Its compressive strength, as that of natural stones, is high, which makes it suitable for members primarily subject to compression, such as columns and arches. On the other hand, again as in natural stones, it is a relatively brittle material whose tensile strength is small compared to its compressive strength. This prevents its economical use in structural members which are subject to tension either entirely (such as tie rods) or over part of their cross sections (such as beams or other flexural members).

To offset this limitation, it has been found possible, in the second half of the nineteenth century, to use steel with its high tensile strength to reinforce concrete, chiefly in those places where its small tensile strength would limit the carrying capacity of the member. The reinforcement usually round steel rods with appropriate surface deformations to provide interlocking, is placed in the forms in advance of the concrete. When completely surrounded by the hardened concrete mass, it forms an integral part of the member. The resulting combination of two materials, known as *reinforced concrete*, combines many of the advantages of each: the relatively low cost, good weather and fire resistance, good compressive strength, and excellent formability of concrete and the high tensile strength and much greater ductility and toughness of steel. It is a combination which allows the almost unlimited range of uses and possibilities of reinforced concrete in the construction of buildings, bridges, dams, tanks, reservoirs, and a host of other structures.

In more recent times it has been found possible to produce steels

relatively low cost, whose yield strength is of the order of 4 times and more that of ordinary reinforcing steel. Likewise, it is possible to produce concrete 2 and 3 times as strong in compression as the more ordinary concretes. There are limits to the strengths of the constituent materials beyond which they can no longer be combined effectively in one member. To be sure, the strength of such a member would increase roughly in proportion to those of the constituent materials. However, the high strains which result from such high stresses, particularly in the steel, would make for large deformations and deflections of such members under load. Equally, if not more important, the large strains in such high-strength reinforcing steel would induce large cracks in the surrounding low-tensile-strength concrete, cracks which would not only be unsightly, but which would expose the steel reinforcement to corrosion by moisture and other chemical action. This limits the useful yield strength of reinforcing steel to about 80 ksi, about twice that of conventional reinforcing steels.

A special way has been found, however, to use steels and concretes of very high strength in combination. This type of construction is known as *prestressed concrete*. The steel, mostly in the shape of wires or strands, but sometimes as bars, is embedded in the concrete under high tension which is held in equilibrium by compression stresses in the surrounding concrete after hardening. Because of this precompression, the concrete in a flexural member will crack on the tension side at a much larger load than when not so precompressed. This reduces radically both the deflections and the tensile cracks at service loads in such structures and thereby enables these high-strength materials to be used effectively. Prestressed concrete is particularly suited to prefabrication on a mass-production basis, although it is being used as well without such prefabrication. Its introduction has extended, to a very significant degree, the range of structural uses of the combination of these two materials.

Figure 1.1 shows simplified sketches of some of the *principal structural forms* of reinforced concrete; pertinent design methods for many of them are discussed later in this volume. A slab, beam, and girder floor, as it is used in many multistory buildings, is shown in (*a*), and a ribbed floor which permits savings of concrete and reuse of standardized metal forms in (*b*). The flat-slab floor of (*c*), distinct in the absence of beams and girders, is frequently used for more heavily loaded buildings, such as warehouses. The rigid-frame structure of (*d*) can be made to span large openings for auditoria, gymnasia, or industrial buildings. Figure 1.1*e* and *f* show a cylindrical shell roof and a folded-plate roof, respectively, forms which, like the other shell roofs in (*h*), (*l*), and (*m*), have been developed in recent years and permit the use of extremely thin surfaces, often thinner, relatively, than an eggshell. Two of the many bridge forms are shown in (*g*) and (*j*), the former a multiarch bridge for large spans, the latter a

Scanned with CamScanner

rigid-frame bridge typical of highway overpasses. The tank or reservo
of (*i*) combines a cylindrical and a spherical shell, the former frequent
prestressed. Representative of the extensive use of reinforced concrete i
foundation work is the counterfort retaining wall of (*k*).

The forms of Fig. 1.1 do not comprise a complete range, but are merel

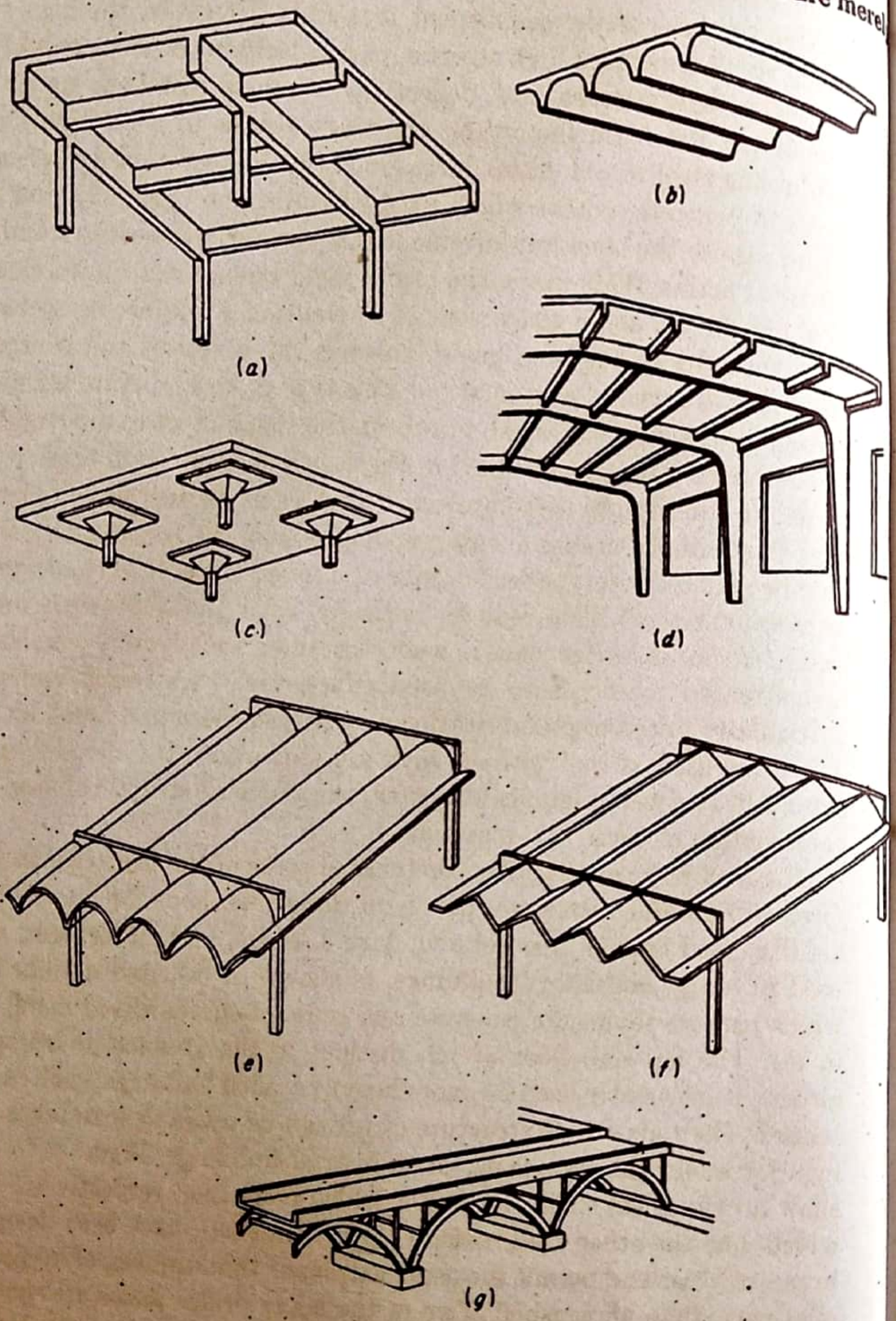


Fig. 1.1 Principal structural forms in reinforced concrete: (*a*) beam-and-girder floo
(*b*) ribbed floor, (*c*) flat-slab floor, (*d*) rigid-frame building, (*e*) cylindrical-shell roo
(*f*) folded-plate roof, (*g*) multiple-arch bridge.

typical of shapes appropriate to the properties and possibilities of concrete structures. They illustrate the adaptability of the material to a great variety of one-dimensional (beams, girders, columns), two-dimensional (slabs, arches, rigid frames), and three-dimensional (shells) structures and structural components. This variability allows the shape of the structure to be adapted to its function in an economical manner and furnishes the architect with a wide range of possibilities for esthetically satisfying structural solutions.

1.2 Cement A cementing material is one which has the adhesive and cohesive properties necessary to bond inert aggregates into a solid mass of adequate strength and durability. This technologically important cate-

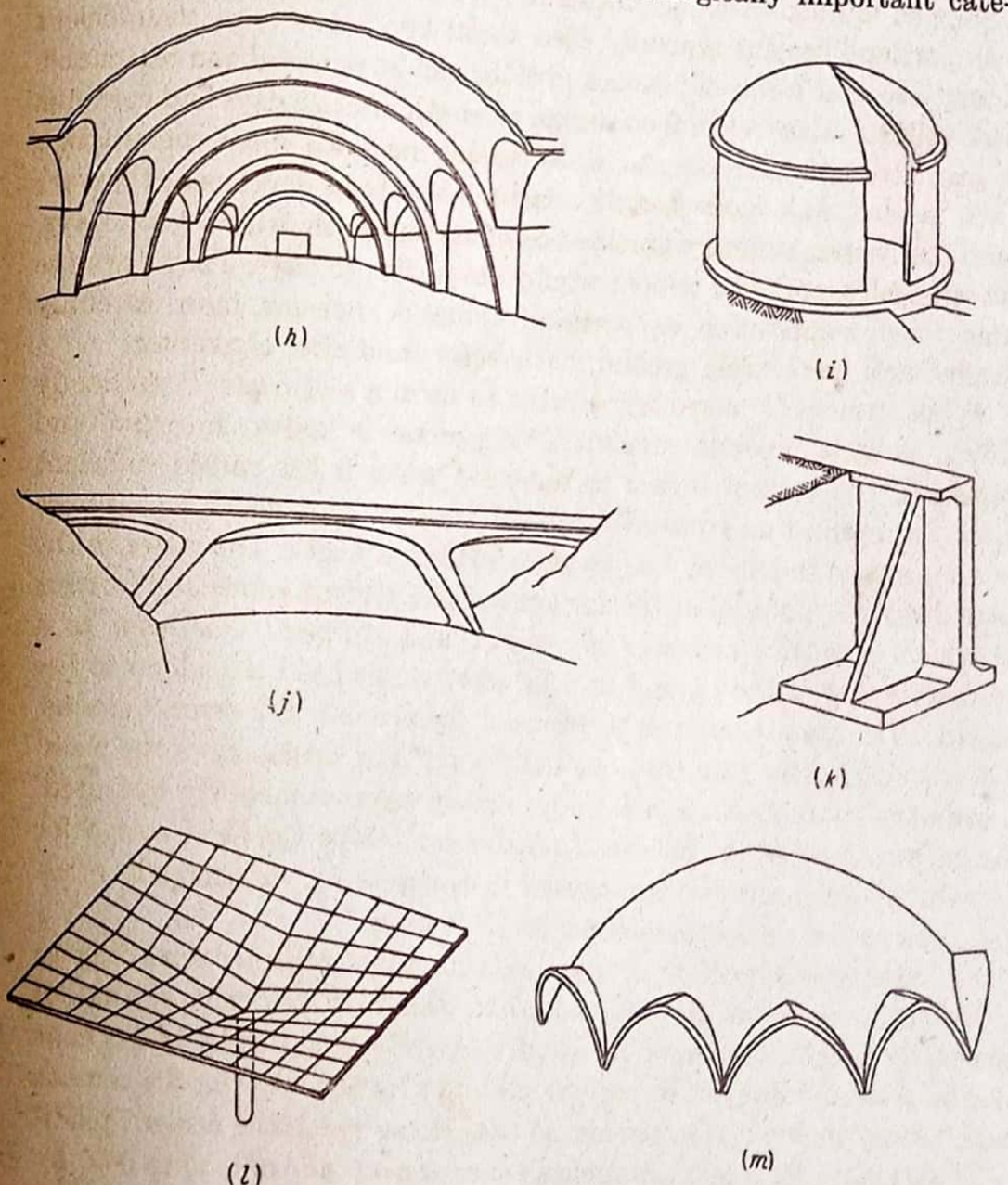


Fig. 1.1 (Continued) Principal structural forms in reinforced concrete: (*h*) shell roof, (*i*) storage tank, (*j*) rigid-frame bridge, (*k*) counterfort retaining wall, (*l*) hyperbolic-paraboloid umbrella shell, (*m*) point-supported dome roof.

Scanned with CamScanner

gory of materials includes not only cements proper, but also limes, asphalts and tars as they are used in road building, and others. For making structural concrete, so-called *hydraulic* cements are used exclusively. Water is needed for the chemical process (hydration) in which the cement powder sets and hardens into one solid mass. Of the various hydraulic cements which have been developed, *portland cement*, which was first patented in England in 1824, is by far the most common.

Portland cement is a finely powdered, grayish material which consists chiefly of calcium and aluminum silicates. The common raw materials from which it is made are limestones, which provide CaO, and clays or shales, which furnish SiO_2 and Al_2O_3. These are ground, blended, fused to clinkers in a kiln, cooled, and ground to the required fineness. The material is shipped in bulk or in bags containing 94 lb of cement. Concretes made with portland cement generally need about two weeks to reach sufficient strength so that forms of beams and slabs can be removed and reasonable loads applied; they reach their design strength after 28 days and continue to gain strength thereafter at a decreasing rate. To speed construction when needed, *high-early-strength cements* have been developed; they are more costly than ordinary portland cement, but reach, within 1 to 3 days, the strength a portland cement would have after 28 days. They have the same basic composition as portland cements, but are more carefully blended and more finely ground, both before and after clinkering.

When cement is mixed with water to form a soft paste, it gradually stiffens until it becomes a solid. This process is known as *setting* and *hardening;* the cement is said to have set when it has gained sufficient rigidity to support an arbitrarily defined pressure, after which it continues for a long time to harden, i.e., to gain further strength. The water in the paste dissolves material at the surfaces of the cement grains and forms a gel which gradually increases in volume and stiffness. This leads to a rapid stiffening of the paste 2 to 4 hr after water has been added to the cement. *Hydration* continues to proceed deeper into the cement grains, at decreasing speed, with continued stiffening and hardening of the mass. In ordinary concrete the cement is probably never completely hydrated. The gel structure of the hardened paste seems to be the chief reason for the volume changes which are caused in concrete by variations in moisture, such as the *shrinkage* of concrete as it dries.

For complete hydration of a given amount of cement, according to H. Rüsch, an amount of water equal to about 25 per cent of that of cement, by weight, is needed chemically. An additional 10 to 15 per cent must be present, however, to provide mobility for the water in the cement paste during the hydration process so that it can reach the cement particles. This makes for a total minimum *water-cement ratio* of 0.35 to 0.40 by weight. This corresponds to 4 to 4.5 gal of water per sack of cement, the more customary way of expressing the water-cement ratio. Water-cement ratios in concretes are generally considerably larger than this minimum, to provide the necessary workability of the concrete mix. Any amount of water above the 25 per cent consumed in the chemical reaction produces pores in the cement paste. The strength of the hardened paste decreases in inverse proportion to the fraction of the total volume occupied by pores. Put differently, since only the solids, and not the voids, resist stress, strength increases directly as the fraction of the total volume occupied by the solids. This is why the strength of the cement paste depends primarily on, and decreases directly with, increasing water-cement ratio.

The chemical process involved in the setting and hardening liberates heat, known as *heat of hydration*. In large concrete masses, such as dams, this heat is dissipated very slowly and results in a temperature rise and volume expansion of the concrete during hydration, with subsequent cooling and contraction. To avoid the serious cracking and weakening which may result from this process, special measures must be taken for its control.

1.3 Aggregates In ordinary structural concretes the aggregates occupy about 70 to 75 per cent of the volume of the hardened mass. The remainder consists of hardened cement paste, uncombined water (i.e., water not involved in the hydration of the cement), and air voids. The latter two evidently do not contribute to the strength of the concrete. In general, the more densely the aggregate can be packed, the better are the strength, weather resistance, and economy of the concrete. For this reason the gradation of the particle sizes in the aggregate, to produce close packing, is of considerable importance. It is also important that the aggregate have good strength, durability, and weather resistance, that its surface be free from impurities such as loam, silt, and organic matter which may weaken the bond with the cement paste, and that no unfavorable chemical reaction take place between it and the cement.

Natural aggregates are generally classified as fine and coarse. *Fine aggregate* or *sand* is any material which will pass a No. 4 sieve, i.e., a sieve with four openings per linear inch. Material coarser than this is classified as *coarse aggregate* or *gravel.* When favorable gradation is desired, aggregates are separated by sieving into two or three size groups of sand and several size groups of coarse aggregate. These can then be combined according to grading charts to result in a densely packed aggregate. The *maximum size of coarse aggregate* in reinforced concrete is governed by the requirement that it shall easily fit into the forms and between the reinforcing bars. For this purpose it should not be larger than one-fifth of the narrowest dimension of the forms nor three-quarters of the minimum distance between reinforcing bars. Authoritative information on aggregate

Scanned with CamScanner

properties, their influence on concrete properties, and their determination, and on selection, preparation, and handling of aggregate is found in the report of ACI Committee 621 (Ref. 1.1).[1]

The *unit weight* of so-called *stone concrete*, i.e., concrete with natural stone aggregate, varies from about 145 to 152 pcf and can generally be assumed as 150 pcf. For special purposes, lightweight concretes on the one hand and heavy concretes on the other are being used with increasing frequency.

Lightweight concrete can be obtained by gas-forming admixtures. However, in American practice they are almost universally produced by using special lightweight aggregates. The use of such concretes, if of strength equal to that of corresponding stone concrete, evidently reduces the dead loads of the structure. Also, the insulating properties of lightweight concrete are generally better than those of stone concrete, so that concretes of extremely light weight, whose strength may no longer be adequate for load-carrying purposes, are often employed as insulating fills.

A variety of lightweight aggregates is available. Natural materials, such as pumice and tuff, or by-products such as cinders, find some use without prior processing except for crushing and grinding. The majority of such aggregates, however, are produced artificially in kilns. Among them are expanded clays (haydite), shales, and slag and sintered fly ash. Some are used primarily for insulating purposes or masonry units; the heavier aggregates, such as expanded clays and shales, are suitable for lightweight structural concrete. Unit weights of lightweight concretes range from 30 to 80 pcf for insulating concrete, 65 to 100 pcf for masonry units, and 65 to 115 pcf for structural concrete. In general, the lower the weight, the lower the strength. The proportioning and control of lightweight aggregate mixes are more delicate than those of stone concrete, and considerable care is needed to assure the desired properties (Refs. 1.2, 1.3).

Heavyweight concrete is frequently required for shielding against gamma and X radiation in nuclear-reactor and similar installations, for protective structures, and for special purposes, such as counterweights of lift bridges. Heavy aggregates are used for such concretes. These consist of heavy iron ores or barite (barium sulfate) rock crushed to suitable sizes. Steel in the form of scrap, punchings, or shot (as fines) is also used. Unit weights of heavyweight concretes with natural heavy rock aggregates range from about 200 to 230 pcf; if iron punchings are added to high-density ores, weights as high as 270 pcf are achieved. The weight may be as high as 330 pcf if ores are used for the fines only, and steel for the coarse aggregate.

[1] References are listed at the end of the chapter.

1.4 Proportioning and Mixing of Concrete The various components of a mix are proportioned so that the resulting concrete has adequate strength, proper workability for placing, and low cost. The latter calls for use of the minimum amount of cement (the most costly of the components) which will achieve adequate properties. The better the gradation of aggregates, i.e., the smaller the volume of voids, the less cement paste is needed to fill these voids. In addition to the water required for hydration (see Art. 1.2), water is needed for wetting the surface of the aggregate. As water is added, the plasticity and fluidity of the mix increases (i.e., its workability improves), but the strength decreases because of the larger volume of voids created by the free water. To reduce the free water while retaining the workability, cement must be added. Therefore, as for the cement paste, the *water-cement ratio* is the chief factor which controls the strength of the concrete. For a given water-cement ratio, one selects that minimum amount of cement, in sacks per cubic yard, which will secure the desired workability.

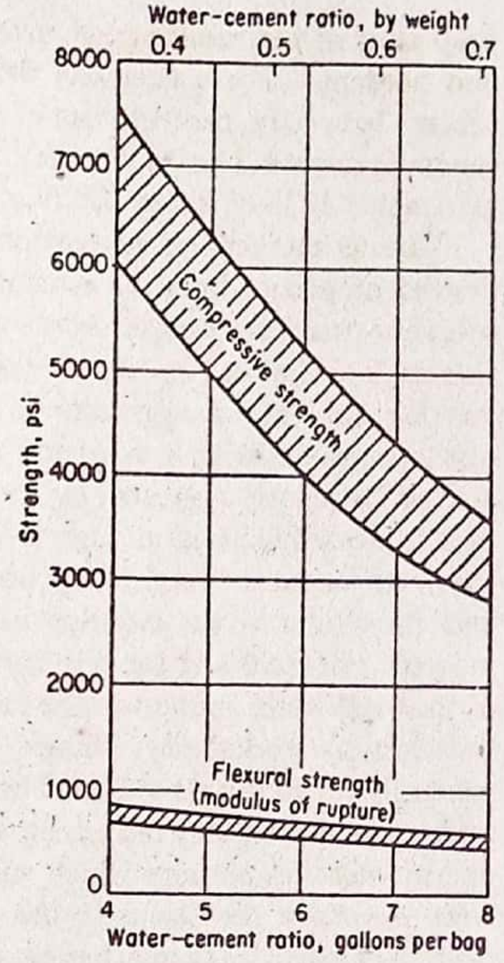


Fig. 1.2 Effect of water-cement ratio on 28-day compressive and flexural strength. (*Adapted from Ref.* 1.4.)

Figure 1.2, adapted from Ref. 1.4, shows the decisive influence of the water-cement ratio on the compressive strength of concrete. Its influence on the tensile strength, as measured by the nominal flexural strength or modulus of rupture, is seen to be pronounced, but much smaller than its effect on compression strength. This seems to be so because, in addition to the void ratio, the tensile strength depends strongly on the strength of bond between coarse aggregate and cement mortar (i.e., cement paste plus fine aggregate). According to tests at Cornell University, this bond strength is relatively slightly affected by the water-cement ratio (Ref. 1.4*a*).

It has been customary to define the *proportions* of a concrete mix by the ratio, by volume or weight, of cement to sand to gravel, for example, 1:2:4. This method refers to the solid components only and, unless the water-cement ratio is specified separately, is insufficient to define the

properties of the resulting concrete either in its fresh state or when set and hardened. For a complete definition of proportions it is now customary to specify, per 94-lb bag of cement, the weight of water, sand, and coarse aggregate. Thus, a mix may be defined as containing (per 94-lb bag of cement) 45 lb of water, 320 lb of sand, and 500 lb of coarse aggregate.

Various methods of proportioning are used to obtain mixes of the desired properties from the cements and aggregates at hand. One is the so-called *trial-batch method*. Selecting a water-cement ratio from information such as that in Fig. 1.2, one produces several small trial batches with varying amounts of aggregate to obtain the required consistency and other properties with a minimum amount of paste. Concrete *consistency* is most frequently measured by the *slump test*. A metal mold in the shape of a truncated cone 12 in. high is filled with fresh concrete in a carefully specified manner. Immediately upon being filled, the mold is lifted off, and the slump of the concrete is measured as the difference in height between the mold and the pile of concrete. The slump is a good measure of the total water content in the mix and should be kept as low as is compatible with workability. Slumps for concretes in building construction generally range from 2 to 6 in. The so-called *ACI method of proportioning* makes use of the slump test in connection with a set of tables which permit one to select proportions which will result in the desired properties for a wide variety of conditions (types of structures, dimensions of members, degrees of exposure to weathering, etc.). Details of this and other methods are beyond the scope of this volume and are fully treated in Refs. 1.4 to 1.6.

In addition to the main components of concretes, *admixtures* are often used for special purposes. There are admixtures to improve workability, to accelerate or retard setting and hardening, to aid in curing, to improve durability, to add color, and to impart other properties. While the beneficial effects of some admixtures are well established, the claims of others should be viewed with caution. *Air-entraining agents* at present are the most important and most widely used admixtures. They cause the entrainment of air in the form of small, well-dispersed bubbles in the concrete. These improve workability and durability, chiefly resistance to freezing and thawing, and reduce segregation during placing. They decrease density because of the increased void ratio and thereby decrease strength; however, this decrease can be partially offset by reduction of mixing water without loss of workability. The chief use of air-entrained concretes is in pavements, but they are also used for structural work, particularly for outdoor structures.

On all but the smallest jobs, *batching* is carried out in special batching plants. Separate hoppers contain cement and the various fractions of aggregate. Proportions are controlled, by weight, by means of manually

operated or automatic dial scales connected to the hoppers. The mixing water is batched either by measuring tanks or by water meters.

The principal purpose of *mixing* is to produce an intimate mixture of cement, water, fine and coarse aggregate, and possible admixtures of uniform consistency throughout each batch. This is achieved in machine mixers of the revolving-drum type. Minimum mixing time is 1 min for mixers of not more than 1 yd^3 capacity, with an additional 15 sec for each additional ½ yd^3. Mixing can be continued for a considerable time without adverse effect. This fact is particularly important in connection with ready-mixed concrete.

On large projects, particularly in the open country where ample space is available, movable mixing plants are installed and operated at the site. On the other hand, in construction under congested city conditions, on smaller jobs, and frequently in highway construction, *ready-mixed concrete* is used. Such concrete is batched in a stationary plant and then hauled to the site in trucks in one of three ways: (1) mixed completely at the stationary plant and hauled in a truck agitator, (2) transit-mixed, i.e., batched at the plant but mixed in a truck mixer, or (3) partially mixed at the plant with mixing completed in a truck mixer. Concrete should be discharged from the mixer or agitator within at most 1½ hr after the water is added to the batch.

1.5 Conveying, Placing, Compacting, Curing *Conveying* of most building concrete from the mixer or truck to the form is done in wheelbarrows or buggies on horizontal runways or by pumping through steel pipelines. The chief danger during conveying is that of *segregation*. The individual components of concrete tend to segregate because of their dissimilarity. In overly wet concrete standing in containers or forms, the heavier gravel components tend to settle, and the lighter materials, particularly water, to rise. Lateral movement, such as flow within the forms, tends to separate the coarse gravel from the finer components of the mix. The danger of segregation has caused the discarding of some previously common means of conveying, such as chutes and conveyor belts, in favor of methods which minimize this tendency.

Placing is the process of transferring the fresh concrete from the conveying device to its final place in the forms. Prior to placing, loose rust must be removed from reinforcement, forms must be cleaned, and hardened surfaces of previous concrete lifts must be cleaned and treated appropriately. Placing and compacting are critical in their effect on the final quality of the concrete Proper placement must avoid segregation, displacement of forms or of reinforcement in the forms, and poor bond between successive layers of concrete. Immediately upon placing, the concrete should be *compacted* by means of hand tools or vibrators. Such

Scanned with CamScanner

compacting prevents honeycombing, assures close contact with forms and reinforcement, and serves as partial remedy to possible prior segregation. Compacting is achieved by hand tamping with a variety of special tools, but now more commonly and successfully with high-frequency, power-driven *vibrators*. These are of the *internal* type, immersed in the concrete, or of the *external* type, attached to the forms. The former are preferable, but must be supplemented by the latter where narrow forms or other obstacles make immersion imposible (Ref. 1.7).

Fresh concrete gains strength most rapidly during the first few days and weeks. Structural design is generally based on the 28-*day strength*, about 70 per cent of which is reached at the end of the first week after placing. The final concrete strength depends greatly on the conditions of moisture and temperature during this initial period. The maintenance of proper conditions during this time is known as *curing*. Thirty per cent of the strength or more can be lost by premature drying out of the concrete; similar amounts may be lost by permitting the concrete temperature to drop to 40°F or lower during the first few days unless the concrete is maintained continuously moist for a long time thereafter. Freezing of fresh concrete may reduce its strength by as much as 50 per cent.

To prevent such damage, concrete should be protected from loss of moisture for at least 7 days and, in more sensitive work, up to 14 days. When high-early-strength cements are used, curing periods can be cut in half. Curing can be achieved by keeping exposed surfaces continually wet through sprinkling, ponding, covering with wet burlap, or the like. Recent methods include the use of sealing compounds which, when properly used, form evaporation-retarding membranes, and waterproof papers. In addition to improved strength, proper moist curing provides better shrinkage control. To protect the concrete against low temperature during cold weather, the mixing water and, occasionally, the aggregates are heated, temperature insulation is used where possible, and special admixtures, particularly calcium chloride, are employed. When air temperatures are very low, external heat may have to be supplied in addition to insulation.

1.6 Tests, Quality Control; Inspection The quality of mill-produced materials, such as structural or reinforcing steel, is guaranteed by the producer, who must exercise systematic quality controls, usually specified by pertinent ASTM (American Society for Testing and Materials) standards. Concrete, in contrast, is produced at or close to the site, and its final qualities are affected by a number of factors which have been briefly discussed. Thus, systematic quality control must be instituted at the construction site.

The main measure of the structural quality of concrete is its *compression strength*. Tests for this property are made on cylindrical specimens

of height equal to twice the diameter, usually 6 × 12 in. Impervious molds of this shape are filled with concrete during the operation of placement as specified by ASTM C172, "Method of Sampling Fresh Concrete," and ASTM C31, "Method of Making and Curing Concrete Specimens in the Field." The cylinders are moist-cured at 70 ± 5°F, generally for 28 days, and then tested in the laboratory at a specified rate of loading. The compression strength obtained from such tests is known as the *cylinder strength* f'_c and is the main property specified for design purposes.

To provide structural safety, continuous control is necessary to ensure that the strength of the concrete as furnished is in satisfactory agreement with the value called for by the designer. The "Building Code Requirements for Reinforced Concrete" of the American Concrete Institute, ACI 318-63 (henceforth referred to as the *ACI Code*), specify that a pair of cylinders shall be tested for each 150 yd³ of concrete. It provides two degrees of control: (1) the average of any five consecutive pairs shall be at least equal to the specified design strength, and not more than 20 per cent of the pairs of tests may have values smaller than specified, and (2) the average of any three consecutive pairs shall be at least equal to the specified design strength, and not more than 10 per cent of the pairs of tests may have values smaller than the specified strength. These requirements provide for adequate average strength as well as for satisfactory uniformity. At the same time they recognize that it is not economically possible to manufacture concrete, or any other material, for that matter, without occasionally producing small quantities of somewhat substandard quality (Ref. 1.15). The more advanced design methods known as *ultimate-strength design* may be used only when control conforms to the more rigorous requirements of (2), above, which also apply to prestressed concrete.

In spite of scientific advances, building in general, and concrete making in particular, retain some elements of an art; they depend on many skills and imponderables. It is the task of systematic *inspection* to ensure close correspondence between plans and specifications and the finished structure. Inspection during construction should be carried out by a competent engineer, preferably the one who produced the design or one who is responsible to the design engineer. The inspector's main functions in regard to materials quality control are sampling, examination, and field testing of materials, control of concrete proportioning, inspection of batching, mixing, conveying, placing, compacting, and curing, and supervision of preparation of specimens for laboratory tests. In addition, he must inspect foundations, formwork, placing of reinforcing steel, and other pertinent features of the general progress of work, keep records of all the inspected items, and prepare periodic reports. The importance of thorough inspection to the correctness and adequate quality of the finished structure cannot be emphasized too strongly.

Scanned with CamScanner

This brief account of concrete technology represents the merest outline of an important subject. Anyone in practice who is actually responsible for any of the phases of producing and placing concrete must familiarize himself with the details in much greater depth. In addition to the literature quoted in the preceeding articles, Refs. 1.8 to 1.11 are relevant in this connection.

1.7 Strength and Deformation of Concrete in Compression

a. Short-time loading Performance of a structure under load depends to a large degree on the stress-strain relationship of the material from which it is made, under the type of stress to which the material is subjected in the structure. Since concrete is used mostly in compression (see Art. 1.1), its compressive stress-strain curve is of primary interest. Such a curve is obtained by appropriate strain measurements in cylinder tests (Art. 1.6) or on the compression side in beams. Figure 1.3 shows a typical set of such curves, obtained at normal, moderate testing speeds on concretes 28 days old, for various cylinder strengths f'_c.

All the curves have somewhat similar character. They consist of an initial relatively straight elastic portion in which stress and strain are closely proportional, then begin to curve to the horizontal, reaching the maximum stress, i.e., the compressive strength, at a strain of approximately 0.002 in. per in., and finally show a descending branch. It is also seen that concretes of lower strength are less brittle, i.e., fracture at a larger maximum strain, than high-strength concretes.

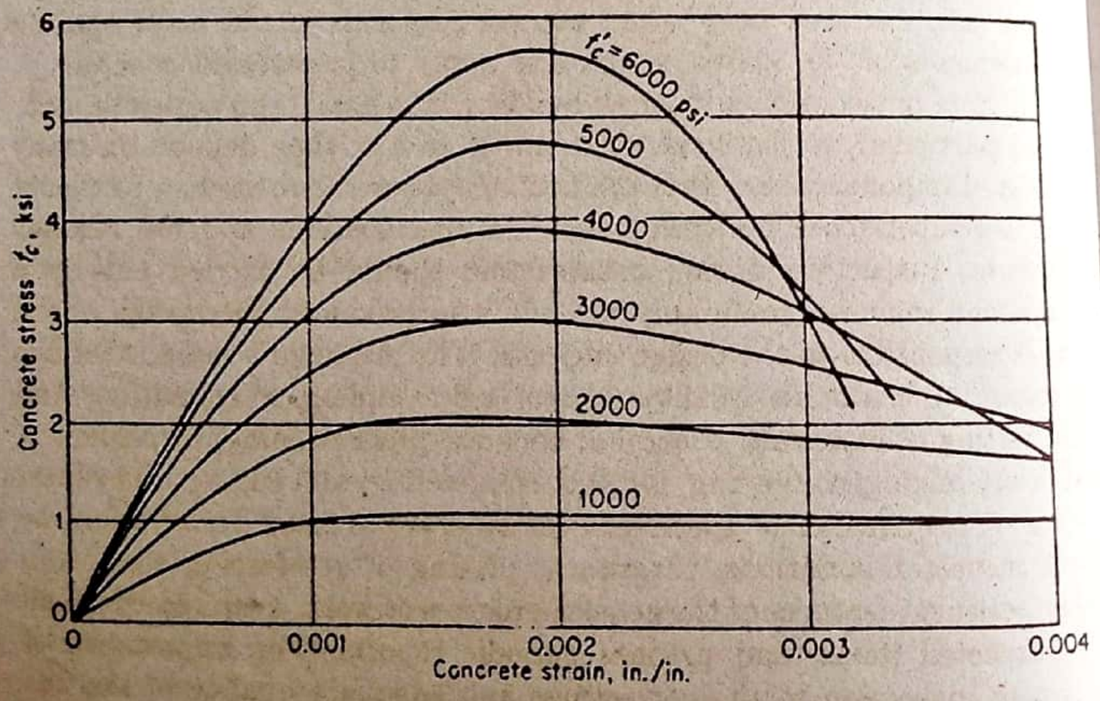


Fig. 1.3 Typical concrete stress-strain curves.

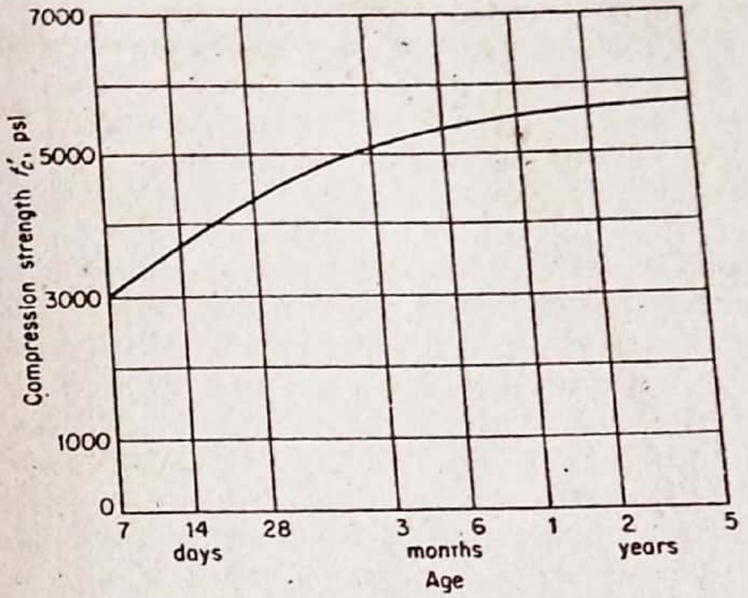


Fig. 1.4 Effect of age on compression strength f'_c. (*From Ref.* 1.4.)

The *modulus of elasticity* E_c (in psi units), that is, the slope of the initial straight portion of the stress-strain curve, is seen to be the larger the higher the strength of the concrete. It can be computed with reasonable accuracy from the empirical equation

$$E_c = 33w^{3/2}\sqrt{f'_c} \tag{1.1}$$

where w is the unit weight of the hardened concrete in pcf, and f'_c its cylinder strength in psi. Equation (1.1) has been obtained by testing structural concretes with values of w from 90 to 155 pcf. For normal sand-and-stone concretes, with $w = 145$ pcf, one obtains

$$E_c = 57{,}500\sqrt{f'_c} \tag{1.2}$$

Information on concrete strength properties such as those discussed is usually obtained through tests made 28 days after pouring. However, cement continues to hydrate, and consequently concrete continues to harden, long after this age, at a decreasing rate. Figure 1.4 shows a typical curve of the gain of concrete strength with age.

In present practice, 28-day cylinder strengths in the range of

$$f'_c = 2500 \text{ to } 5000 \text{ psi}$$

are usually specified for reinforced-concrete structures, with values between 3000 and 4000 being the most common. For prestressed concrete, higher strengths are designated, from about 4000 to 8000 psi, with $f'_c = 5000$ to 6000 psi being most customary.

Scanned with CamScanner

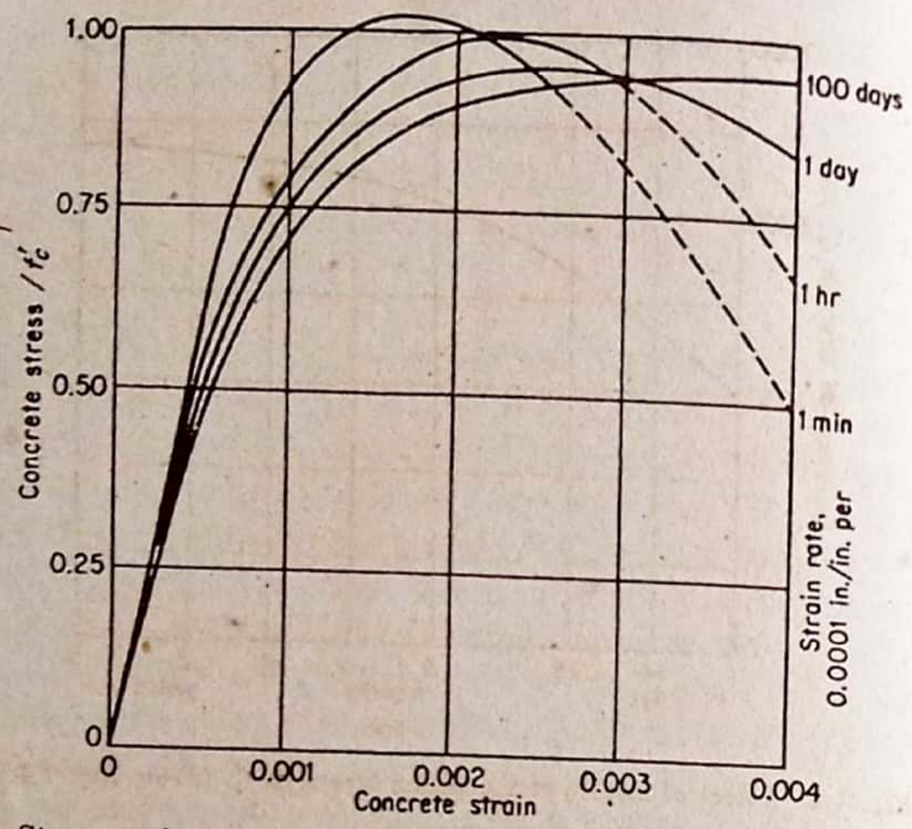


Fig. 1.5 Stress-strain curves at various strain rates, concentric compression. (*Adapted from Ref.* 1.13.)

It should be noted that the shape of the stress-strain curve for various concretes of the same cylinder strength, and even for the same concrete under various conditions of loading, varies considerably. An example of this is shown in Fig. 1.5, where different specimens of the same concrete are loaded at different rates of strain, from one corresponding to relatively fast loading (0.001 in. per in. per min) to one corresponding to an extremely slow application of load (0.001 in. per in. per 100 days). It is seen that the descending branch of the curve, probably indicative of internal disintegration of the material, is much more pronounced at fast than at slow rates of loading. It is also seen that the peaks of the curves, i.e., the maximum strength reached, is somewhat smaller at slower rates of strain.

When compressed in one direction, concrete, like other materials, expands in the direction transverse to that of the applied stress. The ratio of the transverse to the longitudinal strain is known as *Poisson's ratio* and depends on composition and other factors. At stresses lower than about $0.7f_c'$, Poisson's ratio for concrete falls within the limits of 0.15 and 0.20, with 0.17 being the most representative value.

b. Longtime loading In some engineering materials, such as steel, strength and the stress-strain relationship are independent of rate and duration of loading, at least within the usual ranges of rate of stress, temperature, and other variables. In contrast, Fig. 1.5 illustrates the fact that the influence of time, in this case of rate of loading, on the behavior of

concrete under load is pronounced. The main reason for this is that concrete creeps under load, while steel does not exhibit creep under conditions prevailing in buildings, bridges, and similar structures.

Creep is the property of many materials by which they continue deforming over considerable lengths of time at constant stress or load. The nature of the creep process is shown schematically in Fig. 1.6. This particular concrete was loaded at age 28 days with resulting instantaneous strain ϵ_{inst}. The load was then maintained for 230 days, during which time creep is seen to have increased the total deformation to almost 3 times its instantaneous value. If the load were maintained, the deformation would follow the solid curve. If the load is removed, as shown by the dashed curve, the elastic instantaneous strain ϵ_{inst} is, of course, recovered, and some creep recovery is seen to occur. If the concrete is reloaded at some later date, instantaneous and creep deformations develop again as shown.

Creep deformations for a given concrete are practically proportional to the magnitude of the applied stress; at any given stress, high-strength concretes show less creep than lower-strength concretes. As seen in Fig. 1.6, with elapsing time creep proceeds at a decreasing rate and ceases after 2 to 5 years at a final value which, depending on concrete strength and other factors, attains 1.5 to 4 times the magnitude of the instantaneous strain. If, instead of being applied quickly and thereafter kept constant, the load is increased slowly and gradually, as is the case in many structures during and after construction, instantaneous and creep defor-

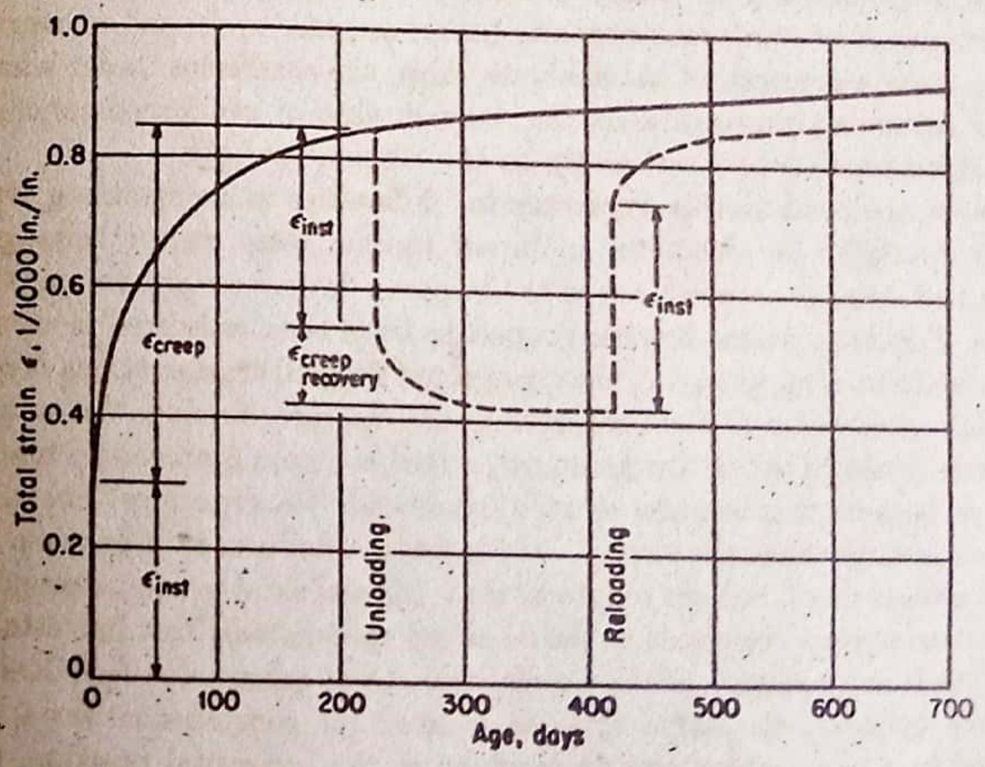


Fig. 1.6 Typical creep curve (concrete loaded to 600 psi at age 28 days).

Scanned with CamScanner

mations proceed simultaneously. The effect is that shown in Fig. 1.5; that is, the previously discussed difference in the shape of the stress-strain curve for various rates of loading is chiefly the result of the creep deformations of concrete.

Sustained loads affect not only the deformation, but also the strength of concrete. The cylinder strength f'_c is determined at normal rates of test loading (about 35 psi per sec). Tests by Rüsch and others have shown that for concentrically loaded, unreinforced concrete prisms or cylinders the *strength under sustained load* is significantly smaller than f'_c, of the order of 75 per cent of f'_c for loads maintained for a year or more.

When concrete is subject to fluctuating rather than sustained loading, its *fatigue strength*, as for all other materials, is considerably smaller than its static strength. When plain concrete in compression is stressed cyclically from zero to maximum stress, its fatigue limit is from 50 to 60 per cent of the static compression strength, for 2,000,000 cycles. A reasonable estimate can be made for other stress ranges using the modified Goodman diagram. For other types of applied stress, such as flexural compression stress in reinforced-concrete beams or flexural tension stress in unreinforced beams or on the tension side of reinforced beams, the fatigue limit likewise appears to be about 55 per cent of the corresponding static strength (Ref. 1.14).

1.8 Tension Strength While concrete is best employed in a manner which utilizes its favorable compression strength, its tension strength is also of consequence in a variety of connections. Thus, the shear and torsion resistance of reinforced-concrete beams appears to depend primarily on the tension strength of the concrete. Also, the conditions under which cracks form and propagate on the tension side of reinforced-concrete flexural members depends strongly on the tension strength.

There are considerable experimental difficulties in determining true tensile strengths for concrete. In direct tension tests, minor misalignments and stress concentrations in the gripping devices are apt to mar the results. For many years, tension properties have been measured in terms of the *modulus of rupture*, i.e., that computed flexural tension stress Mc/I at which a test beam of plain concrete would fracture. Because this nominal stress is computed on the assumption that concrete is an elastic material, and because this bending stress is localized in the outermost fibers, it is apt to be larger than the strength of concrete in uniform axial tension. It is thus a measure of, but not identical with, the real axial tension strength.

In recent years the result of the so-called *split-cylinder* test has established itself as a measure of the tensile strength of concrete. A 6 × 12-in. concrete cylinder, the same type as is used for compression tests, is inserted in a compression-testing machine in the horizontal position, so

that compression is applied uniformly along two opposite generatrices. Plywood pads are inserted between the compression platens of the machine and the cylinder in order to equalize and distribute the pressure. It can be shown that in an elastic cylinder so loaded, a nearly uniform tensile stress of magnitude $2P/\pi dL$ exists at right angles to the plane of load application. Correspondingly, such cylinders, when tested, split into two halves along that plane, at a stress which can be computed from the above expression. P is the applied compression load at failure, and d and L are the diameter and length of the cylinder. Because of local stress conditions at the load lines and the presence of stresses at right angles to the aforementioned tension stresses, the results of the split-cylinder tests likewise are not identical with (but are believed to be a good measure of) the true axial tensile strength. The results of all types of tensile tests show considerably more scatter than those of compression tests.

Tensile strength, whichever way determined, does not correlate well with the compression strength f'_c. It appears that for sand-and-gravel concrete the tensile strength depends primarily on the strength of bond between hardened cement paste and aggregate, whereas for lightweight concretes it depends largely on the tensile strength of the porous aggregate. The compression strength, on the other hand, is much less determined by these particular characteristics.

It appears that a reasonable estimate for the split-cylinder strength f'_{sp} is given by 6 to 7 times $\sqrt{f'_c}$ for sand-and-gravel concretes, and by 4 to 5 times $\sqrt{f'_c}$ for lightweight concretes.[1] The true tensile strength f'_t for the former appears to be of the order of 0.5 to 0.7 times f'_{sp}, and the flexural tension strength f_r (modulus of rupture) from 1.25 to 1.75 times f'_{sp}. The smaller of the foregoing factors apply to higher-strength concretes, and the larger to lower-strength concretes. These approximate expressions show that tension and compression strengths are by no means proportional and that any increase in compression strength, such as that achieved by lowering the water-cement ratio, is accompanied by a much smaller percentage increase in tensile strength (see also Fig. 1.2).

1.9 Strength under Combined Stress In many structural situations concrete is subjected simultaneously to various stresses acting in various directions. For instance, in beams much of the concrete is subject simultaneously to compression and shear stresses, in slabs and footings to compression in two perpendicular directions plus shear. By methods well known in the study of strengths of materials, any such state of combined stress, no matter how complex, can be reduced to three principal stresses

[1] In these expressions, f'_c is expressed in psi, and the resulting f'_{sp} is obtained in psi. For example, for $f'_c = 3600$ psi, $f'_{sp} = 6\sqrt{f'_c}$ to $7\sqrt{f'_c} = 6 \times 60$ to $7 \times 60 = 360$ to 420 psi.

Scanned with CamScanner

acting at right angles to each other on an appropriately oriented elementary cube in the material. Any or all the principal stresses can be either tension or compression. If one of them is zero, a state of *biaxial* stress is said to exist, if two of them are zero, the state of stress is *uniaxial*, either simple compression or simple tension. In most cases only the uniaxial strength properties of a material are known from simple tests, such as the cylinder strength f'_c and the tensile strength f'_t. For predicting the strengths of structures in which concrete is subject to biaxial or triaxial stress, it would be desirable to be able to calculate the strength of concrete in such states of stress, knowing from tests only either f'_c or f'_c and f'_t.

In spite of extensive and continuing research, no reliable theory of the strength of concrete under combined stress has yet emerged. Modifications of various strength theories, such as the maximum-tension-stress, the Mohr, and the octahedral-stress theories, all of which are discussed in strength-of-materials texts, have been adapted with varying partial success to concrete (Refs. 1.16 to 1.19). At this time none of them is free from internal contradictions or of sufficient reliability to be practically useful. One of the reasons for this lies in the highly nonhomogeneous nature of concrete and in the degree to which its behavior at high stresses and at fracture is influenced by microcracking and other discontinuity phenomena (Ref. 1.20).

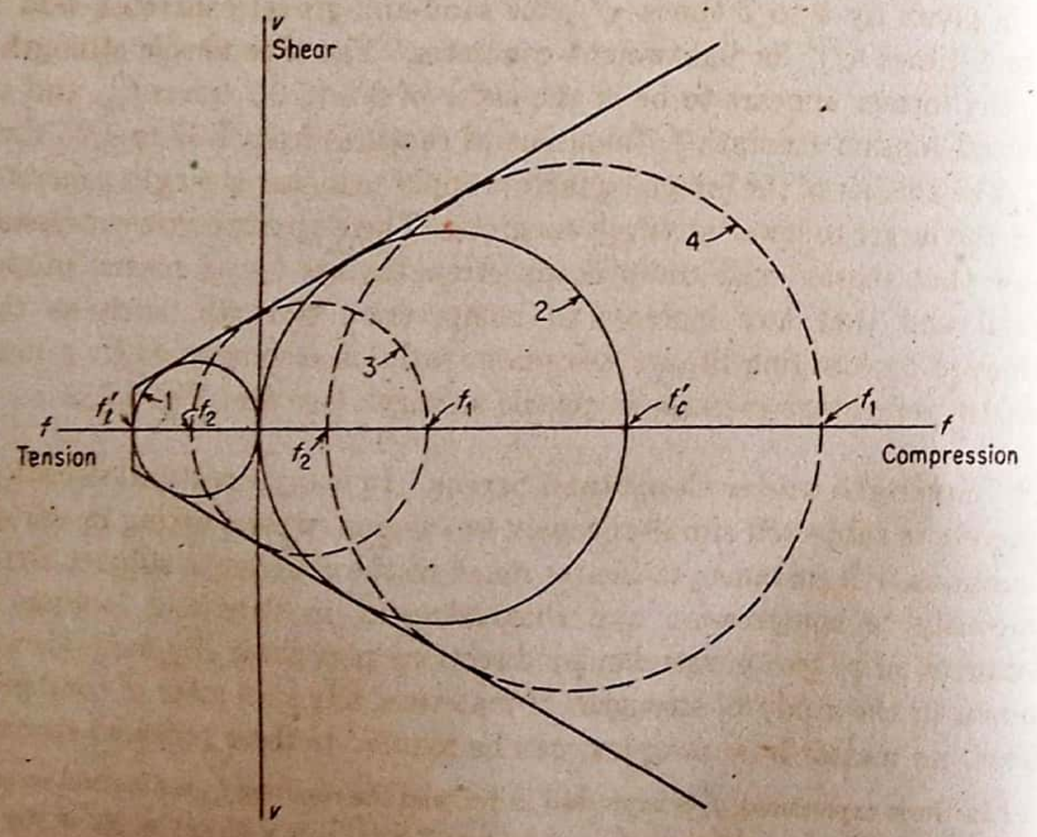


Fig. 1.7 Strength of concrete under combined stress. (*Schematically, according to Ref.* 1.17.)

Qualitatively, the effect of combined stress on strength is easily visualized from Fig. 1.7, which represents a modification of Mohr's strength theory (Ref. 1.16) proposed for concrete by Cowan (Ref. 1.17). In this presentation, circle 1 represents failure in simple tension at a stress f'_t, circle 2 failure in simple compression at a stress f'_c. The dashed circles show two states of combined stress. In circle 3 a principal tension stress f_2 acts at right angles to the principal compression stress f_1. It is seen that $f_1 < f'_c$; that is, when tension acts at right angles to compression, the compressive strength of concrete is reduced as compared to its strength f'_c in simple compression. In circle 4 a smaller principal compression stress f_2 acts at right angles to the larger principal compression stress f_1. It is seen that here $f_1 > f'_c$; that is, when compression acts at right angles to compression, the compressive strength of concrete is increased as compared to its strength f'_c in simple compression. Similar relations can be read off the figure for the strength of concrete in shear as it is affected by simultaneous compression or tension.

The fact that the strength of concrete under combined stress cannot yet be calculated rationally is one of the main reasons for continued reliance on tests. Because of this, the design of reinforced-concrete structures continues to be based on extensive experimental information rather than on consistent analytical theory, particularly in the many situations in which combined stresses occur.

1.10 Volume Changes; Shrinkage, Temperature The deformations discussed in Art. 1.7 were induced by stresses caused by external loads. Influences of a different nature cause concrete, even when free of any external loading, to undergo deformations and volume changes. The most important of these are shrinkage and the effects of temperature variations.

a. Shrinkage As was discussed in Arts. 1.2 and 1.4, any workable concrete mix contains more water than is needed for hydration. If the concrete is exposed to air, the larger part of this free water evaporates in time, the rate and completeness of drying depending on ambient temperature and humidity conditions. As the concrete dries, it shrinks in volume, probably due to the capillary tension which develops in the water remaining in the concrete. Conversely, if dry concrete is immersed in water, it expands, regaining much of the volume loss from prior shrinkage. Shrinkage, which continues at a decreasing rate for several months, depending on the configuration of the member, is a detrimental property of concrete in several respects. When not adequately controlled, it will cause unsightly and often deleterious cracks, particularly in slabs, walls, etc. In structures which are statically indeterminate (and most concrete structures are), it can cause large and harmful stresses. In prestressed concrete it leads to

Scanned with CamScanner

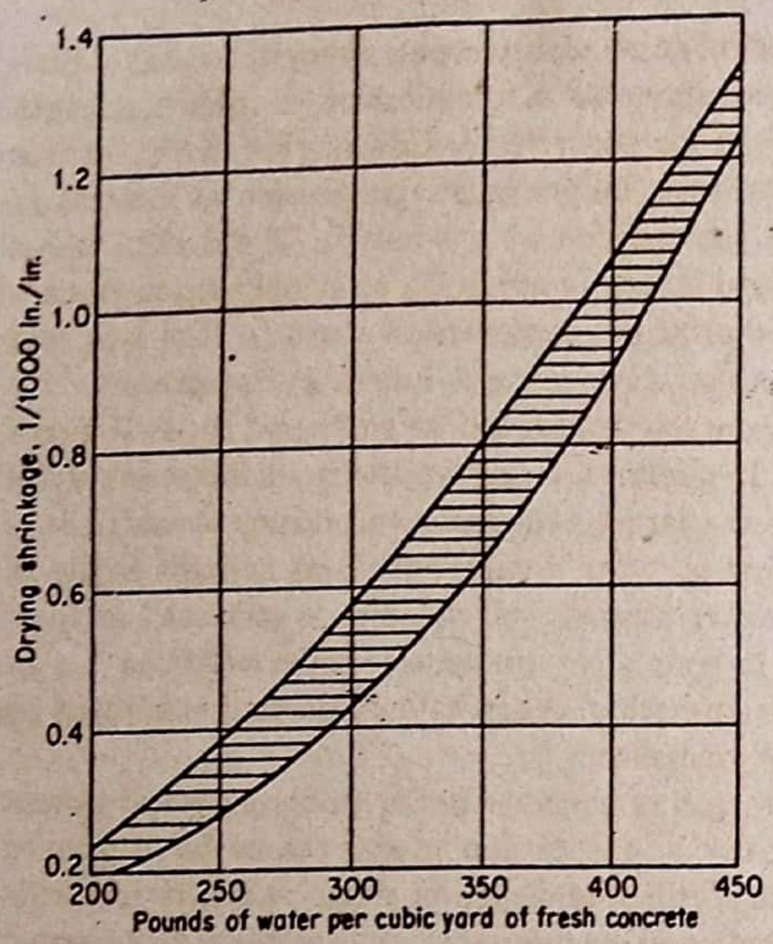


Fig. 1.8 Effect of water content on drying shrinkage. (*Adapted from Ref.* 1.4.)

partial loss of initial prestress. For these reasons it is essential that shrinkage be minimized and controlled.

As is clear from the nature of the process, the chief factor which determines the amount of final shrinkage is the unit water content of the fresh concrete. This is clearly illustrated in Fig. 1.8, which shows the amount of shrinkage in units of 0.001 in. per in. for varying amounts of mixing water. The same aggregates were used for all tests, but in addition to and independently of water content, the amount of cement was also varied, from 4 to 11 sacks per cubic yard of concrete. This very large variation of cement content had only very minor effects on the amount of shrinkage, as compared to the effect of water content; this is evident from the narrowness of the band which comprises the test results for the widely varying cement contents. It is evident from this that the chief means of reducing shrinkage is to reduce the water content of the fresh concrete to the minimum compatible with the required workability. In addition, prolonged and careful curing is beneficial for shrinkage control.

Values of final shrinkage for ordinary concretes are generally of the order of 0.0002 to 0.0007 in. per in., depending on initial water content, ambient temperature and humidity conditions, and the nature of the aggregate. Highly absorptive aggregates, such as some sandstones and slates, result in shrinkage values two and more times those obtained with less absorptive materials, such as granites and some limestones. Some lightweight aggregates, in view of their great porosity, easily result in much larger shrinkage values than ordinary concretes.

b. Temperature changes Like most other materials, concrete expands with increasing temperature and contracts with decreasing temperature. The effects of such volume changes are similar to those caused by shrinkage. That is, temperature contraction can lead to undue cracking, particularly when superposed on shrinkage; in indeterminate structures, deformations due to temperature changes can cause large and occasionally harmful stresses.

The coefficient of expansion varies somewhat, depending on type of aggregate and richness of mix. It is generally within the range of 0.000004 to 0.000006 in. per in. per °F. A value of 0.0000055 is generally accepted as satisfactory for calculating stresses and deformations caused by temperature changes.

1.11 Reinforcing Steels ***a. General*** As compared to concrete, steel is a high-strength material. The useful strength of ordinary reinforcing steels in tension as well as in compression, i.e., the yield strength, is of the order of 10 times the compression strength of common structural concrete, or of the order of 100 times its tensile strength. On the other hand, steel is a high-cost material as compared to concrete. It follows that the two materials are best used in combination if the concrete is made to resist the compression stresses, and the steel the tension stresses. Thus, in reinforced-concrete beams the concrete resists the compression force, longitudinal steel rods are located close to the tension face to resist the tension force, and frequently additional steel bars are so disposed that they resist the inclined tension stresses which are caused by the shear force in the webs of beams. However, reinforcement is also used for resisting compression forces, primarily where it is desired to reduce the cross-sectional dimensions of compression members, as in the lower-floor columns of multistory buildings. Even if no such necessity exists, a minimum amount of reinforcement is placed in all compression members to safeguard them against the effects of small accidental bending moments which might crack and even fail an unreinforced member.

For most effective reinforcing action, it is essential that steel and concrete deform together, i.e., that there be a sufficiently strong *bond* between the two materials so that no relative movements of the steel bars and the surrounding concrete occur. This bond is provided by the relatively large *chemical adhesion* which develops at the steel-concrete interface, by the *natural roughness* of the mill scale of hot-rolled reinforcing bars, and by the closely spaced rib-shaped *surface deformations* with which reinforcing bars are furnished in order to provide a high degree of interlocking of the two materials.

Scanned with CamScanner

Additional features which make for the satisfactory joint performance of steel and concrete are the following: (1) The *thermal expansion coefficients* of the two materials, about 0.0000065 for steel vs. an average of 0.0000055 for concrete, are sufficiently close to forestall cracking and other undesirable effects of differential thermal deformations. (2) While the *corrosion resistance* of bare steel is poor, the concrete which surrounds the steel reinforcement provides excellent corrosion protection, minimizing corrosion problems and corresponding maintainance costs. (3) The *fire resistance* of unprotected steel is impaired by its high thermal conductivity and by the fact that its strength decreases sizably at high temperatures. Conversely, the thermal conductivity of concrete is relatively low. Thus, damage caused by even prolonged fire exposure, if any, is generally limited to the outer layer of concrete, and a moderate amount of concrete cover provides sufficient thermal insulation for the embedded reinforcement.

b. Types of reinforcement The most common type of reinforcing steel in reinforced (as distinct from prestressed) concrete is in the form of round bars. They are available in a large range of diameters, from about ¼ in. to about 1⅜ in. for ordinary applications, and in two recently developed heavy bars of about 1¾ in. and 2¼ in. These bars, with the exception of the ¼-in. size, are furnished with surface deformations for the purpose of increasing the bond strength between steel and concrete. Minimum requirements for these deformations (spacing, projection, etc.) have been developed in lengthy experimental research and are specified in ASTM specification A305. Different bar producers use different patterns, all of which generally satisfy these requirements. Figure 1.9 shows a variety of current types of deformations (type 6 is no longer produced, since the spacing between its deformations exceeds the maximum specified value of 0.7 diam).

Bar sizes are designated by numbers, Nos. 2 through 11 being commonly used, and Nos. 14*S* and 18*S* representing the two special large-size bars previously mentioned. Designation by number, instead of by diameter, has been introduced because the surface deformations make it impossible to define a single easily measured value of the diameter. The numbers are so arranged that the unit in the number designation corresponds closely to ⅛ in. of diameter size. That is, a No. 5 bar has a nominal diameter of ⅝ in., and similarly for the other sizes. Table 1 of Appendix B gives areas, perimeters, and weights of standard bars. Tables 2 to 4 give similar information for groups of bars.

Apart from single reinforcing bars, two other types of reinforcement are in common use for reinforcing slabs and other surfaces, such as shells. One of these is *welded steel wire fabric*. This consists of a series of longitudinal and transverse cold-drawn steel wires at right angles to each other and welded together at all points of intersection. Size and spacing of wires may be the same in both directions or may be different, depending on

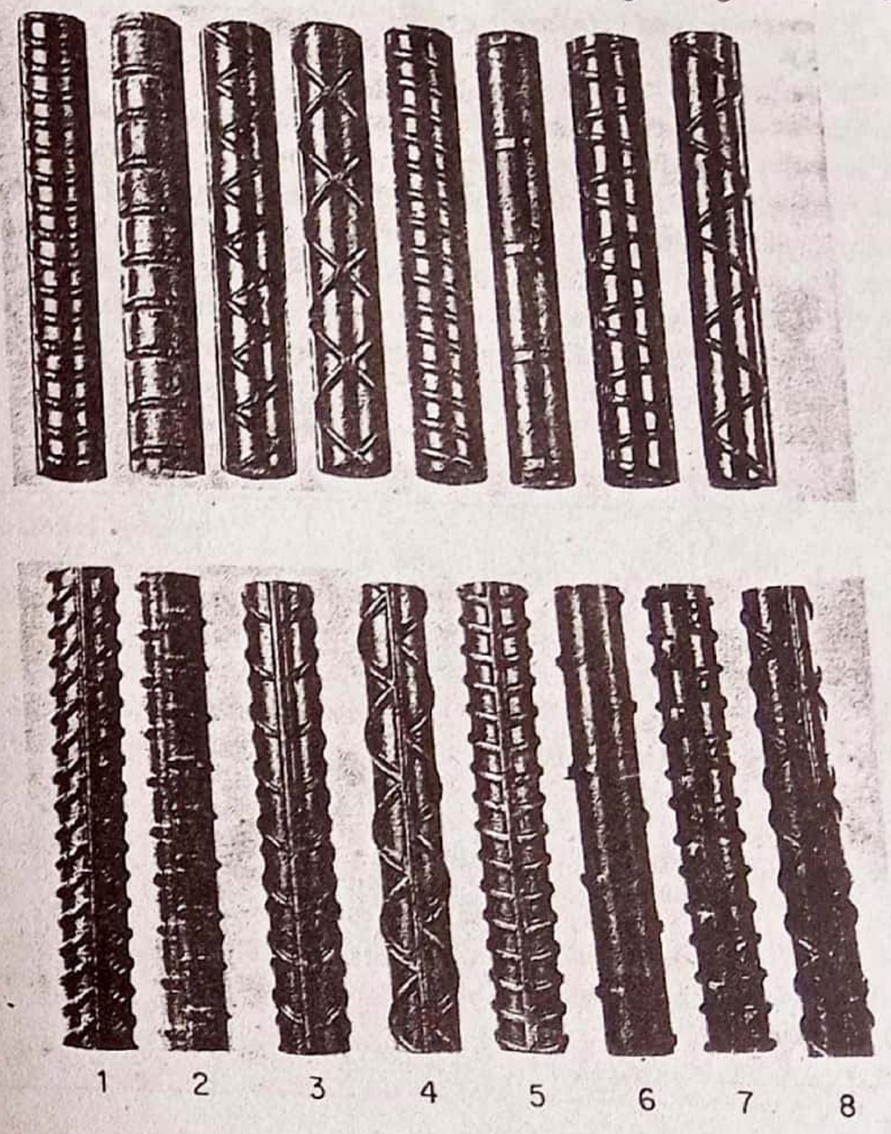


Fig. 1.9 Types of deformed bars.

the requirements of the design. Detailed data can be found in commercial catalogues. A somewhat similar type is known as *bar* or *rod mats*. In these, reinforcing bars or rods are used, instead of cold-drawn wire, to manufacture a grid of longitudinal and transverse bars, connected at their intersections either by welding or by clipping. For prestressed concrete, special forms and grades of reinforcement are used. The main types are *single prestressing wires*, with diameters ranging from 0.192 to 0.276 in., and *prestressing strands*. These are of the seven-wire type, having a center wire enclosed by six helically placed outer wires and ranging in nominal strand diameter from ¼ in. to ½ in. More details on prestressing steels will be found in Chap. 11.

c. Grades and strengths Before the advent of prestressed concrete, almost the only grades of steel which were used for reinforcing bars were low-carbon steels with specified minimum yield points of 33 to 40

Scanned with CamScanner

ksi and minimum tensile strengths of 55 to 70 ksi. Prestressing is most economical when reinforcement of very high strength is used; this brought into use the previously mentioned prestressing wires and strands, with yield strengths of 190 to 210 ksi and tensile strengths of 230 to 270 ksi. In very recent years, particularly with the advent of ultimate-strength design (see Chaps. 2 and 3), deformed reinforcing bars made of higher-strength carbon steels as well as of low-alloy steels have become available, with specified minimum yield points from 50 to 75 ksi and tensile strengths from 80 to 100 ksi.

***Table* 1.1 Standardized reinforcing steels**

Type	Grade	ASTM specification no.	Specified minimum	
			Yield point, ksi	Tensile strength, ksi
Billet or axle	Structural	A15 or A160	33	55
	Intermediate		40	70
	Hard		50	80
Rail	Regular	A16	50	80
	Hard		60	90
Billet	60-ksi yield	A432	60	90
Billet	High-strength	A431	75	100
Cold-drawn wire (e.g., for mesh)	.....	A82	64	80

At the time of writing of this edition, so-called *intermediate-grade* reinforcing steel with a specified yield point of 40 ksi is still the most prevalent, but it is being, and will increasingly be, displaced by reinforcing bars with 60 ksi yield point. The use of high-strength bars with 75 ksi yield point is so far limited by its higher cost and by the fact that, if used in flexural members, it requires special measures of deflection and concrete crack control; the latter is not yet completely understood and at this time is subject to intensive research relative to crack initiation and propagation. The higher-strength reinforcing bars are identified by the producers with rolled-in markings to prevent accidental substitution of the lower-strength intermediate-grade bars. Table 1.1 lists all presently available reinforcing steels (not including prestressing steels which are discussed in Chap. 11), their designations, the ASTM specifications which define their properties in detail, and their two main minimum specified strength values.

The large-size bars No. 14*S* and 18*S*, whose properties are specified in

ASTM A408, are available in the same three grades as the ASTM A15 steels.

d. Stress-strain curves The two chief numerical characteristics which determine the character of reinforcement are its yield point (generally identical in tension and in compression) and its *modulus of elasticity* E. The latter is practically the same for all reinforcing steels (but not for prestressing steels) and is taken as $E = 29{,}000{,}000$ psi.

In addition, however, the shape of the *stress-strain curve*, and particularly of its initial portion, has significant influence on the performance of reinforced-concrete members. Typical stress-strain curves of standardized American reinforcing steels are shown in Fig. 1.10. The curve for a low-alloy reinforcing steel with 90 ksi specified yield point, which at this writing is in the process of development, is also shown in that figure. The complete stress-strain curves are shown in the left part of the figure; the right part gives the initial portions of the curves magnified 10 times.

Low-carbon steels, typified by the 40-ksi curve, show an elastic portion followed by a "yield plateau," i.e., by a horizontal portion of the curve where strain continues to increase at constant stress. For such steels the yield point is that stress at which the yield plateau establishes itself. With further strain the stress begins to increase again, though at a slower rate, a process which is known as *strain-hardening*. The curve flattens out when the tensile strength is reached; it then turns down until fracture occurs. Higher-strength carbon steels, such as those with 60-ksi or 75-ksi yield points, either have a yield plateau of much shorter length or enter strain-hardening immediately without any continued yielding at constant stress. In the latter case the yield point is defined either by a residual strain of 0.2 per cent or by a total strain under load of 0.5 to 0.6 per cent,

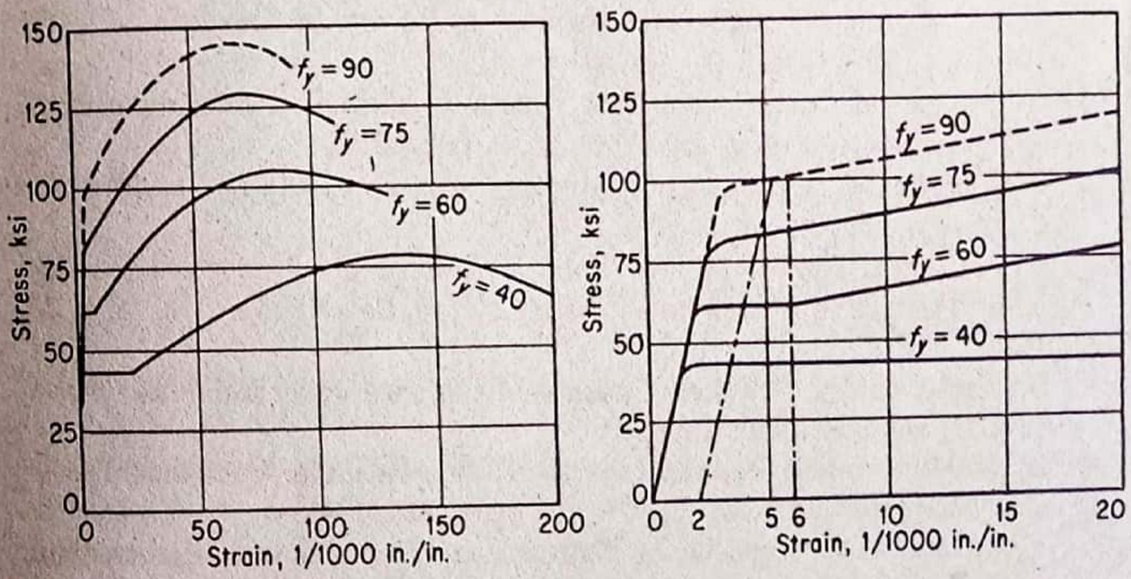


***Fig.* 1.10** Typical stress-strain curves for current reinforcing steels with minimum specified yield points f_y from 40 to 90 ksi.

Scanned with CamScanner

as shown. Low-alloy, high-strength steels, such as the one with $f_y = 90$ ksi, rarely show any yield plateau and usually enter strain-hardening immediately upon beginning to yield.

REFERENCES

1.1 "Selection and Use of Aggregates for Concrete," reported by ACI Committee 621, *J. ACI*, vol. 58, p. 515, 1961.

1.2 G. W. Washa: Properties of Lightweight Aggregates and Concretes, *J. ACI*, vol. 53, p. 375, 1956.

1.3 R. W. Kluge: Structural Lightweight Aggregates and Concretes, *J. ACI*, vol. 53, p. 383, 1956.

1.4 G. E. Troxell and H. E. Davis: "Composition and Properties of Concrete," McGraw-Hill Book Company, Inc., New York, 1956.

1.4*a* T. C. Hsu and F. O. Slate: Tensile Bond Strength between Aggregate and Cement Paste or Mortar, *J. ACI*, vol. 60, p. 465, 1963.

1.5 "Selecting Proportions for Concrete," ACI standard 613.

1.6 "Selecting Proportions for Structural Lightweight Concrete," ACI standard 613A.

1.7 "Consolidation of Concrete," reported by ACI Committee 609, *J. ACI*, vol. 57, p. 985, 1961.

1.8 "Measuring, Mixing and Placing of Concrete," ACI standard 614.

1.9 "Winter Concreting," ACI standard 604.

1.10 "Hot Weather Concreting," ACI standard 605.

1.11 "Selection and Use of Aggregates for Concrete," reported by ACI Committee 621, *J. ACI*, vol. 58, p. 513, 1961.

1.12 E. Hognestad, N. W. Hansson, and D. McHenry: Concrete Stress Distribution in Ultimate Strength Design, *J. ACI*, vol. 55, p. 455, 1955.

1.13 Hubert Rüsch: Research toward a General Flexural Theory for Structural Concrete, *J. ACI*, vol. 57, p. 1, 1960.

1.14 G. M. Nordby: Fatigue of Concrete—a Review of Research, *J. ACI*, vol. 55, p. 191, 1958.

1.15 Evaluation of Compression Test Results of Field Concrete, reported by ACI Committee 214, *J. ACI*, vol. 53, p. 561, 1957.

1.16 S. Timoshenko: "Strength of Materials," part II, 3d ed., D. Van Nostrand Company, Inc., Princeton, N.J., 1956.

1.17 H. J. Cowan: The Strength of Plain, Reinforced and Prestressed Concrete under the Action of Combined Stresses, *Mag. Concrete Res.*, vol. 5, p. 75, 1953.

1.18 B. Bresler and K. S. Pister: Strength of Concrete under Combined Stress, *J. ACI*, vol. 55, p. 321, 1958.

1.19 D. McHenry and J. Karni: Strength of Concrete under Combined Tensile and Compressive Stress, *J. ACI*, vol. 54, p. 829, 1958.

1.20 T. C. Hsu, F. O. Slate, G. M. Sturman, and Geo. Winter: Microcracking of Plain Concrete and the Shape of the Stress-Strain Curve, *J. ACI*, vol. 60, p. 209, 1963.

chapter 2

MECHANICS AND BEHAVIOR OF REINFORCED CONCRETE

2.1 Fundamentals The chief task of the structural engineer is the design of structures. By *design* is meant the determination of the general shape and all specific dimensions of a particular structure so that it will perform the function for which it is created and will safely withstand the influences which will act on it throughout its useful life. These influences are primarily the loads and other forces to which it will be subjected, as well as other detrimental agents, such as temperature fluctuations, foundation settlements, and corrosive influences. *Structural mechanics* is one of the main tools in this process of design. As here understood, it is the body of scientific knowledge which permits one to predict with a good degree of certainty how a structure of given shape and dimensions will

Scanned with CamScanner

behave when acted upon by known forces or other mechanical influences. The chief items of behavior which are of practical interest are (1) the strength of the structure, i.e., that magnitude of loads of a given distribution which will cause the structure to fail, and (2) the deformations, such as deflections and extent of cracking, which the structure will undergo when loaded under service conditions.

In the present chapter, the structural mechanics of reinforced-concrete members will be developed in general terms. Specific methods of design and analysis, based on the information provided by structural mechanics but frequently simplified and conventionalized to various degrees, will be taken up in subsequent chapters.

The fundamental propositions on which the mechanics of reinforced concrete is based are the following:

1. The internal forces, such as bending moments, shear forces, and normal and shear stresses, at any section of a member are in equilibrium with the effects of the external loads at that section. This proposition is not an assumption but a fact, because any body or any portion thereof can be at rest only if all forces acting on it are in equilibrium.

2. The strain in an embedded reinforcing bar (unit extension or compression) is the same as that of the surrounding concrete. Expressed differently, it is assumed that perfect bonding exists between concrete and steel at the interface, so that no slip can occur between the two materials. Hence, as the one deforms, so must the other. With modern deformed bars (see Art. 1.10) a high degree of mechanical interlocking is provided in addition to the natural surface adhesion, so that this assumption is very close to correct.

3. Cross sections which were plane prior to loading continue to be plane in the member under load. Accurate measurements have shown that when a reinforced-concrete member is loaded close to failure, this assumption is not accurate. However, the deviations are usually minor, and the results of theory based on this assumption check well with extensive test information.

4. In view of the fact that the tensile strength of concrete is only a small fraction of its compressive strength (see Art. 1.8), the concrete in that part of a member which is in tension is usually cracked. While these cracks, in well-designed members, are generally so narrow as to be hardly visible (they are known as *hairline* cracks), they evidently render the cracked concrete incapable of resisting tension stress. Correspondingly, it is assumed that concrete is not capable of resisting any tension stress whatever. This assumption is evidently a simplification of the actual situation because, in fact, concrete prior to cracking, as well as the concrete located between cracks, does resist tension stresses of small magnitude. Also, in discussions of the resistance of reinforced-concrete beams to

shear, it will become apparent that under certain conditions this particular assumption is dispensed with and advantage is taken of the modest tension strength which concrete can develop.

5. The theory is based on the actual stress-strain relationships and strength properties of the two constituent materials (see Arts. 1.7 and 1.10) or some reasonable simplifications thereof, rather than on some assumptions of ideal material behavior. This last feature is a relatively new development. It supplants a method of analysis which was based on the assumption that both concrete and steel behave in an elastic manner at all stress levels relevant in calculations. This latter assumption, while leading to relatively simple computational methods, is very far from true (see Figs. 1.3, 1.5, and 1.10). Correspondingly, the newer methods of analysis which recognize the departure from elasticity at the higher stress levels are in much closer agreement with the actual behavior of structures and with very extensive experimental information. At the same time the facts that nonelastic behavior is reflected in modern theory, that concrete is assumed to be ineffective in tension, and that the joint action of the two materials is taken into consideration result in analytical methods which are considerably more complex, but also more challenging, than those which are adequate for members made of a single, substantially elastic material.

These five assumptions permit one to predict by calculation the performance of reinforced-concrete members only for some simple situations. Actually, the joint action of two materials as dissimilar and complicated as concrete and steel is so complex that it has not yet lent itself to purely analytical treatment. For this reason, methods of design and analysis, while utilizing these assumptions, are very largely based on the results of extensive and continuing experimental research. They are modified and improved as additional test evidence becomes available.

2.2 Axial Compression In members which sustain chiefly or exclusively axial compression loads, such as building columns, it is economical to make the concrete carry most of the load. Still, some steel reinforcement is always provided for various reasons. For one, very few members are truly axially loaded; steel is essential for resisting any bending that may exist. For another, if part of the total load is carried by steel with its much greater strength, the cross-sectional dimensions of the member can be reduced, the more so the larger the amount of reinforcement.

The two chief forms of reinforced-concrete columns are shown in Fig. 2.1. In the square column, the four longitudinal bars serve as main reinforcement. They are held in place by transverse small-diameter steel ties which prevent displacement of the main bars during construction operations and counteract any tendency of the compression-loaded bars to

Scanned with CamScanner

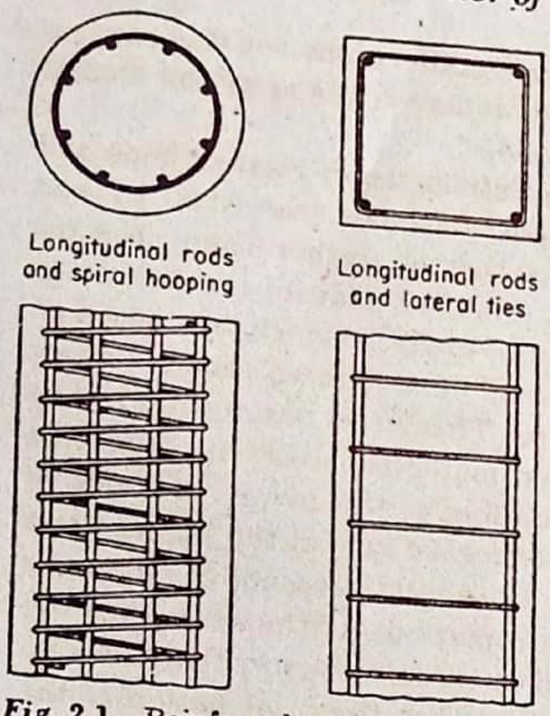


Fig. 2.1 Reinforced-concrete columns.

buckle out of the concrete by bursting the thin outer cover. On the left is shown a round column with eight main reinforcing bars. These are surrounded by a closely spaced spiral which serves the same purpose as the more widely spaced ties and acts to confine the concrete within it, thereby increasing its resistance to axial compression. The discussion which follows applies to tied columns.

When axial load is applied, the compression strain is the same over the entire cross section, and in view of the bonding between concrete and steel, is the same in the two materials (see propositions 2 and 3 of Art. 2.1). To illustrate the action of such a member as load is applied, Fig. 2.2 shows two typical stress-strain curves, one for a concrete with $f'_c = 3000$ psi (3 ksi) and the other for a steel with $f_s = 40{,}000$ psi (40 ksi). The curves for the two materials are drawn on the same graph using different vertical stress scales. Curve b has the shape which would be obtained in a concrete cylinder test. The rate of loading in most structures is considerably slower than that in a cylinder test, and this affects the shape of the curve (see Art. 1.7). Curve c, therefore, is drawn as being characteristic of the performance of concrete under slow or sustained loading. Under these conditions the maximum available compression strength of reinforced concrete is about $0.85f'_c$, as shown.

a. Elastic behavior (working stresses) At low stresses, up to about $f'_c/2$, the concrete is seen to behave nearly elastically, i.e., stresses and strains are quite closely proportional; the straight line d represents this range of behavior with little error for both rates of loading. For the given concrete the range extends to a strain of about 0.00045. The steel, on the other hand, is seen to be elastic nearly to its yield point of 40 ksi, or to the much greater strain of about 0.0013.

Because the compression strain in the concrete, at any given load, is equal to the compression strain in the steel,

$$\epsilon_c = \frac{f_c}{E_c} = \epsilon_s = \frac{f_s}{E_s}$$

from which the relation between the steel stress and the concrete stress is

obtained as

$$f_s = \frac{E_s}{E_c} f_c = nf_c \tag{2.1}$$

where $n = E_s/E_c$ is known as the *modular ratio*.

Let A_c = net area of concrete, i.e., gross area minus area occupied by reinforcing bars
A_g = gross area
A_s = area of reinforcing bars
P = axial load

Then

$$P = f_c A_c + f_s A_s = f_c A_c + nf_c A_s$$

or

$$P = f_c(A_c + nA_s) \tag{2.2}$$

The term $(A_c + nA_s)$ can be interpreted as the area of a fictitious concrete cross section, the so-called *transformed area* which, when sub-

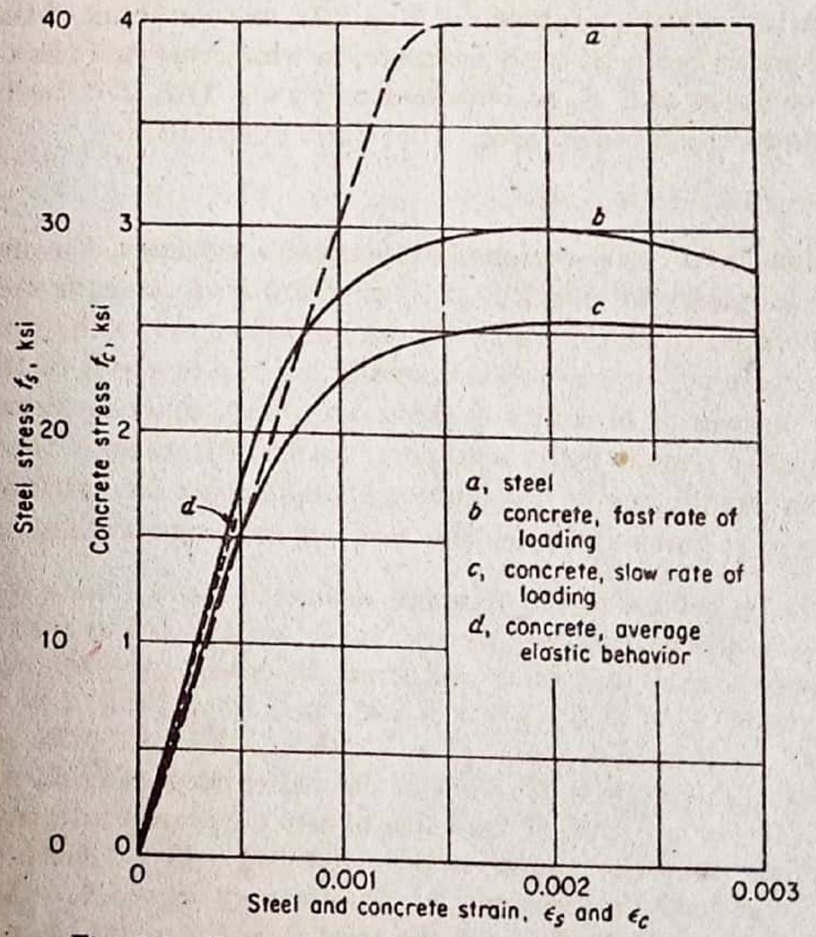


Fig. 2.2 Concrete and steel stress-strain curves.

Scanned with CamScanner

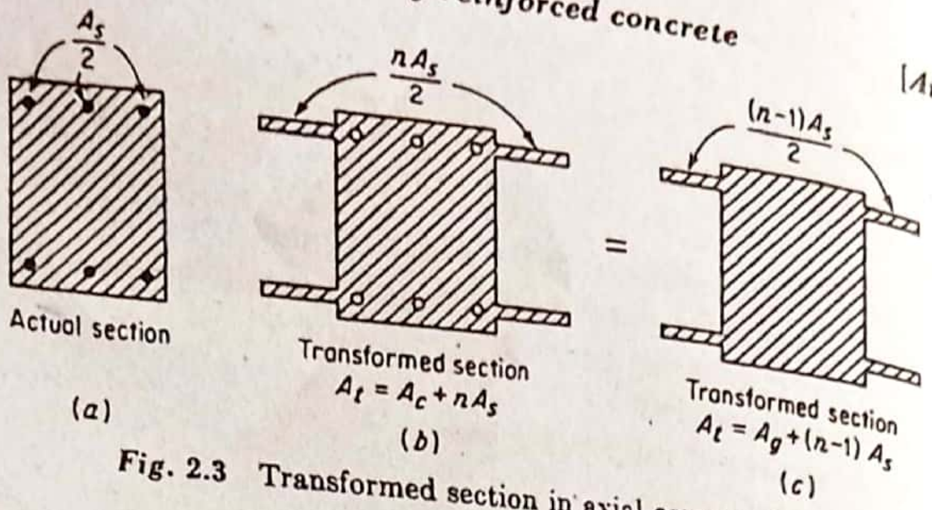


Fig. 2.3 Transformed section in axial compression.

jected to the particular concrete stress f_c, results in the same axial load P as the actual section composed of both steel and concrete. This transformed concrete area is seen to consist of the actual concrete area plus n times the area of the reinforcement. It can be visualized as shown in Fig. 2.3. That is, in Fig. 2.3*b* the three bars along each of the two faces are thought of as removed and replaced, at the same distance from the axis of the section, with added areas of fictitious concrete of total amount nA_s. Alternatively, as shown in Fig. 2.3*c*, one can think of the area of the steel bars as replaced with concrete, in which case one has to add to the gross concrete area A_g so obtained only $(n-1)A_s$ in order to obtain the same total transformed area. Therefore, alternatively,

$$P = f_c[A_g + (n-1)A_s] \tag{2.2a}$$

If load and cross-sectional dimensions are known, the concrete stress can be found by solving Eq. (2.2) or (2.2*a*) for f_c, and the steel stress can be calculated from Eq. (2.1). These relations hold in the range in which the concrete behaves nearly elastically, i.e., up to about 50 to 60 per cent of f'_c. For reasons of safety and serviceability, concrete stresses in structures under design loads are kept within this range. Therefore, these relations permit one to calculate *working stresses*, i.e., stresses which act in a member when it carries the working or design loading.

Example A column of the materials defined in Fig. 2.2 has a cross section of 16 × 20 in. and is reinforced by six No. 9 bars disposed as shown in Fig. 2.3. Determine the axial load which will stress the concrete to 1000 psi.

One finds $A_g = 16 \times 20 = 320$ in.^{2}, and, from Table 2 of Appendix B, $A_s = 6.00$ in. From Eq. (1.2), $E_c = 57{,}500\sqrt{3000} = 3{,}150{,}000$ psi, and $n = 29{,}000{,}000/3{,}150{,}000 = 9$. (In view of the scatter inherent in E_c, it is customary and satisfactory to round off the value of n to the nearest integer.) The load on the column, from Eq. (2.2*a*), is $P = 1000[320 + (9-1)6.00] = 368{,}000$ lb. Of this total load the concrete is seen to carry $P_c = f_cA_c = f_c(A_g - A_s) = 1000(320 - 6) = 314{,}000$ lb, and the steel $P_s = f_sA_s = (nf_c)A_s = 9000 \times 6 = 54{,}000$ lb, which is 14.7 per cent of the total axial load.

b. Inelastic range Inspection of Fig. 2.2 shows that the elastic relationships which have been utilized so far cannot be used beyond a strain of about 0.0005, for the given materials. To obtain information on the behavior of the member at larger strains and, correspondingly, at larger loads, it is therefore necessary to make direct use of the information of Fig. 2.2.

By way of example one may want to calculate the magnitude of the axial load which will produce a strain or unit shortening $\epsilon_c = \epsilon_s = 0.0010$ in the column of the previous example. At this strain the steel is seen to be still elastic, so that the steel stress $f_s = \epsilon_s E_s = 0.001 \times 29{,}000{,}000 = 29{,}000$ psi. The concrete is in the inelastic range, so that its stress cannot be directly calculated, but it can be read from the stress-strain curve for the given value of strain. (1) If the member has been loaded at a fast rate, curve *b* holds at the instant when the entire load is applied. The stress for $\epsilon = 0.001$ can be read as $f_c = 2660$ psi. Consequently, the total load can be obtained from

$$P = f_cA_c + f_sA_s \tag{2.3}$$

which evidently applies in the inelastic as well as in the elastic range. Hence, $P = 2660(320 - 6) + 29{,}000 \times 6 = 835{,}000 + 174{,}000 = 1{,}009{,}000$ lb. Of this total load, the steel is seen to carry 174,000 lb or 17.3 per cent. (2) For slowly applied or sustained loading, curve *c* represents the behavior of the concrete. Its stress at a strain of 0.001 can be read as $f_c = 2250$ psi. Then $P = 2250 \times 314 + 29{,}000 \times 6 = 707{,}000 + 174{,}000 = 881{,}000$ lb. Of this total load, the steel is seen to carry 19.7 per cent.

Comparison of the results for fast and slow loading show the following: Owing to creep of concrete, a given shortening of the column is produced by a smaller load when slowly applied or sustained over some length of time than when quickly applied. More important, the farther the stress is beyond the proportional limit of the concrete, and the more slowly the load is applied or the longer it is sustained, the smaller is the share of the total load carried by the concrete, and the larger that carried by the steel. In the sample column the steel was seen to carry 14.7 per cent of the load in the elastic range, 17.3 per cent for a strain of 0.001 under fast loading, and 19.7 per cent at the same strain under slow or sustained loading.

c. Ultimate strength The one quantity of chief interest to the structural designer is the *ultimate strength*, i.e., the maximum load which his structure or member will carry. Information on stresses, strains, and similar quantities serve chiefly as tools for determining carrying capacity. The performance of the column discussed so far indicates two things: First, in the range of large stresses and strains which precede attainment of ultimate strength and subsequent failure, elastic relationships cannot be utilized. Second, the member behaves differently under fast than under slow or sustained loading and shows less resistance to the latter than to

Scanned with CamScanner

the former. In usual construction, many types of loads, such as the weight of the structure and any permanent equipment housed therein, are sustained, and others are applied at slow rates. For this reason, to calculate a reliable magnitude of ultimate strength, curve *c* of Fig. 2.2 must be used as far as the concrete is concerned.

As for the steel, Fig. 1.10 shows that it reaches its ultimate strength (peak of the curve) at strains of the order of 0.10. However, as load is applied and increased, the compression strains in concrete and steel are the same at all times. Figure 2.2 shows that the maximum stress which the concrete can carry is reached at a strain of 0.002 to 0.003, much smaller than that strain which the steel could sustain by itself. Still larger strains cause the concrete to fail by crushing (cf., Fig. 1.3). Correspondingly, the largest strains to which the steel can be subjected prior to failure of the member are equal to those which the concrete can sustain before crushing, that is, 0.002 to 0.003. It is seen from Fig. 2.2 that the stress in the steel in this range of strains is its yield-point stress. For this reason the yield point is the maximum strength of reinforcement which can be utilized without prior failure of the concrete.

If the small transition curve just prior to yielding is disregarded, the steel strain at which the yield point is reached can be calculated from

$$\epsilon_y = \frac{f_y}{E_s} \tag{2.4}$$

where f_y is the yield point. In the example,

$$\epsilon_y = 40{,}000/29{,}000{,}000 = 0.0014$$

which can also be read from Fig. 2.2. At this strain, the stress in the concrete can be read from curve *c* as 2450 psi, and the load in the member is $P = 2450 \times 314 + 40{,}000 \times 6 = 1{,}010{,}000$ lb. However, curve *c* is seen to continue rising beyond this strain. Consequently, the load can be increased further until the ultimate strength of this concrete is reached at a strain of about 0.002. As was mentioned before, from many tests this maximum strength is assumed to be $0.85f'_c$, or $0.85 \times 3000 = 2550$ psi in the example. During this stage of loading, the steel merely yields at a constant stress, its yield stress, as can be seen from Fig. 2.2.

It is evident from this discussion that, if the yield strain [Eq. (2.4)] is smaller than the strain at which the concrete reaches its ultimate stress $0.85f'_c$, the steel will start yielding and will continue to do so until that strain is reached at which the concrete attains this stress and begins to fail. Correspondingly, the ultimate load[1] of the member is

$$P'_u = 0.85f'_cA_c + f_yA_s \tag{2.5}$$

[1] Throughout this book, quantities which refer to the ultimate strength of a member are primed and furnished with the subscript *u*, for example, P'_u. The prime is used to distinguish these quantities from those which the ACI Code prescribes for use in design. These ultimate design strengths are designated in the code by the subscript *u* without prime, for example, P_u. In order to ensure structural safety, the codified design values such as P_u are smaller than the actual ultimate-strength values, such as P'_u, by percentages which are specified in the code and explained in Chaps. 3 and 5.

Numerous careful tests have shown the reliability of Eq. (2.5) in predicting the ultimate strength of a concentrically loaded reinforced-concrete column, provided its slenderness ratio is small so that buckling will not reduce its strength (Ref. 2.1).

For the particular numerical example, $P'_u = 2550 \times 314 + 40{,}000 \times 6 = 800{,}000 + 240{,}000 = 1{,}040{,}000$ lb. At this stage the steel carries as much as 23 per cent of the load.

Summary In the elastic range of low stresses the steel carries a relatively small portion of the total load of an axially compressed member. As the ultimate strength is approached, there occurs a redistribution of the relative shares of the load resisted, respectively, by concrete and steel, the latter taking an increasing amount. The ultimate load at which the member is on the point of failure consists of the contribution of the steel when it is stressed to the yield point plus that of the concrete when its stress has attained the ultimate strength of $0.85f'_c$, as reflected in Eq. (2.5).

PROBLEM

The same 16 × 20 in. column as in the preceding examples is made of the same concrete and reinforced with the same six No. 9 bars, except that a steel with yield strength $f_y = 60$ ksi is used. The stress-strain diagram of this reinforcing steel is that shown in Fig. 1.10 for $f_y = 60$ ksi. For this column determine: (*a*) the axial load which will stress the concrete to 1000 psi; (*b*) the ultimate strength; (*c*) the share of the total load carried by the reinforcement at these two stages of loading. Compare results with those calculated in the preceding examples for $f_y = 40$ ksi, keeping in mind, in regard to relative economy, that the price per pound for reinforcing steels with 40 ksi and with 60 ksi yield points is about the same.

2.3 Axial Tension It was pointed out in Art. 1.8 that the tension strength of concrete is only a small fraction of its compressive strength. It follows that reinforced concrete is not well suited for use in tension members because the concrete will contribute little, if anything, to their strength. Still, there are situations in which reinforced concrete is stressed in tension, chiefly in tie rods in structures such as arches. Such members consist of one or more bars embedded in concrete in a symmetrical arrangement similar to compression members (cf. Figs. 2.1 and 2.3).

When the tension force in the member is sufficiently small so that the

stress in the concrete is considerably below its tensile strength, both steel and concrete behave elastically. In this situation all the expressions derived for compression in Art. 2.2*a* are identically valid for tension. In particular, Eq. (2.2) becomes

$$P = f_{ct}(A_c + nA_s) \tag{2.6}$$

where f_{ct} is the tensile stress in the concrete.

However, when the load is further increased, the concrete reaches its tensile strength at a stress and strain of the order of one-tenth of what it could sustain in compression. At this stage the concrete cracks across the entire cross section. When this happens, it ceases to resist any part of the applied tension force, since, evidently, no force can be transmitted across the air gap in the crack. At any load larger than that which caused the concrete to crack, the steel is called upon to resist the entire tension force. Correspondingly, at this stage

$$P = f_s A_s \tag{2.7}$$

With further increased load, the tensile stress f_s in the steel reaches the yield point f_y. When this occurs, the tension members cease to exhibit small, elastic deformations but, instead, stretch a sizable and permanent amount at substantially constant load. This does not impair the strength of the member. Its elongation, however, becomes so large (of the order of 1 per cent or more of its length) as to render it useless. Therefore, the maximum useful strength P'_{ut} of a tension member is that force which will just cause the steel stress to reach the yield point. That is,

$$P'_{ut} = f_y A_s \tag{2.8}$$

To provide adequate safety, the force permitted in a tension member under normal service loads should be of the order of $\frac{1}{2}P'_{ut}$. Because the concrete has cracked at loads considerably smaller than this, it does not contribute to the carrying capacity of the member in service. It does serve, however, as a fire and corrosion proofing and often improves the appearance of the structure.

There are situations, though, in which reinforced concrete is used in axial tension under conditions in which the occurrence of tension cracks must be prevented. A case in point is a circular tank (see Fig. 1.1*i*). To provide watertightness, the hoop tension caused by the fluid pressure must be prevented from causing the concrete to crack. In this case, Eq. (2.6) can be used to determine a safe value for the axial tension force P by using, for the concrete tension stress f_{ct}, an appropriate fraction of the tensile strength of the concrete, i.e., of that stress which would cause the concrete to crack.

PROBLEM

A reinforced-concrete water pipe has an inside diameter of 5 ft 0 in. and a wall thickness of 3½ in. The circumferential hoop reinforcement consists of No. 4 bars at 3 in. distance, center to center; the bars are located midway between inside and outside surfaces. The concrete has a compression strength $f'_c = 5000$ psi and a split cylinder strength $f'_{sp} = 450$ psi, for the reinforcement $f_y = 40{,}000$ psi. Determine: (*a*) the allowable water pressure such that there is a safety factor of 1.5 against leakage caused by tension cracks; (*b*) for this allowable water pressure, determine the safety factor against failure of the pipe. *Hint:* To expedite calculations, analyze a 1-ft length of pipe and make use of Tables 2 or 4 of Appendix B. Regarding tension strength of concrete, see Art. 1.8.

2.4 Bending ***a. Bending of homogeneous beams*** Reinforced-concrete beams are nonhomogeneous in that they are made of two entirely different materials. The methods used in the analysis of reinforced-concrete beams are therefore different from those used in the design or investigation of beams composed entirely of steel, wood, or any other structural material. The fundamental principles involved are, however, essentially the same as those relating to homogeneous beams. Briefly, these principles are as follows:

At any cross section there exist internal forces which may be resolved into components normal and tangential to the section. Those components which are normal to the section are the *bending* stresses (tension on one side of the neutral axis and compression on the other). Their function is to resist the bending moment at the section. The tangential components are known as the *shear* stresses, and they resist the transverse or shear forces.

FUNDAMENTAL ASSUMPTIONS

1. A cross section which was plane before loading remains plane under load. This means that the unit strains in a beam, above and below the neutral axis, are proportional to the distance from that axis.

2. The bending stress f at any point depends on the strain at that point in a manner given by the stress-strain diagram of the material. If the beam is made of a homogeneous material whose stress-strain diagram in tension and compression is that of Fig. 2.4*a*, the following holds: If the maximum strain at the outer fibers is smaller than the strain ϵ_p up to which stress and strain are proportional for the given material, then the compression and tension stresses on either side of the axis are proportional to the distance from the axis, as shown in Fig. 2.4*b*. However, if the maximum strain at the outer fibers is larger than ϵ_p, this is no longer true. The situation which then obtains is shown in Fig. 2.4*c*; that is, in the outer portions of the beam, where $\epsilon > \epsilon_p$, stresses and strains are no longer proportional. In these regions the magnitude of stress at any level, such as f_2

Scanned with CamScanner

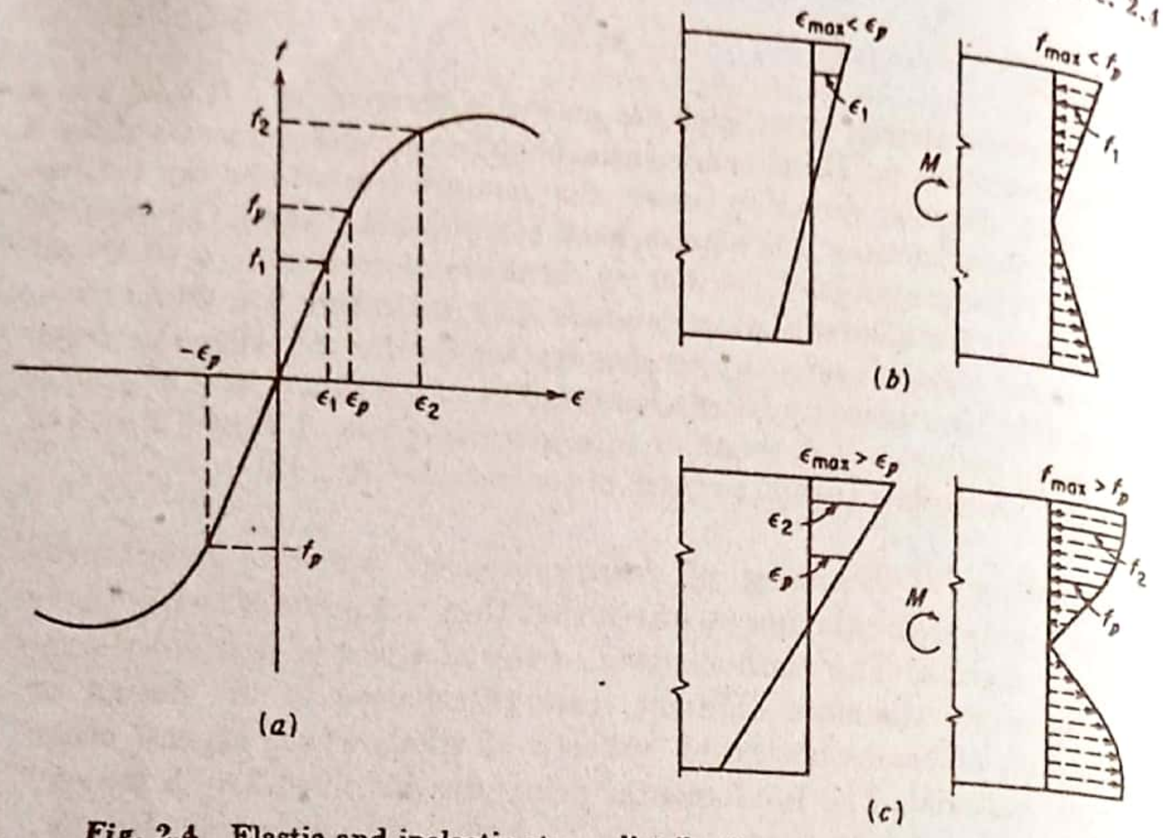


Fig. 2.4 Elastic and inelastic stress distributions in homogeneous beam.

in Fig. 2.4*c*, depends on the strain ϵ_2 at that level in the manner given by the stress-strain diagram of the material. In other words, for a given strain in the beam, the stress at a point is the same as that given by the stress-strain diagram.

3. The distribution of the shear stresses v over the depth of the section depends on the shape of the cross section and of the stress-strain diagram. These shear stresses are largest at the neutral axis and equal to zero at the outer fibers. The shear stresses on horizontal and vertical planes through any point are equal.

4. Owing to the combined action of shear stresses (horizontal and vertical) and flexure stresses, at any point in a beam there are inclined stresses of tension and compression, the largest of which form an angle of 90° with each other. The intensity of the inclined maximum or principal stress at any point is given by the equation

$$t = \frac{f}{2} \pm \sqrt{\frac{f^2}{4} + v^2} \tag{2.9}$$

where f = intensity of normal fiber stress
v = intensity of tangential shearing stress
The inclined stress makes an angle α with the horizontal such that $\tan 2\alpha = 2v/f$.

5. Since the horizontal and vertical shearing stresses are equal and

the flexural stresses are zero at the neutral plane, the inclined tensile and compressive stresses at any point in that plane form an angle of 45° with the horizontal, the intensity of each being equal to the unit shear at the point.

6. When the stresses in the outer fibers are smaller than the proportional limit f_p, the beam behaves *elastically* as shown in Fig. 2.4*b*. In this case the following obtains:

a. The neutral axis passes through the center of gravity of the cross section.

b. The intensity of bending stress normal to the section increases directly with the distance from the neutral axis and is a maximum at the extreme fibers. The stress at any given point in the cross section is represented by the equation

$$f = \frac{My}{I} \tag{2.10}$$

where f = bending stress at a distance y from neutral axis
M = external bending moment at section
I = moment of inertia of cross section about neutral axis
The maximum bending stress occurs at the outer fibers and is equal to

$$f_{max} = \frac{Mc}{I} = \frac{M}{S} \tag{2.11}$$

where c = distance from neutral axis to outer fiber
$S = I/c$ = section modulus of cross section

c. The shear stress (longitudinal equals transverse) v at any point in the cross section is given by

$$v = \frac{VQ}{Ib} \tag{2.12}$$

where V = total shear at section
Q = statical moment about neutral axis of that portion of cross section lying between a line through point in question parallel to neutral axis and nearest face (upper or lower) of beam
I = moment of inertia of cross section about neutral axis
b = width of beam at given point

d. The intensity of shear along a vertical cross section in a rectangular beam varies as the ordinates of a parabola, the intensity being zero at the top and bottom of the beam and a maximum at the neutral axis. The maximum is $\frac{3}{2}V/ba$, since at the neutral axis $Q = ba^2/8$ and $I = ba^3/12$ in Eq. (2.12).

Scanned with CamScanner

The remainder of this article deals only with bending stresses and their effects on reinforced-concrete beams. Shear stresses and their effects are discussed separately in Art. 2.5.

b. Reinforced-concrete beams: behavior under load Plain concrete beams are inefficient as flexural members because the tension strength in bending (modulus of rupture, see Art. 1.8 and Fig. 1.2) is a small fraction of the compression strength. In consequence, such beams fail on the tension side at low loads, long before the strength of the concrete on the compression side has been fully utilized. For this reason, steel reinforcing bars are placed on the tension side as close to the extreme tension fiber as is compatible with proper fire and corrosion protection of the steel. In such a reinforced-concrete beam the tension which is caused by the bending moments is chiefly resisted by the steel reinforcement, while the concrete alone is usually capable of resisting the corresponding compression. Such joint action of the two materials is assured if relative slip is prevented. This is achieved by using deformed bars with their high bond strength at the steel-concrete interface (see Art. 1.11) and, if necessary, by special anchorage of the ends of the bars. A simple example of such a beam, with the customary designations for the cross-sectional dimensions, is shown in Fig. 2.5. For the sake of simplicity the discussion which follows will deal with beams of rectangular cross section, even though members of other shapes are very common in most concrete structures.

When the load on such a beam is gradually increased from zero to that magnitude which will cause the beam to fail, several different stages of behavior can be clearly distinguished. At low loads, as long as the maximum tension stress in the concrete is smaller than the modulus of rupture, the entire concrete is effective in resisting stress, in compression on one side and in tension on the other side of the neutral axis. In addition, the reinforcement, deforming the same amount as the adjacent concrete, is also subject to tension stresses. At this stage all stresses in the concrete are of small magnitude and are proportional to strains. The distribution of strains and stresses in concrete and steel over the depth of the section is as shown in Fig. 2.5*c*.

When the load is further increased, the tension strength of the concrete is soon reached, and at this stage tension cracks develop. These propagate quickly upward to or close to the level of the neutral plane, which, in turn, shifts upward with progressive cracking. The general shape and distribution of these tension cracks is shown in Fig. 2.5*d*. In well-designed beams the width of these cracks is sufficiently small (hairline cracks) so that they are not objectionable either from the viewpoint of corrosion protection or from that of appearance. Their presence, however, affects profoundly the behavior of the beam under load. Evidently, in a cracked

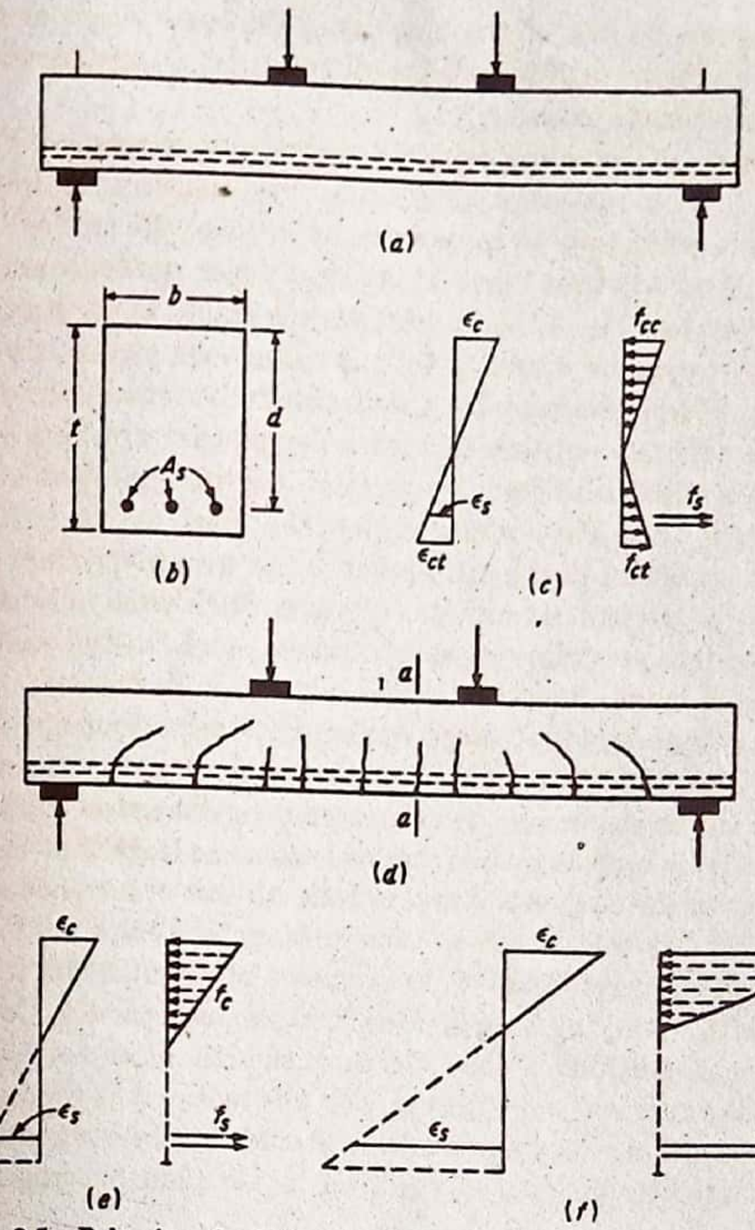


Fig. 2.5 Behavior of reinforced-concrete beam under increasing load.

section, i.e., in a cross section located at a crack such as *a-a* in Fig. 2.5*d*, the concrete does not transmit any tension stresses. Hence, just as in tension members (Art. 2.3), it is the steel which is called upon to resist the entire tension. At moderate loads, if the concrete stresses do not exceed approximately $f'_c/2$, stresses and strains continue to be closely proportional (see Fig. 2.2). The distribution of strains and stresses at or near a cracked section is then that shown in Fig. 2.5*e*. When the load is still further increased, stresses and strains rise correspondingly and are no longer proportional. The ensuing nonlinear relation between stresses and strains is that given by the concrete stress-strain curve. Therefore, just as in homogeneous beams (see Fig. 2.4), the distribution of concrete stresses

Scanned with CamScanner

on the compression side of the beam is of the same shape as the stress-strain curve. Figure 2.5*f* shows the distribution of strains and stresses close to the ultimate load.

Eventually, the carrying capacity of the beam is reached. Failure can be caused in one of two ways. When relatively moderate amounts of reinforcement are employed, at some value of the load the steel will reach its yield point. At that stress the reinforcement yields suddenly and stretches a large amount (see Fig. 1.10), and the tension cracks in the concrete widen visibly and propagate upward, with simultaneous significant deflection of the beam. When this happens, the strains in the remaining compression zone of the concrete increase to such a degree that crushing of the concrete, the so-called *secondary compression failure*, ensues at a load only slightly larger than that which caused the steel to yield. Effectively, therefore, attainment of the yield point in the steel determines the carrying capacity of moderately reinforced beams. Such yield failure is gradual and is preceded by visible signs of distress, such as the widening and lengthening of cracks and the marked increase in deflection.

On the other hand, if large amounts of reinforcement or normal amounts of steel of very high strength are employed, the compression strength of the concrete may be exhausted before the steel starts yielding. Concrete fails by crushing when strains become so large that they disrupt the integrity of the concrete. Exact criteria for this occurrence are not yet known, but it has been observed that rectangular beams fail in compression when the concrete strains reach values of about 0.003 to 0.004 for concretes with f'_c varying from 5000 to 2000 psi, respectively. Compression failure through crushing of the concrete is sudden, of an almost explosive nature, and occurs without warning. For this reason it is good practice to dimension beams in such a manner that, should they be overloaded, failure will be initiated by yielding of the steel rather than by crushing of the concrete.

The analysis of stresses and strength in the different stages just described will be discussed in the next several sections.

c. Stresses elastic, section uncracked As long as the tensile stress in the concrete is smaller than the modulus of rupture so that no tension cracks develop, the strain and stress distribution as shown in Fig. 2.5*c* is essentially the same as in an elastic, homogeneous beam (Fig. 2.4*b*).

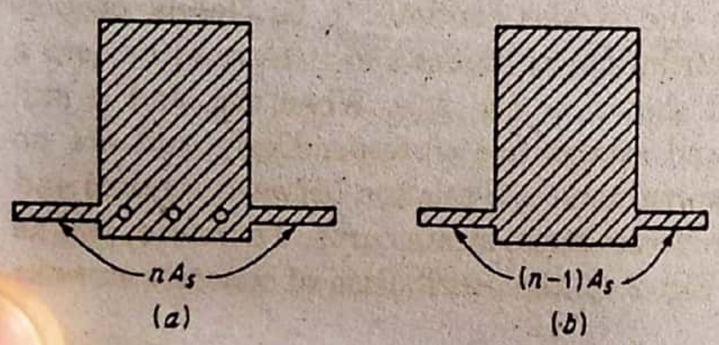


Fig. 2.6 Uncracked transformed section.

The only difference is the presence of another material, the steel reinforcement. As was shown in Art. 2.2*a*, in the elastic range, for any given value of strain, the stress in the steel is n times that of the concrete [Eq. (2.1)]. In the same article it was shown that one can take account of this fact in calculations by replacing the actual steel-and-concrete cross section with a fictitious section thought of as consisting of concrete only. In this "transformed section" the actual area of the reinforcement is replaced with an equivalent concrete area equal to nA_s located at the level of the steel. The transformed, uncracked section pertaining to the beam of Fig. 2.5*b* is shown in Fig. 2.6.

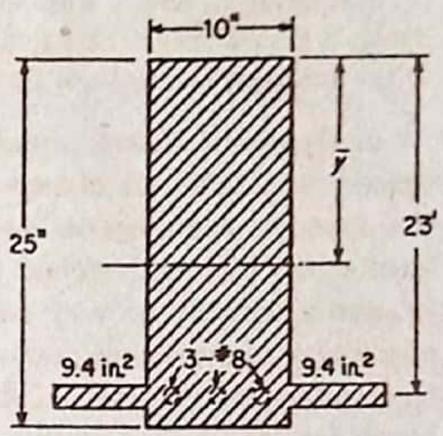


Fig. 2.7

Once the transformed section has been obtained, the usual methods of analysis of elastic homogeneous beams apply. That is, the section properties (location of neutral axis, moment of inertia, section modulus, etc.) are calculated in the usual manner, and, in particular, stresses are computed with Eqs. (2.10) to (2.12).

Example A rectangular beam has the dimensions (see Fig. 2.5*b*) $b = 10$ in., $t = 25$ in., and $d = 23$ in. and is reinforced with three No. 8 bars so that $A_s = 2.35$ in.^{2} The concrete cylinder strength f'_c is 3000 psi, and the tensile strength in bending (modulus of rupture) is 450 psi. The yield point of the steel f_y is 40,000 psi, the stress-strain curves of the materials being those of Fig. 2.2. Determine the stresses caused by a bending moment $M = 40$ ft-kips.

With a value $n = E_s/E_c = 9$ (see the example of Art. 2.2*a*), one has to add to the rectangular outline an area $(n-1)A_s = 8 \times 2.35 = 18.8$ in.^{2}, disposed as shown on Fig. 2.7, in order to obtain the uncracked, transformed section. Conventional calculations show that the location of the neutral axis of this section is given by $\bar{y} = 13.3$ in., and its moment of inertia about this axis is 15,030 in.^{4} For $M = 40$ ft-kips $= 480{,}000$ in-lb, the concrete compression stress at the top fiber is, from Eq. (2.11),

$$f_{ct} = 480{,}000 \times 13.3/15{,}030 = 425 \text{ psi}$$

and, similarly, the concrete tension stress at the bottom fiber is

$$f_{ct} = 480{,}000 \times 11.7/15{,}030 = 374 \text{ psi}$$

Since this value is substantially below the given tensile bending strength of the concrete, 450 psi, no tension cracks will form, and calculation by the uncracked, transformed section is justified. The stress in the steel, from Eqs. (2.1) and (2.10), is

$$f_s = n\frac{My}{I} = 9(480{,}000 \times 9.7/15{,}030) = 2890 \text{ psi}$$

Scanned with CamScanner

By comparing f_c and f_s with the cylinder strength and the yield point, respectively, it is seen that at this stage the actual stresses are quite small as compared to the available strengths of the two materials.

d. Stresses elastic, section cracked When the tension stress f_c exceeds the modulus of rupture, cracks form as shown in Fig. 2.5*d*. If the concrete compression stress is less than approximately $\frac{1}{2}f'_c$ and the steel stress has not reached the yield point, both materials continue to behave elastically or very nearly so. This situation generally obtains in structures under normal service conditions and loads, since at these loads the stresses are generally of the order of magnitude just discussed. At this stage, for simplicity and with little if any error, it is assumed that tension cracks have progressed all the way to the neutral axis, and that sections plane before bending are plane in the bent member. The situation in regard to strain and stress distribution is then that shown in Fig. 2.5*e*.

To compute stresses, and strains if desired, the device of the transformed section can still be used. One need only take account of the fact that all the concrete which is stressed in tension is assumed cracked and, therefore, effectively absent. As shown in Fig. 2.8*a*, the transformed section then consists of the concrete in compression on one side of the axis, and n times the steel area on the other. The distance to the neutral axis, in this stage, is conventionally expressed as a fraction kd of the effective depth d. (Once the concrete is cracked, any material located below the steel is ineffective, which is why d is the effective depth of the beam.) To determine the location of the neutral axis, the moment of the tension area about the axis is set equal to the moment of the compression area, which gives

$$b\frac{(kd)^2}{2} - nA_s(d - kd) = 0 \tag{2.13}$$

Having obtained kd by solving this quadratic equation, one can determine the moment of inertia and other properties of the transformed sec-

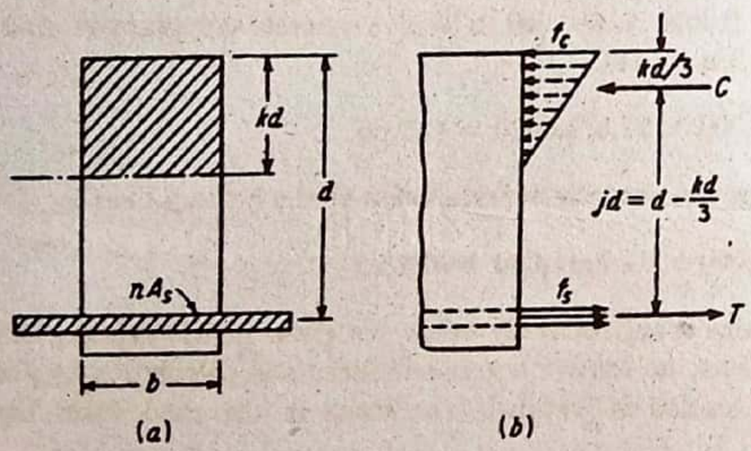


Fig. 2.8 Cracked transformed section.

tion as in the preceding case. Alternatively, one can proceed from basic principles by accounting directly for the forces which act in the cross section. These are shown in Fig. 2.8*b*. The concrete stress, with maximum value f_c at the outer edge, is distributed linearly as shown. The entire steel area A_s is subject to the stress f_s. Correspondingly, the total compression force C and the total tension force T are

$$C = \frac{bkd}{2}f_c \quad \text{and} \quad T = A_s f_s \tag{2.14}$$

The requirement that these two forces must be equal numerically has been taken care of by the manner in which the location of the neutral axis has been determined.

Equilibrium requires that the couple constituted by the two forces C and T be equal numerically to the external bending moment M. Hence, taking moments about C,

$$M = Tjd = A_s f_s jd \tag{2.15}$$

from which the steel stress is

$$f_s = \frac{M}{A_s jd} \tag{2.16}$$

Conversely, taking moments about T,

$$M = Cjd = \frac{bkd}{2}f_c jd = \frac{bd^2}{2}kjf_c \tag{2.17}$$

from which the concrete stress is

$$f_c = \frac{M}{\frac{1}{2}bd^2kj} \tag{2.18}$$

From Fig. 2.8*b* it is seen that $jd = d - kd/3$, or

$$j = 1 - \frac{k}{3} \tag{2.19}$$

Example The beam of the preceding example is subject to a bending moment $M = 80$ ft-kips (rather than 40 ft-kips as previously). Calculate the relevant properties and stresses.

If the section were to remain uncracked, the tension stress in the concrete would now be twice its previous value, that is, 748 ksi. Since this exceeds by far the modulus of rupture of the given concrete (450 psi), cracks will have formed, and the analysis must be adapted appropriately. Equation (2.13), with the known quantities b, n, and A_s inserted, gives the distance to the neutral axis $kd = 7.97$ in., or $k = 7.97/23 = 0.347$. From Eq. (2.19), $j = 1 - 0.347/3 = 0.885$.

Scanned with CamScanner

With these values the steel stress is obtained from Eq. (2.16) as $f_s = 20{,}100$ psi, and the maximum concrete stress from Eq. (2.18) as $f_c = 1175$ psi.

Comparing the results with the pertinent values for the same beam when subject to one-half the moment, as previously calculated, one notices: (1) The neutral plane has migrated upward so that its distance from the top fiber has changed from 13.3 in. to 7.97 in.; (2) even though the bending moment has only been doubled, the steel stress has increased from 2890 psi to 20,100 psi, or about 7 times, and the concrete compression stress has increased from 425 psi to 1175 psi, or 2.7 times; (3) the moment of inertia of the cracked transformed section is easily computed to be 6730 in.^{4}, as compared to 15,030 in.^{4} for the uncracked section. This affects the magnitude of the deflection, as discussed in Art. 2.7. Thus it is seen how radical is the influence of the formation of tension cracks on the behavior of reinforced-concrete beams.

e. Ultimate strength, general analysis It is of interest in structural practice to calculate those stresses and deformations which occur in a structure in service under design load. For reinforced-concrete beams this can be done by the methods just presented, which assume elastic behavior of both materials. It is equally if not more important that the structural engineer be able to predict with satisfactory accuracy the ultimate strength of his structure or structural member. By making this strength larger by an appropriate amount than the largest loads which can be expected during the lifetime of the structure, an adequate margin of safety is assured. Until recent times, methods based on elastic analysis, such as those just presented or variations thereof, have been used for this purpose. It is clear, however, that at or near the ultimate load stresses are no longer proportional to strains. In regard to axial compression this has been discussed in detail in Art. 2.2, and in regard to bending it has been pointed out that at high loads, close to the ultimate, the distribution of stresses and strains is that of Fig. 2.5*f* rather than the elastic distribution of Fig. 2.5*e*. More realistic methods of analysis, based on actual inelastic rather than assumed elastic behavior of the materials and on results of extremely extensive experimental research, have been developed in recent years to predict the ultimate strength. They are used increasingly in structural-design practice.

If the distribution of concrete compression stresses at or near ultimate load (Fig. 2.5*f*) had a well-defined and invariable shape—parabolic, trapezoidal, or otherwise—it would be possible to derive a completely rational theory of ultimate bending strength, just as the theory of elastic bending with its known triangular shape of stress distribution (Figs. 2.4*b* and 2.5*c* and *e*) is straightforward and rational. Actually, inspection of Figs. 1.3 and 2.2, and of many more concrete stress-strain curves which have been published, shows that the geometrical shape of the stress distribution is quite varied and depends on a number of factors, such as the

cylinder strength and the rate and duration of loading. For this and other reasons, a wholly rational flexural theory for reinforced concrete has not yet been developed (Refs. 2.2, 2.3). Present methods of analysis, therefore, are based in part on known laws of mechanics, supplemented, where needed, by extensive test information.

Let Fig. 2.9 represent the distribution of internal stresses and strains when the beam is about to fail. One desires a method to calculate that moment M'_u (ultimate moment) at which the beam will fail either by tension yielding of the steel or by crushing of the concrete in the outer compression fiber. For the first mode of failure the criterion is that the steel stress equal the yield point, $f_s = f_y$. It has been mentioned before that an exact criterion for concrete compression failure is not yet known but that for rectangular beams strains of 0.003 to 0.004 in. per in. have been measured immediately preceding failure. If one assumes, slightly conservatively, that the concrete is about to crush when the maximum strain reaches 0.003, then comparison with a great many tests of beams and columns of a considerable variety of shapes and conditions of loading shows that a satisfactorily accurate and safe prediction of ultimate strength can be made (Ref. 2.4). In addition to these two criteria (yielding of the steel at a stress of f_y and crushing of the concrete at a strain of 0.003), it is not really necessary to know the exact shape of the concrete stress distribution in Fig. 2.9. What is necessary is to know, for a given distance c of the neutral axis, (1) the total resultant compression force C in the concrete and (2) its vertical location, i.e., its distance from the outer compression fiber.

In a rectangular beam the area which is in compression is bc, and the total compression force on this area can be expressed as $C = f_{av}bc$, where f_{av} is the average compression stress on the area bc. Evidently, the average compression stress which can be developed before failure occurs becomes larger the higher the cylinder strength f'_c of the particular con-

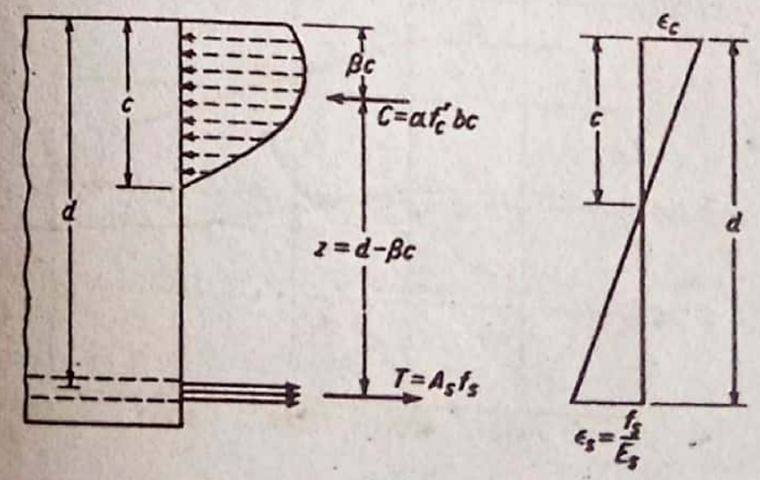


Fig. 2.9 Stress distribution at ultimate load.

Scanned with CamScanner

crete. Let

$$\alpha = \frac{f_{av}}{f'_c}$$

Then

$$C = \alpha f'_c bc \tag{2.20}$$

For a given distance c to the neutral axis, the location of C can be defined as some fraction β of this distance. Thus, as indicated in Fig. 2.9, for a concrete of given strength it is only necessary to know α and β in order to define completely the effect of the concrete compression stresses.

Extensive direct measurements, as well as indirect evaluation of numerous beam tests, have shown that the following values for α and β are satisfactorily accurate (see Ref. 2.4, where α is designated as k_1k_3, and β as k_2):

α equals 0.72 for $f'_c \leq 4000$ psi and decreases by 0.04 for every 1000 psi above 4000.

β equals 0.425 for $f'_c \leq 4000$ psi, and decreases by 0.025 for every 1000 psi above 4000.

The decrease in α and β for high-strength concretes is related to the fact that such concretes are more brittle, i.e., show a more sharply curved stress-strain plot with a smaller near-horizontal portion (see Fig. 1.3). Figure 2.10 shows these simple relations.

If this experimental information is accepted, the ultimate strength can be calculated from the laws of equilibrium and from the assumption that plane cross sections remain plane. Equilibrium requires that

$$C = T \quad \text{or} \quad \alpha f'_c bc = A_s f_s \tag{2.21}$$

(2.22)

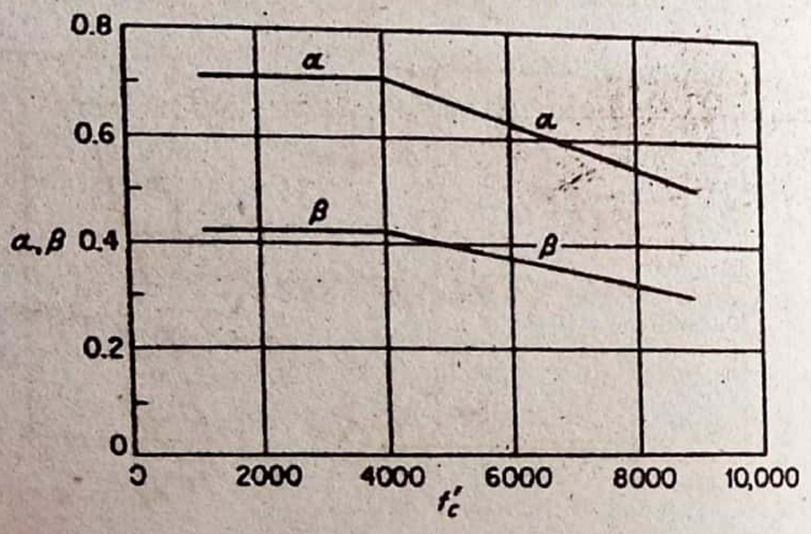


Fig. 2.10

Also, the bending moment, being the couple of the forces C and T, can be written as either

$$M = Tz = A_s f_s(d - \beta c) \tag{2.23}$$

or

$$M = Cz = \alpha f'_c bc(d - \beta c) \tag{2.24}$$

For *tension failure* by yielding of the steel, $f_s = f_y$. Substituting this value in Eq. (2.22), one obtains the distance to the neutral axis:

$$c = \frac{A_s f_y}{\alpha f'_c b} \tag{2.25}$$

It is often convenient to express the steel area nondimensionally as a fraction of the effective area of the section, the so-called *reinforcement ratio:*

$$p = \frac{A_s}{bd} \tag{2.26}$$

Using this quantity, one can also write

$$c = \frac{pf_y}{\alpha f'_c} d \tag{2.25a}$$

as the distance to the neutral axis when tension failure occurs. The ultimate moment M'_u is then obtained from Eq. (2.23), with the value for c just determined, and $f_s = f_y$; that is,

$$M'_u = A_s f_y d\left(1 - \frac{\beta f_y}{\alpha f'_c} p\right) \tag{2.27}$$

With the specific, experimentally obtained values for α and β given previously, this becomes

$$M'_u = A_s f_y d\left(1 - 0.59 \frac{f_y}{f'_c} p\right) \tag{2.27a}$$

On the other hand, for *compression failure* the criterion is that the compression strain in the concrete become $\epsilon_c = 0.003$, as previously discussed. The steel stress f_s, not having reached the yield point, is proportional to the steel strain ϵ_s; that is, according to Hooke's law,

$$\epsilon_s = \frac{f_s}{E_s}$$

From the strain distribution of Fig. 2.9, the distance to the neutral axis is obtained by evaluating the similar triangles and is

$$c = \frac{\epsilon_c}{\epsilon_s + \epsilon_c} d = \frac{0.003}{f_s/E_s + 0.003} d \tag{2.28}$$

Scanned with CamScanner

The ultimate moment of a beam sufficiently heavily reinforced so that failure occurs by compression in the concrete can then be obtained by using the value of c from Eq. (2.28) in Eq. (2.24).

It was noted that compression failure occurs explosively and without warning. For this reason it is good practice to keep the amount of reinforcement sufficiently small so that, should the member be overstressed, it will give adequate warning before failing in a gradual manner by yielding of the steel, rather than by crushing of the concrete. This can be done by keeping the reinforcement ratio $p = A_s/bd$ below a certain limiting value. This value, the so-called *balanced steel ratio* p_b, represents that amount of reinforcement necessary to make the beam fail by crushing of the concrete at the same load which causes the steel to yield. But this means that the neutral axis must be so located that at the load at which the steel starts yielding the concrete reaches its assumed breaking strain of 0.003. Correspondingly, equating the right sides of Eqs. (2.25a) and (2.28) and solving for p, one obtains for the balanced steel ratio

$$p_b = \alpha \frac{0.003}{f_y/E_s + 0.003} \frac{f'_c}{f_y} \tag{2.29}$$

In a well-designed member the actual steel ratio $p = A_s/bd$ is kept well below the balanced ratio p_b.

Example Determine the ultimate moment M'_u at which the beam of the previous example will fail.

For this beam the steel ratio $p = A_s/bd = 2.35/10 \times 23 = 0.0102$. The balanced steel ratio [Eq. (2.29)] is found to be 0.0373. Since the amount of steel in the beam is less than that which would cause failure by crushing of the concrete, the beam will fail in tension by yielding of the steel. Its ultimate moment, from Eq. (2.27a), is found to be

$$M'_u = 2.35 \times 40{,}000 \times 23[1 - 0.59(40{,}000/3000)0.0102]$$
$$= 1.985{,}000 \text{ in.-lb} = 165 \text{ ft-kips}$$

It is interesting to note that when the beam reaches its ultimate strength, the distance to its neutral axis, from Eq. (2.25a), is

$$c = \frac{0.0102 \times 40{,}000}{0.72 \times 3{,}000} 23 = 4.35 \text{ in.}$$

In previous calculations it was found that at low loads, when the concrete had not yet cracked in tension, the neutral axis was located at a distance of 13.3 in. from the compression edge; at higher loads, when the tension concrete was cracked but stresses were still sufficiently small to be elastic, this distance was 7.97 in. Immediately before the beam fails, as has just been shown, this distance has further decreased to 4.35 in. This migration of the neutral axis toward the compression edge as load is

increased is a graphic illustration of the differences among the various stages of behavior through which a reinforced-concrete beam passes as its load is increased from zero to that value which causes it to fail.

f. Ultimate strength, equivalent rectangular stress distribution The preceding method of calculating the ultimate strength, derived from basic concepts of structural mechanics and pertinent experimental research information, also applies to situations other than the case of rectangular beams reinforced on the tension side. It can be used and gives valid answers for beams of other cross-sectional shapes, reinforced in other manners, and for members subject not only to simple bending, but also to the simultaneous action of bending and axial force (compression or tension). However, the pertinent equations for these more complex cases become increasingly cumbersome and lengthy. What is more important, it becomes increasingly difficult for the designer to visualize the physical basis for his design methods and formulas; this could lead to a blind reliance on formulas, with a resulting lack of actual understanding. This is not only undesirable on general grounds but, practically, is more likely to lead to numerical errors in design work than the situation in which the designer at all times has a clear picture of the physical situation in the member which he is dimensioning or analyzing. Fortunately it is possible, essentially by a conceptual trick, to formulate the ultimate-strength analysis of reinforced-concrete members in a different manner which gives the same answers as does the general analysis just developed, but which is much more easily visualized and much more easily applied to cases of greater complexity than that of the simple rectangular beam. Its consistency is shown below, and its application to more complex cases has been checked against the results of a vast number of tests on a great variety of types of members and conditions of loading (Ref. 2.4).

It was noted in the preceding section that the actual geometrical shape of the concrete compression-stress distribution varies considerably and that, in fact, one need not know this shape exactly, provided one does know two things: (1) the magnitude C of the resultant of the concrete compression stresses and (2) the location of this resultant. Information on these two quantities was obtained from the results of experimental research and expressed in the two parameters α and β.

Evidently, then, one can think of the actual complex stress distribution as replaced by a fictitious one of some simple geometrical shape, provided that this fictitious distribution results in the same total compression force C applied at the same location as in the actual member when it is on the point of failure. Historically, a number of simplified, fictitious equivalent stress distributions have been proposed by various investigators in various countries. The one which is finding general acceptance in this

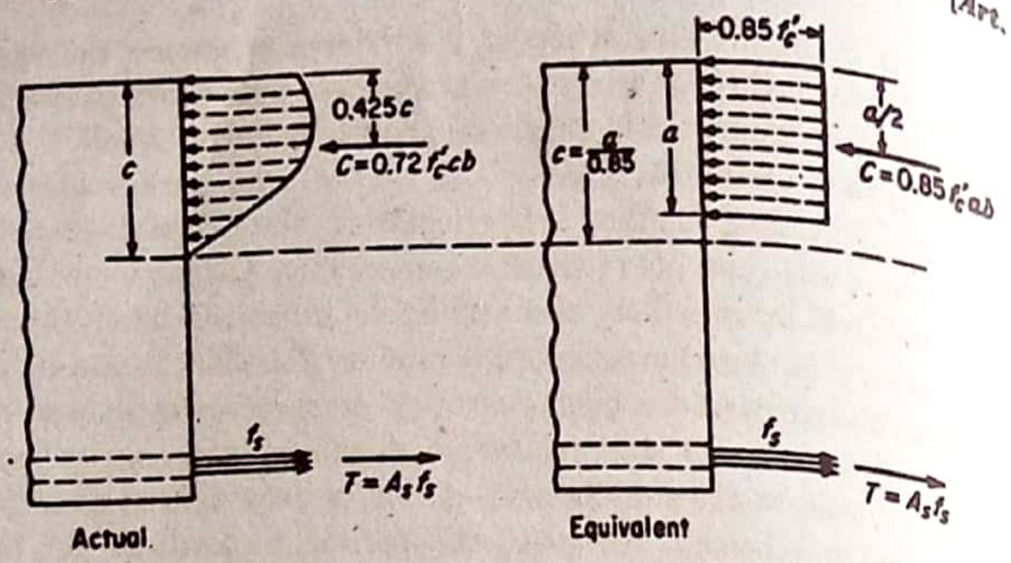


Fig. 2.11 Actual and equivalent rectangular stress distributions at ultimate load (for f'_c less than 4000 psi).

country was first proposed by C. S. Whitney and subsequently elaborated and checked experimentally by others (see, e.g., Ref. 2.4). For concrete with cylinder strength f'_c not exceeding 4000 psi, an actual stress distribution and the fictitious equivalent distribution are shown in Fig. 2.11.

It is seen that the actual distribution is replaced by a fictitious equivalent one of simple rectangular outline. The intensity of this uniform and constant equivalent compression stress is $0.85f'_c$, and it is thought of as acting over a part of the section of depth $a = 0.85c$, where c is the distance to the actual neutral axis. It is in no way maintained that the compression stresses are actually distributed in this most unlikely manner. It is maintained, however that this equivalent distribution gives the answers just derived for the actual situation. Of this one can easily convince oneself. In a rectangular beam of width b the equivalent uniform compression stress $0.85f'_c$ acts on an area ab, so that the total compression force is

$$C = 0.85f'_c ab \tag{2.30}$$

If one expresses the depth a of the rectangular stress block in terms of the distance c to the neutral axis as assumed, that is, $a = 0.85c$, one obtains for the compression force $C = 0.85f'_c \times 0.85c \times b = 0.72f'_c cb$, which is the same as Eq. (2.21) for $\alpha = 0.72$. Further, since the centroid of a rectangle is at middepth, the distance from the compression edge to C is evidently $a/2$. Again expressing a in terms of c as above, one obtains the distance to the compression resultant as $0.5 \times 0.85c = 0.425c$, which is the correct distance for $\beta = 0.425$.

Since the chosen equivalent rectangular stress distribution satisfies the stated requirements (1) and (2), it will give exactly the same answers as were derived previously. This is so for f'_c not exceeding 4000 psi because, in this range of concrete strengths, the parameters α and β are constants

equal, respectively, to 0.72 and 0.425. For concretes of higher strength it has been stated that α and β decrease because of the greater brittleness of such concretes. In the equivalent rectangular stress distribution, this is reflected in the following stipulation:

$$a/c = k_1 = 0.85 \text{ for } f'_c \leq 4000 \text{ psi and decreases by 0.05 for every 1000 psi above 4000} \tag{2.31}$$

This equivalent rectangular stress distribution can be used for deriving the equations which have been developed in the previous section. The failure criteria, of course, are the same as before: yielding of the steel at $f_s = f_y$ or crushing of the concrete at $\epsilon_c = 0.003$. More important, however, because the rectangular stress block is easily visualized and its geometrical properties are extremely simple, many calculations are conveniently carried out directly without reference to formally derived equations.

Example Using the equivalent rectangular stress distribution, calculate directly the ultimate strength of the previously analyzed beam.

The distribution of stresses, internal forces, and strains is as shown in Fig. 2.12. The depth a of the equivalent stress block is found from the equilibrium condition $C = T$. Hence $ab \times 0.85f'_c = A_s f_y$, or $a \times 10 \times 2550 = 2.35 \times 40{,}000$, from which $a = 3.70$ in. The distance to the neutral axis, by the definition of the rectangular stress block, is $c = a/0.85 = 3.70/0.85 = 4.35$ in. One way of determining whether the strength of the beam is governed by yielding of the steel or by crushing of the concrete is to calculate whether the concrete strain in the top fiber is smaller or larger than 0.003 at the instant the steel starts yielding. At that point the strain in the steel is $\epsilon_s = f_y/E_s = 40{,}000/29{,}000{,}000 = 0.00138$. From the similar triangles of the strain distribution, $\epsilon_c = \epsilon_s c/(d - c) = 0.00138(4.35/18.65) = 0.00032$. This value is smaller than the assumed crushing strain of the concrete, and hence failure will be initiated

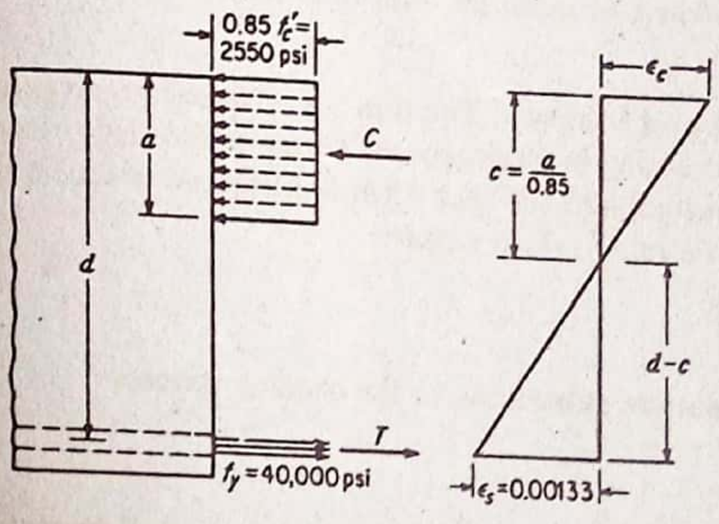


Fig. 2.12

by yielding of the steel. The ultimate moment, then, is $M'_u = T(d - a/2) = 2.35 \times 40{,}000(23.0 - 1.85) = 1{,}985{,}000$ in.-lb = 165 ft-kips.

If one wanted to determine the balanced steel ratio p_b for the given beam, one could proceed as follows: At simultaneous yielding of the steel and crushing of the concrete, it is known that the two pertinent strains are $\epsilon_s = 0.00138$ and $\epsilon_c = 0.003$. Hence, from the similar triangles of the strain distribution, $c/(d - c) = 0.003/0.00138$, from which $c = (3/4.38)d$, and $a = 0.85c = 0.85(3/4.38)23 = 13.4$ in. Hence the tensile force, equal to the compression force, is $T = C = 0.85f'_c ab = 2550 \times 13.4 \times 10 = 342{,}000$ lb. From this the balanced steel ratio is $p_b = A_s/bd = (T/f_y)/bd = 342{,}000/40{,}000 \times 10 \times 23 = 0.0371$. The results of this simple and direct numerical analysis, based on the equivalent rectangular stress distribution, are identical with those previously determined from the general ultimate-strength analysis of beams.

PROBLEM

A simple beam of 20-ft span has the cross section of the preceding examples, 10×25 in., and carries a uniform load of 1900 lb per ft in addition to its own weight. (*a*) Check whether this beam, if reinforced with three No. 8 bars as in the preceding examples, is adequate to carry this load with a minimum factor of safety against failure of 1.85. A different way of stating the same requirement is to stipulate that the ultimate strength of the beam shall be at least equal to 1.85 times the design load. If this requirement is not met, select a three-bar reinforcement of diameter adequate to provide this safety. (*b*) Determine the maximum stress in the steel and in the concrete under working load, i.e., when the beam carries its own weight and the specified uniform design load. (*c*) Will the beam show hairline cracks on the tension side under working load? As before, $f'_c = 3000$ psi, $f_y = 40{,}000$ psi. Use Table 2 of Appendix B for steel areas; assume a unit weight of 150 lb per ft³ for reinforced concrete.

(*Note:* Throughout the remainder of this chapter, additional problems frequently refer to this same beam and loading. To avoid repetitive calculations, the student is advised to retain his computation sheets until reaching the end of the chapter.)

2.5 Shear and Diagonal Tension

a. Homogeneous elastic beams

The stresses acting in homogeneous beams were briefly reviewed in Art. 2.4*a*. It was pointed out that when the material is elastic (stresses proportional to strains), shear stresses

$$v = \frac{VQ}{Ib} \tag{2.12}$$

act in any section in addition to the bending stresses

$$f = \frac{My}{I} \tag{2.10}$$

except for those locations at which the shear force V happens to be zero.

The role of shear stresses is easily visualized by the performance under load of the laminated beam of Fig. 2.13; it consists of two rectangular pieces bonded together along their contact surface. If the adhesive is strong enough, the member will deform as one single beam, as shown in Fig. 2.13*a*. On the other hand, if the adhesive is weak, the two pieces will separate and slide relative to each other as shown in Fig. 2.13*b*. Evidently, then, when the adhesive is effective, there are forces or stresses acting in it which prevent this sliding or shearing. These horizontal shear stresses are shown in Fig. 2.13*c* as they act, separately, on the top and bottom pieces. The same stresses occur in horizontal planes in single-piece beams; they are different in intensity at different distances from the neutral axis.

Figure 2.13*d* shows a differential length of a single-piece rectangular beam acted upon by a shear force of magnitude V. Upward translation is prevented, i.e., vertical equilibrium is provided, by the vertical shear stresses v. Their average value is equal to the shear force divided by the cross-sectional area, $v_{avg} = V/ab$, but their intensity varies over the depth of the section. As is easily computed from Eq. (2.12), the shear stress is zero at the outer fibers and has a maximum of $1.5v_{avg}$ at the neutral axis, the variation being parabolic as shown. Other values and distributions are found for other shapes of the cross section, the shear stress always being zero at the outer fibers and of maximum value at the neutral axis.

If a small square element located at the neutral axis of such a beam

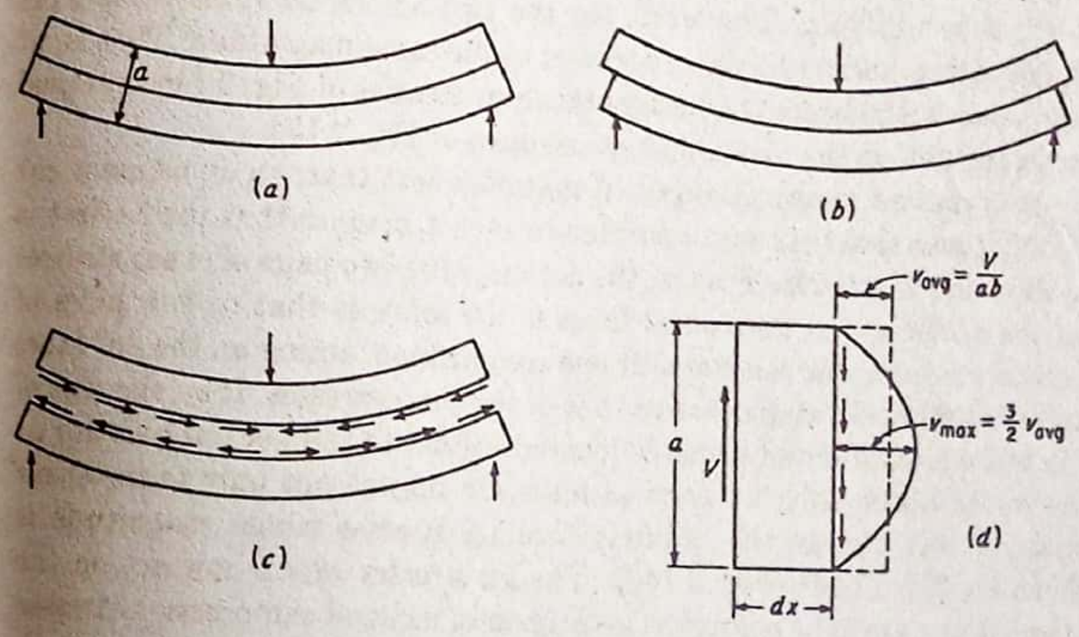


Fig. 2.13 Shear in homogeneous rectangular beam.

Scanned with CamScanner

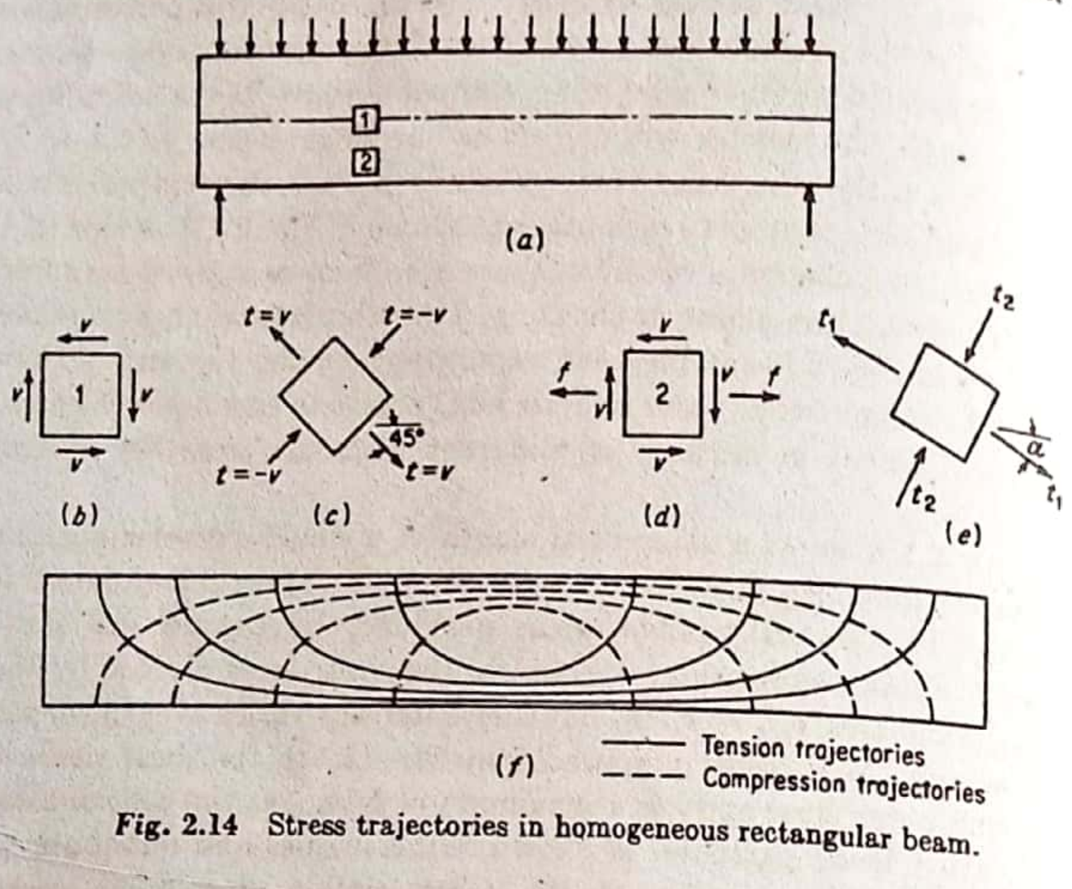


***Fig.* 2.14** Stress trajectories in homogeneous rectangular beam.

is isolated as in Fig. 2.14*b*, the vertical shear stresses on it, equal and opposite on the two faces for reasons of equilibrium, act as shown. However, if these were the only stresses present, the element would not be in equilibrium; it would spin. Therefore, on the two horizontal faces there exist equilibrating horizontal shear stresses of the same magnitude. That is, at any point in the beam the horizontal shear stresses of Fig. 2.14*b* are equal in magnitude to the vertical shear stresses of Fig. 2.13*d*.

It is proved in any strength-of-materials text that, on an element cut at 45°, these shear stresses combine in such a manner that their effect is as shown in Fig. 2.14*c*. That is, the action of the two pairs of shear stresses on the vertical and horizontal faces is the same as that of two pairs of normal stresses, one tension and one compression, acting on the 45° faces and of numerical value equal to that of the shear stresses. If an element of the beam is considered which is located neither at the neutral axis nor at the outer edges, then its vertical faces are subject not only to the shear stresses, but also to the familiar bending stresses whose magnitude is given by Eq. (2.10) (Fig. 2.14*d*). The six stresses which now act on the element can again be combined into a pair of inclined compression stresses and a pair of inclined tension stresses which act at right angles to each other. They are known as *principal* stresses (Fig. 2.14*e*). Their value, as

was mentioned in Art. 2.4*a*, is given by

$$t = \frac{f}{2} \pm \sqrt{\frac{f^2}{4} + v^2} \tag{2.9}$$

and their inclination α by $\tan 2\alpha = 2v/f$.

Since the magnitudes of the shear stresses v and the bending stresses f change both along the beam and vertically with distance from the neutral axis, the inclinations as well as the magnitudes of the resulting principal stresses t also vary from one place to another. Figure 2.14*f* shows, for a rectangular beam uniformly loaded, the inclinations of these principal stresses. That is, these stress trajectories are lines which, at any point, are drawn in that direction in which the particular principal stress, tension or compression, acts at that point. Is is seen that the principal stresses which result from the shear and tension stresses in a beam are always inclined at 45° to the neutral axis. In the vicinity of the outer fibers they are horizontal near midspan.

An important point which follows from this discussion is the following: Tension stresses, which are of particular concern in view of the low tensile strength of the concrete, are not confined to the horizontal bending stresses f which are caused by bending alone. Tension stresses of various inclinations and magnitudes, resulting from shear alone (at the neutral axis) or from the combined action of shear and bending, exist in all parts of a beam and can impair its integrity if not adequately provided for. It is for this reason that the inclined tension stresses, known as *diagonal tension*, must be carefully considered in reinforced-concrete design.

b. Reinforced-concrete beams without shear reinforcement. The discussion of shear in a homogeneous elastic beam applies very closely to a plain concrete beam without reinforcement. As the load is increased in such a beam, a tension crack will form where the tension stresses are largest and will immediately cause the beam to fail. Except for beams of very unusual proportions, the largest tension stresses are those caused at the outer fiber by bending alone, at the section of maximum bending moment. In this case, shear has little, if any, influence on the strength of a beam.

However, when tension reinforcement is provided, the situation is quite different. Even though tension cracks form in the concrete, the required flexural tension strength is furnished by the steel, and much higher loads can be carried. Shear stresses increase proportionally to the loads. In consequence, diagonal tension stresses of significant intensity are created in regions of high shear forces, chiefly close to the supports. The longitudinal tension reinforcement has been so calculated and placed that it is chiefly effective in resisting longitudinal tension near the tension

Scanned with CamScanner

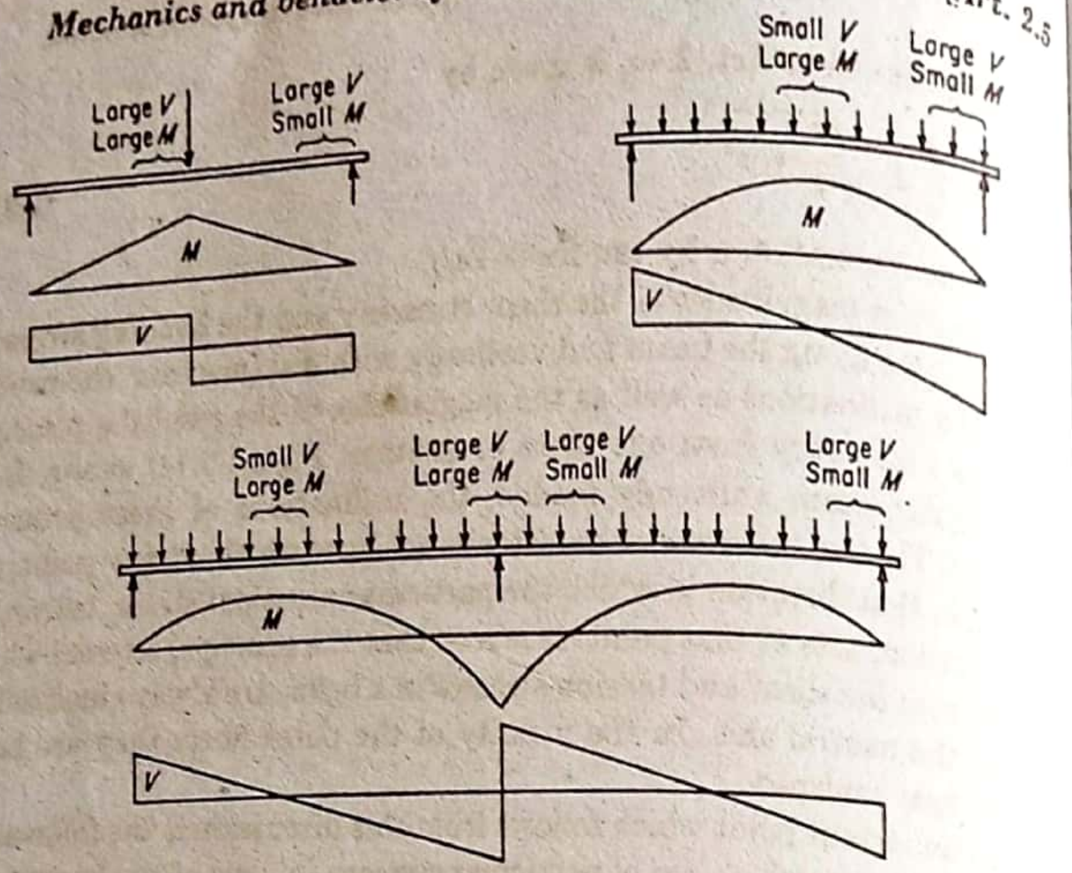


Fig. 2.15 Typical locations of critical combinations of shear and moment.

face. It does not reinforce the tensionally weak concrete against those diagonal tension stresses which occur elsewhere, caused by shear alone or by the combined effect of shear and flexure. Eventually these stresses attain magnitudes sufficient to open additional tension cracks in a direction perpendicular to the local tension stress. These are known as *diagonal* cracks, in distinction to the vertical flexural cracks. The latter occur in regions of large moments, the former in regions in which the shear forces are high. Both types of cracks are shown in Fig. 2.16. In beams in which no reinforcement is provided to counteract the formation of large diagonal tension cracks, their appearance has far-reaching and generally detrimental effects. For this reason methods of predicting the loads at which these cracks will form are desired.

CRITERIA FOR FORMATION OF DIAGONAL CRACKS. It is seen from Eq. (2.9) that the diagonal tension stresses t represent the combined effect of the shear stresses v and the bending stresses f. These, in turn, are, respectively, proportional to the shear force V and the bending moment M at the particular location in the beam [Eqs. (2.10) and (2.12)]. Depending on configuration, support conditions, and load distribution, at a given location in a beam one may find a large moment combining with a small shear force, or the reverse, or large or small values for both shear and moment. Evidently, the relative values of M and V will affect the magnitude as well as the direction of the diagonal tension stresses. Figure 2.15

shows a few typical beams and their moment and shear diagrams and draws attention to locations at which various combinations of high or low V and M occur.

At a location of large shear force V and small bending moment M there will be little flexural cracking, if any, prior to the development of a diagonal tension crack. Consequently, the average shear stress prior to crack formation is

$$v = \frac{V}{bd} \tag{2.32}$$

The exact distribution of these shear stresses over the depth of the cross section is not known. It cannot be computed from Eq. (2.12) because this equation does not account for the influence of the reinforcement, and because concrete is not an elastic homogeneous material. The value computed from Eq. (2.32) must, therefore, be regarded merely as a measure of the average intensity of shear stresses in the section. The maximum value, which occurs at the neutral axis, will exceed this average by an unknown but moderate amount.

If flexural stresses are negligibly small at the particular location, the diagonal tension stresses, as in Fig. 2.14*b* and *c*, are inclined at about 45° and are numerically equal to the shear stresses, with a maximum at the neutral axis. Consequently, diagonal cracks form mostly at or near the neutral axis and propagate from that location as shown in Fig. 2.16*a*. In this situation a diagonal tension crack can be expected to form when the diagonal tension stress in the vicinity of the neutral axis becomes equal to the tension strength of the concrete. The former, as was indicated, is of the order of and somewhat larger than $v = V/bd$; the latter, as discussed in Art. 1.8, varies from about $3.5\sqrt{f'_c}$ to about $5\sqrt{f'_c}$. An evaluation of a very large number of beam tests is in fair agreement with this reasoning (Ref. 2.5). It was found that in regions with large shear and small moment, diagonal tension cracks form at an average or nominal shear stress v_{cr} of about

$$v_{cr} = \frac{V_{cr}}{bd} = 3.5\sqrt{f'_c} \tag{2.33a}$$

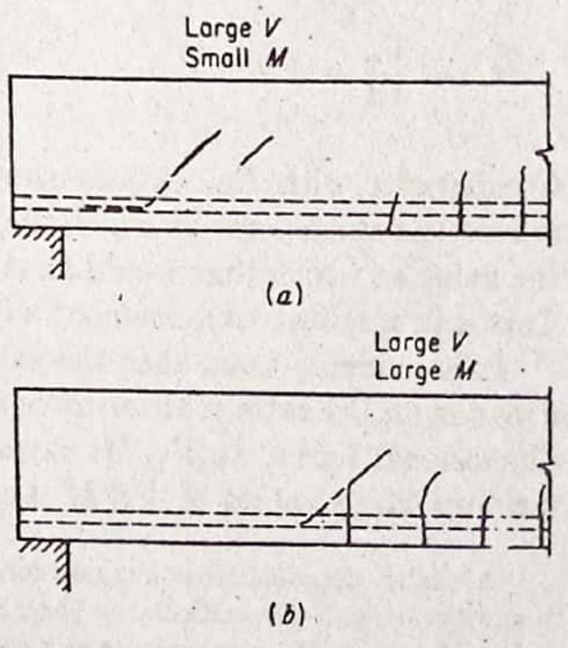


Fig. 2.16 Flexural and diagonal tension cracks.

Scanned with CamScanner

where V_{cr} is that shear force at which the formation of the crack was observed.[1]

The situation is different where both the shear force and the bending moment have large values. At such locations, in a well-proportioned and reinforced beam, flexural tension cracks form first. Their width and length is well controlled and kept small by the presence of longitudinal reinforcement. However, when the diagonal tension stress at the upper end of one or more of these cracks exceeds the tensile strength of the concrete, the crack bends in a diagonal direction and continues to grow in length and width (see Fig. 2.16*b*).

It is evident that at the instant at which a diagonal tension crack of this type develops, the average shear stress is larger than that given by Eq. (2.32). This is so because the preexisting tension crack has reduced the area of uncracked concrete which is available to resist shear to a value smaller than that of the uncracked area bd used in Eq. (2.32). The amount of this reduction will vary, depending on the unpredictable length of the preexisting flexural tension crack. Furthermore, the simultaneous bending stress f combines with the shear stress v to further increase the diagonal tension stress t [see Eq. (2.9)]. No way has been found to calculate reliable values of the diagonal tension stress under these conditions, and recourse must be had to test results.

A large number of beam tests have been evaluated for this purpose (Ref. 2.5). They show that in the presence of large moments (for which adequate longitudinal reinforcement has been provided) the nominal shear stress at which diagonal tension cracks form and propagate is conservatively given by

$$v_{cr} = \frac{V_{cr}}{bd} = 1.9\sqrt{f'_c} \tag{2.33b}$$

Comparison with Eq. (2.33*a*) shows that large bending moments can reduce the shear force at which diagonal cracks form to roughly one-half the value at which they would form if the moment were zero or nearly so. This is in qualitative agreement with the discussion just given.

It is evident, then, that the shear at which diagonal cracks develop depends on the ratio of shear force to bending moment, V/M, or, in nondimensional terms, on Vd/M. Equation (2.33*a*) gives the cracking shear for very large values of Vd/M, and Eq. (2.33*b*) for very small values.

[1] Actually, diagonal tension cracks form at places where a compression stress acts in addition to and perpendicular to the diagonal tension stress, as shown in Fig. 2.14*c* and *e*. The crack, therefore, occurs at a location of biaxial stress, rather than uniaxial tension. However, the effect of this simultaneous compression stress on the cracking strength appears to be small.

Moderate values of Vd/M must be expected to result in magnitudes of v_{cr} intermediate between these extremes. Again, from evaluations of large numbers of tests (Ref. 2.5), it has been found that the nominal shear stress at which diagonal tension cracking develops is conservatively predicted by

$$v_{cr} = \frac{V_{cr}}{bd} = \left(1.9 + 2500\,\frac{pVd}{M\sqrt{f'_c}}\right)\sqrt{f'_c} \le 3.5\sqrt{f'_c} \tag{2.33}$$

where $p = A_s/bd$ as before, and 2500 is an empirical constant in psi units. A graph of this relation is given in Fig. 2.17.

Apart from this influence of Vd/M, it is seen from Eq. (2.33) that increasing amounts of tension reinforcement, i.e., increasing values of the steel ratio p, have a beneficial effect in that they increase the shear at which diagonal cracks develop. This is so because larger amounts of longitudinal steel result in smaller and narrower flexural tension cracks prior to the formation of diagonal cracking, leaving a larger area of uncracked concrete available to resist shear. [For more details on the development of Eq. (2.33), see Ref. 2.5.]

BEHAVIOR OF DIAGONALLY CRACKED BEAMS. In regard to flexural, as distinct from diagonal, tension, it was explained in Art. 2.4 that cracks on the tension side of a beam are permitted to occur and are in no way detrimental to the strength of the member. One might expect a similar situation in regard to diagonal cracking caused chiefly by shear. The analogy, however, is not that simple. Flexural tension cracks are harmless only because adequate longitudinal reinforcement has been provided to resist those flexural tension stresses which the cracked concrete is no longer able to transmit. In contrast, the beams now being discussed, while furnished with the usual longitudinal reinforcement, are not equipped with any other reinforcement to offset the effects of diagonal cracking. Such members, without shear or "web" reinforcement, are frequently used. The very fact, however, that no shear reinforcement is provided makes the diagonal cracks much more decisive in subsequent performance and strength of the beam than the flexural cracks.

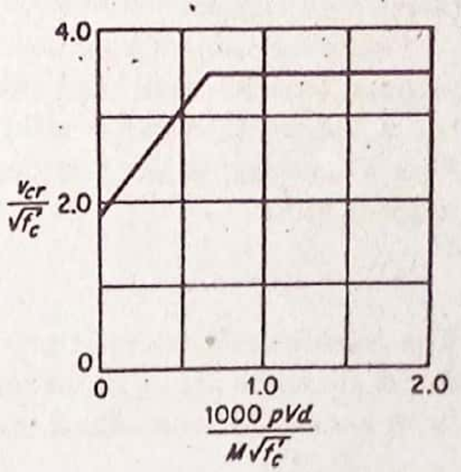


Fig. 2.17

Two types of behavior have been observed in the many tests on which present knowledge is based: (1) The diagonal crack, once formed, spreads either immediately or at only slightly higher load, traversing the entire

Scanned with CamScanner

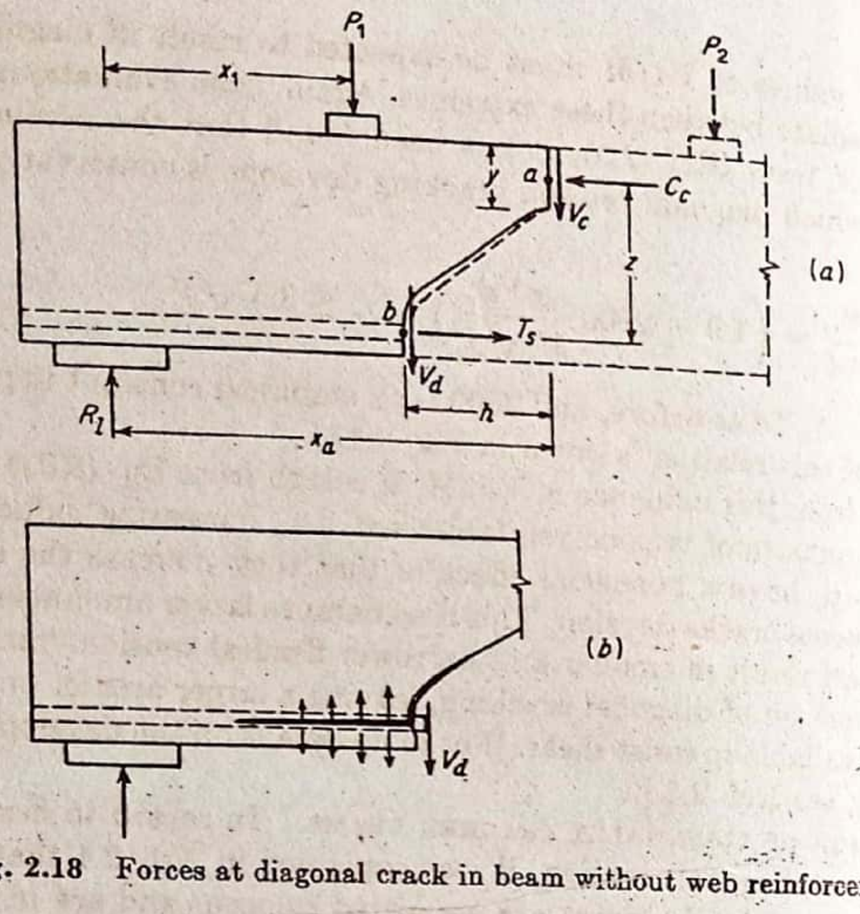


Fig. 2.18 Forces at diagonal crack in beam without web reinforcement.

beam from the tension reinforcement to the compression face, splitting it in two and failing the beam. This process is sudden and without warning and occurs chiefly in the shallower beams, i.e., beams with span-depth ratios of about 8 or more. (2) The diagonal crack, once formed, spreads toward and partially into the compression zone but stops short of penetrating to the compression face. In this case no sudden collapse occurs, and the failure load is usually significantly higher than that at which the diagonal crack first formed. This behavior is chiefly observed in the deeper beams with smaller span-depth ratios and will be analyzed now.

Figure 2.18 shows a portion of a beam, arbitrarily loaded, in which a diagonal tension crack has formed. Consider the part of the beam to the left of the crack, shown in solid lines. There is an external upward shear force V_{ext} acting on this portion, which, for the particular loading shown, happens to be

$$V_{ext} = R_l - P_1$$

The crack cannot transmit any forces, and so the only internal vertical forces are those acting in the uncracked portion of the concrete, V_c, and in or across the longitudinal steel, V_d. Thus, the internal shear force is

$$V_{int} = V_c + V_d$$

Equilibrium requires $V_{int} = V_{ext}$ so that the part of the shear resisted by the uncracked concrete is

$$V_c = V_{ext} - V_d \tag{2.34}$$

In a beam provided with longitudinal reinforcement only, the portion of the shear force resisted by the steel, in dowel action as it were, is usually quite small. In fact, the reinforcing rods on which the dowel force V_d act are supported against vertical displacement chiefly by the thin concrete layer below. The bearing pressure caused by V_d creates, in this concrete vertical tension stresses as shown in Fig. 2.18*b*. Because of these stresses diagonal cracks often result in splitting of the concrete along the tension reinforcement, as shown. Correspondingly, it is likely that most of the shear is resisted by the uncracked portion of concrete at the head of the diagonal crack, or

$$V_c \cong V_{ext} \tag{2.34a}$$

Next, consider moments about point a at the intersection of V_c and C_c; the external moment for the loading shown happens to be

$$(M_{ext})_a = R_l x_a - P_1(x_a - x_1)$$

and the internal moment is

$$(M_{int})_a = (T_s)_b z + (V_d)_b h$$

Here h is the horizontal projection of the diagonal crack, and the designations $(T_s)_b$ and $(V_d)_b$ are meant to emphasize that these two forces in the steel act at point b rather than vertically below point a. Again, equilibrium requires that $(M_{int})_a = (M_{ext})_a$, so that the longitudinal tension in the reinforcement at b is

$$(T_s)_b = \frac{(M_{ext})_a}{z} - \frac{(V_d)_b h}{z} \tag{2.35}$$

Neglecting the dowel force V_d as being only a small fraction of the tension force T_s, one has, with very little error,

$$(T_s)_b \cong \frac{(M_{ext})_a}{z} \tag{2.35a}$$

The formation of the diagonal crack, then, is seen to produce the following redistribution of internal forces and stresses:

1. In the vertical section through a the average shear stress before crack formation was V_{ext}/bd [see Eq. (2.32)]. After crack formation, that same shear force is almost entirely resisted by the much smaller area *by*

Scanned with CamScanner

of the remaining uncracked concrete [see Eq. (2.34*a*) and Fig. 2.18*a*]. Hence, the average shear stress in the concrete has now increased to V_{cr}/by.

2. The diagonal crack, as was described previously, usually rises above the neutral axis and traverses some part of the compression zone before it is arrested by the compression stresses. Consequently, the compression force C_c also acts on an area by smaller than that on which it acted before the crack was formed. Correspondingly, formation of the crack has increased the compression stresses in the remaining uncracked concrete.

3. Prior to diagonal cracking, the tension force in the steel at point b was caused by and was proportional to the bending moment in a vertical section through the same point b. As a consequence of the diagonal crack, however, Eq. (2.35*a*) shows that the tension in the steel at b is now caused by and is proportional to the bending moment at a. Since the moment at a is evidently larger than that at b, formation of the crack has caused a sudden increase in the steel stress at b.

4. The previously described dowel action causes bearing and tension stresses which contribute to the tendency of the concrete to split along the bar toward the nearby support.

If the two materials are capable of resisting these increased stresses, equilibrium will establish itself after internal redistribution, and further load can be applied before failure occurs. Such failure can then develop in various ways. For one, if only enough steel has been provided at b to resist the moment at that section, then the increase of the steel force, in (3) above, will cause the steel to yield because of the larger moment at a, thus failing the beam. If the beam is properly designed to prevent this occurrence, it is usually the concrete at the head of the crack which will eventually crush. This concrete is subject simultaneously to large compression and shear stresses, and this biaxial stress combination is conducive to earlier failure than would take place if either of these stresses were acting alone (Ref. 2.6). Finally, if there is splitting along the reinforcement, it will cause the bond between steel and concrete to weaken to such a degree that the reinforcement may pull loose. This may either be the cause of failure of the beam or, more frequently, may occur simultaneously with crushing of the remaining uncracked concrete.

It was noted earlier that relatively deep beams will usually show continued and increasing resistance after formation of a critical diagonal tension crack, but relatively shallow beams will fail almost immediately upon formation of the crack. The amount of reserve strength, if any, was found to be erratic. In fact, in several test series in which two specimens as identical as one can make them were tested, one failed immediately upon formation of a diagonal crack, while the other reached equilibrium under the described redistribution and failed at a higher load.

For this reason, in modern procedures for designing beams in which no special shear reinforcement is provided, this reserve strength is discounted. Design is based on that shear force V_{cr} or shear stress v_{cr} at which the formation of a diagonal crack must be expected. Thus, Eq. (2.33) has become the criterion for the usable shear strength of such a beam.

PROBLEM

In the problem at the end of Art. 2.4 it was found that a rectangular beam with $b = 10$ in., $t = 25$ in., $d = 23$ in., three No. 9 bars, $f'_c = 3000$ psi, $f_y = 40{,}000$ psi will carry a uniform design load of 1900 lb per ft, plus its own weight with a safety factor slightly larger than the value 1.85 stipulated in that problem. Check whether this beam has a safety factor of at least 2.0 against the formation of diagonal cracks at the indicated load. Decide whether or not shear reinforcement is required. *Explanatory comments:* (*a*) It has been explained that if a beam without web reinforcement fails in shear, collapse is likely to be sudden and complete. On the other hand, if a beam were to be overloaded and to fail in bending, collapse will be gradual and preceded by excessive cracking and deflections which serve as warning of distress. For this reason a larger safety margin is desirable against shear than against flexural failure, as is here stipulated. The detailed manner in which these differential margins are provided in the ACI Code is explained in Chap. 3. (*b*) Tests have shown that diagonal cracks rarely form at a distance from the nearby support smaller than the depth d of the beam, because of the local stress conditions in the immediate vicinity of a support (see also Art. 3.14). For this reason it is now accepted practice that the maximum shear force for which the adequacy of a member must be checked is that acting at a distance d from the face of the support, rather than the larger shear force directly at that face.

c. Reinforced-concrete beams with web reinforcement Economy of design demands, in most cases, that a flexural member be capable of developing its full moment capacity rather than having its strength limited by premature shear failure. This is also desirable in that structures, if overloaded, should not fail in the sudden and explosive manner characteristic of many shear failures, but should show adequate ductility and warning of impending distress. The latter, as was pointed out, obtains for flexural failure caused by yielding of the longitudinal steel, which is preceded by gradual, excessive deflections and noticeable enlargement of cracks. If, then, the available shear strength as given by Eq. (2.33) is not adequate, special shear reinforcement, known as *web reinforcement*, is used to increase this strength.

Web reinforcement may be in either of the two forms shown in Fig. 2.19, or a combination of the two. Figure 2.19*a* shows web reinforcement consisting of vertical stirrups; Fig. 2.19*b* shows inclined bars. The latter

Scanned with CamScanner



Fig. 2.19

can consist of individual stirrups placed at an angle or part of the longitudinal flexural reinforcement bent up where it is no longer needed to furnish moment resistance. A diagonal crack is shown traversed by a number of web bars.

Web reinforcement has no noticeable effect prior to the formation of diagonal cracks. In fact, measurements show that the web steel is practically free of stress prior to crack formation. After diagonal cracks have developed, web reinforcement augments the shear resistance of a beam in three separate ways: (1) Part of the shear force is resisted by the bars which traverse a particular crack. The mechanism of this added resistance is discussed below. (2) The presence of these same bars restricts the growth of diagonal cracks and reduces their penetration into the compression zone. This leaves more uncracked concrete available at the head of the crack for resisting the combined action of shear and compression, already discussed. (3) As seen in the cross section of Fig. 2.19, the stirrups are so arranged that they tie the longitudinal reinforcement into the main bulk of the concrete. This provides some measure of restraint against the splitting of concrete along the longitudinal reinforcement, shown in Fig. 2.18*b*, and increases the share of the shear force resisted in dowel action.

It will be realized from this description that the behavior, once a crack is formed, is quite complex and dependent in its details on the particulars of crack configuration (length, inclination, and location of the main or critical crack). The latter, in turn, is quite erratic and has, so far, defied purely analytical prediction. For this reason, the concepts which underlie present design practice are not wholly rational. They are based partly on rational analysis, partly on test evidence, and partly on successful long-time experience with structures in which certain procedures for designing web reinforcement have resulted in satisfactory performance. Research in this field, both on plain and web-reinforced members, performed mostly between 1945 and 1960, has furnished important experimental data for recent improvements in shear design and analysis It has not yet resulted in a completely consistent rational analysis of shear behavior.

BEAMS WITH VERTICAL STIRRUPS. The web reinforcement being ineffective in the uncracked beam, the magnitude of the shear force or stress which causes cracking to occur is the same as in a beam without web reinforcement and is given by Eq. (2.33). Most frequently, web reinforcement consists of *vertical stirrups;* the forces acting on the portion of such a beam between the crack and the nearby support are shown on Fig. 2.20. They are the same as those of Fig. 2.18, except that each stirrup traversing the crack exerts a force $A_v f_v$ on the given portion of the beam. Here A_v is the cross-sectional area of the stirrup (in the case of the U-shaped stirrup of Fig. 2.19, it is twice the area of one bar), and f_v is the tension stress in the stirrup. Equilibrium in the vertical direction requires

$$V_c + \sum_n A_v f_v + V_d = V_{ext}$$

where n is the number of stirrups traversing the crack. If s is the stirrup spacing, and h the horizontal projection of the crack, as shown, then

$$n = \frac{h}{s}$$

Prior to failure, part of the load, as before, is carried by the uncracked section at the head of the crack. The dowel force V_d will be disregarded, since it is of uncertain and probably minor value. Further opening of the crack is counteracted by the stirrups until the stress in them has reached the yield point f_y. The large stirrup extensions which occur at that stage permit the crack to open and extend, causing the remaining concrete to fail. Consequently, the stirrup stress being f_y when failure occurs, the ultimate shear force V'_u is

$$V'_u = V_c + nA_v f_y$$

While the share of the total shear carried by the stirrups is known, the shear V_c carried by the uncracked concrete at the head of the crack has yet to be defined. It is assumed in present-day methods that this shear, at failure, is the same as that which caused the diagonal crack to form; i.e.,

$$V_c = V_{cr}$$

[V_{cr} is given by Eq. (2.33).] This assumption seems reasonable and conservative. In fact, it has been pointed out that beams without web reinforcement generally fail at loads above that which causes the crack to form, the difference often being insignificant, but under certain conditions sizable. Also, since the presence of stirrups restricts crack growth, the shear resistance of the larger uncracked concrete area in web-reinforced beams should, if anything, exceed that of identical beams without

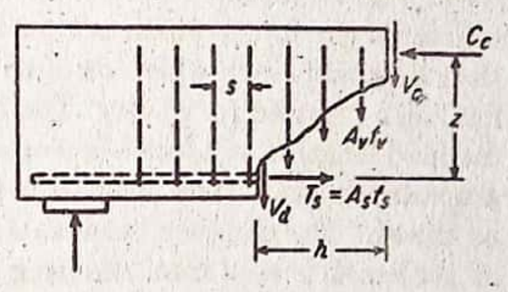


Fig. 2.20 Forces at diagonal crack in beam with vertical stirrups.

Scanned with CamScanner

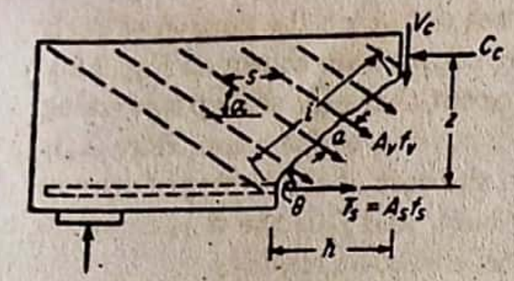


Fig. 2.21 Forces at diagonal crack in beam with inclined web reinforcement.

such reinforcement. In addition, as has been pointed out, the dowel force V_d is likely to be larger in web-reinforced than in plain-web beams. All this points to the fact that in a web-reinforced beam the part of the shear which is not resisted by the stirrups should be at least equal to, and is most likely larger than, the shear force which will cause an identical plain-web beam to crack.

The number of stirrups n spaced a distance s apart was seen to depend on the length h of the horizontal projection of the diagonal crack. If this length is assumed equal to the effective depth of the beam ($h = d$), implying a crack somewhat flatter than 45°, then the above equation for the ultimate shear force V'_u becomes

$$V'_u = V_{cr} + \frac{A_v f_v d}{s} \tag{2.36}$$

Dividing both sides by bd, one obtains the same relation expressed in terms of the nominal ultimate shear stress:

$$v'_u = \frac{V'_u}{bd} = v_{cr} + \frac{A_v f_v}{bs} \tag{2.36a}$$

In Ref. 2.5 the results of 166 beam tests are compared with Eq. (2.36*a*). It is shown that the equation predicts the actual shear strength quite conservatively, the observed strength being on the average 45 per cent larger than predicted; a very few of the individual test beams developed strength just slightly below that of Eq. (2.36*a*). At the same time the very considerable scatter, even though almost entirely on the conservative side, indicates that a deeper and more precise understanding of shear strength has yet to be developed.

BEAMS WITH INCLINED BARS. The function of *inclined web reinforcement*, Fig. 2.19*b*, can be discussed in very similar terms. Figure 2.21 again indicates the forces which act on the portion of the beam to one side of that diagonal crack which results in eventual failure. The dowel force V_d has been omitted for clarity. The crack with horizontal projection h and inclined length $i = h/\cos\theta$ is crossed by inclined bars horizontally spaced a distance s apart. The inclination of the bars is α, and that of the crack θ as shown. The distance between bars measured parallel to the direction of the crack is seen from the irregular triangle to be

$$a = \frac{s}{\sin\theta\,(\cot\theta + \cot\alpha)}$$

The number of bars crossing the crack, $n = i/a$, after some transformation, is obtained as

$$n = \frac{h}{s}(1 + \cot\alpha \tan\theta)$$

The vertical component of the force in one bar or stirrup is $A_v f_v \sin\alpha$, so that the total vertical component of the forces in all bars which cross the crack is

$$V_s = nA_v f_v \sin\alpha = A_v f_v \frac{h}{s}(\sin\alpha + \cos\alpha \tan\theta)$$

As in the case of vertical stirrups, shear failure occurs when the stress in the web reinforcement reaches the yield point. Also, the same assumptions are made as in the case of stirrups, namely that the horizontal projection of the diagonal crack is equal to the effective depth d, and that the concrete, at failure, resists the same force V_{cr} which caused the formation of the diagonal crack. Lastly, the inclination θ of the diagonal crack, which varies somewhat depending on various influences, is generally assumed to be 45°. On this basis, the ultimate strength when failure is caused by shear is obtained as

$$V'_u = V_{cr} + \frac{A_v f_v d(\sin\alpha + \cos\alpha)}{s} \tag{2.37}$$

or, dividing both sides by bd,

$$v'_u = v_{cr} + \frac{A_v f_v(\sin\alpha + \cos\alpha)}{bs} \tag{2.37a}$$

It is seen that Eqs. (2.36) and (2.36*a*), developed for vertical stirrups, are only special cases, for $\alpha = 90°$, of the more general expressions (2.37) and (2.37*a*).

It should be noted that Eqs. (2.36) and (2.37) apply only if web reinforcement is so spaced that any conceivable diagonal crack is traversed by at least one stirrup or inclined bar. Otherwise web reinforcement would not contribute to the shear strength of the beam, because diagonal cracks which could form between widely spaced web reinforcement would fail the beam at the load at which it would fail if no web reinforcement were present. This imposes upper limits on the permissible spacing s to ensure that the web reinforcement is actually effective as calculated.

The inconsistencies in the preceding derivations are fairly evident. For instance, in the case of inclined bars, the assumptions that $h = d$ and $\theta = 45°$ actually mean, by simple geometry, that the diagonal crack has

Scanned with CamScanner

spread all the way to the compression face of the beam. If this were so, no uncracked compression zone would remain available to resist the share V_{cr} of the total shear force. However, this assumption, which is evidently on the unconservative side, appears to be compensated for by other conservative approximations. For one, the share of the shear which is resisted by dowel action has been neglected; for another, as has been pointed out, the share which the uncracked concrete is able to carry has probably been underestimated.

One must conclude that at this time the nature and mechanism of diagonal tension failure are rather clearly understood qualitatively, that some of the quantitative assumptions which have been made cannot be justified by rational analysis, that the calculated results are in acceptable and generally conservative agreement with a very large body of empirical data, and that structures designed on this basis have proved satisfactory.

PROBLEM

The beam discussed in the problem at the end of Art. 2.5*b* ($b = 10$ in., $t = 25$ in., $d = 23$ in., $f'_c = 3000$ psi, span = 20 ft) has been more heavily reinforced with three No. 10 bars, $f_y = 60$ ksi, in order to enable it to carry in flexure a uniform design load of 3300 lb per ft in addition to its own weight, with a minimum safety factor of 1.85. For the section of the beam at a distance d from the support, determine whether web reinforcement is required if a safety factor of at least 2.0 is stipulated against failure by diagonal tension. If so, use vertical U-shaped stirrups as shown on Fig. 2.19*a*, made of No. 2 bars with $f_v = 40$ ksi, and determine the required spacing s at two locations: (1) a distance equal to $d = 23$ in and (2) a distance of 36 in. from the support.

2.6 Bond and Anchorage In a short piece of a beam of length dx shown in Fig. 2.22, the moment at one end will generally differ from tha at the other end by a small amount dM. If this piece is isolated, and if on assumes that after cracking the concrete does not resist any tensio stresses, then the internal forces are those shown in Fig. 2.22*b*. The chang

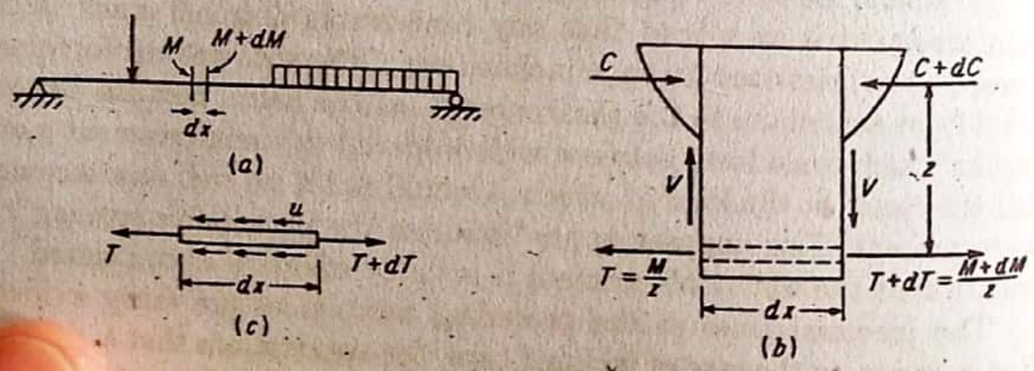


Fig. 2.22

in bending moment dM produces a change in the bar force

$$dT = \frac{dM}{z}$$

Since the bar or bars must be in equilibrium, this change in bar force is resisted at the contact surface between steel and concrete by an equal and opposite force produced by the bond between steel and concrete. If U is the magnitude of this bond force per unit length of bar,

$$U\,dx = (T + dT) - T = dT \tag{a}$$

from which

$$U = \frac{dT}{dx} = \frac{1}{z}\frac{dM}{dx} = \frac{V}{z} \tag{b}$$

Assuming that this bond force per unit length is the resultant of shear-type bond stresses u (see Fig. 2.22*c*) uniformly distributed over the contact area, the nominal bond stress is $u = U/\Sigma_0$ or

$$u = \frac{V}{\Sigma_0 z} \tag{2.38}$$

where Σ_0 is the sum of the perimeters of all the bars. [It is customary to take for the lever arm z the value jd obtained from elastic analysis, Eq. (2.19), so that

$$u = \frac{V}{\Sigma_0 jd} \tag{2.38a}$$

is the more customary form of this equation.] This bond stress is caused by the change dM in bending moment and, for this reason, is known as *flexural bond*.

When plain bars without surface deformations were used, initial bond strength was provided only by the relatively weak chemical adhesion and mechanical friction between steel and concrete. Once adhesion and static friction were overcome at larger loads, small amounts of slip led to interlocking of the natural roughness of the bar with the concrete. However, this natural bond strength is so low that in beams reinforced with plain bars the bond between steel and concrete is frequently broken. Such a beam will collapse as the bar is pulled through the concrete. To prevent this occurrence, end anchorage is provided, chiefly in the form of hooks as in Fig. 2.23. If the anchorage is adequate, such a beam will not collapse even if the bond is broken over the entire length between anchorages.

Scanned with CamScanner

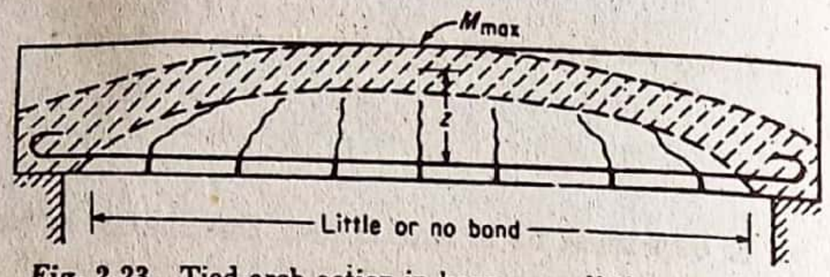


Fig. 2.23 Tied-arch action in beam with little or no bond.

This is so because the member acts as a tied arch, as shown in Fig. 2.23, the uncracked concrete representing the arch (shaded), and the anchored bars the tie rod. In this case, over the length in which the bond is broken, $u = 0$, and, therefore, $dT = 0$. This means that over the entire unbonded length the force in the steel is constant and equal to $T = M_{max}/z$. In consequence, the total steel elongation in such beams is larger than in those in which bond is preserved, resulting in larger deflections and larger widths of cracks.

To improve this situation, deformed bars are now universally used in the United States (see Art. 1.11). With such bars, the shoulders of the projecting ribs bear on the surrounding concrete and result in greatly increased bond strength. It is then possible in most cases to dispense with special anchorage devices such as hooks and anchor plates. In addition, crack widths, as well as deflections, are reduced.

The actual distribution of bond stresses along deformed reinforcing bars is more complex than that represented by Eq. (2.38). In actuality, concrete fails to resist any tension stresses only where a crack is located.

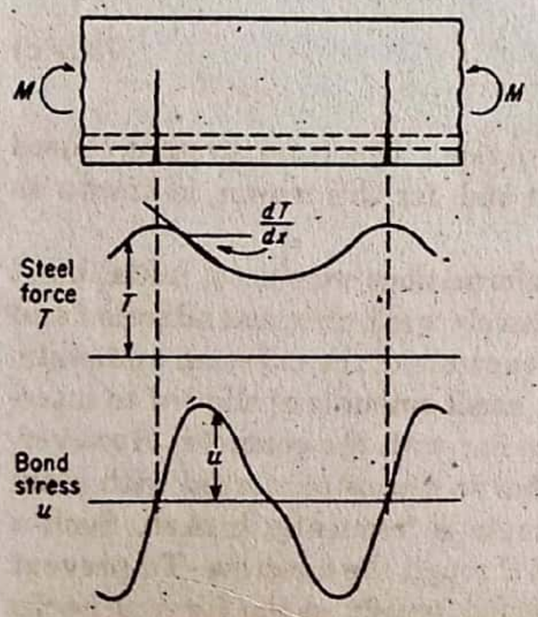
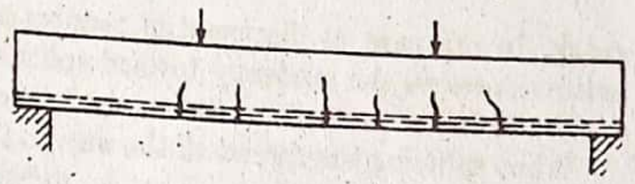


Fig. 2.24 Variation of steel force and bond stress at flexural cracks.

Between cracks, the concrete does resist moderate amounts of tension stress; this reduces the tension force T in the steel, as shown in Fig. 2.24 for a beam portion in pure bending. Since, from Eq. (*b*),

$$u = \frac{dT/dx}{\Sigma_0}$$

local bond stresses, being proportional to the rate of change of the bar force, act in the immediate vicinity of tension cracks and are distributed as shown in Fig. 2.24. Very high values of such bond stresses adjacent to cracks have been measured at Cornell University (Ref. 2.7). They



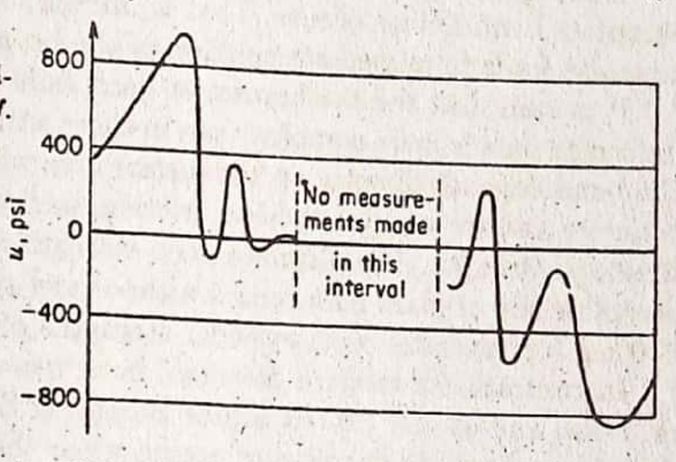


Fig. 2.25 Measured bond-stress distribution. (*From Ref. 2.7.*)

are so high, particularly when high-strength steels are used, that a certain amount of localized slip between steel and concrete occurs at each crack.

If bond stresses become excessive, bond failure ensues. Equation (2.38) shows that this will generally occur where shear forces are large, i.e., in the vicinity of supports. In these regions, bond failure starts at cracks, because there the described localized bond stresses superpose on the flexural bond. Thus, bond stresses at loads close to those which cause bond failure have been measured to be distributed in the general manner shown in Fig. 2.25 (Ref. 2.7).

When bond failure ensues, it results generally in splitting of the concrete along the bars, either in vertical planes as in Fig. 2.26*a*, or in horizontal planes as in Fig. 2.26*b*. Such splitting comes largely from wedging action when the ribs of the deformed bars bear against the concrete. The horizontal type of splitting of Fig. 2.26*b* frequently begins at a diagonal

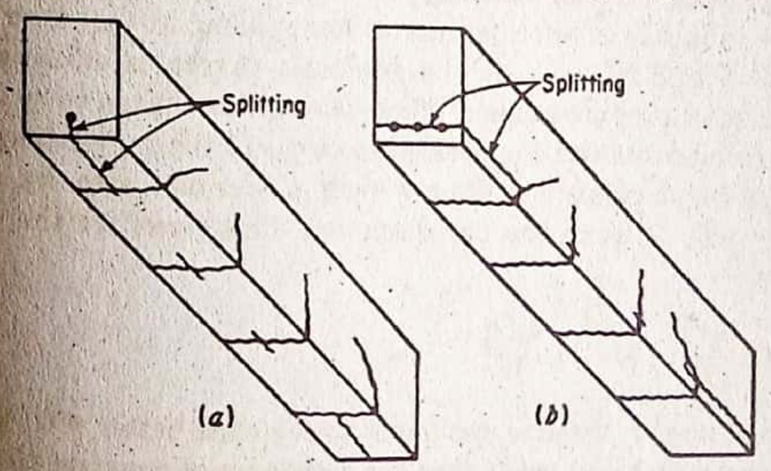


Fig. 2.26 Splitting along reinforcement (schematic).

Scanned with CamScanner

crack. In this case, as discussed in connection with Fig. 2.18*b*, the dowel action increases the tendency toward splitting. This indicates that shear and bond failures are often intricately interrelated.

When splitting has spread all the way to the end of an unanchored bar, complete bond failure occurs. That is, sliding of the steel relative to the concrete leads to immediate collapse of the beam.

It is seen that the mechanism of bond failure in beams with modern deformed bars is more complex than in those with plain bars. In the latter the bond depends directly on the surface area which is in contact with the concrete and for which adhesion, friction, and surface roughness provide the bond strength. The ultimate bond strength u'_u per unit area, at which complete slip of plain bars occurs without any splitting, is of the order of 300 psi for concretes with cylinder strengths of about 3000 to 3500 psi.

In contrast, for modern deformed bars, recent tests at the University of Texas and at the United States Bureau of Standards (Refs. 2.8, 2.9) seem to indicate that splitting occurs when the total bond force U per inch of length of bar, which is transmitted from steel to concrete, reaches a critical value. This ultimate bond force, in pounds per linear inch of bar, is largely independent of bar size or perimeter. The concept of a wedging action is in reasonable conformity with this finding, since the effects of a wedge of given shape depend more on the force with which it is driven than on its size.

It was found that the ultimate average bond force per inch of length of bar is approximately

$$U'_u = 30\sqrt{f'_c} \quad \text{to} \quad 35\sqrt{f'_c} \tag{2.39}$$

Bond forces of this magnitude were observed to result in failure by splitting, in large and excessive slip, or in other prohibitive deformations. These tests were made mostly on beams of the type in Fig. 2.26*a*, with a single bar causing vertical splitting. They do not give adequate information on the influence of such factors as bar spacing in the more realistic situation of Fig. 2.26*b*, nor on the evidently favorable influence which substantial stirrup reinforcement must have on resistance to splitting.

This information can be expressed in terms of the conventional nominal average bond stress per square inch of contact area by dividing U'_u by $\Sigma_0 = \pi D$, D being the bar diameter. This gives, for the ultimate bond stress,

$$u'_u = 9.5\frac{\sqrt{f'_c}}{D} \quad \text{to} \quad 11\frac{\sqrt{f'_c}}{D} \quad \text{psi} \tag{2.40}$$

The fact that bond resistance was found to correlate better with $\sqrt{f'_c}$ than with f'_c agrees with the concept that the resistance of concrete to splitting depends chiefly on its tensile, rather than compressive, strength.

If one considers the large local variations of bond stress caused by flexural and diagonal cracks (see Figs. 2.24 and 2.25), it becomes clear that local bond failures immediately adjacent to cracks will often occur at loads considerably below the failure load of the beam. These result in small local slips and some widening of cracks and increase of deflections, but will be harmless as long as failure does not propagate all along the bar with resultant total slip. In fact, as was discussed in connection with Fig. 2.23, in those cases in which end anchorage is reliable, bond can be severed along the entire length of bar, excluding the anchorages, without endangering the carrying capacity of the beam.

In the beam of Fig. 2.27, the moment, and therefore the steel stress, is evidently zero at the supports and maximal at point a (neglecting the weight of the beam). If one designates the steel stress at a as f_s, the total tension force at that point in a bar of area A_s is $T_s = A_s f_s$, while at the end of the bar it is zero. Evidently, this force has been transferred from the concrete into the bar over the length L by bond stresses on the surface. Therefore, the average bond force over the length L is

$$U = \frac{A_s f_s}{L}$$

If this bond force per unit length is smaller than the ultimate value U'_u of Eq. (2.39), no splitting or other complete failure will occur over the length L.

To put it differently, the minimum length which is necessary to develop, by bond, a given bar force $A_s f_s$ is

$$L_d = \frac{A_s f_s}{U'_u} \tag{2.41}$$

where the ultimate bond force per unit length U'_u is given by Eq. (2.39). This length L_d is known as the *development length* of the bar. In particular, in order to ensure that a bar is securely anchored by bond to develop its maximum usable strength (the yield stress), this development length

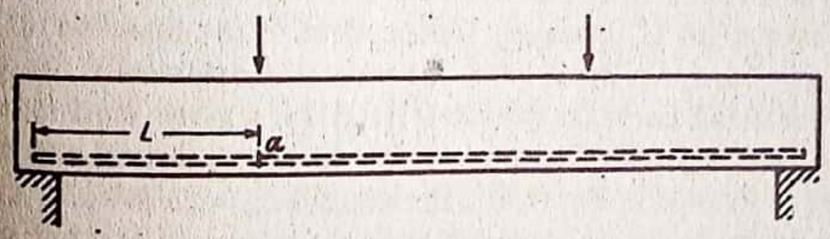


Fig. 2.27 Development length.

Scanned with CamScanner

must be

$$L_{du} = \frac{A_s f_y}{U'_u} \tag{2.41a}$$

Therefore, if, in the beam of Fig. 2.27, the actual length L is equal to or larger than the development length L_{du}, no premature bond failure will occur. That is, the beam will fail by yielding of the steel, rather than by bond failure. This will be so even if, in the immediate vicinity of cracks, local slips may have occurred over small regions along the beam.

From this discussion it is seen that the main requirement for safety against bond failure is this: The length of the bar, from any point of given steel stress (f_s or, at most, f_y) to its nearby free end must be at least equal to its development length as given by Eq. (2.41) or (2.41*a*). If this requirement is satisfied, the magnitude of the nominal flexural bond stress along the beam, as given by Eq. (2.38), is of only secondary importance, since the integrity of the members is assured even in the face of possible minor local bond failures. Conversely, if the actual available length is inadequate for full development, special anchorage, such as by hooks, must be provided to ensure adequate strength.

The development length for a given steel stress f_s, or for the yield strength f_y, can also be written in terms of the conventional nominal bond stress u'_u:

$$L_d = \frac{A_s f_s}{u'_u \Sigma_0} \quad \text{or} \quad L_{du} = \frac{A_s f_y}{u'_u \Sigma_0} \tag{2.41b}$$

where u'_u is given by Eq. (2.40).

It should be noted that the actual local intensity of the bond stress along the embedded length of a bar is not constant. It varies, depending on the crack pattern, on the distance from the section of maximum steel stress, and on other factors. This was illustrated by Figs. 2.24 and 2.25. The ultimate values of Eqs. (2.39) and (2.40) were obtained, from tests with a variety of embedded lengths L, by dividing the bar force by the development length or development surface; that is, $U'_u = A_s f_s/L$ or $u'_u = A_s f_s/L\Sigma_0$. These quantities, therefore, are merely the average values over the embedded length at bond failure, regardless of local variations.

It is seen that U'_u is largely independent of the diameter of the bar. This means that the bond force per inch is substantially the same for large as for small bars. On the other hand, for a given steel stress f_s, the bar force $A_s f_s = f_s \pi D^2/4$ is proportional to the square of the diameter. If this is substituted in Eq. (2.41), the result is $L_d = f_s \pi D^2/4U'_u$; the necessary development length increases with the square of the bar diameter.

Therefore, a beam reinforced with a larger number of small bars requires a smaller development length than a beam reinforced with a small number of large bars of the same total area. This demonstrates the superiority of small bars in developing bond strength.

PROBLEM

Verify whether the beam discussed at the end of Art. 2.5 is adequately designed to provide a safety factor of at least 2.0 against failure in bond. *Notes:* (*a*) For the present purpose it is sufficiently accurate to use the approximate value $j = \frac{7}{8}$ for determining the internal lever arm $z = jd$. (*b*) Bond should be checked both at the support where the flexural bond stress is largest and in reference to the development length. (*c*) For identifying the development length, assume that the beam has a clear span of 20 ft and that the reinforcement is carried 6 in. beyond the face of the support, as shown schematically in Fig. 2.27. (*d*) The maximum steel stress evidently occurs at the point of maximum moment, and development length must be checked for that point. However, in a uniformly loaded beam the bending moment, and thereby the steel stress, at first decrease quite slowly with increasing distance from midspan. For this reason, adequacy of development length should also be checked at one or more additional locations, closer to the supports; it is suggested that this be done for the quarter-points of the span. (*e*) For bar diameters and perimeters see Tables 1 and 3 of Appendix B.

2.7 Deflections at Service Loads In order to serve its intended purpose, a structure must be (1) safe and (2) serviceable. A structure is safe if it is able to resist, without distress and with some margin to spare, all forces which foreseeably will act on it during its lifetime. Serviceability implies, among other things, that deflections and other distortions under load shall be unobjectionably small. For example, excessive beam and slab deflections can lead to objectionable cracking of partitions, ill-fitting doors and windows, poor drainage, misalignment of sensitive machinery or other equipment, excessive vibrations, etc. It becomes important, therefore, to be able to predict deflections with reasonable accuracy, so that members can be dimensioned to ensure both adequate strength and appropriately small deflections.

The deflections of interest are those which occur under normal service conditions. In service, a structure sustains the full dead load plus some fraction or all of the maximum design live load. The usual safety factors provide that under service loading the steel and concrete are not stressed beyond their respective elastic ranges. For this reason the deflections which occur immediately upon application of the load, the so-called *instantaneous deflections*, can be calculated by methods based on the elastic behavior of flexural members as analyzed in Art. 2.4*c* and *d*.

Scanned with CamScanner

It was pointed out in Arts. 1.7 and 1.9 that, in addition to those concrete deformations which occur immediately upon load application, there are other deformations and volume changes which take place gradually and over long intervals of time. These are chiefly creep deformations and shrinkage. In consequence, deflections of reinforced-concrete members continue to increase for some time after load application, at a decreasing rate, and the *longtime deflections* may exceed the instantaneous deflections by a large amount. For this reason, methods for estimating both the instantaneous and the longtime deflections are essential.

a. Instantaneous deflections Elastic deflections can be expressed in the general form

$$\delta = \frac{F\ (\text{loads, spans})}{EI}$$

where EI is the flexural rigidity, and F (loads, spans) is a function of the particular load-and-span arrangement. For instance, the deflection of a uniformly loaded simple beam is $5wL^4/384EI$, so that $F = 5wL^4/384$. Similar deflection equations have been tabulated, or can easily be computed, for many other loadings and span arrangements, simple, fixed, or continuous, and the corresponding functions F may be determined. The particular problem in reinforced-concrete structures is, therefore, the determination of the appropriate flexural rigidity EI for a member consisting of two materials with properties and behavior as widely different as steel and concrete.

If the maximum moment in a flexural member is sufficiently small so that the tension stress in the concrete does not exceed the flexural tensile strength (modulus of rupture, which can be taken as about $7.5\sqrt{f'_c}$), and if the shear stresses are less than v_{cr} [see Eq. (2.33)], neither flexural nor diagonal tension cracks will occur. The full, uncracked section is then available for resisting stress and providing rigidity. This stage of loading has been analyzed in Art. 2.4c. In agreement with this analysis, the effective moment of inertia for this range of low loads is that of the uncracked, transformed section, I_{ut}, and E is the modulus of concrete E_c as given in Art. 1.7. Correspondingly, for this load range,

$$\delta_1 = \frac{F}{E_c I_{ut}} \tag{2.42}$$

At higher loads flexural tension cracks are formed; in addition, if shear stresses are sizable, and web reinforcement is employed to resist them, diagonal tension cracks can exist at service loads. In the region of flexural cracks the position of the neutral axis varies: directly at each crack it is located at the level calculated for the cracked, transformed

section (see Art. 2.4*d*); midway between cracks it dips to a location closer to that calculated for the uncracked, transformed section (Art. 2.4*c*). It does not reach the latter location because, even between cracks, the concrete stress cannot exceed the flexural tensile strength. Correspondingly, flexural tension cracking causes the effective moment of inertia to be that of the cracked, transformed section in the immediate neighborhood of flexural tension cracks, and closer to but smaller than that of the uncracked, transformed section midway between cracks, with a gradual transition between these extremes. Diagonal cracks sometimes extend beyond the calculated location of the neutral axis, reducing the effective rigidity. Also, some redistribution of steel stresses is caused by diagonal cracking (see Art. 2.5) and by localized slip between steel and concrete adjacent to cracks (see Art. 2.6). This is accompanied by an increase in deflections. These effects add to that of flexural tension cracks in further reducing the effective moment of inertia.

It is seen from this brief discussion that, once cracking has started, the effective moment of inertia is close to that of the cracked, transformed section, its actual value depending on the details of crack development. These, in turn, vary with distribution of moments and shears along the beam, magnitude of tensile stresses at service loads depending on the grade of steel used, etc. Tests have shown that in this range, i.e., for loads between the cracking load and the service load, the deflections can be computed from

$$\delta_2 = \frac{F}{E_c k I_{ct}} \tag{2.43}$$

where I_{ct} is the moment of inertia of the cracked, transformed section, and k is a coefficient which varies from about 0.75 to 0.90, depending on severity of cracking. That is, high steel stresses and high shear stresses will result in a lower value of k, and vice versa.

By way of example, it may be recalled that in the particular beam discussed in the example of Art. 2.4, for the uncracked section $I_{ut} = 15{,}030$ in.^{4}, and for the cracked section $I_{ct} = 7630$ in.^{4} It is seen that in this case, once cracks have developed, the rate of deflection is more than twice that observed at low loads for the uncracked beam.

The situation is shown schematically in Fig. 2.28. A reasonable and simple estimate of instantaneous deflections can often be made as follows: If the service load does not (significantly) exceed the cracking load, as is frequently the case in lightly reinforced slabs, the moment of inertia of the uncracked section I_{ut} can be used. Conversely, investigations at Cornell University have shown that, if the service load exceeds the cracking load sizably, instead of calculating separately δ_1 and δ_2 and adding, one may

Scanned with CamScanner

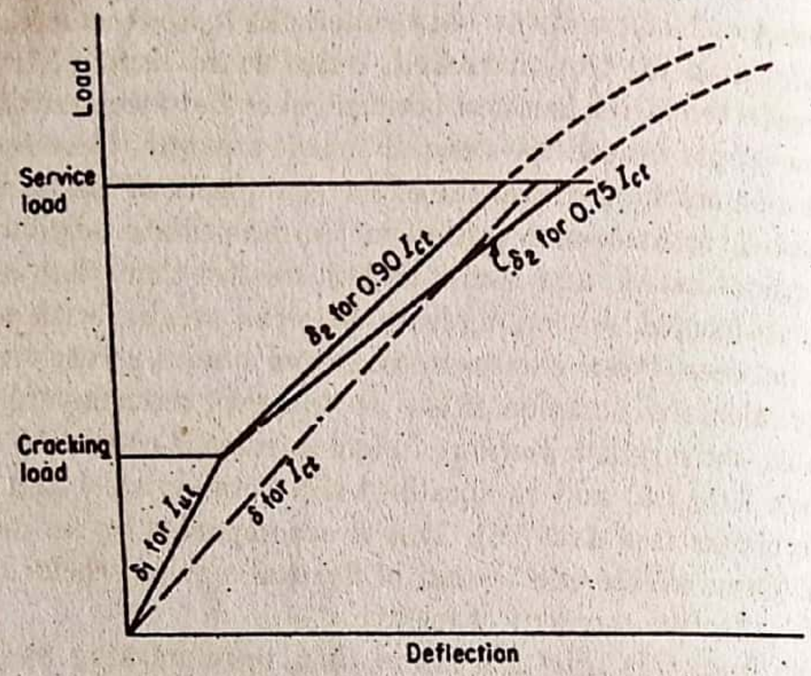


Fig. 2.28 Deflections of reinforced-concrete beams (schematic).

estimate the entire deflection δ by using the moment of inertia I_{ct} of the cracked, transformed section (Refs. 2.10, 2.11). This, likewise, is shown schematically in Fig. 2.28.

b. Longtime deflections Longtime deflections are caused by shrinkage and by creep (chiefly the latter). It was pointed out in Art. 1.7 that creep deformations of concrete are directly proportional to the compression stress. They increase asymptotically with time and, for the same stress, are larger for low- than for high-strength concretes. Correspondingly longtime deflections caused by sustained loads can be estimated by replacing E_c with an equivalent sustained modulus. This modulus must also be used in determining n when calculating I_{ut} or I_{ct}. One such method, including data on the magnitude of this equivalent sustained modulus, is given in Ref. 2.10.

In this same investigation at Cornell University (Ref. 2.10), it was shown from many tests that the following simplified method leads to an adequate estimate of longtime deflections, including the effect of normal shrinkage: (1) Calculate the instantaneous deflection due to the sustained load. (2) Multiply this short-time deflection by a coefficient A; the resulting value is the additional longtime deflection caused by creep and normal shrinkage. That is, (*additional longtime deflection*) $= A \times$ (*instantaneous deflection*).

The coefficient A depends on the duration of the sustained load. It also depends on whether the flexural member carries only reinforcement of amount A_s on the tension side, or whether additional longitudinal reinforcement A_s' is provided on the compression side. In the latter case,

***Table* 2.1 Multiplier A for additional longtime deflections (Ref. 2.10)**

Duration of loading	A_s only	$A_s' = A_s/2$	$A_s' = A_s$
1 month	0.6	0.4	0.3
6 months	1.2	1.0	0.7
1 year	1.4	1.1	0.8
5 years and more	2.0	1.2	0.8

the longtime deflections are much reduced. This is so because, when no compression reinforcement is provided, the compression concrete is subject to unrestrained creep and shrinkage. On the other hand, since steel is not subject to creep, if additional bars are located close to the compression face, they will resist, and thereby reduce, the amount of creep and shrinkage and the corresponding deflection. The appropriate coefficient can be read from Table 2.1.

It will be realized from this discussion that the magnitude of the deflections in reinforced-concrete structures depends on so many influences that no precise calculation is possible. On the other hand, great precision is not necessary practically. From extensive experimental information it can be said that the methods presented here permit deflections to be estimated with an accuracy of about ± 20 per cent, which is adequate for purposes of design.

PROBLEM

For the beam analyzed in the problem at the end of Art. 2.4, estimate the longtime deflection at full service load. Assume that in the particular structure that part of the total service load which acts continually and constitutes the longtime loading consists of the weight of the beam plus 1200 lb per ft. This longtime loading consists of the weight of the floor structure and of other permanent portions of the building supported by the given beam, plus that part of the live load which acts more or less continuously, such as furniture, equipment, the time average of the weight of occupants, etc. The remaining 700 lb per ft are short-duration peak loads, such as the brief peak loading of corridors in an office building at the end of the working day. *Note:* to avoid repetitive calculations, utilize those cross-sectional properties which have been calculated in connection with the problem in Art. 2.4.

2.8 Compression plus Bending The behavior and strength of members which are axially, i.e., concentrically, compressed, have been discussed in Art. 2.2. Such members occur rarely, if ever, in buildings and other structures Components such as columns and arches chiefly carry loads in compression, but simultaneous bending is almost always present.

Scanned with CamScanner

Bending moments are caused by continuity, i.e., by the fact that building columns are parts of monolithic frames in which the support moments of the girders are partly resisted by the abutting columns, by transverse loads such as wind forces, by loads carried eccentrically on column brackets, or in arches when the arch axis does not coincide with the pressure line. Even when design calculations show a member to be loaded purely axially, inevitable imperfections of construction will introduce eccentricities and consequent bending in the member as built. For this reason members which must be designed for simultaneous compression and bending are very frequent in almost all types of concrete structures. Their behavior is easily understood by combining the information and principles of Arts. 2.2 and 2.4.

a. Elastic behavior Up to loads of the order of one-half the ultimate, eccentrically compressed members behave substantially elastically in the manner, and for the reasons, discussed for axially compressed members and for beams. In elastic members made of materials with substantial tension strength, the stresses can be calculated by a simple addition of those caused by axial compression and those caused by bending. A similar situation prevails in eccentrically compressed reinforced-concrete members, provided that no tension cracking has occurred to reduce the effective concrete section. This will be the case if the eccentricity is small enough so that tension stresses in the concrete will not exist or, if present, will be smaller than the bending tension strength f_r (modulus of rupture). This case of small eccentricity will be analyzed first.

(1) SMALL ECCENTRICITY, SECTION UNCRACKED. Figure 2.29*a* shows the cross section of a rectangular eccentrically loaded column, (*b*) its transformed section, and (*c*) the load P acting at a distance (eccentricity) e measured from the centroid of the transformed section. If $A'_s = A_s$, as is most frequently the case and as is assumed here for simplicity of presentation, then the eccentricity is measured from the center line of the column. The eccentric force P can be replaced with an axial force of equal magnitude and a moment $M = Pe$, as shown.

The axial force causes uniform concrete compression stresses

$$f_a = \frac{P}{A_t}$$

and the moment causes maximum concrete bending stresses

$$f_b = \pm \frac{Mc}{I_t} = \pm \frac{Mt/2}{I_t}$$

the first of the two expressions for f_b being general, and the second applying [illegible] $A'_s = A_s$. Here A_t and I_t are, respectively, the area and moment

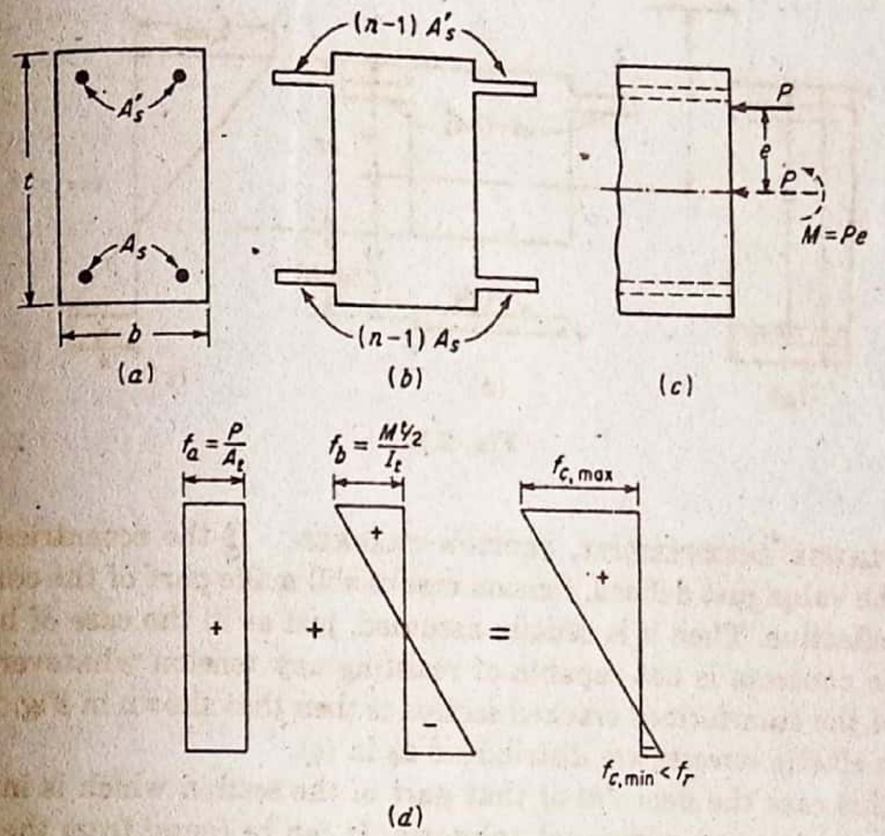


Fig. 2.29

of inertia of the transformed section. Substituting $Pe = M$, the outer fiber stresses in the concrete, by superposition, become

$$f_{c,\substack{\max\\\min}} = \frac{P}{A_t} \pm \frac{Mc}{I_t} = \frac{P}{A_t} \pm \frac{Mt/2}{I_t} \tag{2.44}$$

and are shown in Fig. 2.29*d*. Depending on the relative magnitudes of the two terms, f_{min} can be either positive (compression), in which case the entire cross section is under compression of varying intensity, or negative, in which case a portion of the section is in tension. In the latter case, which is shown in Fig. 2.29*d*, it is assumed that the section remains uncracked as long as the numerically largest tension stress $f_{c,min}$ does not exceed the modulus of rupture f_r. Then the transformed section of Fig. 2.29*b* continues to be correct, and the above analysis applies. Otherwise, if $f_{c,min}$ exceeds f_r in absolute value, tension cracks develop, and the transformed section must be modified accordingly.

It is evident from Eq. (2.44) that, for a given cross section and a given load P, there is a limiting value for the eccentricity e beyond which f_{min} will numerically exceed f_r, causing tension cracks to appear. This limiting eccentricity can be calculated from Eq. (2.44) by substituting $-f_r$ for f_{min}, Pe for M, and solving for e.

Scanned with CamScanner

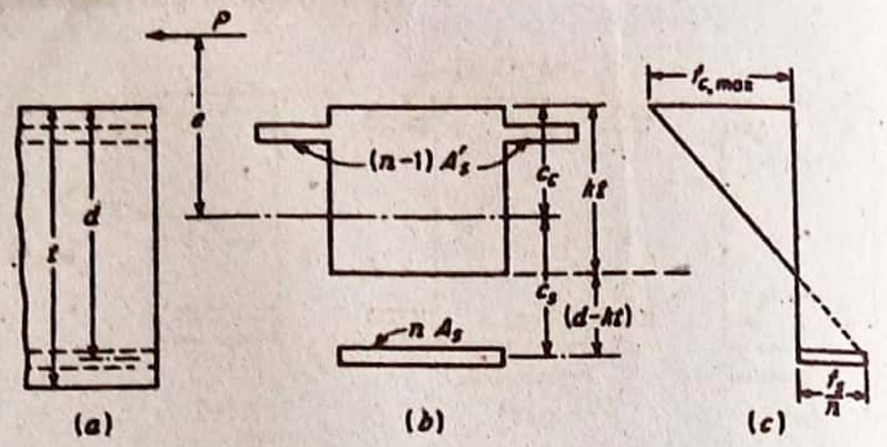


Fig. 2.30

(2) LARGE ECCENTRICITY, SECTION CRACKED. If the eccentricity exceeds the value just defined, tension cracks will make part of the concrete area ineffective. Then it is usually assumed, just as in the case of beams, that the concrete is not capable of resisting any tension whatever. The shape of the transformed cracked section is then that shown in Fig. 2.30b, and the elastic stresses are distributed as in (*c*).

In this case the depth kt of that part of the section which is in compression becomes an additional unknown. It can be found from the equilibrium requirement that the moment of all internal forces about the action line of the external force P must be zero. The internal forces are the stresses shown in Fig. 2.30c acting on the transformed area of (*b*). The mentioned condition

$$M_P = 0$$

results in a cubic equation for kt which can be solved either explicitly or by successive approximation. Once kt is known, the stresses are calculated from the first (general) form of Eq. (2.44). Thus, the maximum concrete stress becomes

$$f_{c,\max} = \frac{P}{A_t} + \frac{Pec_c}{I_t} \tag{2.44a}$$

and the stress in the tension steel

$$f_s = n\left[\frac{P}{A_t} - \frac{Pec_s}{I_t}\right] \tag{2.44b}$$

Here A_t and I_t refer, of course, to the transformed cracked section. The eccentricity e and the fiber distances c_c and c_s for concrete and steel, respectively, are measured from the centroidal axis of the transformed section; compression is designated as positive, tension negative.

b. Ultimate strength In eccentrically compressed members, at loads approaching the ultimate, a nonelastic redistribution of stresses takes place which is similar to that discussed for axially compressed members in Art. 2.2 and for flexural members in Art. 2.4. In compression members, even more than in beams and girders, the designer is chiefly interested in the carrying capacity, i.e., the ultimate strength. Stresses and rigidity at service loads, which govern deflections of flexural members (see Art. 2.7), are of little interest for compression members, whose deflections or other service behavior need rarely be computed. In earlier days, the elastic stresses under service loads, calculated as just described, were taken as a measure of carrying capacity by limiting them to appropriate fractions of f'_c or f_y. Experimental evidence showed, however, that satisfactory correlation of actual strength with elastically computed stresses could not be obtained. This is not surprising if one considers that, as loads become sufficiently large to cause inelastic behavior, not only the magnitude, but also the manner of distribution of the stresses over the cross section, changes decisively. In attempts to account for these discrepancies without upsetting established methods of elastic stress calculation, various arbitrary corrections and adjustments were gradually introduced in these elastic methods. Such methods continue to be used in this and other countries. However, ways of calculating ultimate strength on the basis of inelastic behavior have now been developed for eccentrically compressed members as for other members. Their results are in satisfactory agreement with extensive test evidence. Increasingly, in engineering practice, they are replacing these older and internally inconsistent methods.

If a rectangular column with cross section as in Fig. 2.31a is compressed by an eccentric load P applied as shown, the steel and concrete stresses just prior to failure, i.e., at ultimate load, are distributed in the manner of Fig. 2.31b. That is, with plane sections assumed to remain

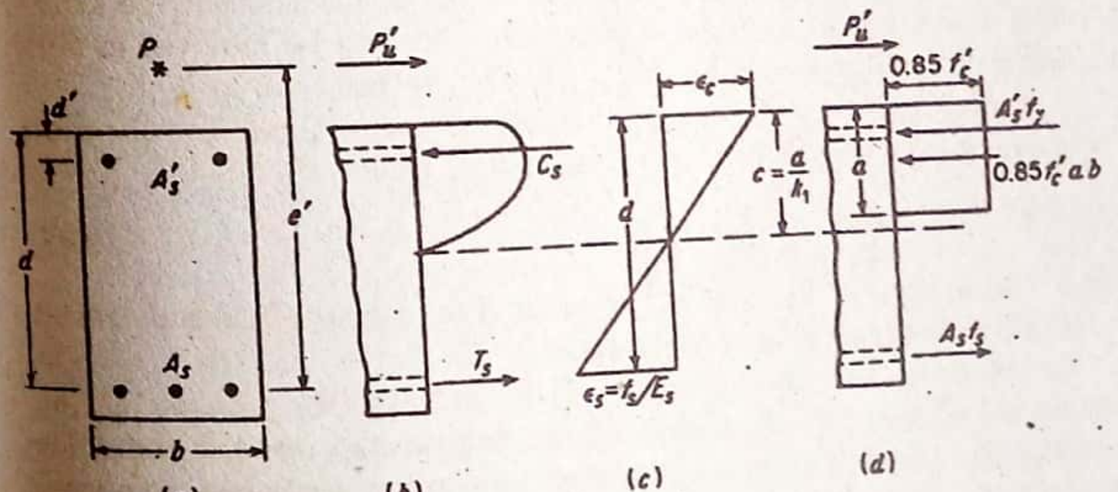


Fig. 2.31 Eccentric compression, ultimate strength.

Scanned with CamScanner

plane, the strains are those shown in Fig. 2.31*c*, which, for the reasons discussed in connection with Fig. 2.9, result in the shown stress distribution. Just as for simple bending, this actual distribution can be replaced, for purposes of calculation, with the equivalent rectangular stress distribution (Fig. 2.31*d*) discussed in Art. 2.4*f* and shown in Fig. 2.11. A large number of tests on columns of a variety of shapes have shown that the ultimate strengths computed on this basis are in satisfactory agreement with test results (Ref. 2.4).

It is assumed in Fig. 2.31*d* that at ultimate load, when the concrete fails in compression, i.e., when $\epsilon_c = \epsilon_u = 0.003$, the compression steel is yielding, so that $f'_s = f'_y$ as shown. For ordinary conditions this is usually the case; it can easily be checked, as will be demonstrated in a numerical example.

Equilibrium between external and internal axial forces requires that

$$P'_u = 0.85f'_c ab + A'_s f'_y - A_s f_s \tag{2.45}$$

Also, the moment about the centroid of the tension steel A_s of the internal stresses must be equal and opposite to the moment of the external force P'_u, so that

$$P'_u e' = 0.85f'_c ab\left(d - \frac{a}{2}\right) + A'_s f'_y(d - d') \tag{2.46}$$

These are the two basic equilibrium relations for rectangular, eccentrically compressed members. The fact that the presence of the compression reinforcement A'_s has displaced a corresponding amount of concrete, of area A'_s, is neglected in Eqs. (2.45) and (2.46). If necessary, particularly for large steel ratios, one can account for this very simply. Evidently, in the above equations a nonexistent concrete compression force of amount $A'_s(0.85f'_c)$ has been included as acting in the displaced concrete at the level of the compression steel. This excess force can be removed in both equations by multiplying A'_s by $(f'_y - 0.85f'_c)$ rather than by f'_y.

For simplicity, the following presentation will be limited to the most frequent case of *symmetrical cross section*, i.e., where

$$A'_s = A_s \qquad \text{and} \qquad f'_y = f_y \tag{2.47}$$

Other conditions, dealt with by the same type of analysis, merely result in lengthier expressions and calculations.

For large eccentricities, failure will be initiated by yielding of the tension steel, followed by a shift of the neutral axis toward the compression side until crushing of the concrete causes a secondary compression failure. Conversely, for small eccentricities, the concrete may crush while the tension steel may be far from yielding. For any cross section of

given dimensions and material strength values, there is one specific eccentricity e' such that a force applied at that distance will cause failure by simultaneous yielding of the tension steel and crushing of the concrete. For this so-called *balanced condition*, let the particular eccentricity be e'_b, and the corresponding ultimate load P_b.

For the *balanced condition*, the concrete strain is $\epsilon_c = \epsilon_u = 0.003$, and simultaneously the strain in the tension steel at the instant at which yielding commences is $\epsilon_s = \epsilon_y = f_y/E_s$. With these values, from the geometry of Fig. 2.31*c*, the distance to the neutral axis is

$$c_b = \frac{\epsilon_u}{\epsilon_y + \epsilon_u} d = \frac{0.003}{f_y/E_s + 0.003} d \tag{2.48}$$

On the other hand, with Eq. (2.47) for symmetrical sections, the depth of the rectangular stress block, from Eq. (2.45), becomes

$$a = \frac{P'_u}{0.85f'_c b} \tag{2.49}$$

Also, by definition of the rectangular stress block [see Eq. (2.31)],

$$a_b = k_1 c_b \tag{2.50}$$

Equating the right sides of Eqs. (2.49) and (2.50), and using c_b from Eq. (2.48), one has, for the ultimate load under balanced conditions,

$$P'_b = 0.85k_1 f'_c bd \frac{0.003}{f_y/E_s + 0.003} \tag{2.51}$$

In particular, for concretes with f'_c not exceeding 4000 psi, from Eq. (2.31), $k_1 = 0.85$, so that in this case

$$P'_b = 0.72f'_c bd \frac{0.003}{f_y/E_s + 0.003} \tag{2.51a}$$

The eccentricity e'_b which results in balanced conditions can then be obtained from Eq. (2.46) by substituting P'_b for P'_u and a_b for a and solving for e'. Loads with eccentricities smaller than e'_b result in primary compression failures at ultimate values larger than P_b; loads with eccentricities larger than e'_b result in primary tension failures at loads smaller than P_b.

(1) FAILURE BY YIELDING OF TENSION STEEL. When $e' > e'_b$, failure is initiated by yielding of the tension steel, followed by lengthening of cracks, shift of the neutral axis, and secondary compression failure by crushing of the concrete. In this case, $f_s = f_y$ and, for a symmetrical section, from Eq. (2.47),

$$A_s f_y = A'_s f'_y$$

Scanned with CamScanner

Therefore, Eqs. (2.45) and (2.46) become

$$P'_u = 0.85f'_c ab \tag{2.45a}$$

$$P'_u e' = P'_u\left(d - \frac{a}{2}\right) + A'_s f'_y(d - d') \tag{2.46a}$$

Solving Eq. (2.45*a*) for the depth of the rectangular stress block, one has

$$a = \frac{P'_u}{0.85f'_c b} \tag{2.52}$$

If this value is substituted in Eq. (2.46*a*), one obtains the following quadratic equation:

$$\frac{P'^2_u}{2 \times 0.85f'_c b} + (e' - d)P'_u - A'_s f_y(d - d') = 0$$

Dividing through by d and solving, one obtains the ultimate load for large eccentricities:

$$P'_u = 0.85f'_c bd\left[-\left(\frac{e'}{d} - 1\right) + \sqrt{\left(\frac{e'}{d} - 1\right)^2 + 2pm\left(1 - \frac{d'}{d}\right)}\right] \tag{2.53}$$

where the parameter

$$m = \frac{f_y}{0.85f'_c} \tag{2.54}$$

is the ratio of the effective strengths of the two materials in connection with the rectangular stress distribution and is useful in this and other connections.

(2) FAILURE BY COMPRESSION OF CONCRETE. When $e' < e'_b$, failure is initiated by crushing of the concrete. That is, when the concrete reaches its ultimate strain $\epsilon_u = 0.003$, the tension steel has not yet reached its yield point, so that $f_s < f_y$. From the geometry of the strain distribution of Fig. 2.31*c* with $\epsilon_c = \epsilon_u$, the depth to the neutral axis is

$$c = \frac{\epsilon_u}{f_s/E_s + \epsilon_u} d \tag{2.55}$$

from which the tension steel stress becomes

$$f_s = E_s\epsilon_u \frac{d - c}{c} = E_s\epsilon_u \frac{d - a/k_1}{a/k_1} \tag{2.55a}$$

If f_s is substituted in Eq. (2.45), and the depth of the stress block a is eliminated between Eqs. (2.45) and (2.46), one obtains a cubic equation in P'_u. From this, the ultimate load for small eccentricities can be determined

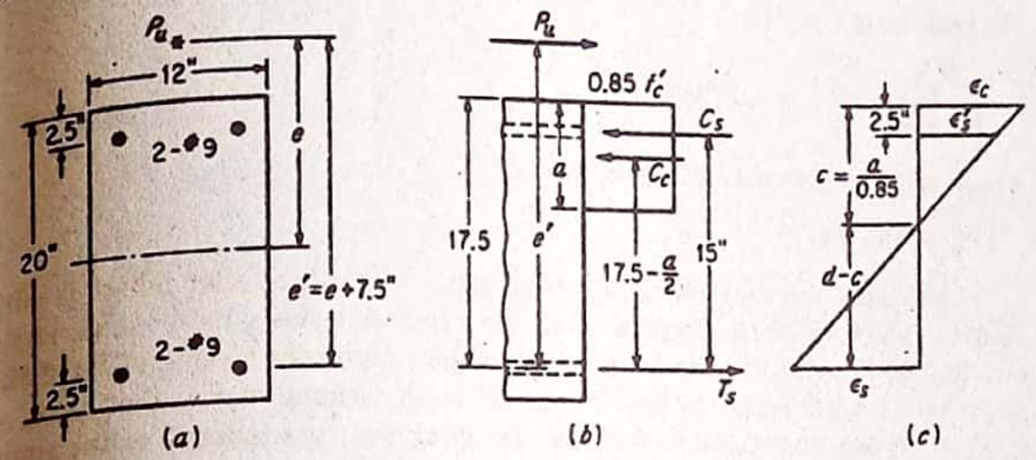


Fig. 2.32

by solving for P'_u either explicitly or, often more quickly, by successive approximation.

Examples The following two examples (in one of which tension governs, and in the other compression) are directly solved numerically, without reference to the previously derived equations. The simplicity of the equivalent rectangular stress block enables such direct numerical analyses, without reference to elaborate formulas, to be carried out for most situations.

The cross section of the column is shown in Fig. 2.32*a*. Four No. 9 bars are used, of 1.0 in.^{2} area each. The cylinder strength is $f'_c = 3000$ psi, and the yield point is $f_y = 40{,}000$ psi.

(1) ECCENTRICITY $e = 15$ IN. FROM CENTERLINE OF COLUMN. The compression force is applied outside the boundaries of the cross section; it is therefore sensible to assume that failure will be initiated by yielding of the tension steel. Assuming the compression steel to yield as well (to be checked later), the three internal forces of Fig. 2.32*b* are:

$$T_s = -2.0 \times 40{,}000 = -80{,}000 \text{ lb}$$
$$C_s = 2.0 \times 40{,}000 = 80{,}000 \text{ lb}$$
$$C_c = 0.85 \times 3000 \times 12a = 30{,}600a$$

As T_s and C_s are equal and opposite, the total internal force being equal and opposite to the external load, P'_u is

$$P'_u = C_c = 30{,}600a$$

from which the depth of the rectangular stress block is

$$a = \frac{P'_u}{30{,}600}$$

Taking moments about the tension steel,

$$P'_u \times 22.5 - 80{,}000 \times 15 - C_c\left(17.5 - \frac{a}{2}\right) = 0$$

Scanned with CamScanner

Substituting P'_u for C_c and $P'_u/30{,}600$ for a, as previously calculated, one obtains the quadratic equation

$$\frac{P'^2_u}{61{,}200} + 5P'_u - 1{,}200{,}000 = 0$$

whose solution gives the ultimate load

$$P'_u = 159{,}000 \text{ lb}$$

It was assumed that the compression steel yields when, after failure is initiated by yielding of the tension steel, the concrete reaches its crushing strain $\epsilon_u = 0.003$. For this to be true, the strain of the compression steel, ϵ'_s of Fig. 2.32c, must be at least equal to that strain at which yielding starts, that is, $\epsilon_y = f'_y/E_s = 40{,}000/29{,}000{,}000 = 0.00138$. To check this, use is made of the strain distribution of Fig. 2.32c.

The depth of the rectangular stress block is

$$a = \frac{P'_u}{30{,}600} = \frac{159{,}000}{30{,}600} = 5.2 \text{ in.}$$

and the depth to the neutral axis is

$$c = \frac{a}{k_1} = \frac{5.2}{0.85} = 6.12 \text{ in.}$$

From similar triangles it is seen that

$$\epsilon'_s = \epsilon_c \frac{c - d'}{c} = 0.003 \frac{6.12 - 2.5}{6.12} = 0.00177 > 0.00138$$

Hence, at the instant at which the ultimate concrete strain is reached, the compression steel strain exceeds the yield strain, verifying the assumption that at ultimate load the compression steel is, in fact, yielding.

(2) ECCENTRICITY $e = 6$ IN. FROM CENTER LINE OF COLUMN. For this small eccentricity it is sensible to assume that failure will be initiated by crushing of the concrete. Proceeding by successive approximations, assume that for this small eccentricity the major part of the cross section is in compression. Thus, try

$$a = 11.0 \text{ in.}$$

Hence

$$c = \frac{a}{k_1} = \frac{11}{0.85} = 12.95 \text{ in.}$$

From the similar triangles of the strain distribution of Fig. 2.32c,

$$\epsilon_s = \frac{f_s}{E_s} = \epsilon_c \frac{d - c}{c}$$

from which the steel stress in the tension reinforcement is

$$f_s = 0.003 \times 29{,}000{,}000 \frac{17.5 - 12.95}{12.95} = 30{,}600 \text{ psi}$$

Taking moments about the centroid of the tension steel,

$$P'_u \times 13.5 = 0.85 \times 3000 \times 11 \times 12(17.5 - 5.5) + 80{,}000 \times 15$$

from which, as a first approximation,

$$P'_u = 388{,}000 \text{ lb}$$

Taking the sum of the axial forces,

$$388{,}000 = 0.85 \times 3000 \times 12a + 2.0 \times 40{,}000 - 2.0 \times 30{,}600$$

from which

$$a = 12.1 \text{ in.}$$

which differs from the assumed value of $a = 11.0$ in.

If this simple calculation is repeated assuming $a = 12.0$ in., one obtains $P'_u = 402{,}500$ lb and $a = 11.9$ in. The latter being satisfactorily close to the assumed value for a, the second approximation,

$$P'_u = 402{,}500 \text{ lb}$$

is taken as the final answer.

Finally, if one computes the ultimate load for balanced conditions from Eq. (2.51*a*), one finds $P'_b = 314{,}000$ lb. For case 1, $P'_u = 159{,}000$ lb $< P'_b$, indicating that failure is, in fact, initiated by yielding of the tension steel; for case 2, $P'_u = 402{,}500$ lb $> P'_b$, indicating that failure is, in fact, caused by crushing of the concrete, as was assumed.

PROBLEM

If the column of the preceding examples is made of high-strength concrete with $f'_c = 5000$ psi and reinforced with high-strength steel with $f_y = 75{,}000$ psi, calculate the ultimate loads. Check whether the substitution of high-strength materials has led to the same percentage increase in carrying capacity for the two conditions of loading. If not, why not? *Note:* As is seen from Table 1.1, steel with $f_y = 75$ ksi is the highest-strength reinforcing steel available at this time under ASTM standards. The stress-strain curve for such steels frequently has the shape shown in Fig. 1.10. For simplicity of calculation, in the given problem assume that the shape of the curve is similar to that for the lower-strength steels, i.e., that it exhibits a horizontal yield plateau before entering the strain-hardening range.

2.9 Prestressed Concrete *a. Prestressing* The successful combination of two materials as unlike in almost every respect as are concrete and steel enables reinforced concrete to occupy an important place in modern construction. Yet there are weaknesses inherent in this combination. They result mainly from the presence of tension cracks which, wherever substantial flexure or shear is present, affect the value of the

Scanned with CamScanner

ultimate load; cracks also occur under service conditions, i.e., at design loads. This has the following disadvantages:

1. In bending, all the concrete on the tension side of the neutral axis, two-thirds or more in flexural members, is lost as a means of resisting stress; its chief structural function is merely to hold the reinforcing bars in place and protect them from corrosion.

2. In shear, as was discussed, the formation of diagonal tension cracks is decisive in limiting the available strength.

3. Deflections being inversely proportional to the moment of inertia of the transformed section, cracked or uncracked as the case may be, beams in which tension cracks have formed show deflections sizably larger than would be the case if cracking could have been prevented.

4. High-strength steels with yield points in excess of 200,000 psi and ultimate strengths of the order of 250,000 psi, 3 to 5 times the strength of ordinary reinforcing steels, are available for use in concrete structures. However, the amount of cracking (width and number of cracks) is roughly proportional to the steel strain, i.e., to the steel stress. Therefore, the high stresses which these steels could sustain cannot be utilized with conventional reinforcement because they would cause an amount of cracking prohibitive with respect to both appearance and corrosion protection and would result in large and frequently prohibitive deflections.

These limitations have been largely overcome by the development of *prestressed concrete*. The essence of prestressing consists in intentionally applying to a structure or structural member forces in a manner which will counteract the effects of the subsequent loads. Specifically, forces are introduced in advance of loading in such a way that they cause internal stresses opposite in sign and distribution to those subsequently produced by the external loads. The resulting total stresses being the sums of those caused by prestressing and those caused by useful load, the performance of the member is improved.

Prestressing steel, in American practice, consists chiefly of seven-wire strands with tension strengths f'_s of 250,000 psi or more and 0.2 per cent offset yield strengths f_y of 200,000 psi or more. Heat-treated, cold-worked alloy-steel bars with tensile strengths of 145,000 psi or more and 0.2 per cent offset yield strengths of about 90 per cent of this value are also utilized. The modulus of elasticity for both types is about 27,000,000 psi.

Suppose a beam is fabricated in the following manner: First, high-strength steel strands are placed in the form and passed through holes in two anchor plates, one at each end. The strands are then pretensioned by applying the *initial prestress force* P_i by a suitable means, such as jacks bearing against abutments (Fig. 2.33*a*). Then the concrete, poured so that the anchor plates bear against the ends of the beam, is allowed to harden. Next the steel strands are secured to the anchor plates, and the jacks

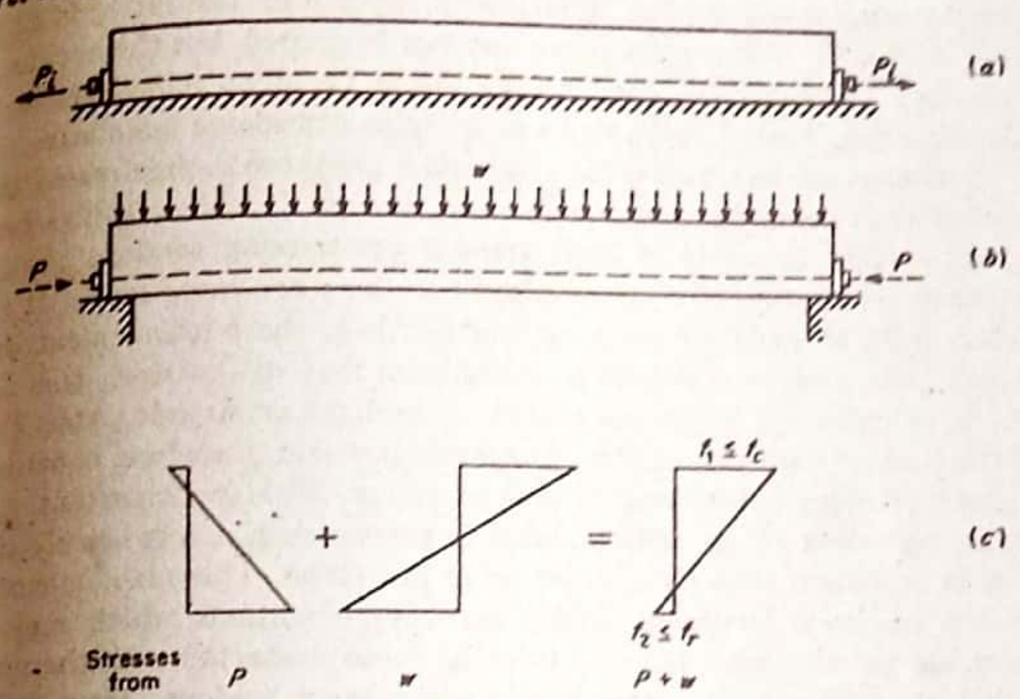


Fig. 2.33 Principle of prestressing.

released. The steel, tending to contract to its original length, is prevented from doing so by the concrete interposed between the anchor plates. Hence, it remains under tension, and this tension is equilibrated by a corresponding compression in the concrete. The effect of the prestressing force, then, is the same as that of an external compression force P applied to the concrete as shown in Fig. 2.33*b*. This stage is known as "transfer"; i.e., the force which equilibrates the steel tension has been transferred from the jacks to the concrete.

After some time has elapsed, the initial prestress P_i will have decreased somewhat, for various reasons which include the elastic compression of the concrete when stressed by the prestressing force, concrete creep and shrinkage, and possible creep of the steel. With current prestressing methods, these losses amount to about 12 to 20 per cent, so that the *final stress* P is smaller by this amount than the initial prestress P_i.

b. Elastic behavior at service loads The principal advantage of a prestressed member is its behavior at service loads. At such loads, stresses in both steel and concrete are kept within the elastic range. The magnitude and location of the prestressing force generally are so arranged that tension cracks will not occur under working loading, dead plus live. In most cases, tension cracking is also prevented, or at least minimized, under temporary conditions such as when a girder, having been fabricated in a prestressing yard, is transported to the site and placed in position, during which time the only load it carries is its own weight. Cracking is prevented by limiting the elastically computed tension stress in the con-

Scanned with CamScanner

crete to some fraction of the modulus of rupture f_r. The latter is of the order of $8\sqrt{f'_c}$. When a crackfree member is desired, but the accidental formation of occasional small cracks would be of no consequence, an allowable maximum tension stress of $6\sqrt{f'_c}$ is considered adequate.

Corrosion protection is of more critical importance in prestressed than in reinforced concrete. This is so for two reasons: (1) Other things being equal, smaller amounts of high-strength prestressing tendons than of ordinary reinforcing rods are employed to carry the same loads. If corrosion were to penetrate to a certain depth in the reinforcement and, thereby, to remove a certain cross-sectional area of the steel, this area would constitute a larger percentage of the light prestressing steel than of the heavier conventional reinforcement; it would, therefore, constitute a greater danger to the integrity of the member. (2) More important, steel under permanent high stress, as used in prestressing, is more easily subject to corrosion than steel under no or low stress. This phenomenon is known as *stress corrosion*. Mildly corrosive conditions which may be harmless to reinforced concrete (such as those connected with the usual hairline cracks) can be damaging to prestressing tendons. Thus, it has been observed that some antifreeze compounds and some high-alumina cements, used chiefly abroad as high-early-strength cements, have led to corrosion difficulties in prestressed concrete, but not in conventionally reinforced concrete. For reasons such as this, it is customary to permit no tensile stresses to occur under service conditions in outdoor structures or in other corrosive environments.

The following discussion of behavior, stresses, and strength of prestressed beams is limited to the situation in the midportions of simple beams, for the sake of simplicity.

In the cross section of a prestressed beam, the prestress force P (Fig 2.34*a*), applied with an eccentricity e below the centroidal axis, gives rise to the compression stess $-P/A_t$ and the bending stress $\pm Pec/I_t$ as shown. (In this discussion, compression stresses are designated as negative, tension as positive.) The bending stress produces a shortening of the bottom fibers and a lengthening of the top fibers, which results in an upward deflection of the beam. In other words, when the prestress force is transferred to the concrete (i.e., in the above described procedure, when the jacks are released), the beam lifts off its soffit, as shown in Fig. 2.34*b*. Then the weight of the girder w_g becomes an active load which, for a prismatic girder, results at midspan in the moment

$$M_g = \frac{w_g L^2}{8}$$

This moment causes additional bending stresses $\pm M_g c/I_t$ of sign opposite

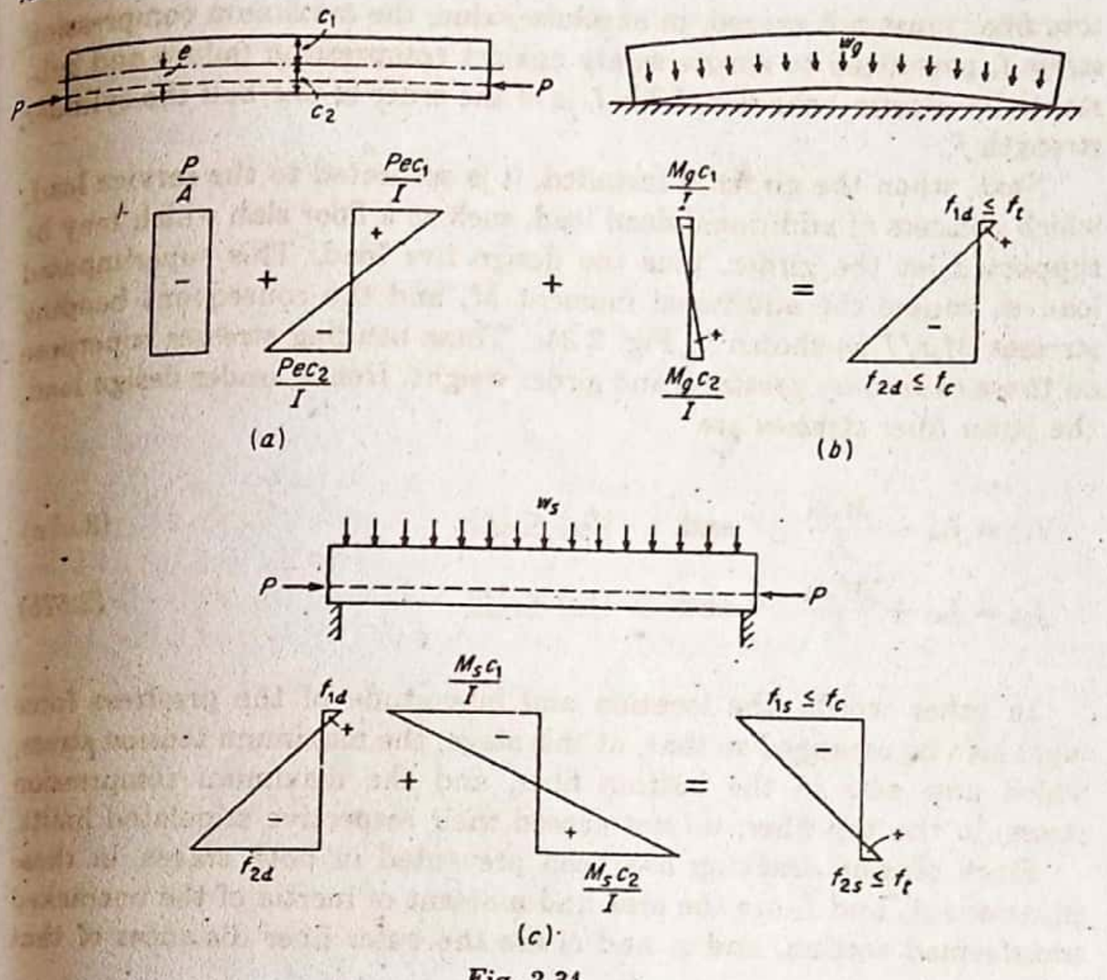


Fig. 2.34

those due to prestress, as shown. These three types of stresses are caused by prestressing and the consequent dead-load stresses resulting from upward deflection; their sums are designated here as f_{1d} and f_{2d} in top and bottom fibers, respectively. They are distributed as shown. In order to prevent cracking, the maximum concrete tension stress, which at this stage occurs at the top fiber, must not exceed the safe value f_t, stipulated as discussed before.

Hence, at this stage, the outer fiber stresses are:

$$f_{1d} = -\frac{P}{A_t} + \frac{Pec_1}{I_t} - \frac{M_g c_1}{I_t} \quad \text{and} \quad |f_{1d}| \leq |f_t| \tag{2.56a}$$

$$f_{2d} = -\frac{P}{A_t} - \frac{Pec_2}{I_t} + \frac{M_g c_2}{I_t} \quad \text{and} \quad |f_{2d}| \leq |f_c| \tag{2.56b}$$

In other words, the location and magnitude of the prestress force must be so arranged that at this stage the tension in the top fiber does not exceed the stipulated maximum f_t. Likewise, the compression at the bot-

Scanned with CamScanner

tom fiber must not exceed, in absolute value, the maximum compression stress f_c permitted to ensure safety against compression failure and substantially elastic behavior. This f_c is of the order of one-half the cylinder strength f'_c.

Next, when the girder is installed, it is subjected to the service load, which consists of additional dead load, such as a floor slab which may be supported on the girder, plus the design live load. This superimposed load w_s causes the additional moment M_s and the consequent bending stresses $M_s c/I$ as shown in Fig. 2.34c. These bending stresses superpose on those caused by prestress and girder weight. Hence, under design load, the outer fiber stresses are

$$f_{1s} = f_{1d} - \frac{M_s c_1}{I_t} \quad \text{and} \quad |f_{1s}| \leq |f_c| \tag{2.57a}$$

$$f_{2s} = f_{2d} + \frac{M_s c_2}{I_t} \quad \text{and} \quad |f_{2s}| \leq |f_t| \tag{2.57b}$$

In other words, the location and magnitude of the prestress force must also be arranged so that, at this stage, the maximum tension stress, which now acts in the bottom fiber, and the maximum compression stress, in the top fiber, do not exceed their respective stipulated limits.

Since tension cracking has been prevented in both stages, in these equations A_t and I_t are the area and moment of inertia of the uncracked transformed section, and c_1 and c_2 are the outer fiber distances of that section.

It will be observed that the stresses caused by prestressing, f_{1d} and f_{2d}, are of opposite sign to those caused by the design load. It is this arrangement which prevents cracking at design loads, so that the entire cross section of the concrete is available to resist stress. In combination with the fact that high-strength steel is used for reinforcement and that high-strength concrete can be used more effectively in prestressed than in reinforced concrete, this leads to sizable reductions in the required quantities of steel and concrete, to corresponding reductions of dead load, to smaller deflections (owing to the fact that the entire uncracked transformed section is available to provide flexural rigidity), and to improved durability and reduced maintenance because of the absence of hairline cracks.

c. Ultimate strength If the design load is significantly exceeded, the maximum tension stress in the concrete will eventually exceed the modulus of rupture. Tension cracks will form, and the beam will behave essentially like an ordinary cracked reinforced-concrete beam, except for the following: (1) In reinforced concrete, under zero load the strain in the reinforcement is, likewise, zero. In prestressed concrete, in contrast, the strain in the tendons at zero load is not zero, but corresponds to the effective prestress after losses; i.e.,

$$\epsilon_{se} = \frac{f_{se}}{E_s} = \frac{P}{A_s E_s}$$

where P and f_{se} are, respectively, the effective prestress force and corresponding stress. Any further steel strain caused by the applied loads adds to this preexisting strain. (2) The stress-strain characteristics of prestressing steel are quite different from those of reinforcing bars. Figure 2.35 shows typical stress-strain curves for prestressing wire and high-tensile bars. It is seen that in contrast to ordinary reinforcing bars (cf. Fig. 1.10) these steels do not show a definite yield plateau, i.e., continued yielding at constant stress. Yielding develops more gradually, and in the inelastic range the stress-strain curve continues to rise smoothly until the tensile strength is reached. Also, the spread between tensile strength f'_s and yield strength f_y is much smaller in prestressing steels than in reinforcing steels, and the total elongation at rupture ϵ'_s is much smaller.

For relatively small steel ratios, failure occurs by rupture of the steel when it has reached its tensile strength f'_s. In this case the beam is said to be *underreinforced*. The ultimate-strength theory, utilizing the equivalent rectangular stress block (Art. 2.4*f*), predicts such failure with ade-

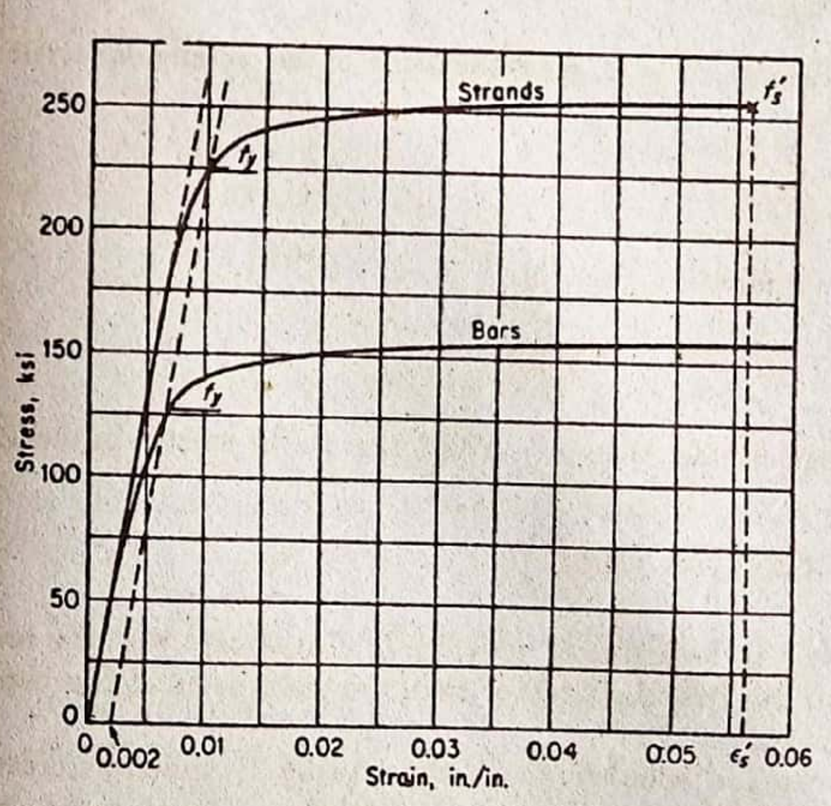


Fig. 2.35 Stress-strain curves for prestressing steels.

Scanned with CamScanner

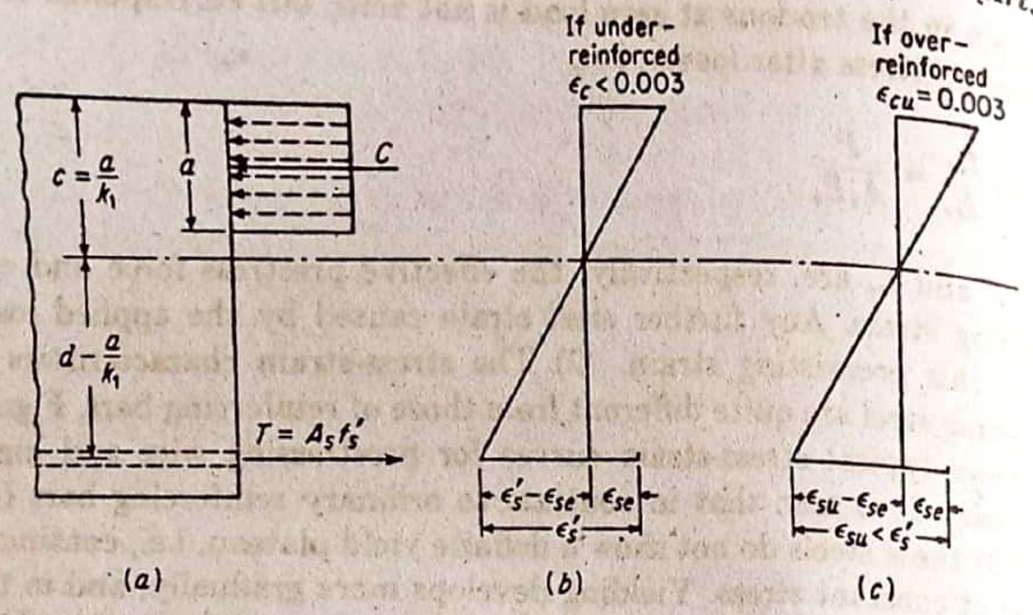


Fig. 2.36

quate accuracy. With reference to Fig. 2.36*a*, the tension force at failure, in this case, is

$$T = A_s f_s'$$

while, for a rectangular section, the compression force is

$$C = 0.85 f_c' ab$$

Equating the two, $T = C$, gives the depth of the rectangular stress block at failure:

$$a = \frac{A_s f_s'}{0.85 f_c' b} \tag{2.58}$$

The ultimate moment, then, is

$$M_u' = T\left(d - \frac{a}{2}\right) = A_s f_s'\left(d - \frac{A_s f_s'}{1.7 f_c' b}\right) \tag{2.59}$$

Introducing the steel ratio $p = A_s/bd$, this can be written in the alternative form

$$M_u' = A_s f_s' d\left(1 - 0.59 p \frac{f_s'}{f_c'}\right) \tag{2.59a}$$

which is seen to be identical with Eq. (2.27*a*), except that the breaking strength of the strand f_s', rather than the yield point of the bars f_y, is seen to govern.

To determine whether the beam actually is underreinforced, one ascertains whether, at the instant of steel failure, i.e., when the steel has reached its ultimate breaking strain ϵ_s', the concrete strain ϵ_c is indeed

smaller than the crushing strain, assumed to be equal to 0.003. Because the steel fractures in the inelastic range, the ultimate strain cannot be obtained by use of Young's modulus; it must be measured on the stress-strain diagram. For prestressing strands, ϵ_s' generally ranges from 0.045 to 0.060. From the strain distribution of Fig. 2.36*b* it is seen that

$$\epsilon_c = (\epsilon_s' - \epsilon_{se}) \frac{a/k_1}{d - a/k_1} \tag{2.60}$$

the depth a having been found from Eq. (2.58). If ϵ_c does not exceed the crushing strain, the beam is underreinforced, and Eqs. (2.59) and (2.59*a*) apply. If ϵ_c exceeds this value, the beam is *overreinforced*. That is, crushing of the concrete will occur before the steel has reached its tensile strength.

In the case of *overreinforced beams*, an explicit calculation of the ultimate moment is not possible for the following reason: The stress in the steel at the moment of concrete failure f_{su}', being smaller than f_s', is not known at the outset. Hence, the depth of the stress block cannot be computed [cf. Eq. (2.58)], making it impossible to calculate the moment of internal forces [cf. Eq. (2.59)]. In this case, successive approximation can be employed as follows: Assume a steel stress f_{su}', read the corresponding strain ϵ_{su} from the stress-strain diagram for the strand, and compute $T = A_s f_{su}'$. Then the depth of the stress block can be calculated from

$$a = \frac{A_s f_{su}'}{0.85 f_c' b} \tag{2.61}$$

and, from the strain relations of Fig. 2.36*c*, the steel strain is

$$\epsilon_{su} = 0.003 \frac{d - a/k_1}{a/k_1} + \epsilon_{se} \tag{2.62}$$

If this value differs from that which corresponds to the assumed steel stress f_{su}', the assumption was incorrect. A new value of ϵ_{su} is assumed on the basis of this first trial, the corresponding next approximation for f_{su}' read from the stress-strain curve, and the procedure repeated until adequate convergence is obtained, usually upon the second, or at most third, trial.

Once the steel stress f_{su}' and the corresponding depth of the stress block a are known, the ultimate moment is

$$M_u' = A_s f_{su}'\left(d - \frac{a}{2}\right) \tag{2.63}$$

The strain distributions of Fig. 2.36*b* and *c* and the calculations based on them neglect the small additional elastic compression strain caused in the concrete at the level of the steel by the prestressing force prior to load application. This strain is of the order of 5 per cent or less of the steel

Scanned with CamScanner

strain at failure, and neglecting it will cause no significant error in the analysis.

When a prestressed beam is underreinforced, failure is preceded by adequate warning, because the large inelastic steel strains cause visible cracking and sagging of the member. The failure of overreinforced beams can occur suddenly and without warning, for which reason this situation is generally avoided, except where special safeguards are used.

A particular, and undesirable, situation may obtain for beams with unusually small steel ratios. In this case, upon formation of tension cracks when the steel has to carry the entire tension, its total breaking strength $A_s f_s'$ may be insufficient to resist that moment at which the tension cracks form. Formation of the first tension crack is then followed by immediate rupture of the steel and sudden collapse of the beam. To guard against this eventuality, the cracking moment can be calculated from Eq. (2.57*b*), with the tension fiber stress f_{cr} taken as the modulus of rupture of the particular concrete. If this cracking moment exceeds the ultimate moment of the cracked section as calculated with Eq. (2.59), the described situation would obtain, and the beam should be redesigned.

These methods of analyzing the ultimate strengths of prestressed rectangular beams assume perfect bonding between steel and concrete. Only in this case is the steel strain equal to the strain in the immediately adjacent concrete so that the strain relationships of Fig. 2.36*b* and *c* hold. For so-called *bonded* members, i.e., where the concrete is poured around and in immediate contact with the strands, nearly perfect bond can be assumed. In some methods of prestressing, unbonded steel is employed. Corrections have been derived (Ref. 2.12) to account for possible slight bond deficiencies in bonded members and for the markedly reduced steel strain in unbonded members. Their design use is discussed in Chap. 11.

Example The beam of Fig. 2.37 is reinforced with prestressing strands whose stress-strain curve is that of Fig. 2.35, with $f_s = 224{,}000$ psi, $f_s' = 256{,}500$, $E_s = 27 \times 10^6$ psi; the concrete cylinder strength is $f_c' = 5000$ psi. The span is 36 ft. Determine (1) the available bending moment for superimposed (useful) loads M_s and (2) the ultimate strength of the beam. Permissible stresses at service load, to avoid cracking and inelastic deformations, are: $f_c = 0.45 f_c' = 2250$ psi and $f_t = 6\sqrt{f_c'} = 425$ psi. Prestress after losses is $f_{se} = 140{,}000$ psi.

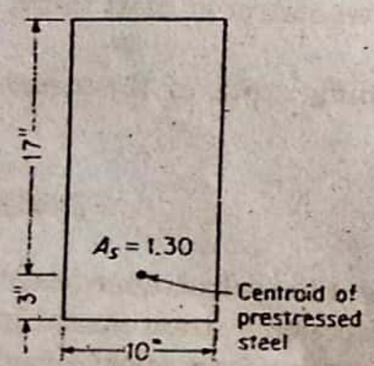


Fig. 2.37

The contribution of the small steel area to the properties of the transformed uncracked section being negligible, those of the gross section will be used. Then $I = 20^3 \times 10/12 = 6670$ in.^{4}; $A = 10 \times 20 = 200$ in.^{2} The prestressing force $P = 140{,}000 \times 1.3 = 182{,}000$ lb. To calculate the maximum moment of the girder due to its own weight, one has weight per foot $= 200/144 \times 150 = 208$ lb per ft, and $M_g = (208 \times 36^2)/8 = 33{,}700$ ft-lb.

Checking the *outer fiber stresses after transfer* of prestress, the girder having deflected away from its soffit [cf. Eqs. (2.56)],

$$f_{\substack{1d \\ 2d}} = -\frac{182{,}000}{200} \pm \frac{182{,}000 \times 7 \times 10}{6670} \mp \frac{33{,}700 \times 12 \times 10}{6670} = \begin{matrix} 405 < & 425 \text{ psi} \\ -2215 < & -2250 \text{ psi} \end{matrix}$$

The moment M_s of the *superimposed loads* is limited to a value which will keep the maximum compression and tension stresses within the stipulated limits. Hence, two values of M_s are computed from Eqs. (2.57), one as governed by the tension stress f_t, and the other by the compression stress f_c. The smaller of the two, evidently, is the maximum admissible moment under design loading. Hence, equating f_{1d} to f_c in Eq. (2.57*a*),

$$-2250 - 405 = -\frac{M_{s1} \times 10}{6670} \qquad M_{s1} = 1{,}775{,}000 \text{ in.-lb}$$

Equating f_{2s} to f_t in Eq. (2.57*b*),

$$425 + 2215 = \frac{M_{s2} \times 10}{6670} \qquad M_{s2} = 1{,}760{,}000 \text{ in.-lb}$$

M_{s2}, being smaller than M_{s1}, is the limiting moment of the superimposed loads under service conditions; i.e.,

$$M_s = 1{,}760{,}000 \text{ in.-lb} = 146{,}700 \text{ ft-lb}$$

To calculate the *ultimate strength*, one must first check whether the beam is underreinforced. If so, it would fail by rupture of the strands at their tension strength of $f_s' = 256{,}500$ psi. Hence, the depth of the rectangular stress block [Eq. (2.58)] is

$$a = \frac{1.30 \times 256{,}500}{0.85 \times 5000 \times 10} = 7.85 \text{ in.}$$

For $f_c' = 5000$, from Eq. (2.31), $k_1 = 0.80$, so that the distance to the neutral axis is $a/k_1 = 7.85/0.80 = 9.8$ in. From Fig. 2.35 it is seen that the ultimate strain of the steel is $\epsilon_s' = 0.056$; the strain due to prestress after losses, $f_{se} = 140{,}000$ psi being in the elastic range of the steel (see Fig. 2.35), is $\epsilon_{se} = 140{,}000/27 \times 10^6 = 0.0052$. Then the maximum compression strain in the concrete [cf. Eq. (2.60)] would be

$$\epsilon_c = (0.056 - 0.0052)9.8/(17.0 - 9.8) = 0.069 > 0.003$$

This strain is seen to exceed by far the assumed ultimate strain of the concrete, which indicates that the concrete would crush before the steel ruptures. In this

sense, then, the beam is overreinforced. Its ultimate strength will, therefore, be calculated by successive approximation.

The steel stress at the moment at which the concrete fails by crushing may be assumed to be $f'_{su} = 225{,}000$ psi; it is seen from Fig. 2.35 that this stress is in the nonlinear, i.e., inelastic, portion of the stress-strain curve. The corresponding steel strain is read from the curve to be $\epsilon_{su} = 0.010$. Then, from Eq. (2.61), $a = 6.9$ in., and, from Eq. (2.62), the corresponding steel strain is $\epsilon_{su} = 0.0081$. The strain read for the assumed f'_{su} from the stress-strain curve (0.010) and that calculated for the same f'_{su} from the strain relationships (0.081) differ by about 20 per cent. Hence, a second approximation is in order.

It will now be assumed that ϵ_{su} is about midway between the two values of the first trial, that is, $\epsilon_{su} = 0.0090$. The corresponding steel stress is read from Fig. 2.35 to be $f_{su} = 220{,}000$ psi. Repeating the steps of the previous calculations, one finds that for this stress $a = 6.75$ in. and, according to the assumed strain relations, $\epsilon_{su} = 0.0086$. It is seen that the two values of the steel strain for this approximation differ by less than 5 per cent. The accuracies of the various data and assumptions involved in this calculation being, at best, of the same order, no further approximation is indicated, and the steel stress at failure can be taken as $f'_{su} = 220{,}000$ psi.

Then, with $a = 6.75$ in., the ultimate moment is [Eq. (2.63)] $M'_u = 1.3 \times 220{,}000 \times 13.13 = 3{,}900{,}000$ in.-lb $= 325{,}000$ ft-lb. The service moment, consisting of that from the weight of the girder M_g and that from the superimposed loads M_s, is

$$M = 33{,}700 + 146{,}700 = 180{,}400 \text{ ft-lb}$$

The ultimate moment is $325/180.4 = 1.8$ times the design or service moment.

It is seen that this method of determining the ultimate strength of prestressed beams, which reflects the actual physical behavior of the member, presupposes a knowledge of the entire stress-strain curve of the particular steel. Even though minimum properties of prestressing steels are standardized in appropriate specifications, details of the shapes of stress-strain curves vary within limits. For this and other reasons, for routine design calculations, simpler approximate formulas have been developed on the basis of experimental information and calculations such as those just presented. These are discussed in Chap. 11.

REFERENCES

2.1 F. E. Richart and R. L. Brown: An Investigation of Reinforced Concrete Columns, *Univ. Illinois Eng. Exp. Sta. Bull.*, no. 267, 1934.

2.2 Hubert Rüsch: Researches toward a General Flexural Theory of Structural Concrete, *J. ACI*, vol. 57, p. 1, July, 1960.

2.3 L. B. Kriz: Ultimate Strength Criteria for Reinforced Concrete, *Proc. ASCE*, vol. 85, no. EM3, 1959; L. B. Kriz and S. L. Lee: Ultimate Strength of Overreinforced Beams, *Proc. ASCE*, vol. 86, no. EM3, 1960.

2.4 A. H. Mattock, L. B. Kriz, and E. Hognestad: Rectangular Concrete Stress Distribution in Ultimate Strength Design, *J. ACI*, vol. 57, p. 875, February, 1961.

2.5 Shear and Diagonal Tension, part 2, Report of ACI-ASCE Committee 326, *J. ACI*, vol. 59, p. 277, 1962 (with extensive bibliography).

2.6 S. A. Guralnick: Shear Strength of Reinforced Concrete Beams, *Trans. ASGE*, vol. 125, p. 603, 1960.

2.7 R. M. Mains: Measurement of the Distribution of Tensile and Bond Stresses along Reinforcing Bars, *J. ACI*, vol. 48, p. 225, 1951.

2.8 P. M. Ferguson and J. N. Thompson: Development Length of High Strength Reinforcing Bars, *J. ACI*, vol. 49, p. 887, 1962.

2.9 R. G. Mathey and David Watstein: Investigation of Bond in Beam and Pullout Specimens with High-yield-strength Deformed Bars, *J. ACI*, vol. 57, p. 1071, 1961.

2.10 W. W. Yu and G. Winter: Instantaneous and Long-time Deflections of Reinforced Concrete Beams under Working Loads, *J. ACI*, vol. 57, p. 29, 1960.

2.11 S. A. Guralnick: High-strength Deformed Steel Bars for Concrete Reinforcement, *J. ACI*, vol. 57, p. 241, 1960.

2.12 J. Warwaruk, M. S. Sozen, and C. P. Siess: Strength and Behavior in Flexure of Prestressed Concrete Beams, *Univ. Illinois Eng. Exp. Sta. Bull.*, no. 464, 1962.

Scanned with CamScanner

chapter 3

BEAMS

GENERAL CONSIDERATIONS

3.1 Working-stress Design and Ultimate-strength Design It is evident from the discussion in Art. 2.4 that the design of reinforced-concrete structures can be performed by either of two alternative methods. The first of these directs attention to *stress conditions* within the structural member under *working loads* and is known as *working-stress design*. The second focuses on the *strength capacity* of the member at conditions corresponding to *failure* and is known as *ultimate-strength design*.

By working-stress methods, allowable stresses are established as some fraction of the stress capacities of the materials, i.e., the yield strength of the steel and the cylinder strength of the concrete. Members are proportioned so that these allowable stresses are not exceeded when working loads are applied. Working load is defined as the sum of the actual dead load of the structure and an estimate of the maximum live load which

will be superimposed at some time during its life. In the concrete stress-strain curves of Fig. 2.2, it is seen that the concrete acts elastically as long as the maximum compressive stress is not more than about $\frac{1}{2}f'_c$. It follows directly that, as long as such stress levels are not exceeded in a reinforced-concrete flexural member, the stress variation in the concrete will be triangular, varying from zero at the neutral axis to a maximum at the extreme compression fiber (see Fig. 2.8*b*). Working-stress design is based on just such a stress distribution, on the grounds that elastic stress limits are not exceeded at working loads.

Ultimate-strength methods, on the other hand, base the design of members on conditions just before failure. Members are proportioned so that the full strength of the cross section is just utilized when the ultimate load is applied. The ultimate load is obtained by multiplying the actual dead load and the anticipated live load by separate overload factors greater than unity. The concrete compressive-stress distribution just before failure is quite different from the triangular distribution described above. At high stress levels, the nonlinearity of the upper part of the concrete stress-strain curve assumes great importance and results in a compressive-stress distribution in the beam such as that shown in Fig. 2.9. Ultimate-strength design is based on the nonlinear compressive-stress variation which is obtained before a member fails.

It may be evident, on further consideration, that working-stress design methods can give no information regarding the actual factor of safety against failure of a reinforced member. The two safety factors often inferred, i.e., (yield stress)/(working stress) in the steel, if steel controls, and (cylinder strength)/(working stress) in the concrete, if concrete controls, are not correct, because in the inelastic range stresses and loads are not proportional. However, elastic analysis does give a realistic representation of conditions in a member at working load and therefore is useful in predicting service-load behavior characteristics such as deflection and crack width. Ultimate-strength methods, on the other hand, permit an accurate appraisal of the strength capacities of members and so permit an evaluation of the actual factor of safety against failure. This is generally the matter of greatest concern to the structural engineer. However, strength procedures give little information about conditions at service load.

Reinforced-concrete structures must perform satisfactorily at working loads but must also be adequately safe against collapse. Consequently, if members are proportioned by working-stress methods, safeguards must be included to ensure that the actual factor of safety against failure is at least as large as implied. Conversely, ultimate-strength design methods must include adequate safeguards to ensure that conditions at working load, particularly crack widths and deflections, are satisfactory.

Scanned with CamScanner

In the chapters which follow, the design of reinforced-concrete members will be treated first from the point of view of ultimate strength, then from the point of view of allowable stresses. While the methods are quite different in fundamental concept, many analogies will be apparent.

3.2 Historical Summary Historically, it is interesting to observe that early proposals for the design of reinforced-concrete members included both working-stress theories and ultimate-strength theories (Ref. 3.1). The theories advanced by Koenen (1886), Neumann (1890), and Coignet and Tedesco (1894) were elastic theories which assumed a linear variation of concrete stress with distance from the neutral axis. The theories of Thullie (1897) and Ritter (1899) were based on a prediction of the ultimate strengths of beams and assumed nonlinear stress distributions.

Because of its relative simplicity, the "straight-line" theory proposed by Coignet and Tedesco gained general acceptance about 1900. It was adopted by code-writing organizations such as the Joint Committee on Standard Specifications for Concrete and Reinforced Concrete (1909), which introduced the concepts of working loads and working stresses. While modifications were made over the ensuing years, the basic concepts of the straight-line theory became firmly established, to the extent that its limitations were generally overlooked.

In the 1930's, however, extensive testing of columns initiated by the American Concrete Institute indicated that measured steel stresses were considerably higher than those predicted by elastic theory. Work by Lyse, Slater, and Richart led to design formulas for columns which could only be described as ultimate-strength formulas in concept, although they were included in modified form in the working-stress design specifications of that time. A 1931 paper by Emperger generated intensive investigation into the ultimate strengths of beams, with significant work done in the United States by Jensen and Whitney.

In the early 1950's, a joint ASCE-ACI committee was organized in the United States to study current knowledge of ultimate-strength design methods and to coordinate research activities. In 1956 that committee published its "Report on Ultimate Strength Design," which contained specific design recommendations. Its proposed formulas were incorporated on an optional basis in the 1956 ACI Building Code (ACI 318-56),[1] and

[1] Throughout this text, repeated reference will be made to the American Concrete Institute and its recommendations. This organization of more than 10,000 members is dedicated to the advancement of concrete technology and of the analysis, design, and construction of reinforced-concrete buildings. As one part of its activity, the American Concrete Institute has published the widely recognized "Building Code Requirements for Reinforced Concrete" (ACI 318-63), which serves as a guide in the design and construction of reinforced-concrete buildings. The Code has no official status in itself. However, it is generally regarded as the most authoritative statement of current good practice in the field of reinforced concrete. As a result, it has been incorporated by law into countless municipal and regional building codes, which do have legal status. Its provisions thereby attain, in effect, legal significance. Most reinforced-concrete structures in the United States and in some other countries are designed in accordance with the current ACI Building Code.

the present ACI Building Code (ACI 318-63) includes a greatly expanded treatment of ultimate-strength design (U.S.D.).

At the same time the present Code continues to include a full set of provisions for working-stress design (W.S.D.). The choice of using U.S.D. or W.S.D. is left to the designer. Over the last two decades, working-stress design has been subjected to a large number of more or less arbitrary adjustments. These were necessary where an analysis based strictly on assumed elastic behavior gave results which had no consistent relation to the actual usable carrying capacity of the member. These adjustments will be discussed in their proper places. Thus, while in earlier times working stresses were calculated on a rational elastic basis but showed no consistent relation to usable strength, the present working-stress design methods in the Code are a mixture of elastic calculations, ultimate-strength concepts, and arbitrary adjustments, all expressed in terms of allowable stresses under design load. In contrast, ultimate-strength design methods are based on a consistent approach which relates the design load that can be allowed on the structure to the actual ultimate strength of the members, as nearly as present knowledge permits this strength to be computed. Working-stress design is retained in the Code primarily because of the long habit of the profession of thinking in terms of elastic stresses. It seems reasonable to assume that the more realistic ultimate-strength methods, which are already widely used today, will become increasingly dominant.

SAFETY PROVISIONS IN REINFORCED-CONCRETE DESIGN

3.3 Safety and Serviceability To serve its purpose, a structure must be safe against collapse and serviceable in use. Serviceability requires that deflections be adequately small, that cracks, if any, be kept to tolerable limits, that vibrations be minimized, etc. Safety requires that the strength of the structure be adequate for all loads which may foreseeably act on it. If the strength of a structure, built as designed, could be predicted with precision, and if the loads and their internal effects (moments, shears, axial forces) were known with equal precision, then safety could be assured by providing a carrying capacity just barely in excess of the known loads. However, there are a number of sources of uncertainty in the analysis, design, and construction of reinforced-concrete structures.

Scanned with CamScanner

These sources of uncertainty, which require a definite margin of safety, may be listed as follows:

1. Actual loads may differ from those assumed in the design.
2. Actual loads may be distributed in a manner different from that assumed in the design.
3. The assumptions and simplifications inherent in any analysis may result in calculated load effects—moments, shears, etc.—different from those which a more rigorous analysis would furnish.
4. The actual structural behavior may differ from that assumed, owing to imperfect knowledge (see Chap. 2).
5. Actual member dimensions may differ from those specified by the designer.
6. Reinforcement may not be in its proper position.
7. Actual material strength may be different from that specified by the designer.

In addition, in establishing a safety specification, consideration must be given to the consequences of failure. In some cases, a failure would merely be an inconvenience. In other cases, loss of life and significant loss of property may be involved. A further consideration should be the nature of the failure, should it occur. A gradual failure, with ample warning permitting remedial measures, is preferable to a sudden, unexpected collapse.

It is evident that the selection of an appropriate margin of safety is not a simple matter. While progress has been made toward rational safety provisions in design codes, the ideal safety specification has not yet been written.

3.4 Applied Loads The loads that act on structures can be divided into two broad categories: *dead load* and *live load*. Dead loads are those which are constant in magnitude and fixed in location. Usually the major part of the dead load is the weight of the structure itself. Live loads, on the other hand, may be either fully or partially in place, or not present at all. They may change in location. Live loads are usually established by local or regional building codes (see Art. 9.2) and include some margin of safety against overload and some allowance for dynamic effect.

If the actual magnitude of live load acting on a structure is plotted against the frequency of occurrence, it is reasonable to expect the results to fall along a curve known as a *normal distribution curve*, as shown in Fig. 3.1*a*. A certain mean value L_m would be observed. Most frequently, the applied load would be close to the mean, but, infrequently, loads considerably larger or smaller than the mean would be observed. A symmetrical distribution would be expected.

If the vertical ordinates were plotted as relative frequency rather than absolute frequency (dividing each ordinate value by the total number of

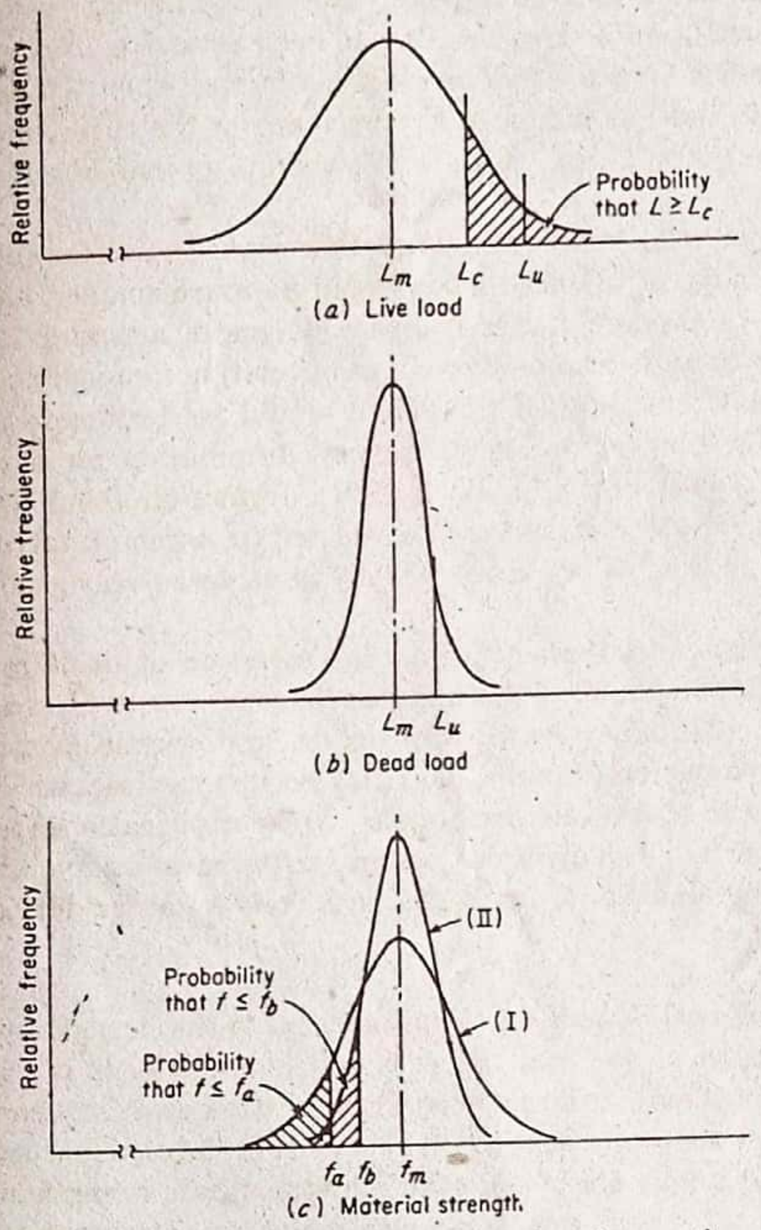


Fig. 3.1 Frequency distribution of loads and strength.

occurrences), then a graph would result which could be used to estimate the probability that the actual load would be greater than, or less than, a certain value. For example, 50 per cent of the area under the curve falls to the left of the mean value; hence there is a 50 per cent probability that a given applied load would be less than the mean value. The properties of normal distribution curves are mathematically defined and have been tabulated in terms of the variability of the given data. It is thus possible to establish the probability that a certain selected load would not be exceeded, knowing the variability of the data and the ratio between that load and the mean load (Ref. 3.2).

It is generally recognized that the value of live load legally specified

Scanned with CamScanner

[Art. 3.

by building codes L_c is considerably above the average value of load $L_$ that will act upon a structure. It has been estimated, for example, tha legally specified loads would be exceeded in only about 10 per cent of th cases. Note that, as indicated by the shape of the curve, no matter ho high the ratio of L_c/L_m, there is still a finite probability that L_c will b exceeded.

A similar relative-frequency function could be plotted for dead loads The variability of the dead loads would be much smaller, however; dead loads can be predicted with a higher degree of accuracy than can liv loads. The total area under the curve of relative frequency would still be 100 per cent, but most of the values would be very close to the mean. Figure 3.1*b* shows a relative-frequency distribution for dead loads, for comparison with Fig. 3.1*a*. With such information about live loads and dead loads, overload factors can be selected to obtain ultimate-load values L_u for design that will be exceeded only in an acceptably small percentage of cases.

An additional consideration in the selection of loads to be used in design is the likelihood of the simultaneous occurrence of various types of loads, e.g., occupancy loads, wind loads, and seismic loads. It appears highly unlikely, for example, that full occupancy load would be acting at the instant of a severe earthquake. Most specifications recognize this. The designer must allow in his design for the most unfavorable distribution and combination of loads that are likely to occur during the life of the structure.

3.5 Structural Strength Fundamental to the strength of a structure is the strength of the material of which it is made. It is convenient to assume that actual material strength, if plotted as a frequency function, would follow a normal distribution curve (Fig. 3.1*c*). The curve would be symmetrical about the mean strength, the mean strength would occur most frequently, and some, but relatively few, strengths far from the mean would occur.

It may be evident that the degree of "peakedness" of the material strength curve would be a function of the quality control of material production. A producer with only average quality control would obtain curve I, while a producer with a higher degree of control would obtain curve II. If a design strength is specified, and if it is stated that in only 1 case in 1000 may the actual strength be less than that specified, producer II could use material with a mean strength much closer to the specified strength than could producer I.

In addition to the strength of the material, structural strength will depend upon the care with which a structure is built, which in turn is a function of the quality of supervision and inspection. Member sizes may

differ from specified dimensions, and reinforcement may be out of position. In this connection, it is observed that care in workmanship is most significant for thin members. If a construction tolerance of ⅛ in. is accepted, for example, and if the thickness of a thin slab is smaller than its specified dimension by the full allowed amount, then this would represent a greater degree of understrength than would the same tolerance applied to a deep beam. The same can be said with regard to the placement of bar reinforcement, which is very critical for slabs as compared with deep beams. Ideally, the selection of safety margin should reflect this difference.

If the distributions of all the uncertainties listed in Art. 3.3 were statistically known in the manner described for loads and material strengths, then a safety margin could be selected as follows: Evidently one cannot design a structure that is 100 per cent safe against collapse, because small probabilities of considerable understrength or unusually high overloads can never be completely eliminated. One could, however, agree on a tolerably small probability of failure, say 1:100,000, and calculate, from the known distribution of uncertainties, that margin of safety which provides this small, specified probability (Ref. 3.2). Because the extensive statistical information necessary for this method exists only fragmentarily at present, today's safety provisions in design codes are a blend of rational approach, past experience, judgment, and compromise.

3.6 Safety Provisions of the ACI Building Code The ACI Code contains recommendations for the design of reinforced-concrete structures by two alternative methods, one based on stress conditions at working loads, and the other based on the ultimate-strength capacity of the structure. The working-stress provisions introduce the safety factor by means of allowable stresses, while the ultimate-strength provisions use separate overload and capacity-reduction factors.

Working-stress provisions The loads used in the design of members by working-stress methods are the computed dead loads and the live loads legally specified by the building code in force at the construction site. Working stresses or allowable stresses, are established at approximately one-half the respective material strengths; they are not to be exceeded at full working loads. The provisions of the Code with respect to allowable stresses are reprinted in Table 3.1 (concrete) and Table 3.2 (steel). Because of the improbability of full occupancy load and full wind or earthquake load occurring at the same moment, members subject to wind or earthquake forces combined with other loads may be proportioned for stresses one-third greater than those specified in Tables 3.1 and 3.2, provided that the section required is not less than that required for the combination of dead and live load.

Scanned with CamScanner

Table 3.1 Allowable stresses in concrete [Art. 3.6

Description		Allowable stresses: For any strength of concrete	For strength of concrete shown below: f'_c = 2500 psi	f'_c = 3000 psi	f'_c = 4000 psi	f'_c = 5000 psi
Modulus of elasticity ratio n		$\frac{29{,}000{,}000}{w^{1.5}33\sqrt{f'_c}}$				
For concrete weighing 145 pcf	n		10	9	8	7
Flexure f_c:						
Extreme fiber stress in compression	f_c	$0.45f'_c$	1125	1350	1800	2250
Extreme fiber stress in tension in plain concrete footings and walls	f_c	$1.6\sqrt{f'_c}$	80	88	102	113
Shear v (as a measure of diagonal tension at a distance d from the face of the support):						
Beams with no web reinforcement*	v_c	$1.1\sqrt{f'_c}$	55*	60*	70*	78*
Joists with no web reinforcement	v_c	$1.2\sqrt{f'_c}$	61	66	77	86
Members with vertical or inclined web reinforcement or combined bent bars and stirrups	v	$5\sqrt{f'_c}$	250	274	316	354
Slabs and footings (peripheral shear)	v_c	$2\sqrt{f'_c}$	100*	110*	126*	141*
Bearing f_c:						
On full area		$0.25f'_c$	625	750	1000	1250
On one-third area or less†		$0.375f'_c$	938	1125	1500	1875

* Special provisions exist for lightweight aggregate concrete.

† This increase shall be permitted only when the least distance between the edges of the loaded and unloaded areas is a minimum of one-fourth the parallel side dimension of the loaded area. The allowable bearing stress on a reasonably concentric area greater than one-third but less than the full area shall be interpolated between the values given.

Table 3.2 Allowable stresses in steel

a. In tension	
For billet-steel or axle-steel concrete reinforcing bars of structural grade	18,000 psi
For main reinforcement, ⅜ in. or less in diameter, in one-way slabs of not more than 12-ft span, 50 per cent of the minimum yield strength specified by the American Society for Testing and Materials for the reinforcement used, but not to exceed	30,000 psi
For deformed bars with a yield strength of 60,000 psi or more and in sizes #11 and smaller	24,000 psi
For all other reinforcement	20,000 psi
b. In compression, vertical column reinforcement	
Spiral columns, 40 per cent of the minimum yield strength, but not to exceed	30,000 psi
Tied columns, 85 per cent of the value for spiral columns, but not to exceed	25,500 psi
Composite and combination columns:	
Structural-steel sections	
For ASTM A36 steel	18,000 psi
For ASTM A7 steel	16,000 psi
Cast-iron sections	10,000 psi
Steel pipe	special provisions
c. In compression, flexural members	special provisions
d. Spirals (yield-strength)	
Hot-rolled rods, intermediate grade	40,000 psi
Hot-rolled rods, hard grade	50,000 psi
Hot-rolled rods, ASTM A432 grade and cold-drawn wire	60,000 psi

Ultimate-strength provisions When designing by ultimate-strength methods, a separation is made between the possibilities of overload and understrength. The computed dead load and the legally specified live load are increased by overload factors to obtain the ultimate loads to be used for design. Overload factors are selected such that these ultimate loads have an acceptably small probability of ever being exceeded. In the selection of overload factors for *live load L*, recognition is given to the fact that legally specified loads themselves include an overload factor (see Fig. 3.1*a*). The recommended factor of increase for live load is 1.8.

Dead loads D have a much smaller variability than live loads. However, there is no prior overload factor included in computed dead loads, as there was for specified live loads. Consistent with these two facts, the overload factor recommended for dead loads is 1.5. The specific recommendation is made that, for structures in such locations and of such proportions that the effects of wind and earthquake may be neglected, the design capacity shall be:

$$U = 1.5D + 1.8L \qquad (A)$$

For structures in whose design *wind loading W* must be included, the

design capacity shall be

$$U = 1.25(D + L + W) \tag{B}$$

or

$$U = 0.9D + 1.1W \tag{C}$$

whichever is greater, provided that no member shall have a capacity less than that required by Eq. (*A*). For structures in which *earthquake loading* E must be considered, E is substituted for W in Eqs. (*B*) and (*C*). The loads L, W, and E are the legally specified loads.

Regarding wind loads, requirement (*C*) governs in those cases in which the dead load tends to stabilize the structure and the wind load tends to produce failure. For instance, the wind load tends to overturn a free-standing smokestack, while its own weight counteracts this tendency. To provide safety, the smallest probable dead load must be combined with the largest probable wind load, which is the reason for requirement (*C*).

In predictions of the ultimate strength of the structure, the Code recognizes that the completed structure or member may be understrength because of understrength materials, inaccuracies in workmanship, manufacturing tolerances, and variations in the degree of supervision and control. Some recognition is given to the relative importance of the members in a structure, i.e., the consequences of failure, and to the state of knowledge of failure mechanisms. The Code provides that the following capacity-reduction factors be applied to the theoretical member strengths calculated for perfect materials and workmanship:

For flexure: $\phi = 0.90$
For diagonal tension, bond, and anchorage: $\phi = 0.85$
For spirally reinforced members with axial loads: $\phi = 0.75$
For tied members with axial load: $\phi = 0.70$

To provide safety, the theoretical ultimate strength, reduced by the coefficient ϕ, must be adequate to resist the ultimate loads specified by Eqs. (*A*) to (*C*).

FLEXURAL DESIGN

3.7 Singly Reinforced Rectangular Beams: Ultimate-strength Design It was shown in Chap. 2 that singly reinforced beams (i.e., beams reinforced with tensile steel only) can fail in two principal ways. If the steel ratio p is relatively low, then at some value of the load the steel will commence yielding. As it yields, the neutral axis migrates upward, the area available to resist compression is reduced, and a secondary

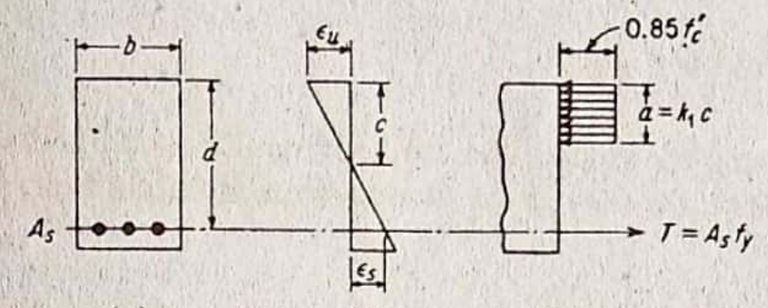


Fig. 3.2

compression failure occurs. If, on the other hand, the steel ratio is high, the concrete will reach its ultimate capacity before the steel yields. While failure due to yielding is a gradual one, with adequate warning of collapse, failure due to crushing of the concrete is sudden and without warning. The first type of failure is therefore preferred. It can be ensured by setting an upper limit on the ratio of tensile reinforcement.[1]

It was shown in the preceding chapter that the balanced steel ratio, such that the steel starts to yield and the concrete reaches its ultimate strain capacity at precisely the same load, is given by the expression

$$p_b = \alpha \frac{0.003}{f_y/E_s + 0.003} \frac{f'_c}{f_y} \tag{2.29}$$

Using the conventional designation $\alpha = 0.85k_1$ and substituting $E_s = 29{,}000{,}000$ psi one obtains the ACI Code equation for balanced steel ratio:

$$p_b = 0.85k_1 \frac{f'_c}{f_y} \frac{87{,}000}{87{,}000 + f_y} \tag{3.1}$$

where $k_1 = 0.85$ for $f'_c \leq 4000$ psi and decreases by 0.05 for every 1000 psi above 4000 psi. The Code specifies that the steel ratio shall not exceed $0.75p_b$, in order that yielding-type failure be ensured. Thus:

$$p_{max} = 0.75p_b \tag{3.2}$$

and, for all sections designed according to this specification, $f_s = f_y$ at failure. Based on the equivalent rectangular compressive-stress distribution described in Art. 2.4*f* and shown in Fig. 3.2, one obtains

$$a = \frac{A_s f_y}{0.85f'_c b} = \frac{pf_y d}{0.85f'_c} \tag{3.3}$$

[1] A third, undesirable, mode of failure may occur in very lightly reinforced beams. If the ultimate resisting moment of the cracked section is less than the moment which produces cracking of the transformed, uncracked section, then the beam will fail immediately upon formation of the crack. In order to avoid this type of failure, which would occur without warning of collapse, the ACI Code establishes a minimum tensile steel ratio equal to $200/f_y$

Scanned with CamScanner

and

$$M'_u = A_s f_y \left(d - \frac{a}{2}\right) \tag{3.4a}$$

By substituting the value of a obtained from Eq. (3.3), and substituting pbd for A_s, into Eq. (3.4a), one obtains the alternative expression

$$M'_u = pf_y bd^2 \left(1 - 0.59p\frac{f_y}{f'_c}\right) \tag{3.4b}$$

which is the same as Eq. (2.27a). In accordance with the safety provisions of the Code, this ultimate-moment capacity M'_u is reduced by the factor ϕ (equal to 0.90 for flexural members) to obtain the ultimate moment M_u to be used in design, so that

$$M_u = \phi A_s f_y \left(d - \frac{a}{2}\right) \tag{3.5a}$$

$$M_u = \phi pf_y bd^2 \left(1 - 0.59p\frac{f_y}{f'_c}\right) \tag{3.5b}$$

Rectangular beam, example 1: ultimate-moment capacity of a given section A rectangular beam has a width of 12 in. and an effective depth to the centroid of the reinforcing steel of 17.5 in. It is reinforced with four No. 9 bars[1] in one row. If $f_y = 60{,}000$ psi and $f'_c = 4000$ psi, what is the ultimate-moment capacity of the beam to be used in design?

The actual steel ratio, $p = 4.00/(12 \times 17.5) = 0.0190$, is found to be less than

$$p_{max} = 0.75 \times 0.85k_1 \frac{f'_c}{f_y}\frac{87{,}000}{87{,}000 + f_y}$$

$$= 0.75 \times 0.85^2 \times \tfrac{4}{60} \times \tfrac{87}{147} = 0.0214$$

Consequently failure by yielding is assured. Then

$$a = \frac{A_s f_y}{0.85f'_c b} = \frac{4.0 \times 60}{0.85 \times 4 \times 12} = 5.89 \text{ in.}$$

$$M_u = \phi A_s f_y \left(d - \frac{a}{2}\right) = 0.90 \times 4.0 \times 60(17.5 - 5.89/2) = 3140 \text{ in.-kips}$$

Rectangular beam, example 2: proportioning a section to resist a given moment Determine the cross section of concrete and area of steel required for a simply supported rectangular beam with a span of 15 ft which is to carry a computed dead load of 1.18 kips per ft and a working live load of 2.30 kips per ft. A 3000-psi concrete is to be used, and the specified steel yield stress is 40,000 psi.

[1] See Table 2, Appendix B, for bar areas.

Overload factors are first applied to the given working loads to obtain the ultimate load for which the beam is to be designed:

Ultimate $w_l = 1.5 \times 1.18 + 1.8 \times 2.30 = 5.92$ kips per ft

$M_u = \frac{1}{8} \times 5.92 \times 15^2 \times 12 = 2000$ in.-kips

The dimensions of the concrete will be directly influenced by the designer's choice of steel ratio. Selecting the maximum steel ratio $p = 0.75p_b$, which will result in the minimum concrete section,

$$p = 0.75 \times 0.85^2 \frac{f'_c}{f_y}\frac{87}{127} = 0.371\frac{f'_c}{f_y}$$

$$M_u = \phi pf_y bd^2 \left(1 - 0.59p\frac{f_y}{f'_c}\right)$$

$$M_u = 0.90 \times 0.371f'_c bd^2(1 - 0.59 \times 0.371) = 0.260f'_c bd^2$$

$$bd^2 = \frac{M_u}{0.260f'_c} = \frac{2000}{0.260 \times 3} = 2560 \text{ in.}^3$$

A concrete section of 10 in. width and 16 in. effective depth will be used. For those dimensions,

$$A_s = pbd = 0.371 \times \tfrac{3}{40} \times 10 \times 16 = 4.44 \text{ in.}^2$$

Three No. 11 bars will be used, providing an area of 4.68 in.^{2}

A somewhat larger beam cross section using less steel may be more economical. In addition, the deflections associated with beams of minimum cross section may be undesirably large. The Code requires a check of deflections if a steel ratio larger than $p = 0.18f'_c/f_y$ is used (see Art. 3.25).

As an alternative solution, the beam will be redesigned with $p = 0.18f'_c/f_y$. In this case,

$$p = 0.18\frac{f'_c}{f_y}$$

$$M_u = 0.90 \times 0.18f'_c bd^2(1 - 0.59 \times 0.18)$$

$$M_u = 0.145f'_c bd^2$$

$$bd^2 = \frac{2000}{0.145 \times 3} = 4600 \text{ in.}^3$$

A beam 11.5 in. wide with an effective depth of 20 in. will be used. For this case,

$$A_s = 0.18 \times \tfrac{3}{40} \times 11.5 \times 20 = 3.11 \text{ in.}^2$$

Four No. 8 bars will be used, providing an area of 3.14 in.^{2}

It is apparent that an infinite number of solutions to the stated problem are possible, depending upon the steel ratio selected. That ratio may vary, according to the Code, from an upper limit of $0.75p_b$ to a lower limit of $200/f_y$.

Scanned with CamScanner

Certain design aids suggest themselves. For example, it would be convenient in practice to graph the relation between the steel ratio p and the value $M_u/\phi bd^2$ for frequently used values of f'_c and f_y. A typical set of such design curves is given by Graph 1, Appendix B.[1] Other ultimate-strength design aids are given in Ref. 3.3.

Rectangular-beam problems can generally be classified as review problems and design problems. The first example illustrated a review problem, in which the section dimensions and material strength capacities were given and it was required to find the moment capacity. The second example illustrated a design problem, in which the design moment was known, as were the material strengths, and it was required to find the proportions of the cross section. There is a certain type of problem which falls into neither category, but which occurs frequently. In this case, the concrete dimensions are given and are known to be adequate to carry the specified moment. It is required only to find the necessary steel area. Typically, this situation obtains at critical design sections of continuous beams, in which the concrete dimensions are often kept constant although the steel reinforcement varies along the span. The concrete dimensions b and d are determined at the maximum moment section, usually at one of the supports. At other supports and at midspan locations, where moments are smaller, the concrete dimensions are known to be adequate, and only the tensile steel is to be found.

Rectangular beam, example 3: determination of steel area for a given moment Using the concrete dimensions of the preceding example ($b = 11.5$ in. and $d = 20$ in.) and the same specified stresses, find the steel area required to resist a design ultimate moment of 1600 in.-kips.

It is possible to obtain a direct solution to this problem by solving Eq. (3.5*b*) for p, which would appear in quadratic form. A somewhat quicker solution may usually be obtained by means of Eq. (3.5*a*). A reasonable value for a is assumed, and A_s is found. By use of Eq. (3.3), a revised estimate of a is obtained, and a modified A_s is obtained from Eq. (3.5*a*). This method can be made to converge

[1] To solve the preceding example by means of Graph 1, for $f_y = 40{,}000$ psi and $f'_c = 3000$ psi, one reads $p_{max} = 0.028$ (at the end of the given curve). The corresponding value of $M_u/\phi bd^2$, from the graph, is 870 psi. Then

$$bd^2 = M_u/(870 \times 0.9) = (2000 \times 1000)/785 = 2560 \text{ in.}^3$$

If $b = 10$ in. and $d = 16$ in. are selected as before, then

$$A_s = pbd = 0.028 \times 10 \times 16 = 4.48 \text{ in.}^2$$

The alternative solution used a steel ratio $p = 0.18f'_c/f_y = 0.18(3/40) = 0.0135$. From the graph, $M_u/\phi bd^2 = 483$, and $bd^2 = 2000 \times 1000/(483 \times 0.9) = 4600$ in.^{3} With $b = 11.5$ in. and $d = 20$ in., $A_s = pbd = 0.0135 \times 11.5 \times 20 = 3.11$ in.^{2}

very rapidly to the final answer. For example,

Assume $a = 4$ in.

$$A_s = \frac{M_u}{\phi f_y(d - a/2)} = \frac{1600}{0.90 \times 40(20 - 2)} = 2.47 \text{ in.}^2$$

Check:

$$a = \frac{A_s f_y}{0.85 f'_c b} = \frac{2.47 \times 40}{0.85 \times 3 \times 11.5} = 3.38 \text{ in.}$$

Assume $a = 3.30$ in.

$$A_s = \frac{1600}{0.90 \times 40 \times (20 - 1.65)} = 2.42 \text{ in.}^2$$

Check:

$$a = 3.38 \times 2.42/2.47 = 3.30 \text{ in.}$$

as assumed. Use $A_s = 2.42$ in.^{2} Four No. 7 bars will be provided.

Problems such as this can readily be solved using Graph 1. The required steel ratio p can be found for the known $M_u/\phi bd^2$. $A_s = pbd$ is then easily determined.

In the design of reinforced-concrete structures, the decision to use either a relatively high- or low-strength concrete or steel depends upon the economics of the particular case, the availability of materials, the importance of special requirements such as minimum member size, and concern for such factors as deflection and crack widths. In general, higher-strength concrete is attained by increasing the amount of cement in the mix. Since cement is the most expensive of the several ingredients, the cost of the concrete increases substantially with increasing strength. On the other hand, high-strength steels, produced either metallurgically or by cold-working lower-strength bars, are available at only slightly increased cost. It can be concluded that, while at the present time steel with a yield stress of 40 ksi is most widely used, in the near future bars of substantially higher strength will come into general use. Concrete strengths will probably remain at about present levels or increase somewhat with improved production methods. The reader may also wish to study Graph 1, Appendix B, with regard to the effect of changes in f_y and f'_c at various steel ratios.

PROBLEMS

U.S.D.: Singly reinforced rectangular beams:

1. A tensile-reinforced beam has a width of 10 in. and an effective depth of 20 in. to the centroid of the bars, which are placed all in one row. If steel with a yield stress of 60,000 psi is used with concrete having $f'_c = 4000$ psi, find the

Scanned with CamScanner

ultimate resisting moment M_u for the following cases: (*a*) $A_s = 2$ No. 8 bars, (*b*) $A_s = 2$ No. 10 bars, (*c*) $A_s = 3$ No. 10 bars.

2. A singly reinforced rectangular beam is to be designed, with effective depth 1.5 times the width, to carry a working live load of 1500 plf, in addition to its own weight, on a 24-ft simple span. Using U.S.D. methods, with $f_y = 40{,}000$ psi and $f'_c = 4000$ psi, determine the required concrete dimensions and steel reinforcement (*a*) for $p = 0.18f'_c/f_y$ and (*b*) for $p = p_{max}$. Comment on your results, and include a sketch of each cross section drawn to scale.

3. A rectangular beam is to span 20 ft between simple supports and must carry a parallel partition weighing 800 plf of beam, in addition to a concentrated live load of 15,000 lb which acts at midspan. Design the beam, using $f_y = 50{,}000$ psi and $f'_c = 5000$ psi.

4. A four-span continuous beam of constant rectangular section is supported at *A*, *B*, *C*, *D*, and *E*. Ultimate moments resulting from analysis are:

At supports, ft-kips		*At midspan, ft-kips*	
M_a	= 92	M_{ab}	= 105
M_b	= 147	M_{bc}	= 92
M_c	= 134	M_{cd}	= 92
M_d	= 147	M_{de}	= 105
M_e	= 92		

Determine the required concrete dimensions for this beam, using $d = 1.75b$, and find the required reinforcement for all critical moment sections. Use a maximum steel ratio of $p = 0.50p_b$, $f_y = 60{,}000$ psi, and $f'_c = 5000$ psi.

3.8 Doubly Reinforced Rectangular Beams: Ultimate-strength Design If a beam is limited in cross section, it may happen that the concrete cannot develop the compression force required to resist the given bending moment. In this case reinforcing is added in the compression zone, resulting in a so-called *doubly reinforced* beam, i.e., one with compression as well as tension reinforcement. Working-stress design indicates in an excessively restrictive manner that compression reinforcement is required for an economically designed beam whenever the steel ratio exceeds the value p_c [Eq. (3.24)]. In contrast, ultimate-strength design recognizes the much larger true compression capacity of the concrete. It calls for compression reinforcement only when the steel ratio exceeds the much larger value $0.75p_b$. In consequence, the use of compression reinforcement has decreased markedly with the introduction and wider use of ultimate-strength design methods. However, there are situations in which it is used for reasons other than strength. It has been found that the inclusion of some compression steel will reduce the long-term deflections of members (see Art. 2.7). In addition, in some cases, bars will be placed in the compression zone for minimum-moment loading (see Art. 8.9) or as stirrup support bars continuous throughout the beam span (see

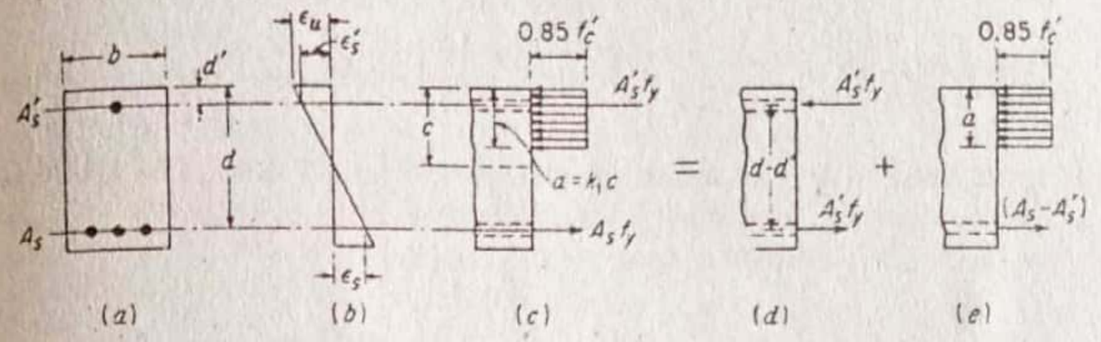


Fig. 3.3 Doubly reinforced rectangular beam.

Art. 3.19). It is often desirable to account for the presence of such reinforcement in flexural design.

If, in a doubly reinforced beam, the tensile-steel ratio p is equal to or less than $p_{max} = 0.75p_b$, the strength of the beam may be approximated within acceptable limits by disregarding the compression bars. The strength of such a beam will be controlled by tensile yielding, and the lever arm of the resisting moment will ordinarily be but little affected by the presence of the compression bars.

If the tensile steel ratio is larger than $0.75p_b$, a somewhat more elaborate analysis is indicated. In Fig. 3.3*a*, a rectangular beam cross section is shown with compression steel A'_s placed a distance d' from the compression face, and with tensile steel A_s at effective depth d. If it is assumed for the moment that both A'_s and A_s are stressed to f_y at failure, the total resisting moment can be thought of as the sum of two parts. The first part, M' is provided by the couple consisting of the force in the compression steel A'_s and the force in an equal area of tension steel:

$$M'_1 = A'_s f_y (d - d') \tag{3.6}$$

as shown in Fig. 3.3*d*. The second part, M'_2, is the contribution of the remaining tension steel $(A_s - A'_s)$ acting with the compression concrete:

$$M'_2 = (A_s - A'_s) f_y \left(d - \frac{a}{2}\right) \tag{3.7}$$

where the depth of the stress block is

$$a = \frac{(A_s - A'_s) f_y}{0.85 f'_c b} \tag{3.8}$$

Defining $p = A_s/bd$ and $p' = A'_s/bd$, this can be written as

$$a = \frac{(p - p') f_y d}{0.85 f'_c} \tag{3.8a}$$

Scanned with CamScanner

The total resisting moment is then [Art. 3.8

$$M'_u = M'_2 + M'_1 = (A_s - A'_s)f_y\left(d - \frac{a}{2}\right) + A'_s f_y(d - d') \tag{3.9}$$

In accordance with the safety provisions of the ACI Code, this ultimate-moment capacity is reduced by the factor ϕ to obtain the ultimate moment M_u to be used in design:

$$M_u = \phi M'_u = \phi\left[(A_s - A'_s)f_y\left(d - \frac{a}{2}\right) + A'_s f_y(d - d')\right] \tag{3.10}$$

This development is predicated on the assumption that both the tension steel and the compression steel are at the yield stress when the beam fails. It is highly desirable, for reasons given earlier, that failure be precipitated by tensile yielding rather than by crushing of the concrete. This can be ensured by setting an upper limit on the tensile steel ratio. The balanced tensile steel ratio for a doubly reinforced beam is $p_b + p'$, where p_b is calculated according to Eq. (3.1). In order to ensure the same margin against brittle-concrete failure in a doubly reinforced beam as in a singly reinforced beam, one should have $p_{max} = 0.75(p_b + p')$. The ACI Code specifies somewhat more liberally that $p_{max} = 0.75p_b + p'$, or

$$(p - p')_{max} = 0.75p_b$$

Whether or not the compression steel will have yielded at failure can be determined as follows: Referring to Fig. 3.3*b*, and taking as the limiting case $\epsilon'_s = \epsilon_y$, one obtains, from geometry,

$$\frac{c}{d'} = \frac{\epsilon_u}{\epsilon_u - \epsilon_y} \quad \text{or} \quad c = \frac{\epsilon_u}{\epsilon_u - \epsilon_y}d'$$

With the neutral axis so established, summing forces in the horizontal direction (see Fig. 3.3*c*) gives:

$$pf_y bd = 0.85k_1 f'_c bc + p'f_y bd$$

$$(p - p') = 0.85k_1\frac{f'_c}{f_y}\frac{c}{d}$$

$$(p - p') = 0.85k_1\frac{f'_c}{f_y}\frac{d'}{d}\frac{\epsilon_u}{\epsilon_u - \epsilon_y} \tag{3.11}$$

Taking $\epsilon_u = 0.003$ as usual and $\epsilon_y = f_y/E_s$, with $E_s = 29{,}000{,}000$ psi, one obtains the minimum value of $(p - p')$ which results in compressive yielding:

$$(p - p') \geq 0.85k_1\frac{f'_c}{f_y}\frac{d'}{d}\frac{87{,}000}{87{,}000 - f_y} \tag{3.11a}$$

If $(p - p')$ is less than this limiting value, the compression steel stress at failure is less than the yield stress, and an analysis taking into account strains and actual stress in the compressive steel is necessary.[1]

If compression bars are used in a flexural member, precautions must be taken to ensure that these bars will not buckle outward under load, spalling off the outer concrete. The ACI Code requires that such bars be anchored by ties or stirrups, which shall not be less than ¼ in. in diameter, spaced not farther apart than 16 bar diameters or 48 tie diameters. At least one tie at each spacing should extend completely around all longitudinal bars, and such stirrups or ties should be used throughout the distance in which the compression reinforcement is required.

Compression-reinforced beam, example 1: ultimate-moment capacity of a given section A rectangular beam has a width of 12 in. and an effective depth to the centroid of the tension reinforcement of 18 in. The tension reinforcement consists of six No. 10 bars in two rows. Compression reinforcement consisting of two No. 9 bars is placed 2½ in. from the compression face of the beam. If $f_y = 50{,}000$ psi and $f'_c = 5000$ psi, what is the ultimate-moment capacity of the beam to be used in design?

$$A_s = 7.59 \qquad p = \frac{A_s}{bd} = \frac{7.59}{12 \times 18} = 0.0352$$

$$A'_s = 2.00 \qquad p' = \frac{A'_s}{bd} = \frac{2.00}{12 \times 18} = 0.0093$$

$$A_s - A'_s = 5.59 \qquad p - p' = \frac{A_s - A'_s}{bd} = \frac{5.59}{12 \times 18} = 0.0259$$

Check:

$$p_b = 0.85k_1\frac{f'_c}{f_y}\frac{87{,}000}{87{,}000 + f_y}$$

$$= 0.85 \times 0.80\,\frac{5}{50}\,\frac{87}{137} = 0.0432$$

$$p_{max} = 0.75 \times 0.0432 = 0.0324$$

Since $p = 0.0352$ is larger than p_{max}, the beam must be analyzed as doubly reinforced. Checking limits on $(p - p')$.

$$(p - p')_{max} = 0.75p_b = 0.0324$$

$$(p - p')_{min} = 0.85k_1\frac{f'_c}{f_y}\frac{d'}{d}\frac{87{,}000}{87{,}000 - f_y}$$

$$= 0.85 \times 0.80\,\frac{5}{50}\,\frac{2.5}{18}\,\frac{87}{37} = 0.0222$$

[1] As an alternative, the contribution of the compression steel could conservatively be neglected in the analysis.

Scanned with CamScanner

Since the actual $(p - p') = 0.0259$ is between these limits, failure will be initiated by tensile yielding, and the compression steel will have yielded at failure. Then

$$M_1 = \phi A_s' f_y (d - d')$$
$$= 0.90 \times 2.00 \times 50(15.5) = 1400 \text{ in.-kips}$$
$$a = \frac{(A_s - A_s')f_y}{0.85 f_c' b} = \frac{5.59 \times 50}{0.85 \times 5 \times 12} = 5.48 \text{ in.}$$
$$M_2 = \phi(A_s - A_s')f_y \left(d - \frac{a}{2}\right)$$
$$= 0.90(5.59)50 \times 15.26 = 3840 \text{ in.-kips}$$
$$M_u = M_1 + M_2 = 1400 + 3840 = 5240 \text{ in.-kips}$$

Compression-reinforced beam, example 2: determination of steel areas for a known moment. A rectangular beam which must carry a working live load of 2.33 kips per ft and a calculated dead load of 0.98 kips per ft on an 18-ft simple span is limited in cross section for architectural reasons to 10 in. width and 20 in. total depth. If $f_y = 40{,}000$ psi and $f_c' = 3000$ psi, what steel area(s) must be provided?

The working loads are first increased by U.S.D. overload factors to obtain the ultimate design load of $1.5 \times 0.98 + 1.8 \times 2.33 = 5.66$ kips per ft. Then $M_u = \frac{1}{8} \times 5.66 \times 18^2 = 229$ ft-kips $= 2750$ in.-kips. To satisfy spacing and cover requirements (see Art. 3.19), it will be assumed that the tension-steel centroid will be 4 in. above the bottom face of the beam, and that compression steel, if required, will be placed $2\frac{1}{2}$ in. below the beam's top surface. Then $d = 16$ in., and $d' = 2\frac{1}{2}$ in.

First, checking the capacity of the section if singly reinforced, using $p = p_{max}$,

$$p_b = 0.85^2 \times \tfrac{3}{40} \times \tfrac{87}{127} = 0.0371$$
$$p_{max} = 0.0278$$
$$A_s = 0.0278 \times 10 \times 16 = 4.44 \text{ in.}^2$$
$$a = \frac{A_s f_y}{0.85 f_c' b} = \frac{4.44 \times 40}{0.85 \times 3 \times 10} = 6.96 \text{ in.}$$
$$M_{max} = \phi A_s f_y \left(d - \frac{a}{2}\right) = 0.90 \times 4.44 \times 40 \times 12.52 = 2000 \text{ in.-kips}^*$$

Since the moment capacity of the singly reinforced beam, 2000 in.-kips, is less than the required capacity, 2750 in.-kips, compression steel is needed. Then

$$M_1 = 2750 - 2000 = 750 \text{ in.-kips}$$
$$A_s' = \frac{M_1}{\phi f_y (d - d')} = \frac{750}{0.90 \times 40 \times 13.5} = 1.54 \text{ in.}^2$$

* Alternatively, the quantity M_{max} may easily be found from Graph 1. For $f_y = 40{,}000$ psi and $f_c' = 3000$ psi, the graph gives $p_{max} = 0.028$, and the corresponding value of $M_u/\phi b d^2$ is 870 psi. Then, for $b = 10$ in. and $d = 16$ in.,

$$M_u = M_{max} = \frac{(0.9 \times 870 \times 10 \times 16^2)}{1000} = 2000 \text{ in.-kips}$$

giving the required compressive-steel area and one part of the tensile-steel area. Denoting the tensile-steel area, tensile-steel ratio, and maximum moment of the singly reinforced beam as $\bar{A}_s$, $\bar{p}_{max}$, and $\bar{M}_{max}$, respectively, the second part of the tensile-steel requirement in the doubly reinforced beam $(A_s - A_s')$ is equal to $\bar{A}_s$. [That is, $(p - p') = \bar{p}_{max}$, and $M_2 = \bar{M}_{max}$.]

$$(A_s - A_s') = 4.44 \text{ in.}^2$$
$$A_s = 4.44 + 1.54 = 5.98 \text{ in.}^2$$

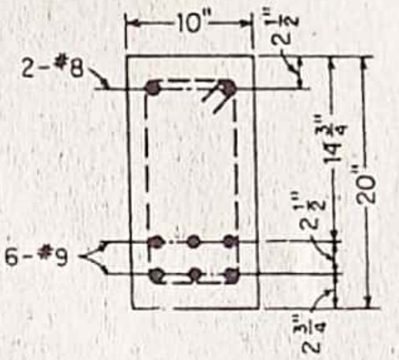


Fig. 3.4

Two No. 8 bars will be used for compression reinforcement, with six No. 9 bars providing the required tensile-steel area, as shown in Fig. 3.4. In order to place the tension bars within the 10 in. beam width, two rows of three bars each are used. Note that in design cases such as this, no check of $(p - p')$ is required, since this quantity is equal to the maximum value of $0.75\,p_b$.

PROBLEMS

U.S.D.: Doubly reinforced rectangular beams:

1. A rectangular concrete beam measures 12 in. in width and has an effective depth to the tensile-steel centroid of 18 in. Compression steel, consisting of two No. 8 bars, is located 2.5 in. from the compression face of the beam. If $f_c' = 4000$ psi and $f_y = 60{,}000$ psi, what is the ultimate moment capacity of the beam, according to ACI Code, for the following alternative tensile-steel areas: (*a*) $A_s =$ 3 No. 10 bars, (*b*) $A_s = 4$ No. 10 bars, (*c*) $A_s = 6$ No. 10 bars.

2. For architectural reasons, a certain rectangular beam of 16 ft span is limited in cross section to a width of 8 in. and a total depth of 16 in. (effective depth = 12 in.). It must carry a total working live load of 1.40 kips per ft, and a total dead load (including its own weight) of 1.10 kips per ft. If $f_c' = 4000$ psi and $f_y = 40{,}000$ psi, what reinforcement is required?

3.9 T Beams: Ultimate-strength Design With the exception of precast systems, reinforced-concrete floors are almost always monolithic. Forms are built for beam soffits and sides and for the underside of slabs, and the entire floor is poured at once, from the bottom of the deepest beam to the top of the slab (see Fig. 1.1*a* and *d*). Beam stirrups and bent bars extend up into the slab. It is evident, therefore, that a part of the slab will act with the upper part of the beam to resist longitudinal compression. The resulting beam cross section is T-shaped rather than rectangular. The slab forms the beam flange, while the part of the beam projecting below the slab forms what is called the *web* or *stem*. The upper part of such a T-beam is stressed laterally in compression as a part of the slab, but this does not reduce its capacity to carry longitudinal compression as a part of the beam.

Scanned with CamScanner

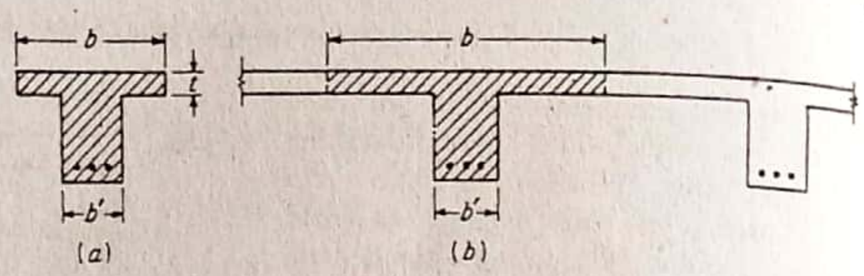


Fig. 3.5 Effective flange widths of T beams.

The first question to be resolved is that of effective width of flange. In Fig. 3.5*a* it is evident that, if the flange is but little wider than the stem width, the entire flange can be considered effective in resisting compression. For the floor system shown in Fig. 3.5*b*, however, it may be equally obvious that elements of the flange midway between the beam stems are less highly stressed in longitudinal compression than those elements directly over the stem. This is so because of shearing deformation of the flange, which relieves the more remote elements of some compressive stress.

While the actual longitudinal compression varies because of this effect, it is convenient in design to make use of an effective flange width which may be smaller than the actual flange width, but which is considered to be uniformly stressed. This effective width has been found to depend primarily on the beam span and on the relative thickness of the slab.

The recommendations for effective width given in the ACI Code are as follows:

1. The effective width b shall not exceed one-fourth the span length of the beam.

2. The overhanging width $(b - b')/2$ on either side of the beam web shall not exceed 8 times the thickness of the slab nor one-half the clear distance to the next beam.

For beams having a flange on one side only, it is recommended that the effective overhanging flange width shall not exceed one-twelfth the span length of the beam, nor 6 times the slab thickness, nor one-half the clear distance to the next beam.

The neutral axis of a T beam may be either in the flange or in the web, depending upon the proportions of the cross section, the amount of tensile steel, and the strengths of the materials. If the calculated depth to the neutral axis is less than or equal to the slab thickness t, the beam can be analyzed as if it were a rectangular beam of width equal to b, the effective flange width. The reason for this is illustrated in Fig. 3.6*a*, which shows a T beam with neutral axis in the flange. The compressive area is indicated by the shaded portion of the figure. If the additional concrete indicated by areas 1 and 2 had been added when the beam was poured, the physical cross section would have been rectangular in shape, with a width b. No

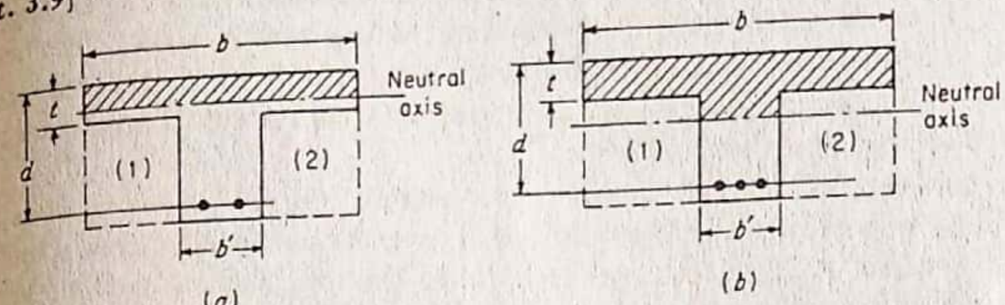


Fig. 3.6 Effective cross sections of T beams.

bending strength would have been added, because areas 1 and 2 are entirely in the tension zone, and tension concrete is disregarded in flexural calculations. The original T beam and the modified rectangular beam are equal in flexural strength, and rectangular beam analysis for flexure applies.

When the neutral axis is in the web, as in Fig. 3.6*b*, the above argument no longer is valid. In this case, methods must be developed which account for the actual T-shaped compressive zone.

Figure 3.7 shows a reinforced-concrete T beam with effective flange width b, web width b', effective depth to the steel centroid d, and flange thickness t. The first step is to locate the neutral axis. Assuming for trial purposes that it will fall in the flange,

$$k_1 c = a = \frac{A_s f_y}{0.85 f'_c b} = \frac{p f_y d}{0.85 f'_c} \tag{3.3}$$

where $p = A_s/bd$. Then

$$c = \frac{p f_y d}{0.85 k_1 f'_c} \tag{3.12}$$

If c is equal to or less than the flange thickness t, the member acts as a rectangular beam of width b and depth d. If c is greater than t, then a T-beam analysis is required.

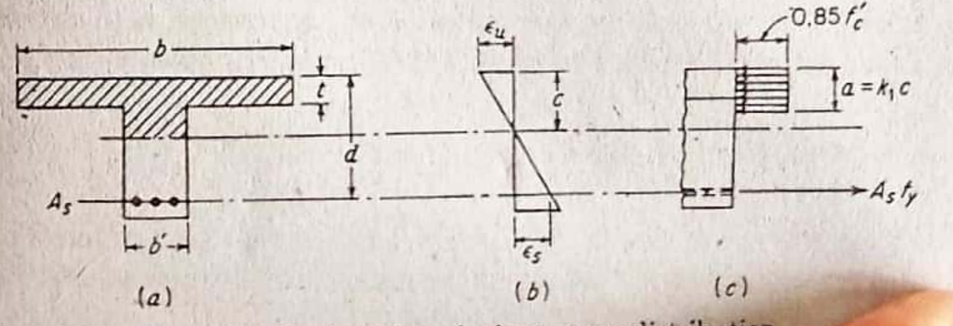


Fig. 3.7 Strain and equivalent stress distribution.

Scanned with CamScanner

It will be assumed in the development that follows that the strength of the T beam is controlled by yielding of the tensile steel. This will usually be the case, because of the large compressive concrete area provided by the flange. In addition, an upper limit can be established for the steel ratio to ensure that this is so.

As a computational device, it is convenient to divide the total tensile steel into two parts. The first part, A_{sf}, represents the steel area which, when stressed to f_y, is required to balance the longitudinal compressive force in the overhanging portions of the flange. Thus

$$A_{sf} = \frac{0.85f'_c(b - b')t}{f_y} \tag{3.13}$$

The force $A_{sf}f_y$ and the equal and opposite force $0.85f'_c(b - b')t$ act with a lever arm $(d - t/2)$ to provide the resisting moment:

$$M'_1 = A_{sf}f_y\left(d - \frac{t}{2}\right) \tag{3.14}$$

The remaining steel area, $(A_s - A_{sf})$, at a stress f_y, is balanced by the compression in the rectangular portion of the beam. The depth of the equivalent rectangular stress block in this zone is found from horizontal equilibrium:

$$a = \frac{(A_s - A_{sf})f_y}{0.85f'_c b'} \tag{3.15}$$

An additional moment M'_2 is thus provided by the forces $(A_s - A_{sf})f_y$ and $0.85f'_c ab'$, acting at the lever arm $(d - a/2)$,

$$M'_2 = (A_s - A_{sf})f_y\left(d - \frac{a}{2}\right) \tag{3.16}$$

and the total resisting moment is the sum of the moments M_1 and M_2:

$$M'_u = M'_1 + M'_2 = A_{sf}f_y\left(d - \frac{t}{2}\right) + (A_s - A_{sf})f_y\left(d - \frac{a}{2}\right) \tag{3.17}$$

This moment is reduced by the factor ϕ in accordance with the safety provisions of the ACI Code to obtain the design ultimate moment:

$$M_u = \phi M'_u = \phi\left[A_{sf}f_y\left(d - \frac{t}{2}\right) + (A_s - A_{sf})f_y\left(d - \frac{a}{2}\right)\right] \tag{3.18}$$

As for rectangular beams, it is desired to ensure that the tensile steel will yield prior to sudden crushing of the compression concrete, as assumed

in the preceding development. Defining

$$p_w = \frac{A_s}{b'd} \tag{3.19}$$

and

$$p_f = \frac{A_{sf}}{b'd} \tag{3.20}$$

the balanced tensile-steel ratio is $p_b + p_f$, where p_b is calculated according to Eq. (3.1). Consistent with the treatment of singly reinforced beams, one should have $p_w \leq 0.75(p_b + p_f)$. According to the ACI Code, $p_w \leq (0.75p_b + p_f)$, or

$$(p_w - p_f) \leq 0.75p_b \tag{3.21}$$

It may be evident that the code provision does not really insure the desired ductility in heavily reinforced cases.

T beam, example 1: ultimate-moment capacity of a given section A floor slab 3 in. thick is supported by reinforced-concrete beams 5 ft on centers which act together with the slab as T beams. The beams are simply supported, and their span is 14 ft. They have a web width of 10 in., an effective depth of 16 in., and a total depth of 20 in. The tensile reinforcement consists of six No. 10 bars in two rows. If $f_y = 60{,}000$ psi and $f'_c = 4000$ psi, what is the ultimate-design-moment capacity of each beam?

The effective flange width cannot exceed

$16t + b' = 16 \times 3 + 10 = 58$ in.
Span/4 $= 14 \times 12/4 = 42$ in.
Center-line beam spacing $= 60$ in.

The flange width is therefore taken equal to 42 in. For six No. 10 bars, $A_s = 7.59$ in.^{2} First checking the location of the neutral axis on the assumption that rectangular-beam formulas may be applied,

$$p = \frac{A_s}{bd} = \frac{7.59}{42 \times 16} = 0.0113$$

$$c = \frac{pf_y d}{0.85k_1 f'_c} = \frac{0.0113 \times 60 \times 16}{0.85 \times 0.85 \times 4} = 3.75 \text{ in.}$$

This exceeds the flange thickness, so a T-beam analysis is indicated.

$$A_{sf} = \frac{0.85f'_c(b - b')t}{f_y} = 0.85 \times \frac{4}{60} \times 32 \times 3 = 5.44 \text{ in.}^2$$

$$(A_s - A_{sf}) = 7.59 - 5.44 = 2.15 \text{ in.}^2$$

$$(p_w - p_f) = \frac{A_s - A_{sf}}{b'd} = \frac{2.15}{10 \times 16} = 0.0134$$

Scanned with CamScanner

Check

$$(p_w - p_f)_{max} = 0.75 \times 0.85k_1 \frac{f'_c}{f_y} \frac{87{,}000}{87{,}000 + f_y}$$

$$= 0.75 \times 0.85^2 \times \tfrac{4}{60} \times \tfrac{87}{147} = 0.0213$$

The actual $(p_w - p_f)$ is seen to be less than this limiting value, ensuring that the beam will fail by tensile yielding. Then

$$M_1 = \phi A_{sf} f_y \left(d - \frac{t}{2}\right) = 0.90 \times 5.44 \times 60 \times 14.50 = 4260 \text{ in.-kips}$$

$$a = \frac{(A_s - A_{sf})f_y}{0.85f'_c b'} = \frac{2.15 \times 60}{0.85 \times 4 \times 10} = 3.80 \text{ in.}$$

$$M_2 = \phi(A_s - A_{sf})f_y \left(d - \frac{a}{2}\right) = 0.90 \times 2.15 \times 60 \times 14.10 = 1640 \text{ in.-kips}$$

$$M_u = M_1 + M_2 = 4260 + 1640 = 5900 \text{ in.-kips}$$

The Code requires that a special check of deflections be made if $(p_w - p_f) > 0.18f'_c/f_y$ or if $f_y > 40{,}000$ psi. In this case,

$$0.18\frac{f'_c}{f_y} = 0.18 \times \frac{4}{60} = 0.0120$$

which is exceeded by the actual steel ratio $(p_w - p_f)$. A check of deflections is, therefore, required by each of these criteria.

In designing T beams, as contrasted to reviewing the capacity of a given section, normally the slab dimensions and beam spacing will have been established by transverse flexural requirements. Consequently, the only additional section proportions that must be determined from flexural considerations are the width and depth of the web and the tensile-steel area.

If the stem dimensions were selected, as for rectangular beams, on the basis of concrete stress capacity in compression, they would be very small because of the large compression flange width furnished by the presence of the slab. Such a design would not represent the optimum solution because of the large tensile-steel requirement resulting from the small effective depth, because of the excessive web reinforcement that would be required for shear, and because of large deflections associated with such a shallow member. It is better practice to select the proportions of the web (1) so as to keep an arbitrarily low web steel ratio $(p_w - p_f)$ or (2) so as to keep web shear stress at desirably low limits or (3) for continuous T beams, on the basis of the flexural requirements at the supports, where the effective cross section is rectangular and of width b'.

T beam, example 2: determination of steel area for a given moment A floor system consists of a 3-in. concrete slab supported by continuous T beams

of 24-ft span, 47 in. on centers. Web dimensions, as determined by negative-moment requirements at the supports, are $b' = 11$ in. and $d = 20$ in. What tensile-steel area is required at midspan to resist an ultimate design moment of 6400 in.-kips if $f_y = 60{,}000$ psi and $f'_c = 3000$ psi?

First determining the effective flange width,

$16t + b' = 16 \times 3 + 11 = 59$ in.
Span/4 $= 24 \times 12/4 = 72$ in.
Center-line beam spacing $= 47$ in.

The center-line T-beam spacing controls in this case, and $b = 47$ in. The concrete dimensions b' and d are known to be adequate in this case, as they have been selected for the larger negative support moment applied to the effective rectangular section $b'd$. The tensile steel at midspan is most conveniently found by trial. Assuming the stress-block depth equal to the flange thickness of 3 in.,

$$d - \frac{a}{2} = 20 - 1.50 = 18.50 \text{ in.}$$

Trial:

$$A_s = \frac{M_u}{\phi f_y(d - a/2)} = \frac{6400}{0.90 \times 60 \times 18.50} = 6.40 \text{ in.}^2$$

$$p = \frac{A_s}{bd} = \frac{6.40}{47 \times 20} = 0.00681$$

$$c = \frac{pf_y d}{0.85k_1 f'_c} = \frac{0.00681 \times 60 \times 20}{0.85 \times 0.85 \times 3} = 3.77 \text{ in.}$$

Since c is greater than t, a T-beam analysis is indicated.

$$A_{sf} = \frac{0.85f'_c(b - b')t}{f_y} = \frac{0.85 \times 3 \times 36 \times 3}{60} = 4.58 \text{ in.}^2$$

$$M_1 = \phi A_{sf} f_y \left(d - \frac{t}{2}\right) = 0.90 \times 4.58 \times 60 \times 18.50 = 4570 \text{ in.-kips}$$

$$M_2 = M_u - M_1 = 6400 - 4570 = 1830 \text{ in.-kips}$$

Assume $a = 4.00$ in.

$$(A_s - A_{sf}) = \frac{M_2}{\phi f_y(d - a/2)} = \frac{1830}{0.90 \times 60 \times 18.00} = 1.88 \text{ in.}^2$$

Check:

$$a = \frac{(A_s - A_{sf})f_y}{0.85f'_c b'} = \frac{1.88 \times 60}{0.85 \times 3 \times 11} = 4.02 \text{ in.}$$

This is satisfactorily close to the assumed value of 4 in.* Then

$$A_s = A_{sf} + (A_s - A_{sf}) = 4.58 + 1.88 = 6.46 \text{ in.}^2$$

* Alternatively, from Graph 1, with

$$\frac{M_u}{\phi bd^2} = \frac{(1830 \times 1000)}{(11 \times 400 \times 0.9)} = 462$$

the steel ratio $(p_w - p_f)$ is found to be 0.0085. Then

$$(A_s - A_{sf}) = (p_w - p_f)b'd = 0.0086 \times 11 \times 20 = 1.88 \text{ in.}^2$$

Scanned with CamScanner

Checking to ensure that tensile yielding will control the strength of the section,

$$(p_w - p_f) = \frac{A_s - A_{sf}}{b'd} = \frac{1.88}{11 \times 20} = 0.00855$$

$$(p_w - p_f)_{max} = 0.75 \times 0.85 k_1 \frac{f'_c}{f_y} \frac{87{,}000}{87{,}000 + f_y}$$

$$= 0.75 \times 0.85^2 \times \tfrac{3}{60} \times \tfrac{87}{147} = 0.0160 > 0.00855$$

The close agreement should be noted between the approximate tensile-steel area of 6.40 in.² found by assuming the stress-block depth equal to the flange thickness and the more exact value of 6.46 in.² found by T-beam analysis. The approximate solution would be satisfactory in many cases.

PROBLEMS

U.S.D.: T beams:

1. A tensile-reinforced T beam is to be designed to carry a uniformly distributed load on a 20-ft simple span. The total ultimate moment at midspan due to all loads is 6240 in.-kips. Concrete dimensions, as governed by web shear and clearance considerations, are $b = 20$ in., $b' = 10$ in., $t = 5$ in., and $d = 20$ in. If $f_y = 60{,}000$ psi and $f'_c = 4000$ psi, what tensile reinforcement is required at midspan?

2. A T beam has an effective flange width of 30 in., web width of 14 in., slab thickness 4 in., and effective depth to the steel centroid of 20 in. If steel having a yield stress of 60,000 psi is used with concrete of $f'_c = 2500$ psi, what is the ultimate-moment capacity of the beam for the following alternative tensile-steel areas: (*a*) $A_s = 3$ No. 11 bars and (*b*) $A_s = 6$ No. 11 bars?

3.10 Singly Reinforced Rectangular Beams: Working-stress Design The design of reinforced-concrete members can also be based on conditions at working load. Working-stress design methods are predicated on the assumption that, at working loads, the concrete stress is sufficiently low so that a linear relation exists between concrete stress and strain. With reference to Fig. 2.8*b*, the following relations have already been derived in Art. 2.4.

$$M = A_s f_s jd \tag{2.15}$$

$$M = \frac{f_c}{2} kjbd^2 \tag{2.17}$$

$$j = 1 - \frac{k}{3} \tag{2.19}$$

If the dimensional properties of the cross section are given, the value of k, which locates the neutral axis, can be found by means of Eq. (2.13).

Substituting $p = A_s/bd$ in that equation, one obtains:

$$b\frac{(kd)^2}{2} - pnbd(d - kd) = 0$$

Dividing through by bd^2,

$$\frac{k^2}{2} - pn(1 - k) = 0$$

from which

$$k = \sqrt{2pn + (pn)^2} - pn \tag{3.22}$$

This expression for k is useful in reviewing the moment capacity of a given beam cross section for which the modular ratio and the steel ratio are known, or for calculating unit stresses in the steel and concrete when a known moment is applied.

If one is *designing* a cross section to resist a given moment, it is often convenient to express k in terms of the desired stresses in the concrete and steel. From the geometry of the strain diagram in Fig. 2.8*c* one obtains

$$\frac{\epsilon_c}{\epsilon_s} = \frac{kd}{d - kd}$$

Substituting $\epsilon_c = f_c/E_c$ and $\epsilon_s = f_s/E_s$,

$$\frac{f_c}{E_c}\frac{E_s}{f_s} = \frac{k}{1 - k}$$

Introducing the modular ratio $n = E_s/E_c$ and the stress ratio $r = f_s/f_c$,

$$\frac{n}{r} = \frac{k}{1 - k}$$

and solving for k,

$$k = \frac{n}{n + r} \tag{3.23}$$

In this case, k is expressed in terms of the modular ratio and the ratio of simultaneous stresses (i.e., the stresses in the concrete and steel at any particular stage of loading). In the design, these stresses would normally be taken as the maximum allowable stresses in the two materials, and the value of k could then be calculated directly from Eq. (3.23).

It may be of interest in certain situations to know the value of p which should be used in designing a beam such that the steel and the concrete

Scanned with CamScanner

will reach their maximum allowable stresses for the same applied moment. This is known as *balanced-stress design*. Equating Eqs. (2.14*a*) and (2.14*b*) and substituting $p = A_s/bd$,

$$\frac{f_c}{2} bkd = pf_s bd$$

Dividing both sides by bd and solving for p, which is then designated as p_e,

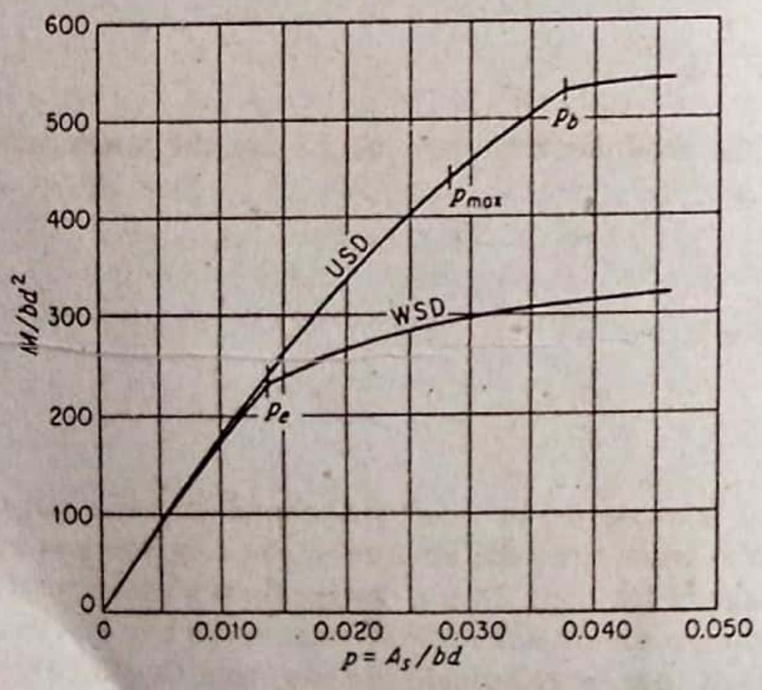
$$p_e = \frac{k}{2}\frac{f_c}{f_s} = \frac{k}{2r}$$

With the desired simultaneous stress values known, Eq. (3.23) can be used to eliminate k, giving

$$p_e = \frac{n}{2r(n + r)} \tag{3.24}$$

The ratio p_e is called the *balanced-stress steel ratio*. If $p < p_e$, the steel will reach its allowable stresses at a lower load than the concrete, and the allowable moment will be determined by Eq. (2.15). If $p > p_e$, the concrete will reach its allowable stress first, and Eq. (2.17) will control.

The relation between beam behavior predicted by W.S.D. theory and that predicted by U.S.D. theory is illustrated by Graph 3.1, which plots resisting moment vs. steel ratio for a singly reinforced beam for f_y = 40,000 psi and f'_c = 3000 psi. Values of M_u predicted by U.S.D. have been



Graph 3.1

divided by a safety factor of 2 in order to permit direct comparison with W.S.D. results.

It is evident from the graph that U.S.D. theory does not differ significantly from elastic theory for values of p smaller than p_e. At that value, elastic theory assumes the resisting moments of steel and concrete to be equal. The bending moment corresponding to p_e can, by that theory, be increased by the addition of tension steel, but this is indicated to be uneconomical, since the steel would be stressed below its allowable value. Any amount of steel in excess of p_e, by elastic theory, provides half as much or less additional strength as does the same amount of steel added to an underreinforced beam with p less than p_e.

U.S.D. theory, confirmed by tests, shows that predictions of flexural capacity by W.S.D. for steel ratios larger than p_e are incorrect. The actual behavior is depicted by the upper curve of Graph 3.1. It shows that additional steel increases the strength of the beam at a practically constant rate until the much larger critical steel ratio p_b is reached. (The maximum steel ratio to be used, according to the ACI Code, is p_{max}, which is also shown on the graph).

The indication of W.S.D. theory that compression reinforcement is required in order to obtain economically moments larger than that corresponding to p_e is incorrect. It is at least partly in order to minimize this feature of W.S.D. that the ACI Code permits the use of compressive steel stress equal to twice the elastic value, thereby reducing the amount of compressive steel required.

Rectangular beam, example 1: allowable moment capacity of a given section A rectangular beam has a width of 12 in. and an effective depth to the centroid of the reinforcing steel of 17.5 in. It is reinforced with three No. 8 bars in one row. If 60,000-psi steel is used at a maximum allowable stress of f_s = 24,000 psi, and 4000-psi concrete is used at an allowable stress of $f_c = 0.45f'_c$ = 1800 psi, what is the maximum working moment that can be resisted?

The steel ratio is $p = A_s/bd = 2.35/(12 \times 17.5) = 0.0112$. With $n = 8$ (see Table 3.1), $pn = 0.0896$, and

$$k = \sqrt{2pn + (pn)^2} - pn = \sqrt{0.1792 + 0.0080} - 0.0896 = 0.343$$

$$j = 1 - \frac{k}{3} = 1 - \frac{0.343}{3} = 0.886$$

If steel stress controls, then from Eq. (2.15),

$$M = A_s f_s jd = 2.35 \times 24 \times 0.886 \times 17.5 = 875 \text{ in.-kips}$$

If concrete stress controls, then from Eq. (2.17),

$$M = \frac{f_c}{2} kjbd^2 = \frac{1.800}{2} 0.343 \times 0.886 \times 12 \times 17.5^2 = 1010 \text{ in.-kips}$$

Scanned with CamScanner

The allowable moment capacity of the beam, controlled by allowable steel stress in this case, is 875 in.-kips. If desired, the actual concrete extreme-fiber stress at a moment of 875 in.-kips can be found as $1800 \times {}^{875}\!/_{1010} = 1560$ psi.

Alternatively, this problem could have been solved by calculating the balanced-stress steel ratio and comparing the actual steel ratio with that value. For example,

$$p_s = \frac{n}{2r(n+r)} = \frac{8}{2(24/1.80)(8+24/1.80)} = 0.0141$$

Since $p = 0.0112 < p_s$, the steel stress controls, and $M = 875$ in.-kips from Eq. (2.15) as before.[1]

Rectangular beam, example 2: proportioning a beam to resist a known moment A rectangular beam must carry a uniformly distributed live load of 680 plf and support the dead load of a wall weighing 380 plf, in addition to its own weight, on a simple span of 24 ft. Design the beam for flexure, using intermediate-grade steel at a working stress of 20,000 psi and 3000-psi concrete at a working stress of 1350 psi.

The total load acting on the beam includes its own weight, which must be estimated. As a first trial a total depth equal to 1 in. per ft of span and a width of one-half that amount are assumed; the beam weight is estimated as $(12 \times 24/144)150 = 300$ plf. The total working load of $680 + 380 + 300 = 1360$ plf produces a maximum moment of

$$M = \tfrac{1}{8} \times 1.36 \times 24^2 = 98.2 \text{ ft-kips}$$

The choice of tensile steel ratio will directly influence the required dimensions of the concrete cross section. Unless circumstances dictate otherwise, the designer using W.S.D. methods would probably use $p = p_s$, such that steel and concrete reach their maximum allowable stresses for the same applied moment. For the given materials, with $p = p_s$,

$$k = \frac{n}{n+r} = \frac{9}{9+20/1.35} = 0.378$$

$$j = 1 - \frac{k}{3} = 1 - \frac{0.378}{3} = 0.874$$

Equating the concrete resisting moment to the total working moment of 98.2 ft-kips = 1180 in.-kips,

$$M = \frac{f_c}{2} kjbd^2$$

$$bd^2 = \frac{2M}{f_c kj} = \frac{2 \times 1180}{1.35 \times 0.378 \times 0.874} = 5290 \text{ in.}^3$$

The relative proportions of b and d may be influenced by architectural factors or by considerations of clearance. In this case, d will be selected equal to 20 in. Then

$$b = {}^{5290}\!/_{400} = 13.2 \text{ in.}$$

and

$$A_s = \frac{M}{f_s jd} = \frac{1180}{20} \times 0.874 \times 20 = 3.38 \text{ in.}^2$$

This area will be provided using two No. 10 bars and one No. 9 bar, all in one row. Concrete dimensions will be rounded off to $b = 13.5$ in. and $d = 20$ in., with a total depth of 22.5 in. As a check, the actual beam dead load is $(13.5 \times 22.5/144) 150 = 316$ plf, which is sufficiently close to the estimated dead load of 300 plf that no revision of moments is necessary.

It is apparent that, had a larger or smaller steel ratio been selected, different concrete dimensions would have resulted. The beam could also have been designed by selecting a steel ratio, finding k and j from Eqs. (3.22) and (2.19), respectively (or from Table 6, Appendix B), and then proceeding as above.

Frequently, in designing continuous beams, it will be required to find the steel area when the concrete dimensions are given and are known to be adequate, since they have been selected for a larger applied moment elsewhere in the span. For this situation, a trial-and-error approach, illustrated by the following example, is quickest.

Rectangular beam, example 3: determination of steel area for a known moment Using the concrete dimensions of the preceding example ($b = 13.5$ in. and $d = 20$ in.), find the steel area required to resist a working moment of 945 in.-kips.

As a first trial, assume that k will take the value for balanced-stress design found from Eq. (3.23). Then

$$k = \frac{n}{n+r} = \frac{9}{9+20/1.35} = 0.378$$

$$j = 1 - \frac{k}{3} = 1 - \frac{0.378}{3} = 0.874$$

$$A_s = \frac{M}{f_s jd} = \frac{945}{20 \times 0.874 \times 20} = 2.70 \text{ in.}^2$$

The values of k and j will now be revised to be consistent with this estimate of

[1] The reader should be aware of design aids included in Appendix B to facilitate the solution of W.S.D. problems. For the present example, with $p = 0.0112$ and $n = 8$, k and j are obtained directly from Table 6 as 0.343 and 0.886, respectively. Since p is less than p_s (obtained from Table 5), steel stress controls, and

$$M = A_s f_s jd = 875 \text{ in.-kips}$$

as before.

Scanned with CamScanner

steel area, using Eqs. (3.22) and (2.19) (or Table 6, Appendix B):

$$p = \frac{A_s}{bd} = \frac{2.70}{13.5 \times 20} = 0.0100$$

$$k = \sqrt{2pn + (pn)^2} - pn = \sqrt{0.180 + 0.008} - 0.090 = 0.343$$

$$j = 1 - \frac{k}{3} = 1 - \frac{0.343}{3} = 0.886$$

A revised estimate of A_s is then obtained:

$$A_s = \frac{945}{20 \times 0.886 \times 20} = 2.66 \text{ in.}^2$$

The difference between the original and revised values of A_s is seen to be negligible.

This example shows that a sufficiently accurate calculation of A_s could be obtained simply by using the balanced-stress value of j. The variation of j with changing steel ratio is not great. In fact, it is likely that the difference between the required steel area and that actually provided will be larger, due to the necessity for using standard bar sizes, than the refinements in calculated values of A_s. In addition, the balanced-stress value of j will always give a conservative estimate of A_s for beams with steel ratios less than the balanced-stress value p_c.

PROBLEMS

W.S.D.: Singly reinforced rectangular beams:

1. A simply supported rectangular beam has a total cross section of 10 × 16 in. and a length of 20 ft. It is reinforced with four No. 5 bars in one row. The distance from the centers of the bars to the lower surface of the beam is 2½ in. With 2500-psi concrete and an allowable stress of 20,000 psi in the steel, what is the resisting moment of the beam?

2. If a concentrated load of 3500 lb were placed on the beam of Prob. 1 at a distance of 7 ft from the support, what would be the maximum unit stress in the concrete and the maximum unit stress in the steel?

3. A simply supported rectangular beam with a span of 18 ft supports a uniform live load of 975 plf and a concentrated load of 3000 lb at the middle of the span. With $f'_c = 3000$ psi and $f_s = 20{,}000$ psi, determine the required cross section and steel area.

4. A simply supported rectangular beam with a span of 17 ft supports a live load which varies uniformly in amount from zero at the left support to 1000 plf at the right support. A 2500-psi concrete and structural-grade reinforcing bars are to be used. Design the beam.

5. A rectangular beam, simply supported, has a width of 14 in. and an effective depth of 26 in. If $n = 9$, and if the allowable unit stresses are 1350 psi and 20,000 psi for the concrete and steel, respectively, what steel area must be used in order that the resisting moment with respect to the strength of the concrete may be the same as the resisting moment with respect to the steel?

6. What would be the resisting moment of the beam in Prob. 5 if the reinforcement consisted of four No. 7 bars?

3.11 Doubly Reinforced Rectangular Beams: Working-stress Design If both steel and concrete are completely elastic, the stress in the compression steel is n times the concrete stress at the same level, since the unit strains in the steel and the adjacent concrete are equal. This allows the compression steel stress to be computed. However, the stresses and strains in the concrete are proportional only at relatively low strains; at higher strains, the stresses no longer increase proportionately. Since the strains in the compression steel and the adjacent concrete remain equal, this means that at higher strain levels the unit stress in the steel, being proportional to the strain, will be larger than it would be if the concrete behaved elastically. This increase in the steel stress over that computed by assuming elastic behavior is accentuated by the fact that concrete, to a certain extent, compresses under constant load or stress (flow or creep). In contrast, steel, if stressed below the yield point, maintains its length essentially unchanged under constant stress. As a result, in a beam reinforced for compression, in the course of time the concrete, by minute flow, transfers part of its compression stress to the steel; the actual stress in the steel becomes higher than that computed on the basis of elastic behavior.

To approximate the effects of the nonlinear concrete stress-strain curve and of plastic flow of the concrete, the ACI Code specifies that the stress in compression reinforcement in beams and eccentric columns be taken as twice the value indicated by the straight-line relation between stress and strain and the appropriate modular ratio, but not of greater value than the allowable stress in tension. This provision is an attempt to compensate in part for the underestimate of the flexural compression strength inherent in working-stress design, as discussed previously.

In Fig. 3.8*a*, a rectangular-beam cross section is shown with com-

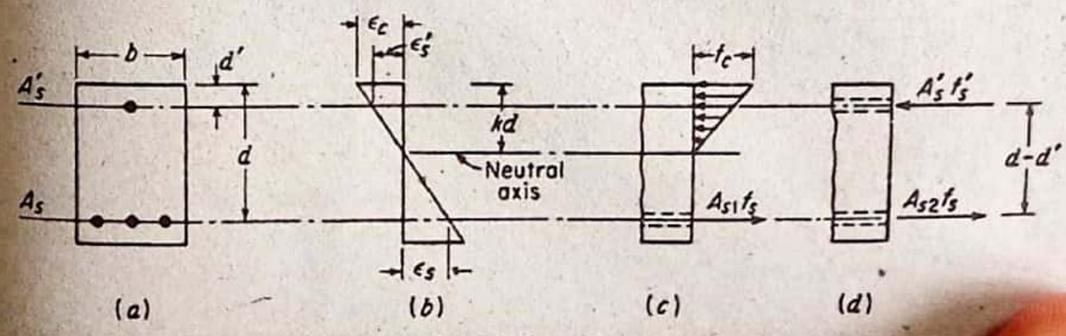


Fig. 3.8 Doubly reinforced rectangular beam.

Scanned with CamScanner

pression steel A'_s placed a distance d' from the compression face and with tensile steel A_s at an effective depth d. The stress in the tensile steel is f_s, while that in the compressive steel is f'_s. It is a design convenience to divide the total resisting moment into two parts. If M is the total resisting moment, and

M_1 = moment that can be developed by given cross section of concrete without compression reinforcement, working with a partial steel area A_{s1} to balance concrete compression

M_2 = moment in excess of M_1, developed by compression reinforcement, acting with additional tensile-steel area A_{s2}

Then

$$M = M_1 + M_2 \qquad \text{and} \qquad A_s = A_{s1} + A_{s2}$$

The moment M_1 depends on the concrete dimensions and allowable stresses and is

$$M_1 = \frac{f_c}{2} kjbd^2 \tag{3.25}$$

where k and j are computed from Eqs. (3.23) and (2.19). The area of tensile steel required for balanced-stress design of a singly reinforced beam having a resisting moment M_1 is

$$A_{s1} = \frac{M_1}{f_s jd} \tag{3.26}$$

A moment M_2 is provided by compressive steel and the remaining tensile steel $A_{s2} = A_s - A_{s1}$, acting with an internal lever arm $(d - d')$:

$$M_2 = A_{s2} f_s (d - d') = A'_s f'_s (d - d') \tag{3.27}$$

The additional moment M_2 may be governed by either the tensile or compressive steel, depending on the stresses in each and their relative areas. From the geometry of Fig. 3.8*b*.

$$\frac{\epsilon_s}{\epsilon'_s} = \frac{d - kd}{kd - d'} = \frac{f_s}{f'_s}$$

Then

$$f'_s = f_s \frac{kd - d'}{d - kd}$$
$$= f_s \frac{k - d'/d}{1 - k}$$

However, as was indicated, the ACI Code recommends that f'_s be taken

equal to twice this value, but not greater than f_s. Thus,

$$f'_s = 2f_s \frac{k - d'/d}{1 - k} \leq f_s \tag{3.28}$$

The moment contribution M_2 can then easily be found from Eq. (3.27).

The above analysis is approximate in that it does not account for the shift in the neutral axis as the compression steel A'_s and the tensile steel A_{s2} are added. The error introduced is so small that it is safely neglected.

Compression-reinforced beam, example 1: allowable moment for a given section A rectangular beam has a width of 12 in. and an effective depth to the centroid of the tensile reinforcement of 18 in. The tension reinforcement consists of four No. 10 bars. Compressive reinforcement is provided by three No. 8 bars, the centroid of which is 2½ in. from the compression face of the beam. If 60,000-psi yield steel is used at a working stress $f_s = 24{,}000$ psi, and $f_c = 1800$ psi (4000-psi concrete), what is the allowable working moment that the beam can resist?

For the balanced-stress beam of 12 in. width and 18 in. effective depth,

$$k = \frac{n}{n + r} = \frac{8}{8 + 24/1.8} = 0.375$$
$$j = 1 - 0.375/3 = 0.875$$

The moment which could be resisted by the beam if singly reinforced with $p = p_s$ is

$$M_1 = \frac{f_c}{2} kjbd^2 = \frac{1.80}{2} 0.375 \times 0.875 \times 12 \times 18^2 = 1150 \text{ in.-kips}$$

and the corresponding steel area is

$$A_{s1} = \frac{M_1}{f_s jd} = \frac{1150}{24 \times 0.875 \times 18} = 3.05 \text{ in.}^2$$

Then $A_{s2} = A_s - A_{s1} = 5.06 - 3.05 = 2.01$ in.^{2}. The stress in the compressive steel is to be taken as twice the modular value, but not to exceed the tensile-steel stress. Thus,

$$f'_s = 2f_s \frac{k - d'/d}{1 - k} = 2 \times 24.0 \frac{0.375 - 2.5/18}{1 - 0.375} = 18.1 \text{ ksi}$$

Since this value is less than $f_s = 24.0$, the compressive steel is assumed to be stressed to 18.1 ksi. Then

$$A_{s2} f_s = 2.01 \times 24.0 = 48.2 \text{ kips}$$
$$A'_s f'_s = 2.35 \times 18.1 = 42.5 \text{ kips}$$

Scanned with CamScanner

The smaller of these two values controls, and

$$M_2 = A_s'f_s'(d - d') = 42.5 \times 15.5 = 660 \text{ in.-kips}$$

The total resisting moment is then the sum of M_1 and M_2:

$$M = 1150 + 660 = 1810 \text{ in.-kips}$$

Compression-reinforced beam, example 2: determination of steel areas to resist a known moment A rectangular beam is limited by architectural considerations to a width of 13 in. and a total depth of 24 in. It must resist a total working moment of 2530 in.-kips. If $f_s = 20{,}000$ psi and $f_c' = 4000$ psi, what reinforcement is required for flexural design?

Under the assumption that two layers of tensile steel will be required, 4 in. will be allowed from the bottom beam face to the tensile-steel centroid. Compressive steel, if required, will be located 3 in. from the compression beam face. For $p = p_c$, the maximum allowable resisting moment of the singly reinforced section is determined: with $f_c' = 4000$ psi, according to the ACI Code, $f_c = 1800$ psi and $n = 8$. Then,

$$k = \frac{n}{n + r} = \frac{8}{8 + 20.0/1.80} = 0.418$$

$$j = 1 - \frac{k}{3} = 1 - \frac{0.418}{3} = 0.861$$

$$M = \frac{f_c}{2} kjbd^2 = \frac{1.80}{2} 0.418 \times 0.861 \times 13 \times 20^2 = 1690 \text{ in.-kips}$$

This is substantially less than the design moment of 2530 in.-kips, indicating the necessity for compression steel. With $M_1 = 1690$,

$$A_{s1} = \frac{M_1}{f_s jd} = \frac{1690}{20.0 \times 0.861 \times 20} = 4.90 \text{ in.}^2$$

$$M_2 = M - M_1 = 2530 - 1690 = 840 \text{ in.-kips}$$

$$A_{s2} = \frac{M_2}{f_s(d - d')} = \frac{840}{20.0 \times 17} = 2.47 \text{ in.}^2$$

$$A_s = A_{s1} + A_{s2} = 4.90 \times 2.47 = 7.37 \text{ in.}^2$$

The stress in the compressive steel is then found:

$$f_s' = 2f_s \frac{k - (d'/d)}{1 - k} = 2 \times 20.0 \frac{0.418 - 3/20}{1 - 0.418} = 18.4 \text{ ksi}$$

but f_s' is not to exceed the stress in the tensile steel. In this case, $f_s' = 18.4$ ksi, and

$$A_s' = \frac{M_2}{f_s'(d - d')} = \frac{840}{18.4 \times 17} = 2.68 \text{ in.}^2$$

The required tensile-steel area of 7.37 in.^{2} will be provided by six No. 10 bars placed in two layers. The compressive steel requirement is met by one No. 8 and two No. 9 bars in one row.

PROBLEMS

W.S.D.: Doubly reinforced beams:

1. A beam of 15 ft simple span carries a uniform live load of 600 plf and a concentrated load of 15,000 lb located 5 ft from the left support. It is limited in size to an overall cross section of 10 × 18 in. What reinforcement must be used if $f_s = 24{,}000$ psi, $f_c = 1800$ psi, and $n = 8$? Assume that the tension steel will be placed in one row, and that the distance from the center of each row to the nearest surface of the beam is 2.5 in.

2. A simply supported rectangular beam with a span of 20 ft has an overall cross section of 8 × 23 in. It is reinforced for compression with two No. 6 bars in one row, the center of which is 2.5 in. from the upper surface of the beam, and for tension with four No. 7 bars in two rows, 2 in. center to center, the center of the lower row being 2.5 in. above the lower surface of the beam. What is the resisting moment of the beam if $f_c = 1125$ psi and $f_s = 20{,}000$ psi, with $n = 10$?

3. If the beam in Prob. 2 supports a single concentrated load at the midspan, what is the maximum safe value of this load?

4. A simply supported beam 10 × 22.5 in. in cross section has a span of 19 ft and is reinforced for tension with six No. 6 bars in two rows, 2 in. center to center, the center of the lower row being 2.5 in. above the lower surface of the beam. The beam also has compression reinforcement consisting of two No. 5 bars with their centers 2 in. from the upper surface of the beam. If $f_s = 18{,}000$ psi and $f_c = 800$ psi, with $n = 15$, what uniform live load per foot can the beam sustain?

3.12 T Beams: Working-stress Design The general discussion of Art. 3.9, with respect to effective width of flange and position of the neutral axis, applies to T beams designed by working-stress methods as well as those designed by ultimate-strength methods. When designing by working-stress methods, however, it is necessary to account for the variable concrete stress in the compression concrete zone. Figure 3.9 shows a T-beam cross section. The compressive force in the web, represented by the area *qrst*, is usually small in comparison with that in the flange and is neglected in the derivation of equations for ordinary design.

On the basis of the geometry of the strain diagram and assumed perfect elasticity of both materials, Eq. (3.23), obtained for rectangular

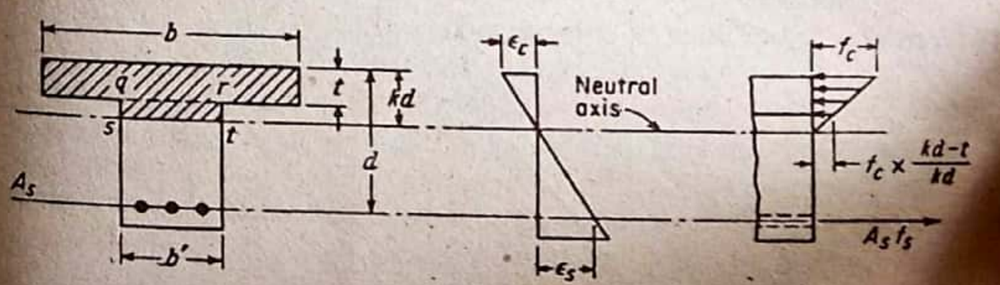


Fig. 3.9 T beam.

Scanned with CamScanner

beams, applies here:

$$k = \frac{n}{n + r} \tag{3.23}$$

This permits the value of k to be calculated easily, provided both n and r are known. Unfortunately, for T beams, the actual $r = f_s/f_c$ is usually not known, even though the maximum allowable stresses are. In a T beam which is a part of a floor system, the compressive area provided by the slab is so large that the actual f_c will be some unknown fraction of its allowable value, and Eq. (3.23) cannot be used directly. In Fig. 3.9 the total tension force is $A_s f_s$, while the total compression force in the flange is

$$\frac{f_c + f_c(kd - t)/kd}{2} bt = f_c \frac{2kd - t}{2kd} bt$$

For horizontal equilibrium, the tension force must equal the compression force, and

$$A_s f_s = pbdf_s = f_c \frac{2kd - t}{2kd} bt \tag{a}$$

From Eq. (3.23),

$$k = \frac{n}{n + r} = \frac{n}{n + f_s/f_c}$$

from which

$$j_c = f_s \frac{k}{n(1 - k)} \tag{b}$$

Substituting this expression for f_c into (*a*) to eliminate unit stresses,

$$k = \frac{np + \frac{1}{2}(t/d)^2}{np + t/d} \tag{3.29}$$

The distance to the center of compression (center of gravity of the trapezoid) from the upper face of the beam is

$$z = \frac{3kd - 2t}{2kd - t} \frac{t}{3} \tag{3.30}$$

and the lever arm of the couple formed by the tensile and compressive forces is

$$jd = d - z \tag{3.31}$$

From the above analysis,

$$j = \frac{6 - 6t/d + 2(t/d)^2 + (t/d)^3(1/2pn)}{6 - 3t/d} \tag{3.32}$$

The resisting moments of the steel and concrete are equal to the product of the lever arm jd of the internal stress couple and the total tension and compression, respectively; hence

$$M = A_s f_s jd \tag{3.33a}$$

or

$$M = f_c \left(1 - \frac{t}{2kd}\right) btjd \tag{3.33b}$$

Approximate equations for resisting moments can be developed as follows: Since the center of gravity of the compression-stress trapezoid is above the middle of the slab, the lever arm jd of the resisting couple is never less than $d - t/2$. The average unit compressive stress

$$f_c \left(1 - \frac{t}{2kd}\right)$$

is never as small as $f_c/2$, except when the neutral axis is at or above the bottom of the slab, in which case rectangular-beam equations apply. Equations (3.33) can be approximated by substituting these limiting values for jd and $f_c(1 - t/2kd)$. Then,

$$M = A_s f_s \left(d - \frac{t}{2}\right) \tag{3.34a}$$

or

$$M = \frac{f_c}{2} bt \left(d - \frac{t}{2}\right) \tag{3.34b}$$

The use of Eqs. (3.34) in *design* is justified for all practical purposes. They must not be used in *review* problems.

T beam, example 1: allowable-moment capacity of a given section A floor slab 4 in. thick is supported by reinforced-concrete beams 9 ft center to center which, together with the slab, act as T beams. The beams are simply supported, and their span is 19 ft. The cross section of each beam below the slab is 10 × 20 in.; the reinforcement consists of six No. 8 bars in two rows, 2 in. center to center vertically, the center of the lower row being 2½ in. above the lower surface of the beam. If a 2500-psi concrete and an allowable steel stress of 20,000 psi are used, what is the maximum allowable working moment of the beam?

For 2500-psi concrete, a working stress $f_c = 1125$ psi is specified by Code, with

Scanned with CamScanner

$n = 10$. The effective width of the compression flange is not to exceed

$$16t + b' = 16 \times 4 + 10 = 74 \text{ in.}$$
$$\frac{\text{Span}}{4} = 19 \times \frac{12}{4} = 57 \text{ in.}$$

Center-line beam spacing = 108 in.
The second criterion controls, and b is taken as 57 in. Then,

$$p = \frac{A_s}{bd} = \frac{4.71}{57 \times 20.5} = 0.00403$$
$$pn = 0.00403 \times 10 = 0.0403$$
$$\frac{t}{d} = \frac{4}{20.5} = 0.195$$
$$k = \frac{pn + 0.5(t/d)^2}{pn + t/d} = \frac{0.0403 + 0.5 \times 0.195^2}{0.0403 + 0.195} = 0.252^*$$

Checking the location of the neutral axis,

$$kd = 0.252 \times 20.5 = 5.16 \text{ in.} > 4.0 \text{ in.}$$

and the beam is, in effect, a T beam as assumed. Then,

$$j = \frac{6 - 6t/d + 2(t/d)^2 + (t/d)^3(1/2pn)}{6 - 3t/d}$$
$$= \frac{6 - 6 \times 0.195 \times 2 \times 0.195^2 + 0.195^3/(2 \times 0.0403)}{6 - 3 \times 0.195} = 0.923^*$$

If the allowable moment is governed by the steel stress, then

$$M = A_s f_s jd = 4.71 \times 20 \times 0.923 \times 20.5 = 1780 \text{ in.-kips}$$

Checking the concrete extreme fiber stress at that moment,

$$f_c = \frac{M}{(1 - t/2kd)btjd}$$
$$= \frac{1{,}780{,}000}{[1 - 4/(2 \times 0.252 \times 20.5)]57 \times 4 \times 0.923 \times 20.5} = 675 \text{ psi}$$

As this is well below the allowable concrete stress of 1125 psi, the working-load capacity of the beam is controlled by the steel as assumed, and the working moment is 1780 in.-kips.

T beam, example 2: determination of steel area for a given moment A floor system consists of a 3-in. concrete slab supported by continuous T beams of 24-ft span, 47 in. on centers. Web dimensions, as determined by negative flexural requirements at the supports, are $b' = 11$ in. and $d = 20$ in. What tensile-steel area is required at midspan to resist a working moment of 2500 in.-kips if $f_s = 20{,}000$ psi and $f'_c = 3000$ psi?

* Values of k and j for T beams may also be found using Graph 12, Appendix B, for known values of the parameters pn and t/d.

As in Example 2 of Art. 3.9, the effective flange width is determined by the 47-in. center-line spacing. For a 3000-psi concrete, the ACI Code specifies that $f_s = 1350$ psi and $n = 9$. The concrete dimensions are known to be adequate, having been selected for the larger negative bending moment at the supports, and only the tensile-steel area need be determined. A trial area is first found, using Eq. (3.34a):

$$A_s = \frac{M}{f_s(d - t/2)} \doteq \frac{2500}{20(20 - 1.50)} = 6.76 \text{ in.}^2$$

If a further refinement is considered necessary, k and j can be found on the basis of this trial steel area, and the steel area refined as indicated:

$$p = \frac{A_s}{bd} = \frac{6.76}{47 \times 20} = 0.0072$$
$$pn = 0.0072 \times 9 = 0.0648$$

Then, with $t/d = 0.15$, from Eqs. (3.29) and (3.32), or from Graph 12, $k = 0.355$ and $j = 0.932$. The revised value of A_s is found from Eq. (3.33a):

$$A_s = \frac{M}{f_s jd} = \frac{2500}{20 \times 0.932 \times 20} = 6.72 \text{ in.}^2$$

The agreement between trial A_s and exact A_s will not always be as close as this, but the trial value will almost always be sufficiently accurate for design purposes. The maximum concrete stress should be checked from Eq. (3.33b):

$$f_c = \frac{M}{(1 - t/2kd)btjd}$$
$$= \frac{2{,}500{,}000}{[1 - 3/(2 \times 0.355 \times 20)]47 \times 3 \times 0.932 \times 20} = 1210 \text{ psi}$$

which is less than the allowed 1350 psi. In order to provide the required A_s of 6.72 in.^{2}, three No. 10 and three No. 9 bars will be used, in two layers.

PROBLEMS

W.S.D.: T beams:

1. A floor slab 4 in. thick is supported by reinforced-concrete beams, 9 ft center to center, which, together with the slab, act as T beams. The beams are simply supported, and their span is 19 ft. The slab supports a live load of 150 psf. The cross section of each beam below the slab is 10 × 20 in.; the reinforcement consists of six No. 7 bars in two rows, 2 in. center to center vertically, the center of the lower row being 2.5 in. above the lower surface of the beam. Determine f_s and f_c, assuming $n = 10$.

2. If each of the beams of Prob. 1 supports a concentrated load of 10,000 lb at midspan in addition to the load from the slab as specified in that problem, determine the revised cross section required and the area of the steel. Assume $f_c = 1350$ psi and $f_s = 20.000$ psi.

Scanned with CamScanner

3. A particular T beam has an effective flange width of 50 in., web width of 11 in., and flange thickness of 4 in. The web depth below the flange is 23 in., and the reinforcement is three No. 11 bars in one row, the center of which is 3 in. above the bottom of the beam. Maximum allowable stresses in the materials are $f_c = 1125$ psi and $f_s = 24{,}000$ psi, with $n = 10$. If the span of the beam is 22 ft, and if it rests freely on brick walls at its ends, what is the maximum uniform load which can be superimposed?

DESIGN FOR SHEAR AND DIAGONAL TENSION

3.13 General Considerations In addition to meeting flexural requirements, beams must be safe against premature failure due to diagonal tension. This mechanism of failure was described in Art. 2.5. Beams may be designed with cross sections sufficiently large that the concrete can resist all the diagonal tension. However, a more economical design will usually result if a smaller cross section is employed, with steel reinforcement provided to carry the excess shear greater than that which can be carried by the concrete alone.

Reinforcement to resist diagonal tensile stresses in a beam may take several forms. A part of the longitudinal steel may be bent up where it is no longer needed to resist flexural tension, as shown in Fig. 3.10*a*. While the ACI Code requires only that the inclined part of any such bar make an angle of at least 30° with the longitudinal part, usually such bars are bent at a 45° angle. Only the center three-fourths of the inclined part of such a bar is to be considered effective as web reinforcement.

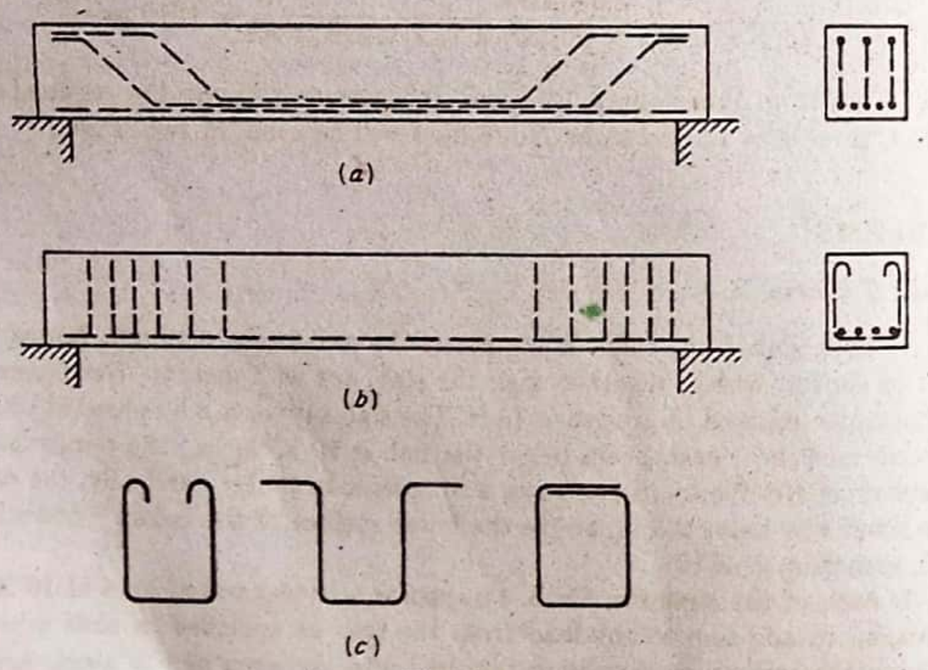


Fig. 3.10

Alternatively, separate web steel may be used, as shown in Fig. 3.10*b*. These separate bars, called *stirrups*, are usually placed perpendicular to the axis of the beam, although they may sometimes be inclined. Where inclined stirrups are used, the code requires that they make an angle of at least 45° with the longitudinal reinforcement and that they be securely anchored against slipping.

Because of the relatively short length of stirrup embedded in the compression zone of a beam, bond requirements (see Art. 3.16) usually dictate the use of special anchorage, obtained by hooking the end of the stirrup. Various forms of stirrups are shown in Fig. 3.10*c*. The 180° and 90° hooks shown in the first two sketches are most common. The closed stirrup shown in the third sketch is convenient when separate straight bars are used for negative flexural reinforcement. These bars can be wired directly to the upper part of the stirrups for temporary support while concrete is poured.

Longitudinal bars at the bottom of a continuous beam are often bent up to provide tensile reinforcement at the top of the beam over the supports. The inclined portions of such bars can be used to provide some or all of the required diagonal tension reinforcement, as previously described. However, because the requirements for longitudinal reinforcement often conflict with those for diagonal tension, and because the saving in steel is usually small, many designers prefer to include separate stirrups to carry all the excess shear, counting on the bent part of the longitudinal bars only to increase the overall safety against diagonal tension failure.

Where vertical stirrups are used, it is undesirable to space them closer than about 4 in.; the size of the stirrups should be chosen so as to avoid a closer spacing. When vertical stirrups are required over a comparatively short distance, it is good practice to space them uniformly over the entire distance, the spacing being calculated for the point of greatest shear (minimum spacing). If the web reinforcement is required over a long distance, and if the shear varies materially throughout this distance, it is more economical to compute the spacings required at several sections and to place the stirrups accordingly, in groups of varying spacing.

Where web reinforcement is needed, the code requires it to be spaced so that every 45° line, representing a potential diagonal crack and extending from the middepth $d/2$ of the member to the longitudinal tension bars, is crossed by at least one line of web reinforcement. When the total working shear stress v exceeds $3\sqrt{f'_c}$ (or when the total ultimate shear stress v_u exceeds $6\phi\sqrt{f'_c}$), every such line must be crossed by at least two lines of web reinforcement. These limitations are shown in Fig. 3.11 for both vertical stirrups and inclined bars, for situations in which the unit shear stress does not exceed the stated limits. For higher shear stresses, the distances s are one-half those shown. The maximum total shear stresses

Scanned with CamScanner

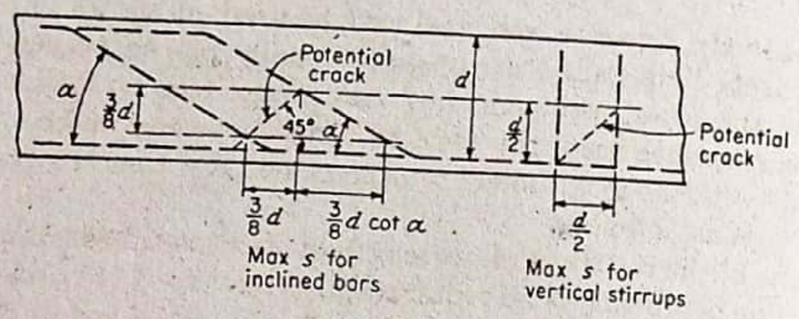


Fig. 3.11

allowed by the ACI Code are a working value of $5\sqrt{f'_c}$ and an ultimate value of $10\phi\sqrt{f'_c}$.

The Code further requires that, where web reinforcement is needed, its area should not be less than $0.0015bs$, where b is the width of the beam, and s is the stirrup spacing. *For beams of* I *or* T *section, only the web width* b' *is considered effective in resisting diagonal tension, and* b' *is to be substituted for* b *in this and all other diagonal-tension formulas.* This minimum area provides a second criterion for maximum spacing:

$$s_{max} = \frac{A_v}{0.0015b}$$

The maximum shear force V, and therefore the maximum calculated shear stress v, generally occur immediately adjacent to a support. Numerous tests have shown, however, that the first diagonal crack occurs not directly at the support, but at some distance from it, of the order of the depth of the beam. This is so because at and adjacent to the supports the additional local stresses caused by reactions counteract crack formation (see Art. 1.9 for strength of concrete under combined stress). *For this reason the ACI Code specifies that the maximum shear stress to be considered is that at a section a distance* d *from the face of the support, where* d *is the effective depth of the beam.* In order that each potential diagonal tension crack originating in the zone of excess shear be contained by web reinforcement, it is required that web reinforcement be provided for a distance d beyond that point at which it is no longer theoretically needed.

Special provisions are included in the Code for cases in which longitudinal stresses are superimposed.

In addition to shear stress resulting from transverse loads, shear stress results from torsional loading of members. Design for this type of shear is treated in Appendix C.

3.14 Ultimate-strength Design for Diagonal Tension

Beams with no web reinforcement Beams which are to be reinforced only for flexural tension must be designed so that shearing stresses throughout the critical portion of the beam are below the value that would result in diagonal tension cracking of the beam web. As discussed

in Art. 2.5*b*, the shear stress causing diagonal cracking can be estimated with the expression

$$v_{cr} = \frac{V_{cr}}{bd} = \left(1.9 + 2500\frac{pVd}{M\sqrt{f'_c}}\right)\sqrt{f'_c} \le 3.5\sqrt{f'_c} \qquad (2.33)$$

where p = longitudinal tensile-steel ratio
d = effective beam depth
V = external shear force at section under consideration
M = external bending moment at section under consideration (not less than Vd)

With V, d, and M in self-consistent units, and $\sqrt{f'_c}$ in psi units, v_{cr} is given in psi units. For reasons of safety, the useful shear capacity of the unreinforced beam web, $v_{uc} = V_{uc}/bd$, is taken as ϕ times the shear stress causing cracking. With a slight rearrangement of terms, one obtains, from Eq. (2.33),

$$v_{uc} = \frac{V_{uc}}{bd} = \phi\left(1.9\sqrt{f'_c} + 2500\frac{pVd}{M}\right) \le 3.5\phi\sqrt{f'_c} \qquad (3.35)$$

The understrength factor ϕ is taken equal to 0.85 for diagonal-tension calculations. As an alternative to Eq. (3.35), the Code permits the use of the simpler, more conservative, but less accurate expression

$$v_{uc} = \frac{V_{uc}}{bd} = 2\phi\sqrt{f'_c} \qquad (3.36)$$

Example 1: beam without web reinforcement A rectangular beam is to be designed to carry an ultimate shear force of 40,000 lb. No web reinforcement is to be used, and f'_c is 4000 psi. What is the minimum beam cross section if controlled by shear?

If no web reinforcement is to be used, it is necessary that the cross-sectional dimensions be selected so that the ultimate shear stress V_u/bd is no larger than the value permitted on the unreinforced web. Adapting Eq. (3.36),

$$v_{uc} = 2\phi\sqrt{f'_c} = 2 \times 0.85\sqrt{4000} = 107 \text{ psi}$$

and

$$bd = \frac{V_u}{v_{uc}} = \frac{40{,}000}{107} = 374 \text{ in.}^2$$

A beam section with $b = 16$ in. and $d = 23.5$ in. will be satisfactory. [Note that Eq. (3.35) may not be used directly in problems of this type because v_{uc} as given by that expression depends upon the section chosen and upon the steel ratio p. Advantage could be taken of the higher permitted value given by Eq. (3.35) by a series of successive trials, however.]

Region in which web reinforcement is required When the unit shearing stress $v_u = V_u/bd$ anywhere in the critical region of a beam exceeds that value which can be resisted by the unreinforced beam web

Scanned with CamScanner

web reinforcement must be provided. For reasons given in Art. 2.5, the shear resistance of the concrete beam web after the first crack has formed can be taken conservatively equal to the shear which caused the first crack, and web reinforcement need be provided only for the excess above that value. For design purposes, the value of shear stress causing cracking is given by Eq. (3.35) or (3.36). The portion of any span through which web reinforcement is required can be found by drawing the shear diagram for the span and superimposing a plot of the value $V_{uc} = v_{uc}bd$.

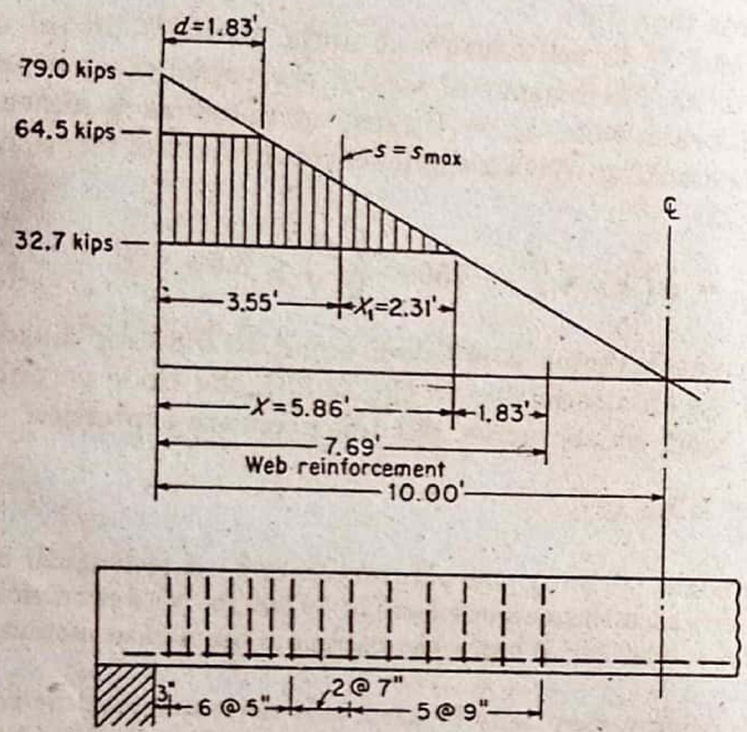


Fig. 3.12

Example 2: limits of web reinforcement A simply supported rectangular concrete beam 16 in. wide, having an effective depth of 22 in., carries a total ultimate load of 7.9 kips per foot on a 20-ft clear span. It is reinforced with 9.86 in.^{2} of tensile steel, which continues uninterrupted into the supports. If $f'_c = 3000$ psi, through what part of the beam is web reinforcement required?

The maximum external shear force occurs at the end of the span, where $V_u = 7.9 \times 20/2 = 79.0$ kips. At the critical section for shear, a distance d from the support, $V_u = 79.0 - 7.9 \times 1.83 = 64.5$ kips. The shear force varies linearly to zero at midspan, as shown in Fig. 3.12*a*. Adopting the simpler criterion of Eq. (3.36),

$$v_{uc} = 2\phi\sqrt{f'_c} = 2 \times 0.85\sqrt{3000} = 93 \text{ psi}$$
$$V_{uc} = v_{uc}bd = 93 \times 16 \times 22 = 32{,}700 \text{ lb}$$

This value is superimposed on the shear diagram, and, from geometry, the point at which web reinforcement theoretically is no longer required is

$$x = 10\,\frac{79.0 - 32.7}{79.0} = 5.86 \text{ ft}$$

from the support face. In accordance with the Code, web reinforcement is carried a distance d beyond this point, and the total distance in which stirrups are provided is $5.86 + 1.83 = 7.69$ ft.

If the more complicated but more accurate Eq. (3.35) is used, the steel ratio, shear force, and bending moment must be known at several points along the span, and the curves of $V_{uc} = v_{uc}bd$ and V_u superimposed to determine the limits of web reinforcement. For the given beam, $p = 9.86/(16 \times 22) = 0.028$. The calculation of v_{uc} and V_{uc} is best done in tabular form as follows:

Distance from support, ft	M, ft-kips	V_u, kips	$v_{uc} = \phi\left(1.9\sqrt{f'_c} + 2500\,\frac{pVd}{M}\right) \le 3.5\phi\sqrt{f'_c}$, psi	$V_{uc} = v_{uc}bd$, kips
0	0	79.0	163	57.4
1	76	71.1	163	57.4
2	142	63.2	137	48.2
3	201	55.3	118	41.6
4	252	47.4	108	38.0
5	296	39.5	103	36.3
6	332	31.6	99	34.8
7	360	23.7	95	33.4
8	379	15.8	93	32.7
9	391	7.9	91	32.0
10	395	0	88	31.0

The ultimate V_u and the shear capacity of the concrete V_{uc} are plotted as functions of the span in Fig. 3.12*b*. Stirrups are required wherever $V_u > V_{uc}$. The point at which stirrups are no longer theoretically required is found, by scaling

Scanned with CamScanner

the diagram, to be 5.70 ft from the support. With the required distance d added to this, the total distance through which stirrups are used is $5.70 + 1.83 = 7.53$ ft.

Design of web reinforcement For beams in which the shear force through the critical region exceeds that which can be resisted by the unreinforced beam web, stirrups or bent bars must be provided to carry the excess. The following equations are developed in Art. 2.5:

For vertical stirrups: $$V_u = V_{cr} + \frac{A_v f_v d}{s} \tag{2.36}$$

For bars inclined at angle α:

$$V_u = V_{cr} + \frac{A_v f_v d(\sin \alpha + \cos \alpha)}{s} \tag{2.37}$$

where V_u = ultimate shear force
V_{cr} = shear force causing cracking of concrete web
A_v = cross-sectional area of web reinforcement
f_v = yield stress of web steel
d = effective beam depth
α = angle of inclination of web reinforcement measured from beam axis
s = spacing of web reinforcement

For design purposes, the predicted strength must be reduced by the understrength factor ϕ. With this modification, and with $V_{uc} = \phi V_{cr}$, Eqs. (2.36) and (2.37) are solved for the required spacing s:

For vertical stirrups: $$s = \frac{A_v f_v \phi d}{(V_u - V_{uc})} \tag{3.37}$$

For bars inclined at angle α: $$s = \frac{A_v f_v \phi d(\sin \alpha + \cos \alpha)}{(V_u - V_{uc})} \tag{3.38}$$

It may be convenient in some cases to express these relationships in terms of the unit shear stress rather than the total shear force. Since

$$(V_u - V_{uc}) = (v_u - v_{uc})bd$$

the last two expressions can be written alternatively as

For vertical stirrups: $$s = \frac{A_v f_v \phi}{(v_u - v_c)b} \tag{3.37a}$$

For bars inclined at angle α: $$s = \frac{A_v f_v \phi(\sin \alpha + \cos \alpha)}{(v_u - v_{uc})b} \tag{3.38a}$$

Example 3: design of web reinforcement Using vertical U stirrups, with $f_v = 40{,}000$ psi, design the web reinforcement for the beam of Example 2.

The solution will be based on the shear diagram in Fig. 3.12*a*. The stirrups must be designed to resist that part of the shear shown shaded. With No. 3

stirrups used for trial, the two maximum spacing criteria are first applied. For $v_u = 64{,}500/(16 \times 22) = 183$ psi, which is less than $6\phi\sqrt{f'_c}$, the spacing must not exceed $d/2 = 23\frac{1}{2} = 11$ in. Also,

$$s_{max} = \frac{A_v}{0.0015b} = \frac{0.22}{0.0015 \times 16} = 9.2 \text{ in.}$$

The second criterion controls in this case, and a maximum spacing of 9 in. is adopted. From the support to a distance d from the support, the excess shear $(V_u - V_{uc}) = 31.8$ kips. In this region, the required spacing is

$$s = \frac{A_v f_v \phi d}{(V_u - V_{uc})} = \frac{0.22 \times 40 \times 0.85 \times 22}{31.8} = 5.2 \text{ in.}$$

This is neither so small that placement problems would result, nor so large that maximum spacing criteria would control, and the choice of No. 3 stirrups is confirmed. Solving Eq. (3.37) for the excess shear at which the maximum spacing can be used,

$$(V_u = V_{uc}) = \frac{A_v f_v \phi d}{s} = \frac{0.22 \times 40 \times 0.85 \times 22}{9} = 18.3 \text{ kips}$$

With reference to Fig. 3.12*a*, this is attained at distance x_1 from the point of zero excess shear, where $x_1 = 5.86 \times 18.3/(79.0 - 32.7) = 2.31$ ft. This is $5.86 - 2.31 = 3.55$ ft from the support face. With this information, a satisfactory spacing pattern can be selected. The first stirrup is usually placed at distance $s/2$ from the support. The following spacing pattern is satisfactory:

1 space	at 3 in.	= 3 in.
6 spaces	at 5 in.	= 30 in.
2 spaces	at 7 in.	= 14 in.
5 spaces	at 9 in.	= 45 in.
Total		92 in.

As an alternative solution, it is possible to plot a curve showing required spacing as a function of distance from the support. Once the required spacing at some reference section, say at the support is determined,

$$s_0 = \frac{A_v f_v \phi d}{(V_u - V_{uc})} = \frac{0.22 \times 40 \times 0.85 \times 22}{46.3} = 3.55 \text{ in.}$$

it is easy to obtain the required spacing elsewhere by a single setting of the slide rule. In Eq. (3.37), only $(V_u - V_{uc})$ changes with distance from the support. For uniform load $(V_u = V_{uc})$ is a linear function of the distance from the point of zero excess shear, 5.86 ft from the support face. Hence, at 1-ft intervals,

$s_1 = 3.55 \times 5.86/4.86 = 4.27$ in.
$s_2 = 3.55 \times 5.86/3.86 = 5.39$ in.
$s_3 = 3.55 \times 5.86/2.86 = 7.27$ in.
$s_4 = 3.55 \times 5.86/1.86 = 11.18$ in.
$s_5 = 3.55 \times 5.86/0.86 = 24.20$ in.

Scanned with CamScanner

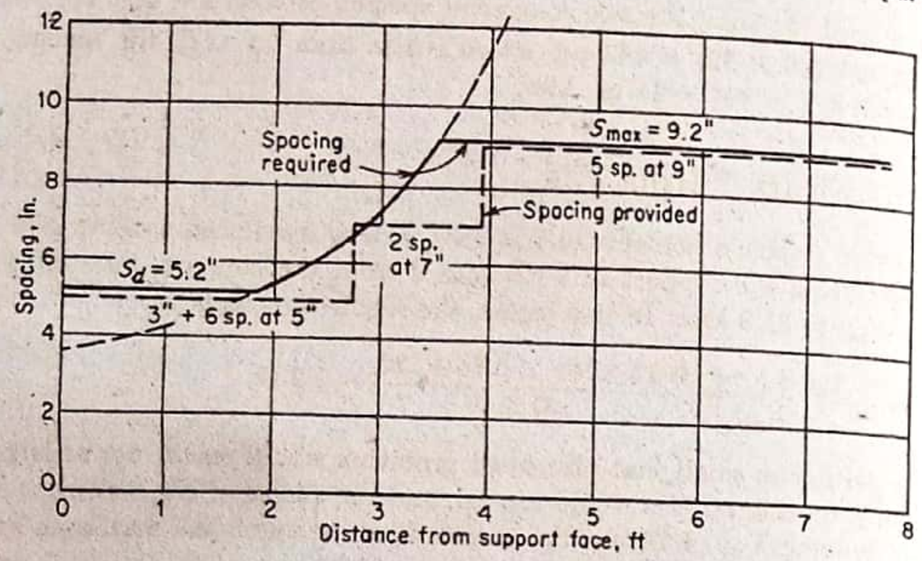


Fig. 3.13

This is plotted in Fig. 3.13, together with the maximum spacing of 9.2 in., and a practical spacing pattern is selected. The spacing at a distance d from the support face is selected as the minimum requirement, in accordance with the ACI Code. The pattern of No. 3 U-shaped stirrups selected (shown on the graph) is identical with the previous solution. In many cases the experienced designer would find it unnecessary actually to plot the spacing diagram of Fig. 3.13 and would select a spacing pattern directly after calculating the required spacing at intervals along the beam.

If the web steel were to be designed on the basis of the excess-shear diagram of Fig. 3.12*b*, the second approach illustrated above would necessarily be selected, and spacings would be calculated at intervals along the span. In this particular case, the maximum permitted spacing of 9.2 in. is less than that required by excess shear anywhere between the point of zero excess shear and a distance d from the support. Consequently, the following spacing could be used:

1 space at 5 in.	= 5 in.
10 spaces at 9 in.	= 90 in.
Total	95 in.

Eleven No. 3 stirrups would be used, rather than the 14 previously calculated, in each half of the span. In designs for which the stress governs the stirrup spacing for both methods rather than the maximum spacing requirements, the saving obtained by the second solution would be even more significant.

PROBLEMS

U.S.D.: Shear and diagonal tension:

1. A beam is to be designed to carry a total ultimate shear of 67,600 lb, using a concrete with $f'_c = 3000$ psi. Proceeding on the basis that the beam cross section will be determined by diagonal tension requirements, select an appropriate width and effective depth (*a*) for a beam in which no web reinforcement is to be used and (*b*) for a beam in which stirrups are used to carry excess shear.

2. A beam of 12 in. width and effective depth 22 in. carries and ultimate uniformly distributed load of 6.0 kips per ft, including its own weight, and is simply supported on an 18-ft span. It is reinforced with three No. 11 bars continuing uninterrupted into the supports. If $f'_c = 4000$ psi, through what part of the beam is web reinforcement required (*a*) if $v_c = 2\phi\sqrt{f'_c}$ and (*b*) if $v_c = (\sqrt{f'_c} + 2500pVd/M)\phi \leq 3.5\phi\sqrt{f'_c}$.

3. In Prob. 2*a*, what effect would a clockwise moment of 200 ft-kips (ultimate) at the right support have on the placement of shear reinforcement previously determined?

4. Design the web reinforcement for the beam of Prob. 2*a* using (*a*) No. 2 stirrups with $f_y = 40{,}000$ psi and (*b*) No. 3 stirrups with $f_y = 40{,}000$ psi. Compare the total weight of web reinforcement for these two alternative designs. Use standard hooks (see Fig. 3.15) at the upper ends of the stirrups. What is your recommendation for the final design?

3.15 Working-stress Design for Diagonal Tension Beams which are to be reinforced only for flexural tension must be designed so that the shearing stresses through the critical portions of the span are below the allowable shearing unit stress permitted on the unreinforced web. This stress is given by

$$v_c = \left(\sqrt{f'_c} + 1300\,\frac{pVd}{M}\right) \leq 1.75\sqrt{f'_c} \tag{3.39}$$

Equation (3.39) will be recognized as being Eq. (3.35) divided by an appropriate safety factor. As an alternative to Eq. (3.39), the Code permits use of the simpler, more conservative, but less accurate

$$v_c = 1.1\sqrt{f'_c} \tag{3.40}$$

When the unit shearing stress anywhere in the critical region of a beam exceeds that value which is allowed on the unreinforced web, as given by Eq. (3.39) or (3.40), web reinforcement must be provided. The shear resistance of the concrete beam web is taken equal to $V_c = v_c bd$, and web reinforcement is provided for the excess above that value.

Working-stress stirrups-spacing formulas, which establish the contribution of web reinforcement in resisting shear, result from a development which is analogous to that used in the derivation of similar ultimate-strength formulas and are:

For vertical stirrups: $$V = V_c + \frac{A_v f_v d}{s} \tag{3.41}$$

For bars inclined at angle α: $$V = V_c + \frac{A_v f_v d(\sin\alpha + \cos\alpha)}{s} \tag{3.42}$$

Scanned with CamScanner

These equations may be solved for the required spacing of web reinforcement:

For vertical stirrups: $$s = \frac{A_v f_v d}{(V - V_c)} \tag{3.43}$$

For bars inclined at angle α: $$s = \frac{A_v f_v d(\sin \alpha + \cos \alpha)}{(V - V_c)} \tag{3.44}$$

It may be convenient in some cases to express the spacing in terms of the unit shear stress rather than the total shear force. Since

$$(V - V_c) = (v - v_c)bd$$

the last two equations can be written

For vertical stirrups: $$s = \frac{A_v f_v}{(v - v_c)b} \tag{3.43a}$$

For bars inclined at angle α: $$s = \frac{A_v f_v(\sin \alpha + \cos \alpha)}{(v - v_c)bd} \tag{3.44a}$$

Example 4: design of web reinforcement A simply supported rectangular beam 16 in. wide, having an effective depth of 22 in., carries a total working load of 5.12 kips per foot on a 20-ft clear span. For $f'_c = 3000$ psi, using vertical U stirrups with $f_v = 20{,}000$ psi, design the web reinforcement.

The shear diagram is shown in Fig. 3.14. Maximum shear, at the support face, is 51.2 kips, and the shear reduces linearly to zero at midspan. At the critical section for shear, a distance d from the support face, the shear is 41.8 kips. Adopting the simpler criterion of Eq. (3.40),

$$v_c = 1.1\sqrt{f'_c} = 1.1\sqrt{3000} = 60 \text{ psi}$$
$$V_c = v_c bd = 60 \times 16 \times 22 = 21{,}200 \text{ lb}$$

The quantity V_c is plotted on the shear diagram of Fig. 3.14; from geometry, the

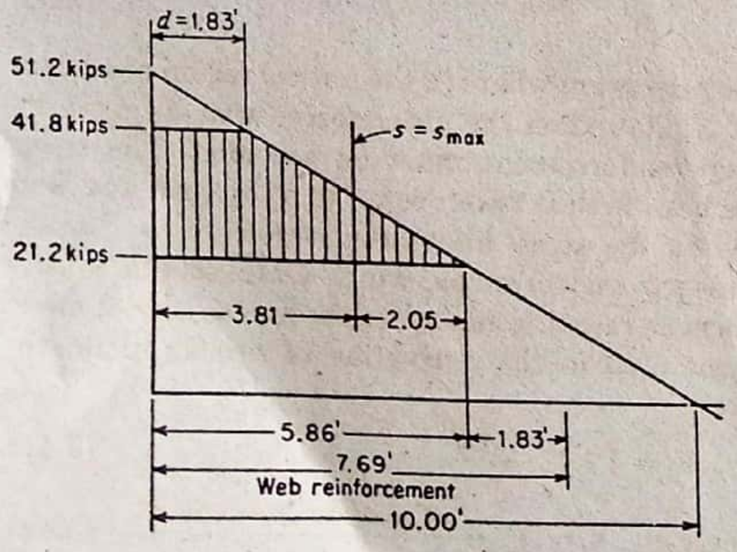


Fig. 3.14

point at which web reinforcement is no longer required is

$$x = 10\,\frac{51.2 - 21.2}{51.2} = 5.86 \text{ ft}$$

from the support face. In accordance with the Code, web reinforcement is carried a distance d beyond this point, for a total distance of 7.69 ft from the support. The stirrups must be designed to resist the shear shown shaded in the figure. With No. 3 stirrups used for trial, the two maximum-spacing criteria are applied as in Example 3 to obtain $s_{max} = 9.2$ in. From the support to a distance d from the support, the required spacing is

$$s = \frac{A_v f_v d}{(V - V_c)} = \frac{0.22 \times 20 \times 22}{20.6} = 4.69 \text{ in.}$$

This is acceptable, and the choice of No. 3 stirrup is confirmed. Solving Eq. (3.43) for the excess shear at which the maximum spacing can be used,

$$(V - V_c) = \frac{A_v f_v d}{s} = \frac{0.22 \times 20 \times 22}{9.2} = 10.5 \text{ kips}$$

This is attained at a distance of 2.05 ft from the point of zero excess shear, or 3.81 ft from the support. With the first stirrup placed at distance $s/2$ from the support face, the following stirrups pattern is selected:

1 space at 2 in.	=	2 in.
6 spaces at 4½ in.	=	27 in.
3 spaces at 6 in.	=	18 in.
5 spaces at 9 in.	=	45 in.
Total		92 in.

BOND AND ANCHORAGE

3.16 General Considerations It was shown in Art. 2.6 that the intensity of the nominal flexural bond stress u on the interface between tensile reinforcement and concrete in a flexural member is

$$u = \frac{V}{\Sigma_0 jd} \quad \text{or} \quad V = u\Sigma_0 jd \tag{2.38a}$$

where V = external shear force
Σ_0 = sum of perimeters of all bars
jd = lever arm of the internal resisting moment
(jd is usually taken as obtained from elastic analysis and often simply as $\frac{7}{8}d$.) To provide for structural safety when designing by ultimate-strength methods, the capacity reduction factor ϕ is introduced. Then the design shear capacity of a beam, if controlled by bond stress, is

$$V_u = \phi u_u \Sigma_0 jd \tag{3.45a}$$

Scanned with CamScanner

[*Art. 3.16*

Conversely, if the designer wishes to calculate the bond stress for a given shear force V_u in the beam for comparison with ultimate bond-stress capacity,

$$u = \frac{V_u}{\phi \Sigma_0 j d} \tag{3.45b}$$

For purposes of bond calculation, the ACI Code specifies that ϕ be taken equal to 0.85.

The critical sections for flexural bond in a beam are at those places where the rate of change in moment is greatest and the total bar perimeter is least. These places are (1) at the face of support, (2) at each point at which tension bars terminate within a span, and (3) at points of inflection. Bent bars that are not more than $d/3$ from the level of the main longitudinal reinforcement may be included in calculating Σ_0, according to Code. While bond stresses exist at the surfaces of both compression and tension bars, those at the interface between compression bars and compression concrete are usually so low that they are not considered in design.

It is useful in many cases to treat the matter of bond in terms of the length of embedment necessary to develop a certain tensile or compressive stress in the bar (see Art. 2.6). This length is

$$L_d = \frac{A_s f_s}{u_u \Sigma_0} \tag{2.41b}$$

where A_s = bar cross-sectional area
f_s = stress to be developed in bar
u_u = ultimate bond-stress capacity
Σ_0 = bar perimeter

On the basis of test evidence [see Eq. (2.40)], the ACI Code specifies the values of flexural or development bond-stress capacity given in Table 3.3, in which f'_c is the specified concrete compressive strength, and D is the diameter of the reinforcing bar. For plain bars, the bond values are one-half those of Table 3.3, with a maximum ultimate value of 250 psi and a maximum working value of 160 psi.

Flexural bond stresses calculated by Eq. (3.45*b*) that are locally considerably higher than estimated bond capacity can be tolerated, provided adequate development length is provided for the reinforcement (see Fig. 2.21). Accordingly, the Code states that flexural bond need not be calculated for the tensile steel when the anchorage bond stress is as low as 0.8 times the limits given in Table 3.3.

Where tensile-steel area is provided using bars of different diameters, the flexural bond stress is different for the different bars. The change in steel stress df_s in a short length dx is essentially the same for all bars. The change of tension force in any bar of diameter D is $dT = df_s \pi D^2/4$. This

Table 3.3

Type of bar	Ultimate bond stress, psi	Working bond stress, psi
Tension bars conforming to ASTM A305:		
Top bars*	$\frac{6.7\sqrt{f'_c}}{D} \le 560$	$\frac{3.4\sqrt{f'_c}}{D} \le 350$
All other bars	$\frac{9.5\sqrt{f'_c}}{D} \le 800$	$\frac{4.8\sqrt{f'_c}}{D} \le 500$
Tension bars conforming to ASTM A408:†		
Top bars*	$4.2\sqrt{f'_c}$	$2.1\sqrt{f'_c}$
All other bars	$6.0\sqrt{f'_c}$	$3\sqrt{f'_c}$
All deformed compression bars	$13\sqrt{f'_c} \le 800$	$6.5\sqrt{f'_c} \le 400$

* Top bars, in reference to bond, are horizontal bars so placed that more than 12 in. of concrete is cast in the member below the bar. The reason for lower values for top bars is that the wet concrete, as it is vibrated, may settle away from under the bar, causing a reduction in effective perimeter. In addition, overvibration may bring excess water to the top of a beam and into contact with the bars, reducing bond-stress capacity.

† These provisions apply to the special large bars No. 14*S* and No. 18*S*. Bond tests of such bars are as yet inconclusive but indicate that substantially lower bond-stress capacity can be expected for such bars than for bars of smaller diameter. In most cases special anchorage is required.

change in tension is balanced by the bond stress acting on the surface of the bar in the length dx, and $dT = u\pi D\,dx$. Equating the right sides of these two expressions,

$$u\pi D\,dx = df_s \pi \frac{D^2}{4}$$

$$u = \frac{df_s}{dx}\frac{D}{4}$$

The intensity of bond stress is seen to be directly proportional to bar diameter for a given stress (or moment) gradient, and the largest bond stress will be at the surface of the largest bar.

If mixed bar sizes are used, the bond stress on each bar can be calculated using Eq. (3.45*b*). If, for example, two sizes are present, the shear force V in that equation can be divided into two parts, V_1 and V_2, pertaining to the bars of diameter D_1 and D_2, respectively. Since

$$V = \frac{dM}{dx} = \frac{dT}{jd\,dx}$$

Scanned with CamScanner

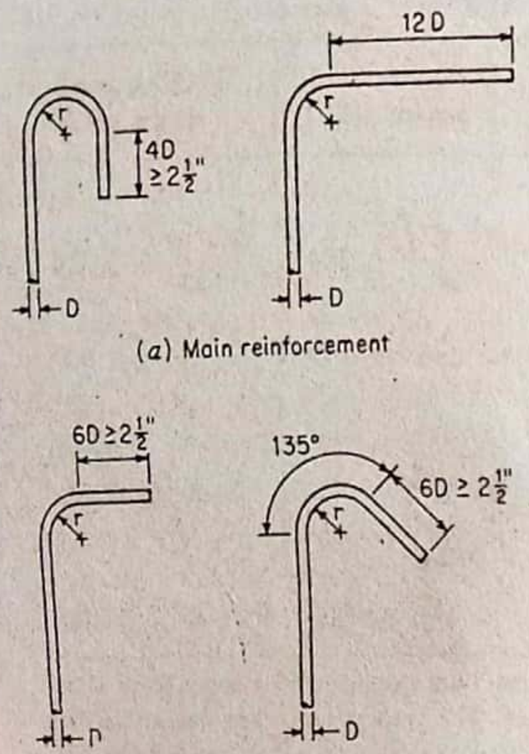


Fig. 3.15 Standard hooks.

these bars is

$$u = \frac{V_2}{\Sigma_{02} jd} = \frac{V(A_{s2}/A_s)}{\Sigma_{02} jd} = \frac{V}{(A_s/A_{s2})\Sigma_{02} jd}$$

But $(A_s/A_{s2})\Sigma_{02}$ is the perimeter that would be obtained if all the area A_s were provided by bars of the larger diameter D_2. Consequently, the bond stress on those bars can be found by Eq. (3.45*b*) using an equivalent perimeter,

$$\Sigma_0' = \frac{A_s}{n_2 \pi D_2^2/4} n_2 \pi D_2 = \frac{4A_s}{D_2}$$

rather than the actual total perimeter.

In the event that the desired stress in a bar cannot be developed by bond alone, it is necessary to provide mechanical anchorage at the end of the bar, usually by means of a 90° bend or a 180° hook. The dimensions and bend radii for hooks have been standardized by the ACI Code as follows (see Fig. 3.15):

1. A semicircular turn plus an extension of at least four bar diameters, but not less than 2½ in. at the free end of the bar, or
2. A 90° turn plus an extension of at least 12 bar diameters at the free end of the bar, or

it is apparent that the shears V_1 and V_2 will be proportional to the tensile forces in the bars of each size, which in turn are proportional to the steel areas provided by the bars of each size.

If A_s = total steel area
A_{s1} = area provided by n_1 bars of diameter D_1
A_{s2} = area provided by n_2 bars of diameter D_2

then

$$V_1 = V\frac{A_{s1}}{A_s} \quad \text{and} \quad V_2 = V\frac{A_{s2}}{A_s}$$

If Σ_{02} is the total perimeter of the larger bars, then the bond stress on

3. For stirrup and tie anchorage only, either a 90° or 135° turn plus an extension of at least six bar diameters, but not less than 2½ in. at the free end of the bar

***Table* 3.4**

Bar No.	*Minimum radius*
3, 4, or 5	2½ bar diameters
6, 7, or 8	3 bar diameters
9, 10, or 11	4 bar diameters
14*S* or 18*S*	5 bar diameters

The minimum radius of bend measured on the inside of the bar for standard hooks must not be less than the values of Table 3.4, except that, for sizes No. 6 through No. 11 inclusive in structural and intermediate grades of bars only, the minimum radius shall be 2½ bar diameters. Such standard hooks in tension may be considered as developing, in the bar, 10,000 psi working stress or 19,000 psi ultimate stress, or may be considered as simple extensions of the bars at the appropriate bond stresses. Hooks are not to be considered effective in adding to the compressive resistance of bars.

3.17 Example: ultimate-strength design for bond A continuous beam with bar details as shown in Fig. 3.16*a* is designed to carry a total uniformly dis-

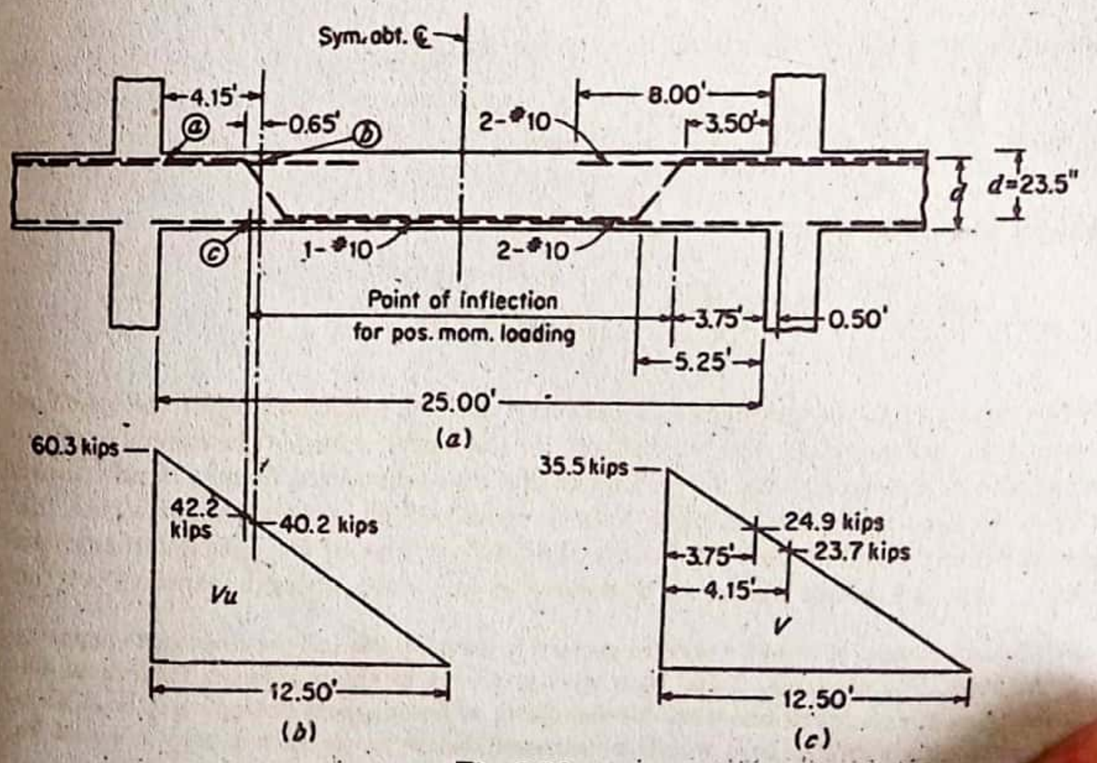


Fig. 3.16

Scanned with CamScanner

tributed ultimate load of 4.83 kips per ft. The resulting shear diagram at ultimate load is shown in Fig. 3.16*b*. If the material strengths f'_c and f_y are 3000 psi and 40,000 psi, respectively, and the point of inflection when the beam is loaded for maximum positive moment is 3.75 ft from the support face, check the intensity of bond stress at all critical points in the beam, and compare these with maximum specified values.

The maximum bond stress at the surface of a tension bar occurs where the shear is greatest and the bar perimeter is least. For simply supported beams, this is at the face of supports. For continuous beams, maximum shear and minimum perimeter do not ordinarily occur at the same location, and it is necessary to check all locations which may be critical. With reference to Fig. 3.16*a*, for negative bars, this will ordinarily be at the face of supports, where the shear is maximum, and at locations where tensile bars are bent downward. In the latter case, although the shear is not so large as at the support, the available perimeter is reduced. The ACI Code specifies that tensile bars within a distance $d/3$ of the main reinforcement may be included in calculating perimeter, so, if bars are bent at 45°, the critical location is a distance $d/3$ beyond the actual bend point. The critical location for positive bars is at the point of inflection. For the given beam,

$$\text{At } (a): \quad u = \frac{V}{\phi \Sigma_o jd} = \frac{60{,}300}{0.85 \times 16.0 \times 0.875 \times 23.5} = 216 \text{ psi}$$

$$\text{At } (b): \quad u = \frac{40{,}200}{0.85 \times 8.0 \times 0.875 \times 23.5} = 286 \text{ psi}$$

$$\text{At } (c): \quad u = \frac{42{,}200}{0.85 \times 5.5 \times 0.875 \times 23.5} = 440 \text{ psi}$$

According to ACI specifications, for the top bars,

$$u_u = \frac{6.7\sqrt{f'_c}}{D} = \frac{6.7\sqrt{3000}}{1.27} = 289 \text{ psi}$$

and for the bottom bars,

$$u_u = \frac{9.5\sqrt{f'_c}}{D} = \frac{9.5\sqrt{3000}}{1.27} = 410 \text{ psi}$$

It is evident that the top bars at locations *a* and *b* are stressed below the specified maximum values, while the bond stress for the bottom bars at location *c* is somewhat above the maximum. According to the Code, however, flexural bond stresses which locally exceed maximum values need not be a concern, provided the development bond stress is not more than 80 per cent of the specified maximum value. For the given beam, to develop the full yield-strength capacity[1] of the

[1] In some cases it would not be necessary to develop the full yield-strength capacity of the bars. For example, if the bars were not bent at the maximum theoretical distance from the support, but were carried closer to the support before being bent, then the remaining straight bars would be stressed below f_y. In such a case it would be necessary only to develop the force $A_s f_s = M/z$.

two No. 7 bars at the point at which the other two bars are bent up,

$$u = \frac{A_s f_y}{\Sigma_o L} = \frac{1.27 \times 40{,}000}{3.99 \times 5.75 \times 12} = 126 \text{ psi}$$

Since this is well below $0.80 \times 410 = 328$ psi, bond failure will not occur in spite of the locally high bond stress, and the beam is satisfactory.

PROBLEM

U.S.D.: Bond and anchorage:

A continuous beam of 24-ft clear span has an effective depth to both positive and negative bars of 24 in. and is 12 in. wide. All bars are 2.5 in. from the nearest beam face. The beam is reinforced for positive bending with three No. 10 bars, two of which are bent up at 45° 5 ft from the support faces to become continuous with negative reinforcement. Additional negative reinforcement consists of three No. 10 bars which are terminated 8 ft from the support faces. The beam carries a working live load of 4.0 kips per ft and a calculated dead load, including its own weight, of 2.0 kips per ft. When loaded for maximum positive moment, the working moments at the face of support are $M_d = 65$ ft-kips and $M_l = 145$ ft-kips. Determine the bond stresses on tension bars at all critical locations for this beam, and compare with the maximum values recommended by ACI Code. Concrete strength is $f'_c = 4000$ psi, and the steel has a yield stress of $f_y = 60{,}000$ psi.

3.18 Example: working-stress design for bond The design of the beam in the preceding example will now be checked for adequacy in bond at a working load of 2.84 kips per ft. Material strengths are as before, and an allowable working stress of 20,000 psi in the tensile steel is assumed.

The shear diagram under working load is shown in Fig. 3.16*c*. The critical locations for bond stress are at (*a*), (*b*), and (*c*) as before. Then

$$\text{At } (a): \quad u = \frac{V}{\Sigma_o jd} = \frac{35{,}500}{16.0 \times 0.875 \times 23.5} = 108 \text{ psi}$$

$$\text{At } (b): \quad u = \frac{23{,}700}{8.0 \times 0.875 \times 23.5} = 144 \text{ psi}$$

$$\text{At } (c): \quad u = \frac{24{,}900}{5.5 \times 0.875 \times 23.5} = 221 \text{ psi}$$

Allowable bond stress for the top bars is

$$u = \frac{3.4\sqrt{f'_c}}{D} = \frac{3.4\sqrt{3000}}{1.27} = 147 \text{ psi}$$

and for the bottom bars is

$$u = \frac{4.8\sqrt{f'_c}}{D} = \frac{4.8\sqrt{3000}}{1.27} = 207 \text{ psi}$$

Scanned with CamScanner

It is seen that the bond stress for the top bars is below the allowable limit at both locations, while the bond stress for the bottom bars exceeds the allowable value. However, assuming that the No. 7 straight bars are fully stressed to f_s at the point at which the other two bars are bent up, the development bond stress is

$$u = \frac{A_s f_s}{\Sigma_0 L} = \frac{1.20 \times 20{,}000}{5.50 \times 5.75 \times 12} = 63 \text{ psi}$$

Since this is well below $0.80 \times 207 = 165$ psi, bond failure will not occur in spite of the locally high stress, and the beam is satisfactory with regard to bond.

DESIGN DETAILS

3.19 Selection of Bars and Bar Spacing The standard reinforcing-bar sizes and types available to the designer were described in Art. 1.10*b*. Common bars range in size from No. 2 to No. 11, with the bar number corresponding approximately to the number of eighth inches of bar diameter. The larger sizes, No. 14*S* (1¾-in. diameter) and No. 18*S* (2¼-in. diameter), are available on special order and are used primarily for column reinforcement. Table 1 of Appendix B gives areas, perimeters, and weights of standard bars; Tables 2 and 3 give information for groups of bars.

It is often desirable to mix bar sizes in order to meet steel-area requirements more closely. In general, mixed bars should be of comparable sizes; for example, it would be bad practice to use No. 11 bars in conjunction with No. 3 bars, while mixing No. 10 bars with No. 8 bars would be perfectly acceptable. There is some practical advantage to minimizing the number of different bar sizes used for a given structure.

Normally it is necessary to maintain a certain minimum distance between adjacent bars in order to ensure proper placement of concrete around them. Air pockets below the steel are to be avoided, and full surface contact between the bars and the concrete is desirable to optimize bond strength.[1] The ACI Code specifies that the minimum clear distance between adjacent bars shall not be less than the nominal diameter of the bars, or 1⅓ times the maximum size of the coarse aggregate, or 1 in. Where reinforcement is placed in two or more layers, the clear distance between layers must not be less than 1 in., and the bars in the upper layer should be placed directly above those in the bottom layer.

In order to provide the steel with adequate concrete protection against fire and corrosion, the designer must maintain a certain minimum thickness of concrete cover outside the outermost steel. The thickness

[1] In some cases bars are placed in direct contact with one another, i.e., "bundled," in order to save space. In such cases special attention must be given to effective perimeter for bond stress; in addition it is desirable that such bundled bars be fully enclosed with stirrups or ties.

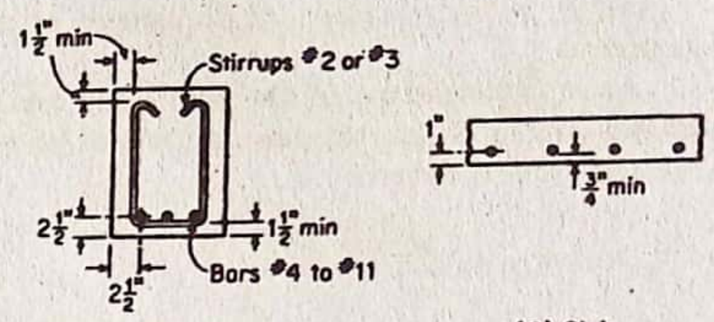


Fig. 3.17 (a) Beam with stirrups (b) Slab

required will vary, depending upon the type of member and conditions of exposure. According to the ACI Code, concrete protection at surfaces not exposed directly to the ground or weather should not be less than ¾ in. for slabs and walls and 1½ in. for beams and girders. If the concrete surface is to be exposed to the weather or in contact with the ground, a protective covering of at least 2 in. is required (1½ in. for No. 5 bars and smaller), except that if the concrete is to be poured in direct contact with the ground, without the use of forms, a covering of at least 3 in. must be furnished.

In general, the centers of bars in beams should be placed at least 2½ in. from the bottom surface of the beam, in order to furnish at least 1½ in. of clear insulation below the bars and the stirrups (see Fig. 3.17). In slabs, 1 in. to the center of the bar is ordinarily sufficient to give the required ¾ in. insulation. Although the distances shown in Fig. 3.17 are not the exact distances required in all cases to furnish the clear insulation specified by the Code, they will almost always satisfy the minimum requirements, and they are sufficiently exact for all design purposes. Total depths of beams should be taken in multiples of not less than ½ in., and preferably 1 in.

3.20 Bar Cutoff and Bend Points Articles 3.7 to 3.12 have dealt with moments, stresses, concrete dimensions, and bar areas at the critical-moment sections of beams. The critical-moment sections are at the face of supports (negative bending) and near the middle of the span (positive bending). Occasionally, "haunched" members of variable depth or width are used so that the concrete flexural capacity will agree more closely with the variation in bending moment along a span or series of spans. Usually, however, prismatic members with constant concrete dimensions are used to simplify formwork and reduce cost.

The steel reinforcement, on the other hand, is easily varied in accordance with requirements for flexure, and it is common practice either to cut off bars where they are no longer required to resist stress, or, in the case of continuous beams, to bend up the bottom steel (usually at 45°)

Scanned with CamScanner

so that it provides tensile reinforcement at the top of the beam over the supports.

As an illustration, in the uniformly loaded, simply supported beam shown in Fig. 3.18*a*, the tensile force to be resisted by the reinforcement at any cross section is

$$T = A_s f_s = \frac{M}{z}$$

where M is the value of bending moment at that section, and z is the internal lever arm of the resisting moment. The lever arm z varies only within narrow limits and is never less than the value obtained at the maximum-moment section. Consequently, the tensile force can be taken

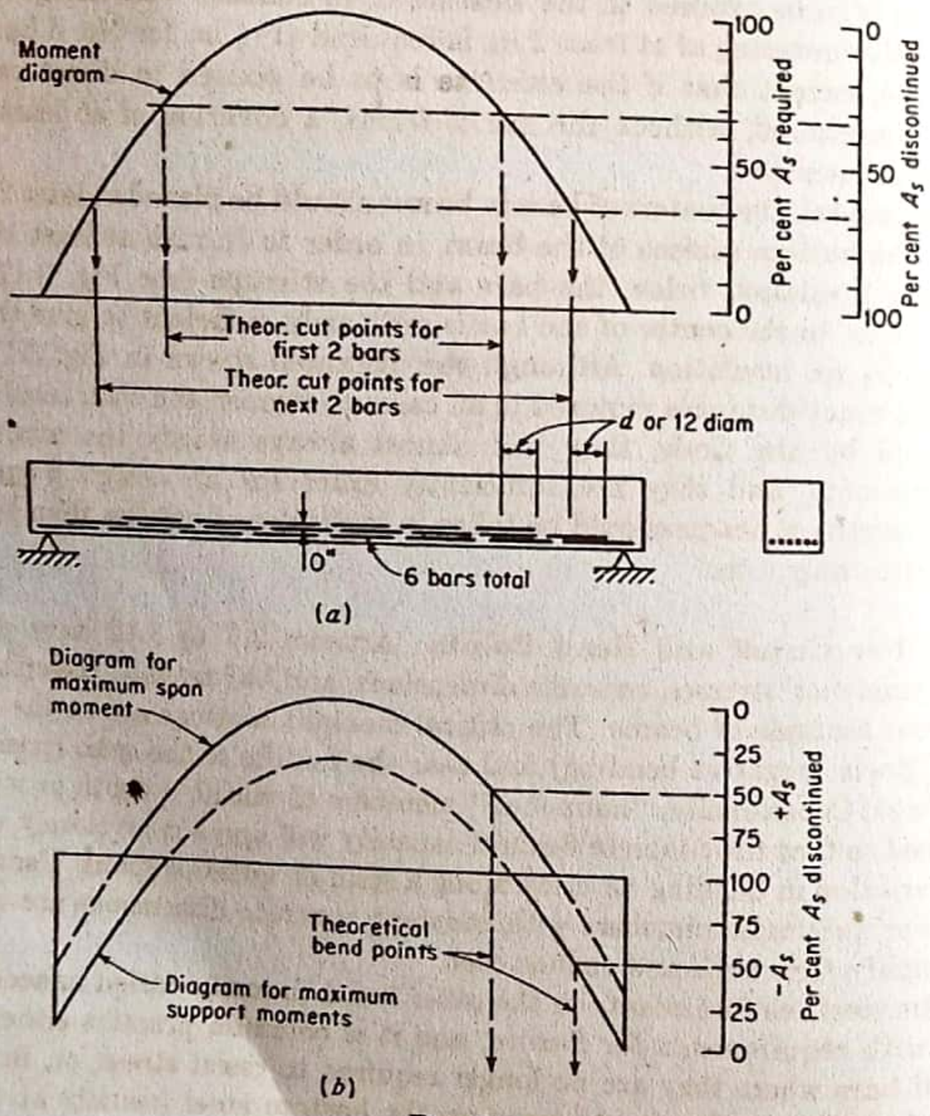


Fig. 3.18

with good accuracy as directly proportional to the bending moment. Since it is desirable to design so that the steel everywhere in the beam is as nearly fully stressed as possible, it follows that the required steel area is very nearly proportional to the bending moment.

The moment diagram of Fig. 3.18*a* can therefore be used as a steel-requirement diagram. At the maximum-moment section, 100 per cent of the tensile steel is required (zero per cent can be discontinued or bent), while at the supports, zero per cent of the steel is theoretically required (100 per cent can be discontinued or bent). The percentage of bars which could be bent elsewhere along the span is obtainable directly from the moment diagram, drawn to scale. To facilitate the determination of bend points for simple spans, Graph 10, Appendix B, has been prepared. It represents a half-moment diagram for a uniformly loaded simple span.

To determine bend points for continuous beams, the moment diagrams resulting from loading for maximum span moment and maximum support moment are drawn. A moment envelope results, which defines the range of values of moment at any section. Bend points can be found from the appropriate moment curve as for simple spans. Figure 3.18*b* illustrates, for example, a continuous beam with moment envelope resulting from alternate loadings to produce maximum span and maximum support moments. The locations of the points at which 50 per cent of the bottom and top steel may theoretically be bent are shown.

According to the ACI Code, uniformly loaded, continuous reinforced-concrete beams of fairly regular span may be designed using moment coefficients (see Table 8.1). These coefficients, analogous to the numerical constant in the expression $\frac{1}{8}wL^2$ for simple beam bending moment, give a conservative approximation of span and support moments for continuous beams. When such coefficients are used in design, bend points may conveniently be found from Graph 11, Appendix B. Moment curves corresponding to the various span- and support-moment coefficients are given at the top and bottom of the chart, respectively.

Actually, in no case should the tensile steel be discontinued exactly at the theoretically described points. It is necessary to develop at least part of the strength of the bar by bond stress before it can carry any tension. Also, as described in Art. 2.6*b* and shown in Fig. 2.18*b*, when diagonal tension cracks form, an internal redistribution of forces occurs in a beam. Prior to cracking, the steel tensile force at any point is proportional to the moment at a vertical section passing through that point. However, after the crack has formed, the tensile force in the steel at the crack is governed by the moment at a section nearer midspan, which may be much larger.

Recognizing these facts, the ACI Code specifies that every bar should be continued at least a distance equal to the effective depth of the beam

Scanned with CamScanner

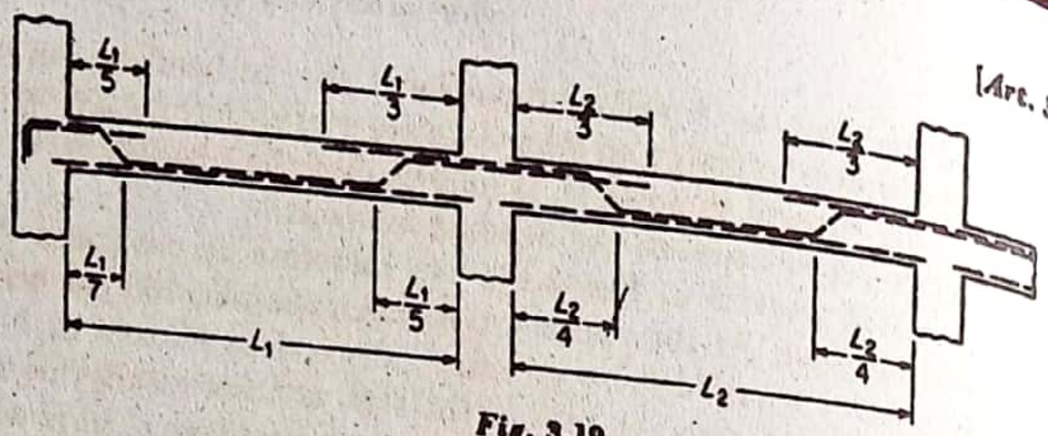


Fig. 3.19

or 12 bar diameters (whichever is larger) beyond the point at which it is theoretically no longer required to resist stress. In addition, it is specified that at least one-third of the bottom tensile steel (one-quarter in the case of continuous beams) must be continued uninterrupted along the same face of the beam a distance of at least 6 in. into the support. At least one-third of the total reinforcement provided for negative moment at the support must be extended beyond the extreme position of the point of inflection a distance not less than one-sixteenth of the clear span or the effective depth of the member, whichever is greater, according to Code.

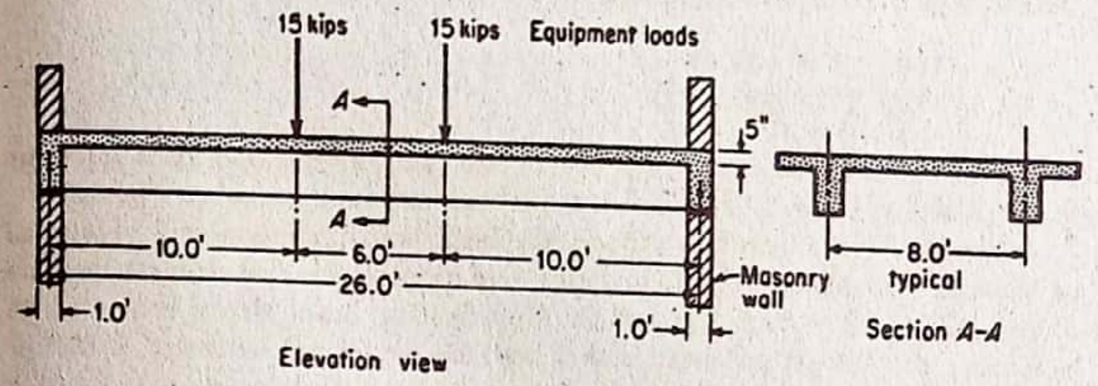
When bars are cut off in a tension zone rather than bent so as to be continuous with steel on the other face of a beam, the Code requires special precautions. It is specified that no flexural bar shall be terminated in a tension zone unless *one* of the following conditions is satisfied:

1. The shear is not over one-half that normally permitted, including allowance for shear reinforcement, if any.
2. Stirrups in excess of those normally required are provided each way from the cutoff a distance equal to three-quarters of the depth of the beam. The excess stirrups shall provide an area not less than $0.0015bs$ where b is the web width, and s the spacing of the stirrups. In addition, the stirrup spacing shall not exceed $d/8r_b$, where r_b is the ratio of the area of bars cut off to the total area of bars at the section.
3. The continuing bars provide twice the area required for flexure at that point or twice the perimeter required for flexural bond.

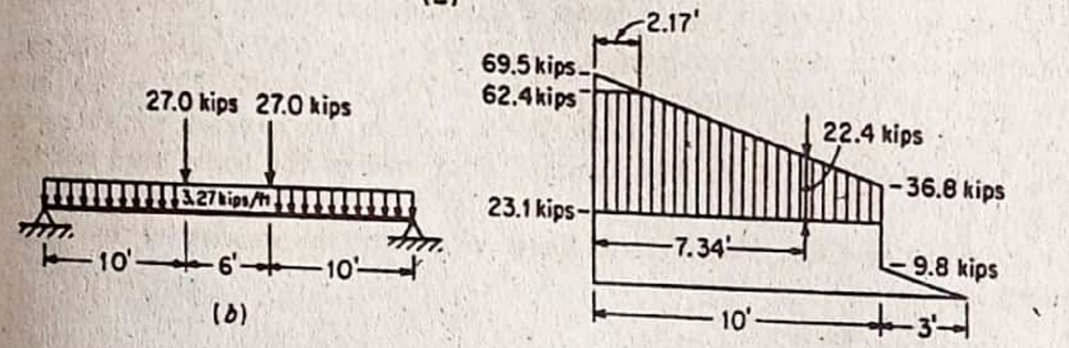
In some cases, particularly for relatively deep beams in which a large percentage of the total bottom steel is to be bent, it may be impossible to locate the bend-up point for bottom bars far enough from the support for the same bars to meet the requirements for top steel. The theoretical points of bend should be checked carefully for both bottom and top steel.

Since the determination of bend points may be a rather tedious matter, particularly for frames which have been analyzed by elastic methods rather than by moment coefficients, many designers specify that bars be bent at more or less arbitrarily defined points which experience has indicated are safe. For nearly equal spans, uniformly loaded, in which not more than about one-half the tensile steel is to be bent, the bend locations shown in Fig. 3.19 are satisfactory.

3.21 Integrated design example A floor system consists of single-span T beams 8 ft on centers, supported by 12-in. masonry walls spaced at 25 ft between inside faces. The general arrangement is shown in Fig. 3.20*a*. A 5-in. monolithic slab carries a uniformly distributed live load of 150 psf. The T beams, in addition to the slab load and their own weight, must carry two 15,000-lb equipment loads applied 3 ft from the span center line as shown. A complete design is to be provided for the T beams, using concrete of 4000 psi strength and bars with 60,000 psi yield stress.

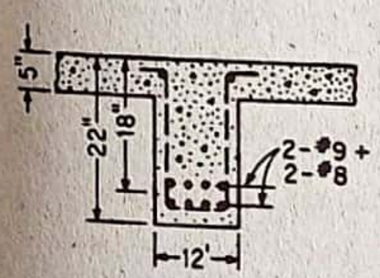


(*a*)

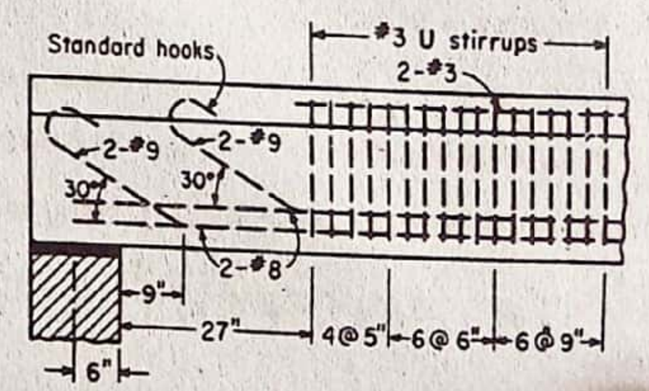


(*b*)

(*c*)



(*d*)



(*e*)

Fig. 3.20

Scanned with CamScanner

According to Code, the span length is to be taken as the clear span plus the beam depth, but not less than the distance between centers of the supports. The latter provision controls in this case, and the effective span is 26 ft. Estimating the beam web dimensions to be 12 × 24 in., the working and ultimate dead loads are

Slab: $\frac{5}{12} \times 150 \times 7 = 440$ plf

Beam: $\frac{12 \times 24}{144} 150 = 300$

$w_{dw} = 740$ plf

$w_{du} = 740 \times 1.5 = 1110$ plf

The uniformly distributed live load is

$w_{lw} = 150 \times 8 = 1200$ plf

$w_{lu} = 1200 \times 1.8 = 2160$ plf

Live-load overload factors are applied to the two concentrated loads to obtain $P_u = 15{,}000 \times 1.8 = 27{,}000$ lb. Ultimate loads are summarized in Fig. 3.20*b*.

In lieu of other controlling criteria, the beam web dimensions will be selected on the basis of shear. The left and right reactions under full ultimate load are $27.0 + 3.27 \times 13 = 69.5$ kips. With the effective beam depth estimated to be 20 in., the maximum shear which need be considered in design is $69.5 - 3.27(0.50 + 1.67) = 62.4$ kips. A maximum shear stress of $6\phi\sqrt{f'_c}$ will be selected (although the Code allows higher values of unit shear) in order to avoid heavy web reinforcement. In the present case, $v_{max} = V/b'd = 6 \times 0.85\sqrt{4000} = 322$ psi, and the required web dimensions are $b'd = V/v_{max} = 62{,}400/322 = 194$ in.^{2} Cross-sectional dimensions $b' = 12$ in. and $d = 18$ in. are selected, providing a total beam depth of 22 in. The assumed dead load of the beam need not be revised.

According to Code, the effective flange width b is the smallest of the three quantities

$$\frac{L}{4} = \frac{26 \times 12}{4} = 78 \text{ in.}$$

$16t + b' = 80 + 12 = 92$ in.

t spacing $= 96$ in.

The first controls in this case. The maximum moment is at midspan, where

$$M_{max} = \tfrac{1}{8} \times 3.27 \times 26^2 + 27.0 \times 10 = 546 \text{ ft-kips}$$

Assuming for trial that the stress-block depth will equal the slab thickness,

$$A_s = \frac{M}{\phi f_y(d - a/2)} = \frac{546 \times 12}{0.90 \times 60 \times 15.5} = 7.82 \text{ in.}^2$$

Then

$$p = \frac{A_s}{bd} = \frac{7.82}{78 \times 18} = 0.0056$$

and

$$c = \frac{pf_y d}{0.85k_1 f'_c} = \frac{0.0056 \times 60 \times 18}{0.85 \times 0.85 \times 4} = 2.10 \text{ in.}$$

The depth to the neutral axis is seen to be less than the slab depth. Since $a = k_1 c = 0.85 \times 2.10 = 1.78$ in., a revised estimate of A_s is

$$A_s = \frac{546 \times 12}{0.90 \times 60 \times 17.11} = 7.10 \text{ in.}^2$$

Four No. 9 and four No. 8 bars will be used, providing a total area of 7.14 in.^{2} They will be arranged in two rows, as shown in Fig. 3.20*d*, with No. 9 bars at the outer end of each row.

Some of this steel can be bent up to assist in resisting diagonal tension stresses. While the Code permits as much as two-thirds of the steel to be bent in simple spans, in the present case only the No. 9 bars will be bent. The bond stress at the face of support on the remaining four No. 8 bars is

$$u = \frac{V_u}{\phi \Sigma_0 jd} = \frac{69{,}500 - (3270 \times 0.5)}{0.85 \times 12.6 \times 0.875 \times 18} = 402 \text{ psi}$$

This is close to, but satisfactorily below, the specified maximum of

$$u = \frac{9.5\sqrt{f'_c}}{D} = \frac{9.5\sqrt{4000}}{1.27} = 473 \text{ psi}$$

confirming that the four No. 9 bars may be bent. They will be bent upward in pairs, in order to maintain symmetry. The moment capacity of the section after two No. 9 bars have been bent up is

$$a = \frac{A_s f_y}{0.85 f'_c b} = \frac{5.14 \times 60}{0.85 \times 4 \times 78} = 1.16 \text{ in.}$$

$$M_u = \phi A_s f_y \left(d - \frac{a}{2}\right) = 0.90 \times 5.14 \times 60(18.0 - 0.58)\tfrac{1}{12} = 403 \text{ ft-kips}$$

After two additional No. 9 bars have been bent, it is

$M_u = 250$ ft-kips

For the present case, with a moment diagram resulting from combined distributed and concentrated loads, the point at which the applied moment is equal to these amounts must be calculated. (In the case of uniformly loaded beams, Graphs 10 and 11 of Appendix B are helpful.) If x_1 is the distance from the support center line to the point at which the moment is 403 ft-kips, then

$$69.5x_1 - 3.27\frac{x_1^2}{2} = 403$$

$$x_1 = 6.95 \text{ ft}$$

Scanned with CamScanner

Similarly, x_2, the distance to the point of 250-ft-kip moment, is 3.95 ft. According to Code, the bent bars must be carried $d = 1.67$ ft or 12 diam = 1.13 ft beyond these theoretical points. Moment requirements will be satisfied if the first two bars are bent $6.95 - 1.67 = 5.28$ ft from the support center line, and the next two bars at 2.28 ft.

The shear diagram resulting from application of ultimate loads is shown in Fig. 3.20*c*. The shear resistance of the uncracked concrete is

$$V_{uc} = 2\phi \sqrt{f'_c}\, b'd = 2 \times 0.85 \sqrt{4000} \times 12 \times 18 = 23{,}100 \text{ lb}$$

Web reinforcement must be provided for that part of the shear diagram shown shaded in the diagram. For bars bent at 30°,

$$(\sin \alpha + \cos \alpha) = 0.500 + 0.866 = 1.37$$

Then, for the bent bars, within a distance d of the support face,

$$s = \frac{1.37 A_v f_v \phi d}{V_u - V_{uc}} = \frac{1.37 \times 2.00 \times 60 \times 0.85 \times 18}{39.3} = 64 \text{ in.}$$

However, governed by the requirement that each potential 45° crack should be crossed by one line of web steel (see Fig. 3.11), the maximum spacing is

$$s_{max} = \tfrac{3}{8} d \left(1 + \frac{1}{\tan \alpha}\right) = \tfrac{3}{8} \times 18(1 + 1.73) = 18.4 \text{ in.}$$

say 18 in. Accordingly, two No. 9 bars will be bent up at a distance $s/2 = 9$ in. from the support face, and two No. 9 bars will be bent at 27 in. from the support face. The bars are anchored in the compression zone, using standard hooks as required by Code.

The first vertical stirrup will be placed at the bend point of the two upper No. 9 bars. At that point, 27 in. from the support center line, the total shear is 62,100 lb. Assuming No. 3 U stirrups,

$$s_{2.25} = \frac{A_v f_v \phi d}{V_u - V_{uc}} = \frac{0.22 \times 60 \times 0.85 \times 18}{62.1 - 23.1} = 5.18 \text{ in.}$$

For No. 3 stirrups, the maximum spacing is $d/2 = 9$ in. or $A_v/0.0015b = 12.2$ in. The first criterion controls. From Eq. (3.37), the maximum spacing of 9 in. can be adopted where the excess shear is no larger than 22.4 kips. This is attained at a distance of 7.34 ft from the support center line (see Fig. 3.20*c*). Stirrups will be provided a distance d beyond the concentrated load. The final spacing of vertical stirrups selected is

1 space at 27 in. =	27 in.
4 spaces at 5 in. =	20 in.
6 spaces at 6 in. =	36 in.
6 spaces at 9 in. =	54 in.
Total	137 in. = 11 ft 5 in.

As an alternative to the present design using bent bars, the longitudinal steel might have been continued straight along the bottom face of the beam and

either cut off where no longer required or continued into the support.[1] Had this been done, only five extra vertical stirrups would have been required to carry the excess shear, the first 2 in. from the face of support, and the remainder at 5 in. spacing. In all probability, the extra cost of bar bending and the extra length of bars associated with the bent-bar design would more than offset the cost of the few stirrups saved, and the use of straight bars with vertical stirrups would be preferred. In continuous beams, in which both positive and negative moments must be provided for, bent bars can often be used advantageously as web reinforcement.

3.22 Splices In general, reinforcing bars are stocked by fabricators in lengths of 60 ft. For this reason, and because it is often more convenient to work with shorter bar lengths, it is frequently necessary to splice bars in the field. Splices in reinforcement at points of maximum stress in slabs, beams, and girders should be avoided wherever possible.

Splices are most often made simply by lapping the bars a sufficient distance to transfer stress by bond from one bar to the other. The lapped bars are usually placed in contact and lightly wired so that they stay in position as the concrete is poured. According to the ACI Code, lapped splices in tension bars must transfer the entire computed stress from bar to bar without exceeding three-fourths of the bond-stress values of Table 3.3. In addition, the minimum requirements of Table 3.5 apply. In determining lap lengths for compression splices, the values of Table 3.5 are to be used.

Alternatively, splicing may be accomplished by welding or by sleeves or mechanical devices which provide positive connection between the bars. An approved welded splice is described by the Code as one in which the bars are butted and welded so that the splice will develop in tension at least 125 per cent of the specified yield strength of the reinforcing bar. Approved connections for bars designed to carry critical tension or compression shall be equivalent in strength to an approved welded splice.

***Table* 3.5 Minimum lap distances* for splices**

Splices	f_y = 40 ksi	f_y = 50 ksi	f_y = 60 ksi	f_y = 75 ksi	But not less than
Tension	24 diam	30 diam	36 diam		12 in.
Compression†	20 diam	20 diam	24 diam	30 diam	12 in.

* Values shown are for bars meeting the requirements of ASTM A305 for deformations. For other bars, minimum lap distances are twice these values.

† If f'_c is less than 3000 psi, increase all values by one-third.

[1] The designer should note the very stringent Code restrictions in cases in which longitudinal steel is cut off in the tension zone of a beam.

Scanned with CamScanner

When bar sizes exceed No. 11, welding or the use of positive mechanical connection devices is required by Code for tension bars and is recommended for compression bars as well.

If lapped tension splices are spaced laterally closer than 12 bar diameters or are located closer than 6 in. or 6 bar diameters to an outside edge, certain precautions are necessary in order to avoid failure by splitting of the concrete along the length of the bars. In such cases, the ACI Code requires that lap length shall be increased by 20 per cent, or that stirrups or closely spaced spirals shall enclose the splice for its full length. Such stirrups are to be excess of those otherwise required for web reinforcement and should have an area at least equal to $0.0015bs$, where b is the width of the beam, and s is the spacing of the stirrups. In addition, the maximum spacing is not to exceed $d/8r_b$, where d is the effective depth of the beam, and r_b is the ratio of the area of the bars spliced to the total bar area at the section. If more than half the area of tension bars is spliced within a length of 40 bar diameters, or if splices are made at points of maximum stress, special precautions must be taken.

In the case of compression splices, compressive stress may be transmitted by bearing of square-cut ends held in concentric contact by a suitably welded sleeve or mechanical device. If a lapped compression splice is used (see Fig. 3.21), and if the bars are offset at the splice, the slope of the inclined axis of the bar is not to exceed 1 in 6, and the portions of the bar above and below the offset are to be parallel to the axis of the column. Horizontal support at the offset bends, provided by ties, spirals, or parts of the floor construction, should be adequate to carry a horizontal thrust assumed equal to 1½ times the horizontal component of the nominal stress in the inclined portion of the bar. In tied columns, the amount of reinforcement spliced by lapping shall not exceed a steel ratio of 0.04 in any 3-ft length of column, according to the Code.

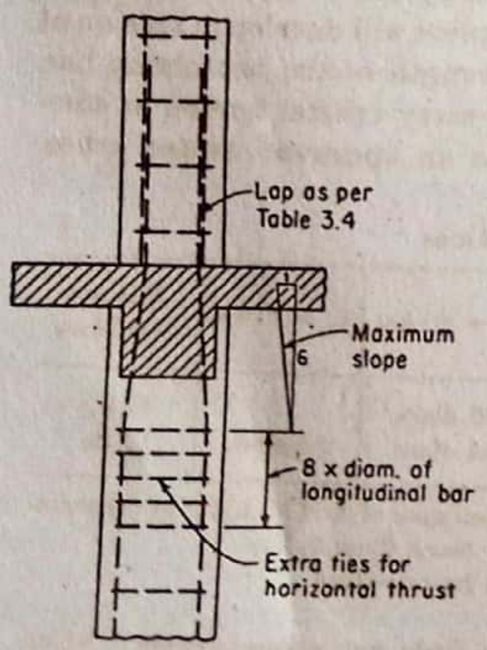


Fig. 3.21

3.23 Control of Cracking With the introduction and increasing use of steels with yield stresses above 40,000 psi, the question of cracking of the tensile portions of reinforced-concrete beams is receiving more attention than it has in the past. The primary concern is not the number of cracks which form, but rather the width of the cracks.

It is desirable to minimize the crack width (1) from the point of view of appearance and (2) because of the detrimental corrosion of the reinforcing steel that may occur if it is exposed by excessively wide cracks.

Extensive investigation of the cracking phenomenon in reinforced-concrete beams is in progress in the United States and abroad. In this country, no final conclusions have been drawn, but, in general, it has been observed (Ref. 3.5) that:

1. The widths of cracks due to loads are essentially proportional to reinforcing-steel stresses.

2. At any given steel stress, the widths of flexural cracks are minimized if the tensile bars are well distributed over the width of the cross section.

It has further been observed in testing at Cornell University that the widths of surface cracks at the level of the tensile steel are porportional to the amount of concrete cover provided for the bars. Placement of bars close to the surface of the beam will result in a larger number of concrete cracks of a smaller width than would be the case if a greater amount of concrete cover were used.

Quantitatively, little has been published to aid the designer in estimating the widths of cracks. The following empirical expression is suggested by Kaar and Mattock:

$$w_{max} = 0.115 \sqrt[4]{A} f_s \times 10^{-6} \quad \text{in.} \tag{3.46}$$

where f_s is the stress in the steel at the load for which the crack widths are to be determined, and A is the area of concrete surrounding one bar. The latter quantity is defined as the total effective concrete area divided by the number of bars, where the total effective concrete area is the area of concrete surrounding the reinforcing bars and having the same centroid as the total main reinforcement. Equation (3.46) fits observed experimental evidence reasonably well for values of A between 3 and 50 in.^{2}.

With regard to crack control, the ACI Code specifies that only deformed bars shall be used (except that plain bars may be used as temperature bars and column spirals, and No. 2 plain bars may be used as stirrups and column ties) and that tension reinforcement shall be well distributed in the zones of maximum concrete tension and in the flanges of T beams. It further specifies that the yield stress for the tension bars shall not exceed 60,000 psi unless it is shown by full-scale tests that the average crack width at service load at the concrete surface of the extreme tension edge does not exceed 0.015 in. for interior members and 0.010 in. for exterior members. The latter provisions give some guide also to current thinking with regard to acceptable crack widths in beams.

Scanned with CamScanner

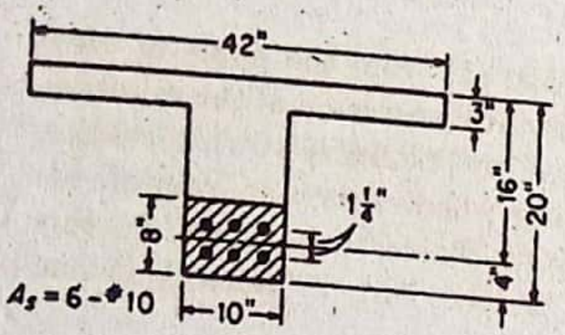


Fig. 3.22

3.24 Design example: control of cracking Estimate the maximum width of crack to be expected at the level of the tensile steel at a working load moment of 3480 in.-kips in the concrete tension zone of the T beam of Example 1, Art. 3.9.

The dimensions of the T beam of Example 1 are shown in Fig. 3.22. The total tensile-steel area provided by the six No. 10 bars is 7.59 in.^{2} The steel stress at working load moment can be closely estimated by taking the internal lever arm equal to the distance $(d - t/2)$:

$$f_s = \frac{M_w}{A_s(d - t/2)} = \frac{3{,}480{,}000}{7.59 \times 14.50} = 31{,}600 \text{ psi}$$

The distance from the steel centroid to the tensile face of the beam is 4 in.; hence the total effective concrete area for purposes of cracking calculations is

$$A_e = 4 \times 2 \times 10 = 80 \text{ in.}^2$$

and the area of concrete surrounding one bar is

$$A = \frac{A_e}{\text{No. of bars}} = \frac{80}{6} = 13.30 \text{ in.}^2$$

The maximum width of crack is then estimated from Eq. (3.46) to be

$$\begin{aligned} w_{max} &= 0.115 \sqrt[4]{A} f_s \times 10^{-6} \\ &= 0.115 \sqrt[4]{13.30} \times 31{,}600 \times 10^{-6} \\ &= 0.0069 \text{ in.} \end{aligned}$$

This value is well below the allowable values of crack width for either exterior or interior members. If the result had been otherwise, a redesign using a larger number of smaller-diameter bars, thus reducing the value of A, would have been indicated.

DEFLECTION OF REINFORCED-CONCRETE MEMBERS

3.25 General Considerations One of the significant results of the more widespread use of ultimate-strength design methods is that the members are often more slender than those designed by working-stress methods. Reasons for this include (1) the economical use of large steel ratios (above p_e) and (2) the economic utilization of high-strength steel and concrete. Recognizing that the deflection of slender members may in some cases exceed desirable limits, the ACI Code specifies that deflection should always be checked when the required net reinforcement ratio p,

$(p - p')$, or $(p_w - p_f)$ exceeds $0.18f'_c/f_y$* or when the specified yield strength exceeds 40,000 psi.

The designer may wish to calculate deflection of a member under one or several loading conditions. For example, it may be important to know the maximum instantaneous deflection under dead load plus full working live load. Or it may be that only the live-load deflection will be of interest. On the other hand, it may be of greatest significance to know the long-term deflection of a member under sustained load. Usually the total working live load will act only infrequently on a member, and the sustained-load deflection should be calculated for dead load plus some fraction of the working live load. The fractional part of the live load to be considered depends upon the type of occupancy. For example, in calculating long-term deflections for a beam carrying the floor of a residential apartment, the designer might reasonably consider about 20 per cent of the live load to be sustained. Longtime deflection for a storage warehouse, on the other hand, should probably be based on 100 per cent of design live load.

Methods for predicting instantaneous and longtime deflections were discussed in Art. 2.7. The usual methods for elastic deflections can be used, with E equal to the usual modulus of elasticity for concrete,

$$E_c = 33w^{1.5}\sqrt{f'_c}$$

and I equal to the moment of inertia of either the uncracked or cracked section, depending upon the condition of the beam under the load for which deflection is to be determined. If the extreme tensile fiber stress in the uncracked transformed section exceeds the modulus of rupture

$$f'_t = 7.5\sqrt{f'_c}$$

then the cracked transformed section should be used in calculating I. If the fiber stress is less than the modulus of rupture, calculations may be based on the moment of inertia of the uncracked transformed section. In lieu of this separate calculation, the ACI Code specifies that calculations be based on the uncracked section if pf_y is equal to or less than 500, and on the cracked section if pf_y is greater than that value. For continuous-beam deflections, it is sufficiently accurate in most cases to use a constant moment of inertia equal to the average of the values at the negative and positive bending regions.

The effects of longtime loads can be estimated using the multipliers of Table 2.1, which express additional longtime deflection as a function of duration of loading. The presence of compressive reinforcement is seen

* This value corresponds to the balanced stress ratio p_e for 40,000-psi yield steel used at a working stress of 20,000 psi, with $f_c = 0.45f'_c$.

Scanned with CamScanner

to be of significance in reducing longtime deflection, and it may sometimes be included for this reason alone. For continuous beams, in which different values of A will ordinarily be obtained at positive and negative bending-moment regions, an average value may be used.

The ACI Code includes the following guide to what may be considered to be upper limits on permissible deflections:

1. Maximum limits for immediate deflection due to live load are:
   a. For roofs which do not support plastered ceilings..... $L/180$
   b. For roofs which support plastered ceilings or for floors which do not support partitions..... $L/360$
2. For a floor or roof construction intended to support or to be attached to partitions or other construction likely to be damaged by large deflections of the floor, the allowable limit for the sum of the immediate deflection due to live load and the additional deflection due to shrinkage and creep under all sustained loads shall not exceed..... $L/360$

3.26 Example: deflection calculation The beam shown in Fig. 3.23*a* is a part of the floor system of an apartment house and is designed to carry a dead

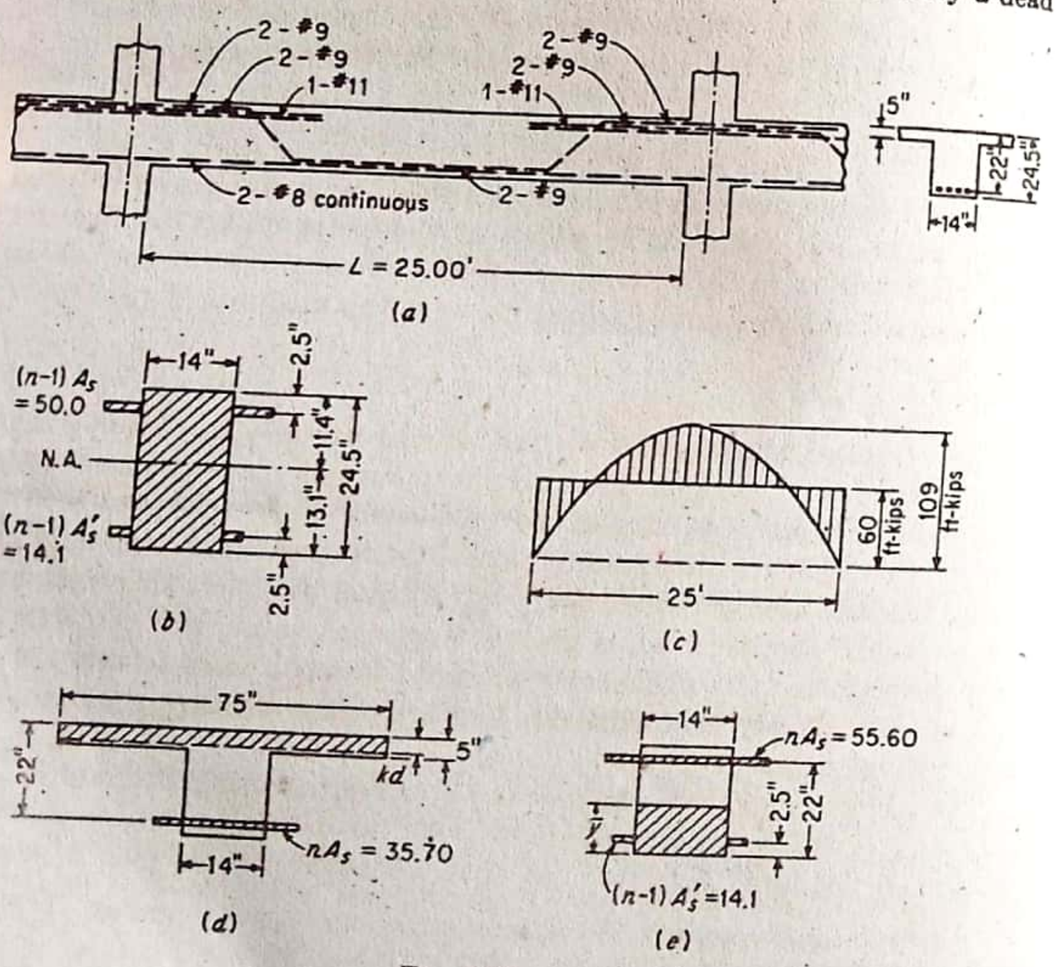


Fig. 3.23

load of 1.0 kip per ft and a working live load of 2.0 kips per ft. Materials of strength $f'_c = 2500$ psi and $f_y = 40{,}000$ psi have been used at working stresses of $f_c = 1125$ psi and $f_s = 20{,}000$ psi, with $n = 10$. Steel is placed 2½ in. from the top and bottom beam faces, as shown in the sketches. It is desired to estimate the deflection of the beam after 5 years of sustained load consisting of full dead load and 20 per cent of the working live load. Under this condition of loading, negative moments are 60 ft-kips at each end of the span.

The beam will first be checked at the supports to determine if cracking occurs under full working load. The ACI moment coefficients (see Table 8.1) are assumed to be applicable, in which case

$$-M = \tfrac{1}{11} wL^2 = \tfrac{1}{11} \times 3.0 \times 25^2 = 171 \text{ ft-kips}$$

With reference to Fig. 3.23*b*, the location of the neutral axis at the support for the uncracked transformed section is found by taking moments about the bottom face of the beam:

$$\bar{y} = \frac{(14 \times 24.5 \times 12.2) + (50 \times 22) + (14.1 \times 2.5)}{(14 \times 24.5) + 50 + 14.1} = 13.1 \text{ in.}$$

Then

$$I_{ut} = (50 \times 8.9^2) + (14.10 \times 10.6^2) + \tfrac{1}{3} \times 14(11.4^3 + 13.1^3) = 22{,}910 \text{ in.}^4$$

and

$$f_{top} = \frac{My_t}{I_{ut}} = \frac{171 \times 12{,}000 \times 11.4}{22{,}910} = 1020 \text{ psi}$$

This substantially exceeds the modulus of rupture, which for this case is $f'_t = 7.5\sqrt{f'_c} = 7.5 \times \sqrt{2500} = 375$ psi, indicating that deflection calculations should be based on the cracked section. Alternatively, applying the ACI criterion,

$$pf_y = \frac{5.56}{14 \times 22} 40{,}000 = 720$$

which substantially exceeds the limiting value of 500 for uncracked analysis. The sustained-load moment diagram, with full dead load and 20 per cent of live load assumed to be acting, is shown in Fig. 3.23*c*. On the basis of this diagram, making use of the second moment-area principle (see Art. 8.3), the instantaneous deflection at midspan is

$$\Delta_i = \frac{1}{EI}\left[\left(\tfrac{1}{3} \times 109 \times 12.5 \times \tfrac{5}{8} \times 12.5\right) - (60 \times 12.5 \times 6.25)\right]$$
$$= \frac{2430}{EI} \quad \text{ft}$$

The modulus of elasticity is

$$E = E_c = 57{,}500\sqrt{f'_c} = 57{,}500\sqrt{2500} = 2{,}880{,}000 \text{ psi}$$

Scanned with CamScanner

[Art. 3.26

At midspan, the effective flange width of the T section is determined, in this case by the restriction that it should not exceed one-quarter of the span length, to be 75 in. In Fig. 3.23*d*, if the neutral axis is in the flange, then

$$p = \frac{3.57}{75 \times 22} = 0.0022$$
$$n = 10$$
$$k = \sqrt{2pn + (pn)^2} - pn = 0.188$$
$$kd = 0.188 \times 22 = 4.14 \text{ in.}$$

which confirms the location of the neutral axis above the bottom of the slab. Then

$$I_{ct} = (\tfrac{1}{3} \times 75 \times 4.14^3) + (35.70 \times 17.86^2) = 13{,}180 \text{ in.}^4$$

At the negative-moment section at the face of the supports, the effective cross section is rectangular and doubly reinforced, and the transformed section is shown in Fig. 3.23*e*. Taking moments about the bottom of the beam face to find the neutral axis,

$$\bar{y} = \frac{(55.60 \times 22) + (14.1 \times 2.5) + 14\bar{y}^2/2}{55.6 + 14.1 + 14\bar{y}} = 9.33 \text{ in.}$$

The moment of inertia is

$$I_{ct} = (55.60 \times 12.67^2) + (14.1 \times 6.83^2) + (\tfrac{1}{3} \times 14 \times 9.33^3) = 13{,}368 \text{ in.}^4$$

The average value of I_{ct} to be used for the calculation of deflection is

$$I_{ct,ave} = \frac{13{,}180 + 13{,}368}{2} = 13{,}274 \text{ in.}^4$$

To account for the sustained nature of the loads, the A factors of Table 2.1 will be used. At midspan, where no compression steel is present, $A = 2.0$. At the support sections, the ratio of compressive to tensile reinforcement is $A_s'/A_s = 1.57/5.56 = 0.283$. By interpolation from Table 2.1, A is found to be 1.5. It is satisfactory to adopt the average of $A = (2.0 + 1.5)/2 = 1.75$ for calculation of the longtime deflection. Then the total deflection due to full dead load and 20 per cent of the live load, after a five-year period of loading, is

$$\Delta_L = \frac{2430}{E_c I_{ct,ave}}(1 + A) = \frac{2430 \times 1728(1 + 1.75)}{2880 \times 13{,}274} = 0.302 \text{ in.}$$

or slightly more than $\frac{1}{4}$ in. If $L/360$ is accepted as a reasonable maximum allowable deflection, then

$$\frac{L}{360} = \frac{25 \times 12}{360} = 0.833 \text{ in.}$$

and it is evident that the proposed construction is satisfactory.

REFERENCES

3.1 *Univ. Illinois Eng. Exp. Sta. Bull.*, no. 399, 1951.

3.2 A. M. Freudenthal: Safety and the Probability of Structural Failures, *Proc. ASCE*, vol. 121, pp. 1337–1397, 1956.

3.3 American Concrete Institute, "Ultimate Strength Design Handbook," 1964.

3.4 American Concrete Institute, "Working Stress Design Handbook," 1964.

3.5 P.-H. Kaar and A. H. Mattock: High Strength Bars as Concrete Reinforcement, *Portland Cement Assoc. Res. Develop. Lab. Develop. Dept. Bull.*, January, 1963.

Scanned with CamScanner

chapter 4

SLABS

4.1 Types of Slabs In reinforced-concrete buildings, slabs are used to provide flat, useful surfaces. A reinforced-concrete slab is a broad, flat plate, usually horizontal, with top and bottom surfaces parallel or nearly so. It may be supported by reinforced-concrete beams (and is usually poured monolithically with such beams), by masonry or reinforced-concrete walls, by structural-steel members, or directly by the ground.

Slabs may be supported on two opposite sides only, as in Fig. 4.1*a*, in which case the structural action of the slab is essentially one-way, the loads being carried by the slab in the direction perpendicular to the supporting beams. On the other hand, there may be beams on all four sides, as in Fig. 4.1*b*, so that two-way action is obtained. Intermediate beams, as shown in Fig. 4.1*c*, may be provided. If the ratio of length to width of one slab panel is larger than about 2, most of the load is carried in the short direction, and one-way action is obtained in effect, even though supports are provided on all sides.

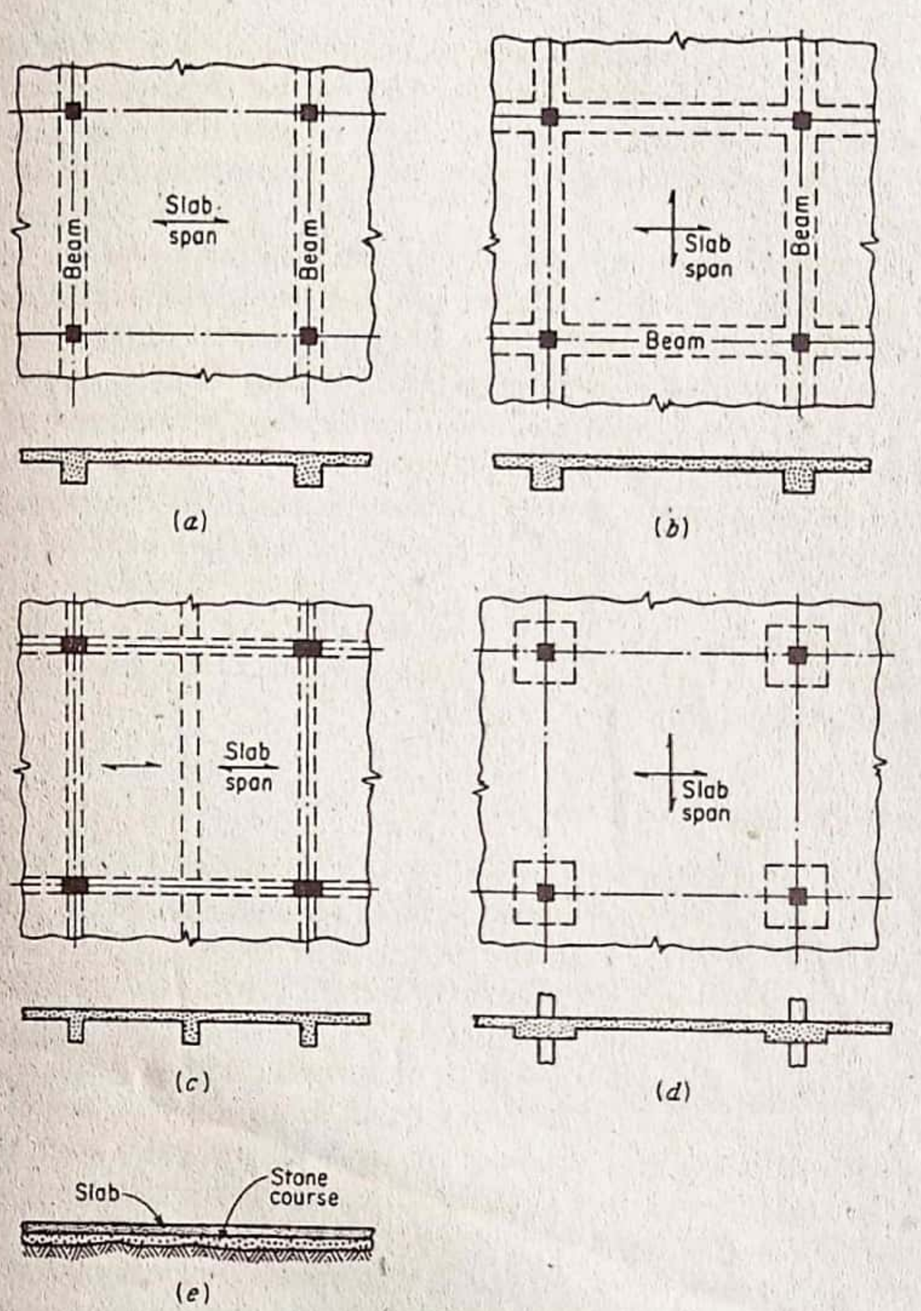


Fig. 4.1

Concrete slabs may in some cases be carried directly by the building columns, as in Fig. 4.1*d*, without the use of beams or girders. The term *flat-slab floor* is used to describe such systems, although in a strict sense all the types described above are flat slabs. In flat-slab floors, the slab may be thickened locally in the vicinity of the columns to reduce stresses due to shear and negative bending. Often the column tops are flared outward for the same reason.

Slabs resting directly on the ground, as in Fig. 4.1*e*, are commonly used in basement or ground floors, for sidewalks, and for highways. While

Scanned with CamScanner

such slabs are often designed by empirical methods, they can be analyzed by methods similar to those developed for beams on elastic foundations. A well-compacted layer of crushed stone or gravel is usually provided under such a slab to ensure uniform support and to provide for proper drainage.

Floor slabs in buildings are usually designed for a uniform live load covering the entire slab area. Concentrated loads on concrete slabs are supported by a width of slab greater than the contact width. Methods of computing the probable distribution of concentrated loads are explained in Art. 12.6. Very heavy, fixed, concentrated loads require supporting beams.

Reinforcing steel for slabs is placed primarily parallel to the surfaces. Straight bar reinforcement may be used, although in continuous slabs bottom bars are often bent up to provide for negative bending over the supports. Welded wire mesh is commonly used for reinforcement of slabs on ground (see Art. 1.10). Bar or rod mats are available for the heavier reinforcement of highway slabs. Slabs may also be prestressed, using high-tensile-strength wires or strands.

ONE-WAY SLABS

4.2 Flexural Analysis A one-way slab is essentially a rectangular beam of comparatively large ratio of width to depth. There are, however, certain factors entering into the design of such slabs which were not considered in the design of rectangular beams. A unit strip of slab cut out at right angles to the supporting beams (shaded area in Fig. 4.2) may be considered as a rectangular beam of unit width, with a depth equal to the thickness of the slab and a length equal to the distance between supports. This strip could be analyzed by the methods which were used in problems dealing with rectangular beams, the bending moment being computed for a unit width, for example. The load per unit area on the slab would then be the load per unit length on the imaginary beam. Since all the load on the slab must be transmitted to the two supporting beams, it follows that all the reinforcing steel should be placed at right angles to these beams, with the exception of any bars that may be placed in the other direction to carry shrinkage and temperature stresses. A one-way slab thus consists of a series of rectangular beams side by side. This simplified analysis, which assumes Poisson's ratio to be zero, is slightly conservative. Actually, longitudinal flexural compression will result in lateral expansion unless the compressed material is restrained. In a one-way slab, this lateral expansion is resisted by the adjacent beam strips, which tend to expand also. The net result is a slight strengthening in the longitudinal direction, but this effect is small and is almost always disregarded.

The ratio of steel in a slab may be determined by dividing the sectional area of one bar by the area of concrete between two successive bars, the latter area being the product of the depth to the center of the bars and the distance between them, center to center. The ratio of steel may also be determined by dividing the average area of steel per foot of width by the effective area of concrete in a 1-ft strip. The average area of steel per foot of width is equal to the area of one bar times the average number of bars in a 1-ft strip (12 divided by the spacing in inches), and the effective area of concrete in a 1-ft (or 12-in.) strip is equal to 12 times the effective depth d.

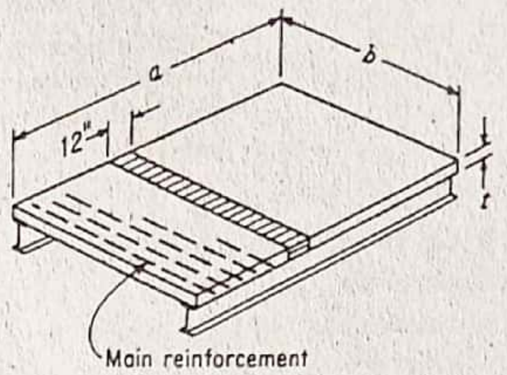


Fig. 4.2

To illustrate the latter method of obtaining the steel ratio p, assume a 5-in. slab with an effective depth of 4 in., with No. 4 bars spaced 4½ in., center to center. The average number of bars in a 12-in. strip of slab is $12/4\frac{1}{2} = 2.7$ bars, and the average steel area in a 12-in. strip is $2.7 \times 0.20 = 0.54$ in.^{2} Hence $p = 0.54/(12 \times 4) = 0.0112$. By the other method, $p = 0.20/(4\frac{1}{2} \times 4) = 0.0112$.

The spacing of bars which is necessary to furnish a given area of steel per foot of width is obtained by dividing the number of bars required to furnish this area into 12. For example, to furnish an average area of 0.46 in.^{2} per ft, with No. 4 bars, requires $0.46/0.20 = 2.3$ bars per foot; the bars must be spaced not more than $12/2.3 = 5.2$ in., center to center.[1]

If the slab is of one span only, and if it rests freely on its supports, the maximum positive moment M, for a uniform load of w psf, is $M = \frac{1}{8}wl^2$. The span length l is taken as the center-to-center distance of supports, but it need not exceed the clear span plus the depth of the slab. If a single-span slab is built monolithically with the supporting beams, the positive and negative moments are computed either by elastic analysis or by moment coefficients (see Art. 8.1) as for continuous beams. Where the width of the support is not known, it may be assumed as 1 ft in obtaining the value of the clear span for use in computing the moments. Such an assumption is usually sufficiently accurate so that no revision is required when the exact width of the support becomes known.

Concrete compression will seldom control the flexural design of one-way slabs, particularly if ultimate-strength design methods are used. Flexural design will ordinarily consist in selecting a slab depth which will permit the use of an economically low steel ratio and which will not allow

[1] The determination of slab steel areas for various combinations of bars and spacing is greatly facilitated by Table 4, Appendix B.

Scanned with CamScanner

Table 4.1 **Minimum slab thicknesses** [*Art.* 4.3

Simply supported	$L/25$
One end continuous	$L/30$
Both ends continuous	$L/35$
Cantilever	$L/12$

unsightly or damaging deflections. The ACI Code specifies the minimum thicknesses in Table 4.1 for all slabs of normal-weight concrete unless calculation of deflections proves that lesser thicknesses may be used without adverse effect. While diagonal tension and bond stresses will seldom influence the design of one-way slabs, these stresses should be checked, particularly for slabs of unusual proportions or loads.

The total slab thickness is usually rounded to the next higher ¼ in. for slabs up to 6 in. thickness, and to the next higher ½ in. for thicker slabs. The concrete protection below the reinforcement should follow the recommendations of the ACI Code (see Art. 3.20) unless conditions warrant some change. In the average slab, a depth of 1 in. below the center of the steel may be used. The lateral spacing of the bars, except those used only to prevent shrinkage and temperature cracks, should not exceed 3 times the thickness of the slab nor 18 in., according to Code. The minimum spacing is given in Art. 3.19.

4.3 Temperature and Shrinkage Reinforcement Concrete shrinks as the cement paste hardens, as was pointed out in Art. 1.9. It is advisable to minimize such shrinkage by using concretes with the smallest possible amounts of water and cement compatible with other requirements, such as strength and workability, and by thorough moist curing of sufficient duration. However, no matter what precautions are taken, a certain amount of shrinkage is usually unavoidable. If a slab of moderate dimensions rests freely on its supports, it can contract to accommodate the shortening of its length produced by shrinkage. Usually, however, slabs and other members are joined rigidly to other parts of the structure and cannot contract freely. This results in tension stresses which are known as *shrinkage stresses*. A decrease in temperature relative to that at which the slab was poured, particularly in outdoor structures such as bridges, may have an effect similar to shrinkage. That is, the slab tends to contract and, if restrained from doing so, becomes subject to tensile stresses.

Since concrete is weak in tension, these temperature and shrinkage stresses are likely to result in cracking. Cracks of this nature are not detrimental, provided their size is limited to what are known as *hairline* cracks. This can be achieved by placing reinforcement in the slab to counteract contraction and distribute the cracks uniformly. As the concrete tends to shrink, such reinforcement resists the contraction and, consequently,

becomes subject to compression. The total shrinkage in a slab so reinforced is less than that in one without reinforcement; in addition, whatever cracks do occur will be of smaller width and more evenly distributed by virtue of the reinforcement.

In one-way slabs the reinforcement provided for resisting the bending moments has the desirable effect of reducing shrinkage and distributing cracks. However, as contraction takes place equally in all directions, it is necessary to provide special reinforcement for shrinkage and temperature contraction in the direction perpendicular to the main reinforcement. This added steel is known as *temperature* or *shrinkage reinforcement*.

Reinforcement for shrinkage and temperature stresses normal to the principal reinforcement should be provided in a structural slab in which the principal reinforcement extends in one direction only. The ACI Code specifies the following minimum ratios of reinforcement area to total concrete area, but in no case shall such reinforcement bars be placed farther apart than 5 times the slab thickness, nor more than 18 in.:

Slabs in which plain bars are used	0.0025
Slabs in which deformed bars with specified yield strengths less than 60,000 psi are used	0.0020
Slabs in which deformed bars with 60,000 psi specified yield strength or welded wire fabric having welded intersections not farther apart in the direction of the stress than 12 in. are used	0.0018

4.4 Example: one-way slab design A reinforced-concrete slab is built integrally with its supports and consists of two equal spans, each with a clear span of 15 ft. The working live load is 100 psf, and 4000-psi concrete is specified for use with steel of yield stress equal to 60,000 psi. Design the slab, using U.S.D. methods, following the provisions of the ACI Code.

The thickness of the slab is first estimated, based on the minimum thickness of Table 4.1: $L/35 = 15 \times 12/35 = 5.15$ in. A trial thickness of 5.25 in. will be used, for which the weight is $150 \times 5.25/12 = 66$ psf. The working live load and computed dead load are then multiplied by the ACI overload factors to obtain ultimate design loads:

Dead load:	$66 \times 1.5 =$	99 psf
Live load:	$100 \times 1.8 =$	180 psf
Total		279 psf

For this case, design moments at critical sections may be found using the ACI moment coefficients (see Table 8.1):

At interior support: $-M = \frac{1}{16} \times 0.279 \times 15^2 = 6.98$ ft-kips
At midspan: $+M = \frac{1}{14} \times 0.279 \times 15^2 = 4.48$ ft-kips
At exterior support: $-M = \frac{1}{24} \times 0.279 \times 15^2 = 2.62$ ft-kips

Scanned with CamScanner

The maximum steel ratio premitted by Code is [Art. 4.4

$$0.75p_b = 0.75 \times 0.85k_1 \frac{f'_c}{f_y} \frac{87{,}000}{87{,}000 + f_y}$$
$$= 0.75 \times 0.85^2 \times \tfrac{4}{60} \times \tfrac{87}{147} = 0.021$$

The minimum required effective depth, as controlled by the negative moment at the interior support, is found from Eq. (3.5*b*) to be

$$d^2 = \frac{M_u}{\phi p f_y b(1 - 0.59 p f_y/f'_c)}$$
$$= \frac{6.98 \times 12}{0.90 \times 0.21 \times 60 \times 12(1 - 0.59 \times 0.021 \times \tfrac{60}{4})}$$
$$= 7.58 \text{ in.}^2$$
$$d = 2.75 \text{ in.}^*$$

This is less than the effective depth of $5.25 - 1.00 = 4.25$ in. required by Code for deflection considerations, and the latter figure will be adopted. At the interior support, assuming the stress-block depth $a = 1.00$ in., the area of steel required per foot of width in the top of the slab is

$$A_s = \frac{M}{\phi f_y(d - a/2)} = \frac{6.98 \times 12}{0.90 \times 60 \times 3.75} = 0.41 \text{ in.}^2$$

Checking the assumed a,

$$a = \frac{A_s f_y}{0.85 f'_c b} = \frac{0.41 \times 60}{0.85 \times 4 \times 12} = 0.60 \text{ in.}$$

A second trial will be made with $a = 0.50$ in. Then

$$A_s = \frac{6.98 \times 12}{0.90 \times 60 \times 4.00} = 0.39 \text{ in.}$$

for which $a = 0.60 \times 0.39/0.41 = 0.57$ in. No further revision is necessary. At other critical moment sections, it will be satisfactory to use the same lever arm, $4.25 - 0.50/2 = 4.00$ in., to determine steel areas, and

At midspan: $A_s = \dfrac{4.48 \times 12}{0.90 \times 60 \times 4.00} = 0.25 \text{ in.}^2$

At exterior support: $A_s = \dfrac{2.62 \times 12}{0.90 \times 60 \times 4.00} = 0.15 \text{ in.}^2$

The maximum shear stress, at the face of the interior support, is

$$V_u = 1.15 \frac{279 \times 15}{2} = 2410 \text{ lb}$$

and

$$v_u = \frac{2410}{12 \times 4.25} = 47 \text{ psi}$$

* This depth is more easily found using Graph 1, Appendix B. For $p = p_{max}$, $M_u/\phi b d^2 = 1050$, from which $d = 2.75$ in.

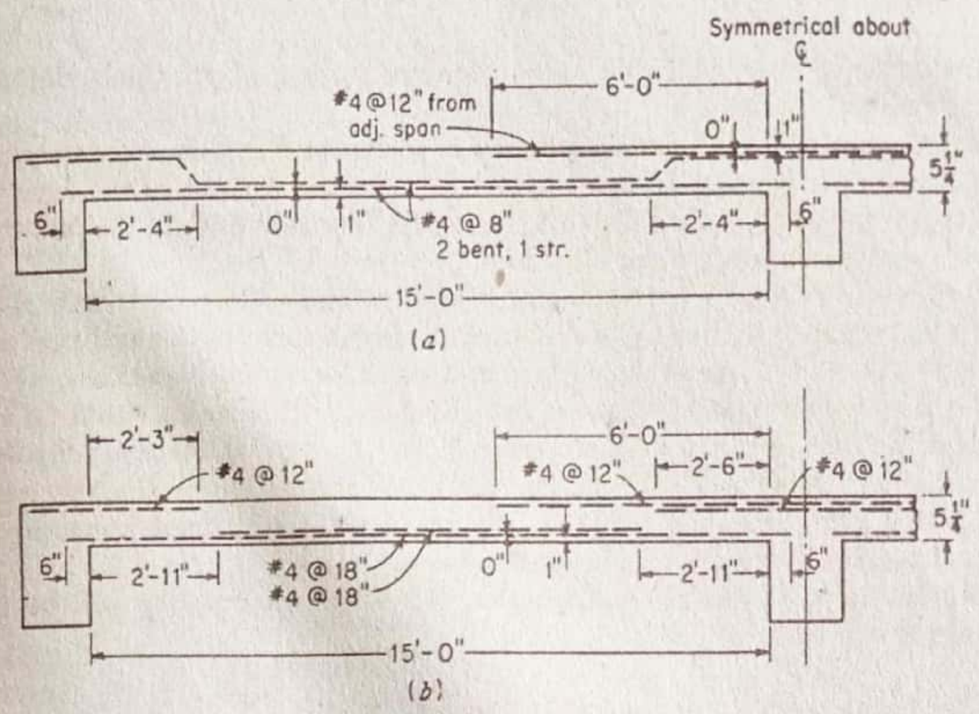


Fig. 4.3

This is well below the permissible value of shear on the unreinforced concrete, which is $v_c = 2\phi\sqrt{f'_c} = 2 \times 0.85\sqrt{4000} = 107$ psi.

The required tensile-steel areas may be provided in a variety of ways, but, whatever the selection, due consideration must be given to actual placing of the steel during construction. The arrangement should be such that the steel may be placed rapidly with the minimum of labor costs even though excess steel is necessary to achieve this end.

Two possible arrangements are shown in Fig. 4.3. In Fig. 4.3*a* bent bars are used, while in Fig. 4.3*b* all bars are straight. The arrangement in (*a*) requires slightly more steel and the additional cost of bending but, on the other hand, requires fewer supporting chairs and permits easier placement, with less likelihood of bar omissions.

In the arrangement of Fig. 4.3*a*, No. 4 bars at 8 in. furnish 0.29 in.^{2} of steel at midspan, slightly more than required. If two-thirds of these bars are bent upward for negative reinforcement over the interior support, the average spacing of such bent bars at the interior support will be $(8 + 16)/2 = 12$ in. Since an identical pattern of bars is bent upward from the other side of the support, the effective spacing of the No. 4 bars over the interior support is 6 in. This pattern provides just the required steel area of 0.39 in.^{2} per ft width of slab over the support. The bars bent at the interior support will also be bent upward for negative reinforcement at the exterior support, providing reinforcement equivalent to No. 4 bars at 12 in., or 0.20 in.^{2} of steel, somewhat in excess of the required 0.15 in.^{2}

Note that it is not considered necessary to achieve uniform spacing of reinforcement in slabs, and that the steel provided can be calculated safely on the basis of average spacing as in the example. Care should be taken to satisfy

Scanned with CamScanner

requirements for both minimum and maximum spacing of principal reinforcement, however.

The locations of bend and cutoff points shown in Fig. 4.3*a* were obtained using Graph 11, Appendix B, as explained in Art. 3.20. A check of the development length provided against Table 8, Appendix B, makes evident the fact that flexural bond stress need not be considered.

The arrangement of Fig. 4.3*b* uses only straight bars. While apparently satisfactory according to the ACI Code, cutting off the shorter positive and negative bars as shown leads to an undesirable condition at the ends of those bars, where there will be concentrations of stress in the concrete. The design would be improved if the negative bars were cut off at 2 ft 11 in. from the face of supports, rather than 2 ft 3 in. and 2 ft 6 in. as shown, and if the positive steel were cut off at 2 ft 3 in., rather than at 2 ft 11 in. This would result in an overlap of approximately $2d$ of the cut positive and negative bars.

Reinforcement to control temperature and shrinkage cracking will be included in the amount of

$$A_s = 0.0018 \times 12 \times 5.25 = 0.11 \text{ in.}^2$$

per 12-in. strip. This requirement is met by using No. 3 bars, at 12 in. spacing, placed directly on top of the main reinforcement in the positive-moment region and directly underneath the main reinforcement in the negative-moment zone.

PROBLEMS

1. A small bridge consisting of a concrete slab supported by steel stringers is to carry a uniformly distributed load of 300 psf in addition to its own weight. The four stringers of the bridge, spanning in the long direction, are spaced 8 ft on centers. The concrete slab spans in the transverse direction and is continuous over the two interior stringers. Find the required thickness of the slab, and design and detail the bar reinforcement, using $f_s = 20{,}000$ psi and $f_c = 1350$ psi, with $n = 9$. Bent bars will be used in preference to all-straight-bar reinforcement. The ACI moment coefficients do not apply.

2. Redesign the bridge of Prob. 1, using ultimate-strength methods, with overload factors of 1.5 and 1.8 applied to dead and live loads, respectively. For the steel, $f_y = 40{,}000$ psi, and the concrete strength is $f'_c = 3000$ psi. Use a maximum steel ratio of $0.50p_b$.

TWO-WAY SLABS

4.5 Performance of Two-way Slabs Most rectangular reinforced-concrete slabs are supported on all four sides by beams, girders, or walls. Figure 1.1*a* shows a typical example of a beam-and-girder floor in which each individual slab panel is so supported. If the proportions of the panel are not too far from square (side ratio up to about 2:1), the slab bends under load into a dished surface rather than into a cylindrical one, as

would be the case for one-way slabs supported only at two opposite sides. This means that at any point the slab is curved in both principal directions, and since bending moments are proportional to curvatures, moments also exist in both directions. To resist these moments, the slab must be reinforced in both directions, by two mutually perpendicular layers of bars parallel, respectively, to the two pairs of edges, one layer resting directly on the other. The slab, then, transmits loads to all four supporting beams, the relative amounts depending on the proportions of the slab and the conditions of continuity at the four edges.

In order to visualize the flexural performance of such a slab, it is convenient to think of it as consisting of two sets of parallel strips, in each of the two directions, intersecting each other. Evidently, part of the load is carried by one set and transmitted to one pair of edge supports, and the remainder by the other. Figure 4.4 shows the two center strips of a rectangular plate with short span A and long span B. If the uniform load is w per ft^2 of slab, each of the two strips acts approximately like a simple beam uniformly loaded by its share of w. Because these imaginary strips actually are part of the same monolithic slab, their deflections at the intersection point must be the same. Equating the center deflections of the short and long strips,

$$\frac{5w_s A^4}{384EI} = \frac{5w_l B^4}{384EI}$$

where w_s = share of load w carried in short direction
w_l = share of load w carried in long direction

Consequently,

$$\frac{w_s}{w_l} = \frac{B^4}{A^4} \tag{4.1}$$

One sees that the larger share of the load is carried in the short direction, the ratio of the two portions of the total load being proportional to the fourth power of the ratio of the spans. This result is approximate because the actual behavior of a slab is more complex than that of the two intersecting strips, but it is a good approximation when the edge conditions are the same on all four sides (e.g., simply supported or rotationally fixed). The two pairs of edge beams can then be designed for the loads w_s and w_l transmitted to them by the slab.

An understanding of the flexural behavior of the slab itself can be

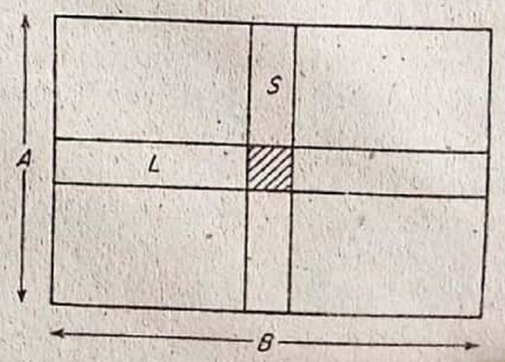


Fig. 4.4

Scanned with CamScanner

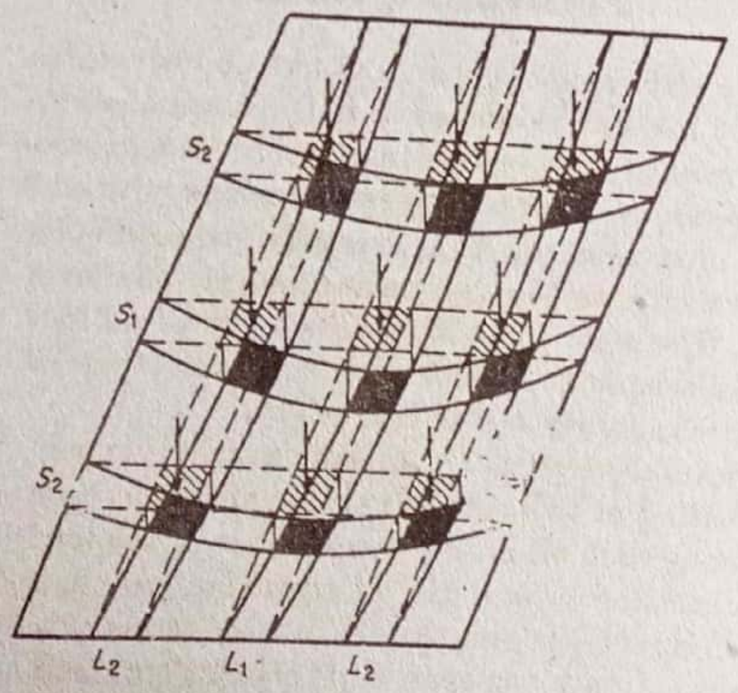


Fig. 4.5 Grid model of uniformly loaded, simply supported slab.

gained from Fig. 4.5, which shows a slab model consisting of two sets of three strips each. It is seen that the two central strips S_1 and L_1 bend in a manner similar to that of Fig. 4.4. The outer strips S_2 and L_2, however, are not only bent, but also twisted. Consider, for instance, one of the intersections of S_2 with L_2. It is seen that at the intersection the exterior edge of strip L_2 is at a higher elevation than the interior edge, while at the nearby end of strip L_2 both edges are at the same elevation; the strip is twisted. This twisting results in torsional stresses and torsional moments which are seen to be most pronounced near the corners. Consequently, the total load on the slab is carried not only by the bending moments in the two directions, but also by the twisting moments. For this reason bending moments in elastic slabs are smaller than would be computed for sets of unconnected strips loaded by w_s and w_l. For instance, for a simply supported square slab, $w_s = w_l = w/2$ [Eq. (4.1)]. If only bending were present, the maximum moment in each strip would be

$$(w/2)A^2/8 = 0.0625wA^2$$

The exact theory of bending of elastic plates shows that actually the maximum moment in such a square slab is only $0.048wA^2$, so that in this case the twisting moments relieve the bending moments by about 25 per cent.

The largest moment occurs where the curvature is sharpest. Figure 4.5 shows this to be the case at midspan of the short strip S_1. Suppose the load is increased until this location is overstressed, so that the steel at the middle of strip S_1 is yielding. If the strip were an isolated beam, it would now fail. Considering the slab as a whole, however, one sees that no immediate failure will occur. The neighboring strips (those parallel as well as those perpendicular to S_1), being actually monolithic with it, will take over that share of any additional load which strip S_1 can no longer carry,

until they, in turn, start yielding. This inelastic redistribution will continue until, in a rather large area in the central portion of the slab, all the steel in both directions is yielding. Only then will the entire slab fail. From this reasoning, which is confirmed by tests, it follows that slabs need not be designed for the absolute maximum moment in each of the two directions (such as $0.048wA^2$ in the example of the preceding paragraph), but only for a smaller average moment in each of the two directions in the central portion of the slab. For instance, one of the several analytical methods provided in the ACI Code permits the above square slab to be designed for a moment of $0.036wA^2$. By comparison with the actual elastic maximum moment, $0.048wA^2$, it is seen that, owing to inelastic redistribution, a moment reduction of 25 per cent is provided.

The flexural behavior of a simply supported slab is summarized in the solid lines of Fig. 4.6. The largest moments occur in the center strips, along 1-1 and 2-2. The moment diagram in the short direction along 1-1 is given by Fig. 4.6*a* and shows a maximum $M_{A,\max}$ at midspan. From Fig. 4.5 it is seen that short strips located closer to the edges (such as S_2) deflect less, are less sharply curved, and consequently have smaller bending moments than the central strip. Therefore, the maximum moment

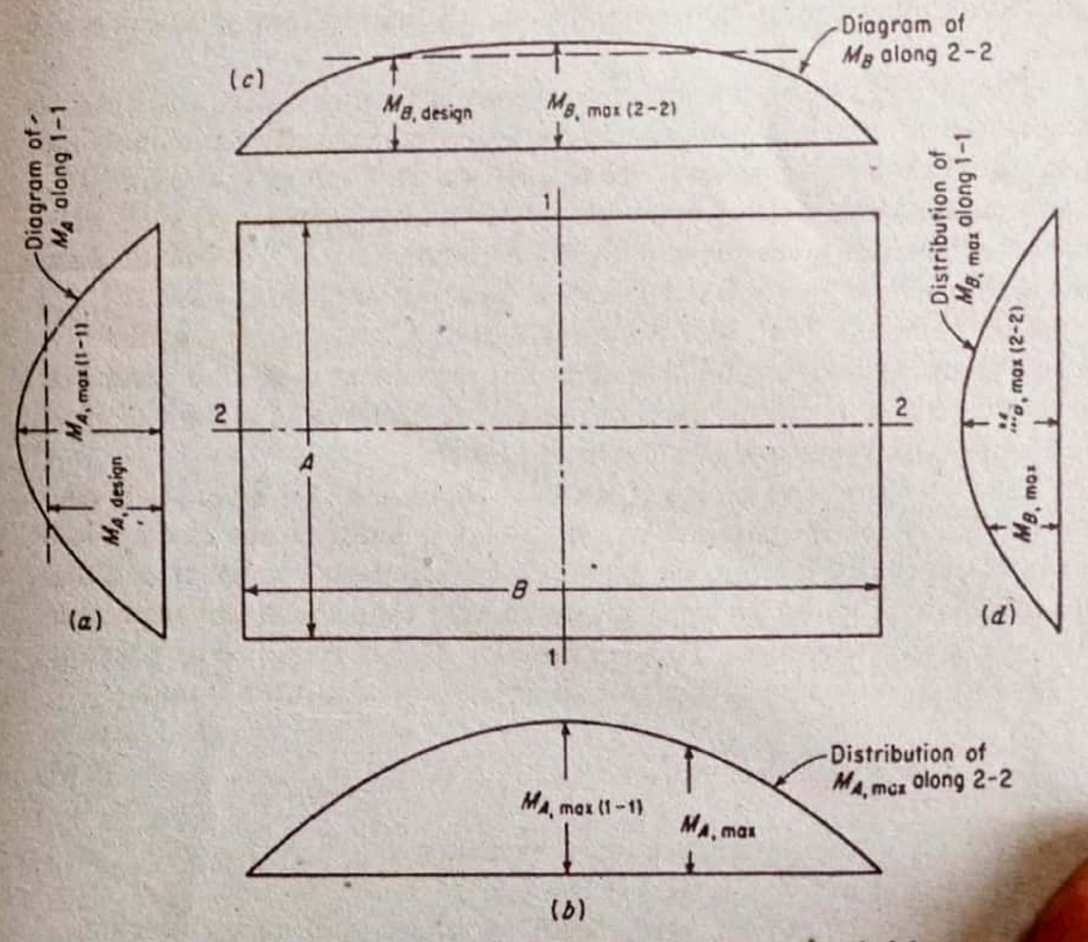


Fig. 4.6 Moments in uniformly loaded, simply supported slab.

Scanned with CamScanner

$M_{A,max}$ at the center of the short strips is distributed longitudinally, as in Fig. 4.6*b*; it is largest at the center and decreases toward zero at the edges. For a slab which departs significantly from square, the moment M_B in the center strip in the long direction is fairly constant in the middle half of the slab. This is seen from Fig. 4.6*c*, which gives the moment diagram along 2-2. Again, inspection of Fig. 4.5 shows that in long strips located closer to the edges (such as L_2) deflection, curvatures, and therefore bending moments are smaller than in the central strip L_1. The distribution of $M_{B,max}$ as it varies in the short direction is shown in Fig. 4.6*d*. As explained before, in view of inelastic redistribution it is not necessary to design for the absolute maximum values of M_A and M_B. The manner in which this and other features are considered in design is discussed in the next article.

4.6 Design of Two-way Slabs by ACI Code The Code provides that slabs with side ratios no larger than 2:1 shall be designed as two-way slabs. From Eq. (4.1) it is seen that for a slab of this proportion the share of the load carried in the long direction is only of the order of one-sixteenth that in the short direction. Hence, such a slab acts almost as if it were spanning in the short direction only. In agreement with this, the Code provides that any slab more oblong than 2:1 shall be treated as a one-way slab.

The precise determination of moments in two-way slabs with various conditions of continuity at the edges is mathematically formidable and not suited to design practice. For this reason the Code provides simplified methods for determining moments, shears, and reactions of such slabs. In fact, the Code gives three different methods for this purpose. Of these, the authors hold method 3 to be the most rational and, generally, the most economical. The older methods 1 and 2, successfully applied over many years, also give reliable results but are not as clear and consistent in approach and assumptions. For reasons of clarity, and in view of space limitations, only method 3 is presented herein.

The Code provides tables of moment coefficients for a variety of conditions. These coefficients are based on elastic analysis but also account for inelastic redistribution. In consequence, the design moment in either direction is smaller by an appropriate amount than the elastic maximum moment in that direction. This is shown by dashed lines in Fig. 4.6*a* and *c*. The design moments in the two directions are computed from

$$M_A = C_A w A^2 \qquad M_B = C_B w B^2 \tag{4.2}$$

where C_A, C_B = tabulated moment coefficients
w = uniform load, psf or lb/ft²
A, B = length of clear span in short and long directions, respectively

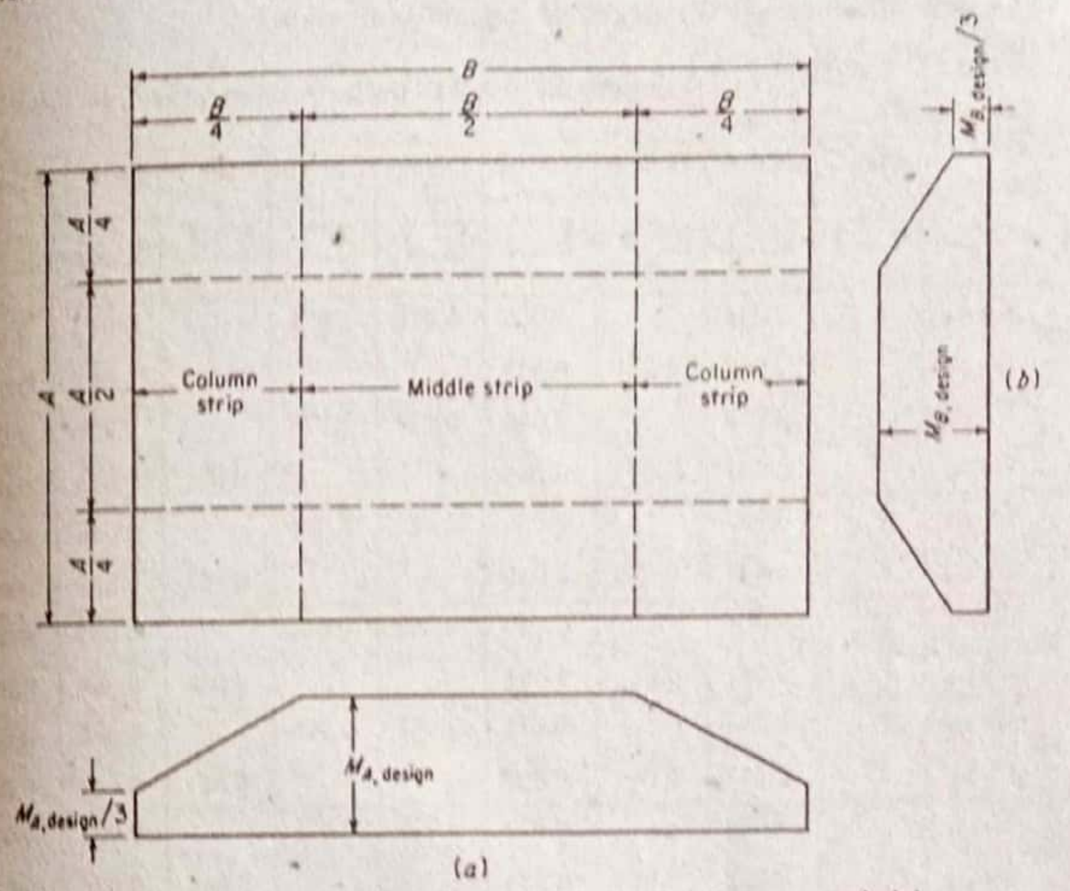


Fig. 4.7 Design moments, ACI method 3, for simply supported slab.

The Code provides that each panel be divided in both directions into a middle strip whose width is one-half that of the panel and two column strips of one-quarter of the panel width (see Fig. 4.7). As discussed before and shown in Fig. 4.6*b* and *d*, the moments in both directions are larger in the center portion of the slab than in regions close to the edges. Correspondingly, it is provided in method 3 that the entire middle strip be designed for the full, tabulated design moment. In the column strips this moment is assumed to decrease from its full value at the edge of the middle strip to one-third of this value at the edge of the panel. This distribution is shown in dashed lines in Fig. 4.7*a* and *b*.

The discussion so far has been restricted to a single panel simply supported at all four edges. An actual situation is shown in Fig. 4.8, in

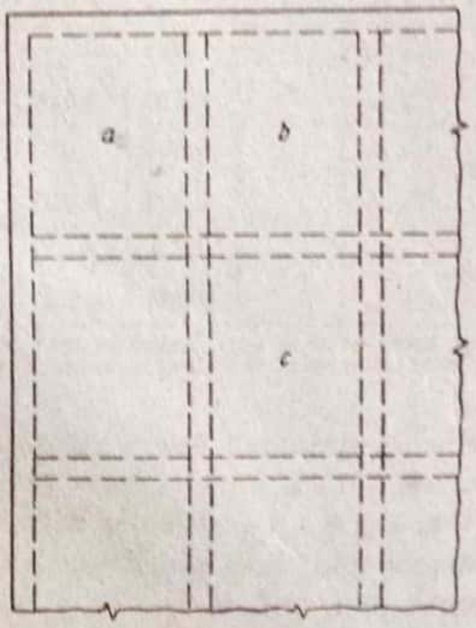


Fig. 4.8 Portion of typical two-way slab floor.

Scanned with CamScanner

Table 4.2 **Coefficients for negative moments in slabs*** [*Art. 4.6*

$M_{A\,neg} = C_{A\,neg} \times w \times A^2$
$M_{B\,neg} = C_{B\,neg} \times w \times B^2$ } where w = total uniform dead plus live load

Ratio $m = \frac{A}{B}$		Case 1	Case 2	Case 3	Case 4	Case 5	Case 6	Case 7	Case 8	Case 9
1.00	$C_{A\,neg}$		0.045		0.050	0.075	0.071		0.033	0.061
	$C_{B\,neg}$		0.045	0.076	0.050			0.071	0.061	0.033
0.95	$C_{A\,neg}$		0.050		0.055	0.079	0.075		0.038	0.065
	$C_{B\,neg}$		0.041	0.072	0.045			0.067	0.056	0.029
0.90	$C_{A\,neg}$		0.055		0.060	0.080	0.079		0.043	0.068
	$C_{B\,neg}$		0.037	0.070	0.040			0.062	0.052	0.025
0.85	$C_{A\,neg}$		0.060		0.066	0.082	0.083		0.049	0.072
	$C_{B\,neg}$		0.031	0.065	0.034			0.057	0.046	0.021
0.80	$C_{A\,neg}$		0.065		0.071	0.083	0.086		0.055	0.075
	$C_{B\,neg}$		0.027	0.061	0.029			0.051	0.041	0.017
0.75	$C_{A\,neg}$		0.069		0.076	0.085	0.088		0.061	0.078
	$C_{B\,neg}$		0.022	0.056	0.024			0.044	0.036	0.014
0.70	$C_{A\,neg}$		0.074		0.081	0.086	0.091		0.068	0.081
	$C_{B\,neg}$		0.017	0.050	0.019			0.038	0.029	0.011
0.65	$C_{A\,neg}$		0.077		0.085	0.087	0.093		0.074	0.083
	$C_{B\,neg}$		0.014	0.043	0.015			0.031	0.024	0.008
0.60	$C_{A\,neg}$		0.081		0.089	0.088	0.095		0.080	0.085
	$C_{B\,neg}$		0.010	0.035	0.011			0.024	0.018	0.006
0.55	$C_{A\,neg}$		0.084		0.092	0.089	0.096		0.085	0.086
	$C_{B\,neg}$		0.007	0.028	0.008			0.019	0.014	0.005
0.50	$C_{A\,neg}$		0.086		0.094	0.090	0.097		0.089	0.088
	$C_{B\,neg}$		0.006	0.022	0.006			0.014	0.010	0.003

*A cross-hatched edge indicates that the slab continues across or is fixed at the support; an unmarked edge indicates a support at which torsional resistance is negligible.

which a system of beams supports a two-way slab. It is seen that some panels, such as panel *a*, have two discontinuous exterior edges, while the other edges are continuous with their neighbors. Panel *b* has one discontinuous and three continuous edges, the interior panel *c* has all edges continuous, and so on. At a continuous edge in a slab, moments are negative, just as at interior supports of continuous beams. Also, the mag-

nitude of the positive moments depends on the conditions of continuity at all four edges.

Correspondingly, Table 4.2, reproduced from the Code, gives moment coefficients C for *negative moments at continuous edges*. The details of the table are self-explanatory. Maximum negative edge moments obtain when both panels adjacent to the particular edge carry full dead and live load.

Table 4.3 **Coefficients for dead-load positive moments in slabs***

$M_{A\,pos\,DL} = C_{A\,DL} \times w \times A^2$
$M_{B\,pos\,DL} = C_{B\,DL} \times w \times B^2$ } where w = total uniform dead load

Ratio $m = \frac{A}{B}$		Case 1	Case 2	Case 3	Case 4	Case 5	Case 6	Case 7	Case 8	Case 9
1.00	$C_{A\,DL}$	0.036	0.018	0.018	0.027	0.027	0.033	0.027	0.020	0.023
	$C_{B\,DL}$	0.036	0.018	0.027	0.027	0.018	0.027	0.033	0.023	0.020
0.95	$C_{A\,DL}$	0.040	0.020	0.021	0.030	0.028	0.036	0.031	0.022	0.024
	$C_{B\,DL}$	0.033	0.016	0.025	0.024	0.015	0.024	0.031	0.021	0.017
0.90	$C_{A\,DL}$	0.045	0.022	0.025	0.033	0.029	0.039	0.035	0.025	0.026
	$C_{B\,DL}$	0.029	0.014	0.024	0.022	0.013	0.021	0.028	0.019	0.015
0.85	$C_{A\,DL}$	0.050	0.024	0.029	0.036	0.031	0.042	0.040	0.029	0.028
	$C_{B\,DL}$	0.026	0.012	0.022	0.019	0.011	0.017	0.025	0.017	0.013
0.80	$C_{A\,DL}$	0.056	0.026	0.034	0.039	0.032	0.045	0.045	0.032	0.029
	$C_{B\,DL}$	0.023	0.011	0.020	0.016	0.009	0.015	0.022	0.015	0.010
0.75	$C_{A\,DL}$	0.061	0.028	0.040	0.043	0.033	0.048	0.051	0.036	0.031
	$C_{B\,DL}$	0.019	0.009	0.018	0.013	0.007	0.012	0.020	0.013	0.007
0.70	$C_{A\,DL}$	0.068	0.030	0.046	0.046	0.035	0.051	0.058	0.040	0.033
	$C_{B\,DL}$	0.016	0.007	0.016	0.011	0.005	0.009	0.017	0.011	0.006
0.65	$C_{A\,DL}$	0.074	0.032	0.054	0.050	0.036	0.054	0.065	0.044	0.034
	$C_{B\,DL}$	0.013	0.006	0.014	0.009	0.004	0.007	0.014	0.009	0.005
0.60	$C_{A\,DL}$	0.081	0.034	0.062	0.053	0.037	0.056	0.073	0.048	0.036
	$C_{B\,DL}$	0.010	0.004	0.011	0.007	0.003	0.006	0.012	0.007	0.004
0.55	$C_{A\,DL}$	0.088	0.035	0.071	0.056	0.038	0.058	0.081	0.052	0.037
	$C_{B\,DL}$	0.008	0.003	0.009	0.005	0.002	0.004	0.009	0.005	0.003
0.50	$C_{A\,DL}$	0.095	0.037	0.080	0.059	0.039	0.061	0.089	0.056	0.038
	$C_{B\,DL}$	0.006	0.002	0.007	0.004	0.001	0.003	0.007	0.004	0.002

*A cross-hatched edge indicates that the slab continues across or is fixed at the support; an unmarked edge indicates a support at which torsional resistance is negligible.

Scanned with CamScanner

Table 4.4 **Coefficients for live-load positive moments in slabs*** [*Art. 4.6*

$M_{A\,pos,\,LL} = C_{A\,LL} \times w \times A^2$
$M_{B\,pos,\,LL} = C_{B\,LL} \times w \times B^2$
} where w = total uniform live load

Ratio $m = \frac{A}{B}$		Case 1	Case 2	Case 3	Case 4	Case 5	Case 6	Case 7	Case 8	Case 9
1.00	$C_{A\,LL}$	0.036	0.027	0.027	0.032	0.032	0.035	0.032	0.028	0.030
	$C_{B\,LL}$	0.036	0.027	0.032	0.032	0.027	0.032	0.035	0.030	0.028
0.95	$C_{A\,LL}$	0.040	0.030	0.031	0.035	0.034	0.038	0.036	0.031	0.032
	$C_{B\,LL}$	0.033	0.025	0.029	0.029	0.024	0.029	0.032	0.027	0.025
0.90	$C_{A\,LL}$	0.045	0.034	0.035	0.039	0.037	0.042	0.040	0.035	0.036
	$C_{B\,LL}$	0.029	0.022	0.027	0.026	0.021	0.025	0.029	0.024	0.022
0.85	$C_{A\,LL}$	0.050	0.037	0.040	0.043	0.041	0.046	0.045	0.040	0.039
	$C_{B\,LL}$	0.026	0.019	0.024	0.023	0.019	0.022	0.026	0.022	0.020
0.80	$C_{A\,LL}$	0.056	0.041	0.045	0.048	0.044	0.051	0.051	0.044	0.042
	$C_{B\,LL}$	0.023	0.017	0.022	0.020	0.016	0.019	0.023	0.019	0.017
0.75	$C_{A\,LL}$	0.061	0.045	0.051	0.052	0.047	0.055	0.056	0.049	0.046
	$C_{B\,LL}$	0.019	0.014	0.019	0.016	0.013	0.016	0.020	0.016	0.013
0.70	$C_{A\,LL}$	0.068	0.049	0.057	0.057	0.051	0.060	0.063	0.054	0.050
	$C_{B\,LL}$	0.016	0.012	0.016	0.014	0.011	0.013	0.017	0.014	0.011
0.65	$C_{A\,LL}$	0.074	0.053	0.064	0.062	0.055	0.064	0.070	0.059	0.054
	$C_{B\,LL}$	0.013	0.010	0.014	0.011	0.009	0.010	0.014	0.011	0.009
0.60	$C_{A\,LL}$	0.081	0.058	0.071	0.067	0.059	0.068	0.077	0.065	0.059
	$C_{B\,LL}$	0.010	0.007	0.011	0.009	0.007	0.008	0.011	0.009	0.007
0.55	$C_{A\,LL}$	0.088	0.062	0.080	0.072	0.063	0.073	0.085	0.070	0.063
	$C_{B\,LL}$	0.008	0.006	0.009	0.007	0.005	0.006	0.009	0.007	0.006
0.50	$C_{A\,LL}$	0.095	0.066	0.088	0.077	0.067	0.078	0.092	0.076	0.067
	$C_{B\,LL}$	0.006	0.004	0.007	0.005	0.004	0.005	0.007	0.005	0.004

*A cross-hatched edge indicates that the slab continues across or is fixed at the support; an unmarked edge indicates a support at which torsional resistance is negligible.

Hence, the moment is computed for this total load. The Code provides that *negative moments at discontinuous edges* shall be assumed equal to one-third of the positive moments for the same direction. One must provide for such moments because some degree of restraint is provided discontinuous edges by the torsional rigidity of the edge beam or by the supporting wall.

As for *positive moments*, there will be little, if any, rotation at the continuous edges if *dead load* alone is acting, because the loads on both adjacent panels tend to produce opposite rotations which cancel, or nearly so. Hence, for this condition the continuous edges can be regarded as fixed, and the appropriate coefficients for the dead-load moments are given in Table 4.3. On the other hand, the maximum *live-load moments* are obtained when live load is placed only on the particular panel, and

Table 4.5 **Ratio of load w in A and B directions for shear in slab and load on supports***

Ratio $m = \frac{A}{B}$		Case 1	Case 2	Case 3	Case 4	Case 5	Case 6	Case 7	Case 8	Case 9
1.00	W_A	0.50	0.50	0.17	0.50	0.83	0.71	0.29	0.33	0.67
	W_B	0.50	0.50	0.83	0.50	0.17	0.29	0.71	0.67	0.33
0.95	W_A	0.55	0.55	0.20	0.55	0.86	0.75	0.33	0.38	0.71
	W_B	0.45	0.45	0.80	0.45	0.14	0.25	0.67	0.62	0.29
0.90	W_A	0.60	0.60	0.23	0.60	0.88	0.79	0.38	0.43	0.75
	W_B	0.40	0.40	0.77	0.40	0.12	0.21	0.62	0.57	0.25
0.85	W_A	0.66	0.66	0.28	0.66	0.90	0.83	0.43	0.49	0.79
	W_B	0.34	0.34	0.72	0.34	0.10	0.17	0.57	0.51	0.21
0.80	W_A	0.71	0.71	0.33	0.71	0.92	0.86	0.49	0.55	0.83
	W_B	0.29	0.29	0.67	0.29	0.08	0.14	0.51	0.45	0.17
0.75	W_A	0.76	0.76	0.39	0.76	0.94	0.88	0.56	0.61	0.86
	W_B	0.24	0.24	0.61	0.24	0.06	0.12	0.44	0.39	0.14
0.70	W_A	0.81	0.81	0.45	0.81	0.95	0.91	0.62	0.68	0.89
	W_B	0.19	0.19	0.55	0.19	0.05	0.09	0.38	0.32	0.11
0.65	W_A	0.85	0.85	0.53	0.85	0.96	0.93	0.69	0.74	0.92
	W_B	0.15	0.15	0.47	0.15	0.04	0.07	0.31	0.26	0.08
0.60	W_A	0.89	0.89	0.61	0.89	0.97	0.95	0.76	0.80	0.94
	W_B	0.11	0.11	0.39	0.11	0.03	0.05	0.24	0.20	0.06
0.55	W_A	0.92	0.92	0.69	0.92	0.98	0.96	0.81	0.85	0.95
	W_B	0.08	0.08	0.31	0.08	0.02	0.04	0.19	0.15	0.05
0.50	W_A	0.94	0.94	0.76	0.94	0.99	0.97	0.86	0.89	0.97
	W_B	0.06	0.06	0.24	0.06	0.01	0.03	0.14	0.11	0.03

*A cross-hatched edge indicates that the slab continues across or is fixed at the support; an unmarked edge indicates a support at which torsional resistance is negligible.

Scanned with CamScanner

not on any of the adjacent panels. In this case some rotation will occur at all continuous edges. As an approximation, the Code assumes 50 per cent restraint for calculating these live-load moments. The corresponding coefficients are given in Table 4.4. Finally, for computing shear in the slab and loads on the supporting beams, Table 4.5 gives the fractions of the total load w which are transmitted in the two directions. It is easily checked that for cases 1 and 2 these fractions are in exact accord with Eq. 4.1. In the other cases they are different, depending on the particular edge conditions.

Since positive-moment steel is placed in two layers, the distance d for the upper layer is smaller than that for the lower layer by one bar diameter (when the same bar size is used for both layers.) Because the moments in the long direction are the smaller ones, it is economical to place the steel in that direction on top of the bars in the short direction. The twisting moments discussed in Art. 4.5 are usually of consequence only in exterior corners, where they tend to crack the slab along 45° lines of the corner panels. For this reason the Code provides that, in addition to the calculated reinforcement, special reinforcement shall be provided at exterior corners in both bottom and top of the slab, for a distance in each direction from the corner equal to one-fifth the long span. The reinforcement in the top of the slab shall be parallel to the diagonal from the corner. The reinforcement in the bottom of the slab shall be at right angles to the diagonal, or it may consist of bars in two directions parallel to the sides of the slab. The reinforcement in each band shall be of size and spacing equivalent to that required for the maximum positive moment in the slab.

The precise locations of inflection points in two-way slabs are not easily determined, since they depend on the side ratio, ratio of live to dead load, and continuity conditions at the edges. A reasonable rule is to assume that a line of inflection exists parallel to any continuous edge at a distance from it of one-sixth the span. The rule may be applied to both the long and the short directions. If bent bars are used, they are generally bent up at these inflection locations.

To limit deflections, the code provides that the minimum thickness of a two-way slab shall be 3.5 in. or the panel perimeter divided by 180, whichever is larger.

4.7 Design example. Design a slab panel 20 ft 0 in. by 25 ft 0 in. to support a uniform live load of 125 psf. The panel is a corner panel of a group. A 3000-psi concrete and steel with $f_y = 60{,}000$ psi are used, in connection with ultimate-strength design.

The minimum thickness, by Code, of $^{90}/_{180} = \frac{1}{2}$ ft = 6 in. will be used. (For heavy loads, such as in warehouses, deeper slabs lead to steel savings which frequently prove more economical than minimum-thickness slabs.) Consequently, the dead load is $\frac{1}{2} \times 150 = 75$ psf, and the design loads for ultimate-strength

design are

Live load:	1.8×125	= 225 psf
Dead load:	1.5×75	= 112.5 psf
Total		337.5 psf

MOMENT CALCULATIONS FOR MIDDLE STRIPS. $m = A/B = {}^{20}/_{25} = 0.80$. The negative moments at continuous edges, from Table 4.2, are

$$M_{A,neg} = 0.071 \times 337.5 \times 20^2 = 9580 \text{ ft-lb} = 115{,}000 \text{ in.-lb}$$
$$M_{B,neg} = 0.029 \times 337.5 \times 25^2 = 6110 \text{ ft-lb} = 73{,}400 \text{ in.-lb}$$

The positive moments, from Tables 4.3 and 4.4, are

Dead load:	$M_{A,pos} = 0.039 \times 112.5 \times 20^2$	= 1755 ft-lb	= 21,000 in.-lb
Live load:	$M_{A,pos} = 0.048 \times 225 \times 20^2$	= 4320 ft-lb	= 51,800 in.-lb
Total			$M_{A,pos}$ = 72,800 in.-lb
Dead load:	$M_{B,pos} = 0.016 \times 112.5 \times 25^2$	= 1125 ft-lb	= 13,500 in.-lb
Live load:	$M_{B,pos} = 0.020 \times 225 \times 25^2$	= 2820 ft-lb	= 33,800 in.-lb
Total			$M_{B,pos}$ = 47,300 in.-lb

The negative moments at discontinuous edges are

$$M_{A,neg} = \tfrac{1}{3}(72{,}800) = 24{,}300 \text{ in.-lb}$$
$$M_{B,neg} = \tfrac{1}{3}(47{,}300) = 15{,}800 \text{ in.-lb}$$

SELECTION OF REINFORCEMENT. From Graph 1, Appendix B:

1. Short direction

a. Span:

$$\frac{M_u}{\phi b d^2} = \frac{72{,}800}{0.9 \times 12 \times 5^2} = 270 \qquad p = 0.0048$$

A_s is equal to $0.0048 \times 12 \times 5 = 0.288$ in.²/ft. From Table 4, Appendix B, No. 4 bars at 7 in. spacing are selected, giving $A_s = 0.34$ in.²/ft.

b. Continuous edge:

$$\frac{M_u}{\phi b d^2} = \frac{115{,}000}{0.9 \times 12 \times 5^2} = 426; \; p = 0.0078$$

A_s is equal to $0.0078 \times 12 \times 5 = 0.468$ in.²/ft. If two of every three positive-moment bars are bent up, and likewise for the adjacent panel, the negative-moment steel area furnished at the continuous edge will be four-thirds the positive-moment steel area in the span, or $A_s = \frac{4}{3} \times 0.34 = 0.453$ in.²/ft. It is seen that this is 3.5 per cent less than the required amount of 0.468. On the other hand, the positive-moment steel furnished, 0.34, represents about 15 per cent more than the required amount. As is discussed in Art. 8.15, the Code permits a certain amount of inelastic moment redistribution, within strictly specified limits. In the case at hand the negative steel furnished suffices for only 96.5 per cent of the calculated moment, but the positive steel permits about 115 per cent of the calcu-

Scanned with CamScanner

lated moment to be resisted. This more than satisfies the conditions for inelastic moment redistribution set by the Code. This situation illustrates how such moment redistribution can be utilized to obtain a simpler and more economical distribution of steel.

c. *Discontinuous edge:* The negative moment at the discontinuous edge is one-third the positive moment in the span; it would be adequate to bend up every third bar from the bottom to provide negative-moment steel at the discontinuous edge. However, this would make for a 21-in. spacing, which is larger than the maximum spacing of $3t = 18$ in. permitted by the Code. Hence, for the discontinuous edge, two of every three bars will be bent up from the bottom steel.

2. Long direction

a. *Span:*

$$\frac{M_u}{\phi bd^2} = \frac{47{,}300}{0.90 \times 12 \times 4.5^2} = 216 \qquad p = 0.0038$$

(The positive-moment steel in the long direction is placed on top of that for the short direction. This makes the depth d for the former one bar diameter smaller than for the latter. This is the reason for using $d = 4.5$ in. for the positive-moment steel in the long direction, and $d = 5$ in. in all other locations.) A_s is equal to $0.0038 \times 12 \times 4.5 = 0.205$ in.²/ft. From Table 4, Appendix B, No. 3 bars at 6 in. spacing are selected, giving $A_s = 0.22$ in.²/ft.

b. *Continuous edge:*

$$\frac{M_u}{\phi bd^2} = \frac{73{,}400}{0.90 \times 12 \times 5^2} = 272; \; p = 0.0048$$

A_s is equal to $0.0048 \times 12 \times 5 = 0.288$ in.²/ft Again, bending up two of every three bottom bars from both panels adjacent to the continuous edge, one has, at that edge, $A_s = \frac{2}{3} \times 0.22 = 0.29$ in.²/ft.

c. *Discontinuous edge:* For the reasons discussed in connection with the short direction, two out of every three bottom bars will, likewise, be bent up at this edge.

The steel selections above refer to the middle strips in both directions. For the *column strips*, as was pointed out, the moments are assumed to decrease linearly from the full calculated value at the inner edge of the column strip to one-third of this value at the edge of the supporting beam or wall. To simplify steel placement, a uniform spacing will be used in the column strips. The average moments in the column strips being two-thirds of the corresponding moments in the middle strips, adequate column strip steel will be furnished if the spacing of this steel is 1½ times that in the middle strip.

According to the recommendation of Art. 4.6, inflection points may be assumed a distance $L/6$ from the continuous edges, that is, 3 ft 4 in. in the short direction and 4 ft 2 in. in the long direction. Two of every three bars are bent up at approximately these locations. The bent-up bars are carried over the support and beyond the inflection point of the adjacent panel a distance not less than

one-sixteenth of the span, or the depth of the member, or 12 bar diameters, whichever is greater. It is customary and slightly conservative, instead, to extend these bars to the quarter point of the adjacent span. This extension will also satisfy the bond requirements of these negative-moment bars at the continuous edges. At the discontinuous edges twice as much steel has been furnished as is needed for the design moments. Therefore, only one-half of the development length of Table 8, Appendix B, must be provided. For the No. 4 bars this length is ½ × 17 = 8.5 in. Flexural bond need not be considered if anchorage bond is no larger than 80 per cent of the permissible value. This will be so if actual development length is no less than 1.25 times this minimum length, or 1.25 × 8.5 = 10.6 in. An 11-in. anchorage length will be used for both No. 4 and No. 3 bars.

The reactions of the slab constitute loads on the edge beams and are calculated from Table 4.5, which indicates that 71 per cent of the load is transmitted in the short direction, and 29 per cent in the long direction. The total load on the panel being $20 \times 25 \times 337.5 = 169{,}000$ lb, the load per foot on the long beam is $(0.71 \times 169{,}000)/(2 \times 25) = 2400$ lb per ft, and on the short beams $(0.29 \times 169{,}000)/(2 \times 20) = 1220$ lb per ft. However, the Code suggests that the short beams be designed for a uniform load not smaller than $wA/3$; in the present case $337.5 \times 2\frac{2}{3} = 2250$ lb per ft exceeds 1220 lb per ft and, therefore, governs. In addition, the edge beams evidently carry their own weight and, in the case of the beams along the continuous edges, the corresponding reactions from the adjacent panels.

PROBLEMS

1. A concrete slab roof is to be designed to cover a transformer vault. The outside dimensions of the vault are 17 × 20 ft, and walls are 8-in. brick. A design live load of 80 psf, uniformly distributed over the roof surface, will be assumed. Design the roof as a two-way slab, using U.S.D. methods, with $f'_c = 4000$ psi and $f_y = 50{,}000$ psi.

2. A concrete warehouse floor is framed by beams on column lines, which are 18 ft on centers in one direction and 24 ft on centers in the other. Beam webs may be assumed to be 12 in. wide. A working live load of 225 psf must be carried. Design a typical interior panel, using U.S.D. methods, with $f'_c = 5000$ psi and $f_y = 60{,}000$ psi.

3. Design a typical exterior and first-interior panel for the warehouse floor of the preceding problem. The 24-ft dimension of the exterior panel is parallel to the outside wall.

FLAT SLABS

4.8 Description of General Type A flat-slab floor, as its name implies, is one consisting of a reinforced-concrete floor slab built monolithically with the columns and supported directly by the columns without the aid of beams and girders. The slab may be of uniform thickness

Scanned with CamScanner

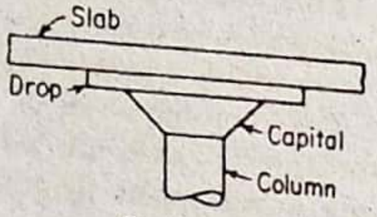


Fig. 4.9

[Art. 4.8

throughout the entire floor area, or a part of it, symmetrical about the column, may be made somewhat thicker than the rest of the slab, the thickened portion of the slab thus formed constituting what is known as a *dropped panel*, or *drop* (see Figs. 4.9, 4.12, and 9.12).

Dropped panels are used to reduce the shearing stress in the slab within the area of the drop. The increase in effective slab thickness provided by the drop also decreases the compression stresses in the concrete and reduces the amount of steel which is required over the column heads. In general, the use of dropped panels is not economical for live loads less than 150 psf.

Dropped panels are square or rectangular. The ACI Code specifies [Art. 2104(*e*), Appendix A] that the side of a drop panel shall be at least 0.33 times the span and that the total thickness to be used in computing the negative steel area for the column strip shall be not more than $1.5t_s$, nor shall the thickness below the slab be more than one-fourth the distance from the edge of the drop panel to the edge of the column capital [Art. 2102(*c*)5, Appendix A]. This usually results in a drop panel with a thickness of one-quarter to one-half the thickness of the slab outside the drop. When drops are used over interior columns, they are normally used over the wall columns also. Such drops should have a width parallel to the wall equal to the corresponding width of the interior-panel drops; at right angles to the wall they should project beyond the center of the column a distance equal to one-half the corresponding total width of the interior drops.

The columns in practically all cases flare out toward the top, forming a capital of a shape somewhat similar to an inverted truncated cone. This capital gives a wider support for the floor slab, which results in a decrease in the bending moment which the slab is called upon the resist and a decrease in the shearing stresses around the perimeter of the column, and tends toward a more rigid structure. The effective diameter of the capital should be taken as the diameter of the circle at the point at which a 45° line from the base of the capital intersects the bottom of the slab or dropped panel. The 45° line must fall within the concrete of the cap at all points.

At the wall columns, a bracket is often used in place of a regular half-capital. The width of the bracket is equal to the width of the column parallel to the wall; the sloping side of the bracket forms an angle of 45° with the horizontal; the projection of the bracket beyond the face of the column is the same as, or somewhat less than, the projection of the interior-column capital.

4.9 Advantages of Flat-slab Floors Structurally, a flat-slab floor has many advantages over an ordinary beam-and-girder floor. The most important of these may be enumerated as follows:

1. For ordinary spans with heavy loads, under average conditions, the flat-slab floor is more economical than the beam-and-girder floor when designed to present Code provisions.
2. In a multistoried building, the same number of stories of a given clear height may be obtained with a smaller total building height, because of the smaller floor thickness.
3. The slab formwork is much simpler.
4. The flat-slab floor, owing to the lack of many sharp corners, is better able to resist continued exposure to fire than the beam-and-girder floor. It has been found by actual experience that the worst damage caused to reinforced concrete by severe fires has occurred at places where there may be spalling, i.e., at exposed edges and sharp corners.
5. Automatic-sprinkler protection may be made more complete under a flat-slab floor, since the nozzles may be placed well up near the under side of the slab without obstruction to the path of the spray.
6. More light may be admitted into the building if desired, by placing the wall beams above the floor level and thus allowing the windows to be extended to the under side of the slab. The absence of deep beams and girders also removes the obstruction to the passage of light within the building.
7. The opportunity for inspecting the position of the reinforcement is excellent, and the conditions attending deposition and placing of the concrete are favorable to securing uniformity and soundness in the concrete.

4.10 Bending Moments in Flat-slab Floors Figure 4.10 represents a portion of a flat-slab floor including four column supports, the load on the floor being uniformly distributed. The full circles represent the column heads underneath the slab. It is evident that the curvature of the slab along any radial line from the column center will be convex upward for a certain distance, then concave upward, then convex upward again. This implies that at some point along each radial line there is a point of inflection where the radial bending

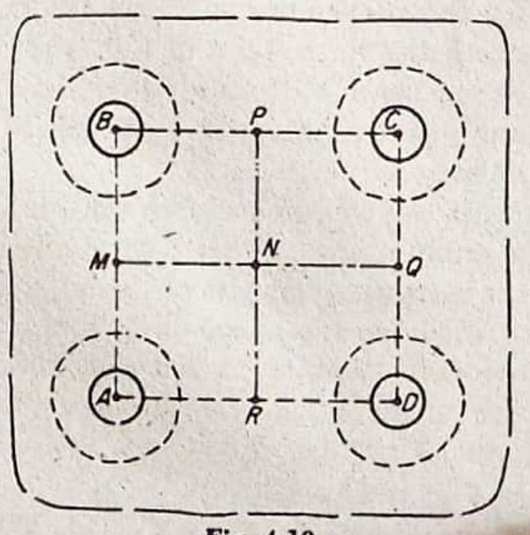


Fig. 4.10

Scanned with CamScanner

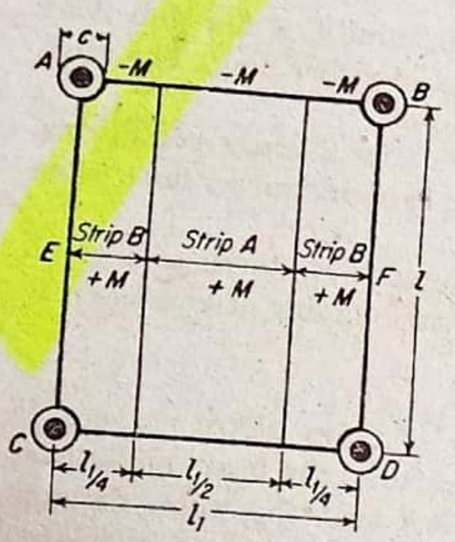


Fig. 4.11

moment changes from positive to negative. The locus of all these points may be represented by the dotted approximate circles centered about the column capitals.

As the slab is loaded, deflection occurs. The point N at the midpoint of the panel, being the farthest away from the support, will deflect more than a point M, P, Q, or R midway between any two adjacent columns. The points M, P, Q, and R will therefore be higher than point N but lower than the supports. This results in a negative moment along the line MQ at M, and a positive moment at N. The condition is similar along line PR.

The analysis of a flat-slab floor is a highly indeterminate problem, and the elastic and inelastic properties of the slab and the relative stiffness of its various parts must be considered in determining accurately the moments and shears in the slab. An arbitrary but satisfactory method of obtaining the theoretical bending moments is to divide each panel into rectangular strips, a middle strip A (Fig. 4.11) with a width equal to $l_1/2$ and two equal column strips B which occupy the outer portions of the panel. Similar strips A' and B' are assumed at right angles to those shown in Fig. 4.11. A system of imaginary beams is thus established, and the load on the panel is transferred to the columns by these beams.

Consider strip A and the two strips B to form one wide but shallow continuous beam, rigidly supported at the four corners by the columns, and partially supported between the columns along the lines AB and CD by the perpendicular strips B'. In this beam, negative moments exist along the lines AB and CD, and positive moments along the line EF. Strips B are obviously stiffer than strip A, and hence both the positive and negative moments in strips B (combined) will be greater than those in strip A.

It is a well-known fact that, in any continuous beam, the sum of the maximum positive moment in any span of the beam and the average of the negative moments at the adjacent supports is equal to the maximum moment in a corresponding simply supported beam. Nichols (Ref. 4.1) recommends that, in flat-slab analysis, the span of the corresponding simply supported beam be taken as $l - \frac{2}{3}c$, where l is the panel length center to center of columns, and c is the diameter of the capital. Thus, in Fig. 4.11,

$$M_{AB} + M_{EF} = \frac{1}{8} w l_1 \left(l - \frac{2}{3} c\right)^2 = \frac{1}{8} W l \left(1 - \frac{2c}{3l}\right)^2 \qquad (4.3)$$

where w = dead and live load on slab, per unit of area
W = total load on one panel
l = distance center to center of columns parallel to strips under consideration
l_1 = distance center to center of columns perpendicular to strips under consideration
c = diameter of column capital

The distribution of this total moment to the positive- and negative-moment sections EF and AB, respectively, must be determined, and then the total positive moment in the section EF and the negative moment in the section AB must be apportioned to the strips A and B. Westergaard and Slater presented a solution of this problem of distribution (Ref. 4.2). For a square interior panel with column capitals but without drop panels, they recommend the following average percentages of the total moment $(M_{AB} + M_{EF})$ for each of the various moment sections:

Column strips, negative moment	48 per cent
Column strips, positive moment	21 per cent
Middle strip, negative moment	17 per cent
Middle strip, positive moment	14 per cent
Total	100 per cent

The effect of a dropped panel is to stiffen the negative-moment portion of the column strip. This causes an increase in the negative moment in strip B and a corresponding decrease in the positive moment at the middle of the strip.

Equation (4.3) can be applied to the determination of moments in square panels and in rectangular panels in which the longer side of the panel is not more than 1.33 times the shorter side. In rectangular panels, separate moments must obviously be computed for the various sections of the two rectangular directions, using for l the length of the side of the panel in the direction parallel to the strip under consideration.[1]

[1] It is interesting to compare the behavior of flat slabs with that of two-way slabs (Art. 4.5). In flat-slab analysis, the full load is assumed to be carried by the slab in each of the two perpendicular directions. This is in apparent contrast to the analysis of two-way slabs, in which the load is divided, one part carried by the slab in the short direction, and the remainder carried by the slab in the long direction. However, in two-way slabs, while only a part of the load is carried by the slab in the short direction, the remainder is transmitted in the perpendicular direction to marginal beams, which then also span in the short direction. Similarly, with part of the load carried by the slab in the long direction, the remainder is transmitted by the slab in the short direction to marginal beams which span in the long direction. It is evident that in two-way slabs, as in flat slabs, conditions of equilibrium require that all the load be carried in each of the two principal directions.

Scanned with CamScanner

4.11 Moments in Interior Panels Any theoretical analysis, such as that outlined above, gives only approximate results, because of the many assumptions which are necessary. Tests of full-sized panels show that the actual stresses in the steel are less than would be obtained from the usual rectangular-beam equations with moments as indicated in Art. 4.10. By comparing the stresses determined by a sound theoretical analysis with those obtained by actual tests, moment coefficients can be obtained which will give rational and safe results. This process has resulted in the development of flat-slab regulations which are part of practically all municipal building codes and technical society standards.

In addition to specifying moment coefficients, these codes usually give minimum requirements for slab thickness, cap and drop dimensions, and column sizes. They specify the arrangement of the reinforcement and outline the method of computing stresses due to shear and bending. The formulas and methods of one code may differ from those of another, but there is sufficient similarity so that the designer who is familiar with the application of the provisions of one code has little difficulty in following those of any other code.

The recommendations of the American Concrete Institute are given in Appendix A. These recommendations provide for two methods of design of flat-slab structures. One method applies to flat-slab floors in which (1) there are three or more panels in each direction, (2) the successive span lengths differ by not more than 20 per cent of the shorter span, and (3) the ratio of length to width of panel does not exceed 1:33. These conditions are usually met in practice. When they do not obtain, the second method is used. This method consists of recommendations governing the analysis of the structure as a series of rigid frames in the two directions of reinforcement (Refs. 4.3, 4.4). Only the former method will be considered in this chapter.

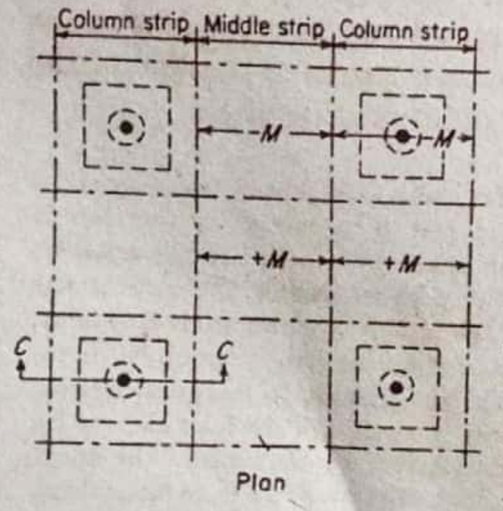


Fig. 4.12

In the ACI Code the total moment $M_{AB} + M_{EF}$ (Fig. 4.11) is specified as about 25 per cent less than the value given in Eq. (4.3), and the distribution varies slightly from the percentages tabulated in Art. 4.10. For convenience in specifying moment coefficients and to simplify the subsequent detailing of the reinforcement, it is desirable to consider two adjoining column strips in adjacent panels as one band. This band is centered about the column line and has a width equal to one-half the panel width. In all the following discussions, any

reference to the "column strip" will imply the combined strips or band described above, as indicated in Fig. 4.12.

The moment distribution for interior panels, as given in the ACI Code, is as follows:

Let $M_0 = M_{AB} + M_{EF}$ (Fig. 4.11), ft-lb
W = total load on panel, including weight of drop, lb
L = span of strip under consideration, center to center of columns, ft
c = diameter of column capital, ft

Then

$$M_0 = 0.09WLF'\left(1 - \frac{2c}{3L}\right)^2 \tag{4.4}$$

where $F = 1.15 - c/L$, but not less than 1.

Moments in interior panels, ACI Code

Strip	Moments in slabs without drops		Moments in slabs with drops	
	Negative	Positive	Negative	Positive
Column strip	$-0.46M_0$	$+0.22M_0$	$-0.50M_0$	$+0.20M_0$
Middle strip	$-0.16M_0$	$+0.16M_0$	$-0.15M_0$	$+0.15M_0$

4.12 Moments in Exterior Panels In wall panels, the strips perpendicular to the wall are analogous to the end spans of a beam which is continuous over a number of supports. In such a beam, if the spans are all equal, the load is uniform, and the ends of the beam rest freely on the end supports, the maximum positive moment in the end spans is greater than in the intermediate spans; the negative moment at the first interior support is greater than the negative moment at any other interior support; the moment at the first support is equal to zero. If the ends of the beam are restrained instead of being freely supported, moments are induced at the end supports, and the maximum positive moments in the end spans as well as the negative moment at the first interior support are affected. The latter two values will normally be greater than the corresponding moments in a typical interior span.

In flat-slab construction, the restraint offered at the end supports may vary considerably. The wall panels may—but seldom do— rest freely on brick walls, they may be built monolithically with the wall columns and with marginal beams (wall beams) along the outer edge of the panels, capable of resisting torsional stresses, or they may be built monolithically

Scanned with CamScanner

with the columns but without the rigid marginal beams. Obviously, the moment coefficients for sections parallel to the wall (strips perpendicular to the wall) would differ materially for these various conditions. The ACI Code provides separate moment coefficients for different support conditions [Art. 2104(*f*), Appendix A].

Since brackets are normally used at exterior columns, and since the sloping face of these brackets usually projects beyond the columns a sufficient amount to make the distance from the center of the column to the extremity of the bracket equal to one-half the diameter of the interior-column capital, the values of c, and hence M_0, for the exterior-panel strips perpendicular to the wall are generally the same as for an interior panel. The moments at the various sections of these strips can therefore usually be obtained by multiplying the moments at the corresponding sections in the interior panel by the ratios of the appropriate moment coefficients given in Art. 2104(*f*), Appendix A.

The moments to be used in the design of the middle strip parallel to the wall in an exterior panel are the same as used for the corresponding sections in an interior panel. The moments to be used in the design of the half-column strip adjacent and parallel to the wall depend upon the relative size of the marginal or wall beam. If the depth of this beam is 1¼ times the thickness of the slab or less, the positive and negative moments are taken as 40 and 38 per cent, respectively, of the corresponding moments specified for a typical interior-panel column strip, and the marginal beam must be designed for 20 per cent of the panel load in addition to the superimposed load from the wall. If the depth of beam is 3 times the thickness of the slab or more, the positive and negative moments are taken as 25 and 26 per cent, respectively, of the corresponding moment specified for a typical interior-panel column strip, and the marginal beam must be designed for 40 per cent of the panel load in addition to the superimposed load from the wall [Table 2104(*f*), Appendix A].

4.13 Shearing Stresses There are two kinds of shearing stress that may be critical in the design of flat-slab structures. The first is the familiar beam-type shear leading to diagonal tension failure. In this case, the slab is considered to act as a wide beam, spanning essentially between supports provided by the perpendicular column strips, with a potential diagonal crack extending in a plane across the entire width of the slab. The critical section is taken a distance d from the face of the column or capital. As for beams, the nominal shear stress V/bd on the unreinforced concrete is not to exceed an allowable working value of

$$v_c = 1.1\sqrt{f'_c}$$

or an ultimate value of

$$v_c = 2\phi\sqrt{f'_c}$$

Alternatively, failure may occur by "punching shear," with the potential diagonal crack following the surface of a truncated cone or pyramid around the column capital or drop panel. In this case, the critical section for shear is taken perpendicular to the plane of the slab and a distance $d/2$ out from the periphery of the support. The nominal shear stress is V/b_0d, where b_0 is the perimeter along the critical section.

At such a critical section, in addition to the shearing stresses and horizontal compressive stresses due to negative bending over the support, vertical or somewhat inclined compressive stress is present, owing to the reaction of the column. The simultaneous presence of vertical and horizontal compression increases the shear resistance of the concrete. Tests have indicated that, when punching shear failure occurs, the shear stress computed on the perimeter of the critical section is larger than in beams or one-way slabs and is approximately equal to $4\sqrt{f'_c}$. Accordingly, the ACI Code specifies that, for punching shear, the nominal shear stress is not to exceed an allowable working value of

$$v_c = 2\sqrt{f'_c}$$

or an ultimate value of

$$v_{uc} = 4\phi\sqrt{f'_c}$$

unless shear reinforcement is provided, in which case an allowable value of $3\sqrt{f'_c}$ an an ultimate value of $6\phi\sqrt{f'_c}$ are permitted.

Shear reinforcement is sometimes used in flat-slab construction and is frequently desirable in flat-plate construction (see Art. 4.18). Such reinforcement may be in the form of bars, rods, or wire and may be designed by conventional methods, except that when such reinforcement is used the allowable stress and design yield strength are taken as one-half their usual values. Such shear reinforcement is not considered effective in members with a total thickness of less than 10 in.

4.14 Thickness of Slab In order to prevent undue deflection, certain limitations are placed on the minimum slab thickness that can be used in a given floor panel. Inasmuch as the actual deflection of a flat slab cannot be computed with any appreciable degree of accuracy, these limitations were developed from a study of the observed deflections in actual structures. The ACI Code specifies that the slab thickness, exclusive of the drop, shall not be less than $\frac{1}{40}$ of the longer dimension for slabs with

Scanned with CamScanner

drops, and not less than 1/36 of the same dimension for slabs without drops.

It further specifies that for a slab with drops the thickness shall not be less than 4 in., nor less than

$$0.024L\left(1-\frac{2c}{3L}\right)\sqrt{\frac{w'}{f'_c/2000}}+1 \tag{4.5a}$$

and that for a slab without drops the thickness shall not be less than 5 in., nor less than

$$0.028L\left(1-\frac{2c}{3L}\right)\sqrt{\frac{w'}{f'_c/2000}}+1\tfrac{1}{2} \tag{4.5b}$$

Of course, the slab must also be thick enough so that allowable unit compressive and shear stresses will not be exceeded. In this connection, the Code requires that a reduced effective width be used in calculating flexural compression stress, in order to allow for the nonuniform variation of bending moment across the width of the critical sections. This reduced effective width is to be taken as three-fourths the width of the strip, except that on a section through a drop panel three-fourths the width of the drop panel is to be used.

4.15 Methods of Reinforcing Flat-slab Floors There are, in the main, four different methods or systems for reinforcing the slab in this type of floor: (1) two-way system, (2) four-way system, (3) three-way system, and (4) circumferential system.

Virtually all flat-slab floors built in this country at the present time have a two-way system of reinforcement. Originally all flat-slab systems were covered by patents. The basic patents have expired, and at present the two-way system is the one in general use. It has the advantage of being simple to design and construct and has proved thoroughly satisfactory. The other systems are chiefly of interest historically and to engineers working on renovations or additions to old buildings.

In the two-way system, bars are placed parallel to the lines of columns over the entire area of the floor at small intervals. The maximum allowable spacing varies in the different codes and specifications. The ACI Code permits a maximum bar spacing of 2 times the slab thickness.

The four-way system consists of two main bands of steel running parallel to the lines of columns, each band centered about the column lines, and two diagonal bands of sufficient width to fill up the floor area left uncovered by the direct bands. In some cases short bars are placed near the top of the slab at right angles to the direct bands over the middle portion of the band to resist the negative moment over that portion; they constitute what are known as the *across-direct* bands.

The three-way system involves a special arrangement of columns such that the lines connecting their center lines form a series of equilateral triangles. The reinforcement then follows the sides of these triangles, each band being centered about one of the panel sides.

In the circumferential system, radial steel emanating from the column head and circumferential steel in the form of concentric rings symmetrical about the column head are used. Concentric rings are also placed about the midpoint of the slab and about the midpoints of the four edges of each panel.

4.16 Factors to Be Considered in the Design of Flat-slab Buildings Flat-slab floors are ordinarily designed to carry only a uniform load over the entire surface, the assumption being that no breaks in the continuity occur. Where heavy concentrated loads are to be sustained in addition to the uniform load, beams should be introduced in such positions as will enable them to carry the weight of the concentrations. Where major openings in the slab occur, they should be framed by beams which will have the effect of restoring continuity to the slab. These beams should be designed to carry a portion of the floor load in addition to any concentrated loads that may rest upon them.

The columns should be designed to provide for bending stresses such as might be caused by unequally loaded panels. This is especially important in the exterior columns, where both the dead and live loads cause continual bending, and where the direct loads are relatively small. The interior roof columns are not likely to be subjected to such eccentric loading, and the ratio of the possible bending stress to the direct load stress decreases as the number of floors to be supported increases. Hence, bending in the interior columns is not so important as in the exterior columns. It should be investigated, however, especially in the upper stories. The amount of bending moment to be assumed is usually stated in the various regulations governing flat-slab design. The spacing of columns is governed by practically the same factors as in the case of beam-and-girder type floors.

To provide proper drainage, a slight pitch may be given to the roof slab without any change in the theoretical computations. Sudden changes in slope, or steps, on the other hand, require special attention.

4.17 Example: flat-slab floor A parking garage, to be designed as a flat-slab structure, is to carry a working live load of 200 psf. Drop panels 8 ft square will be used, and each column capital will consist of a 90° truncated cone with 4-ft diameter at the intersection of the capital with the bottom of the drop panel. Columns are spaced 22 ft on centers in each direction. Design the slab reinforcement, and determine concrete dimensions for a typical interior panel. Steel will be used at a working stress of 20,000 psi; concrete is of 3000 psi strength.

Scanned with CamScanner

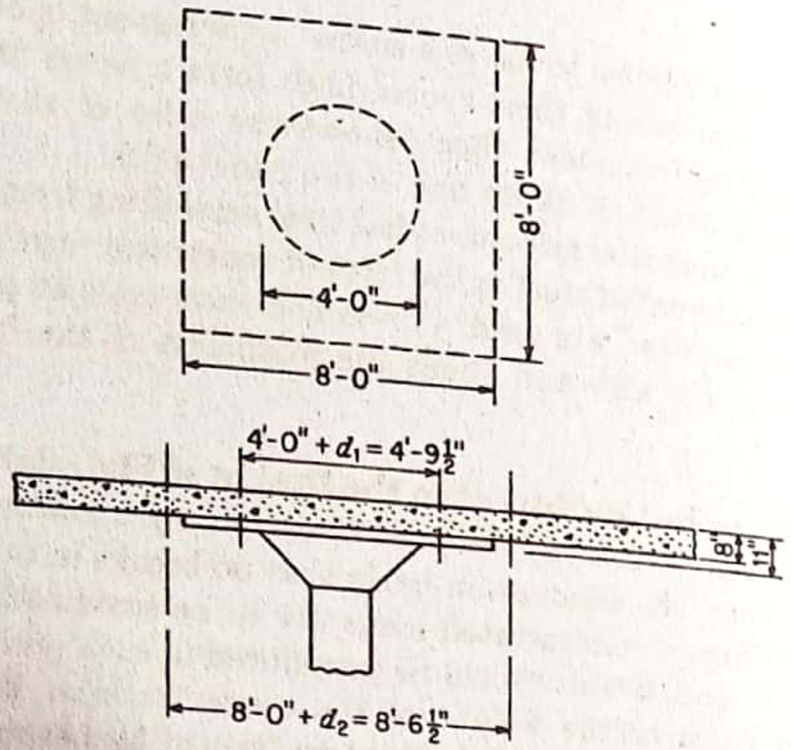


Fig. 4.13

The proposed structure falls within the limitations of the ACI empirical method of Art. 2104, Appendix A, and will be designed in accordance with that specification. The minimum thickness of the slab is established by the smallest of the criteria

$$\frac{L}{40} \quad \text{or} \quad 4 \text{ in.} \quad \text{or} \quad t_2 = 0.024L\left(1 - \frac{2c}{3L}\right)\sqrt{\frac{w'}{f_c'/2000}} + 1$$

With $c = 4$ ft, $L = 22$ ft, and the dead load of the slab estimated to be $150 \times {}^{8}\!/_{12} = 100$ psf,

$$\frac{L}{40} = \frac{22 \times 12}{40} = 6.6 \text{ in.}$$

$$t_2 = 0.024 \times 22(1 - {}^{8}\!/_{66})\sqrt{\frac{100 + 200}{3000/2000}} + 1 = 7.60 \text{ in.}$$

A slab thickness of 8 in. with 3-in. drop panels will be tentatively selected, as shown in Fig. 4.13.

Relative to punching shear, the critical section in the drop panel is at a distance $d_1/2$ from the edge of the column capital.[1] The diameter of the critical section is 4.79 ft. The floor area included within the critical section is $(\pi/4)4.79^2 = 18.0$ ft^2, and the shear force acting on the critical section is

$$V = (22 \times 22 - 18)300 = 140{,}000 \text{ lb}$$

[1] The effective depth is taken as the total depth less ¾ in. protection less 1½ times the diameter of an assumed No. 4 bar.

The nominal shear stress is

$$v = \frac{V}{b_0 d} = \frac{140{,}000}{3.14 \times 4.79 \times 12 \times 9.50} = 82 \text{ psi}$$

According to Code, the allowable shear stress on that section is

$$v_c = 2\sqrt{3000} = 110 \text{ psi} > 82 \text{ psi}$$

A second critical section for punching shear may occur at a distance $d_2/2$ from the edge of the drop panel. The side dimension of the critical section (see Fig. 4.13) is 8.54 ft, and the included area is $8.54^2 = 73$ ft^2. The shear force acting on this critical section is

$$V = (22 \times 22 - 73)300 = 123{,}000 \text{ lb}$$

and

$$v = \frac{V}{b_0 d} = \frac{123{,}000}{4 \times 8.54 \times 12 \times 6.50} = 47 \text{ psi}$$

well below the allowable value of 110 psi.

Beam shear is checked a distance d past the face of the support. Where round columns or capitals are used, the Code specifies that the face of the column be taken as the side of the square having the same area as the actual round support. In the present case, the equivalent square support has a side dimension of $\sqrt{\pi r^2} = 2.0\sqrt{3.14} = 3.54$ ft. At a distance d past that face, the shear force is

$$V = 300 \times 22 \times {}^{23}\!/_{2} - 300 \times 22 \times 2.31 = 57{,}300 \text{ lb}^*$$

and the nominal shear stress is

$$v = \frac{V}{bd} = \frac{57{,}300}{22 \times 12 \times 6.50} = 33 \text{ psi}$$

The permitted shear on this section,

$$v_c = 1.1\sqrt{3000} = 60 \text{ psi}$$

is not exceeded.

The design moments are based on a value of

$$M_0 = 0.09WLF\left(1 - \frac{2c}{3L}\right)^2$$

in which

$$F = 1.15 - \frac{c}{L} \geq 1$$

In the present case, $F = 1.15 - {}^{4}\!/_{22} = 0.97$, so that F is taken equal to unity. Then $W = 300 \times 22^2 = 145{,}000$ lb, and

$$M_0 = 0.09 \times 145{,}000 \times 22(1 - {}^{8}\!/_{66})^2 = 222{,}000 \text{ ft-lb}$$

* The presence of the drop panel over a part of the width of the critical section is neglected.

Scanned with CamScanner

The maximum moment in the slab occurs in the column strip over the support and [see Table 2104(*f*), Appendix A] is $0.50M_0 = 111{,}000$ ft-lb. According to Code, only three-quarters of the width of the drop panel is to be considered effective in resisting flexural compression. The required depth for bending is therefore

$$d_1 = \sqrt{\frac{M}{Kb}} = \sqrt{\frac{111{,}000 \times 12}{223 \times 8 \times 12 \times 0.75}} = 9.11 \text{ in.}$$

The 9.5 in. effective depth provided by an 8-in. slab with 3-in. drop panels will be satisfactory. In the portion of the slab without drop panels, the maximum moment is $0.20M_0 = 44{,}400$ ft-lb. The required depth is

$$d_2 = \sqrt{\frac{44{,}400 \times 12}{223 \times 11 \times 12 \times 0.75}} = 4.92 \text{ in.}$$

The 8 in. total thickness required by other considerations will provide an effective depth of 6.50 in. in the positive-moment region of the column strips, more than satisfactory for flexure.

In flat-slab construction, a slab of any given total thickness will have different effective depths in the two perpendicular directions because of stacking of the bars. While actual depths may be used in the design of rectangular panels in which reinforcement will normally differ in the two directions, in the case of square panels it is convenient if the steel is identical in the two directions. This requires the use of the lesser effective depth in the determination of steel areas. This practice will be followed in the present design.

Using the moment coefficients of Table 2104(*f*), Appendix A, in the column strips, the negative moment is $0.50 \times 222{,}000 = 111{,}000$ ft-lb, and the required steel area is

$$A_s = \frac{M}{f_s jd} = \frac{111{,}000 \times 12}{20{,}000 \times 0.874 \times 9.5} = 8.02 \text{ in.}^2$$

Nineteen No. 6 bars will be used. The positive moment is $0.20 \times 222{,}000 = 44{,}400$ ft-lb, and the required steel is

$$A_s = \frac{44{,}400 \times 12}{20{,}000 \times 0.874 \times 6.50} = 4.70 \text{ in.}^2$$

Eleven No. 6 bars are selected.

In the middle strips, the negative and positive moments are identically $0.15 \times 222{,}000 = 33{,}400$ ft-lb, and the steel requirement is

$$A_s = \frac{33{,}400 \times 12}{20{,}000 \times 0.874 \times 6.50} = 3.53 \text{ in.}^2$$

which will be provided by twelve No. 5 bars. The maximum spacing of $2t = 16$ in. is not exceeded in either the column or middle strips.

Cutting off and bending of slab steel will follow the recommendations of Table 2104(*g*), Appendix A, and are shown in Fig. 4.14. In the column strips, the four straight bottom bars are cut off 12 in. past the face of the drop panel, or 3 ft from the column line. The remaining seven bars are bent up at the quarter point of the span. The straight top bars added over the support are carried $0.33L$ past the column and cut off. The bent bars are terminated $0.30L$ past the column center line.

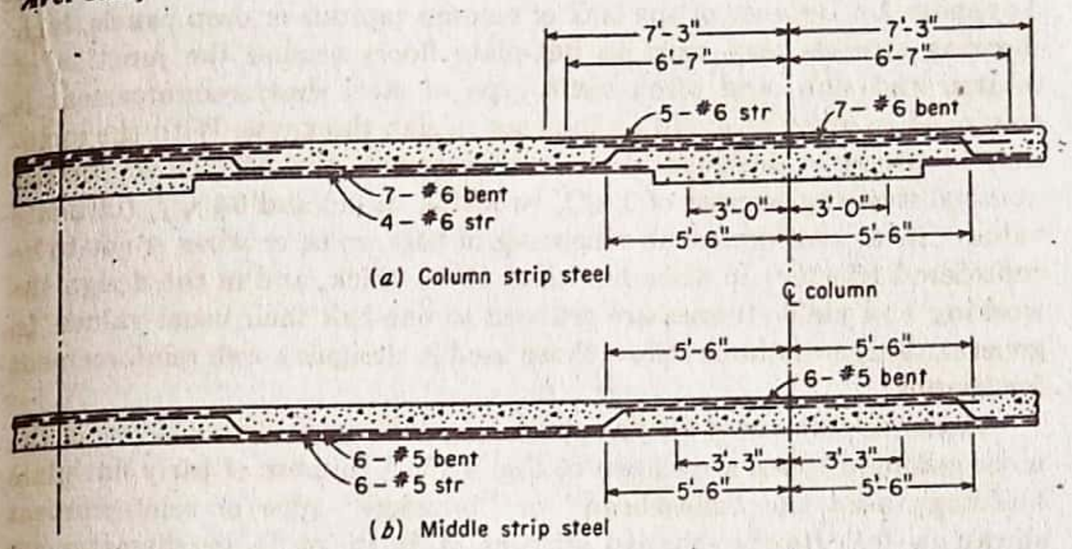


Fig. 4.14

In the middle strips, half the bars are carried straight and cut off $0.15L$ from the support center line. The other half are bent up at the quarter point of the span. Bent-up bars are terminated $0.25L$ past the center line of the column.

From Table 8, Appendix B, it is evident that adequate development length is provided past the point of maximum stress for all bars.

4.18 Flat-plate Construction Flat-plate floors are a variation of flat-slab construction in which neither drop panels nor column capitals are used. The slab, of uniform thickness, is carried directly by columns of constant cross section. Where column spacing is not large, and where design loads are relatively light, a flat-plate design may be most economical. While material quantities may be somewhat greater than for conventional flat-slab or beam-and-girder floors, the savings which accrue from the simplified formwork and the reduction in construction depth often more than offset the increased cost of material. The resulting structural system presents a clean, unbroken appearance; in fact, in many cases, the under surface of the structural slab is used for the ceiling without further treatment. A typical flat-plate building is shown in Fig. 9.13.

The design procedure for flat plates is similar to that for ordinary flat-slab floors. They can be designed either by elastic methods of frame analysis (Art. 2103, Appendix A) or, provided dimensional limitations are met, by the empirical method of moment coefficients (Art. 2104,

Scanned with CamScanner

[*Art. 4.18*

Appendix A). Because of the lack of column capitals or drop panels, high shearing stresses may exist in flat-plate floors around the junction of column and slab, and often some type of steel shear reinforcement is employed in order to avoid an increase in slab thickness. With the inclusion of properly designed shear reinforcement, the ACI Code permits nominal shearing stresses of $3\sqrt{f'_c}$ (working value) and $6\phi\sqrt{f'_c}$ (ultimate value). Shear reinforcement consisting of bars, rods, or wires is not to be considered effective in slabs less than 10 in. thick, and in the design the working and yield stresses are reduced to one-half their usual values. In general, design methods follow those used in designing web reinforcement for beams.

Shear reinforcement for flat plates may take many forms. A few of the more common types are shown in Fig. 4.15. A number of early flat-plate buildings used the "shearhead" or "birdcage" type of reinforcement shown in (*a*). Hairpin-shaped stirrups of $\frac{3}{8}$ in. or $\frac{1}{2}$ in. diameter are welded to horizontal hoops near the top and bottom of the slab. The effectiveness of such reinforcement is questionable, in view of the short length of embedment of each stirrup. Although they are welded to the perpendicular hoops, it is difficult to obtain a reliable weld in such a case.

The bent-bar arrangement of Fig. 4.15*b* is preferred. Usually bent at 45°, such bars are placed over the top of the columns and are additional to the negative-moment reinforcement. They are extended a sufficient distance along the bottom face of the slab to develop their computed stress by bond (Ref. 4.5).

In cases in which a flat plate is supported by steel columns, a weldment fabricated of structural-steel channels may be used, as in Fig. 4.15*c*. Welded to the columns, such assemblies are embedded in the slab and act in the same sense as a column capital to reduce the shear force and increase the shear perimeter for which the slab is to be designed. The critical section for shear is probably about as indicated.

Many flat-plate buildings are constructed by the lift-slab method. A casting bed (often doubling as the ground-floor slab) is poured, steel columns are erected and braced, and at ground level successive slabs, which will later become the upper floors, are cast. A membrane or sprayed parting agent is laid down between successive pours, so that each slab can be lifted in its turn. Jacks placed atop the columns are connected to threaded rods extending down the faces of the columns and connecting, in turn, to lifting collars embedded in the slabs as shown in Fig. 4.15*d*. When a slab is in its final position, the collar is welded to the column. Lifting collars such as that shown, in addition to providing anchorage for the lifting rods, serve to increase the effective size of the support for the slab and consequently reduce the unit shear stress for which the slab must be designed.

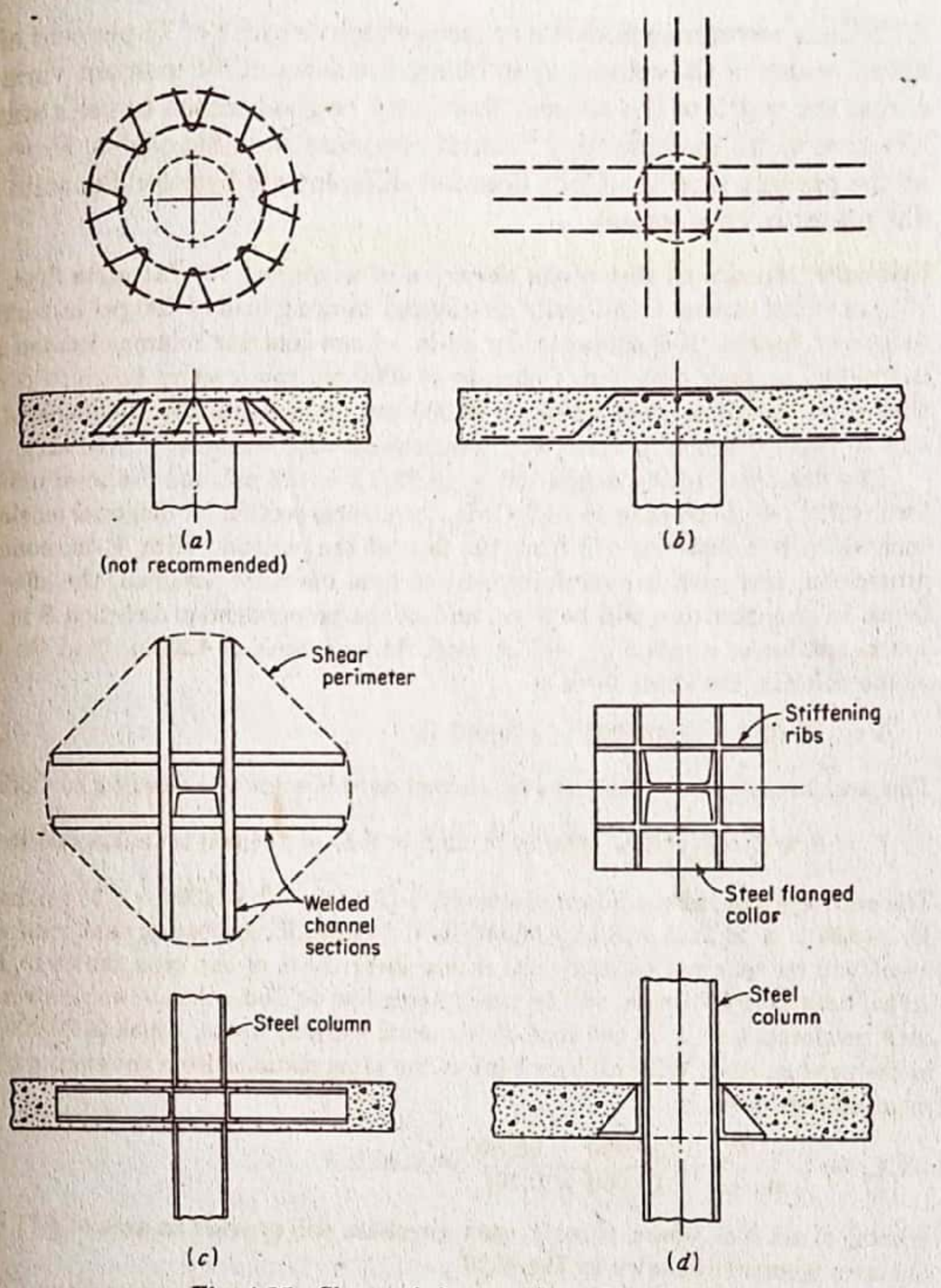


Fig. **4.15** Shear reinforcement for flat plates.

It should be noted that, according to ACI Code, the reinforcement of Fig. 4.15*a* and *b* can be used only in slabs 10 in. or more in thickness, while the devices shown in (*c*) and (*d*) permit a thinner slab to be used.

In flat-plate construction, with characteristically small support area, there is a tendency for the negative moment in the column strips to concentrate over the support. Whereas in ordinary flat-slab construction the

Scanned with CamScanner

ACI Code recommends that a reduced effective width of 75 per cent of the actual width of the column strip be used to account for moment variation across the width of the section, there may be good reason to use a smaller effective width in computing flexural compression in flat plates. However, at the present time the Code does not differentiate between flat slabs and flat plates in this respect.

Example: design of flat-plate shear reinforcement A flat-plate floor slab 10¼ in. thick carries a uniformly distributed working load of 200 psf in addition to its own weight. It is supported by 14-in. square concrete columns located 20 ft on centers in each direction. Concrete of 4000 psi compressive strength is used with steel having a yield stress of 40,000 psi. Investigate the adequacy of the slab to resist diagonal tension, and design shear reinforcement if necessary.

The dead load of the slab is $150 \times 10.25/12 = 125$ psf, and the total uniform load is 325 psf. According to ACI Code, the critical section for diagonal tension in such slabs is a distance $d/2$ from the face of the column. With ¾-in. concrete protection, and with bar reinforcement of 1 in. diameter assumed, the effective depth in one direction will be 9 in., and in the perpendicular direction 8 in. An average value of $d = 8.5$ in. will be used. At a distance of 4.25 in. from the face of the column, the shear force is

$$V_{22.5} = (20^2 - 1.87^2)325 = 129{,}000 \text{ lb}$$

The maximum shear which can be carried at this section, according to Code, is

$$V = 3\sqrt{f'_c}\, b_0 d = 3\sqrt{4000}\,(4 \times 22.5 \times 8.5) = 145{,}000 \text{ lb} > 129{,}000 \text{ lb}$$

The concrete can resist a nominal stress $v_c = 2\sqrt{f'_c} = 2\sqrt{4000} = 126$ psi; hence $V_c = 126 \times 4 \times 22.5 \times 8.5 = 96{,}500$ lb $< 129{,}000$ lb, indicating that reinforcement will be required to carry the excess shear. Bars of the type shown in Fig. 4.15*b*, bent at a 45° angle, will be used. According to Code, the allowable stress in such reinforcement is 50 per cent of the usual working value, which is 20,000 psi in the present case. With all bars bent at the same distance from the support, the required steel area is

$$A_v = \frac{V - V_c}{f_v \sin \alpha} = \frac{129{,}000 - 96{,}500}{10{,}000 \times 0.707} = 4.60 \text{ in.}^2$$

A total of six No. 8 bars, three in each direction, will provide an area of 4.71 in.^{2} The arrangement is shown in Fig. 4.16.

In recognition of the probable pattern of diagonal cracking and the Code requirement that only the center three-quarters of the inclined portion of the bars is to be considered effective as shear reinforcement, the next section to be investigated is a distance $3d/4$ beyond the previous critical section (see Fig. 4.16). The side dimension of this section is 35.30 in., or 2.94 ft. The shear force is

$$V_{35.30} = (20^2 - 2.94^2)325 = 127{,}000 \text{ lb}$$

The concrete can resist

$$V_c = 126 \times 4 \times 35.3 \times 8.5 = 151{,}000 \text{ lb} > 127{,}000 \text{ lb}$$

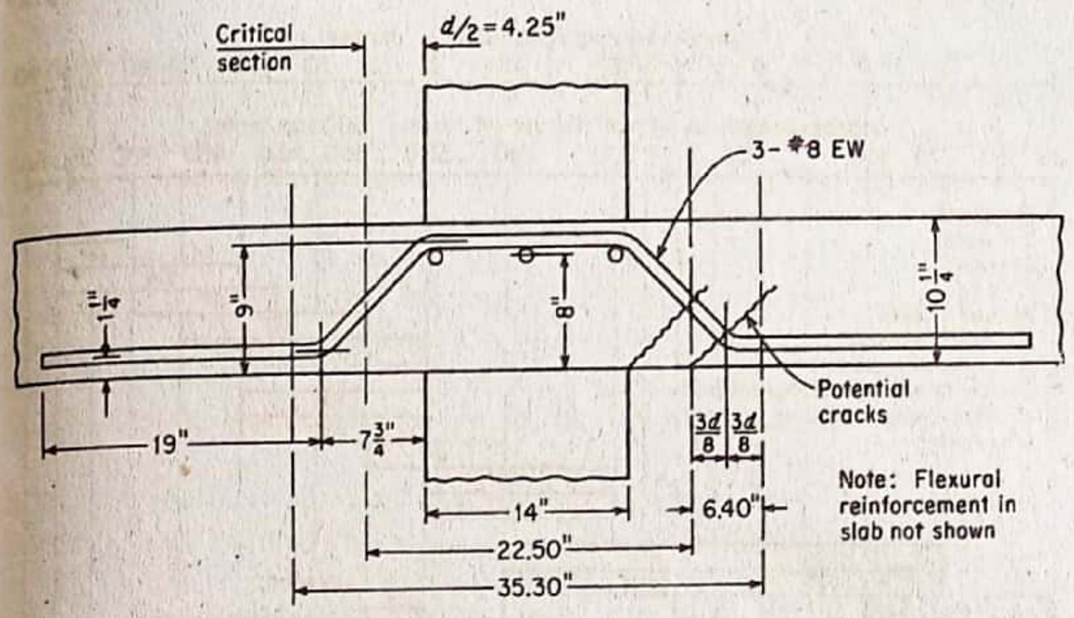


Fig. 4.16

indicating that no additional reinforcement is necessary. The six No. 8 bent bars will provide for all excess shear.

According to Code, bent bars are to be embedded on the compression side of the slab at a distance sufficient to develop by bond the stress for which the bar was designed, but in any case not less than 24 diam. With reference to Table 8, the length required to develop a stress of 10,000 psi is

$$L = 20.6 \times 10{,}000/20{,}000 = 10.3 \text{ in.}$$

The bars will therefore be embedded a distance of $24 \times 1 = 24$ in. in the compression concrete. With approximately 5 in. of length obtained in the sloping part of the bars, a horizontal extension along the bottom of the slab of 19 in. will be used, as shown in the sketch.

PROBLEM

The parking garage described in the example of Art. 4.17 consists of a floor area five bays wide and eight bays long, with all columns spaced 22 ft on centers in each direction. A perimeter beam of 24 in. total depth is used at the outside edge of each exterior panel. Using the ACI moment coefficients for flat slabs (Appendix A), determine the required slab thickness, and design and detail the reinforcement (*a*) for a typical exterior panel at the center of the long edge of the floor and (*b*) for the adjacent first interior panel. Allowable stresses are the same as for the example of Art. 4.17.

SLABS ON GROUND

4.19 General Considerations Concrete slabs are often poured directly on the ground; they receive more or less uniform support from the soil. Roadway and sidewalk slabs, basement floors, and warehouse

Scanned with CamScanner

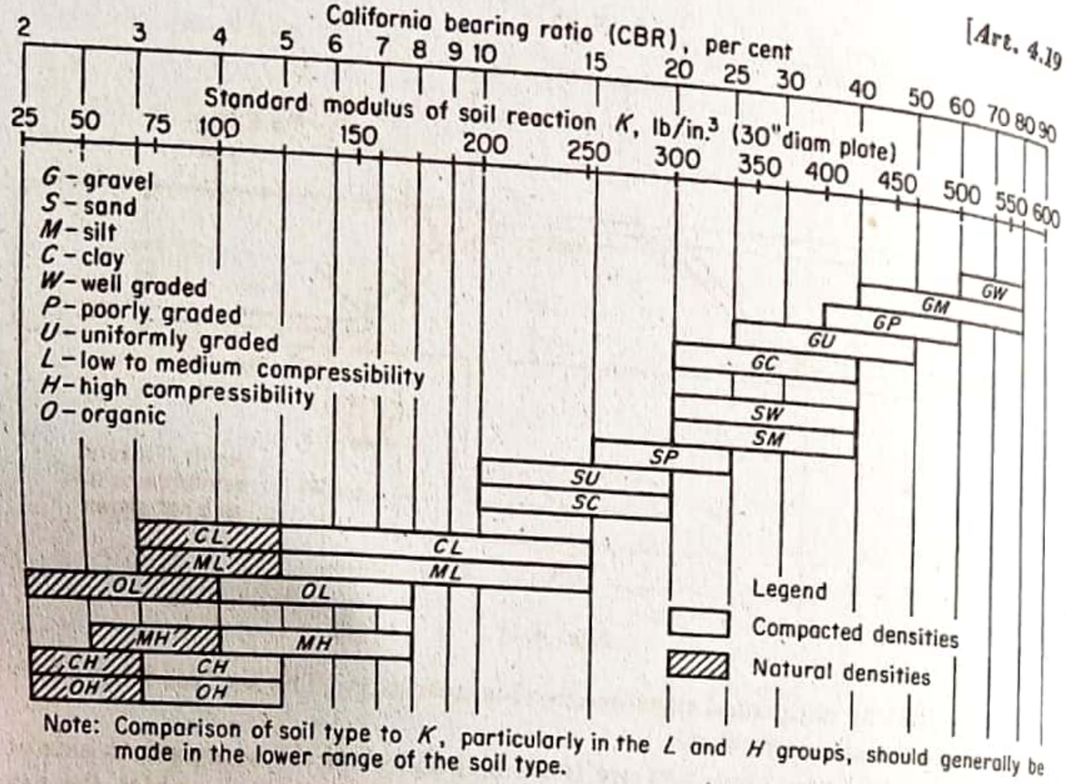


Fig. 4.17 Interrelationships of soil classifications and strength criteria.

floors are common examples of this type of construction. Ordinarily it is desirable to provide a base course of well-compacted crushed stone or gravel. The prepared subgrade, approximately 6 to 12 in. thick, serves (1) to provide more uniform support than if the slab were carried directly on the natural soil, and (2) to improve the drainage of water from beneath the slab. The latter is particularly important in outdoor locations subject to freezing temperatures.

Failures of concrete slabs on ground are not infrequent. Unequal settlement or overloading may cause cracking, as well as restrained shrinkage as volume changes occur. Passage of wheel loads over cracks or improperly made joints may lead to progressive failure by disintegration of the concrete. Failures are not spectacular and do not involve collapse in the usual sense. They may even pass unnoticed for a considerable period of time. Nevertheless, the function of the structure is often impaired, and repairs are both embarrassing and costly.

If the slab is loaded uniformly over its entire area and is supported by an absolutely uniform subgrade, stresses will be due solely to restrained volumetric changes. However, foundation materials are not uniform in their properties. In addition, most slabs are subjected to nonuniform loading. In warehouses, for example, the necessity for maintaining clear aisles for access to stored materials often results in a checkerboard-type load pattern. Wheel loads from trucks and other moving equipment may control the design.

Methods of analysis for such cases are similar to those developed for beams on elastic foundations. Usually the slab is assumed to be homogeneous, isotropic, and elastic; the reaction of the subgrade is assumed to be only vertical and proportional to the deflection. The stiffness of the soil is expressed in terms of the modulus of subgrade reaction k, usually in units of lb per in.^{2} per in., or, simply, lb per in.^{3} The numerical value of k varies widely for different soil types and degrees of consolidation and is generally based on experimental observations; typical values are given in Fig. 4.17. Shown for comparison are values of California bearing ratio, also widely used as a measure of soil consolidation under load.

4.20 Concentrated Loads on Slabs The analysis of slabs supporting concentrated loads is based largely on the work of Westergaard (Refs. 4.6, 4.7). Three separate cases, differentiated on the basis of the location of the load with respect to the edge of the slab, are considered.

Case 1; wheel load close to the corner of a large slab With a load applied at the corner of a slab, the critical stress in the concrete is tension at the top surface of the slab. An approximate solution, due to A. T. Goldbeck, assumes a point load acting at the corner of the slab (see Fig. 4.18). At small distances from the corner, the upward reaction of the soil has little effect, and the slab is considered to act as a cantilever. At a distance x from the corner, the bending moment is Px; it is assumed to be uniformly distributed across the width of the section of slab at right angles to the bisector of the corner angle. For a 90° corner, the width of this section is $2x$, and the bending moment per unit width of slab is

$$\frac{Px}{2x} = \frac{P}{2}$$

If h is the thickness of the slab, the tensile stress at the top surface is

$$f_t = \frac{M}{S} = \frac{P/2}{h^2/6} = \frac{3P}{h^2} \tag{4.6}$$

Equation (4.6) will give reasonably close results only in the immediate vicinity of the slab corner, and only if the load is applied over a small contact area.

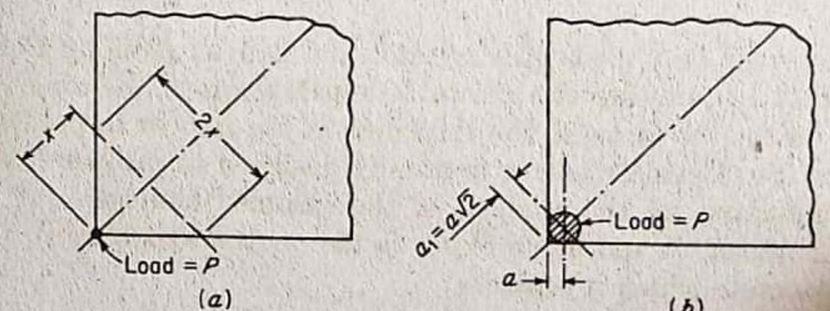


Fig. 4.18

In an analysis which considers the reaction of the subgrade, and which considers the load to be applied over a contact area of radius a (see Fig. 4.18*b*), Westergaard derives the expression for critical tension at the top of the slab, occurring at a distance $2\sqrt{a_1 L}$ from the corner of the slab:

$$f_t = \frac{3P}{h^2}\left[1 - \left(\frac{a\sqrt{2}}{L}\right)^{0.6}\right] \tag{4.7}$$

in which L is the radius of relative stiffness, equal to

$$L = \sqrt[4]{\frac{Eh^3}{12(1-\mu^2)k}} \tag{4.8}$$

where E = elastic modulus of concrete, psi
μ = Poisson's ratio for concrete (approximately 0.15)
k = modulus of subgrade reaction, lb/in.^{3}

The value of L reflects the relative stiffness of the slab and the subgrade. It will be large for a stiff slab on a soft base and small for a flexible slab on a stiff base.

Case 2: wheel load a considerable distance from the edges of a slab With the load is applied some distance from the edges of the slab, the critical stress in the concrete will be tension at the bottom surface. This tension is greatest directly under the center of the loaded area and is given by the expression

$$f_b = 0.316\frac{P}{h^2}[\log h^3 - 4\log(\sqrt{1.6a^2 + h^2} - 0.675h) - \log k + 6.48] \tag{4.9}$$

Case 3: wheel load at an edge of a slab, but removed a considerable distance from a corner When the load is applied at a point along an edge of the slab, the critical tensile stress is at the bottom of the concrete, directly under the load, and is equal to

$$f_b = 0.572\frac{P}{h^2}[\log h^3 - 4\log(\sqrt{1.6a^2 + h^2} - 0.675h) - \log k + 5.77] \tag{4.10}$$

In the event that the tensile stress in the slab, as given by Eqs. (4.7), (4.9), and (4.10), exceeds the allowable tensile stress on the concrete, it is necessary either to increase the thickness of the slab or to provide reinforcement. Such reinforcement is usually designed to provide for all the tension indicated by the analysis of the assumed homogeneous plastic slab. Its centroid should be no closer to the neutral axis than the tension concrete which it replaces.

Example: design of an unreinforced concrete slab on grade A warehouse floor, consisting of an unreinforced slab on ground, is to be designed to support a maximum wheel load of 6000 lb from fork-lift trucks, assumed to apply the load over a contact area of 4-in. radius. Concrete of 4000 psi compressive strength is to be used, with an allowable tensile stress of 200 psi. The slab will be poured in 30-ft-wide strips with construction joints at each edge, and contraction joints will be located every 30 ft in the long direction of the strip. It will be conservatively assumed that no shear transfer is possible across the joints. The wheel load can be applied anywhere within each 900-ft^2 panel. The soil is a clay-gravel with a subgrade modulus of 300 lb per in.^{3}

It will be assumed initially that the critical load location is at the corner of the slab. With

$$E_c = 33w^{1.5}\sqrt{f'_c} = 33 \times 145^{1.5}\sqrt{4000} = 3{,}640{,}000 \text{ psi}$$

and assuming the slab thickness h to be 8 in., the radius of relative stiffness is

$$L = \sqrt[4]{\frac{Eh^3}{12(1-\mu^2)k}} = \sqrt[4]{\frac{3{,}640{,}000 \times 512}{12(1-0.15^2)300}} = 27 \text{ in.}$$

From Eq. (4.7),

$$h^2 = \frac{3P}{f_t}\left[1 - \left(\frac{a\sqrt{2}}{L}\right)^{0.6}\right] = \frac{3 \times 6000}{200}\left[1 - \left(\frac{4\sqrt{2}}{27}\right)^{0.6}\right] = 54.7 \text{ in.}^2$$

$$h = 7.4 \text{ in.}$$

Tentatively a total depth of 7½ in. is selected. If the load is applied centrally within a panel, the tensile stress at the bottom of a 7½-in. slab is, from Eq. (4.9),

$$f_b = \frac{0.316 \times 6000}{56.2}(\log 421 - 4\log 3.96 - \log 300 + 6.48)$$
$$= 144 \text{ psi} < 200 \text{ psi}$$

If the load is applied along the edge of a slab panel, the critical tension at the bottom of the concrete is, from Eq. (4.10),

$$f_b = \frac{0.572 \times 6000}{56.2}(\log 421 - 4\log 3.96 - \log 300 + 5.77)$$
$$= 215 \text{ psi} > 200$$

Since this exceeds the allowable tension by a small amount, a total slab depth of 8 in. will be used.

4.21 Loads Distributed over Partial Areas In addition to concentrated loads, it may be that uniform loads distributed over partial areas of slabs will produce the critical design condition. In warehouses, heavy loads are often stacked about columns, leaving clear aisles midway between the column lines for access, as shown in Fig. 4.19. For moderate column spacing, construction joints are located on column lines only.

Scanned with CamScanner

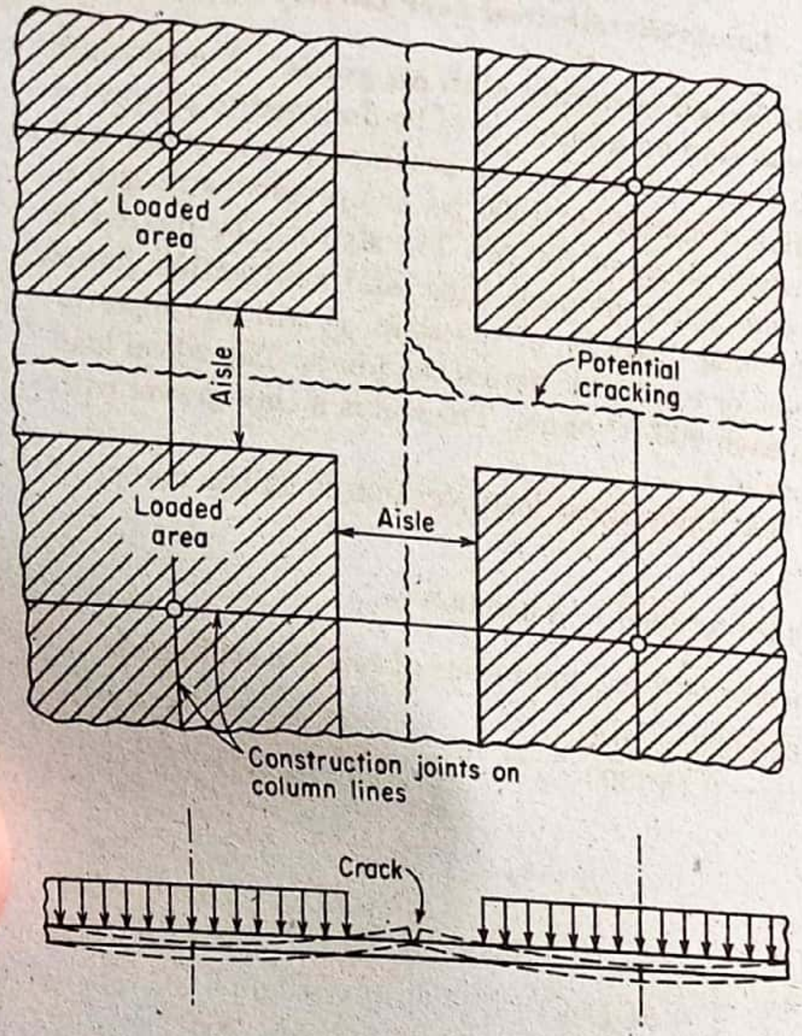


Fig. 4.19

With the loading pattern shown, cracking is likely to occur along the center line of the aisles. In addition, as wheel loads pass over the cracked slab, secondary corner cracks may occur, as shown in one panel.

In an analysis based on the loading and joint arrangement of Fig. 4.19, Rice (Ref. 4.8) derived an expression for the critical negative moment in the slab, which occurs at the center line of the aisle:

$$M_c = \frac{w}{2\lambda^2} e^{-\lambda a} \sin \lambda a \qquad (4.11)$$

where M = slab moment, ft-lb per ft
$\lambda = \sqrt[4]{k/4EI}$, in.$^{-1}$
a = half-aisle width, in.
k = modulus of subgrade reaction, lb per in.^{3}
w = uniform load, psi
e = base of natural logarithms

Recognizing that the width of the aisle cannot always be predicted exactly, Rice suggests that a "critical aisle width" be used. This width is such as to maximize Eq. (4.11) for bending moment. Tables are available (Ref. 4.8) which give critical aisle width and corresponding bending moment for various slab thicknesses and various values of subgrade modulus.

YIELD - LINE THEORY OF SLAB ANALYSIS

4.22 General Considerations Presently the analysis for moments and shears of most reinforced-concrete slabs is based upon elastic theory, somewhat modified for inelastic redistribution. With idealized support conditions, and usually for only a uniformly distribution load, the critical forces and moments can be obtained for rectangular slabs.

While these methods of moment analysis are based essentially on elastic behavior, the actual proportioning of slabs, as for beams and other members, is increasingly being performed by ultimate-strength methods which recognize the inelastic nature of deformations before failure. Although there is a certain inconsistency in combining elastic-moment analysis with ultimate-strength design of sections, this procedure is known to be safe and conservative. It can be shown that a structure analyzed and designed in this way will not fail at a lower load than anticipated (although it may possess substantial reserve strength relative to final collapse; see Art. 8.15).

In recent years, methods have been advanced for moment analysis of reinforced-concrete structures which are based on inelastic considerations, and which direct attention to the conditions that obtain in the structure just prior to failure (see Art. 8.15). In the case of slabs, this failure theory of structural analysis is known as *yield-line theory* (Refs. 4.9, 4.10). It was first proposed by K. W. Johansen. A powerful tool in analysis, it permits the determination of failure moments in slabs of irregular as well as rectangular shapes for a variety of support conditions and loadings.

Figure 4.20*a* shows a simply supported, uniformly loaded, reinforced-concrete slab. For present purposes, it will be assumed to be underreinforced (as are most slabs), with $p < p_b$. The elastic distribution of moments is shown in Fig. 4.20*b*. As the load is gradually increased, and as the maximum applied moment becomes equal to the ultimate-moment capacity of the slab cross section, the tensile steel commences to yield along the transverse line of maximum moment.

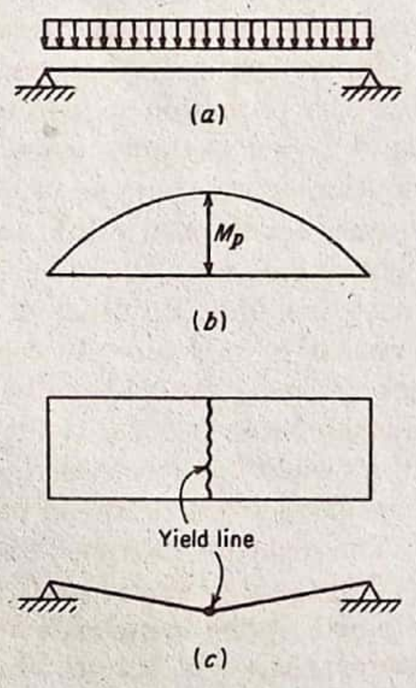


***Fig.* 4.20** Simply supported, uniformly loaded slab.

Scanned with CamScanner

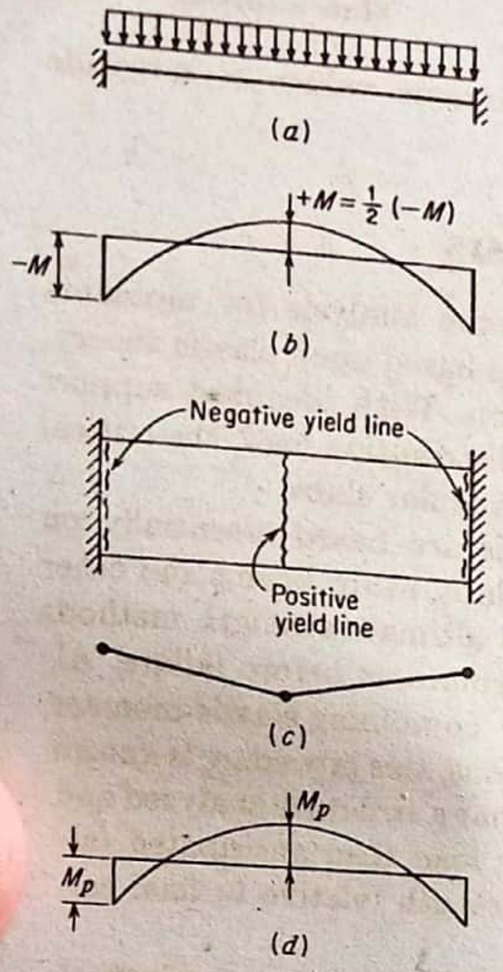


Fig. 4.21 Fixed-end, uniformly loaded slab.

Upon yielding, the curvature of the slab at the yielding section increases sharply, and deflection increases disproportionately. The elastic deformation of the slab is of a small order of magnitude compared with the change in shape of the deflected structure due to the plastic deformation at the yield line. It is acceptable to assume that the slab portions between yield line and supports remain rigid, with all the deformation taking place at the yield line as shown in Fig. 4.20c.

The "hinge" which forms at the yield line rotates at essentially a constant moment. (This moment-rotation relation is shown graphically in Fig. 8.22.) For all practical purposes, the restraining moment at the yielding hinge can be taken equal to the ultimate moment; that is, $M_p = M'_u$.

For a determinate slab such as that of Fig. 4.20, the formation of one yield line is tantamount to failure. A "mechanism" forms (the segments of the slab between the hinge and the supports are able to move without an increase in load), and gross deflection of the structure results.

Indeterminate structures, however, can maintain equilibrium even after the formation of one or more yield lines. The fixed-fixed slab of Fig. 4.21, for example, when loaded uniformly, will have an elastic distribution of moments as in (*b*). As the load is gradually increased (it is assumed for simplicity that the slab is equally reinforced for positive and negative moment), the more highly stressed sections at the supports commence yielding. Rotation of the end tangents occurs, but restraining moments of substantially constant amount M_p continue to act at the support lines. The load can be increased still further, until the moment at midspan becomes equal to the ultimate-moment capacity of the slab, and a third yield line forms as shown in (*c*). This converts the structure into a mechanism and results in collapse.

The moment diagram just before failure is shown in Fig. 4.21*d*. Note that the ratio of elastic positive to negative moments of 1:2 is no longer obtained. Owing to inelastic deformation, the ratio of these moments just before collapse is 1:1 for this particular structure. This is known as *inelastic redistribution of moments.*

Whether or not a concrete structure can sustain rotation and deformation such as to ensure full moment redistribution depends at least in part on the reinforcement ratio. Lightly reinforced members can generally undergo considerable rotation, while overreinforced members may fail by concrete crushing before much rotation occurs. For a more complete discussion of this important aspect of plastic or limit analysis of concrete structures, the reader is referred to Art. 8.15. It will be sufficient for the present to note that most slabs are relatively lightly reinforced, and that the required rotation capacity is normally available.

4.23 Location of Yield Lines The location and orientation of the yield line was evident in the case of the simple slab of Fig. 4.20. Similarly, for the one-way indeterminate slab of Fig. 4.21, the yield lines were easily established. For other cases it is helpful to have a set of guidelines for drawing yield lines and locating axes of rotation. When a slab is on the verge of collapse owing to the existence of a sufficient number of real or plastic hinges to form a mechanism, axes of rotation will be located along the lines of support or over point supports such as columns. The slab segments can be considered to rotate as rigid bodies in space about these axes of rotation. The yield line between any two adjacent slab segments is a straight line, being the intersection of two essentially plane surfaces. Since the yield line (as a line of intersection of two planes) contains all points common to these two planes, it must contain the point of intersection of the two axes of rotation, which is also common to the two planes. That is, the yield line (or yield line extended) must pass through the point of intersection of the axes of rotation of the two adjacent slab segments.

The terms *positive yield line* and *negative yield line* are used to distinguish between those associated with tension at the bottom and tension at the top of the slab, respectively.

Guidelines for establishing axes of rotation and yield lines are summarized as follows:

1. Yield lines are generally straight.

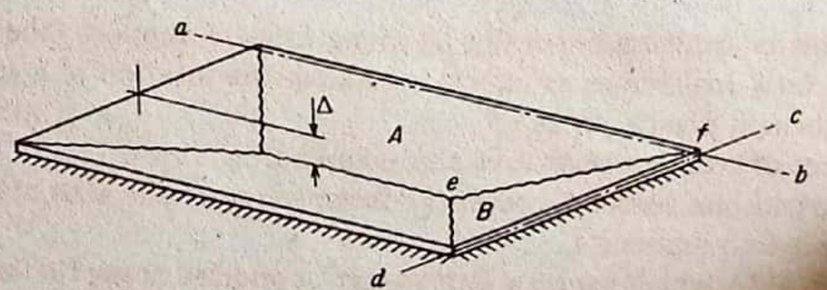


Fig. 4.22 Two-way slab on simple supports.

Scanned with CamScanner

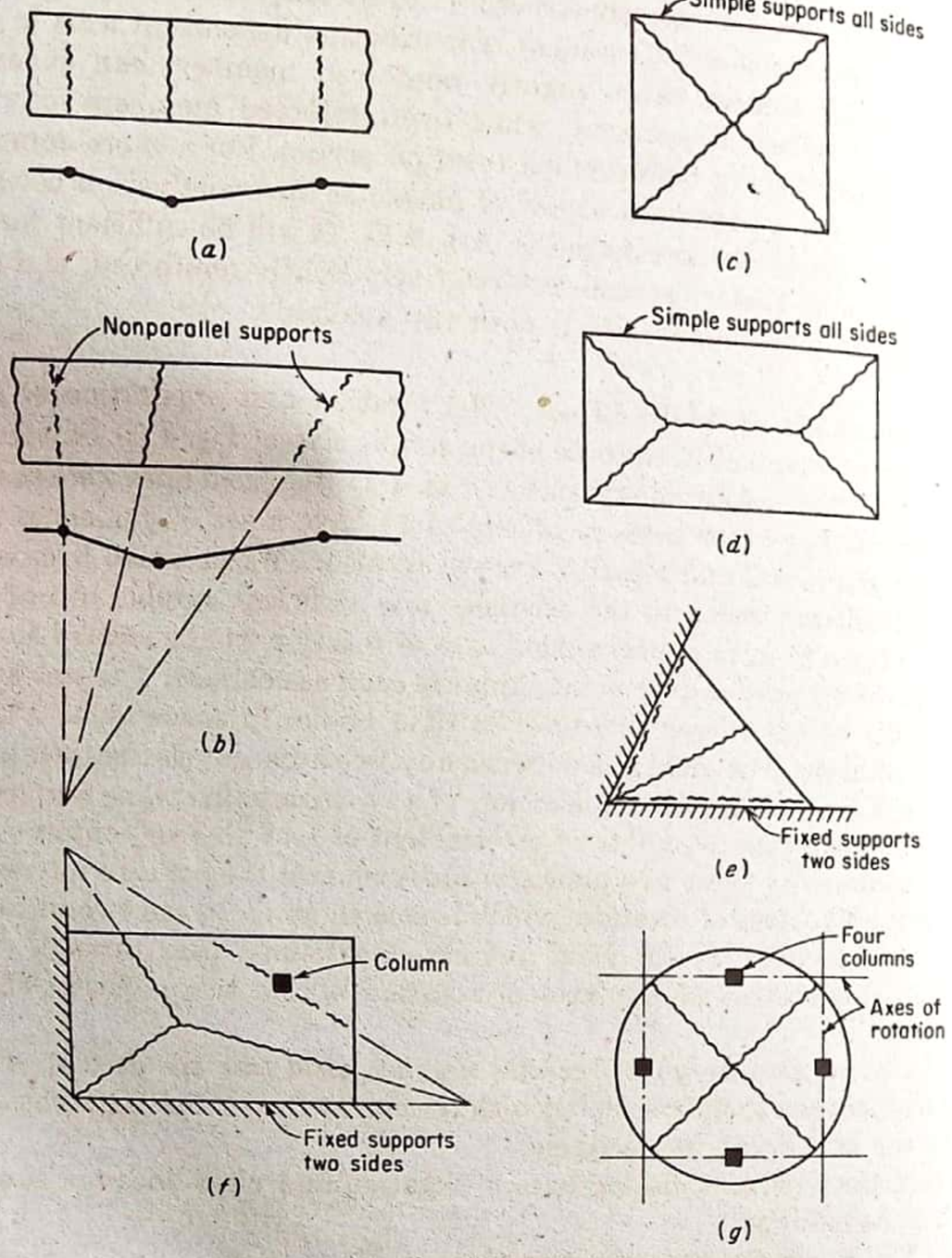


Fig. 4.23 Typical yield-line patterns.

2. Axes of rotation generally lie along lines of support (the support line may be a real hinge, or it may establish the location of a yield line which acts as a plastic hinge).

3. Axes of rotation pass over any columns.

4. A yield line passes through the intersection of the axes of rotation of adjacent slab segments.

In Fig. 4.22, which shows a slab simply supported along its four sides, rotation of slab segments A and B is about ab and cd, respectively. The yield line ef between these two segments is a straight line passing through f, the point of intersection of the axes of rotation.

Illustrations are given in Fig. 4.23 of the application of these guidelines to the establishment of yield-line locations and failure mechanisms for a number of slabs with various support conditions. Shown in (*a*) is a slab continuous over parallel supports. Axes of rotation are situated along the supports (negative yield lines) and near midspan, parallel to the supports (positive yield line). The particular location of the positive yield line in this case and the other cases of Fig. 4.23 depends upon the distribution of loading and the reinforcement of the slab. Methods for determining its location will be discussed later.

For the continuous slab on nonparallel supports, shown in (*b*), the midspan yield line (extended) must pass through the intersection of the axes of rotation over the supports. In (*c*) there are axes of rotation over all four simple supports. Positive yield lines form along the lines of intersection of the rotating segments of the slab. A rectangular two-way slab on simple supports is shown in (*d*). The diagonal yield lines must pass through the corners, while the central yield line is parallel to the two long sides (axes of rotation along opposite supports intersect at infinity in this case).

With this background, the reader should have no difficulty in applying the guidelines to the slabs of Fig. 4.23*e* through *g* to confirm the general pattern of yield lines shown.

4.24 Equilibrium Method of Analysis Once the general pattern of yielding and rotation has been established by applying the guidelines of Art. 4.23, the specific location and orientation of the axes of rotation and the failure load for the slab can be established by either of two methods. The first of these is based on the equilibrium of the various segments of the slab. The second, to be discussed in Art. 4.25, makes use of the principle of virtual work.

The correct locations of axes of rotation and the collapse load of a slab can be found by considerating the equilibrium of the slab segments. Each segment, studied as a free body, must be in equilibrium under the action of the applied loads, the moments along the yield lines, and the reactions or shear along the support lines. It is noted that, because the yield moments are principal moments, twisting moments are zero along the yield lines, and in most cases the shearing forces are also zero. Only the unit moment m generally is considered in writing equilibrium equations.

Example The application of the equilibrium method will be demonstrated first with respect to the one-way, uniformly loaded, continuous slab of Fig. 4.24*a*.

Scanned with CamScanner

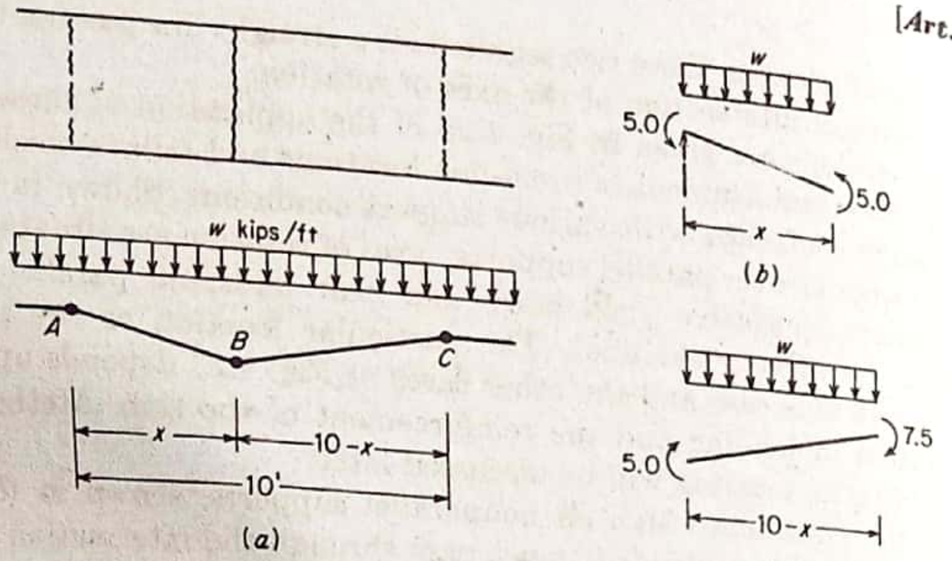


Fig. 4.24 Equilibrium method of analysis for one-way slab.

The slab has a 10-ft span and is reinforced so as to provide a resistance to positive bending of 5.0 ft-kips per ft through the span. In addition, negative steel over the supports provides moment capacities of 5.0 ft-kips per ft at A and 7.5 ft-kips per ft at C. Determine the ultimate load capacity of the slab.

The number of equilibrium equations required will depend upon the number of unknowns. One unknown is always the relation between the ultimate resisting moments of the slab and the load. Other unknowns are needed to define the locations of yield lines. In the present instance, one additional equation will suffice to define the distance of the yield line from the supports. Taking the left segment of the slab as a free body, and writing the equation for moment equilibrium about the left support line (see Fig. 4.24*b*),

$$\frac{wx^2}{2} - 10.0 = 0 \qquad (a)$$

Similarly, for the right slab segment,

$$\frac{w}{2}(10 - x)^2 - 12.5 = 0 \qquad (b)$$

Solving Eqs. (*a*) and (*b*) simultaneously for w and x results in

$$w = 0.89 \text{ kips per ft}^2 \qquad x = 4.75 \text{ ft}$$

If a slab is reinforced identically in orthogonal directions, the ultimate resisting moment is the same in these two directions, as it is along any other line, regardless of its direction. Such a slab is said to be *isotropically* reinforced. If, however, the ultimate strengths are different in two perpendicular directions, the slab is called *orthogonally anisotropic*, or simply *orthotropic*. Only isotropic slabs will be discussed in this section. Johansen has shown (Ref. 4.9) that orthotropic slabs can be reduced to equivalent isotropic cases, for purposes of analysis, by modifying the slab dimensions.

It is convenient in yield-line analysis to represent moments with vectors. The standard convention, in which the moment acts in a clockwise direction when viewed along the vector arrow, will be followed. Treatment of moments as vector quantities will be illustrated by the following example.

Example A square slab is simply supported along all sides and is to be isotropically reinforced. Determine the ultimate resisting moment m per linear foot required just to sustain a uniformly distributed load of w psf.

Conditions of symmetry indicate the yield-line pattern shown in Fig. 4-25*a*. Considering the moment equilibrium of any one of the identical slab segments about its support (see Fig. 4.25*b*), one obtains

$$\frac{wL^2}{4}\frac{L}{6} - 2\frac{mL}{\sqrt{2}}\frac{1}{\sqrt{2}} = 0$$

$$m = \frac{wL^2}{24}$$

4.25 Analysis by Virtual Work Alternative to the method of Art. 4.24 is a method of analysis using the principle of virtual work. Since the moments and loads are in equilibrium when the yield-line pattern has formed, an infinitesimal increase in load will cause the structure to deflect further. The external work done by the loads to cause a small, arbitrary virtual deflection must equal the internal work done as the slab rotates at the yield lines to accomodate this deflection. The slab is therefore given a virtual displacement, and the corresponding rotations at the various yield lines may be calculated. By equating internal and external work, the relation between the applied loads and the ultimate resisting moments of the slab is obtained.

Example Determine the ultimate-load capacity of the one-way, uniformly loaded, continuous slab of Fig. 4.26, using the method of virtual work. The resisting moments of the slab are 5.0, 5.0, and 7.5 ft-kips per ft at A, B, and C, respectively.

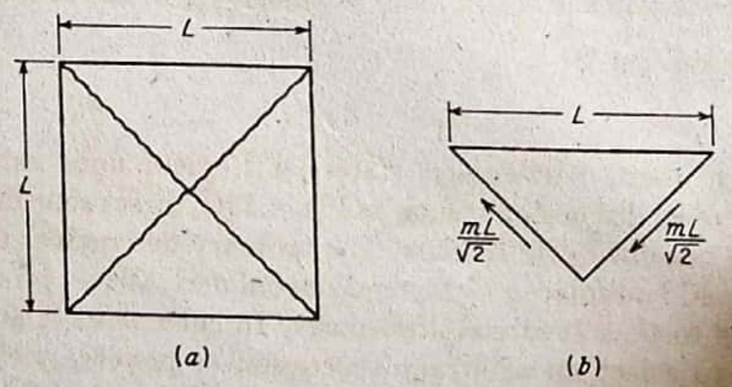


Fig. 4.25

Scanned with CamScanner

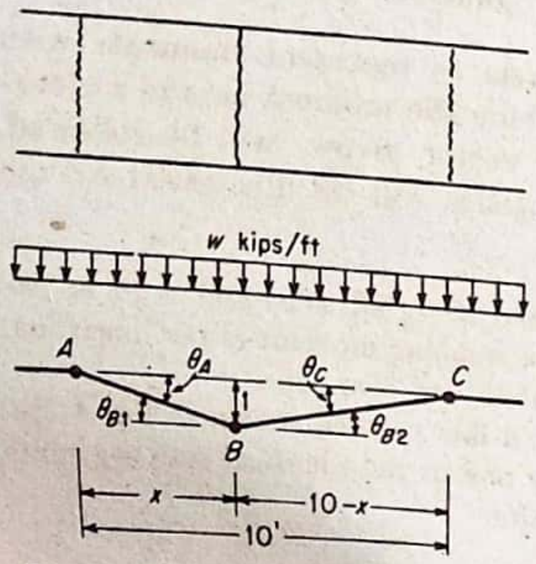


Fig. 4.26 Mechanism method of analysis for one-way slab.

A unit deflection is given to the slab at B (Fig. 4.26). Then the external work done by the load is the sum of the loads times their displacements and is equal to

$$\frac{wx}{2} + \frac{w}{2}(10 - x)$$

The rotations at the hinges are calculated in terms of the unit deflection (see Fig. 4.26) and are

$$\theta_a = \theta_{b1} = \frac{1}{x} \qquad \theta_{b2} = \theta_c = \frac{1}{10 - x}$$

The internal work is the sum of the moments times their corresponding rotation angles:

$$5\frac{1}{x}2 + 5\frac{1}{10 - x} + 7.5\frac{1}{10 - x}$$

Equating the external and internal work,

$$\frac{wx}{2} + 5w - \frac{wx}{2} = \frac{10}{x} + \frac{5}{10 - x} + \frac{7.5}{10 - x}$$

$$5w = \frac{10}{x} + \frac{25}{2(10 - x)}$$

$$w = \frac{2}{x} + \frac{5}{2(10 - x)}$$

To determine the minimum value of w, this expression is differentiated with respect to x and set equal to zero:

$$\frac{dw}{dx} = -\frac{2}{x^2} + \frac{5}{2(10 - x)^2} = 0$$

from which

$$x = 4.75 \text{ ft}$$

Substituting this value in the previous expression for w, one obtains

$$w = 0.89 \text{ kips per ft}^2$$

as before.

In many cases, particularly those with yield lines established by several unknown dimensions (such as Fig. 4.23*f*), direct solution by virtual work would become quite tedious. The ordinary derivatives in the above example would be replaced by several partial derivatives, producing a set of equations to be solved simultaneously. In such cases it is often more convenient to select an arbitrary succession of possible yield-line locations, solve the resulting mechanisms for the unknown load (or unknown moment), and determine the correct minimum load (or maximum moment) by trial.

Example The two-way slab of Fig. 4.27 is simply supported on all four sides and carries a uniformly distributed ultimate load of w psf. Determine the ultimate-moment resistance of the slab, which is to be isotropically reinforced.

Positive yield lines will form in the pattern shown in Fig. 4.27*a*, with the dimension a unknown. The correct dimension a will be such as to maximize the moment resistance required to support the load w. The values of a and m will be found by trial.

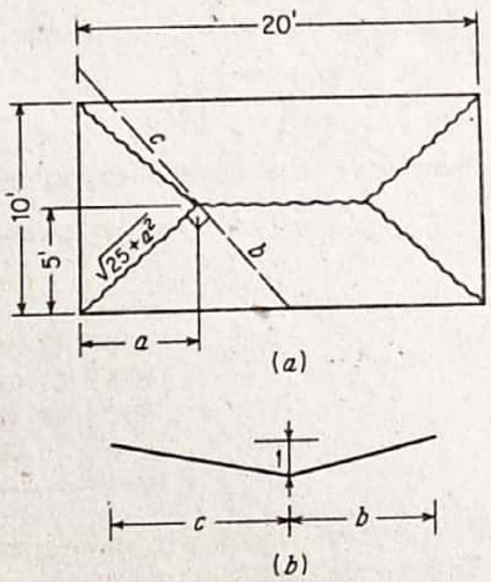


Fig. 4.27

In Fig. 4.27*a*, the length of the diagonal yield is $\sqrt{25 + a^2}$. From similar triangles,

$$b = 5\frac{\sqrt{25 + a^2}}{a} \qquad c = a\frac{\sqrt{25 + a^2}}{5}$$

Then the rotation of the plastic hinge at the diagonal yield line corresponding to a unit deflection at the center of the slab (see Fig. 4.27*b*) is

$$\theta_1 = \frac{1}{b} + \frac{1}{c} = \frac{a}{5\sqrt{25 + a^2}} + \frac{5}{a\sqrt{25 + a^2}} = \frac{1}{\sqrt{25 + a^2}}\left(\frac{a}{5} + \frac{5}{a}\right)$$

The rotation of the yield line parallel to the long edges of the slab is

$$\theta_2 = \tfrac{1}{5} + \tfrac{1}{5} = 0.400$$

For a first trial, let $a = 6$ ft. Then the length of the diagonal yield line is

$$\sqrt{25 + 36} = 7.81 \text{ ft}$$

The rotation at the diagonal yield line is

$$\theta_1 = \frac{1}{7.81}(\tfrac{6}{5} + \tfrac{5}{6}) = 0.261$$

At the central yield line it is $\theta_2 = 0.400$. The internal work done as the incremental deflection is applied is

$$W_i = (m \times 7.81 \times 0.261 \times 4) + (m \times 8 \times 0.400) = 11.36m$$

The external work done during the same deflection is

$$W_e = (10 \times 6 \times \tfrac{1}{2}w \times \tfrac{1}{3} \times 2) + (8 + 5w \times \tfrac{1}{2} \times 2) + (12 \times 5 \times \tfrac{1}{2}w \times \tfrac{1}{3} \times 2) = 80w$$

Scanned with CamScanner

Equating W_i and W_e, one obtains [Art. 4.26

$$m = \frac{80w}{11.36} = 7.05w$$

Successive trials for different values of a result in the following data:

a	W_i	W_e	m
6.0	$11.36m$	$80.0w$	$7.05w$
6.5	$11.08m$	$78.4w$	$7.08w$
7.0	$10.87m$	$76.6w$	$7.04w$
7.5	$10.69m$	$75.0w$	$7.02w$

It is evident that the yield-line pattern defined by $a = 6.5$ ft is critical. The required resisting moment for the given slab is $7.08w$.

In common with the equilibrium method of analysis, the method of virtual work as applied to slabs is an "upper-bound" method in the sense that a yield pattern different from the one assumed may produce a lower failure load or, conversely, may require greater moment capacity to resist a given applied load. To illustrate, the rectangular slab of Fig. 4.28, supported along only three sides and free along the fourth, may fail by either of the two mechanisms shown. An analysis based on yield pattern a may indicate a minimum failure load higher than one based on pattern b. It is necessary to investigate all reasonable failure mechanisms in each case to establish that the correct solution has been found.

4.26 Corner Levers In the preceding discussion it has been assumed that yield lines enter the corners between the two intersecting sides. An alternative possibility is that the yield line forks before it reaches the corner, forming what is known as a *corner lever*, shown in Fig. 4.29*a*.

If the corner is not held down, the triangular element *abc* will pivot about the axis *ab* and lift off the supports. If the corner is held down, a similar situation obtains, except that the line *ab* becomes a yield line. If

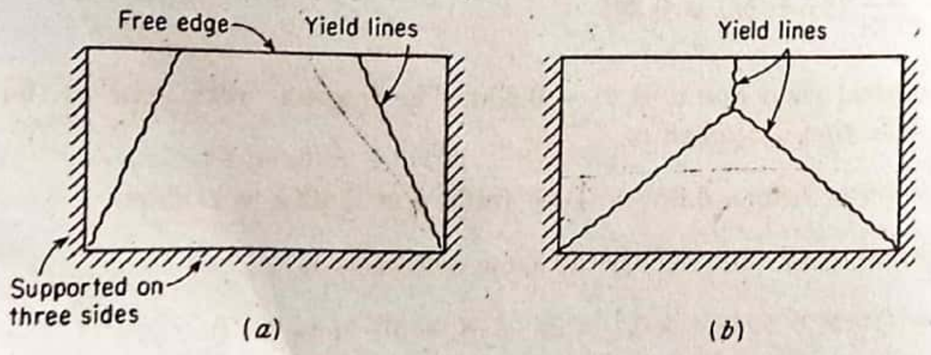


Fig. 4.28

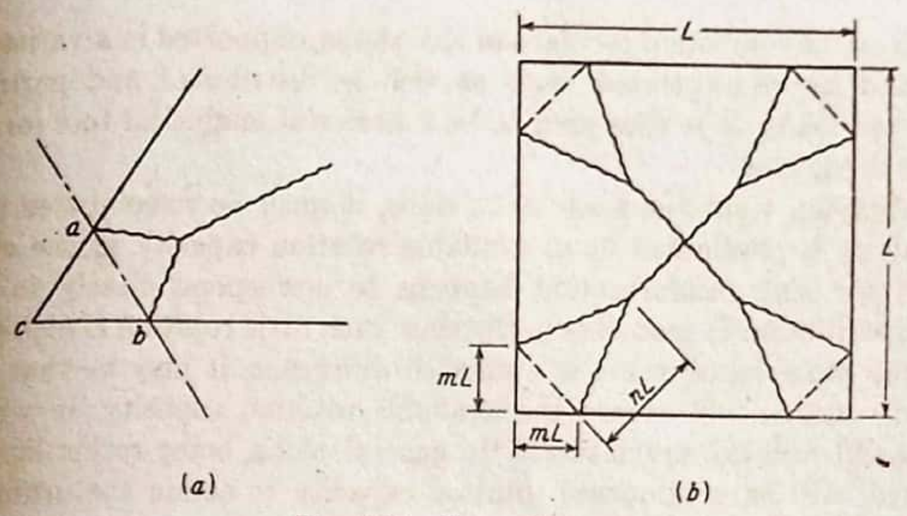


Fig. 4.29 Corner levers.

cracking at the corners of such a slab is to be controlled, top steel, more or less perpendicular to the line *ab*, must be provided. The direction taken by the positive yield lines near the corner indicates the desirability of supplementary bottom slab reinforcement at the corners, placed approximately parallel to the line *ab* (see Art. 4.6).

Although yield-line patterns with corner levers are generally more critical than those without, they are often neglected in yield-line analysis. The analysis becomes considerably more complicated if the possibility of corner levers is introduced, and the error made by neglecting them is usually small.

To illustrate, the uniformly loaded square slab of Art. 4.24, when analyzed for the assumed yield pattern of Fig. 4.25, required an ultimate-moment capacity of $wL^2/24$. The actual yield-line pattern at failure is probably as shown in Fig. 4.29*b*. Since two additional parameters m and n have necessarily been introduced to define the yield-line pattern, a total of three equations of equilibrium are now necessary. These are obtained by summing moments and vertical forces on the segments of the slab. Such an analysis results in a required moment of $wL^2/22$, an increase of about 9 per cent as compared with the results of an analysis neglecting corner levers.[1]

4.27 Limitations of Yield-line Theory The usefulness of yield-line theory is apparent from the preceding articles. In general, elastic solutions are available only for limited conditions, usually uniformly loaded rectangular plates. Even if available, they do not account for the effects of inelastic action. By means of yield-line analysis, a rational solution for the

[1] Analysis indicates (Ref. 4.10) that when the corner is acute the error due to neglect of corner levers may be significant.

Scanned with CamScanner

failure load may be found for slabs of any shape, supported in a variety of ways, and for concentrated loads as well as distributed and partially distributed loads. It is thus seen to be a powerful analytical tool for the structural engineer.

In applying yield-line analysis to slabs, it must be remembered that the analysis is predicated upon available rotation capacity at the yield lines. If the slab reinforcement happens to correspond closely to the elastic distribution of moments in the slab, then little rotation is required. If, on the other hand, there is a marked difference, it may be that the required rotation will exceed the available rotation capacity, in which case the slab will fail prematurely. In general, slabs, being rather lightly reinforced, will have adequate rotation capacity to attain the ultimate loads predicted by yield-line analysis.

It should also be borne in mind that the yield-line analysis focuses attention on the moment capacity of the slab. It is presumed that earlier failure will not occur due to shear, bond, or other causes. In addition, yield-line theory gives no information on stresses, deflections, or severity of cracking under service load conditions.

In spite of these limitations, yield-line analysis provides answers to problems of slab design which cannot be handled by other means, and it will undoubtedly assume a position of increasing importance in engineering practice.

REFERENCES

4.1 J. R. Nichols: Statical Limitations upon the Steel Requirement in Reinforced Concrete Flat Slab Floors, *Trans. ASCE*, vol. 77, 1914.

4.2 H. M. Westergaard and W. A. Slater: Moments and Stresses in Slabs, *Proc. ACI*, vol. 17, 1921.

4.3 D. Peabody, Jr.: Continuous Frame Analysis of Flat Slabs, *J. Boston Soc. Civil Engrs.*, January, 1948.

4.4 "Flat Plate Floors Designed as Continuous Frames," Portland Cement Association Reprint from *R/C*, 1947.

4.5 R. C. Elstner and E. Hognestad: Shearing Strength of Reinforced Concrete Slabs, *J. ACI*, July, 1956.

4.6 H. M. Westergaard: Stresses in Concrete Pavements Computed by Theoretical Analysis, Public Roads, April, 1926.

4.7 H. M. Westergaard: Analytical Tools for Judging Results of Structural Tests of Concrete Pavements, *Public Roads*, December, 1933.

4.8 P. Rice: Design of Concrete Floors on Ground for Warehouse Loading, *J. ACI*, August, 1957.

4.9 E. Hognestad: Yield-line Theory for the Ultimate Flexural Strength of Reinforced Concrete Slabs, *J. ACI*, March, 1953.

4.10 L. L. Jones: "Ultimate Load Analysis of Reinforced and Prestressed Concrete Structures," John Wiley & Sons, Inc., New York, 1962.

chapter 5

COLUMNS: AXIAL COMPRESSION PLUS BENDING

5.1 Types of Columns Concrete compression members whose unsupported length is more than 3 times the least dimension of the cross section are classified as columns. Such members should not be built without reinforcement of some type. In modern construction four types of reinforced-concrete columns are used, namely:

1. Columns reinforced with longitudinal steel and closely spaced spirals
2. Columns reinforced with longitudinal steel and lateral ties
3. Composite columns, in which a structural-steel or cast-iron member is thoroughly encased in a concrete column of type 1
4. Combination columns, in which a structural-steel member is wrapped with wire and encased in at least 2½ in. of concrete over all metal except rivet heads

Scanned with CamScanner

Types 1 and 2 are more generally used, types 3 and 4 being economical with heavy construction loads or extremely heavy permanent loads. Pipe columns, in which a steel pipe is filled with concrete, are sometimes used.

Apart from building columns, there are other structural members that are subject to axial compression, mostly combined with some amount of bending. Among these are arches, variously inclined legs of rigid frames, and compression members in trusses. Even though, for brevity, the term *column* will mostly be used in this chapter, its content applies equally to these other compression members.

For columns of types 1 and 2, above, the ACI Code provides the following *limiting dimensions:* Columns constituting the principal supports of a floor or roof shall have a diameter of at least 10 in. or, for rectangular columns, a least dimension of at least 8 in. and a gross area not less than 96 in. More detailed provisions are given for a number of special cases. It is also provided that the reinforcement ratio of the longitudinal steel shall be not less than 0.01 nor more than 0.08, that at least six bars shall be used for spiral columns and at least four for tied columns, and that the minimum size for longitudinal bars shall be No. 5.

5.2 Columns Reinforced with Ties or Spirals Lateral reinforcement, in the form of individual relatively widely spaced ties or a continuous closely spaced spiral, serves several functions. For one, such reinforcement is needed to hold the longitudinal bars in position in the forms while the concrete is being placed. For this purpose, longitudinal and transverse steel are wired together to form cages, which are then moved into the forms and properly positioned prior to placing of the concrete. For another, transverse reinforcement is needed to prevent the highly stressed, slender longitudinal bars from buckling outward by bursting the thin concrete cover.

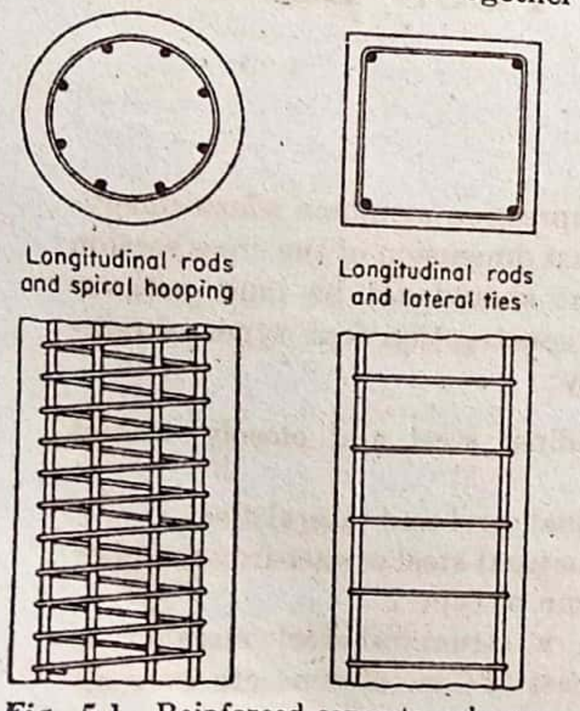


Fig. 5.1 Reinforced-concrete columns.

Closely spaced spirals evidently serve these two functions. Ties, which can be arranged and spaced in various ways, must be so designed that these two requirements are met. This means that the spacing must be sufficiently small to prevent buckling between ties and that, in any tie plane, a sufficient number of ties must be provided to position and hold all bars. On the other hand, in columns with many longitudinal bars, if the column section is crisscrossed by too many ties, they interfere with the placement of concrete in the forms. To achieve adequate tying, yet hold the number of ties to a minimum, the ACI Code gives the following rules for tie arrangement:

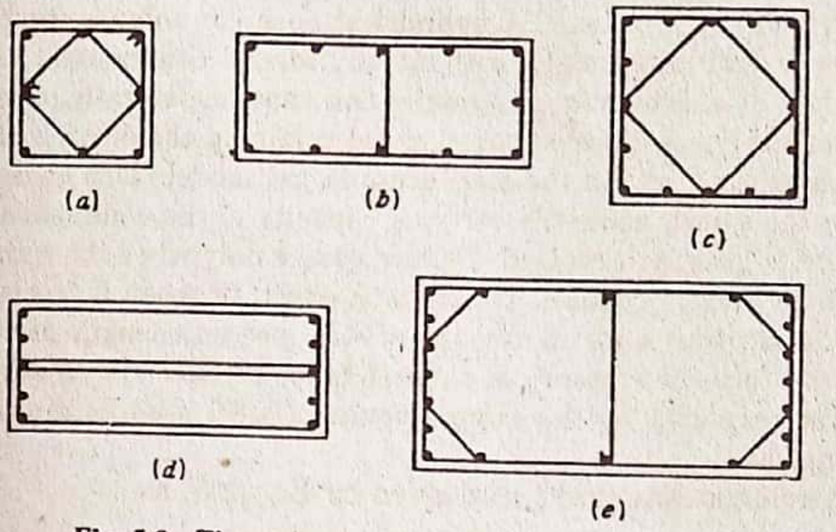


Fig. 5.2 Tie arrangements conforming to ACI Code.

> All bars for tied columns shall be enclosed by lateral ties at least ¼ in. in diameter spaced apart not more than 16 bar diameters, 48 tie diameters, or the least dimension of the column. The ties shall be so arranged that every corner bar and alternate longitudinal bars shall have lateral support provided by the corner of a tie having an included angle of not more than 135°, and no bar shall be farther than 6 in. from such a laterally supported bar. Where the bars are located around the periphery of a circle, a complete circular tie may be used.

Fig. 5.2 shows some tie arrangements which satisfy these requirements.

Spirals, in contrast, are specified to be much more closely spaced than ties, no farther apart than 3 in. or one-sixth of the core diameter. The *core* is that part of the section located within the outer circumference of the spiral. In view of this close spacing, the presence of a spiral affects both the ultimate load and the type of failure as compared with an otherwise identical tied column.

The structural effect of a spiral is easily visualized by considering as a model a steel drum filled with sand (Fig. 5.3). When a load is placed on the sand, a lateral pressure is exerted by the sand on the drum, which causes hoop tension in the steel wall. The load on the sand can be increased until the hoop tension becomes large enough to burst the drum. The sand pile alone, if not confined in the drum, would have been able

Scanned with CamScanner

to support hardly any load. A cylindrical concrete column, to be sure, does have a definite strength without any lateral confinement. As it is being loaded, it shortens longitudinally and expands laterally, depending on Poisson's ratio. A closely spaced spiral confining the column counteracts the expansion, as did the steel drum in the model. This causes hoop tension in the spiral, while the carrying capacity of the confined concrete in the core is greatly increased. Failure occurs only when the spiral steel yields, which greatly reduces its confining effect, or when it fractures. It has been found that a given amount of steel per unit length of column, when in the form of a spiral, is at least twice as effective in adding to the carrying capacity as the same amount of steel used in the form of longitudinal bars.

A tied column fails at the load given by Eq. (2.5) as

$$P'_u = 0.85f'_cA_c + f_yA_s \tag{5.1}$$

At this load the concrete fails by crushing and shearing outward along inclined planes, and the longitudinal steel by buckling outward between ties (Fig. 5.4). In a spiral-reinforced column, when the same load is reached, the longitudinal steel and the concrete within the core are prevented from outward failing by the spiral. The concrete in the outer shell, however, not being so confined, does fail; i.e., the outer shell spalls off when the load P'_u is reached. It is at this stage that the confining action of the spiral takes effect, and, if sizable spiral steel is



Fig. 5.3 Model for action of spiral.



Fig. 5.4 Failure of tied column.

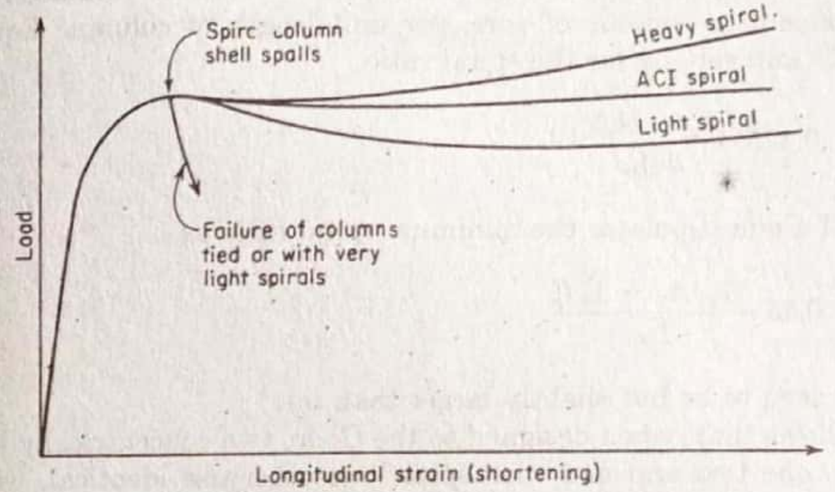


Fig. 5.5 Behavior of spiral and tied columns.

provided, the load which will ultimately fail the column by causing the spiral to yield or burst can be significantly larger than that at which the shell spalled off.

In contrast to the practice in some foreign countries, it is reasoned in American practice that any excess capacity beyond the spalling load of the shell is wasted because the member, although not actually failed, would no longer be considered serviceable. For this reason the Code provides a minimum spiral reinforcement of such amount that its contribution to the carrying capacity is just slightly larger than that of the concrete in the shell. The situation is best understood from Fig. 5.5, which compares the performance of a tied column with that of a spiral column whose spalling load is equal to the ultimate load of the tied column. The failure of the tied column is abrupt and complete. This is true, to almost the same degree, of a spiral column with a spiral so light that its strength contribution is considerably less than the strength lost in the spalled shell. With a heavy spiral the reverse is true, and, with considerable prior deformation, the spalled column would fail at a higher load. The "ACI spiral," its strength contribution about compensating for that lost in the spalled shell, hardly increases the ultimate load. However, by preventing instantaneous crushing of concrete and buckling of steel, it produces a more gradual and ductile failure, i.e., a tougher column.

To determine the right amount of spiral steel, one calculates:

$$\text{Strength contribution of shell} = 0.85f'_c(A_g - A_c) \tag{a}$$

where A_g and A_c are, respectively, the gross and core concrete areas. On the other hand, since spiral steel is at least twice as effective as longitudinal steel, one has conservatively

$$\text{Strength contribution of spiral} = 2p_sA_cf_{sy}$$

Scanned with CamScanner

Here f_{sy} is the spiral yield strength, and p_s is the ratio of volume of spiral reinforcement to volume of core, per unit length of column. Equating (*a*) to (*b*) and solving for the spiral ratio,

$$p_s = 0.425\frac{(A_g - A_c)f'_c}{A_c f_{sy}} \tag{c}$$

The ACI Code stipulates the minimum spiral ratio as

$$p_s = 0.45\,\frac{(A_g/A_c - 1)f'_c}{f_{sy}} \tag{5.2}$$

which is seen to be but slightly larger than (*c*).

It follows that, when designed to the Code, two concentrically loaded columns, one tied and one with spiral but otherwise identical, will fail at about the same load, the former in a sudden and brittle manner, the latter gradually with prior shell spalling and with more ductile behavior. This advantage of the spiral column is much less pronounced if the load is applied with significant eccentricity or when bending from other sources is present simultaneously with axial load. For this reason the Code permits somewhat larger loads on spiral than on tied columns when loaded concentrically or with small eccentricities but reduces this difference for large eccentricities.

ULTIMATE - STRENGTH DESIGN: COMPRESSION PLUS BENDING

5.3 Safety Provisions It was pointed out in Art. 3.7 that in ultimate-strength design adequate safety margins are established by applying overload factors to the design loads and strength-reduction factors to the theoretical ultimate strengths computed for members assumed to be perfect in workmanship and made of materials having exactly the specified strength. It was pointed out that the overload factors apply uniformly, while the strength-reduction factors are different for differently stressed members.

For columns in particular, i.e., for members subject to compression plus bending, the Code provides reduction factors

For tied members: $\phi = 0.70$
For spirally reinforced members: $\phi = 0.75$

The spread between these two values reflects the added safety furnished by the greater toughness of spirally reinforced columns.

There are various reasons why these coefficients are considerably

lower than those for flexure or shear (0.90 and 0.85, respectively). For one, the strength of underreinforced flexural members is not much affected by variations in concrete strength, since it depends primarily on the yield strength of the steel, while the strength of axially loaded members depends strongly on the concrete compression strength [compare, e.g., Eqs. (2.5) and (2.27*a*)]. Because the cylinder strength of concrete under site conditions is less closely controlled than the yield strength of mill-produced steel, a larger occasional strength deficiency must be allowed for. This is particularly true for columns, in which concrete, being placed from the top down the long, narrow form, is more subject to segregation than in horizontally cast beams. Moreover, electrical and other conduits are frequently located in building columns; this reduces their effective cross sections, often unbeknown to the designer, even though this is poor practice and restricted by the Code. Finally, the consequences of a column failure, say in a lower story, would be more catastrophic than of that of a single beam in a floor system of the same building.

Correspondingly, then, the ultimate-strength values to be used for design are

$$P_u = \phi P'_u \tag{5.3a}$$
$$M_u = \phi M'_u \tag{5.3b}$$

where P'_u and M'_u are those simultaneous values of ultimate axial force and ultimate bending moment which are calculated to cause the "perfect" member to fail (see Art. 2.8*b*).

Additionally, the Code recognizes that no members are likely to be found which are purely axially loaded. Even if design calculations show a compression member to be free of any bending moments, imperfections of construction, such as slight beam eccentricities and deviations from straightness or verticality, will cause some unintentional bending moments. For this reason the Code specifies that the minimum load eccentricity for which a compression member must be designed is

For tied members: $e_{min} = 0.10t$
For spirally reinforced members: $e_{min} = 0.05t$

where t is the overall depth of a rectangular section or the outside diameter of a circular section, and $e = M/P$ is the eccentricity referred to the center line of the column. The difference between these values, again, represents a recognition of the greater toughness of spirally reinforced columns with zero or small eccentricities. Evidently, if structural analysis shows eccentricities e to be present which exceed the minimums, these larger design eccentricities must be used in dimensioning the member.

Scanned with CamScanner

5.4 Rectangular Columns For a rectangular column reinforced by A_s and A'_s along the two faces parallel to the axis of bending, it was shown in Eqs. (2.45) and (2.46) that

$$P'_u = \frac{P_u}{\phi} = 0.85f'_c ab + A'_s f'_y - A_s f_s \tag{5.4}$$

$$P'_u e' = \frac{P_u e'}{\phi} = 0.85f'_c ab\left(d - \frac{a}{2}\right) + A'_s f'_y(d - d') \tag{5.5}$$

where the eccentricity e' in Eq. (5.5) is referred to the center of the tension steel. These equations hold for all but very small eccentricities; they assume that the steel A_s on the convex side will be in tension and that only part of the concrete section is in compression (see Fig. 2.31). For very small centroidal eccentricities e, the distance to the neutral axis $c = a/k_1$ may exceed the depth t of the section. Then the entire cross-sectional area will be in compression, so that the stress in the steel A_s will also be compressive, though of magnitude smaller than f'_y. The corresponding distribution of strains and stresses is shown in Fig. 5.6. The stress distribution of Fig. 5.6*b*, which corresponds to the strain distribution of Fig. 5.6*c*, is approximated for purposes of calculation by the rectangular stress distribution of Fig. 5.6*d*. Summing forces, as well as moments, about the steel A_s, it is seen that

$$P'_u = \frac{P_u}{\phi} = 0.85f'_c bt + A'_s f'_y + A_s f_s \tag{5.4a}$$

$$P'_u e' = \frac{P_u e'}{\phi} = 0.85f'_c bt\left(d - \frac{t}{2}\right) + A'_s f'_y(d - d') \tag{5.5a}$$

If, now, the centroidal eccentricity e is reduced to zero, i.e., the column is loaded in concentric compression, then the strains of concrete and steel

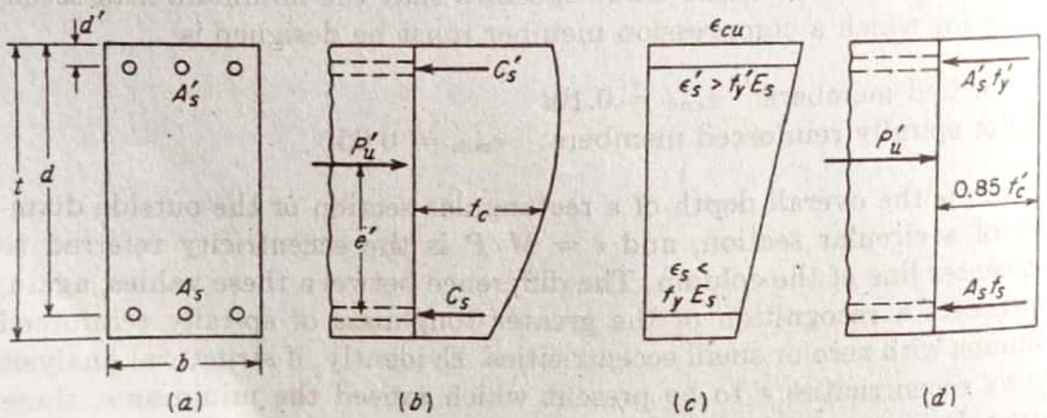


Fig. 5.6 Stresses and strains in eccentric column at failure.

Art. 5.4]

are the same everywhere. Assuming that the yield point of all steel in the section is the same, Eq. (5.4*a*) becomes

$$P'_0 = 0.85f'_c bt + A'_s f'_y + A_s f_y = 0.85f'_c A_c + A_{st} f_y \tag{5.6}$$

Here A_{st} is the total steel area in the section. It is seen that the ultimate load for an axially loaded column (that is, $M = 0$), computed as the limiting case of an eccentrically loaded member, is identical with Eq. (2.5), which was derived for concentric compression and is supported by extensive tests on axially loaded members.

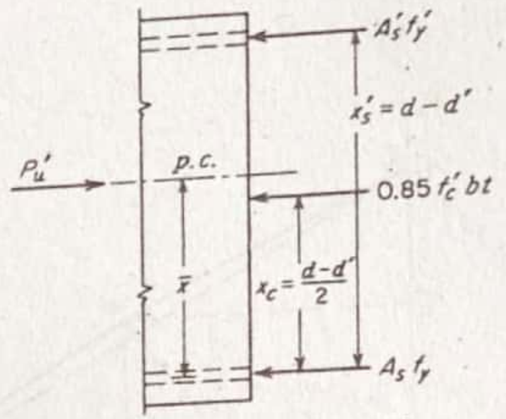


Fig. 5.7 Axis through plastic centroid.

[It should be noted that a concentrically loaded member is one whose eccentricity e about the axis of the cross section is zero. This eccentricity is different from e', used in Eqs. (5.5) and elsewhere, which is measured from the center of the steel A_s. For symmetrically reinforced sections the member is concentrically loaded when the load passes through the center of the section. For an unsymmetrically reinforced section, with $A'_s \neq A_s$, to be concentrically loaded so that Eq. (5.6) is true, the load must pass through a point known as the *plastic centroid*. This point is the location of the resultant of the three internal forces that make up Eq. (5.6). Its distance from the steel A_s can be found from Fig. 5.7 as

$$\bar{x} = \frac{0.85f'_c btx_c + A'_s f'_y x'_s}{0.85f'_c bt + A'_s f'_y + A_s f_y}$$

Evidently, for reasons of equilibrium the external load P must act along the same line as the resultant of all internal forces, i.e., must pass through the plastic centroid. In a symmetrical section the center and the plastic centroid coincide.]

The other limiting case of a member in combined compression plus bending is the situation in which the compression force has become zero, so that bending alone is present. It can be shown, as for the other extreme, that in this case (that is, $P = 0$) the general equations for compression plus bending result in an ultimate bending moment M'_0 equal to that of a simple flexural member with tension reinforcement A_s and compression reinforcement A'_s (see Art. 3.9).

a. Interaction diagram for compression plus bending The information of Art. 2.8, supplemented by the above discussion, shows the considerable complexity of behavior and of corresponding strength calculations for eccentrically loaded members. This behavior ranges

Scanned with CamScanner

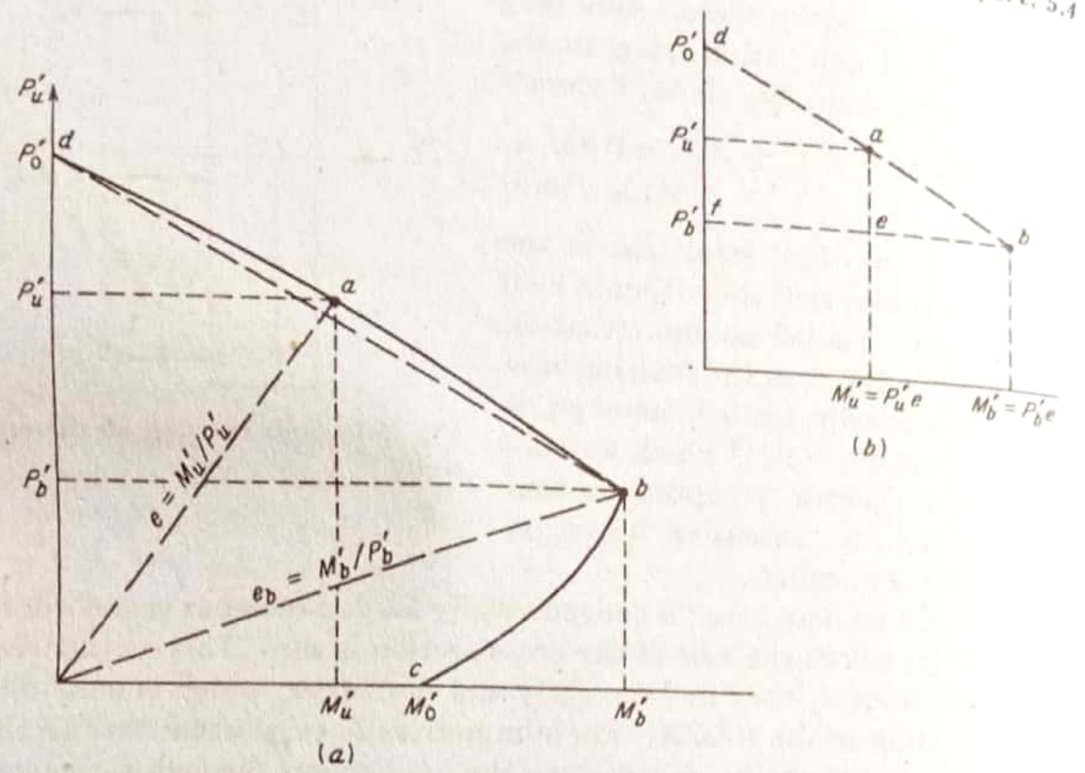


Fig. 5.8 Interaction diagram, compression plus bending, ultimate-strength P'_u and M'_u.

from concentric compression ($P = P'_0$, $M = 0$), over the interval in which failure occurs by crushing of the concrete, through the balanced condition and the interval in which failure occurs by yielding of the steel, to the other extreme of simple bending ($M = M'_0$, $P = 0$). The situation is more easily visualized if the results of the corresponding calculations are graphically depicted in a so-called *interaction diagram*.

For a given cross section and reinforcement, an interaction diagram has the general shape of Fig. 5.8*a*, plotted in terms of ultimate axial loads as ordinates and ultimate moments as abscissas. Moments and eccentricities are here referred to the plastic centroid (for symmetrical sections to the center line of the member), rather than to the center of the tension steel. Any point on the solid curve, such as point *a*, represents a pair of values P'_u and M'_u which, according to the ultimate-strength theory, will just fail the member.

For concentric compression ($M'_u = 0$) the curve starts at *d* with the strength P'_0 of a concentrically loaded member [Eq. (5.6)]. The portion *db* pertains to that range of small eccentricities in which failure is initiated by crushing of the concrete; the corresponding computations were discussed in Art. 2.8*b*. Point *b* represents the balanced condition; i.e., under the simultaneous action of the load P'_b [see Eq. (2.51)] and the corresponding moment M'_b, the concrete will reach its limiting strain (0.003) simultaneously with the tension steel reaching its yield stress f_y. The portion *bc* represents that range in which failure is initiated by yielding of the tension steel (see Art. 2.8*b*). Finally, the end point *c* refers to the moment capacity M'_0 in simple bending, i.e., when $P'_u = 0$. Any inclined line through the origin has a slope whose reciprocal represents the centroidal eccentricity corresponding to the particular combination of ultimate values P'_u and M'_u as shown; that is, $e = M'_u/P'_u$.

It will be observed that in the region *bd* of compression failure, the larger the axial load P'_u, the smaller is the moment M'_u which the section is able to sustain before failing. However, in the region *bc* of tension failures the reverse is true: the larger the axial load, the larger is the simultaneous moment capacity. This is easily understood. In region *bd* failure occurs through overstraining of the concrete. The larger the concrete compression strain caused by the axial load alone, the smaller is the margin of additional strain which can be utilized for the added compression caused by bending. On the other hand, in region *bc* yielding of the steel initiates failure. If a member is loaded in simple bending to the point at which yielding begins in the tension steel, and if an axial compression load is then added, the steel compression stresses caused by this load will superpose on the previous tension stresses. This reduces the total steel stress to a value below the yield strength. Consequently, an additional moment can now be sustained of such magnitude that the combination of the steel stress from the axial load and the increased moment again reaches the yield strength.

b. Design simplifications and Code requirements The lengthy trial-and-error procedures connected with explicit calculations of the strength of eccentrically compressed members call for simplified methods to expedite design. One of these is contained in the ACI Code directly. It consists in replacing the slightly curved line *bd* which covers the compression-failure range with the dashed straight line. This approximation is seen to be on the conservative side, the deviations being quite slight in all but very unusual cases.

In Fig. 5.8*b* this straight line is shown again. From the similarity of the triangles *abe* and *dbf*, the following relations are easily derived:

$$P'_u = \frac{P'_o}{1 + (P'_0/P'_b - 1)e/e_b} \tag{5.7}$$

or, alternatively,

$$P'_u = P'_0 - \frac{(P'_0 - P'_b)M'_u}{M'_b} \tag{5.8}$$

where P'_0 is given by Eq. (5.6), and, for symmetrical reinforcement, P'_b was derived in Eq. (2.51). A general expression for the balanced design

Scanned with CamScanner

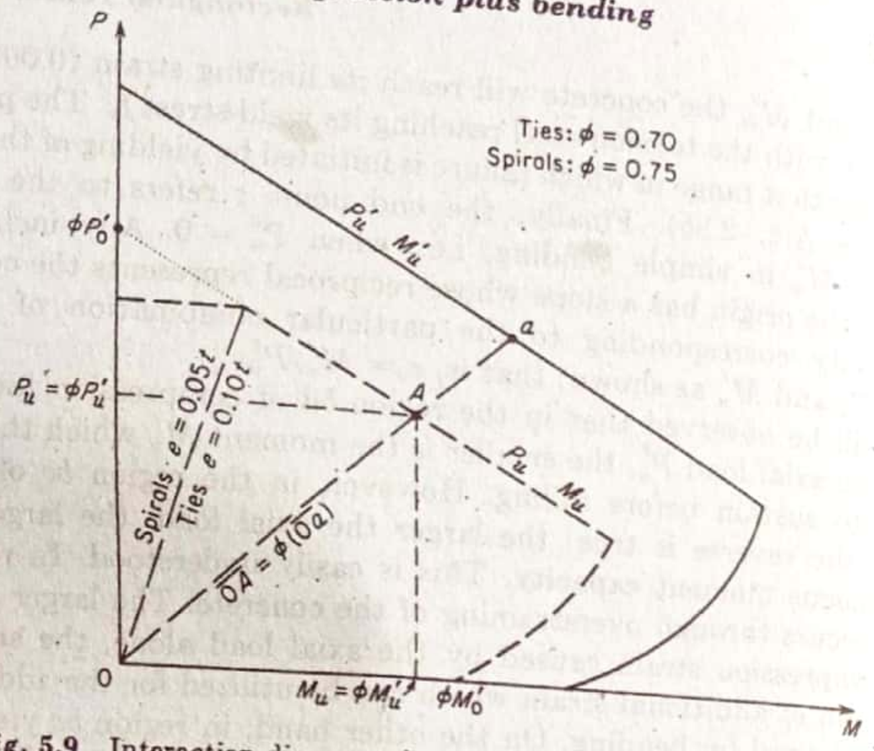


Fig. 5.9 Interaction diagram, design values P_u and M_u by ACI Code.

moment $M_b = \phi M_b'$ can be found as Eq. (19-3) in the Code. For the balanced eccentricity e_b, for symmetrically reinforced rectangular sections, J. G. MacGregor has derived the following approximate expression:

$$e_b = (0.20 + 0.77 p_t m)t \tag{5.9}$$

where $p_t = (A_s + A_s')/bt$

$m = f_y/0.85f_c'$

The *safety provisions of the Code*, as was mentioned in Art. 5.3, include the requirement that the design ultimate load and moment, P_u and M_u, respectively, be obtained by multiplying the calculated strength values P_u' and M_u' by the capacity reduction factor $\phi = 0.70$ [see Eqs. (5.3)]. They also provide that tied columns shall be designed for a minimum eccentricity $e_{min} = 0.10t$. The effect of these provisions is shown in Fig. 5.9, where the solid line of Fig. 5.8 has been redrawn, indicating the calculated ultimate-strength relations and using the simplifying straight-line bd. The dashed curve, which indicates the design ultimate strength according to the Code, is obtained by reducing the length of any radial line Oa by $\phi = 0.70$ to obtain the corresponding length OA. The figure also indicates the stipulated minimum eccentricity $e_{min} = 0.10t$. The Code, as was mentioned before, stipulates that tied columns with design eccentricities smaller than e_{min} be dimensioned for this minimum eccentricity.

c. Design aids In order to reduce the repetitive effort of dimensioning large numbers of columns, such as occur in any tier building frame,

a number of design aids are available in the form of tables or graphs. They are available in handbooks or special pamphlets published by the American Concrete Institute, the Concrete Reinforcing Steel Institute, and the Portland Cement Association. They cover the most common practical cases, i.e., symmetrically reinforced, rectangular tied columns and spirally reinforced, circular and square columns. For other situations the methods of Art. 2.8 and this chapter furnish the necessary principles for direct analysis.

Graphs 2 through 5 of Appendix B represent a set of such design aids for symmetrically reinforced tied columns. They are somewhat approximate in that they have been calculated on the assumption that the compression reinforcement has yielded when ultimate strength is reached. As has been discussed in Art. 2.8, this is not always the case, but is easily verified by a separate calculation. The graphs are seen to consist of interaction diagrams of the type just described. However, instead of plots of P_u' versus M_u', convenient nondimensional parameters have been selected (P_u'/btf_c' versus M_u'/bt^2f_c') which, taken in conjunction with the radial lines for various e/t ratios and the interaction curves drawn for various values of $p_t m$, expedite the dimensioning or analysis of sections. The use of these graphs and associated calculations is illustrated in the following examples.

Example 1 A column is to be designed for 28 kips dead load, 36 kips live load, a moment from dead load of 43.7 ft-kips, and a moment from live load of 37.5 ft-kips; $f_c' = 3000$ psi, and $f_y = 40{,}000$ psi. Design the column.

According to the safety provisions of the ACI Code, the column must be designed for $P_u = 1.5 \times 28 + 1.8 \times 36 = 106.7$ kips and $M_u = 1.5 \times 43.7 + 1.8 \times 37.5 = 133.2$ ft-kips.

A cross section 12×20 in. will be tried, using the graphs for the design. According to the Code, the required ultimate load and moment are $P_u' = P_u/\phi = 106.7/0.70 = 152$ kips and $M_u' = M_u/\phi = 133.2/0.70 = 191.0$ ft-kips. For the selected column size, $e/t = (191.0 \times 12)/(152 \times 20) = 0.75$. To select the correct graph, with 2.5 in. from face to bar center for adequate cover over the stirrups, calculate $d/t = 17.5/20 = 0.875$; hence, it is necessary to interpolate between Graphs 3 and 4. To enter the graphs, calculate $K = 152{,}000/12 \times 20 \times 3000 = 0.21$, and $Ke/t = 0.21 \times 0.75 = 0.157$. Interpolating between the two graphs, one finds $p_t m = 0.23$. Since $p_t = A_s/bt$ and $m = f_y/0.85f_c'$, $A_s = 0.23 \times 12 \times 20(0.85 \times 3000/40{,}000) = 3.52$ in.^{2}. Four No. 9 bars with an area of 4 in.^{2} are selected, one in each corner.

The column has now been designed for the maximum simultaneous values of axial load and moment caused by dead and live load. From the shape of the curves of Graphs 3 and 4, it is evident that if axial load on this column is reduced, its moment capacity will decrease. Consequently, it is generally necessary to check the adequacy for at least one more case

Scanned with CamScanner

of loading, namely that which combines a large moment with a small axial force. At the bottom section of an interior building column, simultaneous maximum moment and maximum load is generally obtained if all floors above that section are fully loaded by dead and live load and only one of the two abutting girders is under live load; this produces maximum joint moment. The other case to be checked is obtained by assuming dead load only on all overlying floors (giving minimal axial load) and again placing live load on one of the two abutting girders to obtain a maximum joint moment.

Example 2 The same column is made of concrete with $f'_c = 5000$ psi and reinforced with steel of $f_y = 75{,}000$ psi. If, as before, the eccentricity about the column axis is $e = 0.75t = 0.75 \times 20 = 15$ in., calculate the design load of the column. (The ACI Code stipulates that steel with yield point in excess of 60 ksi shall be used with a design yield stress equal to 85 per cent of the specified yield stress unless tests show that at the specified yield stress the strain does not exceed 0.003. This is required in order to assure that the concrete will not crush at a strain lower than that at which compression reinforcement begins to yield. It is here assumed that this test requirement has been met. The Code also stipulates safeguards against excessive cracking when high-strength tension reinforcement is used. This requirement is generally more critical for flexural members than for columns.)

To enter the graphs, calculate $p_t m = [4/(12 \times 20)](75{,}000/0.85 \times 5000) = 0.295$. With this value, and with $e/t = 0.75$, interpolating between Graphs 3 and 4, one finds $K = 0.245$. Therefore, the calculated ultimate load is $P'_u = 0.245 \times 12 \times 20 \times 5000 = 294{,}000$ lb, and the ultimate load to be used in design is $P_u = \phi P'_u = 0.70 \times 294{,}000 = 206{,}000$ lb.

From the graphs it is seen that the point representing $K = 0.245$ lies on the lower, curved portion of the $p_t m = 0.295$ curve. From the discussion of Fig. 5.8, it follows that, for the particular loading, failure of this column is initiated by yielding of the tension steel. As has been pointed out, Eq. (2.53), the more elaborate formulas of the Code, and Graphs 2 to 5 are all based on the assumption that in this case the compression steel too has yielded at failure. This should be verified, particularly when, as here, high-strength steel is used.

With reference to Fig. 2.32, which shows a column of the same cross section, if both compression and tension steel are yielding, $P'_u = A'_s f_y - A_s f_y + abf'_c = abf'_c$. From this, the depth of the rectangular stress block is found to be $a = P'_u/bf'_c = 294{,}000/12 \times 5000 = 4.9$ in., and the depth to the neutral axis $c = a/k_1$. For the high-strength concrete used, according to Eq. (2.31), $k_1 = 0.80$, so that $c = 4.9/0.80 = 6.1$ in. At failure the extreme fiber strain of the concrete is assumed to be 0.003, so that from Fig. 2.32*c* the strain in the compression steel is $\epsilon'_s = 0.003(c - 2.5)/c = 0.00167$. On the other hand, the yield strain of the given steel is $\epsilon_y = f_y/E = 75/29{,}000 = 0.00258$. This being larger than ϵ'_s, it is seen that at failure the compression steel is not stressed to the yield point, and the previous calculation is not strictly correct.

For a recalculation, assume by trial that $c = 6.4$ in. (The compression steel

force being smaller than would be the case if the steel were yielding, the concrete has to supply a larger compression force than before; this is the reason for assuming a larger c than was found above.) Then $f'_s = 0.003(3.9/6.4)29{,}000{,}000 = 53{,}000$ psi, and $P'_u = -A_s f_y + A'_s f_s + abf'_c$; with $a = 0.8 \times 6.4 = 5.12$, $P'_u = -2.0 \times 75{,}000 + 2.0 \times 53{,}000 + 5.2 \times 12 \times 5000 = 268{,}000$ lb. If the assumed value for c is correct, then equilibrium requires that the moment of the external force P'_u about the tension steel must be equal to the moment of the internal forces. Hence $M_{ext} = 268{,}000(15.0 + 7.5) = 6{,}040{,}000$ in.-lb, and $M_{int} = A'_s f'_s(d - d') + abf'_c(d - a/2) = 6{,}180{,}000$ in.-lb. It is seen that the difference between external and internal moments is 140,000 in.-lb or 2.3 per cent, an error sufficiently small to be neglected. Consequently, with $P'_u = 266{,}000$, the ultimate load to be used in design is $P_u = 0.7 \times 268{,}000 = 188{,}000$ lb. This compares with the value of 206,000 lb which was calculated from the graphs on the mistaken assumption that the compression steel has yielded at failure. For larger steel ratios than used in this column, errors would be correspondingly larger. This illustrates the special care which must be taken in design when high-strength steel is used for compression reinforcement.

In Example 1 the same column, with moderate-strength materials, was found to have a design ultimate load of 107,000 lb. Compare this with 188,000 lb when high-strength materials are used; the advantage of the latter in increasing carrying capacity, or in reducing member size for a given design load, is immediately evident.

d. Member with small axial load, tension reinforced The majority of columns are symmetrical and symmetrically reinforced. Unsymmetrical members do occur, however. For these, design aids are not usually available, but they can be handled without difficulty by using the basic premises of ultimate-strength design. By way of example, in single-story rigid frames, such as portal frames, large bending moments often combine with relatively small axial loads. In such cases unsymmetrical reinforcement frequently presents the most economical solution. For illustration such a member, reinforced for tension only, is analyzed herein.

For a member with tension reinforcement only, subject to a compression force with an eccentricity e' relative to the center of the tension steel, the ACI Code gives the equation

$$P_u = \phi P'_u = \phi 0.85 f'_c bd \left[-pm + 1 - \frac{e'}{d} + \sqrt{\left(1 - \frac{e'}{d}\right)^2 + \frac{e'pm}{d}} \right]$$

when failure is initiated by yielding of the tension steel. This formula can be derived from Eqs. (2.45) and (2.46) for the special case of $A'_s = 0$ in precisely the same way as Eq. (2.53) was derived for the special case of $A_s f_y = A'_s f'_y$. Whether to use the formula or direct analysis from general principles is a matter of individual preference.

Scanned with CamScanner

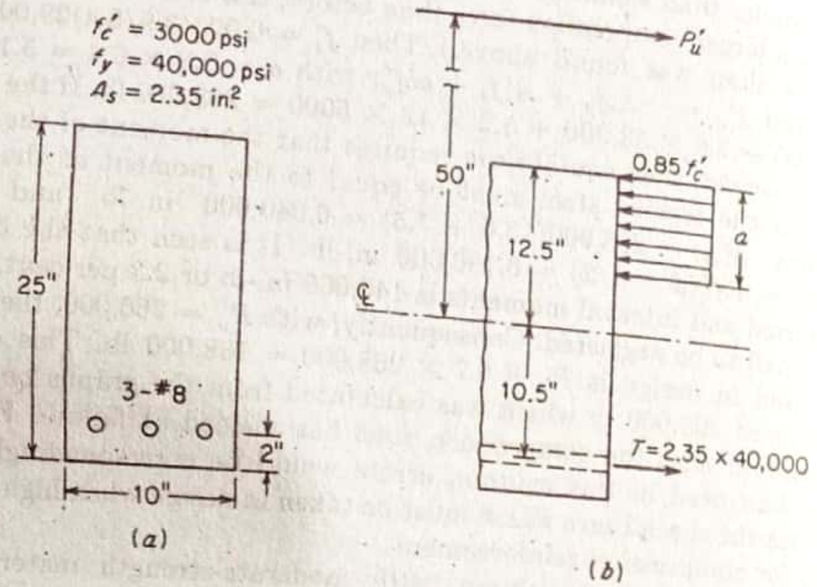


Fig. 5.10

Example The member shown in Fig. 5.10 is subject to a compression force with eccentricity from the center line of $e = 50$ in. Determine the ultimate design load and moment.

With external and internal forces as shown, the two equilibrium equations are written as follows: Taking moments about the center of the steel,

$$P'_u(50 + 10.5) = a \times 10 \times 0.85 \times 3000 \left(23 - \frac{a}{2}\right)$$

and equating internal and external axial forces,

$$P'_u = a \times 10 \times 0.85 \times 3000 - 2.35 \times 40{,}000$$

These two simultaneous equations are solved either explicitly or by successive approximation (assuming a value of a and correcting). They give $a = 5.55$ in., $P'_u = 48{,}000$ lb, and, consequently, $M'_u = 50 \times 48{,}000 = 2{,}400{,}000$ in.-lb. According to the ACI Code, the ultimate values to be used in design are $P_u = 0.70 \times 48{,}000 = 33{,}600$ lb and $M_u = 0.70 \times 2{,}400{,}000 = 1{,}680{,}000$ in.-lb.

The same member, if subject to bending without axial force, would have an ultimate moment of $M'_u = 1{,}985{,}000$ in.-lb (see the example of Art. 2.8*f*). Comparison with $M'_u = 2{,}400{,}000$ in.-lb as calculated above illustrates the fact, discussed previously, that, for flexural members failing in tension, the presence of an axial compression force increases the moment capacity. On this flexural member without axial load, the ultimate moment to be used in design would be

$$M_u = 0.90 \times 1{,}985{,}000 = 1{,}785{,}000 \text{ in.-lb}$$

according to the Code. It is seen that the difference in ϕ values for members in bending and for members in bending plus axial load here leads to

a lack of consistency; namely, the ultimate moment M_u to be used for design of the latter (that is, 1,680,000 in.-lb) is seen to be smaller than that for the former (that is, 1,785,000 in.-lb), in spite of the fact that the situation for the actual ultimate moments M'_u is exactly the reverse. *To avoid this inconsistency, the ACI Code permits, for members subject to bending plus small axial loads, the larger of the two moments M_u to be used, either the one calculated for simultaneous bending plus axial load, or the one calculated for flexure only* [see Art. 1901(*c*) of the Code]. For the case at hand, then, the design values are $P_u = 33{,}600$ lb and $M_u = 1{,}785{,}000$ in.-lb.

e. Contribution of intermediate bars When large bending moments are present, it is most economical to concentrate all or most of the steel along the two outer faces parallel to the axis of bending. Such arrangements are shown in Fig. 5.2*d* and *e*. On the other hand, when axial compression is prevalent and, particularly when a small cross section is desired, it is advantageous to place the steel more uniformly around the perimeter, as in Fig. 5.2*a* to *c*. In this case special attention must be paid to the intermediate bars, i.e., those which are not placed along the two most highly stressed faces. This is so because, when the ultimate-load condition is reached, the stresses in these intermediate bars are frequently below the yield point, even though the bars along either one or both extreme faces may be yielding. To analyze this situation, the distribution of strains over the cross section must be considered, as is illustrated below.

Example The column of Fig. 5.11*a* is loaded eccentrically, with $e = 17.0$ in.; $f'_c = 3.0$ ksi, and $f_y = 60.0$ ksi. Determine the magnitude of the ultimate load.

Trial calculation suggests that the neutral axis is located 13 to 15 in. from the compression edge. A value of $c = 14$ in. is tentatively selected. At the instant the concrete reaches its assumed failure strain of 0.003, the strain distribution is as shown in Fig. 5.11*b*. The strains at the locations of the individual bars are easily found from similar triangles and are shown on the figure.

The yield strain corresponding to the yield point of 60 ksi is $\epsilon_y = 60/29{,}000 = 0.00207$. By comparison of this value with the strains of the individual bar groups, it is seen that the exterior bar groups 1 and 4 have strains exceeding ϵ_y; that is, these bars will yield at failure. On the other hand, interior bar groups 2 and 3 show strains considerably less than ϵ_y. The stresses in these bars at ultimate load can be computed by multiplying their strains by E_s. Thus $f_{s2} = 0.0097 \times 29{,}000 = 28.2$ ksi, and $f_{s3} = 0.00054 \times 29{,}000 = 15.7$ ksi. From the assumed value of c, one finds $a = 0.85 \times 14.0 = 11.9$ in. From Fig. 5.11*c* it will be noted that bar groups 1 and 4, being stressed to the yield point, contribute equal and opposite forces which cancel. Hence

$$P'_u = 0.85f'_cab + f_{s2}A_{s2} + f_{s3}A_{s3}$$
$$= 0.85 \times 3 \times 11.9 \times 12 + 28.2 \times 2.0 - 15.7 \times 2.0 = 389 \text{ kips}$$

The moment of all internal forces about the center line is

$$M'_u = 7.05(0.85f'_cab) + 10.5f_yA_{s1} + 3.5f_{s2}A_{s2} + 3.5f_{s3}A_{s3} + 10.5f_yA_{s4}$$

Scanned with CamScanner

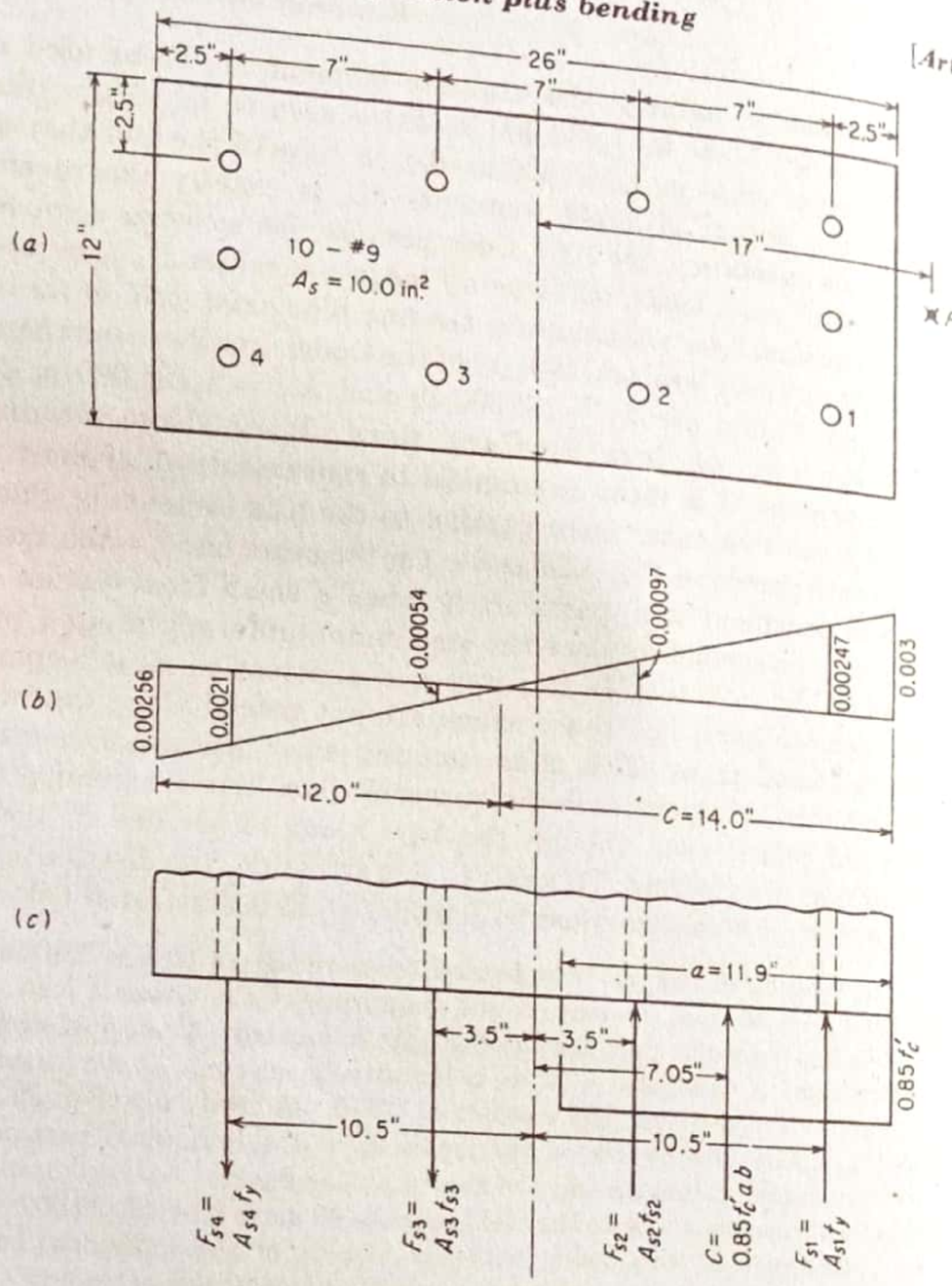


Fig. **5.11**

which, upon substitution of the appropriate numbers, gives

$$M'_u = 6{,}650 \text{ in.-kips}$$

Consequently,

$$e = 6{,}650/389 = 17.1 \text{ in.}$$

This value of the eccentricity differs from the given value $e = 17.0$ in. by less than 1 per cent, indicating that the assumed value of $c = 14$ in. is satisfactory, and no further approximation is needed.

f. Rectangular columns in biaxial bending The methods discussed permit rectangular columns to be designed or analyzed if bending is present about only one of the two principal axes of the section. This situation obtains in the majority of structures. There are other situations, however, and they are by no means exceptional, in which axial compression is accompanied by simultaneous bending about both principal axes of the section. Such is the case, for instance, in corner columns of tier buildings, where beams and girders frame into the column in the directions of both walls and transfer their end moments into the column in two perpendicular planes. Similar situations can occur with respect to interior columns, particularly in irregular column layouts, and in a variety of other structures.

Figure 5.12 shows a rectangular section under the simultaneous action of a concentric load P and biaxial bending by the moments M_x and M_y. The resulting action is the same as when the load P is applied with eccentricities

$$e_x = \frac{M_x}{P} \quad \text{and} \quad e_y = \frac{M_y}{P}$$

about the centroidal x and y axes, respectively, as shown. It is possible to calculate the ultimate load of such a biaxially eccentric column on the basis of the general propositions of ultimate-strength design that have been utilized in all other situations (rectangular equivalent stress block of depth $k_1 c$, ultimate concrete strain $e_u = 0.003$, etc.). The pertinent methods, which are developed in Ref. 5.1, are important as research tools but are cumbersome and not suited to design use.

An approximate design method has been developed by Boris Bresler (Ref. 5.2) and has been satisfactorily verified by comparison with a limited number of test results and with results of extensive computations similar to those in Ref. 5.1.

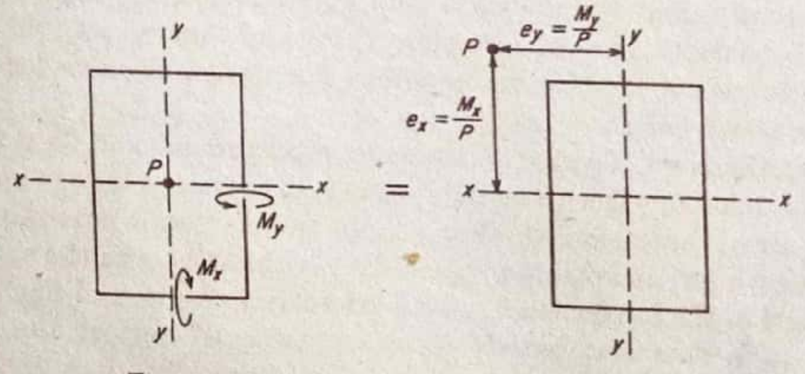


Fig. **5.12** Biaxial bending plus compression.

Scanned with CamScanner

Bresler's equation can be written in the form of an interaction formula, namely,

$$\frac{P'_u}{P'_x} + \frac{P'_u}{P'_y} - \frac{P'_u}{P'_0} = 1 \tag{5.10}$$

where P'_u = ultimate load for biaxial bending with eccentricities e_x and e_y
P'_x = ultimate load when only eccentricity e_x is present ($e_y = 0$)
P'_y = ultimate load when only eccentricity e_y is present ($e_x = 0$)
P'_0 = ultimate load for concentrically loaded column, Eq. (5.6) ($e_x = e_y = 0$)

The nature of this equation is easily illustrated. If, for instance, it were applied in the limit to a column bent only about the x axis, then e_y would equal zero; therefore P'_y would equal P'_0 by the definition of P'_y. If $P'_y = P'_0$ is substituted in Eq. (5.10), one finds $P'_u = P'_x$, as one should. That is, when bending is present in one direction only, the equation gives the correct answer to the effect that the ultimate load is that for uniaxial bending in the particular direction. For another example, assume that $P'_u/P'_0 = 0.20$. This means that the eccentricities are relatively large, so that the ultimate load is a small fraction of that for the concentric column. Assume further that $P'_u/P'_y = 0.40$. Substitution in Eq. (5.10) gives $P'_u/P'_x = 0.80$. That is, the simultaneous bending about the y axis has reduced the ultimate load of this column by 20 per cent as compared to what it would have been had bending been present about the x axis only.

For use in design, the equation can be written in the alternative form

$$\frac{1}{P'_u} = \frac{1}{P'_x} + \frac{1}{P'_y} - \frac{1}{P'_0} \tag{5.10a}$$

which is used as follows:

Given the size and reinforcement of the column and the load eccentricities e_x and e_y, one computes, by the methods of the preceding sections, the ultimate loads P'_x and P'_y for uniaxial bending about the x and y axes, respectively, and the ultimate load P'_0 for concentric loading. Then Eq. (5.10a) permits one to compute $1/P'_u$ and, therefrom, the calculated ultimate load P'_u for biaxial bending. The design ultimate load, as usual, is obtained from $P_u = \phi P'_u$.

Equations (5.10) and (5.10a) are valid provided $P'_u \geq 0.10P'_0$. They are not reliable where biaxial bending is prevalent and is accompanied by an axial force smaller than $P'_0/10$. In the case of strongly prevalent bending, failure is initiated by yielding of the steel, and the situation corresponds to the lowest tenth of the interaction diagram of Fig. 5.8. In this range it is safe and satisfactorily accurate to neglect the axial force entirely and to calculate the section for biaxial bending only (see Art. 5.4d). This is so because, as was discussed before and as is evident from

the shape of the interaction diagram, in the region of tension failure the addition of axial load increases the moment capacity, i.e., contributes to safety. If this contribution is neglected to simplify calculations, the result is on the conservative side.

Example Given the column of Example 2, Art. 5.4. In addition to the eccentricity about the x axis, $e_x = 0.75t_x = 0.75 \times 20 = 15$ in., there is an eccentricity about the y axis, $e_y = 3$ in. Calculate the design load for this column.

From Example 2, $f'_c = 5000$ psi, $f_y = 75{,}000$ psi, $p_t m = 0.295$, and $P'_x = 268$ kips. With $e_y/t_y = 3/12 = 0.295$, interpolation between Graphs 3 and 4 gives $K = 0.635$. Therefore $P'_y = 0.635 \times 12 \times 20 \times 5 = 562$ kips, $P'_0 = 0.85f'_c bt + A_s f_y = 0.85 \times 5 \times 12 \times 20 + 4 \times 75 = 1320$ kips, and, from Eq. (5.10a),

$$P'_u\left(\frac{1}{P'_x} + \frac{1}{P'_y} - \frac{1}{P'_c}\right) = 1$$

Substituting

$$P'_u(1/268 + 1/562 - 1/1320) = 1$$

gives

$$P'_u = 234 \text{ kips}$$

and the ultimate strength to be used in design, in connection with biaxial eccentricities of the stipulated amounts, is

$$P_u = \phi P'_u = 0.70 \times 234 = 164 \text{ kips}$$

This compares with $P_u = 188$ kips found in Example 2 for $e_y = 0$.

5.5 Circular Columns, Spiral Reinforced It was mentioned in Art. 5.2 that spiral-reinforced columns, when load eccentricities are small, show greater toughness, i.e., greater ductility, than tied columns, but that this difference fades out as the eccentricity is increased. For this reason, as was discussed in Art. 5.3, the Code provides a more favorable reduction factor $\phi = 0.75$ for spiral columns, as compared to $\phi = 0.70$ for tied columns. Also, the minimum stipulated design eccentricity for entirely or nearly axially loaded members is $e_{min} = 0.05t$ for spiral-reinforced members, as compared to twice this value for tied members. It follows that spirally reinforced columns permit a somewhat more economical utilization of the materials, particularly for calculated eccentricities smaller than $0.05t$. Further advantages lie in the facts that spirals are available prefabricated, which may save labor in assembling column cages, and that the circular shape is frequently desired by the architect.

Figure 5.13 shows the cross section of a spiral-reinforced column. From six to ten and more longitudinal bars of equal size are provided for longitudinal reinforcement, depending on column diameter. The strain

Scanned with CamScanner

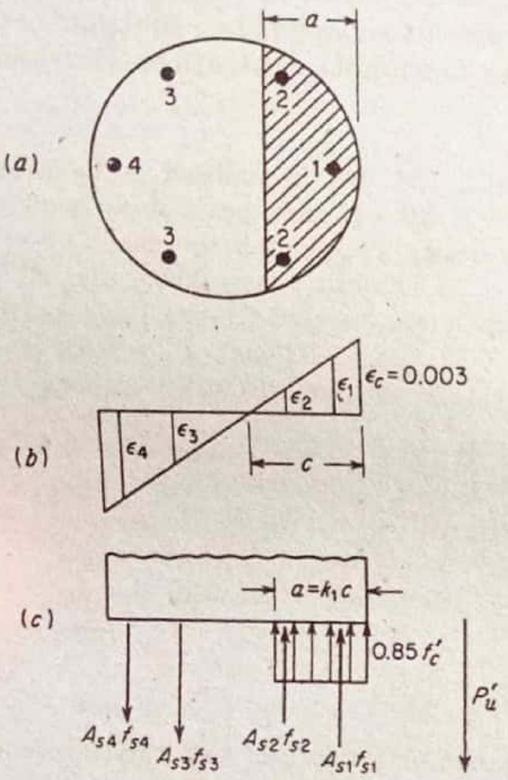


Fig. 5.13 Circular column, compression plus bending.

distribution at the instant at which the ultimate load is reached is shown in Fig. 5.13*b*. Bar groups 2 and 3 are seen to be strained to much smaller values than groups 1 and 4. The stresses in the four bar groups are easily found. For any of the bars with strains in excess of the yield strain $\epsilon_y = f_y/E_s$, the stress at failure is evidently the yield stress of the bar. For those bars with smaller strains, the stress is found from $f_s = \epsilon_s E_s$.

One then has the internal forces shown in Fig. 5.13*c*. They must be in force and moment equilibrium with the external load P'_u. It will be noted that the situation is exactly the same as that discussed, for rectangular columns, in Art. 5.4*f*. Calculations can be carried out exactly as in the example of that article, except that for circular columns the concrete compression zone subject to the equivalent rectangular stress distribution has the shape of a segment of a circle, shown shaded in Fig. 5.13*a*. Though this makes direct calculation awkward, no new principles are involved.

In practice, accurate calculations of this sort need rarely be carried out. The ACI Code gives the following approximate formulas: When tension controls,

$$P_u = \phi \left\{ 0.85 f'_c D^2 \left[\sqrt{\left(\frac{0.85e}{D} - 0.38 \right)^2 + \frac{p_t m D_s}{2.5D}} - \left(\frac{0.85e}{D} - 0.38 \right) \right] \right\} \tag{5.11}$$

When compression controls,

$$P_u = \phi \left[\frac{A_s f_y}{3e/D_s + 1} + \frac{A_g f'_c}{9.6De/(0.8D + 0.67D_s)^2 + 1.18} \right] \tag{5.12}$$

For determining the eccentricity for the balanced case, J. G. MacGregor gives the approximate expression

$$e_b = (0.24 + 0.39 p_t m) D \tag{5.13}$$

Art. 5.6]

where D = overall diameter of circular section
D_s = diameter of circle through centers of longitudinal bars
A_g = gross area of section
e = eccentricity from plastic centroid
$p_t = A_s/A_g$

Proportioning or analysis is usually carried out by means of design aids, such as Graphs 6 to 9 in Appendix B, which have been computed from these formulas. Other more detailed tables and graphs are available, as mentioned in Art. 5.4*c*. These are generally more accurate than the above equations, since they have been calculated on digital computers from an accurate analysis of the situation indicated in Fig. 5.13.

It should be noted that these methods of design and analysis apply only if the steel ratio of the spiral is at least equal to that given by Eq. (5.2) of Art. 5.2, for reasons discussed in that article.

PROBLEMS

1. A column 18 in. square is reinforced with four No. 11 bars; $f'_c = 3$ ksi, and $f_y = 40$ ksi. If the column is axially loaded (design eccentricity $e = 0$), find P_u.

2. The column of Prob. 1 carries a load with an eccentricity $e = 3.5$ in. Find P_u and M_u.

3. If the eccentricity of the column of Prob. 1 is $e = 11.0$ in., find P_u and M_u.

4. A column carries, axially, a dead load of 90 kips and a live load of 70 kips. Using $f'_c = 4$ ksi and $f_y = 60$ ksi, design: (*a*) a square, tied column; (*b*) a circular, spiral column.

5. Redesign the columns of Prob. 4 if the live load is applied with an eccentricity $e = 6$ in.

6. Redesign the columns of Prob. 4 if the live load is applied with an eccentricity of 20 in.

7. For the situation of Prob. 6, design a rectangular, tied column with ratio of long to short side of the order of 2. Compare economy, i.e., compare quantity of concrete and steel, with Prob. 6.

WORKING-STRESS DESIGN OF COLUMNS

5.6 General Historically, the first departure from purely elastic methods in reinforced-concrete design occurred in the analysis of concentrically loaded columns. During the 1930's, elaborate experimental investigations at the University of Illinois under F. E. Richart and at Lehigh University under Inge Lyse showed that there was no recognizable relation between stresses calculated on an elastic basis for working loads [see Eqs. (2.2) and (2.2*a*)] and the actual carrying capacities of axially loaded columns. It was in these investigations that the basic so-called

Scanned with CamScanner

addition law [Eq. (2.5)] was established, to wit

$$P'_u = 0.85f'_cA_c + f_yA_{st} \tag{5.14}$$

where A_{st} is the total area of longitudinal steel. Shortly thereafter the design of axially loaded columns, in the ACI and other codes, was changed to conform to this relationship rather than to presumed elastic behavior.

At the same time, flexural analysis continued to be based on elastic relations. Yet, simple bending on the one hand and simple concentric load on the other are only the two extremes of the general case of simultaneous compression plus bending. If one end point of this continuous range, axial compression, is treated on an ultimate-strength basis [Eq. (5.14)], and the other end point, simple bending, on a purely elastic basis [Eqs. (3.25) to (3.27), for example], it is clear that an inconsistent method must result for the general case of compression plus bending. In consequence, successive editions of the Code have presented ever-changing methods for this case, in repeated attempts to bridge the gap between the two methods by arbitrary adjustments of allowable stresses and other variables. The resulting provisions (by comparison of computed allowable loads with actual carrying capacity) gave safety factors which were mostly excessive, of the order of 3 to 4 and more, but which, for some combinations of eccentricities and steel ratios, were barely larger than 1.

The present (1963) ACI Code, in its ultimate-strength portion, contains a consistent treatment of the entire spectrum from simple bending to simple compression, with uniform and, on the whole, consistent safety provisions. This was discussed in Arts. 5.3 to 5.5. The Code continues to offer an alternative working-stress method of design, the choice between the two being left to the designer. In the 1963 edition the case of combined compression plus bending is once more treated by a method entirely different from those of previous versions. In this method, there is no pretense of calculating actual stresses under working loads by elastic means. The one aim is to obtain a reasonably uniform factor of safety when comparing the allowable working load with the actual carrying capacity as computed on an ultimate-strength basis. Therefore, although the method makes use of such devices of elastic computation as the transformed section (see Fig. 2.29), its chief aim is to make its results consistent with those of ultimate-strength design. A safety factor of 2.5 is aimed at, with actual values confined to the range of about 2.2 to 3.0. This is a considerable improvement over the excessive inconsistencies in previous editions. However, the method is admittedly merely a computational device, entirely usable but devoid of real physical meaning.

It can be assumed that in the foreseeable future ultimate-strength design methods will become prevalent, and methods such as those to be discussed below will eventually pass out of the picture.

Art. 5.7]

5.7 Axially Loaded Columns For concentrically loaded, *spirally reinforced* columns the Code provides the following formula for the allowable load:

$$P = A_g(0.25f'_c + f_sp_g) \tag{5.15}$$

where A_g = gross area of column
$p_g = A_{st}/A_g$
f_s = allowable steel compression stress, equal to $0.40f_y$, but not to exceed 30,000 psi

If this equation is rewritten in the form

$$P = 0.25f'_cA_g + f_sA_{st} \tag{5.15a}$$

and compared with the basic ultimate-strength equation for axially loaded members [Eq. (5.14)], one notices the following: For the reinforcement, a safety factor $f_y/f_s = 2.5$ is employed. For the concrete, the safety factor is $0.85f'_cA_c/0.25f'_cA_g$. With steel ratios in columns limited to the range of 1.0 to 8.0 per cent, $A_c/A_g = 0.99$ to 0.92, so that the safety factor for the contribution of the concrete to the carrying capacity ranges from 3.1 to 3.4. It has been traditional, in working-stress design of columns based on the addition law, to apply such higher safety factors to the concrete contribution, on the assumption that concrete quality is less closely controlled than that of steel. Equation (5.15) holds provided the steel ratio of the spiral is at least that given by Eq. (5.2).

The Code recognizes the greater brittleness of *tied* columns, particularly when axially loaded, and stipulates that their allowable loads shall be 85 per cent of that given by Eq. (5.15); i.e.,

$$P = 0.85A_g(0.25f'_c + f_sp_g) \tag{5.16}$$

Example Design a circular, spiral-reinforced column for a concentric allowable working load of 480 kips, with $f'_c = 4.0$ ksi and $f_y = 60$ ksi for both longitudinal steel and spiral.

It is first necessary to select an approximate steel ratio. In general, lightly reinforced axially loaded columns are more economical than more heavily reinforced ones, except when small column sizes are desired in order to obtain maximum usable floor space. In the present case a moderate steel ratio of about $p_g = 0.02$ will be employed. The allowable steel stress is $f_s = 0.40 \times 60 = 24$ ksi. Thus

$$P = A_g(0.25 \times 4.0 + 24 \times 0.02)$$

or $480 = A_g \times 1.48$. Hence $A_g = 480/1.48 = 324$ in.^{2}

From Table 9, Appendix B, the area of a circular section with diameter $D = 20$ in. is $A_g = 314$ in.^{2} If this size is selected, a steel ratio larger than 0.02 must be provided, to make up for the difference between the furnished and calculated concrete areas.

Scanned with CamScanner

The contribution of the concrete is then $P_c = 314 \times 0.25 \times 4.0 = 314$ kips, and the resistance to be supplied by the steel is $P_s = 480 - 314 = 166$ kips. With an allowable steel stress of 24 ksi, this requires a steel area $A_s = P_s/f_s = 166/24 = 6.9$ in.^{2} Seven No. 9 bars are selected from Table 2, with an area $A_s = 7.0$ in.^{2} The minimum steel ratio of the spiral is computed from Eq. (5.2). With a concrete cover over the spiral of 1.5 in., the core diameter is $D_c = 20 - 3 = 17$ in. Therefore, $A_g = 314$ in.^{2}, and from Table 9 for $D_c = 17$ in., $A_c = 227$ in.^{2} Then $p_s = 0.45(A_g/A_c - 1)f'_c/f_y = 0.45(314/227 - 1)3/60 = 0.0115$. If the pitch of the spiral is g, and the area of the wire a_s, the steel volume in one turn is $a_s\pi D_c$, and the volume of a slice of thickness g of the concrete core is $g\pi D_c^2/4$. (This neglects the small difference between the outside and center-line diameters of the spiral.) The steel ratio is the ratio of these two volumes:

$$p_s = \frac{4a_s}{gD_c}$$

As the ACI Code specifies that the pitch shall not exceed one-sixth of the core diameter, $g = 2.75$ in. is selected. Spirals are usually made of ¼-, ⅜-, ½-, or ⅝-in. wire. A ½ × 2¾ in. spiral, then, gives a steel ratio $p_s = 4 \times 0.20/2.75 \times 17 = 0.0017$. This is in excess of the required amount, but the next smaller size, ⅜ in., would fall short of the requirement.

5.8 Compression plus Bending

It was mentioned in Art. 5.6 that the chief aims of the working-stress design methods for columns in the 1963 ACI Code are to define allowable design loads and moments which furnish a safety factor of about 2.5 when compared with ultimate loads and moments and to formulate the design procedures in terms of conventional elastic analysis. For this purpose, use is made of so-called *interaction equations*.

In an elastic member under compression and bending, but not subject to tension cracking, the maximum fiber stress is found from

$$\frac{P}{A} + \frac{M}{S} = f_{max}$$

from which

$$\frac{P}{f_{max}A} + \frac{M}{f_{max}S} = 1$$

Now, that axial load P_a which, when acting alone without simultaneous bending, results in a given f_{max} is evidently $P_a = f_{max}A$. Likewise, that flexural moment M_f which, when acting alone without simultaneous compression, results in f_{max} is evidently $M_f = f_{max}S$. Hence, the last equation can be rewritten as

$$\frac{P}{P_a} + \frac{M}{M_f} = 1 \qquad (5.17)$$

A plot of this simple interaction equation is shown in Fig. 5.14. While the equation has been derived for elastic stresses, as long as compression governs it is also a good approximation for ultimate strength, as can be seen from the portion *bd* of Fig. 5.8. It relates the resistance to the combined action of P and M to the capacities in compression alone P_a and in flexure alone M_f. It holds only as long as the compression strength of the concrete governs. If cracking of the concrete and yielding of the steel determine failure, entirely different relationships obtain; this corresponds to the fact that in Fig. 5.8 for eccentricities larger than e_b, that is, when tension governs, a curve obtains which is entirely different from *dab* and from its straight-line approximation *db*.

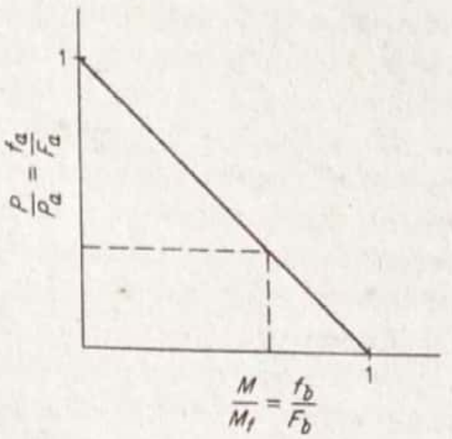


Fig. 5.14 Interaction diagram for elastic stresses, compression plus bending.

a. Concrete compression governs Equation 5.17 is utilized in the Code, for members in which compression governs, by taking $P_a = P'_u/2.5$ (2.5 being the safety factor) and $M_f = 0.45f'_cS_{ut}$. In the latter expression $0.45f'_c$ is the allowable stress in simple bending (see Art. 3.7), and S_{ut} is the section modulus of the uncracked, transformed section (see Fig. 2.3). It is specified that in computing S_{ut} the compression and tension steel areas shall be multiplied by $2n$ rather than by n, as a partial recognition of inelastic action.

If numerator and denominator of the first term in Eq. (5.17) are divided by the gross concrete area A_g, and those of the second term by S_{ut} as just defined, the equation can be written as

$$\frac{f_a}{F_a} + \frac{f_b}{F_b} \leqq 1 \qquad (5.18)$$

where f_a = axial load divided by gross concrete area A_g
f_b = bending moment divided by section modulus of uncracked, transformed section, $2n$ being used for all longitudinal steel
$F_a = 0.34(1 + p_gm)f'_c$ (explained below)
F_b = allowable bending stress for bending alone, that is, $0.45f'_c$

and where $\leqq$ indicates that the section is adequate as long as the left side does not exceed 1.

As was explained, $F_a = P_a/A_g = P'_u/2.5A_g$. Now, Eq. (5.14) can be rewritten as $P'_u = 0.85f'_cA_g[1 + (f_y/0.85f'_c)(A_{st}/A_g)]$. If both sides are divided by A_g, and if the abbreviations $m = f_y/0.85f'_c$ and $p_g = A_{st}/A_g$ are used, one obtains $F_a = 0.34(1 + p_gm)f'_c$ as stated. Here A_{st} is the

Scanned with CamScanner

total area of all longitudinal steel; that is, $A_{st} = A_s + A'_s$. (As a minor simplifying approximation, the gross concrete area A_g instead of the net concrete area A_c is used in these Code provisions.)

Equation 5.18 is applicable in only a limited range of eccentricities $e = M/P$. On the one hand, an upper limit is set on P by Eqs. (5.15) and (5.16), which define the maximum permissible working loads on concentrically compressed columns. If, for small eccentricities, Eq. (5.18) results in a permissible load $P = f_a A_g$ larger than that given by Eq. (5.15) or (5.16), one of the latter governs.

On the other hand, Eq. (5.18) was devised for the situation in which compression of the concrete governs and in which tension cracking, if any, is of minor influence. The Code provides the following upper limits of eccentricity beyond which Eq. (5.18) no longer applies because tension would govern:

For symmetrical tied columns: $$e_b = (0.67 p_g m + 0.17)d \tag{5.19a}$$

For unsymmetrical tied columns: $$e_b = \frac{p'm(d - d') + 0.1d}{(p' - p)m + 0.6} \tag{5.19b}$$

For spiral columns: $$e_b = 0.43 p_g m D_s + 0.14t \tag{5.19c}$$

(It should be noted that these eccentricity values e_b for working-stress design do not have the same significance as and are different in value from the balanced eccentricities e_b in ultimate-strength design, as discussed in Arts. 5.4 and 5.5.)

b. Steel tension governs For a given cross section, knowing e_b from Eqs. (5.19), one can use Eq. (5.18) to calculate the axial force P_b and the corresponding moment $M_b = e_b P_b$ which define the lower end point of the range of validity of Eq. (5.18). For eccentricities larger than e_b, tension begins to govern. At the other extreme, when the axial load P is zero, the section is in simple bending. Consistent with the previous assumptions, the allowable moment for this extreme is defined as 40 per cent of the ultimate moment M'_u in simple bending; i.e., a safety factor of 2.5 is again utilized. These moments M_0 are

For symmetrical tied columns: $$M_0 = 0.40 A_s f_y (d - d') \tag{5.20a}$$
For unsymmetrical tied columns: $$M_0 = 0.40 A_s f_y jd \tag{5.20b}$$
For spiral columns: $$M_0 = 0.12 A_{st} f_y D_s \tag{5.20c}$$

where A_s is the steel on the tension side, and A_{st} the total longitudinal steel. The first of these expressions is simply 40 per cent of M'_u for a compression-reinforced beam with equal tension and compression reinforcement, $A_s = A'_s$ (see Art. 3.9). The other two equations are close approximations to the ultimate moments for the respective cases, also divided by 2.5.

The Code provides that the allowable bending moment M on columns controlled by tension shall be considered to vary linearly with axial load, from M_0 when the section is in simple flexure to M_b when the axial load is equal to N_b. This can be expressed in the nondimensional equation

$$\frac{P}{P_b} = \frac{M - M_0}{M_b - M_0} \tag{5.21}$$

which is easily verified from the geometry of Fig. 5.15 and can be solved for either P or M, as needed.

c. Summary and examples The working-stress design procedure for members in compression plus bending is summarized in Fig. 5.15. The following are shown:

1. For zero or small eccentricities (interval *ea*), the allowable load is that for concentric compression [Eqs. (5.15) and (5.16)].

2. For moderate eccentricities, when compression governs in the interval *ab*, the interaction equation (5.18) applies. It is represented by the straight line connecting P_a (when $M = 0$) and M_f (when $P = 0$). In that range one determines P and M from Eq. (5.18) and compares P with P_{max} as calculated from Eq. (5.15) or (5.16). The smaller of the two is the allowable load.

3. Point b determines the boundary between members governed by compression and those governed by tension. It is found by calculating e_b from Eqs. (5.19), and then P_b from Eq. (5.18).

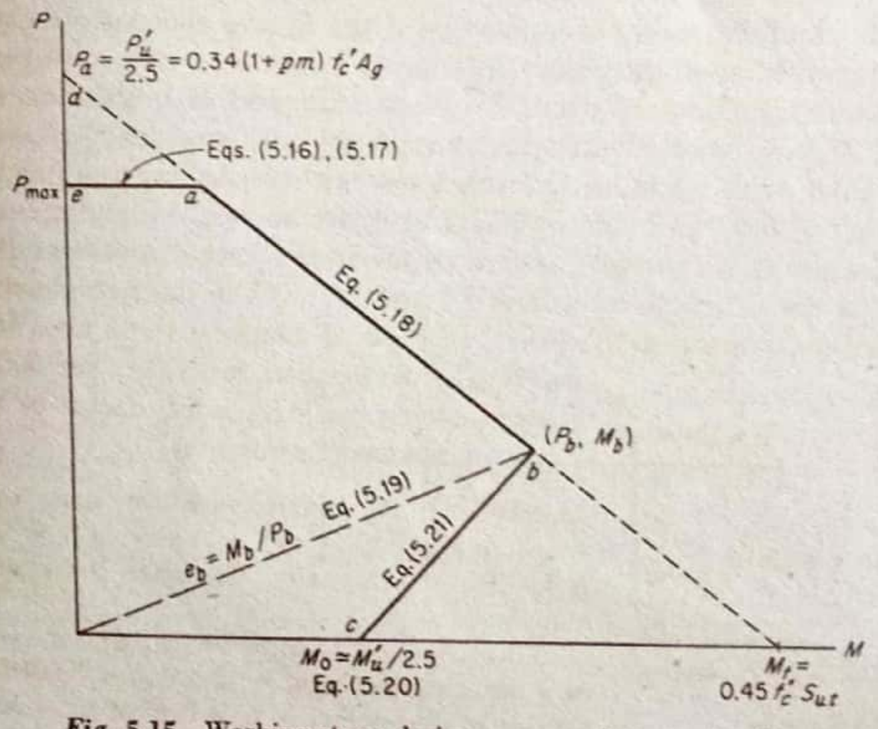


Fig. 5.15 Working-stress design, compression plus bending.

Scanned with CamScanner

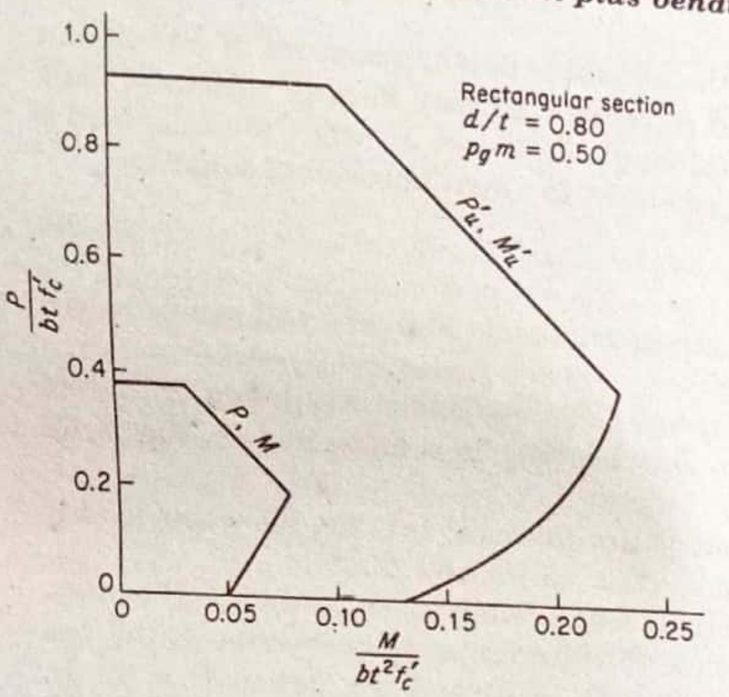


Fig. 5.16 Ultimate strength P_u' and M_u' and allowable values P and M by working-stress design.

4. For large eccentricities, when tension governs, a linear variation is assumed between the moment M_b at the balance point b and M_0 for simple flexure, shown by the straight line bc. Equation (5.21) is used in this range for determining P if M is given, or vice versa.

The general shape of the figure $eabc$, it will be noted, is quite similar to that of the dashed curve in Fig. 5.9. The latter gives the ultimate design values P_u and M_u, and the similarity of the figures comes from the fact that the working-stress design method is devised to give a reasonably constant safety factor of about 2.5 when compared with ultimate values P_u' and M_u'. By way of example, this situation is specifically illustrated in Fig. 5.16, which applies to rectangular sections having the particular values $d/t = 0.80$ and $p_g m = 0.5$. The figure shows, in nondimensional form, the allowable values P and M as specified for working-stress design, as well as the ultimate capacities P_u' and M_u'. While the two figures are not strictly geometrically similar, in view of simplifications used in the working-stress method, it is easily verified that a satisfactorily uniform safety factor of about 2.5 is maintained throughout.

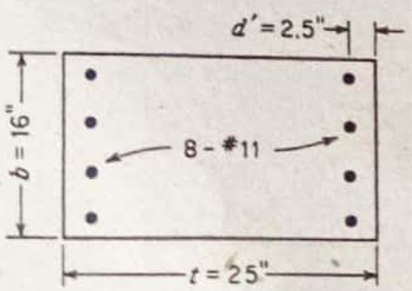


Fig. 5.17

Example 1 A column with the cross section shown in Fig. 5.17, with $f_c' = 4$ ksi and $f_y = 50$ ksi, is loaded concentrically. Calculate the allowable axial load.

With $A_g = 16 \times 25 = 400$ in.^{2} and $A_{st} = 12.5$ in.^{2}, the steel ratio is $p_g = 12.5/400 = 0.0313$. The allowable steel stress is $f_s = 0.40 \times 50 = 20$ ksi.

Then, from Eq. (5.16),

$$P = 0.85 \times 400(0.25 \times 4 + 20 \times 0.313) = 553 \text{ kips}$$

Example 2 If the same column carries a compression load $P = 360$ kips, what is the allowable simultaneous moment?

For this column $m = 50/(0.85 \times 4) = 14.7$, $p_g m = 0.0313 \times 14.7 = 0.460$, and $n = 8$. Assume that compression governs. The section modulus of the transformed, uncracked section is $S_{ut} = I_{ut}/c = (1/c)[bt^3/12 + 2(2n-1)A_s(t/2 - d')^2] = (1/12.5)[16 \times 25^3/12 + 2 \times 15 \times 12.5/2 \times (12.5 - 2.5)^2] = 3160$ in.^{3} (here $A_s = A_{st}/2$). The allowable average compression stress is $F_a = 0.34(1 + p_g m)f_c' = 0.34(1 + 0.460)4 = 1.98$ ksi, and the allowable bending stress is $F_b = 0.45 f_c' = 0.45 \times 4 = 1.80$ ksi. The actual compression stress is $f_a = P/A_g = {}^{360}\!/_{400} = 0.90$ ksi, and the actual bending stress is $f_b = M/S_{ut} = M/3160$. Substituting these values in Eq. (5.18),

$$\frac{f_a}{F_a} + \frac{f_b}{F_b} = \frac{0.90}{1.98} + \frac{M}{3160 \times 1.80} = 1$$

Solving for the allowable moment, one has $M = 3110$ in.-kips.

To check whether compression governs as assumed, one has, from Eq. (5.19a), $e_b = (0.67 \times 0.460 + 0.17)22.5 = 10.75$ in. The actual eccentricity $e = M/P = {}^{3110}\!/_{360} = 8.63$ in. is smaller than e_b, so that compression does, in fact, govern.

Example 3 For the same column, what is the allowable moment if the simultaneous axial load is 100 kips?

Assuming that tension will govern, one first determines P_b and M_b for use in Eq. (5.21). This can be done using Eq. (5.18), which holds for eccentricities up to and including e_b. Hence, with $e_b = 10.75$ in. from Example 2, $P_b/(400 \times 1.98) + 10.75P_b/(3160 \times 1.80) = 1$ gives $P_b = 318$ kips, and $M_b = 10.75 \times 318 = 3420$ in.-kips. Because P is smaller than P_b, tension does, in fact, govern. From Eq. (5.20a), $M_0 = 0.40 \times 6.25 \times 50 \times 20 = 2500$ in.-kips. Solving Eq. (5.21) for M, one has

$$M = M_0 + \frac{P}{P_b}(M_b - M_0) = 2500 + {}^{100}\!/_{318}(3420 - 2500) = 2789 \text{ in.-kips}$$

Note that the allowable moment on the column, $M = 2789$ in.-kips, acting simultaneously with $P = 100$ kips, is now smaller than in Example 2, where the allowable moment was $M = 3110$ in.-kips when the axial load was $P = 360$ kips. As is seen from Figs. 5.15 and 5.16, this is characteristic of columns when tension governs. Consequently, in column design it is necessary to check the adequacy of the selected sections for two arrangements of live load: one which results in simultaneously large axial forces and large moments and one which results in large moments accompanied by small axial loads (see Example 1, Art. 5.4).

Example 4 Design a spiral-reinforced, circular column for $P = 300$ kips, with an eccentricity $e = 6.0$ in., using concrete with $f_c' = 3$ ksi and steel with $f_y = 40$ ksi. Here $n = 9$, $m = 40/(0.85 \times 3) = 15.7$, and $f_s = 0.40 \times 40 = 16$ ksi.

In order to arrive at an estimate of the required dimensions, the cross section of a column loaded concentrically by $P = 300$ kips will first be determined.

Scanned with CamScanner

From Eq. (5.15), with the minimum reinforcement ratio of $p = 0.01$, $A_s = p$
$(0.25f'_c + f_s p_g) = 300/(0.25 \times 3 + 16 \times 0.01) = 330$ in.^{2} Hence, a column of diameter $t = 21$ in. (having $A_g = 346$ in.^{2}), reinforced with six No. 7 bars ($A_s = 3.61$ in.^{2}), would be adequate for axial load alone.

With the stipulated eccentricity, a larger section evidently will be required to accomodate the additional moment eP. A few trial calculations indicate a column with $t = 24$ in., reinforced with ten No. 11 bars with $A_{st} = 15.62$ in.^{2} From Table 9, Appendix B, $A_g = 452$ in.^{2}, so that $p = 15.62/452 = 0.0347$. The section modulus is calculated with the aid of Table 9. The moment of inertia of the uncracked concrete section is 16,280 in.^{4} The table shows for a 24-in. column with $p_g = 0.01$ the moment of inertia of the steel to be 204 in.^{4} Hence, for the given column the steel contributes an amount $100p_g(2n - 1)204 = 3.47(2 \times 9 - 1)204 = 12{,}000$ in.^{4} to the moment of inertia. The section modulus is $S_{ut} = I_{ut}/(t/2) = (16{,}280 + 12{,}000)/12 = 2360$ in.^{3} Further, $F_a = 0.34(1 + 0.0347 \times 15.7)3 = 1.58$ ksi, and $F_b = 0.45 \times 3 = 1.34$ ksi. Hence, according to Eq. (5.18),

$$\frac{300}{452 \times 1.58} + \frac{6.0 \times 300}{2360 \times 1.35} = 0.985 < 1.0$$

It follows that the selected section is adequate.

PROBLEMS

Solve the problems following Art. 5.5 by working-stress design.

d. Rectangular columns in biaxial bending For columns in biaxial bending, when *compression governs*, the Code provides the following expanded form of Eq. (5.18):

$$\frac{f_a}{F_a} + \frac{f_{bx}}{F_b} + \frac{f_{by}}{F_b} \leq 1. \tag{5.22}$$

where f_a, F_a, and F_b are as defined in Art. 5.8*a*, and f_{bx} and f_{by} are the bending moments about the x and y principal axes, divided, respectively, by the section moduli S_{utx} and S_{uty} about the same axes. If a load P is applied at an eccentricity e from the centroid of the section, and if this eccentricity subtends an angle θ with the x axis (Fig. 5.18), then

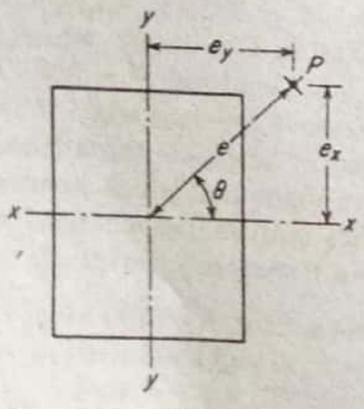


Fig. 5.18 Biaxial bending plus compression.

$$M_x = Pe_x = Pe \sin \theta \tag{5.22a}$$
$$M_y = Pe_y = Pe \cos \theta \tag{5.22b}$$

and f_{bx} and f_{by} are determined for these moments. As in uniaxial bending, the section moduli are calculated for the uncracked, transformed section, $2n$ being used for the longitudinal steel.

A column is considered to be governed by compression if neither e_x nor e_y exceeds the pertinent balanced eccentricity e_{bx} or e_{by} as calculated from Eq. (5.19*a*) or (5.19*b*).

When *tension governs*, a linear variation between the balanced condition and the condition of simple flexure is specified, analogous to that described in Art. 5.8*c* for uniaxial bending. For this linear interpolation, it is first necessary to determine, for biaxial bending, the balanced-condition P_b and M_b on the one hand, and the permissible inclined bending moment M_0 in simple flexure without axial load on the other.

Given the inclination θ of Fig. 5.18, the balanced eccentricity e_b in the direction of e of that figure is taken as either

$$e_b = \frac{e_{bx}}{\sin \theta} \tag{5.23}$$

or

$$e_b = \frac{e_{by}}{\cos \theta} \tag{5.24}$$

whichever is smaller. Here e_{bx} and e_{by} are calculated from Eq. (5.19*a*) or (5.19*b*) for the two principal directions. Then, with Eqs. (5.22) to (5.24) in mind, the balanced load P_b is determined from

$$\frac{P_b}{A_g F_a} + \frac{P_b e_b \sin \theta}{S_{utx} F_b} + \frac{P_b e_b \cos \theta}{S_{uty} F_b} = 1 \tag{5.25}$$

and the corresponding balanced moment is

$$M_b = P_b e_b \tag{5.26}$$

On the other hand, the Code stipulates that the inclined simple flexural moment M_0 in the absence of axial load be determined from

$$\frac{M_0 \sin \theta}{M_{0xx}} + \frac{M_0 \cos \theta}{M_{0yy}} = 1 \tag{5.27}$$

where M_{0xx} = value of M_0 from Eqs. (5.20) for bending about x axis alone
M_{0yy} = value of M_0 from Eqs. (5.20) for bending about y axis alone

Once P_b, M_b, and M_0 are determined, Eq. (5.21) is used as in uniaxial bending to calculate, for biaxial bending, either P or M, as needed.

The authors observe that this Code method will be found quite cumbersome and excessively conservative, resulting in safety factors of 3 and more. They suggest that Bresler's equation (5.10*a*), though not a part of the ACI Code, can be used with equal ease for working-stress and for ultimate-strength design. For the former the equation would take the

Scanned with CamScanner

form

$$\frac{1}{P} = \frac{1}{P_x} + \frac{1}{P_y} - \frac{1}{P_a} \tag{5.28}$$

where P = allowable load in biaxial bending
P_x = allowable load when only eccentricity e_x is present ($e_y = 0$)
P_y = allowable load when only eccentricity e_y is present ($e_x = 0$)
$P_a = 0.34(1 + p_g m)f'_c A_g$, as previously defined

with the proviso that P shall not exceed the value given by Eq. (5.16) as an upper limit. In this manner, P_x and P_y are first calculated for uniaxial bending, as summarized in Art. 5.8*c* and illustrated in the examples; the permissible load in biaxial bending is then obtained from the interaction expression of Eq. (5.28) in the manner illustrated for ultimate-strength design in the example of Art. 5.4*f*.

SLENDER COLUMNS

5.9 General A column is said to be *slender* if its cross-sectional dimensions are small as compared to its length. The degree of slenderness is generally expressed in terms of the *slenderness ratio* h/r, where h is the length of the member, and r the radius of gyration ($r = \sqrt{I/A}$) of its cross section. For square or circular members the value of r is the same about any cross-sectional axis; for other shapes r is smallest about the minor principal axis, and it is generally this value which must be used in determining the slenderness ratio.

It has long been known that a member of great slenderness will collapse under a smaller compression load than a stocky member of the same cross-sectional dimensions. This is so for the following reason: A stocky member, say with $h/r = 10$ (e.g., a square column of length equal to about 3 times its thickness t), when loaded in axial compression, will fail at the load given by Eq. (5.1), because at that load both concrete and steel are stressed to their maximum carrying capacity and give way, respectively, by crushing and by yielding. If a member with the same cross section has a slenderness ratio $h/t = 100$ (e.g., a square column hinged at both ends and of length equal to about 30 times its thickness), it may fail under an axial load of one-half or less of that given by Eq. (5.1). In this case collapse is caused by buckling, i.e., by lateral bending of the member with consequent overstressing of steel and concrete by the bending stresses which superpose on the axial compression stresses.

Until recently, reinforced-concrete columns were rarely so slender that their strengths were significantly affected by buckling. In design, account was taken of the slenderness effect in a very approximate manner by an

equation of the form

$$P_{slender} = RP_{stocky} \tag{5.29}$$

where $P_{slender}$ = carrying capacity under axial load with or without simultaneous bending of member of given slenderness
P_{stocky} = carrying capacity of stocky member of same cross section as slender member
$R = f(h/r) \leq 1$, a reduction factor smaller than 1 which depends on slenderness and is equal to 1 when h/r is so small that no strength reduction occurs

For instance, in past ACI Codes no capacity reduction was prescribed (that is, R was equal to 1) for members with h/t up to 10 (approximately h/r up to 35). For columns with $h/t = 20$ (approximately $h/r = 70$), R became 0.70, and, generally, columns with h/t exceeding 20 were not permitted.

With the introduction of high-strength steels and concretes, and with more accurate design methods (such as ultimate-strength design), it is now possible, for a given amount of axial load with or without simultaneous bending, to design a much smaller cross section than heretofore. This, evidently, makes for more slender members, and it is chiefly because of this that reliable and rational design procedures for slender columns have now become important. In this regard the present ACI Code, while considerably improved, is not entirely satisfactory. It retains provisions of the form of Eq. (5.29), though with more refinements than previously, which lead to more realistic designs. Actually, however, Eq. (5.29) is not the most rational way of accounting for the effects of slenderness. These effects, particularly for an inelastic material such as reinforced concrete, which is also subject to tension cracking in eccentrically compressed members, are of unusual complexity. When more adequate research information is available, a more rational method for designing slender columns will undoubtedly be developed.

5.10 Slenderness Effects ***a. Concentrically loaded columns*** The basic information on the behavior of straight, concentrically loaded, slender columns was developed by Euler more than 200 years ago (Ref. 5.3). In generalized form it states that such a member will fail by buckling at the critical load

$$P_{cr} = \frac{\pi^2 E_t I}{h'^2} \tag{5.30}$$

which, when both sides are divided by the cross-sectional area, gives the

Scanned with CamScanner

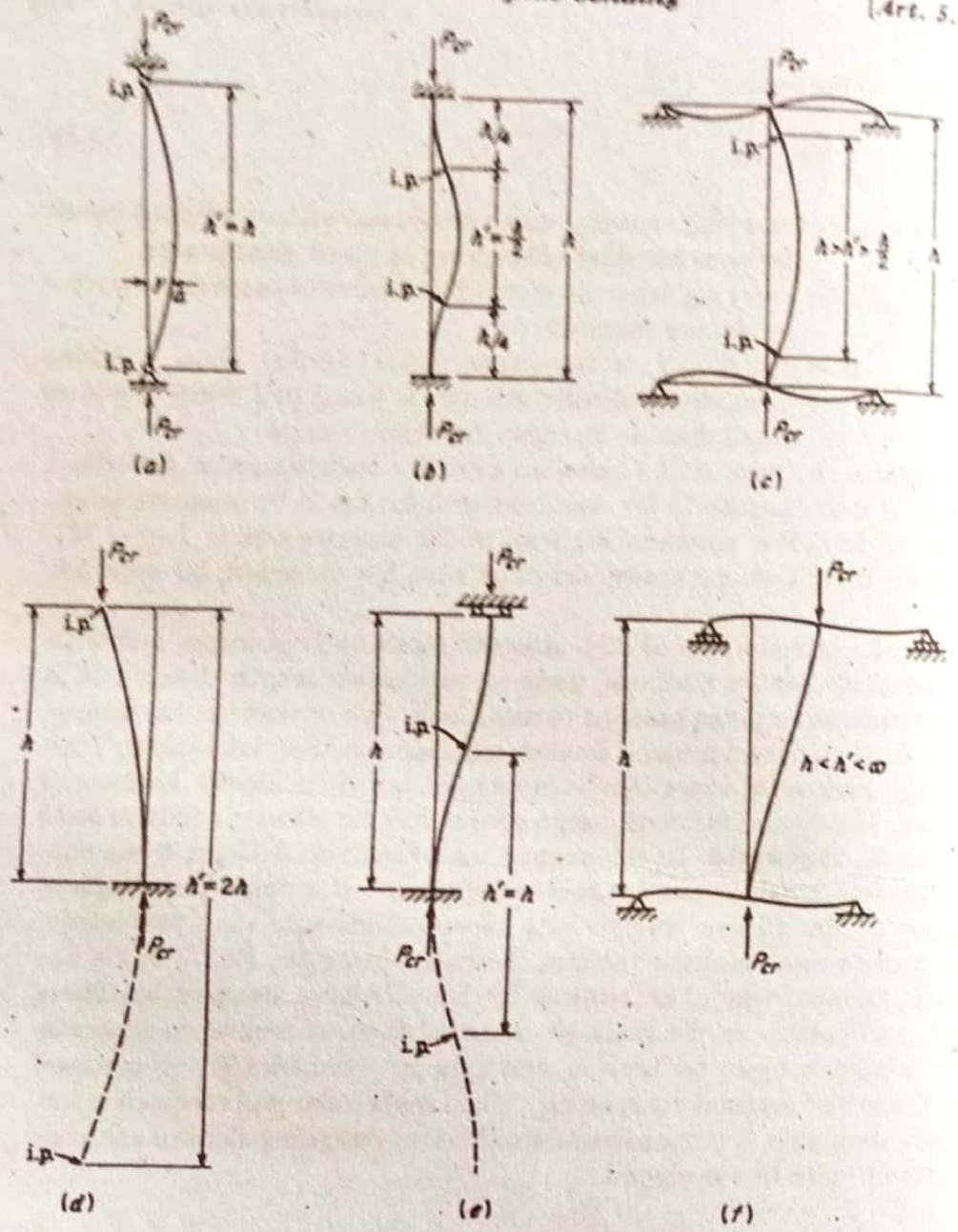


Fig. 5.19 Buckling and effective length of axially loaded columns.

compression stress at which buckling occurs as

$$\left(\frac{P}{A}\right)_{cr} = \frac{\pi^2 E_t}{(h'/r)^2} \tag{5.31}$$

For the simplest case of a column hinged at both ends and constructed of elastic material, E_t becomes simply Young's modulus, and h' is equal

to the actual length h of the column. At the load or stress given by Eq. (5.30) or (5.31) the originally straight member buckles into a half sine wave as in Fig. 5.19a. In this bent configuration, bending moments Py act at any section such as a; y is the deflection at that section. These deflections continue to increase until the bending stress caused by the increasing moment, together with the original compression stress, overstresses and fails the member.

If the stress-strain curve of a short piece of the given member is of the shape of Fig. 5.20a, as it would be for reinforced-concrete columns, E_t is equal to Young's modulus, provided the buckling stress $(P/A)_{cr}$ is below the proportional limit f_p. If it is larger than f_p, buckling occurs in the inelastic range. In this case, in Eqs. (5.30) and (5.31) E_t is the tangent modulus, i.e., the slope of the tangent to the stress-strain curve. As the stress increases, E_t decreases. A plot of the buckling stress versus the slenderness ratio, a so-called *column curve*, therefore has the shape given in Fig. 5.20b, which shows the reduction in buckling strength with increasing slenderness. For very stocky columns one finds that the value of the buckling load or stress, calculated from Eq. (5.30) or (5.31), exceeds the direct crushing strength of the stocky column, given by Eq. (5.1). This is also shown in Fig. 5.20b. Correspondingly, there is a limiting slenderness ratio $(h'/r)_{lim}$. For values smaller than this, failure occurs by simple crushing, regardless of h'/r; for values larger than $(h'/r)_{lim}$, failure occurs by buckling, the buckling load or stress decreasing for greater slenderness.

If the member of Fig. 5.19a is fixed against rotation at both ends, it buckles in the shape of Fig. 5.19b, with inflection points i.p. as shown. The portion between inflection points is in precisely the same situation as the hinge-ended column of Fig. 5.19a, and thus the *effective length* h' of

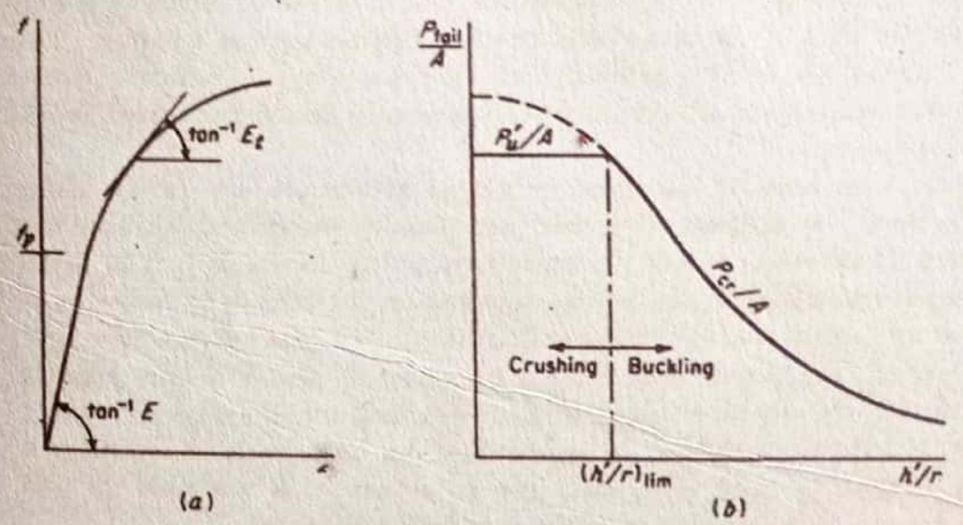


Fig. 5.20 Effect of slenderness on strength of axially loaded columns.

Scanned with CamScanner

the fixed-fixed column, i.e., the distance between inflection points, is seen to be $h' = h/2$. Equation 5.30 shows that an elastic column, when fixed at both ends, will carry 4 times as much load as when hinged.

Columns in real structures are rarely either hinged or fixed, but rather have ends partially restrained against rotation by abutting members. This is schematically shown in Fig. 5.19*c*, from which it is seen that for such members the effective length h', that is, the distance between inflection points, has a value between h and $h/2$. The precise value depends on the degree of end restraint, i.e., on the ratio r' of the rigidity EI/h of the column to the sum of rigidities EI/l of the restraining members at both ends. In the columns of Fig. 5.19*a* to *c* it was assumed that one end was prevented from moving laterally relative to the other end, by horizontal bracing or otherwise. In this case it is seen that the effective length h' is always smaller than, or at most equal to, the real length h.

If a column is fixed at one end and entirely free at the other (cantilever column or flagpole), it buckles as shown in Fig. 5.19*d*. That is, the upper end moves laterally with respect to the lower, a kind of deformation which is known as *sidesway*. It buckles into a quarter of a sine wave and, therefore, is analogous to the upper half of the hinged column of Fig. 5.19*a*. The inflection points, one at the end of the actual column and the other at the imaginary extension of the sine wave, are seen to be a distance $2h$ apart, so that the effective length is $h' = 2h$.

If the column is rotationally fixed at both ends, but one end can move laterally with respect to the other, it buckles as shown in Fig. 5.19*e*, with an effective length $h' = h$. If one compares this column, fixed at both ends but free to sidesway, with a fixed-fixed column which is braced against sidesway (Fig. 5.19*b*), one sees that the effective length of the former is twice that of the latter. By Eq. (5.30), this means that the buckling strength of an elastic fixed-fixed column which is free to sidesway is only one-quarter that of the same column when braced against sidesway. This is an illustration of the general fact that *compression members free to buckle in a sidesway mode are always considerably weaker than when braced against sidesway*.

Again, the ends of columns in actual structures are rarely either hinged, fixed, or entirely free, but are usually restrained by abutting members. If sidesway is not prevented, buckling occurs as in Fig. 5.19*f*, and the effective length, as before, depends on the degree of restraint r'. If the cross beams are very rigid as compared with the column (giving r' close to zero), the case of Fig. 5.19*e* is approached, and h' is only slightly larger than h. On the other hand, if the restraining members are extremely flexible, a hinged condition is approached at both ends. Evidently, a column hinged at both ends and free to sidesway is unstable. It will simply topple, being unable to carry any load whatever.

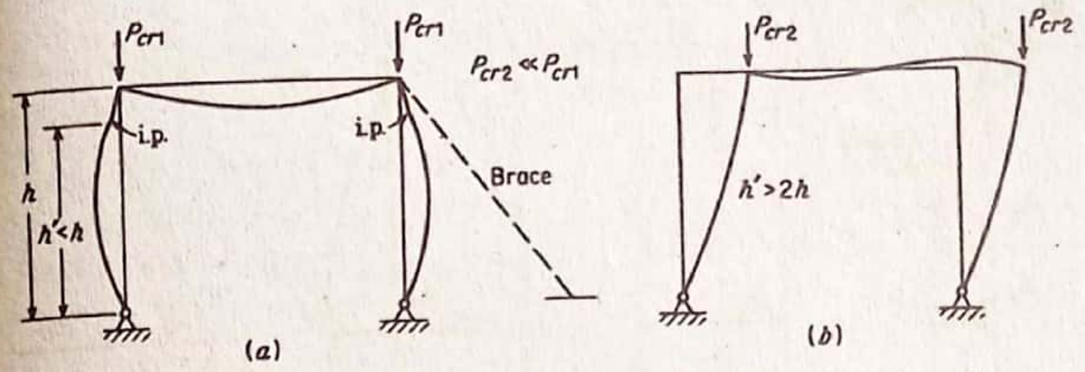


Fig. 5.21 Rigid frame buckling: (*a*) laterally braced; (*b*) unbraced.

In reinforced-concrete structures one is rarely concerned with single members, but rather with rigid frames of various configurations. The manner in which the described relationships affect the buckling behavior of frames is illustrated by the simple portal frame of Fig. 5.21, with loads applied concentrically to the columns. If sidesway is prevented, as indicated schematically by the brace of Fig. 5.21*a*, the buckling configuration will be as shown. The buckled shape of the column corresponds to that of Fig. 5.19*e*, except that the lower end is hinged. It is seen that the effective length h' is smaller than h. On the other hand, if no sidesway bracing is provided to an otherwise identical frame, buckling occurs as in Fig. 5.21*b*. The column is in a situation similar to that of Fig. 5.19*d*, upside down, except that the upper end is not fixed, but only partially restrained by the girder. It is seen that the effective length h' exceeds $2h$ by an amount depending on the degree of restraint. The buckling strength depends on h'/r in the manner shown in Fig. 5.20*b*. In consequence, even though they are dimensionally identical, the unbraced frame will buckle at a radically smaller load than the braced frame.

In summary, the following can be noted:

The strength of concentrically loaded columns decreases with increasing slenderness ratio h'/r.

In columns which are *braced against sidesway* or which are parts of frames braced against sidesway, the effective length h', that is, the distance between inflection points, falls between $h/2$ and h, depending on degree of end restraint.

The effective lengths of columns which are *not braced against sidesway* or which are parts of frames not so braced, are always larger than h, the more so the smaller the end restraint. In consequence, the buckling load of a frame not braced against sidesway is always substantially smaller than that of the same frame when braced.

b. Compression plus bending Most reinforced-concrete compression members are subject to simultaneous flexure, caused by transverse loads or by end moments due to continuity. The behavior of mem-

Scanned with CamScanner

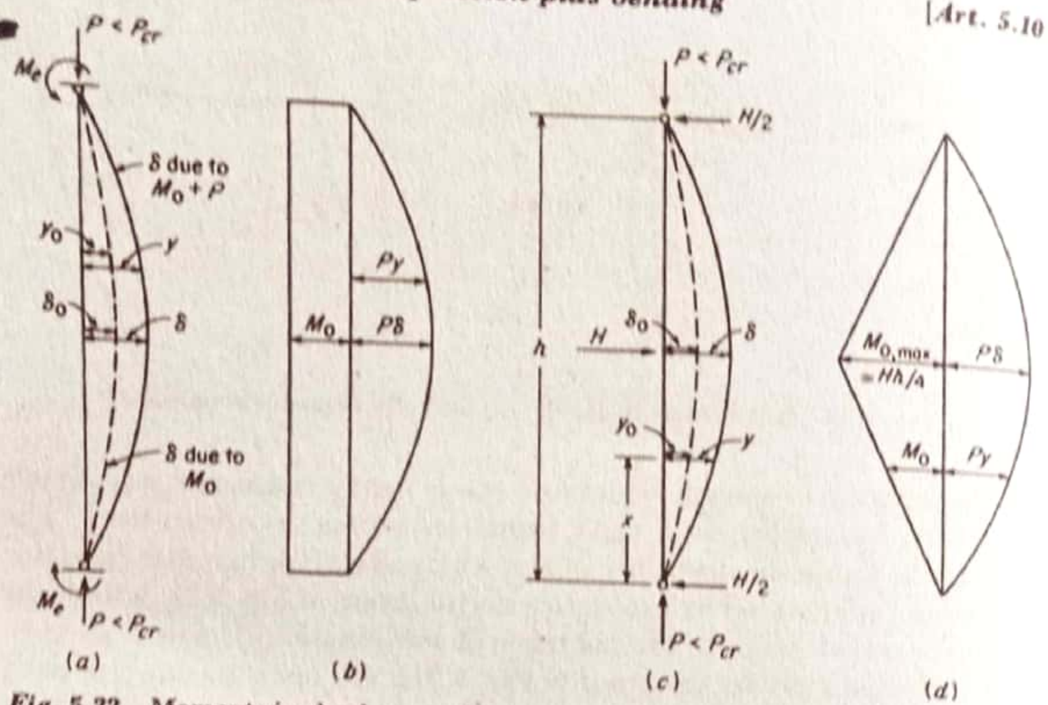


Fig. 5.22 Moments in slender members, compression plus bending, single curvature.

bers subject to such combined loading also depends greatly on their slenderness.

Figure 5.22*a* shows such a member, often known as a *beam-column*, axially loaded by P and bent by equal end moments M_e. If no axial load were present, the moment M_0 in the member would be constant throughout and equal to the end moments M_e. This is shown in Fig. 5.22*b*. In this situation, i.e., in simple bending without axial compression, the member deflects as shown by the dashed curve of Fig. 5.22*a*, where y_0 represents the deflection at any point caused by bending only. When P is applied, the moment at any point increases by an amount equal to P times its lever arm. The increased moments cause additional deflections, so that the deflection curve under the simultaneous action of P and M_0 is the solid curve of Fig. 5.22*a*. At any point, then, the total moment is now

$$M = M_0 + Py \tag{5.32}$$

that is, the total moment consists of the moment M_0 which acts in the absence of P and the additional moment caused by P, equal to P times the deflection.

A similar situation is shown in Fig. 5.22*c*, where bending is caused by the transverse load H. When P is absent, the moment at any point x is $M_0 = Hx/2$, with a maximum at midspan equal to $Hh/4$. The corresponding M_0 diagram is shown in Fig. 5.22*d*. When P is applied, additional

moments Py are caused again, distributed as shown, and the total moment at any point in the beam-column consists of the same two parts as in Eq. (5.32).

The deflections y of elastic beam-columns of the type shown in Fig. 5.22 can be calculated from the deflections y_0 (i.e., from the deflections of the corresponding beam without axial load), using the following expression (see, e.g., Ref. 5.3):

$$y = y_0 \frac{1}{1 - P/P_{cr}} \tag{5.33}$$

If P and P_{cr} in Eq. (5.33) are divided by the area A, and $(P/A)_{cr}$ is replaced with the expression given in Eq. (5.31), then Eq. (5.33) can be rewritten in the form

$$y = y_0 \frac{1}{1 - P(h'/r)^2/A\pi^2E} \tag{5.34}$$

Given the external loading, that is, P and M_0, it is seen from Eqs. (5.32) and (5.34) that the moment M in the member increases with increasing slenderness ratio h'/r. The situation is shown schematically in Fig. 5.23. It indicates that for a given transverse loading, i.e., a given value of M_0, an axial force P causes a larger additional moment in a slender member than in a stocky member.

In the two members in Fig. 5.22, the largest moment caused by P, namely $P\delta$, adds directly to the maximum value of M_0, for example, $M_0 = Hh/4$ in Fig. 5.22*d*. As P increases, the maximum moment at midspan increases at a rate faster than that of P in the manner given by Eqs. (5.32) and (5.34) and shown in Fig. 5.24. The member will fail when the simultaneous values of P and M become equal to P'_u and M'_u, the ultimate strength of the cross section at the location of maximum moment.

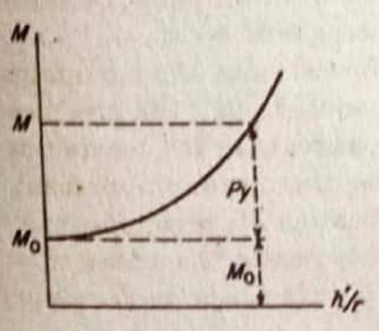


Fig. 5.23 Effect of slenderness on column moments.

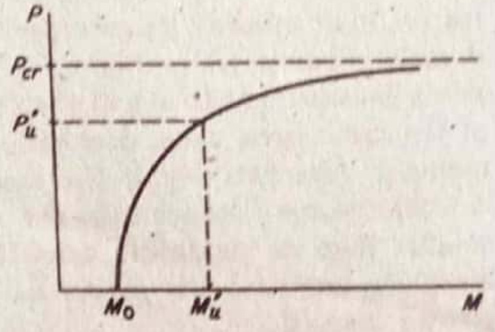


Fig. 5.24 Effect of axial load on column moments.

Scanned with CamScanner

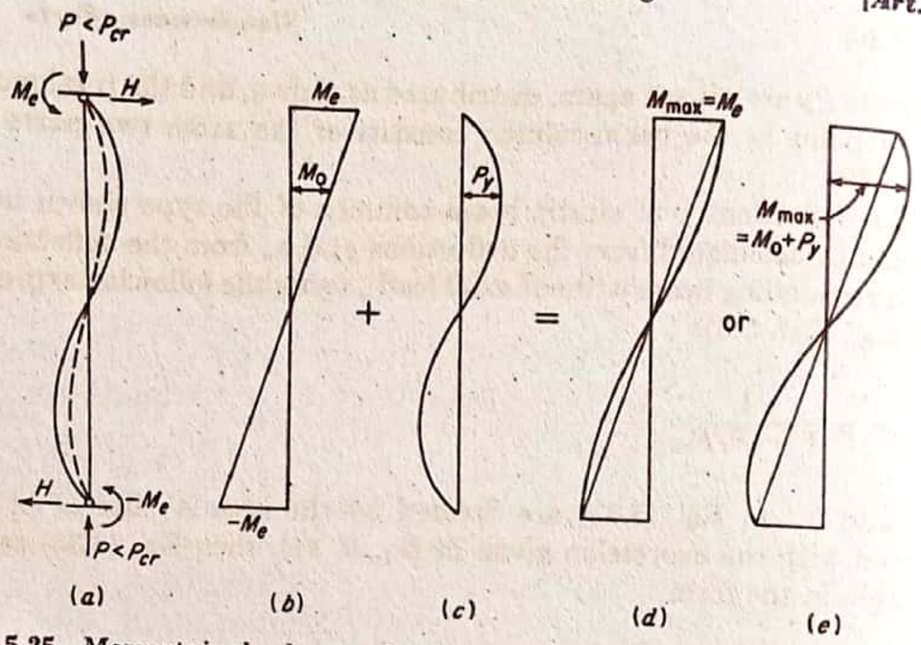


Fig. 5.25 Moments in slender members, compression plus bending, double curvature.

This direct addition of the maximum moment caused by P to the maximum moment caused by transverse load, clearly the most unfavorable situation, does not obtain for all types of deformations. For instance, the member of Fig. 5.25*a*, with equal and opposite end moments, has the M_0 diagram of Fig. 5.25*b*. The deflections caused by M_0 alone are again magnified when an axial load P is applied. In this case, these deflections under simultaneous bending and compression can be approximated by (Ref. 5.3)

$$y = y_0 \frac{1}{1 - P/4P_{cr}} \tag{5.35}$$

By comparison with Eq. (5.33), it is seen that the deflection magnification here is much smaller.

The additional moments Py caused by axial load are distributed as shown in Fig. 5.25*c*. While the M_0 moments are largest at the ends, the Py moments are seen to be largest some distance from the ends. Depending on their relative magnitudes, the total moments $M = M_0 + Py$ are distributed as in either Fig. 5.25*d* or *e*. In the former case, the maximum moment continues to act at the end and to be equal to M_e; the presence of the axial force, then, does not result in any increase in the maximum moment. Alternatively, in the case of Fig. 5.25*e*, the maximum moment is located some distance from the end; at that location M_0 is significantly smaller than its maximum value M_e, and for this reason the added moment Py increases the maximum moment to a value only moderately greater than M_e.

One can generalize as follows by comparing the situation of Fig. 5.22 with that of Fig. 5.25: If the applied moments M_0 alone, without axial force P, cause the member to deflect in single curvature, the addition of an axial force P will greatly magnify the maximum bending moment in the member, the more so the larger the slenderness ratio. On the other hand, if the moments M_0 cause the member to bend in double curvature, with an inflection point somewhere along the member (not necessarily in the middle), the added deflections caused by P are smaller, and the maximum moment either may not be magnified at all by the axial force P (Fig. 5.25*d*) or may be magnified to a generally less significant degree (Fig. 5.25*e*).

What has been said so far refers to *members braced against sidesway*. This includes the frequent case of columns which are parts of structures in which sidesway is prevented in one of various ways: by walls or partitions sufficiently strong and rigid in their own planes effectively to prevent horizontal displacement, by special bracing in vertical planes, such as wind-bracing, in tier buildings by designing the utility core to resist horizontal loads and furnish bracing to the frames, or by bracing the frame against some other essentially immovable support.

If no such bracing is provided, *sidesway can occur only for the entire frame simultaneously*, not for individual columns in the frame. If this is the case, the combined effect of bending and axial load is somewhat different from that in braced columns. For illustration, consider the simple portal frame of Fig. 5.26*a* subject to a horizontal load H, such as a wind load, and compression forces P, such as from gravity loads. The moments M_0 caused by H alone, in the absence of P, are shown in Fig. 5.26*b*; the corresponding deformation of the frame is given in dashed curves. When P is added, additional moments are caused which result in the magnified deformations shown in solid curves and in the moment diagram of Fig. 5.26*c*. It is seen that the maximum values of M_0, both positive and nega-

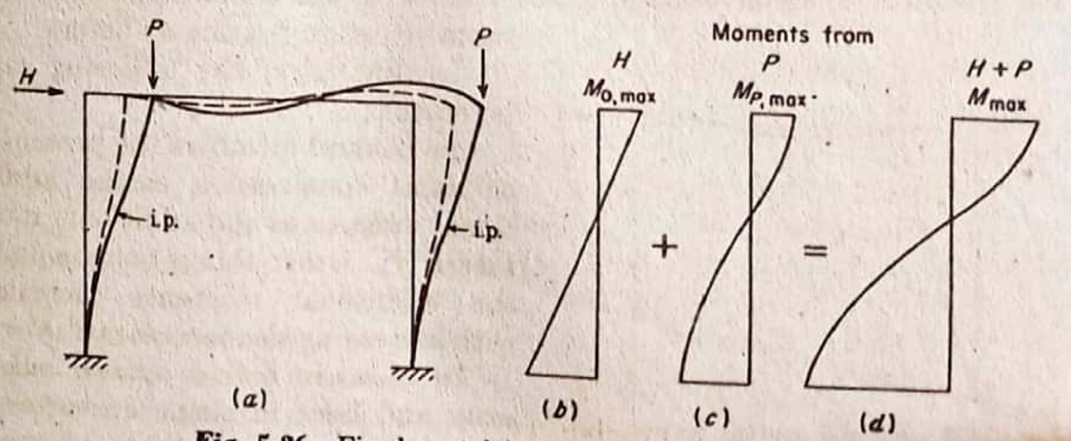


Fig. 5.26 Fixed portal frame, laterally unbraced.

Scanned with CamScanner

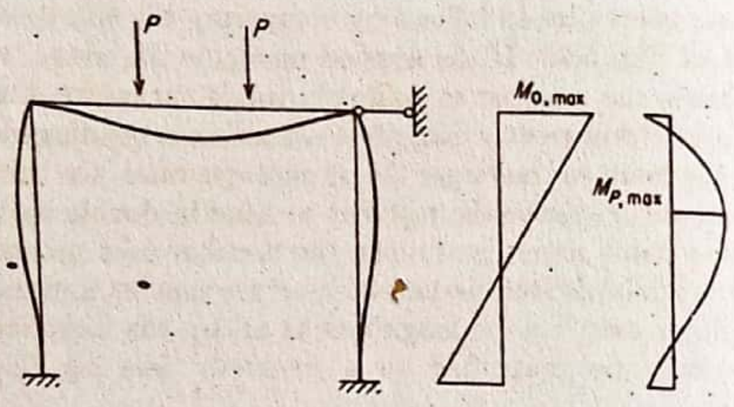


Fig. 5.27 Fixed portal frame, laterally braced.

tive, and the maximum values of the additional moments M_P of the same sign occur at the same locations, namely at the ends of the columns. They are, therefore, fully additive, leading to a large moment magnification. In contrast, if the frame of Fig. 5.26 is laterally braced and vertically loaded, Fig. 5.27 shows that the maximum values of the two different moments occur in different locations; the moment magnification, if any, is therefore much smaller. For the portal hinged at the bottom, as in Fig. 5.28, the discussion of Fig. 5.26 holds: the maximum moments of both kinds are fully additive at the column tops. The difference between the cases of Figs. 5.26 and 5.28, therefore, lies not in the presence or absence of an inflection point, but only in the greater stiffness of the columns fixed at the bottom. This results in the fact that their effective length h' is smaller than that in the hinged situation.

It should be noted that the moments which cause a frame to sidesway need not be caused by horizontal loads as in Figs. 5.26 and 5.28. Asymmetries, either of frame configuration or vertical loading or both, also result in sidesway displacements, as is discussed in Art. 8.6. In this case the presence of axial column loads results in the same deflection and moment magnification as before.

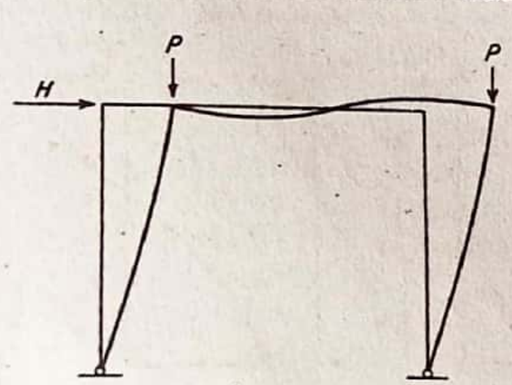


Fig. 5.28 Hinged portal frame, laterally unbraced.

In summary, the following can be stated:

In flexural members the presence of axial compression causes additional deflections and additional moments Py. Other things being equal, the additional moments increase with increasing slenderness ratio h'/r.

In *members braced against sidesway* and bent in single curvature, the maxima of both types of moments, M_0 and Py, occur at the same or at nearby locations and are fully additive; this leads to large moment magnifications. If the M_0 moments result in double curvature (i.e., in the occurrence of an inflection point), the opposite is true, and less or no moment magnification occurs.

In *members of frames not braced against sidesway*, the maximum moments of both kinds, M_0 and Py, almost always occur at the same locations, the ends of the column; they are fully additive, regardless of the presence or absence of an inflection point. Here, too, other things being equal, the additional deflections and the corresponding moments increase with increasing h'/r.

This discussion is merely a simplified presentation of a very complex subject. In particular, Eqs. (5.33) through (5.35) hold only for elastic members. They need modification in detail when applied to inelastic materials, even though the essential behavior, as presented in Figs. 5.23 and 5.29, is the same in both situations. For a material as complex as reinforced concrete, inelastic at relatively low stresses and subject to cracking on the tension side in bent members, an exact analysis of the described situations is not yet possible in most cases. Even if it were, it would be so complex as to need simplification for design purposes. Such a design method, quite possibly oversimplified, is that stipulated in the ACI Code for dealing with slender columns.

5.11 Slender-column Design by ACI Code ***a. General*** Figure 5.20*b* shows that the load capacity, i.e., the buckling load P_{cr}, of an axially compressed slender column is smaller than the ultimate strength P'_u of an axially loaded stocky column, provided the slenderness $h'/r > (h'/r)_{\text{lim}}$. This can be written as

$$P_{cr} = C_P P'_u$$

where $C_P = f_1(h'/r) \leq 1$ is a *load-reduction factor* which expresses the effect of slenderness.

On the other hand, for compression plus bending, the combined information of Figs. 5.23 and 5.24 shows that the maximum bending moment M_0 which can be applied to a slender member by transverse forces or moments is smaller than that moment M'_u which, simultaneously with an axial load P'_u, would fail a stocky member. (A stocky member, in this context, is one for which the moment magnification is so small as to be negligible.) This can be written as

$$M_0 = C_M M'_u$$

where $C_M = f_2(h'/r) \leq 1$ is a *moment-reduction factor* which expresses the effect of slenderness. Both C_P and C_M depend on the slenderness ratio,

Scanned with CamScanner

but the discussion of the preceding article makes clear that they represent different effects.

For simplicity, and partly for reasons of tradition, the *ACI Code applies to both the moment and the axial load the same reduction factor* $R = f(h'/r) \leq 1$. Explicitly, the Code stipulates that

$$P_{\text{slender}} = RP_{\text{stocky}} \tag{5.36}$$
$$M_{\text{slender}} = RM_{\text{stocky}} \tag{5.37}$$

where P_{slender}, M_{slender} = carrying capacity in simultaneous axial compression and bending of member with slenderness ratio h'/r

P_{stocky}, M_{stocky} = carrying capacity in simultaneous axial compression and bending of stocky member of same cross section as slender member

$R = f(h'/r) \leq 1$ = slenderness factor depending on h'/r and defined in more detail below

In design, these relations are used as follows: Let P and M be the axial load and the maximum moment caused in a given member by dead, live, wind, and other loads. P and M are obtained by any of the usual methods of structural analysis, without regard to moment magnification or other slenderness effects. If the slenderness of the member is large enough to reduce the carrying capacity, this reduction is taken care of by designing the member not for P and M, but for the larger quantities P/R and M/R. The member is designed for these increased forces and moments by the methods of ultimate-strength design discussed in Arts. 5.3 to 5.5 or by those of working-stress design as given in Arts. 5.7 and 5.8.

The Code provides that the radius of gyration r is sufficiently accurately given by

For rectangular sections: $r = 0.30t$
For circular sections: $r = 0.25D$

where t is the overall depth in the direction of bending, and D is the diameter of the cross section. For cross sections of other shapes, r may be computed for the gross concrete section, disregarding the reinforcement.

Example A structure is analyzed for the effects of dead and live load in the usual manner, and it is found that a particular member is subject to an axial load $P = 200$ kips and a maximum moment $M = 100$ ft-kips. Preliminary design has furnished approximate cross-sectional dimensions, from which the slenderness ratio h'/r was computed. For this particular slenderness ratio the applicable Code provisions (discussed below) indicate a reduction factor $R = 0.70$. Then the cross section of the member must be dimensioned for an axial load $P/R = 200/0.70 = 286$ kips and a simultaneous moment $M/R = 100/0.70 = 143$ ft-kips.

In agreement with the information given in Art. 5.10, the Code distinguishes between two types of members or, more accurately, between members in two types of structures. On the one hand, there are those structures in which sidesway of one floor or level with respect to the adjacent floor or level is prevented by the presence of adequate bracing. This corresponds to the situation of Figs. 5.21*a* and 5.27. In columns of such frames, *relative lateral displacement of the ends is prevented, and sidesway is not possible.* On the other hand, there are those structures which depend for their lateral stability chiefly or exclusively on the rigidity of the columns, rather than on some other means of bracing. Such frames behave under axial load as shown in Fig. 5.21*b*, or under lateral and axial load as in Figs. 5.26 and 5.28. In columns of such frame *relative lateral displacement of the ends is not prevented, and sidesway possible.*

In structures of the first category, bracing can be provided in various ways: by the rigidity of walls and partitions in their own planes, by special shear walls, by rigid utility cores, by special wind bracing, etc. The Code gives no criteria to define adequate bracing. In most practical cases this is not difficult to decide. Sidesway caused by axial forces alone (Fig. 5.21*b*) can be prevented by relatively light bracing. It has been shown by several investigators, including one of the authors (Ref. 5.4), that bracing capable of resisting a transverse force equal to about 2 per cent or less of the axial force will prevent such sidesway. On the other hand, to prevent sidesway caused by lateral forces alone, such as wind loads, evidently the bracing system by itself must be able to resist these lateral forces. Therefore, the following can be used as a general guide: *To effectively brace a frame against sidesway under the combined action of lateral and vertical forces, the bracing system by itself must be able to resist all the applied lateral loads plus at least 2 per cent of the total vertical load acting at and above the level of the column being designed.*

The discussion which follows deals with columns in which *compression governs* the design of the section, i.e., in which the eccentricity is smaller than e_b. A modification for the case in which tension governs is presented separately later.

b. Sidesway prevented It was shown in Art. 5.10*a* that the effective length h' of a column braced against sidesway ranges from $h/2$ for fixed-fixed conditions to h for hinged-hinged conditions. (Here, as elsewhere, h is defined in the Code as the *clear distance* between the floor at the bottom of the column and the underside of the beam, slab, capital, or drop panel at the top.) The Code ignores this variation of h' in the interest of simplicity and some conservatism. It specifies that *for laterally braced members the entire length* h shall be used for computing the slenderness ratio h'/r.

Scanned with CamScanner

The values of the reduction factors R in the Code were obtained from a simplification and generalization of an elaborate experimental and analytical investigation of the inelastic behavior and strength of slender reinforced-concrete columns (Ref. 5.5).

For *members bent in single curvature* by the applied transverse forces or moments, the Code specifies

$$R = 1.07 - 0.008\frac{h}{r} \leq 1 \tag{5.38}$$

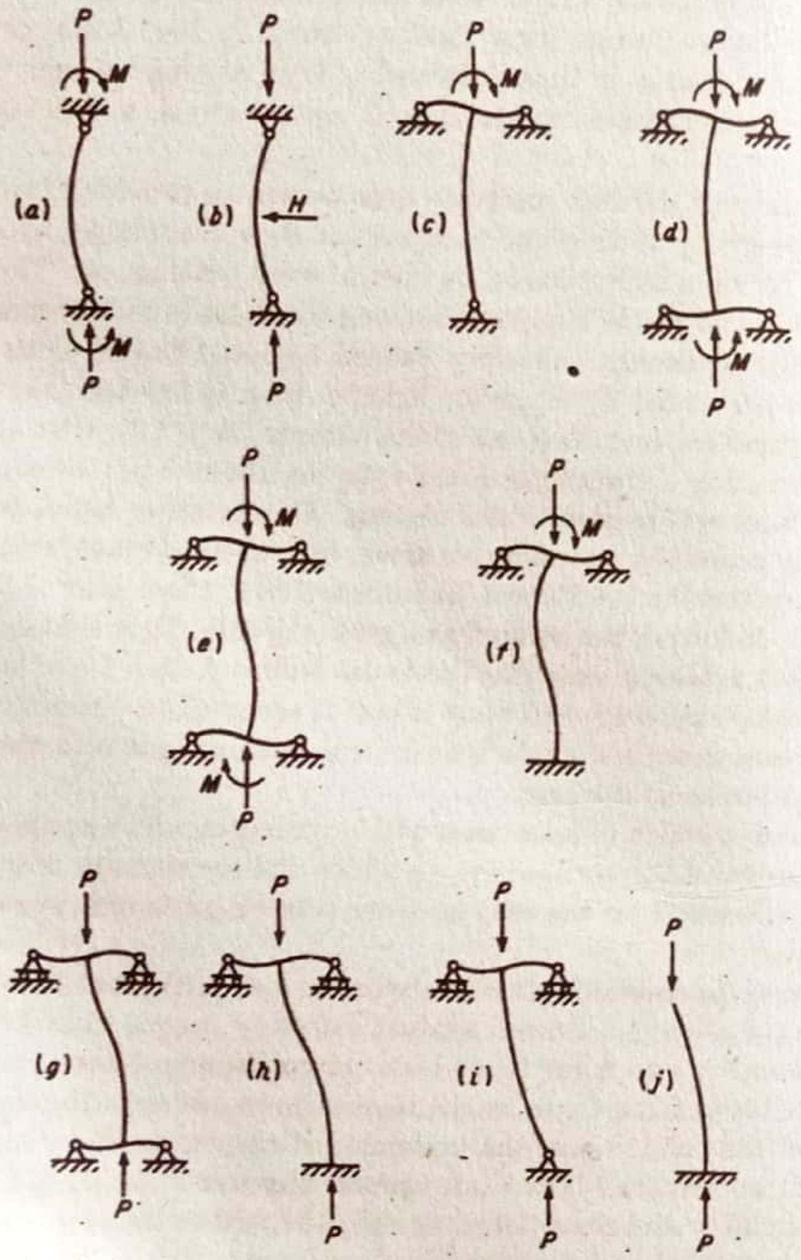


Fig. 5.29 Typical column situations, by ACI Code classification. Equation (5.38) holds for (*a*) to (*d*); Eq. (5.39) holds for (*e*) and (*f*); Eq: (5.42) holds for (*g*) to (*j*).

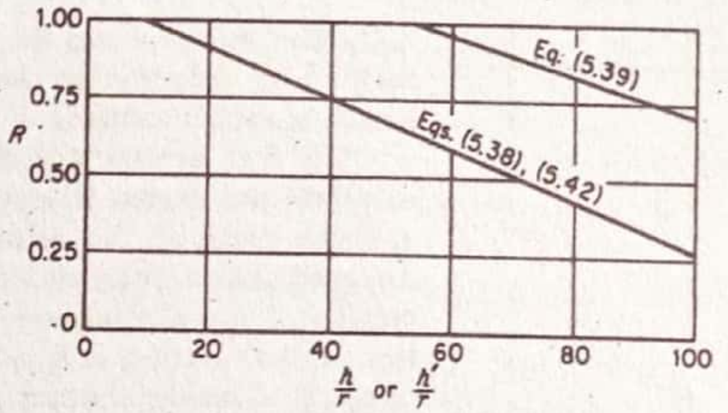


Fig. 5.30 ACI Code slenderness factors.

It was shown in Art. 5.10*b* that it is for this case that the moment magnification is particularly consequential. Hence, the reduction factor R decreases rapidly with increasing slenderness. Specifically, Eq. (5.38) applies to the four situations of Fig. 5.29*a* to *d*.

For *members bent in double curvature* by the applied forces or moments, the Code specifies

$$R = 1.32 - 0.006\frac{h}{r} \leq 1 \tag{5.39}$$

It was shown in Art. 5.10*b* that for this case the moment magnification, if any, is much smaller than that for single curvature. Correspondingly, for any given slenderness ratio the reduction by Eq. (5.39) is much smaller than that by Eq. (5.38). Specifically, Eq. (5.39) applies to the situations of Fig. 5.29*e* and *f*.

The graphs of the two equations are shown in Fig. 5.30. It is seen that the limiting slenderness ratio, up to which no reduction is needed, is $(h/r)_{lim} = 8.75$ for Eq. (5.38) and $(h/r)_{lim} = 53$ for Eq. (5.39). It also shows the much smaller reductions which the Code applies to members bent in double curvature. The authors believe that, while it holds for some cases, this large difference may turn out to be exaggerated for others. Future refinements based on additional research are likely to reflect a more complete spectrum of behavior than is given by these two provisions.

c. Sidesway not prevented It was shown in Art. 5.10*a* that the effective length of a column not braced against sidesway ranges from the actual length h for rotationally fixed ends upward to very large values for the case in which little rotational restraint is provided. In the interest of safety it is, therefore, essential that account be taken of this variation of the effective length.

Based on suitable simplifications of more detailed information (Ref.

Scanned with CamScanner

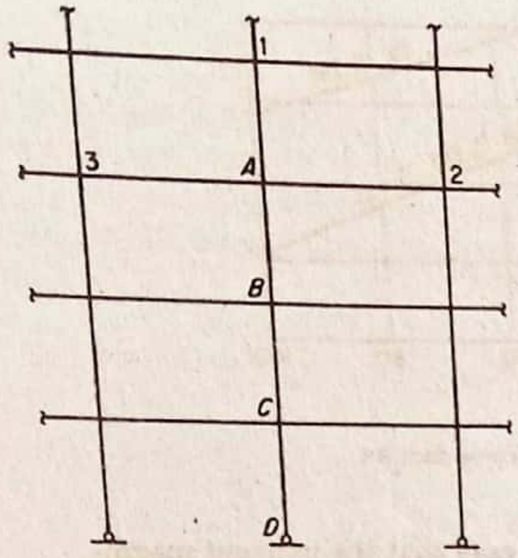


Fig. 5.31 Portion of typical building frame.

5.6), the Code provides the following method for determining the effective length of such a column:

It is first necessary to define and calculate the degree of end restraint at both ends of the column being designed. The rigidity of a structural member, i.e., its resistance to deflection or end rotation, is $K = EI/l$ (see Chap. 8). Consider the part of a building frame shown in Fig. 5.31. The column AB is restrained at its top by the girders $A2$ and $A3$. However, these same girders also provide restraint to the column above, $A1$. Consequently, the two members which tend to buckle, AB and $A1$, are restrained jointly at A by the two girders $A2$ and $A3$. The more rigid the girders in relation to the rigidities of the columns, the larger the degree of restraint against rotation of the columns at A. Therefore, the degree of restraint is $\Sigma K_{\text{girders}}/\Sigma K_{\text{columns}}$, the sums extending over all members in one plane meeting at the joint. In the Code equations, the reciprocal of this degree of restraint is used because it gives simpler expressions. This reciprocal is

$$r' = \frac{\Sigma K \text{ of columns}}{\Sigma K \text{ of girders or other floor members}}$$

the girders or floor members being located in one plane at one end of a column, such as end A of column AB. The magnitude of the end restraint being defined in this manner, the Code gives the effective length h' for *columns restrained against rotation at both ends* as

$$h' = h(0.78 + 0.22r') \geqq h \tag{5.40}$$

In this case, r' is defined as the average of the values at both ends of the given column (AB). It is seen that if r' is equal to or smaller than 1, then $h' = h$. This corresponds to the situation of Fig. 5.19*e*; i.e., the column in this case is regarded as effectively rotationally fixed at both ends. Specifically, Eq. (5.40) applies to the columns of Fig. 5.29*g* and *h*.

Equation (5.40) loses its meaning if one end is hinged, because in this case, at the hinged end, $r' = \infty$. The Code defines a hinged end as one either actually hinged or one in which the restraining members are so flexible that r' exceeds 25. For *columns restrained at one end and hinged at*

the other (such as CD in Fig. 5.31), the effective length is given as

$$h' = 2h(0.78 + 0.22r') \geqq 2h \tag{5.41}$$

in which case r' is the value at the restrained end (end C of CD). Again, if r' is equal to or smaller than 1, this corresponds to the situation of Fig. 5.19*d* upside down; i.e., the column is regarded effectively fixed at one end and free to rotate at the other, resulting in an effective length $h' = 2h$. Specifically, Eq. (5.41) applies to the columns of Fig. 5.29*i* and *j*, the latter giving $h' = 2h$.

It was shown in Art. 5.10*b* that for columns not braced against sidesway the maximum moments of both kinds generally occur at the ends and that, consequently, full moment magnification takes place. For this reason, regardless of whether the column is bent into single or double curvature, the Code specifies the *reduction factor* R *for such unbraced columns* as

$$R = 1.07 - 0.008\frac{h'}{r} \leqq 1 \tag{5.42}$$

the same as is specified for braced columns bent in single curvature [Eq. (5.38)]. The difference is that for the latter the effective length is $h' = h$, whereas for the former h' will in general exceed the actual length h. This results in smaller values of R, that is, in a greater capacity reduction caused by slenderness. It agrees with the information presented in Art. 5.10 that the strength-reducing effects of slenderness are much larger in frames not braced against sidesway than in frames so braced. Specifically, Eq. (5.42) applies to the columns of Fig. 5.29*g* through *j*.

In laterally unbraced frames, the column moments which govern design are often caused by wind loading or, in seismic zones, by earthquake loads. These are loads of short duration as compared not only with dead load, but also with live loads caused by the usual types of occupancy. Deflections from such sustained loads are in part caused by creep (see Art. 2.7). In contrast, the described short-time loads are of such small duration that they do not cause creep deflections. Hence, the total magnitudes of these deflections, and of the moments Py caused by the deflections, are smaller than they would be under the more sustained regime of gravity loads. For this reason, when the *design is governed by lateral loads of short duration*, the Code permits the use of a 10 per cent more favorable reduction factor,

$$R = 1.18 - 0.009\frac{h'}{r} \leqq 1 \tag{5.43}$$

d. Columns governed by tension It is seen from Eq. (5.34) that the additional moment caused by P, that is, the moment magnification,

Scanned with CamScanner

depends not only on the slenderness ratio h'/r, but also on the magnitude of the compression force P. In particular, in the case of a simple, transversely loaded beam without axial force ($P = 0$), the additional moment and the moment magnification vanish, as they should.

On the other hand, the Code expressions for the reduction factor R which have just been presented have been developed for members with relatively large axial loads. For this reason they need modification for application to those members in which bending moments are relatively large and axial forces relatively small. In such a member the capacity of the cross section is governed by tension, i.e., by yielding of the steel. In the limit, for a simple beam with $P = 0$, the reduction factor must be $R = 1$. Correspondingly, the Code stipulates:

> When tension governs the design of the section, the factor R shall be considered to vary linearly from its full value at the balanced condition to a value of 1.0 when the axial load is zero.

Correspondingly, in this range in which the *eccentricity e exceeds the balanced value* e_b, the reduction factor can be obtained from

$$R' = 1 - (1 - R)\frac{e_b}{e} \geq R \tag{5.44}$$

where R' = reduction factor for slender columns failing in tension
R = reduction factor according to applicable equation [Eq. (5.38), (5.39), (5.42), or (5.43)]
e = design eccentricity M/P
e_b = balanced eccentricity [see Eqs. (5.9), (5.13), (5.19)]

It is seen that for the balanced condition, $e = e_b$, Eq. (5.44) gives $R' = R$, the value prescribed for all columns whose strength is governed by compression. At the other extreme, for the case of purely flexural members, when $P = 0$, $e = M/P = \infty$, and Eq. (5.44) gives $R' = 1$. Within this range, R' is seen to increase gradually from R to 1.0, depending on the eccentricity e.

e. Concentrically loaded columns It appears clear from the preceding discussion that the R factors in the ACI Code are chiefly intended to reflect the moment-reduction factors (designated by C_M in Art. 5.11*a*) rather than the load-reduction factors C_P. Most axially compressed members are, in fact, subject to simultaneous bending and should be designed for the combined effect. However, cases do occur in which columns are subject to concentric compression loads without moments. An example is an interior column in a building frame braced against sidesway, with full live load on the floors above and below the column in question. If symmetry prevails, such a column may be entirely free from

calculated moments. In other cases, moments may not be computed by the designer because, by inspection, they are known to be so small as to be negligible.

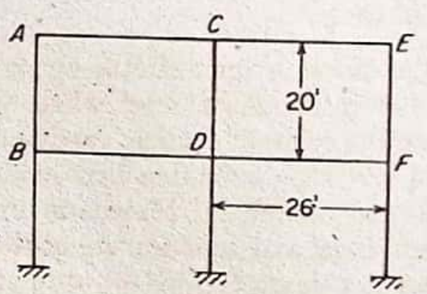
In such cases one cannot decide whether the column is bent in single or double curvature, because no external bending moments act to produce such curvature; consequently, the criterion for applying either Eq. (5.38) or (5.39) does not seem to hold. However, *when sidesway is prevented*, a column will buckle in single curvature (Fig. 5.19*a*) only if it is hinged at both ends. If it is fixed or significantly restrained, inflection points exist between the ends (Fig. 5.19*b* and *c*). Correspondingly, the authors suggest that, for concentrically loaded columns, Eq. (5.38) be used when little or no end restraint is present at either end, and that Eq. (5.39) be used when substantial rotational end restraint is present. One may assume substantial restraint to be present if the average values of r' at both ends are not larger than about 2.0. It is clear from the Code as well as from the preceding discussion of sidesway behavior that Eq. (5.42) applies *when sidesway is not prevented.*

Example In Example 2 of Art. 5.4*c* it was found that a 12 × 20 in. cross section with four No. 9 bars, for which $f'_c = 5000$ psi, $f_y = 75{,}000$ psi, and $p_t m = 0.295$, with an eccentricity $e = 0.75t$, has an ultimate design load $P_u = 188{,}000$ lb. The simultaneous moment is $M_u = 0.75 \times 20 \times 188{,}000$ lb $= 2{,}820{,}000$ in.-lb. It was also found that tension governed the strength. Suppose that this cross section applies to the exterior column AB of the industrial building frame of Fig. 5.32. Gravity loading produces axial forces and moments such that $e/t = 0.75$, as in the quoted example. Determine the load and moment capacity of the column by ultimate-strength design (*a*) when the frame is laterally braced and (*b*) when it is not braced.

a. The radius of gyration of the columns is $r = 0.30 \times 20 = 6.0$ in., and the slenderness ratio in the braced condition, with $h' = h$, is $h/r = 240/6 = 40$. Gravity loads on girders AC and BD cause clockwise moments to act on joints A and B which bend column AB in double curvature. Consequently, when the frame is braced against sidesway, the slenderness reduction factor is found from Eq. (5.39) to be

$$R = 1.32 - 0.0006 \times 40 = 1.08 > 1.0$$

It is seen that no strength reduction is called for on account of slenderness, and the ultimate values to be used in design are equal to the full design strength of the cross section; that is, $P_u = 188{,}000$ lb, and $M_u = 2{,}820{,}000$ in.-lb.



Exterior columns 12 × 20"
Girders 12 × 22"
Distances shown are clear lengths of members

Fig. 5.32

b. When the frame is not laterally braced, it is first necessary to determine the effective length h', depending on the amount of restraint at the ends. For the columns, the moment of inertia of the cross section is $I_c = (12 \times 20^3)/12 = 8000$, and the relative rigidity is $K_c = I_c/h = 8000/(20 \times 12) = 33.3$. The corresponding values for the girders are $I_g = 10{,}900$ and $K_g = 35.0$. (To simplify the example, clear lengths of members have been used to calculate K. In actual design it is customary and more accurate to use center-line distances for determining rigidities.) Hence the restraint factor r' for column AB is

At the top of the column: $r' = 33.3/35.0 = 0.95$
At the bottom of the column: $r' = 2 \times 33.3/35.0 = 1.91$
Average: $r' = (0.95 + 1.91)/2 = 1.43$

Then the effective length, by Eq. (5.42), is

$$h' = 240(0.78 + 0.22 \times 1.43) = 262 \text{ in.}$$

and the slenderness ratio is $h'/r = 262/6 = 43.8$. With this value, the reduction factor is obtained from Eq. (5.42) as

$$R = 1.07 - 0.008 \times 43.8 = 0.72$$

Hence, if compression governed the strength of the section, the slenderness effects would result in a 28 per cent reduction of the carrying capacity. However, for $e/t = 0.75$ it was found that tension governs. To calculate the corresponding reduction factor R' from Eq. (5.44), the balanced eccentricity e_b is needed. Using Eq. (5.9), with $p_t m = 0.295$,

$$e_b = (0.20 + 0.77 \times 0.295)t = 0.43t$$

and

$$R' = 1 - 0.28\frac{0.43t}{0.75t} = 0.84$$

It is seen that the capacity reduction caused by slenderness is 16 per cent, and the values to be used in design are

Ultimate axial load $= 0.84 \times 188{,}000 = 158{,}000$ lb
Ultimate bending moment $= 0.84 \times 2{,}820{,}000 = 2{,}370{,}000$ in.-lb

PROBLEMS

For the frame of the example above (Art. 5.11*e*), design the interior column CD. Maximum moments occur when live load is placed on spans BD and CE; these bend the column in single curvature. Under this loading the axial load from dead load is 70 kips, from live load 50 kips. Because of symmetry, dead load does not cause any moments. Maximum live-load moment in the column at D is 150 ft-kips. Steel and concrete are of the same strengths as in the example.

1. Design column CD by (*a*) ultimate-strength design and (*b*) working-stress design for this load-and-moment combination when the frame is (1) braced and (2) not braced against sidesway.

2. When full live load is placed on the girders on both sides of the column, gravity loads do not cause any moments. However, the axial load is increased by the additional live load which is now placed on girder AC. For this loading condition the axial load from dead load is 70 kips, from live load 100 kips, and the moment is zero. Check the columns designed in Prob. 1 for this condition of loading.

REFERENCES

5.1 A. H. Mattock, L. B. Kriz, and Eivind Hognestad: Rectangular Concrete Stress Distribution in Ultimate Strength Design, *J. ACI*, vol. 57, p. 875, 1961.
5.2 Boris Bresler: Design Criteria for Reinforced Concrete Columns under Axial Load and Biaxial Bending, *J. ACI*, vol. 57, p. 481, 1960; discussion, p. 1612.
5.3 S. P. Timoshenko and J. M. Gere: "Theory of Elastic Stability," 2d ed., McGraw-Hill Book Company, Inc., New York, 1961.
5.4 George Winter: Lateral Bracing of Columns and Beams, *Trans. ASCE*, vol. 125, p. 807, 1960.
5.5 Bengt Broms and I. M. Viest: Long Reinforced Concrete Columns, *Trans. ASCE*, vol. 126, part II, p. 309, 1961.
5.6 "Guide to Design Criteria for Metal Compression Members," Column Research Council, Ann Arbor, Mich., 1960.

Scanned with CamScanner

I am such a asshole Idiot fuckedup dump

chapter **6**

FOOTINGS

6.1 Types and Function of Substructures The substructure, or foundation, is that part of a structure which is usually placed below the surface of the ground and which transmits the load to the underlying soil or rock. All soils compress noticeably when loaded and cause the supported structure to settle. The two essential requirements in the design of foundations are that the total settlement of the structure shall be limited to a tolerably small amount and that differential settlement of the various parts of the structure shall be eliminated as nearly as possible. With respect to possible structural damage, the elimination of differential settlement, i.e., different amounts of settlement within the same structure, is even more important than limitations on uniform overall settlement.

To limit settlements as indicated, it is necessary (1) to transmit the load of the structure to a soil stratum of sufficient strength and (2) to spread the load over a sufficiently large area of that stratum to minimize

bearing pressure. If adequate soil is not found immediately below the structure, it becomes necessary to use deep foundations such as piles or caissons to transmit the load to deeper, firmer layers. If satisfactory soil directly underlies the structure, it is merely necessary to spread the load, by footings or other means. Such substructures are known as *spread* foundations, and it is mainly this type which will be discussed. Information on the more special types of deep foundations can be found in texts on foundation engineering.

6.2 Types of Spread Foundations Footings generally can be classified as wall and column footings. The horizontal outlines of the most common types are given in Fig. 6.1. A wall footing is simply a strip of reinforced concrete, wider than the wall, which distributes its pressure. Single-column footings are usually square, sometimes rectangular, and represent the simplest and most economical type. Their use under exterior columns meets with difficulties if property rights prevent the use of footings projecting beyond the exterior walls. In this case combined footings or strap footings are used which enable one to design a footing which will not project beyond the wall column. Combined footings under two or more columns are also used under closely spaced, heavily loaded interior columns where single footings, if they were provided, would completely or nearly merge.

Such individual or combined column footings are the most frequently used types of spread foundations on soils of reasonable bearing capacity. If the soil is weak and/or column loads are great, the required footing areas become so large as to be uneconomical. In this case, unless a deep foundation is called for by soil conditions, a mat or raft foundation is resorted to. This consists of a solid reinforced-concrete slab which extends under the entire building and which, consequently, distributes the load of the structure over the maximum available area. Such a foundation, in view of its own rigidity, also minimizes differential settlement. It consists, in its simplest form, of a concrete slab reinforced in both directions. A form which provides more rigidity and, at the same time, is often more economical consists of an inverted beam-and-girder floor. Girders are located in the column lines in one direction, with beams in the other, mostly at closer intervals. If the columns are arranged in a square pattern, girders are equally

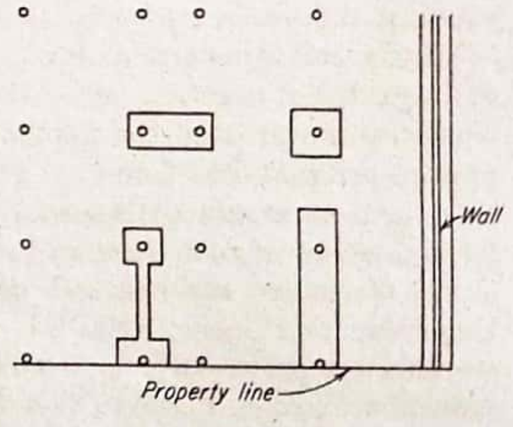


Fig. 6.1 Types of footings.

Scanned with CamScanner

spaced in both directions, and the slab is provided with two-way reinforcement. Inverted flat slabs, with capitals at the bottoms of the columns, are also used for mat foundations.

6.3 Factors Affecting the Design of Concrete Footings In ordinary constructions the load on a wall or column is transmitted vertically to the footing, which, in turn, is supported by the upward pressure of the soil on which it rests. If the load is symmetrical with respect to the bearing area, the bearing pressure is assumed to be uniformly distributed. It is known that this is only approximately true. Under footings resting on coarse-grained soils the pressure is larger at the center of the footing and decreases toward the perimeter. This is so because the individual grains in such soils are somewhat mobile, so that the soil located close to the perimeter can shift very slightly outward in the direction of lower soil stresses. In contrast, in clay soils pressures are higher near the edge than at the center of the footing, since in such soils the load produces a shear resistance around the perimeter which adds to the upward pressure. It is customary to disregard these nonuniformities (1) because their numerical amount is uncertain and highly variable, depending on type of soil, and (2) because the influence of these irregularities on the magnitudes of bending moments and shearing forces in the footing is relatively small.

In order to avoid tilting of footings, the pressures under them should be symmetrically distributed, which implies that columns should be placed at the centers of single footings. For the same reason, for combined footings, the resultant of the column loads should strike at the center of the footing area. If this is not done, uneven pressure distribution will result in uneven settlement, with a corresponding tilting of the footing toward the side of higher soil pressure and possible damage to the superstructure. Only on quite incompressible soils (rock, highly compacted gravels) may exceptions be made to this rule.

The accurate determination of stresses, particularly in single-column footings, is not practical, since they represent relatively massive blocks which cantilever from the column in all four directions. Under uniform upward pressure they deform in a bowl shape, a fact which would greatly complicate an accurate stress analysis. For this reason present procedures for the design of such footings are based almost entirely on the results of two extensive experimental investigations, both carried out at the University of Illinois (Refs. 6.1, 6.2). These tests have recently been reevaluated, particularly in the light of newer concepts of strength in shear and diagonal tension (Refs. 6.2 to 6.4).

6.4 Reinforced-concrete Wall Footings The simple principles of beam action apply to wall footing with only minor modifications. Figure 6.2 shows a wall footing with the forces acting on it. If bending moments were computed from these forces, the maximum moment would be found to occur at the middle of the width. Actually, the very large rigidity of the wall modifies this situation, and the tests cited in Art. 6.3 show that for footings under concrete walls it is satisfactory to compute the moment at the face of the wall (section 1-1). Tension cracks in these tests formed at the locations shown in Fig. 6.2, i.e., under the face of the wall rather than in the middle. For footings supporting masonry walls, the maximum moment is computed midway between the middle and the face of the wall, since masonry is generally less rigid than concrete. The maximum bending moment in footings under concrete walls is, therefore, given by

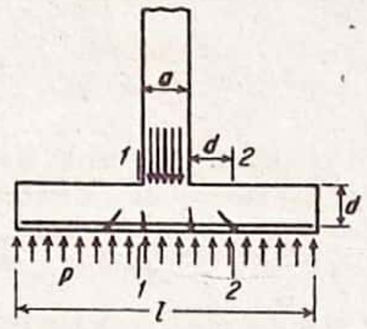


Fig. 6.2 Wall footing.

$$M = \tfrac{1}{8}p(l - a)^2 \tag{6.1}$$

The calculation of bond stresses is based on the shear for the same section, i.e.,

$$V_b = \tfrac{1}{2}p(l - a) \tag{6.2}$$

and the design provisions for bond are the same as for beams and one-way slabs.

For determining shear stresses, the vertical shear force is computed on section 2-2, located, as in beams, at a distance d from the face of the wall. Thus,

$$V_s = p\left(\frac{l - a}{2} - d\right) \tag{6.3}$$

It is generally not economical to use web reinforcement in footings.

Example: design of a wall footing A 16-in. concrete wall supports a total load of 23,100 lb per ft. The allowable bearing pressure of the soil is 2 tons per ft². Design a footing for this wall, using 2500-psi concrete and steel of $f_y = 40{,}000$ psi. Use working-stress design.

Assume the weight of the footing to be 900 lb per ft; the required width is then 24,000/4000 = 6 ft. The net upward pressure caused by the wall load alone (see Art. 6.5 for explanation) is 23,100/6 = 3850 lb per ft. This results in a moment at the critical sections 1-1 of

$$M = \tfrac{1}{8} \times 3850(6 - 1.33)^2 12 = 126{,}000 \text{ in.-lb per ft}$$

Scanned with CamScanner

For the given grades of material, $K = 178$ and $j = 0.866$. The effective depth required for bending is

$$d = \sqrt{\frac{126{,}000}{178 \times 12}} = 7.7 \text{ in.}$$

Assuming temporarily that $d = 8.0$ in., the shear force to be used in computing shear stresses at a distance d from the wall is

$$V_s = 3850[\tfrac{1}{2}(6 - 1.33) - 8.0/12] = 6440 \text{ lb per ft}$$

and the effective depth required for shear is

$$d = \frac{6440}{12 \times 55} = 9.7 \text{ in.}$$

It is seen that shear governs in this case. A depth of $d = 10.5$ in. is selected. *The ACI Code calls for a 3-in. clear insulation for footing bars,* which results in a total depth of 14 in.

The required area of transverse reinforcement is

$$A_s = \frac{126{,}000}{20{,}000 \times 0.866 \times 10.5} = 0.693 \text{ in.}^2 \text{ per ft}$$

Number 6 bars, 7.5 in. on centers, furnish $A_s = 0.71$ in.^{2} per ft. The area of one bar is 0.44 in.^{2}, its perimeter is 2.36 in., and its diameter is 0.75 in. With an allowable bond stress

$$u = \frac{4.8\sqrt{2500}}{0.750} = 320 \text{ psi}$$

the minimum development length required to develop the full allowable tension stress of 20,000 psi is

$$L_d = \frac{0.44 \times 20{,}000}{320 \times 2.36} = 11.6 \text{ in.}$$

The length of the bars, if end cover is 3 in., is $72 - 6 = 66$ in., and the actual development length from the section of maximum moment to the nearby end is

$$\tfrac{1}{2}(66 - 16) = 25 \text{ in.}$$

This being more than twice the required development length, flexural bond need not be checked.

The required longitudinal shrinkage reinforcement is

$$0.002 \times 12 \times 10.5 = 0.25 \text{ in.}^2 \text{ per ft of width of footing.}$$

Number 5 bars spaced 12 in. on centers provide 0.31 in.^{2} per ft and have the added function of spacing the main reinforcement while the concrete is being poured. In addition, they help the footing to bridge accidental weak spots in the soil. For this reason it is good practice to select these bars somewhat in excess of the minimum requirements for shrinkage reinforcement.

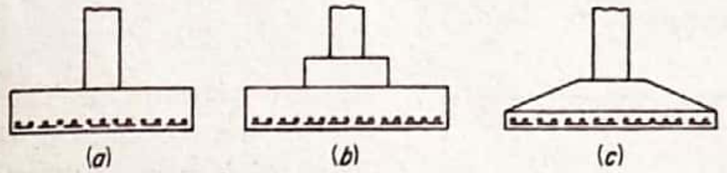


Fig. 6.3 Types of single-column footings.

6.5 Single-column Footings: General Information In plan, single-column footings are usually square. Rectangular footings are used if space restrictions dictate this choice, or if the supported columns are of strongly elongated rectangular cross section. In the simplest form, they consist of a single slab (Fig. 6.3*a*). Another type is that of Fig. 6.3*b*, where a pedestal or cap is interposed between the column and the footing slab; the pedestal provides for a more favorable transfer of load and in many cases is required in order to provide the necessary length for dowels. This form is also known as a *stepped* footing. All parts of a stepped footing must be poured in a single pour, in order to provide monolithic action. Sometimes sloped footings such as those in Fig. 6.3*c* are used. They require less concrete than stepped footings, but the additional labor necessary to produce the sloping surfaces (formwork, etc.) usually makes stepped footings more economical.

Single-column footings represent, as it were, cantilevers projecting out from the column in both directions and loaded upward by the soil pressure. Corresponding tension stresses are caused in both these directions at the bottom surface. Such footings are therefore reinforced by two layers of steel, perpendicular to each other and parallel to the edges.

The required bearing area is obtained by dividing the total load, including the weight of the footing, by the selected bearing pressure. Weights of footings, at this stage, must be estimated and amount usually to 4 to 8 per cent of the column load, the former value applying to the stronger types of soils.

In computing bending moments and shears, only that part of the upward pressure which is caused by the column load is considered. The weight of the footing proper does not cause moments or shears, just as, obviously, no moments or shears are present in a book lying flat on a table.

6.6 Design of Single Footings ***a. Bending moments, reinforcement, and bond*** If a vertical section is passed through a footing, the bending moment which is caused in the section by the net upward soil pressure (i.e., column load divided by bearing area) is obtained from simple statics. Figure 6.4 shows such a section *cd* located along the face of the column. The bending moment about *cd* is that caused by the

Scanned with CamScanner

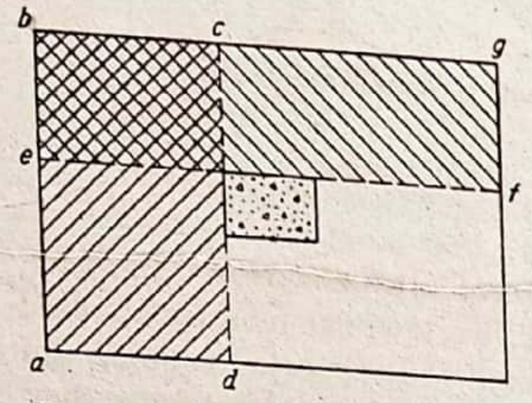


Fig. 6.4 Critical sections for bending and bond.

upward pressure on the area to one side of the section, i.e., the area *abcd*. The reinforcement perpendicular to that section, i.e., the bars running in the long direction, are calculated from this bending moment. Likewise, the moment about section *ef* is caused by the pressure on area *befg*, and the reinforcement in the short direction, i.e., perpendicular to *ef*, is calculated for this bending moment. In footings which support reinforced-concrete columns, these critical sections for bending are located at the faces of the column, as shown.

In footings supporting steel columns, the sections *ab* and *ef* are located, not at the edge of the steel base plate, but halfway between the edge of the column and that of the base plate.

In footings with *pedestals*, the width resisting compression in sections *cd* and *ef* is that of the pedestal; the corresponding depth is the sum of the thicknesses of pedestal and footing. Further sections parallel to *cd* and *ef* are passed at the edge of the pedestal, and the moments determined in the same manner, to check concrete and steel stresses at locations in which the depth is that of the footing only.

For footings with relatively small pedestals, the latter are often discounted in moment and shear computation, and bending is checked at the face of the column, with width and depth equal to that of the footing proper.

In *square footings*, the reinforcement is uniformly distributed over the width of the footing in each of the two layers, i.e., the spacing of the bars is constant. The moments for which the two layers are designed are the same. However, the effective depth d for the upper layer is less by 1 diam than that of the lower layer. Consequently, the required A_s is larger for the upper layer. Instead of using different spacings or different bar diameters in each of the two layers, it is customary to determine A_s for the upper layer and to use the same arrangement of reinforcement for the lower layer.

In *rectangular footings*, the reinforcement in the long direction is again uniformly distributed over the pertinent (shorter) width. In locating the bars in the short direction, one has to consider that the support provided to the footing by the column is concentrated near the middle. Consequently, the curvature of the footing is sharpest, i.e., the moment per foot largest, immediately under the column, and it decreases in the long direction with increasing distance from the column. For this reason

a larger steel area per longitudinal foot is needed in the central portion than near the far ends of the footing. The ACI Code provides, therefore, that:

> In the case of the reinforcement in the short direction that portion [of the reinforcement] determined by Eq. (6.4) shall be uniformly distributed across a band-width (B) centered with respect to the column and having a width equal to the length of the short side of the footing. The remainder of the reinforcement shall be uniformly distributed in the outer portion of the footing.

$$\frac{\text{Reinforcement in band-width } (B)}{\text{Total reinforcement in short direct}} = \frac{2}{(S+1)} \tag{6.4}$$

In Eq. (6.4), S is the ratio of the long side to the short side of the footir

The critical sections for *bond* are the same as those for bending. Bond may also have to be checked at all vertical planes in which changes of section or of reinforcement occur, such as at the edges of pedestals or where part of the reinforcement may be terminated. The shear force to be used for calculating flexural bond is, again, the total upward pressure to one side of the critical section, e.g., the force on the area *abcd* when calculating flexural bond at section *cd*.

b. Shear A column supported by the slab of a simple footing (Fig. 6.5) tends to punch through that slab because of the shear stresses which act in the footing around the perimeter of the column. At the same time the concentrated compression stresses from the column spread out in the footing so that the footing concrete under and adjacent to the column is subject to vertical or somewhat inclined compression, in addition to shear. In consequence, if failure occurs, the fracture takes the shape of the truncated pyramid shown in Fig. 6.5 (or of a truncated cone for round columns), with sides sloping outward at approximately 45°. The average shear stress in the concrete which fails in this manner can

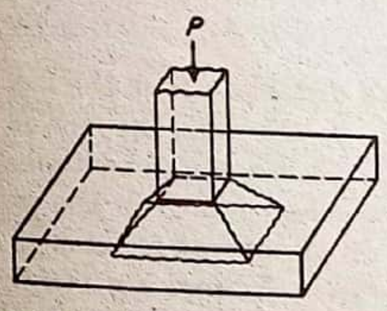


Fig. 6.5 Punching shear failure in single footing.

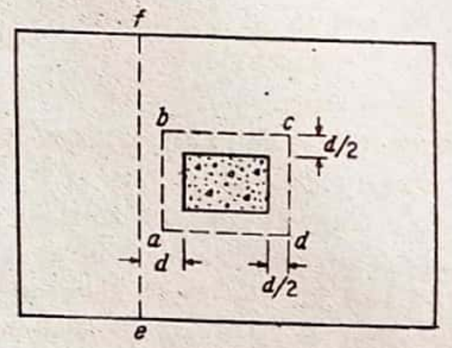


Fig. 6.6 Critical sections for shear.

Scanned with CamScanner

[*Art. 6.6*

be taken as that which acts on vertical planes laid through the footing at a perimeter a distance $d/2$ from the faces of the columns (vertical section through *abcd* in Fig. 6.6). Therefore, the nominal shear stress in the concrete in this critical perimeter section is

$$v = \frac{V}{b_0 d} \tag{6.5}$$

where b_0 = length of perimeter of critical section (*abcd* in Fig. 6.6)
V = shear force acting on that section, i.e., column load minus net upward soil pressure on area *abcd*

In addition to the described shear and vertical compression stresses, horizontal compression stresses caused by the bending moments act above the neutral plane on such a perimeter section. The simultaneous presence of vertical compression spreading out from the column and horizontal compression from bending increases the shear resistance of the concrete (see Art. 1.9). Tests of footings, as well as of flat slabs, have shown, correspondingly, that when a punching-type shear failure occurs the shear stress computed on this perimeter is larger than that in beams or one-way slabs and is approximately equal to $4\sqrt{f'_c}$ (Ref. 6.5). Therefore, the ACI Code stipulates that in ultimate-strength design

$$v_{uc} = \frac{V_u}{b_0 d} \leq 4\phi\sqrt{f'_c} \tag{6.6a}$$

and in working-stress design

$$v_c = \frac{V}{b_0 d} \leq 2\sqrt{f'_c} \tag{6.6b}$$

where V = shear force on perimeter section caused by sum of dead and live loads on column
V_u = sum of dead and live loads multiplied by respective load factors
$\phi = 0.85$

Shear failure can also occur at a section a distance d from the face of the column (such as section *ef* in Fig. 6.6), in the same manner as in beams or one-way slabs. For this reason the Code specifies additionally that shear in sections located at a distance d be checked in the same manner and for the same shear-stress values as in beams. (It will be noticed that these Code provisions for shear in footings are identical with those for slabs supported on columns, such as flat slabs or flat plates; see Art. 4.13.)

The preceding methods for locating the critical sections, both for bending and bond and for shear, are not directly applicable to *footings supporting round columns*, since, in this case, the "face of the column" needs special definition. The ACI Code specifies that for this purpose the face of the columns shall be taken as the side of the square having the same area as the column. The same holds for octagonal columns and for round or octagonal pedestals.

6.7 Transfer of Stress at Base of Column The compressive stress in the longitudinal reinforcement at the base of a reinforced-concrete column is transferred to the footing or pedestal by means of dowels. There should be at least one dowel for each column bar, and the total area of dowels must be at least equal to that of the column bars. The dowels must extend into the footing or pedestal the distance necessary to transfer to the concrete by bond their full working value, i.e., the area of the dowel times the full compression stress allowed on it. The dowels must extend up into the column a distance equal to that required for lapping of longitudinal columns bars; when f'_c is at least 3000 psi, this distance is 20, 24, or 30 diam for steel with specified yield strength of 50,000 psi or less, 60,000, or 75,000 psi, respectively.

When a column rests on a footing or pedestal, it transfers its load only to a part of the total area of the supporting member. The adjacent concrete, which is not under direct load, provides lateral support to the loaded part of the concrete, somewhat analogous to the function of spirals in columns. The permissible bearing stress on such partially loaded areas is, therefore, larger than that permitted in bearing over the full area. The ACI Code specifies the allowable bearing pressure on the full area (such as on the base area of a pedestal) as $0.25f'_c$, and on a partially loaded area (such as the top area of pedestal or footing) as $0.375f'_c$, if the loaded portion is one-third or less of the full area. The allowable stress on an area larger than one-third but less than the full area is obtained by linear interpolation between these two values. If the stress on the bottom surface of a pedestal is larger than $0.25f'_c$, the pedestal must be designed as a reinforced-concrete column. These values are for working-stress design. For ultimate-strength design, 1.9 times these values are to be taken.

6.8 Example: design of a square footing A column 18 in. square, with $f'_c = 4$ ksi, reinforced with eight No. 8 bars of $f_y = 50$ ksi, supports a dead load of 225 kips and a live load of 175 kips. The allowable soil pressure is 5 ksf. Design a square footing with $f'_c = 4$ ksi and $f_y = 50$ ksi. Use ultimate-strength design.

Assume the weight of the footing to be 6 per cent of the column load, or 24 kips; then the required bearing area is $^{42}4\frac{1}{5} = 84.8$ ft². A base 9 ft 3 in. square is selected, furnishing 85.5 ft². With the ultimate-strength load factors, the footing must be designed for a column load $P_u = 1.5 \times 225 + 1.8 \times 175 = 653$ kips. Then the net upward pressure for ultimate-strength design of the footing is $653/85.5 = 7.53$ ksf.

Scanned with CamScanner

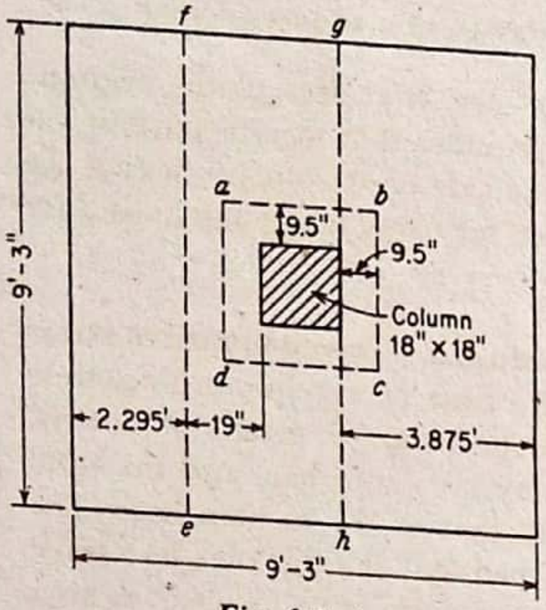


Fig. 6.7

The depth of such footings is usually governed by shear on the critical section *abcd* of Fig. 6.7. After one or two trials, a depth $d = 19$ in. is selected. From Eq. (6.6*a*), the shear stress on this section is not to exceed $4 \times 0.85\sqrt{4000} = 215$ psi. The perimeter length of the critical sections is

$$b_0 = 4(18 + d) = 4(18 + 19) = 148 \text{ in.}$$

and the shear force on this perimeter is the column load minus the net upward pressure on the bearing area located within the perimeter; i.e.,

$$V_u = 653 = (37/12)^2 7.53 = 581 \text{ kips}$$

Therefore, the nominal shear stress on the critical section *abcd* is

$$v_u = \frac{V_u}{b_0 d} = \frac{581{,}000}{148 \times 19} = 207 \text{ psi}$$

This being smaller than the maximum value of 215 psi, the section is adequate for resisting punching shear. It remains to check flexural shear on section *ef* of Fig. 6.7. The distance from that section to the edge is 2.295 ft, so that the nominal shear stress is

$$v_u = \frac{7530 \times 2.295 \times 9.25}{9.25 \times 19} = 76 \text{ psi}$$

The ultimate shear stress to be used in design is the same as in beams; i.e., taking the lower limit and neglecting the influence of moment [Eq. (3.36)],

$$v_c = 2 \times 0.85\sqrt{4000} = 107 \text{ psi}$$

Since this is larger than 76 ksi, section *ef* is adequate in shear.

The moment on section *gh* of Fig. 6.7 is

$$M_u = 7.53 \times 9.25(3.875/2)^2 12 = 628 \text{ in.-kips}$$

The depth required for shear, $d = 19$ in., being greatly in excess of that required for bending, the steel ratio will be low, and the corresponding depth a of the equivalent rectangular stress block small. Assuming it to be $a = 2$ in., the steel area is

$$A_s = \frac{628}{0.9 \times 50(19 - 1)} = 7.75 \text{ in.}^2$$

Checking the depth of the rectangular stress block for this steel area,

$$a = \frac{7.75 \times 50}{0.85 \times 4 \times 9.25 \times 12} = 1.03 \text{ in.}$$

Hence, the lever arm is $c = 19 - 1.03/2 = 18.49$ in. rather than $19 - 1 = 18$ in. as assumed. The error is negligible and on the conservative side, and A_s need not be recomputed. Thirteen No. 7 bars, furnishing 7.82 in.^{2}, will be used in each direction.

The maximum design bond stress is $9.5\sqrt{f'_c}/D = 9.5\sqrt{4000}/0.875 = 685$ psi, and the required development length for No. 7 bars is

$$L_d = \frac{A_s f_y}{u\Sigma_0} = \frac{0.60 \times 50{,}000}{685 \times 2.75} = 15.9 \text{ in.}$$

The actual distance from section *gh* to the end of the bars, assuming 3 in. concrete cover at the ends, is $(3.875 \times 12) - 3 = 43.5$ in. This is greatly in excess of the required development length, and bond is adequate.

For concrete in contact with ground, a minimum cover of 3 in. is required for corrosion protection of the reinforcement. With $d = 19$ in. measured from the top face to the center of the upper layer of No. 7 bars, the total thickness of the footing, in order that 3 in. clear cover for the lower layer be provided, becomes

$$t = 19 + 1.5 \times 0.875 + 3 = 23.2 \text{ in.}$$

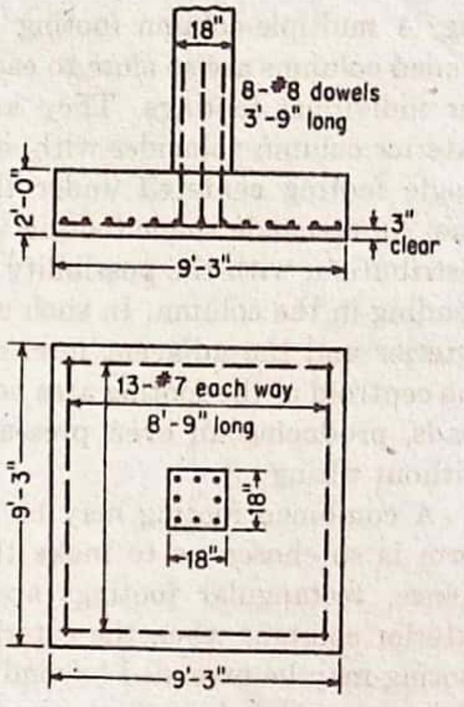


Fig. 6.8

say 24 in. The weight of the footing, $(9.25)^2 2 \times 150 = 25{,}600$ lb, is satisfactorily close to the assumed value of 24,000 lb.

For each of the No. 8 column bars there must be at least one dowel of equal size. With $f_y = 50$ ksi, the dowel must extend at least 24 diam or, for No. 8 bars, 24 in. upward into the column. It must reach downward into the footing at least the full development length. For No. 8 bars the maximum design bond stress is $9.5\sqrt{4000}/1.0 = 600$ psi, and the development length is

$$L_d = \frac{0.79 \times 50{,}000}{600 \times 3.14} = 21 \text{ in.}$$

This can just be accommodated in the 24 in. thickness with 3 in. cover. Had the required development length been greater than the available concrete thickness, a pedestal could have been used, or for each column bar two dowels of smaller diameter could have been provided.

The bearing stress at the interface of column and footing is $653/(18 \times 18) = 2.01$ ksi. This is less than the maximum permissible value of $1.9 \times 0.375 \times 4 = 2.85$ ksi. The footing is shown in Fig. 6.8.

6.9 Multiple-column Footings It is sometimes desirable and quite frequently necessary to support more than one column on the same foot-

Scanned with CamScanner

ing. A multiple-column footing is necessary when two or more heavily loaded columns are so close to each other that there is not sufficient space for individual footings. They are also necessary when the face of an exterior column coincides with, or is close to, the property line so that a single footing centered under the column would project beyond that line. An eccentric single footing would result in unequal bearing-pressure distribution, with the possibility of tilting of the footing and consequent bending in the column. In such cases a combined footing, supporting the exterior and the adjacent interior column, can be so proportioned that the centroid of the footing area coincides with the resultant of the column loads, producing an even pressure distribution and uniform settlement without tilting.

A combined footing may be rectangular in plan or trapezoidal. The form is so chosen as to make the centroid and the resultant coincide. Hence, rectangular footings are suitable for interior columns, or for exterior columns when the exterior column has the lighter load and the footing may be extended beyond the interior column as far as necessary. The trapezoidal shape is required if column loads are unequal and if, for any reason, the footing cannot extend any appreciable distance beyond the heavier column.

Another expedient that is used if an independent footing cannot be centered under an exterior column is to place the exterior-column footing eccentrically and to connect it with the nearest interior-column footing by a beam or strap poured monolithically with both footings. This beam, which is counterweighted by the interior-column load, resists the tilting tendency of the eccentric exterior footing and equalizes the pressure under it. Such constructions are known as *strap*, *cantilever*, or *connected* footings.

6.10 Example: design of a combined footing supporting one exterior and one interior column An exterior 24 × 18 in. column with a total load of 200,000 lb and an interior 24 × 24 in. column with a total load of 300,000 lb are to be supported on a combined rectangular footing whose exterior cannot protrude beyond the outer face of the exterior column (see Fig. 6.1). The distance center to center of columns is 18 ft 0 in., and the allowable soil pressure is 4000 psf. Use working-stress design for a concrete with $f'_c = 3000$ psi and a steel with allowable stress $f_s = 20{,}000$ psi.

It is difficult to estimate the weights of footings of this type. The bearing area, as in single footings, depends only on the column loads and the bearing pressure. The depth, however, is often governed by the longitudinal bending moment, which increases rapidly with increasing distance between columns. Hence, for equal column loads and bearing pressures, larger column spacings result in heavier footings. As a crude rule, 6 to 15 per cent of the combined column loads can be taken as the approximate weight of such footings. In the present case, since the column spacing is relatively large and the bearing capacity

rather low, the footing weight will be assumed as 12 per cent of the column loads, or 60,000 lb. The required bearing area is then 560,000/4000 = 140 ft².

In order to secure uniform soil pressure, the centroid of the bearing area must coincide with the resultant of the column loads. The latter is located at a distance of 300,000 × 18/500,000 = 10.8 ft from the center of the exterior column. The length of the footing must be

$$2(10.8 + 0.75) = 23.1 \text{ ft}$$

A length of 23 ft 3 in. is selected. The required width is then

$$140/23.25 = 6.0 \text{ ft}$$

(see Fig. 6.10).

Longitudinally, the footing represents an upward-loaded beam spanning between columns and cantilevering beyond the interior column. Since this beam is considerably wider than the columns, the column loads are distributed crosswise by transverse beams, one under each column. In the present relatively narrow and long footing it will be found that the required minimum depth for the transverse beams is smaller than is required for the footing in the longitudinal direction. These "beams," therefore, are not really distinct members, but merely represent transverse strips in the main body of the footing, so reinforced that they are capable of resisting the transverse bending moments and the corresponding shears. It then becomes necessary to decide how large the effective width of this transverse beam can be assumed to be. Obviously, the strip directly under the column does not deflect independently and is strengthened by the adjacent parts of the footing. The effective width of the transverse beams is, therefore, evidently larger than that of the column, but cannot be taken as very much larger since the column load must be able to distribute itself reasonably uniformly over the entire width of the beam. In the absence of definite rules for this case, or research results on which to base such rules, the authors recommend that the effective width of such an integral, transverse beam be determined in the following manner: The effective width shall be equal to that of the column plus, on either side of the column, a strip of width equal to one-half that of the column or to one-half the depth of the footing, whichever is smaller. (This rule assumes that the load from the column will spread at an angle of about 30° with the vertical, a rather conservative assumption.)

Design in longitudinal direction The net upward pressure per longitudinal foot is 500,000/23.25 = 21,500 lb per ft. The maximum negative moment between the columns occurs at the section of zero shear. Let x be the distance from the outer edge of the exterior column to this section. Then (see Fig. 6.9)

$$V = 21{,}500x - 200{,}000 = 0$$

results in $x = 9.32$ ft. The moment at this section is

$$M = [21{,}500 \times 9.32^2/2 - 200{,}000(9.32 - 0.75)]12 = -9{,}360{,}000 \text{ in.-lb}$$

The moment at the right edge of the interior column is

$$M = 21{,}500(3.5^2/2)12 = 1{,}575{,}000 \text{ in.-lb}$$

and the details of the moment diagram are as shown in Fig. 6.9.

Scanned with CamScanner

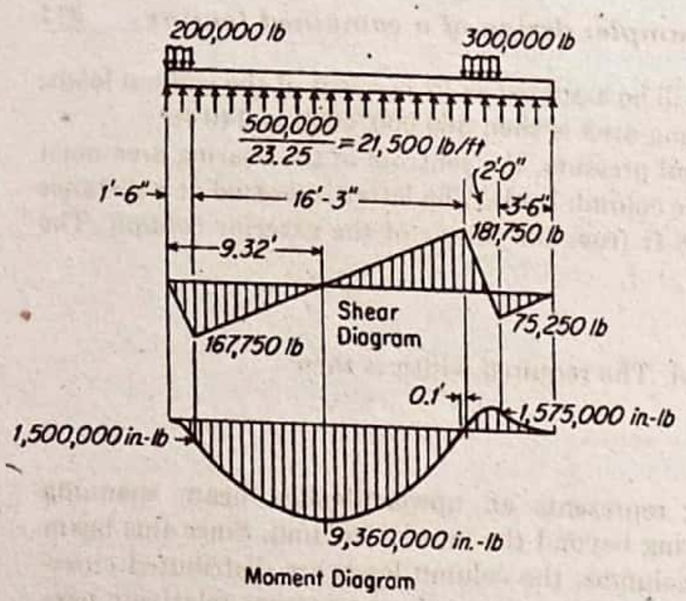


Fig. 6.9

The minimum depth of the footing is that necessary to accommodate the maximum moment without resort to compression reinforcement. With $K = 223$ (see Table 4, Appendix B),

$$d = \sqrt{\frac{9{,}360{,}000}{223 \times 72}} = 24.1 \text{ in.}$$

Trial calculations show that a larger depth is required for shear unless web reinforcement is employed. For footings it is usually more economical to increase d than to resort to web reinforcement. It is found that a depth $d = 28.5$ in. is adequate for that purpose.

From the shear diagram of Fig. 6.9 it is seen that the critical section for flexural shear is at a distance d to the left of the left face of the interior column. At that point, the shear force is

$$V = 181{,}750 - (28.5/12)21{,}500 = 129{,}600 \text{ lb}$$

and the shear stress is

$$v = \frac{129{,}600}{72 \times 28.5} = 63.2 \text{ psi}$$

The allowable shear stress (see Table 3.2) is $v_c = 60$ psi, unless use is made of the more liberal provision of Eq. (3.39). With the latter, the moment at the critical shear section is easily computed to be 450,000 ft-lb. Assuming $p_w = 0.01$ (to be checked later), Eq. (3.39) gives an allowable stress

$$v_c = \sqrt{3000} + 1300\,\frac{0.01 \times 129{,}500(28.5/12)}{450{,}000} = 63.7 \text{ psi}$$

indicating that $d = 28.5$ is adequate.

Additionally, as in single footings, punching shear should be checked on a perimeter section a distance $d/2$ around the column, for which the allowable

shear stress, from Eq. (6.6*b*), is $v_c = 2\sqrt{3000} = 109.5$ psi. Of the two columns, the exterior one with a three-sided perimeter a distance $d/2$ from the column is more critical in regard to this "punching shear." The perimeter is

$$b_0 = 2\left(1.5 + \frac{28.5/12}{2}\right) + (2.0 + 28.5/12) = 9.76 \text{ ft}$$

and the shear force, being the column load minus the soil pressure within the perimeter, is

$$V = 200{,}000 - 2.69 \times 4.38(21{,}500/6) = 157{,}700 \text{ lb}$$

Consequently, the shear stress on the perimeter section is

$$v = \frac{157{,}700}{9.76 \times 12 \times 28.5} = 47.2 \text{ psi}$$

considerably less than the allowable value.

With $d = 28.5$ in., and with 3.5-in. insulation from the center of the bars to the top surface of the footing, the total thickness is 32 in., and its weight is 55,700 lb, which agrees closely with the assumed value.

For the negative moment in the span between the columns, the required steel area is

$$A_s = \frac{9{,}360{,}000}{20{,}000 \times \frac{7}{8} \times 28.5} = 18.8 \text{ in.}^2$$

Fifteen No. 10 bars furnish $A_s = 20.25$ in.^{2} This represents a steel ratio $p = (20.25/72)28.5 = 0.0099$, very close to the value 0.01 assumed for calculating the allowable flexural shear stress from Eq. (3.39). The allowable bond stress for a No. 10 top bar is $3.4\sqrt{3000}/1.27 = 147$ psi, and the corresponding development length is

$$L_d = \frac{1.27 \times 20{,}000}{3.99 \times 147} = 43.5 \text{ in.} = 3.62 \text{ ft}$$

From Fig. 6.9, the distance from the point of maximum moment to the nearer left end of the bars is seen to be $9.32 - \frac{3}{12} = 9.07$ ft, much larger than the required minimum development length. The selected reinforcement is therefore adequate for both bending and bond.

For the portion of the longitudinal beam which cantilevers beyond the interior column,

$$A_s = \frac{1{,}575{,}000}{20{,}000 \times \frac{7}{8} \times 28.5} = 3.15 \text{ in.}^2$$

Eight No. 6 bars, with $A_s = 3.53$ in.^{2}, are selected, and their development length, computed as above but for bottom bars, is found adequate.

Design of transverse beam under interior column The width of the transverse beam under the interior column can now be established by the previously discussed rules to be $24 + 2 \times 12 = 48$ in. The net upward load per

Scanned with CamScanner

linear foot of the transverse beam is 300,000/6 = 50,000 lb per ft. The moment at the edge of the interior column is

$$M = 50{,}000(2^2/2)12 = 1{,}200{,}000 \text{ in.-lb}$$

Since the effective width of the transverse beam was determined as 48 in., the required depth is

$$d = \sqrt{\frac{1{,}200{,}000}{48 \times 223}} = 10.6 \text{ in.}$$

Since the transverse bars are placed on top of the longitudinal bars (see Fig. 6.10), the actual value of d furnished is, to the nearest quarter inch, 28.5 − 0.75 = 27.75 in. Then

$$A_s = \frac{1{,}200{,}000}{20{,}000 \times 0.9 \times 27.75} = 2.40 \text{ in.}^2$$

Seven No. 6 bars are selected and placed within the 48 in. effective width of the transverse beam, at a spacing of about 8 in. They are checked for bond, and it is found that their minimum development length L_d is considerably shorter than the distance from the edge of the column to the end of the bar.

Punching shear at the perimeter a distance $d/2$ from the column has been checked before. The critical section for regular flexural shear, at a distance d from the face of the column, lies beyond the edge of the footing, and, therefore, no further check on shear is needed.

The design of the transverse beam under the exterior column is the same as the design of that under the interior column, except that the effective width is 27 in. The details of the calculations are not shown. It will be easily checked that five No. 6 bars, placed within the 27 in. effective width, satisfy all requirements. Design details are shown in Fig. 6.10.

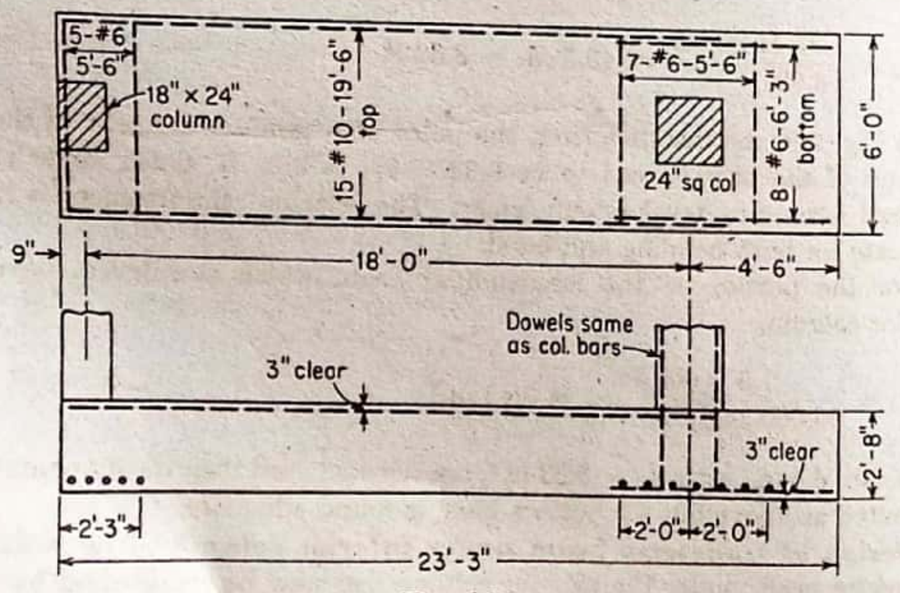


Fig. 6.10

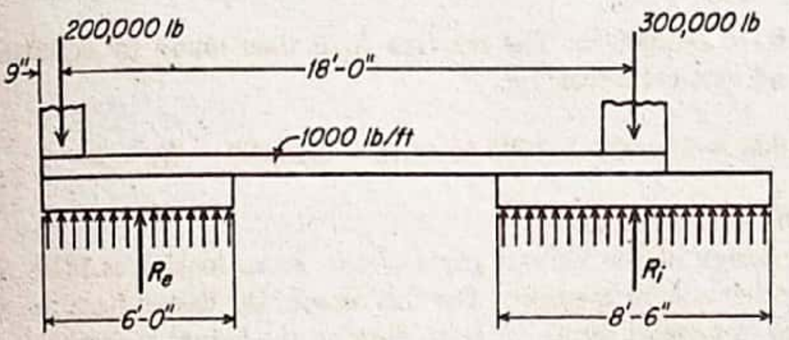


Fig. 6.11

6.11 Design of a Strap Footing In a strap or connected footing, the exterior footing is placed eccentrically under its column, in order that it does not project beyond the property line. Such a position would result in an uneven distribution of the bearing pressure and tipping of the footing. To counteract this tendency, the footing is connected by a beam or strap to the nearest interior footing.

The footing areas are so proportioned that the pressure under each of them is uniform and is the same under both footings. To achieve this, it is necessary, as in other combined footings, that the centroid of the combined area of the two footings coincide with the resultant of the column loads. The strap proper is generally constructed in such a manner that it will not bear directly on the soil.

To illustrate this design, the columns of Art. 6.10 will be so supported. Connected footings for larger column distances generally require less concrete than rectangular footings. Therefore the combined weight will be assumed to be 0.08(300,000 + 200,000) = 40,000 lb. The total required bearing area is 540,000/4000 = 135 ft².

In Art. 6.10 the resultant of the column loads was found to be located 10.8 ft from the center of the exterior column, or 11.55 ft from the exterior face of that column. To distribute the two footing areas so that their total will add up to the required 135 ft² and their centroid will be located at 11.55 ft from the outer edge requires several trial computations. The arrangement shown in Fig. 6.12 was determined by such trials and provides exactly 135 ft² of area. Its centroid is located at a distance $\bar{x} = (72 \times 18.75 + 63 \times 3.0)/135 = 11.40$ ft from the outer edge, which only insignificantly differs from 11.55 ft.

To compute the moments and shears in the various parts of the connected footings, it is first necessary to determine the intensity and location of all external forces and reactions. These are shown in Fig. 6.11. Since the footing areas are so arranged that the pressure on each of them is uniform, the resultants of these net pressures, R_e and R_i, act at the centers of the respective footings. Assuming the weight of the strap to be 1000 lb per ft, R_e is found by equating to zero the moments about the center line of the interior column; i.e.,

$$200{,}000 \times 18.0 + 1000 \times 18.75^2/2 - R_e \times 15.75 = 0$$

Scanned with CamScanner

Hence $R_e = 240{,}000$ lb. The reaction R_i is then found by equating to zero the sum of all vertical forces; i.e.,

$$200{,}000 + 300{,}000 + 1000 \times 18.75 - 240{,}000 - R_i = 0$$

Hence $R_i = 278{,}750$ lb.

The design of the various parts of this strap footing is little different from that of other similar members. For this reason, the design features will merely be discussed in general terms, without showing the actual computations.

Design of strap The strap represents a single-span beam loaded upward by the loads transferred to it by the two footings and supported by downward reactions at the center lines of the two columns. Thus, the upward load in the portion from the exterior edge to a point 6 ft from that edge is simply 240,000/6 = 40,000 lb per ft. A width of $b = 28$ in. is selected. For a column width of 24 in. this permits placing of beam and column bars where the two members intersect and allows the column forms to be supported on the top surface of the strap. With this width, the maximum moment determines the required depth of the strap. The location of maximum moment is determined by equating the shear force to zero and is found to be located 5.13 ft from the exterior edge. The moment decreases toward the interior column and is zero at the center line of that column. Hence, half the strap reinforcement is discontinued where no longer needed, and the other half is carried through the interior column.

In the portion of the strap immediately adjacent to the exterior column, the shear force is larger than that which can be resisted by the concrete alone. Web reinforcement is placed in this region; in view of the large width of the beam, it takes the form of double-looped stirrups (see Fig. 6.12).

Design of footings The *exterior footing* performs exactly like a wall footing of 6-ft length. Even though the column is located at its edge, the balancing action of the strap is such as to transmit the total reaction $R_e = 240{,}000$ lb uniformly over the 6-ft length, thus resulting in the desired uniform soil pressure. The design is carried out exactly as for a wall footing (see Art. 6.4).

The interior footing is loaded in a manner which makes it perform like a square single-column footing (see Arts. 6.6 and 6.8). The main difference is that, because of the presence of the strap, punching cannot occur along the truncated cone surfaces of Fig. 6.5. For this reason, punching shear [according to Eqs. (6.6)] should be checked along a perimeter section located at a distance $d/2$ outward from the longitudinal edges of the strap and from the free face of the column. Flexural shear, as usual, is checked at a distance d from the face of the column.

The weight of this strap footing is 44,700 lb, sufficiently close to the assumed value of 40,000 lb. It is interesting to compare this value with the weight of the combined footing designed in Art. 6.10 for the same situation. This weight was 55,700 lb, or about 25 per cent more than that of the strap footing. The actual saving in using the latter will be somewhat smaller than 25 per cent, since the steel ratio in the strap footing is larger than that in the combined footing, and somewhat more complex formwork is required for the former. Even so, the saving is substantial and would be even larger for greater distances between the two columns.

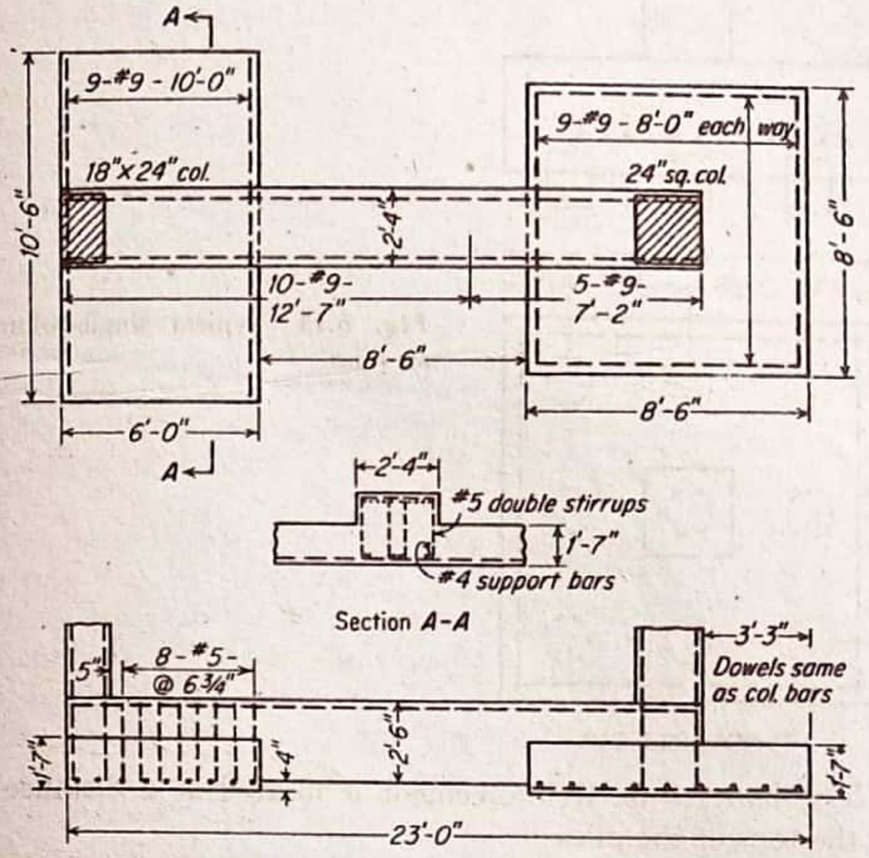


Fig. 6.12

Complete details are shown in Fig. 6.12. The bottom of the strap has been located 4 in. above the bottom of the footings. This permits the bottom planks of the strap forms to be placed on wedges, so that they can be withdrawn after the concrete has hardened. This prevents direct bearing of the strap on soil. Depending on soil conditions, additional stirrups and longitudinal reinforcement at the bottom of the strap may be placed to guard against unforeseen shears and reverse moments due to possible uneven settlement.

6.12 Footings on Piles If soil conditions require the use of piles, these are usually driven in clusters, one to each column, and the load is transferred from the column to the piles by a footing. The design of such pile-supported footings is not much different from that of footings resting directly on soil, except for some special features.

The size of the footing is determined by the required number of piles and by the spacing between them, which usually, for friction piles, is not less than 3 ft for concrete piles or 2.5 ft for timber or H piles. End-bearing piles are sometimes driven at closer distances. The tops of the piles must be securely embedded in the footing. For this purpose the bottom of the footing is located not less than 6 in. below the top of the piles, and the distance from the center of outside piles to the edge of the footing is not

Scanned with CamScanner

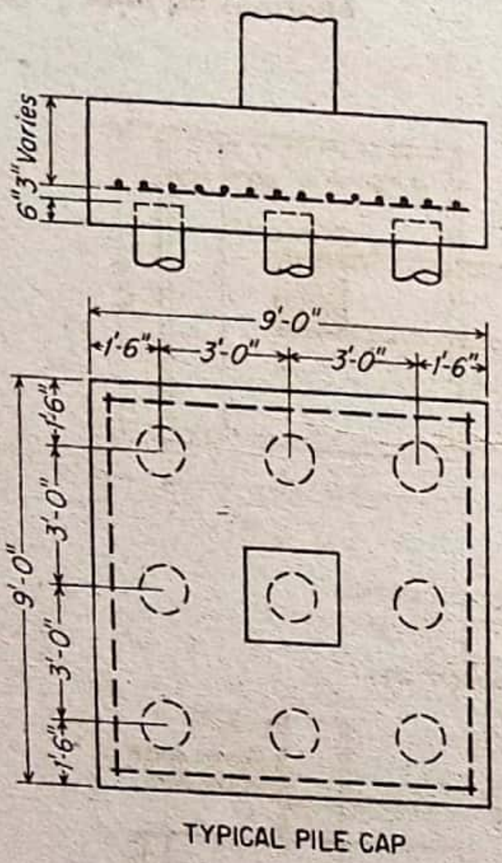


Fig. 6.13 Typical single-column footing on piles.

made less than 1.5 ft. Reinforcement is located at a distance of 3 in. above the tops of the piles.

Occasionally, individual piles are not driven to the design depth, with the result that their tops remain above the planned elevation. Under no circumstances should the footing reinforcement in such cases be bent around the protruding pile. If this were done, the smaller depth of concrete left above the top of such a pile and the complete absence of reinforcement above it would make it possible for the pile to punch through the footing. For this reason such piles must be cut to the required elevation before the footing is poured.

In designing the footing, the load from the column is assumed to be uniformly distributed to all piles in the cluster. For this purpose piles must be arranged symmetrically about the axis of the column. The net load per pile, i.e., the column load divided by the number of piles, is then assumed to act as an upward load on the footing, concentrated at the center of the pile.

The critical sections for moment and bond are the same as for footings resting on soil.

While for bending computations the pile reactions are assumed to be concentrated at the pile centers, in computing shear forces account is taken of the fact that these reactions are actually distributed over the bearing area of the pile. The fact that shear is usually the critical feature which determines the depth of a footing is the reason for the greater refinement in this determination. It is obviously unrealistic to assume

that if the center of a pile is located 1 in. inside the critical section it will not produce any shear on that section, while, if it is located 1 in. outside, its full value will contribute to the shear. Correspondingly, the ACI Code stipulates:

> In computing the external shear, the entire reaction from any pile whose center is located 6 in. or more outside the section shall be assumed as producing shear on the section; the reaction from any pile whose center is located 6 in. or more inside the section shall be assumed as producing no shear on the section. For intermediate positions of the pile center, the portion of the pile reaction to be assumed as producing shear on the section shall be based on straight line interpolation between full value at 6 in. outside the section and zero value at 6 in. inside the section.

Actual pile positions frequently differ from assigned locations. On occasion this happens even with careful construction supervision and workmanship, particularly in irregular soils in which boulders and other obstructions may deflect piles during driving. Such off-location piles may produce moments and shears significantly in excess of the computed values. By the above-quoted rule, unfavorable pile displacements as small as 1 ft may change the shear on the section by an amount equal to the total pile reaction. Pile footings for soils in which such displacements are likely to occur should, therefore, be designed conservatively, that is, with unit stresses considerably below the stipulated values. By this means a strength reserve is created which is available in case actual moments and shears exceed the values computed for perfect pile location. Details of a typical footing on piles are shown in Fig. 6.13.

REFERENCES

6.1 A. N. Talbot: "Reinforced Concrete Wall Footings and Column Footings," *Univ. Illinois Eng. Exp. Sta. Bull.* 67, March, 1913.

6.2 F. E. Richart: Reinforced Concrete Wall and Column Footings, *J. ACI*, vol. 45, pp. 97, 237, 1948.

6.3 E. Hognestad: Shearing Strength of Reinforced Column Footings, *J. ACI*, vol. 50, p. 189, 1953.

6.4 J. Moe: Shearing Strength of Reinforced Concrete Slabs and Footings under Concentrated Loads, *Portland Cement Assoc. Res. Develop. Lab. Dep. Develop. Bull.* D47.

6.5 "Shear and Diagonal Tension," part 3, Slabs and Footings, Report of ACI-ASCE Committee 326, *J. ACI*, vol. 59, p. 353, 1962.

Scanned with CamScanner

chapter 7

RETAINING WALLS

7.1 Function and Types of Retaining Walls Retaining walls are used to hold back masses of earth or other loose material where conditions make it impossible to let those masses assume their natural slopes. Such conditions occur when the width of an excavation, cut, or embankment is restricted by conditions of ownership, use of the structure, or economy. Thus, in railway or highway construction the width of the right of way is fixed, and the cut or embankment must be contained within that width. Similarly, the basement walls of buildings must be located within the property and must retain the soil surrounding the basement.

Free-standing retaining walls, as distinct from those which form parts of structures, such as basement walls, are of various types, the most common of which are shown in Fig. 7.1. The gravity wall (Fig. 7.1*a*) retains the earth entirely by its own weight. The reinforced-concrete cantilever wall (Fig. 7.1*b*) consists of the vertical arm which retains the earth and

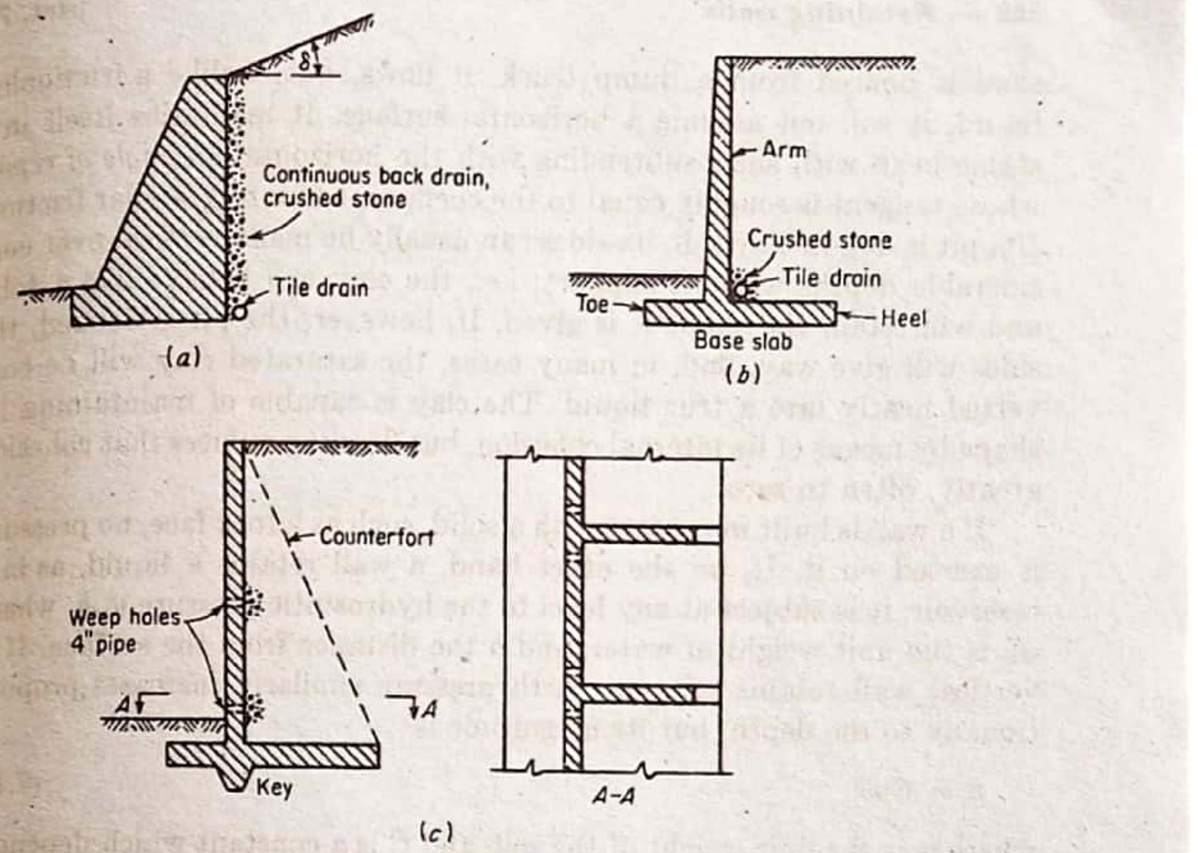


Fig. 7.1 Types of retaining walls and backdrains: (*a*) gravity wall; (*b*) cantilever wall; (*c*) counterfort wall.

is held in position by the footing or base slab. In this case the weight of the fill on top of the heel, in addition to the weight of the wall, contributes to the stability of the structure. Since the arm represents a vertical cantilever, its required thickness increases rapidly with increasing height. To reduce the bending moments in vertical walls of great height, counterforts are used spaced at distances from each other equal to or slightly larger than one-third of the height (Fig. 7.1*c*). Property rights or other restrictions sometimes make it necessary to place the wall at the forward edge of the base slab, i.e., to omit the toe. Wherever it is possible, toe extensions of one-third to one-fourth of the width of the base provide a more economical solution.

Which of the three types of walls is appropriate in a given case depends on a variety of conditions, such as local availability and price of construction materials and property rights. In general, gravity walls are economical only for relatively low walls, possibly up to about 15 ft. Cantilever walls are economical for heights from 10 to 20 ft, while counterforts are indicated for greater heights.

7.2 Earth Pressure In their physical behavior soils and other granular masses occupy a position intermediate between liquids and solids. If

Scanned with CamScanner

sand is poured from a dump truck, it flows, but, unlike a frictionless liquid, it will not assume a horizontal surface. It maintains itself in a stable heap with sides subtending with the horizontal an *angle of repose* whose tangent is roughly equal to the coefficient of intergranular friction. If a pit is dug in clay soil, its sides can usually be made vertical over considerable depths without support; i.e., the clay will behave like a solid and will retain the shape it is given. If, however, the pit is flooded, the sides will give way, and, in many cases, the saturated clay will be converted nearly into a true liquid. The clay is capable of maintaining its shape by means of its internal cohesion, but flooding reduces that cohesion greatly, often to zero.

If a wall is built in contact with a solid, such as a rock face, no pressure is exerted on it. If, on the other hand, a wall retains a liquid, as in a reservoir, it is subject at any level to the hydrostatic pressure $w_w h$, where w_w is the unit weight of water, and h the distance from the surface. If a vertical wall retains soil, the earth pressure similarly increases proportionally to the depth, but its magnitude is

$$p = Cwh \tag{7.1}$$

where w is the unit weight of the soil, and C is a constant which depends on the physical characteristics of the soil.

The pressure which soil exerts on an immovable wall, known as the *rest pressure*, has not been investigated thoroughly. The few measurements that have been made seem to indicate that in this case $C = 0.4$ to 0.5 for uncompacted, noncohesive soils, such as sands and gravels, while it may be as high as 0.8 for the same soils in a highly compacted state. For cohesive clay soils, C appears to be of the order of 0.7 to 1.0.

Usually, however, walls move slightly under the action of the earth pressure. Since walls are constructed of elastic material, they deflect under the action of the pressure, and since they generally rest on compressible soils, they tilt and shift away from the fill. For this reason, the wall is often constructed with a slight batter toward the fill on the exposed face, so that, if and when such tilting takes place, it does not appear evident to the observer. Even if this movement at the top of the wall is only of the order of a fraction of a per cent of the wall height ($\frac{1}{2}$ to $\frac{1}{10}$ per cent according to tests by C. Terzaghi), the rest pressure is materially decreased by it. The magnitude of this pressure against slightly yielding walls is much better explored and known than the rest pressure

If the wall moves away from the fill, a sliding plane ab (Fig. 7.2) forms in the soil mass, and the wedge abc, sliding along that plane, exerts pressure against the wall. Here the angle ϕ is known as the *angle of internal friction;* i.e., its tangent is equal to the coefficient of intergranular friction, which can be determined by appropriate laboratory tests. The corresponding pressure is known as the *active earth pressure*. If, on the other hand, the wall is pushed against the fill, a sliding plane ad is formed, and the wedge acd is pushed upward by the wall along that plane. The pressure which this larger wedge exerts against the wall is known as the *passive earth pressure*. (This latter case will occur, for example, at the left face of the gravity wall of Fig. 7.1 when this wall yields slightly to the left under the pressure of the fill.)

The magnitude of these pressures has been analyzed by Rankine, Coulomb, and others. If the soil surface subtends an angle δ with the horizontal (Fig. 7.1a), then, according to Rankine, the coefficient for active earth pressure is

$$C_a = \cos\delta \frac{\cos\delta - \sqrt{\cos^2\delta - \cos^2\phi}}{\cos\delta + \sqrt{\cos^2\delta - \cos^2\phi}} \tag{7.2}$$

and that for passive pressure is

$$C_p = \cos\delta \frac{\cos\delta + \sqrt{\cos^2\delta - \cos^2\phi}}{\cos\delta - \sqrt{\cos^2\delta - \cos^2\phi}} \tag{7.3}$$

For the frequent case of horizontal surface, that is, $\delta = 0$ (Fig. 7.2), for active pressure,

$$C_{ah} = \frac{1 - \sin\phi}{1 + \sin\phi} \tag{7.4}$$

and for passive pressure,

$$C_{ph} = \frac{1 + \sin\phi}{1 - \sin\phi} \tag{7.5}$$

Rankine's theory is valid only for noncohesive soils such as sand and gravel but, with corresponding adjustments, can also be used successfully for cohesive clay soils.

From Eqs. (7.1) to (7.5) it is seen that the earth pressure at a given depth h depends on the inclination of the surface δ, the unit weight w, and the angle of friction ϕ. The first two of these are easily determined, while little agreement has yet been reached as to the proper values of ϕ. For the ideal case of a dry, noncohesive fill, ϕ could be determined by

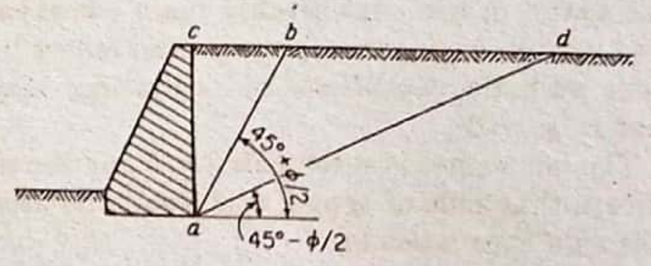


Fig. 7.2

Scanned with CamScanner

laboratory test and then used in the formulas. This is impossible for clays, only part of whose resistance is furnished by intergranular friction while the rest is due to internal cohesion. For this reason their actual ϕ values are often increased by an arbitrary amount to account implicitly for the added cohesion. However, this is often unsafe since, as was shown by the example of the flooded pit, cohesion may vanish almost completely due to saturation and inundation.

In addition, fills behind retaining walls are rarely uniform, and, what is more important, they are rarely dry. Proper drainage of the fill is vitally important to reduce pressures (see Art. 7.5), but even in a well-drained fill the pressure will temporarily increase during heavy storms or sudden thaws. This is due to the fact that even though the drainage may successfully remove the water as fast as it appears, its movement through the fill toward the drains causes additional pressure (seepage pressure). In addition, frost action and other influences may temporarily increase its value over that of the theoretical active pressure. Many walls which were designed without regard to these factors have failed, been displaced, or cracked.

It is good practice, therefore, to select conservative values for ϕ, considerably smaller than the actual test values, in all cases except where extraordinary and usually expensive precautions are taken to keep the fill dry under all conditions. An example of recommended earth-pressure values, which are quite conservative though based on extensive research and practical experience, can be found in Ref. 7.1. Less conservative values are often used in practical designs, but these should be employed with caution in view of the fact that occasional trouble has been encountered with walls so designed.

Table 7.1 gives average values for w and two columns of values for ϕ. The first of these has been adapted by the authors from the information of Ref. 7.1; the second represents magnitudes which are frequently used in engineering practice and, at least for noncohesive soils, are closer to the actual laboratory test values. In contrast to the first, however, these take no account of probable additional pressures due to porewater, seepage, frost, etc. The table also contains values for the coefficient of friction f between concrete and various soils.

It is seen that the values of ϕ according to Ref. 7.1, particularly for soils 4 and 5, are considerably more conservative than the values of ϕ often used in engineering practice and reflect the fact that clays and silts, under suitable conditions of saturation, may become entirely liquid (that is, $\phi = 0$).

The low values of ϕ for soils 3 to 5 and the resulting high soil pressures indicate that soils of type 1 or 2 should be used for backfills of retaining walls wherever possible.

Table 7.1 **Unit weights, effective angles of internal friction ϕ, and coefficients of friction with concrete, f**

Soil*	Unit weight, pcf	ϕ*	ϕ†	f
1. Sand or gravel without fine particles, highly permeable	110–120	35°	33–40°	0.5–0.6
2. Sand or gravel with silt mixture, low permeability	120–130	32°	25–35°	0.4–0.5
3. Silty sand, sand and gravel with high clay content	110–120	26°	23–30°	0.3–0.4
4. Medium or stiff clay	100–120	0‡	25–35°	0.25–0.4
5. Soft clay, silt	90–110	0°	20–25°	0.2–0.3

* Adapted from Ref. 7.1.
† Values often used.
‡ For this case the distance ($h - 4$ ft) should be used instead of h in Eq. (7.1).

7.3 Earth Pressure for Common Conditions of Loading In computing earth pressures on walls, three common conditions of loading are most often met: (1) horizontal surface of fill at the top of the wall, (2) inclined surface of fill sloping up and back from the top of the wall, and (3) horizontal surface of fill carrying a uniformly distributed additional load (surcharge) such as from goods in a storage yard or traffic on a road.

The increase in pressure caused by uniform surcharge s (case 3) is computed by converting its load into an equivalent, imaginary height of earth h' above the top of the wall such that

$$h' = \frac{s}{w} \tag{7.6}$$

and measuring the depth to a given point on the wall from this imaginary surface. This amounts to replacing h with $(h + h')$ in Eq. (7.1).

The distributions of pressure for cases 1 to 3 are shown in Fig. 7.3. The total earth thrust P per linear foot of wall is evidently equal to the area under the pressure-distribution figure, and its line of action passes through the centroid of the pressure. Figure 7.3 gives information, computed in this manner, on magnitude, point of action, and direction of P for these three cases.

Occasionally retaining walls must be built for conditions in which the ground-water level is above the base of the wall, either permanently or seasonally. In that case the pressure of the soil *above* ground water is determined as usual. The part of the wall *below* ground water is subject to the sum of the water pressure and the earth pressure. The former is equal to the full hydrostatic pressure $p_w = w_w h_w$, where w_w and h_w are, respectively, the unit weight of water and the distance from ground-

Scanned with CamScanner

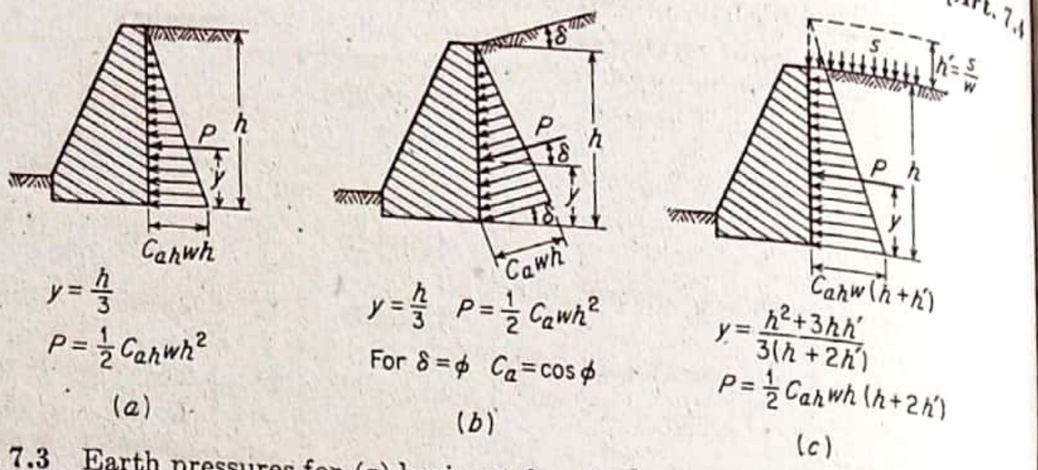


***Fig.* 7.3** Earth pressures for (*a*) horizontal surface; (*b*) sloping surface; (*c*) horizontal surface with surcharge *s*.

water level to the point on the wall. The additional pressure of the soil below ground-water level is computed from Eq. (7.1), where, however, for the portion of the soil below water, w is replaced with $w - w_w$, while h, as usual, is measured from the soil surface. That is, for submerged soil, buoyancy reduces the effective weight in the indicated manner. Pressures of this magnitude, which are considerably larger than those of drained soil, will also occur temporarily after heavy rainstorms or thaws in walls without provision for drainage, or if drains have become clogged.

The seeming simplicity of the determination of earth pressure as here indicated should not lull the designer into a false sense of security and certainty. No theory is more accurate than the assumptions on which it is based. Actual soil pressures are affected by irregularities of soil properties, porewater and drainage conditions, and climatic and other factors which cannot be expressed in formulas. This situation, on the one hand, indicates that involved refinements of theoretical earth-pressure determinations, as sometimes attempted, are of little practical value. On the other hand, the design of a retaining wall is seldom a routine procedure, since the local conditions that affect pressures and safety vary from one locality to another.

7.4 External Stability A wall may fail in two different ways: (1) its individual parts may not be strong enough to resist the acting forces, such as when a vertical cantilever wall is cracked by the earth pressure acting on it, and (2) the wall as a whole may be bodily displaced by the earth pressure, without breaking up internally. To design against the first possibility requires the determination of the necessary dimensions, thicknesses, reinforcements, etc., to resist the moments and shears; this procedure, then, is in no way different from that of determining required dimensions and reinforcements of other types of concrete structures. To

safeguard the wall against bodily displacements, on the other hand, i.e., to ensure its external stability, requires special consideration.

A wall, such as that of Fig. 7.4, together with the soil mass *ijkl* which rests on the base slab, may be bodily displaced by the earth thrust P which acts on plane *ak* by *sliding* along the plane *ab*. Such sliding is resisted by the friction between soil and footing along the same plane. To forestall motion, the forces that resist sliding must exceed those that tend to produce sliding; a factor of safety of 1.5 is generally assumed satisfactory in this connection.

In Fig. 7.4, the force that tends to produce sliding is the horizontal component P_h of the total earth thrust P. The resisting friction force is fR_v, where f is the coefficient of friction between concrete and soil (see Table 7.1), and R_v is the vertical component of the total resultant R; that is, $R_v = W + P_v$. (W = weight of wall plus soil resting on the footing, P_v = vertical component of P.) Hence, to provide sufficient safety,

$$f(W + P_v) \geqq 1.5P_h \tag{7.7}$$

Actually, for the wall to slide to the left, it must push with it the earth *nmb*, which gives rise to the passive earth pressure indicated by the triangle *rmb*. This passive pressure represents a further resisting force which could be added to the left side of Eq. (7.7). However, this should be done only if the proper functioning of this added resistance is ensured. For

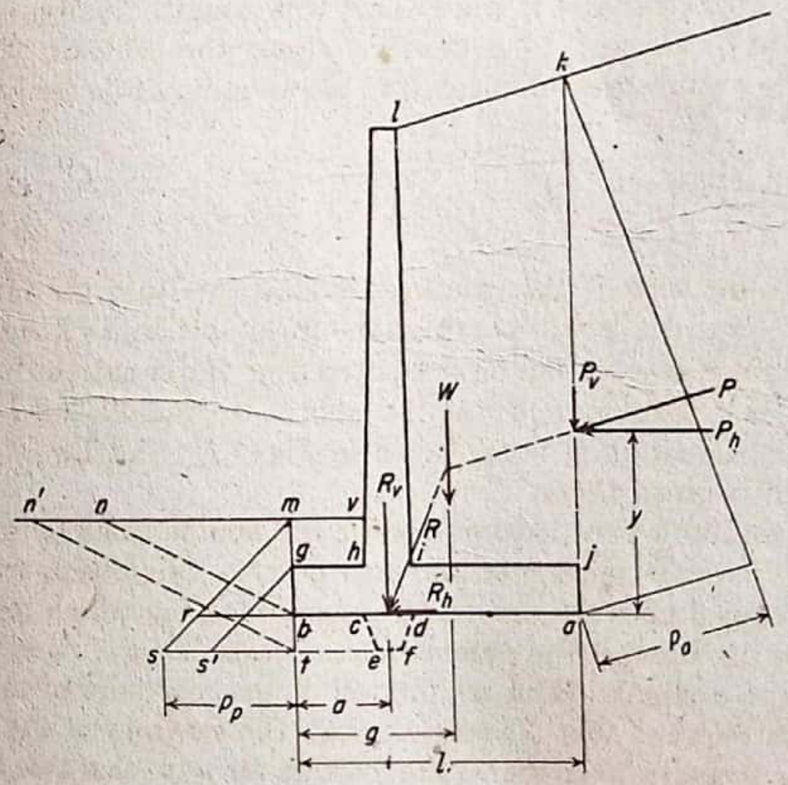


***Fig.* 7.4**

Scanned with CamScanner

that purpose the fill *ghmv* must be placed before the backfill *ijkl* is put in place and must be secure against later removal by scour or other means throughout the lifetime of the wall. If these conditions are not met, it is better not to count on the additional resistance of the passive pressure.

If the required sliding resistance cannot be developed by these means, a key wall *cdef* can be used to increase horizontal resistance. In this case sliding, if it occurs, takes place along the planes *ad* and *tf*. While along *ad* and *ef* the friction coefficient f applies, sliding along *te* occurs within the soil mass. The coefficient of friction that applies in this portion is consequently tan ϕ, where the value of ϕ may be taken from the next to last column in Table 7.1. In this situation sliding of the front soil occurs upward along *tn'* so that, if the front fill is secure, the corresponding resistance from passive soil pressure is represented by the pressure triangle *stm*. If doubt exists as to the reliability of the fill above the toe, the free surface should more conservatively be assumed at the top level of the footing, in which case the passive pressure is represented by the triangle *s'tg*.

Next, it is necessary to ensure that the pressure under the footing does not exceed the *permissible bearing pressure* for the particular soil. Let a (Fig. 7.4) be the distance from the front edge b to the intersection of the resultant with the base plane, and let R_v be the vertical component of R. (This intersection need not be located beneath the vertical arm, as shown, even though an economical wall generally results if it is so located.) Then the base plane *ab*, 1 ft wide longitudinally, is subject to a normal force R_v and to a moment about the centroid $(l/2 - a)R_v$. When these values are substituted in the usual formula for bending plus axial force

$$p_{1,2} = \frac{N}{A} \pm \frac{Mc}{I} \tag{7.8}$$

it will be found that if the resultant is located within the middle third ($a > l/3$), compression will act throughout the section, and the maximum and minimum pressures can be computed from the equations in Fig. 7.5*a*. If the resultant is located just at the edge of the middle third ($a = l/3$), the pressure distribution is as shown in Fig. 7.5*b*, and Eq. (7.8) results in the formula given there.

If the resultant were located outside the middle third ($a < l/3$), Eq. (7.8) would indicate tension at and near point a. Obviously, tension cannot be developed between soil and a concrete footing which merely rests on it. Hence, in this case the pressure distribution of Fig. 7.5*c* will develop, which implies a slight lifting off the soil of the rear part of the footing. Equilibrium requires that R_v pass through the centroid of the pressure-distribution triangle, from which the formula for p for this case can easily be derived.

It is good practice, in general, to have the resultant located within the middle third. This will not only reduce the magnitude of the maximum bearing pressure but will also prevent too large a nonuniformity of pressure. If the wall is founded on a highly compressible soil, such as certain clays, a pressure distribution as in Fig. 7.5*b* would result in a much larger settlement of the toe than of the heel, with a corresponding tilting of the wall. In a foundation on such a soil the resultant, therefore, should strike at or very near the center of the footing. If the foundation is on very incompressible soil, such as well-compacted gravel or rock, the resultant can be allowed to fall outside the middle third (Fig. 7.5*c*).

A third mode of failure is the possibility of the wall *overturning* bodily around the front edge b. For this to occur, the overturning moment yP_h about point b would have to be larger than the restoring moment $(Wg + P_v l)$ in Fig. 7.4, which is the same as saying that the resultant would have to strike outside the edge b. If, as is mostly the case, the resultant strikes within the middle third, adequate safety against overturning exists. and no special check need be made. If the resultant is located outside the middle third, a factor of safety of at least 1.5 should be maintained against overturning; i.e., the restoring moment should be at least 1.5 times the overturning moment.

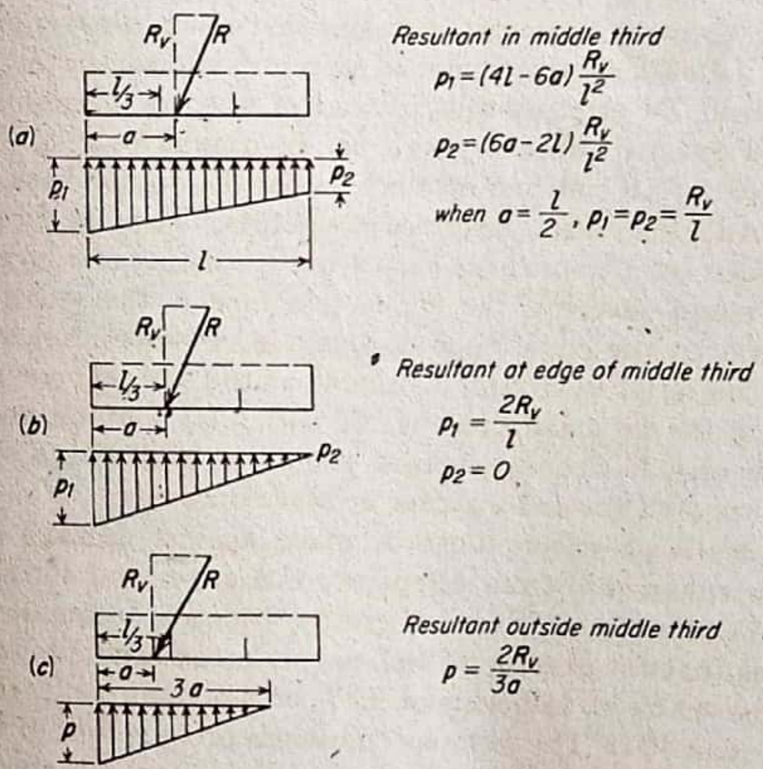


Fig. 7.5 Bearing pressures for different locations of resultant.

Scanned with CamScanner

[*Art. 7.5*

7.5 Drainage and Other Details Such failures or damage to retaining walls as have occasionally occurred were due, in most cases, to one of two causes: overstressing of the soil under the wall with consequent forward tipping or insufficient drainage of the backfill. In the latter case hydrostatic pressure from porewater accumulated during or after rainstorms increases greatly the thrust on the wall; in addition, in subfreezing weather ice pressure of considerable magnitude can develop in such poorly drained soils. The two causes are often interconnected, since large thrusts correspondingly increase the bearing pressure under the footing.

Allowable bearing pressures should be selected with great care. It is necessary, for this purpose, to investigate not only the type of soil immediately underlying the footing, but also the deeper layers. Unless reliable information is available at the site, subsurface borings should be made to a depth at least equal to the height of the wall. The foundation must be laid below *frost depth*, which amounts to 4 to 5 ft and more in the northern states, in order to ensure against heaving by the freezing of soils containing moisture.

Drainage can be provided in various ways. *Weep holes* consisting of 4-in. pipe embedded in the wall, as shown in Fig. 7.1*c*, are usually spaced horizontally at 5 to 10 ft. In addition to the bottom row, additional rows should be provided in walls of substantial height. To facilitate drainage and prevent clogging, 1 ft³ or more of crushed stone is placed at the rear end of each weeper. Care must be taken that the outflow from the weep holes is carried off safely so as not to seep into and soften the soil underneath the wall. To prevent this, instead of weepers, *longitudinal drains* embedded in crushed stone or gravel can be provided along the rear face of the wall (Fig. 7.1*b*) at one or more levels; the drains discharge at the ends of the wall or at a few intermediate points. The most efficient drainage is provided by a *continuous back drain* consisting of a layer of gravel or crushed stone covering the entire rear face of the wall (Fig. 7.1*a*), with discharge at the ends. Such drainage is expensive, however, unless appropriate material is cheaply available at the site. Wherever possible the surface of the fill should be covered with a layer of low permeability and, in case of a horizontal surface, should be laid with a slight slope away from the wall toward a gutter or other drainage.

In long walls provision must be made against damage caused by *expansion or contraction* from temperature changes and shrinkage. The American Association of State Highway Officials recommends in its specifications that for gravity as well as reinforced-concrete walls expansion joints be made at intervals of 90 ft or less, and contraction joints at not more than 30 ft. The same specifications provide that in reinforced-concrete walls horizontal temperature reinforcement of not less than $\frac{1}{8}$ in.² per ft of depth be provided adjacent to the exposed surface.

7.6 Example: design of a gravity retaining wall A gravity wall is to retain a bank 11 ft 6 in. high whose horizontal surface is subject to a live-load surcharge of 400 psf. The soil is a sand-and-gravel mixture with a rather moderate amount of fine, silty particles. It can, therefore, be assumed to be in class 2 of Table 7.1, with the following characteristics: unit weight $w_s = 120$ pcf, $\phi = 30°$ (with adequate drainage to be provided), and base friction coefficient $f = 0.5$. With $\sin 30° = 0.5$, from Eqs. (7.4) and (7.5), the soil-pressure coefficients are $C_{ah} = 0.333$ and $C_{ph} = 3.0$. The allowable bearing pressure is assumed to be 4 tons per ft². This coarse-grained soil has little compressibility, so that the resultant can be allowed to strike near the outer-third point (see Art. 7.4). The weight of the concrete is $w_c = 150$ pcf.

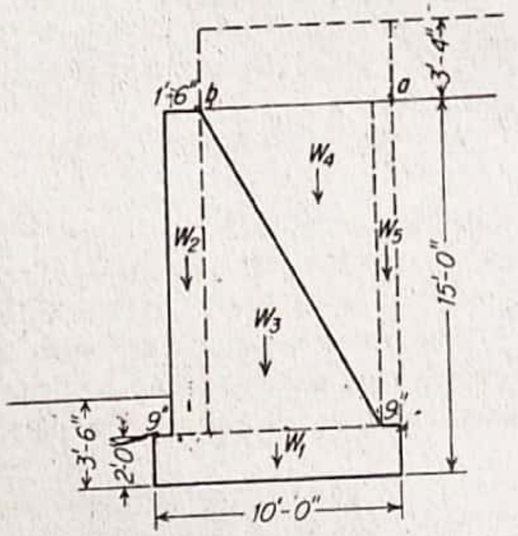


Fig. 7.6

The optimum design of any retaining wall is a matter of successive approximation. Reasonable dimensions are assumed by experience, and the various conditions of stability are checked for these dimensions. On the basis of a first trial, dimensions are readjusted, and one or two additional trials usually result in a favorable design. In the following, only the final design is analyzed in detail. The final dimensions are shown in Fig. 7.6.

The equivalent height of surcharge is $h' = {}^{400}\!/_{120} = 3.33$ ft. From Fig. 7.3*c* the total earth thrust is

$$P = \tfrac{1}{2} \times 0.333 \times 120 \times 15 \times 21.67 = 6500 \text{ lb}$$

and its distance from the base is $y = (225 + 150)/(3 \times 21.67) = 5.77$ ft. Hence, the overturning moment $M_0 = 6500 \times 5.77 = 37{,}500$ ft-lb. To compute the weight W and its restoring moment M_r about the edge of the toe, individual weights are taken, as shown in Fig. 7.6. With x representing the distance of the line of action of each subweight from the front edge, the following computation obtains:

Component weights	W, lb	x, ft	$M_r = xW$, ft-lb
W_1: $10 \times 2 \times 150$	3000	5.0	15,000
W_2: $1.5 \times 13 \times 150$	2930	1.5	4,400
W_3: $\frac{1}{2} \times 13 \times 150$	6830	4.58	31,300
W_4: $\frac{1}{2} \times 13 \times 120$	5460	6.82	37,200
W_5: $0.75 \times 13 \times 120$	1170	9.62	11,250
Total	19,390		99,150

Scanned with CamScanner

The distance of the resultant from the front edge is [Art. 7.7

$$a = (99{,}150 - 37{,}500)/19{,}390 = 3.18 \text{ ft}$$

which is just outside the middle third. The safety factor against overturning, $99{,}150/37{,}500 = 2.64$, is ample. From Fig. 7.5c the maximum soil pressure is $p = (2 \times 19{,}390)/(3 \times 3.18) = 4070$ psf.

The above computations were made for the case in which the surcharge extends only to the rear edge of the wall, point a of Fig. 7.6. If the surcharge extends forward to point b, the following modification obtains:

$$W = 19{,}390 + 400 \times 7.75 = 22{,}490 \text{ lb}$$
$$M_r = 99{,}150 + 400 \times 7.75 \times 6.13 = 118{,}150 \text{ ft-lb}$$
$$a = (118{,}150 - 37{,}500)/22{,}490 = 3.58 \text{ ft}$$

This is inside the middle third, and, from Fig. 7.5a, the maximum bearing pressure is

$$p_1 = (40.0 - 21.5)\ 22{,}490/100 = 4170 \text{ lb per ft}^2$$

The situation most conducive to sliding obtains when the surcharge extends only to point a, since additional surcharge between a and b would increase the total weight and the corresponding resisting friction. The friction force is

$$F = 0.5 \times 19{,}390 = 9690 \text{ lb}$$

Additionally, sliding is resisted by the passive earth pressure on the front of the wall. Although the base plane is 3.5 ft below grade, the top layer of soil cannot be relied upon to furnish passive pressure, since it is frequently loosened by roots and the like, or it could be scoured out by cloudbursts. For this reason the top 1.5 ft will be discounted in computing the passive pressure, which then becomes

$$P_p = \tfrac{1}{2} w_s h^2 C_{ph} = \tfrac{1}{2} \times 120 \times 4 \times 3.0 = 720 \text{ lb}$$

The safety factor against sliding, $(9690 + 720)/6500 = 1.6$, is but slightly larger than the required value 1.5, indicating a favorable design.

7.7 Example: design of a cantilever retaining wall A cantilever is to be designed for the situation of the gravity wall in Art. 7.6. A concrete with $f'_c = 3000$ psi and steel with $f_y = 40{,}000$ psi will be used.

To facilitate computation of weights for checking the stability of the wall, it is advantageous first to ascertain the *thickness of the arm and the footing*. For this purpose the thickness of the footing is roughly estimated, and then the required thickness of the arm is determined at its bottom section. With the bottom of the footing at 3.5 ft below grade and an estimated footing thickness of

1.5 ft, the free height of the arm is 13.5 ft. Hence, with respect to the bottom of the arm (see Fig. 7.3),

$$P = \tfrac{1}{2} \times 120 \times 13.5 \times 20.16 \times 0.333 = 5440 \text{ lb}$$
$$y = \frac{13.5^2 + 3 \times 13.5 \times 3.33}{3(13.5 + 6.66)} = 5.25 \text{ ft}$$
$$M = 5440 \times 5.25 \times 12 = 343{,}000 \text{ in.-lb}$$

For the given grades of concrete and steel, using working-stress design, $K = 223$, and hence the required thickness for bending is $d = \sqrt{343{,}000/(12 \times 223)} = 11.3$ in. A protective covering of 3 in. is required for reinforcement in concrete deposited against ground. Hence, the minimum required thickness of the arm at its base is 15 in. This will be increased to 18 in., since the cost of the excess concrete in such structures is usually more than balanced by the simultaneous saving in steel. The arm is checked for shear at a distance d above the base and is found to be more than adequate.

The thickness of the base is usually the same or slightly larger than that at the bottom of the arm. Hence, the estimated 1.5 ft need not be revised. Since the moment in the arm decreases with increasing distance from the base and is zero at the top, the arm thickness at the top will be made 8 in. It is now necessary to assume lengths of heel and toe slabs and to check the stability for these assumed dimensions. Intermediate trials are omitted here, and the final dimensions are shown in Fig. 7.7a. Trial computations have shown that safety against sliding can be achieved only by an excessively long heel or by a key. The latter, requiring the smaller concrete volume, has been adopted.

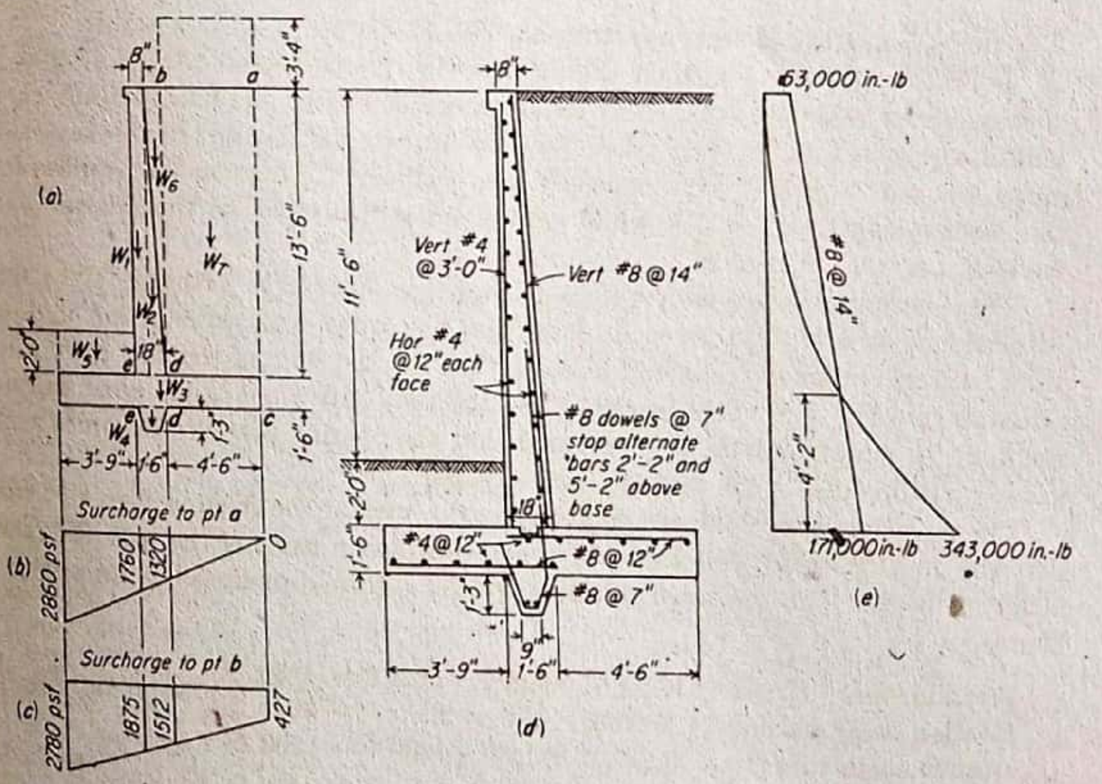


Fig. 7.7

Scanned with CamScanner

Weights and moments about the front edge obtain as follows: [Art. 7.7

Component weights	W, lb	x, ft	M_r, ft-lb
W_1: 13.5 × 0.67 × 150	1,355	4.09	5,550
W_2: 13.5/2 × 0.83 × 150	840	4.70	3,950
W_3: 9.75 × 1.5 × 150	2,195	4.87	10,700
W_4: (1.25 + 0.67)/2 × 1.5 × 150	216	4.50	970
W_5: 3.75 × 2 × 120	900	1.87	1,680
W_6: 13.5/2 × 0.83 × 120	672	4.98	3,350
W_7: 13.5 × 4.5 × 120	7,280	7.50	54,550
Total	13,458		79,750

The total soil pressure on plane ac is the same as for the gravity wall of Art. 7.6, that is, $P = 6500$ lb, and the overturning moment is

$$M_0 = 37{,}500 \text{ ft-lb}$$

The distance of the resultant from the front edge is

$$a = (79{,}750 - 37{,}500)/13{,}458 = 3.14 \text{ ft}$$

which locates the resultant barely outside the middle third. The corresponding maximum soil pressure at the toe, from Fig. 7.5, is

$$p = 2 \times 13{,}458/3 \times 3.14 = 2860 \text{ psf}$$

The factor of safety against overturning, 79,750/37.500 = 2.12, is ample.

To check the safety against sliding, it will be remembered (Art. 7.4) that if sliding occurs it proceeds between concrete and soil along the heel and key (i.e., length $a - e$ in Fig. 7.4) but takes place within the soil in front of the key (i.e., along $t - e$ in Fig. 7.4). Consequently, the coefficient of friction that applies for the former length is $f = 0.5$, while for the latter it is equal to the internal soil friction, i.e., tan 30° = 0.577.

The bearing-pressure distribution is shown in Fig. 7.7*b*. Actually, since the resultant is at a distance $a = 3.14$ ft from the front, i.e., outside the middle third, formal computation would indicate that the last 4 in. of the heel have zero pressure (see Fig. 7.5). This length is so small that only a negligible error will be made if, for simplification, it is assumed that the bearing pressure becomes zero exactly at the edge of the heel, as shown in Fig. 7.7*b*.

The resisting force is then computed as the sum of the friction forces of the rear and front portion, plus the passive soil pressure in front of the wall. For the latter, as in Art. 7.6, the top 1.5-ft layer of soil will be discounted as unreliable. Hence,

Friction, toe:	(2860 + 1760)/2 × 3.75 × 0.577	= 4930 lb
Friction, heel and key:	1760/2 × 6.0 × 0.5	= 2640 lb
Passive earth pressure:	3.25²/2 × 120 × 3.0	= 1900 lb
Total resistance to sliding		= 9470 lb

The factor of safety against sliding, 9470/6500 = 1.46, is less than 3 per cent below the recommended value of 1.5 and can be regarded as adequate.

These computations hold for the case in which the surcharge extends from the right to point a above the edge of the heel. The other case of load distribution, in which the surcharge is placed over the entire surface of the fill up to point b, evidently does not change the earth pressure on the plane ac. It does, however, add to the sum of the vertical forces and increase both the restoring moment M_r and the friction along the base. Consequently, the danger of sliding or overturning is greater when the surcharge extends only to a, for which situation these two cases have been checked and found adequate. In view of the added vertical load, however, the bearing pressure is largest when the surface is loaded to b. For this case,

$$W = 13{,}458 + 400 \times 5.33 = 15{,}590 \text{ lb}$$
$$M_r = 79{,}750 + 400 \times 5.33 \times 7.09 = 94{,}850 \text{ ft-lb}$$
$$a = (94{,}850 - 37{,}500)/15{,}590 = 3.68 \text{ ft}$$

which places the resultant inside the middle third. Hence, from Fig. 7.5,

$$p_1 = (4 \times 9.75 - 6 \times 3.68) \times 15{,}603/9.75^2 = 2780 \text{ psf}$$
$$p_2 = (6 \times 3.68 - 2 \times 9.75) \times 15{,}603/9.75^2 = 427 \text{ psf}$$

which is far below the allowable pressure of 4 tons per ft². The corresponding bearing-pressure distribution is shown in Fig. 7.7*c*.

The external stability of the wall has now been ascertained, and it remains to determine the required reinforcement and to check internal stresses.

Arm and key The moment at the bottom section of the arm has previously been determined as $M = 343{,}000$ in.-lb, and a thickness of 18 in. at the bottom and 8 in. at the top has been selected. With a concrete covering of 3 in. clear, $d = 18 - 3.5 = 14.5$ in. The required steel area at the bottom is

$$A_s = \frac{343{,}000}{\frac{7}{8} \times 14.5 \times 20{,}000} = 1.35 \text{ in.}^2 \text{ per ft}$$

The required area is provided by No. 8 bars at 7 in. center to center.

The bending moment in the arm decreases rapidly with increasing distance from the bottom. For this reason only part of the main reinforcement is needed at higher elevations, and alternate bars will be discontinued where no longer needed. To determine the cutoff point, the moment diagram for the arm has been drawn by computing bending moments at two intermediate levels, 10 ft and 5 ft from the top. These two moments, determined in the same manner as that at the base of the arm, were found to be 160,000 and 30,000 in.-lb, respectively. The resisting moment provided by alternate bars, i.e., by No. 8 bars at 14 in. center to center, at the bottom of the arm is

$$M = \frac{7}{8} \times 14.5 \times 0.675 \times 20{,}000 = 171{,}000 \text{ in.-lb}$$

At the top $d = 8.0 - 3.5 = 4.5$ in., and the resisting moment of the same bars is only $M = 171{,}000(4.5/14.5) = 53{,}000$ in.-lb. Hence, the straight line drawn in Fig. 7.7*e* indicates the resisting moment provided at any elevation by

Scanned with CamScanner

half the number of main bars. The intersection of this line with the moment diagram at a distance of 4 ft 2 in. from the bottom represents the point above which alternate bars are no longer needed. The ACI Code specifies that any bar shall be extended beyond the point at which it is no longer needed to carry flexural stress for a distance equal to d or 12 bar diameters, whichever is greater. In the arm, at a distance of 4 ft 2 in. from the bottom, $d = 11.5$ in., while 12 bar diameters for No. 8 bars are equal to 12 in. Hence, half the bars can be discontinued 12 in. above the point where no longer needed, or a distance of 5 ft 2 in. above the base.

In order to facilitate construction, the footing is poured first, and a construction joint is provided at the base of the arm, as shown in Fig. 7.7*d*. The main bars of the arm, therefore, end at the top of the base slab, and dowels are placed in the latter to be spliced with them. It will be realized that the integrity of the arm depends entirely on the integrity of the splicing of these tension bars. The ACI Code warns specifically against splicing all tension bars in one section by simple contact splices, since this situation can easily lead to splitting of the concrete owing to the stress concentrations at the ends of the spliced bars. One way to avoid this difficulty is to weld all splices; this will entail considerable extra cost.

In this particular wall, another way of placing the reinforcing offers a more economical solution. Because alternate bars in the arm can be discontinued at a distance of 5 ft 2 in. above the base, alternate dowels will be carried up from the top of the base to that distance. These need not be spliced at all, because above that level only alternate No. 8 bars, 14 in. on centers, are needed. These latter bars are placed full length over the entire height of the arm and are spliced at the bottom with alternate shorter dowels. By this means, only 50 per cent of the bars needed at the bottom of the arm are spliced; this is not objectionable.

For tension splices the ACI Code provides that the splice length shall be sufficient to transfer the entire steel stress at three-quarters of the permissible bond stresses, with a minimum of 24 diam for $f_y = 40{,}000$. The allowable bond stress for No. 8 bars is $u = 4.8\sqrt{3000}/1.0 = 263$ psi, and

$$\text{Required splice length} = \frac{0.79 \times 20{,}000}{0.75 \times 263 \times 3.14} = 25.5 \text{ in.}$$

The minimum of 24 diam = 24 in., for No. 8 bars, is less than this, so that 25.5 in. governs. Consequently, alternate dowels are carried a distance of 2 ft 2 in. above the base for splicing with the corresponding bars in the arm, while the intervening dowels are carried to 5 ft 2 in. above the base and terminated without splicing as being no longer needed to carry moments.

Since the dowels had to be extended at least partly into the key to produce the necessary length of embedment, they were bent as shown to provide reinforcement for the key. The exact force which the key must resist is difficult to determine, since probably the major part of the force acting on the portion of the soil in front of the key is transmitted to it through friction along the base of the footing. The relatively strong reinforcement of the key by means of the extended dowels is considered sufficient to prevent separation from the footing.

The sloping sides of the key were provided in order to facilitate excavation

without loosening the adjacent soil. This is necessary in order to ensure proper functioning of the key.

Base slab Toe and heel are designed for moments and shears caused by the bearing pressure, acting upward and counteracted by the superimposed weight of fill and surcharge, including the weight of the footing proper. Since both the bearing pressure and the superimposed weights are different for the two cases of surcharge extending to a and to b, both these conditions must be checked. This has been done, and, for this particular wall, it was found that moments and shears were not much different for the two cases, but that slightly larger values were obtained for surcharge extending to b.

On the *heel*, the combined weights, including surcharge, are

$$13.5 \times 120 + 1.5 \times 150 + 400 = 2245 \text{ lb per ft}$$

The moment produced by this load is counteracted by that from the bearing pressure (Fig. 7.7*c*). Hence,

$$M_d = 2245 \times 4.5^2/2 - 427 \times 4.5^2/2 - (1512 - 427)4.5^2/6$$
$$= 14{,}750 \text{ ft-lb} = 177{,}000 \text{ in.-lb}$$

The 18-in. thickness is ample for concrete bending stresses, as can be seen without computation by comparison with the corresponding value at the base of the arm whose thickness, at that point, is equal to that of the footing. The required steel area,

$$A_s = \frac{177{,}000}{14.5 \times \frac{7}{8} \times 20{,}000} = 0.70 \text{ in.}^2 \text{ per ft}$$

is provided by No. 8 bars at 12 in. center to center, or 0.78 in.^{2} per ft.

The fill above the *toe* will be neglected as being subject to possible erosion. Hence, with only the weight of the footing,

$$1.5 \times 150 = 225 \text{ lb per ft}$$

acting downward,

$$M_e = 1875 \times 3.75^2/2 + (2780 - 1875)3.75^2/3 - 225 \times 3.75^2/2$$
$$= 15{,}800 \text{ ft-lb} = 189{,}500 \text{ in.-lb}$$

Comparison with the moment in the arm, 343,000 in.-lb, again shows the thickness to be ample for bending. The steel area,

$$A_s = \frac{189{,}500}{14.5 \times \frac{7}{8} \times 20{,}000} = 0.75 \text{ in.}^2 \text{ per ft}$$

will again be provided by No. 8 bars at 12 in. center to center, or 0.78 in.^{2} per ft. The required length of embedment beyond points e and d is provided as shown.

Shear has been checked in the arm at a distance d above the footing and in both parts of the footing at a distance d from the front and rear faces of the arm, and has been found to be more than adequate without shear reinforcement.

The No. 4 bars indicated in Fig. 7.7*d* furnish the shrinkage reinforcement and serve to space the main reinforcement. Drainage is to be secured by one of the methods shown in Fig. 7.1, depending on local conditions.

Scanned with CamScanner

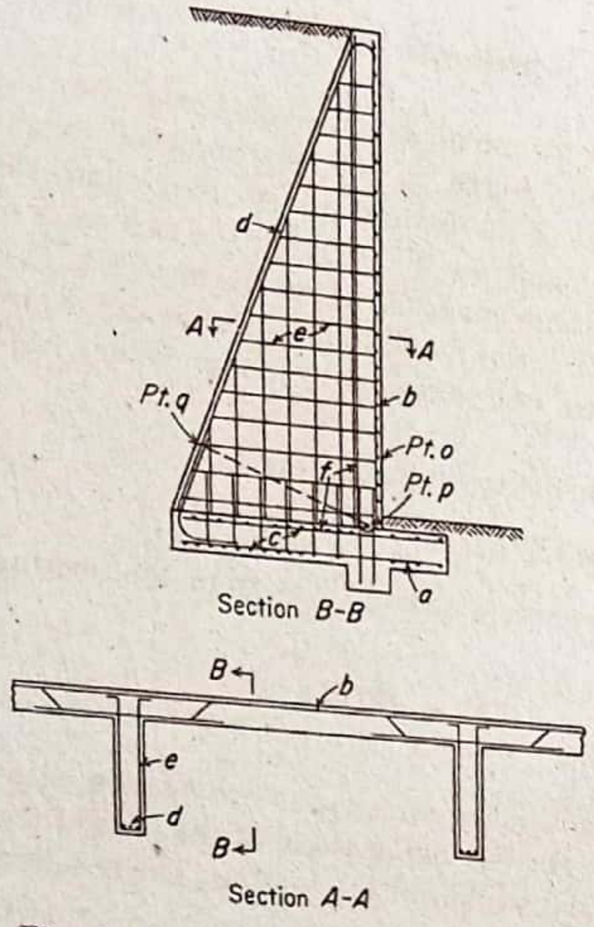


Fig. 7.8 Details of counterfort retaining wall.

in such a slab supported on three sides and nonuniformly loaded is rather involved (Ref. 7.2). It is customary in the design of such walls to disregard the support of the vertical wall by the base slab and to design it as if it were a continuous slab spanning horizontally between counterforts. This procedure is conservative, because the moments obtained by this approximation are larger than those corresponding to the actual conditions of support, particularly in the lower part of the wall. Hence, for very large installations, significant savings may be achieved by a more accurate analysis.

Slab moments are determined for strips 1 ft wide vertically, usually for the strip at the bottom of the wall and for three or four equally spaced additional strips at higher elevations. The earth pressure on the different strips decreases with increasing elevation and is determined from Eq. (7.1). An elaborate moment analysis by moment distribution or some other method is not warranted in view of (1) the approximate assumptions of the design as just discussed and (2) the uncertain magnitude of the earth pressure, which depends, among other influences, on moisture content and may vary from one panel to the next. The authors consider it adequate to assume the positive moments midway between, and the

7.8 Design of Counterfort Retaining Walls

[Art. 7.

The *external stability* of a counterfort retaining wall is determined in the same manner as in the examples of Arts. 7.6 and 7.7. The *toe slab* represents a cantilever built in along the front face of the wall, loaded upward by the bearing pressure, exactly as in the cantilever wall of Art. 7.7. Reinforcement is provided by bars a in Fig. 7.8.

A panel of the *vertical wall* between two counterforts is a slab acted upon by the horizontal earth pressure and supported along three sides, i.e., at the two counterforts and the base slab, while the fourth side, the top edge, is not supported. The earth pressure, of course, increases linearly with distance from the free surface. The exact determination of moments and shears

negative moments at, the counterforts to be equal, and to use for these moments

$$M = \frac{pl^2}{12}$$

for the two lowermost strips and

$$M = \frac{pl^2}{10}$$

for the strips at higher elevations. The smaller moment value for the bottom strips accounts for the fact that the additional support provided by the base slab decreases the moments in the bottom portions of the slab as compared with those which would obtain if this support were absent. Horizontal bars *b* (Fig. 7.8) are provided as required by these moments, with increased spacing or decreased diameter at higher elevations, corresponding to the smaller moments. Alternate bars are bent up to provide for the negative moments at the counterforts, or additional straight bars are placed for them.

The *heel slab* is supported as is the wall slab, i.e., by the counterforts and at the wall. It is loaded downward by the weight of the fill resting on it, its own weight, and such surcharge as there may be. This load is counteracted by the bearing pressure. As in the vertical wall, a simplified analysis consists in neglecting the influence of the support along the third side and in determining moments and shears for strips parallel to the wall, each strip representing a continuous beam supported at the counterforts. With horizontal soil surface, the downward load is constant for the entire heel, whereas the upward load from the bearing pressure is usually smallest at the rear edge and increases frontward. For this reason the span moments are positive (compression on top) and the support moments negative in the rear portion of the heel. Near the wall the bearing pressure often exceeds the vertical weights, resulting in a net upward load. The signs of the moments are correspondingly reversed, and steel must be placed accordingly, i.e., near the top face in the span and near the bottom face at the supports. Bars *c* are provided for these moments.

The *counterforts* are wedge-shaped cantilevers built in at the bottom in the base slab. They support the wall slab and, therefore, are loaded by the total soil pressure over a length equal to the distance center to center between counterforts. They act as a T beam of which the wall slab is the flange and the counterfort the stem. For this reason concrete stresses are always low and need not be checked. The maximum bending moment is that of the total earth pressure, taken about the bottom of the wall slab. This moment is held in equilibrium by the force in the bars *d*, and hence the lever arm of internal forces *jd* is the perpendicular distance *pq*

Scanned with CamScanner

from the center of bars d to the center of the bottom section of the wall slab. Since the moment decreases rapidly in the upper parts of the counterfort, part of the bars d can be discontinued. To find the cutoff points, it is simplest to use the graphical method which was employed for the arm of the cantilever wall (Fig. 7.7*e*). [Art. 7.4

In regard to shear, the ACI Code specifies the critical section to be located a distance d from the support for prismatic members but does not provide any guidance for strongly sloping members, such as these counterforts. The authors suggest the horizontal section oq as a conservative location for checking adequacy in shear. Some modification of the customary shear-stress computation is required for wedge-shaped members. In general, such stresses, on a section parallel to the external load such as oq, are determined by the usual formula $v_c = V_1/bd$, where

$$V_1 = V \pm \frac{M}{d}(\tan\theta + \tan\phi) \tag{7.9}$$

V and M are the shear and moment at the section, and θ and ϕ are the angles which the longitudinal edges subtend with a line perpendicular to the section (Ref. 7 3). The minus sign is to be used when the depth increases with increasing bending moment, as is the case in counterforts. For the example of Fig. 7.8, one of the two angles, say θ, is zero for the front edge, while ϕ is the angle between the vertical and the rear edge. Usually concrete alone is sufficient to carry this shear, although bars e act as stirrups and can be used for resisting excess shear.

The main purpose of bars e is to counteract the pull of the wall slab, and they are thus designed for the full reaction of this slab.

The remaining bars of Fig. 7.8 serve as shrinkage reinforcement, except that bars f have an important additional function. It will be recalled that the wall and heel slabs are supported on three sides. Even though they were designed as if supported only by the counterforts, they develop moments where they join. The resulting tension in and near the reentrant corner is conducive to cracking, which is counteracted by bars f.

REFERENCES

7.1 Terzaghi and Peck: "Soil Mechanics in Engineering Practice," pp. 315–318, John Wiley & Sons, Inc., New York, 1948.

7.2 "Rectangular Concrete Tanks," *Concrete Information ST63*, Portland Cement Association, 1943.

7.3 "Recommended Practice and Standard Specifications for Concrete and Reinforced Concrete," Report of Joint Committee on Standard Specifications for Concrete and Reinforced Concrete, *Proc. ASCE*, part 2, pp. 55–56, June, 1940.

chapter **8**

CONTINUOUS BEAMS AND FRAMES

8.1 Continuity of Reinforced-concrete Structures The individual members which compose a steel or timber structure are fabricated or cut separately and joined together by rivets, bolts, welds, or nails. Unless the joints are especially designed for rigidity, they are too flexible to transfer moments of significant magnitude from one member to another. In contrast, in reinforced-concrete structures as much of the concrete as is practical is poured in one single operation, and reinforcing steel is not terminated at the ends of a member but is carried over at the joints into adjacent members. At construction joints, special care is taken to bond the new concrete to the old by carefully cleaning the latter, carrying reinforcement across the joint, and other means. As a result, such structures represent monolithic or continuous units. Their behavior under load is shown in Fig. 8.1.

Scanned with CamScanner

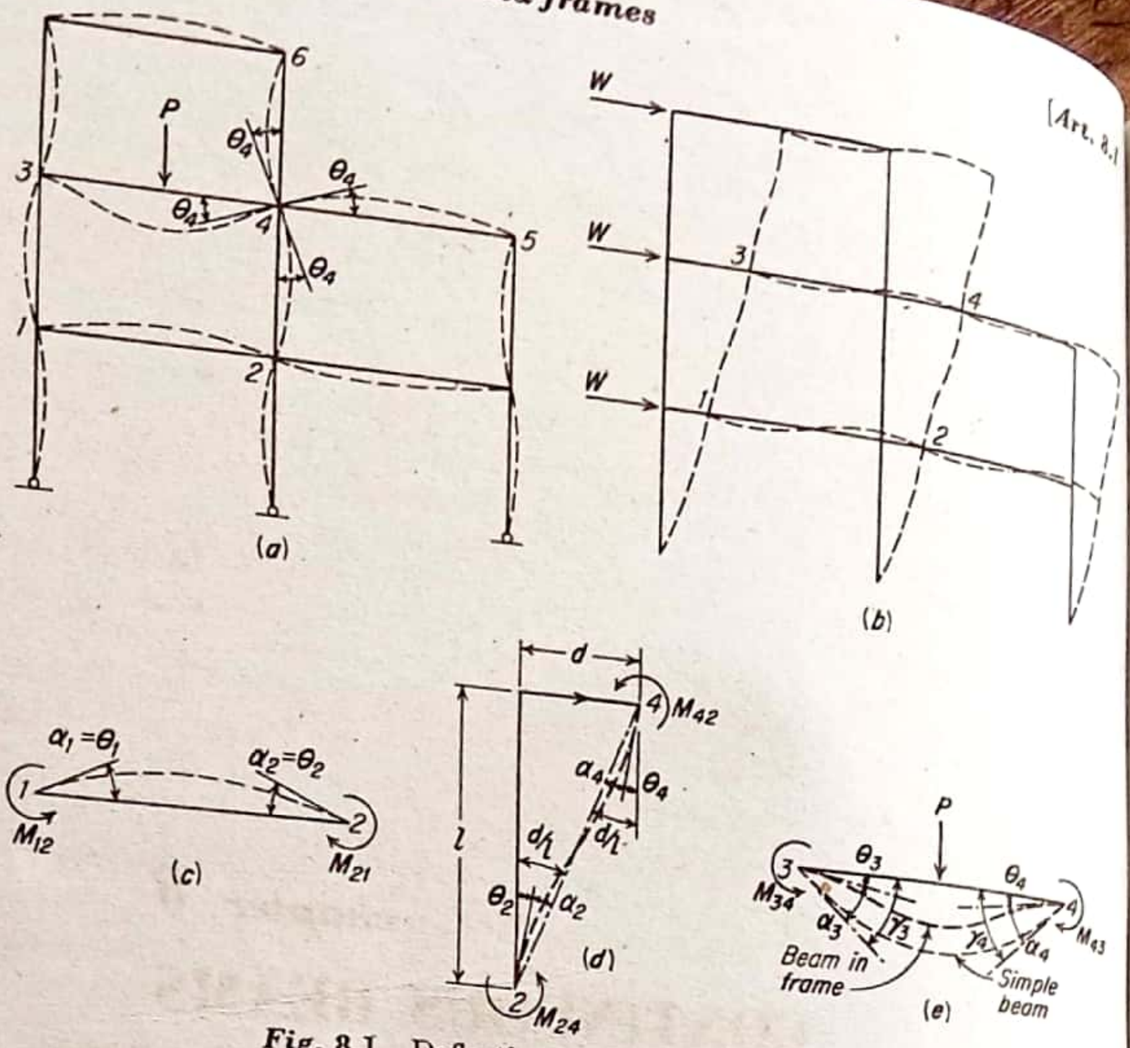


Fig. 8.1 Deflections and slopes of rigid frames.

With simple joints, as provided in steel construction by many types of riveted and bolted connections, only the beam 3-4 would bend in the frame of Fig. 8.1*a*, while all other members would remain essentially straight. With rigid joints, such as in a reinforced-concrete or welded steel frame, the distortion caused by a load on one single member is seen to spread to all other members of the frame, although the magnitude of deformation decreases with increasing distance from the loaded member. Consequently a beam, such as 1-2, even though free from load, bends because its ends are rotated by the amounts α_1 and α_2, as shown in Fig. 8.1*c*. Since curvature is proportional to bending moment ($1/r = M/EI$), this and all other members are subject to bending stresses, even though they are not loaded.

If horizontal forces, such as wind, act on the frame, it deforms as shown in Fig. 8.1*b*. Here, too, all members of the frame distort, even though the forces act only on the left side; the amount of distortion is seen to be about the same for all members, regardless of their distance from points of load, in contrast to the case of vertical loading. A member,

such as 2-4, even though not directly loaded, will experience bending moments caused by the distortions imposed on it, which are shown in Fig. 8.1*d*. It is seen that, in addition to the rotations α_2 and α_4, one end is displaced horizontally with respect to the other by the amount d, resulting in an additional rotation d/l. If, too, a member carries transverse load, such as does beam 3-4, the end rotations γ caused by the load must be superposed on those due to the rotations α caused by the continuity at the joints (Fig. 8.1*e*). The final end slopes θ of each individual member are seen to be the sums of these individual contributions α, d/l, and γ.

In statically determinate structures, such as simple beams, the deflected shape and the moments and shears depend only on the type and magnitude of the loads and the dimensions of the member. In contrast, inspection of Fig. 8.1 shows that in statically indeterminate frames the deflection curve of any member, in addition to the loads, depends on the end slopes θ whose magnitudes, in turn, depend on the distortion of adjacent, rigidly connected members. In particular, for a rigid joint such as joint 4 (Fig. 8.1*a*), the slopes θ of all abutting members must be the same and equal to the rotation of the joint. For a correct design of such frames, it is evidently necessary to determine moments and shears with due consideration of the effect of continuity at the joints.

A number of methods have been developed for such determinations. Those that were available in the early days of concrete design were rather lengthy and tedious. To save time, it became customary to determine moments in continuous structures by using approximate coefficients such as are included in the present ACI Code. Such coefficients are satisfactory if used within their specified limitations. However, with the advent of more practical and efficient methods of analysis, it is now common practice to ascertain moments and shears in continuous structures with a high degree of accuracy and to use approximate moment coefficients only when a closer design would not result in significant economy.

In the following articles the practically useful methods of analysis are discussed as they apply to relatively simple and more or less standard structures. For the more intricate details of this important phase of design, the reader is referred to special texts on analysis of statically indeterminate structures.

8.2 Moments in Continuous Beams The calculation of moments, shears, and reactions for continuous beams may be based on the theorem of three moments. Considering all supports on the same level, the two fundamental equations are (see Fig. 8.2): For uniform loads,

$$M_1 l_1 + 2M_2(l_1 + l_2) + M_3 l_2 = -\tfrac{1}{4} w_1 l_1^3 - \tfrac{1}{4} w_2 l_2^3 \qquad (8.1)$$

Scanned with CamScanner

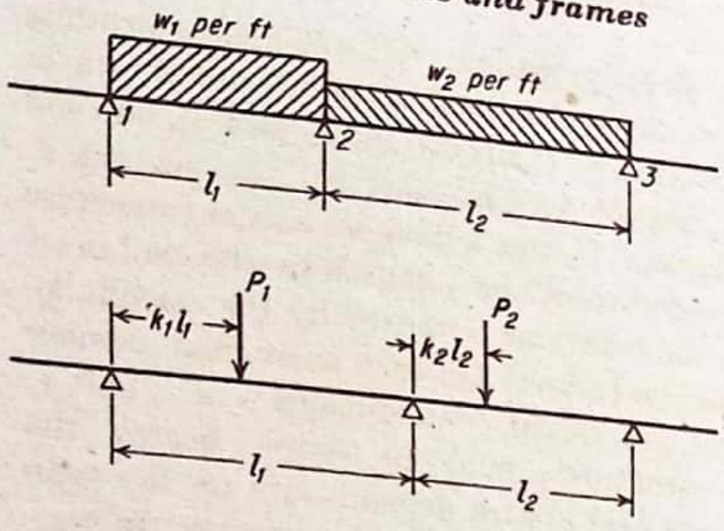


Fig. 8.2

For concentrated loads,

$$M_1 l_1 + 2M_2(l_1 + l_2) + M_3 l_2 = -\Sigma P_1 l_1^2(k_1 - k_1^3) - \Sigma P_2 l_2^2(2k_2 - 3k_2^2 + k_2^3) \quad (8.2)$$

In this simplest form the two equations apply to the most frequent case, that of uniform cross section.

By using a system of such equations, and solving simultaneously for the unknown moments, the bending moments at all the supports may be determined, the reactions computed, and, finally, the bending moment at any section of the beam obtained. From Eq. (8.2), influence lines may be plotted for the moment at any section of the beam, and the loading determined which will produce the maximum moment in that section. In the case of uniform load and equal spans, the exact coefficients of wl^2 for the theoretical maximum moments are given in Table 8.1.

Table 8.1 Moments in continuous, equal-span beams with uniformly distributed load

Number of spans	Intermediate spans and supports				End spans and second support			
	At center, positive moment		At support, negative moment		At center, positive moment		At support, negative moment	
	Dead load	Live load	Dead load	Live load	Dead load	Live load	Dead load	Live load
2					0.070	0.095	0.125	0.125
3	0.025	0.075			0.080	0.100	0.100	0.117
4	0.036	0.081	0.071	0.107	0.071	0.098	0.107	0.120
5	0.046	0.086	0.079	0.111	0.072	0.099	0.105	0.120
6	0.043	0.084	0.086	0.116	0.072	0.099	0.106	0.120
7	0.044	0.084	0.085	0.114	0.072	0.099	0.106	0.120

These coefficients are derived for simple (knife-edge) supports and for the most unfavorable distribution of live loads.

Moment and shear coefficients are given in the ACI Code which are based on exact coefficients given above. They are reprinted in Table 8.2.

Table 8.2 Moment and shear values using ACI coefficients*

Positive moment:	
End spans:	
If discontinuous end is unrestrained	$\frac{1}{11}wl'^2$
If discontinuous end is integral with the support	$\frac{1}{14}wl'^2$
Interior spans	$\frac{1}{16}wl'^2$
Negative moment at exterior face of first interior support:	
Two spans	$\frac{1}{9}wl'^2$
More than two spans	$\frac{1}{10}wl'^2$
Negative moment at other faces of interior supports	$\frac{1}{11}wl'^2$
Negative moment at face of all supports for, (1) slabs with spans not exceeding 10 ft, and (2) beams and girders where ratio of sum of column stiffnesses to beam stiffness exceeds eight at each end of the span	$\frac{1}{12}wl'^2$
Negative moment at interior faces of exterior supports for members built integrally with their supports:	
Where the support is a spandrel beam or girder	$\frac{1}{24}wl'^2$
Where the support is a column	$\frac{1}{16}wl'^2$
Shear in end members at first interior support	$1.15\frac{wl'}{2}$
Shear at all other supports	$\frac{wl'}{2}$

* w = total load per unit length of beam or per unit area of slab.
l' = clear span for positive moment and shear and the average of the two adjacent clear spans for negative moment.

The ACI coefficients were derived with due consideration of the maximum allowable ratio of live to dead load (3:1), maximum allowable span difference (the larger of two adjacent spans not to exceed the shorter by more than 20 per cent), the fact that reinforced-concrete beams are never simply supported but either rest on supports of considerable width, such as walls, or are built monolithically with columns, and other factors. Since all these influences are considered, the ACI coefficients are necessarily quite conservative, so that actual, accurate moments in any particular design are likely to be considerably smaller than indicated. Hence, in many reinforced-concrete structures significant economy can be effected by making a precise analysis of the moments in beams and girders. This becomes mandatory for beams and slabs with spans differing by more than 20 per cent and/or sustaining unsymmetrical loads. Such analyses are more expeditiously carried out by the method of moment distribution (Art. 8.7) than by the use of Eqs. (8.1) and (8.2).

Scanned with CamScanner

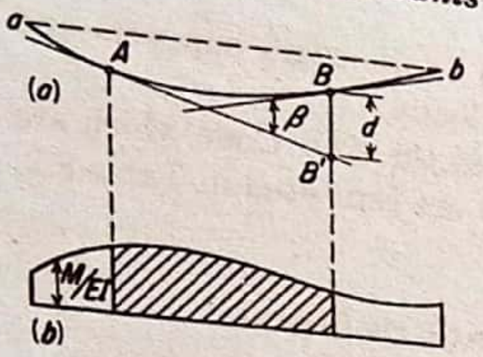


Fig. 8.3

8.3 Moment-area Principles It was indicated in Art. 8.1 that in continuous structures moments and shears caused by imposed deformations, such as the rotation α or the displacements d, superpose on those caused by the direct effect of the load acting on the particular member. To analyze this type of action, it is therefore necessary to establish the relations that exist between bending moments and the corresponding deformations. These are most easily expressed in the form of the two moment-area principles.

In Fig. 8.3*a* let the straight line *ab* represent the original, unloaded shape of an elastic member (beam, girder, column, or the like), and the curve *aABb* its deformed shape or elastic curve. In view of the relation $1/r = M/EI$, this distortion is connected with associated bending moments. Let Fig. 8.3*b* represent the corresponding M/EI diagram, i.e., the graph of the bending moments divided by the respective values of EI. If tangents are drawn to the elastic curve at two points A and B, the moment-area principles state:

1. *The change of slope β between the tangents to the elastic curve at two points A and B is equal to the area of the portion of the M/EI diagram between the two points.*

2. *The distance d of point B from the tangent at point A is equal to the moment about the perpendicular through B of the area of the portion of the M/EI diagram between the two points.*

The corresponding portion of the M/EI diagram is shaded in Fig. 8.3*b*. Note that the distance d is measured perpendicular to the original, undistorted position *ab* of the member (i.e., the line connecting its supports).

For a derivation of these two important principles the reader is referred to any text on the strength of materials.

8.4 Slope-deflection Method In computing moments and shears on isolated beams, the ends are usually considered as freely supported or as fixed. However, there is, even in isolated beams, often an intermediate condition. In frames in which the joints are rigid, such an intermediate condition is commonly encountered. No matter what the degree of restraint, once the end moments are known, moments and shears at any point of the member can be computed from the equations of statics. As is evident from Art. 8.1, the end slopes θ depend on (1) the rotation α of the end tangents to the elastic curve from the position they would have if the member were freely supported (see Fig. 8.1*c*); (2) the relative displacement d of the supports and the corresponding rotation d/l (see

Fig. 8.1*d*); (3) the rotations γ which the direct, transverse loads (if any) would cause if the members were freely supported (see Fig. 8.1*e*). The final end slopes θ are the sums of these individual rotations (see Fig. 8.1*d* and *e*).

In a freely supported beam, the end moments are zero, and the end slopes γ depend on the load and can be computed in the usual manner, e.g., by the moment-area principles (see Art. 8.3). In a fixed-end beam the end slopes are zero, and the end moments are known as the "fixed-end moments" M'. If the beam is an intermediate condition (Fig. 8.1*e*), the end slopes θ obviously have intermediate values (between 0 and γ), and the end moments M have corresponding intermediate values between M' and 0.

Once the end slopes θ are known, the end moments can be determined. Hence, the term "slope deflection" has been applied to this method of analysis, which was developed independently by A. Bendixen in Germany (1914) and G. A. Maney in the United States (1915).

In the discussion that follows, the relations between the end slopes and the end moments are first investigated separately for the three described types of rotations. Two subscripts are used for moments acting on one end of a member, the first indicating the "near" end, on which it acts, and the other indicating the "far" end. Thus (see Fig. 8.4) M_{12} indicates the moment acting on end 1 of beam 1-2.

In Fig. 8.4*a*, a member 1-2 has been isolated from the rest of a rigid frame by passing imaginary cuts around the joints at its two ends. The member then represents a freely supported simple beam. The effect of the adjacent frame members on this beam is to impose certain rotations and deflections on its ends, as can be seen from Fig. 8.1. These effects will be studied individually.

In Fig. 8.4*b* the left support, 1, of the beam has been rotated by the action of moments outside the span 1-2. This rotation causes bending in the beam and produces compression in the upper fiber at 1. In (*c*) the right support, 2, has also been rotated in the same direction by the action of moments outside the beam. This produces tension in the upper fiber at 2. Since

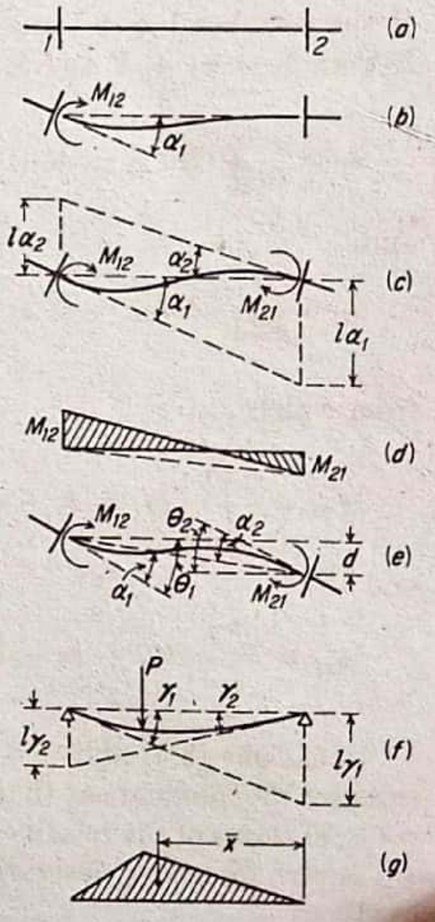


Fig. 8.4

Scanned with CamScanner

the stresses in the upper fiber at 1 and 2 are of opposite sign, there is evidently a point of inflection in the beam, and the moment diagram for the beam is similar to that shown in (*d*).

Since the angles of rotation are small, the distance at 2 from a tangent to the axis of the beam at 1 is $l\alpha_1$, where l is the span 1-2. Then by the principle of moment areas, $l\alpha_1$ is equal to the moment of the M/EI diagram between 1 and 2 about 2. This moment is evidently equal to the algebraic sum of the moments of the shaded areas about 2, that is,

$$l\alpha_1 = \frac{1}{EI}\left(\frac{M_{12}l}{2}\frac{2l}{3} - \frac{M_{21}l}{2}\frac{l}{3}\right) \quad \text{or} \quad \alpha_1 = \frac{l}{6EI}(2M_{12} - M_{21})$$

Similarly,

$$\alpha_2 = \frac{l}{6EI}(2M_{21} - M_{12})$$

In Fig. 8.4*e* the joint 2 has been moved downward a vertical distance d from its original position, the horizontal distance between joints 1 and 2 remaining constant. This has increased the angles between the tangents to the member 1-2 at 1 and 2 and the horizontal by an amount $d/l = R$. If then $\theta_1 = \alpha_1 + R$ and $\theta_2 = \alpha_2 + R$,

$$\theta_1 = \frac{l}{6EI}(2M_{12} - M_{21}) + R \tag{8.3}$$

and

$$\theta_2 = \frac{l}{6EI}(2M_{21} - M_{12}) + R \tag{8.4}$$

from which

$$M_{12} = \frac{2EI}{l}(2\theta_1 + \theta_2 - 3R) \tag{8.5}$$

and

$$M_{21} = \frac{2EI}{l}(2\theta_2 + \theta_1 - 3R) \tag{8.6}$$

Equations (8.5) and (8.6) are the fundamental slope-deflection equations for the moments at the ends of a member sustaining no intermediate loads, in terms of the relative change in slope and displacement of its ends.

In the foregoing derivation the following sign convention has been used:

1. When the rotation of the end tangent is clockwise, the angle measuring this rotation is positive.
2. The deflection of one end with respect to the other is measured normal to the original position of the member and is positive when measured in the same direction as positive angles.
3. External end moments are positive when they tend to rotate the end of the member on which they act in a clockwise direction.

For illustration, in Fig. 8.4*a* to *e* the sense of all rotations, deflections, and moments is positive.

If a transverse load acts on a member, as shown in Fig. 8.4*f*, the corresponding rotations γ must be added to α and R to result in the final rotations θ. From 8.4*f* it is seen that for vertical load and by the sign convention just given, γ_1 is positive, while γ_2 is negative. If F is the area of the moment curve for the simple beam (Fig. 8.4*g*), and $\bar{x}$ the distance of its centroid from support 2, one obtains, from the second moment-area principle,

$$l\gamma_1 = \frac{F\bar{x}}{EI} \quad \text{and} \quad l\gamma_2 = -\frac{F(l-\bar{x})}{EI}$$

If these equations are divided by l and the resulting angles γ added to those of Eqs. (8.3) and (8.4), one obtains, for the case of members carrying transverse loads,

$$\theta_1 = \frac{l}{6EI}(2M_{12} - M_{21}) + R + \frac{F\bar{x}}{EIl} \tag{8.7}$$

and

$$\theta_2 = \frac{l}{6EI}(2M_{21} - M_{12}) + R - \frac{F}{EI}\left(\frac{l-\bar{x}}{l}\right) \tag{8.8}$$

from which

$$M_{12} = \frac{2EI}{l}(2\theta_1 + \theta_2 - 3R) - \frac{2F}{l^2}(3\bar{x} - l) \tag{8.9}$$

and

$$M_{21} = \frac{2EI}{l}(2\theta_2 + \theta_1 - 3R) + \frac{2F}{l^2}(2l - 3\bar{x}) \tag{8.10}$$

These are the complete equations of the slope-deflection method. By comparison with Eqs. (8.5) and (8.6) it is seen that the last terms of Eqs. (8.9) and (8.10) accounts for the influence of transverse loads on the member under consideration. Its physical significance is easily estab-

Scanned with CamScanner

lished in the following manner. If the member of Fig. 8.4 is fixed at its ends, then $\theta_1 = \theta_2 = R = 0$. In this case M_{12} and M_{21} would represent the fixed-end moments of the beam. Equating to zero the indicated terms, it is seen that these fixed-end moments are, respectively, equal to the last terms of Eqs. (8.9) and (8.10). These fixed-end moments will be designated by M^f.

If, in addition, the rigidity I/l of the member is designated by K, and subscripts n and f are used, respectively, for the "near" and "far" ends of the member, Eqs. (8.9) and (8.10) can be written in the following general form:

$$M_{nf} = 2EK(2\theta_n + \theta_f - 3R) + M_{nf}^f \tag{8.11}$$

The sign of M_{nf}^f is established from rule 3, given previously. For instance, the load of Fig. 8.4*f* produces fixed-end moments which tend to rotate the left end of the member counterclockwise and the right end clockwise. Hence, the former is negative, the latter positive, as is correctly reflected in Eqs. (8.9) and (8.10) In the general equation (8.11) they must be substituted with these same signs. (The reader will find that some texts on structural analysis use a sign convention for rotations, deflections, and moments other than that given in Rules 1 to 3. The choice of such a convention is entirely a matter of the designer's preference. One is as good as the other, provided it is consistent in itself and is used consistently.) The determination of the correct sign is greatly facilitated by the use of rough sketches of the deflected shape of the structure, such as Fig. 8.1. By means of such sketches the signs of the moments throughout the frame are easily determined even before an analysis is begun. In fact, the approximate shape of the final moment diagrams can be obtained directly from such sketches, which are of inestimable aid to the designer.

The slope-deflection equations enable one to compute the moments at both ends of all members of a rigid-joint structure by making use of the following requirements:

1. Condition of joint equilibrium: The sum of all moments acting on a joint is zero.
2. Condition of joint continuity: The rotations of the tangents of all members meeting at a joint are equal.
3. Condition of frame equilibrium: The external shears and reactions applied to the frame must be in equilibrium with the applied loads.

8.5 Restraint Conditions and Fixed-end Moments The general slope-deflection equations (8.7) to (8.11) were derived to hold for all conceivable situations, i.e., for any relative magnitudes of θ and M at

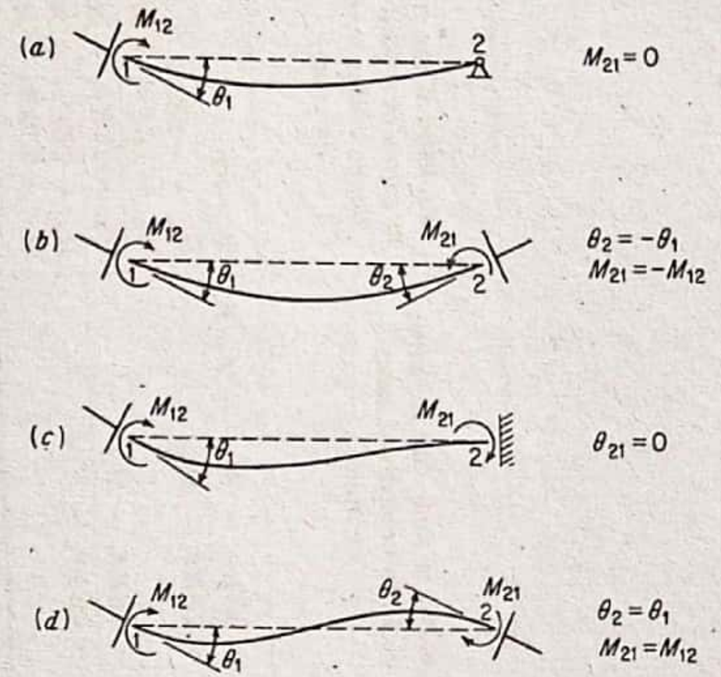


Fig. 8.5

both ends, and for any value of R. The values of θ and M in any particular case depend on the conditions of restraint at both ends, hinged, fixed, or partially restrained. In addition to the general case of partial, unequal restraint at both ends, for which the general equations were derived, there are four special conditions of restraint which are often met in structural analysis. These are shown in Fig. 8.5 and are (*a*) far end hinged, (*b*) symmetrical bending, (*c*) far end fixed, and (*d*) antisymmetrical bending. R equal to zero is assumed for these four simple cases, and the corresponding conditions are shown on the right of Fig. 8.5. By making use of these conditions, simplified equations are easily derived for these four frequent cases.

For instance, for case *a*, noting that $M_{21} = 0$ at the hinged end, Eqs. (8.9) and (8.10) become

$$M_{12} = 2EK(2\theta_1 + \theta_2) + M_{12}^f$$
$$0 = 2EK(2\theta_2 + \theta_1) + M_{21}^f$$

From the second equation,

$$\theta_2 = -\left(\frac{\theta_1}{2} + \frac{M_{21}^f}{4EK}\right)$$

If this value is substituted in the first equation, one obtains

$$M_{12} = 3EK\theta_1 - \left(M_{12}^f + \frac{M_{21}^f}{2}\right)$$

In particular, if no loads act on the member proper, so that bending is caused only by the end moments applied through the joints from

Scanned with CamScanner

Table 8.3 **Moments for different conditions of restraint**

Case (see Fig. 8.5)	Relation between θ angles, no load on span	Moment at near end in terms of θ_1, no load on span	Moment at far end in terms, of θ_1 and θ_2, no load on span	Moment at near end in terms of θ_1, intermediate loads on span	Moment at far end in terms of θ_1 and θ_2, intermediate loads on span
a. Far end hinged.....	$\theta_2 = -\frac{1}{2}\theta_1$	$M_{12} = 3EK\theta_1$	$M_{21} = 0$	$M_{12} = 3EK\theta_1 - (M_{12}^f + M_{21}^f/2)$	$M_{21} = 0$
b. Symmetrical bending...	$\theta_2 = -\theta_1$	$M_{12} = 2EK\theta_1$	$M_{21} = -2EK\theta_1$ $M_{21} = 2EK\theta_2$	$M_{12} = 2EK\theta_1 - M_{12}^f$	$M_{21} = -2EK\theta_1 + M_{21}^f$ $M_{21} = 2EK\theta_2 + M_{21}^f$
c. Far end fixed.....	$\theta_2 = 0$	$M_{12} = 4EK\theta_1$	$M_{21} = 2EK\theta_1$	$M_{12} = 4EK\theta_1 - M_{12}^f$	$M_{21} = 2EK\theta_1 + M_{21}^f$
d. Antisymmetrical bending	$\theta_2 = \theta_1$	$M_{12} = 6EK\theta_1$	$M_{21} = 6EK\theta_1$ $M_{21} = 6EK\theta_2$	$M_{12} = 6EK\theta_1 - M_{12}^f$	$M_{21} = 6EK\theta_1 + M_{21}^f$ $M_{21} = 6EK\theta_2 + M_{21}^f$

adjacent members, $M_{12}^f = M_{21}^f = 0$. In this case the last equation indicates

$$M_{12} = 3EK\theta_1$$

while the next to last results in

$$\theta_2 = -\frac{\theta_1}{2}$$

In a similar manner, such special, simple relations are easily derived for the other three cases. The results are listed in Table 8.3.

If the far end of a member, say end 2, is hinged and subject to joi deflection, one has

$$M_{12} = 2EK(2\theta_1 + \theta_2 - 3R)$$
$$0 = 2EK(2\theta_2 + \theta_1 - 3R)$$

from which

$$M_{12} = 3EK\theta_1 - 3EKR$$

Consequently, *Table* 8.3 *can also be used if joint deflections are present*, by adding $-6EKR$ to the moments M_{12} and M_{21} for cases *b* to *d*, and $-3EKR$ to M_{12} of case *a*.

The use of these relations is easily seen from the following problem. Suppose it is required to find the moment at the fixed end of a beam whose other end is hinged and which carries transverse load. The condition that the left end is fixed while the right end is hinged requires that $\theta_1 = 0$ in case *a* of Table 8.3. Then M_{12} is the moment at the fixed end of that beam and is seen to be

$$M_{12} = -\left(M_{12}^f + \frac{M_{21}^f}{2}\right)$$

This equation indicates that the moment at the fixed end of a beam whose other end is hinged can be expressed in terms of the fixed-end moments of that beam, i.e., the end moments for both ends fixed.

The practical application of the slope-deflection equation obviously requires knowledge of the fixed-end moments M_{n}^f for the particular design loading. It was shown that these fixed-end moments are equal to the last terms of Eqs. (8.9) and (8.10), from which they can be computed for any type of loading. For the most frequent arrangements of load, values of M_{12}^f and M_{21}^f for the left and right end, respectively, are given in Table 8.4. The table also contains for the same loadings, the moments at the fixed end if the other end is hinged, computed from Eq. (8.10).

Scanned with CamScanner

Table 8.4 **Fixed-end moments M^f and moments at fixed ends for beams with other end hinged, for various types of loading**

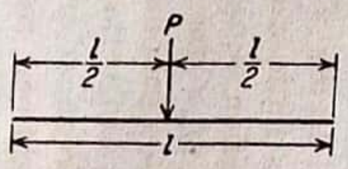
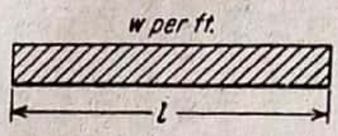
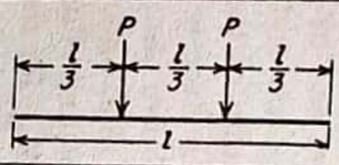
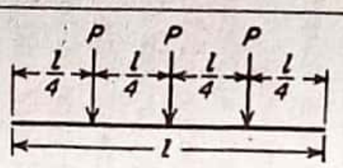
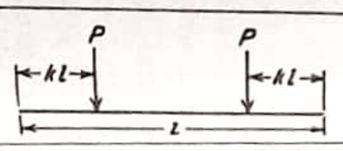
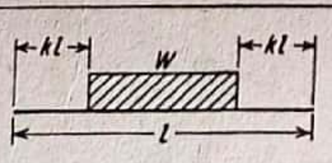
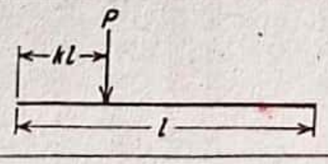
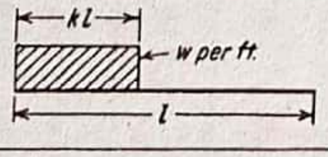
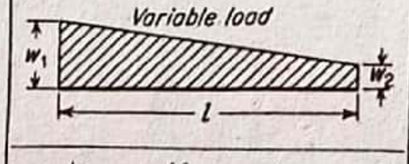
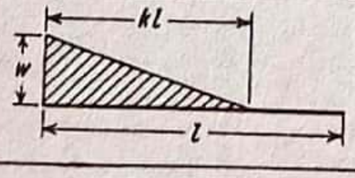
Type of loading	Left fixed-end moment M^f_{12}	Right fixed-end moment M^f_{21}	Moment at left fixed end; right end hinged $M^f_{12} + M^f_{21}/2$	Moment at right fixed end; left end hinged $M^f_{21} + M^f_{12}/2$
	$\frac{1}{8}Pl$	$\frac{1}{8}Pl$	$\frac{3}{16}Pl$	$\frac{3}{16}Pl$
	$\frac{1}{12}wl^2$	$\frac{1}{12}wl^2$	$\frac{1}{8}wl^2$	$\frac{1}{8}wl^2$
	$\frac{2}{9}Pl$	$\frac{2}{9}Pl$	$\frac{1}{3}Pl$	$\frac{1}{3}Pl$
	$\frac{5}{16}Pl$	$\frac{5}{16}Pl$	$\frac{15}{32}Pl$	$\frac{15}{32}Pl$
	$Pkl(1-k)$	$Pkl(1-k)$	$\frac{3}{2}Pkl(1-k)$	$\frac{3}{2}Pkl(1-k)$

Table 8.4 **Fixed-end moments M^f and moments at fixed ends for beams with other end hinged, for various types of loading (*Continued*)**

Type of loading	Left fixed-end moment M^f_{12}	Right fixed-end moment M^f_{21}	Moment at left fixed end; right end hinged $M^f_{12} + M^f_{21}/2$	Moment at right fixed end; left end hinged $M^f_{21} + M^f_{12}/2$
	$\frac{Wl}{12}(1+2k-2k^2)$	$\frac{Wl}{12}(1+2k-2k^2)$	$\frac{Wl}{8}(1+2k-2k^2)$	$\frac{Wl}{8}(1+2k-2k^2)$
	$Pk(1-k)^2l$	$Pk^2(1-k)l$	$\frac{1}{2}P(1-k)(2-k)kl$	$\frac{1}{2}P(1-k^2)kl$
	$\frac{wl^2k^2}{12}(3k^2-8k+6)$	$\frac{wl^2k^3}{12}(4-3k)$	$\frac{1}{8}wl^2k^2(2-k)^2$	$\frac{1}{8}wl^2k^2(2-k^2)$
	$\frac{l^2}{60}(3w_1+2w_2)$	$\frac{l^2}{60}(2w_1+3w_2)$	$\frac{l^2}{120}(8w_1+7w_2)$	$\frac{l^2}{120}(7w_1+8w_2)$
	$\frac{wk^2l^2}{60}(10-10k+3k^2)$	$\frac{wk^3l^2}{60}(5-3k)$	$\frac{wk^2l^2}{120}(20-15k+3k^2)$	$\frac{wk^2l^2}{120}(10-3k^2)$

Scanned with CamScanner

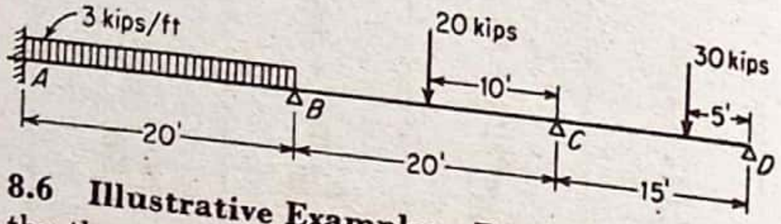


Fig. 8.6

8.6 Illustrative Examples Example 1 Determine the support moments in the three-span, continuous beam of Fig. 8.6. In this beam span, AB is fixed at A, corresponding to case c of table 8.3, while span CD is hinged at D, corresponding to case a. Span BC is partially restrained at both ends, so that for this span Eq. (8.11) must be used.

All moments of inertia are assumed equal. To simplify computations, it is convenient to express all values of K in terms of the K value for one of the members.[1] Thus

$$K_{AB} = \frac{I}{20} \qquad K_{BC} = \frac{I}{20} = K_{AB} \qquad K_{CD} = \frac{I}{15} = 1.33K_{AB}$$

Using the information of Tables 8.3 and 8.4, the fixed-end moments are

$$M_{AB}^f = -M_{BA}^f = -100 \text{ ft-kips}$$
$$M_{BC}^f = -M_{CB}^f = -50 \text{ ft-kips}$$
$$M_{CD}^f = -66.7 \text{ ft-kips}$$

and

$$M_{AB} = 2K_{AB}\theta_B - 100$$
$$M_{BA} = 4K_{AB}\theta_B + 100$$
$$M_{BC} = 2K_{BC}(2\theta_B + \theta_C) - 50 = 4K_{AB}\theta_B + 2K_{AB}\theta_C - 50$$
$$M_{CB} = 2K_{BC}(2\theta_C + \theta_B) + 50 = 4K_{AB}\theta_C + 2K_{AB}\theta_B + 50$$
$$M_{CD} = 3K_{CD}\theta_C - 66.7 = 4K_{AB}\theta_C - 66.7$$

The condition that joints B and C be in equilibrium requires

$$M_{BA} + M_{BC} = 0 \qquad M_{CB} + M_{CD} = 0$$

that is,

$$8K_{AB}\theta_B + 2K_{AB}\theta_C + 50 = 0 \qquad 2K_{AB}\theta_B + 8K_{AB}\theta_C - 16.7 = 0$$

Solving these two simultaneous equations, one obtains

$$K_{AB}\theta_B = -7.23 \qquad K_{AB}\theta_C = +3.89$$

The end moments of the three spans are then obtained by substituting these values in the equations for M_{AB}, M_{BA}, etc.; for example,

$$M_{AB} = 2(-7.23) - 100 = -114.5 \text{ ft-kips}$$

Similarly $M_{BA} = +71.1$, $M_{BC} = -71.1$, $M_{CB} = +51.1$, and $M_{CD} = -51.1$ ft-kips.

[1] In problems other than those involving numerical values of support displacement, relative values of K may be used; thus the units of I and L need not agree. Similarly, the constant E does not affect relative stiffness K and can be omitted.

Example 2 The portal frame of Fig. 8.7*a* is subject to a wind load of 20 kips; determine the moments. As in Example 1 it is convenient to express the rigidities of all members as multiples of one value of K. Thus, for this frame, $K_1 = I_1/20$, $K_2 = 4I_1/40 = 2K_1$, $K_3 = K_1$.

Since changes of length of members due to tension or compression forces cause only negligible effects on the magnitudes of moments, it can be assumed that joints B and C displace the same amount d, as shown in Fig. 8.7*a*. Consequently, $R = d/20$ for both AB and CD. Since the frame is geometrically symmetrical and the top displacements of both legs are equal, both legs distort in precisely the same way and amount, causing the beam BC to deflect in an antisymmetrical shape. (This would not be true if, for example, $I_3 \neq I_1$, or if the lengths of both legs were not equal.) Hence, case d of Table 8.3 applies for member BC, while case c applies for AB and CD, since the bottom ends are fixed. The fixed-end moments are zero for all members, since no loads are applied between ends, but sidesway R is present in members AB and CD. With this information, the slope-deflection equations are

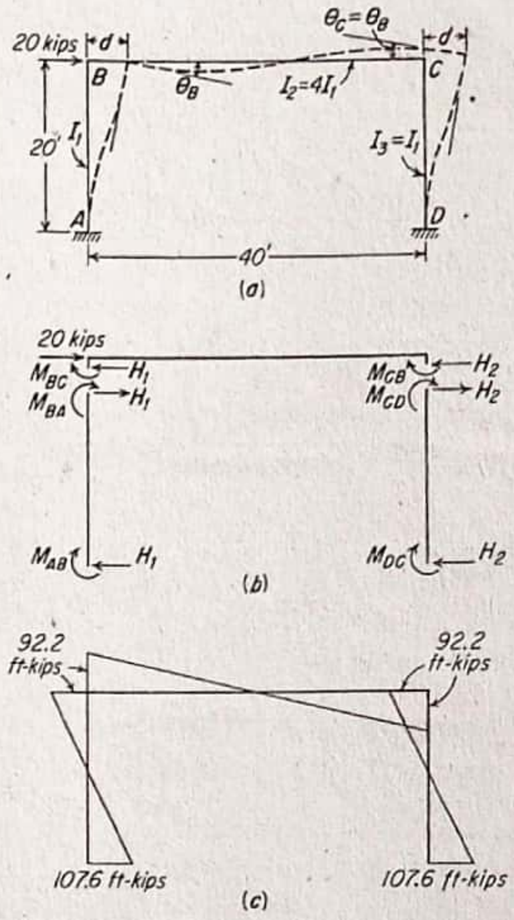


Fig. 8.7

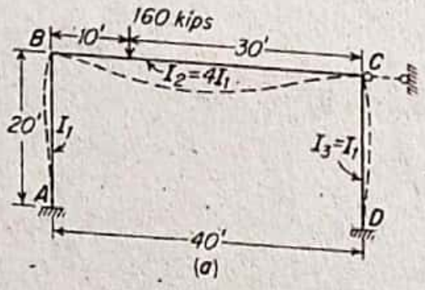
$$M_{AB} = M_{DC} = 2EK_1\theta_B - 6EK_1R$$
$$M_{BA} = M_{CD} = 4EK_1\theta_B - 6EK_1R$$
$$M_{BC} = M_{CB} = 6EK_2\theta_B = 12EK_1\theta_B$$

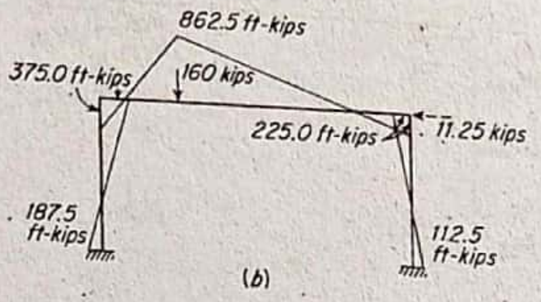
The condition of joint equilibrium, $M_{BA} + M_{BC} = 0$, gives

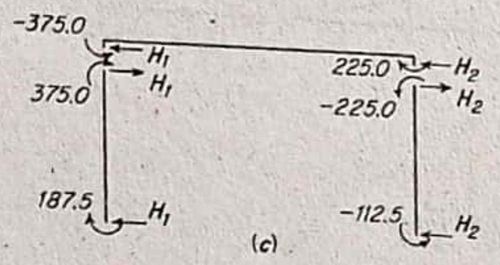
$$16EK_1\theta_B - 6EK_1R = 0$$

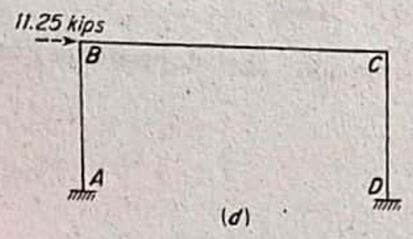
To obtain a second equation for the unknown quantities θ_B and R, use is made of the condition of frame equilibrium, indicating that the sum of the horizontal reactions of both legs must be equal and opposite to the applied horizontal load. In Fig. 8.7*b* are shown the moments and horizontal forces on each leg. At this stage the moments and forces are not known, either in magnitude or direction. For this reason they are all shown in the positive sense, i.e., moments clockwise and forces resulting in positive deflections. In this manner one ensures that the moments and forces resulting from the analysis are obtained with correct sign.

Scanned with CamScanner









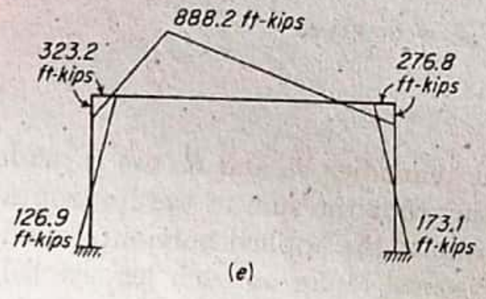


Fig. 8.8

[Art. 8.6

Considering the equilibrium of each leg

$$H_1 = -\frac{M_{AB} + M_{BA}}{20}$$

$$H_2 = -\frac{M_{DC} + M_{CD}}{20}$$

The shears or reactions at the bottoms of the legs must be in equilibrium with the applied horizontal load, or

$$H_1 + H_2 - 20 = 0$$

This expression is often referred to as the *shear* or *bent* equation. Substitution of the values H_1 and H_2 results in

$$M_{AB} + M_{BA} + M_{CD} + M_{DC} + 400 = 0$$

If the values of the moments are substituted in this expression, one obtains a second equation in terms of θ_B and R, namely,

$$3EK_1\theta_B - 6EK_1R + 100 = 0$$

Simultaneous solution with

$$16EK_1\theta_B - 6EK_1R = 0$$

gives

$$EK_1\theta_B = 7.68 \qquad EK_1R = 20.5$$

If these values are substituted in the original moment equations, the following moments result:

$$M_{AB} = M_{DC} = -107.6 \text{ ft-kips}$$
$$M_{BA} = M_{CD} = -92.2 \text{ ft-kips}$$
$$M_{BC} = M_{CB} = 92.2 \text{ ft-kips}$$

The moment diagram is as shown in Fig. 8.7*c*.

Example 3 The frame of Example 2 is loaded as shown in Fig. 8.8*a*. From Table 8.4, with $k = \frac{1}{4}$, the absolute values of the fixed-end moments are $M_{BC}' = 900$ ft-kips and $M_{CB}' = 300$ ft-kips. With proper attention to signs, and noting

that the bottoms of both legs are fixed, the slope-deflection equations are

$$M_{AB} = 2EK_1\theta_B$$
$$M_{BA} = 4EK_1\theta_B$$
$$M_{BC} = 8EK_1\theta_B + 4EK_1\theta_C - 900$$
$$M_{CB} = 8EK_1\theta_C + 4EK_1\theta_B + 300$$
$$M_{CD} = 4EK_1\theta_C$$
$$M_{DC} = 2EK_1\theta_C$$

Joint equilibrium requires

$$M_{BA} + M_{BC} = 0 \qquad \text{and} \qquad M_{CB} + M_{CD} = 0$$

which, upon substitution of the moment values, result in the two simultaneous equations

$$12EK_1\theta_B + 4EK_1\theta_C - 900 = 0$$
$$4EK_1\theta_B + 12EK_1\theta_C + 300 = 0$$

These give

$$EK_1\theta_B = 93.75 \qquad \text{and} \qquad EK_1\theta_C = -56.25$$

If these are substituted in the original moment equations, the following values result:

$$M_{AB} = 187.5 \qquad M_{CD} = -225.0$$
$$M_{CB} = 225.0 \qquad M_{BC} = -375.0$$
$$M_{BA} = 375.0 \qquad M_{DC} = -112.5$$

The corresponding moment diagram is shown in Fig. 8.8*b*.

Since no horizontal loads act on the frame, equilibrium requires that the sum of the horizontal reactions or shears at the bottoms of the legs be zero. In Fig. 8.8*c* are shown the moments acting at the ends of the legs. Since these moments are known from previous computations, they are shown in the correct sense, while the (as yet unknown) shears H are indicated as acting in the positive direction. Considering the equilibrium of both legs, it is seen that

$$H_1 + H_2 = -\frac{375.0 + 187.5}{20} + \frac{225.0 + 112.5}{20} = -11.25 \text{ kips} \neq 0$$

Consequently, the frame is not in equilibrium under the computed distribution of moments. It would be in equilibrium if an additional support were present at the level of the beam, as shown in broken lines in Fig. 8.8*a*, which would prevent horizontal displacement at that level. The reaction in that fictitious support must equilibrate the sum of the shears in the legs and is therefore as shown by the broken arrow in Fig. 8.8*b*. This condition is known as *sidesway prevented* or *no sidesway*. If such a support were physically present, as it sometimes is in bridge frames, the moment diagram of Fig. 8.8*b* would be correct.

In a free-standing frame, however, no such horizontal support exists. To realize the condition of zero horizontal load, it is necessary to apply to the frame a horizontal force equal and opposite to the fictitious horizontal reaction. This

Scanned with CamScanner

means that the correct moments in the free-standing frame are the sum of those computed for no sidesway (Fig. 8.8*b*) plus those resulting from a horizontal force equal to the sum of the horizontal leg reactions (Fig. 8.8*d*).

The latter loading is identical in character with that of Example 2, except that the load is now 11.25 kips instead of 20 kips. No new analysis is needed, since all moments are simply 11.25/20 times the moments of Example 2. Superposition of these sidesway moments on those previously obtained for no sidesway results in final moments as follows:

$$M_{AB} = 187.5 - 107.6 \times 11.25/20 = 126.9$$
$$M_{BA} = 375.0 - 92.2 \times 11.25/20 = 323.2$$
$$M_{BC} = -375.0 + 92.2 \times 11.25/20 = -323.2$$
$$M_{CB} = 225.0 + 92.2 \times 11.25/20 = 276.8$$
$$M_{CD} = -225.0 - 92.2 \times 11.25/20 = -276.8$$
$$M_{DC} = -112.5 - 107.6 \times 11.25/20 = -173.1$$

It can easily be checked that the frame is now in equilibrium, i.e., the sum of the moments at each joint is zero, and the sum of the horizontal reactions at the bottom is zero. These checks should always be made to guard against errors.

The final moment diagram is shown in Fig. 8.8*e*. Comparison with Fig. 8.8*c* shows the sizable difference which obtains between moments computed for no sidesway and those actually occurring in a free-standing frame, i.e., with free sidesway. A correct evaluation of the actual sidesway conditions is therefore a prerequisite for correct analysis. The influence of sidesway is more pronounced the more the frame or the distribution of loads, or both, departs from symmetry. Indeed, if the given portal frame were symmetrically loaded, sidesway would not occur, and the moments determined for no sidesway would be correct. It is the off-center location of the load of Fig. 8.8*a* which causes the frame to sidesway to the right. The direction of this sidesway is that corresponding to the horizontal force of Fig. 8.8*d*; this can also be realized from the fact that to prevent this sidesway it was found that a reaction acting to the left (Fig. 8.8*b*) would be required.

It is of some interest to determine the actual magnitude of such horizontal sidesway displacements. In Example 2 it was found that for a horizontal load of 20 kips, $EK_1R = 20.5$. Since $R = d/20$, one obtains, for the horizontal load of 11.25 kips of Fig. 8.8*e*, the sidesway displacement $d = 20(20.5/EK_1)(11.25/20)$ if all quantities are expressed in kips and feet. If a column section of 24 × 24 in. is required to resist the computed moments and loads, and if $E = 3 \times 10^6$ psi, one finds, with proper attention to units, that the sidesway is $d = 0.127$ in., that is, just over ⅛ in. It is seen that even such small sidesway displacements cause sizable changes in moments. Therefore the assumption of "no sidesway" is justified only if horizontal displacement of the actual structure is prevented by effective connection to a practically unyielding mass, such as solid rock, or to another structure which is very much more rigid than the frame proper.

PROBLEMS

For the following structures (*a*) compute the end moments, (*b*) draw complete moment and shear diagrams, and (*c*) sketch the deflected shape.

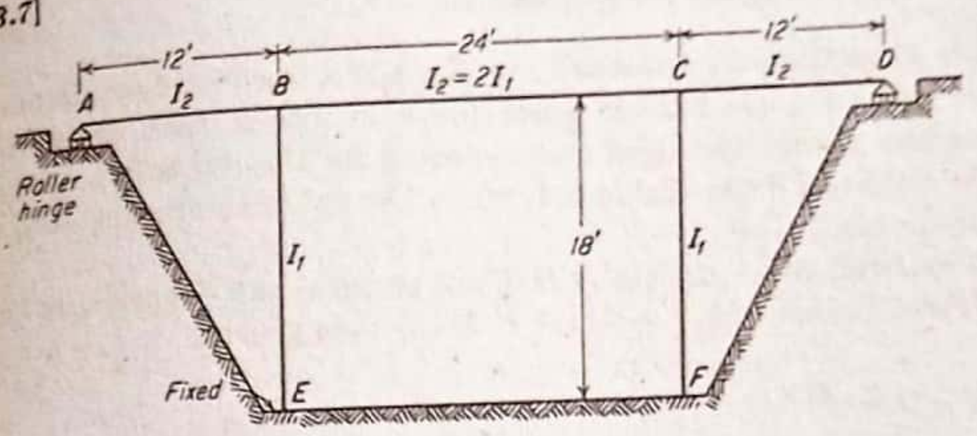


Fig. 8.9 Rigid-frame bridge.

1. The beam of Fig. 8.6, loaded as shown, but with the support C settled ¼ in. relative to the line ABD. Assume a cross section of 12 × 24 in.

2. The bridge frame of Fig. 8.9, subject to a uniform dead load of 1 kip per ft over the entire length. (*Hint:* the symmetry of the structure can be used to simplify computations.)

3. The bridge frame of Fig. 8.9, subject to a horizontal force of 1 kip, applied along the axis of the beam. (Such forces are caused by the inertia of vehicles when brakes are applied.)

4. The bridge frame of Fig. 8.9, subject to a uniform live load of 1 kip per ft on span AB.

8.7 Moment-distribution Method The slope-deflection method is a powerful and relatively simple tool for determining moments in continuous structures, as was illustrated in Art. 8.6. It was shown that this method results in as many simultaneous equations as there are unknown joint rotations and translations (not counting the rotations of hinged joints). If there are not more than three or four such unknowns, the method does not present any practical difficulties. However, in many structures, such as multistory, multibay frames, there may be anywhere from five to twenty or more joints, each with an unknown rotation and many with unknown translations. If the slope-deflection method were used to analyze such structures, the work and time involved in solving large numbers of simultaneous equations would be prohibitive. To overcome this difficulty, Hardy Cross developed and published the moment-distribution method in 1932. Because of the great saving of time it achieves, this method is now very widely used. It is different from most other types of analysis in that no equations are set up and solved unless sidesway is involved. Instead, the final moments are obtained by successive numerical approximations.

Suppose that the four members shown in Fig. 8.10*a* were part of a building frame. For the time being the ends B, C, D, and E will be considered fixed. A temporary fixation against rotation is now introduced

Scanned with CamScanner

at joint A, indicated symbolically in Fig. 8.10*b*. For this state all moments in the structure are known, since the moments at both ends of both girders are simply the fixed-end moments for the respective spans and can be obtained from Table 8.4, while the columns are not subject to any moments.

In general, $M_{AC}{}^f$ and $M_{AE}{}^f$ will not be equal and opposite, so that an *unbalanced moment* $M_A{}^u = M_{AC}{}^f + M_{AE}{}^f$ or in general

$$M_A{}^u = \Sigma_A M^f$$

acts on the joint. The right side of this equation stands for the sum of all fixed-end moments acting on the joint. This unbalanced moment is resisted by the temporary fictitious fixation.

If this fixation is now removed, i.e., the joint is released, it will rotate in the direction of $M_A{}^u$, as indicated in Fig. 8.10*c*, until equilibrium is established. Further rotation is then resisted by the bending rigidity of all members meeting at the joint, each of which exerts on the joint a moment that counteracts the rotation, as shown in Fig. 8.10*d*. For equilibrium to establish itself, the sum of these moments must be equal and opposite to the unbalanced moment, so that the sum of all moments

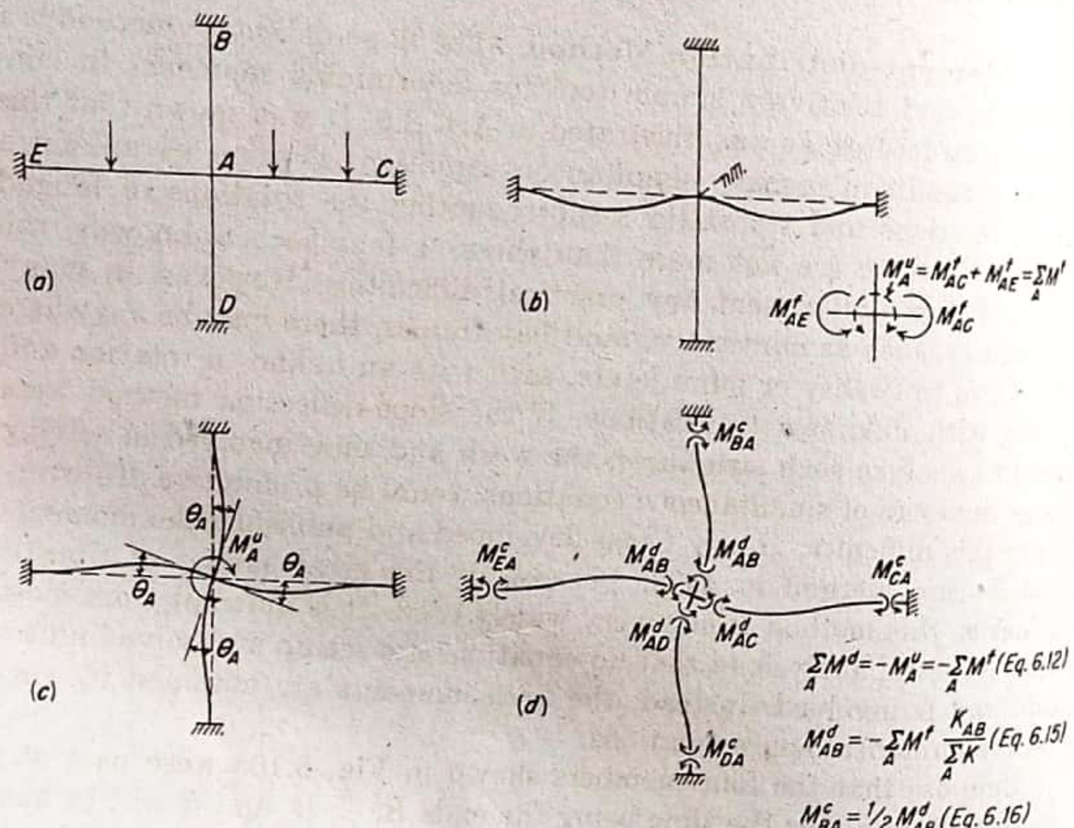


***Fig.* 8.10** Moment distribution at one joint (procedure and formulas).

at the joint is zero. Hence,

$$\Sigma_A M^d = M_{AB}{}^d + M_{AC}{}^d + M_{AD}{}^d + M_{AE}{}^d = -\Sigma_A M^f \tag{8.12}$$

These moments are known as the *distributed moments*, since they represent the fractions of the balancing moment, $-\Sigma_A M^f$, distributed to the respective abutting members.

In Fig. 8.10 all moments are shown in the direction in which they actually act in this particular example, regardless of sign. In connection with the moment-distribution method, *the same sign convention will be used as was established for the slope-deflection method in Art.* 8.4. In particular, the distributed moments in the free-body sketches of the members and joints of Fig. 8.10*d* are all seen to be positive in this case, since they act clockwise on their respective members, or counterclockwise on joint A.

Since joint A is rigid, the angles θ_A of all members (Fig. 8.10*c*) must be equal. From case *c* of Table 8.3, for a member whose far end is fixed, the angle at the near end is

$$\theta_1 = \frac{M_1}{4EK} \tag{8.13}$$

Hence, canceling $4E$, the condition that all end angles are equal can be written as

$$\frac{M_{AB}{}^d}{K_{AB}} = \frac{M_{AC}{}^d}{K_{AC}} = \frac{M_{AD}{}^d}{K_{AD}} = \frac{M_{AE}{}^d}{K_{AE}} \tag{8.14}$$

Using this relation to express all distributed moments in Eq. (8.12) in terms of $M_{AB}{}^d$, one obtains, if the first term is multiplied by (K_{AB}/K_{AB}),

$$M_{AB}{}^d \left(\frac{K_{AB}}{K_{AB}} + \frac{K_{AC}}{K_{AB}} + \frac{K_{AD}}{K_{AB}} + \frac{K_{AE}}{K_{AB}} \right) = -\Sigma_A M^f$$

from which

$$M_{AB}{}^d = (-\Sigma_A M^f) \frac{K_{AB}}{\Sigma_A K} \tag{8.15}$$

Similarly,

$$M_{AC}{}^d = (-\Sigma_A M^f) \frac{K_{AC}}{\Sigma_A K}, \quad \cdots$$

The quantities

$$\frac{K_{AB}}{\Sigma_A K}, \quad \cdots$$

Scanned with CamScanner

are known as the *distribution factors*, since they indicate the fraction of the balancing moment, $-\Sigma_A M^f$, which is distributed to each individual member.

The distributed moments, acting at the near end of each member (at the joint), cause it to bend as shown in Fig. 8.10*d* and result in a moment at the fixed far end. By comparing M_{12} and M_{21} of case *c*, Table 8.3, one sees that the moment M_{21} at the fixed far end is one-half the moment M_{12} applied at the near end. Hence

$$M_{BA^c} = \tfrac{1}{2} M_{AB^d} \qquad M_{CA^c} = \tfrac{1}{2} M_{AC^d} \tag{8.16}$$

The moments M_{AB^c}, etc., are known as the *carry-over moments*, since they are carried over from the near to the far end, and the factor $\frac{1}{2}$ is known as the *carry-over factor*. From the free-body sketches of Fig. 8.10*d* it is seen that the carry-over moments have the same sign as the distributed moments at the other end of the member. In the figure they are positive, since they act clockwise on their respective members, or counterclockwise on their joints B to E.

The *final moments* at either end of any member, then, are the sums of the original fixed-end moments (where they exist, as in the girders) and the distributed moments or the carry-over moments, as the case may be. Thus,

$$\begin{aligned}
M_{AC} &= M_{AC^f} + M_{AC^d} = M_{AC^f} - (\Sigma_A M^f)\frac{K_{AC}}{\Sigma_A K} \\
M_{AB} &= M_{AB^d} = -(\Sigma_A M^f)\frac{K_{AB}}{\Sigma_A K} \\
M_{EA} &= M_{EA^f} + M_{EA^c} = M_{EA^f} - \frac{1}{2}(\Sigma_A M^f)\frac{K_{AE}}{\Sigma_A K} \\
M_{DA} &= M_{EA^c} = -\frac{1}{2}(\Sigma_A M^f)\frac{K_{AD}}{\Sigma_A K}
\end{aligned} \tag{8.17}$$

and similarly for the other four end moments.

The above procedure may seem complicated in general terms. The following numerical example will indicate its actual simplicity. Since, in the moment-distribution method, all computations are carried out numerically rather than in the form of equations, it is important to organize the computing sheets in a systematic manner in order not to get lost in a maze of numbers. Various schemes may be used, at the computer's preference. The authors believe that the scheme employed in the following examples is simple and not conducive to errors.

The left upper sketch in Fig. 8.11 shows the dimensions and loads of the frame. The fixed-end moments (from Table 8.4) are computed as shown, and the stiffnesses K are determined. The moment distribution is carried out on a separate sketch, not necessarily drawn to scale, which

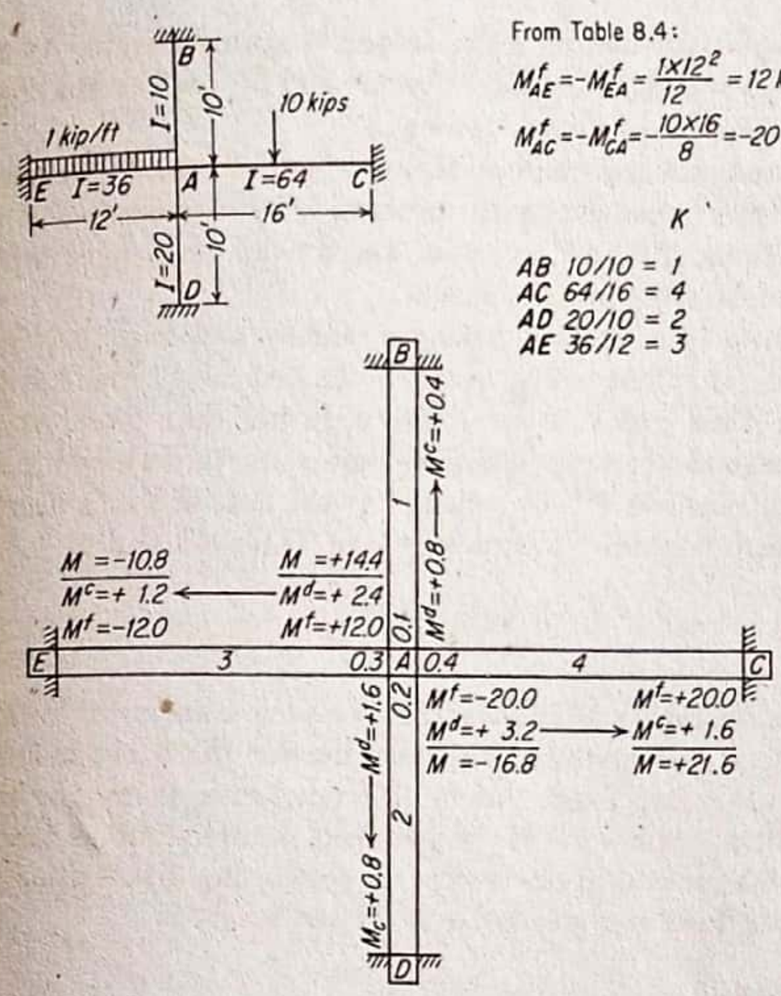


Fig. 8.11 Moment distribution at one joint (calculations).

includes the stiffness of each member (shown at midspan) and the distribution factor (shown near the joints). Fixed-end moments are shown at the sections at which they act. It is advantageous in cases such as this to write all moments in consecutive spans alternatingly on one and the other side of the member. This provides the necessary space to enter all subsequent moments. In the given frame no fixed-end moments act on AD and AB. The balancing moment (equal and opposite to the unbalanced moment at A) is now distributed to the abutting members according to Eq. (8.15); that is, $M_{AB^d} = 8.0 \times 0.1 = 0.8$, $M_{AC^d} = 8.0 \times 0.4 = 3.2$, etc. The carry-over moments at the far ends are one-half the distributed moments [Eq. (8.16)], the carry-over being indicated by arrows. The final moments at each end of all members are obtained by summing the individual entries. Once the distribution is completed, joint A is in equilibrium; i.e., the sum of the final moments is zero:

$$14.4 + 0.8 - 16.8 + 1.6 = 0$$

Scanned with CamScanner

This check should always be made to guard against errors. At the end of members AB and AD the respective M^a and M^c are the final moments, since no fixed-end moments are present.

It is seen that all eight end moments were determined without equations, by a very simple numerical process. With some practice the moment designations (M^f, M^c, etc.) as well as the carry-over arrows can be omitted on the computation sheets.

If the far end of a member is hinged rather than fixed (say end C in Fig. 8.10*a*), the moment it exerts on the locked joint (Fig. 8.10*b*) is the *moment at the fixed end of a beam hinged*, rather than fixed, *at the other end*. In this case the corresponding moments are those listed in the last two columns of Table 8.4. The rotation at the near end of a beam whose far end is hinged is obtained from case *a* of Table 8.3 and is

$$\theta_1 = \frac{M_1}{3EK} \tag{8.18}$$

Comparison with Eq. (8.13) shows that for such a beam the rotation for a given moment is four-thirds the rotation for the same moment M_1 but with the other end fixed. Put in different terms, it may be said that the stiffness of a beam with far end hinged is three-fourths that of the same beam with far end fixed. Hence, for computing distribution factors, the *modified stiffness of a member with far end hinged* is

$$K^m = \frac{3}{4}K = \frac{3}{4}\frac{I}{l} \tag{8.19}$$

rather than I/l for far end fixed. For such members, of course, *no moment is carried over to the hinged end*, since such a support is not capable of resisting a moment.

So far, the moment-distribution method has been discussed only for a structure with one single joint subject to rotation. If more than one such joint is present, each joint is unlocked, balanced, and relocked in turn. With reference to Fig. 8.12, the beam of Example 1, Art. 8.6, will be solved by moment distribution. Fixed-end moments, stiffnesses, and

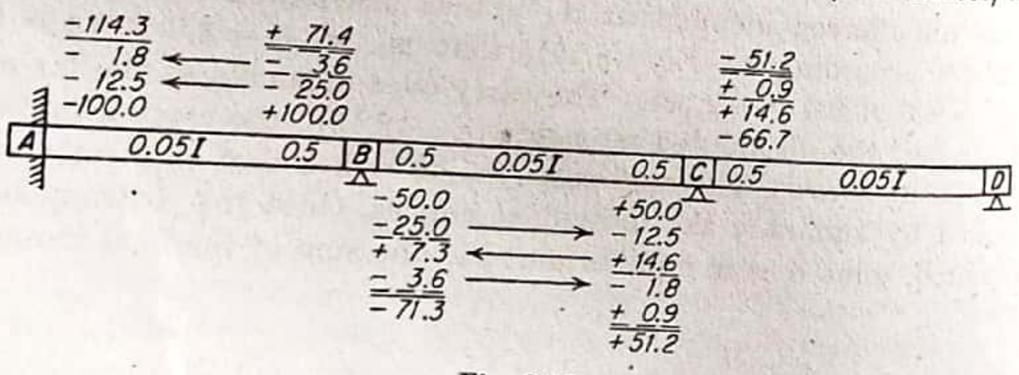


***Fig.* 8.12**

distribution factors are computed and recorded on a separate sketch of the structure. In this particular case, it happens that all the stiffnesses are equal (note the use of modified stiffness for the span CD, with hinged end), so that the distribution factors at all interior joints equal 0.5.

The fixed-end moments are valid only if joints B and C are artificially restrained against rotation. Joint B is first released and permitted to rotate; the unbalanced moment is distributed to members AB and BC in accordance with their stiffnesses, and carry-over moments are recorded at joints A and C. Joint B is then relocked, and joint C is permitted to rotate. To the original unbalance at that joint is added the moment carried over from the rotation of joint B; the entire unbalanced moment is distributed at once, and again the carry-over moment is recorded. Joint C is then relocked, and the cycle is repeated, by returning to joint B, until the successive corrections become negligible. The sum of all moments entered in one column represents the final moment at that end of the member. It should be noted that the moments obtained from Fig. 8.12 differ by only a fraction of a per cent from those obtained by slope deflection in Art. 8.6, namely -114.5, $+71.1$, -71.1, $+51.1$, and -51.1.

It is seen in this example that the correction moments decrease very quickly. In this particular case two distribution cycles have resulted in more than adequate accuracy. In more complicated structures three or four cycles may be required. It is interesting to observe that, for this example, the three-moment method results in three simultaneous equations for M_a, M_b, and M_c, and the slope-deflection method in two simultaneous equations for θ_a and θ_b, while by the moment-distribution method the entire analysis is carried out numerically.

8.8 Moment Distribution for Frames with Joint Displacement (Sidesway) The method discussed in Art. 8.7 permits the determination of moments in structures whose joints, though rotated, are not linearly displaced (translated) under load. When such linear displacements occur, such as from horizontal wind loads or other sources, computations must be correspondingly modified to account for this influence. This process is exactly similar to that employed in Examples 2 and 3, Art. 8.6, except that now moments will be determined by distribution instead of by slope-deflection equations.

If a horizontal force acts on a frame, it will deflect an amount d, as indicated in Fig. 8.13. Even though, for any design, the horizontal force is usually known (say, the wind pressure) it is more convenient in connection with moment distribution to proceed in the reverse order.

The frame is given an arbitrary displacement d of convenient magnitude. Next, the moments due to this displacement and the magnitude

Scanned with CamScanner

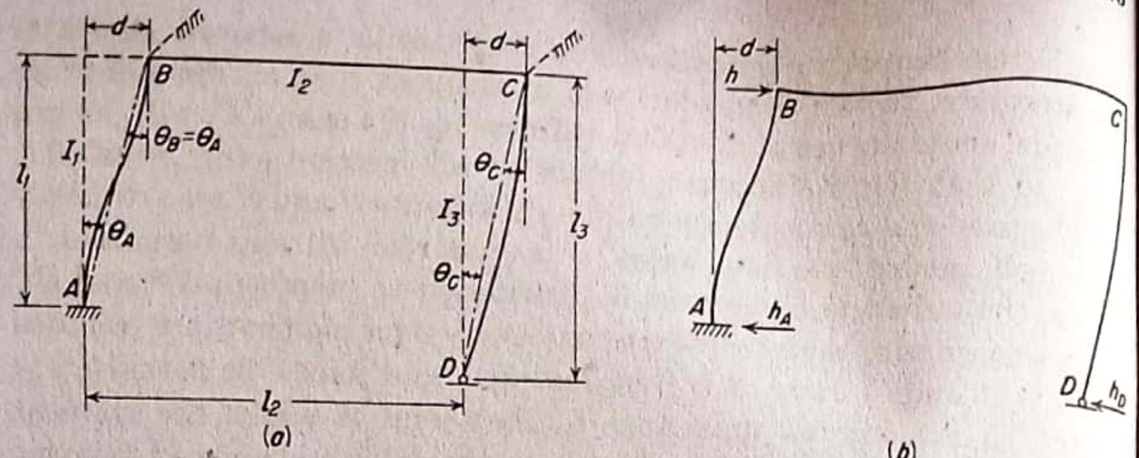


Fig. 8.13

of the force required to produce it are computed. Let the magnitude of this force be h, and the corresponding moments m, while the actual horizontal force is H. Then the actual moments are

$$M = m\frac{H}{h} \tag{8.20}$$

To compute m and h, the joints B and C (Fig. 8.13a) are first locked against rotation and then given an equal arbitrary displacement d. This causes moments m' to occur at A, B, and C (D being hinged in this particular example). Leg AB, with tangents at both ends parallel, bends antisymmetrically, as in Fig. 8.5d. Consequently for a given displacement the moments are obtained from case d of Table 8.3:

$$m'_{AB} = m'_{BA} = 6EK\theta_A = 6K\frac{Ed}{l_1} \tag{8.21}$$

which holds when *the bottom end of the column is fixed*. Column CD, being hinged at one end, corresponds to Fig. 8.5a. Consequently, *for a column with bottom end hinged*, the moment at the top is

$$m'_{CD} = 3EK\theta_C = 3K\frac{Ed}{l_3} \tag{8.22}$$

Next, the temporarily locked joints are released, and the moments m corresponding to the actual configuration of the frame (Fig. 8.13b) are computed by the usual procedure of distributing the moments m'. The horizontal reactions h_A and h_D are now determined by considering individually the equilibrium of each leg (see Fig. 8.7b). Hence,

$$h_A = \frac{m_{AB} + m_{BA}}{l_1} \tag{8.23}$$

and, since D is hinged, so that $m_{DC} = 0$,

$$h_D = \frac{m_{CD}}{l_3} \tag{8.24}$$

The horizontal force corresponding to the arbitrary displacement d is thus

$$h = h_A + h_D \tag{8.25}$$

Since the actual force that acts on the frame is H rather than the fictitious auxiliary force h, the actual moments are then computed from Eq. (8.20).

As was shown in Example 3, Art. 8.6, sidesway and corresponding moments are caused not only by actual horizontal loads, but also by asymmetry of vertical loads and/or of frame configuration.

The analysis of frames with sidesway is illustrated below.

Illustrative example To compute the moments in the frame of Fig. 8.14a, the stiffnesses $K = I/l$ are calculated for all members, except that for the hinged

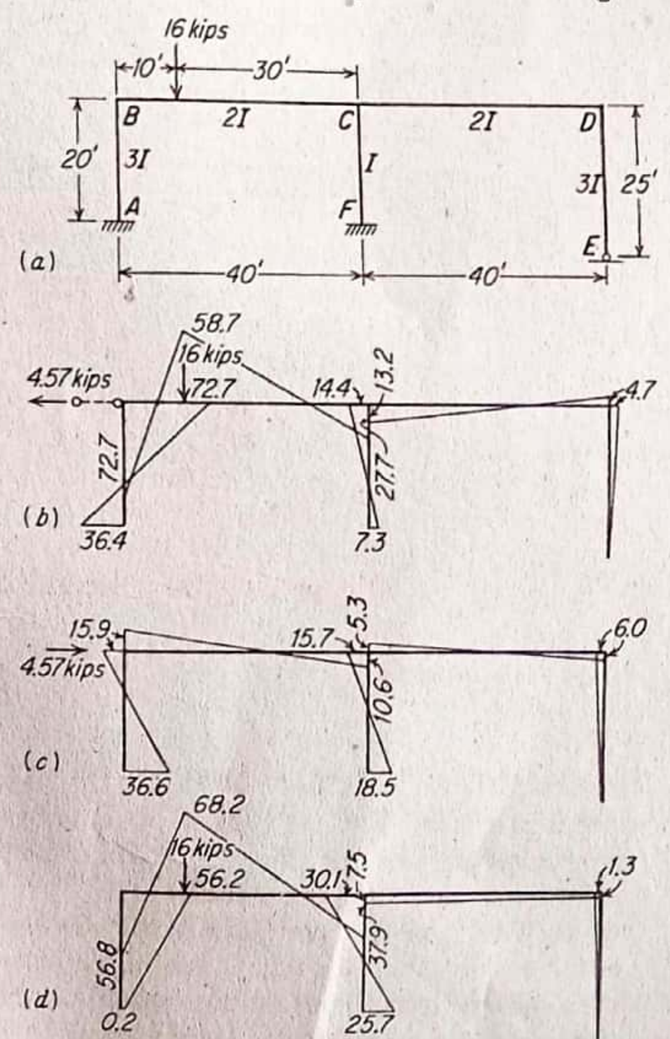
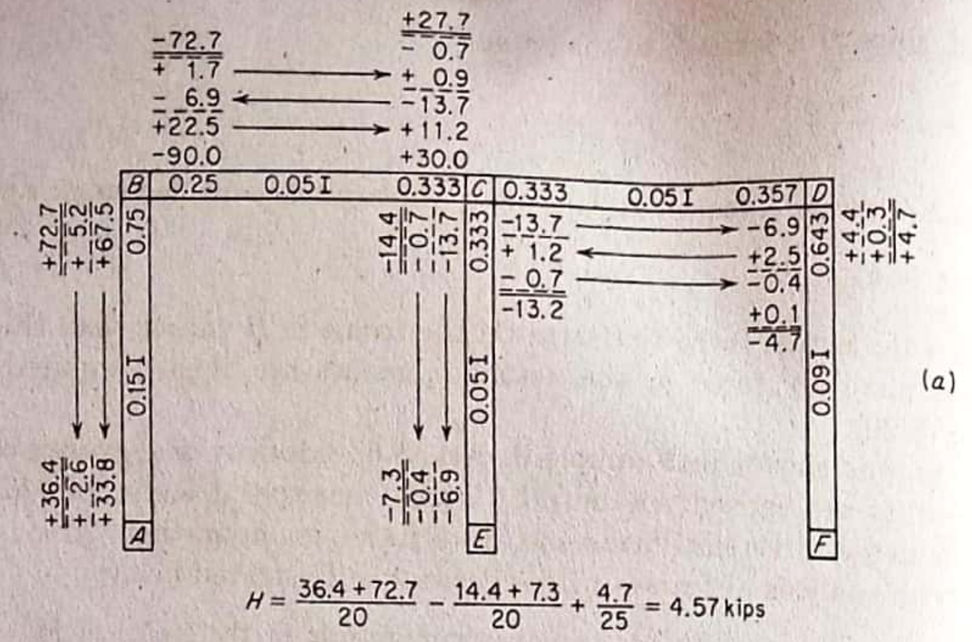


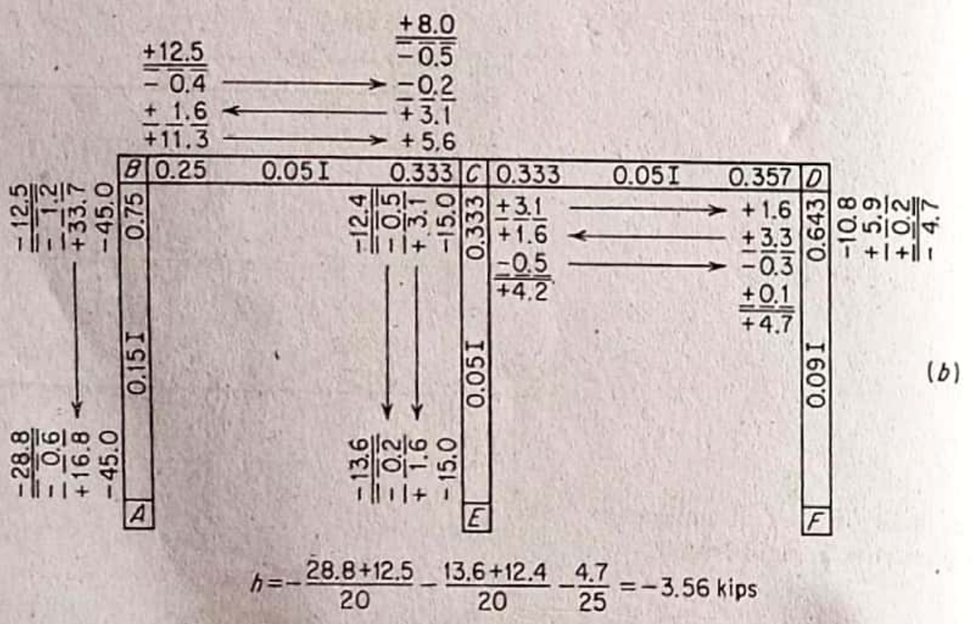
Fig. 8.14 Effect of sidesway on moments in rigid frame.

Scanned with CamScanner



(*a*)

$$H = \frac{36.4 + 72.7}{20} - \frac{14.4 + 7.3}{20} + \frac{4.7}{25} = 4.57 \text{ kips}$$



(*b*)

$$h = -\frac{28.8 + 12.5}{20} - \frac{13.6 + 12.4}{20} - \frac{4.7}{25} = -3.56 \text{ kips}$$

Fig. 8.15

member DE, $K^m = 0.75I/l$. Next, the distribution factors are computed for all members at joints B, C, and D and, together with the stiffnesses, are indicated on the computation sketch, Fig. 8.15*a*. The fixed-end moments for the loaded span BC may be obtained from Table 8.4.

1. With these data the moment distribution of Fig. 8.15*a* is carried out in the usual way for "no sidesway." The distribution was started by unlocking B and then, successively, C and D, then repeating the cycle. It is seen that the corrections produced by the second cycle amount to less than 10 per cent of those of the

first cycle. Since correction moments in successive cycles decrease in about the same proportion, a third cycle, if carried out, would contribute corrections of about 1 per cent or less of the final moments. These can be neglected, so that, in this example, a two-cycle distribution provides satisfactory accuracy.

After completion of the distribution computations, each joint is checked for equilibrium, that is, $\Sigma M = 0$. It is seen that joints B and D check exactly. At joint C there is a discrepancy in the third digit. Such discrepancies in the last digit result frequently from rounding off digits not shown in the computation. If computations are carried to three digits, as they usually are, slight discrepancies in the last digits are obviously negligible.

By computing the shears at the bottoms of the three legs, as shown in Fig. 8.15*a* [see Eqs. (8.23) and (8.24)], an unbalanced force of $H = 4.57$ kips is obtained. In other words, the frame would be in equilibrium under the moments of Fig. 8.15*a* only if an additional support were present to prevent sidesway and to supply a horizontal reaction of 4.57 kips. This fictitious state of loading and the corresponding moment diagram are shown in Fig. 8.14*b*.

2. It is now necessary to determine the "sidesway correction," i.e., to apply a force equal and opposite to H. This amounts to removing the fictitious support at D, which permits the natural sidesway to occur. The sidesway moments caused by H, if superposed on those of Fig. 8.14*b*, give the correct end moments.

To compute these moments, joints B, C, and D are locked and given an arbitrary horizontal displacement. This displacement is so chosen as to result in moments of convenient magnitude; here $Ed = 1000$ serves this purpose. The corresponding end moments for legs AB and CE are computed from Eq. (8.21), and for the hinged leg DF from Eq. (8.22); for $Ed = 1000$, they are -45.0, -15.0, and -10.8 ft-kips, respectively. These moments are applied and distributed in the usual manner, as shown in Fig. 8.15*b*. It is seen that a two-cycle distribution is again sufficient, since a third cycle would add corrections of less than 1 per cent. The horizontal shears are computed as in (1) [see Eqs. (8.23) and (8.24)], and the total horizontal force $h = -3.60$ kips, corresponding to the given deflection $Ed = 1000$, is calculated as indicated in Fig. 8.15*b* [see Eq. (8.25)]. Since the moments of Fig. 8.15*b* are caused by a force of 3.60 kips, while the force required to eliminate the reaction of Fig. 8.14*b* is 4.57 kips, the actual sidesway moments are 4.57/3.60 times those of Fig. 8.15*b* [see Eq. (8.20)]. The corresponding sidesway moment diagram is shown in Fig. 8.14*c*.

3. To obtain the final moments, the sidesway moments of Fig. 8.14*c* are added to those for no sidesway (Fig. 8.14*b*), resulting in the final moment diagram shown in Fig. 8.14*d*. Comparison of Fig. 8.14*b* and *d* shows the very large influence sidesway may have; not only are the magnitudes of the moments changed by 50 per cent and more, but even signs are reversed in some cases, such as at points A and D. Even though the relative influence of sidesway may be considerably smaller in many cases, the present example shows that it is unsafe to neglect sidesway in design except (1) if symmetry of the frame and loading forestall any sidesway tendency or (2) if the structure is so supported as to make sidesway physically impossible.

4. If a real horizontal force of, say, 10 kips, such as a wind load, acts on this frame, from left to right, the moments are 10/4.57 times those of Fig. 8.14*c* or,

Scanned with CamScanner

which amounts to the same, 10/3.60 of those determined by the distribution of Fig. 8.15*b*.

PROBLEMS

Solve Probs. 2 to 4, Art. 8.6, by moment distribution.

8.9 Building Frames: Vertical Loads Rigid frames with a small number of spans, one or at most two stories high, occur frequently in industrial and commercial structures and in bridges. Since the number of joints in such frames is relatively small, their analysis presents no particular difficulty, as is illustrated by the examples of the preceding articles.

In contrast, the frames of multistory apartment or office buildings, warehouses, and the like have a multitude of members and joints, as is seen on the relatively small frame of Fig. 8.16. Such frames are known for short as *building frames* and are composed of columns and of girders or beams. These members must be designed for the largest moments, shears, and, in the case of columns, axial loads which can reasonably be expected to occur during the lifetime of the building. These moments, shears, and axial loads are brought about in part by the weight of the structure (dead load) and in part by live load. While the former is constant, live loads, such as floor loads from human occupancy, can be placed in various ways, some of which will result in larger effects than others.

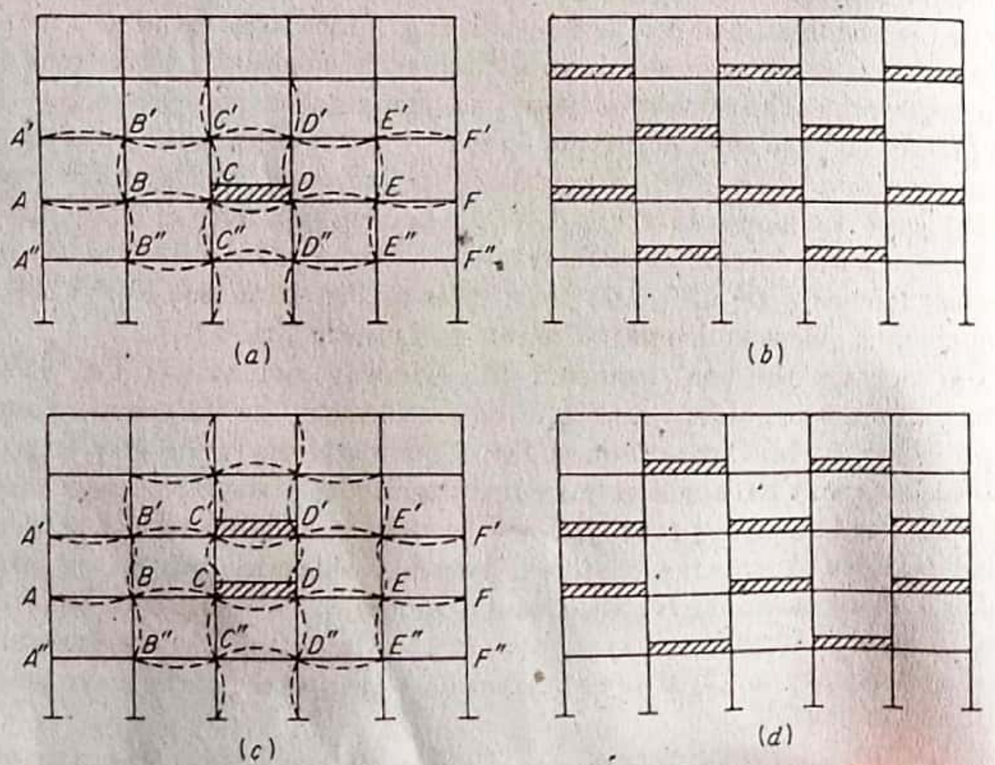


Fig. 8.16

In Fig. 8.16*a*, only span *CD* is loaded by live load. The distortions of the various frame members are seen to be largest in and immediately adjacent to the loaded span and to decrease rapidly with increasing distance from the load. Since bending moments are proportional to curvatures, the moments in more remote members are correspondingly smaller than those in, or close to, the loaded span. However, the loading of Fig. 8.16*a* does not produce the maximum possible positive moment in *CD*. In fact, if additional live load were placed on span *AB*, this span would bend down, *BC* would bend up, and *CD* itself would bend down in the same manner, although to a lesser degree, as it is bent by its own load. Hence, the positive moment in *CD* is increased if *AB* and, by the same reasoning, *EF* are loaded simultaneously. By expanding the same reasoning to the other members of the frame, it is easily seen that the "checkerboard pattern" of live load of Fig. 8.16*b* produces the largest possible positive moments not only in *CD*, but in all loaded spans. Hence, two such checkerboard patterns are required to obtain the maximum positive moments in all spans.

In addition to maximum span moments, it is often necessary to investigate minimum span moments. Dead load, acting as it does on all spans, usually produces only positive span moments. However, live load, placed as in Fig. 8.16*a* and even more so in Fig. 8.16*b*, is seen to bend the unloaded spans upward, i.e., to produce negative moments in the span. If these negative live-load moments are larger than the generally positive dead-load moments, a given girder, depending on load position, may be subject at one time to positive span moments and at another to negative span moments. It must be designed to withstand both types of moments, i.e., it must be furnished with tensile steel at both top and bottom. Thus, the loading of Fig. 8.16*b*, in addition to giving maximum span moments in the loaded spans, gives minimum span moments in the unloaded spans.

Maximum negative moments at the supports of the girders are obtained, on the other hand, if loads are placed on the two spans adjacent to the particular support and in a corresponding pattern on the more remote girders. A separate loading scheme of this type is then required for each support for which maximum negative moments are to be computed.

In each column, the largest moments occur at the top or bottom, as can easily be seen from the examples of the preceding articles. While the loading of Fig. 8.16*c* results in large moments at the ends of columns *CC'* and *DD'*, the reader can easily convince himself with a simple moment distribution that these moments are further augmented if additional loads are placed as shown in Fig. 8.16*d*.

It is seen from this brief discussion that, in order to calculate the

Scanned with CamScanner

maximum possible moments at all critical points of a building frame, live load must be placed in a great variety of different schemes. If a complete moment distribution for the entire frame is carried out for each of these cases, the required amount of computation becomes prohibitive, even for frames with a limited number of spans and stories. The need is apparent, then, for simplified approximate methods which allow the determination of these moments with reasonable accuracy and yet limit the amount of computation. Although such abbreviated methods cannot result in the largest theoretically possible moments, the use of approximations is justified for a variety of reasons.

Thus, even though it is theoretically necessary to load span $B''C''$, among others, to obtain the maximum positive moment in $D'E'$ (Fig. 8.16*b*), the former is so far removed from the latter that its effect on this moment is negligibly small. Hence, the influence on any moments of loads on spans sufficiently far removed can generally be neglected. That such a procedure is legitimate is emphasized also by the fact that it is quite improbable for the exact loading schemes of Fig. 8.16*b* and *d* ever to occur during the lifetime of the structure. Considerations similar to these justify methods in which, to determine any particular moment, only the influence of the adjacent parts of the frame is considered.

In this connection it is also important to realize the difference in the importance of accurate moment determination for girders on the one hand and for columns on the other. In the former the required cross sections are dictated exclusively by moments and shears, and for this reason a relatively accurate determination of these quantities is called for. Columns, on the other hand, must resist the axial loads from overlying parts of the structure, in addition to the bending moments induced in them by the rigidly connected girders. An inaccuracy in determining these moments therefore affects only one of the two factors (loads and moments) which determine the required cross sections and, for this reason, has smaller overall effect than similar inaccuracies in determining girder moments. It should also be noted that the load distribution which results in maximum column moments does not at the same time result in maximum axial forces in the same columns. For instance, even though the loading of Fig. 8.16*d* results in maximum $M_{CC'}$, the axial load on that column would attain its maximum if all, instead of just a few, of the adjacent girder spans in the upper stories were loaded. While such full loading of overlying spans would result in maximum axial force, it would, conversely, cause a smaller moment $M_{CC'}$ than that resulting from Fig. 8.16*d*.

It is evident from this discussion that an approximate method of moment determination is reliable for design use if it permits the determination of girder moments with a relatively high degree of accuracy. For column moments, a cruder approximation is permissible, if such moments

are used in conjunction with maximum axial loads (i.e., all overlying adjacent spans fully loaded, except for such decrease in live load with increasing number of stores as is permitted in most building codes).

Extensive investigation by means of numerous trial computations has shown that, for building frames with reasonably regular outline not involving unusual asymmetry of loading or shape, the influence of sidesway caused by vertical loads can be neglected.

In that case moments are determined with sufficient accuracy by breaking up the entire frame into simpler subframes. Each of these consists of one girder, plus the top and bottom columns framing into that particular girder. Placing the live loads on that girder in the most unfavorable manner permits sufficiently accurate determination of all girder moments and of the moments at the top ends of the bottom columns and at the bottom ends of the top columns. For this partial structure, the far ends of the columns are considered as fixed, except for such first-floor or basement columns where soil and foundation conditions more closely approach hinged ends. Consequently, the ACI Code specifies for floor members, including girders:

> (1) The live load may be considered to be applied only to the floor or roof under consideration, and the far ends of the columns may be assumed as fixed.
> (2) Consideration may be limited to combinations of dead loads on all spans with full live load on two adjacent spans (for negative support moments) and with full live load on alternate spans (for positive span moments).

When investigating the maximum negative moment at any joint, negligible error will result from considering the joints second removed in each direction to be completely fixed. Similarly, in determining maximum or minimum span moments, the joints at the far ends of the adjacent spans may be considered fixed. Thus, individual portions of a frame of many spans may be investigated separately.

In regard to columns, the Code indicates:

> Columns shall be designed to resist the axial forces from loads on all floors, plus the maximum bending due to loads on a single adjacent span of the floor under consideration. Account shall also be taken of the loading condition giving the maximum ratio of bending moment to axial load. In building frames, particular attention shall be given to the effect of unbalanced floor loads on both exterior and interior columns and of eccentric loading due to other causes. In computing moments in columns due to gravity loading, the far ends of columns which are monolithic with the structure may be considered fixed.

The following example illustrates the computation of moments in building frames.

Scanned with CamScanner

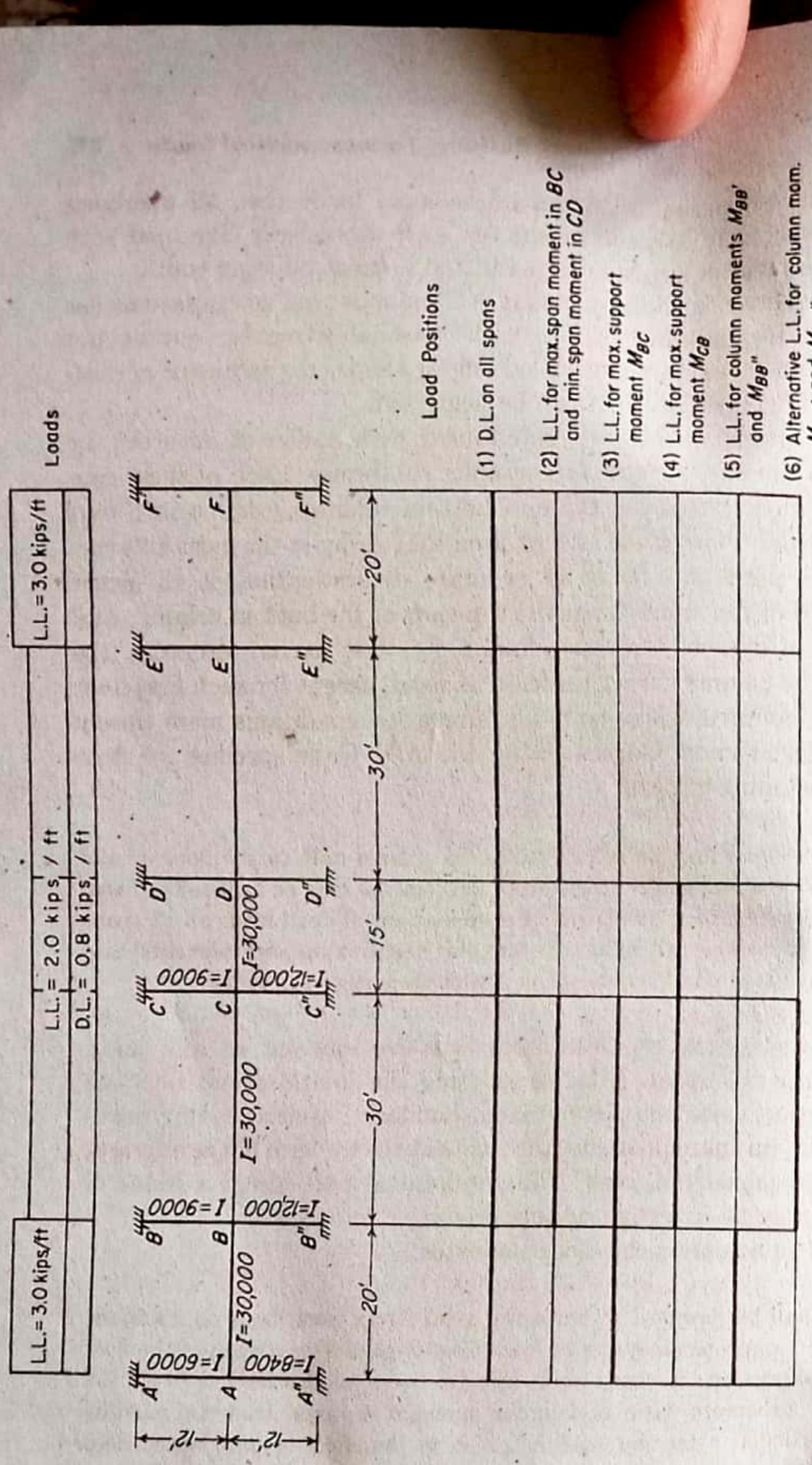


Fig. 8.17 Approximate determination of moments in building frames (vertical load).

Illustrative example The structure shown in Fig. 8.17 represents the second-story girder of the frame of Fig. 8.16, including the abutting top and bottom columns, isolated as just described. Dimensions and moments of inertia are shown in the main sketch, while the magnitude and character of loads are indicated at the top of the figure. Since span lengths differ by more than 20 per cent, and since the ratio of live to dead load, at least for some spans, exceeds 3:1, design by approximate moment coefficients such as those of Table 8.2 would be misleading and unsafe. Moment determination by more accurate frame analysis is, therefore, *mandatory* for this structure. Let it be required to compute all necessary moments for span BC, the minimum span moment for CD, and the column moments $M_{BB'}$ and $M_{BB''}$.

According to the preceding discussion, it is necessary, for this purpose, to determine moments from the six loading schemes shown at the bottom of Fig. 8.17. This would require six separate moment distributions. However, in this particular case considerable simplification can be achieved by noting that (1) all live and dead loads are uniformly distributed, though of varying magnitudes, and (2) the structure is symmetrical. To reduce computations, moments are determined separately for a uniform load of 1 kip per ft placed individually on spans AB, BC, and CD. The moments for all six loadings of Fig. 8.17 can then be computed by simple superposition of the moments obtained from these three distributions. Simplifications such as this depend on the shape of the structure and the type of loading and should always be used when possible.

The fixed-end moments $wl^2/12$ for $w = 1$ kip per ft are 33.3, 75.0, and 18.75 ft-kips for spans AB, BC, and CD, respectively. The stiffnesses and distribution factors are computed in the usual manner from the given lengths and moments of inertia.

For this particular type of moment computation in building frames, a special way of recording the calculations is often found convenient. This scheme is shown in detail in Fig. 8.18*a* and is self-explanatory. It has the advantage that all figures are written in one instead of two directions. Carry-overs along the girders can be indicated by arrows in the usual manner. This would not be possible for carry-overs along columns. However, these are not required, since only moments in the column end sections adjacent to the girder are determined in this special form of distribution. Moment $M_{B'B}$, for instance, would be found, not from this calculation, but from a similar analysis of girder $A'F'$ of Fig. 8.16, with its adjacent columns.

The three distributions for the unit loads on the three spans are given in Fig. 8.18*a* to *c*. In examining these calculations, the following features are noteworthy: (1) It is seen from Fig. 8.18*a* and *b* that moments decrease very rapidly with increasing distance from the loaded span, amounting here to less than 2 per cent of the loaded-span moments at those joints which are twice removed from the loaded span. This reduces very considerably the amount of calculation required for single-span loadings. (2) Two-cycle distribution at the near joints and a single cycle at the more remote joints is seen to result here in satisfactory accuracy, although in some cases more cycles may be required.

For Fig. 8.18*a* the order of joint release was A, B, C, D, A, B, while for Fig. 8.18*b* it was B, C, D, E, A, B, C, D, A, further distribution on each joint being

Scanned with CamScanner

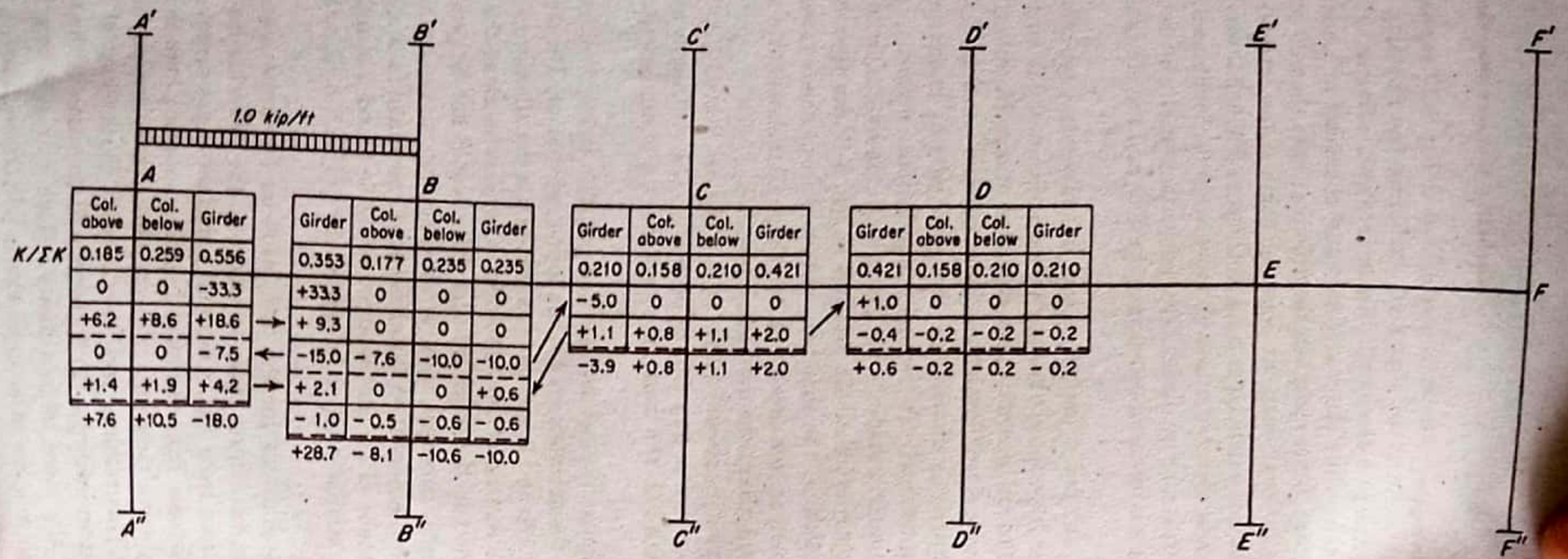


Fig. 8.18a

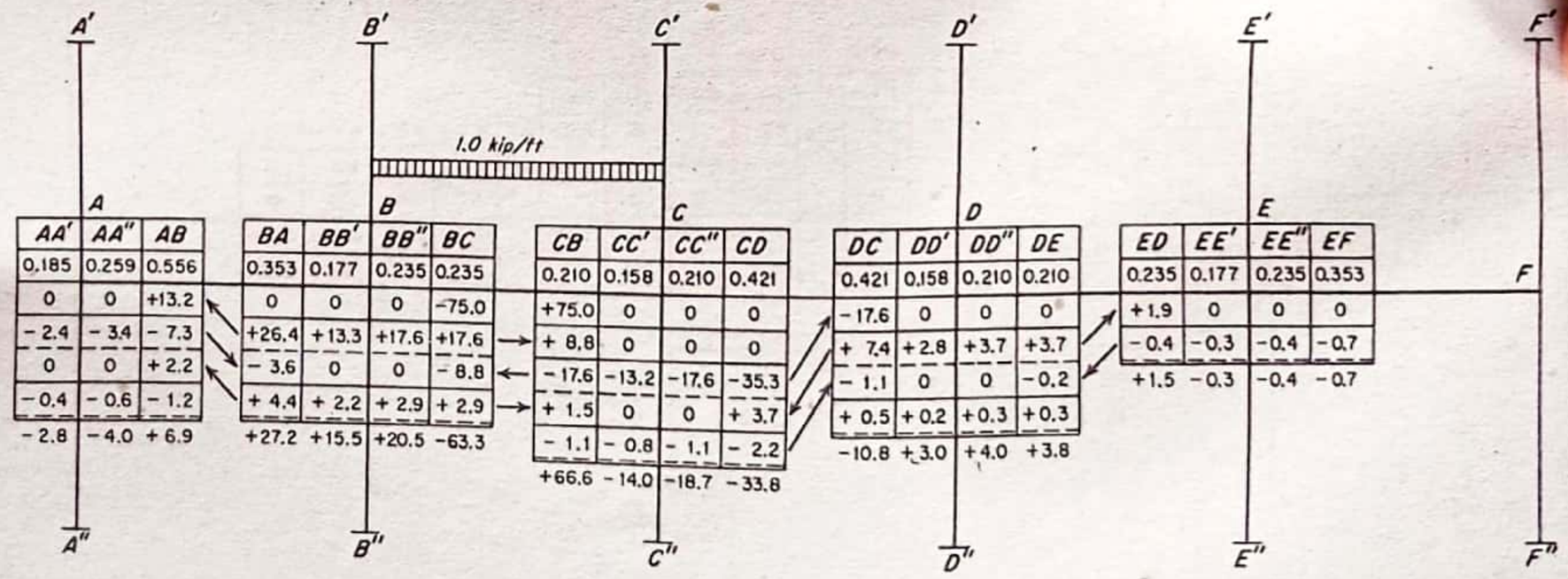


Fig. 8.18b

Scanned with CamScanner

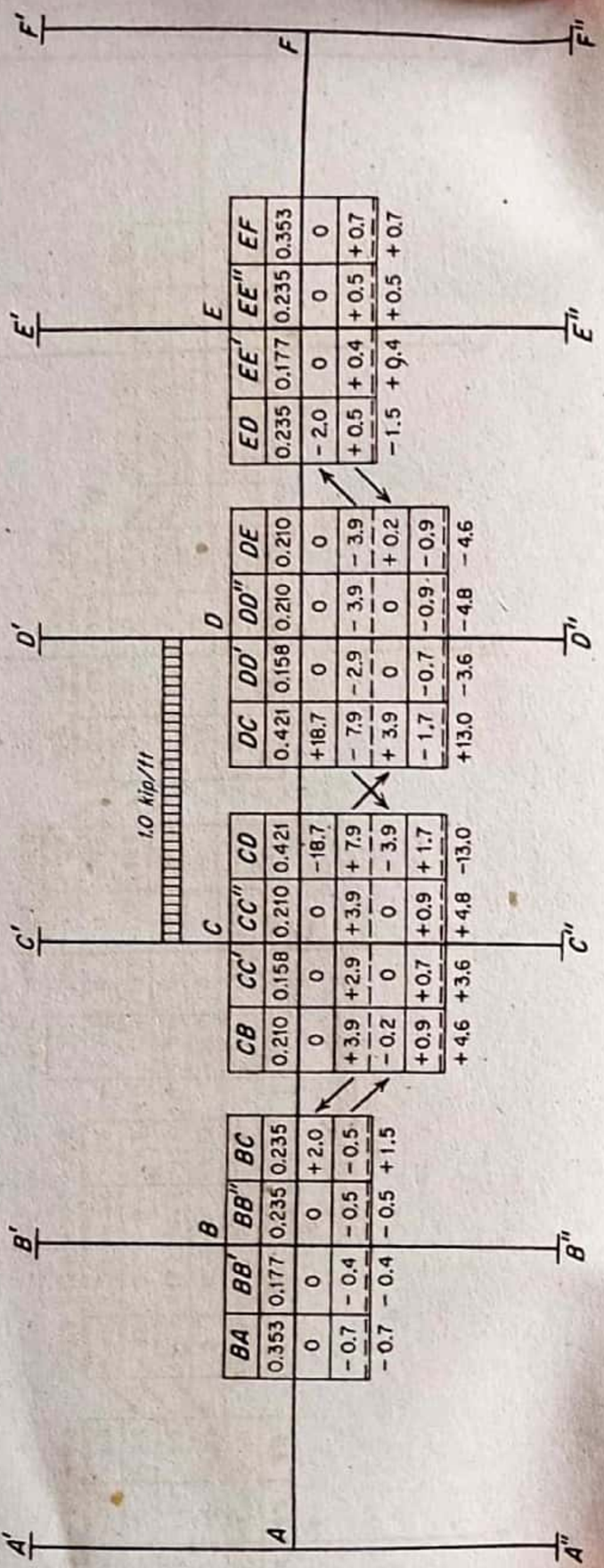


Fig. 8.18c

discontinued as soon as correction moments had decreased sufficiently. For the case of Fig. 8.18c, advantage was taken of symmetry by unlocking symmetrically located joints simultaneously in pairs. Thus C and D were simultaneously released first, next B and E, and finally C and D. It is seen that, if computed in this manner, all component moments on one side are equal and opposite those for the symmetrically located sections on the other side. With some experience such computations in cases of symmetry can be carried out showing only one set of figures. The resulting moments caused by unit loads on individual spans are given in the table below.

Unit load on span	Column moments						Girder moments				
	$M_{AA'}$	$M_{AA''}$	$M_{BB'}$	$M_{BB''}$	$M_{CC'}$	$M_{CC''}$	M_{AB}	M_{BA}	M_{BC}	M_{CB}	M_{CD}
AB	+7.6	+10.5	−8.1	−10.6	+0.8	+1.1	−18.0	+28.7	−10.0	−3.9	−0.6
BC	−2.8	−4.0	+15.5	+20.5	−14.0	−18.7	+6.9	+27.2	−63.3	+66.6	−33.8
CD			−0.4	−0.5	+3.6	+4.8		−0.7	+1.5	+4.6	−13.0
DE			+0.3	+0.4	−3.0	−4.0		+0.7	−1.5	−3.8	+10.8
EF					+0.2	+0.2				+0.2	+0.6
All spans	+4.8	+6.5	+7.3	+9.9	−12.4	−16.6	−11.1	+55.9	−73.3	+63.7	−36.0

The moments for span loads on DE and EF in the table above were obtained as being equal and opposite those for symmetrically located sections for span loads on BC and AB, respectively.

From these moments caused by the unit loads, the actual frame moments are easily computed as follows:

1. Maximum girder moments at supports:

M_{BC}:

D.L. all spans: 0.8 (−73.3) = −58.6
L.L. on BC: 2.0 (−63.3) = −126.6
L.L. on AB: 3.0 (−10.0) = −30.0
Maximum M_{BC} = −215.2 ft-kips

M_{CB}:

D.L. all spans: 0.8 (+63.7) = +51.0
L.L. on BC: 2.0 (+66.6) = +133.2
L.L. on CD: 2.0 (+4.6) = +9.2
Maximum M_{CB} = +193.4 ft-kips

2. Maximum midspan moment in BC:

M_{BC}:

D.L. as in (1) = −58.6
L.L. on BC as in (1) = −126.6
L.L. on DE: 2.0 (−1.5) = −3.0
M_{BC} = −188.2 ft-kips

Scanned with CamScanner

M_{CB}:

D.L. as in (1)	=	+51.0
L.L. on BC as in (1)	=	+133.2
L.L. on DE: 2.0 (−3.8)	=	−7.6
M_{CB}	=	+176.6 ft-kips

Midspan moment:

$$M_{l/2} = 2.8\frac{30^2}{8} - \frac{188.2 + 176.6}{2} = 132.6 \text{ ft-kips}$$

(Since the two end moments differ somewhat, the maximum span moment does not occur at midspan, but at the point of zero shear. In most cases the difference is extremely small.)

3. Minimum midspan moment in CD:

$M_{CD} = -M_{DC}$:

D.L. all spans:	0.8 (−36.6)	= −29.7
L.L. on BC:	2.0 (−33.8)	= −67.6
L.L. on DE:	2.0 (+10.8)	= +21.6
$M_{CD} = -M_{DC}$		= −75.7 ft-kips

Midspan moment:

$$M_{l/2} = 0.8 \times 15^2/8 - 75.7 = -53.2 \text{ ft-kips}$$

(It is seen that the minimum midspan moment in CD is negative so that tension reinforcement is required near the top face of the girder.)

4. Column moments:

$M_{BB'}$:

D.L. all spans:	0.8 (+7.3)	= +5.8
L.L. on BC:	2.0 (+15.5)	= +31.0
$M_{BB'}$		= +36.8 ft-kips

$M_{BB''}$:

D.L. all spans:	0.8 (+9.9)	= + 7.9
L.L. on BC:	2.0 (+20.5)	= +41.0
$M_{BB''}$		= +48.9 ft-kips

(Column moments of opposite sign are caused by live load on AB, instead of BC. It is quickly verified that the absolute values of the column moments at B are larger if live load is placed on BC, rather than on AB. In case of doubt, moments due to live load on either side of the column must be checked; the larger of them governs design.)

Moments at other sections of columns or girders can be computed in the same manner without additional distributions.

If dead and live loads are of different character so that they cannot be obtained as simple multiples of unit loads, and/or if the structure is not symmetrical, it may become necessary actually to carry out separate moment distributions for each case of loading, such as those illustrated in Fig. 8.17. In numerous practical cases, however, simplifications such as those illustrated in the example can be used to shorten computations.

8.10 Building Frames: Horizontal Loads Horizontal loads on building frames are caused primarily by wind pressure. Pressures per square foot of vertical wall surface are specified in building codes and, depending on locality, exposure, etc., vary from 10 to 50 psf. In addition, earthquake shocks produce horizontal sway, which results in inertia forces acting horizontally on the structure. It was found by extensive observation that these horizontal forces, rather than those induced by the simultaneous vertical motion of the ground, are chiefly responsible for structural earthquake damage. For this reason building codes in localities with high earthquake incidence require that structures be designed to resist corresponding horizontal forces. These are specified as stipulated percentages of the total load of the building above the given floor and are of the order of 10 per cent of that load.

In older buildings with massive bearing walls, wind forces are resisted by these walls acting as cantilever beams (loaded in the plane of the wall). In modern frame buildings, light curtain walls are usually employed which do not possess significant strength and stiffness, and horizontal loads must be resisted by the frame proper. With regard to earthquake forces, the older buildings were found to be easily damaged because the heavy and brittle bearing walls did not possess the necessary strength and flexibility to withstand the swaying motion. Correctly designed rigid-frame buildings, on the other hand, were found to stand up very well under such stress.

These horizontal forces, by means of walls and floors acting as rigid diaphragms in their own planes, are transmitted to the joints of the frame. For wind pressures, it is customary to compute the load on a joint from the area of exterior wall surface pertaining to it, i.e., from the rectangle outlined by vertical center lines between adjacent frames and by horizontal center lines between floor levels. Earthquake forces are distributed to individual joints in similar ways. These distributions are not very exact, particularly if the external forces do not act in the planes of the frames and if the outline of the structure is irregular in plan and/or elevation. More accurate ways of distributing the total forces to the individual frames are discussed in the references cited later in this chapter. The references also indicate that the actual distribution of wind forces, in particular, is frequently very different from the assumed uniform pressure on the surface of the windward walls.

For combinations of dead and live loads plus wind or earthquake loads, it must be recognized that the coincidence of full horizontal force with the most unfavorably distributed live load is extremely unlikely.

Scanned with CamScanner

Also, the rarity and temporary nature of the maximum horizontal loads are likely to result in less damage than if those same forces were of greater frequency and extended duration. Accordingly, the ACI Code treats wind and earthquake stresses as somewhat secondary effects, in comparison with the main effects of dead and live load. In working-stress design, an increase in allowable stress is permitted; in ultimate-strength design, reduced load factors are employed when the combined effect of dead, live, and wind load is considered.

Horizontal forces on building frames produce sidesway, and their effects can be accurately computed only by sidesway analysis, as discussed in previous articles. It will be realized that such an analysis, for frames with anywhere from 5 to 20 or more stories, requires very lengthy computations, even by the more rapid moment-distribution method. In most cases, however, such accurate determinations are neither required nor justified. It was pointed out that considerable uncertainty prevails regarding the magnitude as well as the distribution of wind and earthquake forces. It is useless, in analysis, to aim at an accuracy greater than that of the load data and other assumptions. In addition, the somewhat secondary effect of these rate and transitory forces justifies the use of more approximate analytical methods.

A considerable number of such approximate methods has been in use for many years. Although some of them result in slightly better theoretical accuracy than others, in view of the prevailing uncertainties these differences are usually not significant enough to cause the discard of the simpler methods in favor of the more accurate ones. For this reason only the simplest of those methods which are in reasonable agreement with accurate analysis will be discussed here, the approach which is known as the *portal method.*[1]

In simple frames, horizontal forces result in moments distributed as shown in Figs. 8.7*c* and 8.14*c*. It is seen that in all members moments vary linearly and, except in hinged members (*DE* in Fig. 8.14), have opposite signs at the ends (in the sense of the beam sign convention). It is further seen that in these members the points of zero moment (inflection points; see Fig. 8.7*a*) are located reasonably close to the midpoint of each member. In hinged members, of course, zero moment obtains only at the hinge. At the inflection points, only shear and axial forces act on the cross section. For symmetrical portals, such as that of Fig. 8.7, the shear forces are the same in both legs and are equal, each, to half the external horizontal load, as is easily checked from the information on

[1] For more information on other types of analyses, as well as on magnitude and distribution of horizontal forces, the reader is referred to "Wind Bracing in Steel Buildings," Final Report of Sub-committee 31, *Trans. ASCE*, vol. 105, p. 1713, 1940, and Ref. 8.4.

that figure. If one of the legs is more rigid than the other (larger value of K), it would require a larger horizontal force to displace it horizontally by the same amount as the more flexible leg. Consequently the portion of the total shear resisted by the stiffer column is larger than that of the more flexible column. This is easily checked by computing and comparing shears in AB and CF of Fig. 8.14*c*.

In building frames, moments and forces in the girders and columns of each individual story are distributed in substantially the same manner as just discussed for single-story frames. The portal method of computing approximate moments, shears, and axial forces from horizontal loads is, therefore, based on the following three simple propositions:

1. The total horizontal shear in all columns of a given story is equal and opposite to the sum of all horizontal loads acting above that story.
2. The horizontal shear is the same in both exterior columns; the horizontal shear in each interior column is twice that in an exterior column.
3. The inflection points of all members, columns and girders, are located midway between joints.

Although the last of these propositions is commonly applied to all columns, including those of the bottom floor, the authors prefer to deal with the latter separately, depending on conditions of foundation. If the actual conditions are such as practically to prevent rotation (foundation on rock, massive pile foundations, etc.), the inflection points of the bottom columns are above midpoint (see Figs. 8.7*c* and 8.14*c*) and may be assumed to be at a distance $2h/3$ from the bottom. If little resistance is offered to rotation, such as for relatively small footings on compressible soil, the inflection point is located closer to the bottom and may be assumed to be at a distance $h/3$ from the bottom or even lower. (In ideal hinges the inflection point is at the hinge, i.e., at the very bottom.) Since shears and corresponding moments are largest in the bottom story, a judicious evaluation of foundation conditions as they affect the location of inflection points is of considerable importance.

The first of the three cited propositions follows from the requirement that horizontal forces be in equilibrium at any level. The second takes account of the fact that in building frames interior columns are generally more rigid than exterior ones because (1) the larger axial loads require larger cross section and (2) exterior columns are restrained from joint rotation only by one abutting girder, while interior columns are so restrained by two such members. The third proposition is very nearly true because, except for the top and bottom columns and, to a minor degree, for the exterior girders, each member in a building frame is restrained about equally at both ends. For this reason it deflects under horizontal loads in an antisymmetrical manner, with the inflection point at midlength.

Scanned with CamScanner

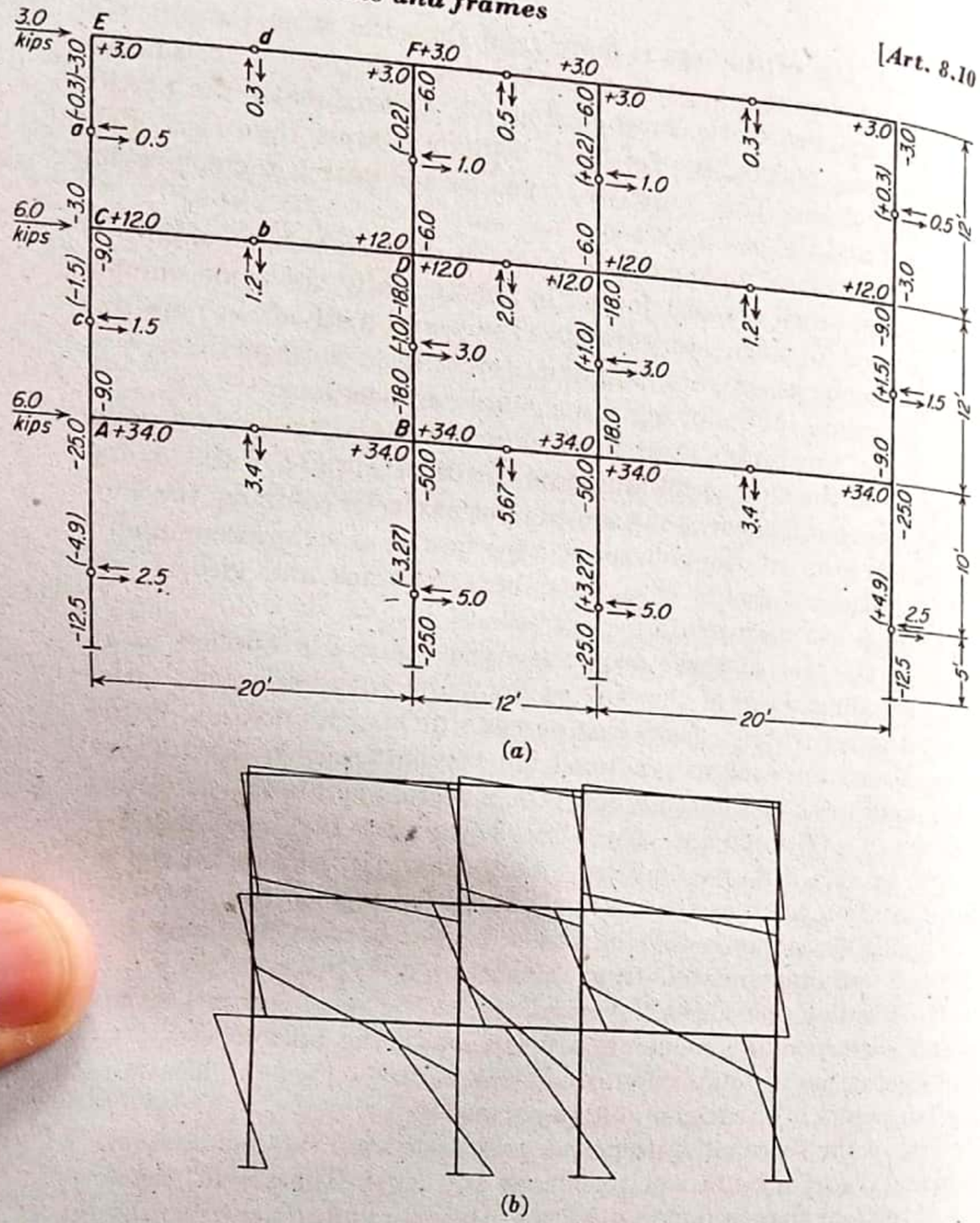


Fig. 8.19 Portal method for determining moments from wind load in building frame.

The actual computations in this method are extremely simple. At an inflection point, with $M = 0$, only shears and axial forces are transmitted from one half of the member to the other. An inflection point is, therefore, equivalent to a hinge, which also transmits only forces, but not moments. Once column shears are determined from propositions 1 and 2, and inflection points (hinges) located from proposition 3, all moments, shears, and forces are simply computed by statics. The process is illustrated in Fig. 8.19*a*.

Consider joints C and D. The total shear in the second story is $3 + 6 = 9$ kips. According to proposition 2, the shear in each exterior column is $9/6 = 1.5$ kips, and in each interior column $2 \times 1.5 = 3.0$ kips. The shears in the other floors, obtained in the same manner, act at the hinges as shown. Consider the equilibrium of the rigid structure between hinges a, b, and c; the column moments, 3.0 and 9.0, respectively, are obtained directly by multiplying the shears by their lever arms, 6 ft. The girder moment at C, to produce equilibrium, is equal and opposite to the sum of the column moments. The shear in the girder is obtained by recognizing that its moment (i.e., shear times half the girder span) must be equal to the girder moment at C. Hence this shear is $12.0/10 = 1.2$ kips. The moment at end D is equal to that at C, since the inflection point is at midspan. At D, column moments are computed in the same manner from the known column shears and lever arms. The sum of the two girder moments, to produce equilibrium, must be equal and opposite to the sum of the two column moments, from which the girder moment to the right of C is $18.0 + 6.0 - 12.0 = 12.0$. Axial forces in the columns also follow from statics. Thus, for the rigid body aEd, a vertical shear of 0.3 kip is seen to act upward at d. To equilibrate it, a tensile force of -0.3 kip is required in the column CE. In the rigid body abc an upward shear of 1.2 kips at b is added to the previous upward tension of 0.3 kip at a. To equilibrate these two forces, a tension force of -1.5 kips is required in column AC. If the equilibrium of all other partial structures between hinges is considered in a similar manner, all moments, forces, and shears are rapidly determined.

In the present case relatively flexible foundations were assumed, and the location of the lowermost inflection points was estimated to be at 1/3 from the bottom. The general character of the resulting moment distribution is shown in Fig. 8.19*b*.

8.11 Effective Span Length In elastic frame analysis, a structure is usually represented by a simple line diagram, based dimensionally on the center-line distances between columns and between floor beams. Actually, the depths of beams and the widths of columns (in the plane of the frame) amount to sizable fractions of the respective lengths of these members; their clear lengths are therefore considerably smaller than their center-line distances between joints.

It is evident that the usual assumption in frame analysis that the members are prismatic, with constant moment of inertia between center lines, is not strictly correct. A beam intersecting a column may be prismatic up to the column face, but from that point to the column center line it has a greatly increased depth, with a moment of inertia which should be considered infinite compared with that of the remainder of the

Scanned with CamScanner

span. A similar variation in width and moment of inertia is obtained for the columns. Thus, to be strictly correct, fixed-end moments, stiffnesses, and carry-over factors which account for the actual variation in member depth should be used in the analysis. Qualitatively, this would increase beam support moments somewhat, and decrease span moments. In addition, it is apparent that the critical section for design for negative bending would be at the face of the support, and not at the center line, since for all practical purposes an unlimited effective depth is obtained in the beam across the width of the support.

It will be observed that, in the case of columns, the moment curve is not very steep, so that the difference between center-line moment and the moment at the top or bottom face of the beam is small and can in most cases be disregarded. However, the moment diagram for the beam is usually quite steep in the region of the support, and there will be a substantial difference between support center-line moment and face moment. If the former were used in proportioning the member, an unnecessarily large section would result. It is desirable, then, to reduce support moments found by elastic analysis to account for the finite width of the supports.

In Fig. 8.20, the change in moment between the support center line and the support face will be equal to the area under the shear diagram between those two points. For knife-edge supports, this shear area is seen to be very nearly equal to $VaL/2$. Actually, however, the reaction is distributed in some unknown way across the width of the support. This will have the effect of modifying the shear diagram as shown by the dashed line; it has been proposed that the reduced area be taken equal to $VaL/3$. The fact that the reaction is distributed will modify the moment diagram as well as the shear diagram, causing a slight rounding of the negative-moment peak, as shown in the figure, and the reduction of $VaL/3$ is properly applied to the moment diagram after the peak has been rounded. This will give nearly the same face moment as would be obtained by deducting the amount $VaL/2$ from the peak moment.

Another effect is present, however: the modification of the moment diagram due to the increased moment of inertia of the beam at the column. This effect is similar to that of a haunch, and it will mean slightly increased negative moment and slightly decreased positive moment. For ordinary values of the ratio a, this shift in the moment curve will be of the order of $VaL/6$.[1] Thus, it is convenient simply to deduct the amount $VaL/3$ from the unrounded peak moment obtained from elastic analysis. This allows for (1) the actual rounding of the shear diagram and the negative-moment peak due to the distributed reaction and (2) the downward shift of the moment curve due to the haunch effect at the supports. The consistent reduction in positive moment of $VaL/6$ is illustrated in Fig. 8.20. In connection with moment reductions, it should be noted that there are certain conditions of support for which no reduction in negative moment is justified. For example, when a continuous beam is carried by a girder of approximately the same depth, the negative moment in the beam at the center line of the girder should be used in designing the negative reinforcing steel.

[1] Thor Germundsson, Effect of Column Width on Continuous Beam Moment. *ACI*, p. 1143, June, 1958.

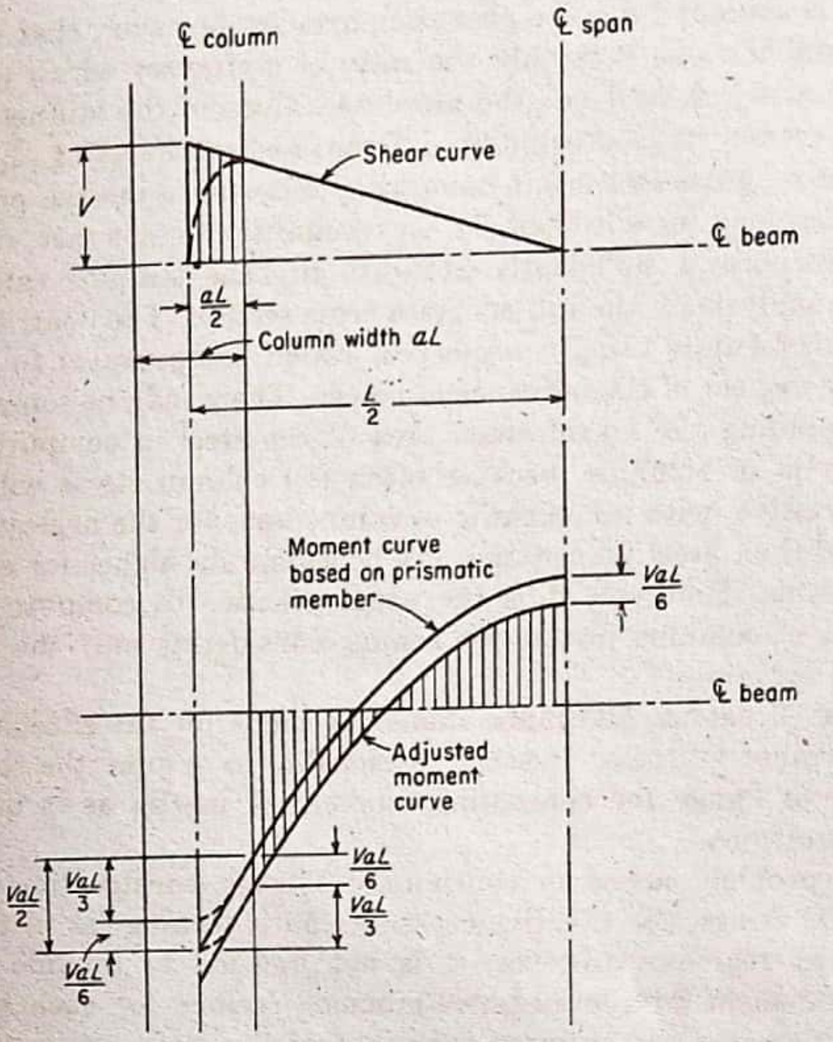


Fig. 8.20

8.12 Moments of Inertia The design of flexural members is based on the cracked section, i.e., on the supposition that the part of the concrete which is in tension is ineffective. Similarly, in calculating deflections (Art. 2.7) the flexural rigidity is based on the moment of inertia of the cracked, transformed section. It would seem, therefore, that moments of inertia to be used in computing stiffnesses K for frame analysis should be determined in the same manner.

Scanned with CamScanner

It is evident from the preceding articles, however, that in most cases in frame analysis it is only the ratio of stiffnesses which influences the elastic analysis, and not the absolute values of the stiffnesses. Stiffness ratios are but little affected by different assumptions (e.g., use of cracked section vs. gross section) in computing moment of inertia, provided there is consistency for all members. In recognition of this fact, it is generally convenient and sufficiently accurate to base stiffness calculations for frame analysis on the full concrete cross section. The contribution of the reinforcement is usually neglected, which compensates to some extent for the neglect of the influence of cracks. There may be some justification for including the transformed area of the steel in computing moments of inertia of columns, because often the column stress will be entirely compressive, with no cracking to compensate for the neglect of the steel. In addition, steel percentages are considerably higher for columns than for beams. However, it is the usual practice to compute moments of inertia of columns just as for beams, considering only the cross section of the concrete.

For T beams, allowance should be made for the effect of the flange on member stiffness. It seems reasonable to assume the same effective width of flange for computing moment of inertia as is used in stress computations.

A problem arises in continuous T-beam construction, in that for flexural design the effective cross section is rectangular in the negative-moment regions. However, it is not unusual to provide compressive reinforcement in the negative-moment regions for such construction. This increases the stiffness over that of the plain rectangular concrete section. Consequently, there is some justification for the common practice of computing stiffnesses of such members on the basis of the gross cross section of the concrete, including flanges, and using this stiffness throught the entire span.

It is somewhat laborious to compute, in every case, the neutral axis of the effective T section and to find the moment of inertia, about that axis, of the unsymmetrical section. In the usual case it is satisfactory to estimate the moment of inertia of the unsymmetrical section under the assumption that it will be some multiple of that of the rectangular cross section of web width b' and total height h. For sections of usual proportions (flange width about 4 to 6 times web width, and flange thickness from 0.2 to 0.4 times total depth), this multiplier will be very close to 2.0.

8.13 Conditions of Support For purposes of analysis, many structures can be divided into a number of two-dimensional frames such as in the example of Art. 8.9. Even for such cases, however, there are situations in which it is impossible to predict with accuracy what the conditions of restraint might be at the ends of a span; yet moments are frequently affected to a considerable degree by the choice made. In many other cases, it is necessary to recognize that structures may be three-dimensional. The rotational restraint at a joint may be influenced or even governed by the characteristics of members framing into that joint at right angles. Adjacent members or frames parallel to the one under primary consideration may likewise influence its performance.

If floor beams are cast monolithically with reinforced-concrete walls (frequently the case when first-floor beams are carried on foundation walls), the moment of inertia of the wall about an axis parallel to its face may be so large that the beam end could be considered completely fixed for all practical purposes. If the wall is relatively thin, or the beam particularly massive, the stiffness of each should be calculated, that of the wall being equal to $I/L = bt^3/12h$, where t is the wall thickness, b the wall width tributary to one beam (i.e., center to center of adjacent panels), and h the wall height. Distribution factors can then be calculated in the usual manner.

If the outer ends of concrete beams rest on masonry walls, as is sometimes the case, an assumption of zero rotational restraint (i.e., hinged support) is probably closest to the actual.

For columns supported on relatively small footings, which in turn rest on compressible soil, a hinged end is generally assumed, since such soils offer but little resistance to rotation of the footing. If, on the other hand, the footings rest on solid rock, or if a cluster of piles is used with their upper portion encased by a concrete cap, the effect is to provide almost complete fixity for the supported column, and this should be assumed in the analysis. Columns supported by a continuous foundation mat should likewise be assumed fixed at their lower ends.

If members framing into a joint in a direction perpendicular to the plane of the frame under analysis have sufficient torsional stiffness, and if their far ends can be considered fixed or nearly so, their effect on joint rigidity should be included in the computations. The torsional stiffness of a member of length L is given by the expression GJ/L, where G is the shear modulus of elasticity of concrete (approximately equal to $E_c/2.2$), and J is the polar moment of inertia of the member. For beams of rectangular cross section, or of sections made up of rectangular elements, J can be taken equal to $(hb^3/3 - b^4/5)$, in which h and b are the cross-sectional dimensions of each rectangular element, b being the lesser dimension in each case. Torsional stiffness at a joint is treated in the same manner as flexural stiffness; the sum of the distribution factors must, as usual, equal unity. When the effect of torsional rigidity is included, it is important to observe that the absolute flexural stiffness $4EI/L$ must be used, rather than relative I/L values.

Scanned with CamScanner

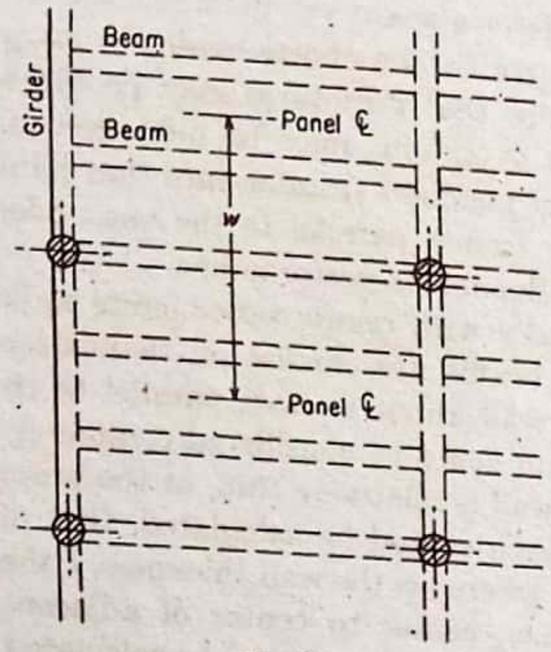


Fig. 8.21

A common situation in beam-and-girder floors and concrete-joist floors is illustrated by Fig. 8.21. The sketch shows a beam-and-girder floor system in which longitudinal beams are placed at the third points of each bay, supported by transverse girders, in addition to the longitudinal beams supported directly by the columns. If the transverse girders are quite stiff, it is apparent that the flexural stiffness of all beams in the width w should be balanced against the stiffness of one set of columns in the longitudinal bent. If, on the other hand, the girders have little torsional stiffness, there would be ample justification for making two separate longitudinal analyses, one for the beams supported directly by the columns, including the I/L values for those beams only, and a second for the beams framing into the girders, in which case simple supports would be assumed. Probably it would generally be sufficiently accurate to consider the girders very stiff torsionally and to add directly the I/L values of all beams tributary to a single column. This has the added advantage that all otherwise identical longitudinal beams will then have the same cross-sectional dimensions and the same reinforcing steel, which will greatly facilitate construction.

8.14 Preliminary Design In making an elastic analysis of a structural framework, it is necessary to know at the outset the cross-sectional dimensions of the members, so that moments of inertia, stiffnesses, and distribution factors can be calculated. Yet the determination of these same cross-sectional dimensions is the precise purpose of the elastic analysis. Obviously, a preliminary estimate of member sizes must be one of the first steps in the analysis. Subsequently, with the results of the analysis at hand, members are proportioned, and the resulting dimensions compared with those previously assumed. If necessary, the assumed section properties are modified, and the analysis is repeated. Since the procedure may become quite laborious, it is obviously advantageous to make the best possible original estimate of member sizes, in the hope of avoiding repetition of the analysis.

In this connection, it is worth repeating that in the ordinary frame analysis one is concerned with relative stiffnesses only, not the absolute stiffnesses. If, in the original estimate of member sizes, the sizes of all

beams and columns are overestimated or underestimated by about the same amount, then correction of these estimated sizes after the first analysis will have little or no effect on the relative stiffnesses. Consequently no revision of the analysis would be required. If, on the other hand, a nonuniform error in estimation is made, and relative stiffnesses differ from assumed values by more than about 30 per cent, a new analysis should be made.

The experienced designer can estimate beam and column sizes with surprising accuracy. Those with little or no experience must rely on trial calculations or arbitrary rules, modified to suit particular situations. In building frames, beam sizes are usually governed by the negative moments and the shears at the supports, where their effective section is rectangular. Moments can be approximated by the fixed-end moments for the particular span, or by using the ACI moment coefficients. In most cases, shears will not differ greatly from simple beam shears. Alternatively, many designers prefer to estimate the depth of beams at about $\frac{3}{4}$ in. per ft of span, with the width about one-half the depth. Obviously, these dimensions are subject to modification, depending on the type and magnitude of the loads, method of design, and material strength.

Column sizes are governed primarily by axial loads, which can be estimated quickly, although the presence of moments in the columns is cause for some increase of the area as determined by axial loads. For interior columns, in which unbalanced moments will not be large, a 10 per cent increase may be sufficient, while for exterior columns, particularly for upper stories, an increase of 50 per cent in area may be appropriate. In deciding on these estimated increases, the following should be considered: Moments are larger in exterior than in interior columns, since, in the latter, dead-load moments from adjacent spans will largely balance, in contrast to the case in exterior columns. In addition, the influence of moments, as compared to that of axial loads, is larger in upper-floor than in lower-floor columns, because the moments are usually of about the same magnitude, while the axial loads are larger in the latter than in the former. Judicious consideration of factors such as these will enable a designer to produce a reasonably accurate preliminary design, which in most cases will permit a satisfactory analysis to be made on the first trial.

8.15 Inelastic Redistribution of Moments Since it is known that concrete does not respond elastically to loads of more than about one-half the ultimate, there is a certain inconsistency in designing reinforced cross sections by ultimate-strength methods (taking into account inelastic behavior) while the moments for which those sections are being designed have been found by elastic analysis. Although this presently accepted

Scanned with CamScanner

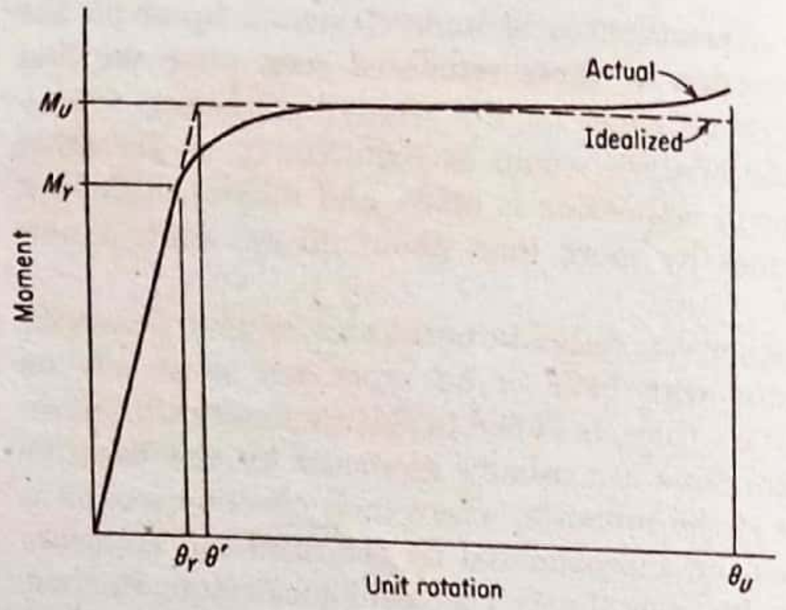


Fig. 8.22

procedure by which elastic analysis is coupled with inelastic design of sections is not consistent, it is safe and conservative. It can be shown that a frame so analyzed and designed will not fail at a lower load than anticipated; on the other hand, because of certain inelastic readjustments that may occur, it may be able to carry a somewhat higher load. The means for utilizing this excess strength is the subject of much current investigation.

If a short segment of a reinforced-concrete beam is subjected to a bending moment, curvature of the beam axis will result, and there will be a corresponding rotation of one face of the segment with respect to the other. It is convenient to express this in terms of an angular change θ per unit length of the member. A representative relation between applied moment M and resulting rotation for an underreinforced section is shown in Fig. 8.22. This relation can be idealized as shown by the dashed lines. As moment is applied, a linear relation between M and θ will be obtained up to that load which produces yielding of the reinforcing steel. A slight further increase in load produces large rotation with little or no increase in resisting moment. The elastic curve of the beam shows an abrupt change in slope at such a section. The beam behaves as if there were a hinge at that point. However, the hinge will not be "friction-free," but will have a fairly constant resistance to rotation, of amount M_u.

If such a plastic hinge forms in a determinate structure, as shown in Fig. 8.23, uncontrolled deflection takes place, and the structure will collapse. The resulting system is referred to as a *mechanism*, in analogy to linkage systems in mechanics. Generalizing, one can say that a

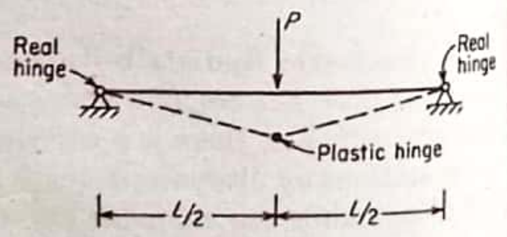


Fig. 8.23

statically determinate system requires the formation of only one plastic hinge in order to become a mechanism.

This is not so for indeterminate structures. In this case, stability may be maintained even though hinges have formed at several cross sections. The formation of such hinges in indeterminate structures permits a redistribution of moments within the beam or frame. It will be assumed for simplicity that the indeterminate beam of Fig. 8.24*a* is symmetrically reinforced, so that the negative bending capacity is the same as the positive. Let the load P be increased gradually until the elastic moment at the fixed support, $\frac{3}{16}PL$, is just equal to the plastic moment capacity of the section M_u. This load is

$$P = P_{el} = \frac{16}{3}\frac{M_u}{L} = 5.33\frac{M_u}{L} \qquad (a)$$

At this load, the positive moment under the load is $\frac{5}{32}PL$, as shown in Fig. 8.24*b*. The beam still responds elastically everywhere but at the left support. At that point, the actual fixed support can be replaced for purposes of analysis with a plastic hinge offering a known resisting moment M_u. Because a redundant reaction has been replaced by a known moment, the beam is now determinate.

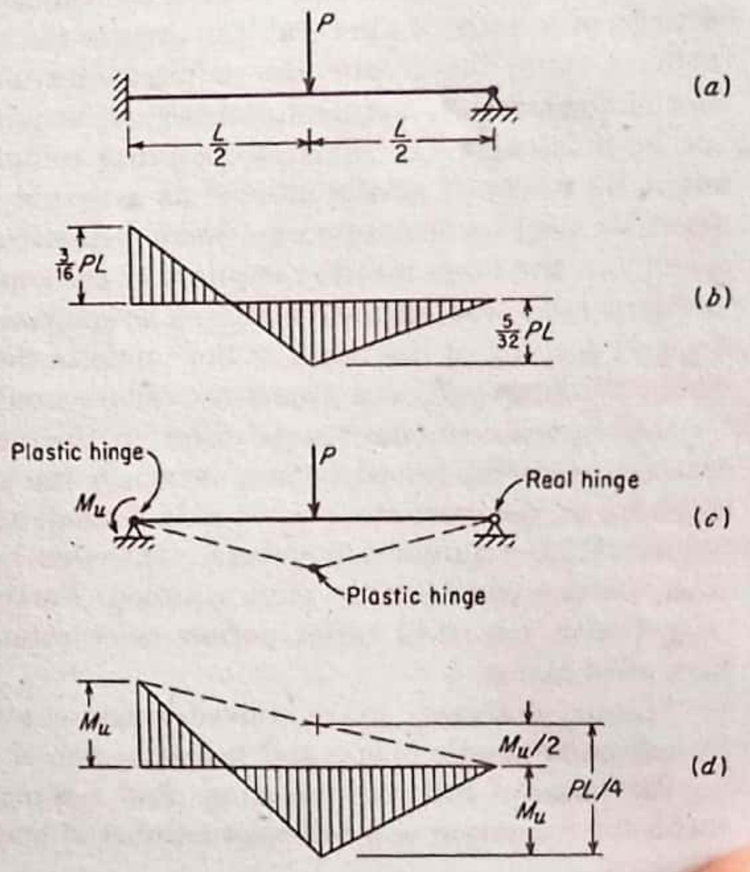


Fig. 8.24

Scanned with CamScanner

The load can be increased further until the moment under the load also becomes equal to M_u, at which load the second hinge forms. The structure is converted into a mechanism, as shown in Fig. 8.24*c*, and collapse occurs. The moment diagram at collapse load is shown in Fig. 8.24*d*. [Art. 8.15

The magnitude of load causing collapse is easily calculated from the geometry of Fig. 8.24*d*:

$$M_u + \frac{M_u}{2} = \frac{PL}{4}$$

from which

$$P = P_u = \frac{6M_u}{L} \qquad (b)$$

By comparison of Eqs. (*b*) and (*a*), it is evident that an increase in P of 12.5 per cent is possible, beyond that load which caused the formation of the first plastic hinge, before the beam will actually collapse. Due to the formation of plastic hinges, a redistribution of moments has occurred such that, at failure, the ratio between positive moment and negative moment is equal to that assumed in reinforcing the structure.

It may be evident that there is a direct relation between the amount of redistribution desired and the rotation capacity required at the critical sections of a beam. In general, the greater the modification of the elastic moment ratio, the greater the required rotation capacity to accomplish that change. In the actual structure, the required rotation may or may not be attainable. To illustrate, a beam completely fixed at both ends might be designed and reinforced as a simply supported span, with no negative steel at the supports. Some redistribution would undoubtedly occur, but the large rotation required at the supports before the assumed moment ratio was realized would be accompanied by such severe cracking and spalling of the beam at the supports that its structural integrity would be destroyed, and premature failure would result.

Reinforced-concrete beams differ in their capacity to permit such rotation. Overreinforced beams, in which the strength is controlled by crushing of the concrete, permit only a small amount of rotation before failure. Underreinforced members, controlled by yielding of the tensile steel, permit considerably more rotation. Furthermore, underreinforced beams with low steel ratios permit more rotation than do those with high steel ratios.

"Limit analysis" in reinforced-concrete structures, based on the formation of plastic hinges and redistribution of moments, could proceed on the basis of full redistribution. *Full redistribution* is understood to mean the formation of a sufficient number of hinges to convert the structure into a mechanism. However, in this case it would have to be shown by special calculations that sufficient rotation capacity is available, at the locations at which the earlier hinges form, to permit all requisite hinges to develop. It would also have to be shown that the resulting structure, at service loads, would not exhibit an objectionable amount of cracking and excessive deflections. Methods for accomplishing this are not yet fully developed. This is in contrast to plastic design in steel structures, where the danger of cracking hardly exists, and where the much greater ductility of the material makes such special checks unnecessary.

On the other hand, in order to limit crack widths and deflections without elaborate proof, while still utilizing most of the advantages of moment redistribution, the designer may avail himself only of a stipulated, limited amount of such redistribution. This amount must be known to be safe in regard to available rotation capacity and crack development at service loads. Because, as was pointed out, rotation capacity increases with decreasing reinforcement ratio, safe conditions for limited redistribution are obtained if suitable limits are set for the steel ratio. This is the manner in which, at the present time, inelastic moment redistribution is now admitted in American and some foreign design codes.

For example, support moments may be reduced or increased 15 per cent from their elastic values, provided the positive moments in the corresponding spans are increased or reduced a statically consistent amount. This permits one to deviate from the moments calculated on the basis of elastic theory. Hence, one can place less steel at one section than is indicated by the elastic moment, if one places at another section more than is indicated to be necessary by elastic analysis. In such a case, when loaded, the beam will yield first where the lesser steel has been provided and will continue to yield until the moments adjust themselves to yield the steel at the second place, leaving the overall strength the same as if one had placed the steel strictly according to the elastic moments.

While most concrete beams have prismatic cross sections, they need not be reinforced equally at all sections. On the contrary, it is quite convenient to match the resisting capacity of the beam, as governed by the reinforcing steel, to the elastic-moment diagram. Accordingly, for the beam of Fig. 8.24*a*, the steel could have been detailed to resist a moment of $\frac{3}{16}PL$ at the support and $\frac{5}{32}PL$ under the load. Hinges would then have formed simultaneously at these two points. It would seem, then, that there would be little advantage in utilizing inelastic moment redistribution for concrete structures, aside from the possibility of thereby more fully utilizing the prismatic concrete section. On further consideration, however, important advantages are apparent. For example, in reinforced-concrete construction, the region in which beams and columns

Scanned with CamScanner

intersect is often very congested with reinforcement. Often beams fram
into the joint from two directions, with substantial negative steel at th
top, and some bottom steel as well. Large column bars must pass through
the same zone. The result is a cage of steel so complex that not only i
bar placement difficult, but often it is impossible to ensure proper deposi
tion of concrete in this important zone. On the other hand, if a redis
tribution of moments is permissible, with negative design moments
reduced and positive moments increased accordingly, an importan
reduction in this congestion of steel at the columns is possible.

A further and perhaps more significant advantage will be evident from study of Fig. 8.25. A three-span continuous beam is shown, with dead load of 1 kip per ft and live load of 2 kips per ft. In order to obtain maximum moments at all critical design sections, it is necessary to consider three alternative loadings. Case *a*, with live and dead load over exterior spans and dead load only over interior span, will produce maximum positive moment in the exterior spans. Case *b*, with dead load on exterior spans and dead and live load on the interior span, will produce the maximum positive moment in the interior span. The maximum negative moment over the interior support is obtained by placing dead and live load on the two adjacent spans and dead load only on the far exterior span, as shown in case *c*.

If it is assumed for purposes of demonstration that a 20 per cent adjustment of support moments is permitted, provided span moments are modified accordingly, an overall reduction in design moments through the entire three-span beam may be possible. Case *a*, for example, produces an elastic maximum span moment in the exterior spans of 109 ft-kips. Corresponding to this is an elastic negative moment of 82 ft-kips at the interior support. Adjusting the support moment upward by 20 per cent, one obtains a negative moment of 98 ft-kips, which results in a downward adjustment of the span moment to 101 ft-kips.

Now consider case *b*; by a similar redistribution of moments, a reduced middle-span moment of 57 ft-kips is obtained through increase of the support moment from 78 to 93 ft-kips.

The moment obtained at the first interior support for loading case *c* can be adjusted in the reverse direction; i.e., the support moment is decreased by 20 per cent to 107 ft-kips, with the positive moments increased in the adjacent spans to 96 ft-kips and 63 ft-kips in the exterior and interior spans, respectively.

Now, it will be observed that the reduction obtained for the span moments in cases *a* and *b* were achieved at the expense of increasing the moment at the first interior support. However, the increased support moment in each case was less than the moment for which that support would have to be designed based on the loading *c*, which produced maxi-

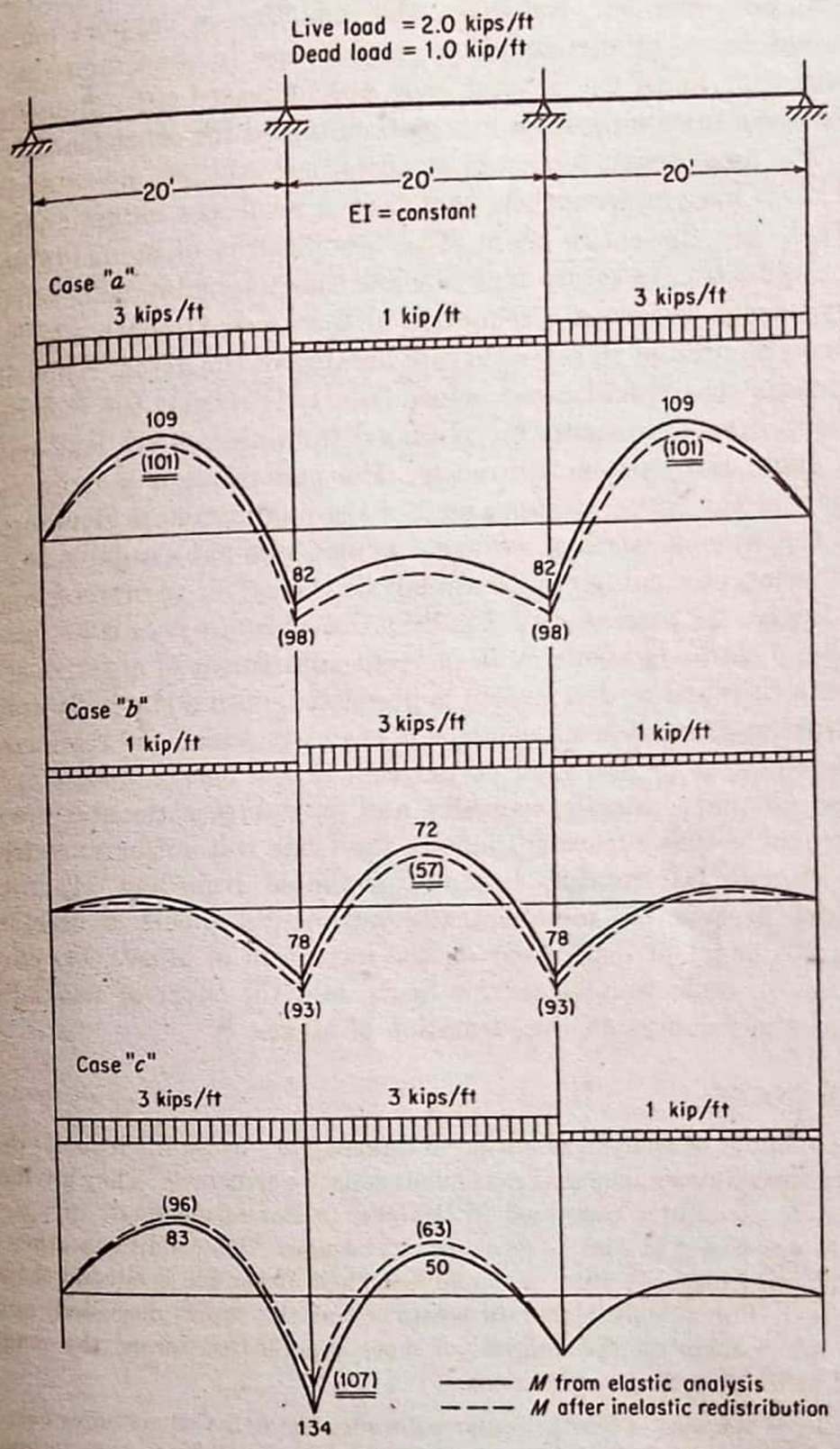


Fig. 8.25

Scanned with CamScanner

mum support moment. Similarly, the reduction in support moment in case *c* was taken at the expense of an increase in span moments in the two adjacent spans. But in each case, the increased span moments were less than the maximum span moments obtained for other loading conditions. The final design moments at all critical sections are underlined in Fig. 8.25. It may be seen, then, that the net result is a reduction in design moments over the entire beam. This modification of moments does not mean a reduction in safety factor below that implied in code safety provisions; rather, it means a reduction of the *excess* strength which would otherwise be present in the structure because of the actual redistribution of moments that would occur before failure. It reflects the fact that the maximum design moments are obtained from alternative load patterns which could not exist concurrently. The end result is a more realistic appraisal of the actual collapse load of the indeterminate structure.

At the time of writing, sufficient evidence is not available to justify the adoption of a complete limit-analysis theory for reinforced concrete. Accordingly, *the present ACI Building Code permits only a limited redistribution of elastic moments*. A 10 per cent adjustment of negative support moments (upward or downward) is permitted, with a statically compatible adjustment in span moments, for beams in which the reinforcement ratio is equal to or less than 50 per cent of the balanced ratio p_b.[1] This ensures adequate rotation capacity and only unobjectionable cracking. It is probable that future editions of the Code will not be so restrictive, as additional information becomes available regarding (1) rotation capacities of concrete members, (2) detrimental effects of cracking at hinges, (3) effect of high shear on the formation of hinges, (4) effect of rotations on deflection at service loads, and (5) effort of triaxiality of stress at the columns on the formation of hinges.

REFERENCES

The methods of analysis discussed in this chapter furnish the tools for dealing with the most common types of continuous concrete structures. They are limited, however, to structures composed of straight, prismatic members, in which all members are either in line or meet at right angles. For conditions other than these, modified methods must be employed. Their discussion is beyond the scope of this text. For a more elaborate treatment of the topics discussed, and for further information on the analysis of more complicated forms, the reader is referred to the following publications:

[1] While, in the case of doubly reinforced beams, the ACI Code requires only that $(p - p')$ be less than $0.50\ p_b$, or equivalently, that $p_{max} = 0.50\ p_b + p'$, in order to ensure the same rotation capacity in doubly reinforced beams as in singly reinforced beams, one should have $p_{max} = 0.50(p_b + p')$. Similarly, in the case of T beams, the Code requirement that $p_{w,max} = 0.50\ p_b + p_f$ might better be stated as $p_{w,max} = 0.50(p_b + p_f)$.

8.1 J. S. Kinney: "Indeterminate Structural Analysis," Addison-Wesley Publishing Company, Inc., Reading, Mass., 1957.

8.2 J. I. Parcel and R. B. B. Moorman: "Analysis of Statically Indeterminate Structures," John Wiley & Sons, Inc., New York, 1955.

8.3 C. K. Wang: "Statically Indeterminate Structures," McGraw-Hill Book Company, Inc., New York, 1953.

8.4 "Continuity in Concrete Building Frames," Portland Cement Association, Chicago.

8.5 "Handbook of Frame Constants," Portland Cement Association, Chicago.

8.6 "Working Stress Design Handbook," American Concrete Institute, Detroit 1964.

8.7 G. C. Ernst and A. R. Riveland: Ultimate Loads and Deflections from Limit Design of Continuous Structural Concrete, *J. ACI*, October, 1959.

8.8 A. H. Mattock: Limit Design for Structural Concrete, *Portland Cement Assoc. Res. Develop. Lab. Develop. Dept. Bull.*, May, 1959.

Scanned with CamScanner

chapter **9**

REINFORCED-CONCRETE BUILDINGS

9.1 Introduction In the conceptual stages of the design of reinforced-concrete structures, it should be borne in mind that reinforced concrete is a material in its own right, with its own unique features and characteristics. To use the material in structural systems which are patterned after articulated structures of steel or timber betrays a lack of design imagination and denies the monolithic nature of concrete construction. From a practical point of view, such imitative design will usually fail to realize the true potential of the material and will often result in highly uneconomical structures.

The advantages of reinforced-concrete construction for buildings are many, but the more significant points are summarized as follows:

Versatility of form Usually placed in the structure in the fluid state, the material is readily adaptable to a wide variety of architectural and functional requirements.

Durability With proper concrete protection of the steel reinforcement, the structure will have long life even under highly adverse climatic or environmental conditions.

Fire resistance With proper protection for the reinforcement, a reinforced-concrete structure provides the maximum in fire protection.

Speed of construction In terms of the entire period from the date of approval of the contract drawings to the date of completion, a concrete building may often be completed in less time than a steel structure. While the field erection of a steel building is more rapid, this phase must necessarily be preceded by prefabrication of all parts in the shop.

Cost In many cases the first cost of a concrete structure is less than that of a comparable steel structure. In almost every case, maintenance costs are less.

Availability of labor and material It is always possible to make use of local sources of labor, and in many inaccessible areas a nearby source of good aggregate can be found, so that only the cement and reinforcement need be brought in from a remote source.

9.2 Floor and Roof Loads The minimum live loads for which the floors and roof of any building should be designed are usually specified in the building code that governs at the site of construction. There are local municipal codes, state codes, and regional codes, as well as "model" codes proposed for general usage. Representative values of minimum live loads to be used in the design of a wide variety of buildings are found in the recommendations of the American Standards Association publication, "Minimum Design Loads in Buildings and Other Structures," a portion of which is reprinted in Table 9.1.

In addition to these uniformly distributed loads, it is recommended, as an alternative to the uniform load, that floors be designed to support safely certain concentrated loads, if these produce a greater stress. For example, office floors are to be designed to carry a load of 2000 lb distributed over an area $2\frac{1}{2}$ ft square, to allow for the weight of a safe or other heavy equipment, and stair treads must safely support a 300-lb load applied on the center of the tread. The specified uniform and concentrated loads are assumed to include adequate allowance for ordinary impact loading. Certain reductions are permitted in live load of 100 psf or less for members supporting 150 ft² of floor or more, on the premise that it is not likely that the entire area would be fully loaded at one time. The reduction specified is at the rate of 0.08 per cent per square foot of area supported by the member, except that no reduction is permitted in places of public assembly. The reduction is not to exceed 60 per cent nor the percentage

$$100\,\frac{D+L}{4.33L}$$

Scanned with CamScanner

Table 9.1 Minimum uniformly distributed live loads [Art. 9.2]

Occupancy or use	Live load, psf
Apartments (see Residential)	
Armories and drill rooms	150
Assembly halls and other places of assembly:	
Fixed seats	60
Movable seats	100
Balcony (exterior)	100
Bowling alleys, poolrooms, and similar recreational areas	75
Corridors:	
First floor	100
Other floors, same as occupancy served except as indicated	
Dance halls	100
Dining rooms and restaurants	100
Dwellings (see Residential)	
Garages (passenger cars)	100
Floors shall be designed to carry 150 per cent of the maximum wheel load anywhere on the floor.	
Grandstands (see Reviewing stands)	
Gymnasiums, main floors, and balconies	100
Hospitals:	
Operating rooms	60
Private rooms	40
Wards	40
Hotels (see Residential)	
Libraries:	
Reading rooms	60
Stack rooms	150
Manufacturing	125
Marquees	75
Office buildings:	
Offices	80
Lobbies	100
Penal institutions:	
Cell blocks	40
Corridors	100
Residential:	
Multifamily houses:	
Private apartments	40
Public rooms	100
Corridors	60
Dwellings:	
First floor	40
Second floor and habitable attics	30
Uninhabitable attics	20
Hotels:	
Guest rooms	40
Public rooms	100
Corridors serving public rooms	100
Public corridors	60
Private corridors	40
Reviewing stands and bleachers	100
Schools:	
Classrooms	40
Corridors	100
Sidewalks, vehicular driveways, and yards subject to trucking	250
Skating rinks	100
Stairs, fire escapes, and exitways	100
Storage warehouse, light	125
Storage warehouse, heavy	250
Stores:	
Retail:	
First floor, rooms	100
Upper floors	75
Wholesale	125
Theaters:	
Aisles, corridors, and lobbies	100
Orchestra floors	60
Balconies	60
Stage floors	150
Yards and terraces, pedestrians	100

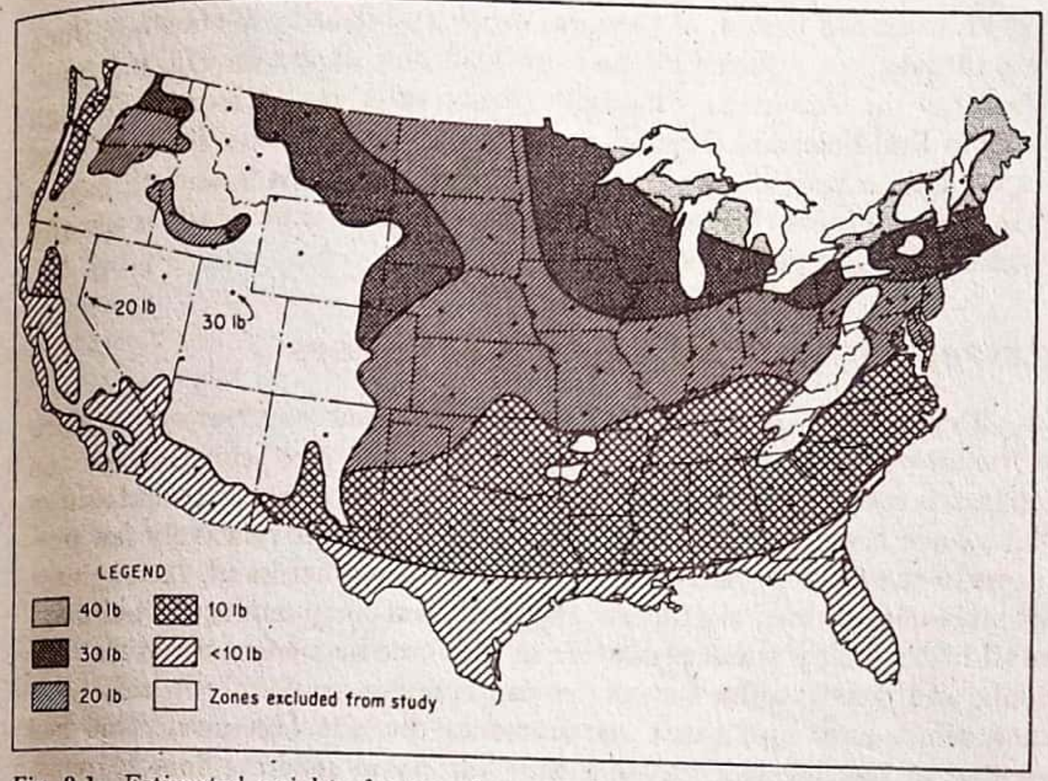


Fig. 9.1 Estimated weight of seasonal snowpack equalled or exceeded one year in ten. (*From "Minimum Design Loads in Buildings and Other Structures," American Standards Association*, 1955.)

in which D is the dead load per square foot of area supported by the member, and L is the live load. No reduction is permitted for loads over 100 psf (characteristic of warehouses and factories, in which cases it is not unlikely that the entire area may be loaded at one time), except that column loads may be reduced 20 per cent.

The specified minimum live loads cannot always be used. The type of occupancy should be considered, and the probable loads computed as accurately as possible. Warehouses for heavy storage may be designed for loads as high as 500 psf or more; unusually heavy operations in manufacturing buildings may require a large increase in the 125-psf value specified in Table 9.1; special provision must be made for all definitely located heavy concentrated loads.

In all cases, the dead weight of the floor must be included in the total design load. When plastered ceilings are specified, an additional allowance of about 10 psf is usual. Floor fill and finish floors together with suspended loads such as piping and lighting fixtures also must be included. If the locations of partitions are not definitely established, an extra allowance of from 10 to 20 psf may be in order.

Snow loads for the design of building roofs are likewise generally specified by local codes. They are preferably based on statistical studies,

Scanned with CamScanner

[*Art. 9.3*

over an extended period, of the local depth and density of snowfall. Such a set of data has resulted in the snow-load map shown in Fig. 9.1, published by the American Standards Association in "Minimum Design Loads in Buildings and Other Structures." A minimum roof load of 20 psf is specified to provide for construction and repair loads and to ensure reasonable stiffness. More detailed information on snow loads is usually available for any particular locality.

REINFORCED-CONCRETE FLOORS AND ROOFS

9.3 Types of Floor Systems The types of concrete floor systems are so numerous as to defy concise classification. In steel construction the designer is usually limited to the utilization of structural plates and shapes which have been standardized in form and size by the relatively few producers in the field. In reinforced concrete, on the other hand, the engineer has more control over the form of the structural components of a building. In addition, many small producers of reinforced-concrete structural elements and construction accessories can compete profitably in this field, since plant and equipment requirements are not excessive. This has resulted in the development of a wide variety of concrete floor systems. Only the more common types can be mentioned in this text.[1]

In general, the commonly used reinforced-concrete floor systems can be classified as follows:

1. One-way reinforcing systems (in which the main reinforcement in each structural element runs in one direction)
   - *a.* One-way solid slabs
     - (1) Slab supported on monolithic concrete beams and girders
     - (2) Slab supported on steel beams (shear connectors may be used to provide for composite action)
     - (3) Slab with light-gage steel decking which serves as form and reinforcement for the concrete
   - *b.* One-way ribbed slabs (also known as concrete joist floors)
   - *c.* Precast systems, including precast slab or beams or both
2. Two-way reinforcing systems (in which the main reinforcement in at least one of the structural elements runs in two directions)
   - *a.* Two-way solid slabs
     - (1) Slab on monolithic concrete beams
     - (2) Slab on steel beams
   - *b.* Two-way ribbed slab on concrete or steel beam supports
   - *c.* Flat-slab systems

[1] For illustrations of several other types of floor systems, see C. G. Ramsey and H. R. Sleeper, "Architectural Graphic Standards," 5th ed., John Wiley & Sons, Inc., New York, 1956.

- (1) Flat slab with drop panels or column capitals or both
- (2) Flat-plate floor with no drop panels or column capitals (may be precast and lifted to final elevation)
- (3) Ribbed flat-slab or flat-plate systems

Each of these types is described in the following articles.

9.4 Monolithic Solid-slab Beam-and-girder Floor A solid-slab beam-and-girder floor consists of a series of parallel beams supported at their extremities by girders which in turn frame into concrete columns placed at more or less regular intervals over the entire floor area. This framework is covered by a one-way reinforced-concrete slab, the load from which is transmitted first to the beams and thence to the girders and columns. The beams are usually spaced so that they come at the midpoints, at the third points, or at the quarter points of the girders, as shown in Fig. 9.2. The arrangement of beams and spacing of columns should be determined by economical and practical considerations. These will be affected by the use to which the building is to be put, the size and shape of the ground area, and the load which must be carried. A comparison of a number of trial designs and estimates should be made if the size of the building warrants, and the most satisfactory arrangement selected. As the slabs, beams, and girders are built monolithically, the beams and girders are designed as T beams, and advantage is taken of continuity.

Beam-and-girder floors, as they are usually called, are adapted to any loads and to any spans that might be encountered in ordinary building construction. The normal maximum spread in live-load values is from 40 to 400 psf, and the normal range in column spacings is from 16 to 32 ft. A complete design of a typical beam-and girder floor panel is given in Arts. 9.23 to 9.26.

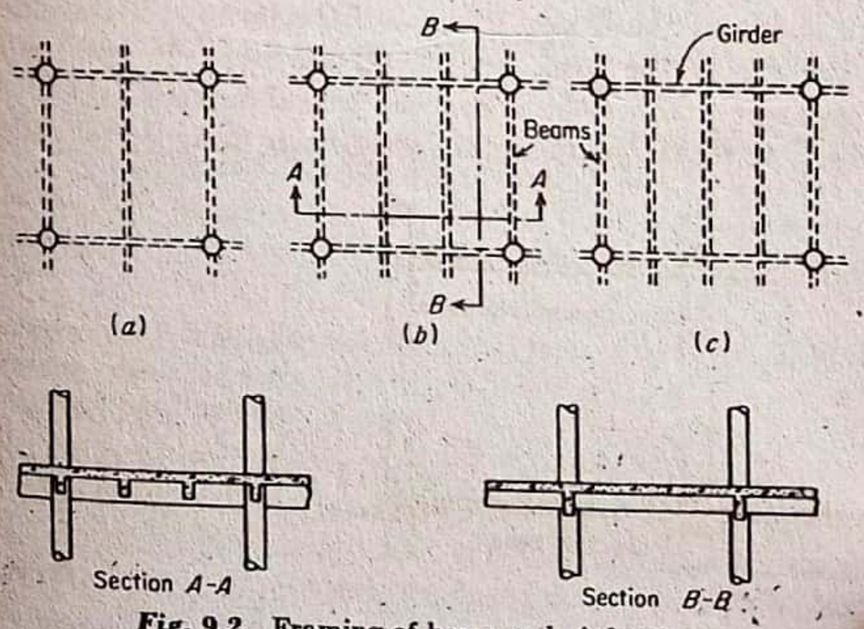


Fig. 9.2 Framing of beam-and-girder floors.

Scanned with CamScanner

In normal beam-and-girder construction the depth of a beam is about twice its stem width. For light loads, however, it may be economical to omit the intermediate beams and deep column-line girders entirely and to have the one-way slab supported by wide, shallow beams which are centered on the column lines and which frame directly into the columns. The interior beam becomes little more than a thickened portion of the slab; this form of construction, in fact, is commonly referred to as *slab-band* construction. There are a number of advantages associated with its use. In the slab span, a haunch is created which aids in resisting the relatively high negative moments that will be present over the interior support. This will both reduce the positive slab moment and the critical negative slab moment at the face of the haunch. While beam steel will be increased because of the reduced effective depth as compared with a beam of normal proportions, cost comparisons have shown that this may often be outweighted by savings in slab steel. Other advantages include a reduced depth of construction, permitting a reduction in overall height of the building, and greater flexibility in locating columns. Formwork is simplified because of the reduction in the number of framing members. In Fig. 9.3 are shown comparative sections through conventional and slab-band floors.

9.5 Concrete-slab Floors on Steel Beams One-way reinforced-concrete slabs are also frequently used in structural-steel framed buildings. Spacing of the steel beams is usually about 6 to 8 ft. Often the slab is poured so that its underside is flush with the underside of the top flange of the beam, as shown in Fig. 9.4*a*. This simplifies construction to a certain extent, as the plywood slab form can be wedged between the upper and lower flanges of the steel beam. Of even greater significance is the fact that positive bracing against lateral buckling is provided for the compressive flange of the beam, whereas if the bottom of the slab were flush with the top of the steel, one would have to rely upon adhesion between the concrete and steel to prevent lateral movement.

Increasingly in recent years buildings are being designed for composite

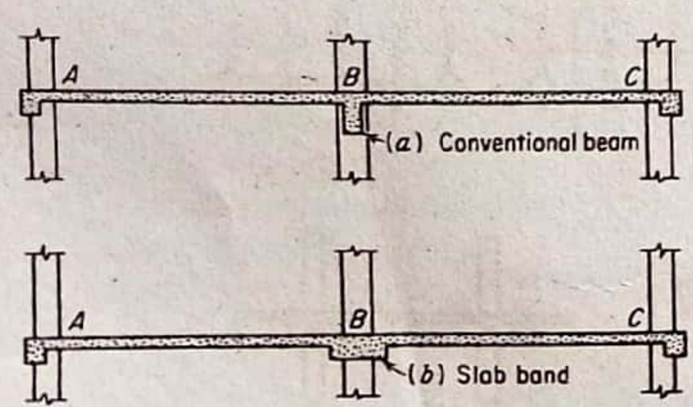


Fig. 9.3 Comparison of sections through conventional and slab-band floors.

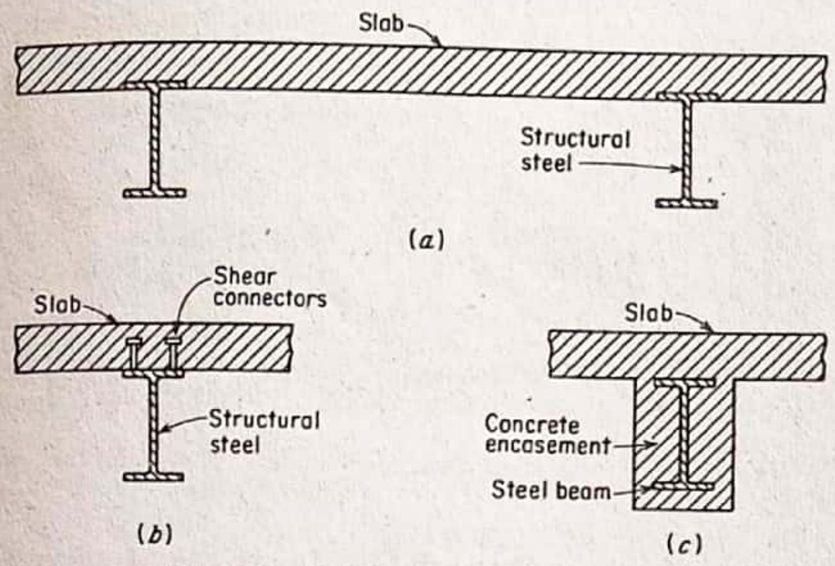


Fig. 9.4 Slab floors with steel beams.

action. Shear connectors are welded to the top of the steel beam and are embedded in the concrete slab, as shown in Fig. 9.4*b*; they prevent relative movement between the concrete and steel in the direction of the beam axis. The entire cross section, consisting of the concrete slab and the steel beam, then acts together in resisting longitudinal flexural stress. Shallower sections can be used which are nevertheless stiffer than their deeper, noncomposite counterparts. The design of composite steel-concrete members is discussed in detail in Chap. 12.

If it is necessary to fireproof a steel frame building, a form may be built around the beam, and the steel encased in concrete as shown in Fig. 9.4*c*. While some composite action undoubtedly exists, this may not be reliable for various reasons, such as the presence of a paint film between the concrete and steel, and the contribution of the concrete is usually disregarded. As an alternative to the solid encasement of the steel, it my be wrapped with expanded-metal lath or wire mesh, which is then troweled or sprayed with a fireproofing vermiculite plaster, affording a substantial reduction in dead load.

9.6 Concrete-slab Floors with Light-gage Steel Decking In recent years considerable use has been made of light-gage steel deck covered with a concrete slab for floors and roofs in steel frame office and apartment buildings. Examples of this type of construction are shown in Figs. 9.5 and 9.6. The steel deck in this case serves a double purpose: (1) it provides a form for the wet concrete, eliminating the necessity for temporary wood forms, and (2) it provides tensile reinforcement for the hardened slab. Often a light welded wire mesh is used in conjunction with the steel deck, to reinforce for shrinkage and temperature stresses in the

Scanned with CamScanner

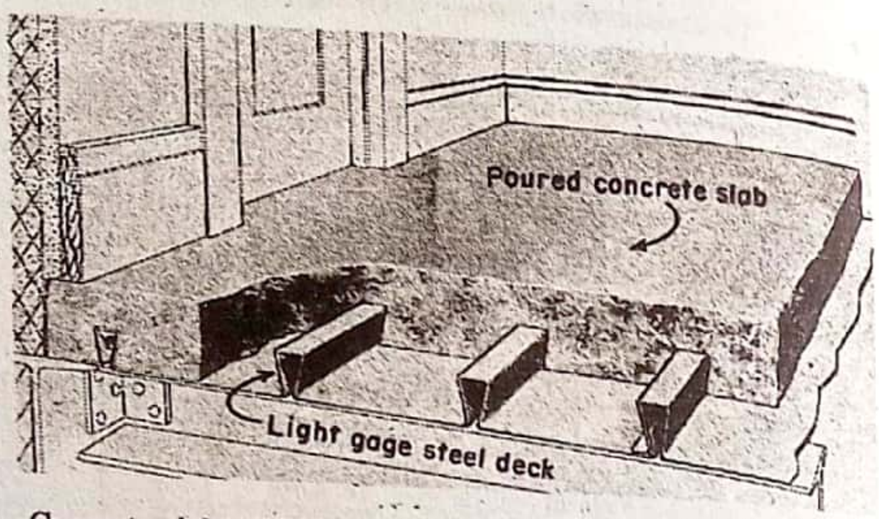


Fig. 9.5 Concrete slab with steel deck reinforcing. (*Fenestra, Inc., Holorib deck*)

direction perpendicular to the deck ribs. In one case, transverse wires are welded to the ridges of corrugated sheet steel, reinforcing shrinkage and temperatures stress as well as improving bond between the panels and the concrete. In some installations, additional negative steel bars are placed over supports; in other cases, the temperature mesh, while not adequate to reinforce for full negative moment, will at least control the cracking which will occur over supports.

The design of steel-deck-reinforced concrete slabs follows the same principles as that of any one-way slab. The steel is assumed to be concentrated at the level of the centroid of the deck cross section. The question of bond between the deck and the concrete becomes of particular

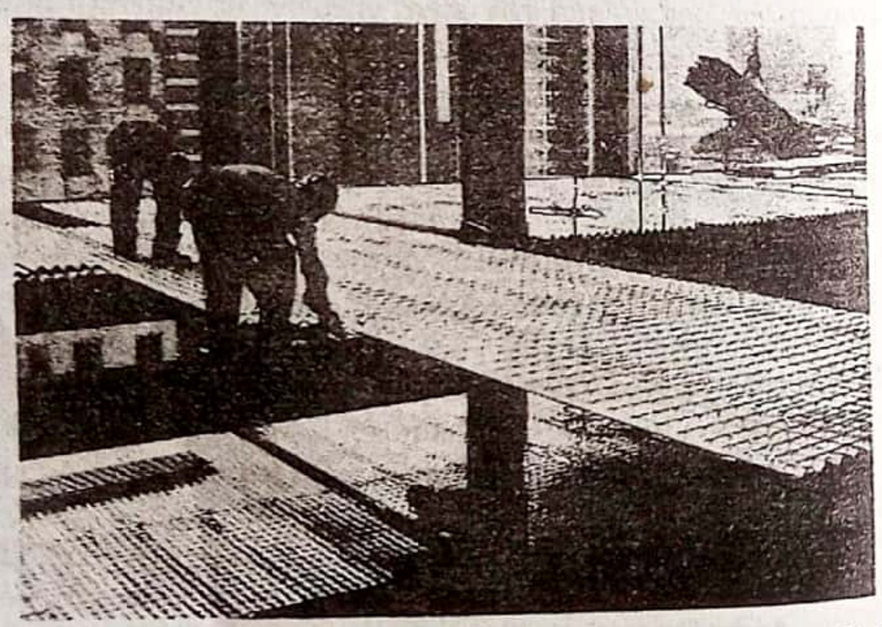
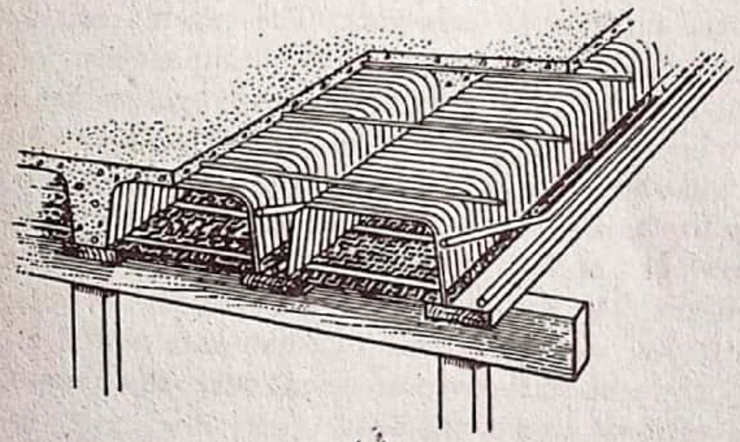


Fig. 9.6 Placing corrugated sheet reinforcing for floor slab. (*Granco Steel Products Co., Cofar deck.*)

importance, and precautions must be taken to ensure that the panels are free of oil film or dirt prior to pouring the slab.

9.7 One-way Ribbed Slabs A ribbed floor consists of a series of small, closely spaced reinforced-concrete T beams, framing into girders which in turn frame into the supporting columns. The T beams (called *joists* or *ribs*) are formed by creating void spaces in what otherwise would be a solid slab. The voids may be formed using wood or specially waterproofed cardboard, but usually special steel pans are used. The girders which support the joists are built as regular T beams.

Since the strength of concrete in tension is small and is commonly neglected in design, elimination of much of the tension concrete in a slab by the use of pan forms results in a saving of weight with little alteration in the structural characteristics of the slab. Ribbed floors are economical for buildings such as apartment houses, hotels, and hospitals, where the live loads are fairly small and the spans comparatively long. They are



(*a*)



(*b*)

Fig. 9.7 Ribbed floors with steel pans.

Scanned with CamScanner

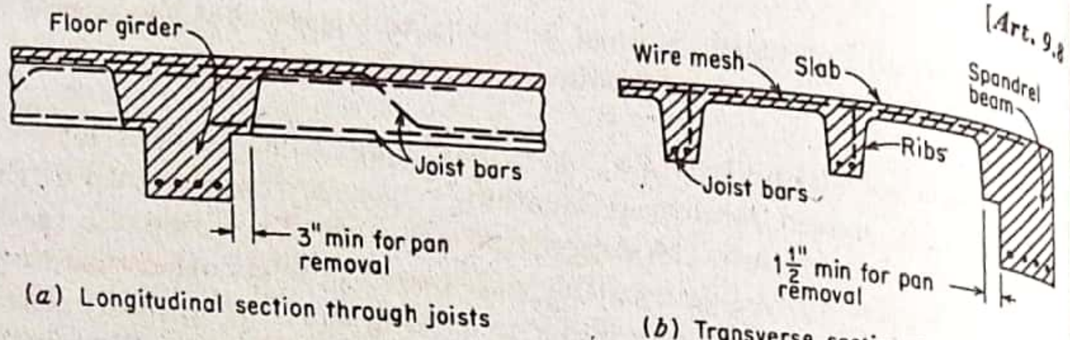


Fig. 9.8 Ribbed-floor cross sections.

not suitable for heavy construction, such as in warehouses, printing plants, and heavy manufacturing buildings.

Steel pan forms are available in depths of 6, 8, 10, 12, and 14 in. They are tapered in cross section, as shown in Fig. 9.7, to facilitate removal and are usually provided with a bottom width of 20 in., although 10- and 30-in. pans are available. Any width of joist may be obtained by varying the width of the soffit form. Figure 9.7*a* and *b* shows steel pan forms in place on wooden falsework. The tapered end pans shown in Fig. 9.7*b* are used where it is desired to obtain a wider joist width near the end supports, because of high shear or negative bending moment.

Concrete is placed on the soffit boards in the space between rows of steel pans, and above the pans to form a slab 2 in. or more thick.[1] After the concrete has hardened, the steel pans are generally removed for reuse. The reinforcement of the joists usually consists of two bars, one bent and one straight. The slab is reinforced, primarily for temperature and shrinkage stresses, with wire mesh or small bars placed at right angles to the joists; the area of the reinforcement is usually about 0.25 per cent of the cross-sectional area of the slab.

The girders which support the joists are rectangular beams or T beams with a maximum flange thickness equal to the total floor thickness, as shown in Fig. 9.8. The rows of pans are stopped at the proper distance from the stem of the girder. End caps are used at each end of each row of pans to form the sides of the girder flange. Figure 9.8 shows transverse and longitudinal cross sections of a typical ribbed-slab floor. A complete ribbed-slab floor design is given in Arts. 9.27 to 9.31.

9.8 Precast-concrete Floor Systems Precast concrete has accounted for a significant portion of building construction in recent years. Although in many cases prestressing is combined with precasting, this is not always so. Many manufacturers produce standard precast members which utilize ordinary reinforcing bars. In general, precast-concrete units can be

[1] The ACI Code specifies a minimum slab thickness of 2 in., but not less than one-half the clear distance between joists.

divided into two categories: (1) those produced as a stock item and adaptable for use under a wide variety of conditions and for many jobs and (2) those produced to a specific shape for a specific job.

Figure 9.9 shows two types of precast members which have become standard in building construction. The concrete joists of Fig. 9.9*a* are commonly available in depths from 6 to 14 in. and are used for spans from 8 to 36 ft. Reinforcement usually consists of a pair of tension bars in the bottom flange, a pair of smaller compression bars in the top flange, and inclined stirrups which are welded to the longitudinal steel. These may be used from about 4 to 8 ft on centers, with either a cast-in-place slab or precast slab units.

Another widely used, standardized precast product is the channel slab shown in Fig. 9.9*b*, which provides a usable floor or roof surface in addition to providing structural strength. A 24-in. width is standard; depths vary, depending upon the span, which may be from 8 to 30 ft, but the shorter-span planks of 2¾- or 3½-in. thickness are most widely used. Main reinforcement consists of one or two longitudinal bars at the bottom of each flange of the channel. A light wire mesh is used to reinforce the channel web.

Precast planks are also provided in rectangular cross section. In some cases, internal longitudinal voids are cast in the rectangular planks by means of collapsible rubber tubes which are withdrawn after the concrete has hardened, thus reducing dead load. In many cases, a lightweight concrete is used.

In contrast to the more or less standard shapes just described, a building may be designed around a precast section or sections that are unique to that particular job. Figure 9.10, for example, shows an unusual precast-concrete load-bearing grill being installed for a large office building in Los Angeles. The units were cast in plastic forms, trucked to the site, and hoisted into final position. In addition to providing an exterior

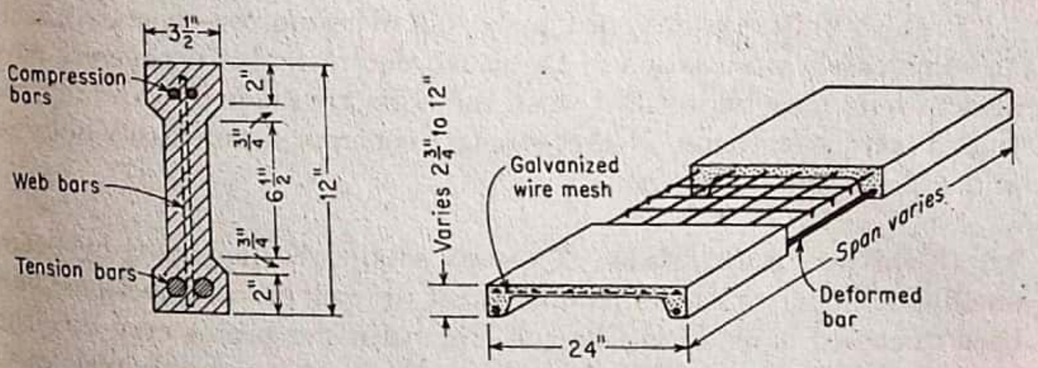


Fig. 9.9 Precast-concrete sections.

Scanned with CamScanner



Fig. 9.10 Precast-concrete load-bearing grill, American Cement Corp. Building. (*Courtesy of Daniel, Mann, Johnson, and Mendenhall, Architect-Engineers, Los Angeles.*)

wall effective in resisting both gravity and seismic loads, they present an attractive facade and desirable shading of sunlight, a requirement overlooked in many contemporary buildings.

Precast units are designed by standard reinforced-concrete theory. In some cases, a relaxation of the usual requirements for concrete cover around bars may be justified when the units are made by carefully controlled factory methods.[1] Higher-strength concrete is more easily obtained under these conditions also.

9.9 Two-way Solid Slabs Two-way solid slabs supported by beams on all four sides, with main reinforcement running in two directions, have been discussed in detail in Chap. 4. The perimeter beams may be either concrete poured monolithically with the slab or structural steel, often

[1] See ACI 711–58, "Precast Concrete Floor and Roof Units."

encased in concrete. Such two-way systems are suitable for intermediate and heavy loads on spans up to about 30 ft. The range of usefulness of two-way slabs corresponds generally to that of flat slabs, described below. The latter are often preferred because of the complete elimination of beams in a flat-slab system. In many concrete buildings designed for other types of reinforcing systems, there occur isolated floor panels which are ideally suited to two-directional reinforcement. An example of this is the floor or roof of a penthouse one bay wide in each direction.

9.10 Two-way Ribbed-slab Floors and Roofs As in one-way slab systems, the dead weight of two-way slabs can be reduced considerably by creating void spaces in what would otherwise be a solid slab. For the most part, the concrete removed is in tension and ineffective, so that the lighter floor will have virtually the same structural characteristics as the corresponding solid floor. Voids are usually formed using dome-shaped steel forms (Fig. 9.11) which are removed after the concrete slab has hardened. The lower flange of each dome contacts that of the adjacent dome, so that the concrete is poured entirely against a metal surface, resulting in good finished appearance of the slab. A waffle-like appearance is imparted to the underside of the floor or roof. Floors of this type are designed as ordinary two-way slabs.

9:11 Flat-slab Floors and Roofs While most slabs dealt with in structural practice are flat, the term *flat-slab* is reserved for a particular form of construction in which the reinforced-concrete slab is supported directly on columns without the aid of beams or girders. Figure 9.12 shows a typical flat-slab floor. Note the thickened portion of the slab, termed a *drop panel*, at the columns and the enlarged sections at the tops of the columns, called *column capitals*. Both the drop panels and column capitals serve the double purpose of reducing shear stress in the slab near the column supports and providing greater effective depth for negative bending moment.

In general, flat-slab construction is economical for live loads of 100 psf

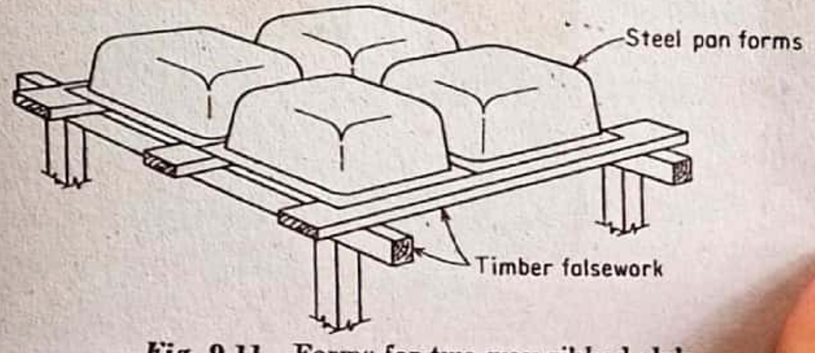


Fig. 9.11 Forms for two-way ribbed slab.

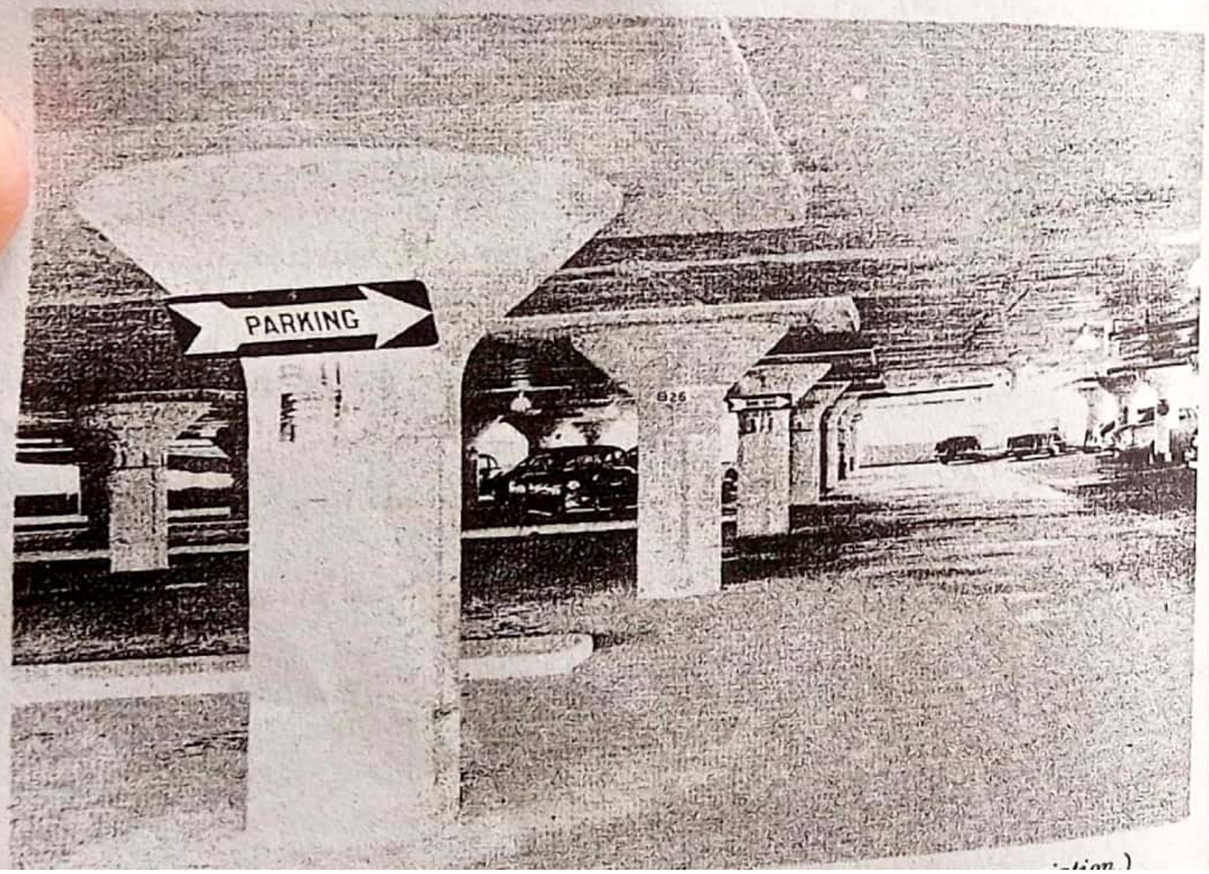
Scanned with CamScanner

[*Art. 9.12*

or more and for spans up to about 30 ft. For lighter loads, such as are found in apartment houses, hotels, and office buildings, some form of ribbed floor construction will usually be less expensive than a flat-slab floor, although in recent years flat slabs have been used economically for a wide range of loading. For spans longer than about 30 ft, beams and girders are desirable because of improved stiffness.

Flat-slab floors are discussed in detail in Chap. 4, and a design example is presented in Arts. 9.32 to 9.46.

9.12 Flat-plate Construction A flat-plate floor is essentially a flat-slab floor with the drop panels and column capitals omitted, so that a floor slab of uniform thickness is carried directly by prismatic columns. Flat-plate floors have been found economical and otherwise advantageous for such uses as apartment buildings, as shown in Fig. 9.13, where the spans are moderate, and the loads relatively light. Construction depth for each floor is held to the absolute minimum, with resultant savings in the overall height of the building. The smooth underside of the slab can be painted directly and left exposed for ceiling, or plaster can be applied to the concrete.



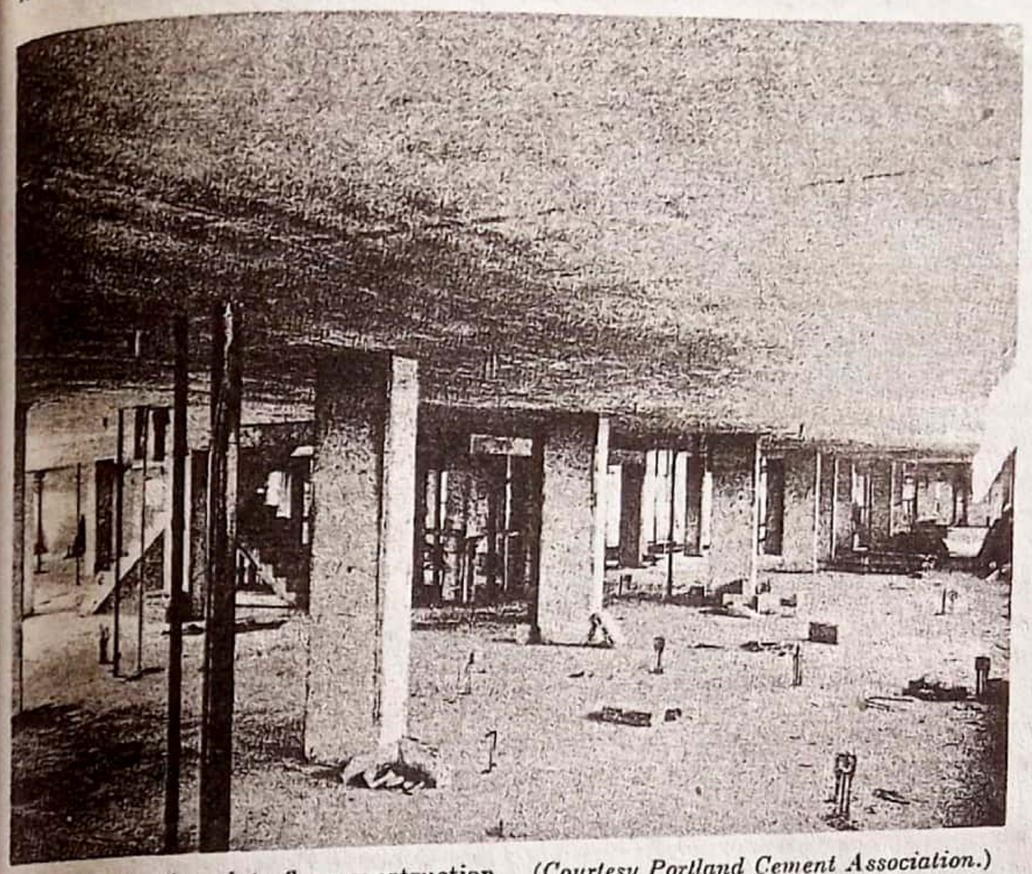


Fig. 9.13 Flat-plate floor construction. (*Courtesy Portland Cement Association.*)

Flat-plate construction is singularly adapted to the precasting of entire floors at ground level. The slabs are cast in layers over the basement or ground-floor slab, with a bond-parting agent between. After the concrete has attained its strength, the slabs are raised to their final elevation by means of jacks set on the columns. With the exception of edge forms, all falsework and forming is eliminated. This is known as *lift-slab* construction.

Certain problems are inherent in flat-plate construction. One of these is the fact that shear stresses in the concrete may be very high near the columns. Often special reinforcement is required in this area in the form of flanged steel weldments, steel beam stubs embedded in the slab, or wire-cage reinforcement. Problems with excessive longtime deflections of the relatively thin slab sections have arisen in a number of recent installations of this type.

9.13 Ribbed Flat-slab Construction The dome forms described in Art. 9.10 have also been used successfully for flat-slab and flat-plate floors, as shown in Fig. 9.14. Inactive tension concrete is removed, with a

Scanned with CamScanner

resultant saving in dead load. A wafflelike appearance results, which has in many instances been used to architectural advantage.

Commonly, dome forms are omitted near the columns, providing a section better able to resist negative bending moment and high shear in that region.

9.14 Floor Surfaces Many types of wearing surfaces are used on concrete floors. Concrete topping ¾ to 2 in. thick is frequently used. Such topping may be either monolithic or bonded. Monolithic finishes should be placed within 45 min after the base slab is poured; bonded finishes are placed on a fully hardened base slab. In order to obtain an effective bond in the latter case, the base slab should be rough, and it should be thoroughly wetted and coated with a neat cement paste before placing the finish. Mix proportions vary, and quite often an artificial hardening agent is added.[1]

A wooden floor may be provided for, if desired, by embedding beveled nailing strips or "sleepers," usually 2 by 4's laid flat, in a layer of cinder concrete on top of the main slab, as shown in Fig. 9.15. A spacing of 16 in. for the sleepers has been found satisfactory for the ordinary floor.

Small vitrified-clay flat tiles embedded in a 2-in. layer of portland-cement mortar also provide a satisfactory floor surface. Asphalt or linoleum tile placed over a smooth cement base is also frequently used.

[1] See Portland Cement Association bulletins "Surface Treatments for Concrete Floors" and "Specifications for Heavy-duty Floor Concrete Floor Finish" for more complete coverage of this important topic.

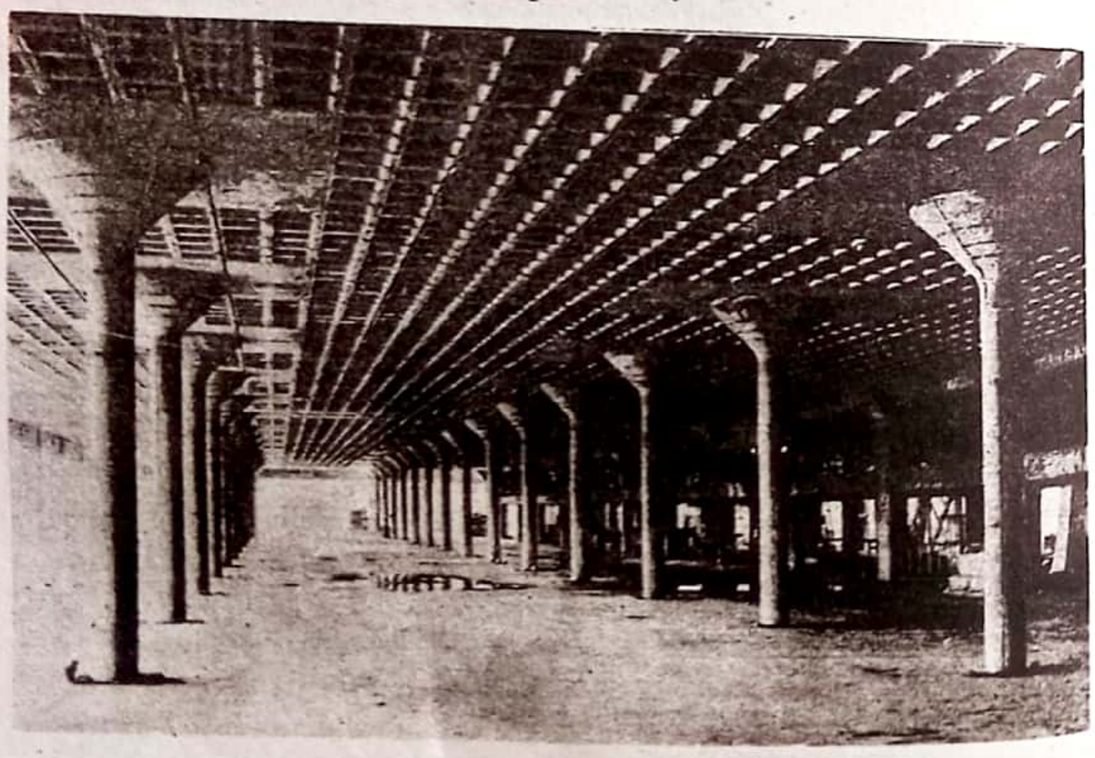


Fig. 9.14 Ribbed flat-slab floor or grid slab.

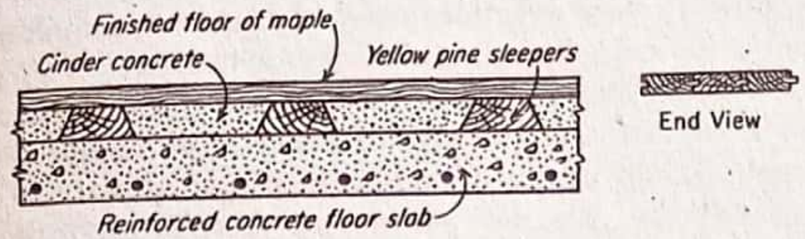


Fig. 9.15 Details of a wooden floor on a concrete slab.

The durability of any wearing surface depends in a large measure upon the method of placing the surface. If not properly constructed, the concrete finish might spall, the wood floor "dry-rot," the tiles curl, and the linoleum crack. In order to ensure the maximum degree of serviceability from a given type of floor surface, a special study of methods which have proved successful for laying that particular type of floor should be made.

9.15 Concrete Roofs The design of roofs is similar to the design of floors. In addition to the structural requirements, however, the roofs must be impervious to the passage of water, provide for adequate drainage, and furnish protection against condensation.

In order to provide adequate drainage, the roof slab may be pitched slightly, or a filling of some light material such as cinder concrete, covered with a suitable roofing material, may be used, the thickness of the filling being varied so as to give the required slope to the roof surface. The amount of slope required for drainage will depend upon the smoothness of the exposed surface. A value of ⅛ in. per ft might be used with a surface of hard tile. Felt and gravel roofs should have a pitch of at least ¼ in. per ft. Some form of flashing is required along the parapets to prevent the drainage from seeping into the building at the edges of the roof slab.

Condensation may best be guarded against by proper ventilation and insulation. The form of insulation to be used will depend upon the particular class of building under consideration.

Imperviousness may best be provided for by the application of some form of separate roof covering, such as a combination of felt and gravel in alternate layers cemented together and to the slab by means of coal-tar pitch or asphalt, vitrified tile embedded in asphalt, or any of the commercial types of built-up roofings. Tin, corrugated iron, or copper roofings are sometimes placed on reinforced-concrete buildings but are usually more expensive and less permanent than other types of coverings.

WALLS AND PARTITIONS

9.16 Panel and Curtain Walls As a general rule, the exterior walls of a reinforced-concrete building are supported at each floor by the skele-

Scanned with CamScanner

ton framework, their only function being to enclose the building. Such walls are called *panel* walls. They may be made of concrete (often precast), cinder concrete block, brick, tile blocks, or insulated metal panels. The latter may be faced with aluminum, stainless steel, or a porcelain-enamel finish over steel, backed by 1 or 2 in. of insulating material and an inner surface sheathing. The thickness of each of these types of panel walls will vary according to the material, type of construction, climatological conditions, and the building requirements governing the particular locality in which the construction takes place.

The pressure of the wind is usually the only load that is considered in determining the structural thickness of a wall panel, although in some cases exterior walls are used as diaphragms to transmit forces caused by horizontal loads down to the building foundations.

Curtain walls are similar to panel walls except that they are not supported at each story by the frame of the building, but are self-supporting. However, they are often anchored to the building frame at each floor to provide lateral support.

9.17 Bearing Walls A bearing wall may be defined as one which carries any vertical load in addition to its own weight. Such walls may be constructed of stone masonry, brick, concrete block, or reinforced concrete. Occasional projections or pilasters add to the strength of the wall and are often used at points of load concentration. In small commercial buildings bearing walls may be used with economy and expediency. In larger commercial and manufacturing buildings, when the element of time is an important factor, the delay necessary for the erection of the bearing wall and the attending increased cost of construction often dictate the use of some other arrangement.

Bearing walls may be of either single or double thickness, the advantage of the latter type being that the air space between the walls renders the interior of the building less liable to temperature variations and makes the wall itself more nearly moistureproof. On account of the greater gross thickness of the double wall, such construction reduces the available floor space. This feature is often sufficient in itself to warrant the selection of the solid wall unless the factors of condensation and temperature are of great importance. Cavity wall construction is usually limited to a total height of about 40 ft.

The thickness of bearing walls varies with the height. The New York City Building Code requires that, for bearing walls made of solid masonry units (brick, stone, concrete brick, etc.) and not more than 75 ft in height, the thickness of the uppermost 55 ft of height shall be at least 12 in., and the thickness below this shall be at least 16 in., except that for walls in buildings of one, two, and three stories the top-story thickness in each

case may be 8 in. In computing wall thicknesses, a maximum story height of 13 ft shall be assumed.

According to the ACI Code, the allowable compressive stress in reinforced-concrete bearing walls shall be

$$f_c = 0.225 f'_c \left[1 - \left(\frac{h}{40t}\right)^3\right] \tag{9.1}$$

in which h is the vertical distance between supports, and t is the thickness of the wall. When the reinforcement in bearing walls is designed, placed, and anchored in position as for tied columns, the allowable stresses shall be those for tied columns, in which the ratio of vertical reinforcement shall not exceed 0.04. For design by ultimate-strength methods, the values from Eq. (9.1) shall be multiplied by 1.9. In the case of concentrated loads, the length of the wall to be considered as effective for each shall not exceed the center-to-center distance between loads, nor shall it exceed the width of the bearing plus 4 times the wall thickness. Reinforced-concrete bearing walls shall have a thickness of at least $\frac{1}{25}$ the unsupported height or width, whichever is shorter. Reinforced-concrete bearing walls of buildings shall be not less than 6 in. thick for the uppermost 15 ft of their height; for each successive 25 ft downward, or fraction thereof, the minimum thickness shall be increased 1 in.

9.18 Basement Walls In determining the thickness of basement walls, the lateral pressure of the earth, if any, must be considered in addition to other structural features. If part of a bearing wall, the lower portion may be designed either as a slab supported by the basement and first floors, or as a retaining wall, depending upon the type of construction. If columns and wall beams are available for support, each basement wall panel of reinforced concrete may be designed to resist the earth pressure as a simple slab reinforced in either one or two directions.

A minimum thickness of 8 in. is generally specified for reinforced-concrete basement walls. In wet ground a minimum thickness of 12 in. should be used. In any case, the thickness cannot be less than that of the wall above.

Care should be taken to brace a basement wall thoroughly from the inside if the earth is backfilled before the wall has obtained sufficient strength to resist the lateral pressure without such assistance or if it is placed before the first-floor slab is in position.

9.19 Partition Walls Interior walls used for the purpose of subdividing the floor area may be made of cinder block, brick, precast concrete, metal lath and plaster, clay tile, or metal. The type of wall selected

Scanned with CamScanner

[Art. 9.2

will depend upon the fire resistance required, flexibility of rearrangement, ease with which electrical conduits, plumbing, etc., can be accomodated, and architectural requirements.

STAIRWAYS

9.20 Types of Concrete Stairs The simplest form of reinforced-concrete stairway consists of an inclined slab supported at the ends upon beams, with steps formed upon its upper surface. Such a stair slab is usually designed as a simple slab with a span equal to the horizontal distance between supports. This method of design requires steel to be placed only in the direction of the length of the slab. Transverse steel, usually one bar to each tread, is used only to assist in distribution of the load and to provide temperature reinforcement. It sometimes becomes necessary to include a platform slab at one or both ends of the inclined slab. Many successful designs made as outlined above for the simple inclined slab indicate that the effect of the angle that occurs in a slab of this type can safely be disregarded.

It is advisable to keep the unsupported span of a stair slab reasonably short. If no break occurs in the flight between floors, intermediate beams, supported by the structural framework of the building, may be employed. If the stair between floors is divided into two or more flights, beams as described above may be used to support the intermediate landing, with these in turn supported as above for the long straight flight, or the intermediate slab may be suspended from a beam at the upper floor level by means of rod hangers. Where conditions permit, the intermediate slab may be supported directly by the exterior walls of the building.

9.21 Building-code Requirements The required number of stairways, and many of the details, are governed to a large extent by the provisions of the governing building code. Among other things, these provisions stipulate the maximum distance from the most remote point in the floor area to the stairway, the minimum width of stairway, the maximum height of any straight flight, the maximum height (or rise) of a single step, the minimum distance (the run) between the vertical faces of two consecutive steps, and the required relation between the rise and the run to give safety and convenience in climbing.

In most codes the minimum width of any stair slab and the minimum dimension of any landing are about 44 in. The maximum rise of a stair step is usually specified as about 7¾ in., and the minimum run or tread width, exclusive of nosing, 9½ in. A rise of less than 6½ in. is not considered generally satisfactory. In order to give a satisfactory and comfortable ratio of rise to run, various rules have been adopted. One requires

Art. 9.23]

that for steps without nosings, the sum of the rise and run shall be 17½ in., but the rise shall not be less than 6½ in. or more than 7¾ in.

The maximum height of a straight flight between landings is generally 12 ft, except for stairways serving as exits from places of assembly, where a maximum of 8 ft is normally specified.

The number of stairways is governed by the width of the stair slab, the number of probable occupants on each floor, and the dimensions of the floor area. One typical code specification is that the distance from any point in an open floor area to the nearest stairway or exit shall not exceed 100 ft, that the corresponding distance along corridors in a particular area shall not exceed 125 ft, and that the combined width of all stairways in any story shall be such that the stairs may accommodate at one time the total number of persons occupying the largest floor area served by such stairs above the floor area under consideration on the basis of one person for each 22 in. of stair width and 1½ treads on the stairs, and one person for each 3½ ft² floor area on the landings and halls within the stairway enclosure.

In all buildings over 40 ft in height, and in all mercantile buildings regardless of height, the required stairways must be completely enclosed by fireproof partitions, and at least one stairway must continue to the roof. An open ornamental stairway can be used from the main entrance floor to the floor next above, provided it is not the only stairway.

9.22 Construction Details The usual practice is to construct the stairways after the main structural framework of the building has been completed, in which event recesses should be left in the beams to support the stair slab, and dowels should be provided to furnish the necessary anchorage. Occasionally, however, the stairs are poured at the same time as the floors, in which event negative-moment reinforcement should be furnished over the supports of the stair slab, as in any continuous-beam construction. The steps are usually poured monolithically with the slab, but they may be molded after the main slab is in place. In the latter instance, provision must be made for securing the step to the slab.

DESIGN OF A BEAM - AND - GIRDER FLOOR

9.23 Data and Specifications In order to illustrate the application of the principles of reinforced-concrete design to the design of a concrete floor of the slab–beam-and-girder type, typical portions of the second floor of the building shown in Figs. 9.17 and 9.18 will be designed. The building is to sustain a live load of 200 psf. The ACI moment coefficients of Table 8.2 are applicable and will be used for this example, although improved economy would undoubtedly result from an elastic analysis of the

Scanned with CamScanner

building frame. The outside faces of all the exterior columns will be kept in the same plane so that the pilasters will have smooth faces, and all the wall beams and girders will be placed flush with the outer face of the pilasters so that the entire outer walls, except for the windows, will be in one plane. A 1-in. bonded wearing surface, which will add to the dead load but will not be considered as part of the effective depth, will be placed on the slab. Steel reinforcement with a yield stress $f_y = 40{,}000$ psi will be used with concrete of strength $f'_c = 3000$ psi. A maximum steel ratio of $p = 0.18f'_c/f_y$ will be adopted.

For purposes of illustration, most of the computations for this design will be presented on computation sheets of the type that are typical in design office practice.

9.24 Design of the Slabs The computations for the design of the floor slabs *S*1 and *S*2 are shown in Computation Sheet 9.1. The clear spans were obtained from the assumptions that the exterior basement columns will be 24 in. deep from the face of the basement wall and that the floor beams will be 8 in. in width. In computing the negative moments at the faces of supports, the average of the two adjacent clear spans was used. A negative-moment coefficient at the interior face of the exterior support of $\frac{1}{24}$ was taken in accordance with Table 8.2. Reinforcing steel is placed with centers 1 in. from the top or bottom of the slab.

From Graph 11, Appendix B:

*S*1:

Fifty per cent positive-moment reinforcement required for

$0.23 \times 7 \text{ ft} - 12 \times \frac{3}{8} \text{ in.} = 1 \text{ ft } 3 \text{ in.}$

from support, bent at 45°, reaching top at 1 ft 1 in. from support. Negative-moment reinforcement required at top,

$0.09 \times 7 \text{ ft} + 4\frac{1}{2} \text{ in.} = 1 \text{ ft } 0 \text{ in.}$

from outer support. At continuous end, 50 per cent positive-moment reinforcement required for 1 ft 3 in. from support, and 50 per cent negative-moment reinforcement at

$0.09 \times 7 \text{ ft} + 4\frac{1}{2} \text{ in.} = 1 \text{ ft } 0 \text{ in.}$

*S*2:

Fifty per cent of positive-moment reinforcement required at

$0.25 \times 6 \text{ ft } 4 \text{ in.} - 4\frac{1}{2} \text{ in.} = 1 \text{ ft } 2\frac{1}{2} \text{ in.}$

Design of floor slab

Live load	$200.0 \times 1.8 = 360$ psf
Dead load (assume 4″ slab + 1″ finish)	$62.5 \times 1.5 = 94$
Total	$= 454$ psf

Clear span for *S*-1 = 7′0″
Clear span for *S*-2 = 6′4″ } Avg clear span = 6′8″

S1

Center:
$M = +\frac{1}{14}(454)(7.0)^2(12) = 19{,}000$ in.-lb
At continuous end:
$M = -\frac{1}{12}(454)(6.67)^2(12) = -20{,}200$ in.-lb
At wall end:
$M = -\frac{1}{24}(454)(7.0)^2(12) = -11{,}050$ in.-lb
From Graph 1
$\frac{M_u}{\phi bd^2} = 483$
$d^2 = \frac{20{,}200}{0.9 \times 12 \times 483} = 3.88$ in.^{2}
$d = 1.97$ in.
Use a minimum d of 3 in.
Slab thickness = 4 in. as assumed.
Center:
$\frac{M_u}{\phi bd^2} = \frac{19{,}000}{0.9 \times 12 \times 9} = 196$
From Graph 1
$p = 0.0051$
$A_s = 0.0051 \times 12 \times 3 = 0.183$ in.^{2}
At continuous end:
$\frac{M_u}{\phi bd^2} = \frac{20{,}200}{0.9 \times 12 \times 9} = 208$
$p = 0.0054$
$A_s = 0.0054 \times 12 \times 3 = 0.194$ in.^{2}
At wall end:
$\frac{M_u}{\phi bd^2} = \frac{11{,}050}{0.90 \times 12 \times 9} = 114$
$p < p_{min} = 0.005$
$A_s = 0.005 \times 12 \times 3 = 0.18$ in.^{2}

S2

Center:
$M = +\frac{1}{16}(454)(6.33)^2(12) = 13{,}600$ in.-lb
At first interior support:
$M = -\frac{1}{12}(454)(6.67)^2(12) = 20{,}200$ in.-lb
At all other interior supports:
$M = -\frac{1}{12}(454)(6.33)^2(12) = 18{,}100$ in.-lb
Use 4-in. slab thickness throughout.

Center:
$\frac{M_u}{\phi bd^2} = \frac{13{,}600}{0.9 \times 12 \times 9} = 140$
$p < p_{min}$
$A_s = 0.005 \times 12 \times 3 = 0.18$ in.^{2}
At first interior support:
$\frac{M_u}{\phi bd^2} = \frac{20{,}200}{0.9 \times 12 \times 9} = 208$
$p = 0.0054$
$A_s = 0.0054 \times 12 \times 3 = 0.19$ in.^{2}
At other interior supports:
$\frac{M_u}{\phi bd^2} = \frac{18{,}100}{0.9 \times 12 \times 9} = 186$
$p < p_{min}$
$A_s = 0.18$ in.^{2}

Outer support	*S*1 center	First interior support	*S*2 center	Other supports
0.18	0.18	0.19	0.18	0.18
#3 straight @ 14″	#3 straight @ 14″	#3 bent @ 7″	#3 bent @ 14″	#3 bent @ 7″
#3 bent @ 14″	#3 bent @ 14″		#3 straight @ 14″	
$A_s = 0.19$	$A_s = 0.19$	$A_s = 0.19$	$A_s = 0.19$	$A_s = 0.19$

Temperature steel
$A_s = 0.002(12)(4) = 0.096$ in.^{2} Use #3 @ 13″

***Computation Sheet* 9.1** Beam-and-girder floor.

from support. Fifty per cent of negative-moment reinforcement required at

$0.09 \times 6 \text{ ft } 4 \text{ in.} + 4\frac{1}{2} \text{ in.} = 0 \text{ ft } 11\frac{1}{2} \text{ in.}$

from support. Number 3 bars at bottom 14 in. center to center are carried into exterior support 6 in. and are continuous over other sup-

Scanned with CamScanner

ports. Alternate No. 3 bars 14 in. center to center are bent up 1 ft 2 in. from face of all supports. Bent-up bars must be extended into the adjacent span a length of

$$0.21 \times 7 \text{ ft} + 4\tfrac{1}{2} \text{ in.} = 1 \text{ ft } 10 \text{ in.}$$

All details for the slab are shown in Fig. 9.17.

9.25 Design of the Beams The computations for the design of beams $B1$ and $B2$ are shown in Computation Sheets 9.2 and 9.3. The clear spans for the beams were obtained using the same assumptions made in the design of the slab, with the further assumption that the beams will be framed into girders 12 in. in width. The beams framing into girders were designed, since these beams have clear spans slightly longer than those framing into columns; however, to simplify the construction, all beams are of the same dimensions. Beams will be proportioned for a maximum steel ratio of $0.18f'_c/f_y$. While a portion of the bottom steel will be bent up in each beam, stirrups will be provided to take all the diagonal tensile stresses.

On the basis of Computation Sheets 9.2 and 9.3, the positive steel requirement of 2.14 in.² for $B1$ will be provided using four No. 7 bars ($A_s = 2.41$). Two of these will be bent up at each end. At the wall end of

Design of beams:

Uniform load per foot from floor $7 \times 454 = 3175$ plf
Dead load of stem (assumed) $210 \times 1.5 = 315$
Total $= 3490$ plf

Clear span for $B1 = 22'6''$
Clear span for $B2 = 22'0''$ } Avg clear span $= 22'3''$

$B1$

Center:
$M = +\frac{1}{14}(3490)(22.5)^2 12 = 1{,}520{,}000$ in.-lb
At continuous end:
$M = -\frac{1}{10}(3490)(22.25)^2 12 = 2{,}080{,}000$ in.-lb
At wall ends:
$M = -\frac{1}{24}(3490)(22.5)^2 12 = 885{,}000$ in.-lb
$V_{max} = \frac{1}{2}(1.15)(3490)22.5 = 45{,}200$ lb
At continuous end:
$p = 0.18 \times \frac{3}{40} = 0.0135$
$\dfrac{M_u}{\phi bd^2} = 483$
$bd^2 = \dfrac{2{,}080{,}000}{0.9 \times 483} = 4790$
Use $b = 12$ in., $d = 20$ in.
$A_s = 0.0135 \times 12 \times 20 = 3.24$ in.²
At wall end:
$\dfrac{M_u}{\phi bd^2} = \dfrac{885{,}000}{0.9 \times 4790} = 206$
$p = 0.0054$
$A_s = 0.0054 \times 240 = 1.30$ in.²
Center:
$A_s = \dfrac{1{,}520{,}000}{0.9 \times 40{,}000(20 - 2)} = 2.35$ in.²
$a = \dfrac{2.35 \times 40}{0.85 \times 3 \times 67.5} = 0.58$ in.
Revised $A_s = 2.35 \times 18/19.71 = 2.14$ in.²

$B2$

Center:
$M = +\frac{1}{16}(3490)(22)^2 12 = 1{,}269{,}000$ in.-lb
At first interior support:
$M = -\frac{1}{11}(3490)(22.25)^2 12 = 1{,}866{,}000$ in.-lb
At all other interior supports:
$M = -\frac{1}{11}(3490)(22)^2 12 = 1{,}842{,}000$ in.-lb
$V_{max} = \frac{1}{2}(3490)22 = 38{,}400$ lb
Beam dimensions will be kept the same throughout.

At first interior support:
$\dfrac{M_u}{\phi bd^2} = \dfrac{1{,}866{,}000}{0.9 \times 4790} = 433$
$p = 0.012$
$A_s = 0.012 \times 240 = 2.88$ in.²

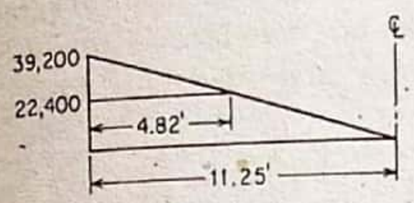
At all other interior supports:
$\dfrac{M_u}{\phi bd^2} = \dfrac{1{,}842{,}000}{0.9 \times 4790} = 428$
$p = 0.0118$
$A_s = 0.0118 \times 240 = 2.84$ in.²

Center:
$A_s = \dfrac{1{,}269{,}000}{0.9 \times 40{,}000(20 - 2)} = 1.96$ in.²
$a = 0.48$
Revised $A_s = 1.96 \times 18/19.76 = 1.79$ in.²

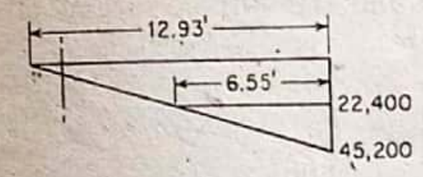
***Computation Sheet* 9.2** Beam-and-girder floor.

$B1$

Shear (use #3 U stirrups):
At wall end:
$V = 39{,}200$ lb
$V_c = 2 \times 0.85\sqrt{3000}\,(12)(20) = 22{,}400$ lb



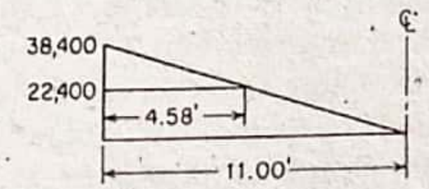
$s_{max} = 29\frac{1}{2} = 10$ in.
$s_{max} = 0.22/0.0015 \times 12 = 12.2$ in.
At distance d:
$V' = 16{,}800 \times 3.15/4.82 = 11{,}000$ lb
$s_d = \dfrac{0.22 \times 0.85 \times 40{,}000 \times 20}{11{,}000}$
$= 13.6$ in. $> s_{max}$
Space 1 @ 5", 8 @ 10".
At continuous end:



At distance d:
$V' = 22{,}800 \times 4.88/6.55 = 17{,}000$ lb
$s_d = \dfrac{0.22 \times 0.85 \times 40{,}000 \times 20}{17{,}000} = 8.80$ in.
Space 1 @ 4", 4 @ 8", 7 @ 10".

$B2$

At either end:



At distance d:
$V' = 16{,}000 \times 2.91/4.58 = 10{,}200$ lb
$s_d = \dfrac{0.22 \times 0.85 \times 40{,}000 \times 20}{10{,}200}$
$= 14.7$ in. $> s_{max}$
Space 1 @ 5", 8 @ 10".

***Computation Sheet* 9.3** Beam-and-girder floor.

Scanned with CamScanner

$B1$, the required area of 1.30 in.² will be met by adding one No. 5 bar to the two No. 7 bent bars ($A_s = 1.51$ in.²). In beam $B2$, the positive steel requirement of 1.79 in.² will be provided by four No. 6 bars ($A_s = 1.77$ in.²), two of which are bent up at each end. At the first interior support, the total requirement is 3.24 in.² Two No. 7 straight bars will be added to the two No. 6 and two No. 7 bent bars ($A_s = 3.29$ in.²). At typical interior supports, where the steel requirement is 2.84 in.², two No. 7 straight bars are added to the two No. 6 bars bent up from each side ($A_s = 2.97$ in.²).

From Graph 11, Appendix B:

$B1$:

Two No. 7 bars can be bent up at

$$0.23 \times 22.5 \times 12 - 20 = 42 \text{ in.}$$

from the face of either support. The remaining two No. 7 bars are continued 6 in. into the support faces. At the wall end, the No. 5 straight bar is continued a distance d beyond the point of inflection and is cut off at

$$0.12 \times 22.5 \times 12 + 20 = 52 \text{ in.}$$

from the support face. At the continuous end, straight bars are cut off at

$$0.28 \times 22.5 \times 12 + 20 = 96 \text{ in.}$$

from the support face.

$B2$:

Two No. 6 bars are bent up at

$$0.25 \times 22 \times 12 - 20 = 46 \text{ in.}$$

from the support faces. The remaining two No. 6 bars are continued 6 in. into the face of the supports. At the first interior support, the four No. 7 straight bars are cut off at

$$0.24 \times 22.25 \times 12 + 20 = 84 \text{ in.}$$

beyond the support face. At all other interior supports, the two No. 7 and two No. 6 straight bars are cut off at

$$0.24 \times 22 \times 12 + 20 = 84 \text{ in.}$$

from the support face.

By inspection of Table 8, Appendix B, it is evident that adequate development length is provided for all bars; therefore, according to Code, flexural bond stress need not be checked.

9.26 Design of the Girders A portion of the sample computations for the design of the girders is shown in Computation Sheets 9.4 and 9.5.

Design of girders

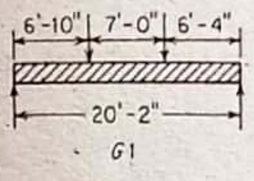
Load from floor beams = 76,800 lb

Live load on girder		360 plf
Dead load of floor finish on girder		19
Dead load of girder (assumed)	$500 \times 1.5 =$	750
	Total =	1129 plf

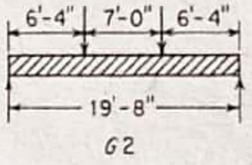
Clear span of $G1$ = 20′2″
Clear span of $G2$ = 19′8″ } Avg clear span used = 19′11″

Simple span maximum moment

$$\tfrac{1}{8}(1129)(19.92)^2 12 = 672{,}000 \text{ in.-lb}$$
$$76{,}800(6.58)12 = 6{,}020{,}000$$
$$M_s = 6{,}692{,}000 \text{ in.-lb}$$



$G1$



$G2$

$G1$

Center:
$M = +\frac{5}{14} M_s = 3{,}820{,}000$ in.-lb

At continuous end:
$M = -\frac{5}{10} M_s = -5{,}350{,}000$ in.-lb

At wall end:
$M = -\frac{5}{16} M_s = -3{,}340{,}000$ in.-lb

$$V_{max} = 1.15\left[76{,}800 + 1129\frac{20.2}{2}\right] = 101{,}000 \text{ lb}$$

Use $p = 0.18 \times \frac{3}{40} = 0.0135$.

At continuous end:

$$\frac{M_u}{\phi bd^2} = 483$$
$$bd^2 = \frac{5{,}350{,}000}{0.9 \times 483} = 12{,}310$$

Use $b = 18$ in., $d = 26.5$ in.

$A_s = 0.0135 \times 18 \times 26.5 = 6.45$ in.²

At wall end:

$$\frac{M_u}{\phi bd^2} = \frac{3{,}340{,}000}{0.9 \times 12{,}310} = 301$$
$$p = 0.0080$$
$A_s = 0.0080 \times 18 \times 26.5 = 3.83$ in.²

At center ($b = 60.5$ in.):

$$A_s = \frac{3{,}820{,}000}{0.9 \times 40{,}000(26.5 - 2)} = 4.33 \text{ in.}^2$$
$$a = \frac{4.33 \times 40}{0.85 \times 3 \times 60.5} = 1.12 \text{ in.}$$

Revised $A_s = 4.33 \times 24.50/25.94 = 4.10$ in.²

$G2$

Center:
$M = +\frac{5}{16} M_s = 3{,}340{,}000$ in.-lb

At ends:
$M = -\frac{5}{11} M_s = -4{,}860{,}000$ in.-lb

$$V_{max} = 76{,}800 + 1129\frac{19.67}{2} = 87{,}500 \text{ lb}$$

Girder dimensions will be kept the same throughout.

At supports:

$$\frac{M_u}{\phi bd^2} = \frac{4{,}860{,}000}{0.90 \times 12{,}310} = 439$$
$$p = 0.0121$$
$A_s = 0.0121 \times 18 \times 26.5 = 5.77$ in.²

At center:

$$A_s = \frac{3{,}340{,}000}{0.9 \times 40{,}000(26.5 - 2)} = 3.78 \text{ in.}^2$$
$$a = \frac{3.78 \times 40}{0.85 \times 3 \times 60.5} = 0.975 \text{ in.}$$

Revised $A_s = 3.78 \times 24.50/26.01 = 3.56$ in.

***Computation Sheet* 9.4** Beam-and-girder floor.

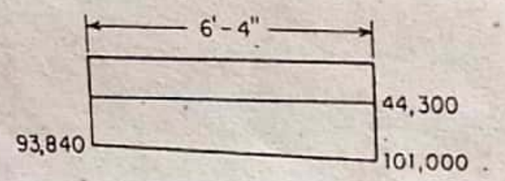
Scanned with CamScanner

The clear spans here were obtained by making use of all previous assumptions and further assuming that the exterior columns supporting the second floor have a depth of 14 in., measured from the face of the wall, and that the interior first-floor columns are 16 in. in diameter. The average clear span was used in computing moments caused by the uniformly distributed load, and the average distance between beams and adjacent columns in $G1$ for computing moments caused by concentrated loads. These assumptions are justifiable since they produce moments slightly larger than those which actually exist in either span. The inherently approximate nature of calculations of this sort does not warrant closer refinement in computations.

$G1$

Shear:

At continued end:



$V_c = 2 \times 0.85 \sqrt{3000} \times 18 \times 26.5 = 44{,}300$ lb

$s_{max} = 26.5/2 = 13.25$ in.

Using #4 U stirrups:

$s_{max} = 0.40/(0.0015 \times 18) = 14.80$ in.

Use $s_{max} = 13$ in.

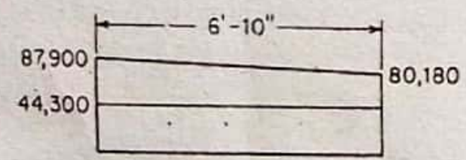
At 26.5 in.:

$V - V_c = 54{,}210$ lb

$$s_d = \frac{0.40 \times 0.85 \times 40{,}000 \times 26.5}{54{,}210} = 6.66 \text{ in.}$$

Space 1 @ 3", 16 @ 6½".

At wall end:



At 26.5 in.:

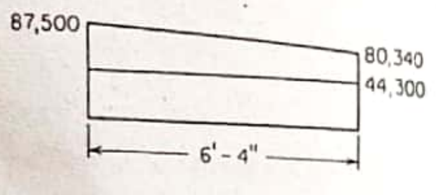
$V - V_c = 41{,}060$ lb

$s_d = 6.66 \times 54{,}210/41{,}060 = 8.78$ in.

Space 1 @ 4", 13 @ 8½".

$G2$

At either end:



At 26.5 in.:

$V - V_c = 40{,}690$ lb

$s_d = 6.66 \times 54{,}210/40{,}690 = 8.88$ in.

Space 1 @ 4", 12 @ 8½".

***Computation Sheet* 9.5** Beam-and-girder floor.

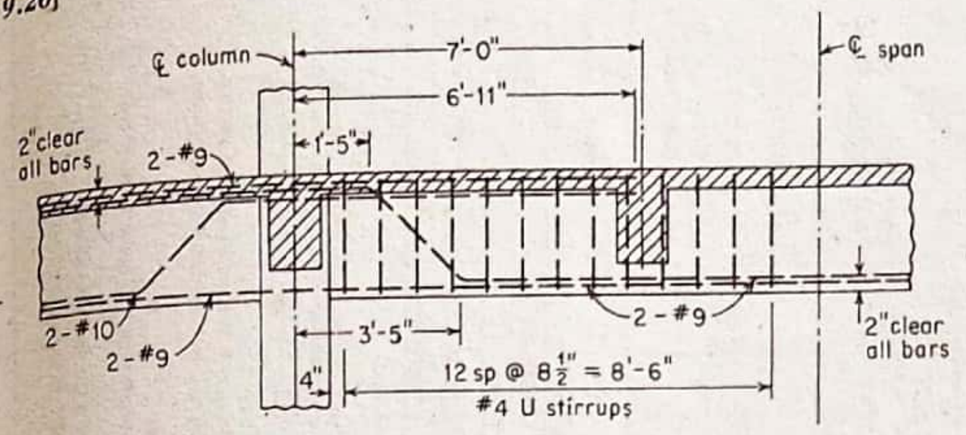


***Fig.* 9.16** Details of girder.

From Computation Sheets 9.4 and 9.5, the positive steel-area requirement for $G1$ of 4.10 in.² will be provided by two No. 9 straight bars and two No. 10 bent bars ($A_s = 4.53$ in.²). At the wall end of $G1$, the requirement of 3.83 in.² is closely met by adding one No. 10 straight bar to the two No. 10 bent bars ($A_s = 3.79$ in.²). In girder $G2$, the positive requirement of 3.56 in.² calls for two No. 9 straight bars and two No. 9 bent bars ($A_s = 4.00$ in.²). At the first interior support, adding two No. 9 straight bars to the two No. 10 and two No. 9 bent bars provides an area of 6.53 in.², very close to the required 6.45 in.² At the typical interior supports, two No. 9 straight bars are added to the two No. 9 bent bars from each adjacent span, providing 6.00 in.², slightly in excess of the required 5.77 in.²

The points at which the bars may be bent up are determined by assuming that the positive moment is zero at a distance of $\frac{2}{3}L/3$ from the concentrated load to the center line of the support, measured toward the support, and that the moment diagram is a straight line between the maximum and zero values. The latter assumption is in error only because of the uniformly distributed weight of the girder; this is very small in comparison with the large concentrated loads. The two No. 9 bars in $G2$ may be bent up at a distance of

$$\tfrac{1}{2} \times \tfrac{2}{3} \times \frac{21 \times 12}{3} = 28 \text{ in.}$$

to the left of the first concentrated load.

A similar assumption for the negative-moment variation can be made; the point of zero negative moment is, therefore, $\frac{2}{3}L/3$ from the center line of the support. The overlapping of the positive and negative moment diagrams which results from these assumptions provides for any variation in the moments that might result from unequal placing of the live load on adjoining spans. The two No. 9 bars at the first interior support of $G2$

Scanned with CamScanner

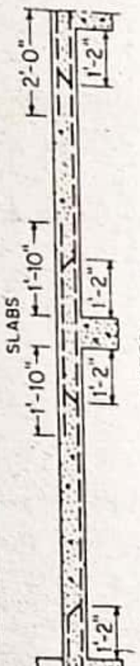
BEAM AND GIRDER SCHEDULE

Mark	Size		Reinforcing					
			Longitudinal			Stirrups		
	b'	d	No. Size	Remarks		No. Size	Spacing from face of support	
B-1	12	22½	2 – #7	Bot.		21 – #3	1@5", 8@10"	wall end
			2 – #7	Bent			1@4", 4@8", 7@10"	cont. end
			1 – #5	Top – Wall end				
			2 – #7	Top – First interior support				
B-2	12	22½	2 – #6	Bot.		18 – #3	1@5", 8@10"	each end
			2 – #6	Bent				
			2 – #7	Top – Typical interior supports				
G-1	18	29	2 – #9	Bot.		31 – #4	1@3", 16@6½"	cont. end
			2 – #10	Bent			1@4", 13@8½"	wall end
			1 – #10	Top – Wall end				
			2 – #9	Top – First interior support				
G-2	18	29	2 – #9	Bot.		26 – #4	1@4", 12@8½"	each end
			2 – #9	Bent				
			2 – #9	Top – Typical interior supports				

SLAB SCHEDULE

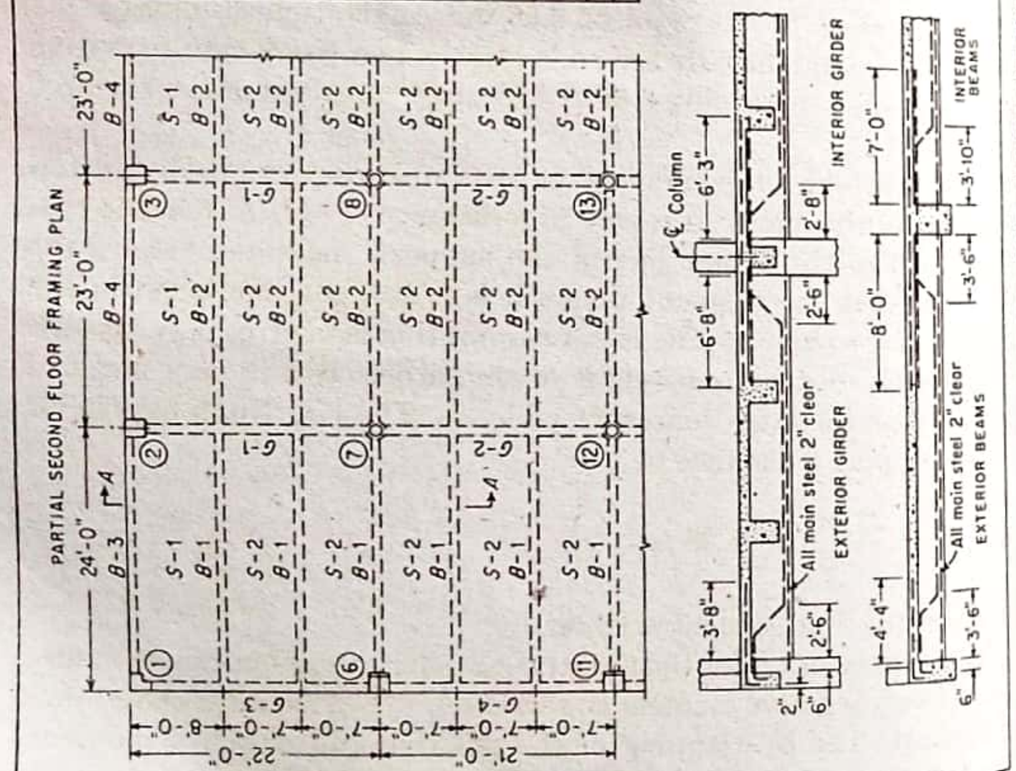
Mark	Depth	Reinforcing		Remarks
		Main steel	Temp. steel	
S-1	4"	#3@7"	#3@13"	Alternate straight and bent.
S-2	4	#3@7"	#3@13"	Alternate straight and bent.

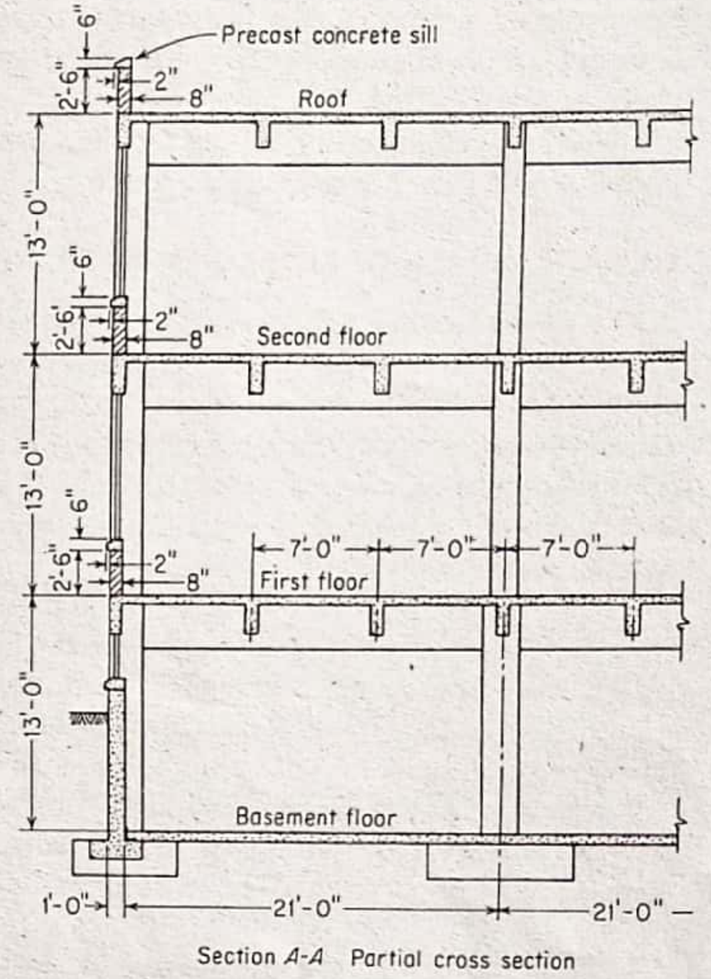
SLABS



NOTES:

1. All concrete to have 3000 pounds per square inch compressive strength in 28 days.
2. Reinforcing steel shall have $f_y = 40{,}000$ psi, with deformation conforming to A.S.T.M. – A305.
3. Bends to be made as shown on diagrams.
4. Place main reinforcing steel so that bottom of steel is 2" above forms in beams and girders and ¾" in slabs.
5. Provide bar supports in accordance with A.C.I. Detailing Manual.
6. Stirrups to have 2 – #3 spacers for length of stirrup spacing





Section *A-A* Partial cross section

Fig. 9.18

may be bent down at a distance of

$$\frac{2.00}{6.53}\,2\,3\,\frac{21 \times 12}{3} = 17 \text{ in.}$$

from the support. Actual bend points are located to satisfy these requirements and are shown in Fig. 9.16. The remaining top bars are carried a distance d past the extreme position of the point of inflection and are cut off

$$\frac{2}{3}\,\frac{21 \times 12}{3} + 26.5 = 83 \text{ in.}$$

from the support as shown. A check of development length for all bars (Table 8, Appendix B) indicates that flexural bond stresses need not be checked.

Vertical No. 4 U stirrups are provided to accommodate all the diagonal tensile stresses, in neglect of the contribution of the bent bars. With reference to the shear diagrams of Computation Sheet 9.5, the excess shear is very nearly constant from the support face to the center line of the con-

Scanned with CamScanner

centrated load. In each case, the spacing required at the critical sectio[n] distance d from the support face is used through the entire region in w[hich] stirrups are required.

Complete engineering details for the portion of the building desig[n] above are shown in Figs. 9.17 and 9.18.

DESIGN OF A RIBBED FLOOR WITH STEEL PAN FORMS

9.27 Dead Loads The weight of a ribbed floor can be computed f[rom] the known concrete dimensions. The general form of the cross sectio[n] the steel tiles must be known, since the taper of the sides and the chan[ge] ing of the upper corners affect the volume of concrete in the ribs or j[oists] The cross section can be obtained from the manufacturers' catalo[gs] The average values in Table 9.2 can be used for joists (or ribs) 5 in. [wide] at the bottom and 25 in. on centers.

The values given in this table do not include the weight of an e[nd] floor finish or a plastered ceiling below the floor. The former can be co[m]puted from the specified thickness of finish or type of floor surface. [In] computing design loads, an allowance of 10 psf is usually made f[or] plastered ceiling. An additional allowance of from 10 to 20 psf is made [for] the weight of partitions not definitely located on the architect's plans [in] where there is a possibility of future rearrangement of partitions. [The] latter condition is very likely to occur in buildings of the types to w[hich]

Table 9.2 **Weight of concrete in ribbed floors with steel pan fillers**

Depth of joist below slab, in.	Thickness of slab, in.	Average weight of floor, psf
6	2	42
	2½	48
8	2	48
	2½	54
10	2	55
	2½	61
12	2	61
	2½	67
	3	73
14	2	69
	2½	75
	3	81

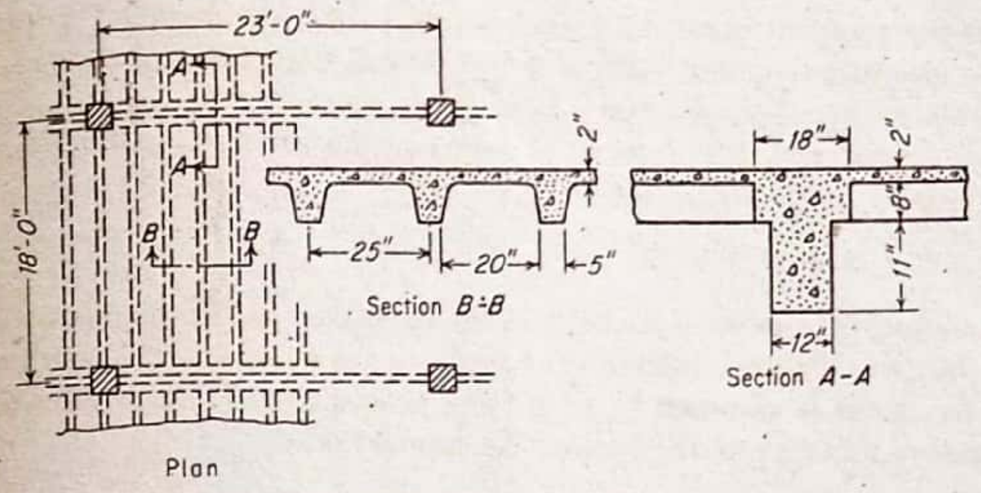


Fig. 9.19 Details of ribbed floor with removable steel pans.

ribbed-floor construction is adapted. When definitely located partitions are parallel with the joists, a joist thicker than the normal 5 in. is usually placed under these partitions, or, if the partition is located between two joists, both these joints are made thicker than the others, and the slab thickness between them is increased. The increased slab thickness is obtained by using shallower pans in the one row, or by lowering the pans in that row. When definitely located partitions are perpendicular to the joists, the partition weight is considered as a concentrated load in designing the joists. Transverse bridging ribs 4 in. wide and the same depth as the joists are commonly used at the center of span of less than 24 ft and at the third points of a longer span to stiffen the joists and distribute concentrated floor loads to adjacent joists.

9.28 Data for Design A typical interior panel of a hotel floor is to be built as a ribbed floor, using removable steel pan forms. The joists are to be supported at the ends on concrete girders, as shown in Fig. 9.19. The span of the girders is 23 ft 0 in., and the distance center to center of girders is 18 ft 0 in. The live load is 50 psf, and allowances for dead loads other than the weight of the concrete are to be made as follows: partitions, 10 psf; plastered ceiling, 10 psf; wood floor, with sleepers in cinder-concrete fill, 15 psf. A 4000-psi concrete is to be used in the floor, with bars for which $f_y = 60{,}000$ psi. It is required to design the panel.

9.29 Design of Joists: ***Computation of moments and shears*** The joists are designed as regular continuous T beams, with a flange width equal to the distance center to center of joists. In order to compute the weight of the floor, the depth of the joists below the slab and the thickness of the slab must be assumed. A combination of 8-in. joists and 2-in. slab will be tried. The weight of the concrete per square foot of floor is 48 psf,

Scanned with CamScanner

and the total ultimate dead load is $(20 + 10 + 15 + 48)1.5 = 140$ psf. The ultimate live load is $50 \times 1.8 = 90$ psf, and the total ultimate load is $140 + 90 = 230$ psf. With 5-in. joists spaced 25 in. on centers, each joist supports $^{25}/_{12} = 2.08$ ft² of floor per foot of joist, and the total ultimate load on each joist is

$$230 \times 2.08 = 478 \text{ plf}$$

The panel is fully continuous, and the effective span for moment is equal to the clear distance between the stems of the girders. If the width of the girder stems is assumed as 12 in., the joist span is 17 ft. The maximum negative moment at the face of the support is

$$M = {}^1/_{11} \times 478 \times 17^2 \times 12 = 151{,}000 \text{ in.-lb}$$

and the maximum positive moment at the center of the span is

$$M = {}^1/_{16} \times 478 \times 17^2 \times 12 = 104{,}000 \text{ in.-lb}$$

The shear at the face of the supporting girder is

$$V_u = 478 \times {}^{17}/_2 = 4070 \text{ lb}$$

Design for shear It is rather difficult to place stirrups in narrow joists, such as are used in this form of construction; hence the shearing unit stress should be kept below the value permitted on the concrete web. Taking this as $v_c = 2\phi\sqrt{f'_c}$, one obtains

$$v_u = 2 \times 0.85\sqrt{4000} = 108 \text{ psi}$$

The effective shearing width of a joist is taken as the width at the bottom of the joist; the increased section due to the side slope of the pans is neglected. If necessary, tapered pans can be used at the ends of each row to increase the shearing area, or deeper joists can be used to serve the same purpose. At the critical section for shear, a distance d (estimated as 8 in.) from the face of supports, the ultimate shear is

$$V_u = 4070 - 478 \times {}^8/_{12} = 3750 \text{ lb}$$

The minimum web area is

$$b'd = \frac{V_u}{v_u} = \frac{3750}{108} = 34.7 \text{ in.}^2$$

If straight end pans are used, with $b' = 5$ in., the minimum effective depth is 6.95 in. With 8-in. joists under a 2-in. slab, the effective depth is $10 - 1{}^1/_8 = 8.87$ in. This will be satisfactory and will allow for a minimum clear insulation under the bars of about $^3/_4$ in.

If the problem of deciding whether to use tapered end pans or deeper pans throughout arises, it should be remembered that the steel area required decreases with an increase in the depth of the joists, and both the cost of the steel and the cost of the concrete should be considered. The cost of the forms can be omitted from the comparison, because this cost does not vary materially.

Computation of steel area At the face of the girder stem, the negative joist moment is 151,000 in.-lb. Then

$$\frac{M_u}{\phi b'd^2} = \frac{151{,}000}{0.9 \times 5 \times 8.87^2} = 427$$

From Graph 1, Appendix B, $p = 0.0076$. Then

$$A_s = pb'd = 0.0076 \times 5 \times 8.87 = 0.33 \text{ in.}^2$$

At midspan, assuming a stress-block depth equal to the slab thickness,

$$\text{Trial } A_s = \frac{M_u}{\phi f_y(d - t/2)} = \frac{104{,}000}{0.9 \times 60{,}000 \times 7.87} = 0.25 \text{ in.}^2$$

The corresponding stress-block depth is

$$a = A_s f_y / 0.85 f'_c b = 0.25 \times 60/(0.85 \times 4 \times 25) = 0.177 \text{ in.}$$

The revised lever arm is 8.78 in., and

$$A_s = 0.25 \times 7.87/8.78 = 0.22 \text{ in.}^2$$

Arrangement of reinforcement As shown in Fig. 9.20, two No. 3 bars ($A_s = 0.22$ in.²) will be used for positive-moment reinforcement. Bending up one bar in each span and adding one No. 3 straight top bar will provide sufficient steel ($A_s = 0.33$ in.²) to meet the negative-moment requirements. In accordance with Graph 11, Appendix B, the positive steel will be bent up at 3.50 ft from the support face and, together with the added straight bars, will be continued a distance of 5.14 ft beyond the

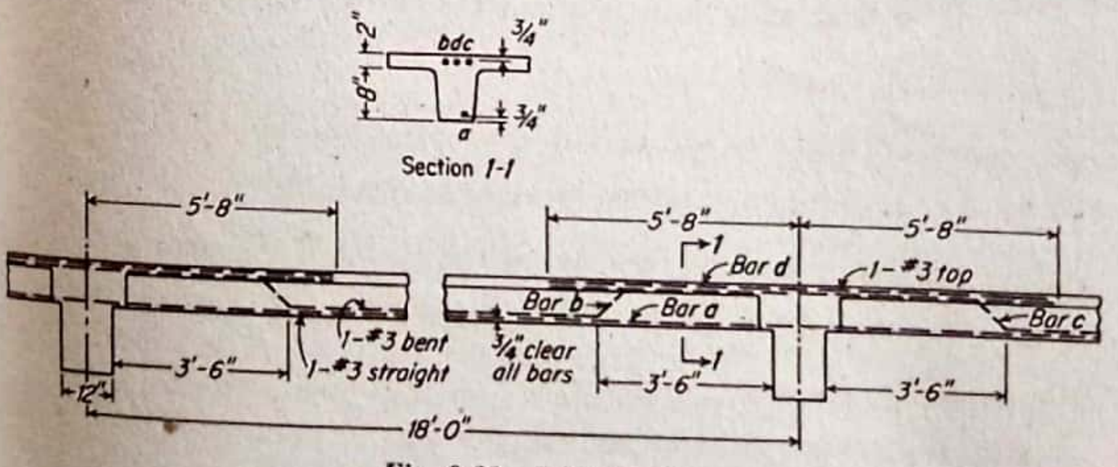


Fig. 9.20 Joist details.

Scanned with CamScanner

far face of the supports. The remaining positive steel will be carried 6 in. into the face of supports. From Table 8, Appendix B, it is evident that adequate development length is provided for both top and bottom steel so that it is unnecessary to check flexural bond stresses.

9.30 Design of Girder: ***Computation of loads*** The loads which are brought to the girder from the joists are theoretically concentrated at the points at which the joists frame into the girder. They are spaced so closely, however, that they may be considered as uniformly distributed throughout the length of the girder without materially affecting the maximum moment in the girder. Each pair of adjoining joists, one on either side of the girder, transmits a load to the girder equal to twice the end shear of one joist, or $2 \times 4070 = 8140$ lb. Since the joists are 25 in., or 2.08 ft, on centers, the uniform load per foot of girder is $8140/2.08 = 3910$ plf. To this must be added the weight of the girder and the floor and ceiling loads directly over and under the girder. With total girder depth assumed to be 22 in., and width 12 in., the weight of the girder is

$$12 \times 22 \times {}^{150}\!/_{144} = 276 \text{ plf}$$

The weights of partitions, ceiling, and fill over the 12-in. girder width add 45 plf. The ultimate dead load is then

$$(276 + 45)1.5 = 480 \text{ plf}$$

The additional ultimate live load directly over the girder is

$$50 \times 1.8 = 90 \text{ plf}$$

and the total ultimate load is

$$3910 + 480 + 90 = 4480 \text{ plf}$$

Computation of moment and shear The girder is continuous at both ends, so that with 18-in. columns the effective span is

$$23 - {}^{18}\!/_{12} = 21.5 \text{ ft}$$

The maximum negative moment at the face of the support is

$$M = {}^{1}\!/_{11} \times 4480 \times 21.5^2 \times 12 = 2{,}260{,}000 \text{ in.-lb}$$

and the maximum positive moment at the center of the span is

$$M = {}^{1}\!/_{16} \times 4480 \times 21.5^2 \times 12 = 1{,}560{,}000 \text{ in.-lb}$$

The maximum shear is

$$V = 4480 \times 21.5/2 = 48{,}200 \text{ lb}$$

Design at supports A maximum steel ratio of

$$0.18\frac{f'_c}{f_y} = 0.18 \times \frac{4}{60} = 0.012$$

will be adopted. Then, from Graph 1,

$$\frac{M_u}{\phi bd^2} = 643$$

from which

$$bd^2 = \frac{M_u}{643\phi} = \frac{2{,}260{,}000}{643 \times 0.9} = 3900 \text{ in.}^3$$

For a girder width of 12 in., the required effective depth is 18.0 in. An effective depth of 18.5 in. will be used, providing an overall girder depth of 21 in. No revision in the assumed dead load is required. The total tension steel required is

$$A_s = 0.012 \times 12 \times 18.0 = 2.59 \text{ in.}^2$$

Design at center The girder is a T beam, but because of the comparatively thick flange, the neutral axis will probably be in the flange, and the girder can be designed for moment as a rectangular beam with a width equal to the width of the flange. Accordingly,

$$\frac{M_u}{\phi bd^2} = \frac{1{,}560{,}000}{0.9 \times 18 \times 18.5^2} = 281$$

From Graph 1, $p = 0.0048$, and

$$A_s = 0.0048 \times 18 \times 18.5 = 1.60 \text{ in.}^2$$

Checking the location of the neutral axis,

$$a = \frac{1.60 \times 60}{0.85 \times 4 \times 18} = 1.57 \text{ in.}$$

well within the depth of the flange as assumed.

The positive-moment requirement of 1.60 in.^{2} will be provided using two No. 6 and one No. 8 bars ($A_s = 1.67$ in.^{2}). The single No. 8 bar will be bent up 4.00 ft from the face of the column, in accordance with Graph 11. At the support, the required area of 2.59 in.^{2} will be provided by adding a single No. 10 straight bar to the two bent-up No. 8 bars ($A_s = 2.84$ in.^{2}). The bent-up bars and the straight bar will be continued 6.75 ft beyond the face of the column.

Adequate development length is provided for all top and bottom bars, so that it is unnecessary to check flexural bond stresses in the girder.

Scanned with CamScanner

[Art. 9.31

Design of web reinforcement Resistance to diagonal tension will be provided using vertical stirrups, in neglect of the contribution of the bent No. 8 bars. The computations are the same as for any uniformly loaded, continuous beam; a typical example is given in Art. 9.25.

9.31 Detail Drawings Each floor plan must show the number of ribs, or joists, in each panel, the number of rows of pans, and the arrangement of the joists. All identical joists are given the same mark, which consists of a numeral indicating the floor, the letter R or J indicating ribs or joists, and a final numeral which is the mark of identity. Thus, $1R22$ would designate first-floor joist No. 22. The outlines of the rows of pans are shown by dotted lines. Where there are several adjacent identical rows forming identical joists, only the end rows and joists in the group are shown, and the numbers of rows and joists are placed on dimension lines with arrows pointing to the boundaries of the group. The depth of the stems of the joists and the thickness of the slab are also given on the floor plan. Temperature steel, usually about No. 2 bars at 10 in. on centers, is placed in the slab at right angles to the joists; this is detailed on the plan in the usual manner. Quite often welded wire mesh is used to reinforce the slab.

A detail floor plan for the typical interior panel which was designed in the preceding articles is shown in Fig. 9.21. The girders are marked on the plan in the usual manner. At least one typical cross section through the joists and through the girders should be given on the drawing. The joists $1R16$ between the columns of Fig. 9.21 are 7 in. wide at the bottom instead of 5 in., in order to fill up the panel. It is usually desirable to have a joist such as $1R16$ between the columns, in order to stiffen the columns in this direction. In tall structures subject to wind pressure, a deeper beam would be used in place of the joist $1R16$ to add to the rigidity of the entire structure.

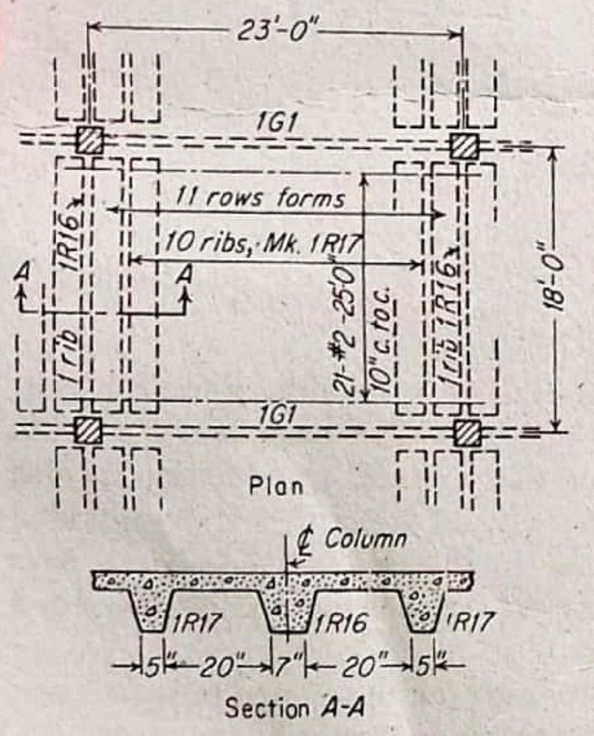


***Fig.* 9.21** Method of detailing ribbed floors with concrete girders.

DESIGN OF A FLAT-SLAB BUILDING

9.32 Data and Specifications The method of design of flat-slab floors and other details involved in a

reinforced-concrete building are illustrated in the following articles, which contain the complete design of a building 66 by 105 ft in plan, consisting of two upper stories and a basement. The height of the upper stories, floor to floor, is 12 ft 0 in., and that of the basement is 10 ft 0 in. The floor plan is shown in Fig. 9.33. The live load to be supported by the floors is 200 psf, and by the roof 40 psf. An additional load of 40 psf is to be considered in the dead weight of the roof, to provide for a cinder-concrete fill and for the roof covering. Adequate drainage will be provided by inclining the exterior slabs in the short direction of the building and by varying the thickness of the surfacing over the middle panel. A 3000-psi concrete will be used for all the construction. The ACI Code will be used in the design of the floor and roof slabs, beams, columns, and footings. Steel of 40,000-psi strength will be used, at a working stress of 20,000 psi.

9.33 Design of Interior Floor Panel: ***Slab*** The thickness of the slab exclusive of the drop panel is

$$t_2 = 0.024 \times 22\left(1 - \frac{2 \times 4.5}{3 \times 22}\right)\sqrt{\frac{300}{3000/2000}} + 1 = 7.33 \text{ in.}$$

A thickness of 8 in. will be tentatively adopted.

Capital Metal cap forms will be used, standard diameters being multiples of 6 in. A diameter c of cap of approximately 0.20 times the average span of the panel will be used.

$$0.20 \times 21.5 \times 12 = 51.6 \text{ in.}$$

Use 4 ft 6 in.

Drop The length of each side of the drop panel will be made approximately equal to 0.33 times the longer span.

$$0.33 \times 22 \times 12 = 87 \text{ in.}$$
$$0.33 \times 21 \times 12 = 83 \text{ in.}$$

A drop 7 ft 6 in. by 7 ft 6 in. will be used.

The thickness of the drop panel will be made 4 in., which is the maximum thickness that can be used in determining the required amount of negative reinforcement in the column strip.

Shearing stresses Article 2102(*c*)2, Appendix A. The unit shearing stress ($v = V/b_0 d$) on a vertical section a distance $d/2$ from the edge of the capital, and concentric with it, shall not exceed $2\sqrt{f'_c} = 110$ psi.

$$\frac{d}{2} = \frac{10.5}{2} = 5.25 \text{ in.} = 0.437 \text{ ft}$$

$$4.50 + 2 \times 0.437 = 5.38 \text{ ft}$$

Scanned with CamScanner

The total load on the panel is

$$300 \times 21 \times 22 + 4/12 \times 150(7.50)^2 = 141{,}300 \text{ lb}$$

At the section described above,

$$V = 141{,}300 - 350\frac{\pi \times 5.38^2}{4} = 133{,}400$$

$$v = \frac{133{,}400}{(\pi \times 5.38 \times 12) \times 10.5} = 62 \text{ psi} < 110 \text{ psi}$$

The unit shearing stress on a vertical section a distance $d/2$ from the edge of the drop panel and parallel with it shall not exceed 110 psi.

$$\frac{d}{2} = \frac{6.5}{2} = 3.25 \text{ in.} = 0.27 \text{ ft}$$

$$750 + 2 \times 0.27 = 8.04 \text{ ft}$$

$$V = (21 \times 22 - 8.04^2)300 = 119{,}000 \text{ lb}$$

$$v = \frac{119{,}000}{(4 \times 8.04 \times 12) \times 6.5} = 48 \text{ psi} < 110 \text{ psi}$$

In checking the unit shearing stress in the slab acting as a wide beam [ACI Code, Art. 1207(*a*)1], the presence of the drop panel over a portion of the width is neglected. The load per foot of slab in the 22-ft span direction is $300 \times 21 = 6300$ plf, and the column reaction is $6300 \times 22/2 = 69{,}300$ lb. At a distance d past the column capital (2.80 ft from the column center line) the shear is

$$69{,}300 - 6300 \times 2.80 = 51{,}600 \text{ lb}$$

and the unit shear is

$$v = \frac{51{,}600}{21 \times 12 \times 6.5} = 32 \text{ psi}$$

The allowable shear stress at this section [Art. 1201(*c*)] is

$$1.1\sqrt{3000} = 61 \text{ psi} > 32 \text{ psi}$$

The assumed dimensions of the capital and drop need no revision.

Bending moments Table 2104(*f*). Since the panel is nearly square, moments and steel areas will be computed for the long direction, and the same steel will be placed in the short direction.

$W = 141{,}300$ lb $\quad l = 22.0$ ft $\quad c = 4.5$ ft

$$M_0 = 0.09WLF\left(1 - \frac{2c}{3L}\right)^2 = 0.09 \times 141{,}300 \times 22.0\left(1 - \frac{2 \times 4.5}{3 \times 22.0}\right)^2$$

$$= 209{,}000 \text{ ft-lb} = 2{,}510{,}000 \text{ in.-lb}$$

Column strip, positive moment: $M = +0.20 \times 2{,}510{,}000 = +502{,}000$ in.-lb

Column strip, negative moment: $M = -0.50 \times 2{,}510{,}000 = -1{,}256{,}000$ in.-lb

Middle strip, positive moment: $M = +0.15 \times 2{,}510{,}000 = +376{,}000$ in.-lb

Middle strip, negative moment: $M = -0.15 \times 2{,}510{,}000 = -376{,}000$ in.-lb

Steel areas In computing steel areas required for those moment sections in which bars are placed in two directions (i.e., the positive-moment section of the middle strip and the negative-moment section of the column strip), the governing row will be assumed as that row farthest from the tension face of the slab. This removes all restrictions as to the order of placing the steel in the two directions. Values of j are obtained from Table 5, Appendix B: $f_s = 20{,}000$; $f_c = 0.45 \times 3000 = 1350$ psi; $n = 9$.

COLUMN-STRIP, POSITIVE-MOMENT SECTION. For No. 5 bars and ¾-in. clear insulation, $d = 8 - 1\frac{1}{16} = 6\frac{15}{16}$ in.

$$A_s = \frac{502{,}000}{20{,}000 \times 0.874 \times 6.93} = 4.16 \text{ in.}^2$$

Fourteen No. 5 bars furnish 4.30 in.²

COLUMN-STRIP, NEGATIVE-MOMENT SECTION. For No. 5 bars and ¾-in. clear insulation, $d = 12 - 1\frac{11}{16} = 10\frac{5}{16}$ in.

$$A_s = \frac{1{,}256{,}000}{20{,}000 \times 0.874 \times 10.31} = 6.96 \text{ in.}^2$$

Twenty-three No. 5 bars furnish 7.06 in.²

Nine bars, or slightly less than two-thirds of the total required for positive moment, will be bent up to provide resistance to negative moment. Hence at each negative-moment section a total of 18 bars is furnished from the two adjacent positive areas. Five straight bars in the top of the slab over the column head are sufficient to complete the steel area required at the negative-moment section (see Fig. 9.22).

Scanned with CamScanner

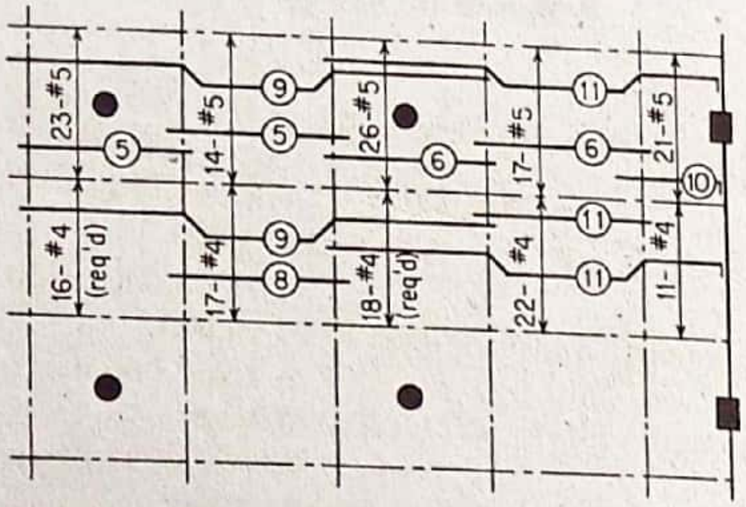


Fig. **9.22** Arrangement of reinforcement in floor slab.

MIDDLE-STRIP, POSITIVE-MOMENT SECTION. For No. 4 bars and ¾-in. clear insulation, $d = 8 - 1\frac{1}{2} = 6\frac{1}{2}$ in.

$$A_s = \frac{376{,}000}{20{,}000 \times 0.874 \times 6.5} = 3.31 \text{ in.}^2$$

Seventeen No. 4 bars furnish 3.33 in.²

MIDDLE-STRIP, NEGATIVE-MOMENT SECTION. For No. 4 bars and ¾-in. clear insulation, $d = 8 - 1 = 7$ in.

$$A_s = \frac{376{,}000}{20{,}000 \times 0.874 \times 7} = 3.08 \text{ in.}^2$$

According to Table 2104(*g*)2, Appendix A, not less than five-tenths of the steel required in the positive-moment section of the middle strip should be bent up at both ends so as to reinforce the two adjacent negative-moment sections. Bending 9 of the 17 bars required in the positive-moment section provides a total of 18 bars in each negative-moment section, which is more than ample in the present case.

Fiber stress in the concrete The critical section is in the negative-moment portion of the column strip. According to Art. 2102(*c*)1, Appendix A, the effective width of the column head section, for compression, shall be taken as three-fourths the width of the dropped panel, 67.5 in.

$$p = \frac{7.06}{67.5 \times 10.31} = 0.0102$$

From Table 5, Appendix B, $k = 0.347$ and $j = 0.885$.

$$f_c = \frac{2 \times 1{,}256{,}000}{0.347 \times 0.885 \times 67.5 \times 10.31^2} = 1140 \text{ psi}$$

The allowable stress is $0.45 \times 3000 = 1350$ psi.

9.34 Design of Exterior Floor Panel From Table 2104(*f*), Appendix A, the following percentages of the interior panel moments are to be used in the exterior panel:

Column-strip negative moment at wall or spandrel: 88
Column-strip negative moment at first row of columns: 112
Column-strip positive moment: 120
Middle-strip negative moment at wall or spandrel: 67
Middle-strip negative moment at first row of columns: 113
Middle-strip positive moment: 133

Hence, the steel areas required at the various sections in the exterior panel (for bands perpendicular to the wall) may be obtained by multiplying the corresponding interior-panel required areas by the above percentages, as follows:

Middle-strip, positive-moment section:

$A_s = 1.33 \times 3.31 = 4.40$ in.²
Twenty-two No. 4 bars furnish 4.32 in.²

Middle-strip, negative-moment section at wall:

$A_s = 0.67 \times 3.08 = 2.06$ in.²
Eleven No. 4 bars furnish 2.16 in.²

Middle-strip, negative-moment section at first interior support:

$A_s = 1.13 \times 3.08 = 3.48$ in.²
Eighteen No. 4 bars furnish 3.54 in.²

Column-strip, positive-moment section:

$A_s = 1.20 \times 4.16 = 5.00$ in.²
Seventeen No. 5 bars furnish 5.22 in.²

Column-strip, negative-moment section at wall:

$A_s = 0.88 \times 6.96 = 6.14$ in.²
Twenty-one No. 5 bars furnish 6.45 in.²

Column strip, negative-moment section at first interior support:

$A_s = 1.13 \times 6.96 = 7.86$ in.²
Twenty-six No. 5 bars furnish 7.98 in.²

9.35 Arrangement of Reinforcement The proposed method of placing and bending the steel so as to furnish the necessary areas at the various sections in both the interior and exterior panels is shown diagrammatically in Fig. 9.22. The points at which the bars are bent are obtained

Scanned with CamScanner

from Fig. 2104(*g*), Appendix A. The minimum spacing is governed by the necessity of allowing space for the concrete to be deposited conveniently and effectively. A minimum spacing of about 3 in. center to center of bars should be maintained if possible. Bars less than ½ in. in diameter are difficult to handle because of their lack of stiffness, and bars greater than ¾ in. in diameter cannot be bent in place.

A complete engineering drawing for the floor slab is shown in Fig. 9.33. This drawing follows the recommendations in the American Concrete Institute "Manual of Standard Practice for Detailing Reinforced Concrete Structures" (ACI 315-57).

9.36 Design of Roof Slab The design of the interior and exterior panels of the roof slab is carried out in a manner similar to that used in the design of the floor slab. The total load on the roof includes the live load (40 psf), the weight of the roofing material (40 psf), and the dead weight of the slab itself. The thickness of slab beyond the drop is 6½ in., and the total thickness through the dropped panel is 10 in. The diameter of the capital is 4 ft 6 in., and the drop is 7 ft 6 in. square in plan.

The number of ½-in. round bars required in the various sections of the slab and the proposed method of placing and bending the bars so as to furnish the required steel areas at all sections are shown diagrammatically in Fig. 9.23. It has been assumed, for simplicity, that the stairway and elevator shaft openings do not extend through the roof.

9.37 Design of Interior Columns The interior columns are to be made of 3000 psi concrete, with reinforcement having $f_y = 40{,}000$ psi. They are to be round, with spirals, and designed in accordance with the ACI specifications. The fundamental principles involved in the design are explained in Chap. 5. In flat-slab construction the columns are an important factor in adding to the rigidity of the slab, and many codes specify a

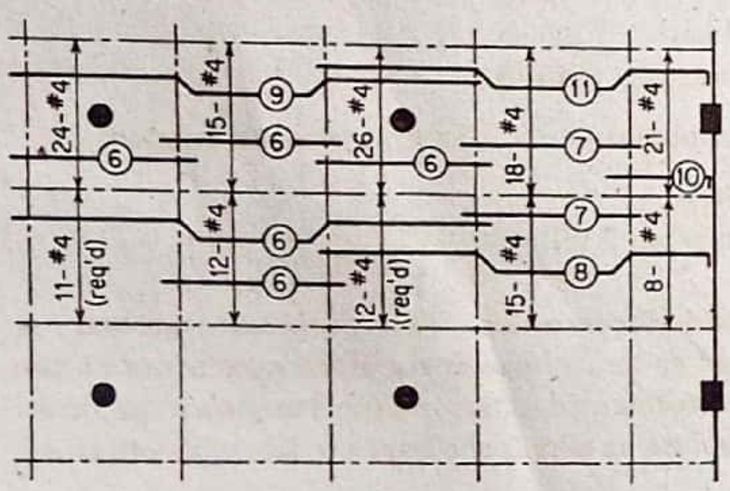


Fig. 9.23 Arrangement of reinforcement in roof slab.

Table 9.3 **Interior columns: design for direct load only**

Column	Load from	Amount of load, kips	Diameter and area of column	Vertical bars	Spirals (Table 10, Appendix B)	Load carried by concrete, kips	Load carried by steel, kips	Total load, kips
Top	Roof	76	16 in.	5-#6	No. 3-1¾ in.	136	35	171
	Column	2	201 in.²	2.21 in.²				
	Capital	2		$p_g = 0.0110$				
	Total	80						
Intermediate	Floor	141	20 in.	8-#6	No. 3-1¾ in.	212	56	264
	Column	3	314 in.²	3.53 in.²				
	Capital	2		$p_g = 0.0112$				
	Total	226						
Basement	Floor	141	24 in.	8-#7	No. 3-2 in.	305	76	381
	Column	4	452 in.²	4.81 in.²				
	Capital	2		$p_g = 0.0106$				
	Total	373						

minimum column size greater than the usual minimum for beam-and-girder floors. For columns supporting heavily loaded floors, a minimum overall dimension of one-fifteenth the average span of the panel is considered satisfactory. Roof columns may be somewhat lighter; one-eighteenth the average span is specified by some codes as a minimum diameter. In the present case $\frac{1}{15} \times 21.5 \times 12 = 17.2$, or 18 in., will be taken as the minimum size for floor columns, and 16 in. for columns supporting the roof.

According to the ACI Code, values of p_g may vary from 0.01 to 0.08 for columns with spirals, but values greater than 0.02 to 0.025 are normally inadvisable because of the crowding of the steel which occurs just above the floor line, where the bars are spliced by lapping. In general, greater overall economy is obtained by the use of the smaller values of p_g. Steel ratios approaching the maximum may be necessary, however, in heavily loaded columns, in order to keep the size of the columns within reasonable limits. In some cases architectural limitations may require a smaller column with the resulting greater steel ratio. Metal column forms, which are generally used for round columns, are available in multiples of 2 in., and column sizes should be selected accordingly.

Table 9.3 gives a summary of the loads (to the nearest thousand pounds) which are carried in each tier of columns. The excess strength of the top column cannot be avoided, since minimum-size columns and the minimum percentage of reinforcement have been used. The excess strength of the intermediate column is required to provide for bending stresses, as shown by the investigation in Art. 9.48.

Scanned with CamScanner

[Art. 9.38

9.38 Investigation for Bending Stresses Bending stresses due to unequally loaded panels are not apt to affect the design of the interior columns, except possibly in the upper tiers. This is because the bending is usually caused by the live load only, and thus the maximum unit stress due to bending is in most cases less than the allowable *increase* in fiber stress as compared with the stress permitted when no bending is considered.

The method of investigation of bending of columns is explained in Chap. 5. With unequally loaded panels the amount of bending moment transferred to the columns depends upon the relative stiffness of the slab on both sides of the column and the columns themselves. The ACI Code [Art. 2104(*b*)2, Appendix A] states that a bending moment[1] of $\frac{1}{40}W_L L$ shall be distributed without further reduction between the columns above and below the floor or roof line under consideration in direct proportion to their stiffness, where W_L is the total live load on one panel, and L the span of the panel.

The maximum combined stress occurs only when the panels at the floor line under consideration are unequally loaded, with a full live load on alternate panels and no load on the remaining panels. A full live load is assumed on all floors above the one considered. In the investigation for the combined stress at the top of any column, the total direct load is equal to the load in Table 9.3 (the full load) minus the weight of the column and minus one-half a live panel load.

Table 9.4 contains a summary of computations which are necessary to determine the adequacy of the interior columns.

For the roof,

$$M = \tfrac{1}{40} \times 40 \times 21 \times 22 \times 21.5 \times 12 = 119{,}000 \text{ in.-lb}$$

[1] The recommended moment of $\frac{1}{40}W_L L$ is based on the following analysis: Due to live load only, the negative moment in a column strip, for two-way slabs with drops and with $c = 0.225L$ (a representative value), is $0.0325W_L L$. This unbalanced moment (assuming live load to be placed only on one side of the columns under consideration) is resisted by the slab on the unloaded side and the columns above and below the floor, more or less in direct proportion to the stiffness factors (I/h) of these members. Assuming that the stiffness factor of the slab is one-third the sum of the stiffness factors of the two columns, the moment to be resisted by the two columns is

$$\tfrac{3}{4} \times 0.0325W_L L = 0.0244W_L L$$

or approximately $\frac{1}{40}W_L L$.

In the investigation of the exterior columns (see Art. 9.49), since there is no slab beyond the wall the entire negative moment in the column strip at the wall is resisted by the two columns. For $c = 0.225L$ this moment is $0.0325WL$, or approximately $\frac{1}{30}WL$. Here the full load (dead plus live) on the panel is used, because both the dead and live loads are unbalanced loads. The total moment of $\frac{1}{30}WL$ is distributed to the columns in direct proportion to the stiffness factors.

Table 9.4 **Interior columns: bending and axial load**

Column	Point	A_g, in.^{2}	N, kips	M, in.-kips	$\frac{e}{t}$	I_t, in.^{4}	F_a, psi	F_b, psi	f_a, psi	f_b, psi	$\frac{f_a}{F_a}$	$\frac{f_b}{F_b}$	Cols. 12 + 13
(1)	(2)	(3)	(4)	(5)	(6)	(7)	(8)	(9)	(10)	(11)	(12)	(13)	(14)
Top	Top	201	69	119	0.108	3787	1200	1350	343	252	0.286	0.187	0.473
	Bottom		80	173	0.135				398	366	0.332	0.270	0.602
Intermediate	Top	314	177	423	0.119	9534	1200	1350	564	449	0.366	0.332	0.689
	Bottom		226	167	0.037				720	175	0.600	0.130	0.730
Basement	Top	452	323	429	0.055	19,970	1120	1350		258	0.595	0.191	0.786
	Bottom		373	0					825	0	0.686	0	0.686

For the other floors,

$$M = \tfrac{1}{40} \times 200 \times 21 \times 22 \times 21.5 \times 12 = 596{,}000 \text{ in.-lb}$$

In the present case, the investigation for bending and direct stress shows that no revision of the original columns, as designed for direct load only, is necessary. It should be noted, however, that in the original selection, some excess strength was intentionally provided in the intermediate column. The amount there provided is shown to be sufficient for the bending. The design as shown in Tables 9.3 and 9.4 is therefore satisfactory.

9.39 Design of Exterior Columns The exterior columns are to be rectangular in section. In addition to the load from the floors, the exterior columns must support the weight of the walls enclosing the story next above. In estimating the weight of the enclosure walls, the wall beams and brick spandrels underneath the windows are assumed 12 in. thick, the spandrel 2 ft 6 in. deep, and the wall beam 2 ft 0 in. deep. The brick parapet wall at the roof is assumed 12 in. thick and 3 ft 6 in. deep. The weight of windows, including sash, is taken as 8 psf. The weight of the brick masonry is assumed as 120 pcf. The general arrangement of a typical wall panel is shown in Fig. 9.24.

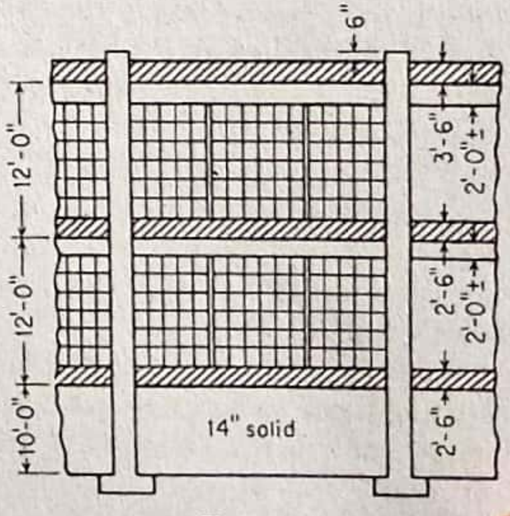


Fig. 9.24

Scanned with CamScanner

[*Art. 9.39*

Bending stresses should always be considered in the design of the exterior columns, especially in the upper tiers. The direct loads on these columns are comparatively small, and the bending moments due to unsymmetrical loading are large since live load and dead load act together in causing these moments. According to Code, the wall columns in flat-slab construction shall be designed to resist a bending moment from the slab of $\frac{1}{30}WL$, where W is the total load (dead and live) on one panel, and L is the average span of the panel. In the present design, at the first- and second-floor levels, $W = 141$ kips, $L = 21.5$ ft, and

$$M = \tfrac{1}{30}(141 \times 21.5 \times 12) = 1215 \text{ in.-kips}$$

At the roof level $W = 76$ kips, and

$$M = \tfrac{1}{30}(76 \times 21.5 \times 12) = 654 \text{ in.-kips}$$

Countermoments due to the weight of the structure that projects beyond the column center lines and countermoments due to the eccentricity of one column with respect to the column beneath may be deducted from the value of $\frac{1}{30}WL$, and the resulting reduced moment is then divided between the two columns immediately above and below a given floor line in proportion to the stiffness factors (I/h) of these columns.

Inasmuch as bending stresses constitute a large proportion of the total stresses in exterior columns, particularly in the upper tiers, it is of no use to design the columns first for direct load only. The general procedure is to assume column sizes and reinforcement, compute the combined extreme fiber stresses, including bending, and then revise the assumed sizes if necessary. Where the concrete is to be left exposed on the exterior face, the dimension along that face should be the same for all tiers of columns and of sufficient amount to give a satisfactory architectural appearance to the face. If this dimension is too small, the building will appear to be unstable or insecure. If it is too large, the building will appear squatty, and the design will be needlessly uneconomical. An elevation drawn to scale, as in Fig. 9.30, will show whether or not an assumed face dimension is satisfactory. Better architectural appearance is obtained by allowing the columns to project 2 in. or more beyond the face of the wall. In the present case, a column width of 22 in. is selected. The minimum required dimension of 18 in. for floor columns and 16 in. for roof columns (see Art. 9.37) will be maintained in the direction perpendicular to the wall. For axially loaded tied columns, steel ratios may vary from 0.01 to 0.04. For tied columns designed to withstand combined bending and axial stress, the steel ratio may vary from 0.01 to 0.08, provided that the amount of steel spliced by lapping shall not exceed a steel ratio of 0.04 in any 3-ft length of column. As stated before, the smaller ratios of reinforcement usually result in more economical designs. Where it is desirable to keep

Table 9.5 Exterior columns: computation of loads

Column	Load from	Amount of load, kips	Size of column, in.	Vertical steel	Load by concrete, kips	Load by steel, kips	Total load, kips
Top	Roof	38	22 × 16	6-#7	190	46	236
	Parapet*	14	$A_g = 352$ in.^{2}	$A_s = 3.61$ in.^{2}			
	Column†	6		$p_g = 0.01025$			
	Total	58					
Intermediate	Floor	71	22 × 18	6-#8	214	61	275
	Wall	12	$A_g = 396$ in.^{2}	$A_s = 4.71$ in.^{2}			
	Column	5		$p_g = 0.0119$			
	Total	146					
Basement	Floor	71	22 × 20	6-#8	238	60	298
	Wall	12	$A_g = 440$ in.^{2}	$A_s = 4.71$ in.^{2}			
	Column	4		$p_g = 0.0107$			
	Total	233					

* This value includes the weight of the stem of the wall beam.

† This value includes the weight of the column above the roof (see Fig. 9.24). The weight of the bracket in each tier has been neglected, since it varies only from about 300 lb for the basement column to 500 lb for the top column.

the column sizes small, larger percentages may be used. The column dimensions and steel areas ultimately selected for trial are shown in Table 9.5.

The countermoment at the top of the intermediate column is equal to the product of the wall load and the distance from the center of the wall beam to the center of the column, plus the moment due to column eccentricity, which is equal to the load on the top column multiplied by the distance between column centers. In the design under consideration, the wall beams are set back 2 in. from the faces of the columns, as shown in Fig. 9.25. At the top of the basement columns the countermoment due to column eccentricity is equal to the load on the intermediate column multiplied by the distance between the column centers, which is $\frac{1}{2}(20 - 18) = 1$ in. In this design the countermoment at the second-floor level is 70,000 in.-lb, and that at the first-floor level is 170,000 in.-lb.

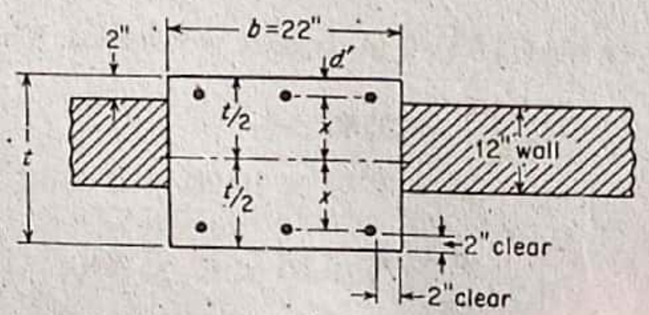


Fig. 9.25

Scanned with CamScanner

Table 9.6 **Exterior columns: bending and axial load** [Art. 9.40]

Column	Point	A_g, in.²	N, kips	M, in.-kips	$\frac{e}{t}$	It, in.⁴	F_a, psi	F_b, psi	f_a, psi	f_b, psi	$\frac{f_a}{F_a}$	$\frac{f_b}{F_b}$	Col. 12 + 13
(1)	(2)	(3)	(4)	(5)	(6)	(7)	(8)	(9)	(10)	(11)	(12)	(13)	(14)
Top	Top	352	54	656	0.759	9,342	1185	1350	*				
	Bottom		58	472†	0.491				*				
Intermediate	Top	396	141	673	0.270	14,052	1210	1350	*				
	Bottom		146	386	0.148				369	247	0.274	0.183	0.457
Basement	Top	440	229	659	0.143	19,164	1190	1350	520	342	0.436	0.254	0.690
	Bottom		233	0	0				530	0	0.445	0	0.445

* Tension governs. Analysis follows the methods of Chap. 5 and indicates the trial column sizes to be satisfactory.

† (Moment from slab) − (countermoment) = 1215 − 70 = 1145 in.-kips

$$\frac{66.4}{(66.4 + 94.6)} \times 1145 = 472 \text{ in.-kips}$$

Tables 9.5 and 9.6 contain a summary of the design. The complete column details are shown in Fig. 9.26.

9.40 Design of Interior-column Footings The interior-column footings are to be square and reinforced in two directions. The allowable soil pressure is 4000 psf.

The interior basement column is a 24-in. round column, with a total load of 373,000 lb. In the design of the footing the round column must be replaced with a square column of the same area. The equivalent square has a side dimension equal to

$$\sqrt{452} = 21.3 \text{ in.} = 1.78 \text{ ft}$$

The bearing area required is

$$(373{,}000 + 28{,}000)/4000 = 100 \text{ ft}^2$$

A base 10 ft 0 in. square is selected. The net upward pressure is

$$\frac{373{,}000}{100} = 3730 \text{ psf}$$

$$M = 3730 \times 10.00 \times 49.3/12 \times 24.6 = 3{,}780{,}000 \text{ in.-lb}$$

$$d = \sqrt{\frac{3{,}780{,}000}{10.00 \times 12 \times 223}} = 11.9 \text{ in.}$$

Assume that, for shear, an effective depth of 19 in. will be adequate.

According to Code, the critical section for shear, with the footing considered to be acting as a broad beam, is at a distance d from the face of the column, that is, $5.00 - (1.78/2 + 19/12) = 2.53$ ft from the edge of the footing. At that section the shear is

$$V = 3730 \times 10 \times 2.53 = 94{,}400 \text{ lb}$$

and the unit shear stress is

$$v = \frac{V}{bd} = \frac{94{,}400}{10 \times 12 \times 19} = 42 \text{ psi}$$

This is well below the allowable shear stress of $1.1\sqrt{3000} = 60$ psi at this section. Alternatively, the shear is computed on a perimeter a distance $d/2$ from the face of the column. The total shearing force is

$$V = 3730(100 - 3.36^2) = 331{,}000 \text{ lb}$$

and the unit shear stress is

$$v = \frac{V}{b_o d} = \frac{331{,}000}{4 \times 3.36 \times 12 \times 19} = 108 \text{ psi}$$

The allowable shearing stress at this section is $2\sqrt{3000} = 110$ psi. The assumed value of 19 in. may be considered satisfactory. The total thick-

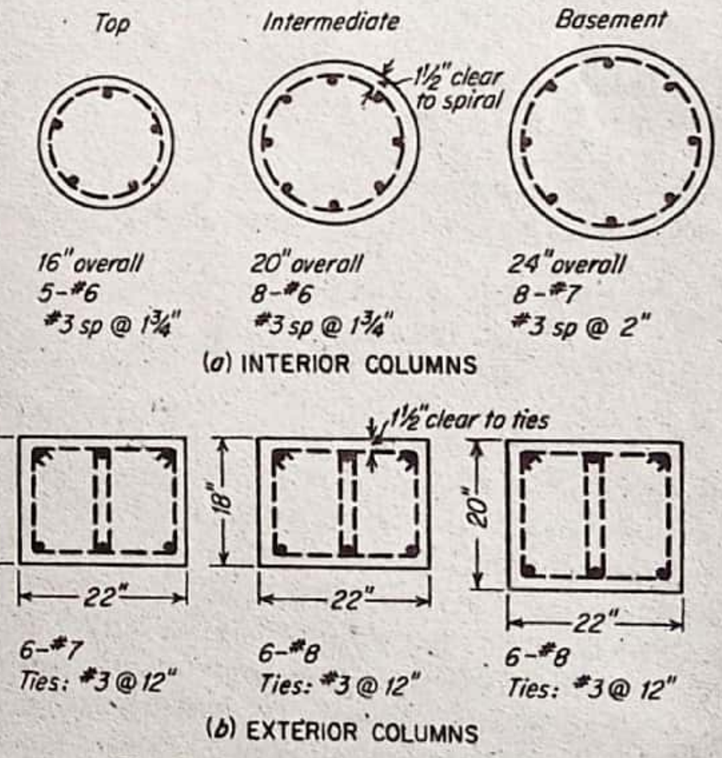


Fig. 9.26 Details of columns.

Scanned with CamScanner

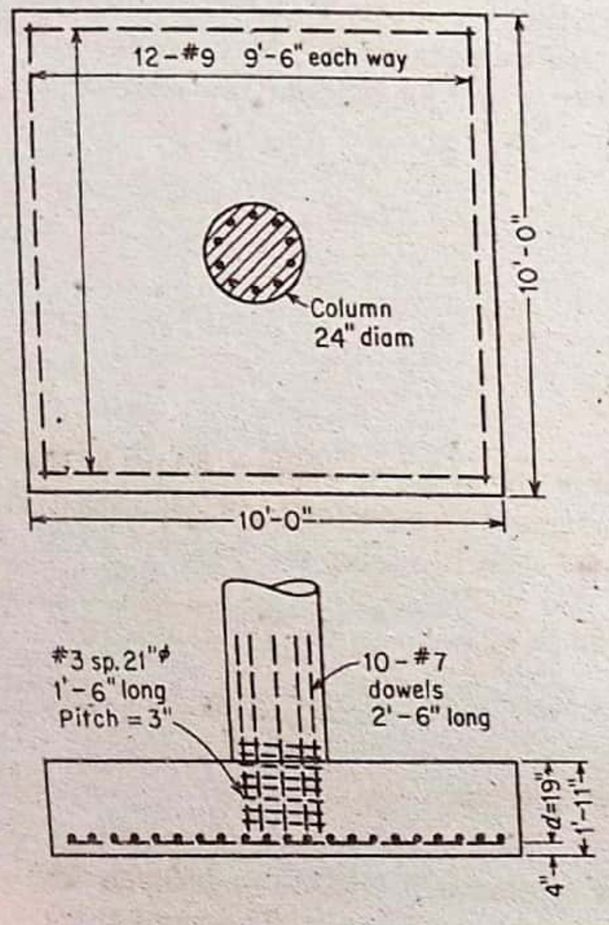


Fig. 9.27 Details of interior-column footing.

ness of the footing is then 23 in., and the weight is 28,800 lb, which agrees with the assumed weight.

$$A_s = \frac{3{,}780{,}000}{20{,}000 \times 0.9 \times 19} = 11.05 \text{ in.}^2$$

The allowable unit bond stress, using No. 9 bars, is 233 psi, and the maximum shear to be used in the equation for unit bond stress is

$$3730 \times 10.00 \times 4.11 = 153{,}000 \text{ lb}$$

$$\Sigma_0 \text{ (required)} = \frac{153{,}000}{233 \times 0.9 \times 19} = 38.4 \text{ in.}$$

Twelve No. 9 bars are selected; $A_s = 12.0$ in.^{2}, and $\Sigma_0 = 42.5$ in. The spacing of the bars is about 9½ in., which is satisfactory.

Ten No. 7 dowels will be placed in the footing. The dowels should extend into the columns 20 bar diameters or, for No. 7 bars, approximately 18 in. The embedment in the footing should be sufficient to develop the full working stress of 13,600 psi, or approximately 12.5 in. This length can be accommodated within the footing; therefore no pedestal is required. A total length of 30 in. will be used. The bearing stress, 373,000/452 = 82[illegible] psi, is less than the allowable value of 1125 psi. The complete details of the footing are shown in Fig. 9.27.

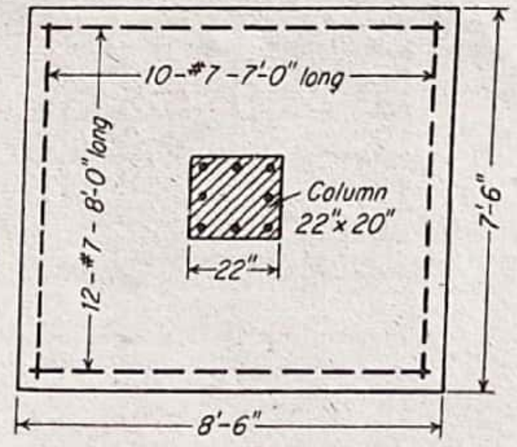


Fig. 9.28 Plan of exterior-column footing.

9.41 Design of Exterior-column Footings The design of the exterior-column footings follows closely the procedure for the interior-column footings. A rectangular concrete block with horizontal dimensions 7.50 × 8.50 ft is used. An effective depth of 15 in. results in a total footing depth of 19 in. Twelve No. 7 bars are used in the long direction of the footing, and ten No. 7 bars in the short direction.

Eight No. 8 dowels 3 ft long are required in each footing. They will project into the footing 15 in., which is sufficient to develop the full working value of each bar. The unit bearing stress at the base of the column is 233,000/22 × 20 = 530 psi, which is much less than the allowable value of 1125 psi. Complete details of the footing are shown in Figs. 9.28 and 9.29.

9.42 Design of Wall Beams With the proposed framing as shown in Figs. 9.30 and 9.33, the unsupported spans of the end wall beams are 19 ft 3 in. and 18 ft 3 in., while those of the intermediate wall beams are 20 ft 2 in. and 19 ft 2 in. for the short and long sides of the building, respectively. Since it is desirable to keep the depth of the wall beams constant throughout the building for architectural appearance, it is first necessary to determine the cross section required for the maximum moment and shear. The width of the beams is taken as 12 in. in all cases.

The maximum shear occurs in the first- and second-floor intermediate

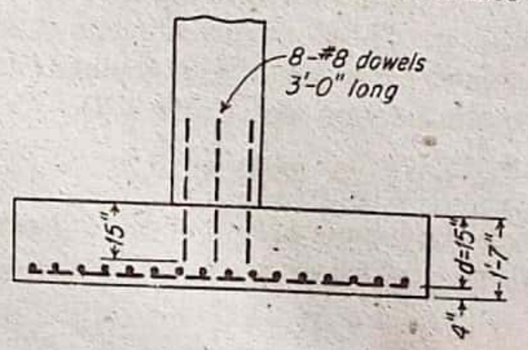


Fig. 9.29 Elevation of exterior-column footing.

Scanned with CamScanner

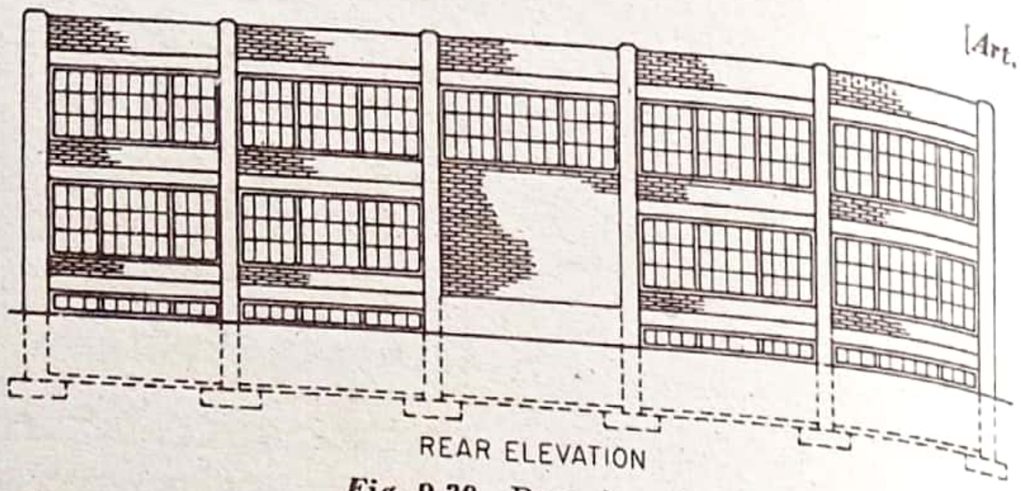


***Fig.* 9.30** Rear elevation.

beams along the short side of the building. According to Table 1004(*f*), Appendix A, a marginal beam having a depth greater than 1¼ and less than 3 times the minimum slab thickness shall carry that proportion of the panel load obtained by interpolation between the proportions assigned to the shallower and deeper beams. In this case the value is 36 per cent. The total load on the wall beam per linear foot is therefore

Brick sill:	$2.5 \times 1 \times 120$	= 300 lb
Windows:	7.5×8	= 60 lb
Stem of beam, assumed		= 170 lb
Floor load:	$0.36 \times 300 \times 21$	= 2270 lb
Total		2800 lb

The maximum shear occurs at the interior supports of the end spans on the short side of the building:

$$V = 1.15 \times 2800 \times 19.25/2 = 31{,}000 \text{ lb}$$

Assuming that web reinforcement will be used, and that the effective depth of the beam is 18 in.,

$$d \text{ (for shear)} = \frac{31{,}000 - {}^{18}\!/_{12} \times 2800}{5\sqrt{3000} \times 12} = 8.15 \text{ in.}$$

The maximum moment occurs in the end spans on the short side of the building. These beams are continuous over one support only and are designed for a negative moment of $\frac{1}{10}wl'^2$, where l' is the average of the two clear spans (see Table 8.2).

$$M = \frac{1}{10} \times 2800 \times 19.71^2 \times 12 = 1{,}305{,}000 \text{ in.-lb}$$

Since the beams are, in effect, T beams with the tee on one side only, the effective width of flange, according to the ACI Code, is

$$b = \frac{1}{12} \times 19.25 \times 12 + 12 = 31.25 \text{ in.}$$

On account of the relatively thick flange, the neutral axis will undoubtedly be in the flange. Under this assumption, the beam must be designed as a rectangular beam 31.25 in. wide, and the required depth is

$$d \text{ (for moment)} = \sqrt{\frac{1{,}305{,}000}{223 \times 31.25}} = 13.5 \text{ in.}$$

In order to give the desired architectural appearance, a total height of 21 in. is adopted for all the wall beams. The effective depth at the center of the beam, allowing for one row of steel with 2½ in. insulation, is 18½ in., and with the proposed arrangement of the steel (Fig. 9.33) the effective depth at the support is 19 in. The weight of the stem per foot is then 165 lb, as assumed.

9.43 Design of *L*1 and *L*2 Since it has been determined above that a cross section of 12 × 21 in. is satisfactory for all wall beams, it is now merely necessary to determine the area of steel required for each beam and to provide for shearing stresses.

The design positive moment in the end beam $L1$ is

$$M = \frac{1}{14} \times 2800 \times 19.25^2 \times 12 = 889{,}000 \text{ in.-lb}$$

and the positive moment in the interior beam $L2$ is

$$M = \frac{1}{16} \times 2800 \times 20.17^2 \times 12 = 853{,}000 \text{ in.-lb}$$

Assuming $j = 0.9$, the required steel areas are as follows:

Beam $L1$, positive-moment section:

$$A_s = \frac{889{,}000}{20{,}000 \times 0.9 \times 18.5} = 2.67 \text{ in.}^2$$

Beam $L1$, interior support:

$$A_s = \frac{1{,}305{,}000}{20{,}000 \times 0.9 \times 19} = 3.81 \text{ in.}^2$$

Beam $L2$, positive-moment section:

$$A_s = \frac{853{,}000}{20{,}000 \times 0.9 \times 18.5} = 2.56 \text{ in.}^2$$

Two No. 7 and two No. 8 bars will be placed in the bottoms of the beams $L1$ and $L2$, providing 2.77 in.² for the positive moment. By bending up the No. 8 bars from each beam and carrying them over the interior support, an area of 3.14 in.² is provided for the negative moment. One more No. 8 bar will provide the additional negative steel required. The No. 8 bars in $L1$ will be bent up at the exterior support, and one No. 9 bar

Scanned with CamScanner

will be added to provide for a negative moment of $\frac{1}{16}wl'^2$. The points at which the bars may be bent and cut off are obtained from Fig. 3.19. The arrangement is shown in Fig. 9.33. The straight bars are carried 6 in. into the columns. A check against Table 8, Appendix B, indicates that adequate development length in bond is provided for all bars.

Since only two bars are bent up in each beam, and these at one place, their strength is disregarded in providing for diagonal tension. Stirrups are placed at suitable intervals to furnish the necessary web strength. With 3000-psi concrete, $V_c = 1.1\sqrt{3000} \times 12 \times 19 = 13{,}700$ lb. At the interior end of $L1$, the distance from the edge of the column in which stirrups are theoretically required is

$$11.1\,\frac{31{,}000 - 13{,}700}{31{,}000} = 6.20 \text{ ft}$$

For No. 3 U stirrups, the maximum spacing is $d/2 = 9.50$ in., but not to exceed $0.22/(0.0015 \times 12) = 12.2$ in. A maximum spacing of 9 in. will be adopted. At a distance d from the face of support, the excess shear is 12,900 lb, and the required stirrup spacing is

$$s = \frac{0.22 \times 20{,}000 \times 19}{12{,}900} = 6.50 \text{ in.}$$

By prorating, the spacing at a point 3 ft from the support is calculated as 9.55 in., which exceeds the maximum spacing. The first stirrup will be placed 4 in. from the support face and followed by four stirrups at 4½ in., three at 6½ in., and six at 9 in., providing web reinforcement over a distance slightly in excess of the theoretical distance plus d as required by Code. At the exterior end of $L1$, the first stirrup is placed 4 in. from the support and followed by nine spaces at 9 in.

In each end of the interior span $L2$, similar calculations indicate spacing from the support face of 4 in., then four spaces at 5½ in., and six at 9 in.

The areas of steel required in the other wall beams, floor, and roof and the arrangement of the web reinforcement are determined in a similar manner. The roof wall beams are made the same depth as those at the second-floor level for architectural reasons. In investigating the beams on the long side of the building, it should be borne in mind that the first interior supports of the line are designed for a moment of $\frac{1}{10}wl'^2$, while at the other interior supports a coefficient of $\frac{1}{11}$ is used. The end supports at the corners of the building are reinforced for negative moments of $\frac{1}{16}wl'^2$. The necessary steel details are shown in Fig. 9.33.

9.44 Design of Stairway Slab The stairway, which extends from the basement to the second-floor level, is located as shown in Fig. 9.33. The

opening made by the stairwell and the future elevator shaft is framed by beams as shown. In order to keep the thickness of the stair slab down to a reasonable minimum, beam $B9$ is placed at the edge of the floor-level landing slab. The stair slab is designed as a simple slab with a span equal to the horizontal distance from the middle of beam $B9$ to the middle of the wall support of the intermediate landing slab.

The dead load on the stair slab is made up of the weight of the intermediate landing slab, the weight of the inclined slab, and the weight of the treads. For purposes of computation it is sufficiently accurate to assume that this total dead load is uniformly distributed over the horizontal span. The live load is assumed as 100 psf of horizontal surface.

The widths of the stair slabs and landing slabs as shown in Fig. 9.35 will prove satisfactory in the ordinary building of this size. With 6-in. bearing allowed on the brick exterior wall, the horizontal span of the stair slab is 12 ft 1 in. The total length of slab between supports is

$$\sqrt{6^2 + 7.66^2} + 3.83 = 13.5 \text{ ft.}$$

Assuming the weight of the slab to be 69 psf, the total load on a 1-ft strip of slab is

Treads:	$9 \times \frac{7.19 \times 10.25}{2 \times 144} \times 150$	= 350 lb
Slab:	13.5×69	= 940
Live load:	12×100	= 1200
Total		= 2490 lb

$$M = \tfrac{1}{8} \times 2490 \times 12.1 \times 12 = 45{,}300 \text{ in.-lb}$$

$$d = \sqrt{\frac{45{,}300}{223 \times 12}} = 4.11 \text{ in.}$$

An effective depth of 4½ in. is selected; with 1-in. insulation the total slab thickness is 5½ in., and the weight is 69 psf, as assumed.

$$A_s = \frac{45{,}300}{20{,}000 \times 0.874 \times 4.50} = 0.575 \text{ in.}^2 \text{ per ft of width}$$

This area is furnished by No. 5 bars, 6 in. center to center. One No. 5 bar, 3 ft 8 in. long, is placed under each tread at right angles to the main reinforcement, as shown in Fig. 9.35.[1]

[1] The detailing shown in Fig. 9.35 assumes that the stairway slab will be poured with the structural frame. A more widely used method of construction places the stair slab after the main structure has been completed. In such cases, recesses must be left in beams $B9$ and in the brick wall in order to furnish support for the future stair slabs, and dowels must be placed in beams $B9$ to project into the stair slabs when they are poured.

Scanned with CamScanner

[Art. 9.45

The floor-level landing slab is made 8 in. thick, and every other bar of the stair-slab reinforcement is continued across this slab. Two No. 5 bars are placed in the intermediate landing slab, at right angles to the main reinforcement, to assist in distributing the load on that slab and to provide for temperature stresses. Negative-moment stresses in the stair slabs across beams *B*9 are provided for by means of short bent bars placed in the tops of the slabs at these points, as shown in Fig. 9.35.

9.45 Design of Beams Framing Stairwell: *Beam B9* (See Fig. 9.31). This beam supports a uniform load along its entire length, consisting of one-half of the stairway-slab load and one-half of the floor-level landing-slab load in addition to its own weight. The span of the beam is 9 ft 5 in., the distance center to center of beams *B*6 and *B*7. The beam is designed as a T beam with the tee on one side only; this is necessary because of the break between the up and down stair slabs at the landing.

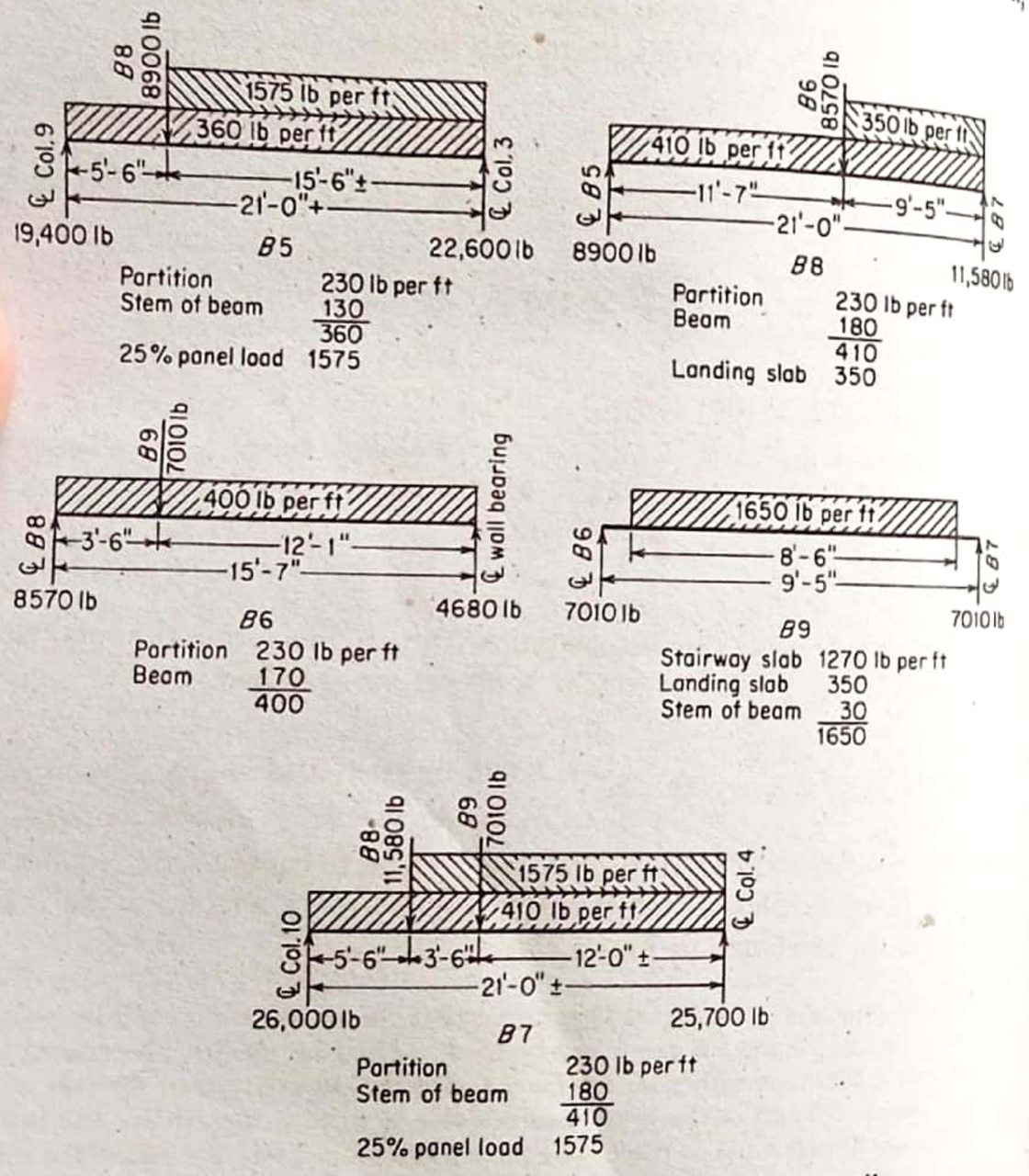


Fig. 9.31 **Loading diagrams for beams framing stairwell.**

Beam B6 This is a simply supported rectangular beam loaded by the weight of a 4-in. hollow tile partition and the concentrated load from *B*9 in addition to its own weight.

Beam B8 This beam carries the concentrated load from beam *B*6, one-half of the load from the landing slab, and the weight of a 4-in. hollow-tile partition, in addition to its own weight. Beam *B*8 has been placed at the edge of the column strip. This fact, together with the improbability of having the full live load on the portion of the floor near it, justifies the assumption that no floor load is supported by *B*8.[1] Because of the open shaft on one side of the beam at the point of maximum moment, it must be designed as a T beam with the tee on one side only. In order to illustrate the method of design when such irregular loads are involved, the design of *B*8 is included below.

The loads on the beam (see Figs. 9.31 and 9.33) are as follows:

Uniform load over entire length of beam:

Partition:	20×11.5	$= 230$ plf
Weight of beam		$= 180$ plf
Total		$= 410$ plf

Additional uniform load from stairway landing slab:

$$\tfrac{1}{2} \times 3.5 \times 200 = 350 \text{ plf}$$

Concentrated load from *B*6 in 8570 lb:

$$R_L = \frac{8570 \times 9.42 + 350 \times 9.42^2/2 + 410 \times 21^2/2}{21} = 8900 \text{ lb}$$

$$R_R = 11{,}580 \text{ lb}$$

The point of zero shear, which locates the point of maximum moment, occurs under the concentrated load. The maximum moment is

$$M = (8900 \times 11.5 - 410 \times 11.58^2/2)12 = 900{,}000 \text{ in.-lb}$$

According to the ACI Code, the effective width of flange is equal to $10 + \frac{1}{12} \times 21 \times 12 = 31$ in. Because of the relatively large thickness of

[1] Since beam *B*8 and the slab adjacent to it are poured at the same time, they cannot act independently of each other. A more conservative design would assume that a part of the adjacent slab load is supported by *B*8.

Scanned with CamScanner

the flange, it is reasonable to assume that the neutral axis is in the flang in which case the equations for rectangular beams apply:

$$d = \sqrt{\frac{900{,}000}{31 \times 223}} = 11.4 \text{ in.}$$

An effective depth of 14 in. will be used, in order to avoid interferenc with the bars in $B6$:

$$b' = \frac{11580 - 1.17 \times 760}{5\sqrt{300} \times 14} = 2.78 \text{ in.}$$

A width of stem of 10 in. will be used, in order to give a reasonable amou of resistance to torsional stresses. With 3 in. of insulation, to provide f two rows of bars, the total height of the beam is 17 in., and the weight p foot is 180 lb, as assumed.

$$A_s = \frac{900{,}000}{20{,}000 \times 0.875 \times 14} = 3.66 \text{ in.}^2$$

Six No. 7 bars are selected (3.61 in.^{2}). With

$$np = \frac{9 \times 3.61}{31 \times 14} = 0.077$$

and $t/d = 14\frac{5}{8} = 0.57$, Graph 12, Appendix B, shows that the neut axis is in the flange, so that, from Table 6, Appendix B, with

$$p = \frac{3.61}{31 \times 14} = 0.0085$$

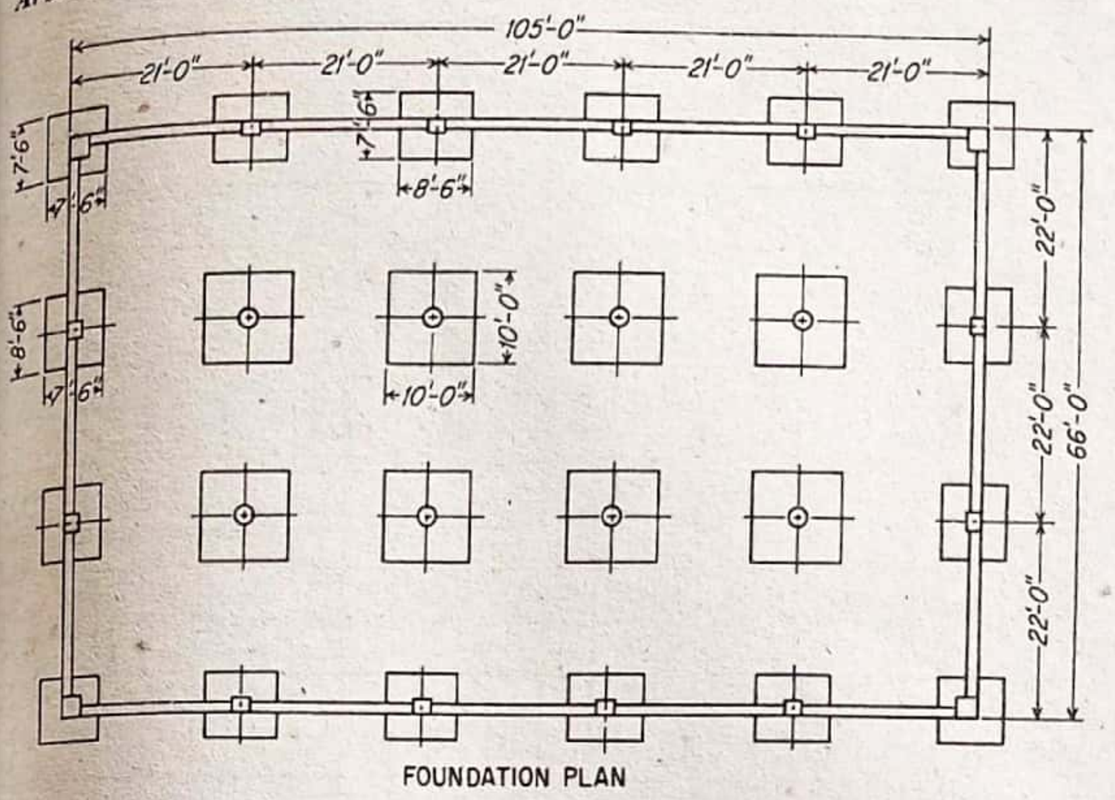
$j = 0.893$, and the revised steel area required is 3.59 in.^{2}. The six No bars are satisfactory.

Since this beam is poured monolithically with the beams supporti it, there will exist some negative moment at the supports. The amount this bending moment is dependent upon too many factors to permit a accurate determination. In order to provide for the stresses of negati moment, one-half the steel is bent up and hooked over the support.

Since only three bars are bent up, and since these are bent at a sing point, they will not be depended upon for diagonal tension resistance, a vertical stirrups will be used wherever web reinforcement is required. T total shear that the concrete can resist is

$$V_c = 1.1\sqrt{3000} \times 10 \times 14 = 8400 \text{ lb}$$

The stirrups will be designed to resist all the shear in excess of t amount.



FOUNDATION PLAN

Fig. 9.32

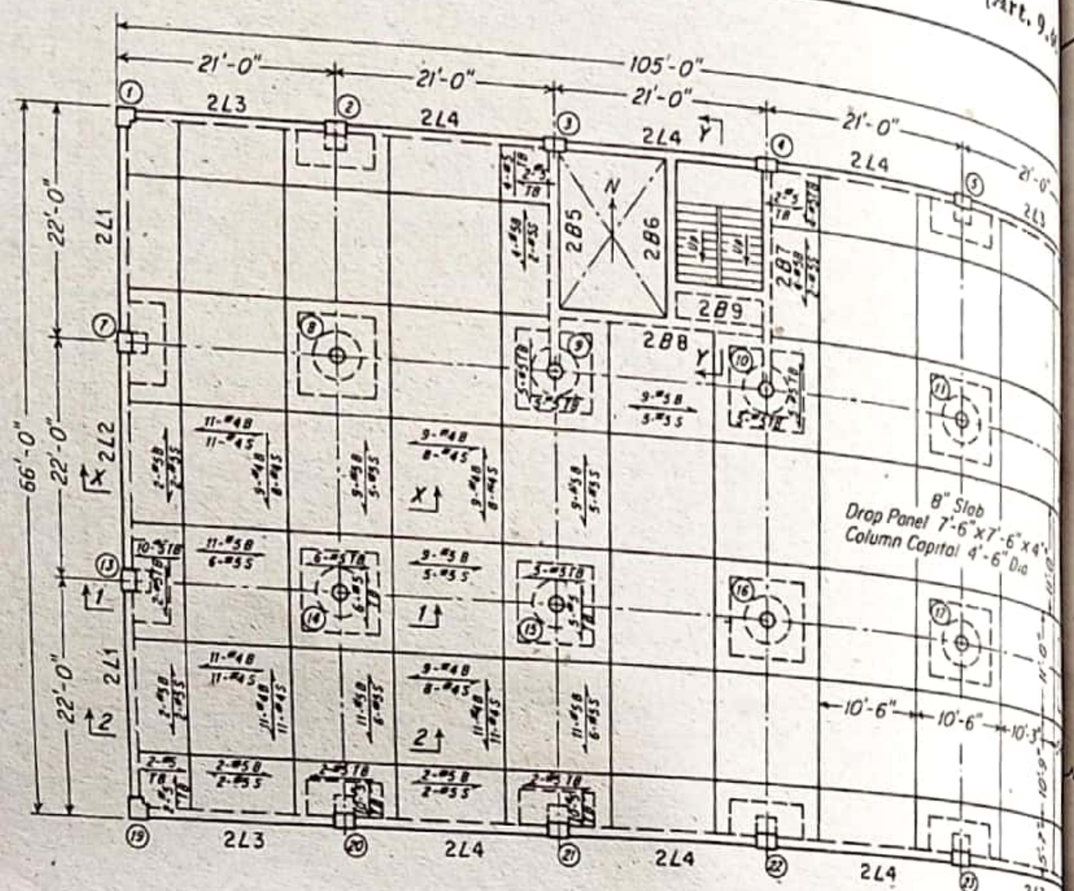
With ¼-in. U stirrups, the required stirrup spacing at the right end of the span is 3 in., followed by 11 spaces at 7 in. At the left end, the first stirrup is placed at 3 in., with four additional stirrups at 7 in.

Beam B5 In addition to supporting the concentration from beam $B8$ and its own weight, beam $B5$ must be designed to support the partition as shown and the required proportion of the floor load. The beam is a T beam, with the tee on one side only.

Beam B7 This beam supports the same loads as beam $B5$, in addition to the concentrated load from beam $B9$. It is a T beam, with the tee on one side only. The complete framing details of the stairway beams are shown in Fig. 9.33.

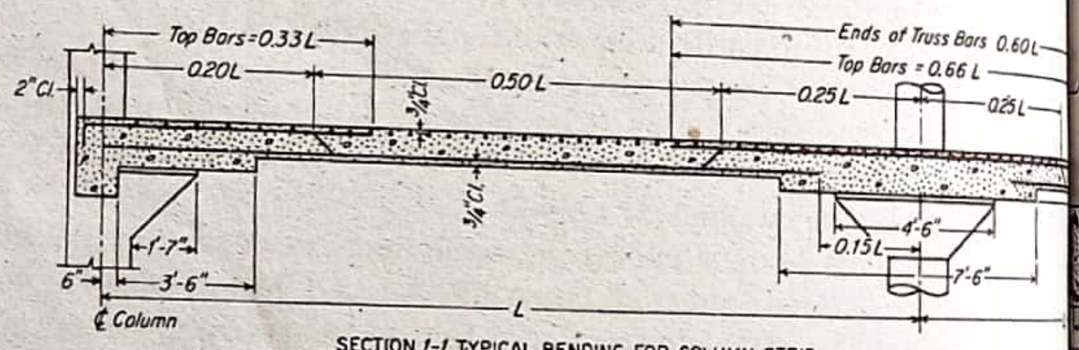
9.46 Engineering Drawings Figure 9.33 is an engineering drawing of the second floor, giving the necessary information on the concrete and steel for the slab and beams at that floor. This is the type of drawing which would be prepared in the design office. The reinforcing-bar fabricator would use this drawing as a basis for preparing a complete detail drawing showing bar lengths and bends and placing instructions. The "Manual of Standard Practice for Detailing Reinforced Concrete Structures" (ACI 315–57) of the American Concrete Institute is usually followed in the preparation of both engineering drawings and fabricator's detail drawings.

Scanned with CamScanner

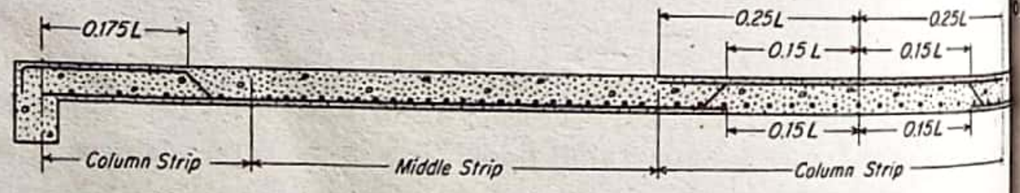


SECOND FLOOR FRAMING PLAN

"B" Denotes bent bar
"S" Denotes stirrup
"TB" Denotes top bar



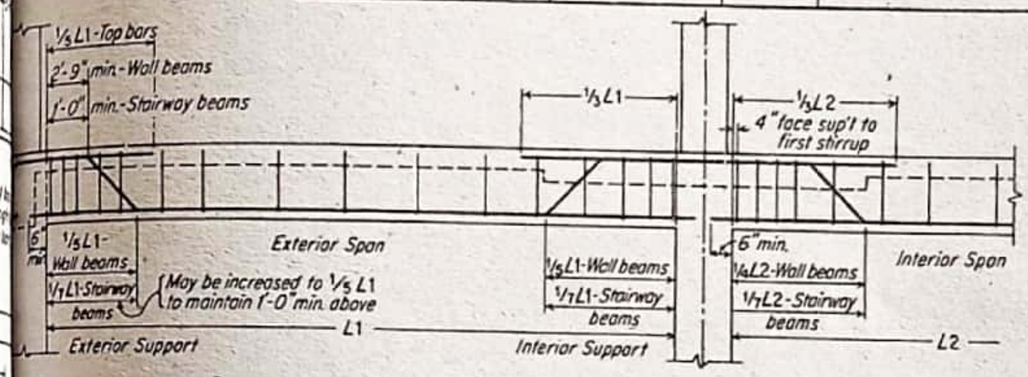
SECTION 1-1 TYPICAL BENDING FOR COLUMN STRIP



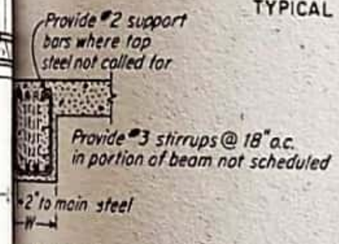
SECTION 2-2 TYPICAL BENDING FOR MIDDLE STRIP

BEAM SCHEDULE

Beam Mark	Size W	Size D	Reinforcing: Longitudinal No.-Size	Reinforcing: Longitudinal Remarks	Reinforcing: Stirrups No.-Size	Reinforcing: Stirrups Spacing from Face of Support
2L1	12	21	2-#7 2-#8 1-#9	Bot. Str. Bent Top Ext. Sup't.	24-#3	4, 9@9 ext. end 4, 4@4½, 3@6½, 6@9 int. end
2L2	12	21	2-#7 2-#8 1-#8	Bot. Str. Bent Top Sup't.	22-#3	4, 4@5½, 6@9, ea. end
2L3	12	21	2-#7 2-#8 1-#7	Bot. Str. Bent Top Ext. Sup't.	16-#3	3@6, 5@9 ea. end
2L4	12	21	2-#6 2-#7	Bot. Str. Bent	16-#3	3@6, 5@9 ea. end
2B5	10	20	3-#9 3-#8	Bot. Str. Bent	14-#3	7@8 south end 3@7, 4@8 north end
2B6	10	16	1-#7 2-#6	Bot. Str. Bent	None	None
2B7	12	22	3-#9 3-#9	Bot. Str. Bent	16-#3	3@6, 3@7, 3@8 south end 3@6, 4@9 north end
2B8	10	17	3-#7 3-#7	Bot. Str. Bent	3-#2	3, 11@7 east end 3, 4@7 west end
2B9	8	12	1-#6 2-#6	Bot. Str. Bent	None	None



TYPICAL BEAM BENDING



AL SECTION
OUGH BEAM

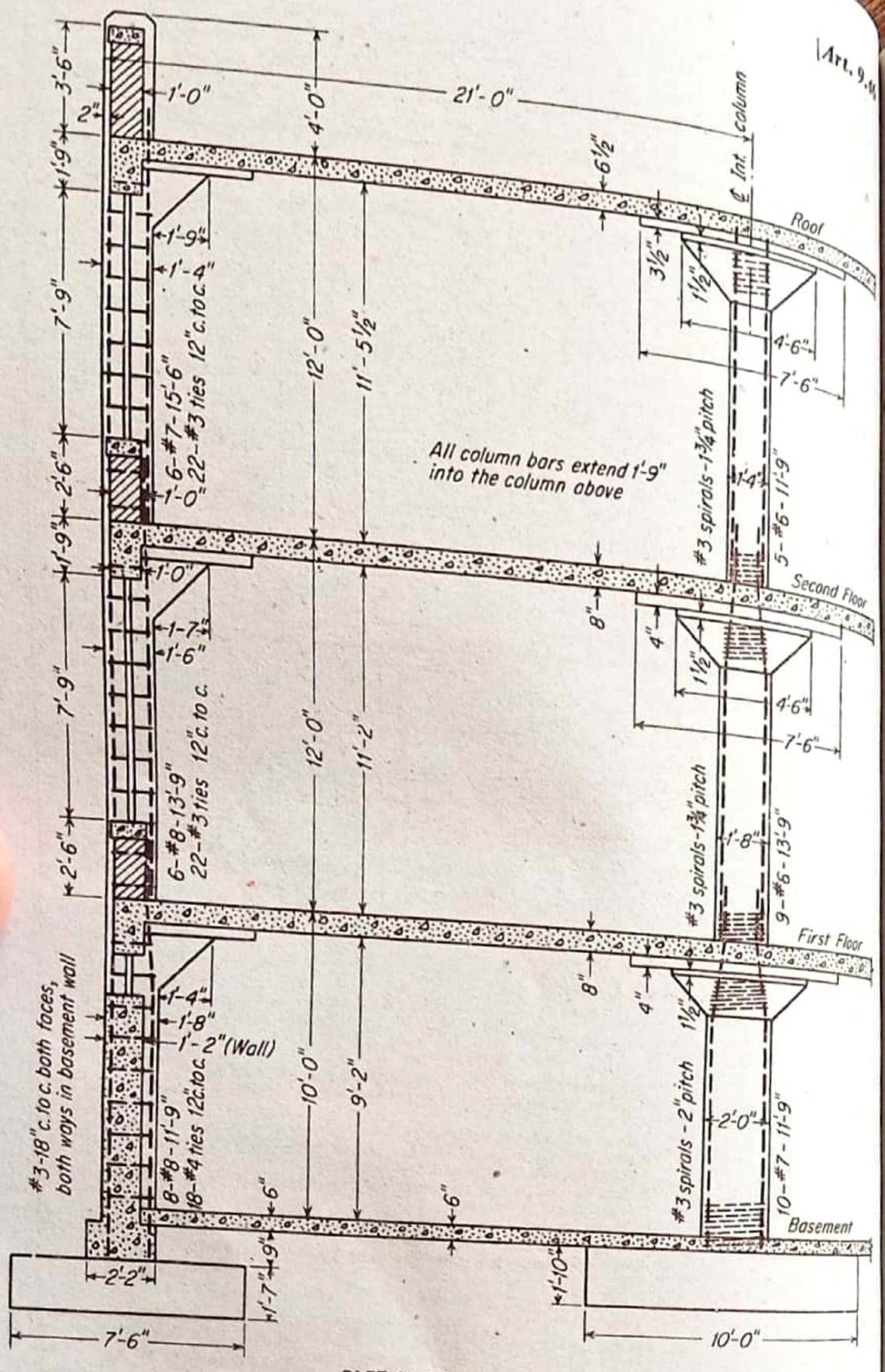
NOTES:

1. All concrete to have 3000 p.s.u. compressive strength at 28 days.
2. Reinforcing steel to have $f_y = 40{,}000$ psi, with deformations conforming to A.S.T.M. – A305.
3. Bends to be made as per diagrams.
4. Terminate non-continuous bent bars in accordance with A C I Code by a hook if required embedment cannot be obtained.
5. Place main reinforcing steel so that bottom of steel is 2" above forms in beams and 3/4" in slabs.
6. All slab and beam steel shall have a minimum extension into the support in accordance with A C I Code.
7. Provide bar supports in accordance with ACI Detailing Manual.

FLAT SLAB BUILDING
SECOND FLOOR FRAMING PLAN

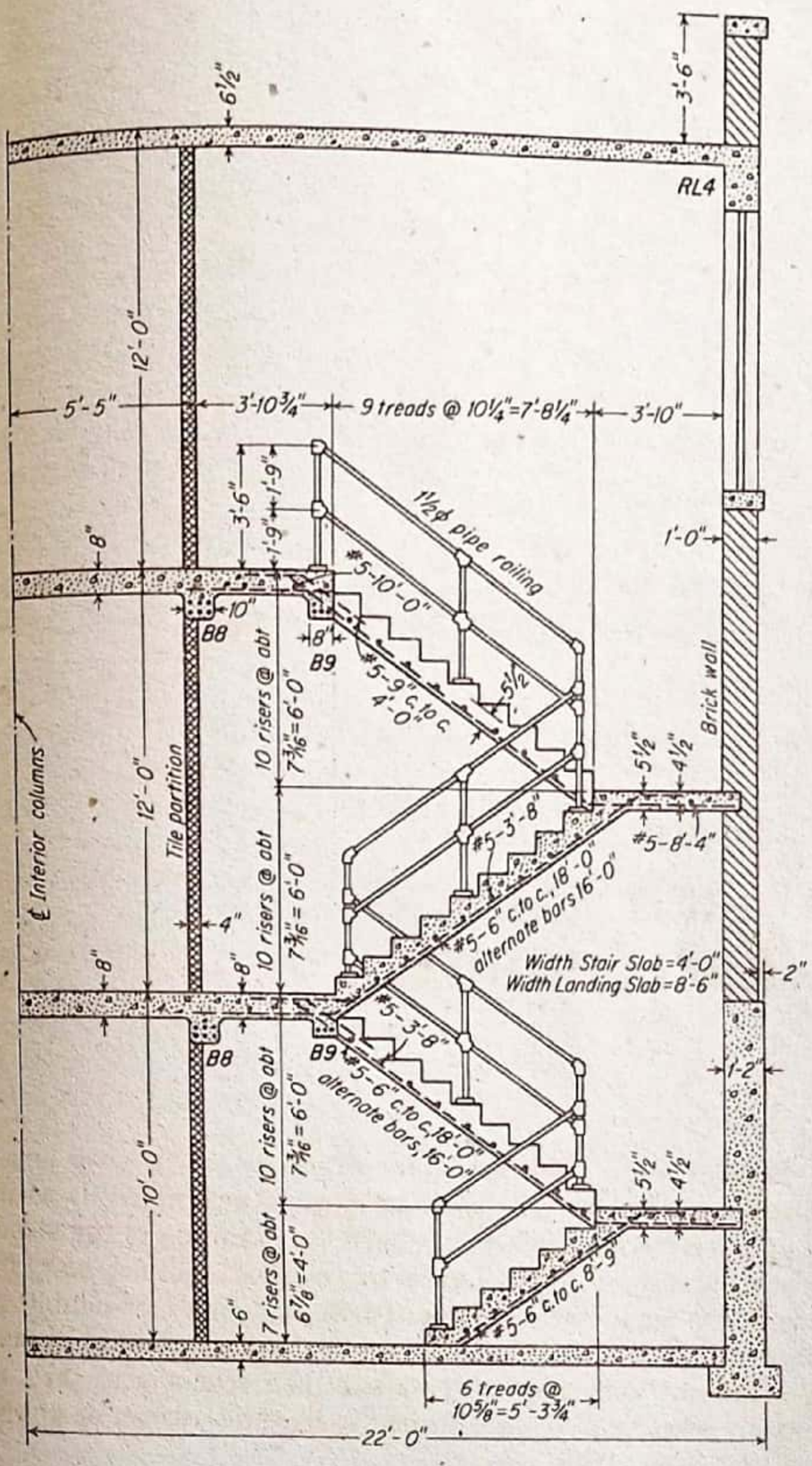
FIG. 9.33

Scanned with CamScanner



PARTIAL CROSS SECTION
SECTION X-X
Showing Column Steel

Fig. 9.34



DETAIL OF STAIRWAY
SECTION Y-Y

Fig. 9.35

Scanned with CamScanner

chapter 10

ARCH AND SHELL ROOFS

10.1 Introduction The search for structures which cover long spans and large areas without intermediate support, and which do so using a minimum of material, has long occupied the attention of the structural-engineering profession. When a plane roof surface is not necessary to meet the functional requirements of the structure, a singly or doubly curved roof form will normally be found to be the most economical of material. These nonlinear, nonplanar systems owe their economy to their unique capacity to resist applied loads primarily by direct stress, as opposed to flexural and shear stress.

In this connection, it is pertinent to observe that the beam is one of the least efficient of structural forms. Commonly, only one cross section of a beam is subjected to the maximum design moment, and consequently if the member is prismatic, only one cross section of the beam is working

at the maximum allowable stress at design load. What is worse, at design load only the extreme fiber of thatunique cross section is stressed to the maximum; all the other fibers are understressed. It is acknowledged that this situation is somewhat improved by continuity, by virtue of which two sections may be subjected to the maximum moment. The situation is further improved by the plasticity of concrete and steel, which results in a nonlinear distribution of stress in the cross section, and which may permit a redistribution of moments to occur within the member which will more fully utilize the prismatic beam. But it is still impossible to compete for efficiency with the simple compression strut, for example, in which every cross section along the length is stressed to the full allowed value over its entire width and depth.

This leads one to select, for those design situations which permit it, a structural form in which direct stress (in the case of concrete, compressive stress) is dominant over flexural and shear stress. The degree to which this is accomplished is a measure of the structural efficiency of the design.

10.2 Arches The use of arches is the oldest structural method for bridging spans too large for straight beams. Arches were introduced by the Romans for their bridges, aqueducts, and large public buildings more than 2000 years ago. Constructed of masonry, concrete, steel, and timber, they have been in wide use ever since.

Modern arches are of three types: the fixed arch, which is rigidly connected to the abutments, the two-hinged arch, which is supported at each end by a hinge resting on the abutment, and the three-hinged arch, which has an additional hinge at the crown. Reinforced-concrete arches are mostly of the first two types.

The structural action and advantage of arches are easily recognized by considering a two-hinged arch. Figure 10.1*a* shows a uniformly loaded simple beam with $M_{max} = wL^2/8$, $V_{max} = wL/2$, and axial force $N = 0$. If this beam is curved, as in Fig. 10.1*b*, M_{max} is the same as before. The

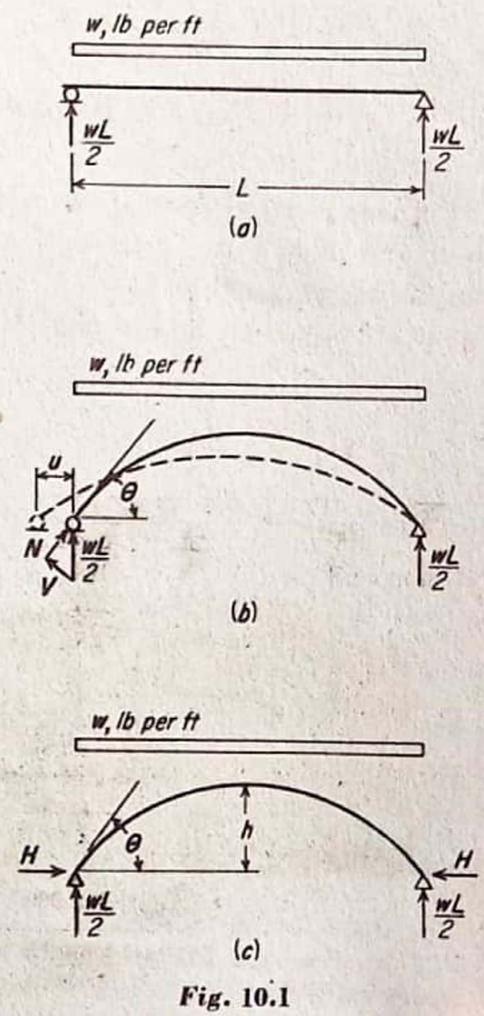


Fig. 10.1

Scanned with CamScanner

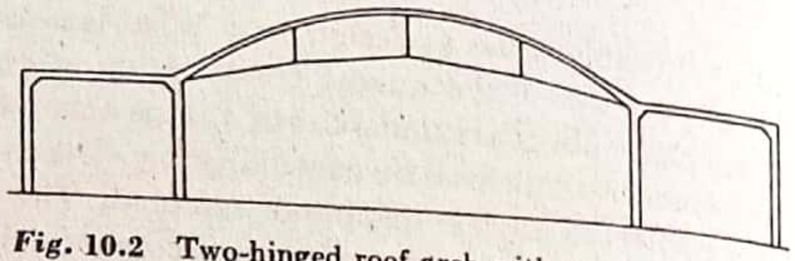


Fig. 10.2 Two-hinged roof arch with cambered tie rod.

shear at the support, however, is decreased to $V_{max} = (wL/2)\cos\theta$; in addition, an axial force is now present in the member which, at the supports, equals $N = (wL/2)\sin\theta$. This curved beam tends to straighten under load since, owing to bending, the bottom fibers are stretched and the top fibers compressed. This action tends to increase the span, as shown in Fig. 10.1*b*. To maintain the original span, as in the two-hinged arch with immovable supports (Fig. 10.1*c*), a horizontal reaction H must be applied. In this two-hinged arch

$$M_{max} = \frac{wL^2}{8} - Hh$$

$$V_{max} = \frac{wL}{2}\cos\theta - H\sin\theta$$

$$N = \frac{wL}{2}\sin\theta + H\cos\theta$$

It is seen that, in comparison with the simple beam, the bending moment and the shear force in the arch are greatly decreased. On the other hand, an axial compression force N, not present in the beam, acts in the arch. It is exactly this state of affairs which is desirable in reinforced concrete,

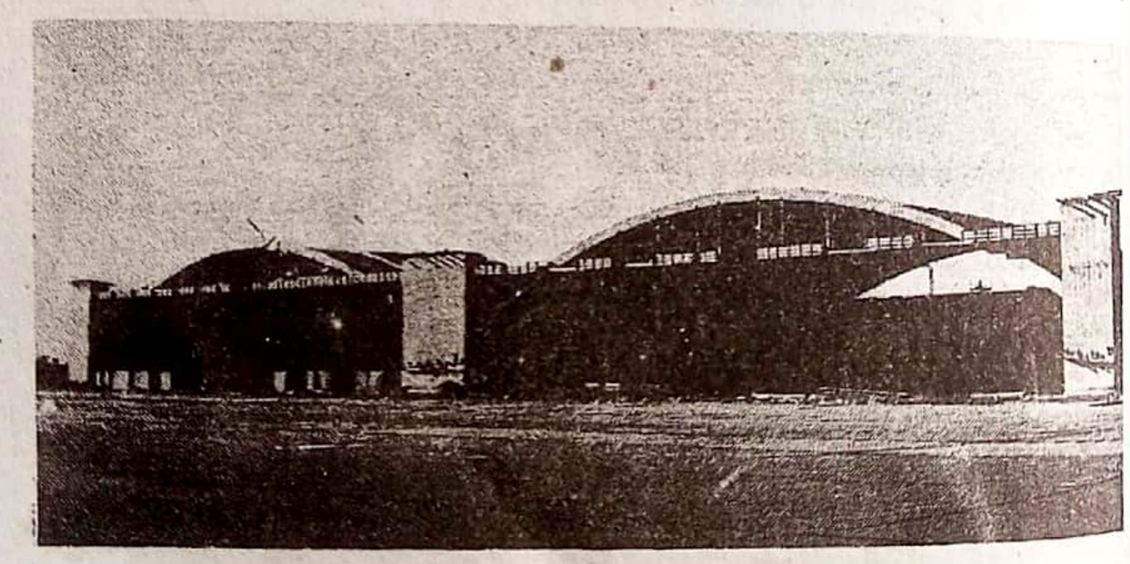


Fig. 10.3 Hangar at Chicago Municipal Airport. Fixed arches spaced at 28 ft 11½ in., clear span 257 ft, height at center 60 ft, thickness of concrete shell between arches varies from 3½ to 6 in. (*Courtesy of Ammann and Whitney.*)

since concrete is relatively weak in tension and shear but strong in compression.

The choice of two-hinged or fixed arches depends on the particular conditions of design. Fixed arches require immovable abutments which prevent not only vertical and horizontal motion, but also rotation of the support. For roof arches resting on columns or walls, it is obviously impossible to fix the supports against rotation, since the rigidity of the supporting structure is not sufficient for this purpose. Two-hinged arches, on the other hand, are insensitive to rotations and to moderate differential settlements of the abutments, which, for this reason, can often be made less substantial than for fixed arches. Tie rods are often provided in two-hinged arches to resist the horizontal reaction H; hence the supports have to resist vertical reactions only, with a corresponding further decrease in their cost. Tied two-hinged arches are obviously advantageous in roof structures of the type shown in Fig. 10.2, where large horizontal reactions would require much heavier columns and frames. Large hangars and halls of the type of Fig. 10.3 have been built both with fixed arches and with tied two-hinged arches; in the latter case tie rods were located below the floor. Effective hinges can be constructed at reasonable cost, provided that the reactions are not excessively large. They may be architecturally undesirable, however, and represent a maintenance problem in some cases. A well-considered decision on the type of arch to be used in a given design depends, therefore, on a balanced evaluation of factors such as those just enumerated.

In contrast to the arch ribs of the previous illustrations, ribless barrel-arch roofs of the type shown in Fig. 10.4 can be used for moderate spans. A strip of unit width may be designed as either a fixed or two-hinged arch.

As was noted in the general discussion of arch action (Fig. 10.1), arch ribs or barrels are subject to compression and bending, and usually only small shear. They are, therefore, designed and analyzed in the same manner as eccentrically compressed columns, with one layer of steel being located near the top surface and another near the bottom. It is economical to keep steel percentages small, on the order of 1 to 2 per cent. Lateral ties for the reinforcement are used in arch ribs as in columns. In barrel arches, transverse reinforcement normal to the main steel is placed near both surfaces and is tied to the main longitudinal steel. This distributes localized loads and acts as temperature and shrinkage reinforcement.

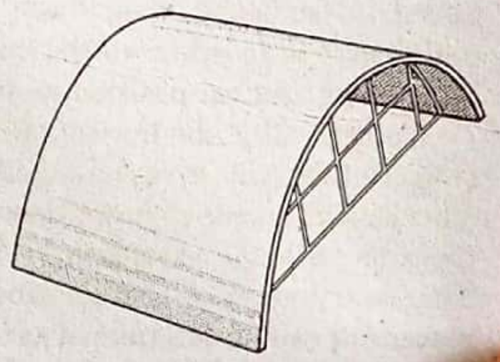


Fig. 10.4 Barrel-arch roof.

Scanned with CamScanner

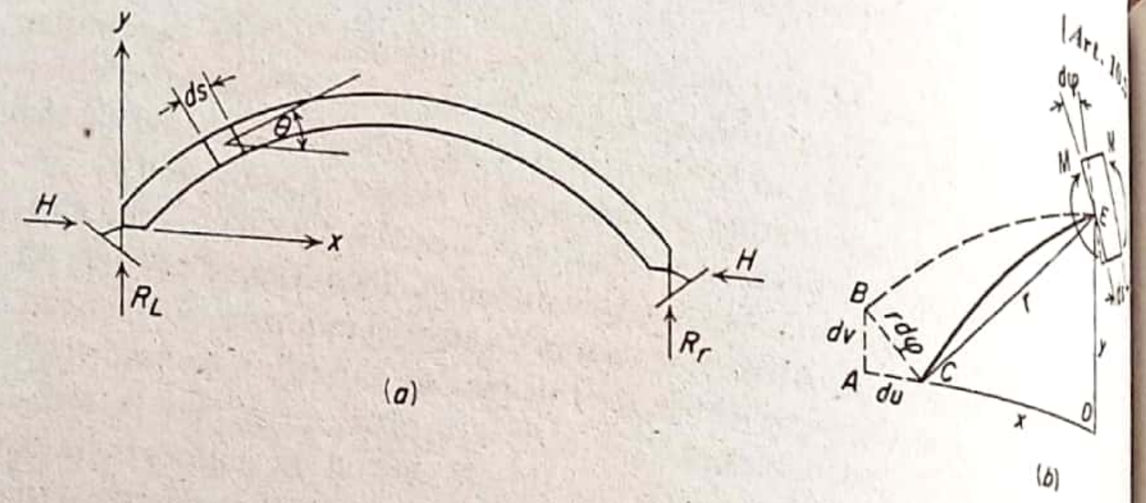


Fig. 10.5

10.3 Theory of Symmetrical, Two-hinged Arches The two-hinged arch (Fig. 10.1*c*) differs from a curved simple beam (Fig. 10.1*b*) in that horizontally immovable hinges or tie rods prevent the spread of supports. The forces in such an arch can be analyzed by introducing a fictitious roller support at one of the hinges, which converts the arch into a simple beam. The horizontal displacement u can then be determined. To convert this fictitious beam into the actual arch, a horizontal force H must be introduced of sufficient magnitude to produce a displacement equal and opposite to u. In other words, this force brings the fictitious roller support back to its original position as it actually is in the arch.

To determine the horizontal displacement u, take a small element ds (Fig. 10.5*a*) of the arch, and consider the effect of the deformation of this one element on the deformation of the arch as a whole. Thus all parts of the arch with the exception of this one element are considered as rigid. The contribution of the deformation of the element ds to the total displacement can be determined as follows. A bending moment M, considered as constant over the small length ds, will cause the left cross section to rotate with respect to the right one by an amount $d\phi$ which can be deter-

mined by the moment-area principle, i.e., from the fact that the rotation of one section with respect to another is equal to the area of the moment curve between them divided by EI. Hence

$$d\phi = \frac{M\,ds}{EI} \tag{10.1}$$

The entire left portion of the arch, rigidly attached as it is to the cross section, will likewise rotate through an angle $d\phi$, as represented by the dotted position of the axis in Fig. 10.5*b*. Consequently, the left end of the arch describes an arc $r\,d\phi$. It will be noted that triangle ABC is similar to triangle CDE. Hence, from simple proportions, $du/r\,d\phi = y/r$, and the horizontal displacement is

$$du = y\,d\phi = \frac{My\,ds}{EI} \tag{10.1a}$$

This is the contribution made to the total displacement u by the angular deformation due to bending of the single element ds. To obtain u itself, it is only necessary to sum these contributions for all elements ds along the arch, or

$$u = \int_0^s \frac{My\,ds}{EI}. \tag{10.2}$$

Let M_0 represent the bending moment due to any external arch loads caused in the fictitious simple curved beam, as in Fig. 10.1*b*. These moments, of course, are the same as those in the straight beam (Fig. 10.1*a*). Then the outward displacement due to these "simple beam moments" is

$$u_{M_0} = \int_0^s \frac{M_0\,y\,ds}{EI} \tag{10.2a}$$

The sign convention is the same as in beam analysis; i.e., moments are considered positive if they produce tension in the bottom fiber. In addition to M_0, the horizontal reaction H causes a moment at section x which is equal to

$$M_H = -Hy$$

and the inward displacement caused by these moments is

$$u_{M_H} = -H\int_0^s \frac{y^2\,ds}{EI} \tag{10.2b}$$

Since, actually, no displacement occurs at the immovable hinge,

$$u_{M_0} = -u_{M_H}$$

Scanned with CamScanner

from which one obtains the magnitude of the horizontal reaction: [Art. 10.3

$$H = -\frac{\int_0^s (M_0\, y\, ds/EI)}{\int_0^s (y^2\, ds/EI)} \tag{10.3}$$

If displacements u were caused exclusively by bending, Eq. (10.3) would furnish all the information necessary for analyzing a two-hinged arch. Since such an arch, as is seen from Fig. 10.1, has only one statically indeterminate reaction H, it is now possible to find moments, shears, and axial forces at any point in the arch from equilibrium conditions only, since the previously unknown force H is given by Eq. (10.3). However, other factors in addition to bending moments may contribute significantly to the magnitude of u and must therefore be considered in determining H.

In addition to bending moments, shear forces and axial thrusts act on element ds. Deformations due to shear in arches are even smaller, relatively, than in beams and can therefore be neglected. Those caused by axial compression forces N, on the other hand, may affect the magnitude of H significantly and must be considered.

Consider an element ds with a concentric force N on both faces, as shown in Fig. 10.5c. The axial shortening $\Delta\, ds$ caused by the normal force N_0 is $N_0\, ds/EA$. N_0 is the component, parallel to the arch axis at the element ds, of all external forces and reactions on the fictitious curved beam to the right or left of the element ds. The component of $\Delta\, ds$ in the direction of u is

$$du = \Delta\, ds \cos\theta \tag{10.4}$$

Hence

$$du_{N_0} = \frac{N_0 \cos\theta\, ds}{EA}$$

and the total displacement due to N_0 is

$$u_{N_0} = -\int_0^s \frac{N_0 \cos\theta\, ds}{EA} \tag{10.5}$$

The minus sign indicates that this displacement is inward, in contrast to the outward displacement u_{M_0}. On the other hand, the horizontal reaction H results in an axial compression, at any point of the arch, of magnitude $H \cos\theta$; thus the inward displacement caused by this action is

$$u_{N_H} = -H \int_0^s \frac{\cos^2\theta\, ds}{EA} \tag{10.6}$$

Temperature changes which may occur in roof arches produce further

deformation of the arch. A uniform temperature increase of $t°$ causes the arch element ds to increase in length by the amount

$$\Delta\, ds = \omega t°\, ds$$

where ω is the temperature coefficient of expansion. Substitution of this expression in Eq. (10.4) and integration over the entire arch give the total support displacement due to a uniform temperature increase:

$$u_t = \omega t° \int_0^s \cos\theta\, ds = \omega t° l \tag{10.7}$$

Another factor which results in inward displacement u is the inevitable shrinkage of concrete. It has been shown, however, that the unfavorable effect of shrinkage is greatly decreased by the longtime plastic flow of concrete, which allows the structure to adapt itself to those stresses which are caused by change of shape, such as shrinkage, rather than by external loads. It has been proposed that limited effect of shrinkage can be accounted for by an equivalent drop in temperature of 15°F added to the actual seasonal temperature drop for which the arch is designed. The temperature coefficient may be taken as $\omega = 5.5 \times 10^{-6}$ per °F.

In addition to the uniform temperature change just considered, a temperature differential may exist between the inside and outside surfaces in roof arches, particularly if, as in the hangar of Fig. 10.3, the roof slab or shell is placed at middepth of the arch ribs. The total temperature changes and corresponding deformations may then be represented as in Fig. 10.5d. The amount by which the bottom fiber ds expands more than the top fiber is $\Delta t°\, \omega\, ds$. It is seen that this results in

$$d\phi = \frac{\Delta t°\, \omega\, ds}{t} \tag{10.8}$$

If this value is substituted in the left equality of Eq. (10.1a), and the result integrated over the arch, the total displacement caused by the temperature gradient becomes

$$u_{\Delta t°} = \omega\, \Delta t° \int_0^s \frac{y\, ds}{t} \tag{10.9}$$

These are all the types of displacements that occur in an arch with immovable hinges. In arches with tie rods, hinges are not immovable, since the force H in the tie rod causes it to stretch. For a tie rod of area A_{tr} and modulus E_{tr}, this stretch amounts to

$$u_{tr} = H \frac{l}{E_{tr} A_{tr}} \tag{10.10}$$

Scanned with CamScanner

For a tied arch, the sum of all other displacements must be equal to the stretch of the tie; i.e.,

$$u_{M_0} + u_{M_H} + u_{N_0} + u_{N_H} + u_{t^\circ} + u_{\Delta t^\circ} = u_{tr}$$

If the proper values are substituted in this equation, the unknown horizontal force H may be found:

$$H = \frac{\int_0^s \frac{M_0\, y\, ds}{I} - \int_0^s \frac{N_0 \cos\theta\, ds}{A} + E\omega\left(t^\circ l + \Delta t^\circ \int_0^s \frac{y\, ds}{t}\right)}{\int_0^s \frac{y^2\, ds}{I} + \int_0^s \frac{\cos^2\theta\, ds}{A} + \frac{El}{E_{tr}A_{tr}}} \tag{10.11}$$

This lengthy expression can usually be simplified by omitting terms which are zero or negligibly small, depending on the particular condition. Thus, for an arch without tie rod the last term in the denominator drops out, since $u_{tr} = 0$. If no temperature gradient can occur between inside and outside surfaces, such as in roof arches located below a well-insulated surface, the term containing Δt° is zero. Furthermore, in many cases the displacements u_{N_0} and u_{N_H} caused by axial compression are very small compared to those caused by bending moments (u_{M_0} and u_{M_H}). For a parabolic arch, S. Timoshenko[1] has computed the amount of error obtained by neglecting the influence of axial compression in determining H. His results are given in the table below, in which t_c is the thickness at the crown:

h/l	1/12			1/8			1/4		
t_c/l	1/10	1/20	1/30	1/10	1/20	1/30	1/10	1/20	1/30
Error, %	17.1	5.1	2.4	8.4	2.2	1.0	1.8	0.4	0.2

Since the usual accuracy of engineering designs is hardly greater than 5 per cent on account of uncertainties of loading, materials properties, and various other factors, the influence of axial compression can be neglected in all but very flat or unusually thick arches. Normally then, the second term in both the numerator and denominator can be dropped as being negligibly small. Hence, for an arch of usual dimensions without tie rod and without temperature gradient, H can be determined with sufficient accuracy from

$$H = \frac{\int_0^s (M_0\, y\, ds/I) + E\omega t^\circ l}{\int_0^s (y^2\, ds/I)} \tag{10.11a}$$

[1] S. Timoshenko, "Strength of Materials," part 1, p. 397, D. Van Nostrand Company, Inc., Princeton, N.J., 1956.

The determination of the integrals in the equation for H is simple, provided that M_0, N_0, I, A, h, and y can be expressed as functions of s and that these functions can be integrated. Ordinarily this is possible for only a few very simple cases in which the arch axis is either a parabola or a circular arc. In most other cases it becomes necessary to approximate these integrals with a finite sum of numerical terms. The details of this procedure will be given after the theory of fixed arches is developed.

10.4 Theory of Symmetrical Fixed Arches The fixed arch shown in Fig. 10.6*a* has a total of six reactions, i.e., a vertical and a horizontal reaction and a moment at each springing. There are, then, three redundant reactions to be determined. If no horizontal loads are present, the condition that the sum of horizontal forces be zero results in $H_l = H_r$.

For purposes of analysis the arch is cut through the crown, and each half arch is regarded as a statically determinate cantilever fixed at its springing. In the plane of separation, in general, a horizontal and a vertical force H_c and V_c and a bending moment M_c will act from one half onto the other. These three quantities are taken as the redundants. They are shown, in Fig. 10.6*b*, acting in the direction and sense which will be assumed as positive in the following derivations. In any other cross section of the structure, M, N, and V will be assumed positive, as shown in Fig. 10.6*b*. If M_c, H_c, and V_c are known, M, N, and V at any point can be determined from statics.

The crown sections of the separate halves, through the action of loads,

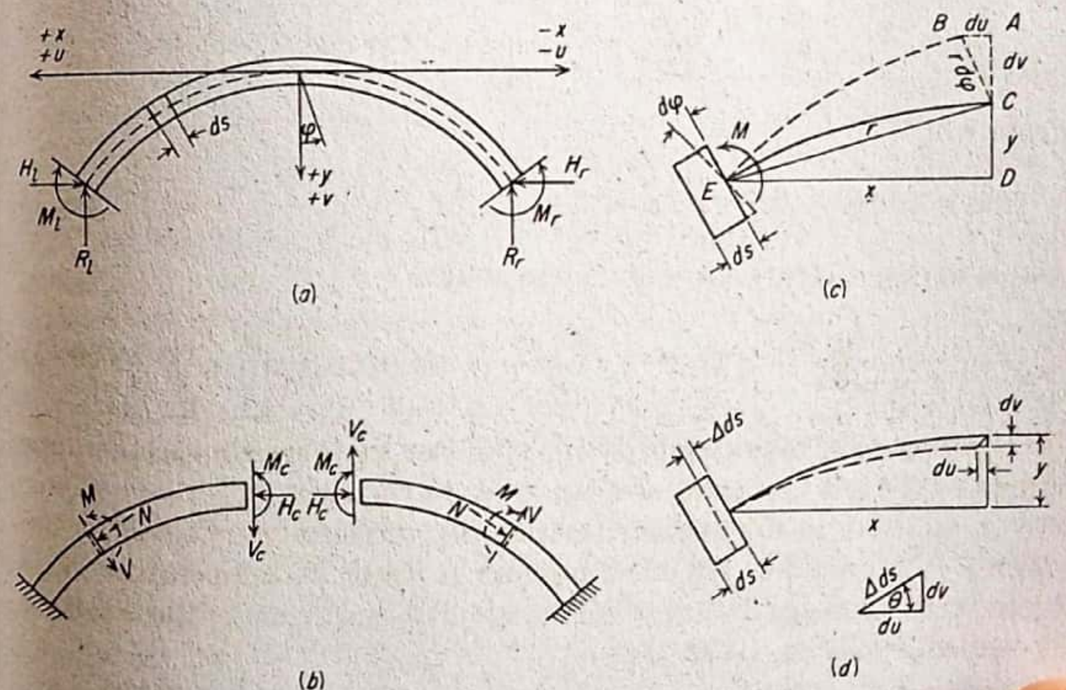


Fig. 10.6

Scanned with CamScanner

temperature, and other influences, will be displaced from their origin
positions. In general, there will be a horizontal displacement u, a vertic
displacement v, and a rotation of the normal to the crown section ϕ. Th
assumed positive directions of these displacements are shown in Fig
10.6*a*. If the structure in fact consisted of two independent cantilever
u, v, and ϕ would, in general, be different for the two halves. Sinc
actually, the arch is one continuous structure, these displacements mus
be equal in magnitude and sign. Consequently,

$$u_l = u_r \qquad v_l = v_r \qquad \phi_l = \phi_r \tag{10.12}$$

where the subscripts l and r refer to the left and right half arch, respec
tively. These three equations permit the determination of the redundant
H_c, V_c, and M_c. In other words, in the arch these three quantities must b
of such magnitude as to join the left and the right cantilevers into on
continuous structure.

Isolating an element ds of the arch (Fig. 10.6*c*), one can determine th
contributions du, dv, and $d\phi$ made to the total displacements u, v, and
by the deformations of this single element. The bending moment M causes
a rotation $d\phi$ which is determined by Eq. (10.1). The part of the arch
between the section and the crown, considered rigid and represented by
its axis in Fig. 10.6*c*, rotates through the same angle $d\phi$, which, con-
sequently, also represents the rotation of the crown section caused by the
deformation of the element ds. Furthermore, since the triangles ABC and
CDE are similar, it is seen that

$$\frac{du}{r\,d\phi} = \frac{y}{r} \quad \text{and} \quad \frac{dv}{r\,d\phi} = \frac{x}{r}$$

from which

$$du = y\,d\phi \qquad dv = x\,d\phi \tag{10.13}$$

Substituting $d\phi$ from Eq. (10.1), one obtains

$$du = \pm\frac{My\,ds}{EI} \qquad dv = \mp\frac{Mx\,ds}{EI} \qquad d\phi = \pm\frac{M\,ds}{EI} \tag{10.13a}$$

In these and the following expressions, if two signs are shown, the upper refers to the left half arch, and the lower to the right.

In addition to the angular rotation $d\phi$, the elements ds will be uniformly compressed or stretched by normal forces N, temperature variations, and shrinkage. If $\Delta\,ds$ is the change of ds due to any of these actions, it is seen, from Fig. 10.6*d*, that

$$du = \Delta\,ds\cos\theta \qquad dv = \Delta\,ds\sin\theta \tag{10.14}$$

An axial force N results in $\Delta\,ds = N\,ds/EA$, and hence in horizontal and vertical displacements

$$du = \frac{N\,ds\cos\theta}{EA} \qquad dv = \frac{N\,ds\sin\theta}{EA} \tag{10.14a}$$

At any point of the arch, x, y, the moment M, and the axial force N are the resultant effects of the three crown quantities M_c, H_c, and V_c and of the external loads acting on the half-arch cantilever in which the particular section is located. They can be calculated by statics (see Fig. 10.6*b*) and are tabulated below:

Force and moment at section x, y

Due to.....	M_c	H_c	V_c	External loads
M	M_c	$H_c y$	$-V_c x$	M_0
N	0	$H_c\cos\theta$	$V_c\sin\theta$	N_0

The signs in this table are valid for both halves of the arch. In this connection it is important to note that for the right half arch x and θ are negative, whereas y is positive by the sign convention given in Fig. 10.6*a*. It should also be noted that external gravity loads result in negative M_0 (see Fig. 10.6*b*). N_0 at any section is the component, in the direction of the tangent to the arch axis, of all the external loads located between that section and the crown; gravity loads therefore result in positive N_0.

By substituting the values M and N from the table into Eqs. (10.13*a*) and (10.14*a*) and integrating for the left half from 0 to $+s/2$, and for the right half from 0 to $-s/2$, one obtains separately the crown displacements u and v for either half. If these are substituted in Eqs. (10.12), they result in three simultaneous equations for H_c, M_c, and V_c. If any particular action, for example, that of H_c, results in equal displacements for both halves, these can obviously be omitted from Eqs. (10.12), since equal terms on both sides of an equation cancel. For example, H_c results in equal vertical displacements v_l and v_r, as is seen directly from Fig. 10.6*c* (the corresponding behavior of the right half is obtained by mirroring the entire figure about the vertical axis through the crown). Hence, the contribution of H_c to the vertical displacements can be omitted in the second of Eqs. (10.12). On the other hand, the horizontal crown displacements caused by H_c are equal in magnitude but opposite in sign, since the crown section of the left cantilever is displaced to the left (see Fig. 10.6*b*), and that of the right cantilever to the right. Hence, these displacements must be entered in the first of Eqs. (10.12).

Scanned with CamScanner

Table 10.1 Crown displacement of half arch of Fig. 10.7: All integrals $\int_0^{+s/2}$ for left half; $\int_0^{-s/2}$ for right half; multiply by $1/E$ [Art. 10.4

Caused by bending

	$+M_c$	$+H_c$	$+V_c$	$+M_0$
u	$\pm M_c \int \frac{y\,ds^*}{I}$	$\pm H_c \int \frac{y^2\,ds}{I}$	Cancels	$\pm \int \frac{M_0 y\,ds}{I}$
v	Cancels	Cancels	$\pm V_c \int \frac{x^2\,ds}{I}$	$\mp \int \frac{M_0 x\,ds}{I}$
ϕ	$\pm M_c \int \frac{ds}{I}$	$\pm H_c \int \frac{y\,ds^*}{I}$	Cancels	$\pm \int \frac{M_0\,ds}{I}$

Caused by arch shortening and temperature

	$+H_c$	$+V_c$	$+N_0$	$+t^\circ$	$+\Delta t^\circ$
u	$\pm H_c \int \frac{\cos^2\theta\,ds}{A}$	Cancels	$\pm N_0 \int \frac{\cos\theta\,ds}{A}$	$\mp\, \omega t^\circ E \int \cos\theta\,ds$	Cancels
v	Cancels	$\pm V_c \int \frac{\sin^2\theta\,ds}{A}$	Cancels	Cancels	$\mp\, \Delta t^\circ\, \omega E \int \frac{x\,ds}{I}$
ϕ	0	0	0	0	$\pm\, \Delta t^\circ\, \omega E \int \frac{ds}{I}$

* These expressions are zero when x and y are measured from the elastic center.

In Table 10.1 are given the crown displacements caused by the various actions, separately for both halves. They must be substituted in Eqs. (10.12) to determine the three redundants. In this table the notation "cancels" designates displacements equal in sign and magnitude for both halves, which cancel if substituted in Eqs. (10.12). For simplicity, all values in the table are multiplied by E.

In addition to the displacements caused by the crown forces and the external loads (which include the weight of the arch), those resulting from temperature changes and shrinkage must be considered just as in the case of the two-hinged arch. In fact, these influences are of more consequence for the fixed than for the two-hinged arch, since the latter, being free to rotate at the supports, is better able to accommodate itself to changes in shape without excessive stress.

A uniform temperature increase of amount t° causes an elongation $\Delta\,ds = \omega t^\circ\,ds$ which, if substituted in Eqs. (10.14) and integrated over the

respective half arches, gives the corresponding crown displacements. Likewise, a temperature differential between top and bottom fiber (Fig. 10.5*d* and *e*) results in a rotation $d\phi$, given by Eq. (10.8). This must be substituted in Eqs. (10.13) and similarly integrated to result in the corresponding crown displacements. These values are shown in Table 10.1. The general information as to range of temperature and method of accounting for shrinkage given in the article on two-hinged arches is valid for the fixed arch.

If the displacements of the table are substituted in Eqs. (10.12), the second equation contains only V_c as an unknown and hence can be solved for this quantity. The first and third equations, however, contain both H_c and M_c, resulting in two simultaneous equations which are awkward to solve and, when solved, lead to rather lengthy expressions for these two quantities. This complication can be overcome by a suitable transformation of coordinates.

Consider the first term of the first row and the second term of the third row of the displacement table; if $\int y\,ds/I$ could be made zero, the first of Eqs. (10.12) would contain only H_c as an unknown, and the third only M_c. Obviously, for the location of the coordinate axes shown in Fig. 10.6*a*, this integral is not zero, since y is positive throughout. It is possible, however, to shift the origin to a position which will make this integral vanish. To visualize the meaning of this shift, assume the arch axis to be loaded by fictitious loads equal to $1/I$ at every point, as shown in Fig. 10.7*a*. Then, since y_1 is the lever arm of any of these forces about the origin, $\int y_1\,ds/I = 0$ shows that the sum of the moments of all these forces about the x axis is to be zero; i.e., the axis is to pass through the center of these forces or is to be coincident with their resultant. The coordinate origin determined in this manner is known as the *elastic center* of the arch. By the general formula for the location of the resultant of parallel forces,

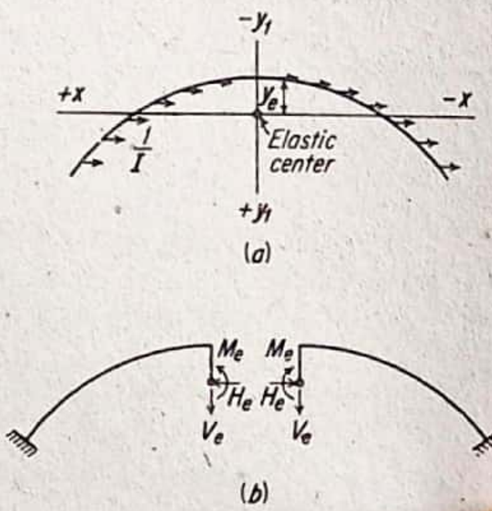


Fig. 10.7

Scanned with CamScanner

the distance y_e of the elastic center from the center of the crown is then found from

$$y_e = \frac{\int_0^{s/2} (y\, ds/I)}{\int_0^{s/2} (ds/I)} \tag{10.15}$$

By symmetry these integrals need be extended only over the half arch.

Let y_1 designate the ordinate of any point on the arch axis measured from this new origin, as shown in Fig. 10.7*a*. Now, assume that the elastic center is joined to the crown section by a rigid, fictitious lever, as shown separately for each half in Fig. 10.7*b*. Instead of introducing the three unknown quantities M_c, H_c, and V_c at the crown, introduce three similar quantities M_e, H_e, and V_e at the ends of these fictitious levers, positive as shown. Then the previously tabulated expressions for u, v, and ϕ refer to the new origin (end of levers) if, in them, y is replaced by y_1, and M_c, H_c, and V_c by M_e, H_e, and V_e. Equations (10.12) are now valid for the ends of these levers. Since the levers are regarded as rigidly connected to their respective crown sections, and the two halves are fitted together to form the complete arch, the ends of the two levers cannot separate, no matter how the arch deforms. Thus the displacements u, v, and ϕ must be the same for the ends of both levers.

Since the origin is now chosen such that $\int y_1\, ds/I = 0$, the first term of the first row and the second term of the third row in Table 10.1 vanish. (These terms are indicated by asterisks in the table.) Hence, if the remaining terms of the first, second, and third rows of the table are substituted, respectively, in the first, second, and third of Eqs. (10.12), each results in one equation with one unknown, H_e, V_e, and M_e in that order. Since in each individual expression the respective integral for the left half arch is added to that for the right half, integration can be extended directly from $-s/2$ to $+s/2$, rather than writing two integrals for each term. The three redundant quantities, referred to the elastic center, then become

$$H_e = \frac{-\int_{-s/2}^{s/2} \frac{M_0 y_1\, ds}{I} - \int_{-s/2}^{s/2} \frac{N_0 \cos\theta\, ds}{A} + Et^\circ \omega l - E\,\Delta t^\circ\, \omega \int_{-s/2}^{s/2} \frac{y_1\, ds}{t}}{\int_{-s/2}^{s/2} \frac{y_1^2\, ds}{I} + \int_{-s/2}^{s/2} \frac{\cos^2\theta\, ds}{A}} \tag{10.16}$$

$$V_e = \frac{\int_{-s/2}^{s/2} (M_0 x\, ds/I) - \int_{-s/2}^{s/2} (N_0 \sin\theta\, ds/A)}{\int_{-s/2}^{s/2} (x^2\, ds/I) + \int_{-s/2}^{s/2} (\sin^2\theta\, ds/A)} \tag{10.17}$$

$$M_e = \frac{-\int_{-s/2}^{s/2} (M_0\, ds/I) - E\,\Delta t^\circ\, \omega \int_{-s/2}^{s/2} (ds/t)}{\int_{-s/2}^{s/2} (ds/I)} \tag{10.18}$$

where all integrals extend over the entire arch, as indicated.

Once these quantities are determined, it is more convenient to work with crown moments and forces (Fig. 10.6*b*) than with those referred to the elastic center (Fig. 10.7*b*). As is seen directly from this figure,

$$H_c = H_e \qquad V_c = V_e \qquad M_c = M_e - H_e y_e \tag{10.19}$$

Equations (10.16) to (10.18) account for all influences that act on symmetrical fixed arches. In any particular design it will often be found that certain of these influences are small compared with others and can be neglected. The analogous situation for the two-hinged arch was discussed in Art. 10.3. As in that case, the influence of rib shortening caused by axial forces N is small except for unusually flat and thick arches. Except for such cases, therefore, the second term in both numerator and denominator of Eqs. (10.16) and (10.17) can be omitted. The last term in the numerator of Eq. (10.16) will often be found to be small in comparison with other terms. Indeed, for an arch with constant cross section this term vanishes. It does so because the elastic center was chosen such that $\int y_1\, ds/I = 0$, which, for constant I, is the same as $\int y_1\, ds = 0$. This makes $\int y_1\, ds/t = 0$ if t is constant. It is seen, therefore, that the magnitude of that term in Eq. (10.16) depends essentially on the ratio of the depths at springing and crown and will usually be negligible. Finally, the term containing Δt° in Eq. (10.18) must be included only in the rather rare case of a roof arch not insulated at the top.

Hence, the following simplified expressions are usually accurate enough for purposes of design:

$$H_e = \frac{-\int_{-s/2}^{s/2} (M_0 y_1\, ds/I) + Et^\circ \omega l}{\int_{-s/2}^{s/2} (y_1^2\, ds/I)} \tag{10.16a}$$

$$V_e = \frac{\int_{-s/2}^{s/2} (M_0 x\, ds/I)}{\int_{-s/2}^{s/2} (x^2\, ds/I)} \tag{10.17a}$$

$$M_e = \frac{-\int_{-s/2}^{s/2} (M_0\, ds/I)}{\int_{-s/2}^{s/2} (ds/I)} \tag{10.18a}$$

A word of warning should be included in connection with these simplified equations. Although under the specific conditions which were enumerated, the omitted terms are usually negligibly small, there is no way of definitely ascertaining this fact except by computing them. It is therefore suggested, particularly for closely designed arches of significant spans, that the simplified equations be used for preliminary design but that in computing final stresses the influence of the omitted terms be at least estimated numerically and included in the final expressions if found significant.

Scanned with CamScanner

10.5 Evaluation of Integrals The integrals which occur in [Art. 10.
expressions for the redundants of both the two-hinged arch [Eqs. (10.1
and (10.11*a*)] and the fixed arch [Eqs. (10.16) to (10.18) and (10.16*a*)
(10.18*a*)] can be evaluated by direct integration only in a few simple cas
For this reason it is necessary, in general, to approximate the integra
with sums of a finite number of terms.

For this purpose the arch axis (not the span) is generally divided in
a number of equal intervals Δs. A maximum of 10 intervals for the ha
arch is generally sufficient; 6 to 8 intervals may often be used for sma
secondary structures. The pertinent quantities entering a particu
integral, such as y_1, M_0, and I for $\int M_0 y_1\, ds/I$, are then computed for t
midpoint of each individual interval Δs. Then

$$\int \frac{M_0 y_1\, ds}{I} \cong \sum \frac{M_{0n} y_{1n}}{I_n}\, \Delta s$$

where the subscript n refers to the values M_0, y_1, and I at the midpo
of the nth interval. The other integrals in Eqs. (10.11) and (10.16)
(10.18) are computed in a similar manner by summation. Attention mu
be paid to the signs of the various quantities. Thus, y_1 is negative
measured upward from the elastic center of the fixed arch (see Fig 10.7
x is negative if measured to the right of the crown of the fixed arch, but
positive throughout for the two-hinged arch, as is evident from Figs. 10.
and 10.5*a*. The importance of this is evident, for instance, in connecti
with Eq. (10.17). If an arch is symmetrically loaded, M_0 and N_0 are equ
at corresponding points of the two half arches. On the other hand, for t
left half arch x and $\sin\theta$ are positive, whereas for the right half they a
negative. Each contribution to the sums of both numerator integrals ma
by an element on the left half is, therefore, canceled by the equal and o
posite contribution made by the corresponding element on the right. Co
sequently, V_e (and thereby V_c) is zero for symmetrical loads, in analo
with a simple beam which has zero shear at midspan, if symmetrical
loaded.

For fixed arches, the location of the elastic center [Eq. (10.15)] is lik
wise calculated by replacing the integrals with corresponding sums. T
computation of these sums is best arranged in tabular form, as demo
strated in the design example of Art. 10.8.

Moments of inertia can be computed for the entire concrete sectio
including the tension portion, without regard to reinforcement.

10.6 Preliminary Arch Design The analysis discussed in the
ceding articles can be carried out only if loads, as well as all dimension
the arch, are definitely known. Before such an analysis can be made, it
therefore necessary to determine the shape and weight of the arch by

preliminary design. In general, only the span, the rise, and the loads superimposed on the arch are known. (In cases in which the designer is free to select the rise it is important to consider that the horizontal thrust decreases as the ratio of rise to span increases, with a consequent saving in cost of abutments.) It is then required to determine the shape of the arch axis and the dimensions of the cross sections at various points and, from these, to find the weight of the arch proper. Once these quantities are preliminarily determined, an exact stress analysis can be made. Should this analysis indicate the necessity for a considerable change in the assumed dimensions, a second, final analysis must be made, based on the corrected dimensions. Since such computations are very time-consuming, it is desirable to determine the shape of the arch by preliminary design as accurately as possible, so that subsequent corrections are held to a minimum.

The axis of the arch is often made to coincide with the equilibrium or string polygon for dead load. If this is done, bending moments are caused by live load only. This polygon can be drawn only after the weight of the arch is determined. For roof arches, in which dead loads are mostly uniform along the axis the parabola is a close approximation to the dead-load polygon, and, with the designations of Fig. 10.9, the equations of the axis and the slope are

$$y = 4rlc^2 \qquad (10.19a)$$

$$\tan\theta = 8rc \qquad (10.19b)$$

Next it is necessary to obtain an estimate of the maximum moments, thrusts, and shears for the purpose of determining the required cross section. To this end superimposed loads are determined, and a rough estimate is made of the weight of the arch proper. If temperature stresses need consideration, the limiting temperatures are also determined. With these data it is possible to determine M, V, and H from Tables 10.2 and 10.3.

For roof arches, the dead load is generally approximately uniformly distributed along the arch axis. The load per horizontal foot of span is therefore distributed as shown in Fig. 10.9. In order that Tables 10.2 and 10.3 may be used this load can be divided into a uniform load g and a variable load of maximum intensity g' at the springing. The tables then allow one to compute separately the influences of each of these two loads,

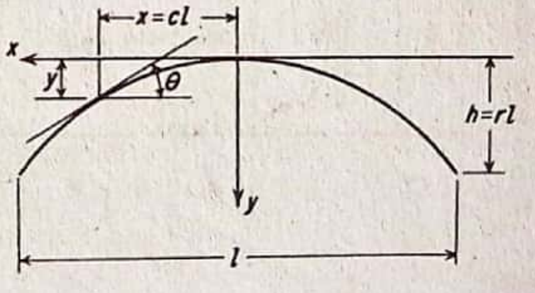
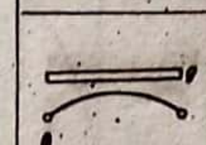
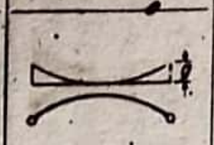
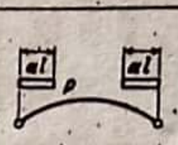
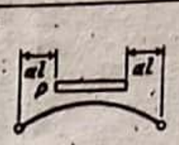
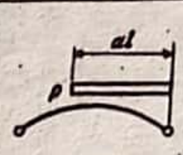
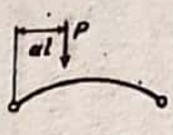


Fig. 10.8

Scanned with CamScanner

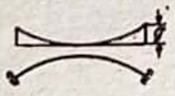
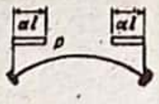
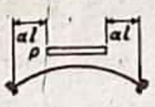
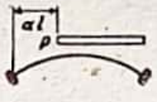
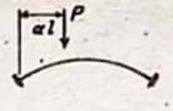
Table 10.2 Moments and reactions of two-hinged parabolic arches*

	Case I	Case II	Case III	Case IV	Case V	Case VI	Case VII	Case VIII	Case IX
								Uniform temperature change	Temperature differential of $\Delta t°$
R_l	$\frac{ql}{2}$	$\frac{q'l}{6}$	pal	$\frac{pl}{2}(1-2\alpha)$	$\frac{pal}{2}(2-\alpha)$	$\frac{pa^2l}{2}$	$P(1-\alpha)$	None	None
R_r	$\frac{ql}{2}$	$\frac{q'l}{6}$	pal	$\frac{pl}{2}(1-2\alpha)$	$\frac{pa^2l}{2}$	$\frac{pal}{2}(2-\alpha)$	$P\alpha$	None	None
H	$\frac{ql^2}{8h}$	$\frac{q'l^2}{42h}$	$\frac{pl^2}{8h}\alpha^2(2\alpha^2-5\alpha^2+5)$	$\frac{-pl^2}{8h}(2\alpha^4-5\alpha^4+5\alpha^2-1)$	$\frac{pl^2}{16h}\alpha^2(2\alpha^2-5\alpha^2+5)$	$\frac{pl^2}{16h}\alpha^2(2\alpha^2-5\alpha^2+5)$	$\frac{5Pl}{8h}\alpha(\alpha^2-2\alpha^2+1)$	$\frac{15EI_c\omega t°}{8h^2}$	$\frac{5EI_c\omega\ \Delta t°}{4l_eh}$
M_e	None	$-\frac{q'l^2}{338}$	$\frac{-pl^2}{8}\alpha^2(2\alpha^2-5\alpha^2+1)$	$\frac{pl^2}{8}\alpha^2(2\alpha^2-5\alpha^2+1)$	.....	.....	$\frac{(1-\alpha)l}{8}P(5\alpha^2-5\alpha+4)$	$\frac{-15EI_c\ \omega t°}{8h}$	$\frac{-5EI_c\omega\ \Delta t°}{4l_e}$
$M_{l/4}$	None	$\frac{q'l^2}{234}$	.....	.....	$\frac{-pl^2}{64}(6\alpha^4-15\alpha^4+23\alpha^2-16\alpha+2)$ †	$\frac{-pl^2}{64}\alpha^2(6\alpha^2-15\alpha^2+7)$ ‡	$\frac{1}{4}(R_nl-Hh)$ ¶ $\frac{1}{4}(R_ll-Hh)$ ¶	$\frac{-45EI_c\ \omega t°}{32h}$	$\frac{-15EI_c\omega\ \Delta t°}{16l_e}$

* According to Eqs. (10.19).

† $\frac{l}{4} \le al \le \frac{l}{2}$ ‡ $\frac{l}{2} \le al \le \frac{3l}{4}$ ¶ $al \le l/4$; $al \ge l/4$

Table 10.3 Moments and reactions of fixed parabolic arches*

	Case I	Case II	Case III	Case IV	Case V	Case VI	Case VII	Case VIII	Case IX
								Uniform temperature change	Temperature differential of $\Delta t°$
R_l	$\frac{ql}{2}$	$\frac{q'l}{6}$	pal	$\frac{pl}{2}(1-2\alpha)$	$\frac{pl}{2}\alpha(\alpha^2-2\alpha^2+2)$	$\frac{pl}{2}(1+\alpha)(1-\alpha)^2$	$P(1-\alpha)^2(1+2\alpha)$	None	None
R_r	$\frac{ql}{2}$	$\frac{q'l}{6}$	pal	$\frac{pl}{2}(1-2\alpha)$	$\frac{pl}{2}\alpha^2(2-\alpha)$	$\frac{pl}{2}(1-2\alpha^2+\alpha^4)$	$P\alpha^2(3-2\alpha)$	None	None
H	$\frac{ql^2}{8h}$	$\frac{q'l^2}{56h}$	$\frac{pl^2}{4h}\alpha^2(6\alpha^2-15\alpha+10)$	$\frac{-pl^2}{8h}(12\alpha^4-30\alpha^4+20\alpha^3-1)$	$\frac{pl^2}{8h}\alpha^2(6\alpha^2-15\alpha+10)$	$\frac{pl^2}{8h}(1-\alpha)^2(6\alpha^2+3\alpha+1)$	$\frac{15}{4}\frac{Pl}{h}\alpha^2(1-\alpha)^2$	$\frac{45EI_c\omega t°}{4h^2}$	None
M_{l_0}	None	$\frac{-q'l^2}{210}$	$-\frac{pl^2}{2}\alpha^2(1-\alpha)^2(1-2\alpha)$	$\frac{pl^2}{2}\alpha^2(1-\alpha)^2(1-2\alpha)$	$-\frac{pl^2}{2}\alpha^2(1-\alpha)^2$	$\frac{pl^2}{2}\alpha^2(1-\alpha)^2$	$-\frac{Pl}{2}\alpha(1-\alpha)^2(2-5\alpha)$	$\frac{15EI_c\omega t°}{2h}$	$\frac{-EI_c\omega\ \Delta t°}{l_e}$
M_{r_0}	None	$\frac{-q'l^2}{210}$	$-\frac{pl^2}{2}\alpha^2(1-\alpha)^2(1-2\alpha)$	$\frac{pl^2}{2}\alpha^2(1-\alpha)^2(1-2\alpha)$	$\frac{pl^2}{2}\alpha^2(1-\alpha)^2$	$-\frac{pl^2}{2}\alpha^2(1-\alpha)^2$	$\frac{Pl}{2}\alpha^2(1-\alpha)(3-5\alpha)$	$\frac{15EI_c\omega t°}{2h}$	$\frac{-EI_c\omega\ \Delta t°}{l_e}$
M_0	None	$-\frac{q'l^2}{560}$	$-\frac{pl^2}{4}\alpha^2(1-2\alpha)(2-\alpha)$	$\frac{pl^2}{4}\alpha^2(1-2\alpha)(2-\alpha)$	$-\frac{pl^2}{8}\alpha^2(1-2\alpha)(2-\alpha)$ †	$\frac{pl^2}{8}\alpha^2(1-2\alpha)(2-\alpha)$ ‡	$-\frac{Pl}{4}\alpha^2(5\alpha^2-10\alpha+3)$	$\frac{15EI_c\omega t°}{4h}$	$\frac{-EI_c\omega\ \Delta t°}{l_e}$

* According to Eqs. (10.19).

† $0 \le al \le \frac{l}{n}$ ‡ $0 \le al \le \frac{l}{n}$

Scanned with CamScanner



g = load per foot of axis
$g/\cos\theta$ = corresponding load per foot of span

Fig. 10.9

which must be added to result in the final M, V, and H. Live load must be so placed as to give maximum moments or forces; this will generally require partial loading of the span. The necessary formulas for partial loading are included in the tables; the load positions, determined by $\alpha = a/l$, are as shown in the sketches. Positions of loads and values of α which result with good accuracy in maximum moments at the crown, quarter point, or springing are given for both types of arches in Fig. 10.10.

In order to obtain simple expressions for Tables 10.2 and 10.3, it was assumed that

$$I = \frac{I_c}{\cos\theta}$$

Even considerable deviation from this relationship has relatively little influence and leads to satisfactory accuracy.

The length of the *half axis* s for parabolic arches is very nearly

$$s = \frac{l}{2}\left(1 + \tfrac{8}{3}r^2\right) \tag{10.20}$$

Once approximate values of M, N, and H are found for the critical sections from Table 10.2 or 10.3, the required cross-sectional dimensions are determined in the usual manner for bending plus axial thrust. Reinforcement is usually provided symmetrically near both faces. For reasons

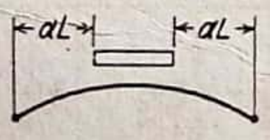
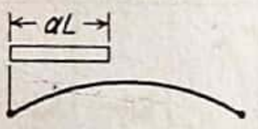
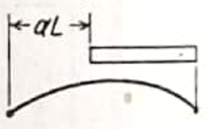
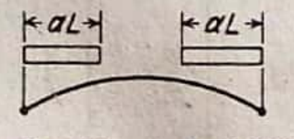
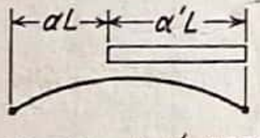
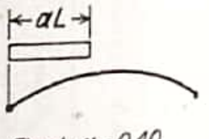
	Crown	Left Quarter Point	Left Springing
Positive Moment	 Two-hinged $\alpha=0.350$ Fixed $\alpha=0.375$	 Two-hinged $\alpha=0.425$ Fixed $\alpha=0.400$	 Fixed $\alpha=0.40$
Negative Moment	 Two-hinged $\alpha=0.350$ Fixed $\alpha=0.375$	 Two-hinged $\alpha'=0.575$ Fixed $\alpha=0.400$	 Fixed $\alpha=0.40$

Fig. 10.10 Live-load positions for maximum moment.

of appearance the depth is often increased gradually from crown to springing or held constant, but it is hardly ever decreased toward the springing.

With dimensions of the cross sections determined as required by strength and appearance, the weight of the arch is computed. If the new total dead load differs materially from that assumed in the beginning, the preliminary design procedure is repeated with adjusted loads, and dimensions are correspondingly corrected.

Since, at this stage, all loads are known, it is now possible to obtain the final location of the arch axis by passing a string polygon for dead load through the midpoints of the crown and springing sections. For this purpose, as well as for the subsequent exact analysis, the half axis is generally divided into six to ten equal sections (see Art. 10.5), and the dead load of each section applied at its center. A smooth curve which is tangent to this string polygon then represents the final location of the arch axis. Accurate values of M, N, and V are now determined by elastic analysis at the crown, quarter point, and springing, and at such additional points as may be necessary. The difference between these accurate values and the approximate ones obtained from the preliminary design will require minor adjustments of cross-sectional dimensions, which can often be made merely by changing the reinforcement without alteration of overall size. Even if the thickness and width of the arch are changed in this stage of design, the elaborate elastic analysis need not be repeated for the adjusted sections unless these adjustments are quite sizable. This is due to the fact that the magnitudes of M, N, and V caused by external loads depend primarily on the ratios of the moments of inertia along the arch to that at the crown, rather than on their absolute values. Only the stresses due to rib shortening and temperature depend directly on the absolute size of the cross section and may have to be recomputed if the dimensions change significantly. The design of a simple roof arch in Art. 10.8 illustrates the above procedure.

10.7 Hinges in Reinforced-concrete Structures It is the function of hinges to transmit safely the thrust N and the shear force S and, at the same time, to offer little resistance to rotation. An ideal hinge should be entirely free to rotate, since only then will the bending moment at the hinge be zero, as assumed in the analysis of hinged structures. Such ideal hinges cannot be constructed, since friction or other inevitable restraining factors cannot be avoided. Practically, however, it is only necessary to ensure that the flexibility of the hinge be considerably greater than that of any other portion of the structure of which it is a part. This will result in very small moments in the hinge as compared to the moments in the structure proper and, therefore, will lead only to negligible errors. The use of hinges is not restricted to arches. They are equally useful in rigid frames,

Scanned with CamScanner

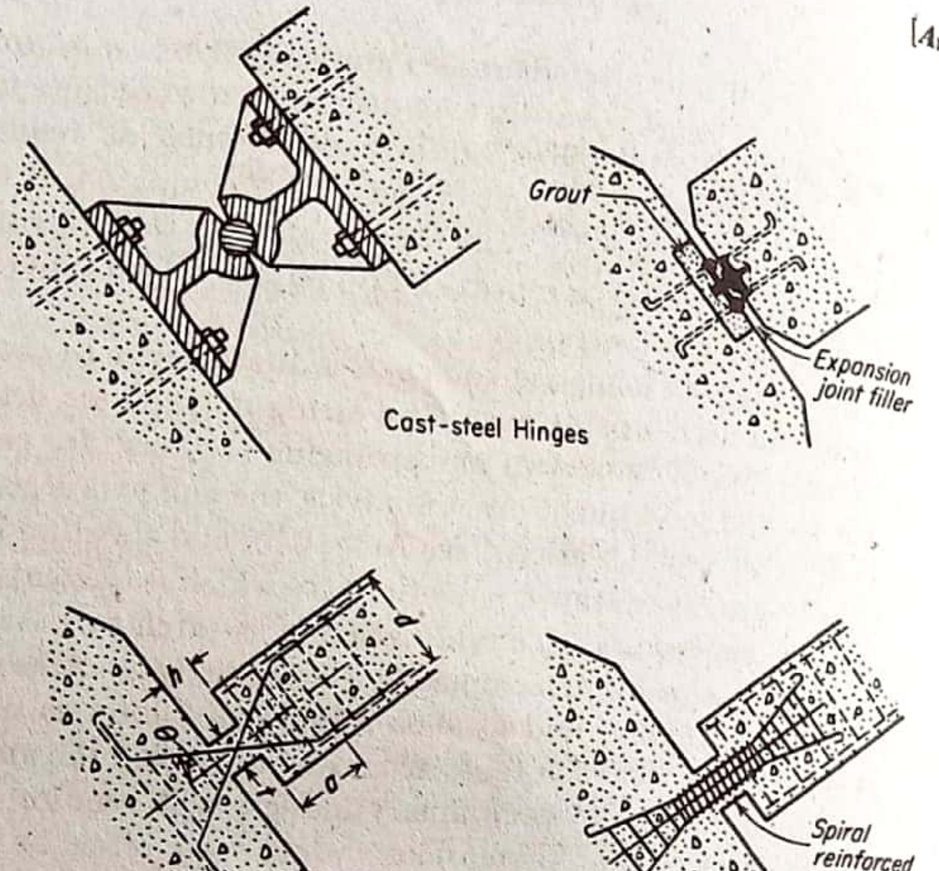


Fig. 10.11 Hinges for concrete structures.

in bridges as well as in buildings, particularly for long-span single-story frames. They reduce or, in the case of three-hinged spans, eliminate the stresses caused by rib shortening, by temperature, and by slight foundation movements. For these reasons a considerable reduction in the dimensions and weight of the structure and foundation can often be achieved by their use.

The main practical types of hinges for concrete structures are given in Fig. 10.11. The steel hinges shown there result in more perfect hinge action than the concrete hinges, but are considerably more expensive. Their use, today, is restricted to unusually heavy structures. Of the two types of concrete hinges, named after the French engineers who developed them, the Mesnager hinge ensures greater freedom of rotation and, except for very large thrusts, is the most satisfactory hinge presently in use.

In order to obtain maximum flexibility in a Mesnager hinge, it has been recommended that the hinge opening h should at least be equal to the concrete thickness t. A value $h = 1.3t$ is recommended by some. However, hinges with smaller openings have been used successfully. For the same purpose of maximum flexibility, the crossed steel bars should not be too

thick and short. On the other hand, if their diameter were too small in relation to their length, they would be likely to buckle. For this reason the slenderness ratio L/r of the hinge bars should be between the limits of 20 and 40, L being the length of the inclined bar between concrete faces (that is, $h/\cos\theta$), and r the radius of gyration of the bar (that is, $D/4$ for round bars of diameter D). The length of embedment of the hinge bars on either side of the hinge should be at least equal to that prescribed for dowels connecting columns to footings.

To find the required area of the hinge bars, it is assumed that they form a triangular truss which transmits the normal and shear forces N and S, as shown in Fig. 10.12. It is easily seen that the compression stress in bars 1 is equal to

$$f'_s = \frac{N}{A'_s \cos\theta} + \frac{S}{A'_s \sin\theta} \tag{10.21}$$

where A'_s is the total combined area of all hinge bars. This stress should not exceed 30 per cent of the yield point of the hinge bars. The large factor of safety, $1/0.3 = 3.33$, is introduced for the following reason: Even though, by the above procedure, the bars are assumed to be subjected only to axial compression, like members of a truss, any rotation actually occurring at the hinge bends the bars and induces corresponding flexural stresses. Such rotations actually do take place during the lifetime of the structure and are caused primarily by changes in live load and in temperature. These flexural stresses superpose on the computed compression and correspondingly increase the values of the actual maximum stresses in the bars. Rather than to attempt computing these additional stresses, it is generally satisfactory to keep the compression stress f'_s sufficiently low so that the bars will not be overstressed by superposed bending.

The inclined bars, transmitting their forces to the concrete by bond along the embedded length, exert a bursting force which must be resisted by lateral reinforcement (stirrups and ties), as shown in Fig. 10.11. Only the part of the lateral reinforcement within a distance $a = 8D$ from the face of the concrete is considered effective in resisting the bursting force. The stress in the lateral reinforcement can be computed from

$$f''_s = \frac{(N/2)\tan\theta + Sa/jd}{0.005ab + A''_s} \tag{10.22}$$

where, in addition to previously defined quantities, A''_s is the combined area of lateral stirrups or ties located within $a = 8D$ from the free face of the hinge, j

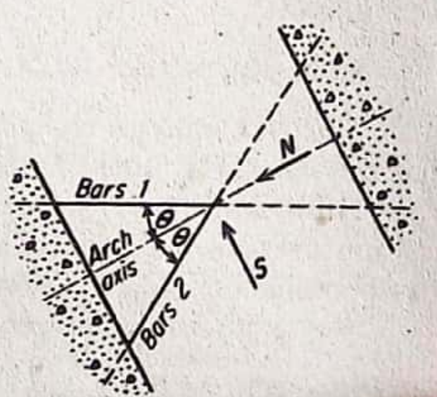


Fig. 10.12

Scanned with CamScanner

can be taken as 0.9, d is shown in Fig. 10.11, and b is the horizontal width of the hinge, equal, in most cases, to the width of the arch rib.

More detailed information on concrete hinges can be found in a paper by G. C. Ernst; most texts on steel bridges give adequate data on steel hinges of the type used for both steel and concrete arches and frames.

10.8 Design of Two-hinged, Tied Roof Arch Arches of the type shown in Fig. 10.2 with 90-ft span are to be spaced at 20-ft intervals, to support a fireproof, insulated roof. The roof itself is to consist of precast slabs spanning between arches and weighing 40 psf. Four-ply tar and gravel roofing to cover the slabs weighs 5 psf. To account for the effects of wind and snow a live load of 35 psf is assumed.

The columns of Fig. 10.2 supporting the arch cannot develop sufficient rigidity to serve as fixed supports. A two-hinged arch is therefore indicated. In addition, if the horizontal thrust were transmitted to the supporting columns and frames, they would become excessively heavy and costly. For this reason a tied arch of the type shown in Fig. 10.13 will be used. A 15-ft rise has been selected, resulting in a rise-span ratio of 1/6, and space. Computations of moments, etc., caused by small secondary loads, such as from the weight of the tie rod and the hangers, have been omitted, since they would complicate and lengthen the illustrative computations without adding new features. In actual design practice the influence of such loads should be included in the computations.

Preliminary design The loads per linear foot of arch axis are:

Dead load:

Concrete slabs:	40×20	= 800 lb per ft
Roofing:	5×20	= 100 lb per ft
Arch (assumed)		= 300 lb per ft
Total		= 1200 lb per ft

Live load:

Snow plus wind:	35×20	= 700 lb per ft

The load, uniform along the axis, results in distribution along the span as shown in Fig. 10.9. With θ computed from Eq. (10.19b), $g' = 380$ lb per ft for dead plus live load, and $g' = 240$ lb per ft for dead load alone. From the information of Table 10.2, the following moments and forces are obtained for the trial design:

Maximum horizontal reaction (loading Fig. 10.14a):

$$H = \frac{gl^2}{8h} + \frac{g'l^2}{42h} = 133 \text{ kips}$$

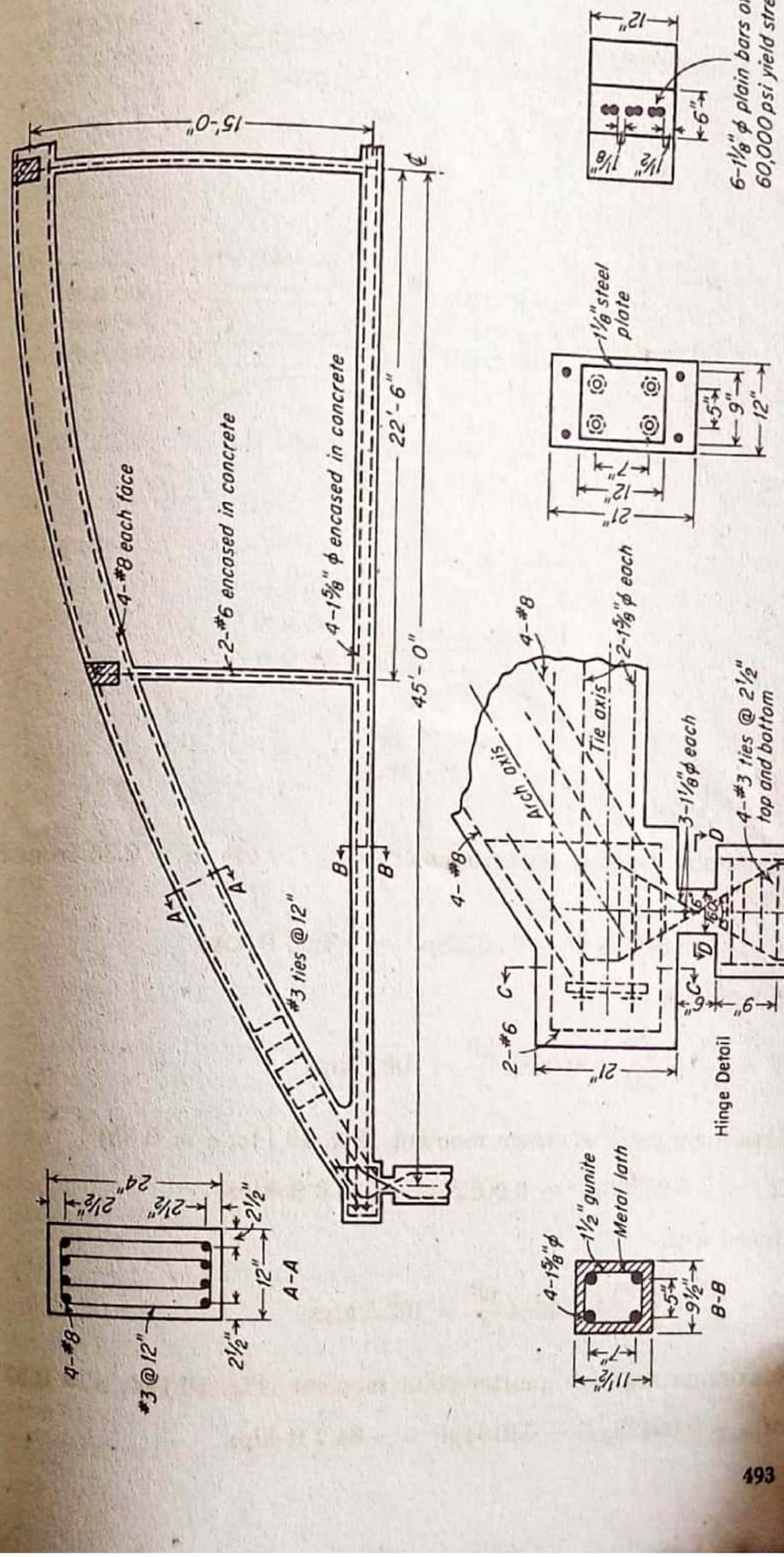


Fig. 10.13 Two-hinged, tied roof arch.

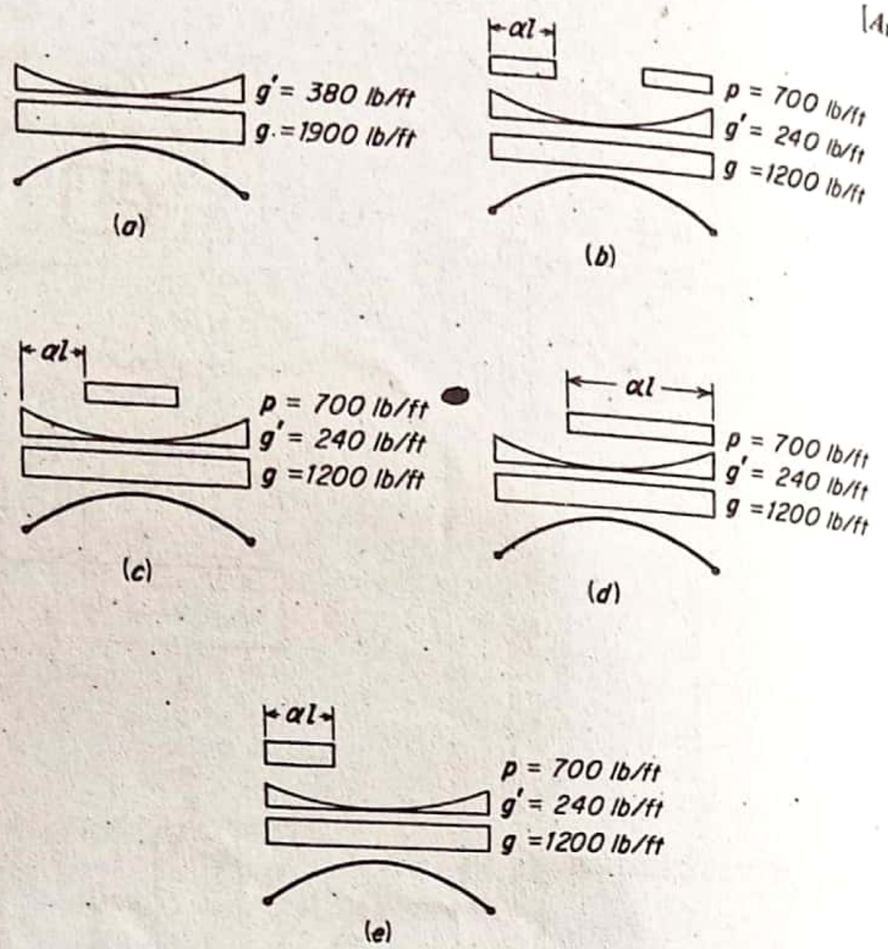


Fig. 10.14

Maximum negative crown moment (Fig. 10.14*b*; $\alpha = 0.35$ from Fig. 10.10):

$$M_c = -0.00296g'l^2 - 0.00725pl^2 = -46.5 \text{ ft-kips}$$

combined with

$$H = \frac{gl^2}{8h} + \frac{g'l^2}{42h} + 0.0685\,\frac{pl^2}{h} = 109.7 \text{ kips}$$

Maximum positive crown moment (Fig. 10.14*c*; $\alpha = 0.35$):

$$M_c = -0.00296g'l^2 + 0.00725pl^2 = 35.0 \text{ ft-kips}$$

combined with

$$H = \frac{gl^2}{8h} + \frac{g'l^2}{42h} + 0.0564\,\frac{pl^2}{h} = 105.5 \text{ kips}$$

Maximum negative quarter-point moment (Fig. 10.14*d*; $\alpha = 0.575$):

$$M_{l/4} = 0.00428g'l^2 - 0.0164pl^2 = -84.2 \text{ ft-kips}$$

combined with

$$H = \frac{gl^2}{8h} + \frac{g'l^2}{42h} + 0.0760\,\frac{pl^2}{h} = 111 \text{ kips}$$

$$R_l = \frac{p\alpha^2 l}{2} + \frac{g'l}{6} + \frac{gl}{2} = 75 \text{ kips}$$

$V_{l/4}$ = vertical shear at quarter point
$= 75 - 22.5 \times 1.2 - 0.240 \times {}^{90}\!/_{8} = 45$ kips

The inclination $\theta = 18°25'$ is determined from Eq. (10.19*b*). Then

$T_{l/4}$ = axial thrust at quarter point
$= V_{l/4} \sin\theta + H\cos\theta$
$= 45 \times 0.316 + 111 \times 0.95 = 119.3$ kips

Maximum positive moment at quarter point (Fig. 10.14*e*; $\alpha = 0.425$):

$$M_{l/4} = 0.00428g'l^2 + 0.0164pl^2 = 100.8 \text{ ft-kips}$$

combined with

$$H = \frac{gl^2}{8h} + \frac{g'l^2}{42h} + 0.0435\,\frac{pl^2}{h} = 100.6 \text{ kips}$$

$$R_l = p\alpha l\left(1 - \frac{\alpha}{2}\right) + \frac{gl}{2} + \frac{g'l}{6} = 86 \text{ kips}$$

$V_{l/4} = 86 - 22.5 \times 1.9 - 0.240 \times {}^{90}\!/_{8} = 41$ kips
$T_{l/4} = 41 \times 0.316 + 102.5 \times 0.95 = 110.5$ kips

Maximum axial thrust at springing (Fig. 10.14*a*):

$H = 133$ kips (as previously computed)
$R_l = 45 \times 1.9 + 15 \times 0.380 = 92.6$ kips
$T_l = R_l \sin\theta + H\cos\theta$
$= 92.6 \times 0.538 + 133 \times 0.834 = 162$ kips

Maximum force in ties: $H = 133$ kips
Maximum crown moment: $M_c = -46.5$ ft-kips
Accompanying crown thrust: $T_c = 109.7$ kips
Maximum quarter-point moment: $M_{l/4} = 100.8$ ft-kips
Accompanying quarter-point thrust: $T_{l/4} = 110.5$ kips
Maximum thrust at springing: $T = 162$ kips

In a structure of this type, in which the entire arch rib is located below an insulated roof, no temperature differential will arise in the rib. In addition, the arch and the tie are always at substantially the same temperature. Any temperature change in the enclosed space will therefore cause the arch and the tie to expand or contract by the same amount and, for this reason, will not cause any temperature stresses in the structure.

Scanned with CamScanner

For simplicity of formwork and for good appearance, an arch of constant cross section will be used. It is consequently only necessary to design the most critical section, which is seen to be that at the quarter point. A concrete with $f'_c = 3000$ psi and intermediate-grade steel will be used.

For a 14 × 22 in. cross section with eight No. 8 bars, $p_g = 0.0204$, $m = 15.7$, and $e_b = 7.51$ in. At the quarter point,

$$e = \frac{100.8 \times 12}{110.5} = 10.95 > e_b$$

indicating that the allowable load is controlled by tension. Following the recommended methods of the ACI Code as described in Art. 5.8, $F_a = 1350$ psi and $F_b = 1350$ psi. These values, together with e_b and I_{uc}, are used in the column-interaction equation to obtain $N_b = 184$ kips and $M_b = 115$ ft-kips. If the given cross section were subjected to pure flexure, M_0 would be 71.4 ft-kips. Accordingly, the axial load of 110.5 kips will permit an allowable moment of 98 ft-kips. While this is slightly below the estimated applied moment of 100.8 ft-kips, the small difference does not justify revision at this stage in the analysis. The weight of this arch rib is 320 lb per ft, as compared with the assumed weight of 300 lb per ft. Since the final location of the arch axis obtained by means of a string polygon is likely to result in a smaller required cross section than determined in this preliminary design, 300 lb per ft will be used for the final analysis.

The tie rod must resist $H_{max} = 133{,}000$ lb. To reduce the stretch of the tie, a low unit stress of about 15,000 psi will be used. Consequently, the required tie area is $A_{tr} = 133{,}000/15{,}000 = 8.9$ in.^{2} Since the final design is likely to result in a smaller H_{max}, four 1⅝-in. plain round bars with upset threaded ends will be used, furnishing an area $A_{tr} = 8.3$ in.^{2}

Final design Since the preliminary design did not result in any change of the weight of the arch rib, as originally assumed, the final design is carried out for the same loads as before, that is, 1200 lb per ft dead load and 700 lb per ft live load.

For the purpose of drawing the dead-load string polygon and for subsequent computations, the length of the arch axis is divided into 20 equal segments Δs. From Eq. (10.20), with $l = 90$ ft and $r = \frac{1}{6}$,

$$\Delta s = l\frac{1 + \frac{8}{3}r^2}{20} = \frac{96.66}{20} = 4.83 \text{ ft}$$

The dead load per segment is $1.2 \times 4.83 = 5.80$ kips. To draw the string polygon, it is simplest first to draw to a large scale the parabolic axis used in the preliminary analysis, which is easily done by computing a sufficient number of points by means of Eq. (10.19*a*). It is sufficient to draw half the arch, as shown in Fig. 10.15. The half axis is next divided into 10 equal parts of 4.83 ft each, and the weight of each such segment, 5.8 kips, is

applied at its midpoint. An accurate string polygon for these loads is then drawn through the midpoints of crown and springing (not shown in Fig. 10.15 so as not to obscure the drawing). A curve tangent to this string polygon represents the final axis. Figure 10.15 shows that for this particular arch the final axis is very close to the original parabola. For subsequent computations the coordinates x and y of the 10 segments are accurately scaled off the drawing.

As is seen from Eq. (10.11*a*), the quantities $y\,\Delta s/I$ and $y^2\,\Delta s/I$ must be computed for the 10 segments of the half arch. For the tentative 14 × 22 in. section, $I = 11{,}600$ in.^{4} The pertinent quantities are assembled in the first four columns of Table 10.4, which summarizes the numerical calculations.

For determining the dimensions of the arch, the tie rod, and the hinges, the forces and moments caused by the following loadings must be computed:

a. MAXIMUM VERTICAL REACTION R AND MAXIMUM FORCE IN TIE ROD H. These are obtained for full live load, being placed over the entire span, so that the load per segment, dead plus live, is 9.2 kips. The corresponding reactions are $R_l = R_r = 92.0$ kips. The beam moments M_0 and the quantities $M_0 y\,\Delta s/I$ are computed at the midpoints of the 10 segments. They are entered in Table 10.4 in the columns headed "Case *a*." By virtue of symmetry, computations can be restricted to half the arch.

b. MAXIMUM POSITIVE QUARTER-POINT MOMENT. The preliminary design has shown that the positive quarter-point moment will govern the dimensions of the arch rib. Since a constant-cross-section arch was chosen,

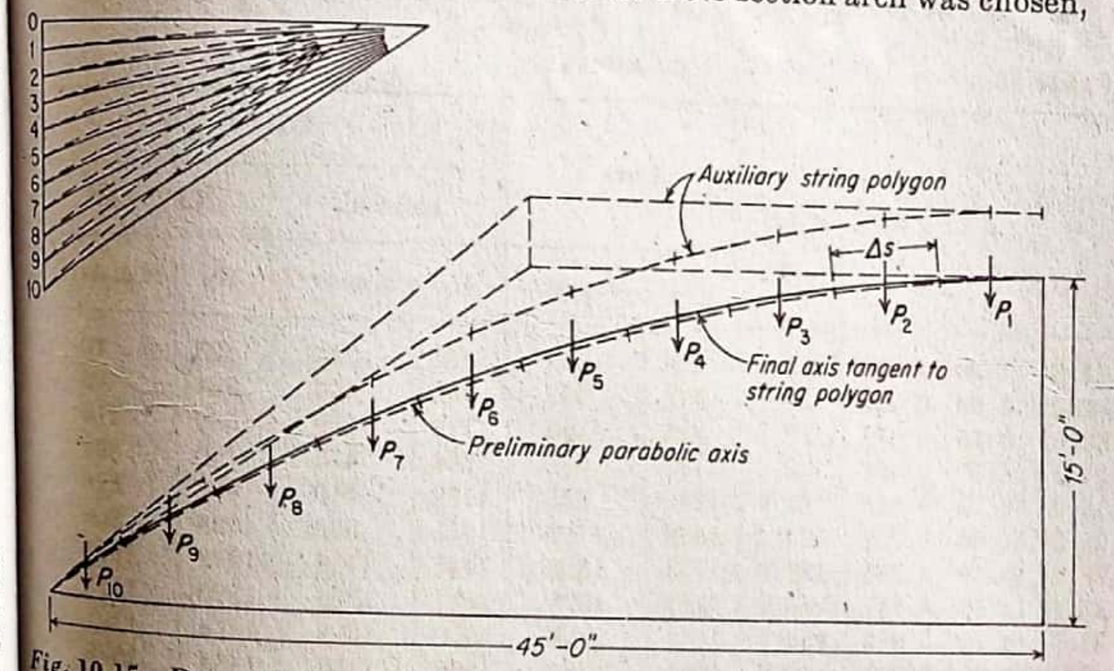


Fig. 10.15 Determination of final location of arch axis by means of dead-load string polygon.

Scanned with CamScanner

it is sufficient for our purposes to investigate only this one loading case. For a more complete investigation, the other loading cases of the preliminary design should also be computed. This is desirable even in the case of a constant-cross-section arch, in view of the approximate character of the preliminary design. It becomes mandatory if the final arch axis differs considerably from the original parabolic shape and, of course, if rib dimensions and reinforcement are varied along the span.

The exact location of the quarter point is at $x = 22.5$ ft. This point does not happen to coincide with any of the centers of the segments. Since moments and thrusts vary only very gradually in an arch subject only to distributed loads, it will be simpler and sufficiently accurate to compute the moment at that segment center located closest to the quarter point, i.e., at $x = 23.5$ ft. According to Fig. 10.10, live load should be placed from the left springing up to $x = 0.425 \times 90 = 38.3$ ft. In the summation process it is quite inconvenient to place loads at locations other than over integer segments. For this reason the first nine segments from the left springing (i.e., up to $x = 40.2$ ft) will be subjected to live load. The error so introduced is entirely negligible. Hence, these nine segments are loaded by 9.2 kips each, the remaining eleven segments by the dead load of 5.8 kips. The corresponding reactions are $R_l = 82.0$ kips and $R_r = 64.4$ kips.

In view of unsymmetrical loading, beam moments M_0 and quantities $M_0 y\ \Delta s/I$ must be computed for both halves of the arch. They are entered in Table 10.4 in the columns headed "Case *b*."

In Table 10.4, x and y are given in feet, $y\ \Delta s/I$ in 1/in., $y^2\ \Delta s/I$ in 1/in.^{2}, M_0 in ft-kips, and $M_0 y\ \Delta s/I$ in ft-kips per in.^{2} (It is advisable to

Table 10.4

x	y	$y\ \Delta s/I$	$y^2\ \Delta s/I$	Case *a*		Case *b*			
						Left half		Right half	
				M_0	$M_0 y\ \Delta s/I$	M_0	$M_0 y\ \Delta s/I$	M_0	$M_0 y\ \Delta s/I$
1.9	1.30	0.078	1.2	174	13	156	12	123	10
6.0	3.90	0.235	10.9	514	121	444	104	364	85
10.2	6.20	0.373	27.6	823	306	713	269	580	216
14.5	8.30	0.498	49.6	1101	553	954	475	790	394
19.0	10.20	0.613	74.9	1349	825	1159	710	976	598
23.5	11.80	0.708	100.2	1556	1102	1321	935	1138	806
28.2	13.10	0.786	123.2	1728	1358	1447	1138	1276	1002
32.9	14.10	0.847	143.2	1862	1578	1531	1298	1390	1178
37.7	14.70	0.882	155.5	1947	1718	1570	1384	1475	1301
42.5	14.95	0.897	160.8	1991	1787	1566	1402	1533	1375
Σ			847.1		9361		7727		6965

select units so as not to obtain unwieldy figures, such as millions on the one hand, or small decimal fractions on the other.)

From the general discussion of Eq. (10.11), it is evident that only the first term in the numerator and the first and last terms in the denominator of that equation need be considered for this particular roof arch. Hence, for determining H, the following equation is used:

$$H = \frac{\Sigma M_0 y\ \Delta s/I}{\Sigma y^2\ \Delta s/I + El/E_{tr}A_{tr}}$$

The denominator then becomes

$$2 \times 848.1 + 4 \times 10^6 \times 90 \times 12/30 \times 10^6 \times 8.3 = 1709.5$$

The maximum force in the tie rod (case *a*) is

$$H_{max} = \frac{2 \times 9361 \times 12}{1709.5} = 131.5 \text{ kips}$$

For the loading which results in maximum quarter-point moment (case *b*),

$$H = \frac{(7727 + 6965)\ 12}{1709.5} = 103.1 \text{ kips}$$

From Table 10.4 the simple beam moment M_0 at $x = 23.5$ ft is seen to be 1321 ft-kips. Hence the moment in the arch rib at that point is

$$M = M_0 - Hy = 1321 - 103.1 \times 11.80 = 103 \text{ ft-kips}$$

Since the point $x = 23.5$ ft is located at the center of the sixth arch segment, the vertical shear at that point is

$$V = 82.0 - 9.2 \times 5.5 = 31.4 \text{ kips}$$

At that point, from Eq. (10.19*b*), $\theta = 17°42'$. The axial thrust at that point then becomes

$$T = 31.4 \times 0.303 + 103.1 \times 0.95 = 107.4 \text{ kips}$$

It will be noticed that the values of H_{max}, M, and T are quite close to those obtained in the preliminary design. Such good coincidence obtains only when, as in this case, the final location of the axis is very close to that used in the preliminary design. Even then, significant differences between preliminary and final results are not infrequent; therefore the accurate analysis by summation should always be carried out.

A 12 × 24 in. section with eight No. 8 bars, shown in Fig. 10.13, is selected for the arch rib. By the methods of Art. 5.8, $p_g = 0.0218$, $m = 15.7$, and $e_b = 8.58$ in. For $M = 103$ ft-kips and $T = 107.4$ kips, $e = 11.5$ in. $> e_b$, indicating tension failure. From the column-interaction

Scanned with CamScanner

equation, with $F_a = 1370$ psi and $F_b = 1350$ psi, $N_b = 173$ kips and $M_b = 124$ ft-kips. If pure bending were applied to the section, M_o would be 79.5 ft-kips. By adopting a straight-line variation of moment from $N = 0$ to $N = N_b$, it is found that for the actual axial load of 107.4 kips, a moment of 107 ft-kips is allowed. This is very close to, and conservatively above, the applied moment of 103 ft-kips, indicating that the section chosen is satisfactory.

With four 1⅝-in. round bars for the tie rod, as obtained in the preliminary design, the stress in the tie is 131,500/8.3 = 15,850 psi. The ends of the tie rods are upset and threaded. The long diameter of the nuts for bars of this size is 3½ in. To accommodate the wrench for tightening the nuts, a 5-in. minimum center-to-center spacing of tie bars is selected.

To transmit the pull of the tie to the concrete, an anchor plate 9 × 12 × 1⅛ in. is provided. Actually, a considerable part of the pull will be transmitted to the concrete by bond over the embedded length of the tie bars; this will be discounted, however, and the anchor designed for the entire pull. The bearing surface is $9 \times 12 - 4 \times 2.1 = 99.6$ in.², and the bearing pressure is 131,500/99.6 = 1320 psi. As is easily computed from the dimensions of Fig. 10.13, the bearing surface represents 39.5 per cent of the cross section of the arch extension in which the anchor is located. For this percentage the ACI Code allows a bearing pressure of 1370 psi. The bending stresses in the anchor plate are investigated in the long direction for a strip 1 in. wide. The maximum negative moment of the portion projecting beyond the center line of the anchors is $1320 \times 2.5^2/2 = 4120$ in.-lb, while the maximum positive moment at the center line of the plate is

$$1320 \times 7^2/8 - 4120 = 3960 \text{ in.-lb}$$

With the section modulus equal to $1.125^2/6 = 0.210$, the maximum bending stress is 4120/0.210 = 19,600 psi, which is slightly smaller than 20,000 psi, the permissible bending stress for structural steel.

The hinges transmit only the vertical reaction $V = 92$ kips, since the horizontal component is resisted by the tie. To reduce the number and size of the hinge bars so as to accommodate them in the limited width, a steel with 60,000-psi yield point will be used, so that the allowable compression stress is $f_s' = 0.3 \times 60{,}000 = 18{,}000$ psi. With an angle $\theta = 30°$ (Fig. 10.12), the required area of hinge bars is computed from Eq. (10.21), that is, $A_s' = 92{,}000/(18{,}000 \times 0.866) = 5.9$ in.² Six No. 9 bars are provided, furnishing an area of 5.95 in.² With a hinge opening of 6 in., as shown in Fig. 10.13, the free length of the hinge bars is $L = 6/0.866 = 6.93$ in., while the radius of gyration is

$$r = 1.125/4 = 0.281$$

Hence the ratio $L/r = 24.7$ is within the limits recommended in Art. 10.7.

The required lateral reinforcement is obtained from Eq. (10.22) where, in this case, $a = 8 \times 1.125 = 9.0$ in., $b = 12$ in., $N = 92{,}000$ lb, and $S = 0$. With an allowable stress $f_s'' = 20{,}000$ psi, the required area becomes $A_s'' = 0.79$ in.² It is seen from Fig. 10.13 that within the length $a = 9$ in. four No. 3 closed ties are provided, which furnish an area of $8 \times 0.11 = 0.88$ in.²

The required length of embedment for the hinge bars is

$$24 \times 1.125 = 27 \text{ in.}$$

beyond the faces of the concrete at either side of the hinge.

In order to avoid bending moments caused by eccentricities, the axes of the arch, the tie, and the hinge must be made to intersect at one common point, as shown in the hinge detail of Fig. 10.13.

10.9 Cylindrical Shells As a further development of the arch principle, shell surfaces provide a structurally efficient solution to the problem of carrying roof loads over long spans. These three-dimensional forms owe their efficiency to the translation of applied loads into tensile and compressive stress and shear stress in the plane of their surface. These are termed *membrane* stresses, and the degree to which membrane stresses are dominant over stresses due to out-of-plane flexure is generally a measure of the structural economy of the system.

One common form of shell surface is the cylindrical shell. This is a developable surface, similar to the barrel arch described in Art. 10.2, but quite different with regard to conditions of support. While the barrel arch normally has continuous support along the lower edges, the cylindrical shell is supported only by transverse diaphragms or ribs, the longitudinal edges being free. Precast units of a cylindrical shell roof are shown in Fig. 10.16. Figure 10.17 shows several of the characteristic types of cylindrical shells. Such shells may be used as single units (Fig. 10.17*a*) supported at the ends and free along the long edges, or as multiple units (Fig. 10.17*b*) joined along the long edges. They may be continuous over one or more intermediate supports (Fig. 10.17*c*). If transverse spans are long, the use of a ribbed cylindrical shell (Fig. 10.17*d*) may be indicated.

Since a cylindrical shell is a space structure, with its internal forces acting in three directions, its analysis becomes quite complicated. However, a qualitative understanding of the fundamental nature of shell behavior can be gained without detailed mathematical analysis. A small element of the shell surface, shown in Fig. 10.18*a* to *c*, must be in equilibrium under the action of the applied load, the membrane forces acting in the plane of the surface, and the out-of-plane shears and moments causing bending in the shell (shown separately in Fig. 10.18*c* for clarity). It

Scanned with CamScanner

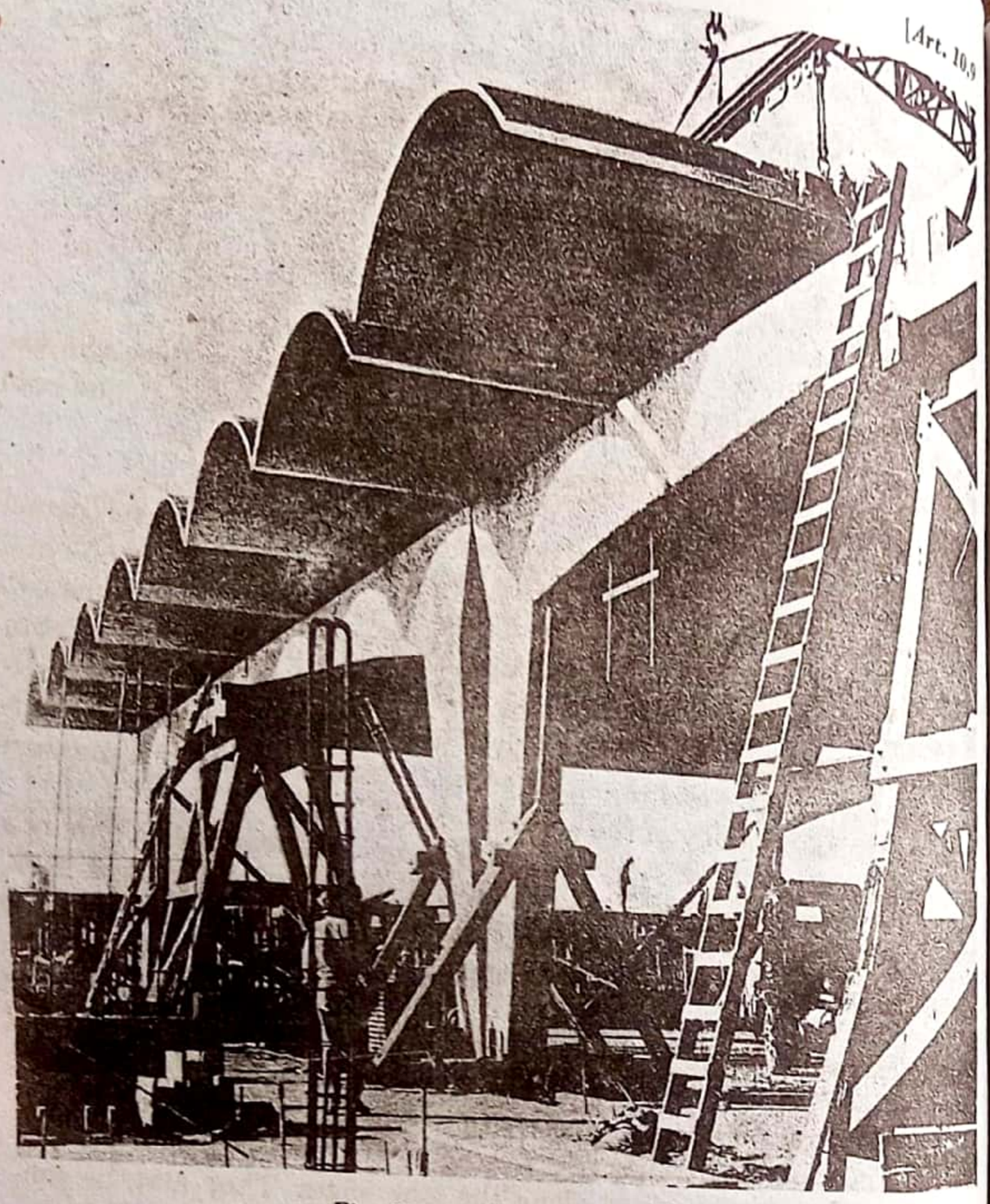


Fig. 10.16 Cylindrical-shell roof.

will be found for most cylindrical shells that the quantities N_x, N_ϕ, M_x, and $M_{x\phi}$ are so small as to be considered negligible, so that the quantities of principal concern are the membrane forces, shown in Fig. 10.8*b*, and the transverse moment M_ϕ. By summing forces in the radial direction, it becomes apparent that the radial component of the load W must be resisted by the radial component of the tangential thrust T_ϕ, while the tangential component must be resisted by the difference between the shears S acting on the two opposite faces of the element, plus the difference in tangential thrust T_ϕ acting on opposite faces. Conditions of equilibrium can be satisfied by the membrane forces alone, so that any load can be

resisted by direct stresses acting wholly in the plane of the surface. Note that it is the presence of the membrane shear stresses which distinguishes shell behavior from that of an arch; because of these shear stresses, a shell can carry loads by direct stress regardless of its shape or the distribution of the loads, while the arch can carry by direct stress only one unique loading. The longitudinal membrane forces T_x are similar to the fiber stress resulting from bending of a beam; in fact, for shells with a suffi-

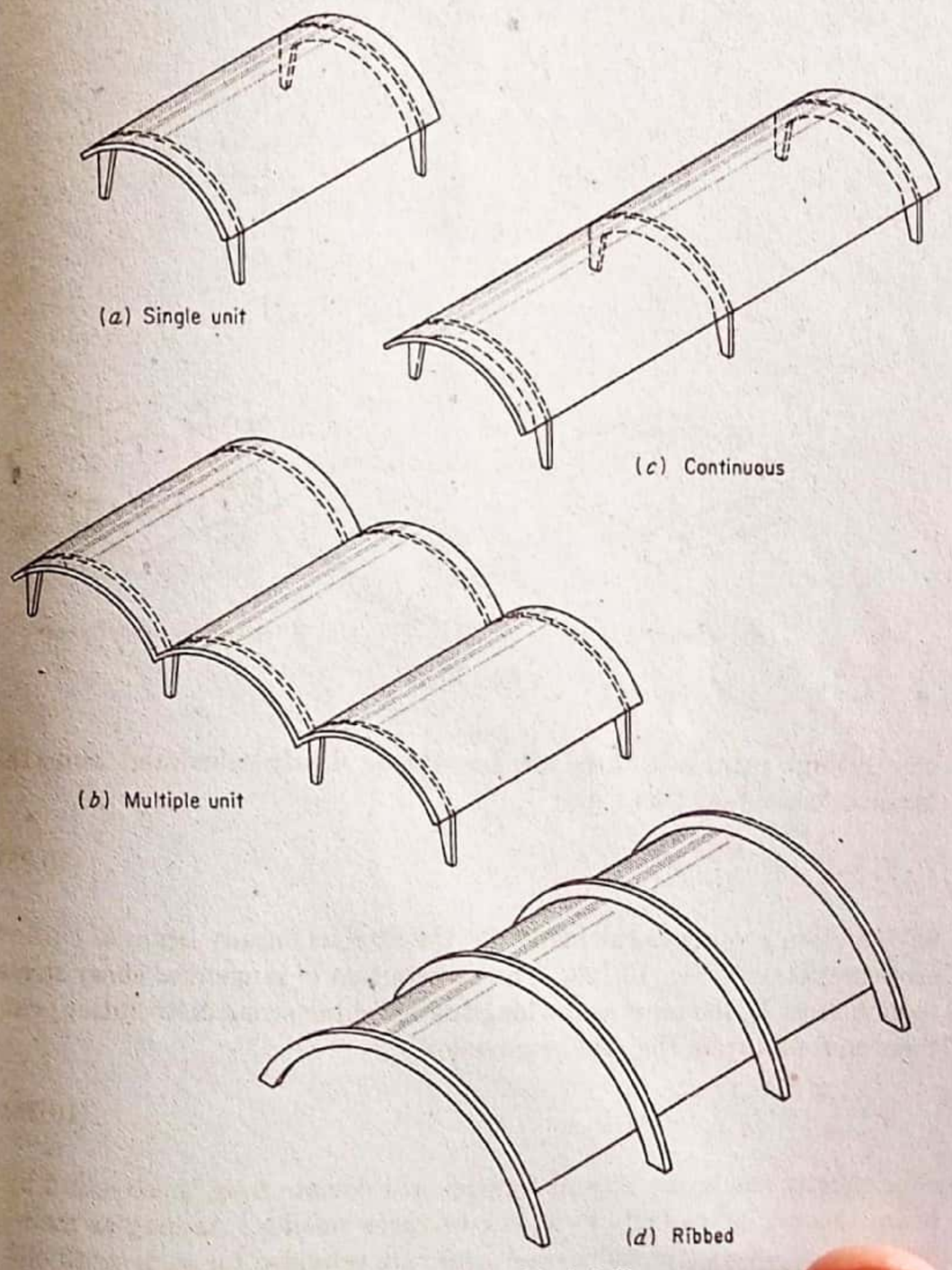
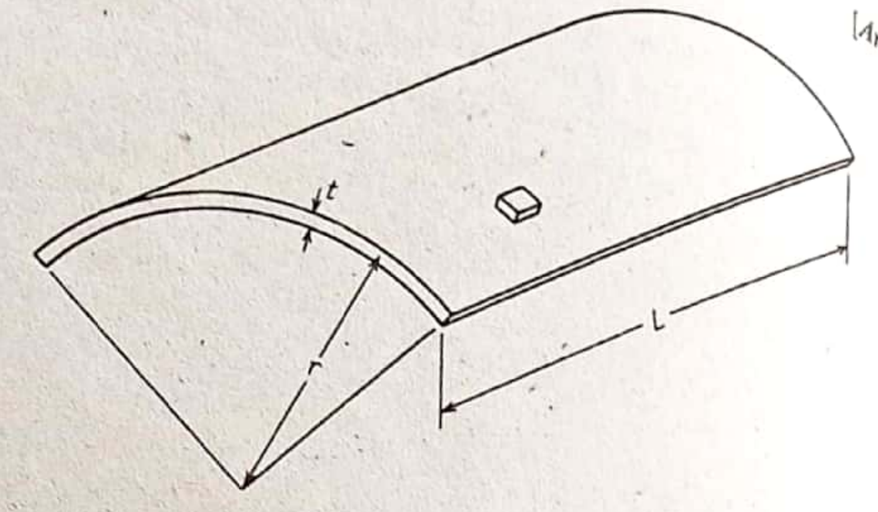
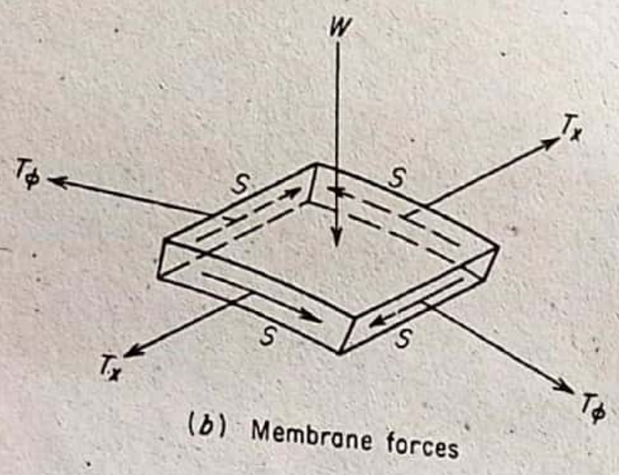


Fig. 10.17 Cylindrical shells.

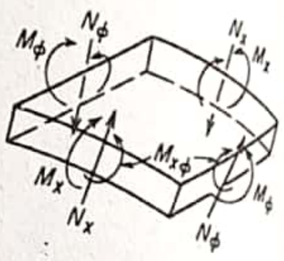
Scanned with CamScanner



(a)



(b) Membrane forces



(c) Out-of-plane forces

Fig. 10.18

ciently high ratio L/r, these stresses can be closely calculated using the familiar beam equation

$$f_z = \frac{T_z}{t} = \frac{My}{I} \tag{10.23}$$

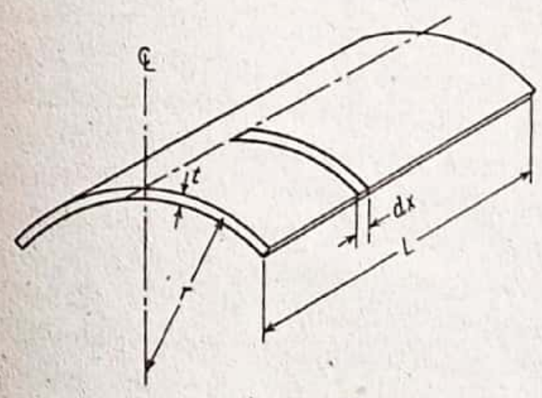
with section properties calculated for the shell as for any beam of curved cross section (see Fig. 10.19*b*). The distribution of tangential shear stress (which must be the same as the longitudinal shear-stress distribution) can then be found from the usual expression,

$$v = \frac{S}{t} = \frac{VQ}{Ib} \tag{10.24}$$

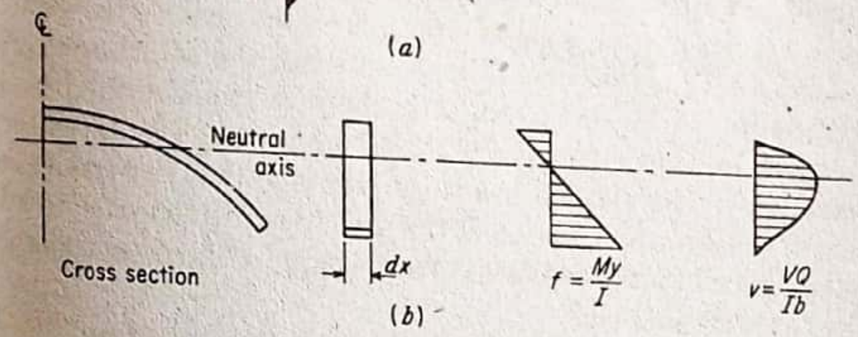
(For shorter shells, the T_z and S forces will deviate from those found by beam theory, increasingly so as L/r becomes smaller.) As long as membrane shear forces and transverse thrust are provided for each small element of the surface, the shell will carry its load almost entirely by mem-

brane stress. But along the free edges, these requirements are no longer met, and it is this condition which brings about the out-of-plane bending forces, principally M_ϕ.

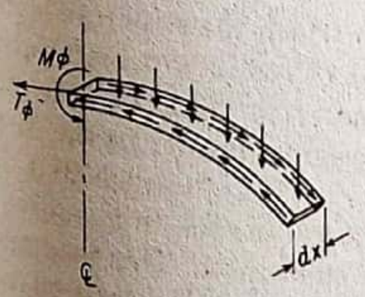
Once the distribution of shear is obtained from beam theory, the transverse moment M_ϕ is calculated from equilibrium of the shell element dx shown in Fig. 10.19*a* and *c*. It is seen that M_ϕ must be equal to the moment of the external load minus the moment of the net tangential shear. It will be found that the difference between these two quantities is small and usually is such as to produce circumferential tension in the top fibers, i.e., the free longitudinal edge will deflect downward and inward under load. It is this relative movement with respect to the crown point which causes the longitudinal stresses T_z, in turn, to deviate from those found by beam theory. Since the free edge deflects more than the crown,



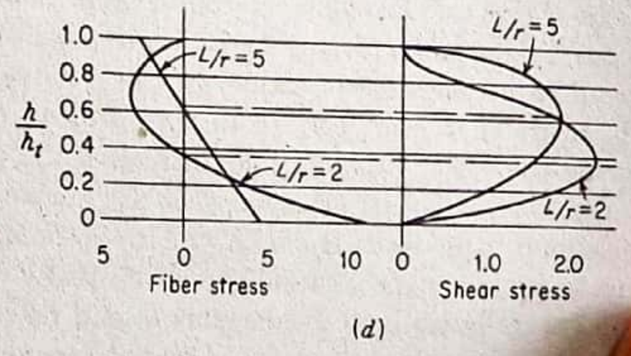
(a)



(b)



(c)



(d)

Fig. 10.19

Scanned with CamScanner

the tensile strains must be larger than those found by beam theory; consequently the tension along the free edge must be increased. But for horizontal equilibrium the compressive stresses above the neutral axis must be increased as well, although the internal moment of these forces must be the same as before. This indicates that the lever arm between the two must decrease; i.e., the center of compression must move down, as must the neutral axis. This effect increases with decreasing L/r, as is shown in Fig. 10.19*d*, which contrasts the longitudinal stress distribution in a shell with $L/r = 5$ with that for a shell with $L/r = 2$.

The change in the longitudinal stress will, in turn, mean a variation in longitudinal (and tangential) shear distribution from that obtained from simple beam theory. Figure 10.19*d* shows the change in shear stress distribution as the L/r ratio is reduced from 5 to 2.

The foregoing qualitative discussion of cylindrical-shell behavior suggests the possibility of a method of solution which has been referred to as the *beam method*. Originally proposed by Lundgren, it is described in detail in Ref. 10.4. In addition to the usual assumptions associated with elastic flexural analysis, Lundgren's method assumes (1) that all points on a transverse cross section deflect the same amount vertically and do not deflect horizontally and (2) that radial moments, torsional moments, and radial shears on transverse cross sections are all negligible. Consistent with these assumptions, it has been observed (Refs. 10.5, 10.6) that the beam method should not be applied to single cylindrical shells with L/r less than about 5, nor to interior units of multiple cylindrical shells with L/r less than about 2. With these conditions satisfied, the solution requires only the calculation of T_x, S, T_ϕ, and M_ϕ, the first two obtained from a beam calculation, and the latter two obtained from what Lundgren terms the *arch calculation*. The method has the advantage that it permits easy visualization of the structural action of the shell in resisting loads; in addition, it can be applied to cross sections of any shape, of variable thickness with or without stiffening ribs.

Alternatively, cylindrical shells can be analyzed by direct application of the theory of elasticity. The solution is analogous to that of a conventional indeterminate frame by superposition, in which the structure is reduced to a determinate frame by the removal of redundant restraints which are then reintroduced in turn and adjusted in value in order to satisfy the stated boundary conditions of the original frame. In the case of the shell, it is first assumed that the surface loads are transmitted to the supports by direct stress only. This is the membrane solution, equivalent to assuming the structure to be statically determinate. This assumption generally leads to displacements and reactions along the long edges which are inconsistent with the stated boundary conditions. To correct this situation, line loads must be applied along the long edges; the stresses

resulting from these line loads are then superimposed on those obtained from the membrane solution to obtain the final stresses in the shell.

The mathematical labor associated with this procedure is greatly reduced by use of data and coefficients available in "Manual of Engineering Practice No. 31—Design of Cylindrical Concrete Shell Roofs," published by the American Society of Civil Engineers in 1952 (Ref. 10.7). This publication includes a set of tables and charts which permit a solution for internal stresses for shells of common proportions and includes a valuable presentation of design theory and a number of detailed examples. In addition to this publication, the reader will find design data of interest in "Coefficients for Design of Cylindrical Concrete Shell Roofs," published by the Portland Cement Association (Ref. 10.8), which extends the "Manual 31" tables, thus avoiding interpolation. Additional discussion and examples are available in Ref. 10.9.

With regard to the reinforcement of the shell, while the analysis is carried out assuming a homogeneous, isotropic material, the concrete has tensile strength so low that it is disregarded, and steel is included to carry all the tension. The bars are in some cases curved to follow the lines of principal stress. While this is theoretically the best arrangement, it leads to difficulty in the field, particularly since fairly large bars may be required. More commonly, the steel is arranged in a rectangular pattern; generally the principal tensile reinforcement is concentrated as near to the lower edge (valley) as possible for greatest economy. Often welded wire mesh is used to provide for transverse moment and thrust. Diagonal bars are used near the ends of the span, in order to provide more efficiently for diagonal tension in those areas. Minimum reinforcement in any direction of about ¼ per cent of the concrete section is used to control shrinkage and temperature cracking. Particular attention should be given to the region in which the thin shell surface joins the more massive end diaphragms or supporting frames, where differential expansion and contraction may require additional reinforcement.

10.10 Folded Plates In an attempt to simplify for work and yet retain many of the advantages characteristic of cylindrical shells, the folded-plate structure has evolved. These surfaces have a deep corrugated form similar to that of cylindrical shells, except that plane elements are used, intersecting in "fold lines" parallel to the span direction. Folded-plate structures have been built, using very thin slabs, spanning clear distances greater than 100 ft. They are not ideal shells, because flexural stresses may have considerable influence on their dimensions and design, but they offer the sizable advantage of simplified formwork as compared to curved shell surfaces.

Folded-plate construction appears to have originated in Germany in

Scanned with CamScanner

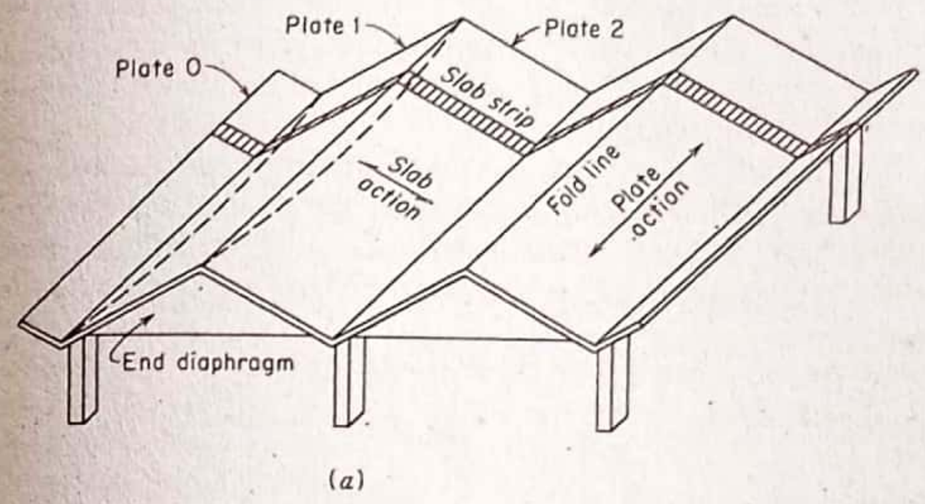


Fig. 10.20 Folded-plate roof.

the 1920's. Following the construction of a number of bunker-type structures using the folded-plate principle, a design theory was developed and published in Europe. The first technical publication on folded plates in the United States was a paper by Winter and Pei (Ref. 10.11) published in 1948. The past 15 years have seen numerous applications of the principles set forth. Figure 10.20 illustrates a recently constructed folded-plate roof of 125-ft span which, in addition to carrying ordinary roof loads, carries the second floor as well from a system of cable hangers. The ground floor is thus kept free of columns.

The action of a folded-plate structure in carrying its loads is illustrated by Fig. 10.21. A surface load applied to the folded-plate structure shown in Fig. 10.21*a* would tend to deflect the individual plates, as indicated by the dotted lines for plate 1, if each plate were free to act independently, the plates spanning as one-way slabs between end diaphragms. The upper edges of plates 1 and 2, for example, would deflect in the directions CC' and CC'', respectively, as in Fig. 10.21*b*. The plates cannot act independently, however. The final location of the deflected edge C must lie at some singular position C_1. This necessitates that plates 1 and 2 undergo deflections Δ_1 and Δ_2, respectively, in their own planes. While the plates have

negligible torsional and flexural stiffness in resisting the deflection components perpendicular to their own planes, they are extremely stiff in resisting in-plane deflections. This resistance to bending about each plate's strong axis results in effective support for the slab along any fold line. A fold line cannot deflect without causing in-plane deflection of one or both of the adjacent plates, a type of deformation which the plates are able to resist effectively. Consequently the plates, rather than spanning in the



(*a*)

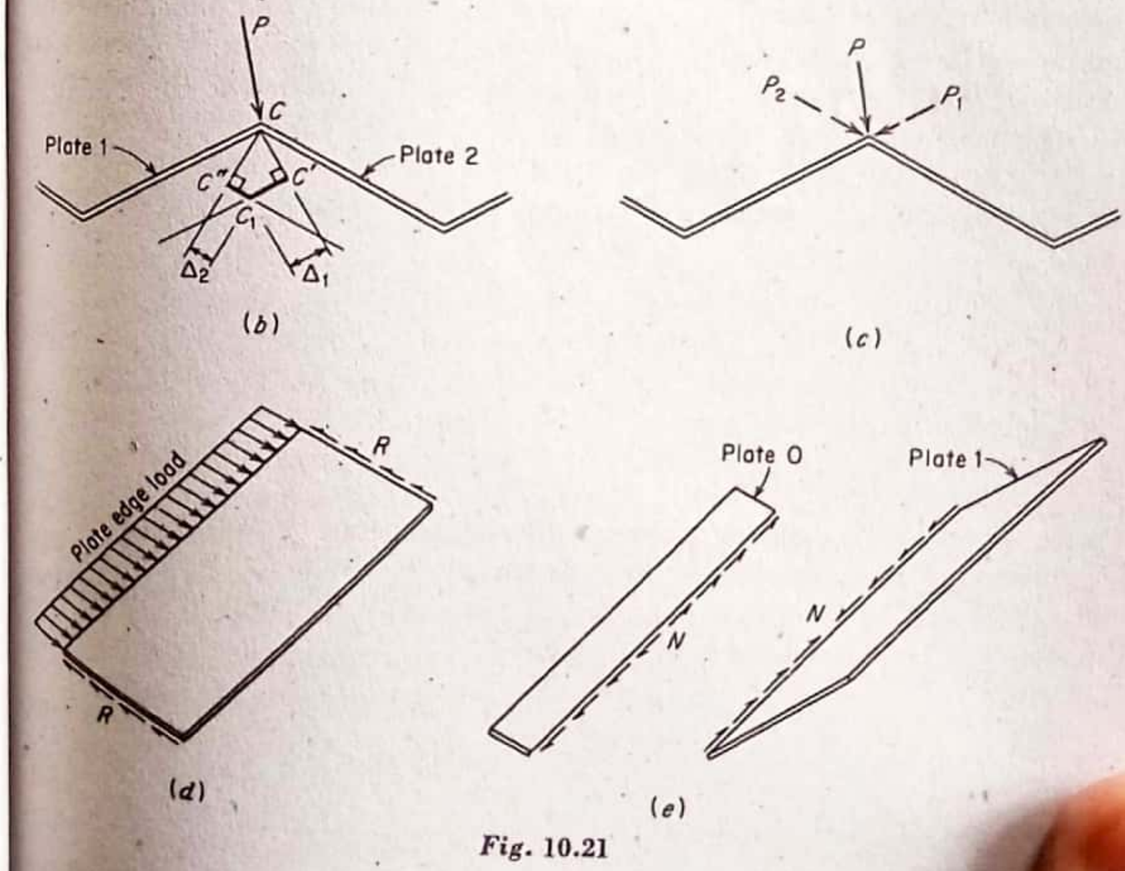


Fig. 10.21

Scanned with CamScanner

long direction of the structure, act as slabs supported at the fold lines as well as the end diaphragms. For most folded plates, the ratio of plate length to width is sufficiently large, in fact, that it is satisfactory to consider all the surface load as carried by the plate in the direction perpendicular to the fold lines. This is termed *slab action*. A typical transverse slab strip is shown in Fig. 10.21*a*.

The reactions from such slab strips are applied as line loads to the fold lines. Because of the negligible torsional and out-of-plane flexural resistance of the plates, the only direction in which each plate can apply a reactive force to resist this line load is parallel to its own surface. The resultant line load P (see Fig. 10.21*c*) therefore resolves into components parallel to the two adjacent plates. The plates in turn carry this edge loading longitudinally between end diaphragms by plate action, as shown in Fig. 10.21*d*. Their behavior may be likened to that of deep, inclined-web girders, laterally braced by adjacent plates. Longitudinal membrane stresses T_x can be found as for any beam. These are termed the *free-edge* stresses.

If conditions are such that the free-edge stresses are the same on both sides of all fold lines, then they are identical with the final stresses. This would be the case, for example, at the edges of an interior unit of a roof consisting of many identical units. If, on the other hand, the initial plate analysis indicates a stress difference on either side of a fold line, an incompatibility is indicated which cannot actually exist, because the strains on either side of a given fold line must be equal. This indicates the presence of longitudinal shears acting along the joint as shown in Fig. 10.21*e*.

For plate 0, the longitudinal stresses at the top and bottom edges, f_{t0} and f_{b0}, resulting from the application of an edge shear N acting as shown, are

$$f_{t0} = -\frac{2N}{A_0} \tag{a}$$

$$f_{b0} = +\frac{4N}{A_0} \tag{b}$$

with + and − indicating tension and compression, respectively, and A_0 indicating the cross-sectional area of the plate. Similarly, the same edge shear N applied to the lower edge of plate 1 in the opposite direction produces the following stresses in plate 1:

$$f_{b1} = -\frac{4N}{A_1} \tag{c}$$

$$f_{t1} = +\frac{2N}{A_1} \tag{d}$$

The edge shear force N must be of such magnitude as to eliminate completely any difference in longitudinal free-edge stresses at the fold line. The total required stress change is therefore equal to

$$f_{b0} - f_{b1} = \frac{4N}{A_0} + \frac{4N}{A_1}$$

The proportion of this change which occurs in plate 0 is

$$\frac{+4N/A_0}{4N/A_0 + 4N/A_1} = \frac{A_1}{A_0 + A_1} = K_0 \tag{e}$$

while that assigned to plate 1 is

$$\frac{4N/A_1}{4N/A_0 + 4N/A_1} = \frac{A_0}{A_0 + A_1} = K_1 \tag{f}$$

The factors K_1 and K_2 are known as the *stress-distribution factors* and are applied to any difference in free-edge stresses to determine the stress change due to edge shear. Similar factors are found for all other joints.

Additionally, it is evident from Eqs. (*a*) through (*d*) that an edge shear causing a given stress change at the near edge of a plate will cause a stress change of one-half that amount, of opposite sign, at the far edge. Thus a *stress carry-over factor* of $-\frac{1}{2}$ is obtained. Stress-distribution factors and stress carry-over factors are applied to the free-edge stresses, in an iterative procedure exactly analogous to the familiar Cross method of moment distribution, to obtain T_x stresses corrected for the presence of edge shears.

In many cases the above analysis is a sufficient basis for design. In other cases, because of the geometry of the structure or the nature of the loads, it is necessary to correct for the relative displacement of the fold lines. This relative displacement amounts to support settlement for the slab strips. While it will usually have little effect on the T_x stresses, there may be a significant change in slab moments M_ϕ and slab shears N_ϕ.

There are several methods for determining the effect of joint translation. The method which is simplest conceptually is an iterative procedure in which the fold-line deflections for the initial plate stresses, calculated as described above, are determined. Slab moments and shears and joint loads resulting from such deflections are found, and the plate stresses resulting from these joint loads are calculated. The associated plate deflections are determined, and the cycle is repeated until sufficient accuracy is obtained. While quite straightforward, the method has the disadvantage that it may converge very slowly, or actually diverge under certain circumstances.

Alternatively, a method analogous to the sidesway analysis of a multistory building is used. Each plate is given an arbitrary rotation in turn,

Scanned with CamScanner

and slab reactions, plate loads, plate stresses, and deflections are found for [*Art. 10.11*
that rotation. A geometrical relation is established between plate deflection and plate rotation which permits the writing of a set of simultaneous equations. From these equations, constants are found which are applied to each of the arbitrary rotation solutions. Final moments and stresses are then found by superposition.

Other methods of solution are available, many particularly adapted for use with digital computers. Additional information of interest to the designer will be found in Refs. 10.13 to 10.15.

10.11 Hyberbolic Paraboloids The possibilities of doubly curved shell roofs have been increasingly exploited in recent years. With both main curvatures in the same direction, say concave downward, such surfaces are termed *synclastic;* with the main curvatures in opposite directions, such as in a saddle surface, they are termed *anticlastic*. The hyperbolic-paraboloid surface is an anticlastic form that has achieved great popularity owing to its economical use of material, relative simplicity of structural action, relatively easy forming, and interesting architectural effect.

With reference to Fig. 10.22, the surface is defined by two intersecting systems of straight-line generators, a and b. The lines AB and CD are termed the *directrixes;* both are parallel to the director plane YOZ, but they are not parallel to each other. The generators a intersect both directrixes and are at the same time parallel to the second director plane XOZ. Similarly, the second set of generators b intersect the directrixes EF and GA and are parallel to the director plane YOZ. The intersection

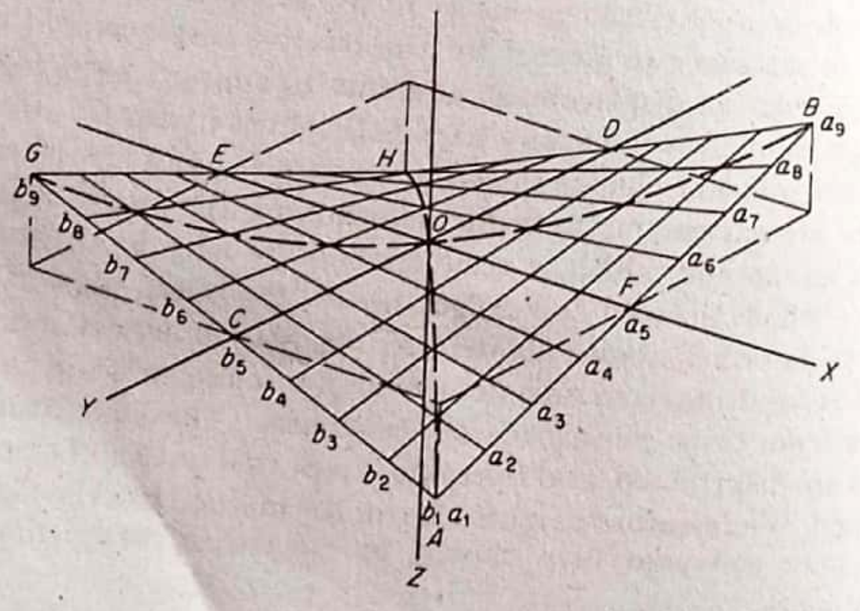


Fig. 10.22

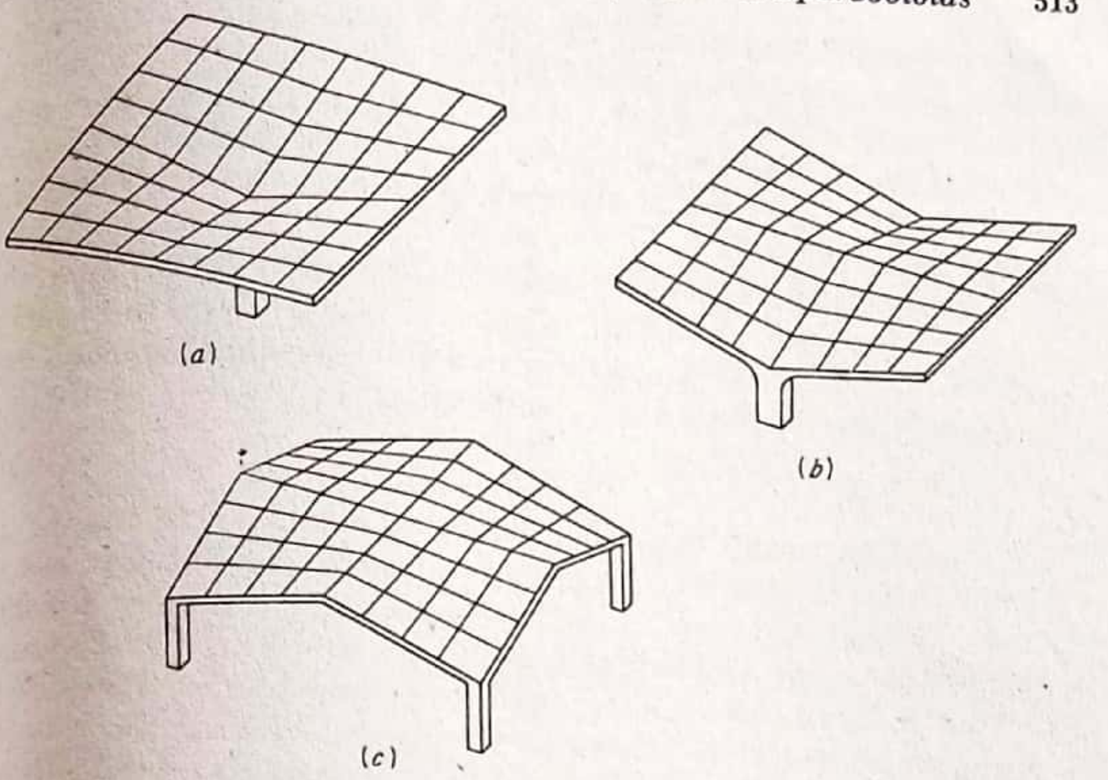


Fig. 10.23

of the two director planes XOZ and YOZ is usually, but not necessarily, a right angle.

In describing the surface, it is convenient to take as coordinate axes the two generators OF and OC, passing through the crown of the surface, and the intersection line OZ of the two director planes. The line OZ is always perpendicular to the plane XOY. The equation of the surface is then

$$z = kxy \tag{10.25}$$

where k is a constant representing the slope of the surface. It is evident that plane sections parallel to the two bisecting planes of the dihedral angle XOY are parabolic; these are termed the *principal parabolas*. They are respectively curved upward (GOB) and downward (AOH); the surface is anticlastic. Plane sections parallel to the plane XOY are hyperbolic; hence the name *hyperbolic paraboloid*.

The geometry of the surface described is most convenient in the building of forms. It is evident that the surface can be formed using straight elements, say 2 by 6's on edge, placed along either system of generators, over which can be laid plank or plywood sheathing thin enough to conform to the warped surface. Many different roof forms can be created either by use of the entire surface or by combining parts of it in various ways. For example, the surface of Fig. 10.22 can be used in its entirety, with a

Scanned with CamScanner

buttress support at A and H; Fig. 10.24 illustrates such an application. Alternatively, segments of the surface can be combined in a number of arrangements, a few of which are shown in Fig. 10.23. In most cases, stiffening ribs are required along the lines of intersection of the segments and along the free edges of the shell to accommodate the substantial thrusts developed.

In analyzing the hyperbolic paraboloid, it is convenient to work with X' and Y' axes, each rotated 45° in a horizontal plane from the original X or Y axis; thus the axes are in the planes of the principal parabolas. The equation of the warped surface then becomes

$$z = 0.5k(x'^2 - y'^2) \tag{10.26}$$

The means by which a hyperbolic paraboloid carries its load may be apparent from its geometry. With two mutually perpendicular sets of parabolic strips, all of exactly the same curvature, it is reasonable to suppose that a load applied to a unit of surface area will be divided equally, half carried by each of the intersection parabolic arch strips. The concave-downward strip carries its share by compression, while the concave-upward strip acts in tension. Since the parabolic axes correspond with the equilibrium polygons for a load distributed uniformly, no bending mo-

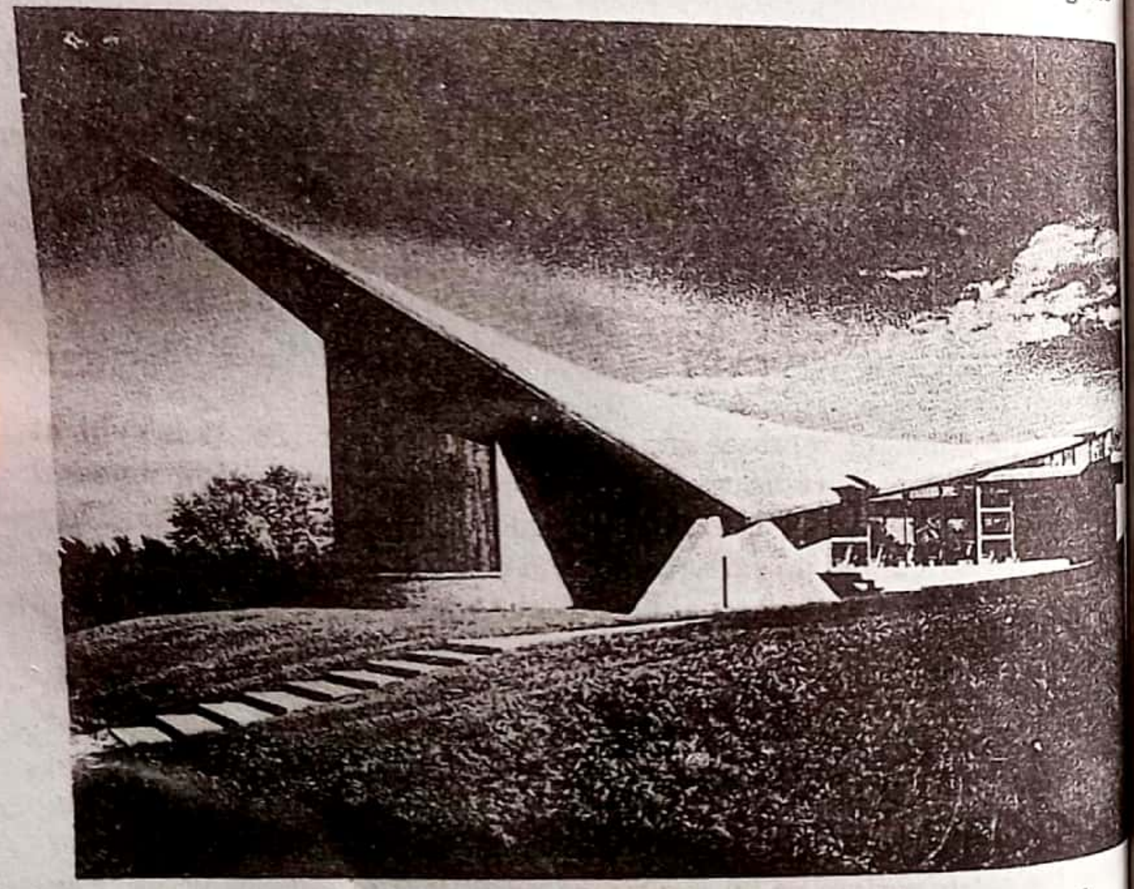


Fig. 10.24 Hyperbolic-paraboloid shell, St. Edmund's Episcopal Church.

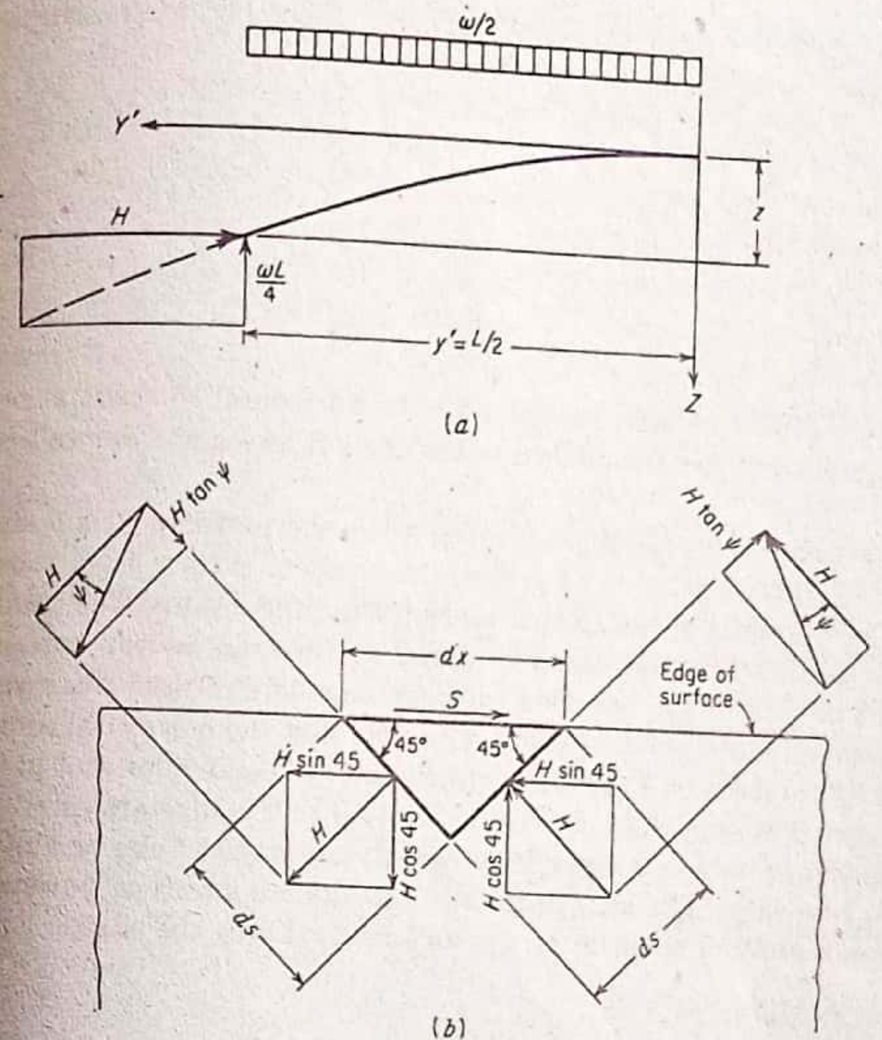


Fig. 10.25

ments or radial shears are developed; that is, the direction of thrust must at any point be tangent to the axis of the parabolic strip. Figure 10.25*a* shows a parabolic compression strip, with a surface load $w/2$ producing a thrust at point (z,y'), with a horizontal component H and a vertical component $wL/4$. With x' a constant value, the equation of the curve is obtained from Eq. (10.26) and is

$$z = k_1 - 0.5ky'^2 \tag{a}$$

where k_1 is a new constant, simply defining the elevation of the vertex. Consider for convenience the parabola which passes through the origin (Fig. 10.22); k_1 is zero, and

$$z = -0.5ky'^2 \tag{b}$$

The slope of the parabola at any point is obtained by differentiation:

$$\frac{dz}{dy'} = -1.0ky' \tag{c}$$

Scanned with CamScanner

At $y' = L/2$, the slope is $-kL/2$. Since the slope of the resultant thrust must coincide with that of the parabola,

$$\frac{wL/4}{H} = \frac{kL}{2}$$

and

$$H = \frac{w}{2k} \tag{10.27}$$

Equation (10.27) is an expression for the horizontal component of tensile or compressive thrust produced in the shell at any point due to a uniform load.

The above analysis is predicated upon the presence of a suitable restraining force, acting on each elemental unit of surface from those adjacent. At the edges of the shell, a special situation obtains. The equilibrium of the small triangular element taken at the edge of the surface (Fig. 10.25*b*) demonstrates the need for edge members to take the thrust that is developed along the free edges. Consider first the horizontal component of thrust, and break that into components perpendicular and parallel to the edge; it is seen that the vectors normal to the edge are equal and act in opposite directions; hence they cancel, and no net force results normal to the free edge. The tangential components are additive, however. If S is the intensity of shear force per unit length along the edge,

$$2H\ ds \sin 45 = S\ dx$$

$$S = 2H \sin 45 \frac{ds}{dx} = 2H \sin^2 45$$

But $H = w/2k$, and $\sin^2 45 = 0.50$, so that

$$S = \frac{w}{2k} \tag{10.28}$$

In considering the effects of the vertical components of thrust, one must take separately the case of an element along a horizontal edge OF or OC (Fig. 10.22) and an element along a sloping edge AF or AC. Along the horizontal edges, since the slope of the axis of one parabola is equal to that of the intersecting parabola but of opposite sign, the vertical components cancel one another (see Fig. 10.25*b*). Consequently, the edge member must resist only a force parallel to its axis. Along the sloping edges, the vertical components do not cancel but rather add, and it is easily shown that the net vertical force is such that, when combined with the horizontal shear, it will produce a force acting along the sloping edge; again an edge member is required to resist axial load only.

The membrane analysis described provides the basis for the principal shell reinforcement. In large hyperbolic paraboloids, careful attention must be given to the question of secondary stresses. These are due to several causes. There are characteristically flat regions in most hyperbolic-paraboloid shells which give rise to significant bending stresses. In addition, the membrane analysis results in an indicated strain incompatibility adjacent to edge members, which may be in compression while the adjacent monolithic shell surface is loaded primarily in shear. The result of this is the development of flexural and shearing stresses in the shell adjacent to the boundary members. Also, concentrated-load effects require special consideration, as well as the effects of temperature changes and support movements. The reader will find further information on hyperbolic-paraboloid shells in Refs. 10.3 and 10.16 to 10.18.

10.12 Spherical Domes Another form of three-dimensional curved roof which has found frequent application is the spherical dome, generated by rotating an arc of a circle about a vertical axis through the center of the circle. The circular arc is termed a *meridian* (see Fig. 10.26*a*), and its plane a *meridian plane*. The movement of a point on the circular arc, as it rotates about the axis of the dome, describes a *parallel*, or a *circle of*

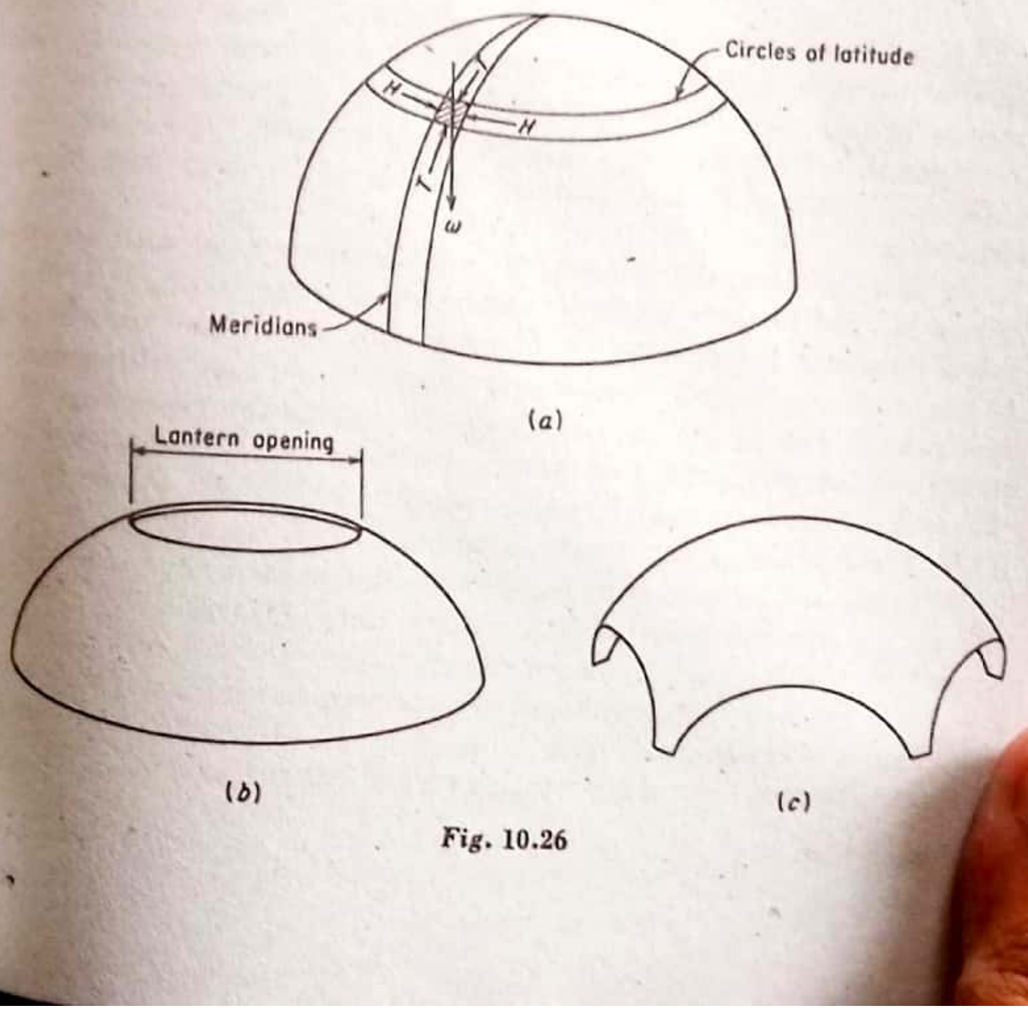


Fig. 10.26

Scanned with CamScanner

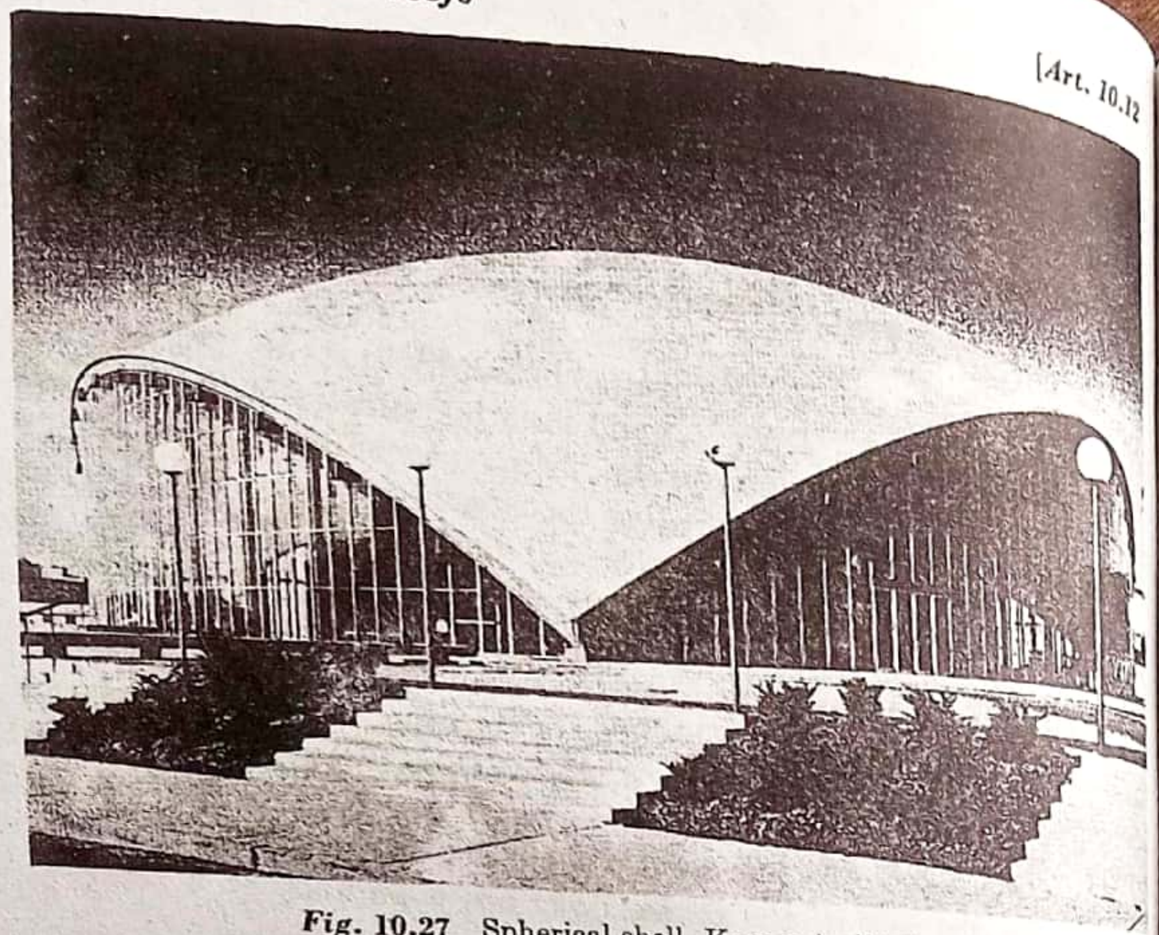


Fig. 10.27 Spherical shell, Kresge Auditorium.

latitude. While simpler to describe geometrically than the hyperbolic paraboloid surface, the dome is considerably more complicated to build, because in the case of the dome there are no straight generators. The forming joists as well as the sheathing must be curved to fit the surface, which adds considerably to the difficulty of construction and cost of such structures.

In spite of this, the economy of material associated with spherical domes has led to their choice in preference to other solutions in many cases. Spherical domes need not be completely closed, as shown in Fig. 10.26*a*, but may include "lantern openings" at the top for purposes of skylighting (Fig. 10.26*b*) or arched openings along the lower edge (Fig. 10.26*c*). A recently completed spherical dome which has attracted considerable attention is the Kresge Auditorium at M.I.T., shown in Fig. 10.27, which is supported at only three points at ground level.

As is the case for hyperbolic paraboloids, domes carry their load almost entirely by membrane stress in the plane tangent to surface, over the greater part of the shell. As a consequence, the shell can be made very thin, even for long spans. Flexural stresses become significant only after axial strains of considerable magnitude occur. In Fig. 10.28*a*, the surface of an annular ring formed by rotating $r\,d\phi$ about the axis is

(*a*)

$$r\,d\phi\,2\pi r\sin\phi$$

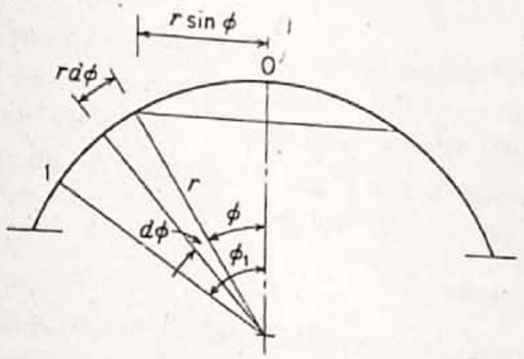
The total surface of the shell above the level of point 1 is found by integrating this expression between the limits zero and ϕ to obtain

$$A = 2\pi r^2(1 - \cos\phi_1) \qquad (b)$$

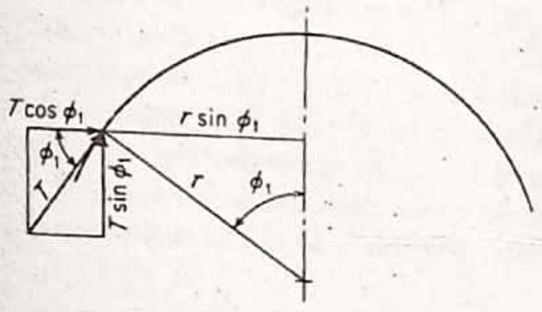
If the load w per unit of surface area is constant, the total load above level 1 is then

$$W = 2\pi r^2 w(1 - \cos\phi_1) \qquad (c)$$

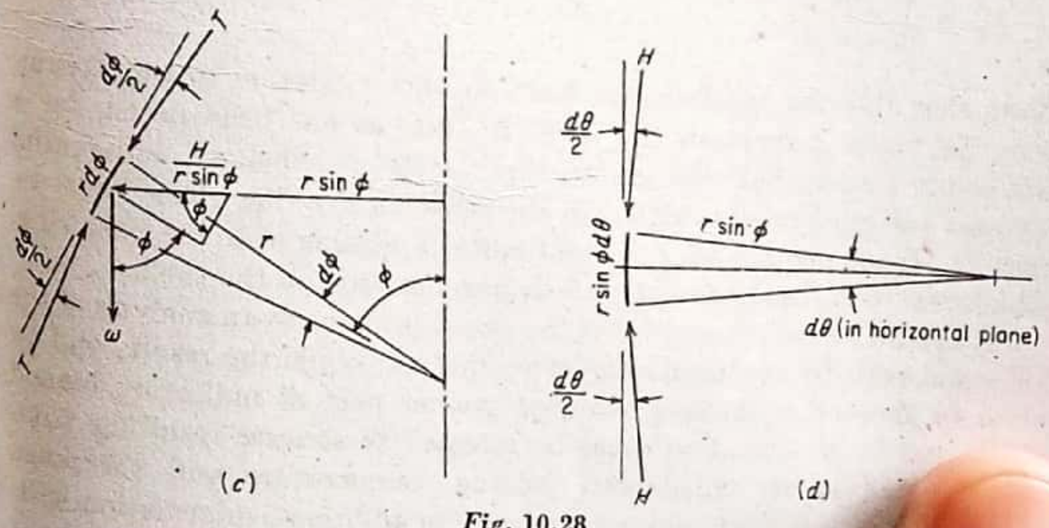
If the total load on the shell above any specified circle of latitude is



(*a*)



(*b*)



(*c*) (*d*)

Fig. 10.28

Scanned with CamScanner

known, the meridianal thrust can be calculated from a consideration of the vertical equilibrium of that portion of the shell. In Fig. 10.28*b* let W be the total weight of the shell above the level concerned, and let T be the meridianal thrust per unit of length. Then

$$W = -2\pi r \sin \phi_1 \, T \sin \phi_1$$

and

$$T = -\frac{W}{2\pi r \sin^2 \phi_1} \tag{10.29}$$

It is noted that the meridianal thrust is always compressive. If the dome is hemispherical, the thrust reaches a maximum value of $W/2\pi r$ at $\phi_1 = 90°$.

The circumferential stress is obtained from the equilibrium of the small element shown shaded in Figs. 10.26*a* and 10.28*c* and *d*. Summing forces in a radial direction, one obtains

$$H = -T - wr \cos \phi_1 \tag{10.30}$$

relating H and T. If one considers the particular case of a dome of uniform thickness and load, one will find that the meridianal thrust, always compressive, varies from a minimum of $-wr/2$ at the crown to $-wr$ if ϕ becomes as large as 90°. The circumferential stress varies from $wr/2$ (compression) at the crown to wr (tension) at $\phi = 90°$. The transition point, at which circumferential stress is zero, occurs at $\phi = 51°50'$.

If the shell is terminated such that ϕ_1 is smaller than 90°, the meridianal thrust will have an outward component which must be resisted by a ring girder subjected to an outward radial force of $T \cos \phi_1$ per unit length. The resulting ring tension is found from the hoop-tension expression and is

$$P_T = \frac{W \cos \phi_1}{2\pi \sin \phi_1} \tag{10.31}$$

Note that the ring tensile stress bears no direct relation to the circumferential stress present in the shell. In fact, as has been noted, for a uniformly loaded shell with ϕ_1 less than 51°50′, the shell circumferential stresses are compressive, although the stress in the ring girder must be tensile. Hence one has an incompatibility of strains near the base ring which results in local bending and shearing stresses in the shell.

It should be kept in mind that the above pertains to an analysis of the spherical shell for membrane stress conditions. While the results will be close to the actual stresses over the greater part of uniformly loaded shells, particular attention must be directed to stresses resulting from concentrated loads, unbalanced loading, temperature and shrinkage effects, and discontinuity along the edges. For additional information with

regard to these and other matters, the reader should consult Refs. 10.2, 10.3, 10.19, and 10.20.

10.13 Conclusion The possibilities of curved two- and three-dimensional structures of reinforced concrete have not yet been fully explored. Great spans can be achieved, and genuine material economy realized; as builders become more familiar with arch and shell construction methods, and as precasting and prestressing techniques are developed more fully, it is to be expected that cost economy will more closely follow economy of material.

While no one would suggest that curved structures offer the best solution to every structural situation, some rather startling and ingenious applications have been found. Already discussed (Fig. 10.20) is a retail store in Florida in which a plane floor system is suspended by cables from a shell roof of 125-ft span. Recently a multistory apartment building was framed using nearly flat hyperbolic paraboloids. Responsible engineers have proposed a concrete building 90 stories high, incorporating thin folded plates in the space between ceiling and floor above to provide long clear spans and using the cellular voids for lighting and utility space. Numerous other possibilities suggest themselves.

The practicing engineer should not be alarmed at the mathematical complications, which in most cases are not as great as supposed. New techniques of analysis are available, as are methods making use of electronic computers, which will greatly abbreviate the labor associated with the solution of stresses in shells. Available also to the structural engineer in general practice are the services of an increasing number of consultants who have made a special study of roof structures and who can, in collaboration with the principal engineer, produce designs of great originality which can be built at a reasonable price.

REFERENCES

10.1 G. C. Ernst: Design of Hinges and Articulations in Reinforced Concrete Structures, *Trans. ASCE*, vol. 106, p. 862, 1941.

10.2 S. Timoshenko and S. Weinowsky-Krieger: "Theory of Plates and Shells," McGraw-Hill Book Company, Inc., New York, 1940.

10.3 A. Pflüger: "Elementary Statics of Shells," McGraw-Hill Book Company, Inc., New York, 1961.

10.4 H. Lundgren: "Cylindrical Shells," vol. 1, Danish Technical Press, Copenhagen, 1951.

10.5 J. Chinn: Cylindrical Shell Analysis Simplified by Beam Method, *J. ACI*, May, 1959.

10.6 M. S. Ketchum, A. L. Parme, H. W. Connor, A. Siev, A. Tedesko, and A. Zweig: Discussion of Ref. 10.5, *J. ACI*, December, 1959.

Scanned with CamScanner

[Art. 10.13

10.7 "Design of Cylindrical Concrete Shell Roofs," American Society of Civil Engineers Manual of Engineering Practice No. 31, 1952.
10.8 "Coefficients for Design of Cylindrical Concrete Shell Roofs," Portland Cement Association, 1959.
10.9 "Design of Barrel Shell Roofs," Portland Cement Association Bull. ST77, 1954.
10.10 A. L. Parme and H. W. Connor: Design Constants for Interior Cylindrical Concrete Shells, *J. ACI*, July, 1961.
10.11 G. Winter and M. Pei: Hipped Plate Construction, *J. ACI*, January, 1947.
10.12 H. Simpson: Design of Folded Plate Roofs, *J. Struct. Div. ASCE*, January, 1958.
10.13 C. S. Whitney, B. G. Anderson, and H. Birnbaum: Reinforced Concrete Folded Plate Construction, *J. Struct. Div. ASCE*, October, 1959.
10.14 E. Traum: The Design of Folded Plates, *J. Struct. Div. ASCE*, October, 1959.
10.15 A. C. Scordelis: Matrix Formulation of the Folded Plate Equations, *J. Struct. Div. ASCE*, October, 1960.
10.16 "Elementary Analysis of Hyperbolic Paraboloid Shells," Portland Cement Association Bull. ST85, 1960.
10.17 A. L. Parme: Shells of Double Curvature, *Proc. ASCE*, vol. 123, p. 989, 1958.
10.18 F. Candella: General Formulas for Membrane Stresses in Hyperbolic Paraboloidical Shells, *J. ACI*, October, 1960.
10.19 "Design of Circular Domes," Portland Cement Association Bull. ST55.
10.20 J. S. Terrington: "Design of Domes," Concrete Publications, Ltd., London, 1946.

chapter 11

PRESTRESSED CONCRETE

11.1 General Modern structural engineering tends to progress toward more economical structures through gradually improved methods of design and the use of higher-strength materials. This results in a reduction of cross-sectional dimensions and consequent weight savings. Such developments are particularly important in the field of reinforced concrete, where the dead load represents a substantial part of the total design load. Also, in multistory buildings, any saving in depth of members, multiplied by the number of stories, can represent a substantial saving in total height, load on foundations, length of heating and electrical ducts, plumbing risers, and wall and partition surfaces. Significant savings can be achieved by the use of high-strength concrete and steel in connection with ultimate-strength design.

However, as was discussed in Art. 2.9, there are limitations to this

Scanned with CamScanner

development, due primarily to the presence of tension cracks which occur under service load conditions and which affect the value of ultimate load. Undesirable features associated with such cracking may be summarized as follows:

1. In flexural members, all concrete on the tension side of the neutral axis, roughly two-thirds of the total volume, does not participate in resisting bending and, in this sense, is wasted.
2. The size of a member is often governed by diagonal tension, a type of stress which concrete is not well suited to resist.
3. The deflection of cracked members is substantially larger than that of uncracked members.
4. The efficient use of high-strength steel is limited by the fact that the amount of cracking (width and number of cracks) is about proportional to the strain, and therefore the stress, in the steel.

These undesirable characteristics of ordinary reinforced concrete have been largely overcome by the development of prestressed concrete. A prestressed-concrete member has been defined as one in which there have been introduced internal stresses of such magnitude and distribution that the stresses resulting from the given external loading are counteracted to a desired degree. Concrete is basically a compressive material, with its strength in tension a low and unreliable value. Prestressing applies a precompression to the member which reduces or eliminates undesirable tensile stresses that would otherwise be present. The entire cross section can be used to resist bending, and cracking under service load conditions can be minimized or even avoided entirely. In addition, it will be shown later that longitudinal precompression greatly reduces the diagonal tension in prestressed-concrete beams.

The first suggestions for prestressing seem to have been made between 1886 and 1908 by the Americans P. H. Jackson and G. R. Steiner, the Austrian J. Mandl, and the German J. Koenen. The use of high-strength steel was first suggested by the Austrian F. von Emperger in 1923, while at about the same time the American R. H. Dill proposed "full prestressing" to eliminate cracks completely. While these proposals remained mainly on paper, the actual development of prestressed reinforced-concrete structures abroad is chiefly due to E. Freyssinet (France, 1928), E. Hoyer (Germany, 1938), and more recently G. Magnel in Belgium. These methods have found very wide application in Europe for bridges with spans of 200 ft and more, floors and roofs, piles, railroad ties, etc. Moderate-sized elements such as prestressed joists, beams, and slabs are successfully mass produced by precasting. In a different field, an independent American method, originated by W. H. Hewitt in 1923, has found wide application. This consists in precompressing the cylindrical shells of water tanks and pipes by surrounding a concrete shell with hoops

of steel which are tightened to a predetermined tension and then covered with a protective concrete layer.

The development in this country has been slower, not for technical but for economic reasons. The European methods achieve great savings of materials, but the methods of prestressing require a great amount of highly qualified labor. This is no particular disadvantage under the high European ratio of material to labor cost. The American ratio is exactly the reverse, which required the development of somewhat different methods more adapted to cost factors in this country. Rapid development in recent years has furnished such techniques, and at the present time considerable quantities of prestressed concrete compete economically with ordinary reinforced concrete and with other materials.

11.2 Sources of Prestress Force Prestress force can be applied to a concrete beam in many ways. Perhaps the most obvious method of precompressing is to use jacks reacting against abutments, as shown in Fig. 11.1*a*. Such a scheme has been employed for large projects. Many variations are possible, including replacing the jacks with compression struts after the desired stress in the concrete is obtained or the use of inexpensive jacks which remain in place in the structure, in some cases with a cement grout used as the hydraulic fluid. The principal difficulty associated with such a system is that even a slight movement of the abutments will drastically reduce the prestress force.

In most cases the same result is more conveniently obtained by tying

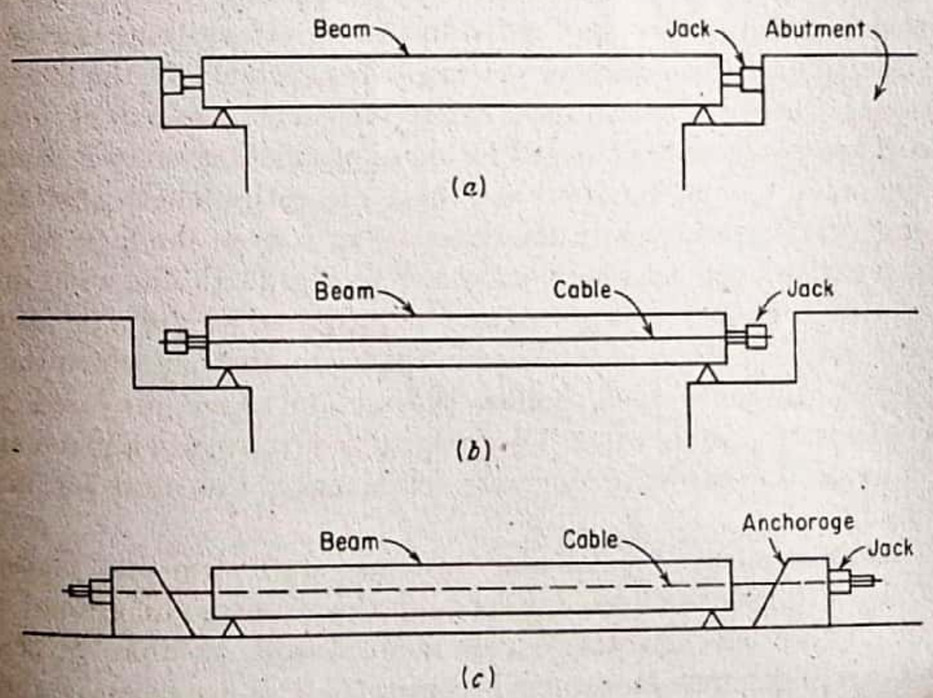


Fig. 11.1

Scanned with CamScanner

the jack bases together with wires or cables, as shown in Fig. 11.1b. These wires or cables may be external, located on each side of the beam; more usually they are passed through a hollow conduit embedded in the concrete beam. Usually one end of the prestressing tendon is anchored, and all the force is applied at the other end. After attainment of the desired amount of prestress force, the wires are wedged against the concrete, and the jacking equipment is removed for reuse. Note that, in this type of prestressing, the entire system is self-contained and is independent of relative displacement of the supports.

Another method of prestressing which is widely used is illustrated by Fig. 11.1c. The prestressing strands are tensioned between massive abutments in a casting yard prior to placing the concrete in the beam forms. The beam is poured around the tensioned strands, and after the concrete has attained sufficient strength, the jacking pressure is released. This transfers the prestressing force to the concrete by bond and friction along the strands, chiefly at the outer ends.

Other means for introducing the desired prestressing force have been attempted on an experimental basis. Thermal prestressing can be achieved by preheating the steel by electrical or other means. Anchored against the ends of the concrete beam while in the extended state, the steel cools and tends to contract. The prestress force is developed through the restrained contraction. The use of expanding cement in concrete members has been tried with varying success. The volumetric expansion, restrained by steel strands or by fixed abutments, produces the prestress force.

Most of the patented systems for applying prestress in current use are variations of those shown in Fig. 11.1b and c. Such systems can generally be classified as *pretensioning* or *posttensioning* systems. In the case of pretensioning, the wires are stressed before the concrete is placed, as in Fig. 11.1c. This system is well suited for mass production, since casting beds can be made several hundred feet long, the entire length cast at once, and individual beams cut to the desired length from the long casting.

In posttensioned construction, shown in Fig. 11.1b, the wires are tensioned after the concrete is placed and has acquired its strength. Usually a hollow conduit or sleeve is provided in the beam, through which the wires are passed. In some cases, hollow box-section beams are used, as are external posttensioning wires. The jacking force is usually applied against the ends of the hardened concrete, eliminating the need for massive abutments.

A large number of pasticular systems, steel elements, jacks, and anchorage fittings have been developed in this country and abroad, many of which differ from each other only in minor details. As far as the designer of prestressed-concrete structures is concerned, it is unnecessary and perhaps even undesirable to specify in detail the technique that is to be

followed and the equipment to be used. It is frequently best to specify only the magnitude and line of action of the prestress force. The contractor is then free, in bidding the work, to receive quotations from several different prestressing subcontractors, with resultant cost savings. It is evident, however, that the designer must have some knowledge of the details of the various systems contemplated for use, so that in selecting cross-sectional dimensions any one of several systems can be accommodated.

As noted in Art. 2.9, the magnitude of prestress force in concrete members is not constant, but diminishes with time at a gradually decreasing rate. The reduction of the initial prestress force P_i to the final effective value P is due to a number of causes. The most significant are elastic shortening of the concrete, concrete creep under sustained load, concrete shrinkage, relaxation of the stress in the steel, frictional loss between the tendons and the concrete during the stressing operation, and loss due to slip of the steel strands as stress is transferred from the prestressing jacks to the anchorages at the ends of the beam. The approximate magnitudes of the various losses and means for predicting stress loss will be discussed in detail in Art. 11.9.

11.3 Prestressing Steels Early attempts at prestressing concrete were unsuccessful because steel of ordinary structural strength was used. The low prestress obtainable in such rods was quickly lost by shrinkage and creep in the concrete.

Such changes in length of concrete have much less effect on prestress force if that force is obtained using highly stressed steel wires or cables. In Fig. 11.2a, a concrete beam of length L is prestressed using steel bars with a yield stress of 40,000 psi, at a working stress of 20,000 psi. With $E_s = 29 \times 10^6$ psi, the unit strain ϵ_s required to produce the desired stress of 20,000 psi is

$$\epsilon_s = \frac{\Delta L}{L} = \frac{f_s}{E_s} = \frac{20{,}000}{29 \times 10^6} = 6.9 \times 10^{-4}$$

But the long-term strain in the concrete due to shrinkage and creep alone may be of the order of 8.0×10^{-4}, which would be sufficient to completely relieve the steel of all stress.

Alternatively, suppose that the beam is prestressed using high-tensile wire with an ultimate strength of 250,000 psi, at a working stress of 150,000 psi. The elastic modulus of steel does not vary greatly, and the same value of 29×10^6 psi will be assumed. Then in this case the unit strain required to produce the working stress in the steel is

$$\epsilon_s = \frac{150{,}000}{29 \times 10^6} = 51.7 \times 10^{-4}$$

Scanned with CamScanner

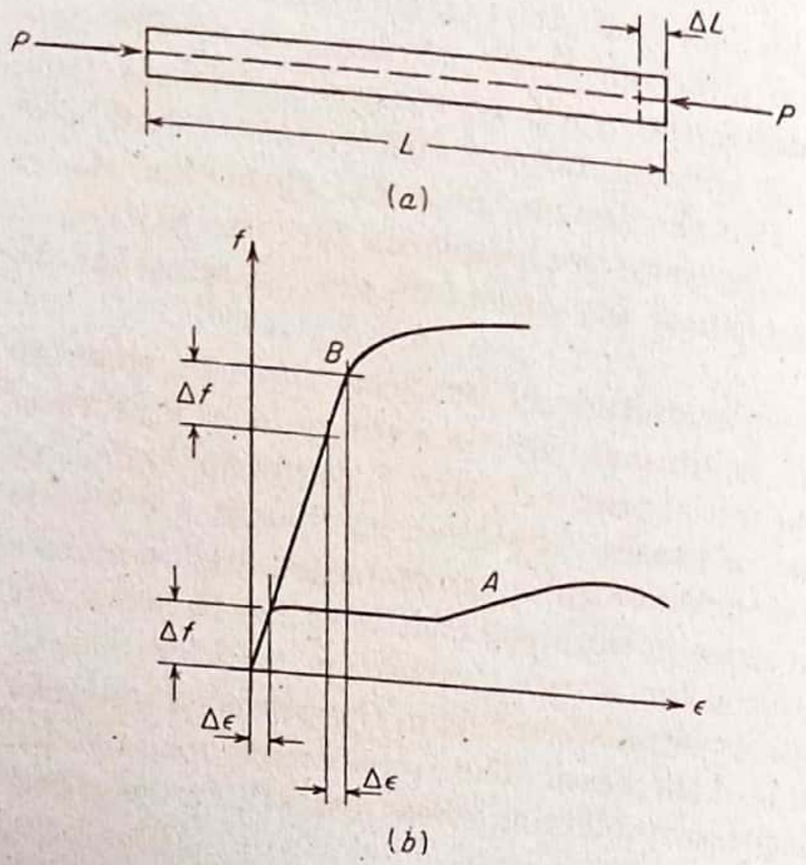


Fig. 11.2

[Art. 11.

If shrinkage and creep strain are the same as before, the net strain in the steel after these losses is

$$\epsilon_s' = (51.7 - 8.0)10^{-4} = 43.7 \times 10^{-4}$$

and the corresponding stress after losses is

$$f_s = \epsilon_s' E_s = 43.7 \times 10^{-4} \times 29 \times 10^6 = 127{,}000 \text{ psi}$$

This represents a stress loss of about 15 per cent, compared with 10 per cent loss in the beam using ordinary steel. It is apparent that the amount of stress lost because of shrinkage and creep is independent of the original stress in the steel. Therefore, the higher the original stress the lower will be the percentage loss. This is illustrated graphically by the stress-strain curves of Fig. 11.2*b*. Curve *A* is representative of ordinary reinforcing rods, with a yield stress between 40,000 and 60,000 psi, while curve *B* represents high-tensile wire, with an ultimate stress of about 250,000 psi. The stress change Δf resulting from a certain change in strain $\Delta\epsilon$ is seen to have much less effect when high steel-stress levels are attained.

Prestressing steel is most commonly used in the form of individual wires of high tensile strength, stranded cable made up of seven or more individual wires, and alloy-steel bars. Prestressing wire is made by rolling steel billets into round rods, which are then passed through dies to reduce the diameter and to produce the required strength. In addition to reducing

the diameter of the wire, the drawing operation changes the internal structure of the wire from crystalline to fibrous and gives the wire great strength through cold-working and strain-hardening. The end product is known as *cold-drawn* wire. For use in prestressing it is almost always subjected to a stress-relieving process. This stress-relieving is not sufficient to reduce materially the strength of the wire, but it does eliminate most of the internal stresses resulting from the drawing operation. A typical stress-strain curve for cold-drawn wire is shown in Fig. 11.3, together with curves for seven-wire stranded cable and for alloy-steel bars. The lack of a well-defined yield point for these materials is apparent, and it is convenient to refer to the "proof-stress" value, established arbitrariiy as that stress which will produce a residual strain of 0.2 per cent.

Stranded cable is usually laid up using seven wires, with the outer six being wound around a seventh wire of slightly larger diameter. The wires may be galvanized (usual for posttensioned construction) or uncoated (usual for pretensioned construction). In the case of stranded cable, stress-relieving is conducted on the finished cable; this eliminates in one operation the internal stresses resulting from both cold-drawing and stranding.

Alloy-steel bars, having a tensile strength somewhat lower than that of cold-drawn wires or stranded cable, are produced by alloying high-carbon steel with other elements, principally manganese and silicon. In addition, cold work is done on the bars during production, further increasing their proportional limit.

A property of steel which is of particular significance in prestressing operations is known as *relaxation*. Most stress-strain curves are obtained from tests conducted at a fairly rapid rate of loading. It is generally

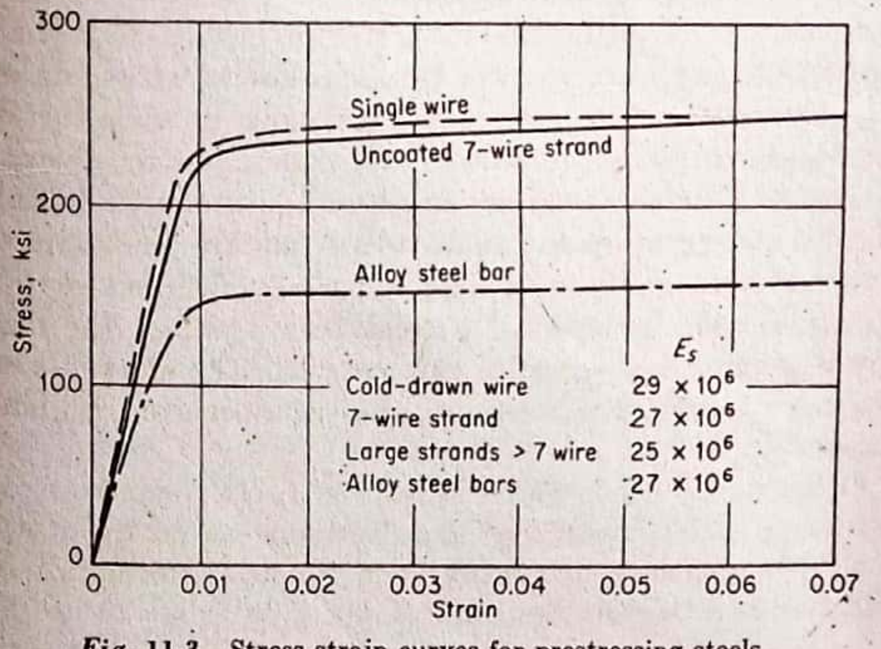


Fig. 11.3 Stress-strain curves for prestressing steels.

Scanned with CamScanner

Table 11.1 Allowable stresses in prestressing steel [Art. 11.

a. *Temporary stresses*	
1. Due to temporary jacking force, but not greater than the maximum value recommended by the manufacturer of steel or of the anchorages	$0.80f'_s$
2. Pretensioning tendons immediately after transfer, or posttensioning tendons immediately after anchoring	$0.70f'_s$
b. *Effective prestress*	$0.60f'_s$, or $0.80f_y$, whichever is smaller

known that if the specimen, be it in the form of wire, strand, or alloy bar is held at a constant high strain, there will be a gradual reduction in stress which approaches some limiting value asymptotically. This phenomenon of relaxation is closely related to, but not quite the same as, creep, which is defined as a gradually changing strain at constant stress. In prestressed beams, the steel undergoes a slightly modified form of relaxation, since the strain is essentially constant but not completely so, as there is a slight reduction in steel strain due to shrinkage and creep of the concrete.

In general, relaxation loss of stress will be higher for high-stress levels than for low. Most present prestressing steel shows only negligible relaxation loss if the stress is below about 50 per cent of ultimate; however, higher stress than this is usually permitted in design. Consequently it is necessary to make some allowance for loss of stress due to relaxation, in addition to other causes.

The tensile stress permitted by the ACI Code in prestressing wires, strands, or bars is dependent upon the stage of loading. With f'_s defined as the ultimate strength of the prestressing steel, and f_{sy} as the nominal yield strength (proof strength), allowable stresses are as shown in Table 11.1.

The justification for higher allowable stresses during the jacking operation and immediately after transfer (the moment at which the wires are cut free of abutments in the case of pretensioning, or when the wires are wedged and jack pressure is removed in the case of posttensioning) lies in the fact that the steel stresses are known quite precisely at this stage. Hydraulic jacking pressure and total steel strain are quantities that are easily measured. In addition, if an accidentally deficient cable should break, it could easily be replaced at small cost; in effect, the tensioning operation is a performance test of the material. The allowable effective prestress, after essentially all losses in stress have occurred, is limited to a more conservative value.

The strength and other characteristics of prestressing wire, strands, and bars very somewhat among manufacturers, as do the methods of grouping the tendons and anchoring them. Typical information is given for illustration in Table 11, Appendix B.

11.4 Concrete for Prestressed Construction Ordinarily, concrete of substantially higher compressive strength is used for prestressed structures than for those constructed of ordinary reinforced concrete. Most prestressed construction in the United States at the present time is designed for a 28-day compressive strength between 4000 and 5000 psi. There are several reasons for this:

1. High-strength concrete normally has a higher modulus of elasticity (see Fig. 1.3). This means a reduction in initial elastic strain under application of prestress force and a reduction in creep strain, which is approximately proportional to elastic strain. This results in a reduction in loss of prestress.

2. In posttensioned construction, high bearing stresses result at the ends of beams, where prestressing force is transferred from the tendons to anchorage fittings, which bear directly against the concrete. This problem can be met by increasing the size of the anchorage fitting or by increasing the bearing capacity of the concrete by increasing its compressive strength. The latter is usually more economical.

3. In pretensioned construction, where transfer by bond is customary, the use of high-strength concrete will permit the development of higher bond stresses.

4. A substantial part of the prestressed construction in the United States is precast, with the concrete mixed, placed, and cured under carefully controlled conditions which facilitate the obtaining of higher strengths.

The strain characteristics of concrete under short-time and sustained loads assume an even greater importance in prestressed structures than in reinforced-concrete structures, because of the influence of strain on loss of prestress force. Strains due to stress, together with volume changes due to shrinkage and temperature changes, may have considerable influence on prestressed structures. In this connection, it is suggested that the reader review Arts. 1.7 to 1.9, which discuss in some detail the compressive and tensile strengths of concrete under short-time and sustained loads and the changes in concrete volume that occur owing to shrinkage and temperature change.

As is the case for prestressing steels, the allowable stresses in the concrete, according to the ACI Code, are dependent upon the stage of loading. These stresses are given in Table 11.2. Here f'_{ci} is the compressive strength of the concrete at the time of initial prestress, f'_c the 28-day compressive strength of the concrete, A_b the bearing area of the anchor plate of the posttensioning steel, and A'_b the maximum area of the portion of the anchorage surface that is geometrically similar to and concentric with the area of the anchor plate of the posttensioning steel.

Scanned with CamScanner

Table 11.2

[Art. 11.5

a. Temporary stresses immediately after transfer, before losses due to creep and shrinkage, shall not exceed the following:

1. Compression ..... $0.60f'_{ci}$
2. Tension stresses in members without auxiliary reinforcement (unprestressed or prestressed) in the tension zone ..... $3\sqrt{f'_{ci}}$

Where the calculated tension stress exceeds this value, reinforcement shall be provided to resist the total tension force in the concrete computed on the assumption of an uncracked section.

b. Stresses at design loads, after allowance for all prestress losses, shall not exceed the following:

1. Compression ..... $0.45f'_c$
2. Tension in the precompressed tension zone:

Members, not exposed to freezing temperatures nor to a corrosive environment, which contain bonded prestressed or unprestressed reinforcement located so as to control cracking ..... $6\sqrt{f'_c}$

All other members 0

These values may be exceeded when not detrimental to proper structural behavior as provided in Art. 104 of ACI Code.

c. The bearing stress on the concrete created by the anchorage in posttensioned concrete with adequate reinforcement in the end regions shall not exceed

$$f_{cp} = 0.6f'_{ci}\sqrt[3]{\frac{A'_b}{A_b}}$$

but not greater than ..... f'_{ci}

11.5 General Equations for Flexural Design It is convenient in treating prestressed members to think of the prestressing forces as a system of external forces acting on the concrete member, which must be in equilibrium under the action of those forces. Figure 11.4*a* shows a simple-span prestressed beam with curved cables, typical of many posttensioned installations. The portion of the beam to the left of a vertical cutting plane x-x is taken as a free body, with forces acting as shown in Fig. 11.4*b*. The force P at the left end is exerted on the concrete through the cable anchorage, while the force P at the cutting plane x-x results from combined shear and normal force acting on the concrete surface at that location. The direction of P is tangent to the curve of the cable at each location. Note the presence of the force N, acting on the concrete from the cable, due to cable curvature. This force will be distributed in some manner along the length of the cable, the exact distribution depending upon the cable profile. Its resultant, and the direction in which the resultant acts, can be found from the force diagram of Fig. 11.4*c*.

It is convenient in working with the prestressing force P to divide it into its components in the horizontal and vertical directions. The horizontal component (Fig. 11.4*d*) is $H = P\cos\theta$, and the vertical component is $V = H\tan\theta = P\sin\theta$, where θ is the angle of inclination of the cable

centroid at the particular section. Since the slope angle is normally quite small, the cosine of θ is very close to unity, and it is sufficient for most calculations to take $H = P$.

In developing equations for flexural stress, the effects of prestress force, dead-load moment, and live-load moment are calculated separately, and the separate stresses are superimposed. When the prestress force P is applied with an eccentricity e below the neutral axis of the cross section with area A and top and bottom fiber distances c_1 and c_2, respectively, it causes the compressive stress $-P/A$ and the bending stresses $+Pec_1/I$ and $-Pec_2/I$ in the top and bottom fibers, respectively (compressive stresses are designated as negative, tensile stresses as positive), as shown in Fig. 11.5*a*. Then, at the top fiber, the stress is

$$f_{1p} = -\frac{P}{A} + \frac{Pec_1}{I} = -\frac{P}{A}\left(1 - \frac{ec_1}{r^2}\right) \tag{11.1}$$

and at the bottom fiber

$$f_{2p} = -\frac{P}{A} - \frac{Pec_2}{I} = -\frac{P}{A}\left(1 + \frac{ec_2}{r^2}\right) \tag{11.2}$$

where r is the radius of gyration of the concrete section. When the dead load of the girder w_g is added, causing additional moment M_g, the total top and bottom fiber stresses become

$$f_{1d} = f_{1P} - \frac{M_g c_1}{I} \tag{11.3}$$

$$f_{2d} = f_{2P} + \frac{M_g c_2}{I} \tag{11.4}$$

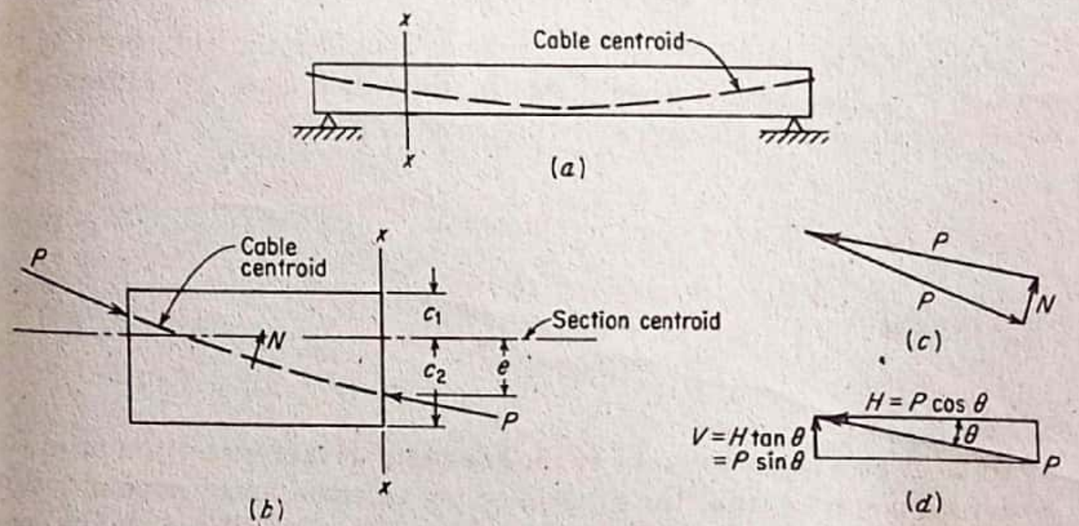


Fig. 11.4

Scanned with CamScanner

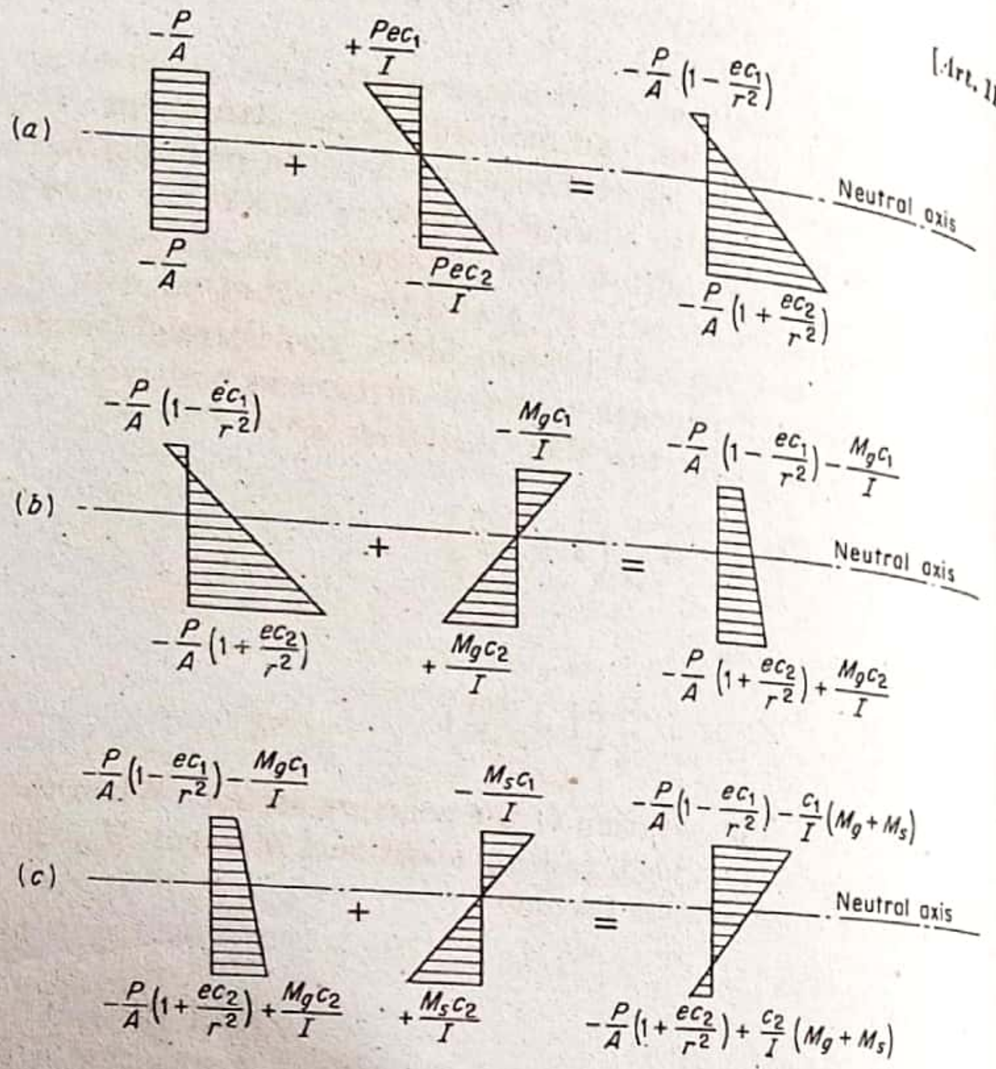


Fig. 11.5 Stress distribution in beams: (*a*) effect of prestress; (*b*) effect of prestress and girder dead load; (*c*) effect of prestress, girder dead load, and service load.

as shown in Fig. 11.5*b*. When the girder is installed and subjected to the service load (dead loads in addition to girder dead load, plus design live load) the stresses in the top and bottom fiber are

$$f_{1s} = f_{1d} - \frac{M_s c_1}{I} \tag{11.5}$$

$$f_{2s} = f_{2d} + \frac{M_s c_2}{I} \tag{11.6}$$

as in Fig. 11.5*c*.

It is necessary, in a review of the adequacy of a cross section or in the design of a section, that the stresses in the extreme fibers remain within the allowable limits under any loading or combination of loadings that can occur. Normally the stress distribution at the section of maximum moment in a properly designed beam will range between the extreme states shown in Fig. 11.6 as the beam passes from the unloaded state to the

loaded state, where f_c is the allowable stress in compression, and f_t the allowable stress in tension.

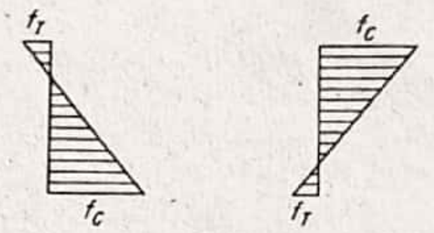


Fig. 11.6 Stress limits.

In calculating the section properties A, I, etc., to be used in the design equations, it is relevant that, in posttensioned construction, the cables are usually grouted in the conduits after tensioning. Before grouting, stresses should be based on the net section with holes deducted. After grouting, the transformed section should be used, with holes considered filled with concrete, and with the steel replaced with an equivalent area of concrete. However, it is satisfactory, unless the holes are quite large, to compute section properties on the basis of the gross concrete section. This tends to underestimate stresses due to prestress and overestimate stresses caused by applied loads; however, each error is small, and the two tend to compensate each other. Similarly, while in pretensioned beams the properties of the transformed section should be used, it makes little difference if calculations are based on properties of the gross concrete section.[1]

In some cases, in the design of prestressed-concrete beams it is useful to establish the location of the upper and lower *kern points* of a cross section. These are defined as the limiting points inside which the prestress-force resultant may be applied without causing tension anywhere in the cross section. Their locations are obtained by writing the expression for the tensile fiber stress due to application of an eccentric prestress force acting alone and setting this expression equal to zero to solve for the required eccentricity. In Fig. 11.7, to locate the upper kern-point distance k_1 from the neutral axis, let the prestress-force resultant P act at that point. Then the bottom fiber stress is

$$f_b = -\frac{P}{A}\left(1 - \frac{ec_2}{r^2}\right) = 0$$

[1] The ACI Code states: "In calculations of section properties prior to bonding of tendons, areas of the open ducts shall be deducted. The transformed area of bonded tendons may be included in pretensioned members and in posttensioned members after grouting."

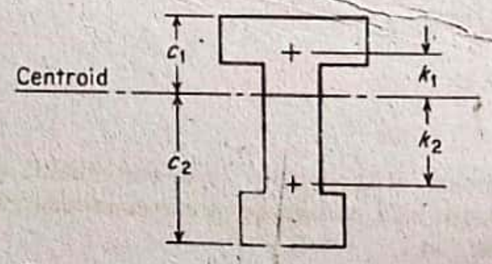


Fig. 11.7 Location of kern points.

Scanned with CamScanner

Set

$$1 - \frac{ec_2}{r^2} = 0$$

and solve for

$$e = k_1 = \frac{r^2}{c_2} \tag{11.7}$$

Similarly, the lower kern-point distance k_2 is

$$k_2 = \frac{r^2}{c_1} \tag{11.8}$$

The region between these two limiting points is known as the *kern*, or in some cases the *core*, of the section.

11.6 Application of Flexural Equations As in reinforced concrete, problems in prestressed concrete can be separated generally into review problems and design problems. For the former, with the applied loads, the concrete cross section, and the amount and point of application of the prestress-force resultant known, the equations of Art 11.5 permit the direct calculation of the resulting stresses. However, if the dimensions of a section and the amount and location of the prestress force are to be found, given the loads and allowable stresses, the problem is more complicated because of the several interrelated variables. More detailed study of these equations will reveal some significant points.

Consider first a simple-span prismatic beam with straight tendons typical of many types of pretensioned construction. Let the allowable concrete stress in tension be f_t, and that in compression f_c.* Straight tendons used with a straight beam result in a constant eccentricity of prestress force below the neutral axis throughout the length of the beam. At the cross section over the supports, neither dead- nor live-load moment is present, and the stresses are due only to the thrust and moment of the prestress force. Using Eqs. (11.1) and (11.2) and setting the top and bottom fiber stresses equal to the maximum allowable tension and compression, respectively,

$$f_{1p} = -\frac{P}{A} + \frac{Pec_1}{I} = f_t$$

$$f_{2p} = -\frac{P}{A} - \frac{Pec_2}{I} = f_c$$

* In writing statements of inequality, it is convenient to designate tensile stress as being larger than zero, and compressive stress smaller than zero. Thus $+450 > -1350$, $-600 > -1140$, etc.

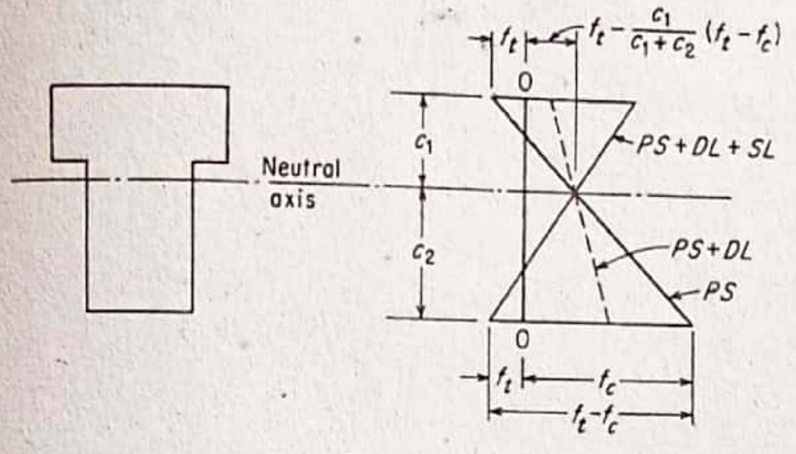


Fig. 11.8

The resulting stress distribution PS is shown in Fig. 11.8. For a given cross section and known allowable stresses, the unknowns in these two equations are P/A and e. Solving simultaneously for these quantities,

$$e = \frac{(f_t - f_c)I}{P(c_1 + c_2)} \tag{a}$$

$$-\frac{P}{A} = f_t - \frac{c_1}{c_1 + c_2}(f_t - f_c) \tag{b}$$

The required prestress force P can be found from Eq. (*b*) as the product of the area times the concrete stress at the section centroid (see Fig. 11.8), and that value of P may be substituted in Eq. (*a*) to obtain the eccentricity.

The section of maximum moment of the beam (usually midspan) will be investigated next under the action of eccentric prestress force and girder dead load. From Eqs. (11.3) and (11.4) the top and bottom fiber stresses are

$$f_{1d} = f_t - \frac{M_g c_1}{I} \qquad f_{2d} = f_c + \frac{M_g c_2}{I}$$

The resulting stress distribution $PS + DL$ is shown in Fig. 11.8. It is evident that, for the type of beam under discussion, this loading state will never be critical, but only represents an intermediate condition between two limiting values which control.

Considering now the maximum-moment section under the action of eccentric prestress force and full service load; from Eqs. (11.5) and (11.6) the top and bottom fiber stresses are

$$f_{1s} = f_{1d} - \frac{M_s c_1}{I} = f_t - \frac{c_1}{I}(M_g + M_s)$$

$$f_{2s} = f_{2d} + \frac{M_s c_2}{I} = f_c + \frac{c_2}{I}(M_g + M_s)$$

Scanned with CamScanner

These stresses must be within the specified allowable stress limits. Thus (designating the section moduli $S_1 = I/c_1$ and $S_2 = I/c_2$) one obtains

$$f_t - \frac{1}{S_1}(M_g + M_s) \geq f_c$$

$$f_c + \frac{1}{S_2}(M_g + M_s) \leq f_t$$

from which

$$S_1 \geq \frac{M_g + M_s}{f_t - f_c} \tag{c}$$

$$S_2 \geq \frac{M_g + M_s}{f_t - f_c} \tag{d}$$

That is, the section moduli of both top and bottom fibers must be at least equal to the total moment $(M_g + M_s)$ divided by the available stress range. The resulting stress distribution $PS + DL + SL$ is shown in Fig. 11.8.

In summary, the significant points of this discussion of prismatic beams with straight tendons are:

1. The required prestress force is the product of the concrete area and the concrete stress at the section centroid.
2. At no place in the beam can the tendon eccentricity be larger than its value at the supports, where only the eccentric prestress force acts.
3. The required section modulus depends upon the sum of the girder moment and service-load moment.

In most cases in actual construction, the prestress force does not act alone on a concrete beam. As the eccentric prestress force is applied, the beam cambers off the supporting form, and stresses due to girder dead load are immediately superimposed on those due to prestress. If straight tendons are used, resulting in a constant eccentricity, it is not possible to take advantage of the superposition of prestress and girder dead-load stresses, because the maximum eccentricity is controlled by the situation at the support, where no dead-load moment acts. On the other hand, if a variable eccentricity is possible, that eccentricity can be made larger near midspan, such that the superimposed prestress and girder dead-load stress distributions will utilize the full stress range from f_t (tension) to f_c (compression).

This is easily done for posttensioned beams by using a curved tendon conduit, wired to the stirrups in the desired profile prior to pouring the concrete. It can also be accomplished (but with somewhat more difficulty) in pretensioned beams, by the use of cable tie-down bars at intervals along the span.

Consider now a simple-span prismatic beam with curved tendons providing a variable eccentricity. All other conditions are the same as in the previous illustration. At the support sections, conditions will be the same as before, with stresses due to prestress force alone, and

$$f_{1p} = -\frac{P}{A} + \frac{Pe_s c_1}{I} = f_t$$

$$f_{2p} = -\frac{P}{A} - \frac{Pe_s c_2}{I} = f_c$$

Accordingly, at the supports,

$$e_s = \frac{(f_t - f_c)I}{P(c_1 + c_2)} \tag{e}$$

$$-\frac{P}{A} = f_t - \frac{c_1}{c_1 + c_2}(f_t - f_c) \tag{f}$$

At the maximum-moment section, girder dead-load stresses are superimposed. The eccentricity of prestress force can therefore be increased such that the limiting stress conditions are attained only under the superimposed load of the girder. Then, at midspan,

$$f_{1d} = -\frac{P}{A} + \frac{Pe_m c_1}{I} - \frac{M_g c_1}{I} = f_t$$

$$f_{2d} = -\frac{P}{A} - \frac{Pe_m c_2}{I} + \frac{M_g c_2}{I} = f_c$$

Solving these two equations simultaneously for the unknowns P/A and e_m,

$$-\frac{P}{A} = f_t - \frac{c_1}{c_1 + c_2}(f_t - f_c) \tag{g}$$

as before, and

$$e_m = \frac{(f_t - f_c)I}{P(c_1 + c_2)} + \frac{M_g}{P} \tag{h}$$

By comparing this expression for e_m with that for e_s at the supports, it is seen that an additional eccentricity in the amount M_g/P has been introduced which will produce a moment due to prestress just equal to the dead-load moment but of opposite sign. The stress distribution $PS + DL$ due to superimposed prestress and girder dead-load stress is shown in Fig. 11.9. The distribution PS due to prestress alone does not exist where dead-load moments act.[1]

[1] In designing on this basis, care must be taken to ensure that the assumed conditions will actually be obtained. For example, a beam cast on soft ground would receive some support along its length even after prestress is applied. A precast beam laid flat on its side during handling would obviously have no dead-load stresses superimposed.

Scanned with CamScanner

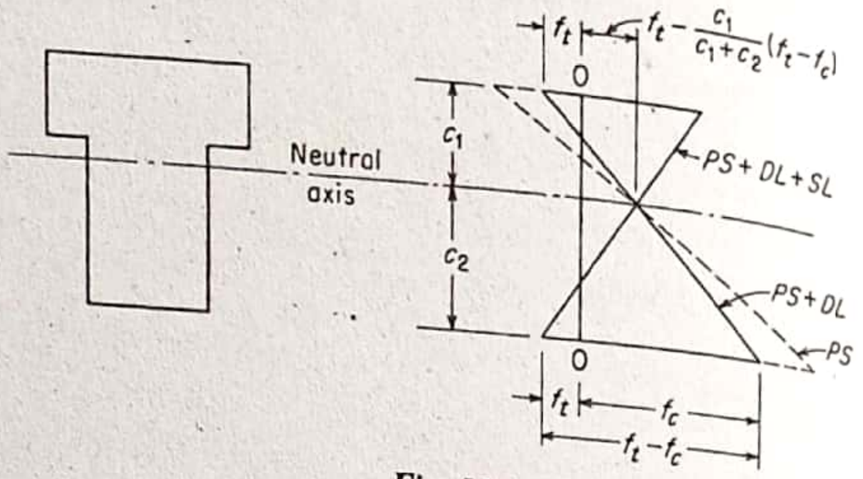


Fig. 11.9

Now, investigating the maximum-moment section under the action of eccentric prestress force and full service load, the top and bottom fiber stresses are

$$f_{1s} = f_{1d} - \frac{M_s c_1}{I} = f_t - \frac{M_s c_1}{I}$$

$$f_{2s} = f_{2d} + \frac{M_s c_2}{I} = f_c + \frac{M_s c_2}{I}$$

These stresses must be within the limits of f_t (tension) and f_c (compression). Thus

$$f_t - \frac{M_s}{S_1} \geq f_c \qquad f_c + \frac{M_s}{S_2} \leq f_t$$

from which

$$S_1 \geq \frac{M_s}{f_t - f_c} \tag{1}$$

$$S_2 \geq \frac{M_s}{f_t - f_c} \tag{2}$$

The section moduli in this case must be at least equal to the superimposed load moment M_s divided by the available stress range. The resulting stress distribution $PS + DL + SL$ is shown in Fig. 11.9.

In summary, the more significant aspects of the second illustration, pertaining to prismatic beams with curved tendons, are:

1. The required prestress force is the product of the concrete area and the concrete stress at the section centroid. (Note that the centroidal stress does not change as moment is applied to the beam.)

2. Conditions at the supports are the same as for beams with straight cables; here prestress force acts alone.

3. Elsewhere along the span, by depressing the centroid of prestress force an amount M_g/P below its lowest possible location at the supports, the dead load of the beam may be fully compensated.

The last feature is of the greatest importance; it explains a large part of the economy of prestressed-concrete members, particularly for long spans. The dead load of the girder is carried entirely "free," at no cost of additional concrete, steel, or prestress force, and the full stress capacity of the material is used in resisting useful load.

Example A simply supported rectangular beam is to span 30 ft and must carry a load, in addition to its own weight, of 500 plf. Allowable concrete stresses are 1800 psi in compression and 200 psi in tension. A prismatic beam with straight, posttensioned wires is to be used. Find the required dimensions of the concrete section, the magnitude of the required prestress force, and the location of the cable centroid.

It is necessary in this case to estimate the dead load of the beam. Assuming a section 12 in. wide and 15 in. deep,

$$w_g = \frac{12 \times 15}{144} 150 = 188 \text{ plf}$$

$$M_g = \tfrac{1}{8} \times 188 \times 30^2 = 21{,}200 \text{ ft-lb}$$

$$w_l = 500 \text{ plf}$$

$$M_s = \tfrac{1}{8} \times 500 \times 30^2 = 56{,}300 \text{ ft-lb}$$

In this case, since straight tendons are specified, the prestress eccentricity can be no larger than that value permissible at the supports, where no girder moments act, and the section modulus depends upon the sum of girder moment and superimposed load moment. Thus

$$S = \frac{M_g + M_s}{f_t - f_c} = \frac{(21{,}200 + 56{,}300)12}{200 + 1800} = 465 \text{ in.}^3$$

$$\frac{bh^2}{6} = 465$$

$$bh^2 = 2790$$

A concrete section 12 in. wide and 15.2 in. deep is selected; the assumed dead load is satisfactory. (In practice, dimensions would be rounded, probably to the next larger inch; however, for the sake of clarity in this example and for comparison with later results, theoretical dimensions will be retained.) Then

$$A = 12 \times 15.2 = 182 \text{ in.}^2$$

$$I = \frac{12 \times 15.2^3}{12} = 3510 \text{ in.}^4$$

$$P = -\left[f_t - \frac{c_1}{c_1 + c_2}(f_t - f_c)\right] A$$

$$= (-200 + \tfrac{1}{2} \times 2000)182 = 146{,}000 \text{ lb}$$

$$e = \frac{(f_t - f_c)I}{P(c_1 + c_2)} = \frac{2000 \times 3510}{146{,}000 \times 15.2} = 3.16 \text{ in.}$$

Scanned with CamScanner

[Art. 11.6

Using stress-relieved solid wires of 0.250-in. diameter (see Table 11, Appendix B) with an effective prestress of 0.60 of the ultimate value, the number of wires required is

$$N = \frac{146{,}000}{0.60 \times 11{,}800} = 20.6$$

Twenty-one wires will be used. A check of top and bottom fiber stresses using Eqs. (11.1) to (11.6) verifies that the specified stress limits have not been exceeded.

Example Design a beam for the same span, load, and stress conditions as for the preceding example; use curved tendons to permit a variable eccentricity.

Under the assumption that dead-load moment can be compensated by additional prestress eccentricity, it is unnecessary to estimate the dead load. The required section modulus is

$$S = \frac{M_s}{f_t - f_c} = \frac{56{,}300 \times 12}{200 + 1800} = 338 \text{ in.}^3$$

$$\frac{bh^2}{6} = 338$$

$$bh^2 = 2030$$

A section 12 in. wide and 13 in. deep is selected, for which

$$A = 12 \times 13 = 156 \text{ in.}^2$$

$$I = \frac{12 \times 13^3}{12} = 2200 \text{ in.}^4$$

$$w_g = {}^{156}\!/_{144} \times 150 = 163 \text{ plf}$$

$$M_g = \tfrac{1}{8} \times 163 \times 30^2 = 18{,}400 \text{ ft-lb}$$

Then

$$P = -\left[f_t - \frac{c_1}{c_1 + c_2}(f_t - f_c)\right] A$$

$$= (-200 + \tfrac{1}{2} \times 2000)156 = 125{,}000 \text{ lb}$$

$$e_s = \frac{(f_t - f_c)I}{P(c_1 + c_2)} = \frac{2000 \times 2200}{125{,}000 \times 13} = 2.71 \text{ in.}$$

$$e_m = e_s + \frac{M_g}{P} = 2.71 + \frac{18{,}400 \times 12}{125{,}000} = 4.48 \text{ in.}$$

In this case, the required number of wires of 0.250 in. diameter is

$$N = \frac{125{,}000}{0.60 \times 11{,}800} = 17.7$$

Eighteen wires will be used. A check of top and bottom fiber stresses, both at the supports and at midspan, indicates that the desired stresses have been attained. In a comparison of these results with those of the previous example, the advantage of curved tendons becomes obvious. By the simple expedient of depressing the centroid of the wires at midspan 1.77 in. below its location at the supports, a saving of over 14 per cent in both concrete and steel is obtained. For longer

spans, with a higher ratio of dead to live load, the saving would be considerably larger.

Example Design a beam with specifications as in the first two examples, except that the span is increased to 60 ft. Use curved tendons to permit a variable eccentricity. The live load is 500 plf, and allowable stresses are 1800 psi in compression and 200 psi in tension as before.

Proceeding as in the second example,

$$M_s = \tfrac{1}{8} \times 500 \times 60^2 = 225{,}000 \text{ ft-lb}$$

$$S = \frac{M_s}{f_t - f_c} = \frac{225{,}000 \times 12}{200 + 1800} = 1350 \text{ in.}^3$$

$$\frac{bh^2}{6} = 1350$$

$$bh^2 = 8110$$

A section 15 in. wide and 23.2 in. deep is selected, for which

$$A = 15 \times 23.2 = 348 \text{ in.}^2$$

$$I = \frac{15 \times 23.2^3}{12} = 15{,}600 \text{ in.}^4$$

$$w_g = {}^{348}\!/_{144} \times 150 = 362 \text{ plf}$$

$$M_g = \tfrac{1}{8} \times 362 \times 60^2 = 163{,}000 \text{ ft-lb}$$

Then

$$P = -\left[f_t - \frac{c_1}{c_1 + c_2}(f_t - f_c)\right] A$$

$$= (-200 + \tfrac{1}{2} \times 2000)348 = 279{,}000 \text{ lb}$$

$$e_s = \frac{(f_t - f_c)I}{P(c_1 + c_2)} = \frac{2000 \times 15{,}600}{279{,}000 \times 23.2} = 4.72 \text{ in.}$$

$$e_m = e_s + \frac{M_g}{P} = 4.72 + \frac{163{,}000 \times 12}{279{,}000} = 11.74 \text{ in.}$$

Note that the half depth of the proposed beam is only 11.60 in., indicating that the centroid of the wire group would have to be outside the cross section in order to satisfy the stated stress conditions. This is obviously not possible, and either the proportions of the beam must be changed or, if the section dimensions are for some reason restricted, the dead load cannot be fully compensated by additional eccentricity of prestress force. Proceeding on the basis that there is no restriction on section dimensions,

$$w_g = \frac{bh}{144} 150 = 1.04bh \quad \text{plf}$$

$$M_g = \tfrac{1}{8} \times 1.04bh \times 60^2 = 468bh \quad \text{ft-lb}$$

$$P = (-200 + \tfrac{1}{2} \times 2000)bh = 800bh \quad \text{lb}$$

Then

$$\frac{M_g}{P} = \frac{468bh \times 12}{800bh} = 7.03 \text{ in.}$$

Scanned with CamScanner

It is interesting to observe here that the added eccentricity M_g/P required to compensate for girder dead load is independent of beam dimensions and depends only on the weight of the material, the span, and the stress at the section centroid. Then

$$e_s = \frac{(f_t - f_c)I}{P(c_1 + c_2)} = \frac{2000bh^3/12}{800bh^2} = 0.208h$$

At this point, it is necessary to establish the amount of concrete that will be required from the tendon centroid to the bottom fiber of the beam. This will depend not only upon the amount of concrete protection needed for the lowest wires (usually 1½ in.), but on the number and arrangement of the wires as well. For present purposes, this distance will be assumed to be $0.10h$. Then

$$e_s + \frac{M_g}{P} + 0.10h = 0.50h$$

$$0.208h + 7.03 + 0.10h = 0.50h$$

$$h = 36.6 \text{ in.}$$

and the corresponding width is

$$b = \frac{6 \times 1350}{36.6^2} = 6.05 \text{ in.}$$

A concrete section 6.05 in. wide and 36.6 in. deep will be used. At the supports the cable eccentricity is $0.208 \times 36.6 = 7.62$ in., and at midspan it is $7.62 + 7.03 = 14.65$ in. The total prestress force required is $800 \times 6.05 \times 36.6 = 177{,}000$ lb.

It is apparent from this example that, for a given span, load, and allowable stress, there is a certain minimum permissible depth which will allow all the dead load to be carried "free." If the section proportions can be modified at will, this is the economical depth to use. If, on the other hand, there are restrictions on maximum depth, as is often the case, or if the ratio of width to depth is limited by other considerations such as lateral stability, then it may be impossible to utilize the full allowable stress under both load conditions, dead load and dead plus live load. This means in turn that the section modulus must be increased to carry at least a portion of the dead-load moment, as well as the live-load moment.

PROBLEMS

1. A rectangular prestressed beam is to be simply supported on a 40-ft span and must carry a superimposed load of 1000 plf. The beam will be pretensioned using straight cables. Concrete of $f'_c = 4000$ psi will be used. The allowable stress in compression is 1800 psi and that in tension is 380 psi. Find the required concrete dimensions, the magnitude of the required prestress force, and the location of the cable centroid.

2. Redesign the beam of Prob. 1 as a posttensioned beam with curved cables permitting a variable eccentricity.

3. A rectangular prestressed beam is to be simply supported on a 60-ft span and must carry a superimposed load of 1000 plf. The beam will be posttensioned with curved cables. Concrete having $f'_c = 4000$ psi will be used at allowable stresses of 1800 psi in compression and 380 psi in tension. Find the required concrete dimensions, the magnitude of the required prestress force, and the location of the cable centroid at the supports and at midspan. Assume that the minimum distance from the tendon centroid to the bottom of the beam is $\frac{1}{10}$ the total beam depth. Comment on your design.

4. Redesign the beam of Prob. 3 using a maximum total depth of 40 in.

11.7 I Sections The discussion up to this point has dealt exclusively with rectangular sections. These are important not only in demonstrating most simply the basic principles of prestressing, but also because rectangular sections are often used for prestressed slabs, for small beams, and for designs in which only a few beams of given dimensions are required. Forming costs are least for rectangular beams. However, for improved material economy it is desirable to use some form of I section for prestressed members, just as in steel design the wide-flange or I shape has proved most efficient. While in ordinary reinforced-concrete design, diagonal tensile stresses restrict the possibility of reduction in web thickness, in prestressed-concrete construction this is not so. It will be demonstrated later that, because of the axial compression over the cross section, diagonal tensile stresses are much reduced. One consequence of this is that the flexurally efficient I or T section can be used. Several common shapes are shown in Figure 11.10. Generally speaking, I, T, and box sections with relatively thin webs and thin flanges are more efficient than members with thicker parts. However several factors limit the gain in efficiency which may be made in proportioning the section, such as the problem of depositing concrete in very thin sections and the question of instability of very thin overhanging compression portions. Cross sections may be either symmetrical or unsymmetrical. If it is possible to utilize the cross section fully (i.e., to achieve the full range of allowable stress in both the top and bottom fibers as the load ranges from dead load only to dead plus live load), then the section should be symmetrical, since it is desirable that $(f_t - f_c) = M_s/S$ should obtain at both top and bottom of the section for

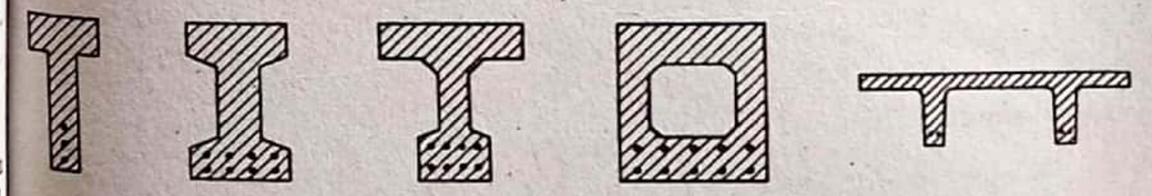


***Fig.* 11.10** Typical nonrectangular sections.

Scanned with CamScanner

the two extreme load conditions. If the situation is such that the d load cannot be fully counteracted by cable eccentricity, then there may good reason to use an unsymmetrical section. A section with a high troid location, providing sufficient depth below the neutral axis to acc modate the cable eccentricity, would be indicated.

In selecting the dimensions of I sections, it is often convenient choose the relative proportions of the section and let all the dimensi vary with one, say the depth, so that all the properties of the sec can be expressed as a numerical constant times some power of the dep The design then closely follows the procedures outlined for rectang sections.

11.8 Cable Profiles The previous discussion has dealt only w critical sections (usually midspan and support sections) in establish cable centroid locations. Most present prestressed construction u members that are essentially prismatic and employs a constant prestr ing force from one end of the beam to the other, although curved or drap tendons are often used. In determining the best location for the centr of such steel through the length of the beam, it is only necessary to ens that the limiting stress states, such as are shown in Fig. 11.6, are nowh violated under any anticipated loading. For a member which is prope designed at the critical sections, it is sufficient elsewhere to ensure th the tendon eccentricity is such that the allowable tensile stress in t concrete is not exceeded.

With no transverse loading applied to a beam, the center of co pression at any cross section will coincide with the center of tension, i the centroid of the prestressing steel. It has been shown that when t girder load is applied, the center of compression will move upward amount M_g/P. Similarly, it can be shown that when the total load applied, the center of compression will rise an amount $(M_g + M_s)$ above its original location.

The upper limit position of the compressive resultant, y_1 above t neutral axis, is such that it produces a tensile stress f_t at the bottom fi of the section. With the compressive resultant at that limiting point, t bottom fiber stress is

$$-\frac{P}{A}+\frac{Pec_2}{I}=f_t$$

from which

$$e = y_1 = \frac{I}{Pc_2}\left(\frac{P}{A}+f_t\right) = \frac{Ar^2}{Pc_2}\left(\frac{P}{A}+f_t\right)$$

$$y_1 = \frac{r^2}{c_2}\left(1+\frac{Af_t}{P}\right) \qquad (11$$

Similarly, the lower limit position of the compressive resultant, y_2 below the neutral axis, is such that it produces the allowable tensile stress f_t at the top fiber, and its location relative to the neutral axis is

$$y_2 = \frac{r^2}{c_1}\left(1+\frac{Af_t}{P}\right) \qquad (11.10)$$

With reference to Fig. 11.11, the location of the steel centroid must therefore be such that it is no less than $(M_g + M_s)/P$ below the level defined by y_1, and no more than M_g/P below the level defined by y_2. In this way the possible range of steel-centroid locations is established. The procedure should be repeated at sufficient intervals along the member to establish cable-centroid envelope curves. Note that, ideally, the upper and lower locations of the steel centroid, found in this way, will coincide. Only for this condition will the full efficiency of the cross section be obtained; i.e., the full allowable stress range will be utilized for both the upper and lower fibers of the beam. Usually this optimum condition is obtained at only one cross section.

A saving in design time is possible if it is noted that the ordinates of the cable envelope curves, measured downward from the limit lines defined by y_1 and y_2, are directly proportional to the ordinates of the respective moment diagrams. For a prismatic beam, for example, the dead load is uniform, and the lower envelope curve will vary parabolically from one end of the span to the other. If the live load is uniformly distributed, the upper envelope curve will likewise be a parabola, passing through established points at midspan and at the two supports. Limiting profiles can be drawn as shown in Fig. 11.12. Figure 11.12*a* illustrates, by the shaded area, the possible range of cable profiles for a uniformly loaded prismatic beam such that the midspan section is fully utilized, with upper and lower cable envelopes coinciding at midspan. Any cable profile falling completely within the shaded zone will be satisfactory from the point of view of flexural stress. Figure 11.12*b* shows the cable zone for a prismatic beam with a single concentrated live load at midspan. The lower cable envelope is a continuous parabola as before, while the upper curve consists

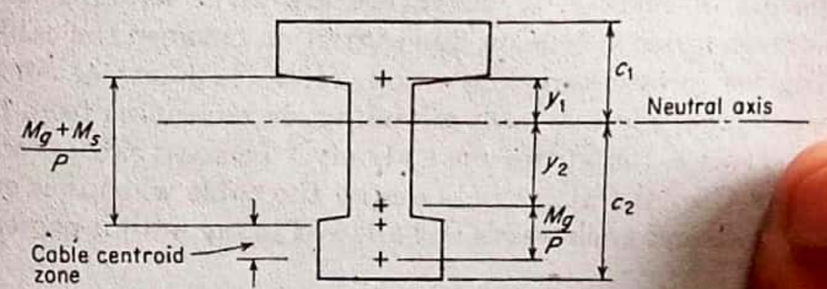


Fig. 11.11

Scanned with CamScanner

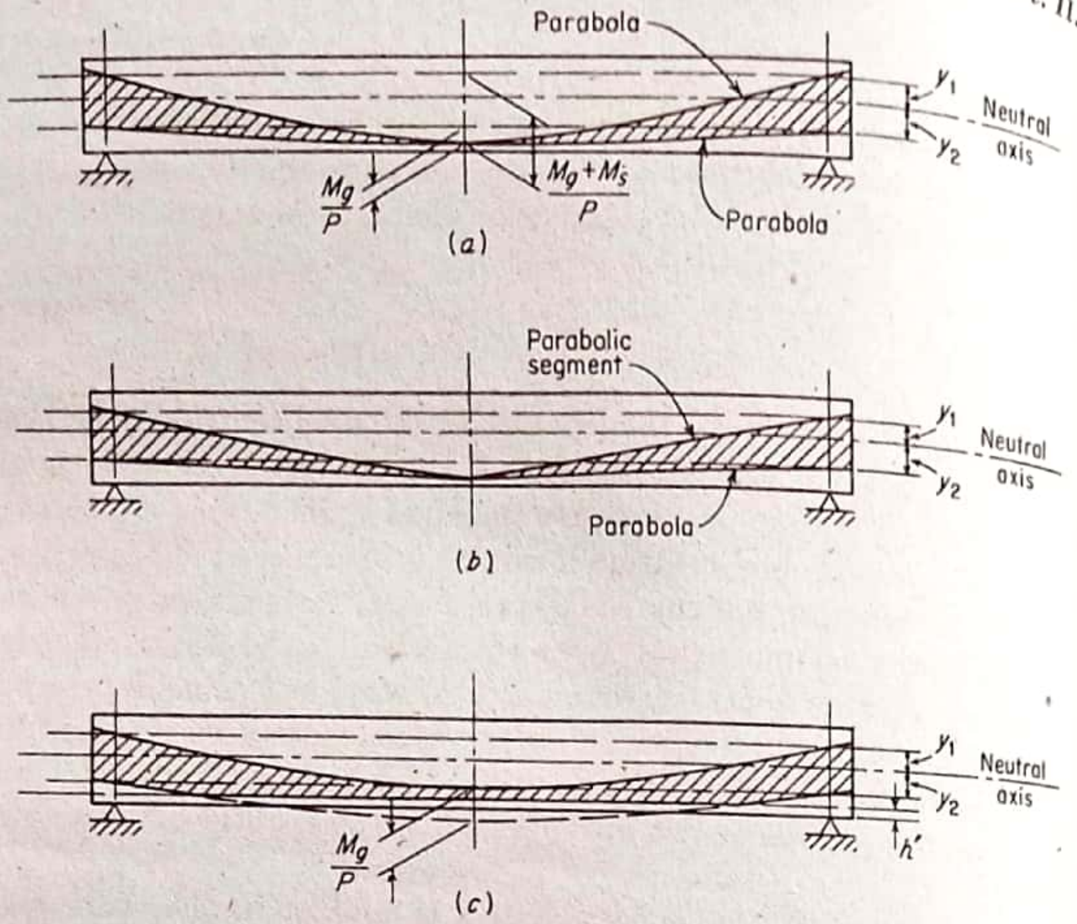


***Fig.* 11.12** Cable-profile zones.

of two parabolic segments with ordinates from the upper limit line proportional to those of the combined dead- and live-load moment diagrams. Figure 11.12*c* shows the situation for a uniformly loaded beam in which depth restrictions prevent the full compensation of dead-load moment. In this case, the distance h' represents the minimum cover to the centroid of the prestressing steel and defines the horizontal cutoff of the lower envelope parabola. As before, any cable shape falling entirely in the shaded zone will satisfy flexural requirements.

From a practical point of view, it is not always wise to adopt any arbitrary shape. In pretensioned construction, cable depressors and cable templates are used to obtain a linear segmental profile. In general, it is desirable to minimize the number of changes in slope. In posttensioned construction, curved-cable alignment can easily be obtained, but, in general, points of reversal of curvature are to be avoided, since these greatly increase losses in tension due to friction between the cable and the duct during the prestressing operation. (If such points of contraflexure cannot be avoided, there is some advantage in tensioning from both ends of the cables, rather than from one end only.) The best cable profile is that which follows the natural curve taken by the cable when it is suspended between the two end anchorages and allowed to sag until it passes through

a single specified low point. To avoid displacing the conduit during concreting, it must be wired to the vertical web reinforcement.

PROBLEMS

1. Determine the cable profile for the beam of Prob. 3, Art. 11.6, giving offset dimensions from the beam centroid to the cable centroid at intervals of one-eighth the span along the beam.
2. Determine the cable profile for the beam of Prob. 4, Art. 11.6, giving offset dimensions from the beam centroid to the cable centroid at intervals of one-eighth the span along the beam.

11.9 Losses in Prestress As was previously mentioned, the prestressing force is not constant but will decrease with time, owing to a variety of causes. Most of these losses take place rapidly at first, and then at a gradually decreasing rate, approaching a limiting value asymptotically. In practice, only initial and final prestress values need be considered, final prestress being that value obtained after all important losses have occurred. It is advisable to check stresses in the member under initial prestress plus girder load, final prestress plus girder load, and final prestress plus service load. Other load combinations may at times be critical. The most important causes of loss in prestress will be discussed briefly in the following paragraphs.

a. Elastic shortening of the concrete In pretensioned members, as the cable force is transferred from the fixed abutments to the concrete beam, elastic instantaneous compressive strain will take place in the concrete, tending to reduce the stress in the bonded prestressing steel. For axially prestressed members, this can be closely estimated by

$$\Delta f_s = n\,\Delta f_c$$

where $\Delta f_c \cong P_i/A_c$ is the change in concrete stress as the prestress force is applied, and n is the modular ratio. It is recognized that the value of Δf_c can only be estimated. It will be found, however, that small errors in predicting Δf_s due to elastic shortening are of little consequence, since the loss in prestress due to that shortening will only be a small percentage of the total prestress.

In posttensioned members, if all the strands are tensioned at one time, there will be no loss due to elastic shortening, because this shortening will occur as the jacking force is applied and before the prestressing force is measured. On the other hand, if various strands are tensioned sequentially, the stress loss in each strand will vary, being a maximum in the first strand tensioned, and zero in the last strand. In such cases, it is sufficiently

Scanned with CamScanner

accurate to calculate the loss in the first cable and to apply one-half that value to all cables.

b. Creep of concrete Shortening of concrete under sustained load has been discussed in detail in Art. 1.7. It is evident that creep will result in loss of prestress force; from the previous discussion, it is known that the creep shortening may be several times the initial elastic shortening. Allowance for loss due to creep is made by using a "creep coefficient" C_c, defined as

$$C_c = \frac{\text{additional longtime deformation}}{\text{initial elastic deformation}}$$

A value of C_c of 1.5 to 2.0 will give satisfactory results under most conditions.

c. Shrinkage of concrete It is apparent that a decrease in the length of a member due to shrinkage of the concrete will be just as detrimental as length changes due to stress, creep, or other causes. As discussed in Art. 1.9, the amount of shrinkage to expect will vary widely, depending upon many factors. Adopting a shrinkage strain of 0.0003 as an average value, the stress loss due to shrinkage is

$$\Delta f_s = 0.0003E_s$$

d. Relaxation of steel The phenomenon of relaxation, similar to creep, was discussed in Art. 11.3. Loss in stress due to relaxation will vary greatly, depending upon the stress in the steel. Since an effective prestress of 60 per cent of the ultimate strength of the steel is generally used, it is apparent from the previous discussion that some allowance must be made for stress loss due to relaxation. A relaxation loss of 3 per cent is typical for steel stressed to $0.60f'_s$.

It is interesting to observe that the largest part of the relaxation loss occurs shortly after the steel is stretched. For stresses of $0.80f'_s$ and higher, even a very short period of loading will produce substantial relaxation, and this, in turn, will reduce the relaxation that will occur later at a reduced stress level. The relaxation rate can thus be artificially accelerated by temporary overtensioning. This technique has sometimes been employed to reduce losses.

e. Frictional losses Losses due to friction, as the cable is stressed in posttensioned members, are usually separated for convenience into two parts: curvature friction and wobble friction. The first is due to intentional bends in the cable profile as specified, and the second to the unintentional variation of the cable from its intended profile. It is apparent that even a "straight" cable duct will have some unintentional misalignment, so that wobble friction must always be considered in posttensioned work. Usually, curvature friction must be considered as well. The force at

Table 11.3

Type of steel	Usual range of observed values		Suggested design values	
	K	μ	K	μ
Wire cables	0.0005–0.0030	0.15–0.35	0.0015	0.25
High-strength bars	0.0001–0.0005	0.08–0.30	0.0003	0.20
Galvanized strand	0.0005–0.0020	0.15–0.30	0.0015	0.25

the jacking end of the cable, P_0, required to produce the force P_x at any point x along the cable, can be found from the expression

$$P_0 = P_x\epsilon^{KL+\mu\alpha}$$

where ϵ = base of natural logarithms
L = cable length from jacking end to point x
α = angular change of cable from jacking end to point x, rad
K = wobble friction coefficient, lb per lb per ft
μ = curvature friction coefficient

There has been much research on frictional losses in prestressed construction, particularly with regard to the values of K and μ. These vary appreciably, depending on construction methods and materials used. The values in Table 11.3 are included in the ACI Code.

The loss of prestress for the entire cable length can be computed by segments, with each segment assumed to consist of either a circular arc or a length of tangent. If one accepts the approximation that the normal pressure on the duct causing the frictional force results from the undiminished initial tension all the way around the curve, then the following simplified expression for loss in tension is obtained:

$$P_0 = P_x(1 + KL + \mu\alpha)$$

where α is the angle between the tangents at the ends. The ACI Code permits the use of the simplified form if the value of $(KL + \mu\alpha)$ is not greater than 0.3.

f. Slip at the anchorages As the load is transferred to the anchorage device in posttensioned construction, a slight inward movement of the cable will occur as the wedges "seat" themselves and as the anchorage itself deforms under stress. The amount of movement will vary greatly, depending on the type of anchorage and on construction techniques. The amount of movement due to "seating" and stress deformation associated with any particular type of anchorage is best established by test. Once

Scanned with CamScanner

Table 11.4 **Summary of losses in prestress, per cent of initial prestress**

Losses	Pretensioned beams		Posttensioned beams	
Before transfer	Shrinkage	3%		
At transfer	Elastic strain in concrete	3%	Elastic strain in concrete (only if multiple strands)	
			Anchor slip	1%
			Bending of beam (usually negligible)	2%
			Friction	2%
After transfer	Shrinkage	4%	Shrinkage	4%
	Concrete creep	7%	Concrete creep	4%
	Steel relaxation	3%	Steel relaxation	3%
Total		20%		16%

this amount ΔL is determined, the stress loss is easily calculated using the equation

$$\Delta f_s = \frac{\Delta L}{L} E_s$$

It is significant to note that the amount of slip is nearly independent of the cable length. For this reason, the stress loss will be large for short cables and relatively small for long cables. The practical consequence of this is that it is most difficult to posttension short wires with any degree of accuracy.

g. Summary of losses As indicated in the above discussion, the magnitude of losses in prestressed construction will vary widely, depending on conditions, and about all one can say is that losses will occur and that they must be considered. Table 11.4 presents a summary of losses for pretensioned and posttensioned beams and is included to present an order of magnitude for the various losses; individual loss figures may vary substantially from the values given.

PROBLEMS

The posttensioned prestressed beam of Fig. 11.13 (Art. 11.10) is used on a simple span of 50 ft. Nine draped strands, having a total cross-sectional area of 1.75 in.^{2}, are used. The steel centroid is 16.0 in. below the top surface of the beam at the supports and is at a 24.5-in. depth at midspan. A desired final prestress of 246,000 lb at midspan will permit a live load of 1000 plf. The average compressive stress at the level of the prestress centroid under normal conditions of loading ($PS + DL$) may be taken as 2000 psi. Strands are tensioned sequentially; at one end only, and are grouted. (1) What is your best estimate of the required initial prestress force? (2) What are the stresses in the concrete at top and bottom fibers at the supports and at midspan immediately after transfer? (3) Comment on and discuss your results. (Note that the curvature of the cable can be approximated by a circular arc in calculating losses due to curvature.)

$E_c = 4 \times 10^6$ psi
$E_s = 28 \times 10^6$ psi
Shrinkage coefficient = 0.0003
Creep coefficient = 2.5
Relaxation of the steel = 4 per cent
Slip at anchorage at transfer = 0.052 in.
$I = 25{,}170$ in.^{4}

11.10 Ultimate Flexural Strength In an ordinary reinforced-concrete beam, the stress in the tensile steel and the compressive force in the concrete increase in proportion to the applied moment up to and somewhat beyond service load, the distance between the two internal force resultants remaining essentially constant. In contrast to this behavior, in a prestressed beam, increased moment is resisted by a proportionate increase in the distance between the compressive and tensile resultant forces, the compressive resultant moving upward as the load is increased. The magnitude of the internal forces remains nearly constant up to and usually somewhat beyond service loads.

This situation is changed drastically upon tensile flexural cracking of the prestressed beam. When the beam cracks, there is a sudden increase in the stress in the steel as the tension which was formerly carried by the concrete is transferred to it. After cracking, the prestressed beam behaves essentially as an ordinary reinforced-concrete beam. The compressive resultant cannot continue to move upward indefinitely, and increasing moment must be accompanied by a nearly proportionate increase in steel stress and compressive force. The ultimate strength of a prestressed beam can therefore be predicted by the methods developed for ordinary reinforced-concrete beams, with minor modifications to account for the differing nature of the stress-strain relationship of prestressing steel as compared to ordinary reinforcing steel.

In Art. 2.9 it was shown that underreinforced prestressed beams will fail when the steel stress reaches its ultimate tensile value f'_s, at which point

$$M_u = A_s f'_s \left(d - \frac{A_s f'_s}{1.7 f'_c b} \right) = A_s f'_s d \left(1 - 0.59 p \frac{f'_s}{f'_c} \right) \qquad (2.59)$$

Whether the beam is underreinforced or overreinforced is determined by calculating the concrete strain in the extreme fiber at the instant of steel rupture. If the concrete strain ϵ_c is less than the crushing strain (usually

Scanned with CamScanner

taken equal to 0.003) when the steel has reached its breaking strain ϵ'_s, then the beam is underreinforced. The concrete strain can be found from the expression

$$\epsilon_c = \epsilon'_s(\epsilon'_s - \epsilon_{se})\frac{a/k_1}{d - a/k_1} \tag{2.60}$$

where

$$a = \frac{A_s f'_s}{0.85 f'_c b} \tag{2.58}$$

If ϵ_c, found in this way, exceeds the crushing strain of the concrete, the beam is said to be overreinforced, in which case the steel stress at failure of the beam is some value $f_{su} < f'_s$. In this case the ultimate strength of the beam can be found by successive approximations as described in detail in Art. 2.9.

The above discussion and that of Art. 2.9 pertain to prestressed beams in which the steel is bonded to the concrete continuously throughout its length. This will normally be the case in pretensioned construction and will be the case in posttensioned construction if the cables are grouted after tensioning, as is usually the case. If a posttensioned beam is not grouted, it is difficult to determine the exact steel stress at failure load. The stress will be uniformly distributed along the entire length of the tendons. Characteristically, there will be a small number of rather wide cracks. These have the effect of reducing the failure load as compared with that of an otherwise identical bonded beam.

The ACI Code states that, if the ratio pf_{su}/f'_c is not more than 0.30, the ultimate flexural strength of prestressed beams can be found from the expression

$$M_u = \phi A_s f_{su}\left(d - \frac{a}{2}\right) \tag{11.11}$$

where

$$a = \frac{A_s f_{su}}{0.85 f'_c b}$$

This is given also in the alternative form

$$M_u = \phi A_s f_{su} d\left(1 - 0.59p\frac{f_{su}}{f'_c}\right) \tag{11.11a}$$

Equation (11.11*a*) is seen to be equivalent to Eq. (2.59), with the substitution of f_{su} for f'_s and the inclusion of the understrength factor ϕ (see Art. 3.7). Where a specific stress-strain curve for the prestressing steel

used is not available, the Code permits the use of the following values of f_{su}:

For bonded members: $$f_{su} = f'_s\left(1 - \frac{0.5pf'_s}{f'_c}\right) \tag{11.12a}$$

For unbonded members: $$f_{su} = f_{se} + 15{,}000 \text{ psi} \tag{11.12b}$$

where f_{se} is the effective steel prestress after losses.

According to the Code, if pf_{su}/f'_c exceeds 0.30, the ultimate moment of the member shall not be taken as greater than

$$M_u = \phi(0.25 f'_c b d^2) \tag{11.13}$$

For flanged members such as I and T beams in which the neutral axis falls outside the flange,[1] the method of determining ultimate flexural strength is exactly analogous to that used for ordinary reinforced-concrete I and T beams. The total steel area is divided into two parts for computational purposes. The first part, at a stress f_{su}, balances the compression in the overhanging portion of the flange, and the remainder, at stress f_{su}, balances the compression in the web. According to Code, in applying the criterion pf_{su}/f'_c to flanged members, p is taken as the steel ratio of only that portion of the total tension-steel area which is required to develop the compressive strength of the web alone. If pf_{su}/f'_c does not exceed 0.30, then

$$M_u = \phi\left[A_{sr} f_{su} d\left(1 - \frac{0.59 A_{sr} f_{su}}{b' d f'_c}\right) + 0.85 f'_c(b - b')t(d - 0.5t)\right] \tag{11.14}$$

where

$$A_{sf} = \frac{0.85 f'_c(b - b')t}{f_{su}}$$

and

$$A_{sr} = A_s - A_{sf}$$

If pf_{su}/f'_c exceeds 0.30, then

$$M_u = \phi[0.25 f'_c b' d^2 + 0.85 f'_c(b - b')t(d - 0.5t)] \tag{11.15}$$

If, after a prestressed beam is designed by working-stress methods, an inadequate factor of safety against failure is obtained, it is possible to include nonprestressed reinforcement in combination with prestressed steel to improve the factor of safety. According to the ACI Code, such nonprestressed steel may be considered to contribute to the tension force in a member at ultimate moment an amount equal to its area times its

[1] This is usually the case where the flange thickness is less than $1.4dpf_{su}/f'_c$.

Scanned with CamScanner

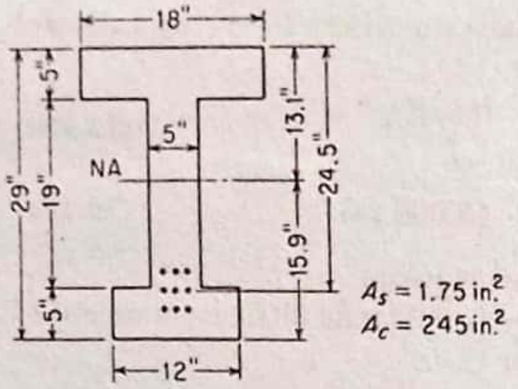


Fig. 11.13

yield point, provided

$$p\frac{f_{su}}{f'_c} + p'\frac{f_y}{f'_c} \leq 0.30$$

where p' is the ratio of unprestressed steel A'_s/bd, and f_y is the yield stress of the unprestressed steel. It is required by Code that the total amount of prestressed and unprestressed reinforcement be adequate to develop an ultimate load in flexure at least equal to 1.2 times the cracking load, calculated on the basis of a modulus of rupture of $7.5\sqrt{f'_c}$.

Example The posttensioned, bonded, prestressed beam shown in cross section in Fig. 11.13 is stressed using wires of ultimate strength $f'_s = 275{,}000$ psi. If the concrete strength is $f'_c = 5000$ psi, what is the ultimate flexural capacity of the member?

With $f'_s = 275{,}000$ psi, the stress in the steel at ultimate load is approximately

$$f_{su} = f'_s\left(1 - \frac{0.5pf'_s}{f'_c}\right)$$

The tensile-steel ratio is

$$p = \frac{A_s}{bd} = \frac{1.75}{18 \times 24.5} = 0.00397$$

Then

$$f_{su} = 275(1 - 0.5 \times 0.00397 \times {}^{275}\!/\!_{5}) = 245 \text{ ksi}$$

It is next necessary to determine the location of the neutral axis. Since

$$1.4dp\frac{f_{su}}{f'_c} = 1.4 \times 24.5 \times 0.00397 \times {}^{245}\!/\!_{5} = 6.68 \text{ in.} > 5.0 \text{ in.}$$

it is concluded that the neutral axis is below the underside of the flange, and equations for flanged members will be used. Then

$$A_s = 0.85\frac{f'_c}{f_{su}}(b - b')t = 0.85 \times {}^{5}\!/\!_{245} \times 13 \times 5 = 1.13 \text{ in.}^2$$

$$A_{sr} = A_s - A_{sf} = 1.75 - 1.13 = 0.62 \text{ in.}^2$$

The ratio

$$p\frac{f_{su}}{f'_c} = \frac{0.62}{5 \times 24}\frac{245}{5} = 0.253$$

is less than 0.30, so the ultimate strength of the member is found from the expression

$$M_u = \phi\left[A_{sr}f_{su}d\left(1 - \frac{0.59A_{sr}f_{su}}{b'df'_c}\right) + 0.85f'_c(b - b')t\left(d - \frac{2}{t}\right)\right]$$

$$= 0.90\left[0.62 \times 245 \times 24.5\left(1 - \frac{0.59 \times 0.62 \times 245}{5 \times 24.5 \times 5}\right) + 0.85 \times 5 \times 13 \times 5 \times 22\right]$$

$$= 8340 \text{ in.-kips}$$

11.11 Shear and Diagonal Tension In prestressed-concrete beams at working loads, there are two factors which greatly reduce the intensity of diagonal tensile stress, as compared with that which would exist if no prestress force were present. The first of these results from the combination of longitudinal compressive stress and shearing stress. An ordinary tensile-reinforced concrete beam under load is shown in Fig. 11.14*a*. The stresses acting on a small element of the beam taken below the neutral axis and near the support are shown in (*b*). It is found by means of Mohr's circle of stress (*c*) that the principal stresses act at 45° to the axis of the beam (*d*) and are numerically equal to the shear-stress intensity; thus

$$t_1 = t_2 = v \tag{a}$$

Now suppose that the same beam, with the same loads, is subjected to a precompression stress in the amount c, as shown in Fig. 11.15*a* and *b*. From Mohr's circle (*c*) the principal tensile stress is

$$t_1 = -\frac{c}{2} + \sqrt{v^2 + \left(\frac{c}{2}\right)^2} \tag{b}$$

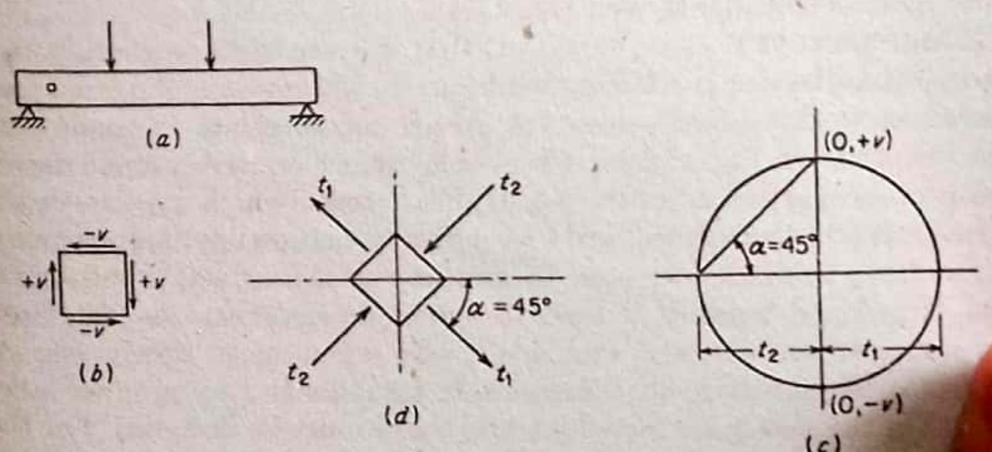


Fig. 11.14

Scanned with CamScanner

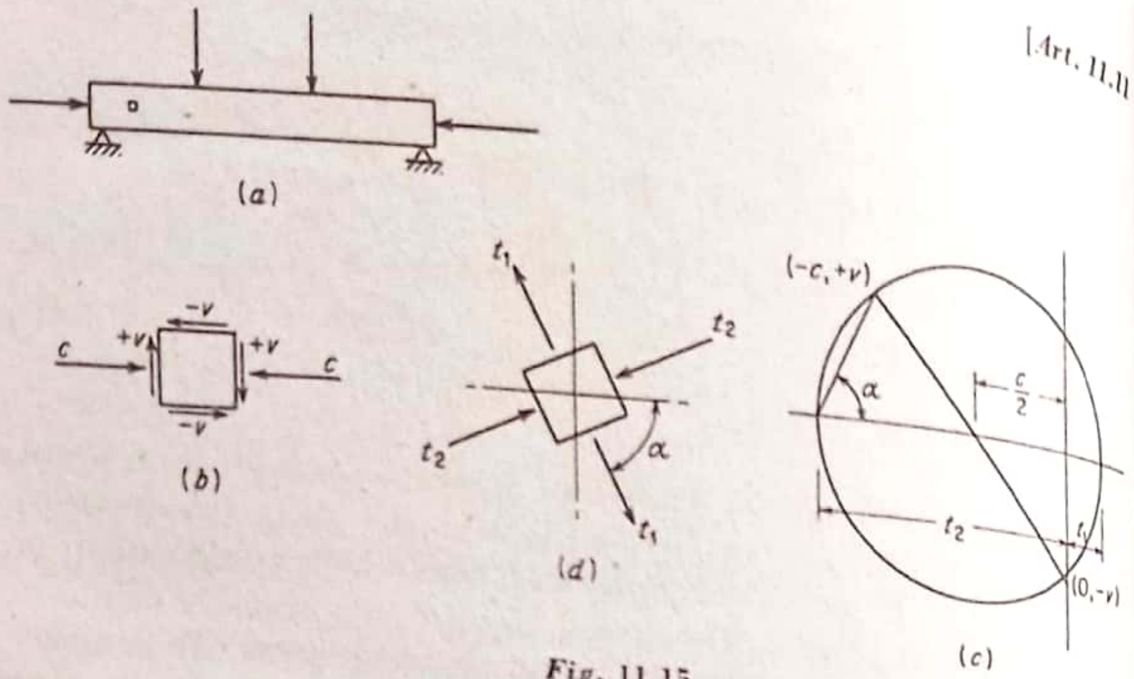


Fig. 11.15

and the direction of the principal tension with respect to the beam axis is

$$\tan 2\alpha = \frac{2v}{c} \tag{c}$$

as shown in (*d*).

Comparison of Eq. (*a*) with (*b*), and Fig. 11.14*c* with 11.15*c*, shows that, with the same shear-stress intensity, the principal tension in the prestressed beam is much reduced.

The second factor working to reduce the intensity of the diagonal tension at working loads results from the curve or slope of the tendons. Normally this slope is such as to produce a shear due to the prestress force which is opposite in direction to the load-imposed shear. The magnitude of this "countershear" is $V_p = P \sin \theta$, where θ is the slope of the tendon at the section considered (see Fig. 11.4).

It is important to note, however, that in spite of these characteristics of prestressed beams at working loads, an investigation of diagonal tensile stresses at working loads does not ensure an adequate factor of safety against failure. In Fig. 11.15*c*, it is evident that a relatively small decrease in compressive stress and increase in shear stress, which may occur when the beam is overloaded, will produce a disproportionately large increase in the resulting principal tension. In addition to this effect, if the countershear of inclined tendons is used to reduce design shear, its contribution does not increase directly with load, but much more slowly (see Art. 11.10). Consequently a small increase in total shear may produce a large increase in the net shear for which the beam must be designed. For these two reasons, it is usual to base design for diagonal tension in prestressed beams on conditions at ultimate load rather than at service load.

At ultimate load, a prestressed beam behaves essentially as an ordinary reinforced-concrete beam. According to ACI Code, the area of shear reinforcement placed perpendicular to the axis of a member is not to be less than

$$A_v = \frac{(V_u - \phi V_c)s}{\phi d f_y} \tag{11.16}$$

nor less than

$$A_v = \frac{A_s}{80}\frac{f'_s}{f_y}\frac{s}{d}\sqrt{\frac{d}{b'}} \tag{11.17}$$

where A_v = area of web reinforcement placed perpendicular to axis of member
V_u = shear due to specified ultimate load
V_c = shear carried by concrete
s = spacing of stirrups
f_y = yield stress of stirrups

The effective depth d, according to Code, is as follows:

1. In members of constant overall depth, d equals the effective depth at the section of maximum moment, and the length of the stirrups at the section under consideration shall be at least equal to the length of the stirrups at the section of maximum moment.

2. In members of varying depth, d equals hd_m/h_m, where d_m and h_m are the effective depth and total depth, respectively, at the section of maximum moment, and h is the total depth at the section under consideration. The stirrups shall extend into the member a distance d from the compression face.

It is seen that Eq. (11.16) is identical with Eq. (3.37) derived for nonprestressed-concrete beams, except that an alternative means for introducing the understrength factor ϕ is used.

The shear resistance of the concrete at ultimate load V_c is taken equal to the shear which caused the first diagonal crack to form in the prestressed beam, as was the case for reinforced-concrete beams (see Art. 2.5). In determining the magnitude of V_c, two types of diagonal tension cracks are recognized:

1. At shear V_{ci} a diagonal crack may result from high principal tension at the head of a flexural crack.

2. At shear V_{cw} a diagonal crack may result from high principal tension in a previously uncracked beam.

The shear force V_c causing cracking is taken as the smaller of V_{ci} and V_{cw}.

Consider first a diagonal tension crack which occurs as a continuation of a previously formed flexural crack (type 1 crack); the principal tensile

Scanned with CamScanner

stress which precipitates such a crack occurs near the centroid of the beam [Art. 11.11
If a 45° crack slope is assumed, a flexural crack at a distance $d/2$ from the section considered may be the initiating cause of the crack. On this basis and on the basis of test observations, the following empirical equation for V_{ci} is derived:

$$V_{ci} = 0.6b'd\sqrt{f'_c} + \frac{M_{cr}}{(M/V - d/2)} + V_d \tag{11.18}$$

V_{ci} is not to be taken less than

$$V_{ci} = 1.7b'd\sqrt{f'_c} \tag{11.19}$$

In Eq. (11.18), M/V is the moment-shear ratio resulting from the distribution of loads causing maximum moment at the section, V_d is the shear due to dead load, and M_{cr} is the net flexural cracking moment, equal to

$$M_{cr} = \frac{I}{y}(6\sqrt{f'_c} + f_{pc} - f_d) \tag{11.20}$$

in which f_{pc} is the compressive stress in the concrete due to prestress only after losses, at the extreme fiber of the section at which tension stresses are caused by applied loads, and f_d is the stress due to dead load at the extreme fiber of the same section.

Because a type 1 diagonal crack is initiated by flexural cracking of the beam, the formation of such a crack will not be affected by the counter-shear, if any, due to tendon inclination.

Now consider type 2 diagonal cracking of a previously uncracked beam section; the shear force causing diagonal tension in the beam to exceed the direct tensile capacity of the concrete can be calculated by an exact principal-stress calculation. This is permitted by Code, with the direct tensile capacity of the concrete taken equal to $4\sqrt{f'_c}$. Alternatively, the Code permits the use of the approximate expression

$$V_{cw} = b'd(3.5\sqrt{f'_c} + 0.3f_{pc}) + V_p \tag{11.21}$$

in which f_{pc} is the compressive stress in the concrete, after losses, at the centroid of the cross section or at the junction of the web and the flange when the centroid lies in the flange. In Eq. (11.21) the effective depth d is taken as the distance from the extreme compression fiber to the centroid of the tendons or as 80 per cent of the overall depth of the member, whichever is greater.

Equations (11.18) to (11.21) were developed for members constructed of normal-weight concrete (about 145 pcf). The ACI Code includes analogous expressions for members made of lightweight concrete.

Other specific provisions of the Code relative to the design of web reinforcement are:

1. Web reinforcement between the face of the support and the section at a distance $d/2$ therefrom shall be the same as that required at that section.
2. Shear reinforcement shall be provided for a distance equal to the effective depth d of the member beyond the point theoretically required.
3. Web reinforcement shall be adequately anchored at both ends.
4. Shear reinforcement not less than determined from Eq. (11.17) shall be provided at all sections and shall be spaced not farther apart than three-fourths the depth of the member or 24 in., whichever is the smaller, except when it is shown by tests that the required ultimate flexural and shear capacity can be developed when the web reinforcement is omitted.
5. A yield strength in excess of 60,000 psi shall not be considered for shear reinforcement.
6. In a pretensioned prestressed beam in which the section distant $d/2$ from the face of the support is closer to the end face of the beam than the transfer length of the wire or strand used, the reduced prestress in the concrete at sections falling within the transfer length should be considered when calculating the diagonal cracking shear V_{cw}. The prestress at the centroid of the section may be assumed to vary linearly from zero at the end face of the beam to a maximum at a distance from the end face equal to the transfer length, assumed to be 50 diam for strand and 100 diam for single wire.

Example The unsymmetrical I section shown in Fig. 11.13 carries an effective prestress force of 288 kips and supports a service load of 1000 plf on a 50-ft span in addition to its own weight of 255 plf. At the maximum moment section of the beam, the effective depth to the steel centroid is 24.5 in. If concrete of strength $f'_c = 5000$ psi and nonprestressed stirrups with $f_y = 40{,}000$ psi are to be used, what is the required spacing of stirrups at a point 5 ft from the support? At that section of the beam, the cable centroid is 19 in. below the compression face of the beam, and the cable slope is $\frac{1}{10}$.

Adopting the more conservative criterion for V_{ci} [Eq. (11.19)],

$$V_{ci} = 1.7b'd\sqrt{f'_c} = 1.7 \times 5 \times 19\sqrt{5000} = 11{,}400 \text{ lb}$$

At the section under consideration,

$$f_{pc} = 288{,}000/245 = 1180 \text{ psi}$$

and

$$V_p = 288{,}000 \times \tfrac{1}{10} = 28{,}800 \text{ lb}$$

Scanned with CamScanner

Then

$$V_{cw} = b'd(3.5\sqrt{f'_c} + 0.3f_{pc}) + V_p$$
$$= 5 \times 0.80 \times 29(3.5\sqrt{5000} + 0.3 \times 1180) + 28{,}800 = 98{,}400$$

Thus

$$V_c = V_{ci} = 11{,}400 \text{ lb}$$

The ultimate shear at the section under consideration is

$$V_u = 1.5 \times 255(25 - 10) + 1.8 \times 1000(25 - 10) = 32{,}750 \text{ lb}$$

Using No. 3 U stirrups,

$$A_v = 2 \times 0.11 = 0.22 \text{ in.}^2$$

$$s = \frac{A_v f_v \phi d}{V_u - \phi V_c} = \frac{0.22 \times 40{,}000 \times 0.90 \times 24.5}{32{,}750 - 0.90 \times 11{,}400} = 8.62 \text{ in.}$$

Open U stirrups similar to those shown in Fig. 3.10c will be used, at a spac of 8½ in.

11.12 Bond There are two separate sources of bond stress in pr stressed-concrete members: (1) flexural bond, which in pretensioned co struction exists between the wires and the concrete, and in grouted pos tensioned construction between the wires and grout and between conc and concrete and (2) prestress transfer bond, usually considered in pr tensioned members only.

Flexural bond The magnitude of bond stress due to flexure w depend significantly on whether or not the beam has cracked. If the bea is uncracked (usually the case at service load), flexural bond stress is lo and in fact need rarely be checked in design. When the beam cracks, sudden increase in bond stress results. The beam then behaves very mu as an ordinary reinforced-concrete beam, and flexural bond stress can b calculated with the equations of Chap. 3. While bond stresses after crac ing are of an order of magnitude higher than those before cracking, th will seldom be a problem in prestressed beams. According to Code, thre or seven-wire pretensioning strand shall be bonded to the concrete fro the cross section under consideration for a distance in inches of not les than

$$l = (f_{su} - \tfrac{2}{3}f_{se})D \qquad (11.2$$

where D is the nominal strand diameter in inches, and the stresses a expressed in kips per square inch. Investigation may be restricted to the cross sections nearest each end of the member that are required to develo their ultimate strength under the specified ultimate load. Equation (11.2 for minimum bonded length is an empirical one based on tests. It seems reflect the general point of view that the actual intensity of flexur

bond stress is not so important as the provision of adequate length of embedment.

Prestress transfer bond In the end regions of pretensioned beams (and in some cases for posttensioned beams), the prestress force from the cables is transferred to the concrete by bond alone. Thus there is a length of transfer at each end of the cables that serves the purpose of cable anchorage. The stress condition in the end zones of such beams is exactly the reverse of that in ordinary reinforced construction. In ordinary reinforced construction, the concrete is poured around an unstressed bar. As the bar is brought into tension, its diameter decreases at the stressed end, owing to Poisson's effect, creating tension normal to the surface of contact between the rod and the concrete. In prestressed beams, on the other hand, the wire is stretched before the concrete is poured around it. As the exposed wire end is cut loose from the anchorage, the stress at the outer end becomes zero. As a consequence, the wire expands as it attempts to regain its original diameter, causing compression normal to the surface of contact with the concrete. The stress in the wires is zero at the free end and increases progressively with distance from that end, approaching its full value at some finite distance, termed the *transfer length*. It is obvious that the free end of the wire must pull into the concrete a certain small distance and that through the extreme end region of the wire there will be relative movement between the wire and the concrete; therefore bond in this region must be completely frictional, with the frictional force enhanced because of the compression normal to the surface of contact. Farther from the free end, within the transfer zone, adhesive bond contributes to slip resistance.

There are as yet insufficient test data available to permit the accurate evaluation of required length of transfer. Fortunately, transfer length does not seem to be a problem in design, except for short members or those in which the loading conditions are such as to cause flexural cracking within the transfer zone, in which case substantial flexural bond stress may add to transfer bond stress to produce failure. The ACI Code states that the transfer length may be assumed to be 50 diam for strand and 100 diam for single wires. These values are based on (1) clean strand or wire surface, (2) gradual release of the prestressing force to the concrete, and (3) steel stress of 150 ksi after transfer. For strand or wire with a slightly rusted surface, the transfer distance can be much shorter. For sudden release of force to the concrete (such as takes place when pretensioned strands are burned through) the transfer length can be at least 20 per cent greater.

11.13 End-block Design In all the foregoing analysis, consideration has been given to resultant stress distribution in the concrete without regard for the fact that the prestress force is actually applied as a con-

Scanned with CamScanner

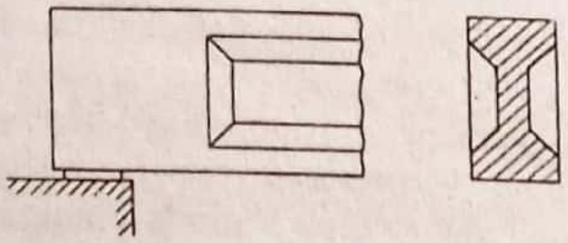


Fig. 11.16 End block for posttensioned beam.

centrated load or as a group of concentrated loads on the end of the member. It has been shown mathematically and experimentally that the effect of such concentration of the load becomes insignificant at a distance from the end of the member approximately equal to the member depth. In pretensioned construction, in which the prestress is normally transferred to the concrete by bond over a length which may about equal the member depth, no problem arises, because of the gradual stress input. However, in posttensioned beams, in which, in many cases, the prestress force is transferred through end anchorages and is applied in full value at the extreme end of the beam, the resulting stress concentrations require special consideration. It is customary in posttensioned I-section beams to cast a solid end block of rectangular cross section (Fig. 11.16), which may extend from the end a distance equal to anywhere from one-half the beam depth to the full beam depth, thus reducing local stresses near the anchorages.

The determination of end-block stress is a complex problem. Theoretical treatments are highly complicated, and in order to obtain workable methods one must introduce simplifications and assumptions which leave the solution at least open to question. Fortunately, one can afford to be quite conservative in reinforcing the end zone against local stress concentration. This will not significantly affect the overall economy of the construction, because even a conservative analysis will usually require only a small amount of mild-steel reinforcement to be placed in a very limited region.

Practically, the problem is to estimate the magnitude and location of the local tensile stresses, which are greatest in the direction at right angles to the prestressing force, and which may be sufficient to cause cracking or splitting of the end of the member. Y. Guyon has published an important mathematical study of end-zone stresses and has presented a set of diagrams for the transverse tension resulting from concentrated longitudinal compressive forces. Examples of such charts, in the form of *isobars*, i.e., curves of equal transverse stress, are shown in Fig. 11.17. These diagrams express the transverse unit tensile stress in terms of the average longitudinal compressive stress $p = H/A$. It is evident from these diagrams that there are two separate zones of transverse tension resulting in the end block. The first, defined as the *bursting* zone, lies deep within the block, along the line of action of the load; the second, the *spalling* zone, is

at the corners of the end block. These tensile zones are separated from each other by a continuous band, shown crosshatched, in which the transverse stress is compressive.

It will be found that in many cases the transverse tensile stress is higher than that which could be tolerated by the concrete, and some form of tensile reinforcement is indicated. Usually this is in the form of ordinary bars, bent in the form of closed stirrups or hoops. The reinforcement to accommodate spalling tension should be located as close to the end face of the beam as is practical. Guyon observes that, for most practical groupings of cable load, the total transverse spalling tension will not exceed $0.03H$, where H is the total longitudinal load, and he recommends that steel be placed in the spalling zone to accommodate that amount of tension. In the bursting zone the amount of steel required to carry tension

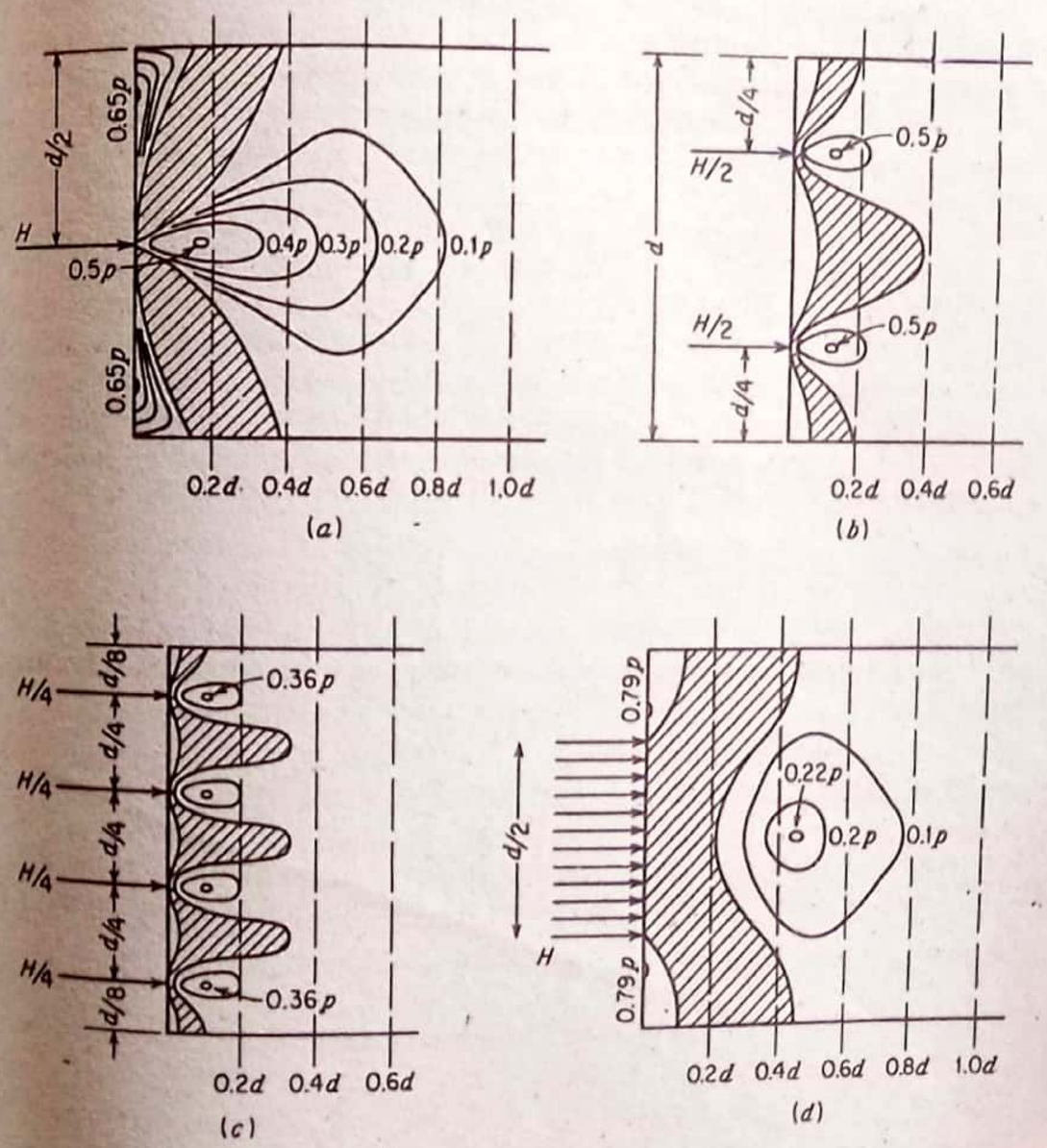


Fig. 11.17 Isobar charts. (*After Ref.* 11.1.)

Scanned with CamScanner

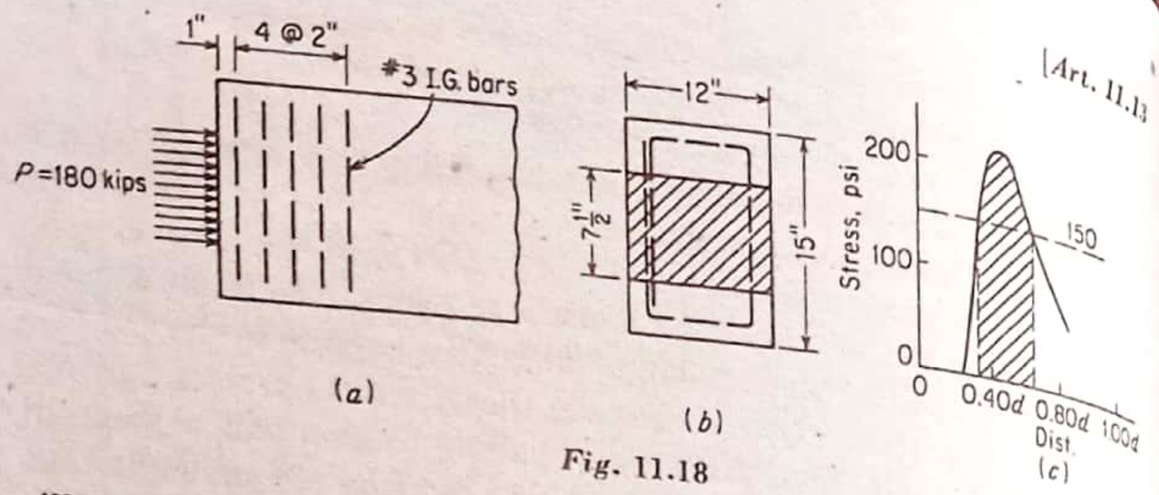


Fig. 11.18

will vary considerably, depending on the pattern of loading. This total tension can be evaluated from diagrams such as Fig. 11.17. Reference 11.1 includes such diagrams covering many specific loading situations.

Example Figure 11.18*a* and *b* show the end zone of a rectangular, posttensioned, prestressed-concrete beam, 12 in. wide and 15 in. deep, stressed by a 180,000-lb prestressing force uniformly distributed over the center half of the depth. It is required to design the end-block reinforcement, with allowable tension in the concrete taken at 150 psi.

The average compressive stress is $p = 180{,}000/(12 \times 15) = 1000$ psi. Then from Fig. 11.17*d* the maximum transverse tension along the middepth center line of the beam is obtained. This is plotted against distance from the beam end in Fig. 11.18*c*. It is seen that the allowable tensile stress in the concrete is exceeded in the region from $0.32d$ to $0.64d$, a horizontal distance of 4.8 in. While the actual tensile stress varies from 150 to 220 psi in that length, use of an average value of 200 psi over the entire distance will not seriously affect the total tension, which is then obtained as

$$200 \times 4.8 \times 12 = 11{,}500 \text{ lb}$$

Number 3 stirrups in the form shown in Fig. 11.18*b*, at working stress $f_s = 20{,}000$ psi, will be used. The number of stirrups required to accommodate bursting tension is

$$N = \frac{11{,}500}{20{,}000 \times 0.22} = 2.6$$

Three stirrups will be used. The spalling tension can be obtained from Fig. 11.17*d*, but it is sufficiently accurate to estimate the total spalling tension as

$$0.03H = 0.03 \times 180{,}000 = 5400 \text{ lb}$$

The number of No. 3 stirrups necessary to accommodate this is

$$N = \frac{5400}{20{,}000 \times 0.22} = 1.23$$

Two additional stirrups are called for; the total of five No. 3 stirrups meets the

requirements of spalling and bursting tension and is arranged as shown in Fig. 11.18*a*.

REFERENCES

The discussion in the preceding articles is limited to the basic features of prestressed-concrete design. A number of points have necessarily been omitted, such as design of continuous prestressed members, composite construction, deflection and camber, partial prestressing, and specific applications such as circular tanks, pipes, and piles. The important problem of selecting the optimum sectional shape for prestressed members has been dealt with only briefly. Additional information with regard to many of these questions can be obtained from the following sources:

11.1 Y. Guyon: "Prestressed Concrete," vols. 1 and 2, John Wiley & Sons, Inc., New York, 1960.
11.2 T. Y. Lin: "Prestressed Concrete Structures," 2d ed.. John Wiley & Sons, Inc., New York, 1963.
11.3 F. Walley: "Prestressed Concrete Design and Construction," Her Majesty's Stationery Office, London, 1953.
11.4 P. W. Abeles: "The Principles and Practice of Prestressed Concrete," Crosby Lockwood & Son, Ltd., London, 1952.
11.5 H. K. Preston: "Practical Prestressed Concrete," McGraw-Hill Book Company, Inc., New York, 1960.
11.6 M. Chi and F. A. Biberstein: "Theory of Prestressed Concrete," Prentice-Hall, Inc., Englewood Cliffs, N.J., 1963.
11.7 T. Y. Lin: Load-balancing Method for Design and Analysis of Prestressed Concrete Structures, *J. ACI*, p. 719, June, 1963.

Scanned with CamScanner

chapter **12**

REINFORCED CONCRETE BRIDGES

12.1 Types of Bridges Reinforced concrete is particularly adaptable for use in highway bridges because of its durability, rigidity, and economy as well as the comparative ease with which a pleasing architectural appearance can be secured. For very short spans, from about 10 to 25 ft,

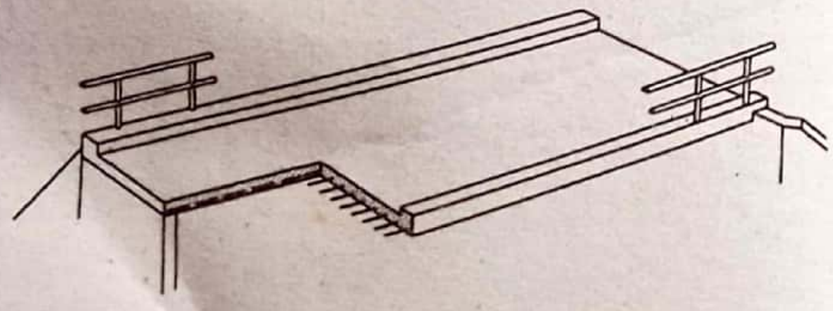


Fig. 12.1 Slab bridge.

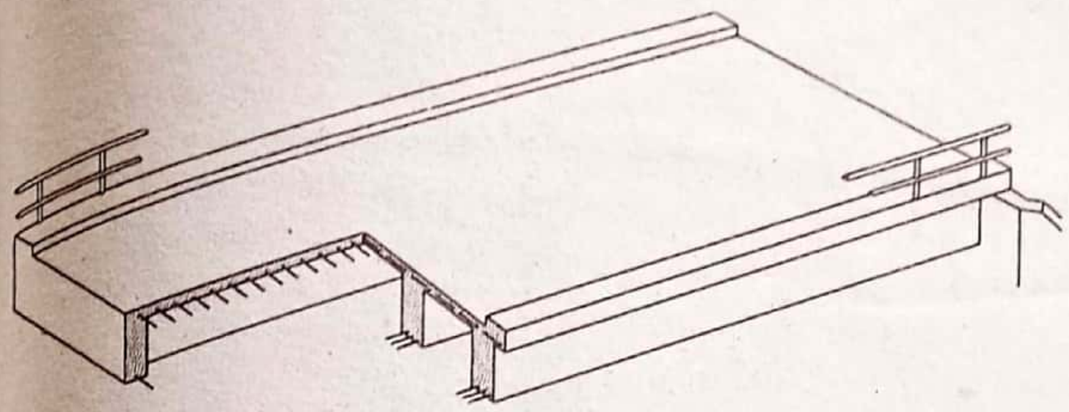


Fig. 12.2 Deck-girder bridge.

one-way slab bridges (Fig. 12.1) are economical. For somewhat longer spans, concrete girder spans (Fig. 12.2) may be used.

Probably most highway spans of medium length, from 40 to 90 ft, presently use composite steel-concrete construction (Fig. 12.3) or prestressed-concrete construction (Fig. 12.4). In composite construction with structural steel, the concrete deck is made to act integrally with supporting steel stringers by means of devices called *shear connectors*, welded to the top flange of the steel section and embedded in the slab. Although such a bridge is not strictly a reinforced-concrete structure, the design of this type of bridge will be discussed in some detail in this section because of its widespread use. Prestressed-concrete bridges frequently make use of composite section characteristics also. Commonly the girders are precast and placed into final location by crane, eliminating the necessity for obstructing traffic by falsework. The deck slab is then cast in place, bonded, and tied to the precast sections by steel dowels.

Bridge spans as long as 320 ft (Fig. 12.5) have been attained using prestressed girders. Other possibilities for long-span concrete bridges are

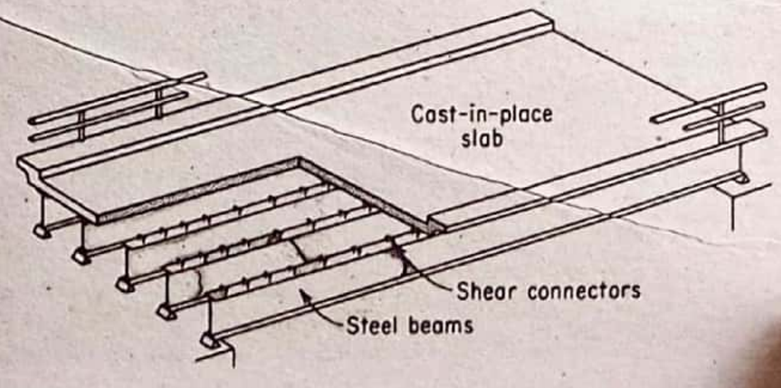


Fig. 12.3 Composite steel-concrete bridge.

Scanned with CamScanner

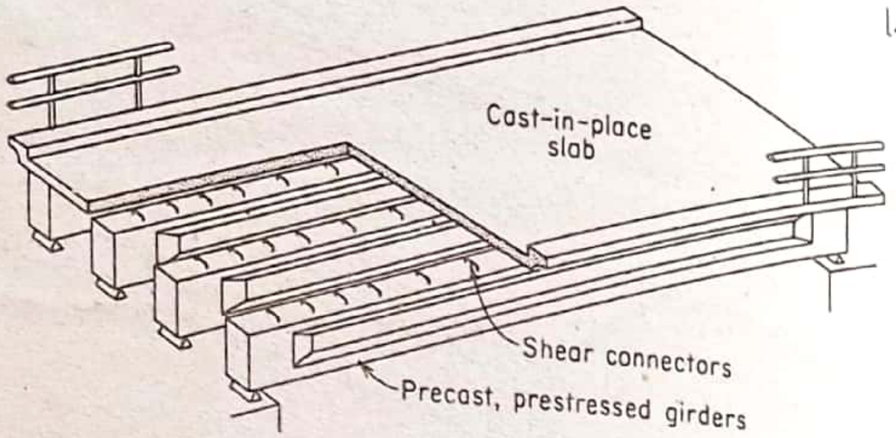


Fig. 12.4 Composite prestressed-concrete bridge.

the various forms of arches, including the barrel arch (Fig. 12.6) and the three-hinged arch (Fig. 12.7).

Structural steel is used more generally than reinforced concrete for bridges which are intended primarily for railroad traffic, except for the shortest spans, for which reinforced-concrete slab bridges are frequently constructed. This chapter will therefore be devoted to a discussion of the details and design of highway bridges only. It is the present practice in the United States to design reinforced-concrete highway structures by working-stress methods rather than on the basis of ultimate strength. Undoubtedly this is due to a feeling that, where repetitive loads are involved, primary attention should be focused on stress conditions at service load levels.

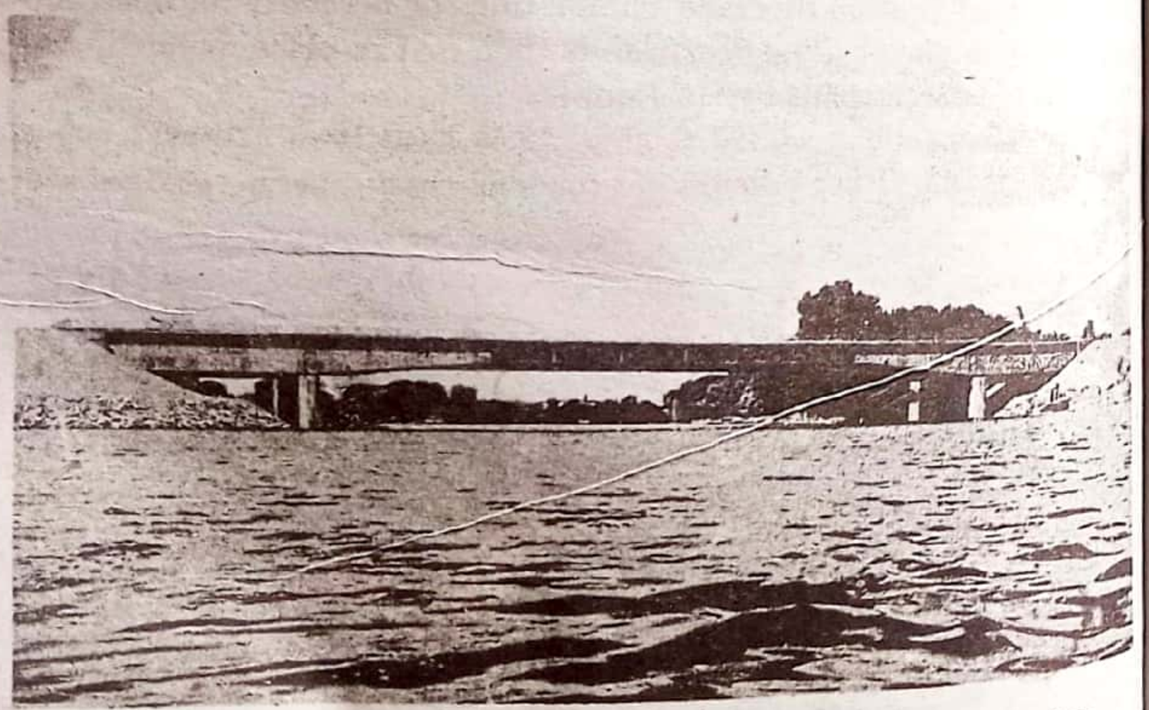


Fig. 12.5 Oneida Lake Bridge: 320-ft span, prestressed-concrete girders.

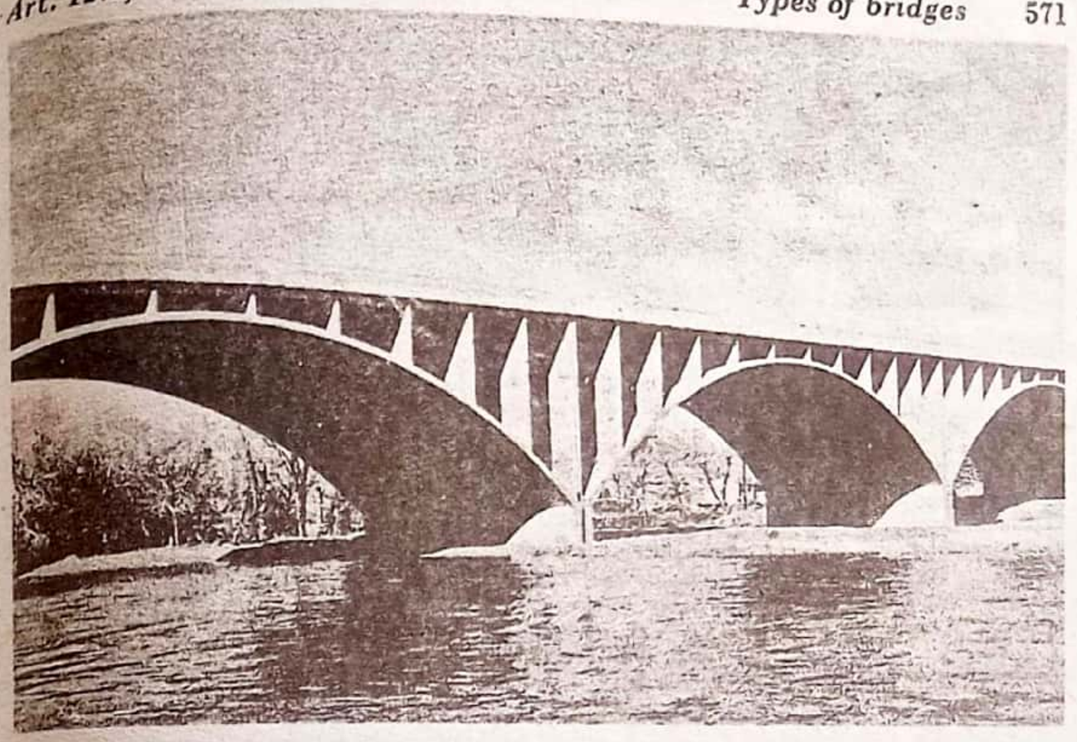


Fig. 12.6 Fox River Valley Bridge: five 178-ft barrel-arch spans.

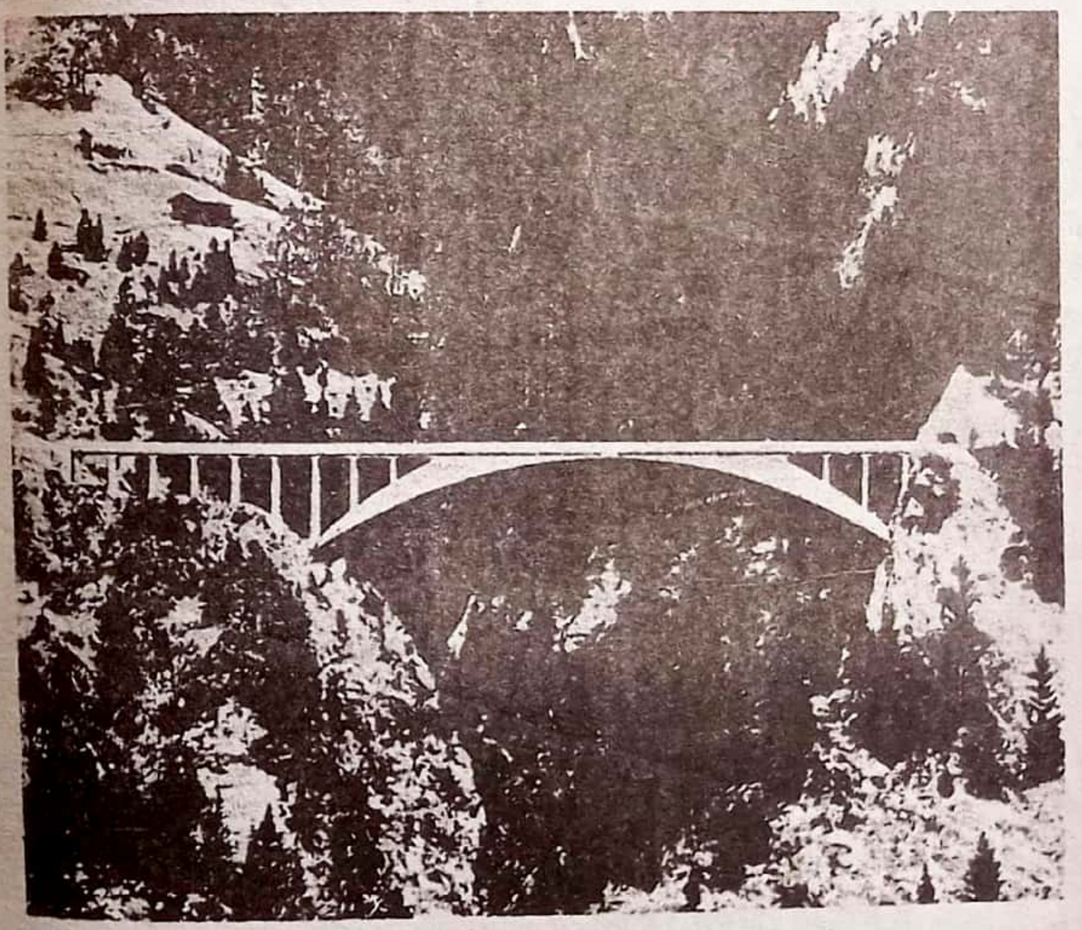


Fig. 12.7 Salgina Bridge, Switzerland: three-hinged arch span.

Scanned with CamScanner

12.2 Live Loads: *Truck loadings* The live loads specified by the American Association of State Highway Officials (Ref. 12.1)—whose specifications control the design of most American highway bridges—consist of standard, idealized trucks or of live loads which are equivalent to a series of trucks. Two systems of loadings are provided: the *H* loadings, as shown in Fig. 12.8, and the *H*-*S* loadings, as shown in Fig. 12.9. The *H* loadings represent a two-axle truck; the *H*-*S* loadings represent a two-axle tractor plus a single-axle semitrailer.

As shown in the figures, the highway loadings are divided into several classes. The number of the loading indicates the gross weight in tons of the truck or tractor. The gross weight is divided between the front and rear axles as shown in Figs. 12.8 and 12.9. For the *H*-*S* loadings the semitrailer axle load is added.

Lane loadings, which are to be used when they produce greater stress then the corresponding truck loadings, are shown in Fig. 12.10. In general,

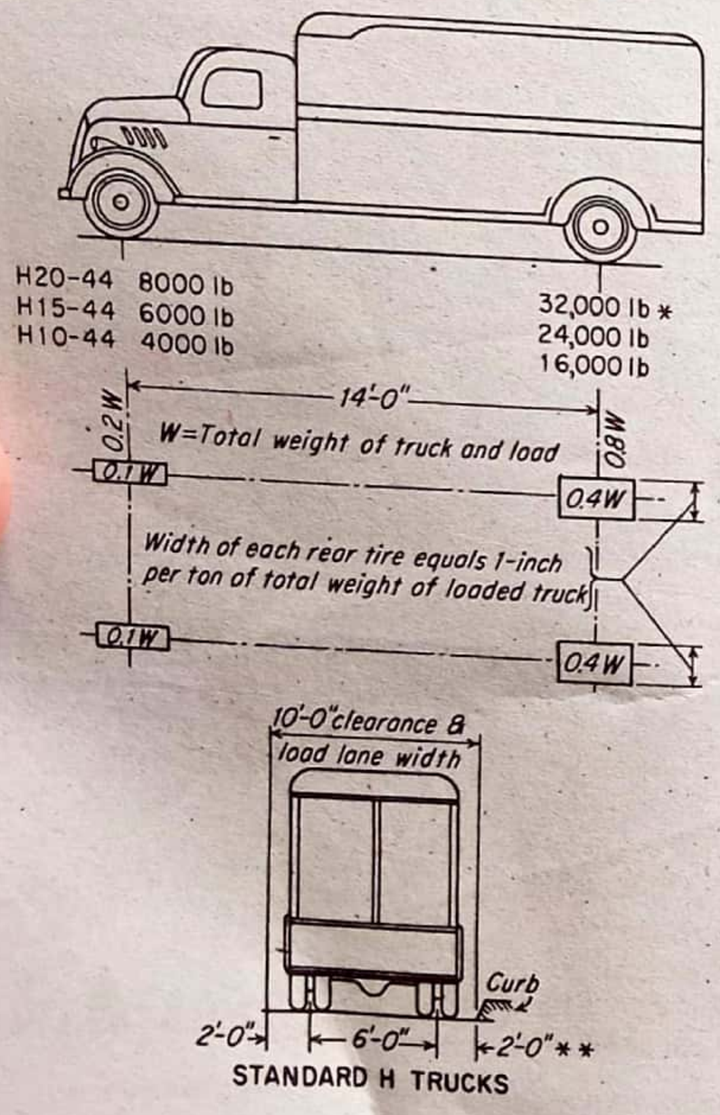


***Fig.* 12.8** Standard *H* truck loadings.

* In the design of steel grid and timber floors for *H*20 or *H*20-*S*16 loading, one axle load of 24,000 lb or two axle loads of 16,000 lb each, spaced 4 ft apart, whichever produces the greater stress, may be used instead of the 32,000-lb axle shown.

** For slab design the center line of the wheel shall be assumed to be 1 ft from the face of the curb.

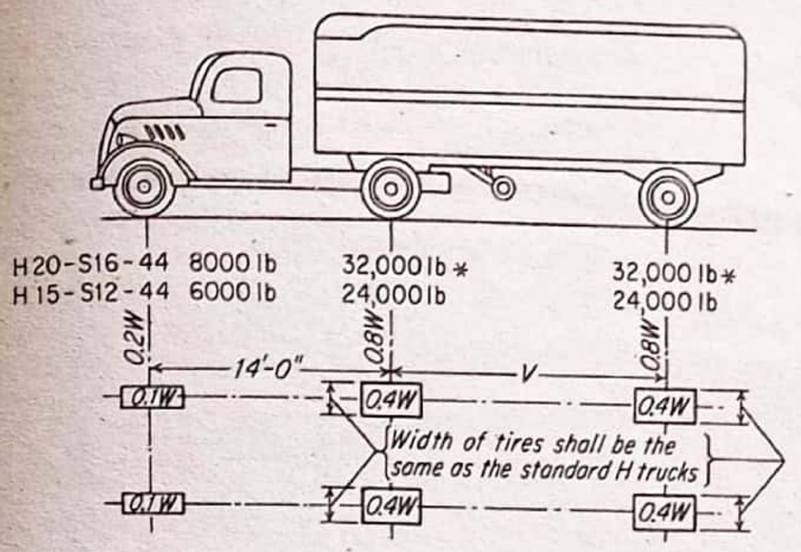


***Fig.* 12.9** Standard *H*-*S* truck loadings.

* In the design of steel grid and timber floors for *H*20 or *H*20-*S*16 loading, one axle load of 24,000 lb or two axle loads of 16,000 lb each, spaced 4 ft apart, whichever produces the greater stress, may be used instead of the 32,000-lb axle shown.

** For slab design the center line of the wheel shall be assumed to be 1 ft from the face of the curb.

the lane loadings, which are designed to approximate the effect of a series of trucks, govern the design of the longer-span bridges.

Other roadway loadings The possibility that the bridge may be required to carry electric railways, railroad freight cars, military vehicles, or other extraordinary vehicles should be considered in design. The class of such traffic shall determine the loads to be used.

Sidewalk loadings Sidewalk floors, stringers, and their immediate supports are usually designed for a live load of at least 85 psf of sidewalk area.

Scanned with CamScanner

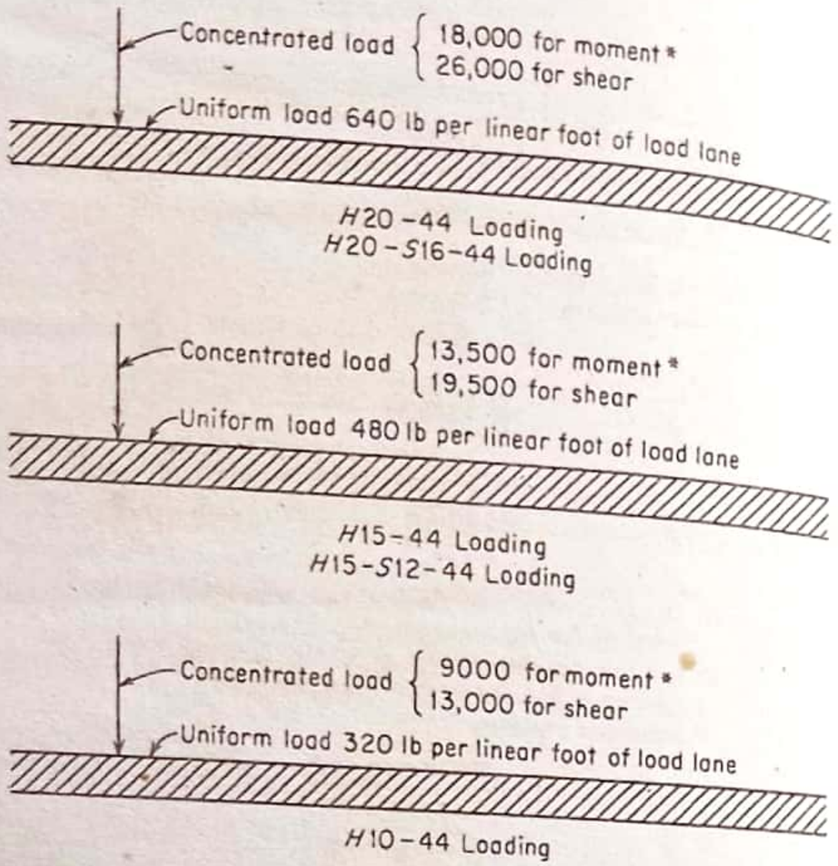


Fig. 12.10 Equivalent lane loadings.

* For continuous spans another concentrated load of equal weight shall be placed in one other span in the series in such a position as to produce maximum negative moment.

Selection of loadings The AASHO specifications state that for truck highways or for other highways which carry heavy truck traffic the minimum live load shall be the *H*15-*S*12 loading. It is common practice at present to design bridge spans on major highways for the *H*20-*S*16 loading, using the lighter loadings only for structures on secondary roads, on which the occurrence of heavy traffic will be negligible.

12.3 Application of Loadings Some of the more important rules for applying the selected AASHO loading follow.

1. The lane loading or standard trucks shall be assumed to occupy a width of 10 ft. They shall be assumed to occupy any position within their design traffic lane which will produce the maximum stress. The width of the design traffic lanes shall be determined from the formula

$$W = \frac{W_c}{N}$$

where W_c = roadway width between curbs, exclusive of median strip
N = number of design traffic lanes as shown in the following table
W = width of design traffic lane

W_c, ft	N
20–30	2
Over 30–42	3
Over 42–54	4
Over 54–66	5
Over 66–78	6
Over 78–90	7
Over 90–102	8
Over 102–114	9
Over 114–126	10

2. Each 10-ft lane loading or single standard truck shall be considered as a unit, and fractional load-lane widths or fractional trucks shall not be used.

3. The number and position of the lane loading or truck loading shall be as specified above. The type of loading to be used—lane loading or truck loading—shall be such as to produce maximum stress subject to the reduction specified below.

Reduction in load intensity Where maximum stresses are produced in any member by loading any number of traffic lanes simultaneously, the following percentages of the resultant live-load stresses shall be used in view of improbable coincident maximum loading:

Number of lanes	*Per cent*
1 or 2	100
3	90
4 or more	75

12.4 Impact Live-load stresses due to truck loading (or equivalent lane loading) are increased to allow for vibration and the sudden application of the load. The increase is computed by the formula

$$I = \frac{50}{l + 125}$$

where I = impact fraction of live-load stress
l = loaded length, ft

The maximum impact allowance to be used shall be 30 per cent.

12.5 Distribution of Loads When a concentrated load is placed on a reinforced-concrete slab, the load is distributed over an area larger than

Scanned with CamScanner

the actual contact area. For example, if a concentrated load with a bearing area of 1 ft² were placed on the slab of a through-girder bridge, it is reasonable to assume that, on account of the stiffness of the slab, the strips of slab at right angles to the girder and adjacent to the 1-ft strip in direct contact with the load would assist in carrying the load. Similarly, with the beams of a T-beam bridge spaced fairly closely, a concentrated load placed directly over one of the beams would not be carried entirely by that beam, for the concrete slab would be sufficiently rigid to transfer part of the load to adjacent beams.

No distribution is assumed in the direction of the span of the member. The effect of any such distribution would be comparatively small.

The following recommendations for the distribution of loads are taken from the specifications of the American Association of State Highway Officials.

12.6 Distribution of Wheel Loads on Concrete Slabs The pertinent rules for the distribution of wheel loads on concrete slabs and some additional design requirements are as follows:

Span lengths For simple spans, the span length shall be the distance center to center of supports but shall not exceed clear span plus thickness of slab.

The following effective span lengths shall be used in calculating the distribution of loads and bending moments for slabs continuous over more than two supports:

Slabs monolithic with beam (without haunches): S = clear span
Slabs supported on steel stringers: S = distance between edges of flanges plus one-half the stringer flange width
Slabs supported on timber stringers: S = clear span plus one-half the thickness of the stringer

Edge distance of wheel load In designing slabs, the center line of the wheel load shall be assumed to be 1 ft from the face of the curb.

Bending moment Bending moment per foot width of slab shall be calculated according to the methods given under Cases 1 and 2. In both cases,

S = effective span length as defined under "span lengths," ft
E = width of slab over which wheel load is distributed, ft
P = load on one rear wheel of truck
P_{15} = 12,000 lb for $H15$ loading
P_{20} = 16,000 lb for $H20$ loading

Case 1: main reinforcement perpendicular to traffic (*spans 2 to 24 ft inclusive*) The live-load moment for simple spans shall be determined by the following formulas (impact not included):

$H20$-$S16$ loading:

$$\frac{S+2}{32}P_{20} = \text{moment in ft-lb per ft width of slab}$$

$H15$-$S12$ loading:

$$\frac{S+2}{32}P_{15} = \text{moment in ft-lb per ft width of slab}$$

In slabs continuous over three or more supports, a continuity factor of 0.8 shall be applied to the above formulas for both positive and negative moments.

Case 2: main reinforcement parallel to traffic Distribution of wheel loads $E = 4 + 0.6S$; maximum 7.0 ft. Lane loads are distributed over a width of $2E$. Longitudinally reinforced slabs shall be designed for the appropriate H-S loading.

For simple spans, the maximum live-load moment per foot width of slab, without impact, is closely approximated by the following formulas:

$H20$-$S16$ loading:

Spans up to and including 50 ft: L.L.M. = $900S$ ft-lb
Spans 50 to 100 ft: L.L.M. = $1000(1.30S - 20.0)$ ft-lb

$H15$-$S12$ loading:

Use three-fourths of the values obtained from the formulas for $H20$-$S16$ loading.

Moments in continuous spans shall be determined by suitable analysis using the truck or appropriate lane loading.

Edge beams (longitudinal) Edge beams shall be provided for all slabs having main reinforcement parallel to traffic. The beam may consist of a slab section additionally reinforced, a beam integral with and deeper than the slab, or an integral reinforced section of slab and curb. It shall be designed to resist a live-load moment of $0.10PS$, where P is the wheel load in pounds (P_{15} or P_{20}) and S is the span length in feet. The moment as stated is for a freely supported span. It may be reduced 20 per cent for continuous spans unless a greater reduction results from a more exact analysis.

Distribution reinforcement Reinforcement shall be placed in the bottoms of all slabs transverse to the main steel reinforcement to provide for the lateral distribution of the concentrated live loads, except that reinforcement will not be required for culverts or bridge slabs when the depth of the fill over the slab exceeds 2 ft. The amount shall be the percentage of the main reinforcement steel required for positive moment as given by the following formulas:

Scanned with CamScanner

For main reinforcement parallel to traffic:

$$\text{Percentage} = \frac{100}{\sqrt{S}} \qquad \text{maximum} = 50 \text{ per cent}$$

For main reinforcement perpendicular to traffic:

$$\text{Percentage} = \frac{220}{\sqrt{S}} \qquad \text{maximum} = 67 \text{ per cent}$$

where S is the effective span length in feet

Shear and bond stress in slabs Slabs designed for bending moment in accordance with the foregoing shall be considered satisfactory in bond and shear.

12.7 Distribution of Wheel Loads to Stringers, Longitudinal Beams, and Floor Beams The following rules govern the distribution of wheel loads affecting longitudinal and transverse concrete beams supporting concrete slabs. The AASHO specification contains additional recommendations for steel and timber flooring which are not reproduced here.

Position of loads for shear In calculating end shears and end reactions in transverse floor beams and longitudinal beams and stringers, no lateral or longitudinal distribution of the wheel shall be assumed for the wheel or axle load adjacent to the end at which the stress is being determined. For loads in other positions on the span, the distribution for shear shall be determined by the method prescribed for moment.

Bending moment in stringers and longitudinal beams In calculating bending moments in longitudinal beams or stringers, no longitudinal distribution of the wheel loads shall be assumed. The lateral distribution shall be determined as follows:

1. *Interior stringers* supporting concrete floors shall be designed for loads determined in accordance with the following table, in which S is the average spacing of stringers in feet:

Floor system	One traffic lane, fraction of a wheel load to each stringer	Two or more traffic lanes, fraction of a wheel load to each stringer
Concrete slab on steel I-beam stringers	$S/7.0$ (S_{max} = 10 ft)*	$S/5.5$ (S_{max} = 14 ft)*
Concrete slab on concrete stringers	$S/6.0$ (S_{max} = 6 ft)*	$S/5.0$ (S_{max} = 10 ft)*
Concrete box girder	$S/8.0$ (S_{max} = 12 ft)*	$S/7.0$ (S_{max} = 16 ft)*

* If S exceeds the value in parenthesis, the load on each stringer shall be the reaction of the wheel loads, under the assumption that the flooring between the stringers acts as a simple beam.

2. The live load supported by *outside stringers* shall be the reaction of the truck wheels, under the assumption that the flooring acts as a simple beam between stringers.

3. The *combined load capacity* of all the beams in a span shall not be less than the total live and dead load in the panel.

Bending moment in floor beams (transverse) In calculating bending moments in floor beams, no transverse distribution of the wheel loads shall be assumed. If longitudinal stringers are omitted and the concrete floor is supported directly on floor beams, the fraction of wheel load allotted to each floor beam is $S/6$, where S equals the spacing of beams in feet. If S exceeds 6 ft, the load on the beam shall be the reaction of the wheel loads, under the assumption that the flooring between beams acts as a simple beam.

12.8 Abutments Bridge abutments serve to transmit the load from the superstructure to the foundation and act as retaining walls to hold back the earth fill behind them.

Bridge seats The bridge seats of abutments which support the fixed ends of concrete highway bridges are quite frequently built as horizontal surfaces without parapets or backwalls, as shown in Fig. 12.11. The slab or the beams of the deck rest directly on the bridge seat; in deck-girder bridges, transverse diaphragm walls are constructed between the beams to hold back the earth above the bridge seat. These diaphragms are thin walls, 6 or 8 in. in thickness, with a nominal amount of reinforcement.

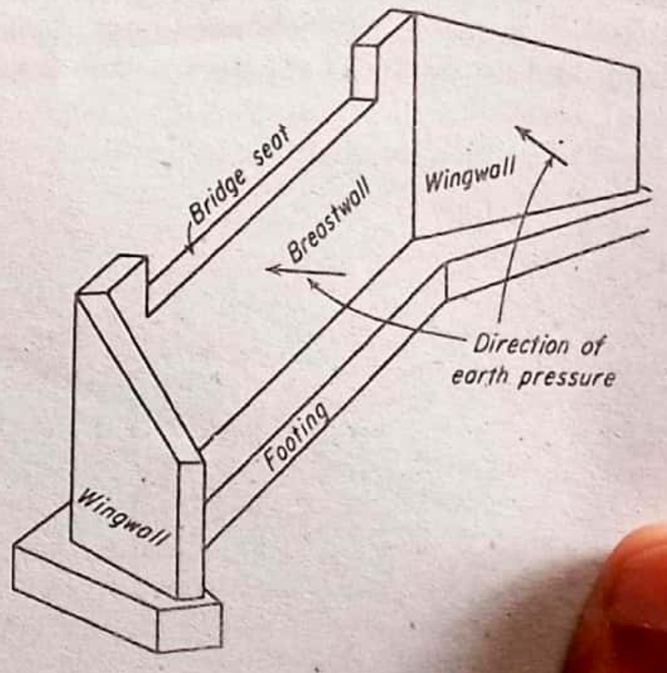


Fig. 12.11 Details of abutment without backwall.

Scanned with CamScanner

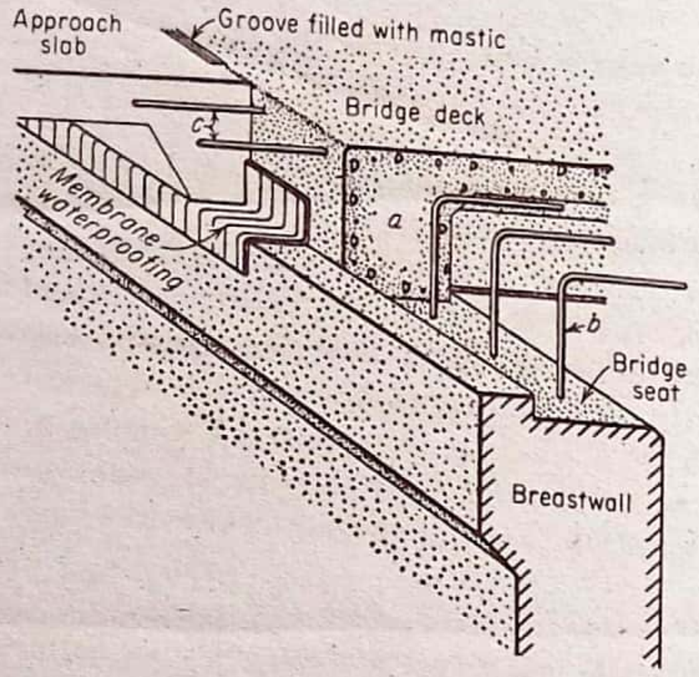


Fig. 12.12 Details of bridge seat with low backwall.

Figure 12.12 shows a modified form of the construction described above in which a very low backwall is used, primarily for the purpose of counteracting the tendency of the abutment to move inward under the deck. The dowels *b* and *c* shown in the abutment and in the deck construction serve to tie the deck, the abutment, and the approach slab together.

Another type of bridge seat is shown in Fig. 12.13. This type is particularly adapted to the fixed ends of deck-girder bridges. The bridge seat is constructed with notches into which the bridge beams are built. Figure 12.13 is a diagrammatic sketch and does not show the final relative positions of the deck and abutment; the two parts of the figure actually fit together as shown by the dotted lines. Ledges are provided in the abutment and at the top of the deck beams to support the approach slab, as

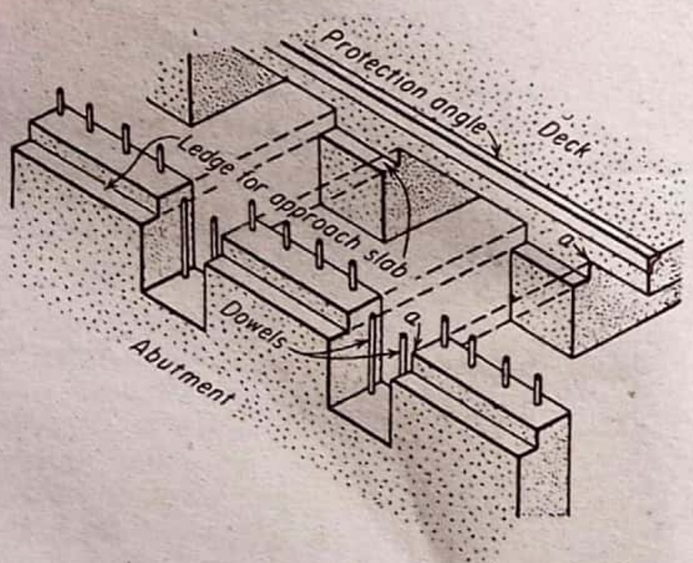


Fig. 12.13 Details of bridge seat with pockets for beams.

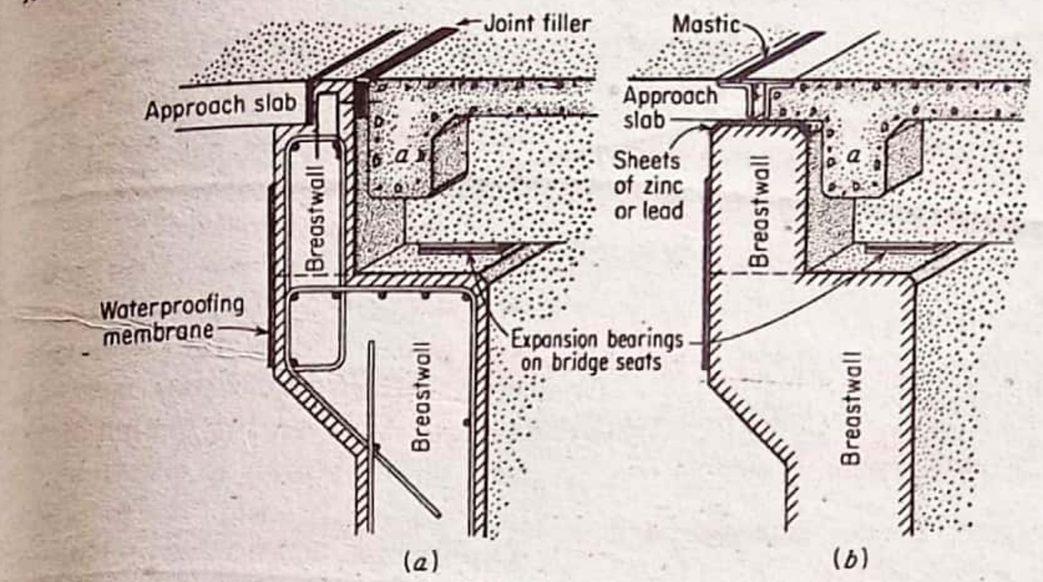


Fig. 12.14 Details of bridge seats with backwalls.

shown in the figure. Dowels are placed in the abutment in such a manner as to project up into the beams and deck slab.

A third type of bridge-seat construction is shown in Fig. 12.14. This is the usual type with backwall, used at the expansion end of the bridge. Two arrangements of joints are shown in the figure. The backwall is extended upward to the roadway surface in (*a*), while it stops at the bottom of the roadway slabs in (*b*). Type *b* is usually preferred, in that only one joint is required in the roadway surface, as compared with two joints in type *a*.

Breast walls The two most common types of breast walls are the cantilever retaining wall of reinforced concrete and the type that acts as a vertical slab supported horizontally by the deck and by the foundation. Buttressed breast walls are rarely used in short-span concrete bridges. Gravity walls of plain concrete are sometimes used, especially where the height of the abutment is not great.

The cantilever breast wall is generally used at the expansion end of the bridge. The type that is supported horizontally by the deck and the footing can be used only at the fixed end; in such cases it is always advisable to have at least a low parapet or back wall, as shown in Fig. 12.12, in order to obtain the direct horizontal resistance which is assumed to be furnished by the deck.

Wing walls Gravity or cantilever-type wing walls may be used. It is advisable to construct vertical expansion joints at the junction of the wing walls and breast wall to avoid unsightly cracks which are apt to form along these planes. Sometimes, instead of an expansion joint, a vertical groove is constructed at the joint; any crack that may develop will the

Scanned with CamScanner

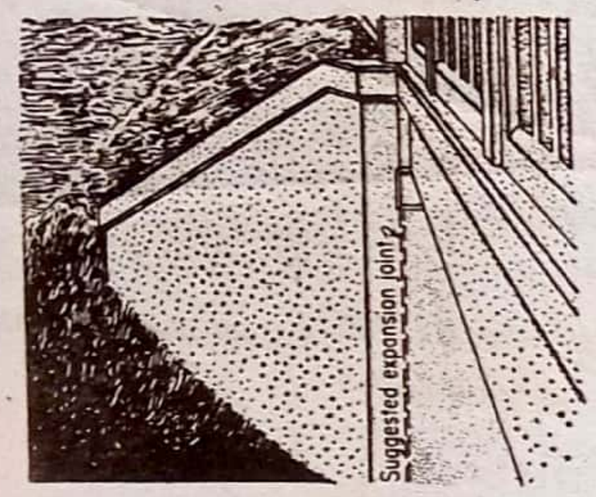


Fig. 12.15 Vertical expansion joint in breast wall.

be inconspicuous. The expansion joint or the groove should preferably be placed at the end of the bridge seat, as shown in Fig. 12.15.

12.9 Miscellaneous Construction Details: *Diaphragms* In deck-girder bridges, thin transverse walls called *diaphragms* are constructed between the beams at the ends of the bridge, as shown at (a) in Figs. 12.12 and 12.14. These diaphragms serve two purposes; first, they furnish lateral support for the beams, and second, when no parapet or back wall is built above the bridge seat, they prevent the earth fill from spilling out on the bridge seat. At the fixed ends, the diaphragms may rest directly on the bridge seat, as shown in Fig. 12.12; at the expansion ends, the diaphragms should be kept clear of the bridge seat, as shown in Fig. 12.14, so as not to develop friction which would interfere with the freedom of longitudinal movement. The diaphragms are usually from 6 to 8 in. thick with a nominal amount of reinforcement.

Intermediate diaphragms should be constructed between the beams of deck-girder bridges with spans greater than 40 ft; the intermediate diaphragms are placed at the center or at the third points of the span.

Fixed bearings Fixed bearings can safely be used at both ends of spans up to 40 ft. Two such bearings are illustrated in Figs. 12.12 and 12.13. The dowels which serve to tie together the deck construction and the abutment are not designed to resist any appreciable amount of bending moment, and hence no joint rigidity can be assumed in the design of the deck or abutment.

Expansion bearings For spans greater than 40 ft, an expansion bearing should be provided at one end of the bridge. A suitable form of expansion bearing for spans up to 50 ft is shown in Fig. 12.14. A pair of steel plates is placed under each girder; the lower plate is anchored to the concrete in the abutment, and the upper plate is fastened to the underside of the girder. Frequently, a thin layer of graphited asbestos, zinc, or copper is placed between the plates to reduce the friction.

For the shorter spans and light loadings, frequently the only expansion device is a layer of tar paper inserted between the bridge seat and the deck. Obviously this is not desirable where provision for expansion is of any importance, because of the questionable efficiency of the construction.

In spans greater than 50 ft, the deflection of the deck may rotate the

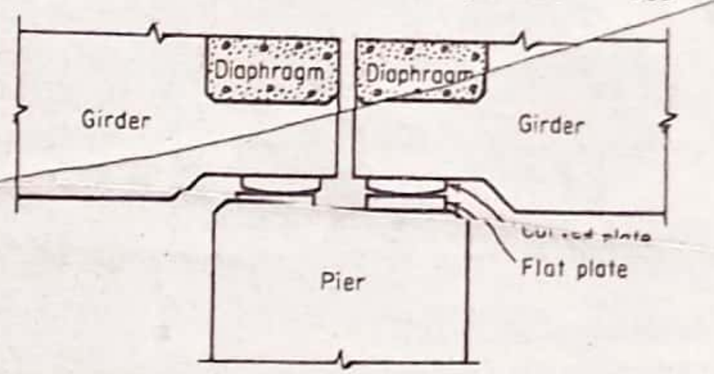


Fig. 12.16 Expansion bearings.

ends of the girders so much that the bearing pressure may become concentrated on a narrow strip along the front edge of the bridge seat and may cause local damage if flat bearing plates are used. In order to counteract this tendency, one plane and one curved plate should be used, as shown in Fig. 12.16.

Deck joints The number of expansion joints in a bridge deck should be kept as low as possible. In single-span bridges of the type under discussion, one such joint usually suffices; that joint is at one end of the bridge. A suitable detail for the joint is shown in Fig. 12.14*b*; in this detail an angle is anchored to the end of the deck slab, and a similar angle is anchored to the end of the approach slab. A tread plate is fastened, by means of rivets or tap screws, to the top of the angle at the end of the deck, and this plate bears on the angle at the end of the approach slab. The tread plate does not cover the latter angle completely, sufficient provision for expansion of the deck slab being made. The groove between the end of the tread plate and the edge of the approach slab is usually filled with mastic, as shown in Fig. 12.14*b*, in order to make the joint watertight. The mastic is soft enough to permit movement of the tread plate, but firm enough to resist displacement.

An enlarged detail of a similar joint is shown in Fig. 12.17; this applies

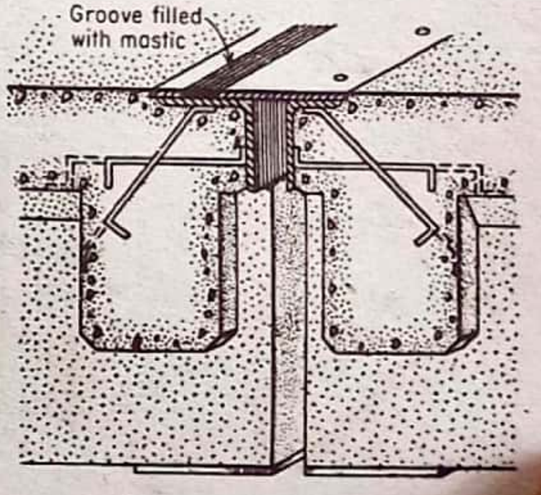


Fig. 12.17 Details of expansion joint.

Scanned with CamScanner



Fig. 12.18 Metal strips for expansion joints.

specifically to the joint between the ends of two adjacent spans in a multispan bridge.

Thin copper or zinc strips, bent in the form of the letter T as shown in Fig. 12.18, are sometimes placed across a joint and embedded in the concrete on either side of the joint to add to the watertightness. The joint is filled with a mastic compound. A detail of this type is shown in Fig. 12.14*a*.

A joint at the fixed end of a span is made watertight by simply filling a groove at the top of the joint with mastic, as shown in Fig. 12.12. The membrane waterproofing which is shown on top of the low parapet in this figure is furnished to ensure watertightness in the horizontal joint.

Drainage Surface water on bridge decks should be disposed of as quickly and as directly as possible. This is accomplished by crowning the roadway about ⅛ in. per ft and pitching the gutters to drain into inlets. In single-span bridges built on a grade, no special provision for longitudinal drainage is ordinarily necessary. The water is carried by the transverse crown to the curbs or gutters and thence to the low end of the bridge, where it can easily be deflected away from the roadway.

If the bridge is horizontal longitudinally, a longitudinal camber can be built into the bridge deck by elevating the middle portion of the span when the forms are erected. This camber will serve to carry the water in the gutters to either end of the span. A camber of about $\frac{1}{10}$ in. per ft is satisfactory for concrete decks.

When necessary, special drain inlets can be constructed by building cast-iron scuppers in the gutters. Two types are shown in Fig. 12.19. The scuppers should be so designed as to prevent the drain water from touching the concrete. Drain inlets are generally necessary in multispan bridges because of the impracticability of carrying the surface water to the ends of the bridge.

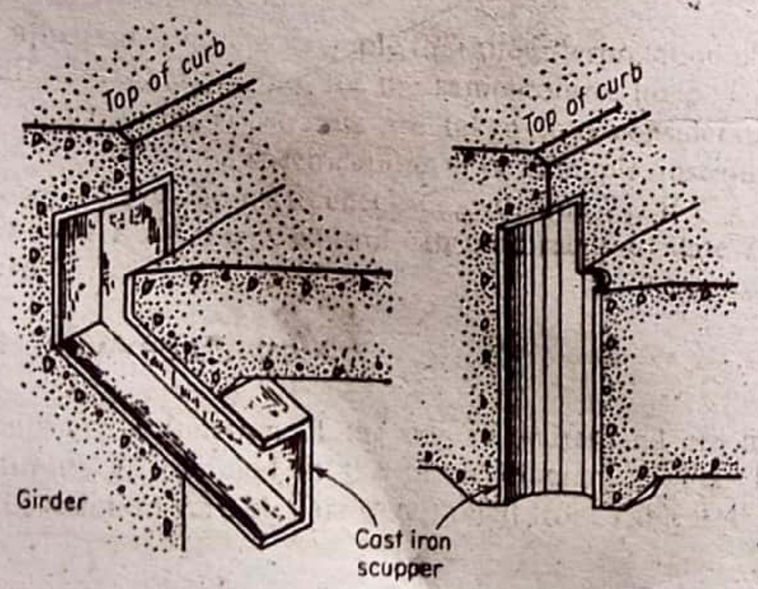


Fig. 12.19 Typical scupper details.

DESIGN OF A SLAB BRIDGE

12.10 Design of a Slab Bridge A slab bridge similar to that shown in Fig. 12.1 is to be designed according to the following data:

Clear span	15 ft
Clear width	26 ft
Live loading	*H*20–*S*16
Wearing surface	30 psf
Concrete strength f'_c	3000 psi
Intermediate-grade reinforcement	

By AASHO specifications, an allowable concrete stress of

$$f_c = 0.40f'_c = 1200 \text{ psi}$$

and an allowable steel stress of 20,000 psi will be used.

The effective span of the slab is assumed as 15 ft + 1 ft = 16 ft, and a total thickness of 12 in. is selected for trial. The total dead load per square foot is then 180 psf, and the dead-load moment is

$$\tfrac{1}{8} \times 180 \times 16^2 = 5760 \text{ ft-lb}$$

The load on each rear wheel is 16,000 lb.

$$E = 4 + 0.06S = 4 + 0.06 \times 16 = 4.96 \text{ ft}$$

The load on a unit width of slab is therefore

$$16{,}000/4.96 = 3230 \text{ lb}$$

and the live-load moment is

$$\frac{PS}{4} = \frac{3230 \times 16}{4} = 12{,}900 \text{ ft-lb}^*$$

The impact coefficient is

$$I = \frac{50}{l + 125} = \frac{50}{16 + 125} = 0.355$$

which is greater than the specified maximum of 0.300. The latter will therefore be used, giving an impact moment of

$$0.300 \times 12{,}900 = 3870 \text{ ft-lb}$$

* Note that this calculation of live-load moments results in a somewhat lower value than the approximate $900S$ = 14,400 ft-lb.

Scanned with CamScanner

The total moment due to dead, live, and impact effects is 22,530 ft-lb.

For the unit stresses specified, $K = 197$ (Table 5, Appendix B), and

$$d = \sqrt{\frac{M}{Kb}} = \sqrt{\frac{22{,}530 \times 12}{197 \times 12}} = 10.7 \text{ in.}$$

With $t = 12$ in., less 1 in. protective covering under the main reinforcement, and less one-half of an assumed bar diameter of 1 in., an effective depth of 10.5 in. is obtained, sufficiently close to the calculated requirement. A 12-in. slab will be used.

The required main reinforcement is

$$A_s = \frac{M}{f_s jd} = \frac{22{,}530 \times 12}{20{,}000 \times 0.875 \times 10.5} = 1.47 \text{ in.}^2 \text{ per ft}$$

which is furnished by No. 8 bars 6 in. on centers ($A_s = 1.57$ in.^{2} per ft). Fifty per cent of these bars will be stopped 15 diam beyond the point at which they are no longer required for moment, or 8 in. short of the face of supports. The remainder will be carried a distance $l = A_s f_s / 2\Sigma_0 u = 9$ in. into the support, in accordance with the AASHO specification. As specified in Art. 12.6, the amount of transverse reinforcement required for proper distribution of concentrated loads (also to provide for shrinkage) is $A_s/\sqrt{S} = 1.47/\sqrt{16} = 0.37$ in.^{2}; No. 5 bars 10 in. on centers are placed directly on top of the longitudinal reinforcement.

In order to facilitate screeding off the slab, the required curbs will not be made monolithic. Required edge beams will consist of an edge slab section additionally reinforced. The dead load carried by the edge beam is

$$\frac{22 \times 24}{144} 150 = 550 \text{ plf}$$

and the dead-load moment is

$$\tfrac{1}{8} \times 550 \times 16^2 = 17{,}600 \text{ ft-lb}$$

The specified live-load moment is

$$0.10 P_{20} S = 0.10 \times 16{,}000 \times 16 = 25{,}600 \text{ ft-lb}$$

giving a total moment of 43,200 ft-lb. The resisting moment of the given section is

$$Kbd^2 = 197 \times 24 \times 10.5^2 \times \tfrac{1}{12} = 43{,}400 \text{ ft-lb}$$

which is just adequate. The steel required is

$$A_s = \frac{43{,}200 \times 12}{20{,}000 \times 0.875 \times 10.50} = 2.82 \text{ in.}^2$$

which will be provided by four No. 8 bars.

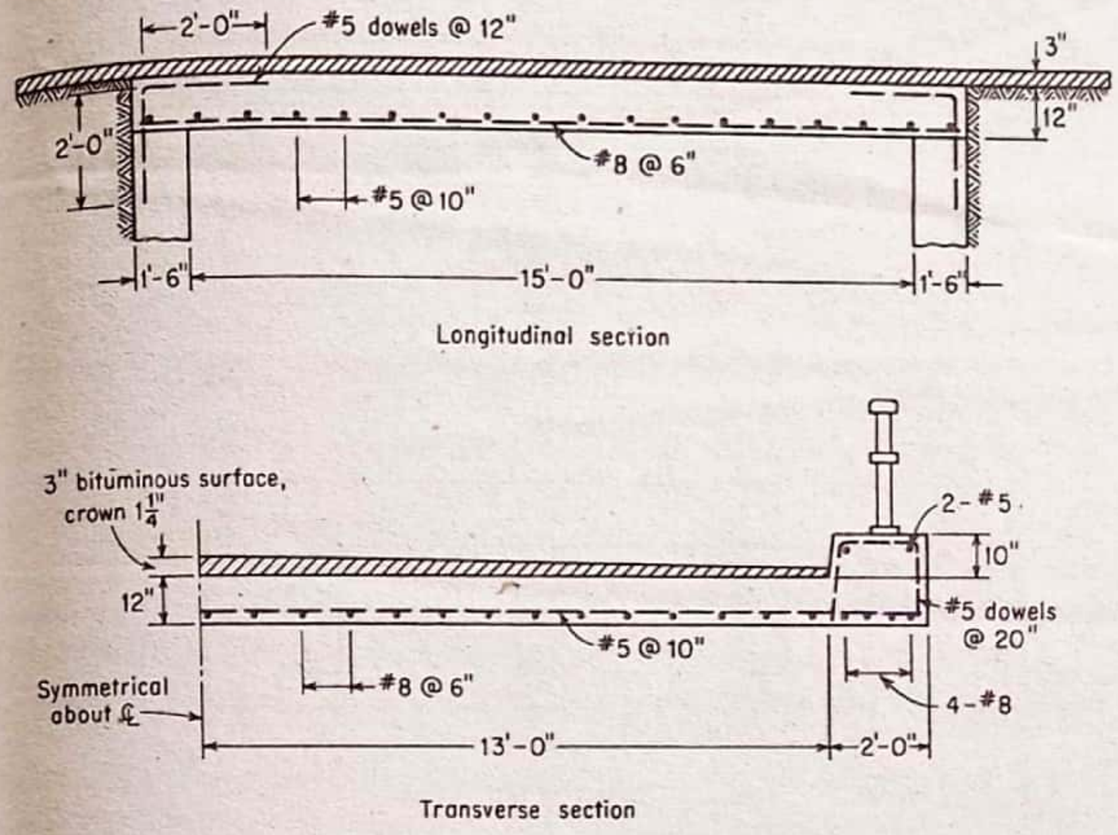


Fig. 12.20 Details of slab bridge.

The crown of the roadway is obtained by varying the thickness of the bituminous wearing surface. No expansion joints are necessary for a span of this length, and a fixed bearing is constructed at each end by placing vertical dowels in the abutment so that they will project up into the concrete deck slab. These are extended horizontally 24 in. to control the cracking that may occur near the edge of the support. The bridge seat is to be coated with a bituminous mixture before the slab is poured. Details are shown in Fig. 12.20.

DESIGN OF A T-BEAM OR DECK-GIRDER BRIDGE

12.11 Data and Specifications A T-beam or deck-girder bridge similar to that shown in Fig. 12.2 is to be designed for the following conditions:

Clear span	48 ft
Clear width	29 ft
Live loading	*H*20–*S*16
Concrete strength f'_c	3000 psi
Intermediate-grade reinforcement	

The design is to meet the AASHO specifications. The bridge will consist of six parallel girders supporting a floor slab, as shown in Fig. 12.21.

Scanned with CamScanner

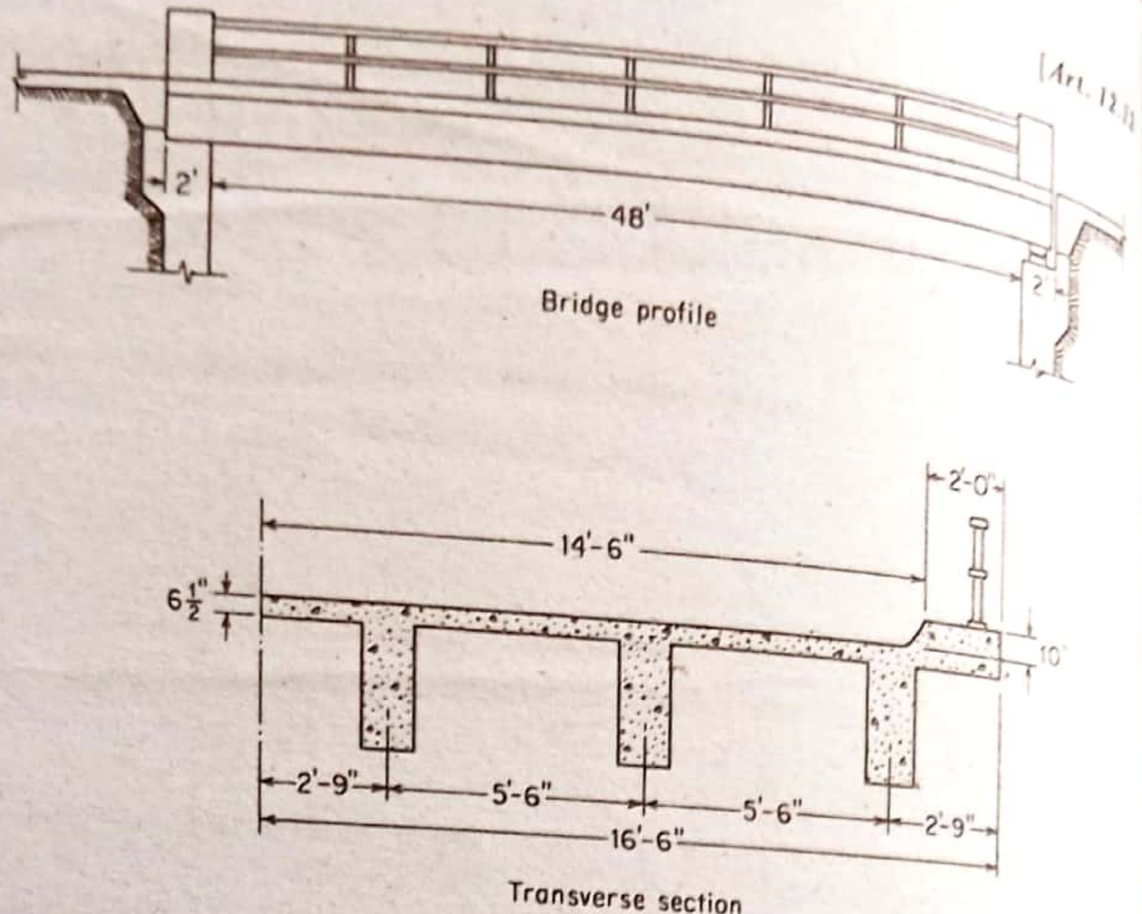


Fig. **12.21** Deck-girder bridge.

12.12 Slab Design Since the slab will be poured monolithically with the girders and will be fully continuous, the span will be taken as the clear distance between girders. Under the assumption that the girders will be 14 in. in width, the clear span will be 4 ft 4 in. For a total thickness of slab of 6 in. (including a ¾-in. wearing surface), with a 15-psf allowance for possible future protective covering, the total dead load is 90 psf. A coefficient of $\frac{1}{10}$ for positive and negative dead-load moments will be assumed in the absence of definite specification values. The dead-load positive and negative moments are

$$\tfrac{1}{10} \times 90 \times 4.33^2 = 169 \text{ ft-lb}$$

For live-load moment computations, Case 1 of Art. 12.6 applies:

$$0.80 \frac{S+2}{32} P_{20} = \frac{0.80 \times 6.33 \times 16{,}000}{32} = 2530 \text{ ft-lb}$$

Since the loaded length is small, the impact coefficient is 0.30, and the impact moment is 760 ft-lb. The total positive and negative moments are 3459 ft-lb. Then

$$d = \sqrt{\frac{3459 \times 12}{197 \times 12}} = 4.19 \text{ in.}$$

With the addition of 1 in. of protective concrete below the center of an assumed ¾-in. bar, and with the ¾-in. wearing surface (not considered structurally effective), the total thickness is 6.32 in. A 6½-in. slab will be used, with an effective depth of 4.37 in. The dead-load estimate need not be revised.

$$A_s = \frac{3459 \times 12}{20{,}000 \times 0.875 \times 4.37} = 0.54 \text{ in.}^2$$

which is furnished by No. 6 bars 10 in. on centers. In order to avoid excessive bending of bars, and since short spans are involved, straight bars will be used in the slab, with No. 6 bars at 10 in. top and bottom. This will provide a surplus of steel in some areas, but the cost of the additional steel will probably be offset by the savings in fabrication and handling of the bent bars which would otherwise be required. Temperature and distribution stresses in the perpendicular direction are provided for by placing five No. 5 bars directly on top of the main slab steel in each slab panel. Complete details of the slab are shown in Fig. 12.26.

12.13 Interior Girders The interior girders are T beams with flange width equal to the center-to-center distance of girders. The required stem dimensions are governed by either the maximum moment or maximum shear. The bridge seats will be assumed 2 ft in width, and the effective span length center to center of bearings taken as 50 ft.

Dead-load moments The weight of the slab per foot of beam is $96 \times 5.5 = 528$ plf. The stem section below the slab is assumed as 14×30 in., which adds weight of 437 plf, making the total 965 plf. The dead-load moment at the center of the span is

$$M_d = \tfrac{1}{8} \times 965 \times 50^2 = 302{,}000 \text{ ft-lb}$$

In order to determine the points at which some of the horizontal steel may be bent up, it is necessary to compute the moment at some sections between the point of maximum moment and the support. At 10 ft from the support, the dead-load moment is 192,800 ft-lb; at 20 ft, 289,000 ft-lb.

Live-load moments The absolute maximum live-load moment will occur with an *H*20-*S*16 truck on the bridge in the position[1] shown in Fig. 12.22. With the distribution of loads as specified in Art. 12.7, each interior girder must support $5.50/5.0 = 1.10$ wheel loads per wheel. Therefore the load from the rear wheel is $1.1 \times 16{,}000 = 17{,}600$ lb, and that from the front wheel is $1.1 \times 4000 = 4{,}400$ lb.

$$R_L = [17{,}600(36.6 + 22.6) + 4400 \times 8.6]\tfrac{1}{50} = 21{,}600 \text{ lb}$$
$$M_{max} = 21{,}600 \times 27.4 - 17{,}600 \times 14 = 346{,}000 \text{ ft-lb}$$

[1] For a discussion of the position of moving loads for absolute maximum moment, see any elementary text in structural theory.

Scanned with CamScanner

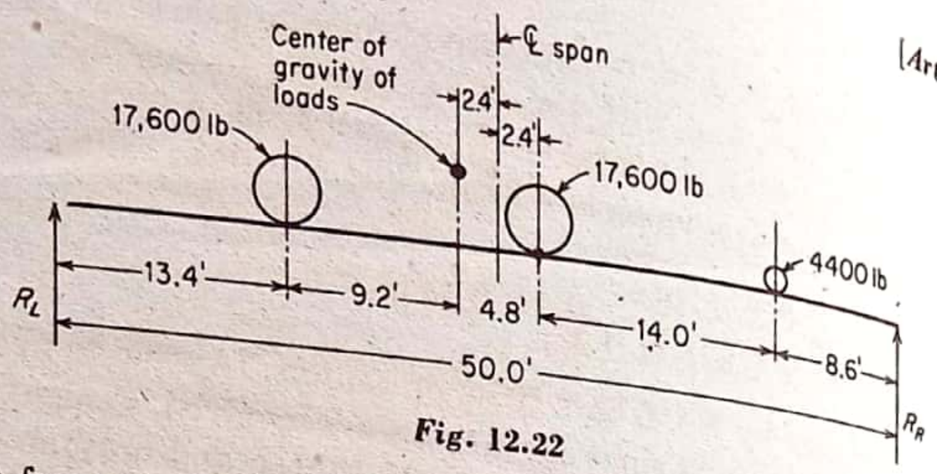


Fig. 12.22

Ten feet from the left support, the maximum live-load moment occurs with the rear trailer wheels at that point and the front wheels 38 ft from the left support. With this position of the loads,

$$R_L = [17{,}600(40 + 26) + 4400 \times 12]\tfrac{1}{50} = 24{,}400 \text{ lb}$$
$$M_{10} = 24{,}400 \times 10 = 244{,}000 \text{ ft-lb}$$

Similarly,

$$M_{20} = 330{,}000 \text{ ft-lb}$$

Impact moments In computing impact moments for a girder such as this, it is usual to consider the whole span as the loaded length. The impact coefficient is therefore $50/(50 + 125) = 0.285$, and the impact moments are as follows:

$$M_{max} = 98{,}700 \text{ ft-lb}$$
$$M_{20} = 94{,}100 \text{ ft-lb}$$
$$M_{10} = 69{,}600 \text{ ft-lb}$$

Maximum total moments The sum of the maximum dead load, live load, and impact moments is 746,700 ft-lb. The total moments at the 20 and 10-ft points are 713,100 and 506,400 ft-lb, respectively.

Dead-load shears The maximum dead-load shear at the end of the beam is $965 \times 25 = 24{,}100$ lb. Ten feet from the support, the shear is 14,450 lb; 20 ft from the support, it is 4800 lb.

Live-load shears The absolute maximum shear occurs with the truck on the span in the position shown in Fig. 12.23. The maximum live-load shear is 30,600 lb. The maximum shears at the 10-, 20-, and 25-ft points are 24,300, 16,400, and 12,700 lb, respectively.

Impact shears For loaded lengths of 50, 40, 30, and 25 ft the impact shears are as follows:

End shear	8700 lb
10-ft section	6900 lb
20-ft section	4700 lb
Midspan section	3600 lb

Total shears The total shears are as follows:

End shear	63,400 lb
10-ft section	45,650 lb
20-ft section	25,900 lb
Midspan section	16,300 lb

Determination of cross section and steel area The maximum shear stress in the beam web will be taken equal to $0.06f'_c = 180$ psi.[1] The area $b'd$ required to sustain this shear is

$$b'd = \frac{V}{vj} = \frac{63{,}400}{180 \times 0.875} = 403 \text{ in.}^2$$

If b' is taken as 14 in., the required d is 28.8 in. If three rows of No. 11 bars are assumed, with 2 in. clear between rows and 2½ in. clear below the bottom row to allow for stirrups and concrete protection, a total depth of 35.42 in. is obtained. A 36-in. total depth will be used, resulting in an effective depth of 29.4 in. The depth of the stem below the slab is then $36 - 6\frac{1}{2} = 29\frac{1}{2}$ in. This is sufficiently close to the assumed value so that the dead-load moments need not be revised. The required tensile-steel area is then found:

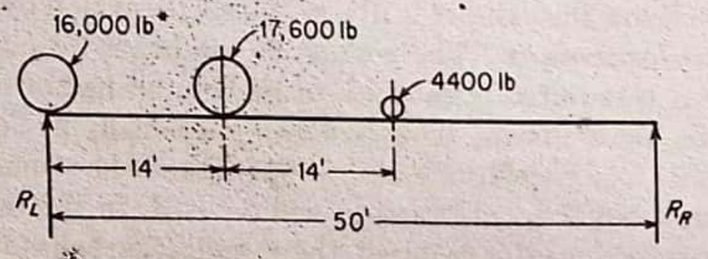
$$A_s = \frac{M}{f_s(d - t/2)} = \frac{746{,}700 \times 12}{20{,}000(29.4 - 5.75/2)} = 16.90 \text{ in.}^2$$

which will be furnished by eleven No. 11 bars.

A check of the maximum stress in the concrete, using Graph 12, Appendix B, shows a maximum compression of 1190 psi, practically equal to the allowable stress of 1200 psi.

The lower four tensile bars, somewhat more than one-third the area, will be extended into the support. The upper two layers will be cut off 15 diam or one-twentieth of the span beyond the point at which they are no longer required, in accordance with the specification. The critical ex-

[1] The AASHO specification permits a unit shear as high as $0.075f'_c$ for beams with web reinforcement.



*See Art 12.7 for prescribed distribution of loads for shear computations.

Fig. 12.23

Scanned with CamScanner

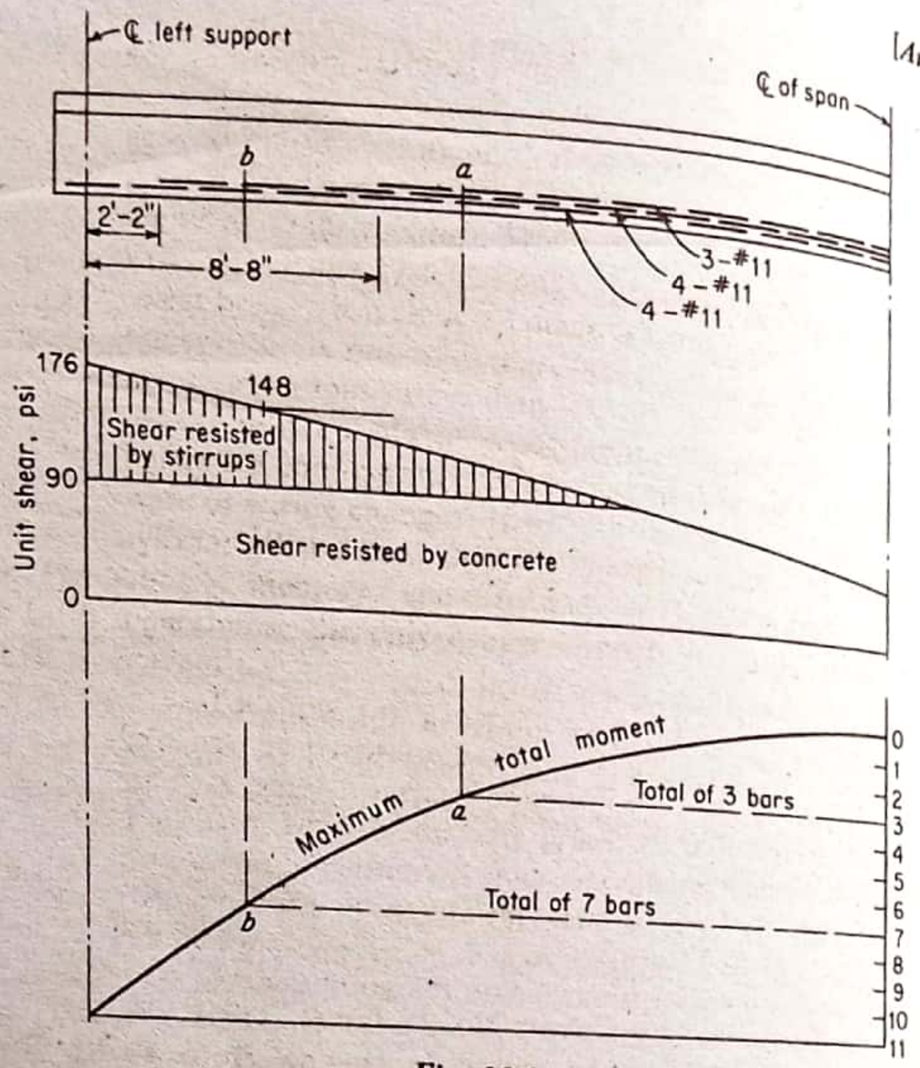


Fig. 12.24

tension in this case is one-twentieth of the span, or 30 in. Cutoff points are found graphically as in Fig. 12.24.

Checking the bond at the center line of supports, where the shear is greatest and the total bar perimeter is least, four No. 11 bars provide a perimeter of 17.7 in., and

$$u = \frac{V}{\Sigma_0 jd} = \frac{63{,}400}{17.7 \times 0.875 \times 29.4} = 139 \text{ psi}$$

which is well below the value of $0.10f'_c = 300$ psi permitted by specification.

Web reinforcement The portion of the beam through which web reinforcement is required is determined by computing the unit shears at various points on the beam. This is shown graphically in Fig. 12.24. The concrete resists a unit shear of $0.03f'_c = 90$ psi, and the remainder is taken up by stirrups. Number 5 U stirrups will be used. In the region through which web reinforcement is required, the specification calls for a maximum spacing of $d/2 = 15$ in. The excess shear corresponding to the spacing is

$$v' = \frac{A_v f_v}{sb'} = \frac{0.61 \times 20{,}000}{15 \times 14} = 58 \text{ psi}$$

and the total shear stress is 148 psi. This is attained 5 ft 3 in. from the support. The maximum spacing in the region in which stirrups are not required to carry shear is $3d/4 = 22\frac{1}{2}$ in. This will apply at a distance of 16 ft 3 in. from the support. At the support, the required spacing is

$$S = \frac{A_v f_v}{v'b} = \frac{0.61 \times 20{,}000}{86 \times 14} = 10.1 \text{ in.}$$

The first stirrup will be placed $s/2 = 5$ in. from the support center line; this will be followed by six stirrups at 10 in., nine at 15 in., and five at 20 in., filling out the distance to the center of the span.

12.14 Exterior Girders The exterior girders are identical in cross section with the interior girders, because the raised curb section will be poured separately and cannot be counted on to participate in carrying loads.

Moments In addition to the 965-plf dead load obtained for the interior girders, the safety curb adds 250 plf, producing a total dead load of 1215 plf and a maximum dead-load moment at the center of the span of 380,000 ft-lb. A portion of each wheel load which rests on the exterior slab panel is supported by the exterior girder. That portion is obtained by placing the wheels as close to the curb as the clearance diagram will permit and treating the exterior slab panel as a simple beam. The position is shown in Fig. 12.25, and the proportion of the load is $4.25/5.50 = 0.773$. The longitudinal position of the load which will produce the absolute maximum bending moment is the same as for the interior girders. The absolute maximum live-load moment can therefore be obtained by direct proportion:

$$M_{max} = (0.773/1.10)346{,}000 = 243{,}000 \text{ ft-lb}$$

The impact moment is $0.285 \times 243{,}000 = 69{,}300$ ft-lb, and the total maximum moment is 692,300 ft-lb.

Shears The maximum dead-load shear is

$$V_D = 1215 \times 25 = 30{,}400 \text{ lb}$$

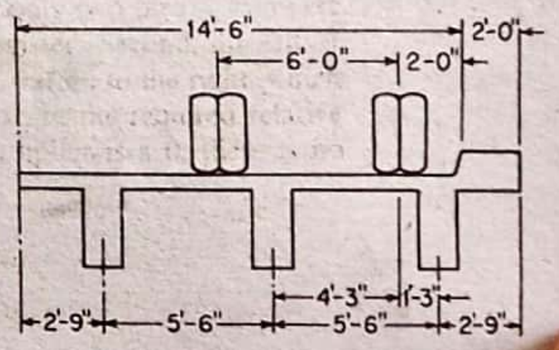


Fig. 12.25

Scanned with CamScanner

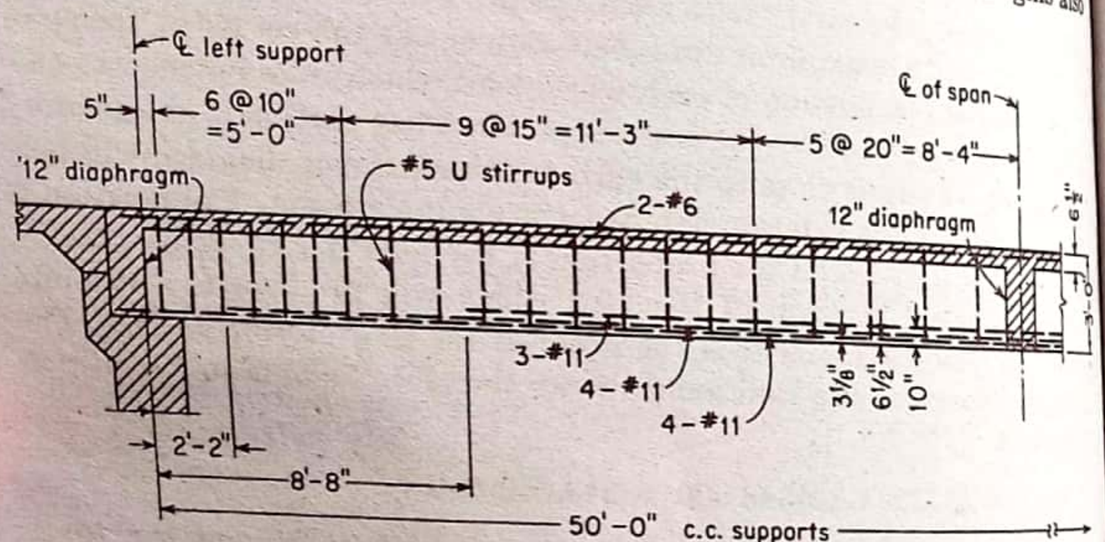
The maximum live-load shear is proportional to the maximum live-load shear in the interior girders:

$$V_L = (0.773/1.10)30{,}600 = 21{,}500 \text{ lb}$$

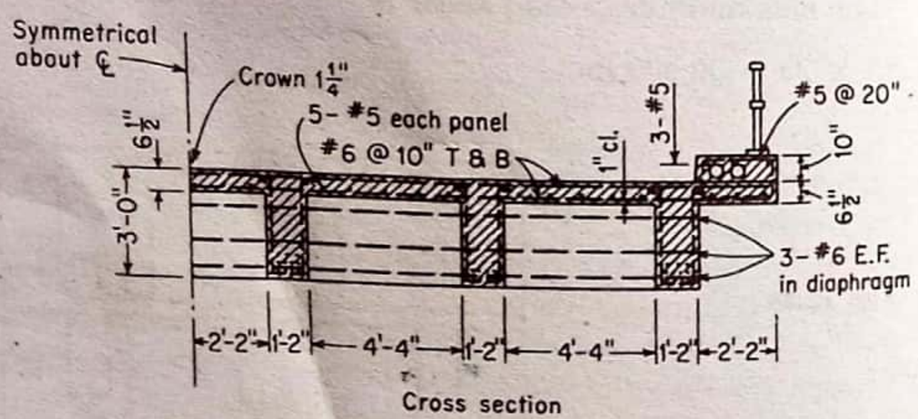
The impact shear at the support is 6100 lb. The total shear at the support is then 58,000 lb. Shears at other points in the span are found similarly.

Determination of cross section and reinforcement Once the shears and moments due to dead and live loads and impact are obtained, the design of the exterior girders follows along the lines of that for the interior girders. The details will not be repeated here.

12.15 Miscellaneous Details: *Diaphragms* A transverse diaphragm (see Figs. 12.12 and 12.14) will be built between the girders at either end of the bridge. The chief function of these diaphragms is to furnish lateral support to the girders; with some abutment details, the diaphragms also



Details of interior girder



Cross section

***Fig.* 12.26** Details of T-beam bridge.

serve to prevent the backfill from spilling out onto the bridge seats. A similar diaphragm will be built between the girders at midspan. Such intermediate diaphragms are recommended for all spans in excess of 40 ft and serve to ensure that all girders act together in resisting the loads.

Fixed bearing A fixed bearing similar to that in Fig. 12.13 is provided at one end. Vertical dowels are placed in the breast wall of the abutment and are bent so as to project into the longitudinal beams or deck slab. Horizontal dowels are embedded in the deck and approach slabs. The diaphragm rests directly on the bridge seat.

Expansion bearing An expansion bearing is provided at one end of the span. Its details are similar to Fig. 12.14*b*. The bottom of the diaphragm is flush with the bottoms of the beams and is not in contact with the bridge seat.

Waterproofing and drainage All joints will be filled with a mastic compound to prevent water from seeping through the joints. Removal of surface water will be accomplished by crowning the roadway 1¼ in. and pitching the gutters toward the ends by providing a camber of 2½ in. at the center. Besides facilitating drainage, this camber serves to prevent the appearance of sag that would be evident if the girders were at the same level throughout the span.

Full details are shown in Fig. 12.26.

COMPOSITE-BRIDGE CONSTRUCTION

12.16 General Description In addition to girder bridges constructed entirely of reinforced concrete, frequently bridges are constructed of longitudinal steel girders with reinforced-concrete decks. If the deck merely rests on the girders, it does not represent an integral part of the transverse cross section. That is, since no provision is made to transfer longitudinal shears from the girder to the deck, the latter does not assist in carrying longitudinal bending moments. In contrast, steel-concrete composite construction (Fig. 12.3), as used in many present-day bridges, consists essentially of three elements: (1) longitudinal steel girders, (2) a reinforced-concrete deck, and (3) devices called *shear connectors* which are welded to the top flanges of the beams and which protrude into the slab to tie slab and beam together and to force them to act as a unit in resisting girder moments and shears. Figure 12.27 shows a typical example of a completed bridge of this type. Simple spans up to about 125 ft and continuous spans up to about 175 ft have been built in this manner.

The principal advantage of this type of construction is that it utilizes the concrete deck, which in normal construction does not contribute to longitudinal strength, to assist in resisting longitudinal bending. The resulting composite section is usually shallower and lighter—but nonethe-

Scanned with CamScanner

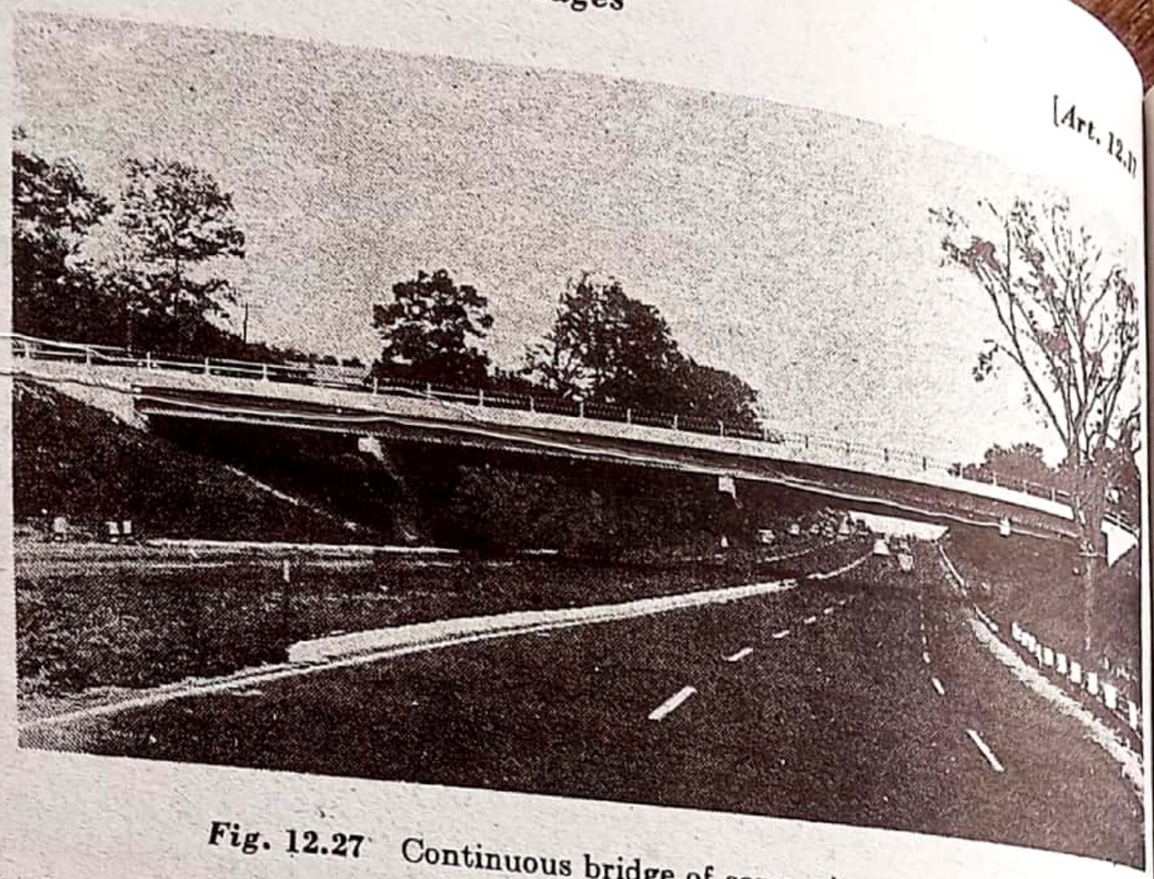


Fig. 12.27 Continuous bridge of composite construction.

less stiffer—than a comparable section of ordinary concrete-slab–steel-stringer construction in which there is no provision for composite action.

The dimension of the concrete slab in composite construction are usually determined by the transverse flexural requirements. Principal reinforcement is in the direction transverse to the axis of the bridge; in the longitudinal direction, only distribution reinforcement is used. The slab design is carried out in the same manner as for noncomposite construction.

The steel beams, spanning longitudinally between abutments or piers, may be rolled sections, rolled sections with cover plates, or built-up plate girders. Unsymmetrical steel sections, such as a rolled W.F. beam with a cover plate on the lower flange only, can be used to advantage. For longer spans, variable-depth sections are often used. The design may be continuous over several supports.

12.17 Shear Connectors Shear connectors are essential to the development of composite action. These must transfer the horizontal shear with extremely small deformation so that the structure deforms as a unit. The closest spacing of shear connectors will normally be near the support, where the shear is greatest, although recent testing indicates that this may not be necessary (Ref. 12.3).

Some of the different types of shear connectors which have been used successfully are shown in Fig. 12.28. These may take the form of a continuous spiral, as in (*a*), welded at the point of contact to the steel beam. Individual pieces of steel channel may be used, as in (*b*), set transverse to

the beam axis and welded to the beam along the back and toe of the channel. The studs shown in (*c*) have been widely used in recent years. Common diameters are $\frac{5}{8}$, $\frac{3}{4}$, and $\frac{7}{8}$ in. They are granular-flux–filled and electrically welded to the steel-beam flange. Whatever the type of shear connector, it must be capable of resisting both horizontal and vertical movement between the concrete and the steel and should extend at least halfway into the slab, but not closer than 1 in. to the top of the slab. Connectors are most economically installed in the fabricating shop. However, the advantages of this procedure may be offset by the possibility of damage during shipment and the difficulty in working along the top of the beams during erection.

Since most shear connectors are of unusual shapes, the ultimate strength in shear has been established experimentally, for the various types. The following expressions are recommended by AASHO (Ref. 12.1):

1. Channels: $Q_{uc} = 180(h + \frac{1}{2}t)w\sqrt{f'_c}$
2. Welded studs with $H/d \geq 4.2$: $Q_{uc} = 330d^2\sqrt{f'_c}$
3. Welded studs with $H/d < 4.2$: $Q_{uc} = 80Hd\sqrt{f'_c}$
4. Spirals: $Q_{uc} = 3840d\sqrt[4]{f'_c}$

where Q_{uc} = ultimate-load capacity of one shear connector or one pitch of spiral bar, lb
h = maximum thickness of channel flange, measured at face of web, in.
t = thickness of web of channel shear connector, in.
w = length of channel shear connector, measured in transverse direction on flange of beam, in.
f'_c = required compressive strength of concrete at 28 days, psi
d = diameter of studs or of round bars used in spirals, in.
H = height of stud, in.

The value of Q_{uc} so obtained represents the ultimate capacity of the connector. AASHO recommends that a safety factor of 4 be applied in arriving at a safe working value Q.

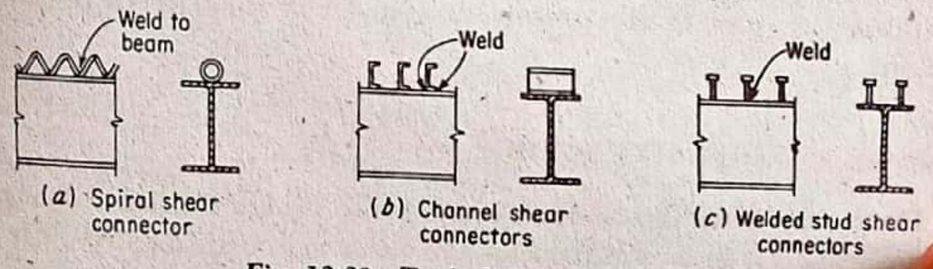


Fig. 12.28 Typical shear connectors.

12.18 Design of Composite Sections The steel stringers alone must support their own dead weight, as well as the dead weight of the formwork and fresh concrete of the deck, unless intermediate shoring is used. The usual principles of steel design apply to the design of the stringers to resist noncomposite dead loads.

A portion of the dead load and all the live load are resisted by composite action. The resisting moment of the composite section is usually computed from the properties of the transformed section obtained by substituting an equivalent amount of steel for the concrete slab.

In transforming the concrete slab into equivalent steel, the depth of the transformed area is held constant, but the width is reduced to $1/n$ times its actual value, where $n = E_s/E_c$. The value of n to be used will depend on whether the loads are long- or short-term. If loads are long-term (such as the composite portion of the dead load), the effects of creep and plastic flow are approximated by reducing E_c to one-third its normal value. Thus, when stresses due to long-term loads are dealt with, the substituted steel area is only one-third what it would otherwise have been.

AASHO recommends that the effective width of the compression-concrete flange be taken not larger than (1) one-fourth the span length of the beam, (2) the distance center to center of beams, or (3) twelve times the least thickness of the slab. For beams having a flange on one side only, the effective flange width shall not exceed one-twelfth the span length of the beam, nor 6 times the thickness of the slab, nor one-half the distance center to center of the next beam.

In composite design, the section must be selected largely by trial and error. While some tables are available giving the section properties for certain combinations of slab and steel beam (Ref. 12.2), and while methods have been developed to reduce the labor of finding an appropriate section (Ref. 12.4), it is not practical to tabulate all desirable combinations of slab width and thickness, steel-beam section, and cover-plate size. Direct design of composite sections is therefore not possible, and the design process is actually a review of an assumed section to determine if the stresses in the concrete and steel are within the allowable range. Stresses due to each type of loading are computed using the appropriate section properties, and these stresses are added algebraically to obtain final values.

DESIGN OF A COMPOSITE BRIDGE

12.19 Data and Specifications A composite bridge similar to that shown in Fig. 12.3 is to be designed for the following conditions.

Span center to center of supports	70 ft
Clear width	28 ft
Live loading	*H*20–*S*16
Wearing surface	30 psf
Concrete strength f'_c	3000 psi
ASTM A7 steel beam	
Intermediate-grade reinforcement	

Welded-stud shear connectors are specified, and a single cover plate will be used on the bottom flange and discontinued where no longer required. The bridge will consist of five parallel girders, as shown in Fig. 12.29.

12.20 Slab Design The design of the slab in the transverse direction follows the procedure presented in Art. 12.12. For the given loads and spans, a slab of 6½-in. total thickness is obtained, reinforced with No. 6 bars 8 in. on centers, top and bottom, in the direction transverse to the supporting beams. In the direction parallel to the girders, six No. 6 bars are equally spaced in each slab panel. Details of the slab are shown in Fig. 12.31.

12.21 Interior Girders The effective width of flange, in accordance with AASHO, is taken equal to the beam spacing of 81 in.

Dead-load moment on steel beams The noncomposite portion

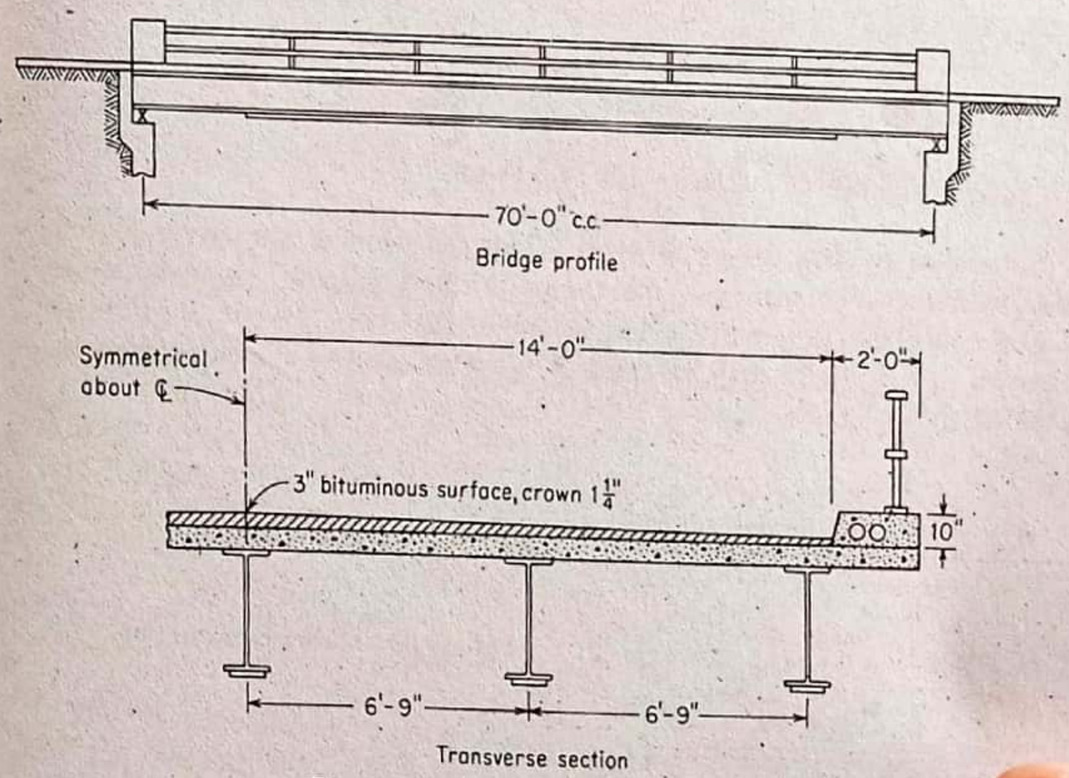


Fig. **12.29** Composite-girder bridge.

Scanned with CamScanner

of the dead load includes the effect of the concrete slab, the estimated girder and cover-plate weight, and the estimated weight of transverse diaphragms. The total weight is estimated at 800 plf, and the noncomposite dead-load moment is

$$M_{DS} = \tfrac{1}{8} \times 800 \times 70^2 = 490{,}000 \text{ ft-lb}$$

Dead-load moment on composite beam The composite dead load includes the weight of bridge rails, safety curbs, and bituminous pavement. These sum up to 300 plf, and the composite dead-load moment is

$$M_{DC} = \tfrac{1}{8} \times 300 \times 70^2 = 184{,}000 \text{ ft-lb}$$

Live-load moment The live-load distribution factor in this case is 6.75/5.5 = 1.23 wheel loads per wheel. The absolute maximum live-load moment will occur when an *H*20-*S*16 truck is located with one of its inner 16,000-lb wheels 2.35 ft from the span center line, and it will occur under that wheel. The live-load moment at that point is

$$M_{max} = 494{,}000 \times 1.23 = 608{,}000 \text{ ft-lb}$$

Impact moment The impact coefficient in this case is

$$50/(70 + 125) = 0.256,$$

and the maximum impact moment is

$$M_{max} = 608{,}000 \times 0.256 = 156{,}000 \text{ ft-lb}$$

Selection of the cross section The selection of the cover-plated cross section is necessarily a matter of trial. A section made up of a 36 W.F.150 plus a single 10 × 1¼ in. cover plate on the bottom flange, as shown in Fig. 12.30, will be tried. Section properties are calculated in Table 12.1.

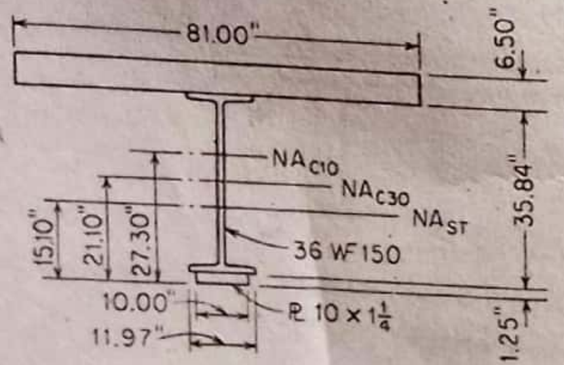


Fig. 12.30 Girder cross section.

Table 12.1 **Properties of section with cover plate**

	I_o	A	y_b NA to bottom	Ay_b	d CG to NA	Ad^2
Steel only:						
36 W.F.150	9012	44.16	19.17	848	4.07	730
Pl 10 × 1¼		12.50	0.63	8	14.47	2630
	9012	56.66		856		3360
						9012
						$I = 12{,}372$
	$\bar{y} = \frac{856}{56.66} = 15.10$			$S_b = \frac{12{,}372}{15.10} = 822$		
	$S_{ts} = \frac{12{,}372}{21.99} = 564$					
Composite with n = 30:						
Steel	12,372	56.66	15.10	856	6.00	2040
Slab	62	17.50	40.34	706	19.24	6480
	12,434	74.16		1562		8,520
						12,434
						$I = 20{,}954$
	$\bar{y} = \frac{1562}{74.16} = 21.10$			$S_b = \frac{20{,}954}{21.10} = 990$		
	$S_{ts} = \frac{20{,}954}{15.99} = 1310$			$S_{tc} = \frac{20{,}954}{22.49} = 929$		
Composite with n = 10:						
Steel	12,372	56.66	15.10	856	12.20	8450
Slab	186	52.50	40.34	2120	13.04	8940
	12,558	109.16		2976		17,390
						12,558
						$I = 29{,}948$
	$\bar{y} = \frac{2976}{109.16} = 27.30$			$S_b = \frac{29{,}948}{27.30} = 1095$		
	$S_{ts} = \frac{29{,}948}{9.79} = 3060$			$S_{tc} = \frac{29{,}948}{16.29} = 1830$		

The stresses due to various loads are shown in Table 12.2. It is seen that the bottom fiber stress is almost equal to the allowable value of 18,000 psi. The top fiber of the steel section is understressed by about 16 per cent. Since the lightest 36-in. section has been selected, the only alternative would be to use a 33-in. rolled section, which would require a heavier cover plate and which would save little if any steel. Consequently

Table 12.2 Total stresses

Load	Moment	f_{sb}	f_{st}	$3nf_c$ or nf_c	f_c
M_{DS}	490,000	7170	10,400		
M_{DC}	184,000	2230	1,690		
M_{LL+I}	764,000	8370	2,990	2380	
Totals		17,770	15,080	5000	80
					500
					580

Table 12.3 Properties of section without cover plate

	I_o	A	y_b NA to bottom	Ay_b	d CG to NA	Ad^2	
Steel only	$S_b = 503$			$S_t = 503$			
Composite with $n = 30$:							
Steel	9012	44.16	17.92	791	5.98	1580	
Slab	62	17.50	39.09	685	15.19	4040	
	9074	61.66		1476		5620	
						9074	
						$I = 14{,}694$	
	$\bar{y} = \frac{1476}{61.66} = 23.90$			$S_b = \frac{14{,}694}{23.90} = 616$			
	$S_{ts} = \frac{14{,}694}{11.94} = 1230$			$S_{tc} = \frac{14{,}694}{18.44} = 798$			
Composite with $n = 10$:							
Steel	9012	44.16	17.92	791	11.48	5820	
Slab	186	52.50	39.09	2050	9.69	4920	
	9198	96.66		2841		10,740	
						9,198	
						$I = 19{,}938$	
	$\bar{y} = \frac{2841}{96.66} = 29.40$			$S_b = \frac{19{,}938}{29.40} = 678$			
	$S_{ts} = \frac{19{,}938}{6.44} = 3090$			$S_{tc} = \frac{19{,}938}{12.94} = 1540$			

the 36 W.F.150 with cover plate 10 × 1¼ in. will be used. The concrete fiber stress is well within the allowable limit.

The cover plate on the lower flange will be discontinued where it is no longer needed to resist stress. Section properties for the beam without cover plate are computed as shown in Table 12.3. Once the section moduli of the beam without cover plate have been found, the point at which the

cover plate can be discontinued without exceeding allowable stresses in the remaining section is found by trial to be 12 ft 9 in. from the support center line. In accordance with specifications, the plate will be continued far enough beyond that point toward the support to develop the capacity of the plate. A 12-in. extension will suffice in this case.

The shear connectors are designed, not for the full shear, but only for that part resulting from the composite portion of the dead load and from the live and impact loads. The horizontal shear between the slab and the top flange of the steel beam can be found from the expression

$$v = \frac{Vm}{I}$$

where V = external shear force acting at given section, lb
m = static moment of concrete cross section (transformed, with $n = 30$ or $n = 10$ as the case may be) about neutral axis of section, in.^{3}
I = moment of inertia of transformed composite section (with $n = 30$ or $n = 10$), in.^{4}
v = unit shear, lb per in.

Note that, in calculations for v, the appropriate value of n must be used in determining the transformed sections for finding m and I; this depends on whether one is dealing with composite dead load or live load.

At the left support, maximum shear is obtained with one 16,000-lb wheel at the support and 16,000- and 4000-lb wheels at 14 and 28 ft from the support, respectively. For this load condition,

$$V_{LL+I} = 44{,}700 \text{ lb}$$
$$v_{LL+I} = \frac{Vm}{I} = \frac{44{,}700 \times 52.50 \times 9.69}{19{,}938} = 1140 \text{ lb per in.}$$
$$V_D = 300 \times 70\tfrac{1}{2} = 10{,}500 \text{ lb}$$
$$v_D = \frac{10{,}500 \times 17.50 \times 15.19}{14{,}694} = 190 \text{ lb per in.}$$
$$v_{\text{total}} = 1140 + 190 = 1330 \text{ lb per in.}$$

For the present design, ¾-in. studs are selected, and, tentatively, four studs per transverse row are used, with studs 4 in. high.

$$\frac{H}{d} = 4.00/0.75 = 5.33$$
$$Q_{uc} = 330d^2\sqrt{f'_c} = 330 \times 0.75^2\sqrt{3000} = 10{,}200 \text{ lb}$$
$$Q = \frac{Q_{uc}}{SF} = \frac{10{,}200}{4} = 2550 \text{ lb}$$

Safe load per group $= 4Q = 10{,}200$ lb

Scanned with CamScanner

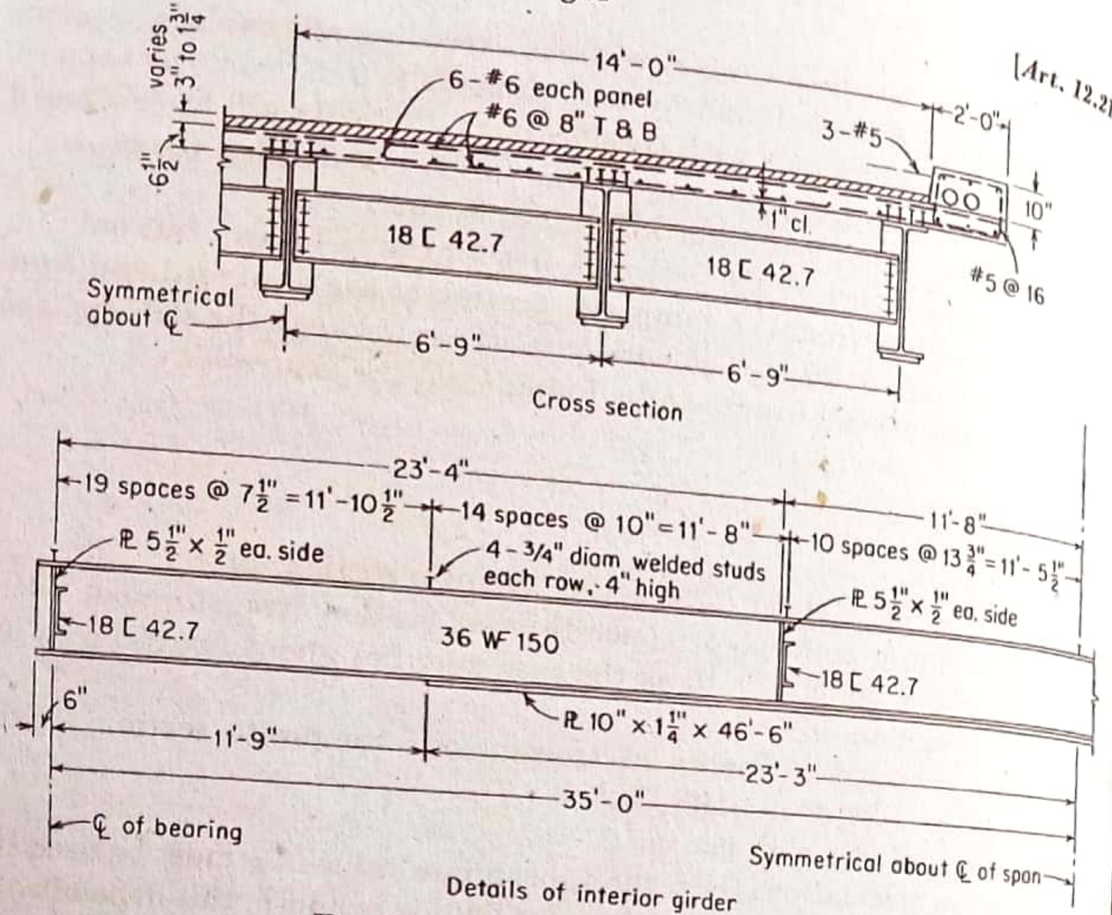


***Fig.* 12.31** Details of composite bridge.

If p is the required pitch (spacing) of connector groups, then

$$vp = 4Q \qquad p = \frac{4Q}{v}$$

and, at the support,

$$p = 10{,}200/1330 = 7.68 \text{ in.}$$

Similar calculations at 7, 14, 21, 28, and 35 ft result in required spacings at those points of 8.50, 10.70, 12.90, 16.20, and 21.80 in., respectively. The maximum spacing permitted by AASHO is 24 in. The stud spacing pattern selected, starting at the left support, is

19 spaces at 7½ in. = 11 ft 10½ in.
14 spaces at 10 in. = 11 ft 8 in.
10 spaces at 13¾ in. = 11 ft 5½ in.

making up the total of 35 ft to midspan. Details are shown in Fig. 12.31.

The spacing of the fillet welds joining the cover plate to the lower flange can likewise be increased as the shear-transfer requirement becomes less. The design method follows that for spacing of the welded studs.

12.22 Exterior Girders The design of the two exterior girders does not differ materially from that for the interior girders, and details will not be presented here. Dead and live loads will differ somewhat; transverse positioning of live load for maximum effect will follow the procedures outlined for the design of exterior girders for the deck-girder bridge (Art. 12.14).

12.23 Miscellaneous Details: *Diaphragms* Transverse diaphragms will be provided at the center line of supports and at the third points of the span. These will consist of 18 C 42.7 members, field-bolted to vertical ribs welded to the girder webs, as shown in Fig. 12.31. In addition to providing safety against overturning of the girders such as might be caused by lateral forces on the roadway, these transverse beams provide some distribution of vertical loads between girders, helping to ensure that the bridge acts as an integral unit.

Bearings A hinged bearing will be provided at one end of each girder, and a rocker bearing at the other, to provide for expansion and contraction of the 70-ft span. A joint detail similar to that shown in Fig. 12.14*b* will be used between the bridge decks and the approach slab.

Drainage The bituminous surface will be crowned to provide lateral drainage, with a depth of 3 in. at the bridge center line and a depth of 1¾ in. at the curbs. A longitudinal camber of 3 in. will ensure that no water stands on the bridge.

Full details of the composite bridge are shown in Fig. 12.31.

REFERENCES

12.1 "Standard Specifications for Highway Bridges," American Association of State Highway Officials, 1961.

12.2 I. M. Viest, R. S. Fountain, and R. C. Singleton: "Composite Construction in Steel and Concrete," McGraw-Hill Book Company, Inc., New York, 1958.

12.3 ACI-ASCE Committee 333: Tentative Recommendations for Design of Composite Beams and Girders for Buildings, *J. ACI*, p. 623, December, 1960.

12.4 R. S. Fountain and I. M. Viest: Selection of the Cross Section for a Composite T Beam, *J. Struct. Div., ASCE*, p. 1313-1, July, 1957.

Scanned with CamScanner

appendix A

FLAT SLABS WITH SQUARE OR RECTANGULAR PANELS (ACI 1963)

2100 Notation

A = distance in direction of span from center of support to intersection of center line of slab thickness with extreme 45° diagonal line lying wholly within concrete section of slab and column or other support, including drop panel, capital and bracket

b_0 = periphery of critical section for shear

c = effective support size [see Art. 2104(c)]

d = distance from extreme compression fiber to centroid of tension reinforcement

f'_c = compressive strength of concrete (see Art. 301)

h = distance from top of slab to bottom of capital

H = story height of the column or support of flat slab center to center of slabs, ft

K = ratio of moment of inertia of column provided to I_c required by Eq. (21-1)

L = span length of flat-slab panel center to center of supports

M_0 = numerical sum of assumed positive and average negative moments at critical design sections of flat slab panel [see Art. 2104(f)1]

Scanned with CamScanner

R_n = factor for increasing negative moment [Art. 2104, Eq. (21-2)]
R_p = factor for increasing positive moment [Art. 2104, Eq. (21-3)]
t = thickness of slab at center of panel, in.
t_1 = thickness of slab without drop panels, or through drop panel, if any, in.
t_2 = thickness of slab with drop panels at points beyond the drop panel, in.
w' = uniformly distributed unit dead and live load
W = total dead and live load on panel
W_D = total dead load on panel
W_L = total live load on panel, uniformly distributed

2101 Definitions and Scope

(*a*) ***Flat slab*** A concrete slab reinforced in two or more directions, generally without beams or girders to transfer the loads to supporting members. Slabs with recesses or pockets made by permanent or removable fillers between reinforcing bars may be considered flat slabs. Slabs with paneled ceilings may be considered as flat slabs provided the panel of reduced thickness lies entirely within the area of intersecting middle strips, and is at least two-thirds the thickness of the remainder of the slab, exclusive of the drop panel, and is not less than 4 in. thick.

(*b*) ***Column capital*** An enlargement of the end of a column designed and built to act as an integral unit with the column and flat slab. No portion of the column capital shall be considered for structural purposes which lies outside of the largest right circular cone with 90° vertex angle that can be included within the outlines of the column capital. Where no capital is used, the face of the column shall be considered as the edge of the capital.

(*c*) ***Drop panel*** The structural portion of a flat slab which is thickened throughout an area surrounding the column, column capital, or bracket.

(*d*) ***Panel strips*** A flat slab shall be considered as consisting of strips in each direction as follows:

A middle strip one-half panel in width, symmetrical about panel center line
A column strip consisting of the two adjacent quarter-panels, one each side of the column center line

(*e*) ***Ultimate strength design*** Flat slabs shall be proportioned by Part IV-A only, except that Part IV-B may be used if the following modifications are made in the design:[1]

1. For either empirical or elastic analysis the numerical sum of the positive and negative bending moments in the direction of either side of a rectangular panel shall be assumed as not less than

$$M_0 = 0.10WLF\left(1 - \frac{2c}{3L}\right)^2$$

in which $F = 1.15 - c/L$ but not less than 1.

2. The thickness of slab shall not be less than shown in Table 2101(*e*).

[1] Parts IV-A and IV-B refer to analysis by W.S.D. and U.S.D. methods, respectively.

Table 2101(*e*)

f_y	Minimum slab thickness	
	With drop panels*	Without drop panels
40,000	$L/40$ or 4 in.	$L/36$ or 5 in.
50,000	$L/36$ or 4 in.	$L/33$ or 5 in.
60,000	$L/33$ or 4 in.	$L/30$ or 5 in.

* To be considered effective, the drop panel shall have a length of at least one-third the parallel span length and a projection below the slab of at least one-fourth the slab thickness.

2102 Design Procedures

(*a*) ***Methods of analysis*** All flat slab structures shall be designed in accordance with a recognized elastic analysis subject to the limitations of Arts. 2102 and 2103, except that the empirical method of design given in Art. 2104 may be used for the design of flat slabs conforming with the limitations given therein. Flat slabs within the limitations of Art. 2104, when designed by elastic analysis, may have resulting analytical moments reduced in such proportion that the numerical sum of the positive and average negative bending moments used in design procedure need not exceed the sum of the corresponding values as determined from Table 2104(*f*).

(*b*) ***Critical sections*** The slab shall be proportioned for the bending moments prevailing at every section except that the slab need not be proportioned for a greater negative moment than that prevailing at a distance A from the support center line.

(*c*) ***Size and thickness of slabs and drop panels***

1. Subject to limitations of Art. 2102(*c*)4, the thickness of a flat slab and the size and thickness of the drop panel, where used, shall be such that the compression due to bending at any section, and the shear about the column, column capital, and drop panel shall not exceed those permitted in Part IV-A or Part IV-B. When designed under Art. 2104, three-fourths of the width of the strip shall be used as the width of the section in computing compression due to bending, except that on a section through a drop panel, three-fourths of the width of the drop panel shall be used. Account shall be taken of any recesses which reduce the compressive area.

2. The shear on vertical sections which follow a periphery b_0 at distance $d/2$ beyond the edges of the column, column capital, or drop panel, and concentric with them, shall be computed as required and limited in Chap. 12 or 17.

3. If shear reinforcement is used, the first line shall be not further than $d/2$ from the face of the support.

4. Slabs with drop panels whose length is at least one-third the parallel span length and whose projection below the slab is at least one-fourth the slab thickness shall be not less than $L/40$ nor 4 in. in thickness.

Scanned with CamScanner

Slabs without drop panels as described above shall be not less than $L/36$ nor 5 in. in thickness.

5. For determining reinforcement, the thickness of the drop panel below the slab shall not be assumed to be more than one-fourth of the distance from the edge of the drop panel to the edge of the column capital.

(*d*) ***Arrangement of slab reinforcement***

1. The spacing of the bars at critical sections shall not exceed 2 times the slab thickness, except for those portions of the slab area which may be of cellular or ribbed construction. In the slab over the cellular spaces, reinforcement shall be provided as required by Art. 807.

2. In exterior panels, except for bottom bars adequately anchored in the drop panel, all positive reinforcement perpendicular to the discontinuous edge shall extend to the edge of the slab and have embedment, straight or hooked, of at least 6 in. in spandrel beams, walls, or columns where provided. All negative reinforcement perpendicular to the discontinuous edge shall be bent, hooked, or otherwise anchored in spandrel beams, walls, or columns.

3. The area of reinforcement shall be determined from the bending moments at the critical sections but shall be not less than required by Art. 807.

4. Required splices in bars may be made wherever convenient, but preferably away from points of maximum stress. The length of any such splice shall conform to Art. 805.

5. Bars shall be spaced approximately uniformly across each panel strip, except:

a. At least 25 per cent of required negative reinforcement in the column strip shall cross the periphery located at a distance of d from the column or column capital.

b. At least 50 per cent of the required negative reinforcement in the column strip shall cross the drop panel, if any.

c. The spacing for the remainder of the column strip may vary uniformly from that required for (*a*) or (*b*) to that required for the middle strip.

(*e*) ***Openings in flat slabs***

1. Openings of any size may be provided in flat slabs if provision is made for the total positive and negative moments and for shear without exceeding the allowable stresses except that when design is based on Art. 2104, the limitations given therein shall not be exceeded.

2. When openings are provided within the area common to two column strips, that part of the critical section shall be considered ineffective which either passes through an opening, or is covered by a radial projection of any opening to the centroid of the support.

(*f*) ***Design of columns***

All columns supporting flat slabs shall be designed as provided in Chap. 14 or 19 with the additional requirements of this chapter.

(*g*) ***Transfer of bending moment between column and slab*** When unbalanced gravity load, wind, or earthquake cause transfer of bending moment between column and slab, the stresses on the critical section shall be investigated by a rational analysis, and the section proportioned accordingly by the requirements of Part IV-A or IV-B. Concentration of reinforcement over the column

head by additional reinforcement or closer spacing may be used to resist the moment of the section. A slab width between lines that are $1.5t$ each side of the column may be considered effective.

2103 Design by Elastic Analysis

(*a*) ***Assumptions*** In design by elastic analysis the following assumptions may be used and all sections shall be proportioned for the moments and shears thus obtained.

1. The structure may be considered divided into a number of bents, each consisting of a row of columns or supports and strips of supported slabs, each strip bounded laterally by the center line of the panel on either side of the center line of columns or supports. The bents shall be taken longitudinally and transversely of the building.

2. Each such bent may be analyzed in its entirety or each floor thereof and the roof may be analyzed separately with its adjacent columns as they occur above and below, the columns being assumed fixed at their remote ends. Where slabs are thus analyzed separately, it may be assumed in determining the bending at a given support that the slab is fixed at any support two panels distant therefrom provided the slab continues beyond that point.

3. The joints between columns and slabs may be considered rigid, and this rigidity (infinite moment of inertia) may be assumed to extend in the slabs from the center of the column to the edge of the capital, and in the column from the top of slab to the bottom of the capital. The change in length of columns and slabs due to direct stress, and deflections due to shear, may be neglected.

4. Where metal column capitals are used, account may be taken of their contributions to stiffness and resistance to bending and shear.

5. The moment of inertia of the slab or column at any cross section may be assumed to be that of the cross section of the concrete. Variation in the moments of inertia of the slabs and columns along their axes shall be taken into account.

6. Where the load to be supported is definitely known, the structure shall be analyzed for that load. Where the live load is variable but does not exceed three-quarters of the dead load, or the nature of the live load is such that all panels will be loaded simultaneously, the maximum bending may be assumed to occur at all sections under full live load. For other conditions, maximum positive bending near midspan of a panel may be assumed to occur under three-quarters of the full live load in the panel and in alternate panels; and maximum negative bending in the slab at a support may be assumed to occur under three-quarters of the full live load in the adjacent panels only. In no case, shall the design moments be taken as less than those occurring with full live load on all panels.

(*b*) ***Critical sections*** The critical section for negative bending, in both the column strip and middle strip, may be assumed as not more than the distance A from the center of the column or support and the critical negative moment shall be considered as extending over this distance.

(*c*) ***Distribution of panel moments*** Bending at critical sections across the slabs of each bent may be apportioned between the column strip and middle strip, as given in Table 2103(*c*). For design purposes, any of these percentages

Scanned with CamScanner

Table 2103(*c*) **Distribution between column strips and middle strips in per cent of total moments at critical sections of a panel**

Strip		Moment section			
		Negative moment at interior support	Positive moment	Negative moment at exterior support	
				Slab supported on columns and on beams of total depth equal to the slab thickness*	Slab supported on reinforced-concrete bearing wall or columns with beams of total depth equal or greater than 3 times the slab thickness*
Column strip		76	60	80	60
Middle strip		24	40	20	40
Half column strip adjacent and parallel to marginal beam or wall	Total depth of beam equal to slabt hickness*	38	30	40	30
	Total depth of beam or wall equal or greater than 3 times slab thickness*	19	15	20	15

*Interpolate for intermediate ratios of beam depth to slab thickness.

Note: The total dead and live reaction of a panel adjacent to a marginal beam or wall may be divided between the beam or wall and the parallel half column strip in proportion to their stiffness, but the moment provided in the slab shall not be less than that given in Table 2103(*c*).

may be varied by not more than 10 per cent of its value, but their sum for the full panel width shall not be reduced.

2104 Empirical Method

(*a*) ***General limitations*** Flat slab construction may be designed by the empirical provisions of this section when they conform to all of the limitations on continuity and dimensions given herein.

1. The construction shall consist of at least three continuous panels in each direction.

2. The ratio of length to width of panels shall not exceed 1.33.

3. The grid pattern shall consist of approximately rectangular panels. The successive span lengths in each direction shall differ by not more than 20 per cent of the longer span. Within these limitations, columns may be offset a maximum of 10 per cent of the span, in direction of the offset, from either axis between center lines of successive columns.

4. The calculated lateral force moments from wind or earthquake may be combined with the critical moments as determined by the empirical method, and the lateral force moments shall be distributed between the column and middle strips in the same proportions as specified for the negative moments in the strips for structures not exceeding 125 ft high with maximum story height not exceeding 12 ft 6 in.

(*b*) ***Columns***

1. The minimum dimension of any column shall be as determined by (*a*) and (*b*) below, but in no case less than 10 in.

a. For columns or other supports of a flat slab, the required minimum average moment of inertia, I_c, of the gross concrete section of the columns above and below the slab shall be determined from Eq. (21-1) and shall be not less than 1000 in.[4] If there is no column above the slab, the I_c of the column below shall be $(2 - 2.3h/H)$ times that given by the formula with a minimum of 1000 in.[4]

$$I_c = \frac{t^3 H}{0.5 + W_D/W_L} \tag{21-1}$$

where t need not be taken greater than t_1 or t_2 as determined in (*d*), H is the average story height of the columns above and below the slab, and W_L is the greater value of any two adjacent spans under consideration.

b. Columns smaller than required by Eq. (21-1) may be used provided the bending moment coefficients given in Table 2104(*f*) are increased in the following ratios:

For negative moments

$$R_n = 1 + \frac{(1 - K)^2}{2.2(1 + 1.4W_D/W_L)} \tag{21-2}$$

For positive moments

$$R_p = 1 + \frac{(1 - K)^2}{1.2(1 + 0.10W_D/W_L)} \tag{21-3}$$

The required slab thickness shall be modified by multiplying w' by R_n in Eq. (21-4) and (21-5).

2. Columns supporting flat slabs designed by the empirical method shall be proportioned for the bending moments developed by unequally loaded panels, or uneven spacing of columns. Such bending moment shall be the maximum value derived from

$$\frac{WL_1 - W_D L_2}{f}$$

Scanned with CamScanner

***Table* 2104(*f*) Moments in flat slab panels in percentages of M_0**

Strip	Column head	Side support type	End support type	Exterior panel: Exterior negative moment	Exterior panel: Positive moment	Exterior panel: Interior negative moment	Interior panel: Positive moment	Interior panel: Negative moment
Column strip	With drop		*A*	44	24	56	20	50
			B	36				
			C	6	36	72		
	Without drop		*A*	40	28	50	22	46
			B	32				
			C	6	40	66		
Middle strip	With drop		*A*	10	20	17*	15	15*
			B	20				
			C	6	26	22*		
	Without drop		*A*	10	20	18*	16	16*
			B	20				
			C	6	28	24*		
Half-column strip adjacent to marginal beam or wall	With drop	1	*A*	22	12	28	10	25
			B	18				
			C	3	18	36		
		2	*A*	17	9	21	8	19
			B	14				
			C	3	14	27		
		3	*A*	11	6	14	5	13
			B	9				
			C	3	9	18		
	Without drop	1	*A*	20	14	25	11	23
			B	16				
			C	3	20	33		
		2	*A*	15	11	19	9	18
			B	12				
			C	3	15	25		
		3	*A*	10	7	13	6	12
			B	8				
			C	3	10	17		

***Table* 2104(*f*) (*Continued*)**

Percentage of panel load to be carried by marginal beam or wall in addition to loads directly superimposed thereon	Type of support listed in Table 2104(*f*): Side support parallel to strip	Side or end edge condition of slabs of depth *t*	End support at right angles to strip
0	1	Columns with no beams	
20	2	Columns with beams of total depth $1\frac{1}{4}t$	*A*
40	3	Columns with beams of total depth $3t$ or more	*B*
		Reinforced concrete bearing walls integral with slab	
		Masonry or other walls providing negligible restraint	*C*

* Increase negative moments 30 per cent of tabulated values when middle strip is continuous across support of type *B* or *C*. No other values need be increased.

Note: For intermediate proportions of total beam depth to slab thicknesses, values for loads and moments may be obtained by interpolation. See also Fig. 2104(*f*)*a* and 2104(*f*)*b*.

L_1 and L_2 being lengths of the adjacent spans ($L_2 = 0$ when considering an exterior column) and f is 30 for exterior and 40 for interior columns.

This moment shall be divided between the columns immediately above and below the floor or roof line under consideration in direct proportion to their stiffness and shall be applied without further reduction to the critical sections of the columns.

(*c*) ***Determination of "c" (effective support size)***

1. Where column capitals are used, the value of c shall be taken as the diameter of the cone described in Art. 2101(*b*) measured at the bottom of the slab or drop panel.

2. Where a column is without a concrete capital, the dimension c shall be taken as that of the column in the direction considered.

3. Brackets capable of transmitting the negative bending and the shear in the column strips to the columns without excessive unit stress may be substituted for column capitals at exterior columns. The value of c for the span where a bracket is used shall be taken as twice the distance from the center of the column to a point where the bracket is $1\frac{1}{2}$ in. thick, but not more than the thickness of the column plus twice the depth of the bracket.

4. Where a reinforced concrete beam frames into a column without capital c

Scanned with CamScanner

bracket on the same side with the beam, for computing bending for strips parallel to the beam, the value of c for the span considered may be taken as the width of the column plus twice the projection of the beam above or below the slab or drop panel.

5. The average of the values of c at the two supports at the ends of a column strip shall be used to evaluate the slab thickness t_1 or t_2 as prescribed in (*d*).

(*d*) *Slab thickness*

1. The slab thickness, span L being the longest side of the panel, shall be at least:

$L/36$ for slab without drop panels conforming with (*e*), or where a drop panel is omitted at any corner of the panel, but not less than 5 in. nor t_1 as given in Eq. (21-4)

$L/40$ for slabs with drop panels conforming to (*e*) at all supports, but not less than 4 in. nor t_2 as given in Eq. (21-5)

2. The total thickness, t_1, in inches, of slabs without drop panels, or through the drop panel if any, shall be at least

$$t_1 = 0.028L\left(1 - \frac{2c}{3L}\right)\sqrt{\frac{w'}{f'_c/2000}} + 1\tfrac{1}{2} \qquad (21\text{-}4)^*$$

3. The total thickness t_2, in inches, of slabs with drop panels, at points beyond the drop panel shall be at least

$$t_2 = 0.024L\left(1 - \frac{2c}{3L}\right)\sqrt{\frac{w'}{f'_c/2000}} + 1 \qquad (21\text{-}5)^*$$

4. Where the exterior supports provide only negligible restraint to the slab, the values of t_1 and t_2 for the exterior panel shall be increased by at least 15 per cent.

(*e*) *Drop panels*

1. The maximum total thickness at the drop panel used in computing the negative steel area for the column strip shall be $1.5t_2$.

2. The side or diameter of the drop panel shall be at least 0.33 times the span in the parallel direction.

3. The minimum thickness of slabs where drop panels at wall columns are omitted shall equal $(t_1 + t_2)/2$ provided the value of c used in the computations complies with (*c*).

(*f*) *Bending moment coefficients*

1. The numerical sum of the positive and negative bending moments in the direction of either side of a rectangular panel shall be assumed as not less than

$$M_0 = 0.09WLF\left(1 - \frac{2c}{3L}\right)^2 \qquad (21\text{-}6)$$

in which $F = 1.15 - c/L$ but not less than 1.

* In these formulas, t_1 and t_2 are in inches and L and c are in feet, and w' is in lb. per ft².

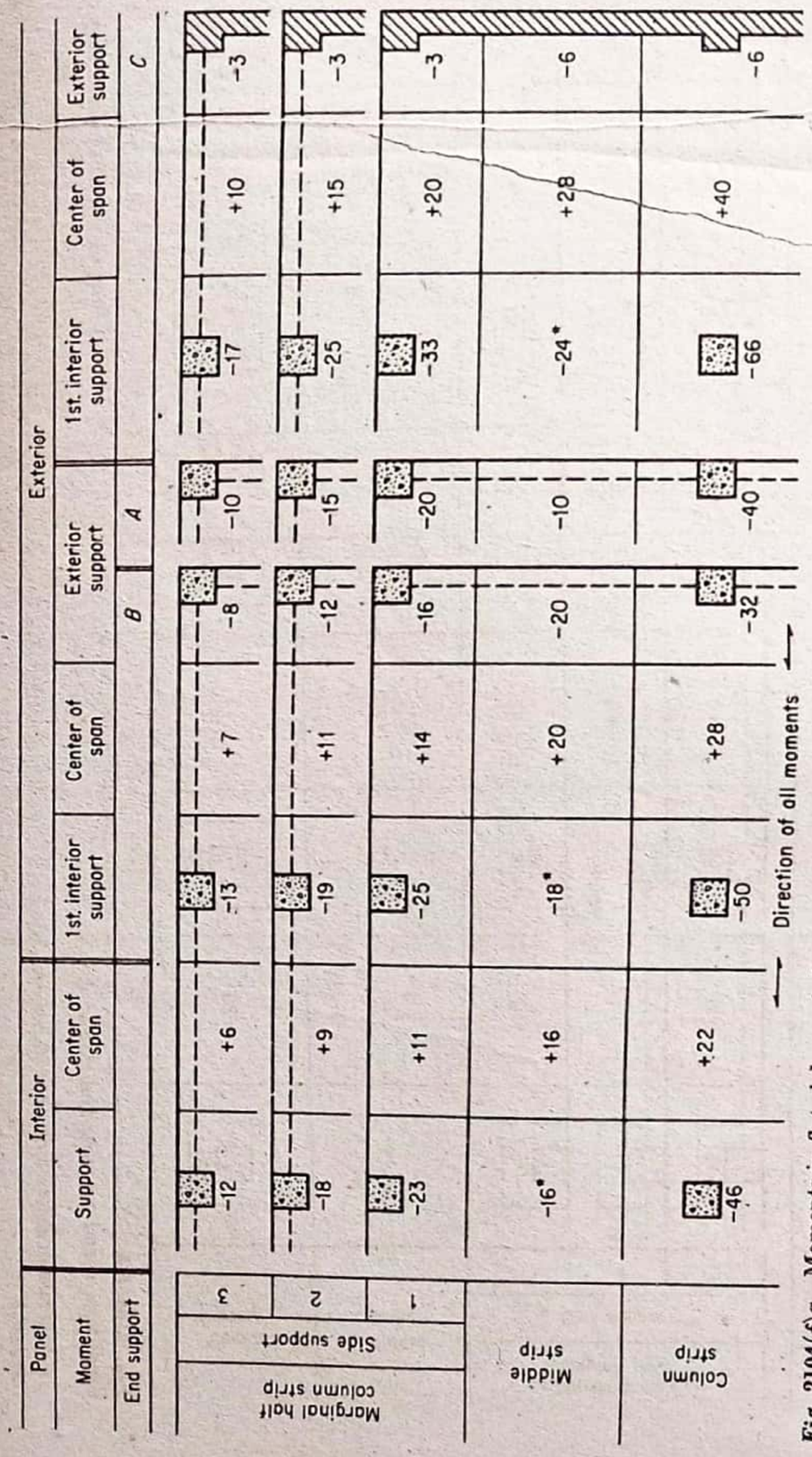


Fig. **2104(*f*)*a*** Moments in flat-slab panels in percentages of M_0, with drops. [See Table 2104(*f*) for notes and classification of conditions of end supports and side supports.]

* Increase negative moments 30 per cent when middle strip is continuous across a support of type B or C; no other values need be increased.

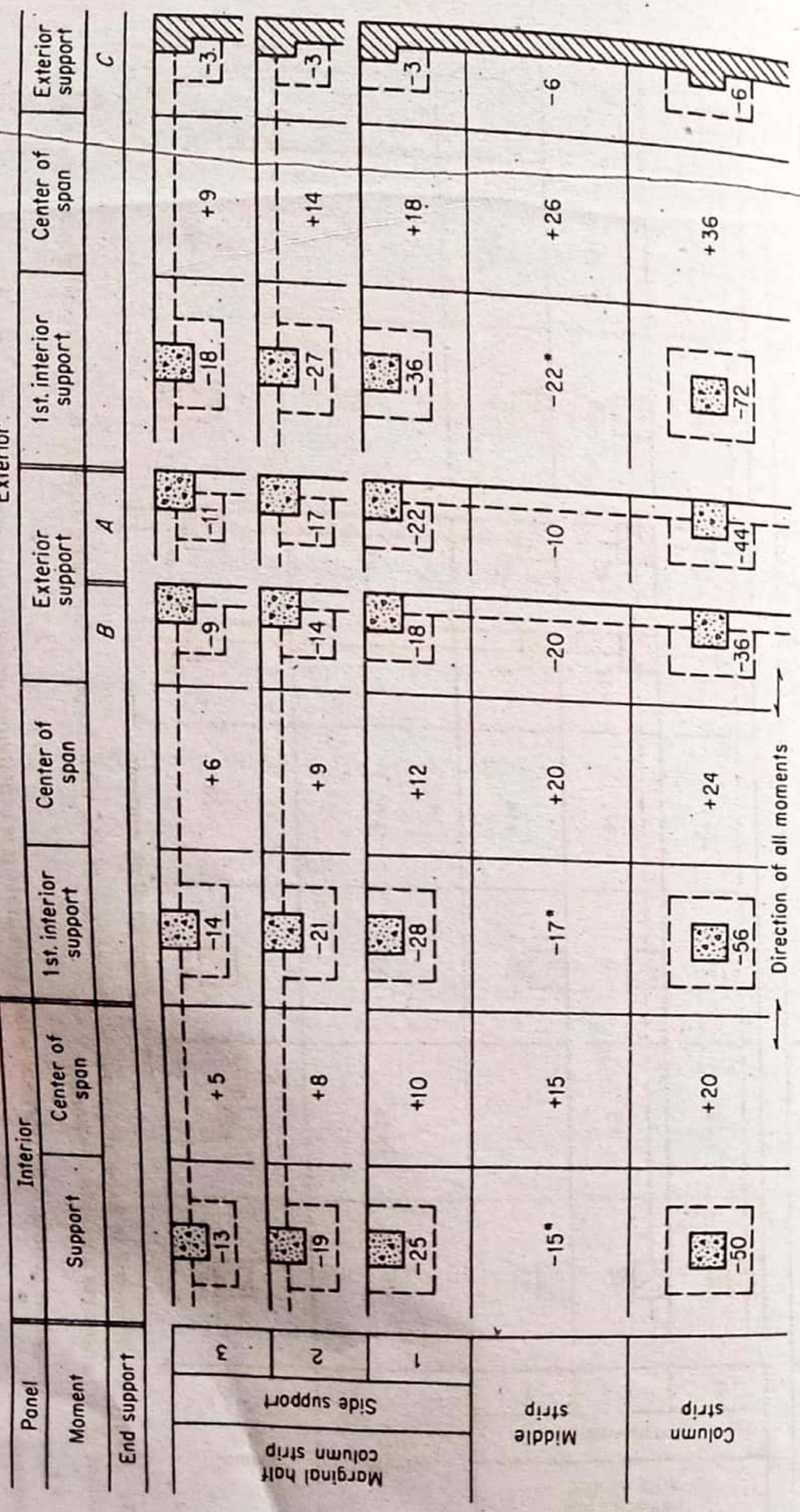


Fig. 2104(*f*)b Moments in flat-slab panels in percentages of M_0, with drops. [See Table 2104(*f*) for notes and classification of conditions of end supports and side supports.]

* Increase negative moments 30 per cent when middle strip is continuous across a support of type B or C; no other values need be increased.

2. Unless otherwise provided, the bending moments at the critical sections of the column and middle strips shall be at least those given in Table 2104(*f*).

3. The average of the values of c at the two supports at the ends of a column strip shall be used to evaluate M_0 in determining bending in the strip. The average of the values of M_0, as determined for the two parallel half column strips in a panel, shall be used in determining bending in the middle strip.

4. Bending in the middle strips parallel to a discontinuous edge shall be assumed the same as in an interior panel.

5. For design purposes, any of the moments determined from Table 2104(*f*) may be varied by not more than 10 per cent, but the numerical sum of the positive and negative moments in a panel shall be not less than the amount specified.

(*g*) ***Length of reinforcement*** In addition to the requirements of Art. 2102(*d*), reinforcement shall have the minimum lengths given in Tables 2104(*g*)1 and 2104(*g*)2. Where adjacent spans are unequal, the extension of negative reinforcement on each side of the column center line as prescribed in Table 2104(*g*)1 shall be based on the requirements of the longer span.

(*h*) ***Openings in flat slabs***

1. Openings of any size may be provided in a flat slab in the area common to two intersecting middle strips provided the total positive and negative steel areas required in (*f*) are maintained.

2. In the area common to two column strips, not more than one-eighth of the width of strip in any span shall be interrupted by openings. The equivalent of all bars interrupted shall be provided by extra steel on all sides of the openings. The shear stresses given in Art. 2102(*c*)2 shall not be exceeded following the procedure of Art. 920(*b*).

3. In any area common to one column strip and one middle strip, openings may interrupt one-quarter of the bars in either strip. The equivalent of the bars so interrupted shall be provided by extra steel on all sides of the opening.

4. Any opening larger than described above shall be analyzed by accepted engineering principles and shall be completely framed as required to carry the loads to the columns.

Scanned with CamScanner

Table 2104(g)1 Minimum length of negative reinforcement

Strip	Percentage of required reinforcing steel area to be extended at least as indicated	Minimum distance beyond center line of support to end of straight bar or to bend point of bent bar*			
		Flat slabs without drop panels		Flat slabs with drop panels	
		Straight	Bend point where bars bend down and continue as positive reinforcement	Straight	Bend point where bars bend down and continue as positive reinforcement
Column strip reinforcement	Not less than 33 per cent	0.30L†		0.33L‡	
	Not less than an additional 34 per cent	0.27L†		0.30L‡	
	Remainder†	0.25L	or 0.20L	0.25L	or To edge of drop but at least 0.20L
Middle strip reinforcement	Not less than 50 per cent	0.25L		0.25L	
	Remainder§	0.25L	or 0.15L	0.25L	or 0.15L

* At exterior supports where masonry walls or other construction provide only negligible restraint to the slab, the negative reinforcement need not be carried further than 0.20L beyond the center line of such support.

† Where no bent bars are used, the 0.27L bars may be omitted, provided the 0.30L bars are at least 50 per cent of total required.

‡ Where no bent bars are used, the 0.30L bars may be omitted provided the 0.33L bars provide at least 50 per cent of the total required.

§ Bars may be straight, bent, or any combination of straight and bent bars. All bars are to be considered straight bars for the end under consideration unless bent at that end and continued as positive reinforcement.

Note: See also Fig. 2104(*g*)a.

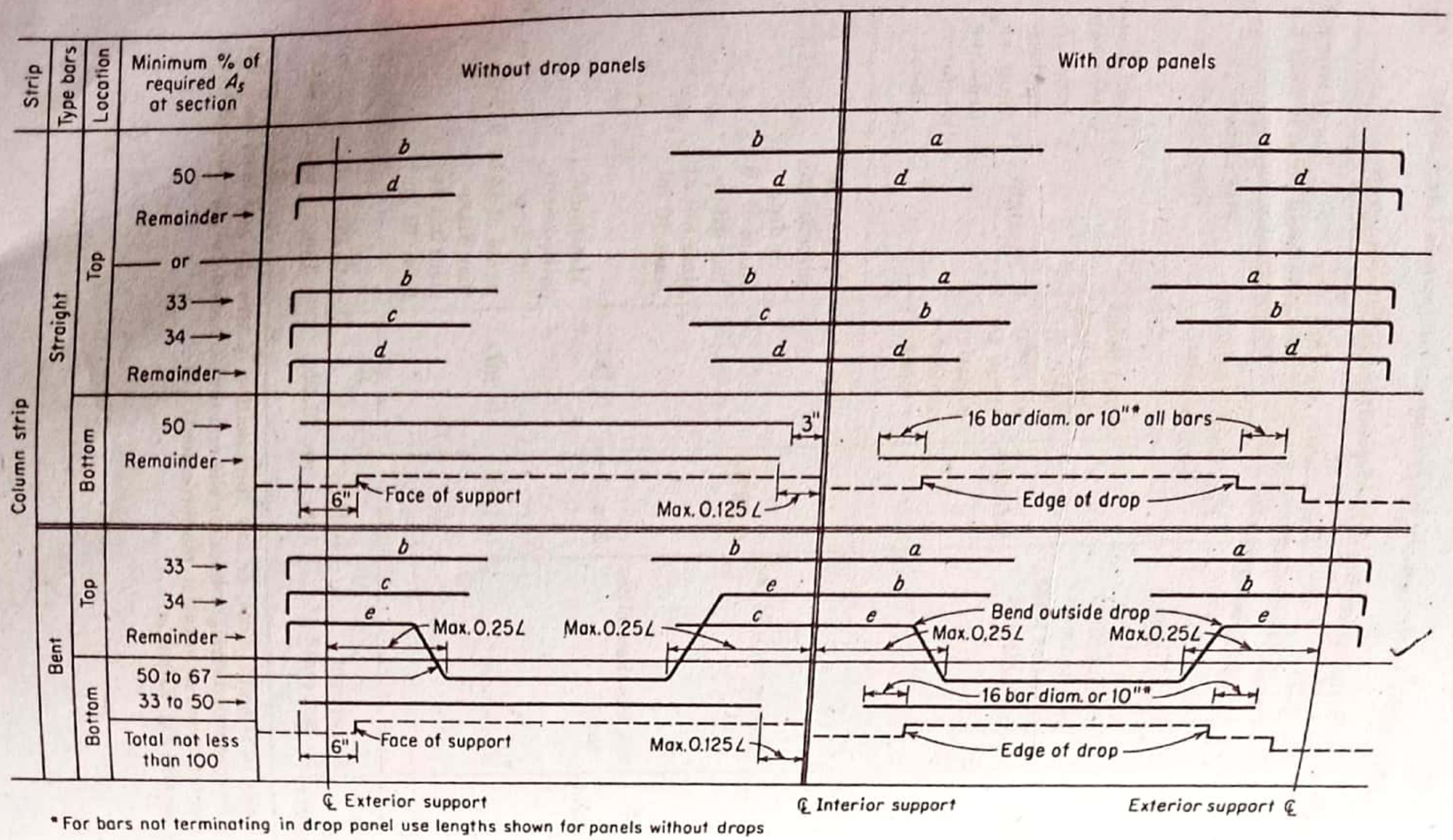
Table 2104(g)2 Minimum length of positive reinforcement

Strip	Percentage of required reinforcing steel area to be extended at least as indicated	Maximum distance from center line of support to end of straight bar or bend point of bent bar			
		Flat slabs without drop panels		Flat slabs with drop panels	
		Straight	Bend point where bars bend up and continue as negative reinforcement	Straight	Bend point where bars bend up and continue as negative reinforcement
Column strip reinforcement	Not less than 33 per cent	0.125L		Minimum embedment in drop panel of 16 bar diameters but at least 10 in.	
	Not less than 50 per cent*	3 in.	or 0.25L		
	Remainder*	0.125L	or 0.25L	Minimum embedment in drop panel of 16 bar diameters but at least 10 in.	or 0.25L
Middle strip reinforcement	50 per cent	0.15L		0.15L	
	50 per cent*	3 in.	or 0.25L	3 in.	or 0.25L

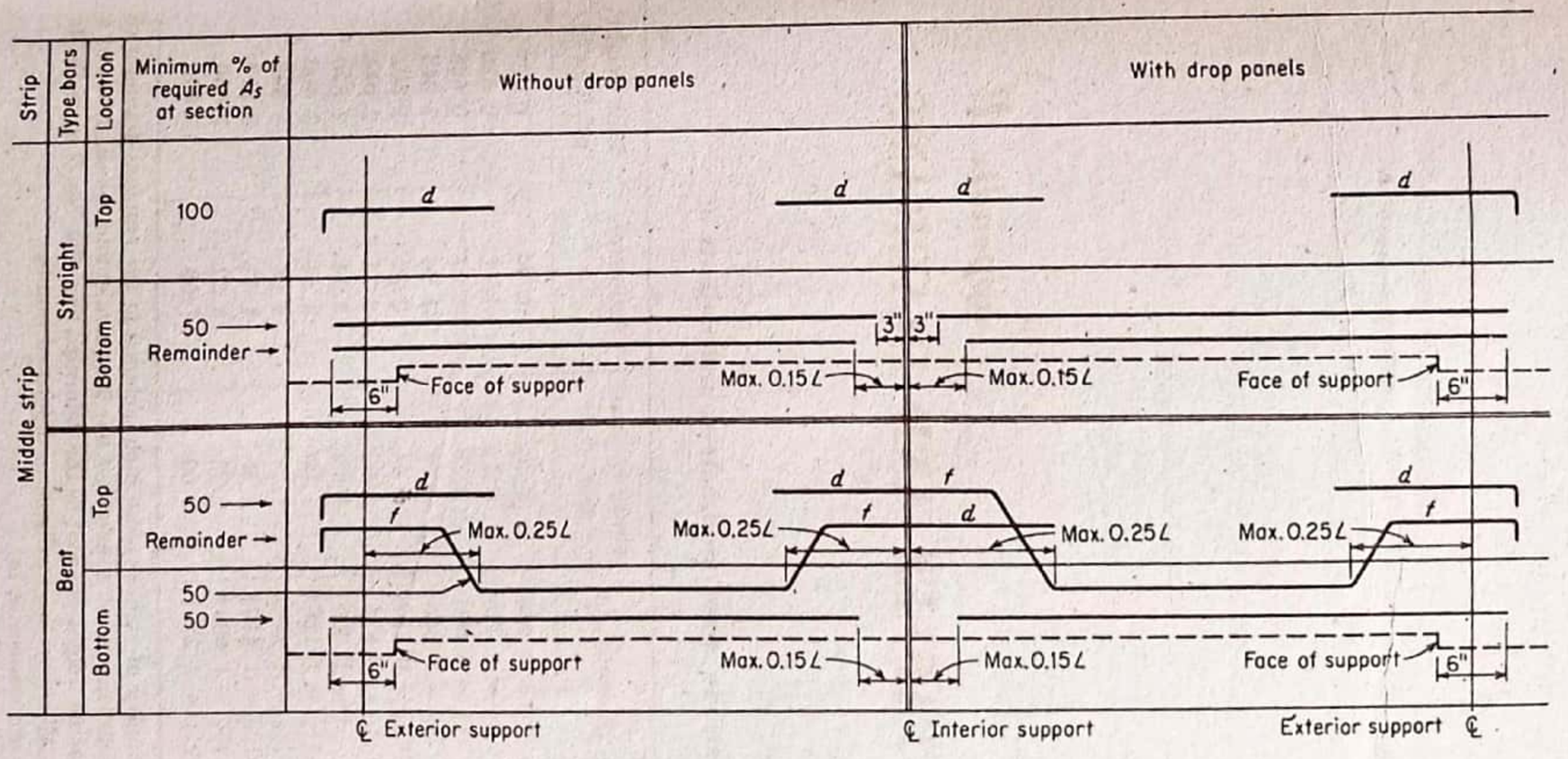
* Bars may be straight, bent, or any combination of straight and bent bars. All bars are to be considered straight bars for the end under consideration unless bent at that end and continued as negative reinforcement.

Note: See also Fig. 2104(*g*)a.

Scanned with CamScanner



*For bars not terminating in drop panel use lengths shown for panels without drops



Minimum length of bar from ℄ support

Mark	a	b	c	d	e	f
Length	0.33L	0.30L	0.27L	0.25L	0.20L	0.15L

At interior supports, L is longer of adjacent spans

Fig.* 2104(*g*)*a Minimum length of flat-slab reinforcement. (At exterior supports, where masonry walls or other construction provides only negligible restraint to the slab; the negative reinforcement need not be carried further than 0.20*L* beyond the center line of such support; any combination of straight and bent bars may be used provided minimum requirements are met.)

Scanned with CamScanner

appendix B

TABLES AND DIAGRAMS

Table 1 **Designations, areas, perimeters, and weights of standard bars**

Bar No.*	Diameter, in.	Cross-sectional area, in.²	Perimeter, in.	Unit weight per foot, lb
2	¼ = 0.250	0.05	0.79	0.167
3	⅜ = 0.375	0.11	1.18	0.376
4	½ = 0.500	0.20	1.57	0.668
5	⅝ = 0.625	0.31	1.96	1.043
6	¾ = 0.750	0.44	2.36	1.502
7	⅞ = 0.875	0.60	2.75	2.044
8	1 = 1.000	0.79	3.14	2.670
9	1⅛ = 1.128†	1.00	3.54	3.400
10	1¼ = 1.270†	1.27	3.99	4.303
11	1⅜ = 1.410†	1.56	4.43	5.313
14*S*	1¾ = 1.693†	2.25	5.32	7.650
18*S*	2¼ = 2.257†	4.00	7.09	13.600

* Based on the number of eighths of an inch included in the nominal diameter of the bars. The nominal diameter of a deformed bar is equivalent to the diameter of a plain bar having the same weight per foot as the deformed bar. Bar No. 2 is available in plain rounds only. All others are available in deformed rounds.

† Approximate to the nearest ⅛ in.

Table 2 **Areas of groups of standard bars in square inches**

Bar No.	Number of bars												
	2	3	4	5	6	7	8	9	10	11	12	13	14
4	0.39	0.58	0.78	0.98	1.18	1.37	1.57	1.77	1.96	2.16	2.36	2.55	2.75
5	0.61	0.91	1.23	1.53	1.84	2.15	2.45	2.76	3.07	3.37	3.68	3.99	4.30
6	0.88	1.32	1.77	2.21	2.65	3.09	3.53	3.98	4.42	4.86	5.30	5.74	6.19
7	1.20	1.80	2.41	3.01	3.61	4.21	4.81	5.41	6.01	6.61	7.22	7.82	8.42
8	1.57	2.35	3.14	3.93	4.71	5.50	6.28	7.07	7.85	8.64	9.43	10.21	11.00
9	2.00	3.00	4.00	5.00	6.00	7.00	8.00	9.00	10.00	11.00	12.00	13.00	14.00
10	2.53	3.79	5.06	6.33	7.59	8.86	10.12	11.39	12.66	13.92	15.19	16.45	17.72
11	3.12	4.68	6.25	7.81	9.37	10.94	12.50	14.06	15.62	17.19	18.75	20.31	21.87
14*S*	4.50	6.75	9.00	11.25	13.50	15.75	18.00	20.25	22.50	24.75	27.00	29.25	31.50
18*S*	8.00	12.00	16.00	20.00	24.00	28.00	32.00	36.00	40.00	44.00	48.00	52.00	56.00

Table 3 **Perimeters of groups of standard bars in inches**

Bar No.	Number of bars												
	2	3	4	5	6	7	8	9	10	11	12	13	14
4	3.1	4.7	6.2	7.8	9.4	11.0	12.6	14.1	15.7	17.3	18.8	20.4	22.0
5	3.9	5.9	7.8	9.8	11.8	13.7	15.7	17.7	19.5	21.6	23.6	25.5	27.5
6	4.7	7.1	9.4	11.8	14.1	16.5	18.8	21.2	23.6	25.9	28.3	30.6	33.0
7	5.5	8.2	11.0	12.7	16.5	19.2	22.0	24.7	27.5	30.2	33.0	35.7	38.5
8	6.3	9.4	12.6	15.7	18.9	22.0	25.1	28.3	31.4	34.6	37.7	40.9	44.0
9	7.1	10.6	14.2	17.7	21.3	24.8	28.4	31.9	35.4	39.0	42.5	46.0	49.6
10	8.0	12.0	16.0	20.0	23.9	27.9	31.9	35.9	39.9	43.9	47.9	51.9	55.9
11	8.9	13.3	17.7	22.2	26.6	31.0	35.4	39.9	44.3	48.7	53.2	57.6	62.0
14*S*	10.6	16.0	21.3	26.6	31.9	37.2	42.6	47.9	53.2	58.5	63.8	69.2	74.5
18*S*	14.2	21.3	28.4	35.5	42.5	49.6	56.7	63.8	70.9	78.0	85.1	93.2	100.3

Table 4 **Areas of bars in slabs in square inches per foot**

Spacing, in.	Bar No.								
	3	4	5	6	7	8	9	10	11
3	0.44	0.78	1.23	1.77	2.40	3.14	4.00	5.06	6.25
3½	0.38	0.67	1.05	1.51	2.06	2.69	3.43	4.34	5.36
4	0.33	0.59	0.92	1.32	1.80	2.36	3.00	3.80	4.68
4½	0.29	0.52	0.82	1.18	1.60	2.09	2.67	3.37	4.17
5	0.26	0.47	0.74	1.06	1.44	1.88	2.40	3.04	3.75
5½	0.24	0.43	0.67	0.96	1.31	1.71	2.18	2.76	3.41
6	0.22	0.39	0.61	0.88	1.20	1.57	2.00	2.53	3.12
6½	0.20	0.36	0.57	0.82	1.11	1.45	1.85	2.34	2.89
7	0.19	0.34	0.53	0.76	1.03	1.35	1.71	2.17	2.68
7½	0.18	0.31	0.49	0.71	0.96	1.26	1.60	2.02	2.50
8	0.17	0.29	0.46	0.66	0.90	1.18	1.50	1.89	2.34
9	0.15	0.26	0.41	0.59	0.80	1.05	1.33	1.69	2.08
10	0.13	0.24	0.37	0.53	0.72	0.94	1.20	1.52	1.87
12	0.11	0.20	0.31	0.44	0.60	0.78	1.00	1.27	1.56

Scanned with CamScanner

Table 5 **Design of rectangular beams and slabs**
$k = n/(n + r)$; $j = 1 - k/3$; $p_c = n/2r(n + r)$; $K = \frac{1}{2}f_c kj$ or $pf_s j$

n and f'_c	f_s	f_c	k	j	p_c	K
	18,000	1000	0.357	0.881	0.0099	157
		1125	0.385	0.872	0.0120	189
10	20,000	1000	0.333	0.889	0.0083	148
(2500)		1125	0.360	0.880	0.0101	178
	24,000	1000	0.294	0.902	0.0061	133
		1125	0.319	0.894	0.0075	160
	18,000	1200	0.375	0.875	0.0125	197
		1350	0.403	0.866	0.0151	235
9	20,000	1200	0.351	0.883	0.0105	186
(3000)		1350	0.377	0.874	0.0128	223
	24,000	1200	0.310	0.897	0.0078	167
		1350	0.336	0.888	0.0095	201
	18,000	1600	0.416	0.861	0.0185	286
		1800	0.444	0.852	0.0222	341
8	20,000	1600	0.390	0.870	0.0156	272
(4000)		1800	0.419	0.860	0.0188	324
	24,000	1600	0.345	0.884	0.0116	246
		1800	0.375	0.875	0.0141	295
	18,000	2000	0.438	0.854	0.0243	374
		2250	0.467	0.844	0.0292	443
7	20,000	2000	0.412	0.863	0.0206	355
(5000)		2250	0.441	0.853	0.0248	423
	24,000	2000	0.368	0.877	0.0154	323
		2250	0.396	0.868	0.0186	387

Table 6 **Review of rectangular beams and slabs**
$k = \sqrt{2pn + (pn)^2} - pn$; $j = 1 - \frac{1}{3}k$

p	$n = 7$		$n = 8$		$n = 9$		$n = 10$	
	k	j	k	j	k	j	k	j
0.0010	0.112	0.963	0.119	0.960	0.125	0.958	0.132	0.956
0.0020	0.154	0.949	0.164	0.945	0.173	0.942	0.180	0.940
0.0030	0.185	0.938	0.196	0.935	0.207	0.931	0.217	0.928
0.0040	0.210	0.930	0.223	0.926	0.235	0.922	0.246	0.918
0.0050	0.232	0.923	0.246	0.918	0.258	0.914	0.270	0.910
0.0054	0.240	0.920	0.254	0.915	0.267	0.911	0.279	0.907
0.0058	0.247	0.918	0.262	0.913	0.275	0.908	0.287	0.904
0.0062	0.254	0.915	0.269	0.910	0.283	0.906	0.296	0.901
0.0066	0.261	0.913	0.276	0.908	0.290	0.903	0.303	0.899
0.0070	0.268	0.911	0.283	0.906	0.298	0.901	0.311	0.896
0.0072	0.271	0.910	0.287	0.904	0.301	0.900	0.314	0.895
0.0074	0.274	0.909	0.290	0.903	0.304	0.899	0.318	0.894
0.0076	0.277	0.908	0.293	0.902	0.308	0.897	0.321	0.893
0.0078	0.280	0.907	0.296	0.901	0.311	0.896	0.325	0.892
0.0080	0.283	0.906	0.299	0.900	0.314	0.895	0.328	0.891
0.0082	0.286	0.905	0.303	0.899	0.317	0.894	0.331	0.890
0.0084	0.289	0.904	0.306	0.898	0.321	0.893	0.334	0.889
0.0086	0.292	0.903	0.308	0.897	0.324	0.892	0.338	0.887
0.0088	0.295	0.902	0.311	0.896	0.327	0.891	0.341	0.886
0.0090	0.298	0.901	0.314	0.895	0.330	0.890	0.344	0.885
0.0092	0.300	0.900	0.317	0.894	0.332	0.889	0.347	0.884
0.0094	0.303	0.899	0.320	0.893	0.335	0.888	0.350	0.883
0.0096	0.306	0.898	0.323	0.892	0.338	0.887	0.353	0.882
0.0098	0.308	0.897	0.325	0.892	0.341	0.886	0.355	0.882
0.0100	0.311	0.896	0.328	0.891	0.344	0.885	0.358	0.881
0.0104	0.316	0.895	0.333	0.889	0.349	0.884	0.364	0.879
0.0108	0.321	0.893	0.338	0.887	0.354	0.882	0.369	0.877
0.0112	0.325	0.892	0.343	0.886	0.359	0.880	0.374	0.875
0.0116	0.330	0.890	0.348	0.884	0.364	0.879	0.379	0.8
0.0120	0.334	0.889	0.353	0.882	0.369	0.877	0.384	0.87
0.0124	0.339	0.887	0.357	0.881	0.374	0.875	0.389	0.870
0.0128	0.343	0.886	0.362	0.879	0.378	0.874	0.394	0.867
0.0132	0.347	0.884	0.366	0.878	0.383	0.872	0.398	0.867
0.0136	0.351	0.883	0.370	0.877	0.387	0.871	0.403	0.866
0.0140	0.355	0.882	0.374	0.875	0.392	0.869	0.407	0.864
0.0144	0.359	0.880	0.378	0.874	0.396	0.868	0.412	0.863
0.0148	0.363	0.879	0.382	0.873	0.400	0.867	0.416	0.861
0.0152	0.367	0.878	0.386	0.871	0.404	0.865	0.420	0.860
0.0156	0.371	0.876	0.390	0.870	0.408	0.864	0.424	0.859
0.0160	0.374	0.875	0.394	0.869	0.412	0.863	0.428	0.857
0.0170	0.383	0.872	0.403	0.867	0.421	0.860	0.437	0.854
0.0180	0.392	0.869	0.412	0.863	0.430	0.857	0.446	0.851
0.0190	0.400	0.867	0.420	0.860	0.438	0.854	0.455	0.848
0.0200	0.407	0.864	0.428	0.857	0.446	0.851	0.463	0.846

Scanned with CamScanner

Table 7 **Permissible bond-stress values** (Top value of each pair is for top bars, bottom for other bars.)

Bar No.	f'_c W.S.D. 2500	3000	4000	5000	6000	U.S.D. 2500	3000	4000	5000	6000
2	160 160	160 160	160 160	160 160	160 160	250 250	250 250	250 250	250 250	250 250
3	350 500	350 500	350 500	350 500	350 500	560 800	560 800	560 800	560 800	560 800
4	340 480	350 500	350 500	350 500	350 500	560 800	560 800	560 800	560 800	560 800
5	272 384	298 421	344 486	350 500	350 500	536 760	560 800	560 800	560 800	560 800
6	227 320	248 351	287 405	321 453	350 496	447 633	489 694	560 800	560 800	560 800
7	194 274	213 300	246 347	275 388	301 425	383 543	419 595	484 687	541 768	560 800
8	170 240	186 263	215 304	240 339	263 372	335 475	367 520	424 601	474 672	519 736
9	151 213	165 233	191 269	213 301	233 330	297 421	325 461	376 533	420 596	460 652
10	134 189	147 207	169 239	189 267	207 293	264 374	289 410	334 473	373 529	409 579
11	121 170	132 186	153 215	171 241	187 264	238 337	260 369	301 426	336 476	368 522
14*S*	105 150	115 164	133 190	148 212	163 232	210 300	230 329	266 379	297 424	325 465
18*S*	105 150	115 164	133 190	148 212	163 232	210 300	230 329	266 379	297 424	325 465
All deformed compression bars	325	356	400	400	400	650	712	800	800	800

Table 8 **Development lengths* in inches**
$L = A_s f_s / \Sigma_0 \times 0.8 \times u_{all}$ (Top value is for top bars, bottom for other bars.)

Bar No.	W.S.D. f_s 20,000	24,000	U.S.D. $f_s = f_y$ 40,000	50,000	60,000
f'_c = 3000:					
2	9.75 9.76	11.7 11.7	13.2 12.5	15.7 15.6	18.8 18.8
3	6.70 4.69	8.04 5.63	8.37 5.86	10.5 7.32	12.6 8.79
4	8.93 6.25	10.7 7.50	11.2 7.81	14.0 9.77	16.7 11.7
5	13.1 9.29	15.7 11.1	14.0 9.77	17.4 12.2	20.9 14.6
6	18.9 13.4	22.7 16.0	19.2 13.5	24.0 16.9	28.7 20.3
7	25.7 18.2	30.8 21.8	26.1 18.4	32.6 23.0	39.1 27.6
8	33.6 23.8	40.3 28.5	34.1 24.0	42.6 30.0	51.1 36.0
9	42.7 30.2	51.2 36.3	43.3 30.6	54.2 38.2	65.0 45.8
10	54.1 38.3	65.0 46.0	54.9 38.7	68.7 48.4	82.4 58.1
11	66.7 47.3	80.1 56.7	67.7 47.8	84.6 59.7	71.6 101.6
14*S*	92.0 64.4	110.4 77.3	92.0 64.4	115.0 80.5	138.0 96.6
18*S*	122.6 85.8	147.2 103.0	122.6 85.8	153.3 107.3	184.0 128.8

* When the bar stress calculated from the bending moment is smaller than the respective maximum values shown in the table, the necessary development length is obtained by reducing the tabulated length in the ratio of calculated steel stress to tabulated steel stress.

Scanned with CamScanner

Table 8 **Development lengths* in inches** (***continued***)
$L = A_s f_s / \Sigma_0 \times 0.8 \times u_{all}$ (Top value is for top bars, bottom for other bars.)

Bar No.	W.S.D. f_s		U.S.D. $f_s = f_y$		
	20,000	24,000	40,000	50,000	60,000
f'_c = 4000:					
2	9.75 9.76	11.7 11.7	13.2 12.5	15.7 15.6	18.8 18.8
3	6.70 4.69	8.04 5.63	8.37 5.86	10.5 7.32	12.6 8.79
4	8.93 6.25	10.7 7.50	11.2 7.81	14.0 9.77	16.7 11.7
5	11.4 8.04	13.6 9.65	14.0 9.77	17.4 12.2	20.9 14.6
6	16.3 11.6	19.6 13.9	16.7 11.7	20.9 14.6	25.1 17.6
7	22.3 15.8	26.7 18.9	22.6 15.9	28.2 19.9	33.9 23.9
8	29.1 20.6	34.9 24.7	29.5 20.8	36.9 26.0	44.2 31.2
9	37.0 26.2	44.4 31.4	37.5 26.5	46.9 33.1	56.3 39.7
10	46.9 33.2	56.3 39.8	47.6 33.6	59.5 41.9	71.4 50.3
11	57.8 40.9	69.3 49.1	58.6 41.4	73.3 51.7	88.0 62.0
14*S*	79.7 55.7	95.6 66.9	79.7 55.8	99.6 69.7	119.5 83.7
18*S*	106.2 74.3	127.5 89.2	106.2 74.3	132.8 92.9	159.3 111.5

* When the bar stress calculated from the bending moment is smaller than the respective maximum values shown in the table, the necessary development length is obtained by reducing the tabulated length in the ratio of calculated steel stress to tabulated steel stress.

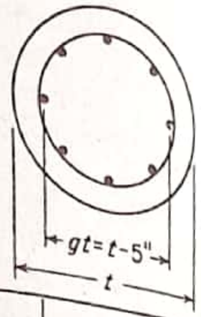
Table 8 **Development lengths* in inches** (***continued***)
$L = A_s f_s / \Sigma_0 \times 0.8 \times u_{all}$ (Top value is for top bars, bottom for other bars.)

Bar No.	W.S.D. f_s		U.S.D. $f_s = f_y$		
	20,000	24,000	40,000	50,000	60,000
f'_c = 5000:					
2	9.75 9.76	11.7 11.7	13.2 12.5	15.7 15.6	18.8 18.8
3	6.70 4.69	8.04 5.63	8.37 5.86	10.5 7.32	12.6 8.79
4	8.93 6.25	10.7 7.50	11.2 7.81	14.0 9.77	16.7 11.7
5	11.2 7.81	9.38 13.4	14.0 9.77	17.4 12.2	20.9 14.6
6	14.6 10.4	17.5 12.4	16.7 11.7	20.9 14.6	25.1 17.6
7	19.9 14.1	23.9 16.9	20.2 14.2	25.3 17.8	30.3 21.4
8	26.0 18.4	31.2 22.1	26.4 18.6	33.0 23.3	39.6 27.9
9	33.1 23.4	39.7 28.1	33.6 23.7	42.0 29.6	50.4 35.5
10	41.9 29.7	50.3 35.6	42.6 30.0	53.2 37.5	63.8 45.0
11	51.7 36.6	62.0 43.9	52.5 37.0	65.6 46.2	78.7 55.5
14*S*	71.3 49.9	85.5 59.9	71.3 49.9	89.1 62.4	106.9 74.8
18*S*	95.0 66.5	11.4 79.8	95.0 66.5	118.7 83.1	142.5 99.7

* When the bar stress calculated from the bending moment is smaller than the respective maximum values shown in the table, the necessary development length is obtained by reducing the tabulated length in the ratio of calculated steel stress to tabulated steel stress.

Scanned with CamScanner

Table 9 **Weights, areas, moments of inertia of circular columns and moments of inertia of column verticals arranged in a circle 5 in. less than the diameter of column**



Diameter of column t, in.	Weight per foot, lb	Area, in.²	I, in.⁴	A_s where $p_g = 0.01$*	I_s, in.⁴†
12	118	113	1,018	1.13	6.92
13	138	133	1,402	1.33	10.64
14	160	154	1,886	1.54	15.59
15	184	177	2,485	1.77	22.13
16	210	201	3,217	2.01	30.40
17	237	227	4,100	2.27	40.86
18	265	255	5,153	2.55	53.87
19	295	284	6,397	2.84	69.58
20	327	314	7,854	3.14	88.31
21	361	346	9,547	3.46	110.7
22	396	380	11,500	3.80	137.2
23	433	416	13,740	4.16	168.4
24	471	452	16,290	4.52	203.9
25	511	491	19,170	4.91	245.5
26	553	531	22,430	5.31	292.7
27	597	573	26,090	5.73	346.7
28	642	616	30,170	6.16	407.3
29	688	661	34,720	6.61	475.9
30	736	707	39,760	7.07	552.3

* For other values of p_g, multiply the value in the table by $100p_g$.

† The bars are assumed transformed into a thin-walled cylinder having the sam sectional area as the bars. Then $I_s = A_s(gt)^2/8$.

Table 10 **Size and pitch of spirals, ACI Code**

Diameter of column, in.	Out to out of spiral, in.	f'_c 2500	f'_c 3000	f'_c 4000	f'_c 5000
f_y = 40,000:					
14, 15	11, 12	⅜–2	⅜–1¾	½–2½	½–1¾
16	13	⅜–2	⅜–1¾	½–2½	½–2
17–19	14–16	⅜–2¼	⅜–1¾	½–2½	½–2
20–23	17–20	⅜–2¼	⅜–1¾	½–2½	½–2
24–30	21–27	⅜–2¼	⅜–2	½–2½	½–2
f_y = 60,000:					
14, 15	11, 12	¼–1¾	⅜–2¾	⅜–2	½–2¾
16–23	13–20	¼–1¾	⅜–2¾	⅜–2	½–3
24–29	21–26	¼–1¾	⅜–3	⅜–2¼	½–3
30	27	¼–1¾	⅜–3	⅜–2¼	½–3¼

Table 11 **Properties of prestressing steel**

A. Uncoated stress-relieved seven-wire strands *(John A. Roebling's Sons Corporation.)*

Nominal diameter, in.	Weight per 1000 ft, lb	Approximate area, in.²	Ultimate strength, lb	Design load, lb	Tensioning load, lb
¼	122	0.0356	9000	5040	6300
5/16	198	0.0578	14,500	8120	10,150
⅜	274	0.0799	20,000	11,200	14,000
7/16	373	0.1089	27,000	15,120	18,900
½	494	0.1438	36,000	20,160	25,200

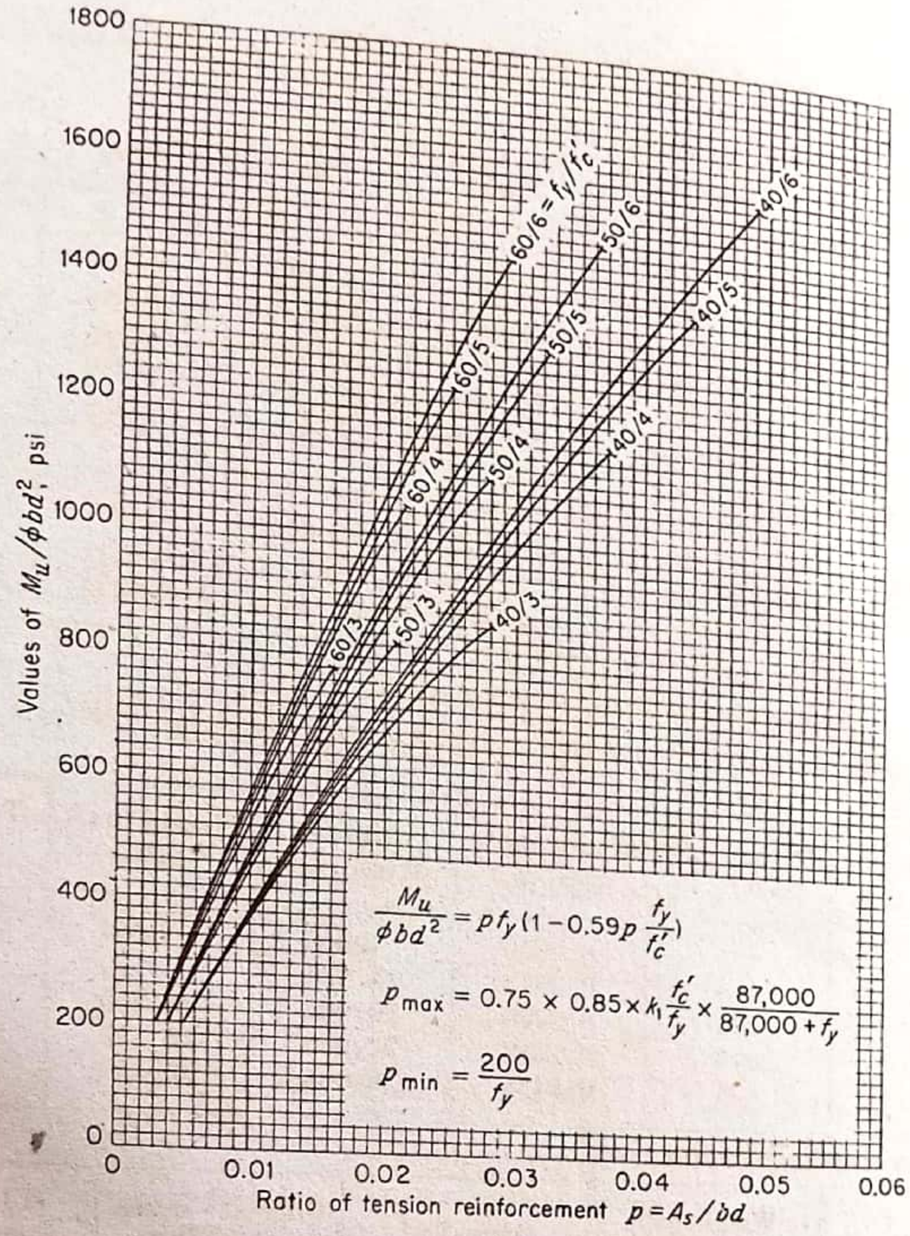
B. Stress-relieved solid wire

Diameter, in.	Weight per 1000 ft, lb	Area, in.²	Ultimate stress, psi	Ultimate strength, lb
0.192	98	0.0290	251,000	7280
0.196	103	0.0302	250,000	7550
0.250	167	0.0491	240,000	11,800
0.276	203	0.0598	236,000	14,100

C. Alloy-steel bars

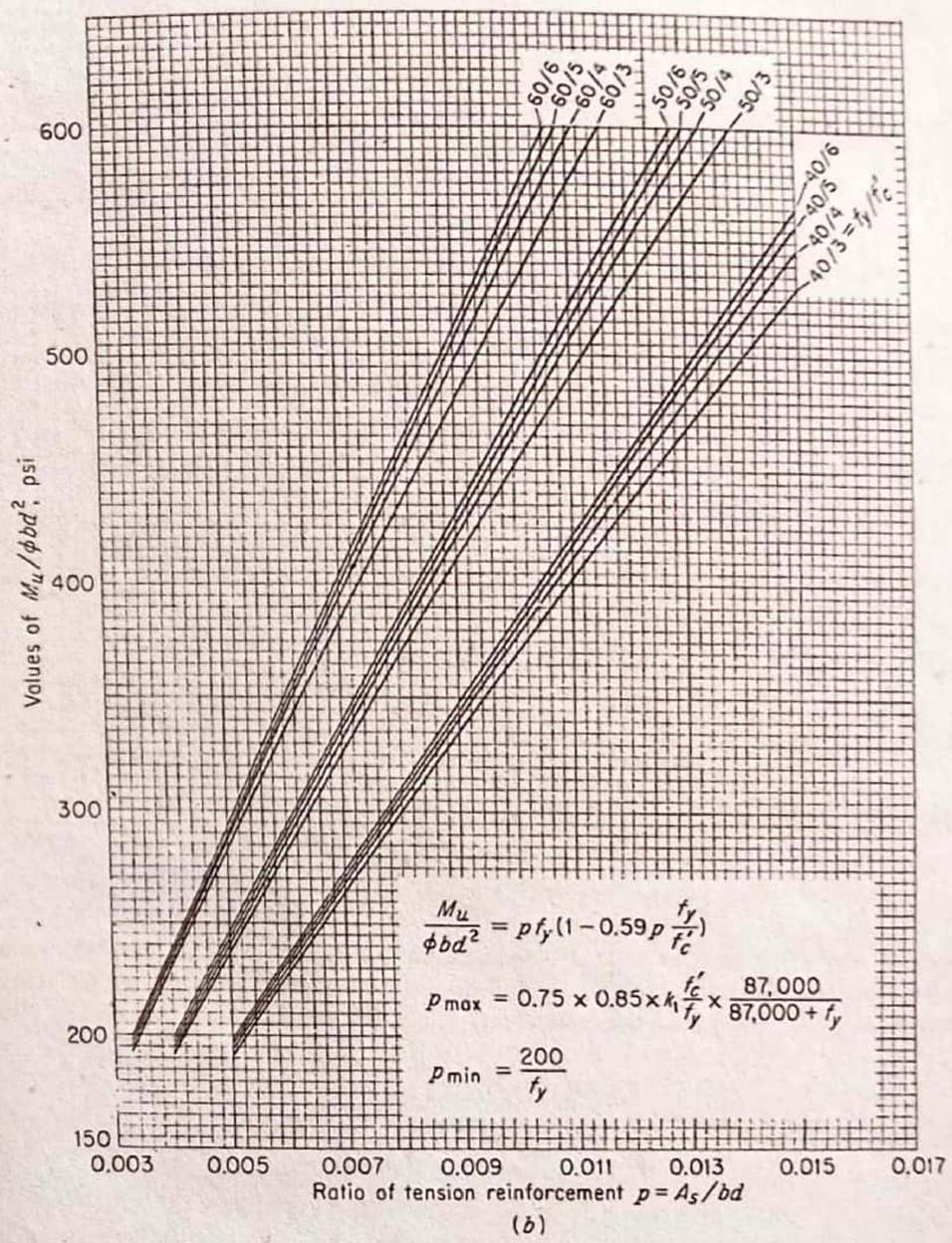
Diameter, in.	Weight per foot, lb	Area, in.²	Ultimate strength, lb
¾	1.50	0.442	64,100
⅞	2.04	0.601	87,100
1	2.67	0.785	113,800
1⅛	3.38	0.994	144,100
1¼	4.17	1.227	177,900

Scanned with CamScanner



(*a*)

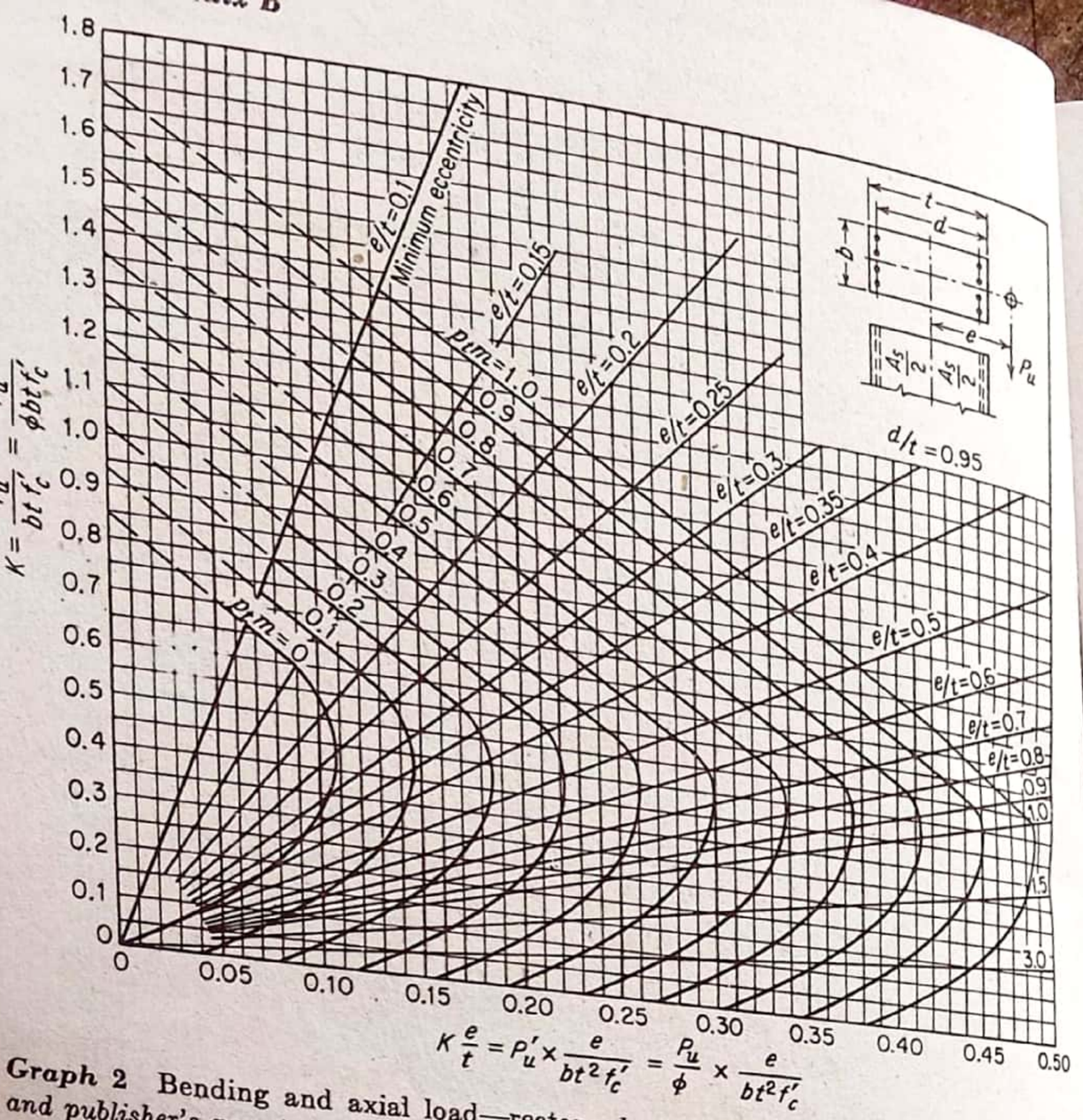
Graph 1a Moment capacity of rectangular sections.



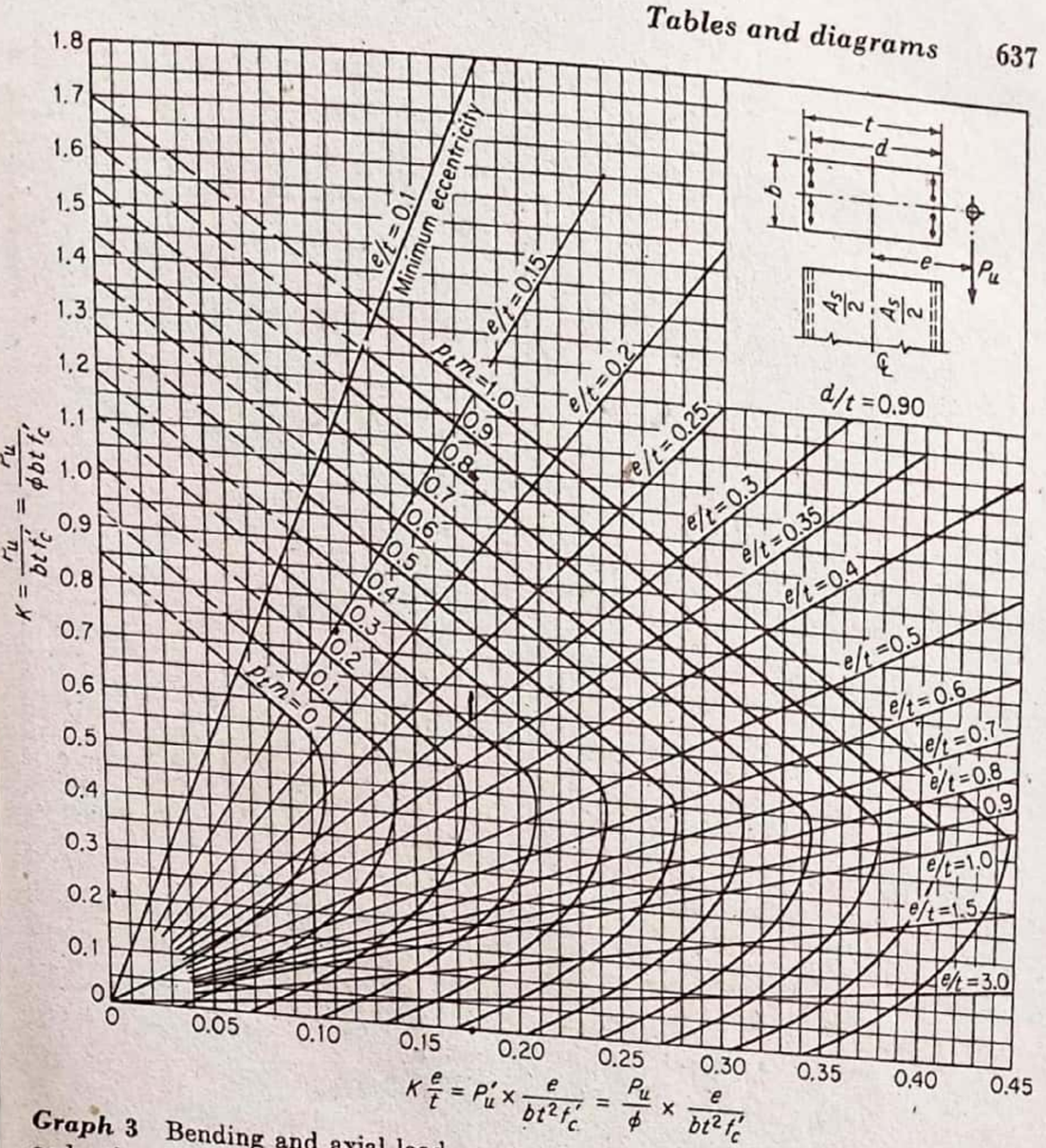
(*b*)

Graph 1b Moment capacity of rectangular sections.

Scanned with CamScanner

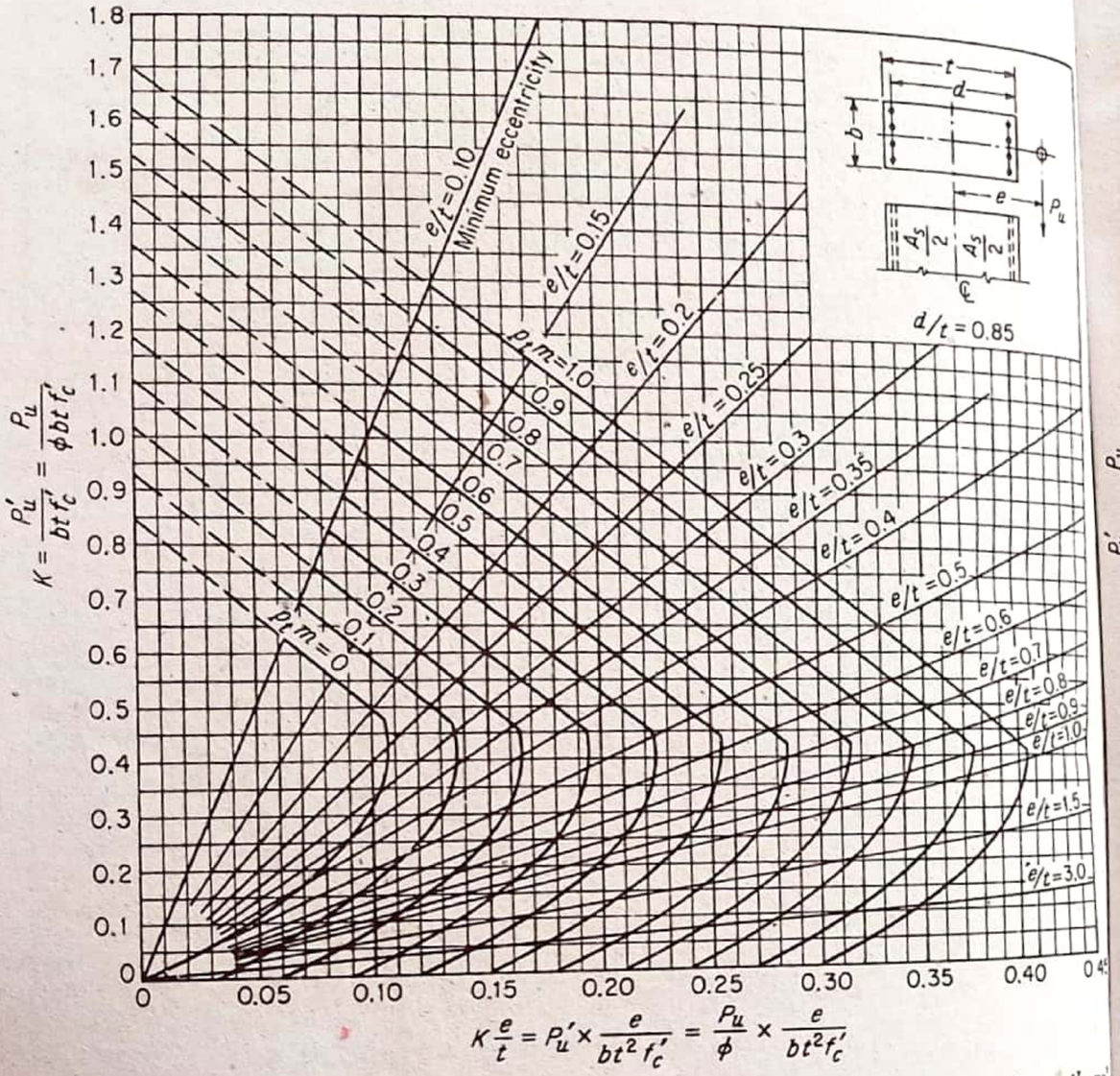


Graph 2 Bending and axial load—rectangular sections. (*Taken, with the authors' and publisher's permission, from C. S. Whitney and Edward Cohen, Guide for Ultimate Strength Design of Reinforced Concrete, J. ACI, vol. 28, no. 5, p. 455, November, 1956.*)

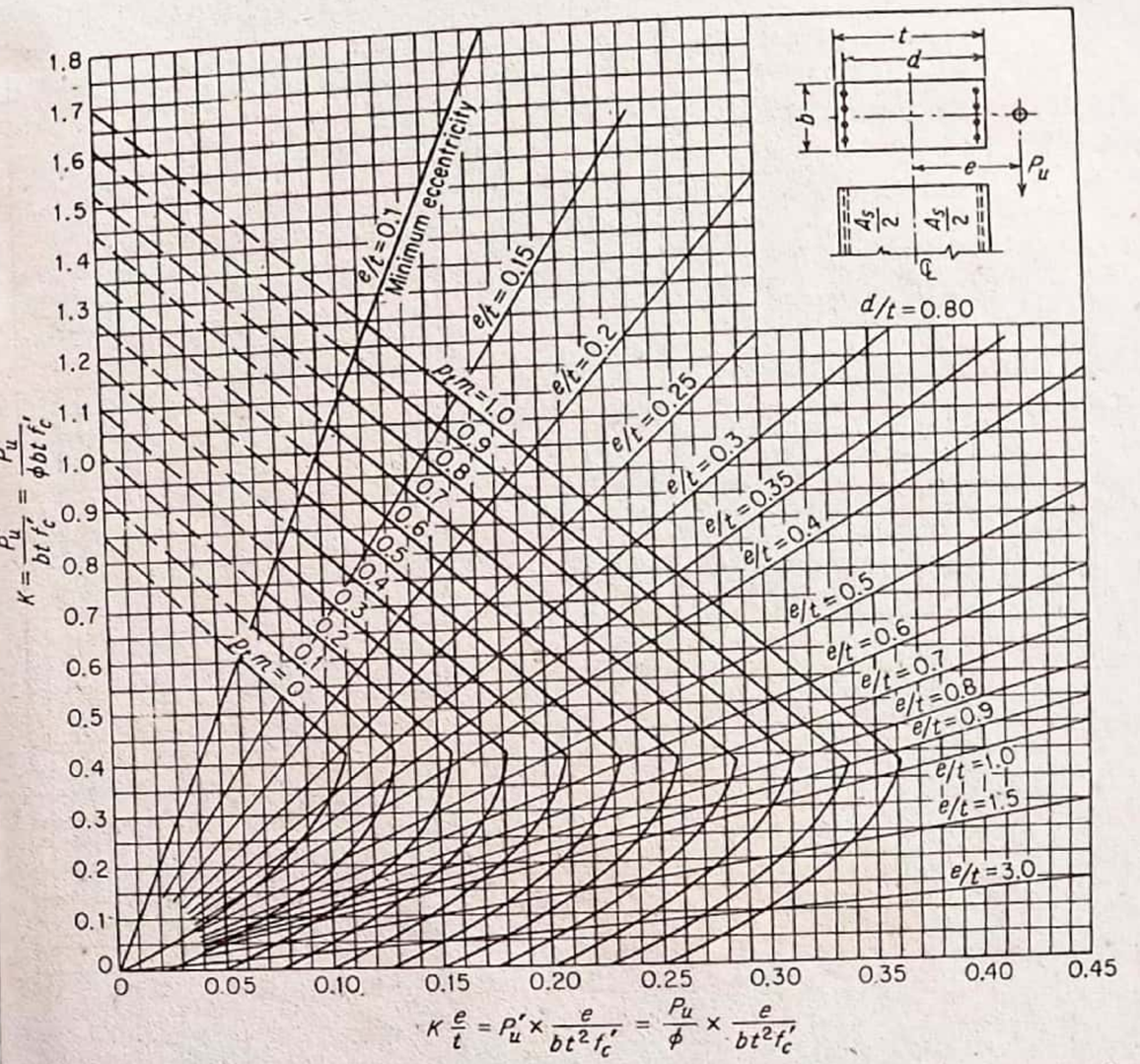


Graph 3 Bending and axial load—rectangular sections. (*Taken, with the authors' and publisher's permission, from C. S. Whitney and Edward Cohen, Guide for Ultimate Strength Design of Reinforced Concrete, J. ACI, vol. 28, no. 5, p. 455, November, 1956.*)

Scanned with CamScanner

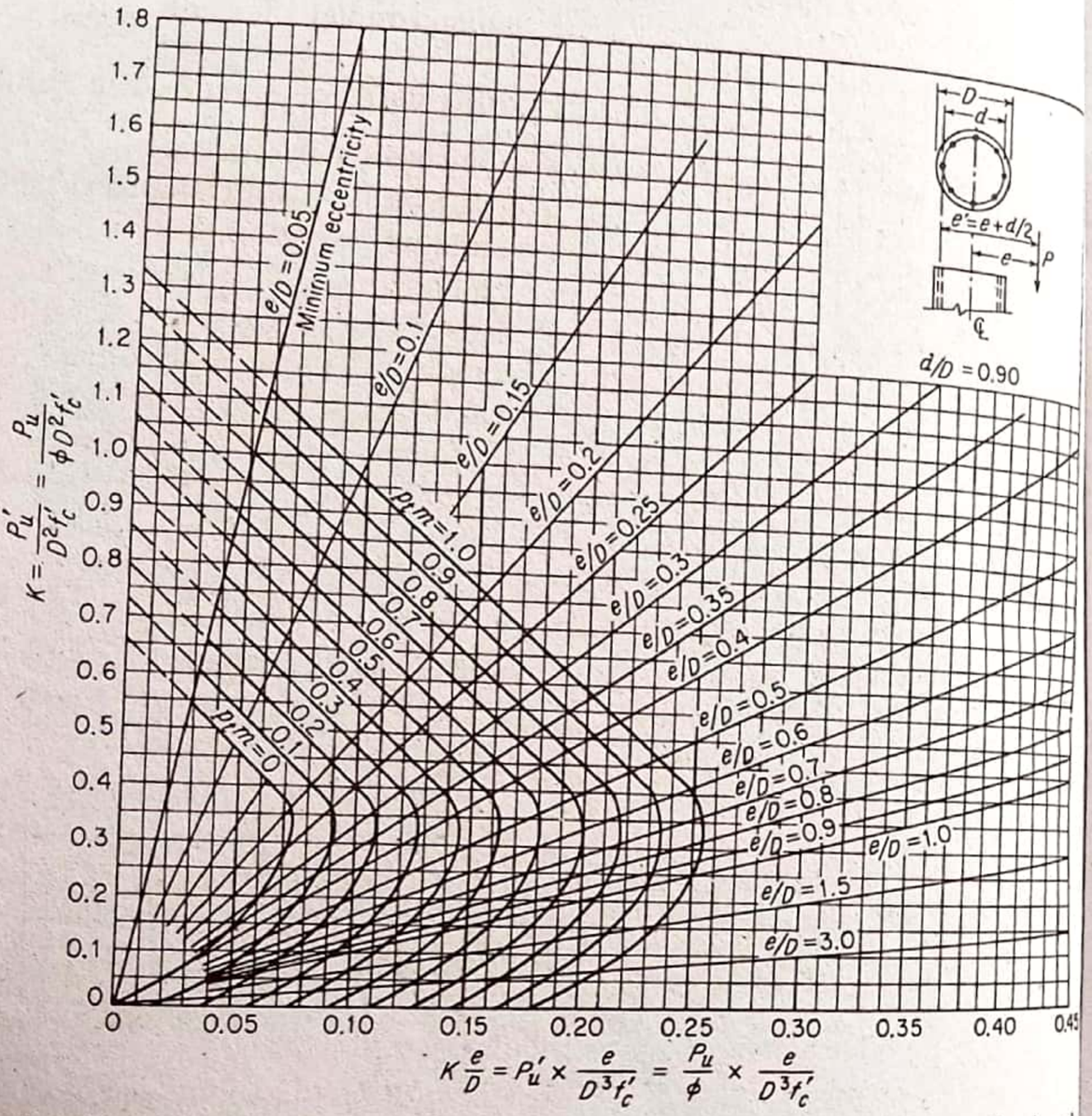


Graph 4 Bending and axial load—rectangular sections. (*Taken, with the authors' and publisher's permission, from C. S. Whitney and Edward Cohen, Guide for Ultimate Strength Design of Reinforced Concrete, J. ACI, vol. 28, no. 5, p. 455, November, 1956.*)

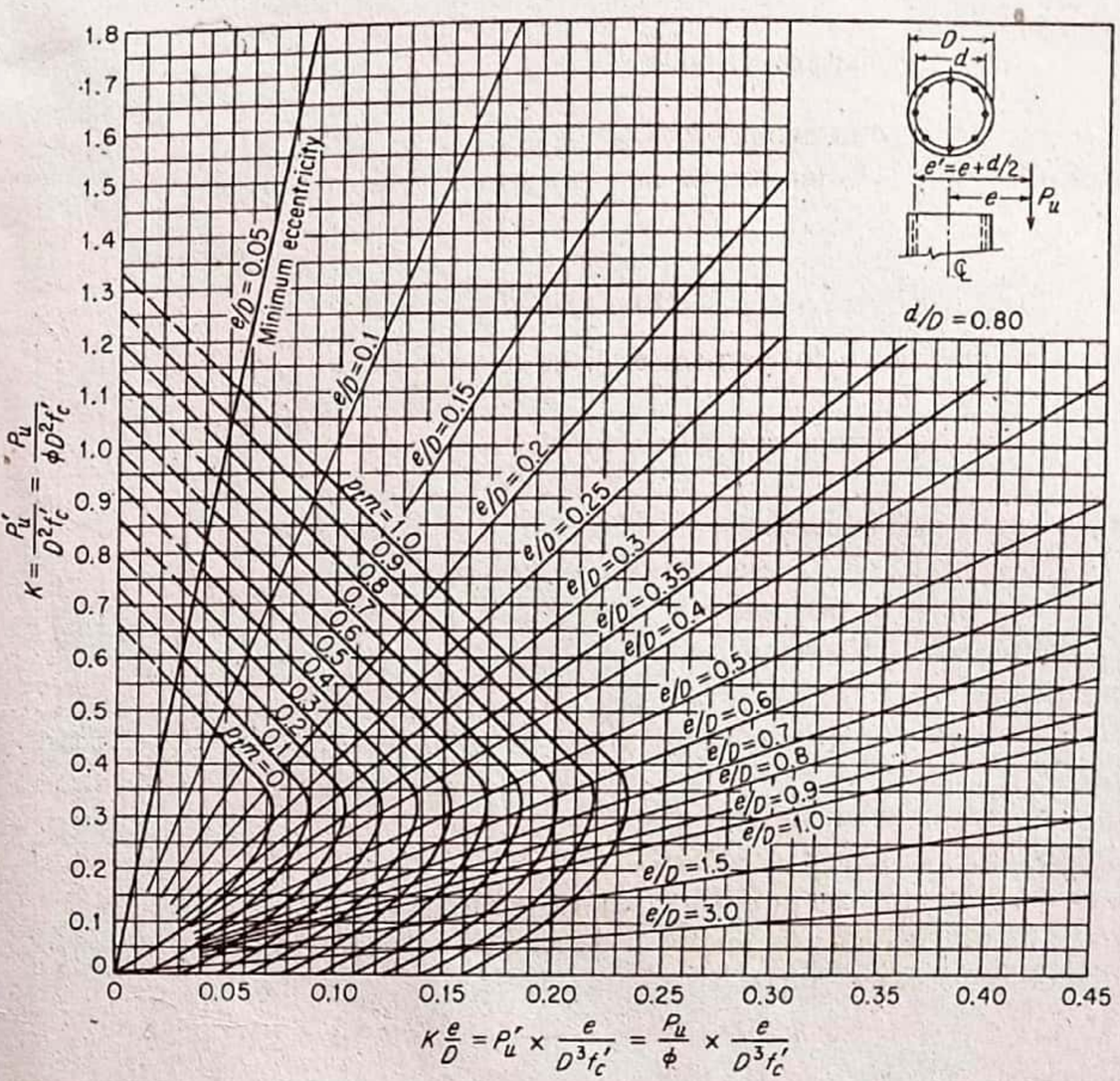


Graph 5 Bending and axial load—rectangular sections. (*Taken, with the authors' and publisher's permission, from C. S. Whitney and Edward Cohen, Guide for Ultimate Strength Design of Reinforced Concrete, J. ACI, vol. 28, no. 5, p. 455, November, 1956.*)

Scanned with CamScanner

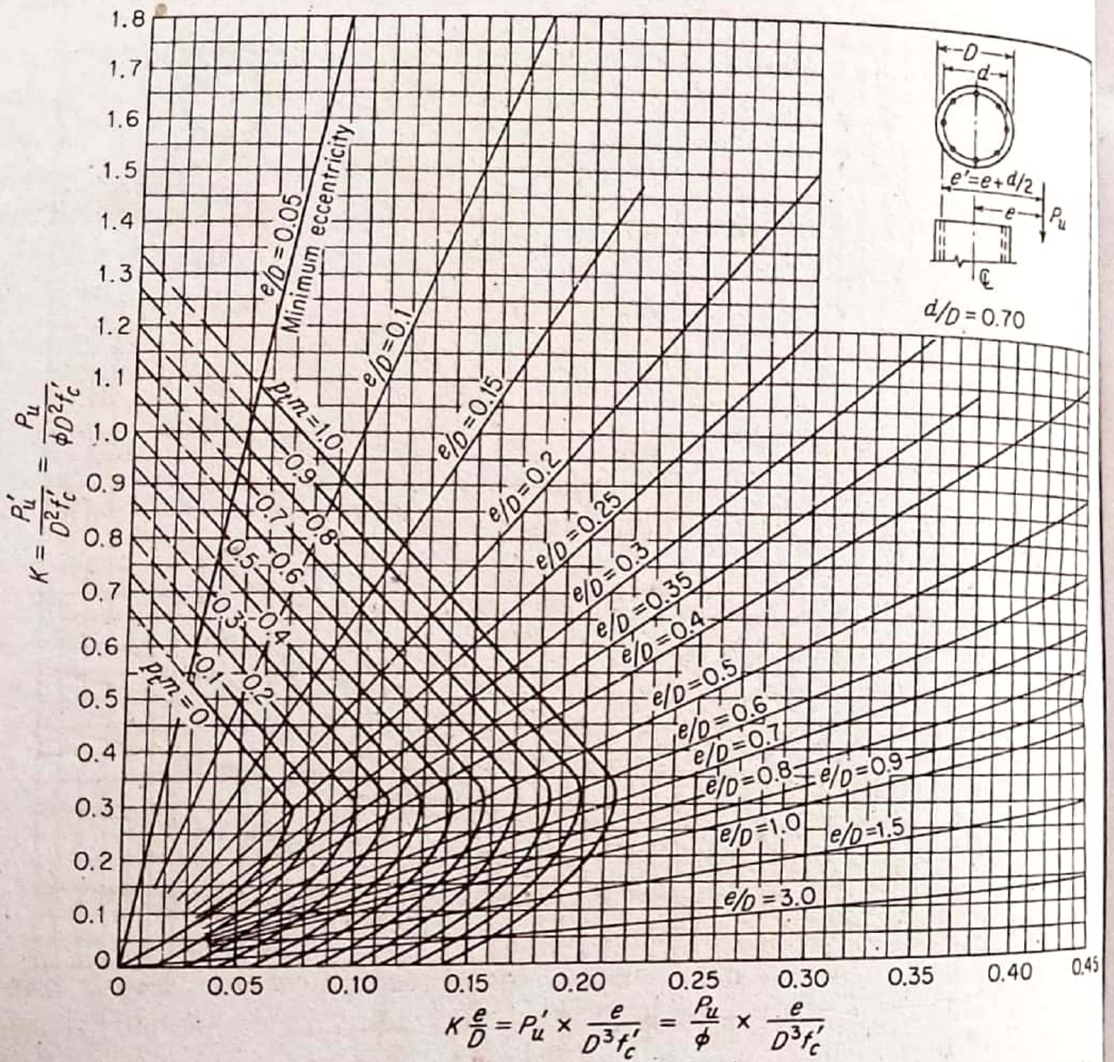


***Graph* 6** Bending and axial load—circular sections. (*Taken, with the authors' and publisher's permission, from C. S. Whitney and Edward Cohen, Guide for Ultimate Strength Design of Reinforced Concrete, J. ACI, vol.* 28, *no.* 5, *p.* 455, *November,* 1956.)

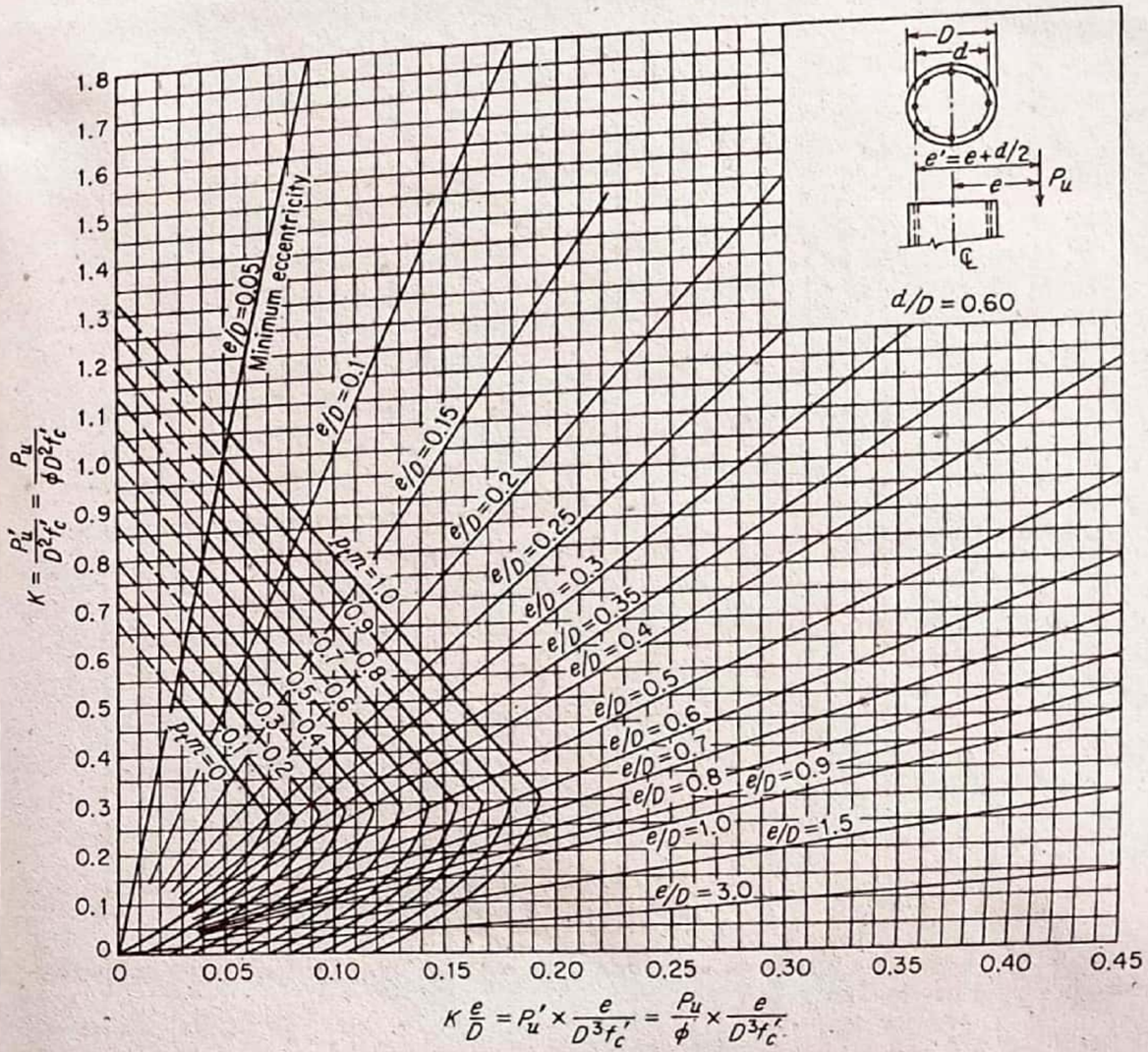


***Graph* 7** Bending and axial load—circular sections with spiral reinforcement. (*Taken, with the authors' and publisher's permission, from C. S. Whitney and Edward Cohen, Guide for Ultimate Strength Design of Reinforced Concrete, J. ACI, vol.* 28, *no.* 5, *p.* 455, *November,* 1956.)

Scanned with CamScanner

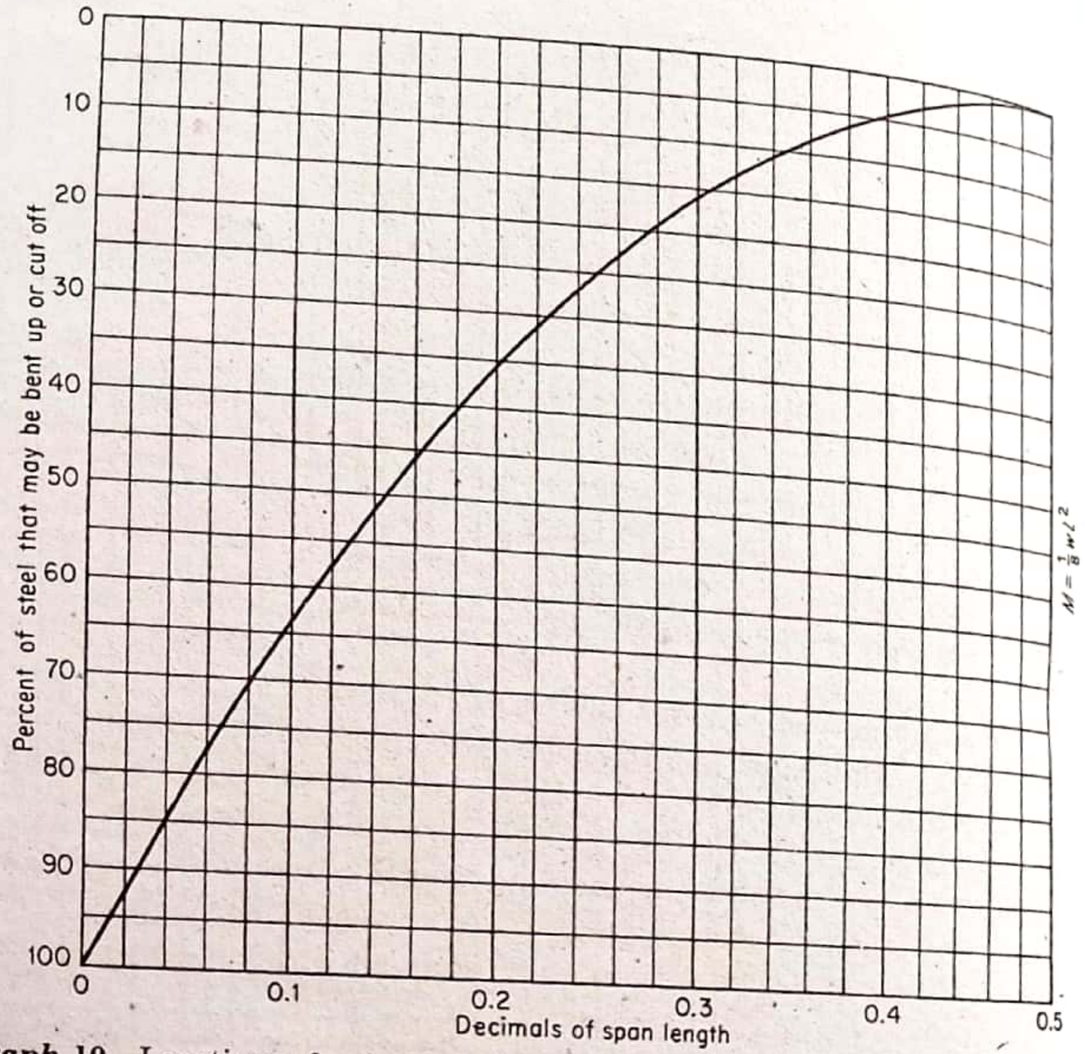


***Graph* 8** Bending and axial load—circular sections with spiral reinforcement. (*Taken, with the authors' and publisher's permission, from C. S. Whitney and Edward Cohen, Guide for Ultimate Strength Design of Reinforced Concrete, J. ACI, vol.* 28, *no.* 5, *p.* 455, *November*, 1956.)

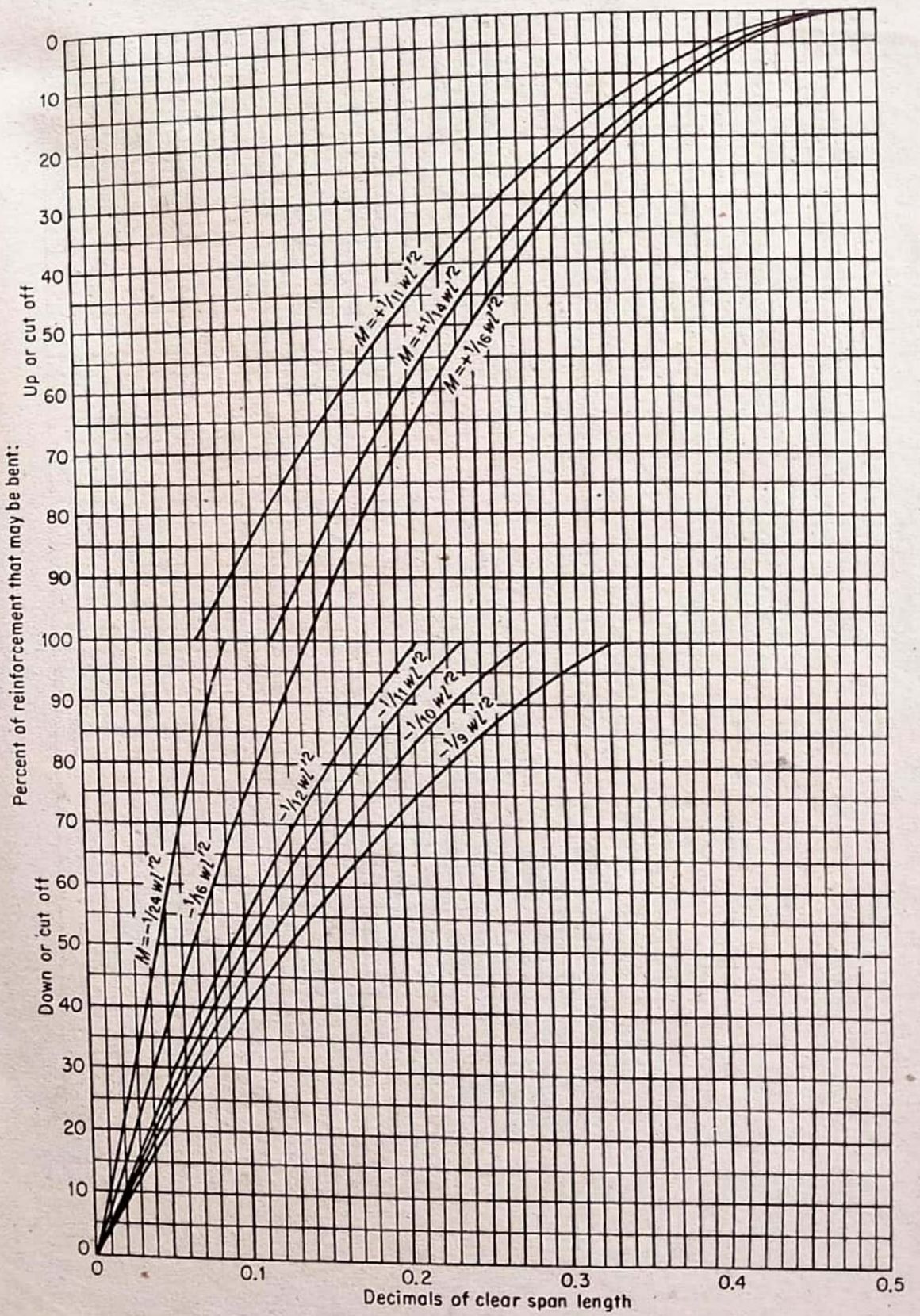


***Graph* 9** Bending and axial load—circular sections with spiral reinforcement. (*Taken, with the authors' and publisher's permission, from C. S. Whitney and Edward Cohen, Guide for Ultimate Strength Design of Reinforced Concrete, J. ACI, vol.* 28, *no.* 5, *p.* 455, *November*, 1956.)

Scanned with CamScanner

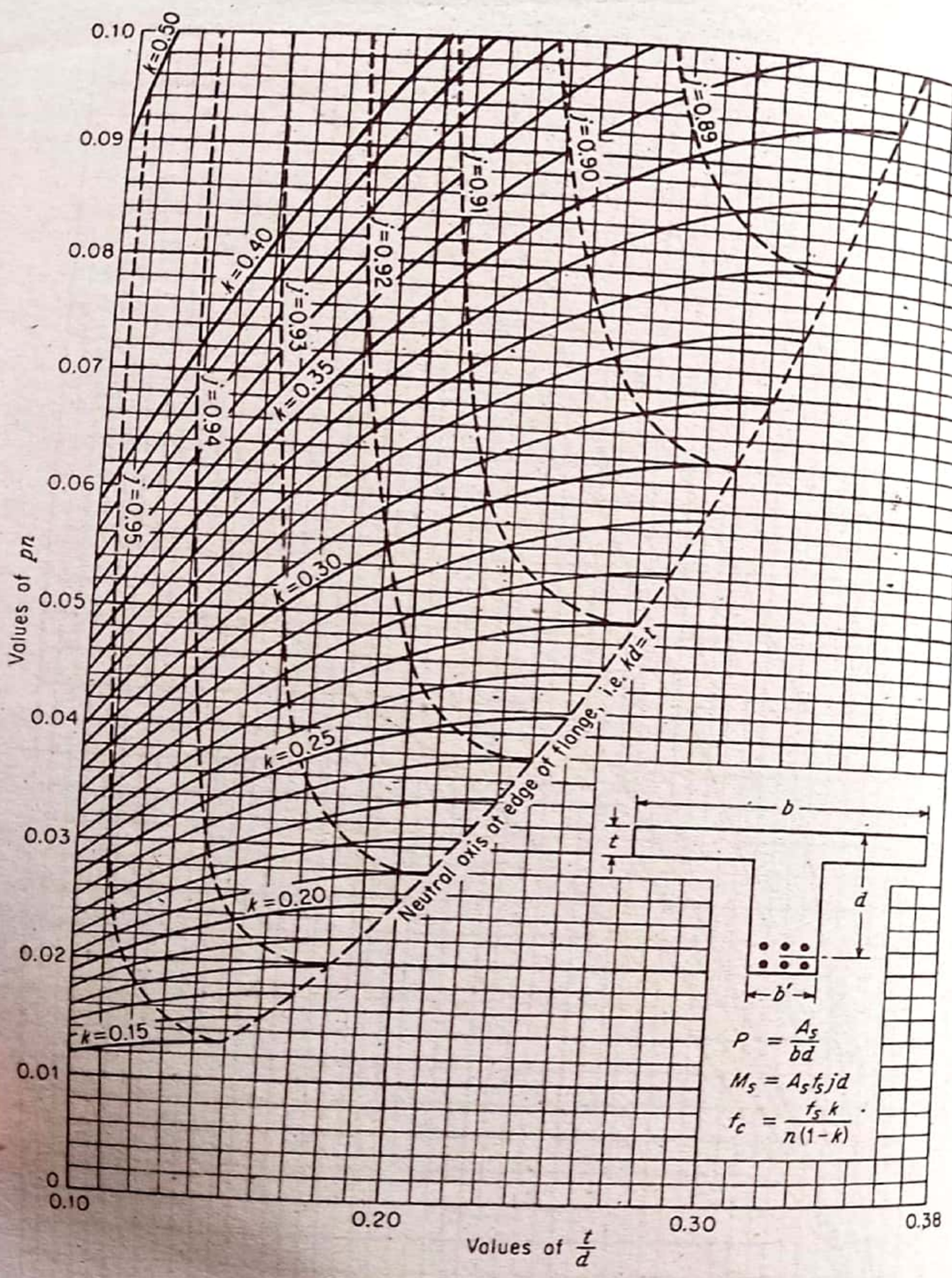


***Graph* 10** Locations of points at which bars may be bent up for simply supported beams uniformly loaded.



***Graph* 11** Approximate locations of points at which bars may be bent up or down or cut off for continuous beams uniformly loaded and built integrally with their supports according to the coefficients of the ACI Code.

Scanned with CamScanner



***Graph* 12** T-beam review.

appendix C

ANALYSIS AND DESIGN OF BEAMS FOR TORSION

C.1 General Considerations In addition to effects considered earlier, concrete beams may be subjected to torsional moments. Torsion rarely occurs alone in reinforced-concrete structures; it is present more often in combination with transverse shear and bending. Torsion may be a primary influence, as in curved beams, but more frequently it is a secondary effect, as in spandrel beams or T beams loaded unsymmetrically. If neglected, torsional stresses can cause distress or failure.

The behavior of concrete members subject to torsion is not completely understood at present, although intensive investigations are in progress in the United States and abroad (Ref. C.1). The present ACI Code mentions torsion only briefly, yet good design practice must account for its effect. In spite of a lack of adequate theoretical and experimental data, foreign code treatment of the subject follows a consistent pattern. These codes focus attention on conditions in the member at working load, and the concrete is presumed to behave elastically. Calculation of torsional stresses is based on the classical theory of Saint-Venant (Ref. C.2).

The Australian Building Code (Ref. C.3) appears to be the most current and reliable guide to the design of members for torsion. The material which follows is patterned after the Australian code, adapted to practice in the United States.

Scanned with CamScanner

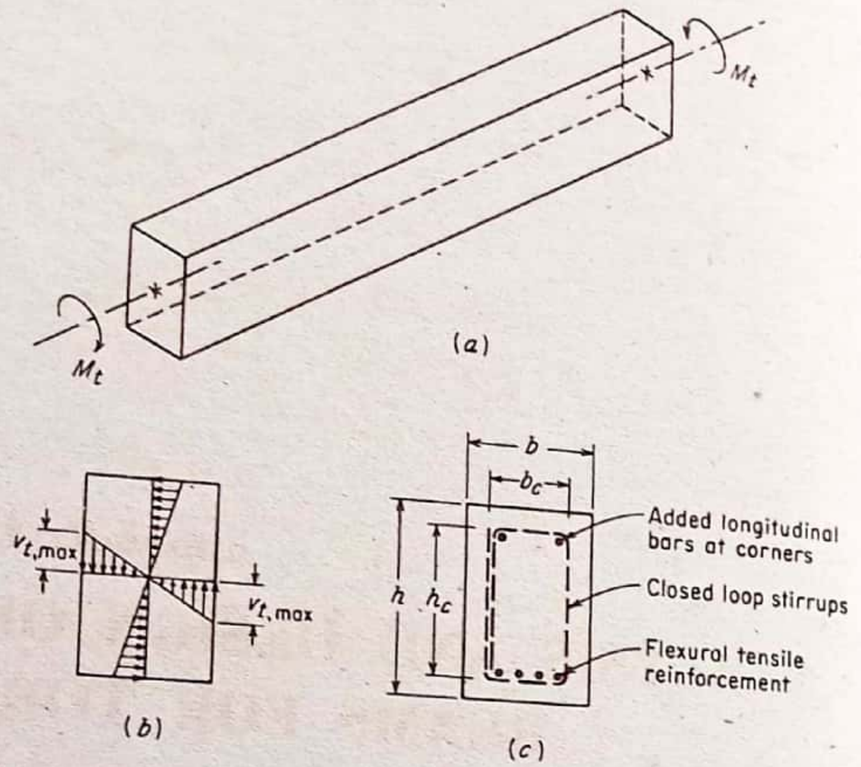


Fig. C.1 (*a*) Rectangular beam subject to torsion; (*b*) distribution of torsional shear along horizontal and vertical centerline of section; (*c*) reinforcement for torsion.

It may serve as a guide to design until such time as the ACI Code will include specific recommendations.

C.2 Torsional Stresses The application of twisting moment to a noncircular prismatic member results in (1) relative rotation of the cross sections and (2) warping of the originally plane cross sections. For a rectangular homogeneous member subject to pure torsion, the application of a twisting moment M_t (see Fig. C.1*a*) results in shearing stresses which vary linearly along any radial line with distance from the section centroid (see Fig. C.1*b*). For a rectangular section, the maximum torsional shear stress obtains at the middle of the long sides. If this shear stress is sufficient in magnitude, diagonal cracks of opposite direction will form near the center of the two long faces. If the section is nearly square, cracks will be evident on all four faces, in a spiral pattern.

In a rectangular section, the maximum flexural shear stress occurs at the neutral axis. Thus, at the center of one long face of such a beam, maximum flexural and torsional shear stresses are additive, while on the opposite face they tend to cancel.

In an elastic rectangular member, the maximum torsional shear stress v_t can be calculated from the expression

$$v_t = \frac{\eta M_t}{b^2 h}$$

in which M_t = torsional moment
b = smaller cross-sectional dimension
h = larger cross-sectional dimension
η = a coefficient which depends on the cross-sectional shape

For rectangular cross sections of usual proportions, η varies from about 3.5 to 4.5. According to the Australian code, η is taken equal to 5, so that

$$v_t = \frac{5M_t}{b^2 h} \tag{C.1}$$

For T, I, and L sections common to reinforced-concrete construction, torsional shear at the face of the web can be approximated by the expression

$$v_t = \frac{3M_t b'}{\Sigma b^3 h} \tag{C.2}$$

in which b' = web width
b = smaller dimension of each component rectangle of the section
h = larger dimension of each component rectangle of the section
$\Sigma b^3 h$ = sum of $b^3 h$ terms of the component rectangles

This equation is based on the assumption that the torsional rigidity of the section is equal to the sum of the torsional rigidities of the component rectangles. While originally intended for application to sections of rather slender proportions, it appears to be satisfactory for thicker sections as well.

Elastic theory indicates that high shear stress occurs at reentrant corners—i.e., where the flange joins the web in T, I, and L sections—and that fillets at these junctions would be desirable. Such fillets complicate construction, however, and are not common. Their omission may be justified by consideration of conditions within the beam when failure is imminent. At that stage of loading, an inelastic redistribution of stresses occurs which tends to equalize torsional shear over the entire cross section.

A problem facing the designer in dealing with torsion is what portion of the slab should be considered as effective flange. There is no reason to suppose that the effective width for torsion is the same as that for flexure. It has been suggested (Ref. C.4) that the entire overhanging portion of the flange may be disregarded in torsion calculations. For beams in which the web width is substantially larger than the slab thickness, this may be satisfactory; in other cases it seems unduly conservative.

C.3 Allowable Torsional Shear To guard against diagonal cracking of members without web reinforcement, it is necessary that torsional shear stress be kept below certain allowable limits. Since torsion produces shear and diagonal tension, permissible torsional shear stresses may be taken the same as values presently prescribed for flexural shear, that is,

For beams: $v_c = 1.1\sqrt{f'_c}$
For joists: $v_c = 1.2\sqrt{f'_c}$ (C.3)

Scanned with CamScanner

If a member is subjected to combined flexural and torsional shear, as in most cases, some codes permit shear stress substantially higher than would be permitted if either flexural or torsional shear were acting alone (Ref. C.1). However, lack of sufficient experimental evidence is reason to be somewhat conservative in this respect. It seems reasonable that there be no *reduction*, at least, in the allowable shear stress for combined cases and that the allowable shear for combined cases be the same as that used when either type of shear is acting alone.

C.4 Reinforcement for Torsion Failure of a concrete member subject to torsion can be delayed by the inclusion within the member of steel reinforcement arranged to cross potential diagonal cracks. The most efficient form of torsion reinforcement would consist of a pair of 45° spirals, one left hand and the other right hand. Such spirals are not often used, for practical reasons.

Diagonal tensile stresses due to torsion differ from those due to transverse shear in that they exist on all four faces of a rectangular section. It is evident that U-shaped stirrups or bent-up bars are not suitable for torsional reinforcement. Closed loops must be used. These are placed perpendicular to the axis of the member. Additional longitudinal bars are placed at the corners of the stirrups to accommodate the longitudinal component of stress and form a closed cage (see Fig. C.1*c*). Stirrup loops must have a sufficient length of embedment at the ends of the bars to ensure that allowable stresses can be developed. In flanged sections, the ends of the stirrups may project into the slab (see Fig. C.2). It is obvious that all such web reinforcement is in addition to that placed for flexural shear, although there is no reason why the two area requirements can not be combined into one set of stirrups.

If adequate reinforcement is provided, nominal torsional-shear stresses computed by Eqs. C.1 or C.2 may exceed the allowable values of Eqs. C.3. A maximum nominal shear stress equal to that permitted for web-reinforced beams subject to flexural shear is appropriate, that is,

$$v = 5\sqrt{f'_c} \tag{C.4}$$

Shear stress, in such a case, is calculated as if the presence of the reinforcement had no effect on stress distribution.

Experimental evidence indicates that if torsional reinforcement is provided, it need be designed only for the excess shear above that permitted on the plain concrete. In cases where torsional and flexural shear combine, the shear resisted by the concrete should be subtracted only once, either from the torsional- or flexural-shear requirement, but not from both. Australian practice is to proportion the reinforcement separately for shear and torsion, with v_c subtracted only from the larger of the shear stresses.

According to Australian code, the total steel area in the two legs of a transverse stirrup used for torsional reinforcement is

$$A_{st} = \frac{M'_t s}{0.8 b_c h_c f_v} \tag{C.5}$$

while the total area of additional longitudinal bars can be found from the equation

$$A_{sl} = \frac{M'_t(b_c + h_c)}{0.8 b_c h_c f_s} \tag{C.6}$$

In the above equations,

M'_t = excess of torsional moment over that resisted by the concrete
s = spacing of stirrups
b_c = smaller dimension of the closed stirrup
h_c = larger dimension of the closed stirrup
f_v = allowable stress for stirrup steel
f_s = allowable stress for longitudinal bars

Present investigations in the United States, as yet incomplete, indicate that the numerical coefficient in the denominator may be taken equal to 0.6 for better agreement with test results.

According to the present ACI Code, at least one longitudinal bar should be placed in each corner of the stirrup cage; these bars are to have a diameter at least equal to that of the stirrup, but in no case less than ½ in.

C.5 Example A reinforced concrete T beam (see Fig. C.2) has an overall depth of 24 in., web width of 12 in., flange width of 36 in., and flange thickness of 5 in. Calculate the amount of torsion reinforcement required if the beam is subject to a twisting moment of 150,000 in.-lb. The concrete strength is $f'_c = 4000$ psi; $f_s = f_v = 20{,}000$ psi.

The allowable torsional shear on the plain concrete may be taken equal to $v_c = 1.1\sqrt{f'_c} = 1.1\sqrt{4000} = 70$ psi. The twisting moment resisted by the concrete alone is found from Eq. C.2:

$$M_{tc} = \frac{v_t}{3b'}\sum b^3 h$$
$$= \frac{70}{3 \times 12}[(12^3 \times 24) + (5^3 \times 12 \times 2)] = 86{,}300 \text{ in.-lb}$$

The addition twisting moment for which web reinforcement must be provided is

$$M'_t = M_t - M_{tc} = 150{,}000 - 86{,}300 = 63{,}700 \text{ in.-lb}$$

Assuming 2 in. from the face of concrete to the center of the stirrup steel,

$b_c = 12 - 4 = 8$ in.
$h_c = 24 - 4 = 20$ in.

Then, from Eq. C.5,

$$A_{st} = \frac{M'_t s}{0.8 b_c h_c f_v} = \frac{63{,}700 \times s}{0.8 \times 8 \times 20 \times 20{,}000} = 0.0248s$$

Scanned with CamScanner

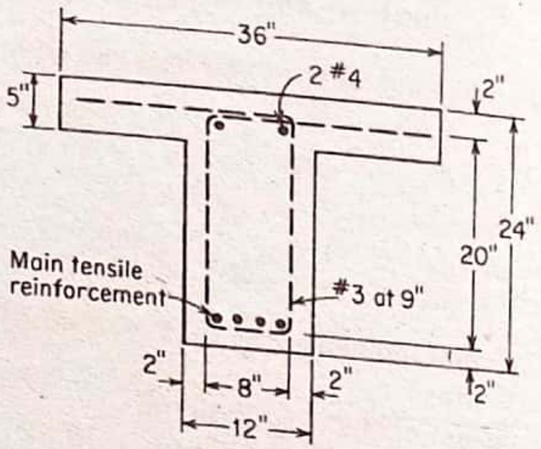


Fig. C.2

For No. 3 stirrups, with two vertical legs per stirrup, $A_{st} = 0.22$ in.^{2} Then, $s = 0.22/0.0248 = 8.88$ in., say 9 in. o.c. From Eq. C.6, the total area of additional longitudinal steel is found:

$$A_{sl} = \frac{M'_t(b_c + h_c)}{0.8 b_c h_c f_s} = \frac{63{,}700 \times 28}{0.8 \times 8 \times 20 \times 20{,}000} = 0.70 \text{ in.}^2$$

Two additional No. 4 bars will be added at the upper stirrup corners; bottom steel will be increased by 0.35 in.^{2} above the requirement for flexural tension. Stirrup legs will be extended into the overhanging flanges. The layout of reinforcement is shown in Fig. C.2.

REFERENCES

C.1 G. P. Fisher and P. Zia: Review of Code Requirements for Torsion Design, *J. ACI*, vol. 61, p. 1, 1964.

C.2 S. Timoshenko and J. N. Goodier: "Theory of Elasticity," chap. 11, McGraw-Hill Book Company, Inc., New York, 1961.

C.3 Australian Standard No. CA. 2, SAA Code for Concrete in Buildings, Standards Association of Australia, Sidney, 1958.

C.4 H. J. Cowan: Design of Beams Subject to Torsion Related to the New Australian Code, *J. ACI*, vol. 56, p. 591, 1960.

INDEX

Aggregates, 7
  coarse, 7
    maximum size of, 7
  fine, 7
  heavyweight, 8
  lightweight, 8
Allowable stresses for concrete and steel, 113
Anchorage, 164
  (*See also* Bond and anchorage)
Arch roofs, 468, 492
  advantages of, 468
  barrel, 471
  two-hinged, design of, 492
Arches, 469
  fixed, analysis of, 477
    elastic center, 481
    equations, general, 482
      simplified, 483
    evaluations of integrals, 484
    moments and reactions, table of, 487
    temperature changes and shrinkage, 480
  hinged, 489
  preliminary design of, 484
Arches, structural action of, 469
  two-hinged, analysis of, 472
    moments and reactions, table of, 486
    shortening, 474
    shrinkage, 475
    temperature changes, 474
    tie rods, 475
  types, choice of, 471
Axial compression, 31
  elastic behavior in, 31
  inelastic behavior, 35
  ultimate strength, 35
  (*See also* Columns)
Axial tension, 37
  prevention of cracks in, 38
  ultimate strength, 38

Beams, 106
  bar cutoff and bend points, 169
  bar spacing and positioning, 168
  bar splices, 177
  bond and anchorage (*see* Bond and anchorage)

Scanned with CamScanner